



ATLAS User's Manual

DEVICE SIMULATION SOFTWARE

SILVACO, Inc.

4701 Patrick Henry Drive, Bldg. 1

Santa Clara, CA 95054

Telephone (408) 567-1000

Internet: www.silvaco.com

April 20, 2010

ATLAS
User's Manual
Copyright 2010

SILVACO, Inc.
4701 Patrick Henry Drive, Building #6
Santa Clara, CA 95054

Phone: (408) 567-1000
Web: www.silvaco.com

The information contained in this document is subject to change without notice.

SILVACO, Inc. MAKES NO WARRANTY OF ANY KIND WITH REGARD TO THIS MATERIAL, INCLUDING, BUT NOT LIMITED TO, THE IMPLIED WARRANTY OF FITNESS FOR A PARTICULAR PURPOSE.

SILVACO, Inc. shall not be held liable for errors contained herein or for incidental or consequential damages in connection with the furnishing, performance, or use of this material.

This document contains proprietary information, which is protected by copyright laws of the United States. All rights are reserved. No part of this document may be photocopied, reproduced, or translated into another language without the prior written consent of SILVACO, Inc.

ACCUCELL, ACCUCORE, ACCUMODEL, ACCUTEST, ATHENA, ATHENA 1D, ATLAS, BLAZE, C-INTERPRETER, CATALYSTDA, CATALYSTAD, CELEBRITY, CELEBRITY C++, CIRCUIT OPTIMIZER, CLARITYRLC, CLEVER, DECKBUILD, DEVEDIT, DEVEDIT3D, DEVICE3D, DISCOVERY, EDA OMNI, EDIF WRITER, ELITE, EXACT, EXPERT, EXPERTVIEWS, FERRO, GATEWAY, GIGA, GIGA3D, GUARDIAN, GUARDIAN DRC, GUARDIAN LVS, GUARDIAN NET, HARMONY, HIPEX, HIPEX-C, HIPEX-NET, HIPEX-RC, HYPERFAULT, LASER, LED, LISA, LUMINOUS, LUMINOUS3D, MAGNETIC, MAGNETIC3D, MASKVIEWS, MC DEPO/ETCH, MC DEVICE, MC IMPLANT, MERCURY, MIXEDMODE, MIXEDMODE3D, MOCASIM, MODELLIB, NOISE, NOMAD, OLED, OPTOLITH, ORGANIC DISPLAY, ORGANIC SOLAR, OTFT, PROMOST, QUANTUM, QUANTUM3D, QUEST, REALTIMEDRC, RESILIENCE, S-PISCES, S-SUPREM3, S-SUPREM4, SCOUT, SDDL, SFLM, SiC, SILOS, SMARTLIB, SMARTSPICE, SMARTSPICE SEE, SMARTSPICERF, SMARTVIEW, SIMULATION STANDARD, SOLVERLIB, SPAYN, SPDB, SPIDER, SPRINT, STELLAR, TCAD DRIVEN CAD, TCAD OMNI, TFT, TFT3D, THERMAL3D, TONYPLOT, TONYPLOT3D, TWISTER, TWISTERFP, VCSEL, UTMOST, UTMOST III, UTMOST IV, UTMOST IV- FIT, UTMOST IV-MEASURE, UTMOST IV- OPTIMIZATION, VICTORY, VICTORYCELL, VICTORYDEVICE, VICTORYPROCESS, VICTORYSTRESS, VIRTUAL WAFER FAB, VWF, VWF AUTOMATION TOOLS, VWF INTERACTIVE TOOLS, VWF MANUFACTURING TOOLS, and VYPER are trademarks of SILVACO, Inc.

All other trademarks mentioned in this manual are the property of their respective owners.

Copyright © 1984 - 2010, SILVACO, Inc.

How to Read this Manual

| Style Conventions | | |
|---|--|--|
| Font Style/Convention | Description | Example |
| • | This represents a list of items or terms. | <ul style="list-style-type: none"> Bullet A Bullet B Bullet C |
| 1. 2. 3. | This represents a set of directions to perform an action. | <p>To open a door:</p> <ol style="list-style-type: none"> Unlock the door by inserting the key into keyhole. Turn key counter-clockwise. Pull out the key from the keyhole. Grab the doorknob and turn clockwise and pull. |
| → | This represents a sequence of menu options and GUI buttons to perform an action. | File→Open |
| Courier | This represents the commands, parameters, and variables syntax. | HAPPY BIRTHDAY |
| New Century Schoolbook Bold | This represents the menu options and buttons in the GUI. | File |
| <i>New Century Schoolbook Italics</i> | This represents the equations. | $abc=xyz$ |
| Note: | This represents the additional important information. | Note: Make sure you save often while running an experiment. |
| NEW CENTURY SCHOOLBOOK IN SMALL CAPS | This represents the names of the SILVACO Products. | ATHENA and ATLAS, . |

Table of Contents

Chapter 1

| | |
|---|------------|
| Introduction | 1-1 |
| 1.1: ATLAS Overview | 1-1 |
| 1.2: Features And Capabilities of ATLAS | 1-2 |
| 1.2.1: Comprehensive Set of Models | 1-2 |
| 1.2.2: Fully Integrated Capabilities | 1-2 |
| 1.2.3: Sophisticated Numerical Implementation | 1-2 |
| 1.3: Using ATLAS With Other Silvaco Software | 1-3 |
| 1.4: The Nature Of Physically-Based Simulation | 1-4 |

Chapter 2

| | |
|--|-------------|
| Getting Started with ATLAS | 2-1 |
| 2.1: Overview | 2-1 |
| 2.2: ATLAS Inputs and Outputs | 2-2 |
| 2.3: Modes of Operation | 2-3 |
| 2.3.1: Interactive Mode With DeckBuild | 2-3 |
| 2.3.2: Batch Mode With DeckBuild | 2-3 |
| 2.3.3: No Windows Batch Mode With DeckBuild | 2-3 |
| 2.3.4: Running ATLAS inside Deckbuild | 2-4 |
| 2.3.5: Batch Mode Without DeckBuild | 2-4 |
| 2.3.6: TMA Compatibility Mode | 2-4 |
| 2.3.7: ISE Compatibility Mode | 2-4 |
| 2.4: Accessing The Examples | 2-5 |
| 2.5: The ATLAS Syntax | 2-7 |
| 2.5.1: Statements and Parameters | 2-7 |
| 2.5.2: The Order of ATLAS Commands | 2-7 |
| 2.5.3: The DeckBuild Command Menu | 2-8 |
| 2.5.4: PISCES-II Quick Start | 2-8 |
| 2.6: Defining A Structure | 2-10 |
| 2.6.1: Interface From ATHENA | 2-10 |
| 2.6.2: Interface From DevEdit | 2-11 |
| 2.6.3: Using The Command Language To Define A Structure | 2-11 |
| 2.6.4: Automatic Meshing (Auto-meshing) Using The Command Language | 2-16 |
| 2.6.5: Modifying Imported Regions | 2-23 |
| 2.6.6: Remeshing Using The Command Language | 2-23 |
| 2.6.7: Specifying 2D Circular Structures | 2-25 |
| 2.6.8: Specifying 3D Structures | 2-29 |
| 2.6.9: Specifying 3D Cylindrical Structures | 2-29 |
| 2.6.10: Extracting 2D Circular Structures From 3D Cylindrical Structures | 2-33 |
| 2.6.11: General Comments Regarding Grids | 2-34 |
| 2.6.12: Maximum Numbers Of Nodes, Regions, and Electrodes | 2-34 |
| 2.6.13: Quadrilateral REGION Definition | 2-35 |
| 2.7: Defining Material Parameters And Models | 2-36 |
| 2.7.1: Specifying Contact Characteristics | 2-36 |
| 2.7.2: Specifying Material Properties | 2-39 |
| 2.7.3: Specifying Interface Properties | 2-40 |
| 2.7.4: Specifying Physical Models | 2-40 |
| 2.7.5: Summary Of Physical Models | 2-42 |
| 2.8: Choosing Numerical Methods | 2-46 |

| | |
|--|-------------|
| 2.8.1: Numerical Solution Techniques | 2-46 |
| 2.9: Obtaining Solutions | 2-50 |
| 2.9.1: DC Solutions | 2-50 |
| 2.9.2: The Importance Of The Initial Guess | 2-51 |
| 2.9.3: Small-Signal AC Solutions | 2-53 |
| 2.9.4: Transient Solutions | 2-54 |
| 2.9.5: Advanced Solution Techniques | 2-55 |
| 2.9.6: Using DeckBuild To Specify SOLVE Statements | 2-57 |
| 2.10: Interpreting The Results. | 2-58 |
| 2.10.1: Run-Time Output | 2-58 |
| 2.10.2: Log Files | 2-59 |
| 2.10.3: Parameter Extraction In DeckBuild | 2-60 |
| 2.10.4: Functions In TonyPlot | 2-61 |
| 2.10.5: Solution Files | 2-62 |
| 2.10.6: Technology Specific Issues in ATLAS | 2-64 |

Chapter 3

| | |
|---|-------------|
| Physics | 3-1 |
| 3.1: Basic Semiconductor Equations. | 3-1 |
| 3.1.1: Poisson's Equation | 3-1 |
| 3.1.2: Carrier Continuity Equations | 3-1 |
| 3.1.3: The Transport Equations | 3-2 |
| 3.1.4: Displacement Current Equation | 3-4 |
| 3.2: Basic Theory of Carrier Statistics | 3-5 |
| 3.2.1: Fermi-Dirac and Boltzmann Statistics | 3-5 |
| 3.2.2: Effective Density of States | 3-5 |
| 3.2.3: Intrinsic Carrier Concentration | 3-6 |
| 3.2.4: Evaluation of Fermi-Dirac Integrals | 3-7 |
| 3.2.5: Rules for Evaluation of Energy Bandgap | 3-7 |
| 3.2.6: The Universal Energy Bandgap Model | 3-8 |
| 3.2.7: Passler's Model for Temperature Dependent Bandgap | 3-8 |
| 3.2.8: General Ternary Bandgap Model with Bowing | 3-9 |
| 3.2.9: Bandgap Narrowing | 3-9 |
| 3.2.10: The Universal Bandgap Narrowing Model | 3-11 |
| 3.2.11: Bennett-Wilson and del Alamo Bandgap models. | 3-11 |
| 3.3: Space Charge from Incomplete Ionization, Traps, and Defects | 3-12 |
| 3.3.1: Incomplete Ionization of Impurities | 3-12 |
| 3.3.2: Low Temperature Simulations | 3-14 |
| 3.3.3: Traps and Defects | 3-14 |
| 3.4: The Energy Balance Transport Model | 3-26 |
| 3.4.1: The Energy Balance Equations | 3-26 |
| 3.4.2: Density of States | 3-28 |
| 3.4.3: Energy Density Loss Rates | 3-29 |
| 3.4.4: Temperature Dependence of Relaxation Times | 3-30 |
| 3.4.5: Energy Dependent Mobilities | 3-31 |
| 3.5: Boundary Physics. | 3-32 |
| 3.5.1: Ohmic Contacts | 3-32 |
| 3.5.2: Schottky Contacts | 3-32 |
| 3.5.3: Floating Contacts | 3-39 |
| 3.5.4: Current Boundary Conditions. | 3-40 |
| 3.5.5: Insulating Contacts | 3-40 |
| 3.5.6: Neumann Boundaries | 3-40 |
| 3.5.7: Lumped Element Boundaries. | 3-41 |
| 3.5.8: Distributed Contact Resistance | 3-43 |

| | |
|--|--------------|
| 3.5.9: Energy Balance Boundary Conditions | 3-44 |
| 3.6: Physical Models | 3-45 |
| 3.6.1: Mobility Modeling | 3-45 |
| 3.6.2: Mobility Model Summary | 3-83 |
| 3.6.3: Carrier Generation-Recombination Models | 3-84 |
| 3.6.4: Impact Ionization Models | 3-101 |
| 3.6.5: Band-to-Band Tunneling | 3-116 |
| 3.6.6: Gate Current Models | 3-126 |
| 3.6.7: Device Level Reliability Modeling | 3-153 |
| 3.6.8: The Ferroelectric Permittivity Model | 3-154 |
| 3.6.9: Epitaxial Strain Tensor Calculations in Zincblende | 3-155 |
| 3.6.10: Epitaxial Strain Tensor Calculation in Wurtzite | 3-156 |
| 3.6.11: Polarization in Wurtzite Materials [26] | 3-157 |
| 3.6.12: Stress Effects on Bandgap in Si | 3-158 |
| 3.6.13: Low-Field Mobility in Strained Silicon | 3-161 |
| 3.6.14: Light Absorption in Strained Silicon | 3-162 |
| 3.7: Quasistatic Capacitance - Voltage Profiles | 3-164 |
| 3.8: Conductive Materials | 3-165 |
| 3.8.1: Conductors with Interface Resistance | 3-165 |
| 3.8.2: Importing Conductors from ATHENA | 3-165 |
| 3.9: Optoelectronic Models | 3-166 |
| 3.9.1: The General Radiative Recombination Model | 3-166 |
| 3.9.2: The Default Radiative Recombination Model | 3-167 |
| 3.9.3: The Standard Gain Model | 3-167 |
| 3.9.4: The Empirical Gain Model | 3-168 |
| 3.9.5: Takayama's Gain Model | 3-169 |
| 3.9.6: Band Structure Dependent Optoelectronic Models | 3-170 |
| 3.9.7: Unstrained Zincblende Models for Gain and Radiative Recombination | 3-171 |
| 3.9.8: Strained Zincblende Gain and Radiative Recombination Models | 3-174 |
| 3.9.9: Strained Wurtzite Three-Band Model for Gain and Radiative Recombination | 3-175 |
| 3.9.10: Lorentzian Gain Broadening | 3-177 |
| 3.9.11: Ishikawa's Strain Effects Model | 3-178 |
| 3.10: Optical Index Models | 3-181 |
| 3.10.1: The Sellmeier Dispersion Model | 3-181 |
| 3.10.2: Adachi's Dispersion Model | 3-181 |
| 3.10.3: Tauc-Lorentz Dielectric Function with Optional Urbach Tail Model for Complex Index of Refraction | 3-182 |
| 3.11: Carrier Transport in an Applied Magnetic Field | 3-184 |
| 3.12: Anisotropic Relative Dielectric Permittivity | 3-186 |
| 3.13: Single Event Upset Simulation | 3-188 |
| 3.14: Field Emission from Semiconductor Surfaces | 3-191 |
| 3.15: Conduction in Silicon Nitride | 3-192 |
| Chapter 4 | |
| S-Pisces: Silicon Based 2D Simulator | 4-1 |
| 4.1: Overview | 4-1 |
| 4.2: Simulating Silicon Devices Using S-Pisces | 4-2 |
| 4.2.1: Simulating MOS Technologies | 4-2 |
| 4.2.2: Simulating Silicon Bipolar Devices | 4-5 |
| 4.2.3: Simulating Non-Volatile Memory Technologies (EEPROMs, FLASH Memories) | 4-7 |
| 4.2.4: Simulating SOI Technologies | 4-8 |

Chapter 5

| | |
|---|-------------|
| Blaze: Compound Material 2D Simulator | 5-1 |
| 5.1: Overview | 5-1 |
| 5.1.1: Basic Heterojunction Definitions | 5-1 |
| 5.1.2: Alignment | 5-2 |
| 5.1.3: The Drift Diffusion Transport Model | 5-12 |
| 5.1.4: The Thermionic Emission and Field Emission Transport Model | 5-13 |
| 5.1.5: Temperature Dependence of Electron Affinity | 5-15 |
| 5.2: The Physical Models | 5-16 |
| 5.2.1: Common Physical Models | 5-16 |
| 5.2.2: Recombination and Generation Models | 5-19 |
| 5.3: Material Dependent Physical Models | 5-20 |
| 5.3.1: Cubic III-V Semiconductors | 5-20 |
| 5.3.2: Gallium Arsenide (GaAs) Physical Models | 5-26 |
| 5.3.3: Al(x)Ga(1-x)As System | 5-28 |
| 5.3.4: In(1-x)Ga(x)As(y)P(1-y) System | 5-30 |
| 5.3.5: The Si(1-x)Ge(x) System | 5-32 |
| 5.3.6: Silicon Carbide (SiC) | 5-34 |
| 5.3.7: GaN, InN, AlN, Al(x)Ga(1-x)N, In(x)Ga(1-x)N, Al(x)In(1-x)N, and Al(x)In(y)Ga(1-x-y)N | 5-37 |
| 5.3.8: The Hg(1-x)Cd(x)Te System | 5-45 |
| 5.3.9: CIGS (CuIn(1-x)Ga(x)Se ₂), CdS, and ZnO | 5-46 |
| 5.4: Simulating Heterojunction Devices with Blaze | 5-47 |
| 5.4.1: Defining Material Regions with Positionally-Dependent Band Structure | 5-47 |
| 5.4.2: Defining Materials and Models | 5-48 |

Chapter 6

| | |
|--|------------|
| 3D Device Simulator | 6-1 |
| 6.1: 3D Device Simulation Programs | 6-1 |
| 6.1.1: DEVICE3D | 6-1 |
| 6.1.2: GIGA3D | 6-1 |
| 6.1.3: TFT3D | 6-1 |
| 6.1.4: MIXEDMODE3D | 6-1 |
| 6.1.5: QUANTUM3D | 6-2 |
| 6.1.6: LUMINOUS3D | 6-2 |
| 6.2: 3D Structure Generation | 6-3 |
| 6.3: Model And Material Parameter Selection in 3D | 6-4 |
| 6.3.1: Mobility | 6-4 |
| 6.3.2: Recombination | 6-4 |
| 6.3.3: Generation | 6-4 |
| 6.3.4: Carrier Statistics | 6-4 |
| 6.3.5: Boundary Conditions | 6-4 |
| 6.3.6: Optical | 6-5 |
| 6.3.7: Single Event Upset Simulation | 6-5 |
| 6.3.8: Boundary Conditions in 3D | 6-5 |
| 6.3.9: TFT3D Models | 6-5 |
| 6.3.10: QUANTUM3D Models | 6-5 |
| 6.3.11: LUMINOUS3D Models | 6-5 |
| 6.4: Numerical Methods for 3D | 6-6 |
| 6.4.1: DC Solutions | 6-6 |
| 6.4.2: Transient Solutions | 6-6 |
| 6.4.3: Obtaining Solutions In 3D | 6-6 |
| 6.4.4: Interpreting the Results From 3D | 6-6 |
| 6.4.5: More Information | 6-6 |

Chapter 7

| | |
|--|-------------|
| Giga: Self-Heating Simulator | 7-1 |
| 7.1: Overview | 7-1 |
| 7.1.1: Applications | 7-1 |
| 7.1.2: Numerics | 7-1 |
| 7.2: Physical Models | 7-2 |
| 7.2.1: The Lattice Heat Flow Equation | 7-2 |
| 7.2.2: Specifying Thermal Conductivity | 7-2 |
| 7.2.3: Specifying Heat Capacity | 7-7 |
| 7.2.4: Specifying Heat Sink Layers | 7-8 |
| 7.2.5: Non-Isothermal Models | 7-9 |
| 7.2.6: Heat Generation | 7-12 |
| 7.2.7: Thermal Boundary Conditions | 7-13 |
| 7.2.8: Temperature Dependent Material Parameters | 7-15 |
| 7.2.9: Phase Change Materials (PCMs) | 7-16 |
| 7.2.10: C-Interpreter Defined Scattering Law Exponents | 7-20 |
| 7.3: Applications of GIGA | 7-21 |
| 7.3.1: Power Device Simulation Techniques | 7-21 |
| 7.3.2: More Information | 7-21 |

Chapter 8

| | |
|--|-------------|
| Laser: Edge Emitting Simulator | 8-1 |
| 8.1: Overview | 8-1 |
| 8.2: Physical Models | 8-2 |
| 8.2.1: Scalar Helmholtz Equation | 8-2 |
| 8.2.2: Vector Helmholtz Equation | 8-4 |
| 8.2.3: Local Optical Gain | 8-5 |
| 8.2.4: Stimulated Emission | 8-5 |
| 8.2.5: Photon Rate Equations | 8-5 |
| 8.2.6: Spontaneous Recombination Model | 8-7 |
| 8.2.7: Optical Power | 8-7 |
| 8.2.8: Gain Saturation | 8-7 |
| 8.3: WAVEGUIDE Statement | 8-8 |
| 8.4: Solution Techniques | 8-9 |
| 8.5: Specifying Laser Simulation Problems | 8-10 |
| 8.5.1: LASER Statement Parameters | 8-10 |
| 8.5.2: Numerical Parameters | 8-11 |
| 8.6: Semiconductor Laser Simulation Techniques | 8-12 |
| 8.6.1: Generation of Near-Field and Far-Field Patterns | 8-12 |

Chapter 9

| | |
|---|------------|
| VCSEL Simulator | 9-1 |
| 9.1: Overview | 9-1 |
| 9.2: Physical Models | 9-2 |
| 9.2.1: Reflectivity Test Simulation | 9-2 |
| 9.2.2: Helmholtz Equation | 9-4 |
| 9.2.3: Local Optical Gain | 9-6 |
| 9.2.4: Photon Rate Equations | 9-6 |
| 9.3: Simulating Vertical Cavity Surface Emitting Lasers | 9-8 |
| 9.3.1: Specifying the Device Structure | 9-8 |
| 9.3.2: Specifying VCSEL Physical Models and Material Parameters | 9-11 |
| 9.3.3: Enabling VCSEL Solution | 9-12 |
| 9.3.4: Numerical Parameters | 9-13 |

| | |
|---|-------------|
| 9.3.5: Alternative VCSEL Simulator | 9-13 |
| 9.3.6: Far Field Patterns | 9-14 |
| 9.4: Semiconductor Laser Simulation Techniques | 9-15 |

Chapter 10

| | |
|--|--------------|
| Luminous: Optoelectronic Simulator | 10-1 |
| 10.1: Overview | 10-1 |
| 10.2: Ray Tracing | 10-2 |
| 10.2.1: Ray Tracing in 2D | 10-2 |
| 10.2.2: Ray Tracing in 3D | 10-4 |
| 10.2.3: Reflection and Transmission | 10-6 |
| 10.2.4: Diffusive Reflection [272] | 10-8 |
| 10.2.5: Light Absorption and Photogeneration | 10-9 |
| 10.2.6: Outputting the Ray Trace | 10-9 |
| 10.3: Matrix Method | 10-10 |
| 10.3.1: Characteristic Matrix | 10-10 |
| 10.3.2: Reflectivity, Transmissivity, and Absorptance | 10-11 |
| 10.3.3: Transfer Matrix and Standing Wave Pattern | 10-12 |
| 10.3.4: Transfer Matrix with Diffusive Interfaces | 10-14 |
| 10.4: Beam Propagation Method in 2D | 10-18 |
| 10.4.1: Using BPM | 10-18 |
| 10.4.2: Light Propagation In A Multiple Region Device | 10-19 |
| 10.4.3: Fast Fourier Transform (FFT) Based Beam Propagation Algorithm | 10-19 |
| 10.5: Finite Difference Time Domain Analysis [269] | 10-21 |
| 10.5.1: Physical Model | 10-21 |
| 10.5.2: Beam and Mesh | 10-23 |
| 10.5.3: Boundary Conditions [224] | 10-23 |
| 10.5.4: Static Solutions and Error Estimation | 10-27 |
| 10.6: User-Defined Photogeneration | 10-30 |
| 10.6.1: User-Defined Beams | 10-30 |
| 10.6.2: User-Defined Arbitrary Photogeneration | 10-32 |
| 10.6.3: Exponential Photogeneration | 10-33 |
| 10.6.4: Tabular Photogeneration (Luminous2D only) | 10-34 |
| 10.7: Photocurrent and Quantum Efficiency | 10-35 |
| 10.8: Defining Optical Properties of Materials | 10-36 |
| 10.8.1: Setting Single Values For The Refractive Index | 10-36 |
| 10.8.2: Setting A Wavelength Dependent Refractive Index | 10-36 |
| 10.9: Anti-Reflective (AR) Coatings for Ray Tracing and Matrix Method | 10-38 |
| 10.9.1: Anti-Reflective Coatings in LUMINOUS3D | 10-40 |
| 10.10: Specifying Lenslets | 10-41 |
| 10.11: Frequency Conversion Materials (2D Only) | 10-46 |
| 10.12: Simulating Photodetectors | 10-49 |
| 10.12.1: Defining Optical Sources | 10-49 |
| 10.12.2: Specifying Periodicity in the Ray Trace | 10-50 |
| 10.12.3: Defining Luminous Beam Intensity in 2D | 10-50 |
| 10.12.4: Defining Luminous3D Beam Intensity | 10-51 |
| 10.12.5: Monochromatic or Multispectral Sources | 10-51 |
| 10.12.6: Solar Sources | 10-53 |
| 10.12.7: Extracting Dark Characteristics | 10-54 |
| 10.12.8: Extracting Detection Efficiency | 10-55 |
| 10.12.9: Obtaining Quantum Efficiency versus Bias | 10-55 |
| 10.12.10: Obtaining Transient Response to Optical Sources | 10-56 |
| 10.12.11: Obtaining Frequency Response to Optical Sources | 10-56 |
| 10.12.12: Obtaining Spatial Response | 10-57 |

| | |
|---|--------------|
| 10.12.13: Obtaining Spectral Response | 10-57 |
| 10.12.14: Obtaining Angular Response | 10-58 |
| 10.13: Simulating Solar Cells | 10-59 |
| 10.13.1: Solar Spectra | 10-59 |
| 10.13.2: Solar Optical Propagation Models | 10-59 |
| 10.13.3: Solar Cell Extraction | 10-62 |

Chapter 11

| | |
|--|-------------|
| LED: Light Emitting Diode Simulator | 11-1 |
| 11.1: Overview | 11-1 |
| 11.2: Defining Light Emitting Devices (LEDs) | 11-2 |
| 11.3: Specifying Light Emitting Diode Models | 11-4 |
| 11.3.1: Specifying Polarization and Piezoelectric Effects | 11-4 |
| 11.3.2: Choosing Radiative Models | 11-4 |
| 11.3.3: Using k.p Band Parameter Models in Drift Diffusion | 11-5 |
| 11.4: Data Extraction | 11-6 |
| 11.4.1: Extracting Luminous Intensity | 11-6 |
| 11.4.2: Extracting Emission Spectra | 11-7 |
| 11.4.3: Extracting Emission Wavelength | 11-8 |
| 11.5: Reverse Ray-Tracing | 11-9 |
| 11.6: The LED Statement | 11-15 |
| 11.6.1: User-Definable Emission Spectra | 11-15 |

Chapter 12

| | |
|--|-------------|
| MixedMode: Mixed Circuit and Device Simulator | 12-1 |
| 12.1: Overview | 12-1 |
| 12.1.1: Background | 12-1 |
| 12.1.2: Advantages of MixedMode Simulation | 12-2 |
| 12.2: Using MixedMode | 12-3 |
| 12.2.1: General Syntax Rules | 12-3 |
| 12.2.2: Circuit and Analysis Specification | 12-4 |
| 12.2.3: Device Simulation Syntax | 12-7 |
| 12.2.4: Recommendations | 12-7 |
| 12.3: A Sample Command File | 12-12 |
| 12.4: MixedMode Syntax | 12-14 |
| 12.4.1: Circuit Element Statements | 12-14 |
| 12.4.2: Control and Analysis Statements | 12-29 |
| 12.4.3: Transient Parameters | 12-44 |
| 12.4.4: Expressions | 12-49 |

Chapter 13

| | |
|--|-------------|
| Quantum: Quantum Effect Simulator | 13-1 |
| 13.1: Quantum Effects Modeling | 13-1 |
| 13.2: Self-Consistent Coupled Schrodinger Poisson Model | 13-2 |
| 13.3: Density Gradient (Quantum Moments Model) | 13-7 |
| 13.4: Bohm Quantum Potential (BQP) | 13-9 |
| 13.4.1: Calibration against Schrodinger-Poisson Model | 13-10 |
| 13.4.2: Post Calibration runs | 13-11 |
| 13.5: Quantum Correction Models | 13-14 |
| 13.5.1: Hansch's Model | 13-14 |
| 13.5.2: Van Dort's Model | 13-14 |
| 13.6: General Quantum Well Model | 13-16 |
| 13.7: Quantum Transport: Non-Equilibrium Green's Function Approach | 13-18 |

| | |
|--|--------------|
| 13.7.1: Mode Space NEGF Approach | 13-18 |
| 13.7.2: Planar NEGF approach | 13-21 |
| 13.8: Drift-Diffusion Mode-Space Method (DD_MS) | 13-22 |

Chapter 14

| | |
|--|-------------|
| TFT: Thin-Film Transistor Simulator | 14-1 |
| 14.1: Polycrystalline and Amorphous Semiconductor Models | 14-1 |
| 14.2: Simulating TFT Devices | 14-2 |
| 14.2.1: Defining The Materials | 14-2 |
| 14.2.2: Defining The Defect States | 14-2 |
| 14.2.3: Density of States Model | 14-2 |
| 14.2.4: Trapped Carrier Density | 14-4 |
| 14.2.5: Steady-State Trap Recombination | 14-6 |
| 14.2.6: Transient Traps | 14-6 |
| 14.2.7: Continuous Defects | 14-10 |
| 14.2.8: Discrete Defects | 14-10 |
| 14.2.9: Amphoteric Defects | 14-11 |
| 14.2.10: Amphoteric Defect Generation | 14-15 |
| 14.2.11: Light Induced Defect Generation | 14-15 |
| 14.2.12: Plotting The Density Of States Versus Energy | 14-16 |
| 14.2.13: Using the C-Interpreter to define DEFECTS | 14-16 |
| 14.2.14: Setting Mobility and Other Models | 14-17 |

Chapter 15

| | |
|--|--------------|
| Organic Display and Organic Solar: Organic Simulators | 15-1 |
| 15.1: Organic Device Simulation | 15-1 |
| 15.1.1: Organic Display | 15-1 |
| 15.1.2: Organic Solar | 15-3 |
| 15.2: Organic Materials Physical Models | 15-5 |
| 15.2.1: Organic Defects Model | 15-5 |
| 15.2.2: Hopping Mobility Model | 15-9 |
| 15.2.3: Poole-Frenkel Mobility Model | 15-10 |
| 15.2.4: Bimolecular Langevin Recombination Model | 15-13 |
| 15.3: Singlet and Triplet Excitons | 15-14 |
| 15.3.1: Dopants | 15-17 |
| 15.3.2: Light Generation of Excitons | 15-18 |
| 15.3.3: Exciton Dissociation | 15-18 |
| 15.3.4: Metal Quenching | 15-19 |

Chapter 16

| | |
|--|-------------|
| NOISE: Electronic Noise Simulator | 16-1 |
| 16.1: Introduction | 16-1 |
| 16.2: Simulating Noise in ATLAS | 16-2 |
| 16.3: Circuit Level Description of Noise | 16-3 |
| 16.3.1: Noise "Figures of Merit" for a Two-Port Device | 16-4 |
| 16.4: Noise Calculation | 16-6 |
| 16.4.1: The Impedance Field | 16-6 |
| 16.4.2: Microscopic Noise Source | 16-7 |
| 16.4.3: Local Noise Source | 16-7 |
| 16.5: ATLAS Models | 16-8 |
| 16.5.1: Diffusion Noise | 16-8 |
| 16.5.2: Generation-Recombination Noise | 16-9 |
| 16.5.3: Flicker Noise | 16-11 |

| | |
|-------------------------------|--------------|
| 16.6: Output | 16-13 |
| 16.6.1: Log Files | 16-13 |
| 16.6.2: Structure Files | 16-14 |

Chapter 17

| | |
|--|-------------|
| Thermal 3D: Thermal Packaging Simulator | 17-1 |
| 17.1: Overview | 17-1 |
| 17.1.1: 3D Structure Generation | 17-1 |
| 17.2: Model and Material Parameter Selection | 17-2 |
| 17.2.1: Thermal Simulation Model | 17-2 |
| 17.2.2: Setting Thermal Conductivity | 17-2 |
| 17.3: Numerical Methods | 17-3 |
| 17.4: Obtaining Solutions In THERMAL3D | 17-4 |
| 17.5: Interpreting The Results From THERMAL3D | 17-5 |
| 17.6: More Information | 17-6 |

Chapter 18

| | |
|---|--------------|
| Mercury: Fast FET Simulator | 18-1 |
| 18.1: Introduction | 18-1 |
| 18.1.1: Accessing Mercury | 18-1 |
| 18.2: External Circuit | 18-2 |
| 18.3: Device | 18-4 |
| 18.4: Quasi-2D Simulation | 18-6 |
| 18.4.1: Poisson Equation | 18-6 |
| 18.4.2: Channel Simulation | 18-9 |
| 18.5: DC and Small-Signal AC | 18-13 |
| 18.5.1: Small-Signal AC | 18-13 |
| 18.6: Harmonic Balance | 18-14 |
| 18.6.1: Non-Linearity | 18-15 |
| 18.6.2: Harmonic Balance | 18-16 |
| 18.7: NETWORK | 18-19 |
| 18.8: POISSON | 18-27 |
| 18.9: SURFACE | 18-31 |

Chapter 19

| | |
|--|--------------|
| MC Device | 19-1 |
| 19.1: What is MC Device | 19-1 |
| 19.2: Using MC Device | 19-2 |
| 19.3: Input Language and Syntax | 19-4 |
| 19.3.1: The Input Language | 19-4 |
| 19.3.2: Statement allocation and usage | 19-4 |
| 19.3.3: Migrating From MOCA Input Format | 19-5 |
| 19.3.4: Commonly-Used Statements | 19-6 |
| 19.3.5: List of Statements | 19-11 |
| 19.3.6: Accessing The Examples | 19-13 |
| 19.4: Bulk Simulation | 19-15 |
| 19.5: Device Simulation | 19-16 |
| 19.5.1: Device Geometry | 19-16 |
| 19.5.2: Ohmic Contacts | 19-22 |
| 19.5.3: Estimators | 19-23 |
| 19.5.4: Initial Conditions | 19-25 |
| 19.5.5: Bipolar | 19-26 |

| | |
|---|--------------|
| 19.5.6: Track Boundary Crossings | 19-26 |
| 19.5.7: Time Step Regions | 19-26 |
| 19.5.8: Importing Data | 19-26 |
| 19.6: Statistical Enhancement | 19-29 |
| 19.6.1: LOTHRE | 19-29 |
| 19.6.2: HITHRE | 19-30 |
| 19.6.3: RELTHRE | 19-30 |
| 19.6.4: RATIO, N | 19-30 |
| 19.6.5: Particle Compression | 19-31 |
| 19.6.6: Statistical Enhancement Statements | 19-31 |
| 19.7: Physical Models | 19-32 |
| 19.7.1: Self-Consistent Simulation | 19-32 |
| 19.7.2: Band Structure | 19-39 |
| 19.7.3: Electron Dispersion and Equations of Motion | 19-42 |
| 19.7.4: Coulomb Interaction | 19-48 |
| 19.7.5: Phonon Scattering | 19-51 |
| 19.7.6: Impurity Scattering | 19-57 |
| 19.7.7: Tunneling | 19-60 |
| 19.7.8: Size Quantization | 19-64 |
| 19.7.9: Schottky Barrier Injection | 19-68 |
| 19.7.10: Gather/Scatter Algorithm | 19-69 |
| 19.7.11: Interpolation Schemes | 19-70 |
| 19.7.12: WKB Formula | 19-73 |
| 19.7.13: Strain | 19-74 |
| 19.8: Tips | 19-79 |

Chapter 20

| | |
|--|--------------|
| Numerical Techniques | 20-1 |
| 20.1: Overview | 20-1 |
| 20.2: Numerical Solution Procedures | 20-2 |
| 20.3: Meshes | 20-3 |
| 20.3.1: Mesh Regridding | 20-3 |
| 20.3.2: Mesh Smoothing | 20-4 |
| 20.4: Discretization | 20-5 |
| 20.4.1: The Discretization Process | 20-5 |
| 20.5: Non-Linear Iteration | 20-6 |
| 20.5.1: Newton Iteration | 20-6 |
| 20.5.2: Gummel Iteration | 20-6 |
| 20.5.3: Block Iteration | 20-7 |
| 20.5.4: Combining The Iteration Methods | 20-7 |
| 20.5.5: Solving Linear Subproblems | 20-7 |
| 20.5.6: Convergence Criteria for Non-linear Iterations | 20-8 |
| 20.5.7: Error Measures | 20-8 |
| 20.5.8: Terminal Current Criteria | 20-9 |
| 20.5.9: Convergence Criteria | 20-10 |
| 20.5.10: Detailed Convergence Criteria | 20-12 |
| 20.6: Initial Guess Strategies | 20-18 |
| 20.6.1: Recommendations And Defaults | 20-19 |
| 20.7: The DC Curve-Tracer Algorithm | 20-20 |
| 20.8: Transient Simulation | 20-21 |
| 20.9: Small Signal and Large Signal Analysis | 20-22 |
| 20.9.1: Frequency Domain Perturbation Analysis | 20-22 |
| 20.9.2: Fourier Analysis Of Transient Responses | 20-23 |
| 20.9.3: Overall Recommendations | 20-24 |

| | |
|---|-------|
| 20.10: Differences Between 2D and 3D Numerics | 20-25 |
|---|-------|

Chapter 21

| | |
|--|-------------|
| Statements. | 21-1 |
| 21.1: Input Language | 21-1 |
| 21.1.1: Syntax Rules | 21-1 |
| 21.2: A.MESH, R.MESH, X.MESH, Y.MESH, Z.MESH | 21-4 |
| 21.3: BEAM | 21-6 |
| 21.4: COMMENT, # | 21-21 |
| 21.5: CONTACT | 21-22 |
| 21.6: CURVETRACE | 21-30 |
| 21.7: DBR | 21-33 |
| 21.8: DEFECTS | 21-38 |
| 21.9: DEGRADATION | 21-44 |
| 21.10: DOPING | 21-45 |
| 21.11: DOSEXTRACT | 21-66 |
| 21.12: ELECTRODE | 21-68 |
| 21.13: ELIMINATE | 21-73 |
| 21.14: EXTRACT | 21-75 |
| 21.15: EYE.DIAGRAM | 21-76 |
| 21.16: FDX.MESH, FDY.MESH | 21-78 |
| 21.17: FOURIER | 21-79 |
| 21.18: GO | 21-81 |
| 21.19: IMPACT | 21-82 |
| 21.20: INTDEFECTS | 21-98 |
| 21.21: INTERFACE | 21-104 |
| 21.22: INTTRAP | 21-113 |
| 21.23: LASER | 21-118 |
| 21.24: LED | 21-125 |
| 21.25: LENS | 21-130 |
| 21.26: LOAD | 21-134 |
| 21.27: LOG | 21-136 |
| 21.28: LX.MESH, LY.MESH | 21-141 |
| 21.29: MATERIAL | 21-142 |
| 21.30: MEASURE | 21-183 |
| 21.31: MESH | 21-186 |
| 21.32: METHOD | 21-190 |
| 21.33: MOBILITY | 21-203 |
| 21.34: MODELS | 21-226 |
| 21.35: MQW | 21-266 |
| 21.36: NITRIDECHARGE | 21-270 |
| 21.37: ODEFECTS | 21-272 |
| 21.38: OINTDEFECTS | 21-275 |
| 21.39: OPTIONS | 21-279 |
| 21.40: OUTPUT | 21-281 |
| 21.41: PHOTOGENERATE | 21-290 |
| 21.42: PML | 21-292 |
| 21.43: PROBE | 21-294 |
| 21.44: QTREGION | 21-305 |
| 21.45: QTX.MESH, QTY.MESH | 21-308 |
| 21.46: QUIT | 21-309 |

| | |
|---|--------|
| 21.47: REGION | 21-310 |
| 21.48: REGRID | 21-321 |
| 21.49: SAVE | 21-326 |
| 21.50: SET | 21-333 |
| 21.51: SINGLEEVENTUPSET | 21-334 |
| 21.52: SOLAR | 21-337 |
| 21.53: SOLVE | 21-339 |
| 21.54: SPX.MESH, SPY.MESH, SPZ.MESH | 21-359 |
| 21.55: SYMBOLIC | 21-360 |
| 21.56: SPREAD | 21-361 |
| 21.57: SYSTEM | 21-364 |
| 21.58: THERMCONTACT | 21-365 |
| 21.59: TITLE | 21-367 |
| 21.60: TONYPLOT | 21-368 |
| 21.61: TRAP | 21-369 |
| 21.62: UTMOST | 21-372 |
| 21.63: VCSEL | 21-377 |
| 21.64: WAVEFORM | 21-379 |
| 21.65: WAVEGUIDE | 21-381 |

Appendix A

C-Interpreter Functions A-1

| | |
|---------------------|-----|
| A.1: Overview | A-1 |
|---------------------|-----|

Appendix B

Material Systems B-1

| | |
|--|------|
| B.1: Overview | B-1 |
| B.2: Semiconductors, Insulators, and Conductors | B-2 |
| B.2.1: Semiconductors | B-2 |
| B.2.2: Insulators | B-2 |
| B.2.3: Conductors | B-2 |
| B.2.4: Unknown Materials | B-2 |
| B.2.5: Specifying Unknown or User-Defined Materials in ATLAS | B-2 |
| B.3: ATLAS Materials | B-4 |
| B.3.1: Specifying Compound Semiconductors Rules | B-5 |
| B.4: Silicon and Polysilicon | B-7 |
| B.5: The Al(x)Ga(1-x)As Material System | B-10 |
| B.6: The In(1-x)Ga(x)As(y)P(1-y) System | B-11 |
| B.7: Silicon Carbide (SiC) | B-12 |
| B.8: Material Defaults for GaN/InN/AlN System | B-13 |
| B.9: Material Defaults for Compound Semiconductors | B-20 |
| B.10: Miscellaneous Semiconductors | B-27 |
| B.11: Insulators | B-31 |
| B.12: Metals/Conductors | B-33 |
| B.13: Optical Properties | B-34 |
| B.13.1: SOPRA Database | B-35 |
| B.14: User Defined Materials | B-46 |

Appendix C

| | |
|---|------------|
| RF and Small Signal AC Parameter Extraction[239] | C-1 |
|---|------------|

Appendix D

| | |
|------------------------|------------|
| MC Device Files | D-1 |
|------------------------|------------|

| | |
|---|------------|
| D.1: The Default Configuration File: defaults.in | D-1 |
|---|------------|

| | |
|--------------------------|------------|
| D.2: File Formats | D-7 |
|--------------------------|------------|

| | |
|-----------------------------|-----|
| D.2.1: Silvaco Output Files | D-7 |
|-----------------------------|-----|

| | |
|-----------------------------|-----|
| D.2.2: General Output Files | D-9 |
|-----------------------------|-----|

| | |
|-----------------------------|------|
| D.2.3: Current Output Files | D-11 |
|-----------------------------|------|

| | |
|--------------------------------|------|
| D.2.4: Scattering Output Files | D-12 |
|--------------------------------|------|

| | |
|-----------------------------|------|
| D.2.5: Quantum Output Files | D-13 |
|-----------------------------|------|

| | |
|---|------|
| D.2.6: Miscellaneous Input And Output Files | D-14 |
|---|------|

| | |
|-----------------------------------|------|
| D.2.7: Band Structure Input Files | D-14 |
|-----------------------------------|------|

| | |
|----------------------|-------------|
| D.3: Examples | D-16 |
|----------------------|-------------|

| | |
|--|------|
| D.3.1: Bulk n-type Silicon: mcdeviceex01 | D-16 |
|--|------|

| | |
|---------------------------------------|------|
| D.3.2: A 25-nm n-MOSFET: mcdeviceex02 | D-17 |
|---------------------------------------|------|

| | |
|---|------|
| D.3.3: A 25-nm n-MOSFET with Quantum Correction: mcdeviceex03 | D-19 |
|---|------|

| | |
|---------------------------------------|------|
| D.3.4: A 25-nm p-MOSFET: mcdeviceex04 | D-21 |
|---------------------------------------|------|

| | |
|---|------|
| D.3.5: An imported 25-nm n-MOSFET: mcdeviceex05 | D-23 |
|---|------|

Appendix E

| | |
|-----------------------|------------|
| Hints and Tips | E-1 |
|-----------------------|------------|

This page is intentionally left blank.

1.1: ATLAS Overview

ATLAS provides general capabilities for physically-based two (2D) and three-dimensional (3D) simulation of semiconductor devices. If you're new to ATLAS, read this chapter and Chapter 2: "Getting Started with ATLAS" to understand how ATLAS works. Once you've read these chapters, you can refer to the remaining chapters for a detailed understanding of the capabilities of each ATLAS product.

Those who have used earlier versions of ATLAS may find it helpful to review the updated version history in Appendix D: "ATLAS Version History".

ATLAS is designed to be used with the VWF INTERACTIVE TOOLS. The VWF INTERACTIVE TOOLS are DECKBUILD, TONYPLOT, DEVEDIT, MASKVIEWS, and OPTIMIZER. See their respective manuals on how to use these products. See Section 1.3: "Using ATLAS With Other Silvaco Software" for more information about using ATLAS with other Silvaco tools.

ATLAS is supplied with numerous examples that can be accessed through DECKBUILD. These examples demonstrate most of ATLAS's capabilities. The input files that are provided with the examples are an excellent starting point for developing your own input files. To find out how to access the example, see Chapter 2: "Getting Started with ATLAS", Section 2.4: "Accessing The Examples".

1.2: Features And Capabilities of ATLAS

1.2.1: Comprehensive Set of Models

ATLAS provides a comprehensive set of physical models, including:

- DC, AC small-signal, and full time-dependency.
- Drift-diffusion transport models.
- Energy balance and Hydrodynamic transport models.
- Lattice heating and heatsinks.
- Graded and abrupt heterojunctions.
- Optoelectronic interactions with general ray tracing.
- Amorphous and polycrystalline materials.
- General circuit environments.
- Stimulated emission and radiation
- Fermi-Dirac and Boltzmann statistics.
- Advanced mobility models.
- Heavy doping effects.
- Full acceptor and donor trap dynamics
- Ohmic, Schottky, and insulating contacts.
- SRH, radiative, Auger, and surface recombination.
- Impact ionization (local and non-local).
- Floating gates.
- Band-to-band and Fowler-Nordheim tunneling.
- Hot carrier injection.
- Quantum transport models
- Thermionic emission currents.

1.2.2: Fully Integrated Capabilities

ATLAS works well with other software from SILVACO. For example, ATLAS

- Runs in the DECKBUILD interactive run-time environment.
- Is interfaced to TONYPLOT, the interactive graphics and analysis package.
- Accepts input from the ATHENA and SSUPREM3 process simulators.
- Is interfaced to UTMOST parameter extraction and device modeling software.
- can be used in experiments with the VWF AUTOMATION TOOLS.

1.2.3: Sophisticated Numerical Implementation

ATLAS uses powerful numerical techniques, including:

- Accurate and robust discretization techniques.
- Gummel, Newton, and block-Newton nonlinear iteration strategies.
- Efficient solvers, both direct and iterative, for linear subproblems.
- Powerful initial guess strategies.
- Small-signal calculation techniques that converge at all frequencies.
- Stable and accurate time integration.

1.3: Using ATLAS With Other Silvaco Software

ATLAS is best used with the VWF INTERACTIVE TOOLS. These include DECKBUILD, TONYPLOT, DEVEDIT, MASKVIEWS, and OPTIMIZER. DECKBUILD provides an interactive run time environment. TONYPLOT supplies scientific visualization capabilities. DEVEDIT is an interactive tool for structure and mesh specification and refinement. MASKVIEWS is an IC Layout Editor. The OPTIMIZER supports black box optimization across multiple simulators.

ATLAS, however, is often used with the ATHENA process simulator. ATHENA predicts the physical structures that result from processing steps. The resulting physical structures are used as input by ATLAS, which then predicts the electrical characteristics associated with specified bias conditions. The combination of ATHENA and ATLAS makes it possible to determine the impact of process parameters on device characteristics.

The electrical characteristics predicted by ATLAS can be used as input by the UTMOST device characterization and SPICE modeling software. Compact models based on simulated device characteristics can then be supplied to circuit designers for preliminary circuit design. Combining ATHENA, ATLAS, UTMOST, and SMARTSPICE makes it possible to predict the impact of process parameters on circuit characteristics.

ATLAS can also be used as one of the simulators within the VWF AUTOMATION TOOLS. VWF makes it convenient to perform highly automated simulation-based experimentation. VWF is used in a way that reflects experimental research and development procedures using split lots. It therefore links simulation very closely to technology development, resulting in significantly increased benefits from simulation use.

1.4: The Nature Of Physically-Based Simulation

ATLAS is a physically-based device simulator. Physically-based device simulation is not a familiar concept for all engineers. This section will briefly describe this type of simulation.

Physically-based device simulators predict the electrical characteristics that are associated with specified physical structures and bias conditions. This is achieved by approximating the operation of a device onto a two or three dimensional grid, consisting of a number of grid points called nodes. By applying a set of differential equations, derived from Maxwell's laws, onto this grid you can simulate the transport of carriers through a structure. This means that the electrical performance of a device can now be modeled in DC, AC or transient modes of operation.

There are three physically-based simulation. These are:

- It is predictive.
- It provides insight.
- It conveniently captures and visualizes theoretical knowledge.

Physically-based simulation is different from empirical modeling. The goal of empirical modeling is to obtain analytic formulae that approximate existing data with good accuracy and minimum complexity. Empirical models provide efficient approximation and interpolation. They do not provide insight, or predictive capabilities, or encapsulation of theoretical knowledge.

Physically-based simulation has become very important for two reasons. One, it is almost always much quicker and cheaper than performing experiments. Two, it provides information that is difficult or impossible to measure.

The drawbacks of physically-based simulation are that all the relevant physics must be incorporated into a simulator. Also, numerical procedures must be implemented to solve the associated equations. These tasks have been taken care of for ATLAS users.

Those who use physically-based device simulation tools must specify the problem to be simulated. In ATLAS, specify device simulation problems by defining:

- The physical structure to be simulated.
- The physical models to be used.
- The bias conditions for which electrical characteristics are to be simulated.

The subsequent chapters of this manual describe how to perform these steps.

2.1: Overview

ATLAS is a physically-based two and three dimensional device simulator. It predicts the electrical behavior of specified semiconductor structures and provides insight into the internal physical mechanisms associated with device operation.

ATLAS can be used standalone or as a core tool in SILVACO's VIRTUAL WAFER FAB simulation environment. In the sequence of predicting the impact of process variables on circuit performance, device simulation fits between process simulation and SPICE model extraction.

This chapter will show you how to use ATLAS effectively. It is a source of useful hints and advice. The organization of topics parallels the steps that you go through to run the program. If you have used earlier versions of ATLAS, you will still find this chapter useful because of the new version.

This chapter concentrates on the core functionality of ATLAS. If you're primarily interested in the specialized capabilities of a particular ATLAS tool, read this chapter first. Then, read the chapters that describe the ATLAS tools you wish to use.

2.2: ATLAS Inputs and Outputs

Figure 2-1 shows the types of information that flow in and out of ATLAS. Most ATLAS simulations use two input files. The first input file is a text file that contains commands for ATLAS to execute. The second input file is a structure file that defines the structure that will be simulated.

ATLAS produces three types of output files. The first type of output file is the run-time output, which gives you the progress and the error and warning messages as the simulation proceeds. The second type of output file is the log file, which stores all terminal voltages and currents from the device analysis. The third type of output file is the solution file, which stores 2D and 3D data relating to the values of solution variables within the device at a given bias point.

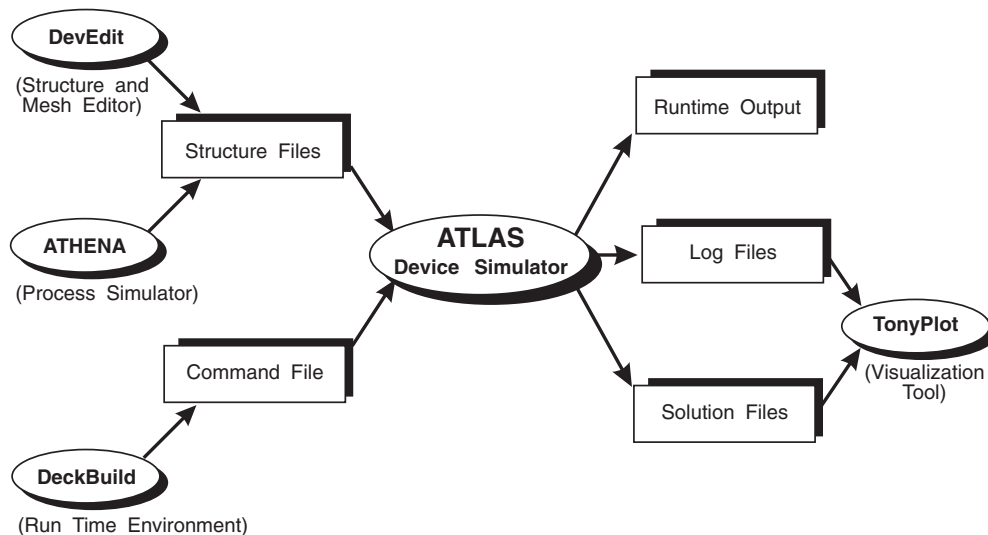


Figure 2-1: ATLAS Inputs and Outputs

2.3: Modes of Operation

ATLAS is normally used in conjunction with the DECKBUILD run-time environment, which supports both interactive and batch mode operation. We strongly recommend that you always run ATLAS within DECKBUILD. In this section, we present the basic information you need to run ATLAS in DECKBUILD. The DECKBUILD USER'S MANUAL provides a more detailed description of the features and capabilities of DECKBUILD.

2.3.1: Interactive Mode With DeckBuild

To start ATLAS in DECKBUILD, type:

```
deckbuild -as
```

at the UNIX system command prompt. The command line option, `-as`, instructs DECKBUILD to start ATLAS as the default simulator.

If you want to start from an existing input file, start DECKBUILD by typing:

```
deckbuild -as <input filename>
```

The run-time output shows the execution of each ATLAS command and includes error messages, warnings, extracted parameters, and other important output for evaluating each ATLAS run. When ATLAS runs in this mode, the run-time output is sent to the output section of the DeckBuild Window and can be saved as needed. Therefore, you don't need to save the run-time output explicitly. The following command line, however, specifies the name of a file that will be used for storing the run-time output.

```
deckbuild -as <input filename> -outfile <output filename>
```

In this case, the run-time output is sent to the output file and to the output section of the DeckBuild Window.

2.3.2: Batch Mode With DeckBuild

To use DECKBUILD in a non-interactive or batch mode, add the `-run` parameter to the command that invokes DECKBUILD. A prepared command file is required for running in batch mode. We advise you to save the run-time output to a file, since error messages in the run-time output would otherwise be lost when the batch job completes. For example:

```
deckbuild -run -as <input filename> -outfile <output filename>
```

Using this command requires a local X-Windows system to be running. The job runs inside a DECKBUILD icon on the terminal and quits automatically when the ATLAS simulation is complete. You can also run DECKBUILD using a remote display. For example:

```
deckbuild -run -as <input file> -outfile <output file> -display<hostname>:0.0
```

2.3.3: No Windows Batch Mode With DeckBuild

For completely non-X Windows operation of DECKBUILD, use the `-ascii` parameter. For example:

```
deckbuild -run -ascii -as <input filename> -outfile <output filename>
```

This command directs DECKBUILD to run the ATLAS simulation without the DeckBuild Window or icon. This is useful for remote execution without an X Windows emulator or for replacing UNIX-based ATLAS runs within framework programs.

When using batch mode, use the UNIX command suffix, `&`, to detach the job from the current command shell. To run a remote ATLAS simulation under DECKBUILD without display and then logout from the system, use the UNIX command, `nohup`, before the DECKBUILD command line. For example:

```
nohup deckbuild -run -ascii -as <input filename> -outfile <output filename> &
```

2.3.4: Running ATLAS inside Deckbuild

Each ATLAS run inside DECKBUILD should start with the line:

```
go atlas
```

A single input file may contain several ATLAS runs each separated with a `go atlas` line. Input files within DECKBUILD may also contain runs from other programs such as ATHENA or DEVEDIT along with the ATLAS runs.

Running a given version number of ATLAS

The `go` statement can be modified to provide parameters for the ATLAS run. To run version 5.14.0.R, the syntax is:

```
go atlas simflags="-V 5.14.0.R"
```

Starting Parallel ATLAS

The `-P` option is used to set the number of processors to use in a parallel ATLAS run. If the number set by `-P` is greater than the number of processors available or than the number of parallel thread licenses, the number is automatically reduced to this cap number. To run on 4 processors, use:

```
go atlas simflags="-V 5.14.0.R -P 4"
```

2.3.5: Batch Mode Without DeckBuild

You can run ATLAS outside the DECKBUILD environment. But this isn't recommended by SILVACO. If you don't want the overhead of the DeckBuild Window, use the No Windows Mode. Many important features such as variable substitution, automatic interfacing to process simulation, and parameter extraction are unavailable outside the DECKBUILD environment. To run ATLAS directly under UNIX, use the command:

```
atlas <input filename>
```

To save the run-time output to a file, don't use the UNIX redirect command (`>`). Simply specify the name of the output file. For example:

```
atlas <input filename> -logfile <output filename>
```

Note: The standard examples supplied with ATLAS will not run correctly outside of DECKBUILD.

2.3.6: TMA Compatibility Mode

You can add the `-TMA` command line flag to the `atlas` command to direct the ATLAS simulator to operate in TMA Compatibility Mode. In this mode, the default material models and parameters are altered to closely agree with those of TMA's Medici[®] simulator.

2.3.7: ISE Compatibility Mode

You can add the `-ISE` command line flag to the `atlas` command to direct the ATLAS simulator to operate in ISE Compatibility Mode. In this mode, the default material models and parameters are altered to closely agree with those of ISE's Dessis[®] simulator.

2.4: Accessing The Examples

ATLAS has a library of standard examples that demonstrate how the program is used to simulate different technologies. These examples are a good starting point for creating your own simulations. The examples are accessed from the menu system in DECKBUILD. To select and load an example:

1. Start DECKBUILD with ATLAS as the simulator, which is described in the previous section.
2. Use left mouse button to pull down the **Main Control** menu.
3. Select **Examples**. An index will then appear in a Deckbuild Examples Window (see Figure 2-2).

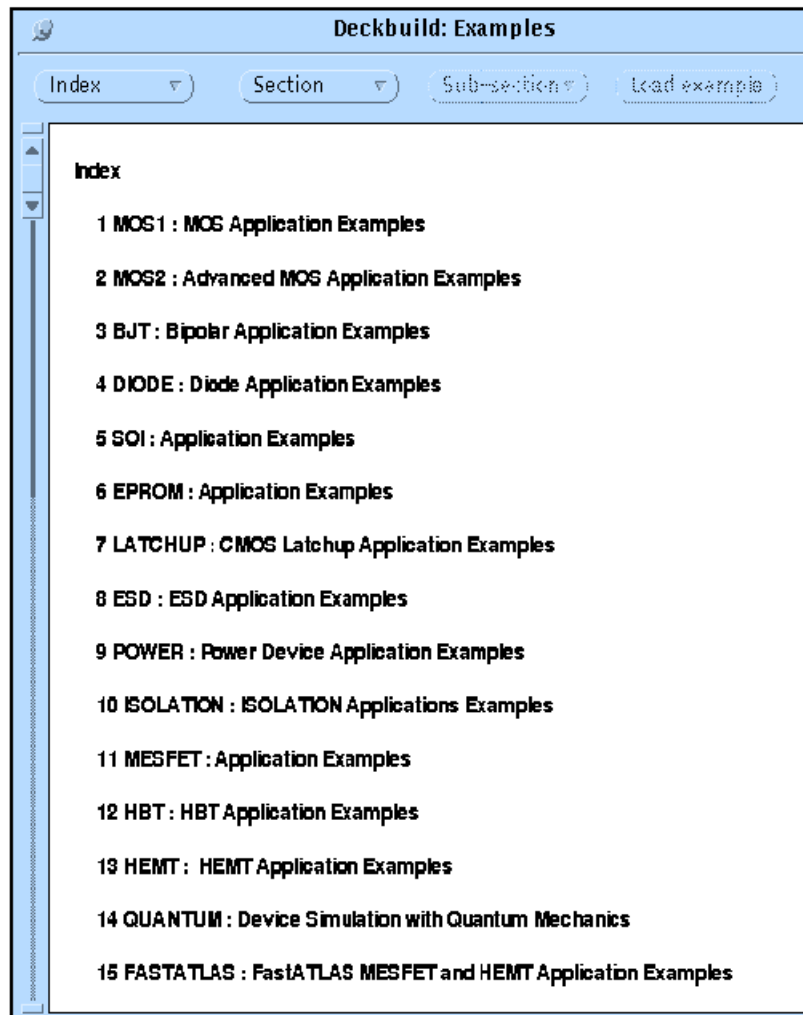


Figure 2-2: Examples Index in DeckBuild

The examples are divided by technology or technology group. For instance, the most common technologies are individually listed (e.g., MOS are under BJT), while others are grouped with similar devices (e.g., IGBT and LDMOS are under POWER, and solar cell and photodiode are under OPTOELECTRONICS).

4. Choose the technology by double clicking the left mouse button over that item. A list of examples for that technology will appear. These examples typically illustrate different devices, applications, or types of simulation.

You can also search for an example by selecting the Index button. Wildcards can be used in the search.

5. Choose a particular example by double clicking the left mouse button over that item in the list. A text description of the example will appear in the window. This text describes the important physical mechanisms in the simulation and the details of the ATLAS syntax used. You should read this information before proceeding.
6. Press the **Load example** button. The input command file for the example will be copied into your current working directory together with any associated files. A copy of the command file will be loaded into DECKBUILD. Note that the **Load example** button remains faded out until this step is performed correctly.
7. Press the **run** button in the middle frame of the DECKBUILD application window to run the example. Alternatively, most examples are supplied with results that are copied into the current working directory along with the input file. To view the results, select (highlight) the name of the results file and select **Tools-Plot**. See the TONYPLOT USER'S MANUAL for details on using TONYPLOT.

2.5: The ATLAS Syntax

An ATLAS command file is a list of commands for ATLAS to execute. This list is stored as an ASCII text file that can be prepared in DECKBUILD or in any text editor. Preparing an input file in DECKBUILD is preferred. You can create an input file by using the DeckBuild Commands menu in the DeckBuild Window.

2.5.1: Statements and Parameters

The input file contains a sequence of statements. Each statement consists of a keyword that identifies the statement and a set of parameters. The general format is:

```
<STATEMENT>    <PARAMETER>=<VALUE>
```

With a few exceptions, the input syntax is not case sensitive. One important exception is that commands described in this manual as being executed by DECKBUILD rather than ATLAS are case sensitive. These include EXTRACT, SET, GO, and SYSTEM. Also, filenames for input and output under UNIX are case sensitive.

For any <STATEMENT>, ATLAS may have four different types for the <VALUE> parameter. These are: Real, Integer, Character, and Logical.

An example of a statement line is:

```
DOPING UNIFORM N.TYPE CONCENTRATION=1.0e16 REGION=1 OUTFILE=my.dop
```

The statement is DOPING. All other items are parameters of the DOPING statement. UNIFORM and N.TYPE are Logical parameters. Their presence on the line sets their values to true. Otherwise, they take their default values (usually false). CONCENTRATION is a Real parameter and takes floating point numbers as input values. REGION is an Integer parameter taking only integer numbers as input. OUTFILE is a Character parameter type taking strings as input.

The statement keyword must come first but the order of parameters within a statement is unimportant.

You only need to use enough letters of any parameter to distinguish it from any other parameter on the same statement. Thus, CONCENTRATION can be shortened to CONC. REGION. It can't be shortened to R, however, since there's a parameter called RATIO associated with the DOPING statement.

You can set logical parameters to false by preceding them with the ^ symbol. Any line beginning with a # is ignored. These lines are used as comments.

ATLAS can read up to 256 characters on one line. But it is better to spread long input statements over several lines to make the input file more readable. The \ character at the end of a line indicates continuation.

For more information about statements and parameters in ATLAS, see Chapter 21: "Statements".

2.5.2: The Order of ATLAS Commands

The order in which statements occur in an ATLAS input file is important. There are five groups of statements that must occur in the correct order (see Figure 2-3). Otherwise, an error message will appear, which may cause incorrect operation or termination of the program. For example, if the material parameters or models are set in the wrong order, then they may not be used in the calculations.

The order of statements within the mesh definition, structural definition, and solution groups is also important. Otherwise, it may also cause incorrect operation or termination of the program.

| <i>Group</i> | | <i>Statements</i> |
|----------------------------------|------|--|
| 1. Structure Specification | ———— | MESH REGION ELECTRODE DOPING |
| 2. Material Models Specification | ———— | MATERIAL MODELS CONTACT INTERFACE |
| 3. Numerical Method Selection | ———— | METHOD |
| 4. Solution Specification | ———— | LOG SOLVE LOAD SAVE |
| 5. Results Analysis | ———— | EXTRACT TONYPLOT |

Figure 2-3: ATLAS Command Groups with the Primary Statements in each Group

2.5.3: The DeckBuild Command Menu

The DeckBuild Command Menu (Command Menu) can help you to create input files. This menu is found under the **Commands** button on DECKBUILD's main screen. The Commands Menu is configured for ATLAS whenever ATLAS is the currently active simulator in DECKBUILD. When ATLAS is active, which is indicated in the lower bar of the DeckBuild Window, an ATLAS command prompt will appear in the DECKBUILD output section.

The Command Menu gives you access to pop-up windows where you type information. When you select the **Write** button, syntactically correct statements are written to the DECKBUILD text edit region. The DeckBuild Command Menu does not support all possible ATLAS syntax, but aims to cover the most commonly used commands.

2.5.4: PISCES-II Quick Start

This section is a quickstart for those who may be familiar with the syntax and use of the Stanford University PISCES-II program or other device simulators derived from this program.

The major differences between ATLAS and PISCES-II are:

- all graphics are handled by a separate interactive graphics program, TONYPLOT. By using TONYPLOT, you no longer need to run the device simulator simply to plot or alter graphics.
- no need to separate individual ATLAS simulations into separate input files. Multiple runs of ATLAS are possible in the same input file separated by the line `go atlas`. There's also no need to separate process and device simulation runs of SILVACO products into separate input files. A single file containing ATHENA and ATLAS syntax is permitted in DECKBUILD.
- the interface from process to device simulation is handled though a single file format compatible with other programs. The file read by ATLAS is the default output file format of ATHENA. No special file format for the interface is required.
- when defining a grid structure within ATLAS, the `NODE` and `LOCATION` syntax to define exact grid line numbers in X and Y is not recommended. A more reliable and easier to use syntax using `LOCATION` and `SPACING` is available.

- using the `REGRID` command is not recommended due to the creation of obtuse triangles. A standalone program, such as `DEVEDIT`, can be used as a grid pre-processor for ATLAS.
- all numerical method selection commands and parameters are on the `METHOD` statement. The `SYMBOLIC` statement is not used. Historically, `SYMBOLIC` and `METHOD` were used as a coupled pair of statements, but it is more convenient to use a single statement (`METHOD`) instead. Most of the old parameters of the `SYMBOLIC` statement have the same meaning and names, despite this move to a single statement. One notable change in ATLAS is that you can combine numerical methods together.

See the “Pisces-II Compatibility” section on page 2-49 for more information concerning the translation of PISCES-II numerics statements.

- various general purpose commands are actually part of the `DECKBUILD` user environment. These include `SET`, `EXTRACT`, `GO`, `SYSTEM`, and `SOURCE`. These commands can be interspersed inside ATLAS syntax.
- Variable substitution is supported for both numerical and string variables using the `SET` statement and the `$` symbol. To avoid confusion, the `#` symbol is preferred over the `$` symbol for comment statements.

In addition to these changes, the physical models are generally different in ATLAS. Most of the original PISCES-II models have been preserved but often are not the default or the recommended models to use. See the on-line examples for technology specific information about models.

2.6: Defining A Structure

There are three ways to define a device structure in ATLAS.

The first way is to read an existing structure from a file. The structure is created either by an earlier ATLAS run or another program such as ATHENA or DEVEDIT. A MESH statement loads in the mesh, geometry, electrode positions, and doping of the structure. For example:

```
MESH INFILE=<filename>
```

The second way is to use the **Automatic Interface** feature from DECKBUILD to transfer the input structure from ATHENA or DEVEDIT.

The third way is create a structure by using the ATLAS command language. See Chapter 21: “Statements” for more information about the ATLAS syntax.

2.6.1: Interface From ATHENA

When ATHENA and ATLAS are run under DECKBUILD, you can take advantage of an automatic interface between the two programs. Perform the following steps to load the complete mesh, geometry, and doping from ATHENA to ATLAS.

1. Deposit and pattern electrode material in ATHENA.
2. Use the ELECTRODE statement in ATHENA to define contact positions. Specify the X and Y coordinates as cross-hairs to pin-point a region. The whole region is then turned into electrode. In many cases, only the X coordinate is needed. For example:

```
ELECTRODE NAME=gate X=1.3 [Y=-0.1])
```

There is a special case to specify a contact on the bottom of the structure. For example:

```
ELECTRODE NAME=substrate BACKSIDE
```

3. Save a structure file while ATHENA is still the active simulator. For example:

```
STRUCTURE OUTF=nmos.str
```
4. Start ATLAS with the go atlas command written in the same input deck. This will automatically load the most recent structure from ATHENA into ATLAS.

If you need to load the structure saved in step 4 into ATLAS without using the auto-interface capability, use the MESH command. For example:

```
MESH INF=nmos.str
```

ATLAS inherits the grid used most recently by ATHENA. With a careful choice of initial mesh or by using the grid manipulation techniques in ATHENA, you can produce a final mesh from ATHENA that will give good results in ATLAS. But, a grid that is appropriate for process simulation isn't always appropriate for device simulation. If the final ATHENA mesh is inappropriate for ATLAS, use either DEVEDIT to re-mesh the structure or the REGRID command.

Note: There's no need to specify a MESH command in ATLAS when using the Automatic Interface of Deckbuild.

2.6.2: Interface From DevEdit

A 2D or 3D structure created by DEVEDIT can be read into ATLAS using the following statement.

```
MESH INF=<structure filename>
```

This statement loads in the mesh, geometry, electrode positions, and doping of the structure. ATLAS will automatically determine whether the mesh is 2D for S-PISCES or BLAZE, or 3D for DEVICE3D or BLAZE3D.

If the structure coming from DEVEDIT were originally created by ATHENA, then define the electrodes in ATHENA as described in the previous section. If the structure is created in DEVEDIT, the electrode regions should be defined in the **Region/Add region** menu of DEVEDIT.

2.6.3: Using The Command Language To Define A Structure

To define a device through the ATLAS command language, you must first define a mesh. This mesh or grid covers the physical simulation domain. The mesh is defined by a series of horizontal and vertical lines and the spacing between them. Then, regions within this mesh are allocated to different materials as required to construct the device. For example, the specification of a MOS device requires the specification of silicon and silicon dioxide regions. After the regions are defined, the location of electrodes is specified. The final step is to specify the doping in each region.

When using the command language to define a structure, the information described in the following four sub-sections must be specified in the order listed.

Specifying The Initial Mesh

The first statement must be:

```
MESH SPACE.MULT=<VALUE>
```

This is followed by a series of X.MESH and Y.MESH statements.

```
X.MESH LOCATION=<VALUE> SPACING=<VALUE>
.
Y.MESH LOCATION=<VALUE> SPACING=<VALUE>
.
```

The SPACE.MULT parameter value is used as a scaling factor for the mesh created by the X.MESH and Y.MESH statements. The default value is 1. Values greater than 1 will create a globally coarser mesh for fast simulation. Values less than 1 will create a globally finer mesh for increased accuracy. The X.MESH and Y.MESH statements are used to specify the locations in microns of vertical and horizontal lines, respectively, together with the vertical or horizontal spacing associated with that line. You must specify at least two mesh lines for each direction. ATLAS automatically inserts any new lines required to allow for gradual transitions in the spacing values between any adjacent lines. The X.MESH and Y.MESH statements must be listed in the order of increasing x and y. Both negative and positive values of x and y are allowed.

Figure 2-4 illustrates how these statements work. On the left hand plot, note how the spacing of the vertical lines varies from 1 μm at $x=0$ and $x=10 \mu\text{m}$ to 0.5 μm at $x=5 \mu\text{m}$. On the right hand plot, note how specifying the SPACE.MULT parameter to have a value of 0.5 has doubled the density of the mesh in both the X and Y directions.

You can specify the PERIODIC parameter on the MESH statement to mean that the structure and mesh are periodic in the x direction.

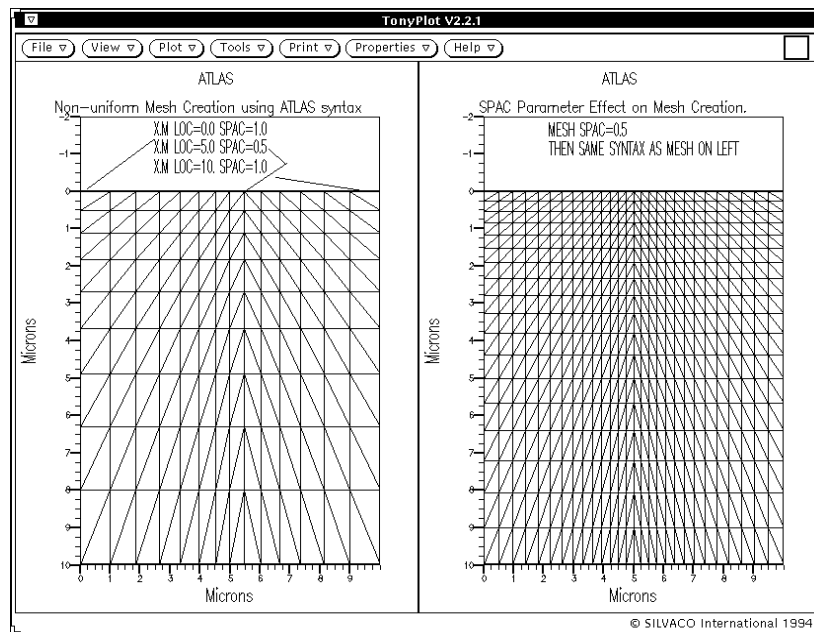


Figure 2-4: Non-uniform Mesh Creation using ATLAS Syntax

After an initial mesh has been defined, you can remove grid lines in specified regions. This is typically done in regions of the device where a coarse grid is expected to be sufficient such as the substrate. The removal of grid lines is accomplished using the `ELIMINATE` statement. The `ELIMINATE` statement removes every second mesh line in the specified direction from within a specified rectangle. For example, the statement:

```
ELIMINATE COLUMNS X.MIN=0 X.MAX=4 Y.MIN=0.0 Y.MAX=3
```

removes every second vertical grid line within the rectangle bounded by $x=0$, $x=4$, $y=0$ and $y=3$ microns.

Specifying Regions And Materials

Once the mesh is specified, every part of it must be assigned a material type. This is done with `REGION` statements. For example:

```
REGION number=<integer> <material_type> <position parameters>
```

Region numbers must start at 1 and are increased for each subsequent region statement. You can have up to 200 different regions in ATLAS. A large number of materials is available. If a composition-dependent material type is defined, the x and y composition fractions can also be specified in the `REGION` statement.

The position parameters are specified in microns using the `X.MIN`, `X.MAX`, `Y.MIN`, and `Y.MAX` parameters. If the position parameters of a new statement overlap those of a previous `REGION` statement, the overlapped area is assigned as the material type of the new region. Make sure that materials are assigned to all mesh points in the structure. If this isn't done, error messages will appear and ATLAS won't run successfully.

You can use the `MATERIAL` statement to specify the material properties of the defined regions. But you must complete the entire mesh and doping definition before any `MATERIAL` statements can be used. The specification of material properties is described in Section 2.7.2: "Specifying Material Properties".

Cylindrical Coordinates

Cylindrical coordinates are often used when simulating discrete power devices. In this mode, ATLAS operates with $x=0$ as the axis of symmetry around which the cylindrical geometry is placed. Many of the default units change when cylindrical coordinates are used. The calculated current is in Amps rather than the usual Amps per micron. External elements are specified in absolute units (e.g., Farads, not Farads/micron for capacitors).

The MESH statement must be used to specify cylindrical symmetry. The following statement creates a mesh, which contains cylindrical symmetry.

```
MESH NX=20 NY=20 CYLINDRICAL
```

There are 20 mesh nodes along the X axis and 20 mesh nodes along the Y axis.

The following statement imports a mesh, which contains cylindrical symmetry.

```
MESH INF=mesh0.str CYLINDRICAL
```

Note: The CYLINDRICAL parameter setting isn't stored in mesh files. Therefore, this parameter must be specified each time a mesh file, which contains cylindrical symmetry, is loaded.

Specifying Electrodes

Once you have specified the regions and materials, define at least one electrode that contacts a semiconductor material. This is done with the ELECTRODE statement. For example:

```
ELECTRODE NAME=<electrode name> <position_parameters>
```

You can specify up to 50 electrodes. The position parameters are specified in microns using the X.MIN, X.MAX, Y.MIN, and Y.MAX parameters. Multiple electrode statements may have the same electrode name. Nodes that are associated with the same electrode name are treated as being electrically connected.

Some shortcuts can be used when defining the location of an electrode. If no Y coordinate parameters are specified, the electrode is assumed to be located on the top of the structure. You also can use the RIGHT, LEFT, TOP, and BOTTOM parameters to define the location. For example:

```
ELECTRODE NAME=SOURCE LEFT LENGTH=0.5
```

specifies the source electrode starts at the top left corner of the structure and extends to the right for the distance LENGTH.

Specifying Doping

You can specify analytical doping distributions or have ATLAS read in profiles that come from either process simulation or experiment. You specify the doping using the DOPING statement. For example:

```
DOPING <distribution_type> <dopant_type> <position_parameters>
```

Analytical Doping Profiles

Analytical doping profiles can have uniform, gaussian, or complementary error function forms. The parameters defining the analytical distribution are specified in the DOPING statement. Two examples are shown below with their combined effect shown in Figure 2-5.

```
DOPING UNIFORM CONCENTRATION=1E16 N.TYPE REGION=1
```

```
DOPING GAUSSIAN CONCENTRATION=1E18 CHARACTERISTIC=0.05 P.TYPE \
  X.LEFT=0.0 X.RIGHT=1.0 PEAK=0.1
```

The first DOPING statement specifies a uniform n-type doping density of 10^{16} cm^{-3} in the region that was previously labelled as region #1. The position parameters X.MIN, X.MAX, Y.MIN, and Y.MAX can be used instead of a region number.

The second DOPING statement specifies a p-type Gaussian profile (see Equation 21-3) with a peak concentration of 10^{18} cm^{-3} . This statement specifies that the peak doping is located along a line from $x = 0$ to $x = 1$ microns. Perpendicular to the peak line, the doping drops off according to a Gaussian distribution with a standard deviation of $(0.05/\sqrt{2}) \mu\text{m}$. At $x < 0$ or $x > 1$, the doping drops off laterally with a default standard deviation that is $(70/\sqrt{2})\%$ of CHARACTERISTIC. This lateral roll-off can be altered with the RATIO.LATERAL parameter. If a Gaussian profile is being added to an area that was already defined with the opposite dopant type, you can use the JUNCTION parameter to specify the position of the junction depth instead of specifying the standard deviation using the CHARACTERISTIC parameter.

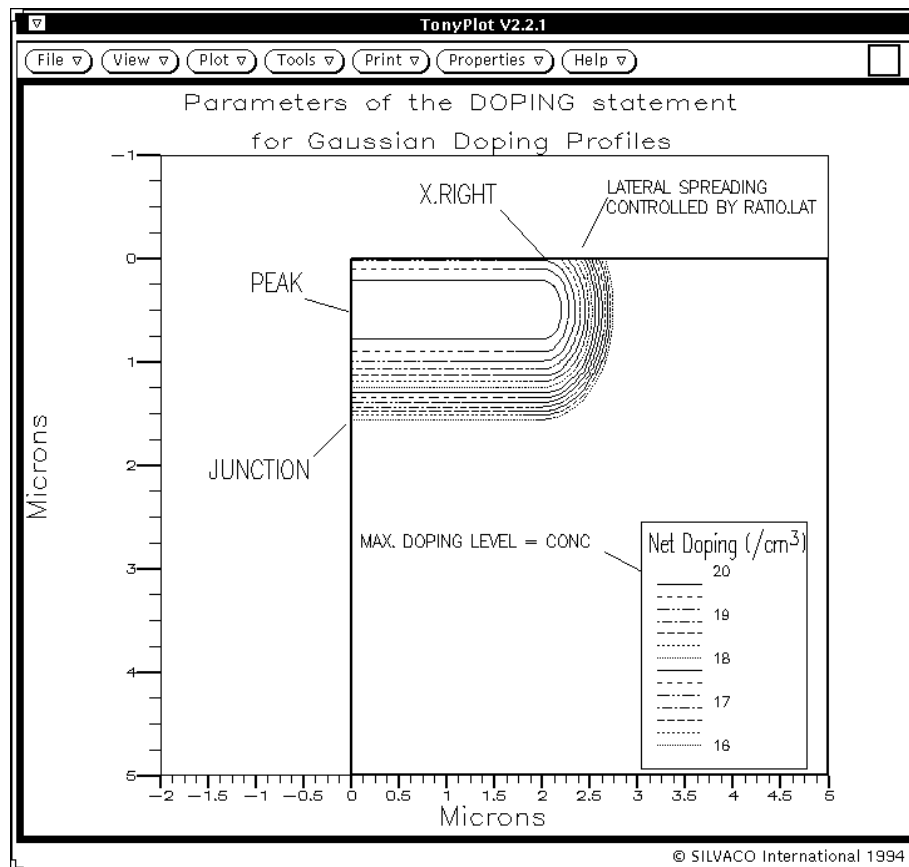


Figure 2-5: Analytical specification of a 2D Profile

The other analytical doping profile available is the complementary error function. This is defined as

$$\operatorname{erfc}(z) = \frac{2}{\sqrt{\pi}} \int_z^{\infty} \exp(-y^2) dy \quad 2-1$$

where the z variable is the distance scaled by the characteristic distance defined by the CHAR parameter.

The following example show DOPING statements that use this analytical form.

```
DOPING ERFC N.TYPE PEAK=0.5 JUNCTION=1.0 CONC=1.0E19 X.MIN=0.25 \
      X.MAX=0.75 RATIO.LAT=0.3 ERFC.LAT
DOPING P.TYPE CONC=1E18 UNIFORM
```

This sets up a donor profile with a peak concentration of $1.0\text{E}19 \text{ cm}^{-3}$ at $X = 0.5$ microns. The CHAR parameter, which determines the rate of change of the doping level with distance, is not directly set on the DOPING profile. Instead, it is calculated so that the net doping level at the position given by the JUNCTION parameter is zero. In this example, the acceptor concentration is $1.0 \times 10^{18} \text{ cm}^{-3}$ everywhere and so we require a donor density of $1.0 \times 10^{18} \text{ cm}^{-3}$ at a position of 1 micron to create the p-n junction there. The value of CHAR is calculated from the formula

$$\operatorname{erfc}([\text{JUNCTION} - \text{PEAK}] / \text{CHAR}) = 0.1 \quad 2-2$$

which results in a value of CHAR of approximately 0.43 microns.

Additionally, the donor concentration falls off in the lateral direction outside the range of 0.25 to 0.75 microns. The lateral falloff parameter is defined to be 0.3 times the principal falloff parameter and has the shape of the complementary error function.

Importing 1D SSUPREM3 Doping Profiles

One-dimensional doping profiles can be read into ATLAS from a SSUPREM3 output file. The doping data must have been saved from SSUPREM3 using the statement:

```
STRUCTURE OUTFILE=<output filename>
```

at the end of the SSUPREM3 run.

In ATLAS, the MASTER parameter of the DOPING statement specifies that a SSUPREM3 file will be read by ATLAS. Since this file will usually contain all the dopants from the SSUPREM3 simulation, the desired dopant type must also be specified. For example, the statement:

```
DOPING MASTER INFILE=mydata.dat BORON REGION=1
```

specifies that the boron profile from the file mydata.dat should be imported and used in region #1. SSUPREM3 profiles are imported into ATLAS one at a time (i.e., one DOPING statement is used for each profile or dopant). The statements:

```
DOPING MASTER INFILE=mydata.dat BORON OUTFILE=doping.dat
DOPING MASTER INFILE=mydata.dat ARSENIC X.RIGHT=0.8 RATIO=0.75
DOPING MASTER INFILE=mydata.dat ARSENIC X.LEFT=2.2 RATIO=0.75
```

offset the arsenic doping from boron to create a 2D doping profile from a single SSUPREM3 result.

It is advisable to include the OUTFILE parameter on the first DOPING statement to create a 2D3D doping file. This file will then be used in the next section to interpolate doping on a refined mesh after a REGRID. This file, however, can't be plotted in TONYPLOT. The position parameters and the RATIO.LATERAL parameter are used in the same manner as for analytical doping profiles to set the extent of the 1D profile.

2.6.4: Automatic Meshing (Auto-meshing) Using The Command Language

Automatic meshing provides a simpler method for defining device structures and meshes than the standard method described in Section 2.6.3: “Using The Command Language To Define A Structure”. Auto-meshing is particularly suited for epitaxial structures, especially device structures with many layers (for example, a VCSEL device). Auto-meshing unburdens you from the delicate bookkeeping involved in ensuring that the locations of mesh lines in the Y direction are consistently aligned with the edges of regions. This is done by specifying the locations of Y mesh lines in the REGION statements. The following sections will show how auto-meshing is done, using a few simple examples.

Specifying The Mesh And Regions

In the first example, we use a simple device to show you the fundamental concepts of auto-meshing. The first statements in this example are as follows:

```
MESH AUTO
X.MESH LOCATION=-1.0 SPACING=0.1
X.MESH LOCATION=1.0 SPACING=0.1
```

These statements are similar to the ones used in the standard method that described a mesh using the command language as shown in Section 2.6.3: “Using The Command Language To Define A Structure”. There are, however, two key differences. The first difference is the inclusion of the AUTO parameter in the MESH statement. You need this parameter to indicate that you want to use auto-meshing. The second and more important difference is that in this example we will not specify any Y.MESH statements. This is because the locations of Y mesh lines will be automatically determined by the parameters of the REGION statements.

You can still specify one or more Y.MESH statements. Such defined mesh lines will be included in the mesh. But including Y.MESH statements is optional in auto-meshing.

In the next few statements of the example, we will show you several new concepts that will explain how auto-meshing works. The following four lines describe the regions in the example device:

```
REGION TOP THICKNESS=0.02 MATERIAL=GaN NY=5 DONOR=1E16
REGION BOTTOM THICKNESS=0.1 MATERIAL=AlGaAs NY=5 DONOR=1E17 X.COMP=0.2
REGION TOP THICKNESS=0.08 MATERIAL=AlGaAs NY=4 ACCEPTOR=1E17 X.COMP=0.2
REGION BOTTOM THICKNESS=0.5 MATERIAL=AlGaAs NY=10 DONOR=1E18 X.COMP=0.2
```

New Concepts

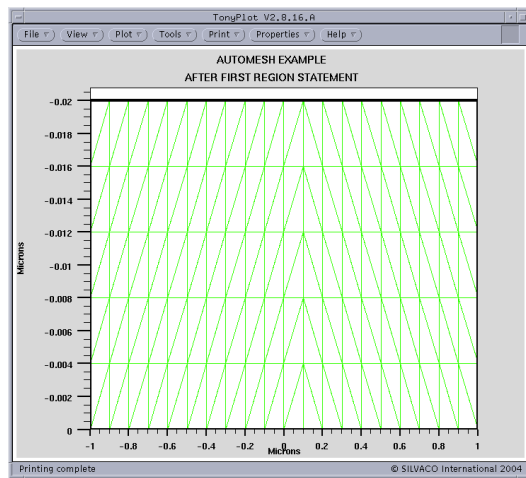
First, it appears that composition and doping are being specified in the REGION statement. This is the case for the DONOR, ACCEPTOR, X.COMPOSITION and Y.COMPOSITION parameters in the REGION statement that specify uniform doping or composition or both over the specified region. These parameters are also available to the standard methods described in Section 2.6.3: “Using The Command Language To Define A Structure”, but are more amenable to specification of epitaxial structures such as we are describing in this example.

Next, you should notice several other new parameters. These are the TOP, BOTTOM, THICKNESS and NY parameters. All of these are used to describe the relative locations and thicknesses of the layers as well as the locations of the Y mesh lines. The most intuitive of these parameters is the THICKNESS parameter, which describes the thickness in microns, in the Y direction of each layer. As for the extent in the X direction, in the absence of any specified X.MIN or X.MAX parameters, it is assumed that the region extends over the full range of the X mesh described above in the X.MESH statements.

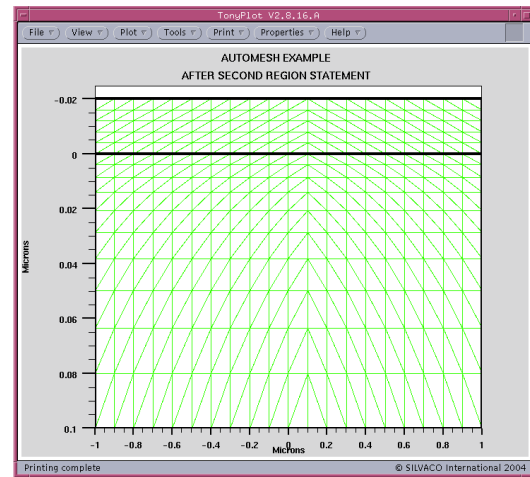
The NY parameter describes how many Y mesh lines are contained in the region so that the Y mesh lines are evenly spaced over the region. You can use the SY parameter instead of NY to specify the spacing in microns between Y mesh lines in the region. Make sure the value of SY does not exceed the value of THICKNESS. Generally, the relationship between SY, NY and THICKNESS can be expressed by the following:

$$SY = \text{THICKNESS}/NY$$

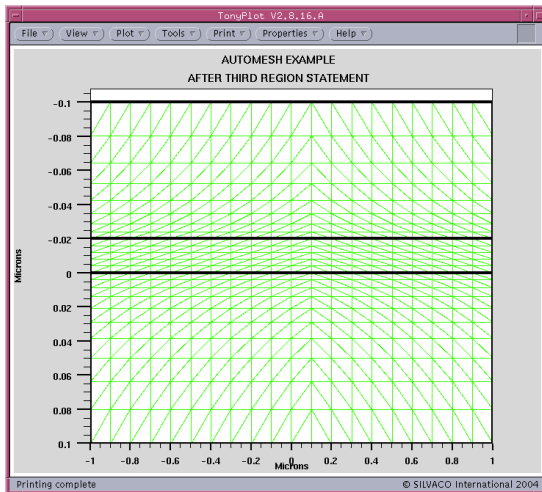
Figure 2-6 shows the meanings of the TOP and BOTTOM parameters.



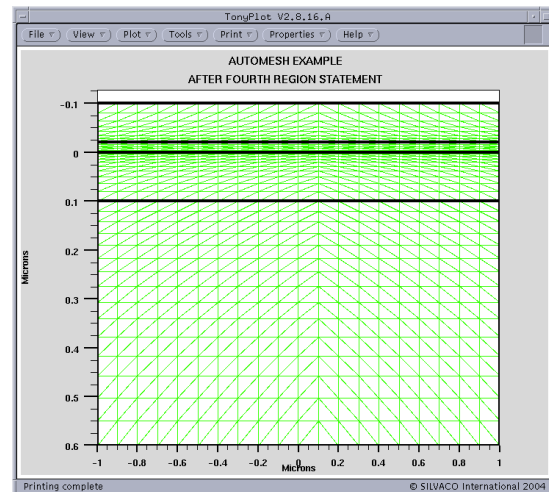
a) Structure after 1st REGION Statement



b) Structure after 2nd REGION Statement



c) Structure after 3rd REGION Statement



d) Structure after 4th REGION Statement

Figure 2-6: Simple Example of Auto-meshing Showing Sequence of Structure Development.

This figure shows a progression of representations of how the structure's mesh and region outlines appear after each REGION statement. This figure should give you an intuitive feel of how the regions are alternately placed on the top or bottom of the structure according to the specification of the TOP or BOTTOM parameters. It is important to keep in mind that the ATLAS coordinate convention for the Y axis is that positive Y is directed down into the device. This is similar to using the TOP and BOTTOM parameters of the ELECTRODE statement.

One thing you might notice in this figure is that the number of Y mesh lines in each region does not always match the number specified. This is because at each interface between regions, the Y mesh line spacing is ambiguously defined and the auto-meshing algorithm will always pick the smaller spacing between the two at each interface. Then, the spacing between Y mesh lines varies continuously between subsequent interfaces in a similar way as it does for mesh spacings specified by the LOCATION and SPACING parameters in the X.MESH and Y.MESH statements.

The auto-meshing algorithm maintains the "notion" of the current Y locations of the "top" and "bottom". Let's call these locations "Y_{top}" and "Y_{bottom}".

Before any REGION statements are processed, "Ytop" and "Ybottom" are both defined to be equal to zero. As the REGION statements are processed, the following cases are addressed:

- If you place the region on the top, as specified by the TOP parameter, the region will extend from "Ytop" to "Ytop"-THICKNESS (remember positive Y points down) and "Ytop" will move to the new location "Ytop"-THICKNESS.
- If you place the region on the bottom, as specified by the BOTTOM parameter, the region will extend from "Ybottom" to "Ybottom"+THICKNESS and "Ybottom" will move to the new location "Ybottom"+THICKNESS.

The auto-meshing algorithm will ensure that all regions are perfectly aligned to their neighboring regions and there are no inconsistencies between the locations of Y mesh lines and the region edges that they resolve.

Non-uniformity In The X Direction and Auto-meshing

In some cases, you may want to define a device with material discontinuities in the X direction. Such discontinuities may represent etched mesa structures or oxide apertures. There are a couple of ways to do this in auto-meshing. For example, you want to etch out a region from the structure of the previous example, from X=0 to the right and from Y=0 to the top. You can add the statement

```
REGION MATERIAL=Air X.MIN=0.0 Y.MAX=0.0
```

In this statement, we are not using the auto-meshing features but are using syntax of the standard meshing methods described in Section 2.6.3: "Using The Command Language To Define A Structure". ATLAS supports mixing the standard syntax with auto-meshing but be careful when doing this as we will explain shortly. Figure 2-7 shows the resulting structure and mesh after adding this statement. In this figure, we see that we have obtained the desired result.

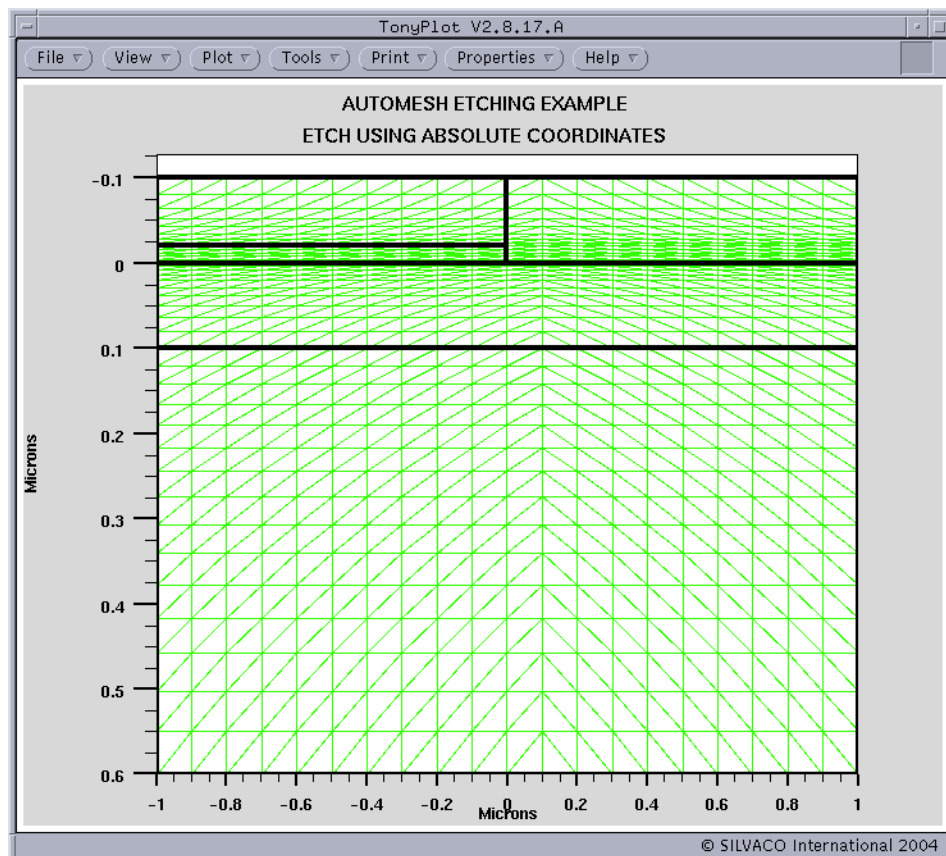


Figure 2-7: Structure Etch Example in Auto-meshing

The potential pitfall in using absolute Y coordinates in auto-meshing is that the location you choose, for example, by summing up thicknesses may not match the location your computer has calculated with its inherent numerical imprecision. The result is not only that the resulting structure may not exactly match what you desire. More importantly, you may end up accidentally creating a mesh with Y mesh lines closely spaced (usually in the order of the machine precision). This can cause numerical instability (poor convergence) and can overflow or underflow in certain models. What's worse is that this situation is difficult to detect.

There is, however, one situation where we can absolutely predict the location of an edge or Y mesh line. That is at $Y=0$. This is exactly what we have done in our example. So if you want to use auto-meshing with specifications of an absolute value of Y, then arrange your device structure so that the specification of Y will be at zero.

This also applies to the location of a recessed electrode. Make sure it is located at $Y=0$ if you are using auto-meshing.

There is another method of providing for discontinuities in material in the X direction that is absolutely safe from the previously discussed problems. In this approach, we use another parameter called `STAY` in the `REGION` statement in conjunction with the `TOP` or `BOTTOM` parameters.

The following describes the effect of the `STAY` parameter in the `REGION` statement.

- If you place the region on the top, as specified by the `TOP` parameter, and the `STAY` parameter is specified, the region will extend from "`Ytop`" to "`Ytop`"-`THICKNESS` and "`Ytop`" will remain in its current position.
- If you place the region on the bottom, as specified by the `BOTTOM` parameter, and the `STAY` parameter is specified, the region will extend from "`Ybottom`" to "`Ybottom`" + `THICKNESS` and "`Ybottom`" will remain in its current position.

The use of the `STAY` parameter can best be illustrated by the following example. In this example, we will reproduce the same structure discussed in the last example but this time using only `STAY` parameters and by not using any specification of absolute Y coordinates. The new `REGION` specifications are as follows:

```
REGION BOTTOM    THICKNESS=0.1  MATERIAL=AlGaIn NY=5  DONOR=1E17    X.COMP=0.2
REGION BOTTOM    THICKNESS=0.5  MATERIAL=AlGaIn NY=10  DONOR=1E18    X.COMP=0.2
REGION TOP STAY  THICKNESS=0.02 MATERIAL=GaN    NY=5    DONOR=1E16
REGION TOP       THICKNESS=0.02 MATERIAL=Air     NY=5    X.MIN=0.0
REGION TOP STAY  THICKNESS=0.08 MATERIAL=AlGaIn NY=4    ACCEPTOR=1E17 X.COMP=0.2
REGION TOP       THICKNESS=0.08 MATERIAL=Air     NY=4    X.MIN=0.0
```

In this example, we slightly rearranged the `REGION` statements for clarity and split one region into two. Figure 2-8 shows the results.

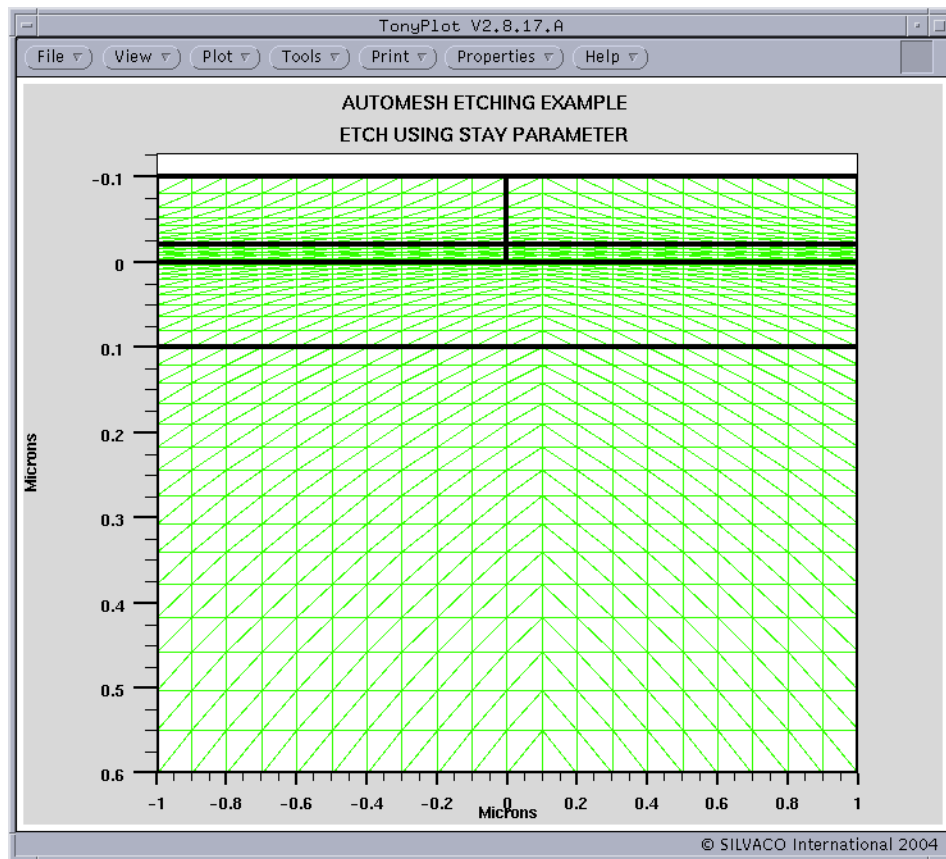


Figure 2-8: Structure Etching Example Using The STAY Parameter

The following describes the operation of the STAY parameter in this example:

- The STAY parameter in the third REGION statement means that the fourth REGION will start at the same Y coordinate as the third.
- Since the THICKNESS and NY parameters are the same in the third and fourth regions, they will have the same range of Y values and the same Y mesh.
- The specification of X.MIN in the fourth REGION statement means that the region will not completely overlap the third region but will only overlap to a minimum X value of 0.
- The lack of a STAY parameter in the fourth REGION statement means that the fifth region will lie directly atop the third and fourth regions.
- The STAY parameter in the fifth REGION statement means that the sixth REGION will start at the same Y coordinate as the fifth.
- Since the THICKNESS and NY parameters are the same in the fifth and sixth regions, they will have the same range of Y values and the same Y mesh.
- The specification of X.MIN in the sixth REGION statement means that the region will not completely overlap the fifth region but will only overlap to a minimum X value of 0.

As you can see, using the STAY parameter carefully avoids the problems of specifying values of Y coordinates and the potential problems involved. By doing so, you can specify arbitrary stepped structures.

Grading of Composition and Doping

We have provided another method for specifying composition or doping or both in the `REGION` statement that is available for both auto-meshing and meshing using the standard method described in Section 2.6.3: “Using The Command Language To Define A Structure”. This method allows linear grading of rectangular regions. Eight new parameters of the `REGION` statement support this function. They are `ND.TOP`, `ND.BOTTOM`, `NA.TOP`, `NA.BOTTOM`, `COMPX.TOP`, `COMPX.BOTTOM`, `COMPY.TOP`, and `COMPY.BOTTOM`. In the syntax of these parameter names, “`TOP`” refers to the “top” or extreme Y coordinate in the negative Y direction, and “`BOTTOM`” refers to the “bottom” or extreme Y coordinate in the positive Y direction. With this in mind, the following rules apply:

- If you specify `ND.TOP` and `ND.BOTTOM` in a `REGION` statement, the donor doping in the region will vary linearly from the value specified by `ND.TOP` at the “top” of the device to the value specified by `ND.BOTTOM` at the “bottom” of the device.
- If you specify `NA.TOP` and `NA.BOTTOM` in a `REGION` statement, the acceptor doping in the region will vary linearly from the value specified by `NA.TOP` at the “top” of the device to the value specified by `NA.BOTTOM` at the “bottom” of the device.
- If you specify `COMPX.TOP` and `COMPX.BOTTOM` in a `REGION` statement, the X composition fraction in the region will vary linearly from the value specified by `COMPX.TOP` at the “top” of the device to the value specified by `COMPX.BOTTOM` at the “bottom” of the device.
- If you specify `COMPY.TOP` and `COMPY.BOTTOM` in a `REGION` statement, the Y composition fraction in the region will vary linearly from the value specified by `COMPY.TOP` at the “top” of the device to the value specified by `COMPY.BOTTOM` at the “bottom” of the device.

Note: Any subsequent `DOPING` statements will add to the doping specified by the doping related parameters on the `REGION` statement.

Superlattices and Distributed Bragg Reflectors DBRs

For auto-meshing, we have provided a convenient way of specifying a certain class of superlattices or as they are commonly used distributed Bragg reflectors (DBRs). This class of superlattice includes any superlattice that can be described as integer numbers of repetitions of two different layers. By different, we mean that the two layers may have different thicknesses, material compositions, or dopings, or all. These "conglomerate" structures are specified by the DBR or SUPERLATTICE statement. Actually, SUPERLATTICE is a synonym for DBR. Therefore in the following discussion, we will use the DBR syntax and recognize that SUPERLATTICE and DBR can be used interchangeably.

Most of the syntax of the DBR statement is similar to the syntax of the REGION statement, except the syntax is set up to describe two regions (or two sets of regions). As you will see, we differentiate these regions (or sets of regions) by the indices 1 and 2 in the parameter's name.

The following example should make this concept clear.

```
MESH AUTO
X.MESH LOCATION=-1.0 SPACING=0.1
X.MESH LOCATION=1.0 SPACING=0.1

DBR TOP LAYERS=4 THICK1=0.1 THICK2=0.2 N1=2 N2=3 MAT1=GaAs MAT2=AlGaAs \
X2.COMP=0.4
DBR BOTTOM LAYERS=3 THICK1=0.05 THICK2=0.075 N1=3 N2=3 MAT1=AlGaAs \
MAT2=GaAs X1.COMP=0.4
```

In this example, we can see we are using auto-meshing because of the appearance of the AUTO parameter in the MESH statement. The DBR statements should be familiar since the functionality and syntax are similar to the REGION statement. We will not discuss those similarities here. We will only discuss the important differences. For more information about the similarities, see Chapter 21: "Statements".

The main new parameter is the LAYERS parameter. This parameter specifies the total number of regions added. The region indexed "1" is always added first, then the region indexed "2" is added, and depending on the value of LAYERS, the sequence of regions continues 1, 2, 1, 2, 1, ...

Figure 2-9 shows the functionality of the DBR statement, which gives the resulting structure and mesh from the example.

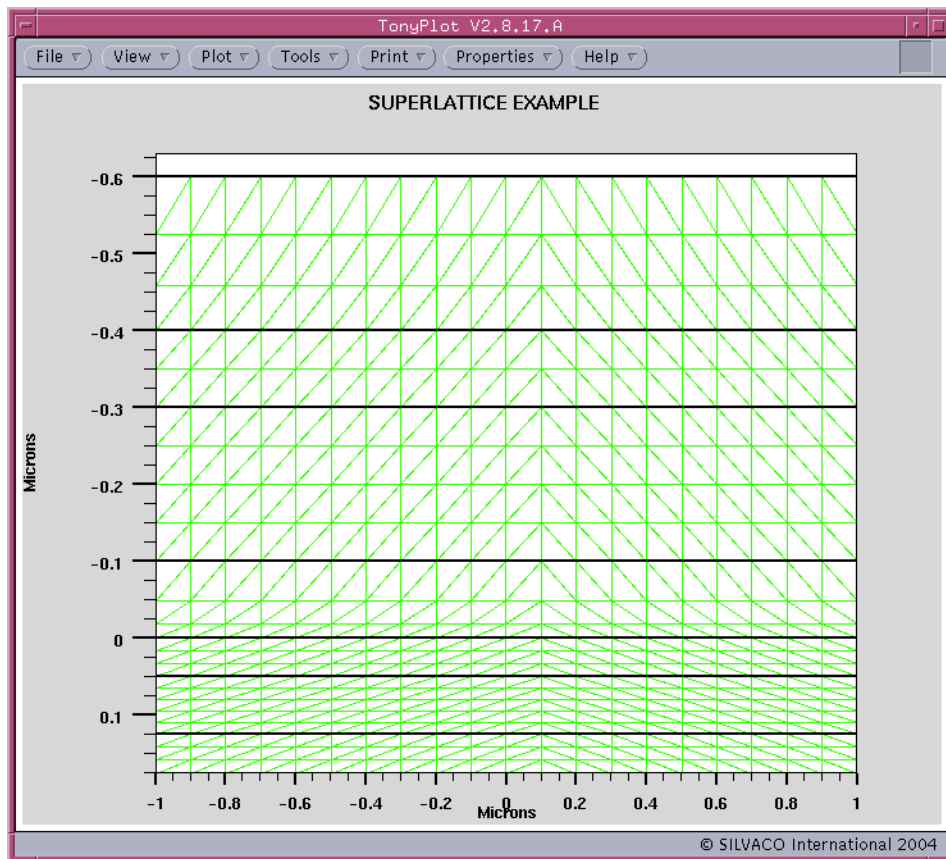


Figure 2-9: Superlattice Example Structure

2.6.5: Modifying Imported Regions

If you import a device structure from a file using the `INFILE` parameter of the `MESH` statement, you may want to modify some of the characteristics of one or more of the regions in the structure. To do this, specify a `REGION` statement with the `MODIFY` parameter and the `NUMBER` or `NAME` parameter assigned to the region number of interest. You can specify/respecify any of the following `REGION` statement parameters: `STRAIN`, `WELL.CNBS`, `WELL.VNBS`, `WELL.GAIN`, `POLAR.SCALE`, `QWELL`, `LED`, `WELL.FIELD`, and `POLARIZATION`.

2.6.6: Remeshing Using The Command Language

It can be difficult to define a suitable grid when specifying a structure with the command language. The main problem is that the meshes required to resolve 2D doping profiles and curved junctions are quite complicated. Simple rectangular meshes require an excessive number of nodes to resolve such profiles. If a device structure only includes regions of uniform doping, then there's usually no need to regrid. But when realistic 2D doping profiles are present, a regrid may be necessary.

Note: The recommended solution for defining complex mesh structures for ATLAS is to use the standalone program, `DEVEDIT`.

Regrid On Doping

ATLAS includes a regridding capability that generates a fine mesh only in a localized region. You specify a quantity on which the regrid is to be performed. The mesh is then refined in regions where the specified quantity varies rapidly. Whenever a specified quantity (usually doping) changes quickly, the regridding will automatically grade the mesh accordingly. You can get a regrid on doping before any solutions are obtained. You can do this by using the statement:

```
REGRID LOGARITHM DOPING RATIO=2 SMOOTH.KEY=4 DOPFILE=<filename1> \
OUTFILE=<filename2>
```

This statement must be used after the MESH, REGION, MATERIAL, ELECTRODE, and DOPING statements described previously. The effects of this REGRID statement on a simple diode structure are shown in Figure 2-10.

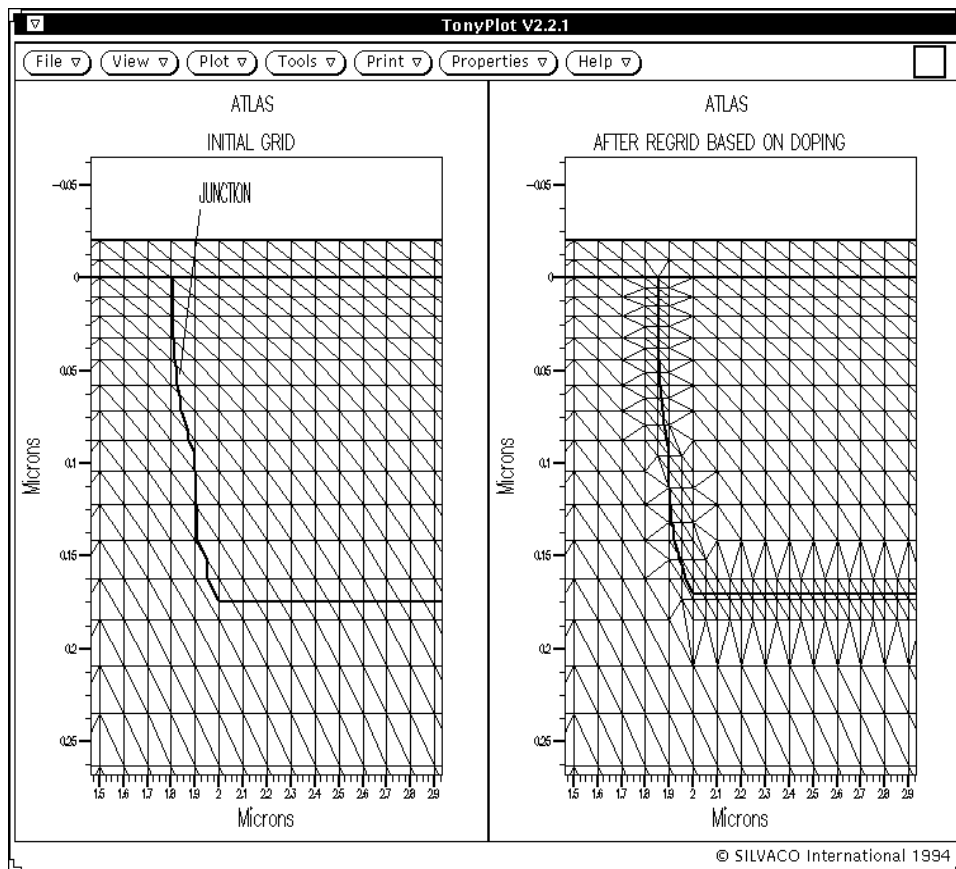


Figure 2-10: Regrid on doping provides improved resolution of junction

In this statement, the regridding will resolve doping profiles to two orders of magnitude in change.

The doping file, *filename1*, must be specified in the first DOPING statement with the OUTFILE parameter. The results of the regrid are saved in the file, *filename2*. The SMOOTH.KEY parameter value selects a smoothing algorithm. A value of 4 is typically best as this algorithm tends to produce the fewest obtuse triangles. For a complete description of the various smoothing algorithms, see Chapter 20: “Numerical Techniques”.

Regrid Using Solution Variables

The `REGRID` statement can use a wide range of solution variables as the basis for mesh refinement. A regrid on solution variables can only be used after a solution has been obtained. After a regrid on a solution variable, the solution must be re-solved at the same bias in ATLAS.

For example:

```
REGRID POTENTIAL RATIO=0.2 MAX.LEVEL=1 SMOOTH.K=4 DOPFILE=<filename1>
SOLVE PREV
```

Regrid on potential is often used for high voltage power devices.

Note: You can use the `REGRID` statement any number of times on a structure. But we advise you to quit and restart ATLAS between regrids on electrical quantities. You can use the `go atlas` statement to do this. This should be followed by a `MESH` statement, loading the output file of the `REGRID` command, and a re-setting of all material and model parameters.

2.6.7: Specifying 2D Circular Structures

In some situations, it may be desirable to construct a device with a circular cross section. This is possible by using `DEVEDIT` and by using the `MESH` statement in the ATLAS command language. Make sure to put the `MESH` statement first in the input deck and specify the `CIRCULAR` parameter.

The radial mesh spacing is then given by a series of `R.MESH` statements and the angular mesh given by a series of `A.MESH` statements. The angles are specified in degrees between 0 and 360.

For example

```
MESH CIRCULAR

R.MESH LOC=0.0  SPAC=0.05
R.MESH LOC=0.2  SPAC=0.05
R.MESH LOC=0.35 SPAC=0.025
R.MESH LOC=0.39 SPAC=0.01
R.MESH LOC=0.4  SPAC=0.01

A.MESH LOC=0    SPAC=30
A.MESH LOC=360  SPAC=30
```

would create a circular mesh with major angular spacing of 30° and a radial spacing, which is relatively coarse near to the origin and becomes finer towards the edge of the device.

The angular spacing defines a set of major spokes radiating out from the origin with the number of elements between each spoke increasing with distance from the origin. The mesh spacing may be irregular, although a regular mesh spacing suffices for most problems.

The spacing in the radial direction will in general be irregular. This can result in the creation of obtuse elements, particularly if the spacing decreases rapidly with increasing radius. The `MINOBTUSE` parameter on the `MESH` statement deploys an algorithm to reduce the occurrence of obtuse elements, particularly obtuse boundary elements. It is set to true by default, but you can clear it by using the syntax `^MINOBTUSE`.

For some device structures, you can reduce the size of the solution domain by using symmetry arguments. ATLAS allows you to create a wedge shaped device by using the `MAXANGLE` parameter.

For example

```
MESH CIRCULAR MAXANGLE=150
```

would create a circular wedge with an angle at the origin of 150°.

Note: MAXANGLE should not exceed 180°.

Once a circular mesh has been created, it may be subdivided into regions using the R.MIN, R.MAX, A.MIN and A.MAX parameters on the REGION statement.

R.MIN is the inner radius of the region. R.MAX is the outer radius of the region. Both are in the units of microns. A.MIN and A.MAX define the minimum and maximum angular limits of the region respectively, both in degrees.

For example

```
REGION NUM=1 MATERIAL=SILICON A.MIN=0 A.MAX=360.0 R.MAX=0.4
REGION NUM=2 MATERIAL=OXIDE A.MIN=30 A.MAX=150.0 R.MIN=0.35 R.MAX=0.4
```

will enforce the area between angular limits of 30 and 150 degrees and radial limits of 0.35 and 0.4 microns to be an oxide region, and the rest of the mesh defined above to be a silicon region.

Similarly, the ELECTRODE and DOPING statements have R.MIN, R.MAX, A.MIN, and A.MAX parameters. Support for doping of circular meshes is extended from that described in Section 2.6.3: “Using The Command Language To Define A Structure” to allow analytical doping profiles in the radial direction (UNIFORM, GAUSS, ERFC) with optional lateral fall off in the angular (i.e., at constant radius) direction. The lateral falloff is GAUSSIAN unless ERFC.LAT is specified to change it to the complementary error function. The usual parameters for specifying the analytical profile apply with the principal direction being the radial direction.

If you set MAX.ANGLE to 180° and add the following lines, you will obtain the structure as shown in Figure 2-11.

```
ELECTRODE NAME=DRAIN R.MIN=0.35 A.MIN=0.0 A.MAX=30.0
ELECTRODE NAME=SOURCE R.MIN=0.35 A.MIN=150.0 A.MAX=180.0
ELECTRODE NAME=GATE A.MIN=60.0 A.MAX=120.0 R.MIN=0.39 R.MAX=0.4
```

If you further add the DOPING statement below, then you will obtain the doping profile as shown in Figure 2-12.

```
DOPING GAUSS N.TYPE CONC=1.0e19 CHAR=0.05 R.MIN=0.15 R.MAX=0.2 A.MIN=0.0
A.MAX=180.0
```

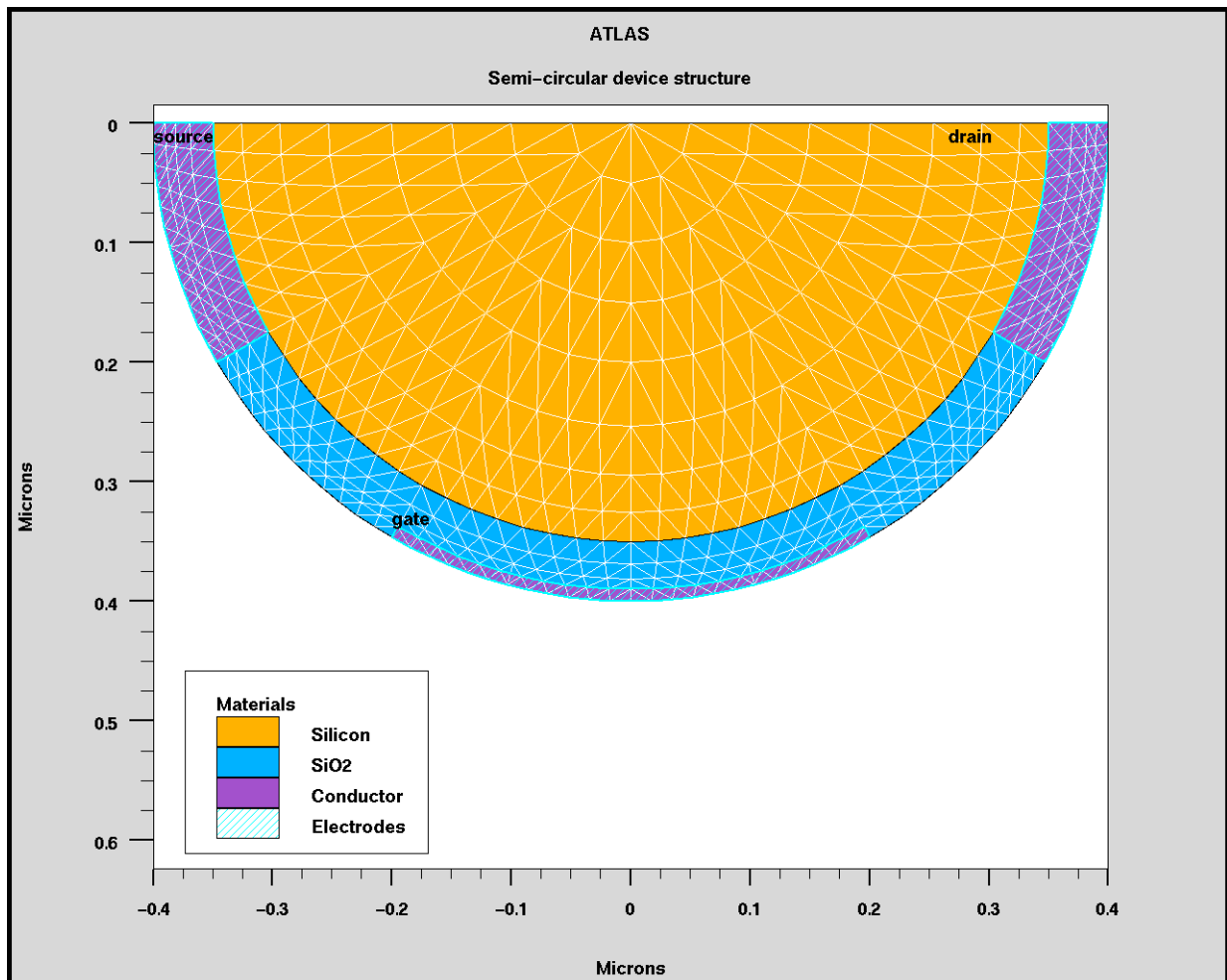


Figure 2-11: Semi-circular structure created using ATLAS command syntax.

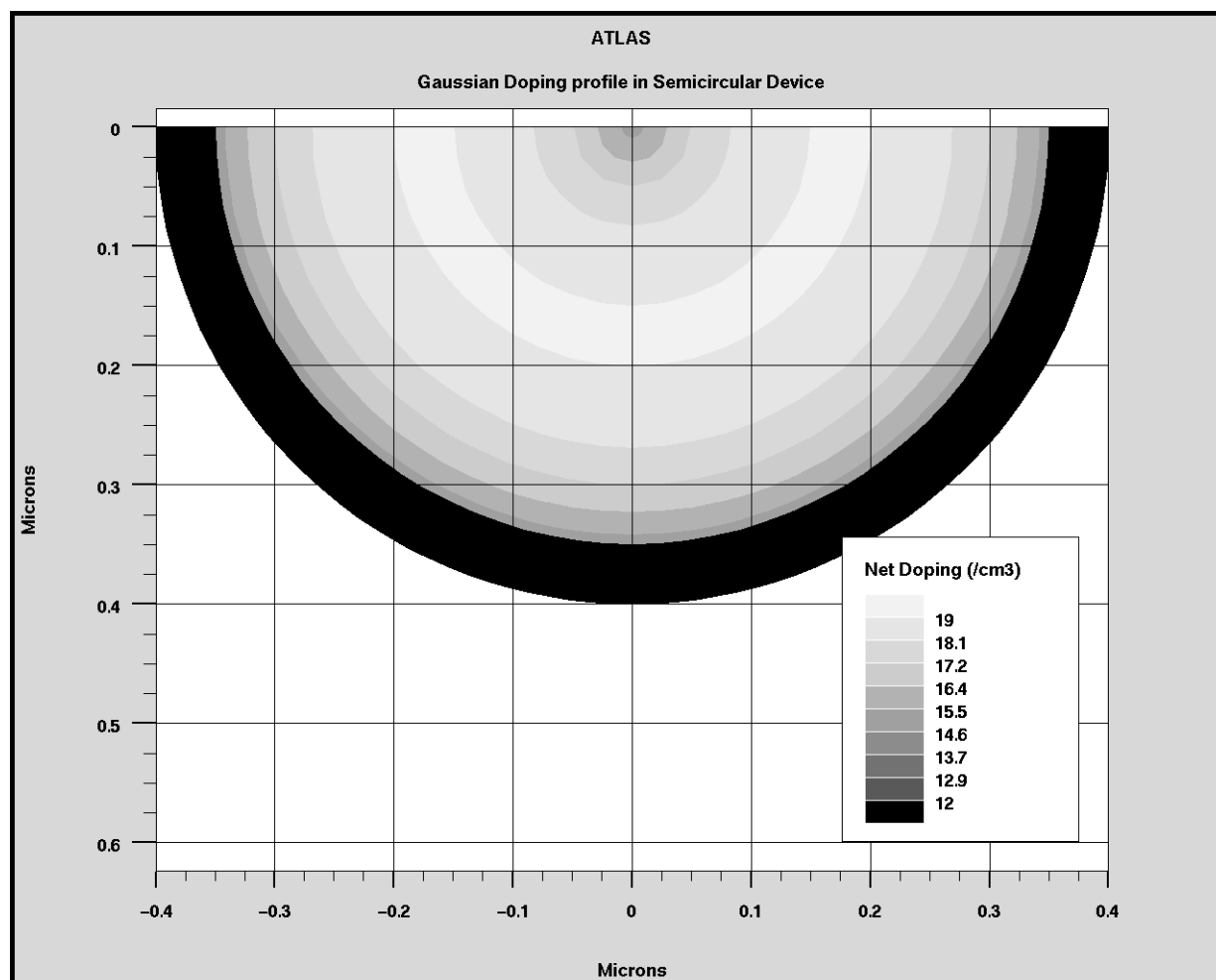


Figure 2-12: Gaussian doping profile applied to the semi-circular structure of Figure 2-11.

Note: To obtain the best results, align region and electrode boundaries with existing meshlines (radial or major spokes).

2.6.8: Specifying 3D Structures

The syntax for forming 3D device structures is an extension of the 2D syntax described in the previous section. The MESH statement should appear as:

```
MESH THREE.D
```

The THREE.D parameter tells ATLAS that a three dimensional grid will be specified. The other statements used to specify 3D structures and grids are the same as for 2D with the addition of Z direction specifications. The statements:

```
MESH THREE.D
X.MESH LOCATION=0 SPACING=0.15
X.MESH LOCATION=3 SPACING=0.15
Y.MESH LOCATION=0 SPACING=0.01
Y.MESH LOCATION=0.4 SPACING=0.01
Y.MESH LOCATION=3 SPACING=0.5
Z.MESH LOCATION=0 SPACING=0.1
Z.MESH LOCATION=3 SPACING=0.1
```

define a 3D mesh that is uniform in the X and Z directions and varies in the Y direction.

Position parameters for the Z direction (Z.MIN and Z.MAX) are also used on REGION, ELECTRODE, or DOPING statements.

2.6.9: Specifying 3D Cylindrical Structures

As mentioned in Section 2.6.3: “Using The Command Language To Define A Structure”, you can model a quasi-3D cylindrical structure in ATLAS2D by specifying the CYLINDRICAL parameter on the MESH statement. This has the drawback that the resulting device structure and solution has no dependence on the angle around the axis of rotation. In ATLAS3D, the CYLINDRICAL parameter enables you to create a general cylindrical structure. The MESH statement must appear as:

```
MESH THREE.D CYLINDRICAL
```

where the THREE.D parameter informs the simulator to create a fully 3D mesh.

When specifying the CYLINDRICAL parameter, you must now specify the structure in terms of radius, angle, and cartesian Z coordinates.

There are three mesh statements analogous to those used for general structures that are used to specify mesh in radius, angle and Z directions. The R.MESH statement is used to specify radial mesh. The A.MESH statement is used to specify angular mesh. The Z.MESH statement is used to specify mesh in the Z direction.

For example:

```
MESH THREE.D CYLINDRICAL

R.MESH LOCATION=0.0 SPACING=0.0004
R.MESH LOCATION=0.0028 SPACING=0.00005
R.MESH LOCATION=0.004 SPACING=0.0002

A.MESH LOCATION=0 SPACING=45
A.MESH LOCATION=360 SPACING=45

Z.MESH LOCATION=-0.011 SPACING=0.001
Z.MESH LOCATION=0.011 SPACING=0.001
```

Here, the R.MESH lines are similar to the familiar X.MESH, Y.MESH, and Z.MESH except the R.MESH locations and spacings are radial relative to the Z axis in microns.

The locations and spacings on the A.MESH lines specify locations and spacings in degrees of rotation about the Z axis. The Z.MESH lines are exactly the same as have been already discussed.

For 3D cylindrical structure, specifying the REGION and ELECTRODE statements also are modified to allow specification of ranges in terms of radius, angle and z location. The range parameters are R.MIN, R.MAX, A.MIN, A.MAX, Z.MIN and Z.MAX. R.MIN, R.MAX, Z.MIN and Z.MAX are all in units of microns. A.MIN and A.MAX are in degrees.

To continue the example, we will specify a surround gate nano-tube as follows:

```

REGION NUM=1 MATERIAL=silicon \
  Z.MIN=-0.1 Z.MAX=0.1 A.MIN=0 A.MAX=360.0 R.MAX=0.0028

REGION NUM=2 MATERIAL=oxide \
  R.MIN=0.0028 R.MAX=0.004 Z.MIN=-0.011 Z.MAX=0.011 A.MIN=0 A.MAX=360.0

ELECTRODE NAME=DRAIN Z.MIN=-0.011 Z.MAX=-0.01 R.MAX=0.0028

ELECTRODE NAME=SOURCE Z.MIN=0.01 Z.MAX=0.011 R.MAX=0.0028

ELECTRODE NAME=GATE Z.MIN=-0.004 Z.MAX=0.004 R.MIN=0.0038 MATERIAL=aluminum

```

Here, we defined a central core of silicon surrounded by an oxide cladding. The device has a surrounding gate with a source and drain at either end.

Figure 2-13 shows a cutplane normal to the Z axis at z=0 for this device.

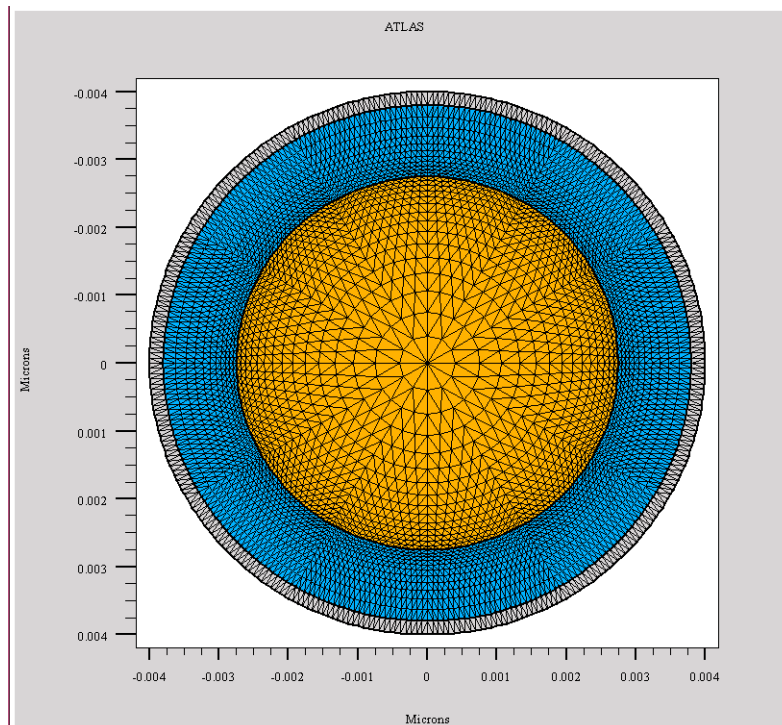


Figure 2-13: Cutplane of 3D Cylindrical Simulation

In some instances, you can reduce the size of the cylindrical device by using symmetry arguments. So if the device has mirror symmetry about some plane through its axis of rotation, it suffices to model only half of the cylinder. You can tell the simulator to do this by using the parameter `MAX.ANGLE`, which restricts the angular extent of mesh.

For example:

```
MESH THREE.D CYLINDRICAL MAX.ANGLE=180
```

will result in a semi-cylinder.

The value of `MAX.ANGLE` should not be greater than 180° and must satisfy the condition that the angular range of the device must start and end on major spokes of the radial mesh. In other words, `MAX.ANGLE` must be equal to a integral multiple of angular mesh spacing. For example, if the angular mesh spacing was 45°, then `MAX.ANGLE` can be 45, 90, 135 or 180°. ATLAS will automatically adjust the value of `MAX.ANGLE` if it is necessary.

If the mesh spacing in the radial direction is regular, then the resulting mesh will usually have no obtuse elements. If the mesh spacing in the radial direction decreases with increasing radius, then it is possible that some obtuse triangular elements will be formed. Use the parameter `MINOBTUSE` to try to reduce the number of obtuse triangular elements.

The `DOPING` statement has been modified to accept the parameters `R.MIN`, `R.MAX`, `A.MIN` and `A.MAX`. These apply to the analytic doping `PROFILES`, namely `UNIFORM`, `GAUSSIAN`, and `ERFC`. `R.MIN` and `R.MAX` specify the minimum and maximum radial extents in microns. `A.MIN` and `A.MAX` specify the minimum and maximum angular extents in degrees. The principal direction for the `GAUSSIAN` and `ERFC` dependence is the `Z` direction. Thus the usual `DOPING` parameters, such as `CHAR`, `PEAK`, `DOSE`, `START` and `JUNCTION` all apply to the `Z` direction with `R.MIN`, `R.MAX`, `A.MIN`, `A.MAX` defining the extents at which lateral fall off occurs.

The lateral fall-off in the radial and angular directions can be controlled by the `LAT.CHAR` or `RATIO.LAT` parameters.

For example:

```
DOPING GAUSSIAN N.TYPE START=0.25 CONC=1.0e19 CHAR=0.2 LAT.CHAR=0.2 \  
R.MIN=0.4 R.MAX=0.6 A.MIN=0.0 A.MAX=360
```

produces a gaussian doping profile in the `Z` direction, with a peak at `Z=0.25` microns, and with a lateral gaussian fall-off in the radial direction when it is outside a radius of between 0.4 and 0.6 microns. Figure 2-14 shows the radial and angular distribution. Figure 2-15 shows the radial and `z`-variation. The `Z` direction corresponds to the vertical direction on the cutplane.

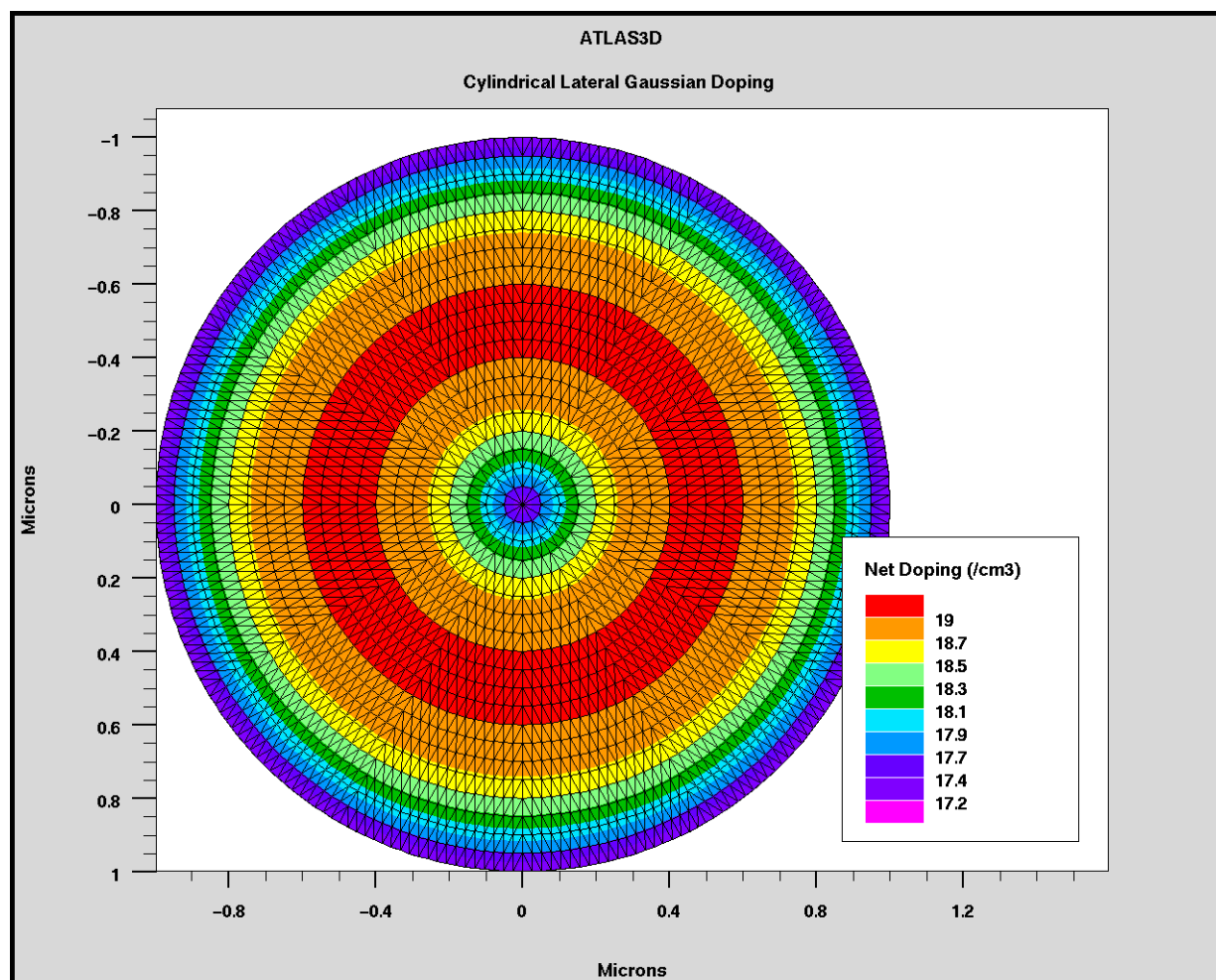


Figure 2-14: Cylindrical gaussian doping profile on a cutplane perpendicular to the Z axis.

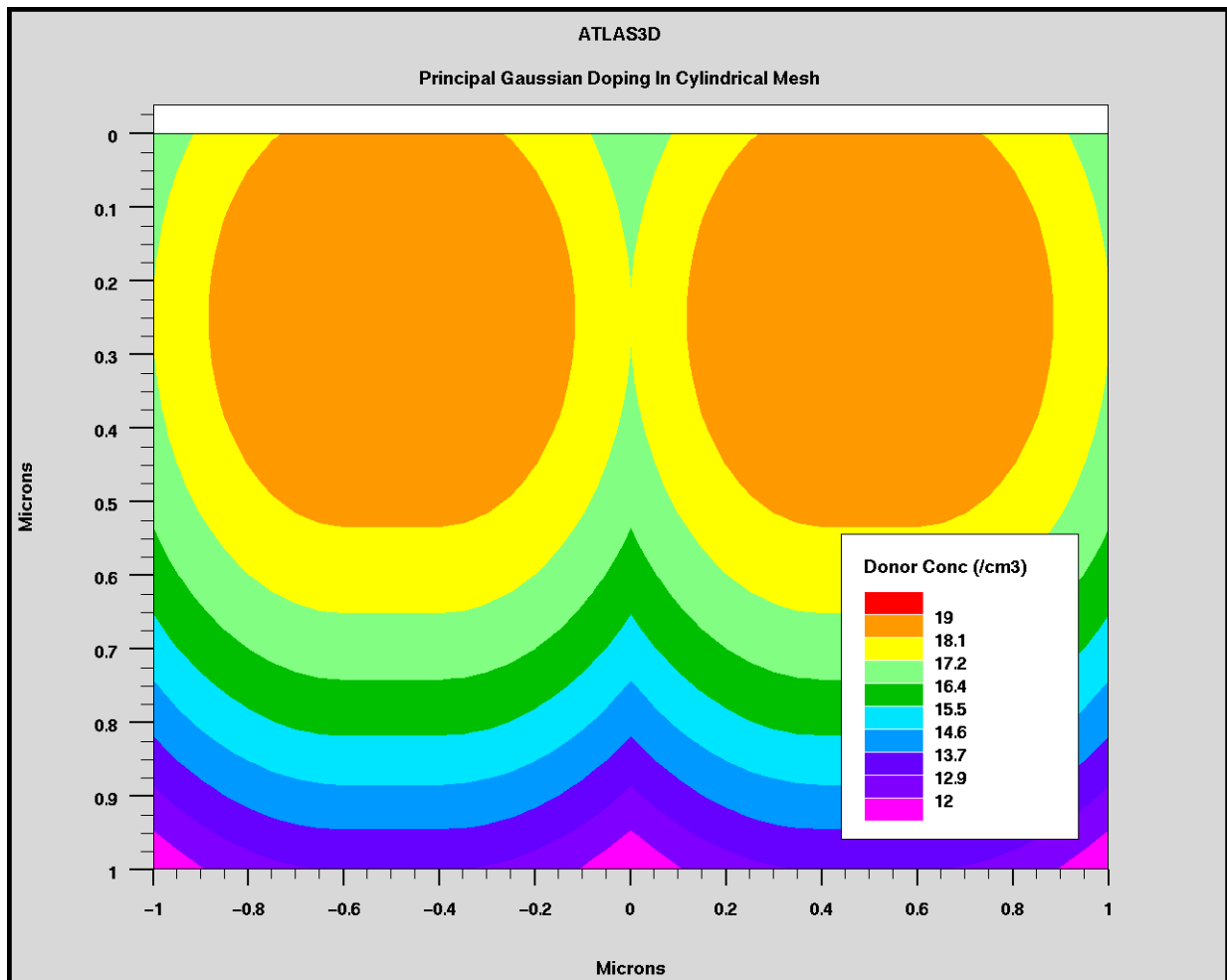


Figure 2-15: Cylindrical gaussian doping profile on a cutplane containing the Z axis.

2.6.10: Extracting 2D Circular Structures From 3D Cylindrical Structures

To simulate circular structures in 2D that are analogous to the 3D meshing described above, use the cutplane feature in structure saving. To do this, specify the `CUTPLANE` and `Z.CUTPLANE` parameters of the `SAVE` statement. The logical parameter `CUTPLANE` specifies that you are interested in outputting a 2D cutplane from a 3D structure. The `Z.CUTPLANE` specifies the Z coordinate value in microns of the location where you want the cutplane.

For example, Figure 2-13 was generated by the following syntax:

```
SAVE CUTPLANE Z.CUTPLANE=0.0
```

2.6.11: General Comments Regarding Grids

Specifying a good grid is a crucial issue in device simulation but there is a trade-off between the requirements of accuracy and numerical efficiency. Accuracy requires a fine grid that resolves the structure in solutions. Numerical efficiency is greater when fewer grid points are used. The critical areas to resolve are difficult to generalize because they depend on the technology and the transport phenomena. The only generalization possible is that most critical areas tend to coincide with reverse-biased metallurgical junctions. Typical critical areas are:

- High electric fields at the drain/channel junction in MOSFETs
- The transverse electric field beneath the MOSFET gate
- Recombination effects around the emitter/base junction in BJTs
- Areas of high impact ionization
- Around heterojunctions in HBTs and HEMTs.

The CPU time required to obtain a solution is typically proportional to N^α , where N is the number of nodes and α varies from 2 to 3 depending on the complexity of the problem. Thus, the most efficient way is to allocate a fine grid only in critical areas and a coarser grid elsewhere.

The three most important factors to look for in any grid are:

- Ensure adequate mesh density in high field areas
- Avoid obtuse triangles in the current path or high field areas
- Avoid abrupt discontinuities in mesh density

For more information about grids, see Chapter 20: “Numerical Techniques”, Section 20.3: “Meshes”.

2.6.12: Maximum Numbers Of Nodes, Regions, and Electrodes

ATLAS sets some limits on the maximum number of grid nodes that can be used. But this shouldn't be viewed as a bottleneck to achieving simulation results. In the default version, 2D ATLAS simulations have a maximum node limit of 100,000. 3D ATLAS simulations have an upper limit of 40,000,000 nodes with no more than 100,000 nodes in any one Z plane and a maximum number of Z planes of 2,000.

This limit is high enough that for almost all simulations of conventional devices, running out of nodes is never an issue. For most 2D simulations, you can obtain accurate results with somewhere between 2,000 and 4,000 node points properly located in the structure.

If you exceed the node limits, error messages will appear and ATLAS will not run successfully. There are two options to deal with this problem. The first option is to decrease the mesh density because simulations with the maximum nodes take an extremely long time to complete. The second option is to contact your local SILVACO office (support@silvaco.com).

A node point limitation below these values might be seen due to virtual memory constraints on your hardware. For each simulation, ATLAS dynamically allocates the virtual memory. See the SILVACO INSTALLATION GUIDE for information about virtual memory requirements. The virtual memory used by the program depends on the number of nodes and on items, such as the models used and the number of equations solved.

Also, there is a node limit for the number of nodes in the X or Y directions in 2D and 3D ATLAS. In the standard version, this limit is 20,000 nodes. This is applicable to meshes defined in the ATLAS syntax using X.MESH and Y.MESH statements.

The maximum number of regions defined in both 2D and 3D ATLAS is 1,000. The maximum number of definable electrodes is 100. Again, if you need to include more than the maximum number of regions or electrodes, contact your local SILVACO office (support@silvaco.com).

2.6.13: Quadrilateral REGION Definition

In addition to the rectangular shaped regions, which we have considered so far, you can create regions with sloping sides. Although it is possible to make complicated overall region shapes using rectangular regions as building blocks, this task is made easier by being able to specify the co-ordinates of each of the four corners of the REGION. To do this, use the P1.X, P1.Y, P2.X, P2.Y, P3.X, P3.Y, P4.X, and P4.Y parameters on the REGION statement. Then, (P1.X, P1.Y) are the XY coordinates of the first corner of the region and so on.

The region must lie entirely within the device limits as defined by the mesh. To obtain best results, these corner coordinates must coincide with valid mesh points as created by the X.MESH and Y.MESH statements.

Because the overall mesh shape will still be rectangular, you may need to use VACUUM regions as padding to get a non-rectangular shaped device. Alternatively, use DEVEDIT to get a non-rectangular overall device shape.

Example:

```
REGION NUMBER=3 MATERIAL=SILICON P1.X=0.0 P1.Y=1.0 P2.X=3.0 P2.Y=1.0 P3.X=3.5
P3.Y=2.5 P4.X=0.0 P4.Y=2.0
```

| Table 2-1. Quadrilateral Shaped REGION Definition | | | | |
|---|-----------|------|---------|---------|
| Statement | Parameter | Type | Default | Units |
| REGION | P1.X | Real | | Microns |
| REGION | P1.Y | Real | | Microns |
| REGION | P2.X | Real | | Microns |
| REGION | P2.Y | Real | | Microns |
| REGION | P3.X | Real | | Microns |
| REGION | P3.Y | Real | | Microns |
| REGION | P4.X | Real | | Microns |
| REGION | P4.Y | Real | | Microns |

2.7: Defining Material Parameters And Models

Once you define the mesh, geometry, and doping profiles, you can modify the characteristics of electrodes, change the default material parameters, and choose which physical models ATLAS will use during the device simulation. To accomplish these actions, use the `CONTACT`, `MATERIAL`, and `MODELS` statements respectively. Impact ionization models can be enabled using the `IMPACT` statement. Interface properties are set by using the `INTERFACE` statement.

Many parameters are accessible through the SILVACO C-INTERPRETER (SCI), which is described in Appendix A: “C-Interpreter Functions”. This allows you to define customized equations for some models. For more information about the `INTERFACE` and `MODELS` statements, see Chapter 21: “Statements”, Sections 21.21: “INTERFACE” and 21.34: “MODELS”.

2.7.1: Specifying Contact Characteristics

Workfunction for Gates or Schottky Contacts

An electrode in contact with semiconductor material is assumed by default to be ohmic. If a work function is defined, the electrode is treated as a Schottky contact. The `CONTACT` statement is used to specify the metal workfunction of one or more electrodes. The `NAME` parameter is used to identify which electrode will have its properties modified.

The `WORKFUNCTION` parameter sets the workfunction of the electrode. For example, the statement:

```
CONTACT NAME=gate WORKFUNCTION=4.8
```

sets the workfunction of the electrode named `gate` to 4.8eV. The workfunctions of several commonly used contact materials can be specified using the name of the material. You can specify workfunctions for `ALUMINUM`, `N.POLYSILICON`, `P.POLYSILICON`, `TUNGSTEN`, and `TU.DISILICIDE` in this way. The following statement sets the workfunction for a n-type polysilicon gate contact.

```
CONTACT NAME=gate N.POLYSILICON
```

Aluminum contacts on heavily doped silicon is usually ohmic. For this situation, don't specify a workfunction. For example, MOS devices don't specify:

```
CONTACT NAME=drain ALUMINUM /* wrong */
```

The `CONTACT` statement can also be used to specify barrier and dipole lowering of the Schottky barrier height. To enable barrier lowering, specify the `BARRIER` parameter, while specifying dipole lowering using the `ALPHA` parameter. For example, the statement:

```
CONTACT NAME=anode WORKFUNCTION=4.9 BARRIER ALPHA=1.0e-7
```

sets the work function of the Schottky contact named `anode` to 4.9eV enables barrier lowering and sets the dipole lowering coefficient to 1 nm.

Note: When a Schottky barrier is defined at a contact, we recommend that a fine y mesh is present just beneath the contact inside the semiconductor. This allows the Schottky depletion region to be accurately simulated.

Setting Current Boundary Conditions

The `CONTACT` statement is also used to change an electrode from voltage control to current control. Current controlled electrodes are useful when simulating devices, where the current is highly sensitive to voltage or is a multi-valued function of voltage (e.g., post-breakdown and when there is snap-back).

The statement:

```
CONTACT NAME=drain CURRENT
```

changes the drain electrode to current control. The `BLOCK` or `NEWTON` solution methods are required for all simulations using a current boundary condition. For more information about these methods, see Chapter 20: “Numerical Techniques”, Section 20.5: “Non-Linear Iteration”.

Defining External Resistors, Capacitors, or Inductors

Lumped resistance, capacitance, and inductance connected to an electrode can be specified using the `RESISTANCE`, `CAPACITANCE`, and `INDUCTANCE` parameters in the `CONTACT` statement. For example, the statement:

```
CONTACT NAME=drain RESISTANCE=50.0 CAPACITANCE=20e-12 INDUCTANCE=1e-6
```

specifies a parallel resistor and capacitor of 50 ohms and 20 pF respectively in series with a 1 μ H inductor. Note that in 2D simulations, these passive element values are scaled by the width in the third dimension. Since in 2D ATLAS assumes a 1 μ m width, the resistance becomes 50 $\Omega\text{-}\mu\text{m}$.

Distributed contact resistance for an electrode can be specified using the `CON.RESIST` parameter. For example, the statement:

```
CONTACT NAME=source CON.RESISTANCE=0.01
```

specifies that the source contact has a distributed resistance of 0.01 Ωcm^2 .

Note: Simulations with external resistors, capacitors, or inductors must be solved using the `BLOCK` or `NEWTON` solution method.

Floating Contacts

The `CONTACT` statement is also used to define a floating electrode. There are two distinctly different situations where floating electrodes are important. The first situation is for floating gate electrodes used in EEPROM and other programmable devices. The second situation is for contacts directly onto semiconductor materials such as floating field plates in power devices.

To enable floating gates, specify the `FLOATING` parameter on the `CONTACT` statement. For example, the statement:

```
CONTACT NAME=fgate FLOATING
```

specifies that the electrode named `fgate` will be floating and that charge boundary conditions will apply.

For contacts directly onto semiconductor, the `FLOATING` parameter cannot be used. This type of floating electrode is best simulated by specifying current boundary conditions on the `CONTACT` statement. For example, the statement:

```
CONTACT NAME=drain CURRENT
```

specifies current boundary conditions for the electrode named `drain`. On subsequent `SOLVE` statements, the drain current boundary condition will default to zero current. Therefore, floating the contact.

You can also make a floating contact to a semiconductor using a very large resistor attached to the contact instead. For example:

```
CONTACT NAME=drain RESIST=1e20
```

Note that extremely large resistance values must be used to keep the current through the insignificant contact. Using a lumped resistor will allow the tolerance on potential to move slightly above zero. For example, if the tolerance is 10^{-5}V and the defined resistance was only $10\text{M}\Omega\mu\text{m}$, then a current of $10^{-12}\text{A}/\mu\text{m}$ may flow through the contact, which may be significant in breakdown simulations.

Shorting Two Contacts Together

It is possible in ATLAS to tie two or more contact together so that voltages on both contacts are equal. This is useful for many technologies for example dual base bipolar transistors. There are several methods for achieving this depending on how the structure was initially defined.

If the structure is defined using ATLAS syntax, you can have multiple `ELECTRODE` statements with the same `NAME` parameter defining separate locations within the device structure. In this case, the areas defined to be electrodes will be considered as having the same applied voltage. A single current will appear combining the current through both `ELECTRODE` areas.

Also, if two separate metal regions in ATHENA are defined using the `ATHENA ELECTRODE` statement to have the same name, then in ATLAS these two electrodes will be considered as shorted together.

If the electrodes are defined with different names, the following syntax can be used to link the voltages applied to the two electrodes.

```
CONTACT NAME=base1 COMMON=base
.
SOLVE VBASE=0.1
```

Here, the electrode, `base1`, will be linked to the electrode, `base`. The applied 0.1V on `base` will then appear on `base1`. ATLAS, however, will calculate and store separate currents for both `base` and `base1`. This can be a useful feature. But in some cases, such as where functions of the currents are required in `EXTRACT` or `TONYPLOT`, it is undesirable. You can add the `SHORT` parameter to the `CONTACT` statement above to specify so that only a single base current will appear combining the currents from `base` and `base1`. Note that the electrode specified by the `COMMON` parameter should preferably have a name that exactly matches one of those specified in the `ELECTRODE` statement (see the `NAME` description in Section 21.12: “ELECTRODE”). Additionally, the electrode specified by the `NAME` parameter should not have a bias applied directly to it. You should always apply the bias to the electrode specified by the `COMMON` parameter.

You can also specify the voltages on the linked electrodes to be different, but have a constant `OFFSET` relative to the bias on the electrode specified by the `COMMON` parameter.

The statement

```
CONTACT name=base1 COMMON=base FACTOR=0.5
```

ensures the bias on `base1` will be equal to the bias on `base` + 0.5 V. If you also specify the `MULT` parameter on this statement, then `FACTOR` will be interpreted as multiplicative rather than additive. In this case, the bias applied to `base1` will be one-half of the bias applied to `base`. If `FACTOR` (and optionally `MULT`) is applied to a contact for which current boundary conditions are being used, then it has no effect. Any existing bias differences between the linked electrodes are, however, maintained under current boundary conditions. To apply additive or multiplicative relationships between currents on linked electrodes, remove the `CONTACT` statements linking them. Then, directly specify the required values of the currents on the `SOLVE` statement.

When loading a structure from ATHENA or DEVEDIT, where two defined electrode regions are touching, ATLAS will automatically short these and use the electrode name that was defined first.

Making an Open Circuit Contact

It is often required to perform a simulation with an open circuit on one of the defined electrodes. There are three different methods to make an open circuit contact. The first method is to entirely deleting an electrode from the structure file. The second method is to add an extremely large lumped resistance. For example, $10^{20}\Omega$ onto the contact to be made open circuit. The third method is to switch the boundary conditions on the contact to be made open circuit from voltage controlled to current controlled. Then, specifying a very small or zero current through that electrode.

Each of these methods are feasible. If a floating region, however, is created within the structure, then numerical convergence may be affected. As a result, we normally recommend that you use the second method because it ensures better convergence.

2.7.2: Specifying Material Properties

Semiconductor, Insulator, or Conductor

All materials are split into three classes: semiconductors, insulators and conductors. Each class requires a different set of parameters to be specified. For semiconductors, these properties include electron affinity, band gap, density of states and saturation velocities. There are default parameters for material properties used in device simulation for many materials.

Appendix B: “Material Systems” lists default material parameters and includes a discussion on the differences between specifying parameters for semiconductors, insulators, and conductors.

Setting Parameters

The `MATERIAL` statement allows you to specify your own values for these basic parameters. Your values can apply to a specified material or a specified region. For example, the statement:

```
MATERIAL MATERIAL=Silicon EG300=1.12 MUN=1100
```

sets the band gap and low field electron mobility in all silicon regions in the device. If the material properties are defined by region, the region is specified using the `REGION` or `NAME` parameters in the `MATERIAL` statement. For example, the statement:

```
MATERIAL REGION=2 TAUN0=2e-7 TAUP0=1e-5
```

sets the electron and hole Shockley-Read-Hall recombination lifetimes for region number two (see Chapter 3: “Physics”, the “Shockley-Read-Hall (SRH) Recombination” section on page 3-85 for more information about this type of recombination). If the name, `base`, has been defined using the `NAME` parameter in the `REGION` statement, then the statement:

```
MATERIAL NAME=base NC300=3e19
```

sets the conduction band density of states at 300 K for the region named `base`.

The description of the `MATERIAL` statement in Chapter 21: “Statements”, Section 21.29: “`MATERIAL`” provides a complete list of all the material parameters that are available.

Heterojunction Materials

The material properties of heterojunctions can also be modified with the `MATERIAL` statement. In addition to the regular material parameters, you can define composition dependent material parameters. For example, composition dependent band parameters, dielectric constants, and saturation velocities.

For heterojunction material systems, the bandgap difference between the materials is divided between conduction and valence bands. The `ALIGN` parameter specifies the fraction of this difference applied to the conduction band edge. This determines the electron and hole barrier height and overrides any electron affinity specification. For example, the statement:

```
MATERIAL MATERIAL=InGaAs ALIGN=0.36
MATERIAL MATERIAL=InP      ALIGN=0.36
```

specifies that 36% of the bandgap difference between InGaAs and InP is applied to the conduction band and 64% is applied to the valence band. For example, if the band gap difference (ΔE_g) for this material system is 0.6 eV, then the conduction band barrier height is 0.216 eV and the valence band barrier height is 0.384 eV.

For heterojunction devices, the transport models may be different for each material. You can specify these models and their coefficients for each material using the `MODELS` statement. See Section 2.7.4: “Specifying Physical Models” for a description of this option.

2.7.3: Specifying Interface Properties

The `INTERFACE` statement is used to define the interface charge density and surface recombination velocity at interfaces between semiconductors and insulators. For example, the statement:

```
INTERFACE QF=3e10
```

specifies that all interfaces between semiconductors and insulators have a fixed charge of $3 \cdot 10^{10} \text{cm}^{-2}$. In many cases, the interface of interest is restricted to a specific region. This can be accomplished with the `X.MIN`, `X.MAX`, `Y.MIN`, and `Y.MAX` parameters on the `INTERFACE` statement. These parameters define a rectangle, where the interface properties apply. For example, the statement:

```
INTERFACE QF=3e10 X.MIN=1.0 X.MAX=2 Y.MIN=0.0 Y.MAX=0.5
```

restricts the interface charge to the semiconductor-insulator boundary within the specified rectangle. In addition to fixed charge, surface recombination velocity and thermionic emission are enabled and defined with the `INTERFACE` statement. For more information about this statement, see Chapter 21: “Statements”, Section 21.21: “INTERFACE”.

2.7.4: Specifying Physical Models

Physical models are specified using the `MODELS` and `IMPACT` statements. Parameters for these models appear on many statements including: `MODELS`, `IMPACT`, `MOBILITY`, and `MATERIAL`. The physical models can be grouped into five classes: mobility, recombination, carrier statistics, impact ionization, and tunneling. Chapter 3: “Physics”, Section 3.6: “Physical Models” contains details for each model.

Tables 2-2 to 2-6 give summary descriptions and recommendations on the use of each model. Table 2-7 is a guide for compatibility between models.

All models with the exception of impact ionization are specified on the `MODELS` statement. Impact ionization is specified on the `IMPACT` statement. For example, the statement:

```
MODELS CONMOB FLDMOB SRH FERMIDIRAC
IMPACT SELB
```

specifies that the standard concentration dependent mobility, parallel field mobility, Shockley-Read-Hall recombination with fixed carrier lifetimes, Fermi Dirac statistics and Selberherr impact ionization models should be used.

ATLAS also provides an easy method for selecting the correct models for various technologies. The `MOS`, `BIP`, `PROGRAM`, and `ERASE` parameters for the `MODELS` statement configure a basic set of mobility, recombination, carrier statistics, and tunneling models. The `MOS` and `BIP` parameters enable the models for MOSFET and bipolar devices, while `PROGRAM` and `ERASE` enable the models for programming and erasing programmable devices. For example, the statement:

```
MODELS MOS PRINT
```

enables the `CVT`, `SRH`, and `FERMIDIRAC` models, while the statement:

```
MODELS BIPOLAR PRINT
```

enables the `CONMOB`, `FLDMOB`, `CONSRH`, `AUGER`, and `BGN`.

Note: The `PRINT` parameter lists to the run time output the models and parameters, which will be used during the simulation. This allows you to verify models and material parameters. We highly recommend that you include the `PRINT` parameter in the `MODELS` statement.

Physical models can be enabled on a material by material basis. This is useful for heterojunction device simulation and other simulations where multiple semiconductor regions are defined and may have different characteristics. For example, the statement:

```
MODEL MATERIAL=GaAs FLDMOB EVSATMOD=1 ECRITN=6.0e3 CONMOB
MODEL MATERIAL=InGaAs SRH FLDMOB EVSATMOD=1 \
ECRITN=3.0e3
```

change both the mobility models and critical electric field used in each material. For devices based on advanced materials, these model parameters should be investigated carefully.

Energy Balance Models

The conventional drift-diffusion model of charge transport neglects non-local effects, such as velocity overshoot and reduced energy dependent impact ionization. ATLAS can model these effects through the use of an energy balance model, which uses a higher order approximation of the Boltzmann Transport Equation (see Chapter 3: “Physics”, Section 3.1.3: “The Transport Equations”). In this equation, transport parameters, such as mobility and impact ionization, are functions of the local carrier temperature rather than the local electric field.

To enable the energy balance transport model, use the `HCTE`, `HCTE.EL`, or `HCTE.HO` parameters in the `MODELS` statement. These parameters enable the energy transport model for both carriers, electrons only, or holes only respectively. For example, the statement:

```
MODELS MOS HCTE
```

enables the energy balance transport model for both electrons and holes in addition to the default MOSFET models.

2.7.5: Summary Of Physical Models

| Table 2-2. Carrier Statistics Models | | |
|--------------------------------------|------------|--|
| Model | Syntax | Notes |
| Boltzmann | BOLTZMANN | Default model |
| Fermi-Dirac | FERMI | Reduced carrier concentrations in heavily doped regions (statistical approach). |
| Incomplete Ionization | INCOMPLETE | Accounts for dopant freeze-out. Typically, it is used at low temperatures. |
| Silicon Ionization Model | IONIZ | Accounts for full ionization for heavily doped Si. Use with INCOMPLETE. |
| Bandgap Narrowing | BGN | Important in heavily doped regions. Critical for bipolar gain. Use Klaassen Model. |

| Table 2-3. Mobility Models | | |
|---|----------|---|
| Model | Syntax | Notes |
| Concentration Dependent | CONMOB | Lookup table valid at 300K for Si and GaAs only. Uses simple power law temperature dependence. |
| Concentration and Temperature Dependent | ANALYTIC | Caughey-Thomas formula. Tuned for 77-450K. |
| Arora's Model | ARORA | Alternative to ANALYTIC for Si |
| Carrier-Carrier Scattering | CCSMOB | Dorkel-Leturq Model. Includes n, N and T dependence. Important when carrier concentration is high (e.g., forward bias power devices). |
| Parallel Electric Field Dependence | FLDMOB | Si and GaAs models. Required to model any type of velocity saturation effect. |
| Tasch Model | TASCH | Includes transverse field dependence. Only for planar devices. Needs very fine grid. |
| Watt Model | WATT | Transverse field model applied to surface nodes only. |
| Klaassen Model | KLA | Includes N, T, and n dependence. Applies separate mobility to majority and minority carriers. Recommended for bipolar devices |

Table 2-3. Mobility Models

| Model | Syntax | Notes |
|----------------------|-----------|---|
| Shirahata Model | SHI | Includes N , E_{\perp} . An alternative surface mobility model that can be combined with KLA. |
| Modified Watt | MOD.WATT | Extension of WATT model to non-surface nodes. Applies constant E_{\perp} effects. Best model for planar MOS devices |
| Lombardi (CVT) Model | CVT | Complete model including N , T , E_{\parallel} , and E_{\perp} effects. Good for non-planar devices. |
| Yamaguchi Model | YAMAGUCHI | Includes N , E_{\parallel} and E_{\perp} effects. Only calibrated for 300K. |

Table 2-4. Recombination Models

| Model | Syntax | Notes |
|-------------------------|------------|---|
| Shockley-Read-Hall | SRH | Uses fixed minority carrier lifetimes. Should be used in most simulations. |
| Concentration Dependent | CONSRH | Uses concentration dependent lifetimes. Recommended for Si. |
| Auger | AUGER | Direct transition of three carriers. Important at high current densities. |
| Optical | OPTR | Band-band recombination. For direct materials only. |
| Surface | S.N S.P | Recombination at semiconductor to insulator interfaces. This is set in the INTERFACE statement. |

Table 2-5. Impact Ionization

| Model | Syntax | Notes |
|--------------------|----------------|--|
| Selberherr's Model | IMPACT SELB | Recommended for most cases. Includes temperature dependent parameters. |
| Grant's Model | IMPACT GRANT | Similar to Selberherr's model but with different coefficients. |
| Crowell-Size | IMPACT CROWELL | Uses dependence on carrier scattering length. |
| Toyabe Model | IMPACT TOYABE | Non-local model used with Energy Balance. Any IMPACT syntax is accepted. |

Table 2-5. Impact Ionization

| Model | Syntax | Notes |
|-----------|----------------------|---|
| Concannon | N.CONCAN P.CONCAN | Non-local model developed in Flash EEPROM technologies. |

Table 2-6. Tunneling Models and Carrier Injection Models

| Model | Syntax | Notes |
|--------------------------------------|----------------------|---|
| Band-to-Band (standard) | BBT.STD | For direct transitions. Required with very high fields. |
| Concannon Gate Current Model | N.CONCAN P.CONCAN | Non-local gate model consistent with Concannon substrate current model. |
| Direct Quantum tunneling (Electrons) | QTUNN.EL | Quantum tunneling through conduction band barrier due to an insulator. |
| Direct Quantum tunneling (Hole) | QTUNN.HO | Quantum tunneling through valence band barrier due to an insulator. |
| Fowler-Nordheim (electrons) | FNORD | Self-consistent calculation of tunneling through insulators. Used in EEPROMs. |
| Fowler-Nordheim (holes) | FNHOLES | Same as FNORD for holes. |
| Klaassen Band-to-Band | BBT.KL | Includes direct and indirect transitions. |
| Hot Electron Injection | HEI | Models energetic carriers tunneling through insulators. Used for gate current and Flash EEPROM programming. |
| Hot Hole Injection | HHI | HHI means hot hole injection. |

Note: In the notes in Tables 2-2 through 2-6, n is electron concentration, p is hole concentration, T is lattice temperature, N is dopant concentration, E_{||} is parallel electric field, and E_⊥ is perpendicular electric field.

Table 2-7. Model Compatibility Chart

| | CONMOB | FLDMOB | TFLDMB2 | YAMAGUCHI | CVT | ARORA | ANALYTIC | CCSMOB | SURMOB | LATTICE H | E.BALANCE |
|----------------|--------|-----------------|-----------------|-----------|-----|-------|----------|--------|--------|-----------|-----------|
| CONMOB [CM] | — | OK | OK | YA | CV | AR | AN | CC | OK | OK | OK |
| FLDMOB [FM] | OK | — | TF ¹ | YA | CV | OK | OK | OK | OK | OK | OK |
| TFLDMB2 [TF] | OK | TF ¹ | — | YA | CV | OK | OK | TF | TF | OK | OK |
| YAMAGUCHI [YA] | YA | YA | YA | — | CV | YA | YA | YA | YA | NO | NO |

Table 2-7. Model Compatibility Chart

| | CONMOB | FLDMOB | TFLDMB2 | YAMAGUCHI | CVT | ARORA | ANALYTIC | CCSMOB | SURMOB | LATTICE H | E.BALANCE |
|----------------|--------|--------|---------|-----------|-----|-------|----------|--------|--------|-----------|-----------|
| CVT [CV] | CV | CV | CV | CV | — | CV | CV | CV | CV | OK | OK |
| ARORA [AR] | AR | OK | OK | YA | CV | — | AR | CC | OK | OK | OK |
| ANALYTIC [AN] | AN | OK | OK | YA | CV | AR | — | CC | OK | OK | OK |
| CCSMOB [CC] | CC | OK | TF | YA | CV | CC | CC | — | OK | OK | OK |
| SURMOB [SF] | OK | OK | TF | YA | CV | OK | OK | OK | — | OK | OK |
| LATTICE H [LH] | OK | OK | OK | NO | OK | OK | OK | OK | OK | — | OK |
| E.BALANCE [EB] | OK | OK | OK | NO | OK | OK | OK | OK | OK | OK | 2 |

Key To Table Entries

MODEL ABBREVIATION = The model that supersedes when a combination is specified. In some cases, a warning message is issued when a model is ignored.

OK = This combination is allowed.

NO = This combination is not allowed.

NOTES:

1. Uses internal model similar to FLDMOB

2. When models including a parallel electric field dependence are used with energy balance the electric field term is replaced by a function of carrier temperature.

Using the C-Interpreter to Specify Models

One of the ATLAS products is a C language interpreter that allows you to specify many of the models used by ATLAS. To use these functions, implement the model in C as equations in a special file called an *ATLAS lib file*. You can access the default ATLAS template file by typing:

```
atlas -T <filename>
```

at the UNIX command prompt. This creates a default template file with the name specified by the <filename> parameter. See Appendix A: “C-Interpreter Functions” for a listing of the default C-INTERPRETER functions. To use the interpreter functions, give the corresponding parameters in the statements containing the name of the C language file with the model given as the parameter value. For example, the statement:

```
MATERIAL NAME=Silicon F.MUNSAT=munsat.lib
```

specifies that the file, *munsat.lib*, contains the C-INTERPRETER function for the specification of the parallel field dependent electron mobility model.

2.8: Choosing Numerical Methods

2.8.1: Numerical Solution Techniques

Several different numerical methods can be used for calculating the solutions to semiconductor device problems. Numerical methods are given in the `METHOD` statements of the input file. Some guidelines for these methods will be given here. For full details, however, see Chapter 20: “Numerical Techniques”.

Different combinations of models will require ATLAS to solve up to six equations. For each of the model types, there are basically three types of solution techniques: (a) decoupled (`GUMMEL`), (b) fully coupled (`NEWTON`) and (c) `BLOCK`. The `GUMMEL` method will solve for each unknown in turn keeping the other variables constant, repeating the process until a stable solution is achieved. The `NEWTON` method solve the total system of unknowns together. The `BLOCK` methods will solve some equations fully coupled while others are de-coupled.

Generally, the `GUMMEL` method is useful where the system of equations is weakly coupled but has only linear convergence. The `NEWTON` method is useful when the system of equations is strongly coupled and has quadratic convergence. The `NEWTON` method may, however, spend extra time solving for quantities, which are essentially constant or weakly coupled. `NEWTON` also requires a more accurate initial guess to the problem to obtain convergence. Thus, a `BLOCK` method can provide for faster simulations times in these cases over `NEWTON`. `GUMMEL` can often provide better initial guesses to problems. It can be useful to start a solution with a few `GUMMEL` iterations to generate a better guess. Then, switch to `NEWTON` to complete the solution. Specification of the solution method is carried out as follows:

```
METHOD GUMMEL BLOCK NEWTON
```

The exact meaning of the statement depends on the particular models it applied to. This will be discussed in the following sections.

Basic Drift Diffusion Calculations

The isothermal drift diffusion model requires the solution of three equations for potential, electron concentration, and hole concentration. Specifying `GUMMEL` or `NEWTON` alone will produce simple Gummel or Newton solutions as detailed above. For almost all cases, the `NEWTON` method is preferred and it is the default.

Specifying:

```
METHOD GUMMEL NEWTON
```

will cause the solver to start with `GUMMEL` iterations. Then, switch to `NEWTON` if convergence is not achieved. This is a robust but a more time consuming way of obtaining solutions for any device. This method, however, is highly recommended for all simulations with floating regions such as SOI transistors. A floating region is defined as an area of doping, which is separated from all electrodes by a pn junction.

`BLOCK` is equivalent to `NEWTON` for all isothermal drift-diffusion simulations.

Drift Diffusion Calculations with Lattice Heating

When the lattice heating model is added to drift diffusion, an extra equation is added. The `BLOCK` algorithm solves the three drift diffusion equations as a `NEWTON` solution. Follows this with a `GUMMEL` solution of the heat flow equation. The `NEWTON` algorithm solves all four equations in a coupled manner. `NEWTON` is preferred once the temperature is high. `BLOCK`, however, is quicker for low temperature gradients. Typically, the combination used is:

```
METHOD BLOCK NEWTON
```

Energy Balance Calculations

The energy balance model requires the solution of up to 5 coupled equations. GUMMEL and NEWTON have the same meanings as with the drift diffusion model. In other words, GUMMEL specifies a de-coupled solution and NEWTON specifies a fully coupled solution.

But BLOCK performs a coupled solution of potential, carrier continuity equations followed by a coupled solution of carrier energy balance, and carrier continuity equations.

You can switch from BLOCK to NEWTON by specifying multiple solution methods on the same line. For example:

```
METHOD BLOCK NEWTON
```

will begin with BLOCK iterations. Then, switch to NEWTON if convergence is still not achieved. This is the most robust approach for many energy balance applications.

The points where the algorithms switch is pre-determined, but can be changed in the METHOD statement, the default values set by SILVACO work well for most circumstances.

Energy Balance Calculations with Lattice Heating

When non-isothermal solutions are performed in conjunction with energy balance models, a system of up to six equations must be solved. GUMMEL or NEWTON solve the equations iteratively or fully coupled respectively. BLOCK initially performs the same function as with energy balance calculations, then solves the lattice heating equation in a de-coupled manner.

Setting the Number of Carriers

ATLAS can solve both electron and hole continuity equations, or only for one or none. You can make this choice by using the CARRIERS parameter. For example:

```
METHOD CARRIERS=2
```

specifies a solution for both carriers is required. This is the default. With one carrier, the ELEC or HOLE parameter is needed. For example, for hole solutions only:

```
METHOD CARRIERS=1 HOLE
```

To select a solution for potential, only specify:

```
METHOD CARRIERS=0
```

Note: Setting the number of carriers using the syntax, MODEL NUMCARR=<n>, is obsolete and should not be used.

Important Parameters of the METHOD Statement

You can alter all of the parameters relevant to the numerical solution process. This, however, isn't recommended unless you have expert knowledge of the numerical algorithms. All of these parameters have been assigned optimal values for most solution conditions. For more information about numerical algorithms, see Chapter 20: "Numerical Techniques".

The following parameters, however, are worth noting at this stage:

- `CLIMIT` or `CLIM.DD` specify minimal values of concentrations to be resolved by the solver. Sometimes, you need to reduce this value to aid solutions of breakdown characteristics. A value of `CLIMIT=1e-4` is recommended for all simulations of breakdown, where the pre-breakdown current is small. `CLIM.DD` is equivalent to `CLIMIT` but uses the more convenient units of cm^{-3} for the critical concentration. `CLIM.DD` and `CLIMIT` are related by the following expression.

$$\text{CLIM.DD} = \text{CLIMIT} * \sqrt{N_c N_v} \quad 2-3$$

- `DVMAX` controls the maximum update of potential per iteration of Newton's method. The default corresponds to 1V. For power devices requiring large voltages, you may need an increased value of `DVMAX`. `DVMAX=1e8` can improve the speed of high voltage bias ramps.
- `CLIM.EB` controls the cut-off carrier concentration below, which the program will not consider the error in the carrier temperature. This is applied in energy balance simulations to avoid excessive calculations of the carrier temperature at locations in the structure where the carrier concentration is low. Setting this parameter too high, where ATLAS ignores the carrier temperature errors for significant carrier concentrations, will lead to unpredictable and mostly incorrect results .

Restrictions on the Choice of METHOD

The following cases require `METHOD NEWTON CARRIERS=2` to be set for isothermal drift-diffusion simulations:

- current boundary conditions
- distributed or lumped external elements
- AC analysis
- impact ionization

Both `BLOCK` or `NEWTON` or both are permitted for lattice heat and energy balance.

Note: Simulations using the `GUMMEL` method in these cases may lead to non-convergence or incorrect results.

Pisces-II Compatibility

Previous releases of ATLAS (2.0.0.R) and other PISCES-II based programs use the `SYMBOLIC` command to define the solution method and the number of carriers included in the solution. In this version of ATLAS, the solution method is specified completely on the `METHOD` statement.

The `COMB` parameter, which was available in earlier ATLAS versions, is no longer required. It has been replaced with either the `BLOCK` method or the combination of `GUMMEL` and `NEWTON` parameters. Table 2-8 identifies direct translations of old syntax to new.

Note: These are direct translations and not necessarily the best choices of numerical methods.

| Table 2-8. Parameter Syntax Replacements | |
|---|---|
| Old Syntax (V2.0.0.R) | New Syntax |
| <code>symbolic newton carriers=2</code> | <code>method newton</code> |
| <code>symbolic newton carriers=1 elec</code> | <code>method newton carriers=1 electron</code> |
| <code>symbolic gummel carriers=0</code> | <code>method gummel carriers=0</code> |
| <code>symbolic newton carriers=2</code> <code>method comb</code> | <code>method gummel newton</code> |
| <code>models lat.temp</code> <code>symbolic newton carriers=2</code> <code>method comb</code> | <code>models lat.temp</code> <code>method block</code> |
| <code>models hcte</code> <code>symbolic gummel carriers=2</code> <code>method comb</code> | <code>models hcte</code> <code>method block</code> |

2.9: Obtaining Solutions

ATLAS can calculate DC, AC small signal, and transient solutions. Obtaining solutions is similar to setting up parametric test equipment for device tests. You usually define the voltages on each of the electrodes in the device. ATLAS then calculates the current through each electrode. ATLAS also calculates internal quantities, such as carrier concentrations and electric fields throughout the device. This is information that is difficult or impossible to measure.

In all simulations, the device starts with zero bias on all electrodes. Solutions are obtained by stepping the biases on electrodes from this initial equilibrium condition. As will be discussed, due to the initial guess strategy, voltage step sizes are limited. This section concentrates on defining solution procedures. To save results, use the LOG or SAVE statements. Section 2.10: "Interpreting The Results" on how to analyze and display these results.

2.9.1: DC Solutions

In DC solutions, the voltage on each electrode is specified using the SOLVE statement. For example, the statements:

```
SOLVE VGATE=1.0  
SOLVE VGATE=2.0
```

solves a single bias point with 1.0V and then 2.0V on the gate electrode. One important rule in ATLAS is that when the voltage on any electrode is not specified in a given SOLVE statement, the value from the last SOLVE statement is assumed.

In the following case, the second solution is for a drain voltage of 1.0V and a gate voltage of 2.0V.

```
SOLVE VGATE=2.0  
SOLVE VDRAIN=1.0
```

When the voltage on a particular electrode is never defined on any SOLVE statement and voltage is zero, you don't need to explicitly state the voltage on all electrodes on all SOLVE statements. For example, in a MOSFET, if VSUBSTRATE is not specified, then V_{bs} defaults to zero.

Sweeping The Bias

For most applications, a sweep of one or more electrodes is usually required. The basic DC stepping is inconvenient and a ramped bias should be used. To ramp the base voltage from 0.0V to 1.0V with 0.05V steps with a fixed collector voltage of 2.0V, use the following syntax:

```
SOLVE VCOLLECTOR=2.0  
SOLVE VBASE=0.0 VSTEP=0.05 VFINAL=1.0 NAME=base
```

The NAME parameter is required and the electrode name is case-sensitive. Make sure the initial voltage, VSTEP and VFINAL, are consistent. A badly specified ramp from zero to 1.5V in 0.2V steps will finish at 1.4V or 1.6V.

Generating Families of Curves

Many applications such as MOSFET Id/Vds and bipolar Ic/Vce simulations require that a family of curves is produced. This is done by obtaining solutions at each of the stepped bias points first, and then solving over the swept bias variable at each stepped point. For example, in MOSFET Id/Vds curves, solutions for each Vgs value are obtained with Vds=0.0V. The output from these solutions are saved in ATLAS solution files. For each gate bias, the solution file is loaded and the ramp of drain voltage performed.

The family of curves for three 1V gate steps and a 3.3V drain sweep would be implemented in ATLAS as follows:

```
SOLVE VGATE=1.0  OUTF=solve_vgate1
SOLVE VGATE=2.0  OUTF=solve_vgate2
SOLVE VGATE=3.0  OUTF=solve_vgate3

LOAD INFILE=solve_vgate1
LOG OUTFILE=mos_drain_sweep1
SOLVE NAME=drain VDRAIN=0 VFINAL=3.3 VSTEP=0.3

LOAD INFILE=solve_vgate2
LOG OUTFILE=mos_drain_sweep2
SOLVE NAME=drain VDRAIN=0 VFINAL=3.3 VSTEP=0.3

LOAD INFILE=solve_vgate3
LOG OUTFILE=mos_drain_sweep3
SOLVE NAME=drain VDRAIN=0 VFINAL=3.3 VSTEP=0.3
```

The LOG statements are used to save the Id/Vds curve from each gate voltage to separate files. We recommend that you save the data in this manner rather than to a single LOG file (see Section 2.10: “Interpreting The Results”).

2.9.2: The Importance Of The Initial Guess

To obtain convergence for the equations used, supply a good initial guess for the variables to be evaluated at each bias point. The ATLAS solver uses this initial guess and iterates to a converged solution. For isothermal drift diffusion simulations, the variables are the potential and the two carrier concentrations. If a reasonable grid is used, almost all convergence problems in ATLAS are caused by a poor initial guess to the solution.

During a bias ramp, the initial guess for any bias point is provided by a projection of the two previous results. Problems tend to appear near the beginning of the ramp when two previous results are not available. If one previous bias is available, it is used alone. This explains why the following two examples eventually produce the same result. The first will likely have far more convergence problems than the second.

```
1. SOLVE VGATE=1.0 VDRAIN=1.0 VSUBSTRATE=-1.0
2. SOLVE VGATE=1.0
   SOLVE VSUBSTRATE=-1.0
   SOLVE VDRAIN=1.0
```

In the first case, one solution is obtained with all specified electrodes at 1.0V. In the second case, the solution with only the gate voltage at 1.0V is performed first. All other electrodes are at zero bias. Next, with the gate at 1.0V, the substrate potential is raised to -1.0V and another solution is obtained. Finally, with the substrate and the gate biased, the drain potential is added and the system solved again. The advantage of this method over the first case is that the small incremental changes in voltage allow for better initial guesses at each step.

Generally, the projection method for the initial guess gives good results when the I-V curve is linear. But it may encounter problems if the IV curve is highly non-linear or if the device operating mode is changing. Typically, this may occur around the threshold or breakdown voltages. At these biases, smaller voltage steps are required to obtain convergence. As will be described, ATLAS contains features such as the TRAP parameter and the curve tracer to automatically cut the voltage steps in these highly non-linear area.

Numerical methods are described in Section 2.8: “Choosing Numerical Methods” and Chapter 20: “Numerical Techniques”.

In many cases, these methods are designed to overcome the problems associated with the initial guess. This is particularly important in simulations involving more than the three drift diffusion variables. Generally, coupled solutions require a good initial guess, whereas de-coupled solutions can converge with a poor initial guess.

The Initial Solution

When no previous solutions exist, the initial guess for potential and carrier concentrations must be made from the doping profile. This is why the initial solution performed must be the zero bias (or thermal equilibrium) case. This is specified by the statement:

```
SOLVE INIT
```

But if this syntax isn't specified, ATLAS automatically evaluates an initial solution before the first SOLVE statement. To aid convergence of this initial guess, the solution is performed in the zero carrier mode solving only for potential.

The First and Second Non-Zero Bias Solutions

From experience with ATLAS, it is found that the first and second non-zero bias solutions are the most difficult to obtain good convergence. Once these two solutions are obtained, the projection algorithm for the initial guess is available and solutions should all have a good initial guess.

These first two solutions, however, must use the result of the initial solution as the basis of their initial guess. Since the initial solution is at zero bias, it provides a poor initial guess.

The practical result of this is that the first and second non-zero bias solutions should have very small voltage steps. In the following example, the first case will likely converge whereas the second case may not.

```
1. SOLVE INIT
   SOLVE VDRAIN=0.1
   SOLVE VDRAIN=0.2
   SOLVE VDRAIN=2.0
2. SOLVE INIT
   SOLVE VDRAIN=2.0
```

The Trap Parameter

Although ATLAS provides several methods to overcome a poor initial guess and other convergence problems, it is important to understand the role of the initial guess in obtaining each solution. The simplest and most effective method to overcome poor convergence is by using:

```
METHOD TRAP
```

This is enabled by default. Its effect is to reduce the bias step if convergence problems are detected. Consider the example from the previous section:

```
SOLVE INIT
SOLVE VDRAIN=2.0
```


If the second `SOLVE` statement does not converge, `TRAP` automatically cuts the bias step in half and tries to obtain a solution for $V_d = 1.0V$. If this solution does not converge, the bias step will be halved again to solve for $V_d = 0.5V$. This procedure is repeated up to a maximum number of tries set by the `METHOD` parameter `MAXTRAPS`. Once convergence is obtained, the bias steps are increased again to solve up to $2.0V$. The default for `MAXTRAPS` is 4 and it is not recommended to increase it, since changing the syntax to use smaller bias steps is generally much faster.

This trap facility is very useful during bias ramps in overcoming convergence difficulties around transition points such as the threshold voltage. Consider the following syntax used to extract a MOSFET I_d/V_{gs} curve.

```
SOLVE VGATE=0.0 VSTEP=0.2 VFINAL=5.0 NAME=gate
```

Assume the threshold voltage for the device being simulated is $0.7V$ and that `ATLAS` has solved for the gate voltages up to $0.6V$. The next solution, at $0.8V$, may not converge at first. This is because the initial guess was formed from the two sub-threshold results at $V_{gs}=0.4V$ and $0.6V$ and the solution has now become non-linear. The trap facility will detect the problems in the $0.8V$ solution and cut the bias step in half to $0.7V$ and try again. This will probably converge. The solution for $0.8V$ will then be performed and the bias ramp will continue with $0.2V$ steps.

2.9.3: Small-Signal AC Solutions

Specifying AC simulations is a simple extension of the DC solution syntax. AC small signal analysis is performed as a post-processing operation to a DC solution. Two common types of AC simulation in `ATLAS` are outlined here. The results of AC simulations are the conductance and capacitance between each pair of electrodes. Tips on interpreting these results is described in Section 2.10: “Interpreting The Results”.

Single Frequency AC Solution During A DC Ramp

The minimum syntax to set an AC signal on an existing DC ramp is just the `AC` flag and the setting of the small signal frequency. For example:

```
SOLVE VBASE=0.0 VSTEP=0.05 VFINAL=1.0 NAME=base AC FREQ=1.0e6
```

Other AC syntax for setting the signal magnitude and other parameters are generally not needed as the defaults suffice. One exception is in 1D MOS capacitor simulations. To obtain convergence in the inversion/deep depletion region, add the `DIRECT` parameter to access a more robust solution method.

Ramped Frequency At A Single Bias

For some applications, such as determining bipolar gain versus frequency, you need to ramp the frequency of the simulation. This is done using the following syntax:

1. `SOLVE VBASE=0.7 AC FREQ=1e9 FSTEP=1e9 NFSTEPS=10`
2. `SOLVE VBASE=0.7 AC FREQ=1e6 FSTEP=2 MULT.F NFSTEPS=10`

The first case ramps the frequency from $1GHz$ to $11GHz$ in $1GHz$ steps. A linear ramp of frequency is used and `FSTEP` is in Hertz. In the second example, a larger frequency range is desired and so a geometrical step of frequency is used. The `MULT.F` parameter is used to specify that `FSTEP` is a unitless multiplier for the frequency. This doubles the frequency in successive steps from $1MHz$ to $1.024GHz$.

You can combine the following syntax for ramping the frequency of the AC signal with the syntax for ramping the bias. The frequency ramps are done at each bias point during the DC ramp.

```
SOLVE VBASE=0.0 VSTEP=0.05 VFINAL=1.0 NAME=base AC FREQ=1.0e6 \  
FSTEP=2 MULT.F NFSTEPS=10
```

2.9.4: Transient Solutions

Transient solutions can be obtained for piecewise-linear, exponential, and sinusoidal bias functions. Transient solutions are used when a time dependent test or response is required. To obtain transient solutions for a linear ramp, specify the `TSTOP`, `TSTEP`, and `RAMPTIME` parameters.

Figure 2-16 shows the syntax of the transient voltage ramp. The `RAMPTIME` specifies the time that the linear ramp should obtain its final value. `TSTOP` specifies the time that solutions will stop. `TSTEP` specifies the initial step size.

Subsequent time steps are calculated automatically by ATLAS. For example, the statement:

```
SOLVE VGATE=1.0 RAMPTIME=1E-9 TSTOP=10e-9 TSTEP=1e-11,
```

specifies that the voltage on the gate electrode will be ramped in the time domain from its present value to 1.0V over a period of 1 nanoseconds.

Time domain solutions are obtained for an additional 9 nanoseconds. An initial time step of 10 picoseconds is specified. Note that if you specify subsequent transient solutions, don't reset the time to zero.

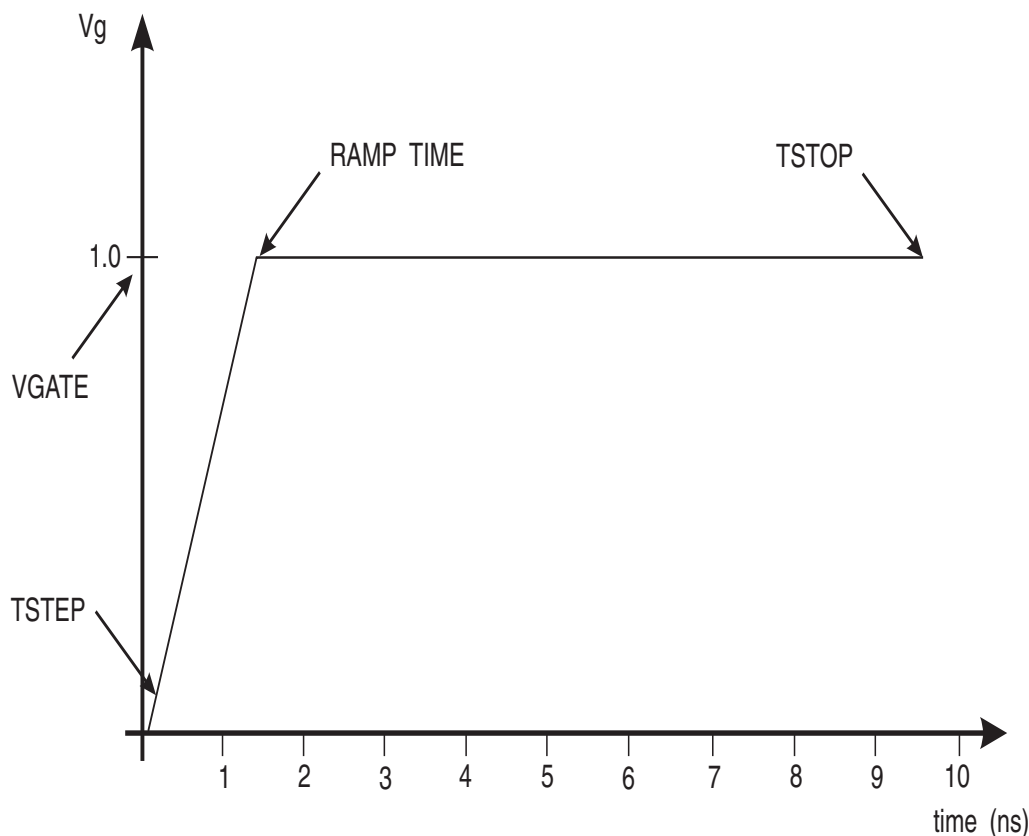


Figure 2-16: Diagram showing syntax of Transient Voltage Ramp in ATLAS

2.9.5: Advanced Solution Techniques

Obtaining Solutions Around The Breakdown Voltage

Obtaining solutions around the breakdown voltage can be difficult using the standard ATLAS approach. It requires special care when choosing voltage steps and interpreting the results. The curve tracer described in “The Curvetrace Capability” section on page 2-56 is the most effective method in many cases.

A MOSFET breakdown simulation might be performed using the following standard syntax for ramping the drain bias. Note that the setting of CLIMIT is recommended for breakdown simulations when the pre-breakdown leakage is low.

```
IMPACT SELB
METHOD CLIMIT=1e-4
SOLVE VDRAIN=1.0 VSTEP=1.0 VFINAL=20.0 NAME=drain
```

If the breakdown were 11.5V, then convergence problems will be expected for biases higher than 11.0V. Although it depends on technology used, it is common for the breakdown curve to be flat up to a voltage very close to breakdown and then almost vertical. The current changes by orders of magnitude for very small bias increments.

This produces some problems for ATLAS using the syntax described above. If the breakdown occurs at 11.5V, there are no solutions for voltages greater than this value. ATLAS is trying to ramp to 20.0V. Therefore, it is inevitable that ATLAS will fail to converge at some point. This is usually not a problem since by that point the breakdown voltage and curve have been obtained.

Above 11V, bias step reduction will take place due to the TRAP parameter. ATLAS will continually try to increase the drain voltage above 11.5V and those points will fail to converge. But it will solve points asymptotically approaching $V_{ds}=11.5V$ until it reaches the limit set by the MAXTRAPS parameter. If you use the default of 4 traps, the minimum allowed voltage step will be $1.0 \times (0.5)^4$ or 0.004V. This is normally enough accuracy for determining the breakdown point. But the simulation might not allow the current to reach a sufficiently high level before MAXTRAPS is needed.

Typically in device simulation, the breakdown point is determined once the current is seen to increase above the flat pre-breakdown leakage value by two orders of magnitude in a small voltage increment. If you want to trace the full breakdown curve up to high current values, apply more advanced techniques than the simple voltage ramp. Two of these techniques are described in the following subsections. These methods may use extra CPU time.

Using Current Boundary Conditions

In all of the examples considered in the basic description of the SOLVE statement, it was assumed that voltages were being forced and currents were being measured. ATLAS also supports the reverse case through current boundary conditions. The current through the electrode is specified in the SOLVE statement and the voltage at the contact is calculated. Current boundary conditions are set using the CONTACT statement as described in Section 2.7: “Defining Material Parameters And Models”.

The syntax of the SOLVE statement is altered once current boundary conditions are specified.

```
SOLVE IBASE=1e-6
```

The syntax above specifies a single solution at a given current.

```
SOLVE IBASE=1e-6 ISTEP=1e-6 IFINAL=5e-6 NAME=base
```

This sets a current ramp similar in syntax to the voltage ramp described earlier.

```
SOLVE IBASE=1e-10 ISTEP=10 IMULT IFINAL=1e-6 NAME=base
```

This is similar to the previous case. The `IMULT` parameter, however, is used to specify that `ISTEP` should be used as a multiplier for the current rather than a linear addition. This is typical for ramps of current since linear ramps are inconvenient when several orders of magnitude in current may need to be covered.

Important points to remember about current boundary conditions are that the problems of initial guess are more acute when very small (noise level) currents are used. Often, it is best to ramp the voltage until the current is above $1\text{pA}/\mu\text{m}$ and then switch to current forcing.

When interpreting the results, it is important to remember the calculated voltage on the electrode with current boundary conditions is stored as the internal bias. In other words, `base int.bias` in `TONYPLOT` or `vint.base` in `DECKBUILD`'s `extract` syntax.

The Compliance Parameter

Compliance is a parameter used to limit the current or voltage through or on an electrode during a simulation. You can set an electrode compliance. After reaching this limit, the bias sweep will stop. This is similar to parametric device testing when we stop a device from being over-stressed or destroyed. The compliance refers to the maximum resultant current or voltage present after obtaining a solution. If you set an electrode voltage, the compliance will then refer to the electrode current. If there are current boundary conditions, you can set a voltage compliance.

The statements:

```
SOLVE VGATE=1.0
SOLVE NAME=drain VDRAIN=0 VFINAL=2 VSTEP=0.2 COMPL=1E-6 CNAME=drain
```

solve for IV on the gate and then ramps the drain voltage towards 2V in 0.2V steps. The simulation will stop if it reaches $1\mu\text{A}/\mu\text{m}$ of drain current before $V_d=2\text{V}$. Thus, as in parametric testing, you can define a particular level and set the simulation to solve up to that point. Once ATLAS reaches the compliance limit, it will simulate the next statement line in the command file.

The Curvetrace Capability

The automatic curve tracing algorithm can be invoked to enable ATLAS to trace out complex IV curves. The algorithm can automatically switch from voltage to current boundary conditions and vice versa. You can use a single `SOLVE` statement to trace out complex IV curves, such as breakdown curves and CMOS latch-up including the snapback region and second breakdown. The algorithm is based upon a dynamic load line approach.

For example, typical `CURVETRACE` and `SOLVE` statements to trace out an IV curve for the breakdown of a diode would look like:

```
CURVETRACE CONTR.NAME=cathode STEP.INIT=0.5 NEXTST.RATIO=1.2 \
          MINCUR=1e-12 END.VAL=1e-3 CURR.CONT
SOLVE CURVETRACE
```

`CONTR.NAME` specifies the name of the electrode, which is to be ramped. `STEP.INIT` specifies the initial voltage step. `NEXTST.RATIO` specifies the factor used to increase the voltage step in areas on the IV curve away from turning points. `MINCUR` sets a small current value above that activates the dynamic load line algorithm. Below the `MINCUR` level, using the `STEP.INIT` and `NEXTST.RATIO` determines the next solution bias. `END.VAL` stops the tracing if the voltage or current of the ramped electrode equals or exceeds `END.VAL`. Using `VOLT.CONT` or `CURR.CONT` specify whether `END.VAL` is a voltage or current value.

When you plot the log file created by the `CURVETRACE` statement in `TONYPLOT`, select the internal bias labeled `int.bias` for the ramped electrode instead of plotting the applied bias, which is labeled Voltage.

2.9.6: Using DeckBuild To Specify SOLVE Statements

The DeckBuild Solve menu can be used generate SOLVE statements. The menu has a spreadsheet style entry. To access this menu, select the **Command/Solutions/Solve...** button in DECKBUILD. To define a test, click the right mouse button in the worksheet and select the **Add new row** option. This will add a new row to the worksheet. This procedure should be repeated once per electrode in your device structure. The entry for each cell can then be edited to construct a SOLVE statement.

Some cells require the selection using a pop menu or the entry of numerical values. The electrode name is specified in the first cell. To edit the electrode name, use a popup menu by pressing the right mouse button on the cell. The second cell specifies whether the electrode will be a voltage (V), current (I) or charge (Q) controlled. The third cell specifies whether the SOLVE statement is to be a single DC solve (CONST), a swept DC variable (VAR1), a stepped DC variable (VAR2), or a transient solution (PULSE). The remaining cells specify the parameter values that are required for the type of solution desired.

The pop-up window to specify the solution file names are accessed through the **Props...** button. You can construct several SOLVE statements to create solve sequences, which define a test. This test may be saved in a file and read in using the **Save...** and **Load...** buttons.

2.10: Interpreting The Results

As already described in Section 2.2: “ATLAS Inputs and Outputs”, ATLAS produces three different types of output files. These files are also described in the following sections.

2.10.1: Run-Time Output

Run-time output is provided at the bottom of the DeckBuild Window. If it's run as a batch job, the run-time output can be stored to a file.

Errors occurring in the run-time output will be displayed in this window. Note that not all errors will be fatal (as DECKBUILD tries to interpret the file and continue). This may cause a statement to be ignored, leading to unexpected results. We recommend that you check the run-time output of any newly created input file the first time it runs to intercept any errors.

If you specify the `PRINT` option within the `MODELS` statement, the details of material parameters and constants and mobility models will be specified at the start of the run-time output. This is a useful way of checking what parameters values and models are being applied in the simulation. We recommend that you always specify `MODELS PRINT` in input files.

During `SOLVE` statements, the error numbers of each equation at each iteration are displayed (this is a change from the previous ATLAS version). It isn't vital for you to understand the iteration information. It can, however, provide important insights in the case of convergence problems.

The output can be interpreted as follows:

```

proj      psi      n      p      psi      n      p
direct    x        x        x      rhs      rhs      rhs

  i   j   m  -5.00*  -5.00*  -5.00*  -26.0*  -17.3*  -17.3*
- - - - -
1     N  -1.932 -2.934 -1.932  -25.2   -10.19  -9.876
2     N  -4.741 -5.64* -4.267  -28.8*  -16.67  -15.47
3     A  -11.3* -11.7* -9.63*  -28.8*  -16.67  -18.0*

Electrode  Va (V)          Jn (A/um)          Jp (A/um)          Jc (A/um)          Jt (A/um)
=====
gate       0.000e+00      -0.000e+00      -0.000e+00      0.000e+00      0.000e+00
source     0.000e+00      -3.138e-13      -1.089e-35      -3.138e-13      -3.138e-13
drain      1.000e-01       3.139e-13       1.076e-23       3.139e-13       3.139e-13
substrate  0.000e+00      -6.469e-19      -8.853e-17      -8.918e-17      -8.918e-17

```

The top left value, `proj`, indicates the initial guess methodology used. The default projection method is used here. Alternatives are `previous`, `local`, or `init`. The second value, `direct`, indicates the solver type. This will either be `direct` or `iterative`.

The first three column headings: `i`, `j`, and `m` indicate the iteration numbers of the solution and the solution method. `i` indicates the outer loop iteration number for decoupled solutions. `j` indicates the inner loop number. `m` indicates the solution method by a single letter, which are:

- G = gummel
- B = block
- N = newton
- A = newton with autonr
- S = coupled Poisson-Schrodinger solution

The remaining column headings indicate which column lists the `XNORM` and `RHSNORM` errors for the equations being solved. See Chapter 20: “Numerical Techniques”, Section 20.5.7: “Error Measures” for a full description of these errors. The values printed in each error column under the hashed line are the logarithm to base 10 of the error. Earlier PISCES versions would print the floating point value. The values printed above the dashed line in each column are the tolerances used.

When the star * symbol appears as the least significant digit in the number, it means this error measure has met its tolerance.

After achieving convergence, ATLAS lists the results by electrode. The column, V_a , lists the voltage at the contact surface. This will differ from the applied voltage if external resistors or the curvetracer are used. All relevant current components are listed. Here, only electron, hole, conduction, and total currents are given. In other modes of simulation, these columns may differ.

The output of AC analysis, `MIXEDMODE`, and 3D simulations differ from this standard. See Chapter 12: “MixedMode: Mixed Circuit and Device Simulator” for more information about `MIXEDMODE`.

ATLAS may produce a very large amount of run-time output for complex simulations. You can save run-time output to a file as shown in Section 2.3: “Modes of Operation”.

2.10.2: Log Files

Log files store the terminal characteristics calculated by ATLAS. These are current and voltages for each electrode in DC simulations. In transient simulations, the time is stored. In AC simulations, the small signal frequency and the conductances and capacitances are saved. For example, the statement:

```
LOG OUTF=<FILENAME>
```

is used to open a log file. Terminal characteristics from all `SOLVE` statements after the `LOG` statement are then saved to this file along with any results from the `PROBE` statement.

To not save the terminal characteristics to this file, use another `LOG` statement with either a different log filename or the `OFF` parameter.

Typically, a separate log file should be used for each bias sweep. For example, separate log files are used for each gate bias in a MOS I_d/V_{ds} simulation or each base current in a bipolar I_c/V_{ce} simulation. These files are then overlaid in `TONYPLOT`.

Log files contain only the terminal characteristics. They are typically viewed in `TONYPLOT`. Parameter extraction of data in log files can be done in `DECKBUILD`. Log files cannot be loaded into ATLAS to re-initialize the simulation.

Units of Currents In Log files

Generally, the units of current are written into the log file. In `TONYPLOT`, it is Amperes per micron. This is because ATLAS is a two-dimensional simulator. It sets the third dimension (or Z direction) to be one micron. Thus, if you compare ATLAS 2D simulation results for a MOSFET versus the measured data from a MOSFET of width 20 micron, you need to multiply the current in the log file by 20.

There are four exceptions:

- In the 3D modules of ATLAS, the width is defined in the 3D structure. Therefore, the units of the current are Amperes.
- In `MIXEDMODE`, set the width of devices. The current is also in Amperes.
- When cylindrical coordinates are used, the current written to the log file is integrated through the cylinder and is also in Amperes.
- When the `WIDTH` parameter in the `MESH` statement is used, the current is scaled by this factor and is in Amperes.

Similar rules apply for the capacitance and conductance produced by AC simulations. These are usually in $1/(\text{ohms.microns})$ and Farads/micron respectively.

UTMOST Interface

ATLAS log files can be read directly into the batch mode, UTMOST. The following commands in UTMOST are used to read in a set of IV curves stored in separate log files.

```
INIT INF=<filename> MASTER
INIT INF=<filename> MASTER APPEND
```

Note: The UTMOST statement in ATLAS is no longer recommended for interfacing to UTMOST.

2.10.3: Parameter Extraction In DeckBuild

The EXTRACT command is provided within the DECKBUILD environment. It allows you to extract device parameters. The command has a flexible syntax that allows you to construct specific EXTRACT routines. EXTRACT operates on the previous solved curve or structure file. By default, EXTRACT uses the currently open log file. To override this default, supply the name of a file to be used by EXTRACT before the extraction routine. For example:

```
EXTRACT INIT INF="<filename>"
```

A typical example of using EXTRACT is the extraction of the threshold voltage of an MOS transistor. In the following example, the threshold voltage is extracted by calculating the maximum slope of the I_d / V_g curve, finding the intercept with the X axis and then subtracting half of the applied drain bias.

```
EXTRACT NAME="nvt" XINTERCEPT(MAXSLOPE(CURVE (V."GATE", (I."DRAIN")))) \
- (AVE(V."DRAIN"))/2.0)
```

The results of the extraction will be displayed in the run-time output and will be by default stored in the file `results.final`. To store the results in a different file at the end of EXTRACT command, use the following option:

```
EXTRACT...DATAFILE="<filename>"
```

Cut-off frequency and forward current gain are of particular use as output parameters. These functions can be defined as follows:

```
# MAXIMUM CUTOFF FREQUENCY
EXTRACT NAME="FT_MAX" MAX(G."COLLECTOR" "BASE" / (6.28*C."BASE" "BASE"))

#FORWARD CURRENT GAIN
EXTRACT NAME="PEAK GAIN" MAX(I."COLLECTOR" / I."BASE")
```

Note: Over 300 examples are supplied with ATLAS to provide many practical examples of the use of the EXTRACT statement.

AC Parameter Extraction

You can perform basic analysis of the capacitance and conductance matrix produced by ATLAS using DECKBUILD or TONYPLOT. The capacitance between gate and drain will be labeled as Cgate>drain in TONYPLOT or c."gate" "drain" in DECKBUILD'S EXTRACT.

The total capacitance on any electrode is defined as Celectrode>electrode. Thus, the magnitude of Cgate>gate is the total gate capacitance.

The LOG statement also includes options for small-signal, two-port RF analysis including s-parameter extraction. The solutions are saved into the log file and in the run-time output. The list of options for RF analysis are:

```
s.param, y.param, h.param, z.param, abcd.param gains
```

Terminal impedance and parasitics are accounted for by adding any of the following:

```
impedance=<val>, rin=<val>, rout=<val>, rcommon=<val> or  
rground=<val>, lin=<val>, lout=<val>,  
lcommon=<val> or lground=<val>, width=<val>
```

The width defaults to 1µm and impedance defaults to 50Ω. All parasitics default to zero.

The Stern stability factor, k, is calculated along with current gain (h21), GUmax, and GTmax when the GAINS option is added to the LOG statement.

The run-time output for AC analysis has been modified to only list the analysis frequency and electrode conductance/capacitance values. If one of the two-port options is added to the LOG statement (e.g., S.PARAM), the two-port parameters are also included in the run-time output.

Note: AC parameter conversion utilities in the UTMOST statement have been discontinued.

See Appendix C: "RF and Small Signal AC Parameter Extraction[239]" for more information.

Additional Functions

EXTRACT has two additional important functions. The first function is to provide data for the VWF database. In other words, to store device parameters to the VWF database, you must evaluate them using EXTRACT. The second function is when using the DeckBuild Optimizer to tune parameters, use the EXTRACT statements as the optimization targets.

2.10.4: Functions In TonyPlot

The **Edit/Functions** Menu in TONYPLOT allows you to specify and plot functions of the terminal characteristics in the **Graph Function** text fields. For example, you can calculate transconductance using the following function:

```
dydx (drain current, gate voltage)
```

Current gain can be evaluated as:

```
collector current / base current
```

When creating functions, the key to correct syntax is that the name for any variable in a function is the same as that in the **Y Quantities** list on the **Display** menu.

2.10.5: Solution Files

Solution files or structure files provide an image of the device at a particular bias point (DC solution or transient solution point). This gives you the ability to view any evaluated quantity within the device structure in question, from doping profiles and band parameters to electron concentrations and electric fields. These files should be plotted using TONYPLOT.

The syntax used to generate these files is of two forms:

- (1) `SAVE OUTFILE=<filename>`
- (2) `SOLVE OUTFILE=<filename>.sta MASTER [ONEFILEONLY]`

Here in the second form, a file named <filename> will be saved with data from the previously solved bias point.

In this case, a structure file will be saved at each bias point solved in the solve statement. The last letter of the file name will be automatically incremented alphabetically (i.e., *.sta, *.stb, *.stc..., and so on). If you need the solution for the last bias point, you can add the `onefileonly` parameter to the command. The <filename>.sta file will be overwritten at each solution point.

Structure files can be large (1 - 2 MB), depending on the mesh density and quantities saved. It is recommended that unwanted structure files be deleted.

If many solution files have been written from a long simulation, it is often confusing to find out which solution file belongs to which bias point or transient time. The solution files should be plotted in TONYPLOT. In TONYPLOT, you can create 2D contour plots and 1D cutlines. To find out the bias of any solution file in TONYPLOT, select the plot, and press **b** on the keyboard.

Interpreting Contour Plots

Some quantities saved in the solution files are not evaluated at the node points during solutions. They are evaluated at the center of the sides of each triangle in the mesh. Values of quantities at each node are derived from averaging the values from the sides of triangles connected to that node. The weighting method used to do the averaging can be selected with options in the `OUTPUT` statement. It is possible that for some meshes, smoother contour plots can be obtained by choosing a non-default averaging method.

When interpreting the contour plots, it's important to remember that the solution file contains values only at each node point. The color fills seen in TONYPLOT are simply interpolations based on the node values. This may lead to occasional strange contour values. In these cases, check the node values using the probe in TONYPLOT.

The primary solution variables (potential, carrier concentration, lattice temperature and carrier temperatures) are calculated on the nodes of the ATLAS mesh. Therefore, they are always correct in TONYPLOT. But since ATLAS doesn't use nodal values of quantities, such as electric field and mobility, the actual values used in calculations cannot be determined from TONYPLOT or the structure files. The `PROBE` statement allows you to directly probe values at given locations in the structure. This provides the most accurate way to determine the actual values used in ATLAS calculations.

Customizing Solution Files (OUTPUT Statement)

Several quantities are saved by default within a structure file. For example, doping, electron concentration, and potential. You can also specify additional quantities (such as conduction band potential) by using the `OUTPUT` statement. This must precede the `SAVE` statement in question. For example, to save the conduction and valence band potentials, the following command would be used at some point before the relevant `SAVE`.

```
OUTPUT CON.BAND VAL.BAND
```

Saving Quantities from the Structure at each Bias Point (PROBE statement)

Structure files provide all data from the structure at a single bias point. The log files provide terminal characteristics for a set of bias points. Use the `PROBE` statement to combine these and allow certain structural quantities to be saved at each bias point.

The `PROBE` statement allows you to specify quantities to be saved at given XY locations. You can also save the maximum or minimum of certain quantities. The value from the `PROBE` at each bias point in DC or timestep in transient mode is saved to the log file. The syntax:

```
PROBE NAME=mycarriers N.CONC X=1 Y=0.1
```

saves the electron concentration at (1, 0.1) for each solution in the log file. When `TONYPLOT` displays the log file, the value will be labelled `mycarriers`. You can then plot `mycarriers` versus terminal bias or current or other probed quantities.

Certain direction dependent quantities, such as electric field and mobility, can be probed. In these cases, specify a direction for the vector quantity using the `DIR` parameter.

The `PROBE` statement provides the only way to extract the actual values of quantities, which are calculated along the sides of each triangle in ATLAS. The `PROBE` statement actually stored the triangle side value closest to the probed location, while taking into account the direction for vector quantities.

Note: Specifying the probe location exactly at a material or region interface will often lead to erroneous results. It is best to slightly offset the location of the probe inside the material or region of interest.

Re-initializing ATLAS at a Given Bias Point

Each `SOLVE` statement will begin with the device biased at the previous value solved. To begin a solution at a previously solved bias point, re-load the structure file saved at that point. This is accomplished in the following manner:

```
LOAD INFILE=<filename> MASTER
```

Information about that solution point will be displayed in the Output Window.

This command is useful for solving a set of I/V curves. For example, to solve a family of I_d / V_d (at various V_g), ramp the gate with zero drain bias. A structure file is then saved at each desired value of V_g . These structure files can be reloaded in turn while a V_d sweep is performed.

Note: An ATLAS input file cannot start with a `LOAD` statement. Before loading the structure file, use the `MESH` statement to load the device mesh for the same structure. Also, the same `MODELS`, `MATERIAL`, and `CONTACT` settings are required when the files are saved by ATLAS.

2.10.6: Technology Specific Issues in ATLAS

This chapter was designed to give an overview to the basic use of ATLAS without regard to the details required for a given technology. Requirements for ATLAS simulation vary considerably. The needs of the sub-micron MOS device engineer, the 1000V power device engineer, and the III-V RF device engineer differ and cannot all be covered in one chapter. SILVACO provides many references to individual technology problems using ATLAS. These are:

- A library of standard examples that can be accessed on-line from DECKBUILD. Look at these examples not only for their technology but also related ones. For example, different aspects of high frequency analysis is covered in the MESFET and silicon bipolar example sections.
- The chapters for each ATLAS module in this manual.
- The Simulation Standard, a newsletter distributed by SILVACO. To make sure you're on the mailing list, contact your local SILVACO office or go to www.silvaco.com.
- The SILVACO website also provides detailed information. It contains on-line versions of the articles in our newsletter, on-line searchable index of the examples, links to other TCAD web sites, and a section on solutions to known problems with all SILVACO programs.
- For more information about suggested technology specific strategies, contact your local SILVACO support engineer at support@silvaco.com.

3.1: Basic Semiconductor Equations

Years of research into device physics have resulted in a mathematical model that operates on any semiconductor device [177]. This model consists of a set of fundamental equations, which link together the electrostatic potential and the carrier densities, within some simulation domain. These equations, which are solved inside any general purpose device simulator, have been derived from Maxwell's laws and consist of Poisson's Equation (see Section 3.1.1: "Poisson's Equation"), the continuity equations (see Section 3.1.2: "Carrier Continuity Equations") and the transport equations (see Section 3.1.3: "The Transport Equations"). Poisson's Equation relates variations in electrostatic potential to local charge densities. The continuity and the transport equations describe the way that the electron and hole densities evolve as a result of transport processes, generation processes, and recombination processes.

This chapter describes the mathematical models implemented in ATLAS. Note that a discretization of the equations is also performed so that they can be applied to the finite element grid used to represent the simulation domain.

3.1.1: Poisson's Equation

Poisson's Equation relates the electrostatic potential to the space charge density:

$$\text{div}(\varepsilon \nabla \psi) = -\rho \quad 3-1$$

where ψ is the electrostatic potential, ε is the local permittivity, and ρ is the local space charge density. The reference potential can be defined in various ways. For ATLAS, this is always the intrinsic Fermi potential ψ_i which is defined in the next section. The local space charge density is the sum of contributions from all mobile and fixed charges, including electrons, holes, and ionized impurities.

The electric field is obtained from the gradient of the potential (see Equation 3-2).

$$\vec{E} = -\nabla \psi \quad 3-2$$

3.1.2: Carrier Continuity Equations

The continuity equations for electrons and holes are defined by equations:

$$\frac{\partial n}{\partial t} = \frac{1}{q} \text{div} \vec{J}_n + G_n - R_n \quad 3-3$$

$$\frac{\partial p}{\partial t} = -\frac{1}{q} \text{div} \vec{J}_p + G_p - R_p \quad 3-4$$

where n and p are the electron and hole concentration, \vec{J}_n and \vec{J}_p are the electron and hole current densities, G_n and G_p are the generation rates for electrons and holes, R_n and R_p are the recombination rates for electrons and holes, and q is the magnitude of the charge on an electron.

By default ATLAS includes both Equations 3-3 and 3-4. In some circumstances, however, it is sufficient to solve only one carrier continuity equation. The specification of which continuity equations are to be solved is performed in the METHOD statement by turning off any equation that is not to be solved. The syntax, ^ELECTRONS or ^HOLES, turns off the electron continuity equation and the hole continuity equation respectively.

3.1.3: The Transport Equations

Equations 3-1, 3-3, and 3-4 provide the general framework for device simulation. But further secondary equations are needed to specify particular physical models for: \vec{J}_n , \vec{J}_p , G_n , R_n , G_p and R_p .

The current density equations, or charge transport models, are usually obtained by applying approximations and simplifications to the Boltzmann Transport Equation. These assumptions can result in a number of different transport models such as the drift-diffusion model, the Energy Balance Transport Model or the hydrodynamic model. The choice of the charge transport model will then have a major influence on the choice of generation and recombination models.

The simplest model of charge transport that is useful is the Drift-Diffusion Model. This model has the attractive feature that it does not introduce any independent variables in addition to ψ , n and p . Until recently, the drift-diffusion model was adequate for nearly all devices that were technologically feasible. The drift-diffusion approximation, however, becomes less accurate for smaller feature sizes. More advanced energy balance and hydrodynamic models are therefore becoming popular for simulating deep submicron devices. ATLAS supplies both drift-diffusion and advanced transport models.

The charge transport models and the models for generation and recombination in ATLAS make use of some concepts associated with carrier statistics. These concepts are summarized in a further section of this chapter that deals with the carrier statistics.

Drift-Diffusion Transport Model

Derivations based upon the Boltzmann transport theory have shown that the current densities in the continuity equations may be approximated by a drift-diffusion model [207]. In this case, the current densities are expressed in terms of the quasi-Fermi levels ϕ_n and ϕ_p as:

$$\vec{J}_n = -q\mu_n n \nabla \phi_n \quad 3-5$$

$$\vec{J}_p = -q\mu_p p \nabla \phi_p \quad 3-6$$

where μ_n and μ_p are the electron and hole mobilities. The quasi-Fermi levels are then linked to the carrier concentrations and the potential through the two Boltzmann approximations:

$$n = n_{ie} \exp\left[\frac{q(\psi - \phi_n)}{kT_L}\right] \quad 3-7$$

$$p = n_{ie} \exp\left[\frac{-q(\psi - \phi_p)}{kT_L}\right] \quad 3-8$$

where n_{ie} is the effective intrinsic concentration and T_L is the lattice temperature. These two equations may then be re-written to define the quasi-Fermi potentials:

$$\phi_n = \psi - \frac{kT_L}{q} \ln \frac{n}{n_{ie}} \quad 3-9$$

$$\phi_p = \psi + \frac{kT_L}{q} \ln \frac{p}{n_{ie}} \quad 3-10$$

By substituting these equations into the current density expressions, the following adapted current relationships are obtained:

$$\vec{J}_n = qD_n \nabla n - qn\mu_n \nabla \psi - \mu_n n (kT_L \nabla (\ln n_{ie})) \quad 3-11$$

$$\vec{J}_p = -qD_p \nabla p - qp\mu_p \nabla \psi + \mu_p p (kT_L \nabla (\ln n_{ie})) \quad 3-12$$

The final term accounts for the gradient in the effective intrinsic carrier concentration, which takes account of bandgap narrowing effects. Effective electric fields are normally defined whereby:

$$\vec{E}_n = -\nabla \left(\psi + \frac{kT_L}{q} \ln n_{ie} \right) \quad 3-13$$

$$\vec{E}_p = -\nabla \left(\psi - \frac{kT_L}{q} \ln n_{ie} \right) \quad 3-14$$

which then allows the more conventional formulation of drift-diffusion equations to be written (see Equations 3-15 and 3-16).

$$\vec{J}_n = qn\mu_n \vec{E}_n + qD_n \nabla n \quad 3-15$$

$$\vec{J}_p = qp\mu_p \vec{E}_p - qD_p \nabla p \quad 3-16$$

It should be noted that this derivation of the drift-diffusion model has tacitly assumed that the Einstein relationship holds. In the case of Boltzmann statistics this corresponds to:

$$D_n = \frac{kT_L}{q} \mu_n \quad 3-17$$

$$D_p = \frac{kT_L}{q} \mu_p \quad 3-18$$

If Fermi-Dirac statistics are assumed for electrons, Equation 3-17 becomes:

$$D_n = \frac{\left(\frac{kT_L}{q} \mu_n \right) F_{1/2} \left\{ \frac{1}{kT_L} [\varepsilon_{Fn} - \varepsilon_C] \right\}}{F_{-1/2} \left\{ \frac{1}{kT_L} [\varepsilon_{Fn} - \varepsilon_C] \right\}} \quad 3-19$$

where F_α is the Fermi-Dirac integral of order α and ε_{Fn} is given by $-q\phi_n$. An analogous expression is used for holes with Fermi-Dirac statistics.

Note: See Section 3.2.9: “Bandgap Narrowing” for more information on the effects resulting from bandgap narrowing and their implementation.

Energy Balance Transport Model

A higher order solution to the general Boltzmann Transport Equation consists of an additional coupling of the current density to the carrier temperature, or energy. The current density expressions from the drift-diffusion model are modified to include this additional physical relationship. The electron current and energy flux densities are then expressed as:

$$\vec{J}_n = qD_n \nabla n - q\mu_n n \nabla \psi + qnD_n^T \nabla T_n \quad 3-20$$

$$\vec{S}_n = -K_n \nabla T_n - \left(\frac{k\delta_n}{q} \right) \vec{J}_n T_n \quad 3-21$$

$$\vec{J}_p = -qD_p \nabla p - q\mu_p p \nabla \psi - qpD_p^T \nabla T_p \quad 3-22$$

$$\vec{S}_p = -K_p \nabla T_p - \left(\frac{k\delta_p}{q} \right) \vec{J}_p T_p \quad 3-23$$

where T_n and T_p represent the electron and hole carrier temperatures and S_n and S_p are the flux of energy (or heat) from the carrier to the lattice. The energy balance transport model includes a number of very complex relationships and therefore a later section of this chapter has been devoted to this model.

3.1.4: Displacement Current Equation

For time domain simulation, the displacement current is calculated and included in the structure, log file and the run time output. The expression for displacement current is given as:

$$\vec{J}_{dis} = \varepsilon \left(\frac{\partial \vec{E}}{\partial t} \right) \quad 3-24$$

3.2: Basic Theory of Carrier Statistics

3.2.1: Fermi-Dirac and Boltzmann Statistics

Electrons in thermal equilibrium at temperature T_L with a semiconductor lattice obey Fermi-Dirac statistics. That is the probability $f(\varepsilon)$ that an available electron state with energy ε is occupied by an electron is:

$$f(\varepsilon) = \frac{1}{1 + \exp\left(\frac{\varepsilon - E_F}{kT_L}\right)} \quad 3-25$$

where E_F is a spatially independent reference energy known as the Fermi level and k is Boltzmann's constant.

In the limit, $\varepsilon - E_F \gg kT_L$, Equation 3-25 can be approximated as:

$$f(\varepsilon) = \exp\left(\frac{E_F - \varepsilon}{kT_L}\right) \quad 3-26$$

Statistics based on the use of Equation 3-26 are referred to as Boltzmann statistics [271, 109]. The use of Boltzmann statistics instead of Fermi-Dirac statistics makes subsequent calculations much simpler. The use of Boltzmann statistics is normally justified in semiconductor device theory, but Fermi-Dirac statistics are necessary to account for certain properties of very highly doped (degenerate) materials.

The Fermi-Dirac statistics have been implemented in ATLAS in a similar form to Boltzmann statistics.

The remainder of this section outlines derivations and results for the simpler case of Boltzmann statistics which are the default in ATLAS. You can have ATLAS use Fermi-Dirac statistics by specifying the `FERMIDIRAC` parameter in the `MODEL` statement.

3.2.2: Effective Density of States

Integrating the Fermi-Dirac statistics over a parabolic density of states in the conduction and valence bands, whose energy minimum is located at energies E_C and E_V respectively, yields the following expressions for the electron and hole concentrations:

$$n = N_C F_{1/2}\left(\frac{E_F - E_C}{kT_L}\right) \quad 3-27$$

$$p = N_V F_{1/2}\left(\frac{E_V - E_F}{kT_L}\right) \quad 3-28$$

where $F_{1/2}(\eta)$ is referred to as the Fermi-Dirac integral of order 1/2. If Equation 3-26 is a good approximation, then Equations 3-27 and 3-28 can be simplified to

$$n = N_C \exp\left(\frac{E_F - E_C}{kT_L}\right) \quad 3-29$$

$$p = N_V \exp\left(\frac{E_V - E_F}{kT_L}\right) \quad 3-30$$

which are referred to as the Boltzmann approximation.

N_C and N_V are referred to as the effective density of states for electrons and holes and are given by:

$$N_C(T_L) = 2 \left(\frac{2\pi m_e^* k T_L}{h^2} \right)^{\frac{3}{2}} M_c = \left(\frac{T_L}{300} \right)^{NC.F} \text{ NC300} \quad 3-31$$

$$N_V(T_L) = 2 \left(\frac{2\pi m_h^* k T_L}{h^2} \right)^{\frac{3}{2}} = \left(\frac{T_L}{300} \right)^{NV.F} \text{ NV300} \quad 3-32$$

where M_c is the number of equivalent conduction band minima. NC300 and NV300 are user-definable on the MATERIAL statement as shown in Table 3-1.

In some circumstances, the lattice temperature, T_L , is replaced by the electron temperature, T_n , in Equation 3-31 and hole temperature, T_p , in Equation 3-32.

| Table 3-1. User-Definable Parameters for the Density of States | | | |
|--|-----------|-----------------------|------------------|
| Statement | Parameter | Default | Units |
| MATERIAL | NC300 | 2.8×10^{19} | cm^{-3} |
| MATERIAL | NV300 | 1.04×10^{19} | cm^{-3} |
| MATERIAL | NC.F | 1.5 | |
| MATERIAL | NV.F | 1.5 | |

3.2.3: Intrinsic Carrier Concentration

Multiplying Equations 3-29 and 3-30 yields:

$$np = n_{ie}^2 \quad 3-33$$

where n_{ie} is the intrinsic carrier concentration and is given for Boltzmann statistics by:

$$n_{ie} = \sqrt{N_C N_V} \exp\left(\frac{-E_g}{2kT_L}\right) \quad 3-34$$

$E_g = E_C - E_V$ is the band-gap energy.

For intrinsic (undoped) material, $p = n$. By equating Equations 3-29 and 3-30 and solving for E_F yields:

$$E_F = E_i = -q\psi_i = \frac{E_C + E_V}{2} + \left(\frac{kT_L}{2}\right) \ln\left(\frac{N_V}{N_C}\right) \quad 3-35$$

where E_i is the Fermi level for intrinsic doped silicon, and ψ_i is the intrinsic potential. Equation 3-35 also defines the intrinsic potential under non-equilibrium conditions. As indicated previously, for ATLAS the ψ used in Equation 3-1 is the intrinsic potential.

The electron and hole concentrations can be expressed in terms of the intrinsic carrier concentration as:

$$n = n_{ie} \exp \left[\frac{q(\psi - \phi_n)}{kT_L} \right] \quad 3-36$$

$$p = n_{ie} \exp \left[\frac{-q(\psi - \phi_p)}{kT_L} \right] \quad 3-37$$

where ψ is the intrinsic potential and ϕ is the potential corresponding to the Fermi level (i.e., $E_F = q\phi$).

The expression for intrinsic carrier concentration, n_{ie} , can be generalized to Fermi-Dirac statistics using Equations 3-27 and 3-28. Specifying the `NI.FERMI` parameter in the `MODELS` statement will cause ATLAS to calculate n_{ie} using Fermi-Dirac statistics.

3.2.4: Evaluation of Fermi-Dirac Integrals

In addition to the Fermi-Dirac integral of order $\frac{1}{2}$ as used in Equations 3-27 and 3-28, ATLAS also needs to evaluate the Fermi-Dirac integrals of order $-\frac{3}{2}, -\frac{1}{2}, \frac{3}{2}$. There are simple, quickly calculated, but relatively poor approximations available for these integrals. You can also evaluate them to machine precision; however, the amount of computation required makes the evaluations relatively slow. ATLAS uses a Rational Chebyshev approximation scheme, which is efficient in terms of CPU use and also has accuracy close to the machine precision. In the worst case, the approximation differs from the actual values by 1 part in 10^{10} and is typically much better.

3.2.5: Rules for Evaluation of Energy Bandgap

In the ATLAS simulator, there are several ways to evaluate the value of energy bandgap for a given material. To uniquely define the approach used, there is a set of rules that are followed in a hierarchical manner. The following is a description of this hierarchy:

1. For each material or material system, there may be a default approach. To determine the default for a given material or material system, refer to the descriptions given in Section 5.3: "Material Dependent Physical Models". If the material system is not listed in this section, then look for default energy bandgap model constants in Appendix B: "Material Systems".
2. If you set the `EG300` parameter of the `MATERIAL` statement to a value greater than zero and you do not set the `PASSLER` parameter of the `MODELS` statement, the universal energy bandgap model described in Section 3.2.6: "The Universal Energy Bandgap Model" will be used.
3. If you set the `EG300` parameter of the `MATERIAL` statement to a value greater than zero and you set the `PASSLER` parameter of the `MODELS` statement, then Passler's model for temperature dependent energy bandgap described in Section 3.2.7: "Passler's Model for Temperature Dependent Bandgap" will be used.
4. If you specify the `K.P` parameter of the `MODELS` statement for materials in the InAlGaN system, then the bandgap is taken as the minimum transition energy calculated following the approach given by the strained zincblende two band model described in Section 3.9.8: "Strained Zincblende Gain and Radiative Recombination Models" or the strained wurtzite 3 band model described in Section 3.9.9: "Strained Wurtzite Three-Band Model for Gain and Radiative Recombination".
5. If you assign the `F.BANDCOMP` parameter of the `MATERIAL` statement to a valid filename, the `C` interpreter function for energy bandgap will be used.
6. If you assign the `EG12BOW` parameter to a non-zero value, the general ternary bowing model described in Section 3.2.8: "General Ternary Bandgap Model with Bowing" will be used.

3.2.6: The Universal Energy Bandgap Model

The temperature dependence of the bandgap energy is modeled in ATLAS as follows [223]:

$$E_g(T_L) = E_g(0) - \frac{EGALPHA(T_L^2)}{T_L + EGBETA} = EG300 + EGALPHA \left[\frac{300^2}{300 + EGBETA} - \frac{T_L^2}{T_L + EGBETA} \right] \quad 3-38$$

You can specify EG300, EGALPHA and EGBETA parameters in the MATERIAL statement (see Table 3-2).

| Table 3-2. User-Specifiable Parameters for Equation 3-38 | | | |
|--|-----------|-----------------------|------------------|
| Statement | Parameter | Default | Units |
| MATERIAL | EG300 | 1.08 | eV |
| MATERIAL | EGALPHA | 4.73×10 ⁻⁴ | eV/K |
| MATERIAL | EGBETA | 636 | K |
| MATERIAL | NC300 | 2.8×10 ¹⁹ | cm ⁻³ |
| MATERIAL | NV300 | 1.04×10 ¹⁹ | cm ⁻³ |

The default values are material dependent, which can be found in Appendix B: “Material Systems”. Table 3-2 displays the defaults for Silicon only.

3.2.7: Passler's Model for Temperature Dependent Bandgap

An alternative temperature dependent bandgap model by Passler [172] can be enabled by the PASSLER parameter of the MODELS statement.

The bandgap is given by

$$Eg(T) = Eg(0) - \frac{A.PASSLER \cdot T.PASSLER}{2} \quad 3-39$$

$$\left\{ \left[\left(\frac{2 \cdot T}{T.PASSLER} \right)^{1/P.PASSLER} + 1 \right]^{P.PASSLER} - 1 \right\}$$

where Eg(T) is the lattice temperature dependent bandgap, T is the lattice temperature, A.PASSLER, T.PASSLER and P.PASSLER are user-specified parameters on the MATERIAL statement and Eg(0) is given by

$$Eg(0) = EG300 - \frac{A.PASSLER \cdot T.PASSLER}{2} \quad 3-40$$

$$\left\{ \left[\left(\frac{2 \cdot 300}{T.PASSLER} \right)^{1/P.PASSLER} + 1 \right]^{P.PASSLER} - 1 \right\}$$

where EG300 is a user specified parameter on the MATERIAL statement.

3.2.8: General Ternary Bandgap Model with Bowing

For Ternary compound semiconductors, you can use a bandgap model that continuously and non-linearly interpolates between the bandgaps of the two binary extremes in composition. To enable this model, you must specify the EG12BOW, EG1300 and EG2300 parameters of the MATERIAL statement. EG1300 is the 300K bandgap of the binary compound at a composition fraction of $x=0$. EG2300 is the 300K bandgap of the binary compound at a composition fraction of $x=1$. EG12BOW is the bowing factor. The bandgap as a function of composition is given by Equation 3-41.

$$E_g = EG2300 * x + EG1300 * (1 - x) - EG12BOW * x * (1 - x) \quad 3-41$$

where x is the composition fraction.

You can include the effects of temperature in the Bowing model by specifying the EG1ALPH, EG1BETA, EG2ALPH and EG2BETA parameters of the MATERIAL statement. These parameters are used in Equations 3-53 through 3-55 to calculate the bandgap.

$$E_{g1} = EG1300 + EG1ALPH \left[\frac{300^2}{300 + EG1BETA} - \frac{T_L^2}{T_L + EG1BETA} \right] \quad 3-42$$

$$E_{g2} = EG2300 + EG2ALPH \left[\frac{300^2}{300 + EG2BETA} - \frac{T_L^2}{T_L + EG2BETA} \right] \quad 3-43$$

$$E_g = E_{g2} * x + E_{g1} * (1 - x) - EG12BOW * x * (1 - x) \quad 3-44$$

3.2.9: Bandgap Narrowing

In the presence of heavy doping, greater than 10^{18}cm^{-3} , experimental work has shown that the pn product in silicon becomes doping dependent [217]. As the doping level increases, a decrease in the bandgap separation occurs, where the conduction band is lowered by approximately the same amount as the valence band is raised. In ATLAS this is simulated by a spatially varying intrinsic concentration n_{ie} defined according to Equation 3-45.

$$n_{ie}^2 = n_i^2 \exp\left(\frac{\Delta E_g}{kT}\right) \quad 3-45$$

Bandgap narrowing effects in ATLAS are enabled by specifying the BGN parameter of the MODELS statement. These effects may be described by an analytic expression relating the variation in bandgap, ΔE_g , to the doping concentration, N . The expression used in ATLAS is from Slotboom and de Graaf [218]:

$$\Delta E_g = BGN \cdot E \left\{ \ln \frac{N}{BGN \cdot N} + \left[\left(\ln \frac{N}{BGN \cdot N} \right)^2 + BGN \cdot C \right]^{\frac{1}{2}} \right\} \quad 3-46$$

You can specify the BGN.E, BGN.N, and BGN.C parameters in the MATERIAL statement. The default values from Slotboom [218] and Klaassen [122] are shown in Table 3-3. The Klaassen defaults will be used if you specify the BGN.KLA parameter in the MODELS statement. Otherwise, the Slotboom values will be used (by default). You can select a second set of defaults by specifying BGN.KLAASSEN.

Table 3-3. User-Definable Parameters of Bandgap Narrowing Model

| Statement | Parameter | Defaults (Slotboom) | Defaults (Klaassen) | Units |
|-----------|-----------|------------------------|------------------------|------------------|
| MATERIAL | BGN.E | 9.0×10^{-3} | 6.92×10^{-3} | V |
| MATERIAL | BGN.N | 1.0×10^{17} | 1.3×10^{17} | cm ⁻³ |
| MATERIAL | BGN.C | 0.5 | 0.5 | |

The variation in bandgap is introduced to the other physical models by subtracting the result of Equation 3-47 from the bandgap, E_g . In addition an adjustment is also made to the electric field terms in the transport models as described earlier. The adjustment takes the form:

$$\vec{E}_n = -\nabla \left(\psi + \frac{kT_L}{q} \ln n_{ie} \right) \quad 3-47$$

$$\vec{E}_p = -\nabla \left(\psi - \frac{kT_L}{q} \ln n_{ie} \right) \quad 3-48$$

The variation in the energy bandgap is also applied partially to the electron affinity, χ . The effective electron affinity, χ_{eff} given as follows:

$$\chi_{eff} = \chi + \Delta E_g \times \text{ASYMMETRY} \quad 3-49$$

where ASYMMETRY is a user-specifiable asymmetry factor. You can specify the value of the asymmetry factor using the ASYMMETRY parameter of the MATERIAL statement.

Note: In addition to this in-built model for bandgap narrowing, ATLAS allows you to use its C-INTERPRETER module. You can write an external file with C-code that defines an equation for bandgap narrowing. The filename is specified with the F.BGN parameter in the MODEL statement. See Appendix A: "C-Interpreter Functions" for more information on C-INTERPRETER.

3.2.10: The Universal Bandgap Narrowing Model

A universal bandgap narrowing model has been suggested [179]. This model given in Equation 3-50 relates the change in bandgap to the material effective masses, m_c and m_v , and the static dielectric constant ϵ_s . The `UBGN.C` and `UBGN.B` parameters are fitting parameters to define in the `MATERIAL` statement. To enable the model, specify `UBGN` on the `MODELS` statement.

$$\Delta E_g = -\text{UBGN.C} \left[\frac{\epsilon_s^5}{N} \left(m_0 \frac{m_c + m_v}{m_c m_v} + \text{UBGN.B} T^2 \frac{\epsilon_s}{N} \right) \right]^{-\frac{1}{4}} \quad 3-50$$

In Equation 3-50, N is the net doping concentration. The default values for `UBGN.C` and `UBGN.B` are $3.9 \times 10^{-5} \text{ eV cm}^{3/4}$ and $3.10 \times 10^{12} \text{ cm}^{-3} \text{ K}^{-2}$.

3.2.11: Bennett-Wilson and del Alamo Bandgap models

These are variations of the Slotboom and de Graaf model. The Bennett-Wilson formula [25] is

$$\Delta E_g = -\text{BGN.E} [\log(N/\text{BGN.N})]^2 \quad 3-51$$

and the del-Alamo formula [5],[222] is

$$\Delta E_g = -\text{BGN.E} [\log(N/\text{BGN.N})] \quad 3-52$$

where N is the total doping concentration. In both cases, the formula is only used for $N > \text{BGN.N}$, otherwise it is set at zero. Table 3-4 shows the default values of `BGN.E` and `BGN.N` for Silicon.

| Table 3-4. Silicon Default Values for Bennett-Wilson and del Alamo Bandgap models | | | | |
|---|--------------------|------------------|------------------------|-----------------------|
| Statement | Parameter | Units | Default (Bennett) | Default (Del Alamo) |
| MATERIAL | <code>BGN.E</code> | cm^{-3} | 6.84×10^{-3} | 1.87×10^{-2} |
| MATERIAL | <code>BGN.N</code> | cm^{-3} | 3.162×10^{18} | 7.0×10^{17} |

To enable the Bennett-Wilson model, use the `BGN.BENNETT` flag on the `MODELS` statement. To enable the del Alamo model, use the `BGN.ALAMO` flag on the `MODELS` statement.

3.3: Space Charge from Incomplete Ionization, Traps, and Defects

Poisson's Equation (Equation 3-1) including the carrier concentrations, the ionized donor and acceptor impurity concentrations N_D^+ and N_A^- , charge due to traps and defects, Q_T , has the form:

$$\text{div}(\epsilon \nabla \psi) = q(n - p - N_D^+ + N_A^-) - Q_T \quad 3-53$$

In ATLAS the default is to assume full impurity ionization (i.e., $N_D^+ = N_{D, \text{total}}$ and $N_A^- = N_{A, \text{total}}$), and to set Q_T equal to zero.

ATLAS also provides the options of accounting for incomplete ionization of impurities and accounting for additional charge associated with traps and defects.

3.3.1: Incomplete Ionization of Impurities

ATLAS can account for impurity freeze-out [108] with appropriate degeneracy factors GCB and GVB for conduction and valence bands. The ionized donor and acceptor impurity concentrations are then given by:

$$N_D^+ = \frac{N_D}{1 + \text{GCB} \exp\left(\frac{\epsilon_F - (E_C - \text{EDB})}{kT_L}\right)} \quad 3-54$$

$$N_A^- = \frac{N_A}{1 + \text{GVB} \exp\left(\frac{E_V + \text{EAB} - \epsilon_F}{kT_L}\right)} \quad 3-55$$

where EDB and EAB are the dopant activation energies and N_D and N_A are net compensated n-type and p-type doping, respectively. Net compensated doping is defined as follows:

If

$$N_{\text{total}} \equiv (N_{D, \text{total}} - N_{A, \text{total}}) > 0 \quad 3-56$$

then

$$N_D = |N_{\text{total}}| \text{ and } N_A = 0 \quad 3-57$$

Otherwise

$$N_D = 0 \text{ and } N_A = |N_{\text{total}}| \quad 3-58$$

The INCOMPLETE parameter of the MODELS statement is used to select incomplete ionization and the parameters.

| Table 3-5. User-Specifiable Parameters for Equations 3-54 and 3-55 | | |
|--|-----------|-------|
| Statement | Parameter | Units |
| MATERIAL | GCB | |
| MATERIAL | EDB | eV |
| MATERIAL | GVB | |
| MATERIAL | EAB | eV |

To properly handle incomplete ionization in silicon for high doping levels, a new incomplete ionization model has been added.

The models that form incomplete ionization of impurities given by Equations 3-54 and 3-55 give good physical results for low to moderately doped semiconductors. For heavily (greater than $3 \times 10^{18} \text{ cm}^{-3}$) doped semiconductors, these models fail to predict experimental results of complete ionization. For silicon, an optional model has been introduced that better matches experimental results. This model is set by the `IONIZ` parameter of the `MODELS` statement.

In this model, the activation energies of the dopants in Equations 3-54 and 3-55 have been modified for doping dependence as given in the following equations:

$$\text{EDB}(eV) = A \cdot \text{EDB} - B \cdot \text{EDB} N_D^{1/3} \quad 3-59$$

$$\text{EAB}(eV) = A \cdot \text{EAB} - B \cdot \text{EAB} N_A^{1/3} \quad 3-60$$

At doping concentrations above $3 \times 10^{18} \text{ cm}^{-3}$, the model predicts complete ionization. At doping concentrations between 10^{18} cm^{-3} and $3 \times 10^{18} \text{ cm}^{-3}$, the model predicts a linearly interpolated value between the above expressions and complete ionization.

The default value for the parameters of Equations 3-59 and 3-60 were chosen to represent reasonable values for silicon and are given in Table 3-5.

| Table 3-6. User-Specifiable Parameters for Equations 3-59 and 3-60 | | |
|--|-----------|----------|
| Statement | Parameter | Units |
| MATERIAL | A.EDB | 0.044 |
| MATERIAL | B.EDB | 3.6e-8 |
| MATERIAL | A.EAB | 0.0438 |
| MATERIAL | B.EAB | 3.037e-5 |

For general semiconductors, you can use Equations 3-59 and 3-60 without the transitions to complete ionization. To enable this model, specify `INC.ION` in the `MODEL` statement.

3.3.2: Low Temperature Simulations

In conjunction with Fermi-Dirac statistics and impurity freeze-out, ATLAS simulates device behavior under low operating temperatures. In general, simulations can be performed at temperatures as low as 50K without loss of quadratic convergence. Below this temperature, carrier and ionization statistics develop sharp transitions which cause slower convergence. Since many more iterations will probably be required if temperatures below 50K are specified, the `ITLIMIT` parameter of the `METHOD` statement should be increased.

Due to the limited exponent range on some machines, ATLAS can have trouble calculating the quasi-Fermi level of minority carriers. As the temperature decreases, the intrinsic carrier concentration also decreases. In quasi-neutral regions, the minority carrier concentration can easily underflow. Such situations were handled in the past by setting these concentrations to zero. This method does not allow an accurate subsequent calculation of minority carrier quasi-Fermi levels. In order to accurately

calculate quasi-Fermi levels, majority carrier concentration and the relation, $np = n_{ie}^2$ is used to obtain minority carrier concentrations in case of an underflow. Despite these efforts, spurious glitches are occasionally observed at low temperatures in the minority quasi-Fermi levels.

3.3.3: Traps and Defects

Semiconductor materials exhibit crystal flaws, which can be caused by dangling bonds at interfaces or by the presence of impurities in the substrate. The presence of these defect centers, or traps, in semiconductor substrates may significantly influence the electrical characteristics of the device. Trap centers, whose associated energy lies in a forbidden gap, exchange charge with the conduction and valence bands through the emission and capture of electrons. The trap centers influence the density of space charge in semiconductor bulk and the recombination statistics.

Device physics has established the existence of three different mechanisms, which add to the space charge term in Poisson's equation in addition to the ionized donor and acceptor impurities. These are interface fixed charge, interface trap states and bulk trap states. Interface fixed charge is modeled as a sheet of charge at the interface and therefore is controlled by the interface boundary condition. Interface traps and bulk traps will add space charge directly into the right hand side of Poisson's equation. This section describes the definition of bulk trap states and the implementation of these bulk trap states into ATLAS for both steady state and transient conditions.

A donor-type trap can be either positive or neutral like a donor dopant. An acceptor-type trap can be either negative or neutral like an acceptor dopant. A donor-like trap is positively charged (ionized) when empty and neutral when filled (with an electron). An empty donor-type trap, which is positive, can capture an electron or emit a hole. A filled donor-type trap, which is neutral, can emit an electron or capture a hole. An acceptor-like trap is neutral when empty and negatively charged (ionized) when filled (with an electron). A filled acceptor-like trap can emit an electron or capture a hole. An empty acceptor-like trap can capture an electron or emit a hole. Unlike donors, donor-like traps usually lie near the valence band. Likewise, acceptor-like traps usually lie near the conduction band.

Figure 3-1 shows the terminology used within ATLAS to define the type of trap. The position of the trap is defined relative to the conduction or valence bands using `E.LEVEL` so for instance, an acceptor trap at 0.4eV would be 0.4eV below the conduction band.

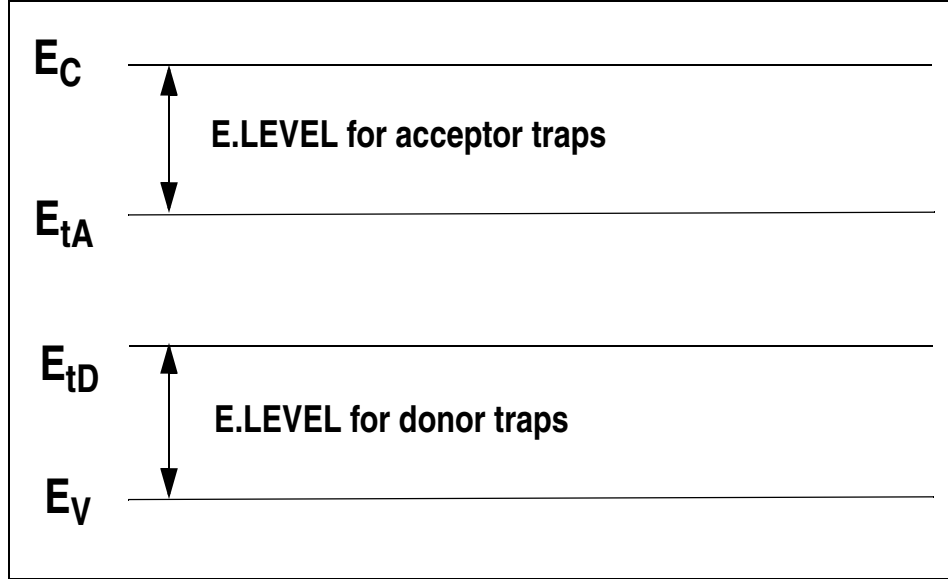


Figure 3-1: Definition of the trap energy level for acceptor and donor traps in reference to the conduction and valence band edges.

Calculation of Trapped Charge in Poisson's Equation

The total charge caused by the presence of traps is subtracted from the right hand side of Poisson's equation. The total charge value is defined by:

$$Q_T = q(N_{tD}^+ - N_{tA}^-) \quad 3-61$$

where N_{tD}^+ and N_{tA}^- are the densities of ionized donor-like and acceptor-like traps respectively. The ionized density depends upon the trap density, DENSITY, and its probability of ionization, F_{tA} and F_{tD} . For donor-like and acceptor-like traps respectively, the ionized densities are calculated by the equations:

$$N_{tD}^+ = \text{DENSITY} \times F_{tD} \quad 3-62$$

$$N_{tA}^- = \text{DENSITY} \times F_{tA} \quad 3-63$$

In the case where multiple traps at multiple trap energy levels are defined the total charge becomes:

$$N_{tD}^+ = \sum_{\alpha=1}^k N_{tD\alpha}^+, N_{tA}^- = \sum_{\beta=1}^m N_{tA\beta}^- \quad 3-64$$

where k is the number of donor-like traps and m is the number of acceptor-like traps.

The probability of ionization assumes that the capture cross sections are constant for all energies in a given band and follows the analysis developed by Simmons and Taylor [216]. The probability of ionization is given by the following equations for acceptor and donor-like traps.

$$F_{tA} = \frac{v_n \text{SIGN } n + e_{pA}}{v_n \text{SIGN } n + v_p \text{SIGP } p + e_{nA} + e_{pA}} \quad 3-65$$

$$F_{tD} = \frac{v_p \text{SIGP } p + e_{nD}}{v_n \text{SIGN } n + v_p \text{SIGP } p + e_{nD} + e_{pD}} \quad 3-66$$

where SIGN and SIGP are the carrier capture cross sections for electrons and holes respectively, v_n and v_p are the thermal velocities for electrons and holes. For donor like traps, the electron and hole emission rates, e_{nD} and e_{pD} , are defined by:

$$e_{nD} = \frac{1}{\text{DEGEN.FAC}} v_n \text{SIGN } n_i \exp \frac{E_t - E_i}{kT_L} \quad 3-67$$

$$e_{pD} = \text{DEGEN.FAC } v_p \text{SIGP } n_i \exp \frac{E_i - E_t}{kT_L} \quad 3-68$$

where E_i is the intrinsic Fermi level position, E_t is the trap energy level as defined by E.LEVEL and DEGEN.FAC is the degeneracy factor of the trap center. The latter term takes into account that spin degeneracy will exist, that is the “empty” and “filled” conditions of a defect will normally have different spin and orbital degeneracy choices. For acceptor like traps, the electron and hole emission rates, e_{nA} and e_{pA} , are defined by:

$$e_{nA} = \text{DEGEN.FAC } v_n \text{SIGN } n_i \exp \frac{E_t - E_i}{kT_L} \quad 3-69$$

$$e_{pA} = \frac{1}{\text{DEGEN.FAC}} v_p \text{SIGP } n_i \exp \frac{E_i - E_t}{kT_L} \quad 3-70$$

Table 3-7. User-Specifiable Parameters for Equations 3-62 to 3-68

| Statement | Parameter | Units |
|-----------|-----------|------------------|
| TRAP | E.LEVEL | eV |
| TRAP | DENSITY | cm ⁻³ |
| TRAP | DEGEN.FAC | |
| TRAP | SIGN | cm ² |
| TRAP | SIGP | cm ² |

Trap Implementation into Recombination Models

To maintain self-consistency, you need to take into account that electrons are being emitted or captured by the donor and acceptor-like traps. Therefore, the concentration of carriers will be affected. This is accounted for by modifying the recombination rate in the carrier continuity equations.

The standard SRH recombination term (see “Shockley-Read-Hall (SRH) Recombination” section on page 3-85) is modified as follows:

$$R = \sum_{\alpha=1}^l R_{D\alpha} + \sum_{\beta=1}^m R_{A\beta} \quad 3-71$$

where l is the number of donor-like traps, m is the number of acceptor-like traps. For donor-like traps, the function R is:

$$R_{D\alpha} = \frac{pn - n_{ie}^2}{\text{TAUN} \left[p + \text{DEGEN} \cdot \text{FAC} n_{ie} \exp\left(\frac{E_i - E_t}{kT_L}\right) \right] + \text{TAUP} \left[n + \frac{1}{\text{DEGEN} \cdot \text{FAC}} n_{ie} \exp\left(\frac{E_t - E_i}{kT_L}\right) \right]} \quad 3-72$$

For acceptor like traps the function R is:

$$R_{A\beta} = \frac{pn - n_{ie}^2}{\text{TAUN} \left[p + \frac{1}{\text{DEGEN} \cdot \text{FAC}} n_{ie} \exp\left(\frac{E_i - E_t}{kT_L}\right) \right] + \text{TAUP} \left[n + \text{DEGEN} \cdot \text{FAC} n_{ie} \exp\left(\frac{E_t - E_i}{kT_L}\right) \right]} \quad 3-73$$

The electron and hole lifetimes TAUN and TAUP are related to the carrier capture cross sections SIGN and SIGP through the equations:

$$\text{TAUN} = \frac{1}{\text{SIGN} v_n \text{DENSITY}} \quad 3-74$$

$$\text{TAUP} = \frac{1}{\text{SIGP} v_p \text{DENSITY}} \quad 3-75$$

The thermal velocities v_n and v_p are calculated from the following electron and hole effective masses.

$$v_n = \left(\frac{3kT}{m_n m_0} \right)^{1/2} \quad 3-76$$

$$v_p = \left(\frac{3kT}{m_p m_0} \right)^{1/2} \quad 3-77$$

To specify the effective masses directly, use the M.VTHN and M.VTHP parameters from the **MATERIAL** statement. If M.VTHN or M.VTHP or both are not specified, the density of states effective mass is extracted from the density of states (N_c or N_v) using Equations 3-31 and 3-32. In the case of silicon if M.VTHN or M.VTHP are not specified, the effective masses are calculated from:

$$m_n = 1.045 + 4.5 \times 10^{-4} T \quad 3-78$$

$$m_p = 0.523 + 1.4 \times 10^{-3} T - 1.48 \times 10^{-6} T^2 \quad 3-79$$

where T is the lattice temperature.

Table 3-8. User-Specifiable Parameters for Equations 3-72-3-75

| Statement | Parameter | Units |
|-----------|-----------|-------|
| TRAP | TAUN | s |
| TRAP | TAUP | s |

The TRAP statement activates the model and is used to:

- Specify the trap type DONOR or ACCEPTOR
- Specify the energy level E.LEVEL parameter
- Specify the density of the trap centers DENSITY
- Specify the degeneracy factor DEGEN.FAC
- Specify either the cross sections, SIGN and SIGP, or the electron and hole lifetimes TAUN and TAUP.

Trap-Assisted Tunneling

Trap-Assisted Tunneling models the trap-to-band phonon-assisted tunneling effects for Dirac wells. At high electric fields, tunneling of electrons from the valence band to the conduction band through trap or defect states can have an important effect on the current.

Trap-assisted tunneling is modeled by including appropriate enhancement factors [99] (Γ_n^{DIRAC} and Γ_p^{DIRAC}) in the trap lifetimes in Equation 3-72. These enhancement factors modify the lifetimes so that they include the effects of phonon-assisted tunneling on the emission of electrons and holes from a trap. This model is enabled by specifying TRAP.TUNNEL in the MODELS statement.

For donor like traps, the recombination term for traps becomes:

$$R_D = \frac{pn - n_{ie}^2}{\frac{TAUN}{1 + \Gamma_n^{DIRAC}} \left[p + DEGEN.FAC n_{ie} \exp\left(\frac{E_i - E_t}{kT_L}\right) \right] + \frac{TAUP}{1 + \Gamma_p^{DIRAC}} \left[n + \frac{1}{DEGEN.FAC} n_{ie} \exp\left(\frac{E_t - E_i}{kT_L}\right) \right]} \quad 3-80$$

For acceptor like traps, the recombination term becomes:

$$R_A = \frac{pn - n_{ie}^2}{\frac{TAUN}{1 + \Gamma_n^{DIRAC}} \left[p + \frac{1}{DEGEN.FAC} n_{ie} \exp\left(\frac{E_i - E_t}{kT_L}\right) \right] + \frac{TAUP}{1 + \Gamma_p^{DIRAC}} \left[n + DEGEN.FAC n_{ie} \exp\left(\frac{E_t - E_i}{kT_L}\right) \right]} \quad 3-81$$

The field-effect enhancement term for electrons is given by:

$$\Gamma_n^{DIRAC} = \frac{1}{kT_L} \int_0^1 \exp\left(\frac{\Delta E n}{kT_L} u - K_n u^{3/2}\right) du \quad 3-82$$

while the field-effect enhancement term for hole is:

$$\Gamma_p^{DIRAC} = \frac{1}{kT_L} \int_0^1 \exp\left(\frac{\Delta E p}{kT_L} u - K_p u^{3/2}\right) du \quad 3-83$$

where u is the integration variable, ΔE_n is the energy range where tunneling can occur for electrons, ΔE_p is the tunneling energy range for holes, and K_n and K_p are defined as:

$$K_n = \frac{4}{3} \sqrt{\frac{2m_0^{\text{MASS.TUNNEL}} \Delta E_n^3}{q \hbar |E|}} \quad 3-84$$

$$K_p = \frac{4}{3} \sqrt{\frac{2m_0^{\text{MASS.TUNNEL}} \Delta E_p^3}{q \hbar |E|}} \quad 3-85$$

\hbar is the reduced Planck's constant, m_0 is the rest mass of an electron and `MASS.TUNNEL` is the effective mass. You can specify `MASS.TUNNEL` by setting the `MASS.TUNNEL` parameter in the `MODELS` statement.

Table 3-9 shows the user-specifiable parameter for Equations 3-84 and 3-85.

| Table 3-9. User-Specifiable Parameters for Equations 3-84 and 3-85 | | | |
|--|-------------|---------|-------|
| Statement | Parameter | Default | Units |
| MODELS | MASS.TUNNEL | 0.25 | |

Non-local Trap Assisted Tunneling

The Trap-assisted-tunneling model in the previous section uses values of the field effect enhancement factors I_n^{DIRAC} and I_p^{DIRAC} which are approximate. They are evaluated using an approximation for the tunneling probability. It is assumed that the value at each node point depends only on the local field strength there, and that the field is assumed to be constant over the range of the tunneling. This gives Airy function solutions for the tunneling probabilities. A further approximation is also made by replacing the Airy function with the leading term of its high field asymptotic behavior. The integration over allowed tunneling energies is also evaluated approximately. A more accurate expression for I_n^{DIRAC} is

$$I_n^{\text{DIRAC}} = \frac{1}{kT} \int_0^{\Delta E_n} e^{E/kT} T(E) dE \quad 3-86$$

where $T(E)$ is the probability that an electron with energy E tunnels elastically to the conduction band from the trap position.

The exponential term gives the probability that the electron will gain energy $(\Delta E_n - E)$ from phonon interactions before tunneling. In Equation 3-86, the reference of energy is the conduction band edge and ΔE_n is the maximum energy below this for which the tunneling is possible, or the trap depth if less than this maximum (see Figure 3-2). There is a similar expression for holes. The tunneling probability is evaluated using a Wentzel-Kramers-Brillouin (WKB) method. The integral in Equation 3-86 is evaluated numerically in order to give the I_n^{DIRAC} and I_p^{DIRAC} terms.

The trap energy is at the Intrinsic Fermi energy in each material, unless you specify the parameter `TAT.NLDEPTH` on the `MODELS` statement. `TAT.NLDEPTH` has units of energy in Electron Volts. If you specify `TAT.NLDEPTH` and `TAT.RELEI` on the `MODELS` statement, then the value of `TAT.NLDEPTH` will be added to the Intrinsic Fermi energy to give the trap energy level. If `TAT.NLDEPTH` is specified without

TAT.RELEI, then the trap energy is calculated by subtracting TAT.NLDEPTH from the conduction band energy as follows:

$$E_T = E_c - \text{TAT.NLDEPTH} \quad 3-87$$

To model Trap Assisted Tunneling through heterojunctions, you must use the TAT.RELEI parameter if you want to use the TAT.NLDEPTH parameter.

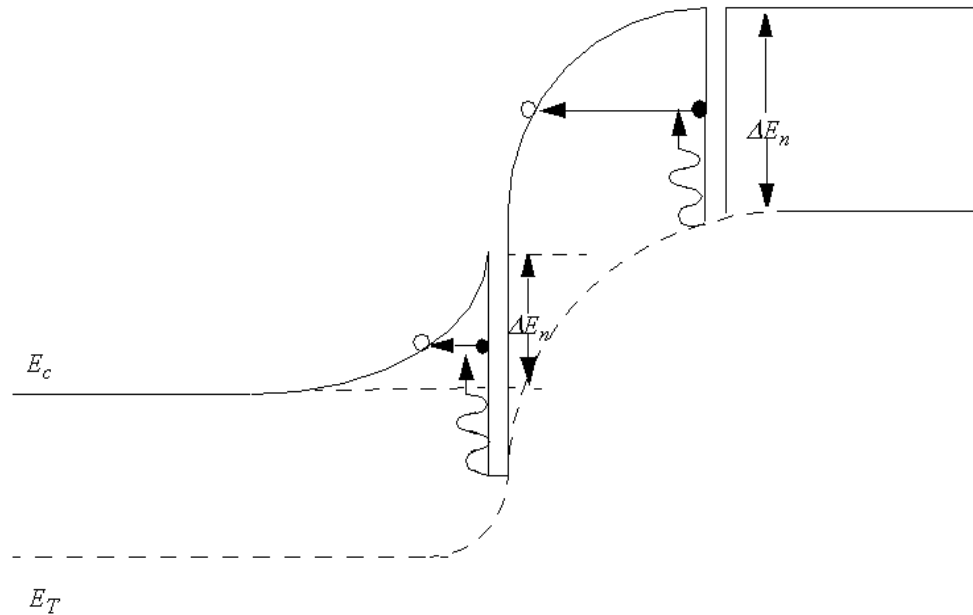


Figure 3-2: Schematic of Phonon assisted electron tunneling from a trap to the conduction band

The Γ_n^{DIRAC} and Γ_p^{DIRAC} terms are then used in Equations 3-80 and 3-81. The values of wavevector used in the tunneling probability calculation are evaluated using the density of states effective mass. To use different masses, then use the ME.TUNNEL and MH.TUNNEL parameters on the MATERIAL statement. Using ME and MV on the MATERIAL statement will also change the masses used but may affect the behavior of other models. For example, if you specify both ME and ME.TUNNEL, the evaluation of the Γ factor will use the value of ME.TUNNEL.

To use this model, specify an extra rectangular mesh encompassing the region where the Γ terms are to be evaluated. To position the special mesh, use the QTX.MESH and QTY.MESH statement. You must then set the required direction of the quantum tunneling using the QTUNN.DIR parameter on the MODELS statement. Outside this mesh, the local model of the previous section will be used to evaluate the Γ terms.

For example

```
qtx.mesh loc=0.0 spac=0.01
qtx.mesh loc=1.0 spac=0.01

qty.mesh loc=1.0 spac=1.0
qty.mesh loc=9.0 spac=1.0
```


will set up a mesh in the rectangle bounded by $x=0.0$, $x=1.0$, $y=1.0$ and $y=9.0$. The tunneling will be assigned to be in the X direction using the `QTUNN.DIR (=1)` parameter on the `MODELS` statement. All the required values are interpolated from the values on the `ATLAS` mesh. In this case, they are interpolated onto each slice in the X direction.

You can also use one or more `QTREGION` statements to set up the special meshes required for this model. The syntax is exactly the same as described in the “Non-local Band-to-Band Tunneling” section on page 3-119. This enables you to model non-local Trap-Assisted tunneling for more than one p-n junction and for p-n junctions with complicated shapes.

To enable the model, specify `TAT.NONLOCAL` on the `MODELS` statement. You also need to specify `QTUNN.DIR` on the `MODELS` statement to determine the direction of tunneling if you have used `QTX.MESH` and `QTY.MESH` to set up the special mesh.

To output the calculated values of Γ_n^{DIRAC} and Γ_p^{DIRAC} to a structure file, specify `NLTAT.GAMMA` on the `OUTPUT` statement. This allows you to visualize their values when interpolated back onto the device mesh.

Table 3-10. Non-local Trap Assisted Tunneling Parameters for the MODELS Statements

| Parameter | Type | Default |
|---------------------------|---------|---------|
| <code>TAT.RELEI</code> | Logical | False |
| <code>TAT.NONLOCAL</code> | Logical | False |
| <code>TAT.NLDEPTH</code> | Real | 0 |
| <code>QTUNN.DIR</code> | Real | 0 |

Table 3-11. Non-local Trap Assisted Tunneling Parameters for the MATERIAL Statement

| Parameter | Type | Default |
|------------------------|------|---------|
| <code>ME.TUNNEL</code> | Real | |
| <code>MH.TUNNEL</code> | Real | |

Poole-Frenkel Barrier Lowering for Coulombic Wells

The Poole-Frenkel barrier lowering effect enhances the emission rate for trap-to-band phonon-assisted tunneling as well as pure thermal emissions at low electric fields. The Poole-Frenkel effect occurs when the Coulombic potential barrier is lowered due to the electric field, and only occurs when there is a Coulomb interaction between the trap and the carrier.

The following interactions are Coulombic.

- Between an empty (positive) donor-type trap and an electron.
- Between a filled (negative) acceptor-type trap and a hole.

The following interactions are short-range (Dirac).

Between a filled (neutral) donor-type trap and a hole.

Between an empty (neutral) acceptor-type trap and an electron.

The Poole-Frenkel effect is modeled by including field-effect enhancement for Coulombic wells (Γ_n^{COUL} and Γ_p^{COUL}) and thermal emission (χ_F) [144] in the trap lifetimes in Equation 3-72. The trap-assisted tunneling effects for Dirac wells remains unmodified. To enable this model, specify `TRAP.COULOMBIC` in the `MODELS` statement.

The recombination term for traps now becomes:

$$R_A = \frac{pn - n_{ie}^2}{\frac{TAUN}{\chi_F + \Gamma_n^{COUL}} \left[p + \frac{1}{DEGEN.FAC} n_{ie} \exp\left(\frac{E_i - E_t}{kT_L}\right) \right] + \frac{TAUP}{1 + \Gamma_p^{DIRAC}} \left[n + DEGEN.FAC n_{ie} \exp\left(\frac{E_t - E_i}{kT_L}\right) \right]} \quad 3-88$$

$$R_D = \frac{pn - n_{ie}^2}{\frac{TAUN}{1 + \Gamma_n^{DIRAC}} \left[p + DEGEN.FAC n_{ie} \exp\left(\frac{E_i - E_t}{kT_L}\right) \right] + \frac{TAUP}{\chi_F + \Gamma_p^{COUL}} \left[n + \frac{1}{DEGEN.FAC} n_{ie} \exp\left(\frac{E_t - E_i}{kT_L}\right) \right]} \quad 3-89$$

where the Poole-Frenkel thermal emission enhancement factor, χ_F , is given by:

$$\chi_F = A.TRAPCOULOMBIC \exp\left(\frac{\Delta E_{fp}}{kT_L}\right) \quad 3-90$$

ΔE_{fp} is the barrier lowering term for a Coulombic well (see Equation 3-91).

$$\Delta E_{fp} = \sqrt{\frac{B.TRAPCOULOMBIC q^3 |E|}{\pi \epsilon}} \quad 3-91$$

The Coulombic field-enhancement terms, Γ_n^{COUL} and Γ_p^{COUL} , are defined as:

$$\Gamma_n^{COUL} = \frac{\Delta E n}{kT_L} \int_{\frac{\Delta E_{fp}}{\Delta E_n}}^1 \exp\left(\frac{\Delta E n}{KT_L} u - k_p u^{3/2} \left[1 - \left(\frac{\Delta E_{fp}}{u \Delta E_n} \right)^{5/3} \right]\right) du \quad 3-92$$

$$\Gamma_p^{COUL} = \frac{\Delta E p}{kT_L} \int_{\frac{\Delta E_{fp}}{\Delta E_p}}^1 \exp\left(\frac{\Delta E p}{KT_L} u - k_p u^{3/2} \left[1 - \left(\frac{\Delta E_{fp}}{u \Delta E_p} \right)^{5/3} \right]\right) du \quad 3-93$$

Table 3-12. User-Specifiable Parameters for Equations 3-90 and 3-91

| Statement | Parameter | Default | Units |
|-----------|-----------------|---------|-------|
| MATERIAL | A.TRAPCOULOMBIC | 1.0 | |
| MATERIAL | B.TRAPCOULOMBIC | 1.0 | |

Transient Traps

In the time domain the acceptor and donor traps do not reach equilibrium instantaneously but require time for electrons to be emitted or captured. This is taken account of inside ATLAS by solving an additional differential rate equation whenever a transient simulation is performed. These rate equations for donor and acceptor traps are given in Equations 3-94 and 3-95 [255]:

$$\begin{aligned} \frac{dN_{tD}^+}{dt} = & \text{DENSITY} \left\{ v_p \text{SIGP} \left[p(1 - F_{tD}) - F_{tD} n_i \text{DEGEN.FAC} \exp \frac{E_i - E_t}{kT} \right] \right. \\ & \left. - v_n \text{SIGN} \left[n F_{tD} - \frac{(1 - F_{tD}) n_i \exp \frac{E_t - E_i}{kT}}{\text{DEGEN.FAC}} \right] \right\} \end{aligned} \quad 3-94$$

$$\begin{aligned} \frac{dN_{tA}^-}{dt} = & \text{DENSITY} \left\{ v_n \text{SIGN} \left[n(1 - F_{tA}) - \text{DEGEN.FAC} F_{tA} n_i \exp \frac{E_t - E_i}{kT} \right] \right. \\ & \left. - v_p \text{SIGP} \left[p F_{tA} - \frac{(1 - F_{tA}) n_i \exp \frac{E_i - E_t}{kT}}{\text{DEGEN.FAC}} \right] \right\} \end{aligned} \quad 3-95$$

A transient trap simulation using this model is more time consuming than using the static model but gives a much more accurate description of the device physics. It may sometimes be acceptable to perform transient calculations using the static trap distribution and assume that traps reach equilibrium instantaneously. If this is the case, a flag (FAST) on the TRAP statement will neglect the trap rate equation from the simulation.

As may be seen from Equations 3-94 and 3-95, each trap species has a net electron capture rate and a net hole capture rate. The former arise from the terms proportional to $v_n \text{SIGN}$ and the latter from terms proportional to $v_p \text{SIGP}$. These capture rates enter the transient current continuity Equations 3-3 and 3-4 as components of the R_n and R_p terms respectively. In some circumstances, they will be generation rates rather than recombination rates, but by convention they are still referred to as R_n and R_p with negative values. In steady state, the trap occupation is constant and therefore the electron and hole capture rates are equal for each trap species. By substituting Equations 3-65 to 3-70 into the right hand sides of Equations 3-94 and 3-95, you obtain the expressions for steady state recombination, namely Equations 3-72 and 3-73. Under transient simulation conditions R_n and R_p have different values. This difference leads to the change over time of the trap occupation densities.

To view the values of R_n and R_p summed over the trap species present in a transient simulation, ATLAS provides two options. To output the rates to a standard structure file for SAVE statements, you specify U.TRANTRAP on the OUTPUT statement. You specify E.TRANTRAP on the PROBE statement to obtain a probe of R_n and H.TRANTRAP on the PROBE statement to obtain a probe of R_p .

| Table 3-13. Output of Transient Recombination Rates | | | |
|---|------------|---------|---------|
| Statement | Parameter | Type | Default |
| OUTPUT | U.TRANTRAP | Logical | False |
| PROBE | E.TRANTRAP | Logical | False |
| PROBE | H.TRANTRAP | Logical | False |

Hysteresis of Interface Traps

The default implementation of traps at a semiconductor-insulator interface assumes that the traps are located exactly at the interface. Their rate of response to changes in the energy of the Quasi-Fermi level in the semiconductor depends linearly on the values of the carrier capture cross-sections, `SIGN` and `SIGP`, as Equations 3-94 and 3-95 show.

In the `HEIMAN` model, the traps are assumed to have a uniform distribution in depth in the insulator [93]. They are further assumed to have values of `SIGN` and `SIGP` that depend on their distance into the insulator, d , as

$$\text{SIGN}(d) = \text{SIGN} e^{-\kappa_e d} \quad 3-96$$

$$\text{SIGP}(d) = \text{SIGP} e^{-\kappa_h d} \quad 3-97$$

where

$$\kappa_e^2 = \frac{2m_e^*(E_c - E_{tA})}{\hbar^2} \quad 3-98$$

and

$$\kappa_h^2 = \frac{2m_h^*(E_{tD} - E_v)}{\hbar^2} \quad 3-99$$

are the evanescent wavevectors of the semiconductor electron and hole states as they tunnel into the insulator. The capture cross-sections decrease with depth, d , in the insulator. Consequently the spatially deeper the trap, the more slowly it will respond to changes of carrier concentration at the semiconductor-insulator interface. For example, if the traps are initially full and the device is biased to empty them, then after a certain time the traps up to a certain depth will be empty and deeper traps will still be full. Heiman demonstrates that the transition distance between the two cases is very narrow with a length scale of approximately $1/(2\kappa_e)$ for electrons and $1/(2\kappa_h)$ for holes [93].

To enable this model you specify `HEIMAN` on the `INTTRAP` statement. The trap parameters are set up as usual for interface traps with the additional specification of the `DEPTH` parameter. This determines the extent of the uniform trap density distribution into the insulator and is in units of microns with a default value of 0.005 microns. The number of equally spaced internal points describing the internal trap distribution for each interface node is the `HPOINTS` parameter. This is optionally specified on the `INTTRAPS` statement and has a default value of 10. For each interface node, the trap distribution is calculated at each of the `HPOINTS` internal points. The average occupancy of the interface charge at each interface point is obtained by taking the arithmetic mean over these internal points.

These averages can be output by using the parameters `FTACC.TRAP` and `FTDON.TRAP` on the `PROBE` statement. The `PROBE` must be positioned on the semiconductor-insulator interface where hysteresis traps are present.

The `HEIMAN` model only applies to steady-state bias ramps at present. You must specify the total simulation timespan for the bias ramp using the `TIMESPAN` parameter on the `SOLVE` statement. The assumed time to sweep the bias through `VSTEP` volts is thus `VSTEP*TIMESPAN/(VFINAL-V(initial))` seconds. To simulate a hysteresis cycle, you need two consecutive `SOLVE` statements—one to ramp the voltage to the desired final value and the other to return it to the initial value. The value of `TIMESPAN` can be different for the two `SOLVE` statements. Any `SOLVE` statement executed without a `TIMESPAN` parameter will cause the trap occupation probabilities to be set to their steady-state values consistent with the device bias state.

Note: Changes in the quasi-Fermi levels at the semiconductor interface cause trap occupation changes up to a distance d into the insulator. Distance d depends on the natural logarithm of the measurement time `TIMESPAN` divided by the trap capture lifetime. Traps that are situated deep in the insulator therefore require a large value of `TIMESPAN`. The `DEPTH` parameter, therefore, should not be set to too high a value.

Table 3-14. Parameters for the HEIMAN Model

| Statement | Parameter | Type | Default | Units |
|-----------|-----------|---------|---------|---------------|
| INTTRAP | HEIMAN | Logical | False | |
| INTTRAP | DEPTH | Real | 5.0e-3 | μm |
| INTTRAP | HPOINTS | Real | 10 | |
| SOLVE | TIMESPAN | Real | | seconds |

3.4: The Energy Balance Transport Model

The conventional drift-diffusion model of charge transport neglects non-local transport effects such as velocity overshoot, diffusion associated with the carrier temperature and the dependence of impact ionization rates on carrier energy distributions. These phenomena can have a significant effect on the terminal properties of submicron devices. As a result ATLAS offers two non-local models of charge transport, the energy balance, and hydrodynamic models.

The Energy Balance Transport Model follows the derivation by Stratton [219,220] which is derived starting from the Boltzmann Transport Equation. By applying certain assumptions, this model decomposes into the hydrodynamic model [155,12,13].

The Energy Balance Transport Model adds continuity equations for the carrier temperatures, and treats mobilities and impact ionization coefficients as functions of the carrier temperatures rather than functions of the local electric field.

3.4.1: The Energy Balance Equations

The Energy Balance Transport Model introduces two new independent variables T_n and T_p , the carrier temperature for electrons and holes. The energy balance equations consist of an energy balance equation with the associated equations for current density and energy flux $\vec{S}_{n,p}$.

For electrons the Energy Balance Transport Model consists of:

$$\text{div} \vec{S}_n = \frac{1}{q} \vec{J}_n \cdot \vec{E} - W_n - \frac{3k}{2} \frac{\partial}{\partial t} (\lambda_n^* n T_n) \quad 3-100$$

$$\vec{J}_n = q D_n \nabla n - q \mu_n n \nabla \psi + q n D_n^T \nabla T_n \quad 3-101$$

$$\vec{S}_n = -K_n \nabla T_n - \left(\frac{k \delta_n}{q} \right) \vec{J}_n T_n \quad 3-102$$

and for holes:

$$\text{div} \vec{S}_p = \frac{1}{q} \vec{J}_p \cdot \vec{E} - W_p - \frac{3k}{2} \frac{\partial}{\partial t} (\lambda_p^* p T_p) \quad 3-103$$

$$\vec{J}_p = -q D_p \nabla p - q \mu_p p \nabla \psi - q p D_p^T \nabla T_p \quad 3-104$$

$$\vec{S}_p = -K_p \nabla T_p - \left(\frac{k \delta_p}{q} \right) \vec{J}_p T_p \quad 3-105$$

where \vec{S}_n and \vec{S}_p are the energy flux densities associated with electrons and holes, and μ_n and μ_p are the electron and hole mobilities.

The remaining terms, D_n and D_p , are the thermal diffusivities for electrons and holes as defined in Equations 3-106 and 3-113 respectively. W_n and W_p are the energy density loss rates for electrons and holes as defined in Equations 3-129 and 3-130 respectively. K_n and K_p are the thermal conductivities of electrons and holes as defined in Equations 3-110 and 3-117 respectively.

$$D_n = \frac{\mu_n k T_n}{q} \lambda_n^* \quad 3-106$$

$$\lambda_n^* = \frac{F(1/2)(\eta_n)}{F_{-1/2}(\eta_n)}, \quad \eta_n = \frac{\varepsilon F_n - \varepsilon_c}{k T_n} = F_{1/2}^{-1}\left(\frac{n}{N_c}\right) \quad 3-107$$

$$D_n^T = \left(\mu_{2n} - \frac{3}{2} \lambda_n^* \mu_n \right) \frac{k}{q} \quad 3-108$$

$$\mu_{2n} = \mu_n \left(\frac{5}{2} + \xi_n \right) \frac{F_{\xi_n} + 3/2(\eta_n)}{F_{\xi_n} + 1/2(\eta_n)} \quad 3-109$$

$$K_n = q \ n \ \mu_n \left(\frac{k}{q} \right)^2 \Delta_n T_n \quad 3-110$$

$$\Delta_n = \delta_n \left[\left(\xi_n + \frac{7}{2} \right) \frac{F_{\xi_n} + 5/2(\eta_n)}{F_{\xi_n} + 3/2(\eta_n)} - \left(\xi_n + \frac{5}{2} \right) \frac{F_{\xi_n} + 3/2(\eta_n)}{F_{\xi_n} + 1/2(\eta_n)} \right] \quad 3-111$$

$$\delta_n = \frac{\mu_{2n}}{\mu_n} \quad 3-112$$

Similar expressions for holes are as follows:

$$D_p = \frac{\mu_p k T_p}{q} \lambda_p^* \quad 3-113$$

$$\lambda_p^* = \frac{F(1/2)(\eta_p)}{F_{-1/2}(\eta_p)}, \quad \eta_p = \frac{\varepsilon_v - \varepsilon_f}{k T_p} = F_{1/2}^{-1}\left(\frac{p}{N_V}\right) \quad 3-114$$

$$D_p^T = \left(\mu_{2p} - \frac{3}{2} \lambda_p^* \mu_p \right) \frac{k}{q} \quad 3-115$$

$$\mu_{2p} = \mu_p \left(\frac{5}{2} + \xi_p \right) \frac{F_{\xi_p} + 3/2(\eta_p)}{F_{\xi_p} + 1/2(\eta_p)} \quad 3-116$$

$$K_p = q \ p \ \mu_p \left(\frac{k}{q} \right)^2 \Delta_p T_p \quad 3-117$$

$$\Delta_p = \delta_p \left[\left(\xi_p + \frac{7}{2} \right) \frac{F_{\xi_p} + 5/2(\eta_p)}{F_{\xi_p} + 3/2(\eta_p)} - \left(\xi_p + \frac{5}{2} \right) \frac{F_{\xi_p} + 3/2(\eta_p)}{F_{\xi_p} + 1/2(\eta_p)} \right] \quad 3-118$$

$$\delta_p = \frac{\mu_{2p}}{\mu_p} \quad 3-119$$

If Boltzmann statistics are used in preference to Fermi statistics, the above equations simplify to:

$$\lambda_n^* = \lambda_p^* = 1 \quad 3-120$$

$$\Delta_n = \delta_n = \left(\frac{5}{2} + \xi_n\right) \quad 3-121$$

$$\Delta_p = \delta_p = \left(\frac{5}{2} + \xi_p\right) \quad 3-122$$

$$\xi_n = \frac{d(\ln \mu_n)}{d(\ln T_n)} = \frac{T_n}{\mu_n} \frac{\partial \mu_n}{\partial T_n} \quad 3-123$$

$$\xi_p = \frac{d(\ln \mu_p)}{d(\ln T_p)} = \frac{T_p}{\mu_p} \frac{\partial \mu_p}{\partial T_p} \quad 3-124$$

The parameters ξ_n and ξ_p are dependent on the carrier temperatures. Different assumptions concerning ξ_n and ξ_p correspond to different non-local models. In the high-field saturated-velocity limit, that corresponds to velocity saturation, the carrier mobilities are inversely proportional to the carrier temperatures.

$$\xi_n = \xi_p = -1 \quad 3-125$$

and this corresponds to the Energy Balance Transport Model.

If instead the choice $\xi_n = \xi_p = 0$ was chosen this would correspond to the simplified Hydrodynamic Model. The parameters, ξ_n and ξ_p , can be specified using the KSN and KSP parameters on the MODELS statement.

Boundary conditions for n, p, and ψ are the same as for the drift diffusion model. Energy balance equations are solved only in the semiconductor region. Electron and hole temperatures are set equal to the lattice temperature on the contacts. On the other part of the boundary, the normal components of the energy fluxes vanish.

Hot carrier transport equations are activated by the MODELS statement parameters: HCTE.EL (electron temperature), HCTE.HO (hole temperature), and HCTE (both carrier temperatures).

3.4.2: Density of States

The calculation of the effective density of states is modified for the Energy Balance Transport Model. The electron and hole temperatures replace the lattice temperature in Equations 3-31 and 3-32. For example:

$$N_c = \left(\frac{2 \pi m_e^* k T_n}{h^2} \right)^{\frac{3}{2}} = \left(\frac{T_n}{300} \right)^{\frac{3}{2}} NC(300) \quad 3-126$$

$$N_v = \left(\frac{2 \pi m_n^* k T_p}{h^2} \right)^{\frac{3}{2}} = \left(\frac{T_p}{300} \right)^{\frac{3}{2}} NV(300) \quad 3-127$$

3.4.3: Energy Density Loss Rates

The energy density loss rates define physical mechanisms by which carriers exchange energy with the surrounding lattice environment. These mechanisms include carrier heating with increasing lattice temperature as well as energy exchange through recombination processes (SRH and Auger) and generation processes (impact ionization). If the net generation-recombination rate is written in the form:

$$U = R_{srh} + R_n^A + R_p^A - G_n - G_p \quad 3-128$$

where R_{srh} is the SRH recombination rate, R_n^A are R_p^A Auger recombination rates related to electrons and holes, G_n and G_p are impact ionization rates, then the energy density loss rates in Equations 3-100 and 3-103 can be written in the following form:

$$W_n = \frac{3}{2} n \frac{k(T_n - T_L)}{\text{TAUREL}.\text{EL}} \lambda_n + \frac{3}{2} k T_n \lambda_n R_{SRH} + E_g (G_n - R_n^A) \quad 3-129$$

$$W_p = \frac{3}{2} p \frac{k(T_p - T_L)}{\text{TAUREL}.\text{HO}} \lambda_p + \frac{3}{2} k T_p \lambda_p R_{SRH} + E_g (G_p - R_p^A) \quad 3-130$$

where

$$\lambda_n = F_{\frac{3}{2}}(\eta_n) / F_{\frac{1}{2}}(\eta_n) \quad 3-131$$

$$\lambda_p = F_{\frac{3}{2}}(\eta_p) / F_{\frac{1}{2}}(\eta_p) \quad 3-132$$

(and are equal to 1 for Boltzmann statistics), $\text{TAUREL}.\text{EL}$ and $\text{TAUREL}.\text{HO}$ are the electron and hole energy relaxation times, E_g is the bandgap energy of the semiconductor. The relaxation parameters are user-definable on the `MATERIAL` statement, which have their defaults shown in Table 3-15.

The relaxation times are extremely important as they determine the time constant for the rate of energy exchange and therefore precise values are required if the model is to be accurate. But, this is an unmeasurable parameter and Monte Carlo analysis is the favored method through which values can be extracted for the relaxation time.

It's also important to take into consideration that different materials will have different values for the energy relaxation time but within `ATLAS`, the relaxation time will always default to the value for silicon.

Table 3-15. User-Specifiable Parameters for Equations 3-129 and 3-130

| Statement | Parameter | Default | Units |
|-----------------------|------------------------|---------------------|-------|
| <code>MATERIAL</code> | <code>TAUREL.EL</code> | 4×10^{-13} | s |
| <code>MATERIAL</code> | <code>TAUREL.HO</code> | 4×10^{-13} | s |

3.4.4: Temperature Dependence of Relaxation Times

ATLAS doesn't provide an explicit default model for the temperature dependence of energy relaxation times. Two methods exist, however, to make the relaxation time a function of carrier energy.

For the first method, use a built-in model by specifying the `TRE.T1`, `TRE.T2`, `TRE.T3`, `TRE.W1`, `TRE.W2`, and `TRE.W3` parameters in the `MATERIAL` statement. Then, activate the electron temperature (electron energy) dependent energy relaxation time by using `E.TAUR.VAR` in the `MODELS` statement. Electron energy relaxation time will then be:

$$\tau_e = \begin{cases} \text{TRE.T1}, & W < \text{TRE.W1} \\ \text{TRE.T2}, & W = \text{TRE.W2} \\ \text{TRE.T3}, & W > \text{TRE.W3} \end{cases} \quad 3-133$$

where:

$$W = \frac{3}{2}kT_n \quad 3-134$$

For $\text{TRE.W1} < W < \text{TRE.W2}$ the energy relaxation time varies quadratically between `TRE.T1` and `TRE.T2`. For $\text{TRE.W2} < W < \text{TRE.W3}$ energy relaxation time varies quadratically between `TRE.T2` and `TRE.T3`. The corresponding parameter for hole energy relaxation time in the `MODELS` statement is `H.TAUR.VAR`. Other parameters are listed in Table 3-16.

| Table 3-16. User- Specifiable Parameters for Variable Energy Relaxation Time. | | | |
|---|-----------|------------------------|-------|
| Statement | Parameter | Default | Units |
| MATERIAL | TRE.T1 | 8×10^{-13} | s |
| MATERIAL | TRE.T2 | 1.92×10^{-12} | s |
| MATERIAL | TRE.T3 | 1×10^{-12} | s |
| MATERIAL | TRE.W1 | 0.06 | eV |
| MATERIAL | TRE.W2 | 0.3 | eV |
| MATERIAL | TRE.W3 | 0.45 | eV |
| MATERIAL | TRH.T1 | 1×10^{-12} | s |
| MATERIAL | TRH.T2 | 1×10^{-12} | s |
| MATERIAL | TRH.T3 | 1×10^{-12} | s |
| MATERIAL | TRH.W1 | 1×10^{10} | eV |
| MATERIAL | TRH.W2 | 1×10^{10} | eV |
| MATERIAL | TRH.W3 | 1×10^{10} | eV |

For the second method, use the C-INTERPRETER to apply a user-defined model for energy relaxation time as a function of carrier energy. In the MODELS statement, assign the F.TAURN and F.TAURP parameters with the names of external files that contain the user-defined C-INTERPRETER function for the energy relaxation time. You should also specify E.TAUR.VAR and H.TAUR.VAR flags in the MODELS statement when using C-INTERPRETER functions for the energy relaxation times.

3.4.5: Energy Dependent Mobilities

The Energy Balance Transport Model requires the carrier mobility to be related to the carrier energy. This has been achieved through the homogeneous steady state energy balance relationship that pertains in the saturated velocity limit. This allows an effective electric field to be calculated, which causes the carriers in a homogeneous sample to attain the same temperature as at the node point in the device. The effective electric fields, $E_{eff,n}$ and $E_{eff,p}$, are calculated by solving the equations:

$$q\mu_n(E_{eff,n})E_{eff,n}^2 = \frac{3}{2} \frac{k(T_n - T_L)}{TAUMOB.EL} \quad 3-135$$

$$q\mu_p(E_{eff,p})E_{eff,p}^2 = \frac{3}{2} \frac{k(T_p - T_L)}{TAUMOB.HO} \quad 3-136$$

for $E_{eff,n}$ and $E_{eff,p}$. These equations are derived from the energy balance equations by stripping out all spatially varying terms. The effective electric fields are then introduced into the relevant field dependent mobility model. A full description of the available models is given in Section 3.6.1: “Mobility Modeling”.

ATLAS2D provides a general C-interpreter function allowing you to specify carrier mobility as a function of Perpendicular field, carrier temperature, Lattice temperature, carrier concentration and donor and acceptor concentrations.

For electron mobility, the parameter is F.ENMUN, which can be set in either the MATERIAL or MOBILITY statement. The corresponding parameter for hole mobility is F.ENMUP, which can be set in either the MATERIAL or MOBILITY statement. The respective C-functions are `endepmun()` and `endepmup()`. The examples of these functions are provided in ATLAS.

3.5: Boundary Physics

ATLAS supports several boundary conditions: Ohmic contacts, Schottky contacts, insulated contacts, and Neumann (reflective) boundaries. Voltage boundary conditions are normally specified at contacts. Current boundary conditions can also be specified. Additional boundary conditions have been implemented to address the needs of specific applications. You can connect lumped elements between applied biases and semiconductor device contacts. A true distributed contact resistance is included to account for the finite resistivity of semiconductor contacts.

3.5.1: Ohmic Contacts

Ohmic contacts are implemented as simple Dirichlet boundary conditions, where surface potential, electron concentration, and hole concentrations (ψ_s , n_s , p_s) are fixed. Minority and majority carrier quasi-Fermi potentials are equal to the applied bias of the electrode (i.e., $\phi_n = \phi_p = V_{applied}$). The potential ψ_s is fixed at a value that is consistent with space charge neutrality. For example:

$$n_s + N_A^- = p_s + N_D^+ \quad 3-137$$

Equation 3-137 can be solved for ψ_s , n_s , and p_s , since ϕ_n and ϕ_p are known. If Boltzmann statistics are used, the substitution of Equations 3-36 and 3-37 into Equation 3-137 will yield:

$$n_s = \frac{1}{2} \left[\left(N_D^+ - N_A^- \right) + \sqrt{\left(N_D^+ - N_A^- \right)^2 + 4n_{ie}^2} \right] \quad 3-138$$

$$p_s = \frac{n_{ie}^2}{n_s} \quad 3-139$$

$$\psi_s = \phi_n + \frac{kT_L}{q} \ln \frac{n_s}{n_{ie}} = \phi_p - \frac{kT_L}{q} \ln \frac{p_s}{n_{ie}} \quad 3-140$$

Note: If you don't specify a work function, the contacts will be Ohmic regardless of its material.

3.5.2: Schottky Contacts

To specify a Schottky contact [193], specify a workfunction using the `WORKFUN` parameter of the `CONTACT` statement. The surface potential of the Schottky contact is given by:

$$\psi_s = \text{AFFINITY} + \frac{E_g}{2q} + \frac{kT_L}{2q} \ln \frac{N_C}{N_V} - \text{WORKFUN} + V_{applied} \quad 3-141$$

where `AFFINITY` is the electron affinity of the semiconductor material, E_g is the bandgap, N_C is the conduction band density of states, N_V is the valence band density of states, and T_L is the ambient temperature. In practice, the workfunction is defined as:

$$\text{WORKFUN} = \text{AFFINITY} + \phi_B \quad 3-142$$

where ϕ_B is the barrier height at the metal-semiconductor interface in eV.

Table 3-17. User-Specifiable Parameters for Equation 3-142

| Statement | Parameter | Units |
|-----------|-----------|-------|
| CONTACT | WORKFUN | eV |
| MATERIAL | AFFINITY | eV |

For example, if the Schottky contact were aluminum with a workfunction difference to the silicon of 4.2 eV and a barrier height of 0.7eV, then you would define the Schottky contact with the statement:

```
CONTACT NAME=GATE WORKFUN=4.9
```

Note: You can also define the workfunction using a C-Interpreter function. This function is referenced by the F.WORKE parameter of the CONTACT statement. The function defines workfunction as a function of electric field.

You can enable the thermionic emission model by specifying any of the following parameters of the CONTACT statement: SURF.REC, E.TUNNEL, VSURFN, VSURFP, or BARRIERL. In this case, the quasi-Fermi levels, ϕ_n and ϕ_p , are no longer equal to $V_{applied}$. Instead, these parameters are defined by a current boundary conditions at the surface [52]:

$$J_{sn} = qVSURFN(n_s - n_{eq})\exp\left(\frac{\Delta\phi_b}{kT}\right) \quad 3-143$$

$$J_{sp} = qVSURFP(p_s - p_{eq})\exp\left(\frac{\Delta\phi_b}{kT}\right) \quad 3-144$$

Table 3-18. User-Specifiable Parameters for Equations 3-143 to 3-144

| Statement | Parameter | Units |
|-----------|-----------|-------|
| CONTACT | VSURFN | cm/s |
| CONTACT | VSURFP | cm/s |

where J_{sn} and J_{sp} are the electron and hole currents at the contact, n_s is the surface electron concentration and p_s is the surface hole concentrations. The terms, n_{eq} and p_{eq} , are the equilibrium electron and hole concentrations assuming infinite surface recombination velocity ($\phi_n = \phi_p = V_{applied}$). If VSURFN and VSURFP are not specified on the CONTACT statement, their values will be calculated using:

$$VSURFN = \frac{ARICHN T_L^2}{q N_C} \quad 3-145$$

$$VSURNP = \frac{ARICHP T_L^2}{q N_V} \quad 3-146$$

Table 3-19. User-Specifiable Parameters for Equations 3-145 to 3-146

| Statement | Parameter | Default | Units |
|-----------|-----------|---------|-----------------------------------|
| MATERIAL | ARICHN | 110 | A/cm ² /K ² |
| MATERIAL | ARICHP | 30 | A/cm ² /K ² |

Here, ARICHN and ARICHP are the effective Richardson constants for electrons and holes, taking account of quantum mechanical reflections and tunneling, N_C and N_V are the conduction and valence band density of states. The ARICHN and ARICHP parameters are user-definable as shown in Table 3-19 and N_C and N_V are functions of the lattice temperature, T_L , according to Equations 3-31 and 3-32.

The schottky thermionic emission model also accounts for field-dependent barrier-lowering mechanisms. These mechanisms are caused by image forces and possible static dipole layers at the metal-semiconductor interface [223]. If the barrier height is defined as:

$$\phi_{bn} = \text{WORKFUN} - \text{AFFINITY} \quad 3-147$$

$$\phi_{bp} = \text{AFFINITY} + \frac{E_g}{q} - \text{WORKFUN} \quad 3-148$$

With barrier lowering, the amount of energy by which these barrier heights are lowered is defined by:

$$\Delta\phi_b = \text{BETA} \left[\frac{q}{4\pi\epsilon_s} \right]^2 E^{1/2} + \text{ALPHA} \times E^{\text{GAMMA}} \quad 3-149$$

Table 3-20. User-Specifiable Parameters for Equation 3-149

| Statement | Parameter | Default | Units |
|-----------|-----------|---------|-------|
| CONTACT | ALPHA | 0.0 | cm |
| CONTACT | BETA | 1.0 | |
| CONTACT | GAMMA | 1.0 | |

Here, E is the magnitude of the electric field at the interface and ALPHA is the linear, dipole barrier lowering coefficient. The Barrier Lowering Model can be turned on with the BARRIER parameter in the CONTACT statement. Typical values of ALPHA may be found in [10]. Note that the term with the square root dependence on electric field corresponds to the image force, while the linear term corresponds to the Dipole Effect [223].

Thermionic emission is implemented on a triangle-by-triangle basis, which means using the surface recombination velocity and geometrical data. A thermionic emission component is then calculated for each triangle so that an element of interest is connected. Using the electric field for each triangle, an adjusted recombination thermionic emission term can be computed if barrier lowering is incorporated. This is in contrast to where a single field value for the electrode node is used to compute total thermionic emission value [199].

You can take electron or hole tunneling through the barrier into account by specifying the `E.TUNNEL` or `H.TUNNEL` parameter in the `CONTACT` statement. The electron tunneling current (J_{tn}) is given by the Tsu-Esaki Model (Equation 3-150) and is applied to the contact as a current boundary condition.

$$J_{tn} = -\frac{4 \pi q \text{ME.TUNNEL } m_0 k T_L}{h^3} \int_0^{\phi_{bn}} P(E_Z) N(E_Z) dE_Z \quad 3-150$$

Here, ϕ_{bn} is the barrier height, `ME.TUNNEL` is the relative effective mass for electrons, m_0 is the electron rest mass, h is Planck's constant, k is Boltzmann's constant, q is the electron charge, and $N(E_Z)$ is given by:

$$N(E_Z) = \ln \left(\frac{1 + e^{\left(\frac{E_F - E_Z}{k T_L} \right)}}{1 + e^{\left(\frac{E_F - E_Z - qV}{k T_L} \right)}} \right) \quad 3-151$$

The transmission probability $P(E_Z)$ is given by the *WKB* [223] approximation for a triangular barrier and is expressed as:

$$P(E_Z) = \exp \left(\frac{-8 \pi (2 \text{ME.TUNNEL } m^*)^{\frac{1}{2}} (\phi_{bn} - E_Z)^{\frac{3}{2}}}{3 q h E} \right) \quad 3-152$$

The `ME.TUNNEL` parameter is user-definable in the `CONTACT` statement.

Similar expressions for Equations 3-150 through 3-152 exist for hole tunneling. You can specify the `MH.TUNNEL` parameter on the `CONTACT` statement for the hole relative mass for tunneling.

For example, to specify a thermionic emission schottky contact with tunneling and barrier lowering, the command would be:

```
CONTACT NAME=GATE SURF.REC E.TUNNEL BARRIER
```

Parabolic Field Emission Model

For wide bandgap materials such as SiC the parabolic field emission model is suggested [51,67]. Equation 3-153 describes the current as a function of applied bias voltage V . Equation 3-154 describes the tunneling probability $T(E)$.

$$J = \frac{A^*T}{k_B} \int_0^\infty T(E) \ln \left[\frac{1 + \exp\left(\frac{-E - E_n}{k_B T}\right)}{1 + \exp\left(\frac{-E - qV - E_n}{k_B T}\right)} \right] dE \quad 3-153$$

$$T(E) = \begin{cases} \exp\left(\frac{2}{\hbar q} \sqrt{\frac{m^* e}{N}} \left[E \ln \left(\frac{\sqrt{E_b^*} + \sqrt{E_b^* - E}}{\sqrt{E}} \right) - \sqrt{E_b^*} \sqrt{E_b^* - E_b} \right] \right) & \text{for } (E < E_b^*) \\ 1 & \text{for } (E > E_b^*) \end{cases} \quad 3-154$$

Here A^* is Richardson's constant, E_b is the barrier height on the metal side, N is the semiconductor doping concentration, $E_n = E_c - E_f = kT^* \ln(N_c/N)$ is the quasi fermi level energy $V_{bi} = (E_b - E_n)/q$ is the built in voltage, and $E_b^* = q(V_{bi} - V) = E_b - E_n - qV$ is the barrier height on the semiconductor side.

Richardson's constant A^* is given by $\frac{4\pi m^* q k^2}{h^3}$ where m is the effective mass.

The effective mass is generally taken from the density of states. You can, however, specify a mass for this tunneling calculation only by the `ME.TUNNEL` and `MH.TUNNEL` parameters of the `CONTACT` statement. To enable the model, use the `PARABOLIC` parameter of the `CONTACT` statement. To turn on the tunneling components independently for electrons and holes, specify the `E.TUNNEL` and `H.TUNNEL` parameters of the `CONTACT` statement. To enable the model, specify the `NSURF.REC` or `PSURF.REC` parameters of the `CONTACT` statement.

Universal Schottky Tunneling (UST) Model

In the Universal Schottky Tunneling (UST) Model [102, 152], the tunneling current is represented by localized tunneling rates at grid locations near the Schottky contact. For electrons, this is illustrated in Figure 3-3. The tunneling component of current can be described by Equation 3-155.

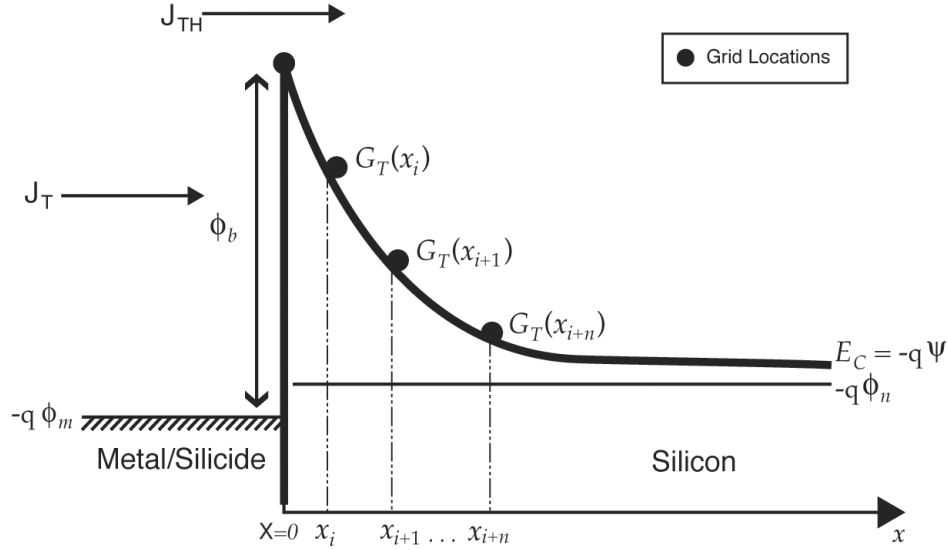


Figure 3-3: Local tunneling generation rate representation of the universal Schottky tunneling model

$$J_T = \frac{A^* T_L}{k} \int_{-\infty}^{\infty} \Gamma(E) \ln \left[\frac{1 + f_s(E)}{1 + f_m(E)} \right] dE \quad (3-155)$$

Here, J_T is the tunneling current density, A^* is the effective Richardson's coefficient, T_L is the lattice temperature, $\Gamma(E)$ is the tunneling probability, $f_s(E)$ and $f_m(E)$ are the Maxwell-Boltzmann distribution functions in the semiconductor and metal and E is the carrier energy.

You can then apply the transformation [102] given in Equation 3-156 to obtain the localized tunneling rates, G_T

$$G_T = \frac{1}{q} \nabla J_T \quad (3-156)$$

Applying the transformation given in Equations 3-155 and 3-156, you can obtain the expression given in Equation 3-157.

$$G_T = \frac{A^* T_L \vec{E}}{k} \Gamma(x) \ln \left[\frac{1 + n / \gamma_n N_c}{1 + \exp[-(E_c - E_{FM}) / k T_L]} \right] \quad (3-157)$$

Here, \vec{E} is the local electric field, n is the local electron concentration, N_c is the local conduction band density of states, γ_n is the local Fermi-Dirac factor, E_c is the local conduction band edge energy and E_{FM} is the Fermi level in the contact.

The tunneling probability $\Gamma(x)$ can be described by Equation 3-158.

$$\Gamma(x) = \exp \left[\frac{-2\sqrt{2m}}{\hbar} \int_0^x (E_c(x') - E_c(x)) dx' \right] \quad (3-158)$$

In Equation 3-158, m is the electron effective mass for tunneling, and $E_c(x)$ is the conduction band edge energy as a function of position.

Assuming linear variation of E_c around a grid location, Equation 3-158 can be reduced to Equation 3-159.

$$\Gamma(x) = \exp\left[\frac{-4\sqrt{2m}\hbar}{3\hbar}(E_{FM} + q\phi_b - E_c(x))^{1/2}\right] \quad 3-159$$

In Equation 3-159, ϕ_b is the barrier height. Similar expressions to Equations 3-155 through 3-159 exist for holes.

To enable the universal Schottky tunneling model you should specify `UST` on the `MODELS` statement. You are also required to specify `SURF.REC` on the `CONTACT` statement for each contact that you wish the model to apply. Once enabled, this model automatically applies to both electrons and holes. For a given grid point, however, the model will only apply to one carrier according to the relative direction of the local electric field.

Once you enable the model, for each electrode with thermionic emission, the model will be applied to all grid points within a specified distance of the electrode. To specify this distance, use `D.TUNNEL` parameter of the `MATERIAL` statement. The default value of `D.TUNNEL` is 10^{-6} in units of cm.

Phonon-assisted Tunneling Model for GaN Schottky Diodes

It has been found that the reverse I-V characteristics of some Gallium Nitride (GaN) diodes can best be explained by using a phonon-assisted electron tunneling model [178]. The electrons are assumed to be emitted from local levels in the metal-semiconductor interface and give a contribution to the current of

$$J = Q_{PIP.NT} W \quad 3-160$$

where `PIP.NT` gives the occupied state density near the interface in units of cm^{-2} . The rate of phonon-assisted tunneling, W , is given by

$$W = \frac{qF}{8ME_{TUNNEL}PIP_{ET}} \left[(1 + \gamma^2)^{1/2} - \gamma \right]^{1/2} [1 + \gamma^2]^{-1/4} \quad 3-161$$

$$\times \exp\left\{ \frac{-4(2ME_{TUNNEL})^{1/2}}{3qF\hbar} PIP_{ET}^{3/2} \left[(1 + \gamma^2)^{1/2} - \gamma \right]^2 \times \left[(1 + \gamma^2)^{1/2} + \frac{\gamma}{2} \right] \right\}$$

where

$$\gamma = \frac{(2ME_{TUNNEL})^{1/2} \Gamma^2}{8q\hbar F(PIP_{ET})^{1/2}} \quad 3-162$$

F is the field strength at the interface and Γ is the energy width of the absorption band given by

$$\Gamma^2 = 8PIP_{ACC}(PIP_{OMEGA})^2 (2n + 1) \quad 3-163$$

and n is the phonon density.

To enable the model, use the keyword `PIPINYS` on the `CONTACT` statement. The default value of `PIP.NT` is 0 and so you must set a finite value for this quantity in order for the model to have any effect. The other parameters may be specified on the `MATERIAL` statement. Although the model was developed specifically for reverse bias current in GaN, ATLAS does not restrict use of the model to that material. `PIP.OMEGA` is the phonon energy, `PIP.ACC` is the electron-phonon interaction constant, and `PIP.ET` is the trap depth.

Table 3-21. User-Specifiable Parameters for the Pipinys model.

| Statement | Parameter | Type | Default | Units |
|-----------|-----------|------|---------|-----------------|
| MATERIAL | PIP.OMEGA | Real | 0.07 | eV |
| MATERIAL | PIP.ACC | Real | 2.0 | |
| MATERIAL | PIP.ET | Real | 1.0 | eV |
| MATERIAL | PIP.NT | Real | 0.0 | cm ² |

3.5.3: Floating Contacts

A contact that isn't connected to a current or voltage source and is totally insulated by dielectric is called a floating contact. ATLAS accounts for floating contacts such as floating gates in EPROM devices by using a distributed charge boundary condition, which is applied to all nodes of the floating electrode (see Equation 3-164).

$$\int_s D \cdot dS = Q_{FG} \quad 3-164$$

where D is the electric displacement vector, s represents the external surface of the floating gate, and Q_{FG} is the injected charge.

ATLAS performs an integration over the entire surface of the electrode and forces the potential on the floating nodes to produce the correct total charge on the electrode. The total charge when performing a simulation is by default zero but can be defined using the `SOLVE` statement. The total charge may change if you activate a Charge Injection Model. For more information about this model, see Section 3.6.6: "Gate Current Models". To define a contact as a floating contact, use:

```
CONTACT NAME=fgate FLOATING
```

Note: When specifying a floating contact, use the Newton scheme as the numerical technique. See Chapter 20: "Numerical Techniques", Section 20.5.1: "Newton Iteration".

3.5.4: Current Boundary Conditions

In some devices, the terminal current is a multi-valued function of the applied voltage. This means that for some voltage boundary conditions, the solution that is obtained depends on the initial guess. An example of this is the CMOS latch-up trigger point. At the trigger point the I-V curve changes from being flat to vertical and may exhibit a negative slope. The solution will then have three different solutions of current for one applied bias. The particular solution which the model finishes in will depend upon the initial conditions.

This trigger point is difficult to determine using a simple voltage boundary condition. In addition, it is almost impossible to compute any solutions in the negative resistance regime when using voltage boundary conditions. Some of these problems can be overcome using current boundary conditions.

Calculation of current boundary conditions is activated by the `CURRENT` parameter in the `CONTACT` statement.

The current boundary conditions are described by the Kirchhoff relation:

$$J_s - \Sigma(J_n + J_p) = 0 \quad 3-165$$

where J_s is the applied current, J_n and J_p are given by Equations 3-11 and 3-12, and the summation is taken over all grid points incident on the boundary. This relation is solved for the boundary potential. The ohmic conditions in Equations 3-138 and 3-139 apply for electron and hole concentrations.

The voltage boundary condition should be used in regions where dI/dV is small. The current boundary condition may be preferable for operating regimes where dI/dV is large. It is common for the negative resistance regime of a device to have a slope dI/dV very close to 0. Such behavior should be considered when using a current source to trace out an entire I-V curve. In these cases, use the `CURVETRACE` option in ATLAS.

Note: When a current boundary condition has been specified, choose the Newton numerical scheme on the `METHOD` statement. You can perform ac small signal analysis with current boundary conditions.

3.5.5: Insulating Contacts

Insulating contacts are contacts that are completely surrounded by insulator. They may be connected to a voltage source (tied contact) or they may be floating.

Insulating contacts that are connected to a voltage source generally have a work function that dictates a value for ψ_s similar to that given by Equation 3-141. Electron and hole concentrations within the insulator and at the insulating contact are forced to be zero (i.e., $n_s=p_s=0$).

3.5.6: Neumann Boundaries

Along the outer (non-contact) edges of devices, homogeneous (reflecting) Neumann boundary conditions are imposed so that current only flows out of the device through the contacts. In the absence of surface charge along such edges, the normal electric field component becomes zero. Current isn't permitted to flow from the semiconductor into an insulating region except via oxide tunneling models. At the interface between two different materials, the difference between the normal components of the respective electric displacements must be equal to any surface charge according to:

$$\hat{n} \cdot \epsilon_1 \nabla \psi_1 - \hat{n} \cdot \epsilon_2 \nabla \psi_2 = \rho_s \quad 3-166$$

where n is the unit normal vector, ϵ_1 and ϵ_2 are the permittivities of the materials on either side of the interface and ρ_s is the sheet charge at the interface.

3.5.7: Lumped Element Boundaries

ATLAS supports some simple configurations of lumped elements. These are indicated in Figure 3-4.

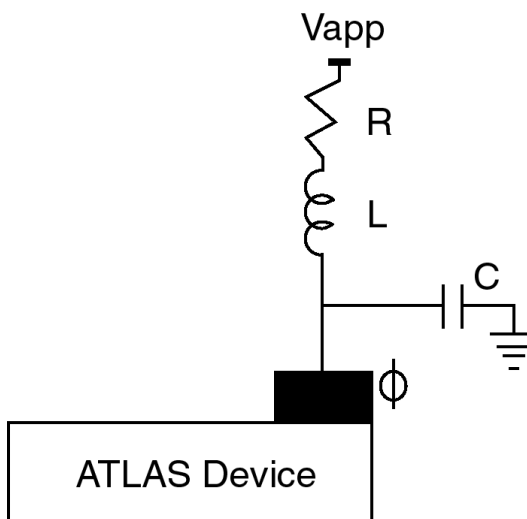


Figure 3-4: The Lumped elements supported by ATLAS

Lumped elements can be extremely useful when simulating CMOS or MOSFET structures. For example, the p-tub contact in the CMOS cross-section might be tens or hundreds of microns away from the active area of an embedded vertical npn bipolar transistor, which may only be 10-20 μm on a side. If the whole structure were simulated, a tremendous number of grid points (probably more than half) are essentially wasted in accounting for a purely resistive region of the device.

In the case of a MOSFET substrate, you would not want to include grid points all the way to the back side of a wafer. In either of these cases, a simple lumped resistance can be substituted [187].

Table 3-22 shows the user-specifiable parameters for Figure 3-4.

| Table 3-22. User-Specifiable Parameters for Figure 3-2. | | | |
|---|-----------|-------------|---------------------|
| Symbol | Statement | Parameter | Units |
| C | CONTACT | CAPACITANCE | F/ μm |
| R | CONTACT | RESISTANCE | $\Omega\mu\text{m}$ |
| L | CONTACT | INDUCTANCE | H μm |

Resistance is specified in $\Omega\mu\text{m}$, capacitance is specified in F/ μm , and inductance is specified in H μm .

The following combinations are possible: resistance only, resistance and capacitance, inductance and resistance and inductance, capacitance and resistance. For the case of inductance or capacitance only, ATLAS adds a small resistance as well. For more complicated circuit configurations, use the MIXEDMODE module of ATLAS.

The boundary condition for a lumped resistance boundary is analogous to the current boundary condition described in Section 3.5.4: “Current Boundary Conditions” and is given by:

$$\frac{V_a - V_s}{R} - \Sigma(J_n + J_p) = 0 \quad 3-167$$

where V_a is the applied potential, R is the lumped resistance, and J_n and J_p are the electron and hole currents given by Equations 3-11 and 3-12. V_s is the boundary potential or "internal bias" solution. The summation is taken over all grid points incident on the boundary. The ohmic conditions in Equations 3-138 and 3-139 apply for electron and hole concentrations.

Note: Capacitance increases with device width (into the Z plane) while resistance decreases. Except for the case of extremely large resistances where the arrangement becomes similar to a pure current source, no convergence degradation has been observed for a lumped element boundary in comparison to a simple Ohmic contact. Transient simulation therefore becomes easier and is more well-defined.

You should use the simulator to calculate any resistance (or capacitance) components that might be included as lumped elements. When performing CMOS simulations, you could simulate just the p-tub with Ohmic contacts at either end. From the plot of terminal current (in A/ μm) versus voltage, resistance can be directly extracted from the slope. Be very careful to consider any three-dimensional effects (e.g., current spreading) before using a resistance value in further simulations.

When looking at the results of simulation with lumped elements it's important to distinguish between the applied voltage (V_{app}) and the internal bias (ϕ) in the log file produced by ATLAS.

The lumped element boundary conditions can also be used with AC small signal analysis (see Section 20.9.2: "Fourier Analysis Of Transient Responses"). In this case, the driving voltage is a harmonic signal of small amplitude and the capacitance shown in Figure 3-4 is connected to AC ground. Because some of the AC current goes to this ground, the measured admittances may not always sum to zero.

An alternative circuit arrangement is also available. If you specify the `RESONANT` parameter on a `CONTACT` statement, then for that contact the capacitance will also be connected to the driving voltage.

In this case, the lumped elements form a parallel resonant circuit with the series resistor and inductance in parallel with the capacitance. Also in this case, current continuity will be explicitly satisfied.

The susceptance may be inductive rather than capacitive if inductors are present in the lumped elements. This manifests itself as a negative capacitance (i.e., the conductance and capacitance are of different signs). You can easily convert the output capacitance to an inductance using the formula

$$L = 1/(\omega^2 C) \quad 3-168$$

where ω is the angular frequency, C is the capacitance in farads and L the inductance in henrys.

3.5.8: Distributed Contact Resistance

Since contact materials have finite resistivities, the electrostatic potential isn't always uniform along the metal-semiconductor surface. To account for this effect, a distributed contact resistance can be associated with any electrode. This is in contrast to the lumped contact resistance described in the previous section.

ATLAS implements this distributed contact resistance by assigning a resistance value to each surface element associated with the contact. If each surface element is a different length, a different value for the contact resistance will be assigned. ATLAS calculates a resistance value of R_i for each surface element from the value of `CON.RESIST`, as specified on the `CONTACT` statement. The units of `CON.RESIST` are Ωcm^2 and R_i calculated as:

$$R_i = \frac{\text{CON.RESIST}}{d_i \text{ WIDTH}} \quad 3-169$$

where R_i is the resistance at node i , P_c is specified by the `CON.RESIST` parameter, d_i is the length of the contact surface segment associated with node i and `WIDTH` is the width of the device. The effect of the resistance, R_i is to add an extra equation to be satisfied to node i .

This equation is given by:

$$\frac{1}{R_i} \left[V_{\text{applied}} - \left(\psi_i \pm \frac{kT_L}{q} \ln(N/n_{ie}) \right) \right] - (I_n + I_p + I_{\text{disp}}) = 0 \quad 3-170$$

where V_{applied} is the external applied voltage, ψ_i is the surface potential, N is the net doping, n_i is the intrinsic electron concentration, and I_n , I_p , I_{disp} are the electron, hole and displacement currents at node i . This equation simply balances the current in and out of the resistor added to each i node.

As with the case for lumped elements, ATLAS can print out a value of contact resistance for each contact in the run time output. Since the actual value depends on the length of each surface segment for distributed contacts, ATLAS prints out the value of `CON.RESIST/WIDTH` which is the same for all contact surface segments. This runtime output is enabled by adding the `PRINT` option on the `MODELS` statement.

Table 3-23. User-Specifiable Parameters for Equation 3-169

| Statement | Parameter | Units |
|----------------------|-------------------------|----------------------|
| <code>CONTACT</code> | <code>CON.RESIST</code> | $\Omega\text{-cm}^2$ |
| <code>MESH</code> | <code>WIDTH</code> | μm |

Note: AC small signal analysis cannot be performed when any distributed contact resistance has been specified. Also, only the `NEWTON` numerical scheme should be chosen on the `METHOD` statement.

3.5.9: Energy Balance Boundary Conditions

When the Energy Balance Transport Model is applied, special boundary conditions are applied for carrier temperatures. By default at the contacts, Dirichlet boundary conditions are used for carrier temperatures:

$$T_n = T_p = T_L \quad 3-171$$

You can treat contacts as Neumann (reflective) boundaries with respect to carrier temperature by specifying `REFLECT` on the `CONTACT` statement.

Elsewhere on the boundary, the normal components of the energy fluxes vanish. The boundary conditions for (ψ, n, p) are the same as for the drift-diffusion model.

3.6: Physical Models

3.6.1: Mobility Modeling

Electrons and holes are accelerated by electric fields, but lose momentum as a result of various scattering processes. These scattering mechanisms include lattice vibrations (phonons), impurity ions, other carriers, surfaces, and other material imperfections. Since the effects of all of these microscopic phenomena are lumped into the macroscopic mobilities introduced by the transport equations these mobilities are therefore functions of the local electric field, lattice temperature, doping concentration, and so on.

Mobility modeling is normally divided into: (i) low-field behavior, (ii) high field behavior, (iii) bulk semiconductor regions and (iv) inversion layers.

The low electric field behavior has carriers almost in equilibrium with the lattice and the mobility has a characteristic low-field value that is commonly denoted by the symbol $\mu_{n0,p0}$. The value of this mobility is dependent upon phonon and impurity scattering. Both of which act to decrease the low-field mobility.

The high electric field behavior shows that the carrier mobility declines with electric field because the carriers that gain energy can take part in a wider range of scattering processes. The mean drift velocity no longer increases linearly with increasing electric field, but rises more slowly. Eventually, the velocity doesn't increase any more with increasing field but saturates at a constant velocity. This constant velocity is commonly denoted by the symbol v_{sat} . Impurity scattering is relatively insignificant for energetic carriers, and so v_{sat} is primarily a function of the lattice temperature.

Modeling mobility in bulk material involves: (i) characterizing μ_{n0} and μ_{p0} as a function of doping and lattice temperature, (ii) characterizing v_{sat} as a function of lattice temperature, and (iii) describing the transition between the low-field mobility and saturated velocity regions.

Modeling carrier mobilities in inversion layers introduces additional complications. Carriers in inversion layers are subject to surface scattering, extreme carrier-carrier scattering, and quantum mechanical size quantization effects. These effects must be accounted for in order to perform accurate simulation of MOS devices. The transverse electric field is often used as a parameter that indicates the strength of inversion layer phenomena.

You can define multiple non-conflicting mobility models simultaneously. You also need to know which models are over-riding when conflicting models are defined.

Low-Field Mobility Models

The low-field carrier mobility can be defined in five different ways.

The first way is use the `MUN` and `MUP` parameters to set constant values for electron and hole mobilities and optionally specify temperature dependence. The second way is by using a look-up table model (`CONMOB`) to relate the low-field mobility at 300K to the impurity concentration. The third way is by choosing the analytic low-field mobility models, `ANALYTIC`, `ARORA`, or `MASETTI`, to relate the low-field carrier mobility to impurity concentration and temperature. The fourth way is by choosing a carrier-carrier scattering model (`CCSMOB`, `CONWELL`, or `BROOKS`) that relates the low-field mobility to the carrier concentrations and temperature. The fifth way is to use a unified low-field mobility model (`KLAASSEN`) that relates the low-field mobility to donor, acceptor, lattice, carrier-carrier scattering, and temperature.

Constant Low-Field Mobility Model

In ATLAS, the choice of mobility model is specified on the `MODELS` statement. The parameters associated with mobility models are specified on a separate `MOBILITY` statement. One or more mobility models should always be specified explicitly. The default is to use constant low-field mobilities within each region of a device. This default model is independent of doping concentration, carrier densities and electric field. It does account for lattice scattering due to temperature according to:

$$\mu_{n0} = \text{MUN} \left(\frac{T_L}{300} \right)^{-\text{TMUN}} \quad 3-172$$

$$\mu_{p0} = \text{MUP} \left(\frac{T_L}{300} \right)^{-\text{TMUP}} \quad 3-173$$

where T is the lattice temperature. The low-field mobility parameters: `MUN`, `MUP`, `TMUN` and `TMUP` can be specified in the `MOBILITY` statement with the defaults as shown in Table 3-24.

| Table 3-24. User-Specifiable Parameters for the Constant Low-Field Mobility Model | | | |
|---|-----------|---------|---|
| Statement | Parameter | Default | Units |
| MOBILITY | MUN | 1000 | $\text{cm}^2 / (\text{V} \cdot \text{s})$ |
| MOBILITY | MUP | 500 | $\text{cm}^2 / (\text{V} \cdot \text{s})$ |
| MOBILITY | TMUN | 1.5 | |
| MOBILITY | TMUP | 1.5 | |

Concentration-Dependent Low-Field Mobility Tables

ATLAS provides empirical data for the doping dependent low-field mobilities of electrons and holes in silicon at $T_L=300\text{K}$ only. This data is used if the `CONMOB` parameter is specified in the `MODELS` statement. The data that is used is shown in Table 3-25.

| Table 3-25. Mobility of Electrons and Holes in Silicon at T=300K | | |
|--|--|-------|
| Concentration (cm^{-3}) | Mobility ($\text{cm}^2/\text{V} \cdot \text{s}$) | |
| | Electrons | Holes |
| 1.0×10^{14} | 1350.0 | 495.0 |
| 2.0×10^{14} | 1345.0 | 495.0 |
| 4.0×10^{14} | 1335.0 | 495.0 |
| 6.0×10^{14} | 1320.0 | 495.0 |
| 8.0×10^{14} | 1310.0 | 495.0 |
| 1.0×10^{15} | 1300.0 | 491.1 |
| 2.0×10^{15} | 1248.0 | 487.3 |

Table 3-25. Mobility of Electrons and Holes in Silicon at T=300K

| Concentration (cm ⁻³) | Mobility (cm ² /V·s) | |
|-----------------------------------|---------------------------------|--------|
| | Electrons | Holes |
| 4.0×10 ¹⁵ | 1200.0 | 480.1 |
| 6.0×10 ¹⁵ | 1156.0 | 473.3 |
| 8.0×10 ¹⁵ | 1115.0 | 466.9 |
| 1.0×10 ¹⁶ | 1076.0 | 460.9 |
| 2.0×10 ¹⁶ | 960.0 | 434.8 |
| 4.0×10 ¹⁶ | 845.0 | 396.5 |
| 6.0×10 ¹⁶ | 760.0 | 369.2 |
| 8.0×10 ¹⁶ | 720.0 | 348.3 |
| 1.0×10 ¹⁷ | 675.0 | 331.5 |
| 2.0×10 ¹⁷ | 524.0 | 279.0 |
| 4.0×10 ¹⁷ | 385.0 | 229.8 |
| 6.0×10 ¹⁷ | 321.0 | 2103.8 |
| 8.0×10 ¹⁷ | 279.0 | 186.9 |
| 1.0×10 ¹⁸ | 252.0 | 178.0 |
| 2.0×10 ¹⁸ | 182.5 | 130.0 |
| 4.0×10 ¹⁸ | 140.6 | 90.0 |
| 6.0×10 ¹⁸ | 113.6 | 74.5 |
| 8.0×10 ¹⁸ | 99.5 | 66.6 |
| 1.0×10 ¹⁹ | 90.5 | 61.0 |
| 2.0×10 ¹⁹ | 86.9 | 55.0 |
| 4.0×10 ¹⁹ | 83.4 | 53.7 |
| 6.0×10 ¹⁹ | 78.8 | 52.9 |
| 8.0×10 ¹⁹ | 71.6 | 52.4 |
| 1.0×10 ²⁰ | 67.8 | 52.0 |
| 2.0×10 ²⁰ | 52.0 | 50.8 |
| 4.0×10 ²⁰ | 35.5 | 49.6 |
| 6.0×10 ²⁰ | 23.6 | 48.9 |
| 8.0×10 ²⁰ | 19.0 | 48.4 |
| 1.0×10 ²¹ | 17.8 | 48.0 |

Analytic Low-Field Mobility Model

The following analytic function based upon the work of Caughey and Thomas [37, 208] can be used to specify doping- and temperature-dependent low-field mobilities.

$$\mu_{n0} = \text{MU1N.CAUG} \cdot \left(\frac{T_L}{300K} \right)^{\text{ALPHAN.CAUG}} \quad 3-174$$

$$+ \frac{\text{MU2N.CAUG} \cdot \left(\frac{T_L}{300K} \right)^{\text{BETAN.CAUG}} - \text{MU1N.CAUG} \cdot \left(\frac{T_L}{300K} \right)^{\text{ALPHAN.CAUG}}}{1 + \left(\frac{T_L}{300K} \right)^{\text{GAMMAN.CAUG}} \cdot \left(\frac{N}{\text{NCRITN.CAUG}} \right)^{\text{DELTAN.CAUG}}}$$

$$\mu_{p0} = \text{MU1P.CAUG} \cdot \left(\frac{T_L}{300K} \right)^{\text{ALPHAP.CAUG}} \quad 3-175$$

$$+ \frac{\text{MU2P.CAUG} \cdot \left(\frac{T_L}{300K} \right)^{\text{BETAP.CAUG}} - \text{MU1P.CAUG} \cdot \left(\frac{T_L}{300K} \right)^{\text{ALPHAP.CAUG}}}{1 + \left(\frac{T_L}{300K} \right)^{\text{GAMMAP.CAUG}} \cdot \left(\frac{N}{\text{NCRITP.CAUG}} \right)^{\text{DELTAP.CAUG}}}$$

where N is the local (total) impurity concentration in cm^{-3} and T_L is the temperature in degrees Kelvin.

This model is activated by specifying **ANALYTIC** in the **MODELS** statement. The parameters of this model are specified in the **MOBILITY** statement. The default parameters are for silicon at $T_L = 300\text{K}$.

Table 3-26. User-Specifiable Parameters for Equations 3-174 and 3-175

| Statement | Parameter | Default | Units |
|-----------|-------------|---------|---|
| MOBILITY | MU1N.CAUG | 55.24 | $\text{cm}^2 / (\text{V} \cdot \text{s})$ |
| MOBILITY | MU1P.CAUG | 49.7 | $\text{cm}^2 / (\text{V} \cdot \text{s})$ |
| MOBILITY | MU2N.CAUG | 1429.23 | $\text{cm}^2 / (\text{V} \cdot \text{s})$ |
| MOBILITY | MU2P.CAUG | 479.37 | $\text{cm}^2 / (\text{V} \cdot \text{s})$ |
| MOBILITY | ALPHAN.CAUG | 0.0 | arbitrary |
| MOBILITY | ALPHAP.CAUG | 0.0 | arbitrary |
| MOBILITY | BETAN.CAUG | -2.3 | arbitrary |
| MOBILITY | BETAP.CAUG | -2.2 | arbitrary |
| MOBILITY | GAMMAN.CAUG | -3.8 | arbitrary |

Table 3-26. User-Specifiable Parameters for Equations 3-174 and 3-175

| Statement | Parameter | Default | Units |
|-----------|-------------|------------------------|------------------|
| MOBILITY | GAMMAP.CAUG | -3.7 | arbitrary |
| MOBILITY | DELTAN.CAUG | 0.73 | arbitrary |
| MOBILITY | DELTAP.CAUG | 0.70 | arbitrary |
| MOBILITY | NCRITN.CAUG | 1.072×10^{17} | cm^{-3} |
| MOBILITY | NCRITP.CAUG | 1.606×10^{17} | cm^{-3} |

Arora Model for Low-Field Mobility

Another analytic model for the doping and temperature dependence of the low-field mobility is available in ATLAS. This model, which is due to Arora [16], has the following form:

$$\mu_{n0} = \text{MU1N.ARORA} \left(\frac{T_L}{300} \right)^{\text{ALPHAN.ARORA}} + \frac{\text{MU2N.ARORA} \left(\frac{T_L}{300} \right)^{\text{BETAN.ARORA}}}{1 + \frac{N}{\text{NCRITN.ARORA} \cdot \left(\frac{T_L}{300} \right)^{\text{GAMMAN.ARORA}}}} \quad 3-176$$

$$\mu_{p0} = \text{MU1P.ARORA} \left(\frac{T_L}{300} \right)^{\text{ALPHAP.ARORA}} + \frac{\text{MU2P.ARORA} \left(\frac{T_L}{300} \right)^{\text{BETAP.ARORA}}}{1 + \frac{N}{\text{NCRITP.ARORA} \cdot \left(\frac{T_L}{300} \right)^{\text{GAMMAP.ARORA}}}} \quad 3-177$$

where N is the total local dopant concentration.

This model is activated by specifying ARORA in the MODELS statement. The parameters of the model are specified in the MOBILITY statement. The default parameters are for silicon at $T_L=300\text{K}$.

Table 3-27. User-Specifiable Parameters for Equations 3-176 and 3-177

| Statement | Parameter | Default | Units |
|-----------|--------------|---------|---|
| MOBILITY | MU1N.ARORA | 88.0 | $\text{cm}^2 / (\text{V} \cdot \text{s})$ |
| MOBILITY | MU1P.ARORA | 54.3 | $\text{cm}^2 / (\text{V} \cdot \text{s})$ |
| MOBILITY | MU2N.ARORA | 1252.0 | $\text{cm}^2 / (\text{V} \cdot \text{s})$ |
| MOBILITY | MU2P.ARORA | 407.0 | $\text{cm}^2 / (\text{V} \cdot \text{s})$ |
| MOBILITY | ALPHAN.ARORA | -0.57 | |
| MOBILITY | ALPHAP.ARORA | -0.57 | |
| MOBILITY | BETAN.ARORA | -2.33 | |

Table 3-27. User-Specifiable Parameters for Equations 3-176 and 3-177

| Statement | Parameter | Default | Units |
|-----------|--------------|------------------------|------------------|
| MOBILITY | BETAP.ARORA | -2.33 | |
| MOBILITY | GAMMAN.ARORA | 2.546 | |
| MOBILITY | GAMMAP.ARORA | 2.546 | |
| MOBILITY | NCRITN.ARORA | 1.432×10^{17} | cm^{-3} |
| MOBILITY | NCRITP.ARORA | 2.67×10^{17} | cm^{-3} |

Masetti Model For Low-Field Mobility

Masetti et al. [151] modeled the dependence of mobility on carrier concentration over a range of 8 orders of magnitude in carrier concentration from approximately 10^{13} cm^{-3} to 10^{21} cm^{-3} . They found that their model required different parameter sets for the electron mobility in Arsenic and Phosphorous n-doped Silicon. The model is optimized for room temperature, although it does model temperature dependence to some extent.

The functional form of the electron mobility is

$$\mu_n = \text{MTN.MIN1} \exp\left(-\frac{\text{MTN.PC}}{N}\right) + \frac{\text{MTN.MAX} - \text{MTN.MIN2}}{1 + \left(\frac{N}{\text{MTN.CR}}\right)^{\text{MTN.ALPHA}}} - \frac{\text{MTN.MU1}}{1 + \left(\frac{\text{MTN.CS}}{N}\right)^{\text{MTN.BETA}}} \quad 3-178$$

where N is the total or ionized doping level. The functional form of the hole mobility is

$$\mu_p = \text{MTP.MIN1} \exp\left(-\frac{\text{MTP.PC}}{N}\right) + \frac{\text{MTP.MAX} - \text{MTP.MIN2}}{1 + \left(\frac{N}{\text{MTP.CR}}\right)^{\text{MTP.ALPHA}}} - \frac{\text{MTP.MU1}}{1 + \left(\frac{\text{MTP.CS}}{N}\right)^{\text{MTP.BETA}}} \quad 3-179$$

where N is the total dopant concentration. MTN.MAX and MTP.MAX are given a lattice temperature dependence as in Equations 3-172 and 3-173 respectively. These equations are functionally equivalent to the bulk mobility term in the Lombardi CVT model (Equations 3-227 and 3-228). To use it as a stand alone mobility model, use the `MASETTI` parameter on the `MODELS` statement for both electron and hole mobility.

`N.MASETTI` on the `MOBILITY` statement enables it for electrons. `P.MASETTI` on the `MOBILITY` statement enables it for holes.

For electron mobility, there is a choice of two default parameter sets. The set for arsenic doping are used unless you set the `MSTI.PHOS` parameter on the `MOBILITY` statement to use the set corresponding to Phosphorous. The following tables show default sets for electron mobility and for Boron doping (p-type).

Table 3-28. Parameter Set for Electron Mobility with Arsenic Doping in Silicon.

| Statement | Parameter | Default | Units |
|-----------|-----------|-----------------------|---------------------------|
| MOBILITY | MTN.MIN1 | 52.2 | $\text{cm}^2/(\text{Vs})$ |
| MOBILITY | MTN.MIN2 | 52.2 | $\text{cm}^2/(\text{Vs})$ |
| MOBILITY | MTN.MAX | 1417 | $\text{cm}^2/(\text{Vs})$ |
| MOBILITY | MTN.MU1 | 43.4 | $\text{cm}^2/(\text{Vs})$ |
| MOBILITY | MTN.PC | 0.0 | cm^{-3} |
| MOBILITY | MTN.CR | 9.68×10^{16} | cm^{-3} |
| MOBILITY | MTN.CS | 3.34×10^{20} | cm^{-3} |
| MOBILITY | MTN.ALPHA | 0.68 | |
| MOBILITY | MTN.BETA | 2.0 | |

Table 3-29. Parameter Set for Electron Mobility with Phosphorous Doping in Silicon (MSTI.PHOS set)

| Statement | Parameter | Default | Units |
|-----------|-----------|-----------------------|---------------------------|
| MOBILITY | MTN.MIN1 | 68.5 | $\text{cm}^2/(\text{Vs})$ |
| MOBILITY | MTN.MIN2 | 68.5 | $\text{cm}^2/(\text{Vs})$ |
| MOBILITY | MTN.MAX | 1414 | $\text{cm}^2/(\text{Vs})$ |
| MOBILITY | MTN.MU1 | 56.1 | $\text{cm}^2/(\text{Vs})$ |
| MOBILITY | MTN.PC | 0.0 | cm^{-3} |
| MOBILITY | MTN.CR | 9.2×10^{16} | cm^{-3} |
| MOBILITY | MTN.CS | 3.41×10^{20} | cm^{-3} |
| MOBILITY | MTN.ALPHA | 0.711 | |
| MOBILITY | MTN.BETA | 1.98 | |

Table 3-30. Parameter Set for Hole Mobility with Boron doping in Silicon.

| Statement | Parameter | Default | Units |
|-----------|-----------|---------|---------------------------|
| MOBILITY | MTP.MIN1 | 44.9 | $\text{cm}^2/(\text{Vs})$ |
| MOBILITY | MTP.MIN2 | 0.0 | $\text{cm}^2/(\text{Vs})$ |
| MOBILITY | MTP.MAX | 470.5 | $\text{cm}^2/(\text{Vs})$ |

Table 3-30. Parameter Set for Hole Mobility with Boron doping in Silicon.

| Statement | Parameter | Default | Units |
|-----------|-----------|-----------------------|------------------------|
| MOBILITY | MTP.MU1 | 29.0 | cm ² / (Vs) |
| MOBILITY | MTP.PC | 9.23×10 ¹⁶ | cm ⁻³ |
| MOBILITY | MTP.CR | 2.23×10 ¹⁷ | cm ⁻³ |
| MOBILITY | MTP.CS | 6.1×10 ²⁰ | cm ⁻³ |
| MOBILITY | MTP.ALPHA | 0.719 | |
| MOBILITY | MTP.BETA | 2.0 | |

Carrier-Carrier Scattering Models For Low-Field Mobility

Dorkel and Leturcq Models

The Dorkel and Leturcq Model [59] for low-field mobility includes the dependence on temperature, doping, and carrier-carrier scattering. This model is activated by specifying the CCSMOB parameter of the MODELS statement. The parameters of the model are specified in the MOBILITY statement. This model has the form:

$$\mu_{n0,p0} = \mu_{n,p}^L \left[\frac{1.025}{1 + \left[2.126 \left(\frac{\mu_{n,p}^L}{\mu_{n,p}^{IC}} \right) \right]^{0.715}} - 0.025 \right] \quad 3-180$$

where L is the lattice scattering, I is the ionized impurity scattering, and C is the carrier-carrier scattering. Here, $\mu_{n,p}^{IC}$ is defined as:

$$\mu_{n,p}^{IC} = \left[\frac{1}{\mu_C} + \frac{1}{\mu_{n,p}^I} \right]^{-1} \quad 3-181$$

where:

$$\mu_C = \frac{1.04 \cdot 10^{21} \left(\frac{T_L}{300} \right)^{3/2}}{\sqrt{np} \ln \left[1 + 7.45 \cdot 10^{13} \left(\frac{T_L}{300} \right)^2 (np)^{-1/3} \right]} \quad 3-182$$

$$\mu_n^I = \frac{AN \cdot CCS(T_L)^{3/2}}{N_T} f \left[\frac{BN \cdot CCS(T_L)^2}{n+p} \right] \quad 3-183$$

$$\mu_p^I = \frac{AP \cdot CCS(T_L)^{3/2}}{N_T} f \left[\frac{BP \cdot CCS(T_L)^2}{n+p} \right] \quad 3-184$$

Here, N_T is the total concentration, T_L is the lattice temperature and n, p are the electron and hole carrier concentrations respectively.

$$f(x) = \left[\ln(1+x) - \frac{x}{1+x} \right]^{-1} \quad 3-185$$

The values of the lattice scattering terms, $\mu_{N,P}^L$ are defined by Equations 3-172 and 3-173.

| Table 3-31. User-Specifiable Parameters for Equations 3-183 and 3-184 | | | |
|---|-----------|-----------------------|------------------|
| Statement | Parameter | Default | Units |
| MOBILITY | AN.CCS | 4.61×10^{17} | cm^{-3} |
| MOBILITY | AP.CCS | 1.0×10^{17} | cm^{-3} |
| MOBILITY | BN.CCS | 1.52×10^{15} | cm^{-3} |
| MOBILITY | BP.CCS | 6.25×10^{14} | cm^{-3} |

Conwell-Weisskopf Model

This model adapts Conwell-Weisskopf theory to carrier-carrier scattering [40]. According to this model, the carrier-carrier contribution to mobility is

$$\mu_{ccs} = \frac{D.CONWELL \left(\frac{T}{300} \right)^{3/2}}{\sqrt{pn} \left(\ln \left(1 + \frac{F.CONWELL}{(pn)^{(1/3)}} \left(\frac{T}{300} \right)^2 \right) \right)} \quad 3-186$$

where T is the Lattice temperature in Kelvin, n is the electron concentration, and p is the hole concentration. This is then combined with other enabled low-field mobility models (if any) using Matthiessens rule, giving overall low-field mobilities as follows

$$\frac{1}{\mu_n} = \frac{1}{\mu_{n0}} + \frac{1}{\mu_{ccs}} \quad 3-187$$

$$\frac{1}{\mu_p} = \frac{1}{\mu_{p0}} + \frac{1}{\mu_{ccs}} \quad 3-188$$

To enable the model for both electrons and holes, specify CONWELL on the MODELS statement. Alternatively, N.CONWELL on the MOBILITY statement enables it for electron mobility. P.CONWELL on the MOBILITY statement enables it for hole mobility.

| Table 3-32. MOBILITY Statement Parameters | | | |
|---|---------|------------------------|------------------------------------|
| Parameter | Type | Default | Units |
| D.CONWELL | Real | 1.04×10^{21} | $(\text{cmV} \cdot \text{s})^{-1}$ |
| F.CONWELL | Real | 7.452×10^{13} | cm^{-2} |
| N.CONWELL | Logical | False | |
| P.CONWELL | Logical | False | |

Brooks-Herring Model

Like the Conwell-Weisskopf model, this adds in the effects of carrier-carrier scattering to the low-field mobility using Matthiesen's rule. The carrier-carrier contribution to mobility is

$$\mu_{ccs} = \frac{A.BROOKS \left(\frac{T}{300} \right)^{\frac{3}{2}}}{\sqrt{pn} \phi(\eta)} \quad 3-189$$

where

$$\phi(\eta) = \log(1 + \eta) - \frac{\eta}{1 + \eta} \quad 3-190$$

and

$$\eta(T) = \frac{B.BROOKS \left(\frac{T}{300} \right)^2}{N_c F_{-1/2} \left(\frac{n}{N_c} \right) + N_v F_{-1/2} \left(\frac{p}{N_v} \right)} \quad 3-191$$

$F_{-1/2}$ is the Fermi-Dirac function of order $-1/2$, N_c and N_v are the conduction band and valence band effective densities of states, n is the electron concentration, p is the hole concentration, and T is the Lattice temperature.

To enable the model for both electrons and holes, specify BROOKS on the MODELS statement. Alternatively, N.BROOKS on the MOBILITY statement enables it for electron mobility. P.BROOKS on the MOBILITY statement enables it for hole mobility.

| Table 3-33. MOBILITY Statement Parameters | | | |
|---|---------|-----------------------|------------------------------------|
| Parameter | Type | Default | Units |
| A.BROOKS | Real | 1.56×10^{21} | $(\text{cmV} \cdot \text{s})^{-1}$ |
| B.BROOKS | Real | 7.63×10^{19} | cm^{-3} |
| N.BROOKS | Logical | False | |
| P.BROOKS | Logical | False | |

Incomplete Ionization and Doping Dependent Mobility

The default in ATLAS is to use the total doping ($N_A + N_D$) in the formulae for the doping concentration dependence of low-field mobility (e.g., ARORA model). As an alternative, ATLAS can use the ionized dopant concentration.

The ionized doping concentration is obtained automatically and used in calculating the charge density when you set the `INCOMPLETE` parameter on the `MODELS` statement. See Section 3.3.1: “Incomplete Ionization of Impurities” for more information.

ATLAS has a `MOB.INCOMPL` parameter on the `MODELS` statement. This allows you to use the ionized dopant concentration to calculate doping dependent mobilities. Specifying this parameter automatically sets the `INCOMPLETE` parameter. This ensures that the solution is consistent with an ionized rather than total doping concentration.

For high doping levels, the difference between total doping and ionized doping concentrations can be large and so this can result in quite different mobility values.

If it is required to use the ionized dopant concentration for mobility calculations and the total dopant concentration for calculating the charge density in Poisson's equation, then specify `MOB.INCOMPL ^INCOMPLETE` on the `MODELS` statement to explicitly clear this flag. This combination of parameters is not recommended.

`MOB.INCOMPL` affects the `ANALYTIC`, `ARORA`, `MASETTI`, `YAMAGUCHI`, `CVT`, `KLAASSEN`, `ALBRECHT` and tabulated Low-Field Mobility Models.

Klaassen's Unified Low-Field Mobility Model

The model by D. B. M. Klaassen [120, 121], provides a unified description of majority and minority carrier mobilities. In so doing, it includes the effects of lattice scattering, impurity scattering (with screening from charged carriers), carrier-carrier scattering, and impurity clustering effects at high concentration. The model shows excellent agreement between the modeled and empirical data for:

- majority electron mobility as a function of donor concentration over the range of 10^{14} cm^{-3} to 10^{22} cm^{-3}
- minority electron mobility as a function of acceptor concentration over the range of 10^{17} cm^{-3} to 10^{20} cm^{-3}
- minority hole mobility as a function of donor concentration from 10^{17} cm^{-3} to 10^{20} cm^{-3}
- temperature dependence over the range of 70 K to 500 K

The Klaassen Model accounts for a broader set of effects and has been calibrated over a wider range of conditions than any other of the low-field bulk mobility models. This is the recommended model for both MOS and bipolar simulation and is the default model for silicon when you set `MOS2` or `BIPOLAR2` in the `MODELS` statement. You can enable or disable the model by using the `KLA` parameter in the `MODELS` statement, or independently for electrons and holes by the `KLA.N` and `KLA.P` parameters of the `MOBILITY` statement.

The total mobility can be described by its components using Matthiessen's rule as:

$$\mu_{n0}^{-1} = \mu_{nL}^{-1} + \mu_{nDAP}^{-1} \quad 3-192$$

$$\mu_{p0}^{-1} = \mu_{pL}^{-1} + \mu_{pDAP}^{-1} \quad 3-193$$

μ_n and μ_p are the total low-field electron and hole mobilities, μ_{nL} and μ_{pL} are the electron and hole mobilities due to lattice scattering, μ_{nDAP} and μ_{pDAP} are the electron and hole mobilities due to donor (D), acceptor (A), screening (P) and carrier-carrier scattering.

The lattice scattering components, μ_{nL} and μ_{pL} are given as:

$$\mu_{nL} = \text{MUMAXN.KLA} \left(\frac{300}{T_L} \right)^{\text{THETAN.KLA}} \quad 3-194$$

$$\mu_{pL} = \text{MUMAXP.KLA} \left(\frac{300}{T_L} \right)^{\text{THETAP.KLA}} \quad 3-195$$

where T_L is the temperature in degrees Kelvin. MUMAXN.KLA, MUMAXP.KLA, THETAN.KLA, and THETAP.KLA are user-definable model parameters which can be specified as shown in Table 3-34.

| Table 3-34. User-Specifiable Parameters for Equations 3-194 and 3-195 | | | |
|---|------------|---------|-------------------------|
| Statement | Parameter | Default | Units |
| MOBILITY | MUMAXN.KLA | 1417.0 | cm ² / (V·s) |
| MOBILITY | MUMAXP.KLA | 470.5 | cm ² / (V·s) |
| MOBILITY | THETAN.KLA | 2.285 | |
| MOBILITY | THETAP.KLA | 2.247 | |

The impurity-carrier scattering components of the total mobility are given by:

$$\mu_{nDAP} = \mu_{N,n} \frac{N_{nsc}}{N_{nsc,eff}} \left(\frac{\text{NREF1N.KLA}}{N_{nsc}} \right)^{\text{ALPHA1N.KLA}} + \mu_{nc} \left(\frac{n+p}{N_{nsc,eff}} \right) \quad 3-196$$

$$\mu_{pDAP} = \mu_{N,p} \frac{N_{psc}}{N_{psc,eff}} \left(\frac{\text{NREF1P.KLA}}{N_{psc}} \right)^{\text{ALPHA1P.KLA}} + \mu_{pc} \left(\frac{n+p}{N_{psc,eff}} \right) \quad 3-197$$

| Table 3-35. User-Specifiable Parameters for Equations 3-196 and 3-197 | | | |
|---|-------------|-----------------------|-----------------|
| Statement | Parameter | Default | Units |
| MOBILITY | ALPHA1N.KLA | 0.68 | |
| MOBILITY | ALPHA1P.KLA | 0.719 | |
| MOBILITY | NREF1N.KLA | 9.68×10 ¹⁶ | cm ³ |
| MOBILITY | NREF1P.KLA | 2.23×10 ¹⁷ | cm ³ |

The impurity scattering components, $\mu_{N,n}$ and $\mu_{N,p}$, are given by:

$$\mu_{N,n} = \frac{\text{MUMAXN.KLA}^2}{\text{MUMAXN.KLA} - \text{MUMINN.KLA}} \left(\frac{T_L}{300} \right)^{(3 \times \text{ALPHA1N.KLA} - 1.5)} \quad 3-198$$

$$\mu_{N,p} = \frac{\text{MUMAXP.KLA}^2}{\text{MUMAXP.KLA} - \text{MUMINP.KLA}} \left(\frac{T_L}{300} \right)^{(3 \times \text{ALPHA1P.KLA} - 1.5)} \quad 3-199$$

where T_L is the temperature in degrees Kelvin. MUMINN.KLA and MUMINP.KLA are user-defined parameters shown in Table 3-36, and the other parameters are as described in Tables 3-34 and 3-35.

| Table 3-36. User-Specifiable Parameters for Equations 3-198 and 3-199 | | | |
|---|------------|---------|---|
| Statement | Parameter | Default | Units |
| MOBILITY | MUMINN.KLA | 52.2 | $\text{cm}^2 / (\text{V}\cdot\text{s})$ |
| MOBILITY | MUMINP.KLA | 44.9 | $\text{cm}^2 / (\text{V}\cdot\text{s})$ |

The carrier-carrier scattering components, μ_{nc} and μ_{pc} , are given by:

$$\mu_{nc} = \frac{\text{MUMINN.KLA} \times \text{MUMAXN.KLA}}{\text{MUMAXN.KLA} - \text{MUMINN.KLA}} \left(\frac{300}{T_L} \right)^{0.5} \quad 3-200$$

$$\mu_{pc} = \frac{\text{MUMINP.KLA} \times \text{MUMAXP.KLA}}{\text{MUMAXP.KLA} - \text{MUMINP.KLA}} \left(\frac{300}{T_L} \right)^{0.5} \quad 3-201$$

The N_{nsc} and N_{psc} parameters of Equations 3-196 and 3-197 are given by:

$$N_{nsc} = N_D + N_A + p \quad 3-202$$

$$N_{psc} = N_D + N_A + n \quad 3-203$$

where N_D is the donor concentration in cm^{-3} , N_A is the acceptor concentration in cm^{-3} , n is the electron concentration in cm^{-3} and p is the hole concentration in cm^{-3} .

The parameters of Equations 3-196 and 3-197 are given by:

$$N_{nsc, eff} = N_D + G(P_n)N_A + \left(\frac{p}{F(P_n)} \right) \quad 3-204$$

$$N_{psc, eff} = N_A + G(P_p)N_D + \left(\frac{n}{F(P_p)} \right) \quad 3-205$$

where N_D is the donor concentration in cm^{-3} , N_A is the acceptor concentration in cm^{-3} and n is the electron concentration in cm^{-3} and p is the hole concentration in cm^{-3} . The two functions, $G(P)$ and $F(P)$, are functions of the screening factors, P_n and P_p , for electrons and holes. The function, $G(P)$, in Equations 3-204 and 3-205 are given by:

$$G(P_n) = 1 - \frac{\text{S1.KLA}}{\left[\text{S2.KLA} + P_n \left(\frac{(T_L/300)}{\text{ME.KLA}} \right)^{\text{S4.KLA}} \right]^{\text{S3.KLA}}} + \frac{\text{S5.KLA}}{\left[P_n \left(\frac{\text{ME.KLA}}{(T_L/300)} \right)^{\text{S7.KLA}} \right]^{\text{S6.KLA}}} \quad 3-206$$

$$G(P_p) = 1 - \frac{\text{S1.KLA}}{\left[\text{S2.KLA} + P_p \left(\frac{(T_L/300)}{\text{MH.KLA}} \right)^{\text{S4.KLA}} \right]^{\text{S3.KLA}}} + \frac{\text{S5.KLA}}{\left[P_p \left(\frac{\text{MH.KLA}}{(T_L/300)} \right)^{\text{S7.KLA}} \right]^{\text{S6.KLA}}} \quad 3-207$$

Here, T_L is the temperature in degrees Kelvin, m_e and m_h are the electron and hole masses and the parameters $S1.KLA$ through $S7.KLA$ are user-specifiable model parameters as shown in Table 3-37..

| Table 3-37. User-Specifiable Parameters for Equations 3-206 and 3-207 | | | |
|---|-----------|----------|-------|
| Statement | Parameter | Default | Units |
| MOBILITY | $S1.KLA$ | 0.89233 | |
| MOBILITY | $S2.KLA$ | 0.41372 | |
| MOBILITY | $S3.KLA$ | 0.19778 | |
| MOBILITY | $S4.KLA$ | 0.28227 | |
| MOBILITY | $S5.KLA$ | 0.005978 | |
| MOBILITY | $S6.KLA$ | 1.80618 | |
| MOBILITY | $S7.KLA$ | 0.72169 | |

The functions, $F(P_n)$ and $F(P_p)$, in Equations 3-204 and 3-205 are given by:

$$F(P_n) = \frac{R1.KLA P_n^{R6.KLA} + R2.KLA + R3.KLA \frac{ME.KLA}{MH.KLA}}{P_n^{R6.KLA} + R4.KLA + R5.KLA \frac{ME.KLA}{MH.KLA}} \quad 3-208$$

$$F(P_p) = \frac{R1.KLA P_p^{R6.KLA} + R2.KLA + R3.KLA \frac{MH.KLA}{ME.KLA}}{P_p^{R6.KLA} + R4.KLA + R5.KLA \frac{MH.KLA}{ME.KLA}} \quad 3-209$$

where the parameters, $R1.KLA$ through $R6.KLA$, are user-specifiable as shown in Table 3-38.

| Table 3-38. User-Specifiable Parameters for Equations 3-208 and 3-209 | | | |
|---|-----------|---------|-------|
| Statement | Parameter | Default | Units |
| MOBILITY | $ME.KLA$ | 1.0 | |
| MOBILITY | $MH.KLA$ | 1.258 | |
| MOBILITY | $R1.KLA$ | 0.7643 | |
| MOBILITY | $R2.KLA$ | 2.2999 | |
| MOBILITY | $R3.KLA$ | 6.5502 | |
| MOBILITY | $R4.KLA$ | 2.3670 | |
| MOBILITY | $R5.KLA$ | -0.8552 | |
| MOBILITY | $R6.KLA$ | 0.6478 | |

The screening parameters, P_n and P_p , used in Equations 3-208 and 3-209 are given by:

$$P_n = \left[\frac{\text{FCW.KLA}}{P_{CW,n}} + \frac{\text{FBH.KLA}}{P_{BH,n}} \right]^{-1} \quad 3-210$$

$$P_p = \left[\frac{\text{FCW.KLA}}{P_{CW,p}} + \frac{\text{FBH.KLA}}{P_{BH,p}} \right]^{-1} \quad 3-211$$

Here, the FCW.KLA and FBH.KLA parameters are user-specifiable model parameters as shown in Table 3-39.

| Table 3-39. User-Specifiable Parameters for Equations 3-210 and 3-211 | | | |
|---|-----------|---------|-------|
| Statement | Parameter | Default | Units |
| MOBILITY | FCW.KLA | 2.459 | |
| MOBILITY | FBH.KLA | 3.828 | |

The functions, $P_{BH,n}$ and $P_{BH,p}$, $P_{CW,n}$, and $P_{CW,p}$ are given by the following equations.

$$P_{BH,n} = \frac{1.36 \times 10^{20}}{n} (\text{ME.KLA}) \left(\frac{T_L}{300} \right)^2 \quad 3-212$$

$$P_{BH,p} = \frac{1.36 \times 10^{20}}{p} (\text{MH.KLA}) \left(\frac{T_L}{300} \right)^2 \quad 3-213$$

$$P_{CW,n} = 3.97 \times 10^{13} \left\{ \frac{1}{Z_n^3 N_D} \left(\frac{T_L}{300} \right)^3 \right\}^{\frac{2}{3}} \quad 3-214$$

$$P_{CW,p} = 3.97 \times 10^{13} \left\{ \frac{1}{Z_p^3 N_A} \left(\frac{T_L}{300} \right)^3 \right\}^{\frac{2}{3}} \quad 3-215$$

where T_L is the temperature in degrees Kelvin, m_e/m_0 and m_h/m_0 are the normalized carrier effective masses, and n and p are the electron and hole concentrations in cm^{-3} .

Also here, N_D and N_A are the donor and acceptor concentrations in cm^{-3} , T_L is the temperature in degrees Kelvin, and Z_n and Z_p are clustering functions given by:

$$Z_n = 1 + \frac{1}{\text{CD.KLA} + \left(\frac{\text{NREFD.KLA}}{N_D} \right)^2} \quad 3-216$$

$$Z_p = 1 + \frac{1}{CA.KLA + \left(\frac{NREFA.KLA}{N_A}\right)^2} \quad 3-217$$

where N_D and N_A are the donor and acceptor concentrations in cm^{-3} and $CD.KLA$, $CA.KLA$, $NREFD.KLA$, and $NREFA.KLA$ are user-definable parameters as given in Table 3-40.

Table 3-40. User-Specifiable Parameters for Equations 3-216 and 3-217

| Statement | Parameter | Default | Units |
|-----------|-----------|----------------------|---------------|
| MOBILITY | CD.KLA | 0.21 | |
| MOBILITY | CA.KLA | 0.50 | |
| MOBILITY | NREFD.KLA | 4.0×10^{20} | cm^3 |
| MOBILITY | NREFA.KLA | 7.2×10^{20} | cm^3 |

Note: When the Klaassen low-field mobility is used, remember that it has been calibrated to work with Klaassen's models for bandgap narrowing, $KLAAUG$ recombination, and $KLASRH$ recombination. These models are described in the Section 3.6.3: "Carrier Generation-Recombination Models".

Uchida's Low-Field Model for Ultrathin SOI

The model by Uchida et.al. [229], provides a mobility limit in ultrathin-body MOSFET transistors with SOI thickness less than 4 nm. This mobility limit is due to thickness fluctuations in the nano scale SOI film. The model for electrons and holes is given by Equations 3-218 and 3-219.

$$\mu_{nu} = CN.UCHIDA \cdot TN.UCHIDA^6 \quad 3-218$$

$$\mu_{pu} = CP.UCHIDA \cdot TP.UCHIDA^6 \quad 3-219$$

The parameters $CN.UCHIDA$, $CP.UCHIDA$ are calibrated from the reference to a default value of $0.78125 \text{ cm}^2/(\text{V}\cdot\text{s}\cdot\text{nm}^6)$. The parameters $TN.UCHIDA$ and $TP.UCHIDA$ represent the thickness of the SOI in μm . This value should as close as possible to match the physical thickness of the SOI layer in the simulated structure file. To enable this model for electrons and holes, specify values for $TN.UCHIDA$ and $TP.UCHIDA$, and specify the logical parameters $UCHIDA.N$ or $UCHIDA.P$ or both on the **MOBILITY** statement. Table 3-41 lists the user specifiable parameters.

Table 3-41. User-Specifiable Parameters for Equations 3-187 and 3-188

| Statement | Parameter | Default | Units |
|-----------|-----------|---------|--|
| MOBILITY | CN.UCHIDA | 0.78125 | cm ² / (V·s·nm ⁶) |
| MOBILITY | CP.UCHIDA | 0.78125 | cm ² / (V·s·nm ⁶) |
| MOBILITY | TN.UCHIDA | 4.0 | nm |
| MOBILITY | TP.UCHIDA | 4.0 | nm |

Perpendicular Field Mobility Model

Mobility degradation effects due to perpendicular fields can be accounted for using a simple perpendicular field dependent mobility model. To enable this model described by Equations 3-220 and 3-221, specify PRPMOB on the MODELS statement.

$$\mu_n = \text{GSURFN} \cdot \frac{\mu_{0n}}{\sqrt{1 + \frac{E_{\perp}}{\text{ECN} \cdot \text{MU}}}} \quad 3-220$$

$$\mu_p = \text{GSURFP} \cdot \frac{\mu_{0n}}{\sqrt{1 + \frac{E_{\perp}}{\text{ECN} \cdot \text{MP}}}} \quad 3-221$$

The default values for the user specifiable parameters of Equations 3-220 and 3-221 are described in Table 3-42.

Table 3-42. User Specifiable Parameters of the Perpendicular Field Mobility Model

| Statement | Parameter | Default | Units |
|-----------|-----------|----------------------|-------|
| MOBILITY | GSURFN | 1.0 | |
| MOBILITY | GSURFP | 1.0 | |
| MOBILITY | ECN.MU | 6.48×10 ⁴ | V/cm |
| MOBILITY | ECP.MU | 1.87×10 ⁴ | V/cm |

Inversion Layer Mobility Models

To obtain accurate results for MOSFET simulations, you need to account for the mobility degradation that occurs inside inversion layers. The degradation normally occurs as a result of the substantially higher surface scattering near the semiconductor to insulator interface.

This effect is handled within ATLAS by three distinct methods:

- a surface degradation model SURFMOB
- a transverse electric field model SHIRAHATA
- specific inversion layer mobility models CVT, YAMAGUCHI, and TASCH

The CVT, YAMAGUCHI, and TASCH models are designed as stand-alone models which incorporate all the effects required for simulating the carrier mobility.

Lombardi CVT Model

The inversion layer model from Lombardi [143] is selected by setting CVT on the MODEL statement. This model overrides any other mobility models which may be specified on the MODELS statement. In the CVT model, the transverse field, doping dependent and temperature dependent parts of the mobility are given by three components that are combined using Matthiessen's rule. These components are μ_{AC} , μ_{sr} and μ_b and are combined using Matthiessen's rule as follows:

$$\mu_T^{-1} = \mu_{AC}^{-1} + \mu_b^{-1} + \mu_{sr}^{-1} \quad 3-222$$

The first component, μ_{AC} , is the surface mobility limited by scattering with acoustic phonons:

$$\mu_{AC, n} = \frac{BN.CVT}{\left(\frac{E_{\perp}}{E_1}\right)^{EN.CVT}} + \left(\frac{CN.CVT \left(\frac{N}{N_1}\right)^{TAUN.CVT}}{\left(\frac{E_{\perp}}{E_1}\right)^{DN.CVT}} \right) \frac{T_1}{T_L} \quad 3-223$$

$$\mu_{AC, p} = \frac{BP.CVT}{\left(\frac{E_{\perp}}{E_1}\right)^{EP.CVT}} + \left(\frac{CP.CVT \left(\frac{N}{N_1}\right)^{TAUP.CVT}}{\left(\frac{E_{\perp}}{E_1}\right)^{DP.CVT}} \right) \frac{T_1}{T_L} \quad 3-224$$

where T_L is the temperature, E_{\perp} is the perpendicular electric field, and N is the total doping concentration. In E_1 is 1V/cm, N_1 is 1cm^{-3} , and T_1 is 1K. You can define the parameters BN.CVT, BP.CVT, CN.CVT, CP.CVT, DN.CVT, DP.CVT, TAUN.CVT, and TAUP.CVT in the MOBILITY statement (see Table 3-43 for their defaults).

The second component, μ_{sr} , is the surface roughness factor and is given by:

$$\frac{1}{\mu_{sr, n}} = \frac{\left(\frac{E_{\perp}}{E_1}\right)^{KN.CVT}}{DELN.CVT} + \frac{\left(\frac{E_{\perp}}{E_1}\right)^3}{FELN.CVT} \quad 3-225$$

for electrons and

$$\frac{1}{\mu_{sr, p}} = \frac{\left(\frac{E_{\perp}}{E_1}\right)^{KP.CVT}}{DELP.CVT} + \frac{\left(\frac{E_{\perp}}{E_1}\right)^3}{FELP.CVT} \quad 3-226$$

for holes.

The default values of FELN.CVT and FELP.CVT are set so high that the second terms are negligible. The KN.CVT, KP.CVT, DELN.CVT, DELP.CVT, FELN.CVT and FELP.CVT parameters are user-definable (see Table 3-43 for their defaults).

The third mobility component, μ_b , is the mobility limited by scattering with optical intervalley phonons. This component is given by:

$$\mu_{b, n} = MU0N.CVT \exp\left(\frac{-PCN.CVT}{N}\right) + \frac{\left[MUMAXN.CVT \left(\frac{T_L}{300}\right)^{-GAMN.CVT} - MU0N.CVT \right]}{1 + \left(\frac{N}{CRN.CVT}\right)^{ALPHN.CVT}} \quad 3-227$$

$$- \frac{MU1N.CVT}{1 + \left(\frac{CSN.CVT}{N}\right)^{BETAN.CVT}}$$

$$\mu_{b, p} = MU0P.CVT \exp\left(\frac{-PCP.CVT}{N}\right) + \frac{\left[MUMAXP.CVT \left(\frac{T_L}{300}\right)^{-GAMP.CVT} - MU0P.CVT \right]}{1 + \left(\frac{N}{CRP.CVT}\right)^{ALPHP.CVT}} \quad 3-228$$

$$- \frac{MU1P.CVT}{1 + \left(\frac{CSP.CVT}{N}\right)^{BETAP.CVT}}$$

Here, N is the total density of impurities and T_L is the temperature in degrees Kelvin.

Because μ_{AC} and μ_{sr} are related to interaction with an interface, you can specify a typical distance from the interface over which these components are significant [190]. If you specify the N.LCRIT or P.LCRIT parameters or both then factors

$$FE = \exp(-l/N.LCRIT) \quad 3-229$$

and

$$FH = \exp(-l/P.LCRIT) \quad 3-230$$

are obtained, where l is the shortest distance to the nearest interface from the point at which the mobility will be calculated. These factors are then used to modify the Matthiesen's rule of Equation 3-222 to

$$\frac{1}{\mu_T} = \frac{FE}{\mu_{AC}} + \frac{FE}{\mu_{sr}} + \frac{1}{\mu_b} \quad 3-231$$

for electrons and

$$\frac{1}{\mu_T} = \frac{FH}{\mu_{AC}} + \frac{FH}{\mu_{sr}} + \frac{1}{\mu_b} \quad 3-232$$

for holes. Far from the interface, the mobility is the same as the bulk mobility.

| Table 3-43. User-Specifiable Parameters for Equations to 3-228 | | | |
|--|-----------|-------------------------|---|
| Statement | Parameter | Default | Units |
| MOBILITY | ALPHN.CVT | 0.680 | |
| MOBILITY | ALPHP.CVT | 0.71 | |
| MOBILITY | BETAN.CVT | 2.00 | |
| MOBILITY | BETAP.CVT | 2.00 | |
| MOBILITY | BN.CVT | 4.75×10^7 | $\text{cm}^2 / (\text{V} \cdot \text{s})$ |
| MOBILITY | BP.CVT | 9.925×10^6 | $\text{cm}^2 / (\text{V} \cdot \text{s})$ |
| MOBILITY | CN.CVT | 1.74×10^5 | $\text{cm}^2 / (\text{V} \cdot \text{s})$ |
| MOBILITY | CP.CVT | 8.842×10^5 | $\text{cm}^2 / (\text{V} \cdot \text{s})$ |
| MOBILITY | CRN.CVT | 9.68×10^{16} | cm^{-3} |
| MOBILITY | CRP.CVT | 2.23×10^{17} | cm^{-3} |
| MOBILITY | CSN.CVT | 3.43×10^{20} | cm^{-3} |
| MOBILITY | CSP.CVT | 6.10×10^{20} | cm^{-3} |
| MOBILITY | DELN.CVT | 5.82×10^{14} | $\text{cm}^2 / (\text{V} \cdot \text{s})$ |
| MOBILITY | DELP.CVT | 2.0546×10^{14} | $\text{cm}^2 / (\text{V} \cdot \text{s})$ |
| MOBILITY | DN.CVT | 0.333 | |
| MOBILITY | DP.CVT | 0.333 | |
| MOBILITY | EN.CVT | 1.0 | |
| MOBILITY | EP.CVT | 1.0 | |
| MOBILITY | FELN.CVT | 1.0×10^{50} | $\text{cm}^2 / (\text{V} \cdot \text{s})$ |
| MOBILITY | FELP.CVT | 1.0×10^{50} | $\text{cm}^2 / (\text{V} \cdot \text{s})$ |

Table 3-43. User-Specifiable Parameters for Equations to 3-228

| Statement | Parameter | Default | Units |
|-----------|------------|------------------------|-------------------------|
| MOBILITY | KN.CVT | 2.0 | |
| MOBILITY | KP.CVT | 2.0 | |
| MOBILITY | GAMN.CVT | 2.5 | |
| MOBILITY | GAMP.CVT | 2.2 | |
| MOBILITY | MU0N.CVT | 52.2 | cm ² / (V·s) |
| MOBILITY | MU0P.CVT | 44.9 | cm ² / (V·s) |
| MOBILITY | MU1N.CVT | 43.4 | cm ² / (V·s) |
| MOBILITY | MU1P.CVT | 29.0 | cm ² / (V·s) |
| MOBILITY | MUMAXN.CVT | 1417.0 | cm ² / (V·s) |
| MOBILITY | MUMAXP.CVT | 470.5 | cm ² / (V·s) |
| MOBILITY | N.LCRIT | 1.0 | cm |
| MOBILITY | P.LCRIT | 1.0 | cm |
| MOBILITY | PCN.CVT | 0.0 | cm ⁻³ |
| MOBILITY | PCP.CVT | 9.23×10 ⁻¹⁶ | cm ⁻³ |
| MOBILITY | TAUN.CVT | 0.125 | |
| MOBILITY | TAUP.CVT | 0.0317 | |

Note: The CVT model when activated will also, by default, apply the Parallel Electric Field Mobility Model which is described in the “Parallel Electric Field-Dependent Mobility” section on page 3-77. In this model, the low-field mobility is supplied from the CVT model.

Darwish CVT Model

The CVT model already described has been successfully used in many device simulations. Lately, an improved version of this model has been proposed by Darwish et al. [54] where several modifications have been implemented. The first modification is that the bulk mobility is calculated using Klaassen’s model (see “Klaassen’s Unified Low-Field Mobility Model” section on page 3-55) to take into account coulomb screening effects. The second modification is a new expression for surface roughness is used.

The new model for surface roughness replaces Equations 3-225 and 3-226 with:

$$\frac{1}{\mu_{sr, n}} = \frac{\left(\frac{E_{\perp}}{E_2}\right)^{\gamma_n}}{\text{DELN.CVT}} + \frac{\left(\frac{E_{\perp}}{E_2}\right)^3}{\text{FELN.CVT}} \quad 3-233$$

$$\frac{1}{\mu_{sr,p}} = \frac{\left(\frac{E_{\perp}}{E_2}\right)^{\gamma_p}}{\text{DELP.CVT}} + \frac{\left(\frac{E_{\perp}}{E_2}\right)^3}{\text{FELP.CVT}} \quad 3-234$$

where:

$$\gamma_n = \text{AN.CVT} + \frac{\text{ALN.CVT} \times (n+p)}{\left(\frac{N}{N_2}\right)^{\text{ETAN.CVT}}} \quad 3-235$$

$$\gamma_p = \text{AP.CVT} + \frac{\text{ALP.CVT} \times (n+p)}{\left(\frac{N}{N_2}\right)^{\text{ETAP.CVT}}} \quad 3-236$$

Here, N is the total doping density ($N_D + N_A$), N_2 is 1cm^{-3} , and E_2 is 1 V/cm .

Table 3-44 shows the default parameters for the new equations.

| Table 3-44. Default parameters for the surface roughness components of new CVT model. | | | |
|---|-----------|------------------------|---------------|
| Parameter | Statement | Default | Units |
| AN.CVT | MOBILITY | 2.58 | |
| AP.CVT | MOBILITY | 2.18 | |
| ALN.CVT | MOBILITY | 6.85×10^{-21} | cm^3 |
| ALP.CVT | MOBILITY | 7.82×10^{-21} | cm^3 |
| ETAN.CVT | MOBILITY | 0.0767 | |
| ETAP.CVT | MOBILITY | 0.123 | |

Next, in the Darwish model, the expressions for acoustic phonon scattering are modified as shown in Equations 3-237 and 3-238.

$$\mu_{AC,n} = \frac{\text{BN.CVT}}{\left(\frac{E_{\perp}}{E_2}\right)^{\text{EN.CVT}}} + \left(\frac{\text{CN.CVT} \left(\frac{N}{N_2}\right)^{\text{TAUN.CVT}}}{\left(\frac{E_{\perp}}{E_2}\right)^{\text{DN.CVT}}} \right) \frac{1}{T'_n} \quad 3-237$$

$$\mu_{AC,p} = \frac{\text{BP.CVT}}{\left(\frac{E_{\perp}}{E_2}\right)^{\text{EP.CVT}}} + \left(\frac{\text{CP.CVT} \left(\frac{N}{N_2}\right)^{\text{TAUP.CVT}}}{\left(\frac{E_{\perp}}{E_2}\right)^{\text{DP.CVT}}} \right) \frac{1}{T'_p} \quad 3-238$$

where

$$T'_n = (T_L/300)^{\text{KAPPAN.CVT}} \quad 3-239$$

$$T_p' = (T_L/300)^{\text{KAPPAP.CVT}}$$

3-240

Table 3-45 shows the default values for KAPPAN.CVT and KAPPAP.CVT.

| Table 3-45. Default Parameter Values for Equations 3-239 and 3-240. | | | |
|---|------------|---------|-------|
| Statement | Parameter | Default | Units |
| MOBILITY | KAPPAN.CVT | 1.7 | |
| MOBILITY | KAPPAP.CVT | 0.9 | |

Finally, the default values for many of the parameters are changed from those listed Table 3-43. Table 3-31 lists the defaults used for the Darwish model.

| Table 3-46. Default Parameters for the Darwish model. | | | |
|---|-----------|-----------------------|---|
| Statement | Parameter | Default | Units |
| MOBILITY | BN.CVT | 3.61×10^7 | cm/s |
| MOBILITY | BP.CVT | 1.51×10^7 | cm/s |
| MOBILITY | CN.CVT | 1.7×10^4 | |
| MOBILITY | CP.CVT | 4.18×10^3 | |
| MOBILITY | TAUN.CVT | 0.0233 | |
| MOBILITY | TAUP.CVT | 0.0119 | |
| MOBILITY | DELN.CVT | 3.58×10^{18} | $\text{cm}^2 / (\text{V} \cdot \text{s})$ |
| MOBILITY | DELP.CVT | 4.1×10^{15} | $\text{cm}^2 / (\text{V} \cdot \text{s})$ |

You can enable the Darwish model for electrons and holes by specifying NEWCVT.N or NEWCVT.P on the MOBILITY statement.

Yamaguchi Model

The Yamaguchi Model [265] is selected by setting YAMAGUCHI in the MODELS statement. This model overrides any mobility model specifications other than the CVT model. The model consists of calculating the low-field, doping dependent mobility. Surface degradation is then accounted for based upon the transverse electric field before including the parallel electric field dependence.

The low-field part of the Yamaguchi Model is given as follows:

$$\mu_{n0} = \text{MULN.YAMA} \left[1 + \frac{N}{\frac{N}{\text{SN.YAMA}} + \text{NREFN.YAMA}} \right]^{-\frac{1}{2}}$$

3-241

$$\mu_{p0} = \text{MULP.YAMA} \left[1 + \frac{N}{\frac{N}{\text{SP.YAMA}} + \text{NREFP.YAMA}} \right]^{-\frac{1}{2}} \quad 3-242$$

where N_i is the total impurity concentration. The equation parameters: MULN.YAMA, MULP.YAMA, SN.YAMA, SP.YAMA, NREFP.YAMA, and NREFP.YAMA are user-definable in the MOBILITY statement (see Table 3-47 for their defaults).

The transverse electric field dependence is accounted for as follows:

$$\mu_{s,n} = \mu_{n0} (1 + \text{ASN.YAMA } E_{\perp})^{-\frac{1}{2}} \quad 3-243$$

$$\mu_{s,p} = \mu_{p0} (1 + \text{ASP.YAMA } E_{\perp})^{-\frac{1}{2}} \quad 3-244$$

where E_{\perp} is the perpendicular electric field and the equation parameters, ASN.YAMA and ASP.YAMA, are user-definable in the MOBILITY statement (see Table 3-47 for their defaults).

The final calculation of mobility takes into account the parallel electric field dependence which takes the form:

$$\mu_n = \mu_{s,n} \left[1 + \left(\frac{\mu_{s,n} E}{\text{ULN.YAMA}} \right)^2 \left(\text{GN.YAMA} + \frac{\mu_{s,n} E}{\text{ULN.YAMA}} \right)^{-1} + \left(\frac{\mu_{s,n} E}{\text{VSN.YAMA}} \right)^2 \right]^{-\frac{1}{2}} \quad 3-245$$

$$\mu_p = \mu_{s,p} \left[1 + \left(\frac{\mu_{s,p} E}{\text{ULP.YAMA}} \right)^2 \left(\text{GP.YAMA} + \frac{\mu_{s,p} E}{\text{ULP.YAMA}} \right)^{-1} + \left(\frac{\mu_{s,p} E}{\text{VSP.YAMA}} \right)^2 \right]^{-\frac{1}{2}} \quad 3-246$$

where E is the parallel electric field and the equation parameters: ULN.YAMA, ULP.YAMA, VSN.YAMA, VSP.YAMA, GN.YAMA, and GP.YAMA are user-definable in the MOBILITY statement (see Table 3-47 for their defaults).

Table 3-47. User-Specifiable Parameters for Equations to 3-246

| Statement | Parameter | Default | Units |
|-----------|------------|----------------------|---|
| MOBILITY | SN.YAMA | 350.0 | |
| MOBILITY | SP.YAMA | 81.0 | |
| MOBILITY | NREFP.YAMA | 3.0×10^{16} | cm^{-3} |
| MOBILITY | NREFP.YAMA | 4.0×10^{16} | cm^{-3} |
| MOBILITY | MULN.YAMA | 1400.0 | $\text{cm}^2 / (\text{V} \cdot \text{s})$ |
| MOBILITY | MULP.YAMA | 480.0 | $\text{cm}^2 / (\text{V} \cdot \text{s})$ |

Table 3-47. User-Specifiable Parameters for Equations to 3-246

| Statement | Parameter | Default | Units |
|-----------|-----------|-----------------------|-------|
| MOBILITY | ASN.YAMA | 1.54×10^{-5} | cm/V |
| MOBILITY | ASP.YAMA | 5.35×10^{-5} | cm/V |
| MOBILITY | VSN.YAMA | 1.036×10^7 | cm/s |
| MOBILITY | VSP.YAMA | 1.2×10^7 | cm/s |
| MOBILITY | ULN.YAMA | 4.9×10^6 | cm/s |
| MOBILITY | ULP.YAMA | 2.928×10^6 | cm/s |
| MOBILITY | GN.YAMA | 8.8 | |
| MOBILITY | GP.YAMA | 1.6 | |

The Tasch Model

S-PISCES includes an improved local field-dependent mobility model. This model, which was originally derived and published by Tasch et. al [212,213] has been designed explicitly for MOSFETs. It defines the mobility as a function of the perpendicular and parallel electric fields, the interface charge, the lattice temperature and the doping concentration. To activate this model, is activated use the TASCH parameter on the MODELS statement. This mobility model is given by the following expressions:

$$\mu_n = \Gamma_n + (E_{perp} - E_0) \frac{d\Gamma_n}{dE_{perp}} \quad 3-247$$

$$\mu_p = \Gamma_p + (E_{perp} - E_0) \frac{d\Gamma_p}{dE_{perp}} \quad 3-248$$

where E_{perp} is the transverse electric field and E_0 is the transverse electric field at the edge of the inversion layer. The functions $\Gamma_{n,p}$ are defined as:

$$\Gamma_n = \frac{\mu_{eff,n}}{\left(1 + \left(\frac{\mu_{eff,n} E_{\parallel}}{VSATN}\right)^{BETAN}\right)^{1/BETAN}} \quad 3-249$$

$$\Gamma_p = \frac{\mu_{eff,p}}{\left(1 + \left(\frac{\mu_{eff,p} E_{\parallel}}{VSATP}\right)^{BETAP}\right)^{1/BETAP}} \quad 3-250$$

The carrier mobilities $\mu_{eff,n}$ and $\mu_{eff,p}$ are defined by three components μ_{ph} , μ_{sr} and μ_c which are combined by Mathiessen's rule according to:

$$\mu_{eff} = \left[\frac{1}{\mu_{ph}} + \frac{1}{\mu_{sr}} + \frac{1}{\mu_c} \right]^{-1} \quad 3-251$$

The term μ_{ph} takes account of the degradation in mobility due to acoustic phonon scattering through the expressions:

$$\mu_{ph,n}^{-1} = \left(\text{MUBN} \cdot \text{TAS} \left(\frac{T_L}{300} \right)^{-\text{TMUBN} \cdot \text{TAS}} \right)^{-1} + \left(Z_n / \text{DN} \cdot \text{TAS} Y_n \left(\frac{T_L}{300} \right)^{1/2} \right)^{-1} \quad 3-252$$

$$\mu_{ph,p}^{-1} = \left(\text{MUBP} \cdot \text{TAS} \left(\frac{T_L}{300} \right)^{-\text{TMUBP} \cdot \text{TAS}} \right)^{-1} + \left(Z_p / \text{DP} \cdot \text{TAS} Y_p \left(\frac{T_L}{300} \right)^{1/2} \right)^{-1} \quad 3-253$$

The function, $Z_{n,p}$, is defined as:

$$Z_n = \text{Z11N} \cdot \text{TAS} \left(\frac{T_L}{300} \right) E_{eff,n}^{-1} + \text{Z22N} \cdot \text{TAS} E_{eff,n}^{-\frac{1}{3}} \quad 3-254$$

$$Z_p = \text{Z11P} \cdot \text{TAS} \left(\frac{T_L}{300} \right) E_{eff,p}^{-1} + \text{Z22P} \cdot \text{TAS} E_{eff,p}^{-\frac{1}{3}} \quad 3-255$$

where:

$$E_{eff,n} = \frac{(E_{perp} + \text{RN} \cdot \text{TAS} - 1) \cdot E_0}{\text{RP} \cdot \text{TAS}} \quad 3-256$$

$$E_{eff,p} = \frac{(E_{perp} + \text{RN} \cdot \text{TAS} - 1) \cdot E_0}{\text{RP} \cdot \text{TAS}} \quad 3-257$$

Also, the function $Y_{n,p}$, is defined as:

$$Y_n = \text{P1N} \cdot \text{TAS} \left(\frac{T_L}{300} \right)^{\text{B1N} \cdot \text{TAS}} + \text{P2N} \cdot \text{TAS} n + \text{B2N} \cdot \text{TAS} \left(\frac{T_L}{300} \right)^{-1} N_f \quad 3-258$$

$$Y_p = \text{P1P} \cdot \text{TAS} \left(\frac{T_L}{300} \right)^{\text{B1P} \cdot \text{TAS}} + \text{P2P} \cdot \text{TAS} p + \text{B2P} \cdot \text{TAS} \left(\frac{T_L}{300} \right)^{-1} N_f \quad 3-259$$

Mobility degradation due to surface roughness is accounted for by the term μ_{sr} which is calculated according to:

$$\mu_{sr,n} = \left(\frac{\text{ESRN} \cdot \text{TAS}}{E_{eff,n}} \right)^{\text{BETAN} \cdot \text{TAS}} \quad 3-260$$

$$\mu_{sr,p} = \left(\frac{\text{ESRP} \cdot \text{TAS}}{E_{eff,p}} \right)^{\text{BETAP} \cdot \text{TAS}} \quad 3-261$$

The final term, μ_C , models Coulombic scattering with the expressions:

$$\mu_{C,n} = \frac{\text{N2N} \cdot \text{TAS} \cdot \left(\frac{T_L}{300} \right)^{1.5}}{N_A \ln(1 + \gamma_{BH,n}) - \frac{\gamma_{BH,n}}{(1 + \gamma_{BH,n})}} \quad 3-262$$

$$\mu_{C,p} = \frac{N2P.TAS \cdot \left(\frac{T_L}{300}\right)^{1.5}}{N_D \ln(1 + \gamma_{BH,p}) - \frac{\gamma_{BH,p}}{(1 + \gamma_{BH,p})}} \quad 3-263$$

Here:

$$\gamma_{BH,n} = \frac{N1N.TAS}{n} \cdot \left(\frac{T_L}{300}\right)^{ALPHAN.TAS} \quad 3-264$$

$$\gamma_{BH,p} = \frac{N1P.TAS}{p} \cdot \left(\frac{T_L}{300}\right)^{ALPHAP.TAS} \quad 3-265$$

T_L is the lattice temperature in degrees Kelvin, N_f is the fixed interface charge at the gate dielectric-silicon interface (cm^{-2}), N_A is the channel acceptor doping concentration in cm^{-3} , N_D is the channel donor doping concentration in cm^{-3} , n and p are the electron and hole concentrations per unit volume in the inversion layer (cm^{-3}). The default parameters within each equation is defined in the `MOBILITY` statement. The default parameters are shown in Table 3-47.

Table 3-48. Parameters for Equations 3-247 through 3-265

| Statement | Parameter | Default | Units |
|-----------|-----------|-----------------------|-------|
| MOBILITY | RN.TAS | 2 | |
| MOBILITY | RP.TAS | 3 | |
| MOBILITY | BETAN | 2 | |
| MOBILITY | BETAP | 1 | |
| MOBILITY | MUBN.TAS | 1150 | |
| MOBILITY | MUBP.TAS | 270 | |
| MOBILITY | TMUBN.TAS | 2.5 | |
| MOBILITY | TMUBP.TAS | 1.4 | |
| MOBILITY | DN.TAS | 3.2×10^{-9} | |
| MOBILITY | DP.TAS | 2.35×10^{-9} | |
| MOBILITY | P1N.TAS | 0.09 | |
| MOBILITY | P1P.TAS | 0.334 | |
| MOBILITY | B1N.TAS | 1.75 | |
| MOBILITY | B1P.TAS | 1.5 | |
| MOBILITY | P2N.TAS | 4.53×10^{-8} | |
| MOBILITY | PEP.TAS | 3.14×10^{-7} | |

Table 3-48. Parameters for Equations 3-247 through 3-265

| Statement | Parameter | Default | Units |
|-----------|------------|-----------------------|-------|
| MOBILITY | B2N.TAS | -0.25 | |
| MOBILITY | B2P.TAS | -0.3 | |
| MOBILITY | Z11N.TAS | 0.0388 | |
| MOBILITY | Z11P.TAS | 0.039 | |
| MOBILITY | Z22N.TAS | 1.73×10^{-5} | |
| MOBILITY | Z22P.TAS | 1.51×10^{-5} | |
| MOBILITY | ESRN.TAS | 2.449×10^7 | |
| MOBILITY | ESRP.TAS | 1.0×10^8 | |
| MOBILITY | BETAN.TAS | 2 | |
| MOBILITY | BETAP.TAS | 1 | |
| MOBILITY | N2N.TAS | 1.1×10^{21} | |
| MOBILITY | N2P.TAS | 1.4×10^{18} | |
| MOBILITY | N1N.TAS | 2.0×10^{19} | |
| MOBILITY | N1P.TAS | 8.4×10^{16} | |
| MOBILITY | ALPHAN.TAS | 2 | |
| MOBILITY | ALPHAP.TAS | 3.4 | |

Perpendicular Electric Field-Dependent Mobility

The Watt Model

A surface mobility model derived by J.T.Watt [247] is available in ATLAS. This mobility model is activated when the parameter SURFMOB is specified on the MODELS statement. The default model parameters are tuned to describe the measured mobilities in silicon at 300K. You can modify model parameters by using the MOBILITY statement.

The Watt model takes into consideration the following primary scattering mechanisms in the inversion layer:

1. Phonon scattering which results primarily from the interaction between two-dimensional inversion layer carriers and bulk phonons.
2. Surface roughness scattering caused by the interaction between inversion layer carriers and deviations from ideal planarity at the interface.
3. Charged impurity scattering caused by the interaction between inversion layer carriers and ions located in the oxide, at the interface, or in the bulk

The phonon and surface roughness components are functions of effective electric field. The charged impurity component is a function of the channel doping density.

The effective mobilities for electrons and holes are given by Equations 3-266 and 3-267.

$$\begin{aligned} \frac{1}{\mu_{eff,n}} = & \frac{1}{MREF1N.WATT} \left(\frac{1}{E_{eff,n}} \right)^{AL1N.WATT} \\ & + \frac{1}{MREF2N.WATT} \left(\frac{1}{E_{eff,n}} \right)^{AL2N.WATT} \\ & + \frac{1}{MREF3N.WATT} \left(\frac{1}{N_B} \right)^{-1} \left(\frac{1}{N_i} \right)^{AL3N.WATT} \end{aligned} \quad 3-266$$

$$\begin{aligned} \frac{1}{\mu_{eff,p}} = & \frac{1}{MREF1P.WATT} \left(\frac{1}{E_{eff,p}} \right)^{AL1P.WATT} \\ & + \frac{1}{MREF2P.WATT} \left(\frac{1}{E_{eff,p}} \right)^{AL2P.WATT} \\ & + \frac{1}{MREF3P.WATT} \left(\frac{1}{N_B} \right)^{-1} \left(\frac{1}{N_i} \right)^{AL3N.WATT} \end{aligned} \quad 3-267$$

Here, N_B is the surface trapped charge density, N_i is the inversion layer charge density and E_{eff} is the effective electric field given by:

$$E_{eff,n} = E_{\perp} + ETAN.WATT(E_0 - E_{\perp}) \quad 3-268$$

$$E_{eff,p} = E_{\perp} + ETAP.WATT(E_0 - E_{\perp}) \quad 3-269$$

Here, E_{\perp} is the electric field perpendicular to the current flow and E_0 is the perpendicular electric field at the insulator-semiconductor interface. The equation parameters and their defaults are listed in Table 3-49.

The terms on the right side of Equations 3-266 and 3-267, describe (in order) the three scattering mechanisms previously discussed. Each component contains two constants: a pre-exponential factor and the exponent of the principal independent parameter. The charge impurity scattering component is assumed to be inversely proportional to doping density.

The expression for effective mobility contains a number of normalizing constants. These normalizing constants are included to allow easy comparison of constants. The first two terms in this mobility model are dependent on E_{eff} and represent the universal mobility-field relationship. The third term accounts for deviation from the universal relationship resulting from charged impurity scattering.

Table 3-49. User-Specifiable Parameters for Equations 3-266 - 3-269

| Statement | Parameter | Default | Units |
|-----------|-------------|---------|-------------------------|
| MOBILITY | ETAN.WATT | 0.50 | |
| MOBILITY | ETAP.WATT | 0.33 | |
| MOBILITY | MREF1N.WATT | 481.0 | cm ² / (V·s) |
| MOBILITY | MREF1P.WATT | 92.8 | cm ² / (V·s) |
| MOBILITY | MREF2N.WATT | 591.0 | cm ² / (V·s) |
| MOBILITY | MREF2P.WATT | 124.0 | cm ² / (V·s) |
| MOBILITY | MREF3N.WATT | 1270.0 | cm ² / (V·s) |
| MOBILITY | MREF3P.WATT | 534.0 | cm ² / (V·s) |
| MOBILITY | AL1N.WATT | -0.16 | |
| MOBILITY | AL1P.WATT | -0.296 | |
| MOBILITY | AL2N.WATT | -2.17 | |
| MOBILITY | AL2P.WATT | -1.62 | |
| MOBILITY | AL3N.WATT | 1.07 | |
| MOBILITY | AL3P.WATT | 1.02 | |

Modifications to the Watt's Model

By default the Watt mobility model is a surface model that applies, only to those grid points on the silicon/ oxide interface. A modification has been added that now applies the Watt model to points below the interface. This extension to the Watt model is enabled using the MOD.WATT.N and MOD.WATT.P parameters of the MOBILITY statement.

The distance over which the model is applied can be controlled by using the YMAXN.WATT and the YMAXP.WATT parameters of the MOBILITY statement. These parameters specify the maximum value of the Y coordinate over which the model is applies below the interface for electrons and holes respectively.

The XMINN.WATT, XMINP.WATT, XMAXN.WATT and XMAXP.WATT of the MOBILITY statement can be used to limit the range of the model in the X direction, to prevent the model from applying to the source and drain regions. The MIN.SURF parameter of the MODELS statement can also be used for this purpose. When enabled, the MIN.SURF parameter will ensure that the Watt model will only apply to minority regions.

The logical parameters `EXP.WATT.N` and `EXP.WATT.P` of the `MOBILITY` statement can also be used to enable an additional modification to the Watt model. When these parameters are enabled the effective normal electric field becomes a function of the depth beneath the silicon/oxide interface according to:

$$E_{\perp,n} = E_y \exp \frac{-(y - y_{int})}{YCHARN.WATT} \quad 3-270$$

$$E_{\perp,p} = E_y \exp \frac{-(y - y_{int})}{YCHARP.WATT} \quad 3-271$$

where E_{\perp} is the perpendicular electric field, E_y is the perpendicular electric field at the interface, y is the local Y coordinate and y_{int} is the Y coordinate of the silicon/oxide interface. The `YCHARN.WATT` and `YCHARP.WATT` parameters are user-definable in the `MOBILITY` statement.

Table 3-50. User-Specifiable Parameters for Equations 3-194 and 3-195

| Statement | Parameter | Default | Units |
|-----------|-------------|-----------------------|---------|
| MOBILITY | XMINN.WATT | -1.0×10^{32} | microns |
| MOBILITY | XMAXN.WATT | 1.0×10^{32} | microns |
| MOBILITY | YMAXN.WATT | -1.0×10^{32} | microns |
| MOBILITY | XMINP.WATT | -1.0×10^{32} | microns |
| MOBILITY | XMAXP.WATT | 1.0×10^{32} | microns |
| MOBILITY | YMAXP.WATT | -1.0×10^{32} | microns |
| MOBILITY | YCHARN.WATT | 1.0×10^{32} | microns |
| MOBILITY | YCHARP.WATT | 1.0×10^{32} | microns |

Shirahata's Mobility Model

The Shirahata Mobility Model [214] is a general purpose MOS mobility model that accounts for screening effects in the inversion layer and uses an improved perpendicular field dependence for thin gate oxides. In the original paper, the authors present the model as a combination of portions of Klaassen's model for low-field mobility contributions and an empirically fit expression for the perpendicular field dependent mobility in the inversion layer. In this implementation, if the Klaassen Low-Field Model is used with the Shirahata model, the lattice scattering term in the Klaassen model is omitted and Matthiesen's rule is used to combine the Klaassen and Shirahata mobilities. But for other low-field models, at any given location, the lesser of the low-field and the Shirahata mobilities are used.

To enable the Shirahata Mobility Model, use the `SHI` parameter of the `MODELS` statement. You can also enable it individually for electrons and holes using the `SHI.N` and `SHI.P` parameters of the `MOBILITY` statement.

The Shirahata models for electrons and holes are given by:

$$\mu_n = \frac{\text{MU0N.SHI} \left(\frac{T_L}{300} \right)^{-\text{THETAN.SHI}}}{\left[1 + \frac{|E_{\perp}|}{\text{E1N.SHI}} \right]^{\text{P1N.SHI}} + \left[\frac{|E_{\perp}|}{\text{E2N.SHI}} \right]^{\text{P2N.SHI}}} \quad 3-272$$

$$\mu_p = \frac{\text{MU0P.SHI} \left(\frac{T_L}{300} \right)^{-\text{THETAP.SHI}}}{\left[1 + \frac{|E_{\perp}|}{\text{E1P.SHI}} \right]^{\text{P1P.SHI}} + \left[\frac{|E_{\perp}|}{\text{E2P.SHI}} \right]^{\text{P2P.SHI}}} \quad 3-273$$

where E_{\perp} is the perpendicular electric and the equation parameters: MU0N.SHI, MU0P.SHI, E1N.SHI, E1P.SHI, E2N.SHI, E2P.SHI, P1N.SHI, P1P.SHI, P2N.SHI, P2P.SHI, THETAN.SHI and THETAP.SHI are user-definable in the MOBILITY statement (see Table 3-51 for their defaults).

Table 3-51. User-Specifiable Parameters for Equations 3-272 and 3-273

| Statement | Parameter | Default | Units |
|-----------|------------|----------------------|-------------------------|
| MOBILITY | MU0N.SHI | 1430.0 | cm ² / (V·s) |
| MOBILITY | MU0P.SHI | 500.0 | cm ² / (V·s) |
| MOBILITY | E1N.SHI | 6.3×10 ³ | V/cm |
| MOBILITY | E1P.SHI | 8.0×10 ³ | V/cm |
| MOBILITY | E2N.SHI | 0.77×10 ⁶ | V/cm |
| MOBILITY | E2P.SHI | 3.9×10 ⁵ | V/cm |
| MOBILITY | P1N.SHI | 0.28 | |
| MOBILITY | P1P.SHI | 0.3 | |
| MOBILITY | P2N.SHI | 2.9 | |
| MOBILITY | P2P.SHI | 1.0 | |
| MOBILITY | THETAN.SHI | 2.285 | |
| MOBILITY | THETAP.SHI | 2.247 | |

Note: If the maximum low-field mobility has been user-defined, then it's important to also define this value inside the Shirahata model with the MU0N.SHI and MU0P.SHI parameters in the MOBILITY statement.

Parallel Electric Field-Dependent Mobility

As carriers are accelerated in an electric field their velocity will begin to saturate when the electric field magnitude becomes significant. This effect has to be accounted for by a reduction of the effective mobility since the magnitude of the drift velocity is the product of the mobility and the electric field component in the direction of the current flow. The following Caughey and Thomas Expression [37] is used to implement a field-dependent mobility. This provides a smooth transition between low-field and high field behavior where:

$$\mu_n(E) = \mu_{n0} \left[\frac{1}{1 + \left(\frac{\mu_{n0} E}{VSATN} \right)^{BETAN}} \right]^{\frac{1}{BETAN}} \quad 3-274$$

$$\mu_p(E) = \mu_{p0} \left[\frac{1}{1 + \left(\frac{\mu_{p0} E}{VSATP} \right)^{BETAP}} \right]^{\frac{1}{BETAP}} \quad 3-275$$

Here, E is the parallel electric field and μ_{n0} and μ_{p0} are the low-field electron and hole mobilities respectively. The low-field mobilities are either set explicitly in the `MOBILITY` statement or calculated by one of the low-field mobility models. The `BETAN` and `BETAP` parameters are user-definable in the `MOBILITY` statement (see Table 3-52 for their defaults).

The saturation velocities are calculated by default from the temperature-dependent models [204]:

$$VSATN = \frac{ALPHAN.FLD}{1 + THETAN.FLD \exp\left(\frac{T_L}{TNOMN.FLD}\right)} \quad 3-276$$

$$VSATP = \frac{ALPHAP.FLD}{1 + THETAP.FLD \exp\left(\frac{T_L}{TNOMP.FLD}\right)} \quad 3-277$$

But, you can set them to constant values on the `MOBILITY` statement using the `VSATN` and `VSATP` parameters.

In this case, no temperature dependence is implemented. Specifying the `FLDMOB` parameter on the `MODELS` statement invokes the field-dependent mobility. `FLDMOB` should always be specified unless one of the inversion layer mobility models (which incorporate their own dependence on the parallel field) are specified.

You can invoke a `C-INTERPRETER` function for the saturation velocities. The `F.VSATN` and `F.VSATP` parameters in the `MATERIAL` statement can be set to provide the filenames of two text files containing the particular functions. These functions allow you to include the temperature dependence. See Appendix A: “C-Interpreter Functions” for more details.

Canali Modification

The Canali model [35] has been implemented as an alternative to using fixed values of BETAN and BETAP in the Caughey-Thomes model. This uses the exponent BETA, which depends on lattice temperature (TL), and will calculate the values of BETAN and BETAP as

$$\text{BETAN} = \text{N.BETA0} * (\text{TL}/300)^{(\text{N.BETAEXP})} \quad 3-278$$

$$\text{BETAP} = \text{P.BETA0} * (\text{TL}/300)^{(\text{P.BETAEXP})} \quad 3-279$$

The Canali model can be used for Silicon up to 430 K.

To enable the model, use the N.CANALI and P.CANALI parameters on the MOBILITY statement. You should also set the FLDMOB flag on the MODELS statement. The EVSATMOD and HVSATMOD should also have their default values of 0.

| Table 3-52. User-Definable Parameters in the Field-Dependent Mobility Model | | | |
|---|------------|-------------------|-------|
| Statement | Parameter | Default | Units |
| MOBILITY | ALPHAN.FLD | 2.4×10^7 | cm/s |
| MOBILITY | ALPHAP.FLD | 2.4×10^7 | cm/s |
| MOBILITY | BETAN | 2.0 | |
| MOBILITY | BETAP | 1.0 | |
| MOBILITY | N.BETAEXP | 0.66 | |
| MOBILITY | N.BETA0 | 1.109 | |
| MOBILITY | N.CANALI | False | |
| MOBILITY | P.BETAEXP | 0.17 | |
| MOBILITY | P.BETA0 | 1.213 | |
| MOBILITY | P.CANALI | False | |
| MOBILITY | THETAN.FLD | 0.8 | |
| MOBILITY | THETAP.FLD | 0.8 | |
| MOBILITY | TNOMN.FLD | 600.0 | K |
| MOBILITY | VSATN | | cm/s |
| MOBILITY | VSATP | | cm/s |
| MOBILITY | TNOMP.FLD | 600.0 | K |

Note: Equation 3-277, which was derived for the drift-diffusion approximation, ensures that velocity overshoot cannot occur. To model velocity overshoot in silicon, apply the Energy Balance Transport Model. This model follows the above implementation but with the electric field term replaced by a new “effective” field calculated from the carrier temperature see the following section for more details.

Note: BLAZE includes a different field dependent mobility model that does simulate velocity overshoot in GaAs. See Chapter 5: “Blaze: Compound Material 2D Simulator” for more information.

Carrier Temperature Dependent Mobility

The Energy Balance Transport Model allows the carrier mobility to be related to the carrier energy. This has been achieved through the homogeneous steady state energy balance relationship that pertains in the saturated velocity limit. This allows an effective electric field to be calculated, which is the uniform electric field value that causes the carriers in a homogeneous sample to attain the same temperature as at the node point in the device. The effective electric fields, $E_{eff,n}$ and $E_{eff,p}$, are calculated by solving the equations:

$$q\mu_n(E_{eff,n})E_{eff,n}^2 = \frac{3}{2} \frac{k(T_n - T_L)}{TAUMOB.EL} \quad 3-280$$

$$q\mu_p(E_{eff,p})E_{eff,p}^2 = \frac{3}{2} \frac{k(T_p - T_L)}{TAUMOB.HO} \quad 3-281$$

for $E_{eff,n}$ and $E_{eff,p}$. These equations are derived from the energy balance equations by stripping out all spatially varying terms. The effective electric fields are then introduced into the relevant field dependent mobility model. The TAUMOB.EL and TAUMOB.HO parameters can be set on the MODELS statement and have the default values shown in Table 3-53.

Note: The TAUMOB.EL and TAUMOB.HO parameters are distinct from the energy balance relaxation time parameters: TAUREL.EL and TAUREL.HO. But, if the E.TAUR.VAR and H.TAUR.VAR parameters are set on the MODELS statement, then TAUREL.EL and TAUREL.HO are used in place of TAUMOB.EL and TAUMOB.HO.

Table 3-53. User-Specifiable Parameters for Equations 3-280 and 3-281

| Statement | Parameter | Default | Units |
|-----------|-----------|-----------------------|-------|
| MODELS | TAUMOB.EL | 2.5×10^{-13} | s |
| MODELS | TAUMOB.HO | 2.5×10^{-13} | s |

Four different models have been implemented into the ATLAS Energy Balance Transport Model which can be chosen by the parameter EVSATMOD on the MODELS statement. These models shall be described next.

Setting `EVSATMOD=0` implements, the default model for silicon based upon the Caughey-Thomas field-dependent mobility model in Equation 3-274. The resultant relationship between the carrier mobility and the carrier temperature is in the forms:

$$\mu_n = \frac{\mu_{n0}}{\left(1 + X_n^{\text{BETAN}}\right)^{\frac{1}{\text{BETAN}}}} \quad 3-282$$

$$\mu_p = \frac{\mu_{p0}}{\left(1 + X_p^{\text{BETAP}}\right)^{\frac{1}{\text{BETAP}}}} \quad 3-283$$

$$X_n^{\text{BETAN}} = \frac{1}{2}(\alpha_n^{\text{BETAN}}(T_n - T_L)^{\text{BETAN}} + \sqrt{\alpha_n^{2\text{BETAN}}(T_n - T_L)^{2\text{BETAN}} - 4\alpha_n^{\text{BETAN}}(T_n - T_L)^{\text{BETAN}}}) \quad 3-284$$

$$X_p^{\text{BETAP}} = \frac{1}{2}(\alpha_p^{\text{BETAP}}(T_p - T_L)^{\text{BETAP}} + \sqrt{\alpha_p^{2\text{BETAP}}(T_p - T_L)^{2\text{BETAP}} - 4\alpha_p^{\text{BETAP}}(T_p - T_L)^{\text{BETAP}}}) \quad 3-285$$

$$\alpha_n = \frac{3}{2} \frac{k_B \mu_{n0}}{q \text{VSATN}^2 (\text{TAUREL_EL})} \quad 3-286$$

$$\alpha_p = \frac{3}{2} \frac{k_B \mu_{p0}}{q \text{VSATP}^2 (\text{TAUREL_HO})} \quad 3-287$$

where μ_{n0} and μ_{p0} are the low-field carrier mobilities and `VSATN` and `VSATP` are the saturated velocities for electrons and holes. The `VSATN`, `VSATP`, `BETAN`, and `BETAP` parameters are user-definable in the `MOBILITY` statement. The terms, `TAUREL_EL` and `TAUREL_HO`, are the energy relaxation times for electrons and holes and can be defined in the `MATERIAL` statement.

Setting `EVSATMOD=0` with the additional parameter, `MOBTEM.SIMPL`, allows you to apply a simplified form of the above model. This form is:

$$\mu_n = \frac{\mu_{n0}}{\sqrt{1 + \alpha_n^2 (T_n - T_L)^2}} \quad 3-288$$

$$\mu_p = \frac{\mu_{p0}}{\sqrt{1 + \alpha_p^2 (T_p - T_L)^2}} \quad 3-289$$

where μ_{n0} and μ_{p0} are again the low-field carrier mobilities and $a_{n,p}$ are as defined above.

Setting `EVSATMOD=1` implements the GaAs carrier temperature dependent mobility model. See Chapter 5: “Blaze: Compound Material 2D Simulator” for more information about this model.

Setting EVSATMOD=2 will apply the simple velocity limiting model based upon the electric field. In other words, the temperature dependent mobility is turned off and the standard electric field based mobility model is applied.

Note: If the YAMAGUCHI or TASCH mobility models are chosen in the MODEL statement, then no energy dependence is applied. No energy dependence is included in any perpendicular electric field model, such as SHIRAHATA or SURFMOB.

Table 3-54. User-Specifiable Parameters for Equations 3-282– 3-289

| Statement | Parameter | Units |
|-----------|-----------|-------------------------|
| MOBILITY | MUN | cm ² / (V·s) |
| MOBILITY | MUP | cm ² / (V·s) |
| MATERIAL | VSATN | cm/s |
| MATERIAL | VSATP | cm/s |

Meinerzhagen-Engl Model

The Meinerzhagen-Engl model is another velocity saturation model in which the mobility depends on the carrier temperature [156].

$$\mu_n = \frac{\mu_{n0}}{(1 + \alpha_n^\beta (T_n - T_L)^\beta)^{1/\beta}} \quad 3-290$$

$$\mu_p = \frac{\mu_{p0}}{(1 + \alpha_p^\beta (T_p - T_L)^\beta)^{1/\beta}} \quad 3-291$$

where α_n and α_p are the same as in Equations 3-286 and 3-287. If $\beta=2$, then you have the same result as in Equations 3-288 and 3-289. The exponent β , however, may now depend on lattice temperature (T_L).

As in the Canali model, the values of BETAN and BETAP are calculated as

$$\text{BETAN} = \text{N.BETA0} * (\text{TL}/300)^{(\text{N.BETAEXP})} \quad 3-292$$

$$\text{BETAP} = \text{P.BETA0} * (\text{TL}/300)^{(\text{P.BETAEXP})} \quad 3-293$$

although the default values differ from the Canali model (see Table 3-55).

To activate the model, specify FLDMOB on the MODELS statement and additionally N.MEINR or P.MEINR or both on the MOBILITY statement. You must at least solve for one of the electron or hole temperatures. The exponent β is constant unless you enable Lattice temperature too.

Table 3-55. User specifiable parameters for Meinerzhagen-Engl model.

| Statement | Parameter | Default |
|-----------|-----------|---------|
| MOBILITY | N.MEINR | False |
| MOBILITY | P.MEINR | False |
| MOBILITY | N.BETA0 | 0.6 |
| MOBILITY | P.BETA0 | 0.6 |
| MOBILITY | N.BETAEXP | 0.01 |
| MOBILITY | P.BETAEXP | 0.01 |

Complete C-Interpreter Functions for Mobility

ATLAS provides some C-Interpreter functions that allows you to completely specify the mobility. These can be considered as stand-alone mobility specifications as they are not combined with other mobility parameters.

First, there is a C-Interpreter function that allows the input of a mobility function, which depends explicitly on position. The parameters supplied to the function include the (X, Y, Z) coordinates of each node point, acceptor and donor concentrations, electric field, electrical potential, lattice temperature and carrier temperature.

For electron mobility, use the `F.LOCALMUN` parameter on the `MATERIAL` or `MOBILITY` statement. For hole mobility, use the `F.LOCALMUP` parameter on the `MATERIAL` or `MOBILITY` statement.

There is also a C-Interpreter function that allows you to supply a mobility, which depends explicitly on perpendicular electric field (as in a surface mobility model) and on parallel field (as in a velocity saturation model). Other parameters that are supplied are dopant densities, carrier densities, lattice temperature and composition fractions. For electron mobility, use the `F.TOFIMUN` parameter on the `MATERIAL` or `MOBILITY` statement. For hole mobility, use the `F.TOFIMUP` parameter on the `MATERIAL` or `MOBILITY` statement.

For details about C-Interpreter functions, see Appendix A: “C-Interpreter Functions” and the C-Interpreter templates, which come with your ATLAS distribution.

3.6.2: Mobility Model Summary

Tables 3-56 and 3-57 shows a brief description of the mobility models.

| Table 3-56. Mobility Models Summary | | |
|---|------------|---|
| Model | Syntax | Notes |
| Concentration Dependent | CONMOB | Lookup table valid at 300K for Si and GaAs only. Uses simple power law temperature dependence. |
| Concentration and Temperature Dependent | ANALYTIC | Caughey-Thomas formula. Tuned for 77-450K. |
| Arora's Model | ARORA | Alternative to ANALYTIC for Si. |
| Carrier-Carrier Scattering | CCSMOB | Dorkel-Leturq Model. Includes n, N and T dependence. Important when carrier concentration is high (e.g., forward bias power devices). |
| Parallel Electric Field Dependence | FLDMOB | Si and GaAs models. Required to model any type of velocity saturation effect. |
| Tasch Model | TASCH | Includes transverse field dependence. Only for planar devices. Needs very fine grid. |
| Watt Model | WATT | Transverse field model applied to surface nodes only. |
| Klaassen Model | KLA | Includes N, T, and n dependence. Applies separate mobility to majority and minority carriers. Recommended for bipolar devices |
| Shirahata Model | SHI | Includes N, E_{\perp} . An alternative surface mobility model that can be combined with KLA. |
| Modified Watt | MOD . WATT | Extension of WATT model to non-surface nodes. Applies constant E_{\perp} effects. Best model for planar MOS devices |
| Lombardi (CVT) Model | CVT | Complete model including N, T, E_{\parallel} and E_{\perp} effects. Good for non-planar devices. |
| Yamaguchi Model | YAMAGUCHI | Includes N, E_{\parallel} and E_{\perp} effects. Only for 300K. |

| Table 3-57. Mobility Models Summary | | | | | | | | | | | |
|-------------------------------------|--------|-----------------|-----------------|-----------|-----|-------|----------|--------|---------|-----------|--------------|
| | CONMOB | FLDMOB | TFLDMB2 | YAMAGUCHI | CVT | ARORA | ANALYTIC | CCSMOB | SURFACE | LATTICE H | E.BALANCE |
| CONMOB [CM] | — | OK | OK | YA | CV | AR | AN | CC | OK | OK | OK |
| FLDMOB [FM] | OK | — | TF ¹ | YA | CV | OK | OK | OK | OK | OK | OK |
| TFLDMB2 [TF] | OK | TF ¹ | — | YA | CV | OK | OK | TF | TF | OK | OK |
| YAMAGUCHI [YA] | YA | YA | YA | — | CV | YA | YA | YA | YA | NO | NO |
| CVT [CV] | CV | CV | CV | CV | — | CV | CV | CV | CV | OK | OK |
| ARORA [AR] | AR | OK | OK | YA | CV | — | AR | CC | OK | OK | OK |
| ANALYTIC [AN] | AN | OK | OK | YA | OK | | — | CC | OK | OK | OK |
| CCSMOB [CC] | CC | OK | TF | YA | CV | CC | CC | — | OK | OK | OK |
| SURFMOB [SF] | OK | OK | TF | YA | CV | OK | OK | OK | — | OK | OK |
| LATTICE H [LH] | OK | OK | OK | NO | OK | OK | OK | OK | OK | — | OK |
| E.BALANCE [EB] | OK | OK | OK | NO | OK | OK | OK | OK | OK | OK | ² |

Table 3-57. Mobility Models Summary

| | CONMOB | FLDMOB | TFLDMB2 | YAMAGUCHI | CVT | ARORA | ANALYTIC | CCSMOB | SURFACE | LATTICE H | E.BALANCE |
|--|--------|--------|---------|-----------|-----|-------|----------|--------|---------|-----------|-----------|
|--|--------|--------|---------|-----------|-----|-------|----------|--------|---------|-----------|-----------|

Key to Table Entries:

MODEL ABBREVIATION = The model that supersedes when a combination is specified. In some cases, but not all, a warning message is issued when a model is ignored.

OK = This combination is allowed.

NO = This combination isn't allowed.

NOTES:

1. Uses internal model similar to FLDMOB
2. When models including a parallel electric field dependence are used with energy balance the electric field term is replaced by a function of carrier temperature.

3.6.3: Carrier Generation-Recombination Models

Carrier generation-recombination is the process through which the semiconductor material attempts to return to equilibrium after being disturbed from it. If we consider a homogeneously doped semiconductor with carrier concentrations n and p to the equilibrium concentrations n_0 and p_0 then at equilibrium a steady state balance exists according to:

$$n_0 p_0 = n_i^2 \quad 3-294$$

Semiconductors, however, are under continual excitation whereby n and p are disturbed from their equilibrium states: n_0 and p_0 . For instance, light shining on the surface of a p-type semiconductor causes generation of electron-hole pairs, disturbing greatly the minority carrier concentration. A net recombination results which attempts to return the semiconductor to equilibrium. The processes responsible for generation-recombination are known to fall into six main categories:

- phonon transitions
- photon transitions
- Auger transitions
- surface recombination
- impact ionization
- tunneling

The following sections describes the models implemented into ATLAS that attempts the simulation of these six types of generation-recombination mechanisms.

Shockley-Read-Hall (SRH) Recombination

Phonon transitions occur in the presence of a trap (or defect) within the forbidden gap of the semiconductor. This is essentially a two step process, the theory of which was first derived by Shockley and Read [215] and then by Hall [86]. The Shockley-Read-Hall recombination is modeled as follows:

$$R_{SRH} = \frac{pn - n_{ie}^2}{\text{TAUPO} \left[n + n_{ie} \exp \left(\frac{\text{ETRAP}}{kT_L} \right) \right] + \text{TAUNO} \left[p + n_{ie} \exp \left(\frac{-\text{ETRAP}}{kT_L} \right) \right]} \quad 3-295$$

where ETRAP is the difference between the trap energy level and the intrinsic Fermi level, T_L is the lattice temperature in degrees Kelvin and TAUNO and TAUPO are the electron and hole lifetimes. This model is activated by using the SRH parameter of the MODELS statement. The electron and hole lifetime parameters, TAUNO and TAUPO, are user-definable in the MATERIAL statement. The default values for carrier lifetimes are shown in Table 3-58. Materials other than silicon will have different defaults. A full description of these parameters are given in Appendix B: “Material Systems”.

| Table 3-58. User-Specifiable Parameters for Equation 3-295 | | | |
|--|-----------|--------------------|-------|
| Statement | Parameter | Default | Units |
| MATERIAL | ETRAP | 0 | eV |
| MATERIAL | TAUNO | 1×10^{-7} | s |
| MATERIAL | TAUPO | 1×10^{-7} | s |

Note: This model only presumes one trap level which, by default, is ETRAP=0 and it corresponds to the most efficient recombination centre. If the TRAP statement is used to define specific trap physics then separate SRH statistics are implemented as described earlier in “Trap Implementation into Recombination Models” section on page 3-17.

SRH Concentration-Dependent Lifetime Model

The constant carrier lifetimes that are used in the SRH recombination model above can be made a function of impurity concentration [197,137,72] using the following equation:

$$R_{SRH} = \frac{pn - n_{ie}^2}{\tau_p \left[n + n_{ie} \exp \left(\frac{\text{ETRAP}}{kT_L} \right) \right] + \tau_n \left[p + n_{ie} \exp \left(\frac{-\text{ETRAP}}{kT_L} \right) \right]} \quad 3-296$$

where:

$$\tau_n = \frac{\text{TAUNO}}{\text{AN} + \text{BN} \left(\frac{N_{total}}{\text{NSRHN}} \right) + \text{CN} \left(\frac{N_{total}}{\text{NSRHN}} \right)^{\text{EN}}} \quad 3-297$$

$$\tau_p = \frac{\text{TAUPO}}{\text{AP} + \text{BP} \left(\frac{N_{total}}{\text{NSRHP}} \right) + \text{CP} \left(\frac{N_{total}}{\text{NSRHP}} \right)^{\text{EP}}} \quad 3-298$$

Here, N is the local (total) impurity concentration. The TAUN0, TAUP0, NSRHN, and NSRHP parameters can be defined on the MATERIAL statement (see Table 3-59 for their default values). This model is activated with the CONSRH parameter of the MODELS statement.

| Table 3-59. User-Specifiable Parameters for Equations 3-296 to 3-298 | | | |
|--|-----------|----------------------|------------------|
| Statement | Parameter | Default | Units |
| MATERIAL | TAUN0 | 1.0×10^{-7} | s |
| MATERIAL | NSRHN | 5.0×10^{16} | cm^{-3} |
| MATERIAL | TAUP0 | 1.0×10^{-7} | s |
| MATERIAL | NSRHP | 5.0×10^{16} | cm^{-3} |
| MATERIAL | AN | 1.0 | |
| MATERIAL | AP | 1.0 | |
| MATERIAL | BN | 1.0 | |
| MATERIAL | BP | 1.0 | |
| MATERIAL | CN | 0.0 | |
| MATERIAL | CP | 0.0 | |
| MATERIAL | EN | 0.0 | |
| MATERIAL | EP | 0.0 | |

You can choose an alternate set of default values for the concentration dependent SRH model as suggested by Law et.al. [137]. Specifying CONSRH, LAW on the MODEL statement will select the use of the alternate default values shown in Table 3-60.

| Table 3-60. Alternate default values for Equations 3-296 to 3-298 | | | |
|---|-----------|---------------------|------------------|
| Statement | Parameter | Default | Units |
| MATERIAL | TAUN0 | 30×10^{-6} | s |
| MATERIAL | TAUP0 | 10×10^{-6} | s |
| MATERIAL | NSRHN | 1×10^{17} | cm^{-3} |
| MATERIAL | NSRHP | 1×10^{17} | cm^{-3} |

Klaassen's Concentration Dependent Lifetime Model

The Klaassen Concentration and Temperature-dependent SRH Lifetime Model [121] is enabled by setting the KLASRH logical parameter in the MODELS statement. The lifetimes for electrons and holes in this model are given by the equations:

$$\tau_{AUN0}^{-1} = (\text{KSRHTN}^{-1} + \text{KSRHCN} \times N) \left(\frac{300}{T_L} \right)^{\text{KSRHGN}} \quad 3-299$$

$$\tau_{AUP0}^{-1} = (\text{KSRHTP}^{-1} + \text{KSRHCP} \times N) \left(\frac{300}{T_L} \right)^{\text{KSRHGP}} \quad 3-300$$

Here, N is the local (total) impurity concentration. You can define the KSRHTN, KSRHTP, KSRHCN, KSRHCP, KSRHGN, and KSRHGP parameters in the MATERIAL statement. Their default values are given in Table 3-61.

| Table 3-61. User-Specifiable Parameters for Equations 3-299 to 3-300 | | | |
|--|-----------|-------------------------|------------------------|
| Statement | Parameter | Default | Units |
| MATERIAL | KSRHTN | 2.5×10^{-3} | s |
| MATERIAL | KSRHTP | 2.5×10^{-3} | s |
| MATERIAL | KSRHCN | 3.0×10^{-13} | cm^3/s |
| MATERIAL | KSRHCP | 11.76×10^{-13} | cm^3/s |
| MATERIAL | KSRHGN | 1.77 | |
| MATERIAL | KSRHGP | 0.57 | |

Scharfetter Concentration Dependent Lifetime Model

This is another model for the dependence of recombination lifetimes on total doping level. To enable this model, use the flag SCHSRH on the MODELS statement. The lifetimes are given by

$$\tau_n(N) = N \cdot \text{SCH} \cdot \text{MIN} + \frac{(N \cdot \text{SCH} \cdot \text{MAX} - N \cdot \text{SCH} \cdot \text{MIN})}{\left[1 + (N \cdot \text{SCH} \cdot \text{NREF})^{\text{N} \cdot \text{SCH} \cdot \text{GAMMA}} \right]} \quad 3-301$$

and

$$\tau_p(N) = P \cdot \text{SCH} \cdot \text{MIN} + \frac{(P \cdot \text{SCH} \cdot \text{MAX} - P \cdot \text{SCH} \cdot \text{MIN})}{\left[1 + (P \cdot \text{SCH} \cdot \text{NREF})^{\text{P} \cdot \text{SCH} \cdot \text{GAMMA}} \right]} \quad 3-302$$

where N is the Total doping density. Table 3-62 shows the MATERIAL statement parameters.

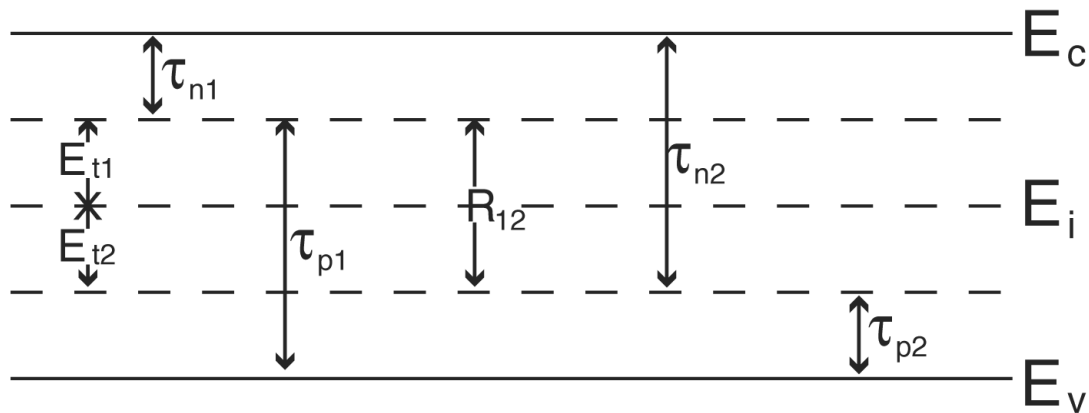
Table 3-62. User Specifiable Parameters for Equations 3-301 and 3-302

| Statement | Parameter | Units | Default |
|-----------|-------------|------------------|----------------------|
| MATERIAL | N.SCH.MIN | s | 0.0 |
| MATERIAL | P.SCH.MIN | s | 0.0 |
| MATERIAL | N.SCH.MAX | s | 1.0×10^{-5} |
| MATERIAL | P.SCH.MAX | s | 3.0×10^{-6} |
| MATERIAL | N.SCH.GAMMA | s | 1.0 |
| MATERIAL | P.SCH.GAMMA | s | 1.0 |
| MATERIAL | N.SCH.NREF | cm^{-3} | 1.0×10^{16} |
| MATERIAL | P.SCH.NREF | cm^{-3} | 1.0×10^{16} |

Coupled Defect Level Recombination Model

This model is a modification of the SRH model to the situation where there is charge transfer between two defect levels. This can lead to large excess currents in devices. The model has explained some anomalous diode characteristics [200].

Figure 3-5 shows the assumptions about the trap levels.

**Figure 3-5: Trap Level Assumptions**

If there is no coupling between the two defect levels, then the recombination total recombination rate is just the sum of two SRH terms, $R_1 + R_2$, where

$$R_1 = \frac{np - n_i^2}{r_1} \quad 3-303$$

and

$$R_2 = \frac{np - n_i^2}{r_2} \quad 3-304$$

where the denominators are

$$r_k = \tau_{nk}(p + p_k) + \tau_{pk}(n + n_k):k = 1, 2 \quad 3-305$$

Assuming Boltzmann statistics apply, the quantities n_1 , n_2 , p_1 and p_2 are given by

$$\left. \begin{aligned} n_1 &= n_i \exp\left(\frac{E_{t1}}{kT}\right) \\ p_1 &= n_i \exp\left(\frac{-E_{t1}}{kT}\right) \\ n_2 &= n_i \exp\left(\frac{E_{t2}}{kT}\right) \\ p_2 &= n_i \exp\left(\frac{-E_{t2}}{kT}\right) \end{aligned} \right\} \quad 3-306$$

If r_{12} is non-zero, then the total recombination rate is given by

$$R = R_1 + R_2 + \left(\sqrt{R_{12}^2 - S_{12} - R_{12}} \right) \quad 3-307$$

$$\times \frac{\text{CDL} \cdot \text{TN1} \cdot \text{CDL} \cdot \text{TP2}(n + n_2)(p + p_1) - \text{CDL} \cdot \text{TN2} \cdot \text{CDL} \cdot \text{TP1}(n + n_1)(p + p_2)}{r_1 r_2}$$

where

$$R_{12} = \frac{r_1 r_2}{2 \times \text{CDL} \cdot \text{COUPLING} \cdot \text{CDL} \cdot \text{TN1} \cdot \text{CDL} \cdot \text{TN2} \cdot \text{CDL} \cdot \text{TP1} \cdot \text{CDL} \cdot \text{TP2}(1 - \varepsilon)} \quad 3-308$$

$$+ \frac{\text{CDL} \cdot \text{TN1}(p + p_1) + \text{CDL} \cdot \text{TP2}(n + n_2)}{2 \text{CDL} \cdot \text{TN1} \cdot \text{CDL} \cdot \text{TP2}(1 - \varepsilon)}$$

$$+ \frac{\varepsilon[\text{CDL} \cdot \text{TN2}(p + p_2) + \text{CDL} \cdot \text{TP1}(n + n_1)]}{2 \text{CDL} \cdot \text{TN2} \cdot \text{CDL} \cdot \text{TP1}(1 - \varepsilon)}$$

and

$$S_{12} = \frac{1}{\text{CDL} \cdot \text{TN1} \cdot \text{CDL} \cdot \text{TP2}(1 - \varepsilon)} \left(1 - \frac{\text{CDL} \cdot \text{TN1} \cdot \text{CDL} \cdot \text{TP2} \varepsilon}{\text{CDL} \cdot \text{TN2} \cdot \text{CDL} \cdot \text{TP1}} \right) (np - n_i^2) \quad 3-309$$

The factor ε is given by

$$\varepsilon = \exp\left(\frac{-(|E_{t2} - E_{t1}|)}{K_B T}\right) \quad 3-310$$

and will generally be less than 1. It can be shown that as r_{12} becomes small, the total recombination rate simplifies to $R_1 + R_2$ as required.

You can set all the relevant parameters in ATLAS. To set the rate r_{12} , use `CDL.COUPLING` on the `MATERIAL` statement. To set the carrier lifetimes, use `CDL.TN1`, `CDL.TN2`, `CDL.TP1` and `CDL.TP2` on the `MATERIAL` statement. To set the energies of the defect levels relative to the intrinsic level, use `CDL.ETR1` and `CDL.ETR2` on the `MATERIAL` statement.

With reference to the energies shown in Figure 3-5, `CDL.ETR1` will be positive and `CDL.ETR2` will be negative. Table 3-63 shows these quantities and the units and default values.

To enable the model, use either the `CDL` parameter or the `CONCDL` parameter on the `MODELS` statement. If you set `CDL`, then the values used for the lifetimes are those set by `CDL.TN1`, `CDL.TN2`, `CDL.TP1` and `CDL.TP2`. If you set `CONCDL`, then the lifetimes used are doping dependent and are derived from Equations 3-297 and 3-298 with the lifetimes being `CDL.TN1`, `CDL.TN2`, `CDL.TP1` and `CDL.TP2`, instead of `TAUN0` and `TAUP0`. The default values for the other parameters are shown in Table 3-59.

`SRH` and `CDL` are mutually exclusive parameters. If you enable `CDL`, the `CDL` recombination rate is output to a structure file in the `SRH` slot and are added to the output of total recombination rate.

| Table 3-63. Material Parameters for Coupled Defect Level Model | | | | |
|--|--------------|------|----------------------------------|---------|
| Statement | Parameter | Type | Units | Default |
| MATERIAL | CDL.ETR1 | Real | eV | 0.0 |
| MATERIAL | CDL.ETR2 | Real | eV | 0.0 |
| MATERIAL | CDL.TN1 | Real | s | 1.0 |
| MATERIAL | CDL.TN2 | Real | s | 1.0 |
| MATERIAL | CDL.TP1 | Real | s | 1.0 |
| MATERIAL | CDL.TP2 | Real | s | 1.0 |
| MATERIAL | CDL.COUPLING | Real | s ⁻¹ cm ⁻³ | 1.0 |

The individual lifetimes cannot be output to a structure file.

Trap Assisted Auger Recombination

This model adds in a dependence of recombination lifetime on carrier density, and will only be significant at fairly high carrier densities [73].

The carrier lifetimes are reduced according to the following formula

$$\tau_n = \frac{\tau_n}{(1 + TAA.CN(n + p)\tau_n)} \quad 3-311$$

$$\tau_p = \frac{\tau_p}{(1 + TAA.CP(n + p)\tau_p)} \quad 3-312$$

where n is the electron density and p the hole density. To enable the model, specify `TRAP.AUGER` on the `MODELS` statement. It will then apply to the `SRH` model if enabled or to the `CDL` model if enabled.

You can set the parameters on the MATERIAL statement with the defaults as shown in Table 3-64.

| Table 3-64. Parameters for Trap assisted Auger model | | | |
|--|-----------|--------------------|-----------------------|
| Statement | Parameter | Units | Default |
| MATERIAL | TAA.CN | cm ³ /s | 1.0×10 ⁻¹² |
| MATERIAL | TAA.CP | cm ³ /s | 1.0×10 ⁻¹² |

Trap-Assisted Tunneling

In a strong electric field, electrons can tunnel through the bandgap via trap states. This trap-assisted tunneling mechanism is enabled by specifying TRAP.TUNNEL on the MODELS statement and is accounted for by modifying the Shockley-Read-Hall recombination model.

$$R_{SRH} = \frac{pn - n_{ie}^2}{\frac{TAUP0}{1 + \Gamma_p^{DIRAC}} \left[n + n_{ie} \exp\left(\frac{ETRAP}{kT_L}\right) \right] + \frac{TAUN0}{1 + \Gamma_n^{DIRAC}} \left[p + n_{ie} \exp\left(\frac{-ETRAP}{kT_L}\right) \right]} \quad 3-313$$

Here, Γ_n^{DIRAC} is the electron field-effect enhancement term for Dirac wells, and Γ_p^{DIRAC} is the hole field-effect enhancement term for Dirac wells. Γ_n^{DIRAC} and Γ_p^{DIRAC} are defined in Equations 3-82 and 3-83.

Schenk Model for Trap Assisted Tunneling [202]

The Schenk model gives the field-effect enhancement factors as an analytic function. Before using this analytic function, however, ATLAS works out several intermediate quantities. The first is an effective trap level E_t given by

$$E_t = \frac{1}{2}Eg(T) + \frac{3}{4}kT \ln\left(\frac{m_c}{m_v}\right) - E_{TRAP} - \left(32R_c \hbar^3 \Theta^3\right)^{1/4} \quad 3-314$$

for electrons

$$E_t = \frac{1}{2}Eg(T) + \frac{3}{4}kT \ln\left(\frac{m_c}{m_v}\right) + E_{TRAP} + \left(32R_v \hbar^3 \Theta^3\right)^{1/4} \quad 3-315$$

for holes. The quantities R_c and R_v are the effective Rydberg energies given by

$$R_c = m_c \left(\frac{Z_{SCHENK}}{\text{PERMITTIVITY}} \right)^2 \times 13.6eV \quad 3-316$$

$$R_v = m_v \left(\frac{Z_{SCHENK}}{\text{PERMITTIVITY}} \right)^2 \times 13.6eV \quad 3-317$$

The quantity Θ is known as the electro-optical frequency and is given as

$$\Theta = \left(\frac{q^2 F^2}{2 \hbar m_{O, ME, TUNNEL}} \right)^{1/3}$$

$$\Theta = \left(\frac{q^2 F^2}{2 \hbar m_{O, MH, TUNNEL}} \right)^{1/3}$$
3-318

where F is the electric field. If you do not specify `ME.TUNNEL`, then a value of $0.5 * (MT1 + MT2)$ will be used for silicon and the density of states effective electron mass for other materials. If you do not specify `MH.TUNNEL`, then the density of states effective hole mass will be used.

The next quantity is the lattice relaxation energy given by

$$\varepsilon_R = \text{HUANG_RHYS} \times \text{PHONON_ENGRY}$$
3-319

From this is derived the quantity ε_F given by

$$\varepsilon_K = \frac{(2 \varepsilon_R k T)^2}{(\hbar \Theta)^3}$$
3-320

ATLAS then calculates the optimum horizontal transition energy, E_0 . This is the energy at which the tunneling probability for carriers to tunnel from the trap level to the band edge has a maximum. It is given by

$$E_0 = 2 \sqrt{\varepsilon_F} \sqrt{\varepsilon_F + E_t + \varepsilon_R} - 2 \varepsilon_F - \varepsilon_R$$
3-321

The field enhancement factor for electrons is then given by

$$\Gamma_n = \left[1 + \frac{(\hbar \Theta)^{3/2} \sqrt{E_t - E_0}}{E_{O, \text{PHONON_ENERGY}}} \right]^{-1/2} \frac{(\hbar \Theta)^{3/4} (E_t - E_0)^{1/4}}{2 \sqrt{E_t E_0}} \left(\frac{\hbar \Theta}{k T} \right)^{3/2}$$

$$\times \exp \left[\frac{-(E_t - E_0)}{\text{PHONON_ENERGY}} + \frac{\text{PHONON_ENERGY} - k T}{2 \text{PHONON_ENERGY}} \right]$$

$$+ \frac{E_t + k T / 2}{\text{PHONON_ENERGY}} \ln(E_t / E_r) - \frac{E_0 \ln(E_0 / E_r)}{\text{PHONON_ENERGY}} \Bigg]$$

$$\times \exp \left(\frac{E_t - E_0}{k T} \right) \exp \left[-\frac{4}{3} \left(\frac{E_t - E_0}{k T} \right)^{3/2} \right]$$
3-322

The field enhancement factor for holes is obtained using Equation 3-322 but with E_t replaced by $E_{g(T)} - E_i$. The default effective masses used in the above calculation are correct for Silicon with the electric field in the <100> direction. They are also accurate for the <110> direction, but for the <111> direction a value of

$$m_c = 3 \left(\frac{1}{m_{t1}} + \frac{1}{m_{t2}} + \frac{1}{m_l} \right)^{-1} \quad 3-323$$

should be used for electrons. To enable the model, specify SCHENK.TUN on the MODELS statement and the parameters shown in Table 3-65.

| Table 3-65. User Definable Parameters for Schenk Trap Assisted Tunneling Model | | | |
|--|---------------|-------|---------|
| Statement | Parameter | Units | Default |
| MATERIAL | PHONON. ENRGY | eV | 0.068 |
| MATERIAL | Z. SCHENK | | 1.0 |
| MATERIAL | HUANG. RHYS | | 3.5 |

Poole-Frenkel Barrier Lowering for Coulombic Wells

The Poole-Frenkel effect can enhance the emission rate for Coulombic wells. If the TRAP.COULOMBIC parameter is specified in the MODELS statement, the Shockley-Read-Hall electron and hole recombination model becomes:

$$R_{n, SRH} = \frac{p_n - n_{ie}^2}{\left(\frac{TAUP0}{1 + \Gamma_p^{DIRAC}} \right) \left[n + n_{ie} \exp\left(\frac{ETRAP}{kT_L}\right) \right] + \left(\frac{TAUN0}{\chi_F + \Gamma_n^{COUL}} \right) \left[p + n_{ie} \exp\left(\frac{-ETRAP}{kT_L}\right) \right]} \quad 3-324$$

$$R_{p, SRH} = \frac{p_n - n_{ie}^2}{\left(\frac{TAUP0}{\chi_F + \Gamma_n^{COUL}} \right) \left[n + n_{ie} \exp\left(\frac{ETRAP}{kT_L}\right) \right] + \left(\frac{TAUN0}{1 + \Gamma_p^{DIRAC}} \right) \left[p + n_{ie} \exp\left(\frac{-ETRAP}{kT_L}\right) \right]} \quad 3-325$$

The Poole-Frenkel thermal emission factor, χ_F , is defined in Equation 3-90. The Coulombic field-enhancement terms, Γ_n^{COUL} and Γ_p^{COUL} are defined in Equations 3-92 and 3-93.

Optical Generation/Radiative Recombination

The next physical mechanisms we have to consider for generation/recombination are photon transition. This mechanism occurs primarily in one step and is therefore a direct generation/recombination mechanism. There are two partial processes involved. For radiative recombination, an electron loses energy on the order of the band gap and moves from the conduction band to the valence band. For optical generation, an electron moves from the valence band to the conduction. In silicon, band to band generation/recombination is insignificant. This effect, however, is important for narrow gap semiconductors and semiconductors whose specific band structure allows direct transitions. By assuming a capture rate C_c^{OPT} and an emission rate C_e^{OPT} , the involved partial processes can be written as

$$R_{np}^{OPT} = C_c^{OPT} n_p, \quad 3-326$$

for recombination and

$$G_{np}^{OPT} = C_e^{OPT} \quad 3-327$$

for generation.

These rates must be equal in thermal equilibrium so that

$$C_{np}^{OPT} = C_c^{OPT} n_{ie}^2. \quad 3-328$$

The total band to band generation/recombination is the difference of the partial rates, which equates to

$$R_{np}^{OPT} = C_c^{OPT} (np - n_{ie}^2). \quad 3-329$$

In ATLAS, C_c^{OPT} can be defined by COPT on the MATERIAL statement or implemented using a C-Interpreter routine. To turn on the optical recombination/ generation model, define the OPTR keyword on the MODELS statement.

Auger Recombination

Auger recombination occurs through a three particle transition whereby a mobile carrier is either captured or emitted. The underlying physics for such processes is unclear and normally a more qualitative understanding is sufficient [207].

Standard Auger Model

Auger Recombination is commonly modeled using the expression [60]:

$$R_{Auger} = AUGN (pn^2 - nn_{ie}^2) + AUGP (np^2 - pn_{ie}^2) \quad 3-330$$

where the model parameters AUGN and AUGP are user-definable in the MATERIAL statement (see Table 3-66 for its default value). You can activate this model with the AUGER parameter from the MODELS statement.

| Table 3-66. User-Specifiable Parameters for Equation 3-330 | | | |
|--|-----------|-----------------------|------------------------|
| Statement | Parameter | Default | Units |
| MATERIAL | AUGN | 2.8×10^{-31} | cm^6/s |
| MATERIAL | AUGP | 9.9×10^{-32} | cm^6/s |

Klaassen's Temperature-Dependent Auger Model

The Klaassen Auger Recombination Model [122] is activated by specifying the `KLAAUG` parameter of the `MODELS` statement. The form of this model is:

$$R_{Auger} = C_n(pn^2 - nn_{ie}^2) + C_p(np^2 - pn_{ie}^2) \quad 3-331$$

where the Auger coefficients are temperature dependent according to:

$$C_n = \text{KAUGCN} \left(\frac{T_L}{300} \right)^{\text{KAUGDN}} \quad 3-332$$

$$C_p = \text{KAUGCP} \left(\frac{T_L}{300} \right)^{\text{KAUGDP}} \quad 3-333$$

Here, the `KAUGCN`, `KAUGCP`, `KAUGDN`, and `KAUGDP` parameters are user-definable in the `MATERIAL` statement and have the defaults shown in Table 3-67.

| Table 3-67. User-Specifiable Parameters for Equation 3-332 and 3-333 | | | |
|--|-----------|------------------------|------------------------|
| Statement | Parameter | Default | Units |
| MATERIAL | KAUGCN | 1.83×10^{-31} | cm^6/s |
| MATERIAL | KAUGCP | 2.78×10^{-31} | cm^6/s |
| MATERIAL | KAUGDN | 1.18 | |
| MATERIAL | KAUGDP | 0.72 | |

Narrow Bandgap Auger Model

An alternative model for the Auger recombination coefficients that is more suitable for modeling Auger processes in narrow bandgap semiconductors can be enabled by setting the parameters AUGKN and AUGKP on the MATERIAL statement and by specifying AUGER on the MODELS statement. The model in ATLAS is a simplification of that by Beattie [22] and takes the form:

$$R_{Auger} = C_n(pn^2 - nn_{ie}^2) + C_p(np^2 - pn_{ie}^2) \quad 3-334$$

where the Auger coefficients are concentration dependent according to:

$$C_n = \frac{AUGN}{1 + AUGKN \cdot n} \quad 3-335$$

$$C_p = \frac{AUGP}{1 + AUGKP \cdot p} \quad 3-336$$

Here, n and p are the electron and hole carrier concentrations and the new parameters, AUGKN and AUGKP, are user-definable on the MATERIALS statement.

Auger Recombination Model for High and Low Injection Conditions [48,116]

The Auger recombination rate given in equation 3-327 can be modified to account for high and low injection conditions. In this model, the Auger rate coefficients, C_n and C_p , are carrier and doping concentration dependent and are given by:

$$C_n = AUG \cdot CNL \left(\frac{N_D}{N_D + p} \right) + \frac{AUG \cdot CHI}{2} \left(\frac{p}{N_D + p} \right) \quad 3-337$$

$$C_p = AUG \cdot CPL \left(\frac{N_A}{N_A + p} \right) + \frac{AUG \cdot CHI}{2} \left(\frac{p}{N_A + p} \right) \quad 3-338$$

Here, you can specify the AUG.CNL, AUG.CPL, and AUG.CHI parameters on the MATERIAL statement and have defaults described in Table 3-66.

| Table 3-68. User Specifiable Parameters for Equations 3-330 and 3-331. | | | |
|--|-----------|------------------------|------------------------|
| Statement | Parameter | Default | Units |
| MATERIAL | AUG.CNL | 2.2×10^{-31} | cm^6/s |
| MATERIAL | AUG.CPL | 9.2×10^{-32} | cm^6/s |
| MATERIAL | AUG.CHI | 1.66×10^{-30} | cm^6/s |

To enable this model, specify PIC.AUG on the MODELS statement.

Auger Recombination Model With Temperature and Concentration Dependent Coefficients

The rate of Auger recombination is usually given by

$$R_{Auger} = C_n(n^2 p - n n_{ie}^2) + C_p(p^2 n - p n_{ie}^2) \quad 3-339$$

The coefficients are dependent on both lattice temperature and carrier density [97]. The carrier density dependence is such that the coefficients are reduced in size as carrier density increases. The physical explanation of this dependence is that carrier-carrier interactions become more significant at higher values of carrier density and reduce the Auger recombination rate [85].

The coefficients are given by

$$C_n(T, n) = [\text{HNS} \cdot \text{AE} + \text{HNS} \cdot \text{BE}(T/300) + \text{HNS} \cdot \text{CE}(T/300)^2] \\ \times [1 + \text{HNS} \cdot \text{HE}[\exp(-n/\text{HNS} \cdot \text{NOE})]] \quad 3-340$$

$$C_p(T, p) = [\text{HNS} \cdot \text{AH} + \text{HNS} \cdot \text{BH}(T/300) + \text{HNS} \cdot \text{CH}(T/300)^2] \\ \times [1 + \text{HNS} \cdot \text{HH}[\exp(-p/\text{HNS} \cdot \text{NOH})]] \quad 3-341$$

where n is electron density, p is hole density, and T is lattice temperature.

To enable the model, set the flag `HNSAUG` on the `MODELS` statement. You can change all the parameters by specifying them on the `MATERIAL` statement. Table 3-70 shows the default values. Setting `HNS.HE=0` and `HNS.HH=0` will remove the carrier density dependence if required.

Table 3-69. User-Specifiable Parameters for Equations 3-341 to 3-342

| | | | |
|----------|---------|------------------------|--------------------|
| MATERIAL | HNS.AE | 6.7×10 ⁻³² | cm ⁶ /s |
| MATERIAL | HNS.AH | 7.2×10 ⁻³² | cm ⁶ /s |
| MATERIAL | HNS.BE | 2.45×10 ⁻³¹ | cm ⁶ /s |
| MATERIAL | HNS.BH | 4.5×10 ⁻³³ | cm ⁶ /s |
| MATERIAL | HNS.CE | -2.2×10 ⁻³² | cm ⁶ /s |
| MATERIAL | HNS.CH | 2.63×10 ⁻³² | cm ⁶ /s |
| MATERIAL | HNS.HE | 3.4667 | |
| MATERIAL | HNS.HE | 8.25688 | |
| MATERIAL | HNS.NOE | 1.0×10 ¹⁸ | cm ⁻³ |
| MATERIAL | HNS.NOH | 1.0×10 ¹⁸ | cm ⁻³ |

Surface Recombination

In addition to generation-recombination within the bulk of the semiconductor, electrons or holes may recombine or be generated at interfaces. The rate of surface recombination may be even greater than within the bulk. The standard method is to model interface recombination in a similar manner as the bulk generation-recombination rate [82] where:

$$R_{surf} = \frac{pn - n_{ie}^2}{\tau_p^{eff} \left[n + n_{ie} \exp \left(\frac{ETRAP}{kT_L} \right) \right] + \tau_n^{eff} \left[p + n_{ie} \exp \left(\frac{-ETRAP}{kT_L} \right) \right]} \quad 3-342$$

Here:

$$\frac{1}{\tau_n^{eff}} = \frac{1}{\tau_n} + \frac{d_i}{A_i} S.N \quad 3-343$$

and

$$\frac{1}{\tau_p^{eff}} = \frac{1}{\tau_p} + \frac{d_i}{A_i} S.P \quad 3-344$$

τ_n^i is the bulk lifetime calculated at node i along the interface and which may be a function of the impurity concentration as well. The d_i and A_i parameters are the length and area of the interface for node i . The $S.N$ and $S.P$ parameters are the recombination velocities for electrons and holes respectively, which are user-definable in the `INTERFACE` statement. The `X.MIN`, `X.MAX`, `Y.MIN`, and `Y.MAX` parameters can also be set in the `INTERFACE` statement to define the region, where the specified values of the surface recombination velocities apply. This model is activated by the presence of the recombination velocities in the `INTERFACE` statement.

Table 3-70. User-Specifiable Parameters for Equations 3-343 to 3-344

| Statement | Parameter | Default | Units |
|-----------|-----------|---------|-------|
| INTERFACE | S.N | 0 | cm/s |
| INTERFACE | S.P | 0 | cm/s |

Zamdmmer Model for LT-GaAs

Low temperature grown GaAs (LT-GaAs) is GaAs grown at a temperature of 200 - 300°, usually with a slight excess of Arsenic. The properties of LT-GaAs depend on the growth temperature and depend on the degree of post-growth annealing [147]. It can be produced with high resistivity and with sub-picosecond carrier lifetime, which makes it ideal for ultrafast photodetectors that are based on displacement current. In that category of device, the response time is limited by the recombination lifetime of photogenerated carriers. It has been observed that operating these devices under high bias conditions tends to increase the response time [274].

One possible explanation of this effect is the effective decrease in the capture cross-section with field of the recombination centers as also observed in SiO₂ [162]. According to [274], this causes an increase in the electron lifetime with electric field, F , which can be modeled as

$$\tau(F) = \tau(0) \left(\frac{T_e(F)}{T_L} \right)^{1.5} \left(\frac{r(0)}{r(F)} \right)^3 \quad 3-345$$

where $\tau(0)$ is the electron lifetime with no field present. The variable r is the radius of the coulombic potential well caused by the trapping centers. With zero applied field, this radius is isotropic but as a field is applied, it becomes anisotropic and you can define a minimum and maximum radius in the direction of the field. $r(F)$ is the minimum radius defined as the minimum radius at which the potential between two trapping centers is equal to the maximum potential between them minus

$2 K_B T/q$. The ratio $\frac{T_e(F)}{T_L}$ is the ratio of electron temperature to lattice temperature. The electron

temperature is approximated as

$$T_e = T_L + \frac{\lambda F e}{K_B} \quad 3-346$$

where λ is the optical phonon mean free path and K_B is Boltzmanns constant.

The model is designed for discrete traps. These are created by either the TRAPS statement or the TRAPS parameter on the DOPING statement. You enable the model by setting the ZAMDMMER parameter on the MODELS statement. You set the distance between the recombination centers using the ZAMDMMER.Z0 field on the MATERIAL statement, and set the value of λ with the IG.LRELE parameter on the MODELS statement.

The model evaluates the recombination lifetime at every point in the LT-GaAs according to the value of electric field there. An example of the amount by which the electron lifetime is enhanced as a function of field is given in Figure 3-6.

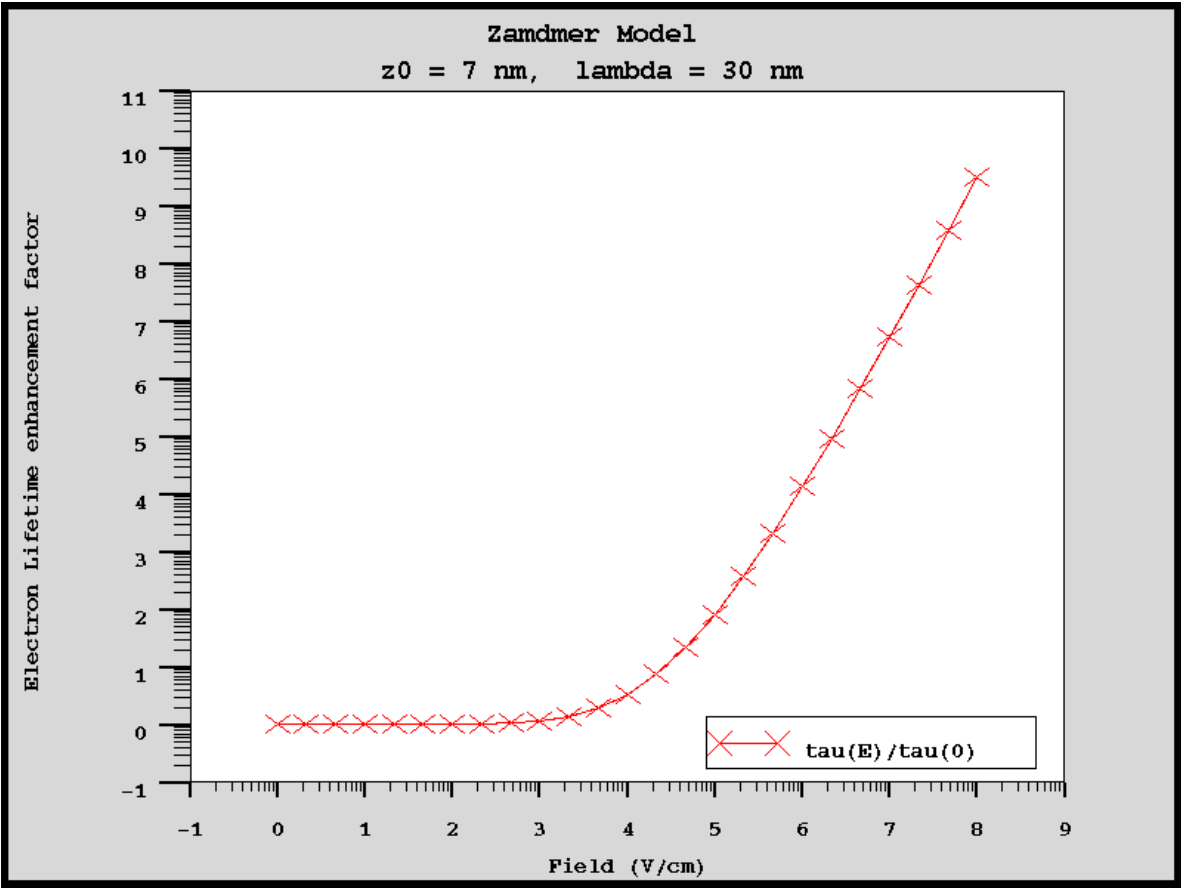


Figure 3-6: Log-Log plot of lifetime enhancement factor as a function of electric field. The trap separation is 7 nm and the value of λ is 30 nm for this example.

A summary of the parameters used for the ZAMDMER model are given in Table 3-71.

| Table 3-71. Parameters for the ZAMDMER Model | | | | |
|--|------------|---------|----------------------|-------|
| Statement | Parameter | Type | Default | Units |
| MODELS | ZAMDMER | Logical | False | |
| MODELS | IG.LRELE | Real | 2.0×10^{-6} | cm |
| MATERIAL | ZAMDMER.Z0 | Real | 7.0×10^{-7} | cm |

3.6.4: Impact Ionization Models

In any space charge region with a sufficiently high reverse bias, the electric field will be high enough to accelerate free carriers up to a point where they will have acquired sufficient energy to generate more free carriers when in collision with the atoms of the crystal. In order to acquire sufficient energy, two principle conditions must be met.

First, the electric field must be sufficiently high. Then, the distance between the collisions of the free carrier must be enough to allow acceleration to a sufficiently high velocity

In other words, the carrier must gain the ionization energy E_i between collisions. If the generation rate of these free carriers is sufficiently high this process will eventually lead to avalanche breakdown.

The general impact ionization process is described by the Equation 3-347.

$$G = \alpha_n |\vec{J}|_n + \alpha_p |\vec{J}|_p \quad 3-347$$

Here, G is the local generation rate of electron-hole pairs, $\alpha_{n,p}$ are the ionization coefficient for electrons and holes and $J_{n,p}$ are their current densities. The ionization coefficient represents the number of electron-hole pairs generated by a carrier per unit distance travelled. The accurate calculation of this parameter has been researched because it is vital if the effects related to impact ionization, such as substrate current and device breakdown, are to be simulated. These models can be classified into two main types: local and non-local models.

The former assume that ionization at any particular point within the device is a function only of the electric field at that position. Non-local models, however, perform a more rigorous approach by taking into account the energy that the carrier gains.

Geometrical Considerations for Impact Ionization Models

In all the available models discussed in the following sections, the ionization coefficients are dependent on electric field. There are several different ways to consider the interaction between electric field and current implied by Equation 3-347.

During simulation, currents and fields are calculated both as scalar values on the edges of triangles and as vector quantities on the triangles themselves. ATLAS allows three different ways of looking at Equation 3-347.

The first model uses Equation 3-348.

$$G = \alpha_n (|E_{tri}|) J_{ntri} + \alpha_p (|E_{tri}|) J_{ptri} \quad 3-348$$

Here, E_{tri} is the vector field on the triangle, J_{ntri} is the electron current vector on the triangle, and J_{ptri} is the hole current vector on the triangle. In ATLAS3D, electric field is combined with the z-component of the field at each corner of the prism to give an overall field modules at each node. To select this model, specify `E.VECTOR` of the `IMPACT` statement.

A simpler model can be selected by specifying `E.SIDE` on the `IMPACT` statement (see Equation 3-349).

$$G = \alpha_n (|E_{side}|) J_{nside} + \alpha_p (|E_{side}|) J_{pside} \quad 3-349$$

Here, E_{side} is the scalar field along the side of a triangle, J_{nside} is the electron current along the side and J_{pside} is the hole current along the side. This model is the most non-physical but has the advantages of better robustness and calculation speed and is compatible with older device simulators. This model is only supported in ATLAS2D.

The most complex and physically sound model is selected by specifying `E.DIR` on the `IMPACT` statement (see Equation 3-350).

$$G = \alpha_n \left(\left| \frac{E_{tri} \cdot J_{ntri}}{J_{ntri}} \right| \right) J_{ntri} + \alpha_p \left(\left| \frac{E_{tri} \cdot J_{ptri}}{J_{ptri}} \right| \right) J_{ptri} \quad 3-350$$

In this model, the ionization coefficients are a function of the field in the direction of the current. If the dot product of E and J is negative, then the field component is taken as 0. Consequently, impact ionization may only occur when a current is dominated by the drift term. This model is the most physically sound and is the default model for the field dependence of the impact ionization coefficients.

Another option is to abandon the use of the Electric field and adopt the gradient of the Quasi-Fermi levels to use when calculating the ionization coefficients.

$$G = \alpha_n (|\nabla \phi_n|) J_n + \alpha_p (|\nabla \phi_p|) J_p \quad 3-351$$

The modulus of the quasi-Fermi level gradients across each triangle are used, which is similar to the E.VECTOR electric field model. Using the gradient of quasi-Fermi level has the advantage that built-in electric fields (such as those existing across highly doped n - p junctions) do not result in an artificially high ionization rate at low contact biases. In the situation where the current is dominated by drift rather than diffusion, the gradient of quasi-fermi level will be essentially equal to the electric field. The impact ionization coefficients calculated from gradient of quasi-fermi level are in that case the same as the E.DIR or E.VECTOR options. To enable this model, specify GRADQFL on the IMPACT statement.

Local Electric Field Models for Impact Ionization

Selberherr's Impact Ionization Model

The ionization rate model proposed by Selberherr [207] is a variation of the classical Chynoweth model [46]. Activate this model by using the SELB parameter of the IMPACT statement, which is based upon the following expressions [236]:

$$\alpha_n = \text{AN} \exp \left[- \left(\frac{\text{BN}}{E} \right)^{\text{BETAN}} \right] \quad 3-352$$

$$\alpha_p = \text{AP} \exp \left[- \left(\frac{\text{BP}}{E} \right)^{\text{BETAP}} \right] \quad 3-353$$

Here, E is the electric field in the direction of current flow at a particular position in the structure and the parameters AN, AP, BN, BP, BETAN, and BETAP are defined on the IMPACT statement and have the default values shown in Table 3-72. In the case of AN, AP, BN, and BP you can define a value of electric field, EGRAN V/cm, where for electric fields, >EGRAN V/cm, the parameters are: AN1, AP1, BN1, BP1, while for electric fields, <EGRAN V/cm, the parameters become AN2, AP2, BN2, and BP2.

The AN and BN parameters are also a function of the lattice temperature in this model [150]. The temperature dependence of these coefficients is defined as follows:

$$\text{AN} = \text{AN}_{1,2} \left(1 + \text{A.NT} \left[\left(\frac{T_L}{300} \right)^{\text{M.ANT}} - 1 \right] \right) \quad 3-354$$

$$\text{AP} = \text{AP}_{1,2} \left(1 + \text{A.PT} \left[\left(\frac{T_L}{300} \right)^{\text{M.APT}} - 1 \right] \right) \quad 3-355$$

$$\text{BN} = \text{BN}_{1,2} \left(1 + \text{B.NT} \left[\left(\frac{T_L}{300} \right)^{\text{M.BNT}} - 1 \right] \right) \quad 3-356$$

$$BP = BP_{1,2} \left(1 + B.P.T \left[\left(\frac{T_L}{300} \right)^{M.BPT} - 1 \right] \right) \quad 3-357$$

The parameters associated with these equations are shown in Table 3-73.

An alternative model for temperature dependence of AN and AP is given by the following expressions:

$$AN = AN_{1,2} + CN2 \cdot T + DN2 \cdot T^2 \quad 3-358$$

$$AP = AP_{1,2} + CP2 \cdot T + DP2 \cdot T^2 \quad 3-359$$

where T is temperature and CN2, CP2, DN2, and DP2 are user-specifiable parameters on the IMPACT statement. By default, the temperature model of Equations 3-354 and 3-355 are used and the values of CN2, CP2, DN2 and DP2 are all zero. You can use the temperature dependence models described in Equations 3-358 or 3-359 or both by specifying non-zero values for CN2, CP2, DN2 and DP2.

The critical fields given by BN and BP may be modeled based on band gap and optical phonon mean free paths using the following expressions:

$$BN = \frac{E_g}{q\lambda_n^0} \quad 3-360$$

$$BP = \frac{E_g}{q\lambda_p^0} \quad 3-361$$

where $q\lambda_n^0$ and $q\lambda_p^0$ are the optical phonon mean free paths for electrons and holes and E_g is the local temperature dependent band gap. The free paths are modeled using the following expressions:

$$\lambda_n^0 = LAMDAH \frac{\tanh[q_{OPPHE}/2kT_L]}{\tanh[q_{OPPHE}/2k300]} \quad 3-362$$

$$\lambda_p^0 = LAMDAE \frac{\tanh[q_{OPPHE}/2kT_L]}{\tanh[q_{OPPHE}/2k300]} \quad 3-363$$

where T is the lattice temperature and LAMDAE, LAMDAH, OPPHE are user-specifiable parameters listed in Table 3-74. To enable the models described by Equations 3-356, 3-357, 3-358 and 3-359, either specify BN_{1,2} or BP_{1,2} or both as zero.

| Table 3-72. User-Definable Parameters in the Selberherr Impact Ionization Model | | |
|---|-----------|------------------------------------|
| Statement | Parameter | Default |
| IMPACT | AN1 | $7.03 \times 10^5 \text{ cm}^{-1}$ |
| IMPACT | AN2 | $7.03 \times 10^5 \text{ cm}^{-1}$ |
| IMPACT | AP1 | $6.71 \times 10^5 \text{ cm}^{-1}$ |
| IMPACT | AP2 | $1.58 \times 10^6 \text{ cm}^{-1}$ |
| IMPACT | BN1 | $1.231 \times 10^6 \text{ V/cm}$ |

Table 3-72. User-Definable Parameters in the Selberherr Impact Ionization Model

| Statement | Parameter | Default |
|-----------|-----------|--------------------------|
| IMPACT | BN2 | 1.231×10^6 V/cm |
| IMPACT | BP1 | 1.693×10^6 V/cm |
| IMPACT | BP2 | 2.036×10^6 V/cm |
| IMPACT | BETAN | 1.0 |
| IMPACT | BETAP | 1.0 |
| IMPACT | EGRAN | 4×10^5 V/cm |

Table 3-73. Temperature Coefficient Parameters of the Selberherr Impact Ionization Model for Silicon in Equations 3-354 to 3-357

| Statement | Parameter | Default |
|-----------|-----------|---------|
| IMPACT | A.NT | 0.588 |
| IMPACT | B.NT | 0.248 |
| IMPACT | A.PT | 0.588 |
| IMPACT | B.PT | 0.248 |
| IMPACT | M.ANT | 1.0 |
| IMPACT | M.BNT | 1.0 |
| IMPACT | M.APT | 1.0 |
| IMPACT | M.BPT | 1.0 |

Table 3-74. User specifiable parameters for the optical phonon mean free path model in Equations 3-362 and 3-363.

| Statement | Parameter | Default | Units |
|-----------|-----------|----------------------|-------|
| IMPACT | LAMDAE | 6.2×10^{-7} | cm |
| IMPACT | LAMDAH | 3.8×10^{-7} | cm |
| IMPACT | OPPHE | 0.063 | eV |

Van Overstraeten–de Man Impact Ionization Model

Based on the Chynoweth law [46], this model is very similar to the Selberherr model. The differences, however, are that the exponents `BETAN` and `BETAP` are set equal to unity. The lattice temperature dependence of the coefficients is also different. The functional forms of the ionization rate are

$$\alpha_n = \gamma_n^{\text{AN}} \exp\left[\frac{-\gamma_n^{\text{BN}}}{E}\right] \quad 3-364$$

$$\alpha_p = \gamma_p^{\text{AP}} \exp\left[\frac{-\gamma_p^{\text{BP}}}{E}\right] \quad 3-365$$

where the γ factors depend on Lattice temperature, or device temperature if `GIGA` is not enabled. They are calculated as

$$\gamma_n = \frac{\tanh\left(\frac{\text{N.VANHW}}{2k(300)}\right)}{\tanh\left(\frac{\text{N.VANHW}}{2kT}\right)} \quad 3-366$$

$$\gamma_p = \frac{\tanh\left(\frac{\text{P.VANHW}}{2k300}\right)}{\tanh\left(\frac{\text{P.VANHW}}{2kT}\right)} \quad 3-367$$

and will be unity if the device is at a uniform 300 K. The same parameters are used as in the Selberherr model but the `BETAN` and `BETAP` are fixed at unity. The other parameters are in Table 3-75. To activate the model, use the `VANOVERS` parameter on the `IMPACT` statement.

| Table 3-75. van Overstraeten–de Man model Parameters | | | |
|--|-----------|---------|-------|
| Statement | Parameter | Default | Units |
| IMPACT | N.VANHW | 0.063 | eV |
| IMPACT | P.VANHW | 0.063 | eV |
| IMPACT | VANOVERS | False | -- |

Valdinoci Impact Ionization Model

Valdinoci et al. [233] reported on a measurement technique to calibrate the temperature dependence of impact ionization models and proposed a new model based on their study. Their model of both electron and hole ionization coefficients was calibrated for silicon for temperature ranging from 25 to 400°C. This model is based on the following:

$$\alpha_{n,p} = \frac{E}{a_{n,p}(T_L) + b_{n,p}(T_L) \exp[d_{n,p}(T_L)/(E + c_{n,p}(T_L))]} \quad 3-368$$

where E is the electric field along the current flow lines. The parameters in Equation 3-368 depend on temperature as follows:

$$a_n(T_L) = \text{VAL}.\text{AN0} + \left(\text{VAL}.\text{AN1} \cdot T_L^{\text{VAL}.\text{AN2}} \right) \quad 3-369$$

$$b_n(T_L) = \text{VAL}.\text{BN0} \exp(\text{VAL}.\text{BN1} \cdot T_L) \quad 3-370$$

$$c_n(T_L) = \text{VAL}.\text{CN0} + \left(\text{VAL}.\text{CN1} \cdot T_L^{\text{VAL}.\text{CN2}} \right) + \text{VAL}.\text{CN3} \cdot T_L^2 \quad 3-371$$

$$d_n(T_L) = \text{VAL}.\text{DN0} + \text{VAL}.\text{DN1} \cdot T_L + \text{VAL}.\text{DN2} \cdot T_L^2 \quad 3-372$$

$$a_p(T_L) = \text{VAL}.\text{AP0} + \left(\text{VAL}.\text{AP1} \cdot T_L^{\text{VAL}.\text{AP2}} \right) \quad 3-373$$

$$b_p(T_L) = \text{VAL}.\text{BP0} \exp(\text{VAL}.\text{BP1} \cdot T_L) \quad 3-374$$

$$c_p(T_L) = \text{VAL}.\text{CP0} + \left(\text{VAL}.\text{CP1} \cdot T_L^{\text{VAL}.\text{CP2}} \right) + \text{VAL}.\text{CP3} \cdot T_L^2 \quad 3-375$$

$$d_p(T_L) = \text{VAL}.\text{DP0} + \text{VAL}.\text{DP1} \cdot T_L + \text{VAL}.\text{DP2} \cdot T_L^2 \quad 3-376$$

Our default parameters for silicon are shown in Table 3-76. These parameters are also taken from Valdinoci et al. [233]. To enable this model, specify the logical parameter, VALDINOCI, in the IMPACT statement.

| Table 3-76. Default Parameters for Valdinoci Impact Ionization Model | | | | |
|--|-----------|------|--------------------------|-------|
| Statement | Parameter | Type | Default | Units |
| IMPACT | VAL.AN0 | Real | 4.3383 | |
| IMPACT | VAL.AN1 | Real | -2.42×10 ⁻¹² | |
| IMPACT | VAL.AN2 | Real | 4.1233 | |
| IMPACT | VAL.BN0 | Real | 0.235 | |
| IMPACT | VAL.BN1 | Real | 0.0 | |
| IMPACT | VAL.CN0 | Real | 1.6831×10 ⁴ | |
| IMPACT | VAL.CN1 | Real | 4.3796 | |
| IMPACT | VAL.CN2 | Real | 1.0 | |
| IMPACT | VAL.CN3 | Real | 0.13005 | |
| IMPACT | VAL.DN0 | Real | 1.233735×10 ⁶ | |

Table 3-76. Default Parameters for Valdinoci Impact Ionization Model

| Statement | Parameter | Type | Default | Units |
|-----------|-----------|------|------------------------|-------|
| IMPACT | VAL.DN1 | Real | 1.2039×10 ³ | |
| IMPACT | VAL.DN2 | Real | 0.56703 | |
| IMPACT | VAL.AP0 | Real | 2.376 | |
| IMPACT | VAL.AP1 | Real | 0.01033 | |
| IMPACT | VAL.AP2 | Real | 1.0 | |
| IMPACT | VAL.BP0 | Real | 0.17714 | |
| IMPACT | VAL.BP1 | Real | -0.002178 | |
| IMPACT | VAL.CP0 | Real | 0.0 | |
| IMPACT | VAL.CP1 | Real | 0.00947 | |
| IMPACT | VAL.CP2 | Real | 2.4924 | |
| IMPACT | VAL.CP3 | Real | 0.0 | |
| IMPACT | VAL.DP0 | Real | 1.4043×10 ⁶ | |
| IMPACT | VAL.DP1 | Real | 2.9744×10 ³ | |
| IMPACT | VAL.DP2 | Real | 1.4829 | |

Zappa's Model for Ionization Rates in InP

A model for temperature and field dependent ionization rates in InP was proposed by Zappa et. al. [275]. To enable this model, specify ZAPPA in the IMPACT statement. The model is described for electrons and holes by Equations 3-377 through 3-391:

$$\alpha_n = \frac{qE}{ZAP_AN} \exp \left\{ 0.217 \left(\frac{ZAP_AN}{E_n} \right)^{1.14} - \left[\left(0.217 \left(\frac{ZAP_AN}{E_n} \right)^{1.14} \right)^2 + \left(\frac{ZAP_AN}{qE\lambda_n} \right)^2 \right]^{0.5} \right\} \quad 3-377$$

$$\lambda_n = ZAP_BNTanh \left(\frac{ZAP_CN}{2kT} \right) \quad 3-378$$

$$E_n = ZAP_DNTanh \left(\frac{ZAP_EN}{2kT} \right) \quad 3-379$$

$$\alpha_p = \frac{qE}{ZAP_AP} \exp \left\{ 0.217 \left(\frac{ZAP_AP}{E_p} \right)^{1.14} - \left[\left(0.217 \left(\frac{ZAP_AP}{E_p} \right)^{1.14} \right)^2 + \left(\frac{ZAP_AP}{qE\lambda_p} \right)^2 \right]^{0.5} \right\} \quad 3-380$$

$$\lambda_p = ZAP_BPTanh \left(\frac{ZAP_CP}{2kT} \right) \quad 3-381$$

$$E_p = ZAP_DP \tanh\left(\frac{ZAP_EP}{2kT}\right) \quad 3-382$$

where E is the local electric field and T is the local temperature. Table 3-77 describes the user-specifiable parameters for Zappa's model.

| Table 3-77. User-Specifiable parameters for Zappa's Ionization Rate Model | | | | |
|---|-----------|------|---------|-----------|
| Statement | Parameter | Type | Default | Units |
| IMPACT | ZAP.AN | Real | 1.9 | eV |
| IMPACT | ZAP.BN | Real | 41.7 | angstroms |
| IMPACT | ZAP.CN | Real | 46.0 | meV |
| IMPACT | ZAP.DN | Real | 46.0 | meV |
| IMPACT | ZAP.EN | Real | 46.0 | meV |
| IMPACT | ZAP.AP | Real | 1.4 | eV |
| IMPACT | ZAP.BP | Real | 41.3 | angstroms |
| IMPACT | ZAP.CP | Real | 36.0 | meV |
| IMPACT | ZAP.DP | Real | 36.0 | meV |
| IMPACT | ZAP.EP | Real | 36.0 | meV |

Grant's Impact Ionization Model

The second ionization model has the same form as the Selberherr model but a simpler implementation where:

$$\alpha_n = AN \exp\left[-\left(\frac{BN}{E}\right)\right] \quad 3-383$$

$$\alpha_p = AP \exp\left[-\left(\frac{BP}{E}\right)\right] \quad 3-384$$

This implementation has three key differences:

- The model has a low-field, an intermediate field and a high field region.
- The coefficients for silicon are different.
- There is no temperature dependence.

This model was developed after investigations by Baraff [20] suggested the existence of a low, intermediate and high field response region for electron and hole ionization rates. The coefficients implemented into this model match the experimental data of Grant [63], which suggested that the three different regions existed.

This model is activated with the `GRANT` parameter of the `IMPACT` statement. The model parameters: `AN`, `AP`, `BN`, and `BP` aren't user-definable. Instead, the three electric field regions have in-built values as follows:

1) **Low Electric Field** $E < 2.4 \times 10^5 \text{ V/cm}$ 3-385

$$AN = 2.6 \times 10^6 \quad AP = 2.0 \times 10^6$$

$$BN = 1.43 \times 10^6 \quad BP = 1.97 \times 10^6$$

2) **Intermediate Electric Field** $2.4 \times 10^5 > E > 5.3 \times 10^5 \text{ V/cm}$ 3-386

$$AN = 6.2 \times 10^5 \quad AP = 2.0 \times 10^6$$

$$BN = 1.08 \times 10^6 \quad BP = 1.97 \times 10^6$$

3) **High Electric Field** $E > 5.3 \times 10^5 \text{ V/cm}$ 3-387

$$AN = 5.0 \times 10^5 \quad AP = 5.6 \times 10^5$$

$$BN = 9.9 \times 10^6 \quad BP = 1.32 \times 10^6$$

Crowell-Size Impact Ionization Model

Crowell and Size [53] have proposed a more physical relationship between the electric field and the ionization rates. This model represents ionization coefficients as follows:

$$\alpha_{n,p} = \frac{1}{\lambda_{n,p}} \exp \left[C_0(r) + C_1(r)x + C_2(r)x^2 \right] \quad 3-388$$

$$C_0 = -1.92 + 75.5r - 75.7r^2 \quad 3-389$$

$$C_1(r) = -1.75 \times 10^{-2} - 11.9r + 46r^2 \quad 3-390$$

$$C_2(r) = 3.9 \times 10^{-4} - 1.17r + 11.5r^2 \quad 3-391$$

where:

$$r = \frac{\text{OPPHE}}{E_i}; \quad x = \frac{E_i}{q\lambda_{n,p}E} \quad 3-392$$

$$E_i = \begin{cases} 1.1\text{eV} & \text{for electrons} \\ 1.8\text{eV} & \text{for holes} \end{cases} \quad 3-393$$

$$\lambda_n^o = \text{LAMDAE} \frac{\tanh[q\text{OPPHE}/2kT_L]}{\tanh[q\text{OPPHE}/2k300]} \quad 3-394$$

$$\lambda_n^o = \text{LAMDAH} \frac{\tanh[qE_r/2kT_L]}{\tanh[qE_r/2k300]} \quad 3-395$$

The Crowell-Size Model for impact ionization is selected by setting the `CROWELL` parameter of the `IMPACT` statement.

Table 3-78. Crowell-Size Impact Ionization Model Parameters.

| Statement | Parameter | Default |
|-----------|-----------|-------------------------|
| IMPACT | LAMDAE | 6.2×10^{-7} cm |
| IMPACT | LAMDAH | 3.8×10^{-7} cm |

Okuto-Crowell Impact Ionization Model

This is another empirical model with temperature dependent coefficients where the ionization coefficients take the following forms:

$$\alpha_n = \text{ANOKUTO}(1 + \text{CNOKUTO}(T - 300)) \cdot F^{\text{NGAMOKUTO}} \times \exp \left(- \left(\frac{\text{BNOKUTO}(1 + \text{DNOKUTO}(T - 300))}{F} \right)^{\text{NDELOKUTO}} \right) \quad 3-396$$

$$\alpha_p = \text{APOKUTO}(1 + \text{CPOKUTO}(T - 300)) \cdot F^{\text{PGAMOKUTO}} \times \exp \left(- \left(\frac{\text{BPOKUTO}(1 + \text{DPOKUTO}(T - 300))}{F} \right)^{\text{PDELOKUTO}} \right) \quad 3-397$$

where F is the effective electric field.

The parameters are optimized to fit in the Electric Field Range 10^5 to 10^6 V/cm but the same ones are used for the whole range of field. It uses a relatively large set of parameters and so you can easily adjust the default values (applicable to silicon) to fit other materials [166].

To enable the model, use the OKUTO parameter on the IMPACT statement. The adjustable model parameters are given in Table 3-79.

Table 3-79. Okuto-Crowell Model Parameters

| Statement | Parameter | Default | Units |
|-----------|-----------|-----------------------|-------|
| IMPACT | ANOKUTO | 0.426 | /V |
| IMPACT | APOKUTO | 0.243 | /V |
| IMPACT | BNOKUTO | 4.81×10^5 | V/cm |
| IMPACT | BPOKUTO | 6.53×10^5 | V/cm |
| IMPACT | CNOKUTO | 3.05×10^{-4} | /K |
| IMPACT | CPOKUTO | 5.35×10^{-4} | /K |
| IMPACT | DNOKUTO | 6.86×10^{-4} | /K |
| IMPACT | DPOKUTO | 5.67×10^{-4} | /K |

Table 3-79. Okuto-Crowell Model Parameters

| Statement | Parameter | Default | Units |
|-----------|-----------|---------|-------|
| IMPACT | NGAMOKUTO | 1.0 | |
| IMPACT | PGAMOKUTO | 1.0 | |
| IMPACT | NDELOKUTO | 2.0 | |
| IMPACT | PDELOKUTO | 2.0 | |

Note: If NGAMOKUTO or PGAMOKUTO is different from 1.0, the units of ANOKUTO or APOKUTO will be different from /V.

Lackner Impact Ionization Model

This is another, more recent, impact ionization model based on Chynoweth's law [129]. It is similar to the van Overstraeten - de Man model but with an extra factor Z, dividing the ionization rate. The factor Z and the ionization coefficients are

$$Z = 1 + \frac{\text{GAMMAN} \cdot \text{BNLACKNER}}{F} \exp\left(-\frac{\text{GAMMAN} \cdot \text{BNLACKNER}}{F}\right) + \frac{\text{GAMMAP} \cdot \text{BPLACKNER}}{F} \exp\left(-\frac{\text{GAMMAP} \cdot \text{BPLACKNER}}{F}\right) \quad 3-398$$

$$\alpha_n = \frac{\text{GAMMAN} \cdot \text{ANLACKNER}}{Z} \exp\left(-\frac{\text{GAMMAN} \cdot \text{BNLACKNER}}{F}\right) \quad 3-399$$

$$\alpha_p = \frac{\text{GAMMAP} \cdot \text{APLACKNER}}{Z} \exp\left(-\frac{\text{GAMMAP} \cdot \text{BPLACKNER}}{F}\right) \quad 3-400$$

$$\text{GAMMAN} = \frac{\tanh\left(\frac{\text{N} \cdot \text{LACKHW}}{2k300}\right)}{\tanh\left(\frac{\text{N} \cdot \text{LACKHW}}{2kT}\right)}, \text{GAMMAP} = \frac{\tanh\left(\frac{\text{P} \cdot \text{LACKHW}}{2k300}\right)}{\tanh\left(\frac{\text{P} \cdot \text{LACKHW}}{2kT}\right)} \quad 3-401$$

To enable the model, use the LACKNER parameter on the IMPACT statement. The adjustable model parameters are given in Table 3-80.

Table 3-80. LACKNER Model Parameters

| Statement | Parameter | Default | Units |
|-----------|-----------|-----------------------|-------|
| IMPACT | ANLACKNER | 1.316×10 ⁶ | /cm |
| IMPACT | APLACKNER | 1.818×10 ⁶ | /cm |
| IMPACT | BNLACKNER | 1.474×10 ⁶ | V/cm |

Table 3-80. LACKNER Model Parameters

| Statement | Parameter | Default | Units |
|-----------|-----------|---------------------|-------|
| IMPACT | BPLACKNER | 2.036×10^6 | V/cm |
| IMPACT | N.LACKHW | 0.063 | eV |
| IMPACT | P.LACKHW | 0.063 | eV |

Non-Local Carrier Energy Models for Impact Ionization

All local electric field based models will normally overestimate the rate of impact ionization. This occurs because lucky electron theory inherently assumes that a carrier is traveling through a constant electric field E . As a result it will predict a distance $\Delta x = E_i/qE$ over which the carrier will gain the ionization energy E_i . In real devices, however, the electric field is never constant but is normally sharply peaked at metallurgical junctions. Therefore, as a carrier passes through the peaked electric field the lucky electron model will predict the ionization distance Δx to be too small. As a result the ionization rate is overestimated. The effect of this is that all the simulated breakdown voltages will be underestimated and substrate currents overestimated.

The Energy Balance Transport Model can be used to improve the simulation of impact ionization by implementing ionization models based upon the carrier temperature instead of the electric field. The carrier temperature is a more meaningful basis as the velocity-field relationship is more closely modeled. This allows a non-local dependence on the electric field within the impact ionization model. Energy Balance Transport Models will therefore result in more accurate simulations of breakdown voltage and substrate current. Two different impact ionization models have been implemented into ATLAS, the first is based upon the classical Chynoweth relationship, modified to include carrier temperature, but the second is a more advanced non-Maxwellian approach based upon carrier temperatures.

When the energy balance transport model is applied, only two impact ionization models are available. These are the Toyabe model and the Concannon model.

Toyabe Impact Ionization Model

The temperature dependent impact ionization model is founded on the Selberherr model and is similar to that suggested by Toyabe [112]. The carrier temperature is used to calculate an effective electric field based upon the homogeneous temperature-field relation. To maintain self-consistency within the energy balance transport model this is the same relationship used for the effective electric field within the carrier temperature dependent mobility. This model is the default model for impact ionization with energy balance transport and is activated with the TOYABE parameters on the IMPACT statement. The ionization rates now have the form:

$$\alpha_n = A_N \exp\left(\frac{-B_N}{E_{eff, n}}\right) \quad 3-402$$

$$\alpha_p = A_P \exp\left(\frac{-B_P}{E_{eff, p}}\right) \quad 3-403$$

where the model parameters: A_N , A_P , B_N , and B_P are user-definable in the IMPACT statement. The A_N , A_P , B_N , and B_P parameters have the same default values as $AN1$, $AP1$, $BN1$, and $BP1$ listed in Table 3-72.

The effective electric field is calculated according to:

$$E_{eff, n} = \frac{3}{2} \frac{kT_n}{qL_{REL, EL}} \quad 3-404$$

$$E_{eff,p} = \frac{3}{2} \frac{kT_p}{q_{LREL.HO}} \quad 3-405$$

where the energy relaxation lengths, LREL.EL and LREL.HO, can be explicitly defined in the IMPACT statement, or can be calculated according to:

$$LREL.EL = VSATN * TAUSN \quad 3-406$$

$$LREL.HO = VSATP * TAUSP \quad 3-407$$

VSATN and VSATP are the saturation velocities for electrons and holes, and TAUSN and TAUSP correspond to the electron energy relaxation times (TAUREL.EL and TAUREL.HO) in Equations 3-286 and 3-287. You must set the LENGTH.REL flag to use the values of LREL.EL and LREL.HO specified in the IMPACT statement.

Table 3-81. User-Specifiable Parameters for Equations 3-404-3-407

| Statement | Parameter | Units |
|-----------|-----------|-------|
| IMPACT | LREL.EL | μm |
| IMPACT | LREL.HO | μm |
| MATERIAL | VSAT | cm/s |
| MATERIAL | VSATN | cm/s |
| MATERIAL | VSATP | cm/s |
| IMPACT | TAUSN | s |
| IMPACT | TAUSP | s |

Note: As an added level of flexibility, the relaxation times used for the energy balance equation and those used in the impact ionization model are separated into two user-definable parameters. In contrast to TAUREL.EL and TAUREL.HO, which are used in different formulae, the TAUSN and TAUSP parameters are only applicable in the impact ionization expression in Equations 3-404 and 3-405. By default, TAUREL.EL=TAUSN and TAUREL.HO=TAUSP.

It can also be argued that the AN, AP, BN, and BP parameters should also be a function of the carrier temperature. But, no clear theoretical basis for this has been proposed and accepted. Instead, the C-INTERPRETER within ATLAS has been extended to include two C-INTERPRETER functions. These functions are specified via the F.EDIIN and F.EDIIP parameters of the IMPACT statement. These parameters specify the filename of a text file containing a C-INTERPRETER function that describes the dependence of the model parameters AN, AP, BN and BP as a function of the carrier temperatures. These values will then be used within Toyabe's energy dependent impact ionization model.

Concannon's Impact Ionization Model

The previous non-local impact ionization model inherently assumes a Maxwellian shape to the distribution of hot carriers. Recent work by Fiegna et. al. [69] using Monte Carlo simulations suggests a non-Maxwellian high energy tail to the energy distribution function. To accurately model these effects, a non-Maxwellian based model from Concannon [50] has been implemented. Based upon this energy distribution the model calculates the probability of a carrier having sufficient energy to cause impact ionization. The model results show good agreement with measured results for a 0.9μm flash EPROM device [50].

To enable the Concannon substrate current for the electron and hole continuity equations, specify the `N.CONCANNON` and `P.CONCANNON` parameters in the `IMPACT` statement.

The generation rate is a function of the carrier temperature and concentration is given by:

$$G_n(x, y) = \text{CSUB.N} \times n \int_{\text{ETH.N}}^{\infty} F(\varepsilon, T_n(x, y)) d\varepsilon \quad 3-408$$

$$G_p(x, y) = \text{CSUB.P} \times p \int_{\text{ETH.P}}^{\infty} F(\varepsilon, T_p(x, y)) d\varepsilon \quad 3-409$$

where $n(x,y)$ and $p(x,y)$ are the electron and hole carrier concentrations within the semiconductor, ε is energy, $T_n(x,y)$ and $T_p(x,y)$ are the electron and hole carrier temperatures in the semiconductor, F is given in Equation 3-410, `CSUB.N`, `CSUB.P`, `ETH.N`, and `ETH.P` are user-specifiable parameters as given in Table 3-82.

| Table 3-82. User-Specifiable Parameters for Equations 3-408 and 3-409 | | | |
|---|-----------|----------------------|-------|
| Statement | Parameter | Default | Units |
| IMPACT | CSUB.N | 2.0×10^{14} | |
| IMPACT | CSUB.P | 4.0×10^{14} | |
| IMPACT | ETH.N | 1.8 | eV |
| IMPACT | ETH.P | 3.5 | eV |

The function, $F(\varepsilon, T)$, in Equations 3-408 and 3-409 is given by the product of the density of states function, $g(\varepsilon)$, and the energy distribution function $f(\varepsilon)$ as:

$$F = \frac{g(\varepsilon)f(\varepsilon)}{\int_0^{\infty} g(\varepsilon)f(\varepsilon)} \quad 3-410$$

The density of states function is given by:

$$g(\varepsilon) = \varepsilon^{1.25} \quad 3-411$$

The energy distribution functions for electrons and holes are:

$$f_n(\varepsilon) = \left[\exp\left(\frac{-\text{CHIA} \varepsilon^3}{T_n^{1.5}}\right) + \text{C0} \exp\left(\frac{-\text{CHIB} \varepsilon^3}{T_n^{1.5}}\right) \right] \quad 3-412$$

$$f_p(\varepsilon) = \exp\left(\frac{-\text{CHI.HOLES} \varepsilon^3}{T_p^{1.5}}\right) \quad 3-413$$

Here, ε is energy, $T_{n,p}$ are the carrier temperatures, CHIA, CHIB, and C0 are user-specifiable parameters (see Table 3-83).

| Table 3-83. User-Definable Parameters for the Energy Distribution Functions | | | |
|---|-----------|-----------------------|-------|
| Statement | Parameter | Default | Units |
| IMPACT | CHIA | 3.0×10^5 | |
| IMPACT | CHIB | 5.0×10^4 | |
| IMPACT | C0 | 2.5×10^{-10} | |
| IMPACT | CHI.HOLES | 4.6×10^4 | |

Two other parameters in the IMPACT statement are user-definable, which may affect the result of the numeric integration. The ENERGY.STEP parameter specifies the energy step size in eV used during the numeric integration. The default step size is 25 meV. The INFINITY parameter sets the upper limit of the integration and specifies ratio of the increment added to the integral divided by the current value of the integral. The default value of the INFINITY parameter is 0.001.

Note: To maintain self-consistent results, implement this model if the Concannon model is being used for the simulation of gate current.

Other Hydrodynamic Models

You can also use the Lackner, Okuto-Crowell, and van Overstraeten - de Man models with the hydrodynamic model. To use this model, set the command line flag -ISE instead of the ATLAS default model (Equations 3-404 and 3-405). The ATLAS default model assumes the effective field used to calculate impact ionization rate is directly proportional to carrier Temperature.

A more physical relationship between effective field and carrier temperature is given by

$$E_{eff, n} = \frac{1.5k_B(T_n - T_L)}{\text{TAUREL} \cdot \text{EL} \cdot \text{NISELAMBD} \cdot \text{VSATN}} \quad 3-414$$

$$+ \alpha_n(E_{eff, n})^{\text{N.UPSILON}} (E_g(T_L) + \text{NISEDELTA} k_B T_n)$$

$$E_{eff,p} = \frac{1.5k_B(T_p - T_L)}{\text{TAUREL.HO PISELAMBDA VSATP}} + \alpha_p(E_{eff,p})P. \text{UPSILON}(E_g(T_L) + \text{PISEDELTA}k_B T_p) \quad 3-415$$

The parameters N.UPSILON and P.UPSILON can be either 0(unset) or 1(set). The default for Silicon is 1. It is 0 for other materials. In the case where UPSILON is unity, the equation becomes a transcendental one because it contains α as a function of E_{eff} . In this case, the equation is solved iteratively in order to obtain α . If no solution is found, then an error message will output and you must set N.UPSILON=0 or P.UPSILON=0. The user adjustable parameters are given in Table 3-84.

| Table 3-84. Hydrodynamic Model Parameters | | | |
|---|------------|----------------------|----------------------|
| Statement | Parameter | Default | Units |
| IMPACT | N.UPSILON | True (in silicon) | False (otherwise) |
| IMPACT | P.UPSILON | True (in silicon) | False (otherwise) |
| IMPACT | NISELAMBDA | 1.0 | |
| IMPACT | PISELAMBDA | 1.0 | |
| IMPACT | NISEDELTA | 1.5 | |
| IMPACT | PISEDELTA | 1.5 | |

3.6.5: Band-to-Band Tunneling

Standard Models

If a sufficiently high electric field exists within a device local band bending may be sufficient to allow electrons to tunnel, by internal field emission, from the valence band into the conduction band. An additional electron is therefore generated in the conduction band and a hole in the valence band. This generation mechanism is implemented into the right-hand side of the continuity equations. The tunneling generation rate is [98,99,100,119] as:

$$G_{BBT} = \text{BB.A} E^{\text{BB.GAMMA}} \exp\left(-\frac{\text{BB.B}}{E}\right) \quad 3-416$$

where E is the magnitude of an electric field and BB.A, BB.B, and BB.GAMMA are user-definable parameters. In ATLAS there are three different sets of values that may be applied to the model parameters.

The model parameters can be set to the standard model [98] by specifying BBT.STD on the MODELS statement. The parameter defaults for the standard model are as follows:

$$\text{BB.A} = 9.6615\text{e}18 \text{ cm}^{-1} \text{ V}^{-2} \text{ s}^{-1} \quad \text{BB.B} = 3.0\text{e}7 \text{ V/cm} \quad \text{BB.GAMMA} = 2.0$$

The model parameters may also be set to the Klaassen Model [98,119,99] by specifying BBT.KL on the MODELS statement. The parameter defaults for the Klaassen model are as follows:

$$\text{BB.A} = 4.00\text{e}14 \text{ cm}^{-1/2} \text{ V}^{-5/2} \text{ s}^{-1} \quad \text{BB.B} = 1.9\text{e}7 \text{ V/cm} \quad \text{BB.GAMMA} = 2.5$$

In application, use the standard model with direct transitions while using the Klaassen model with indirect transitions.

You can modify the basic band-to-band tunneling given in Equation 3-416 by the generation rate GBBT with the D factor as suggested in [98]. The D factor is given by:

$$D = (\exp[\phi_p - q\psi / KT] + 1)^{-1} - (\exp[\phi_n - q\psi / KT] + 1)^{-1} \quad 3-417$$

where ϕ_n and ϕ_p are the electron and hole quasi-Fermi levels as given in Equations 3-9 and 3-10 and ψ is the electrostatic potential. To enable this modification, specify `BBT.HURKX` in the `MODELS` statement.

Another modification allows these model parameters to be calculated from the first principles by specifying the `AUTOBBT` parameter in the `MODELS` statement. In this case, the parameters are calculated according to:

$$BB.A = \frac{q^2 \sqrt{(2 \times \text{MASS.TUNNEL } m_0)}}{h^2 \sqrt{EG300}} \quad 3-418$$

$$BB.B = \frac{\pi^2 EG300^{\frac{3}{2}} \sqrt{\frac{\text{MASS.TUNNEL } m_0}{2}}}{qh} \quad 3-419$$

Here:

$$BB.GAMMA = 2 \quad 3-420$$

where q is the electronic charge, h is Planck's constant, E_g is the energy bandgap, m_0 is the rest mass of an electron and `MASS.TUNNEL` is the effective mass. The parameter `MASS.TUNNEL` may be set on the `MODELS` statement and the bandgap at 300K, `EG300`, is defined on the `MATERIAL` statement.

| Table 3-85. User-Definable Parameters in the Band-to-Band Tunneling Model | | | |
|---|-----------|----------------------|--|
| Statement | Parameter | Default | Units |
| MODELS | BB.A | 4.0×10^{14} | $\text{cm}^{-1/2} \text{ V}^{-5/2} \text{ s}^{-1}$ |
| MODELS | BB.B | 1.9×10^7 | V/cm |
| MODELS | BB.GAMMA | 2.5 | |

Schenk Band to Band Tunneling Model

A comprehensive study of band-to-band tunneling was carried out by Schenk [203]. A rigorous theory was developed and then an approximate result suitable for use in device simulations was derived. The result shows that phonon assisted band-to-band tunneling rate is generally dominant compared to the band-to-band tunneling that doesn't involve a phonon scattering event. The direct band-to-band tunneling is thus neglected. The model also assumes that the electric field is constant over the tunneling length. Therefore, it is a local model.

The recombination-generation rate is given by

$$G_{BBT}^{SCHENK} = A_BBT_SCHENK F^{7/2} S \left(\frac{(A^{\mp})^{-3/2} \exp\left(\frac{A^{\mp}}{F}\right)}{\exp\left(\frac{HW_BBT_SCHENK}{kT}\right) - 1} + \frac{(A^{\pm})^{-3/2} \exp\left(\frac{A^{\pm}}{F}\right)}{1 - \exp\left(\frac{-HW_BBT_SCHENK}{kT}\right)} \right) \quad 3-421$$

where $A^{\pm} = B_BBT_SCHENK(\hbar\omega \pm HW_BBT_SCHENK)^{3/2}$, S is a statistical factor dependent on carrier concentrations, and $\hbar\omega$ is the energy of the transverse acoustic phonon. The upper sign refers to tunneling generation of electron-hole pairs (reverse biased junction). The lower sign refers to tunneling recombination of electron-hole pairs (forward bias).

You can set parameters from Table 3-86 on the `MODELS` or `MATERIAL` statement. To enable the model, specify `SCHENK.BBT` on the `MODELS` statement.

Table 3-86. Schenk Band to Band Tunneling Model Parameters

| Statement | Parameter | Type | Default | Units |
|-----------------|---------------|------|------------------------|--|
| MATERIAL/MODELS | A.BBT.SCHENK | Real | 8.977×10^{20} | $\text{cm}^2 \text{s}^{-1} \text{V}^2$ |
| MATERIAL/MODELS | B.BBT.SCHENK | Real | 2.14667×10^7 | $\text{eV}^{-3/2} \text{Vcm}^{-1}$ |
| MATERIAL/MODELS | HW.BBT.SCHENK | Real | 0.0186 | eV |

Kane Band-To-Band Tunneling Model

Another local field band-to-band tunneling model is based on the work of Kane [111]. In this model, the tunneling generation rate is given by

$$G_{BBT} = \frac{BBT_A_KANE}{\sqrt{E_g}} F^{BBT_GAMMA} \exp\left(-BBT_B_KANE \frac{E_g^2}{F}\right) \quad 3-422$$

where E_g is the position dependent bandgap and F is the magnitude of the electric field. It is similar to the standard models, except that it automatically includes a dependence on bandgap.

To enable this model specify `BBT.KANE` on the `MODELS` statement. The parameters are also aliased as indicated in Table 3-87.

Table 3-87. Parameters (with aliases) for the BBT.KANE Model

| Statement | Parameter | Alias | Type | Default | Units |
|-----------|------------|--------|---------|----------------------|---|
| MODELS | BBT.KANE | BTBT | Logical | False | |
| MODELS | BBT.A_KANE | A.BTBT | Real | 3.5×10^{21} | $\text{eV}^{1/2} / \text{cm} \cdot \text{s} \cdot \text{V}^2$ |
| MODELS | BBT.B_KANE | B.BTBT | Real | 2.25×10^7 | $\text{V} / \text{cm} \cdot \text{eV}^{3/2}$ |
| MODELS | BBT.GAMMA | | Real | 2.5 | |

Non-local Band-to-Band Tunneling

The band-to-band tunneling models described so far in this section calculate a recombination-generation rate at each point based solely on the field value local to that point. For this reason, we refer to them as local models. To model the tunneling process more accurately, you need to take into account the spatial variation of the energy bands. You also need to take into account that the generation/recombination of opposite carrier types is not spatially coincident. Figure 3-9 illustrates this for a reverse biased p-n junction where it is assumed that the tunneling process is elastic. For degenerately doped p-n junctions, you can obtain tunneling current at forward bias and consequently can obtain negative differential resistance in the forward I-V curve.

The ATLAS Non-local Band-To-Band tunneling model, `BBT.NONLOCAL`, allows modeling of the forward and reverse tunneling currents of degenerately doped p-n junctions.

It is less suitable for lightly doped p-n junctions. It is not suitable for application to the unipolar, high-field regions of a device. It is currently only available in ATLAS2D.

The first step in using `BBT.NONLOCAL` is in defining the areas where it will be applied.

These areas must each contain a single p-n junction, which may be either planar or non-planar. They have a mesh that interpolates data from the underlying device mesh and performs the band-to-band tunneling calculations on the interpolated data.

`BBT.NONLOCAL` thus assumes that the tunneling takes place on a series of 1D slices through the junction, each slice being locally perpendicular to the junction. The slices themselves will be approximately parallel to their neighbors.

ATLAS has two methods of setting up these areas of slices. The first method is only applicable to planar junctions parallel to the x or y-axes. It allows you to set up a rectangular area using the `QTX.MESH` and `QTY.MESH` statements. You also specify the number of tunneling slices and the number of mesh points along the slices.

For example:

```
QTX.MESH LOCATION=0.0 SPACING=0.25
QTX.MESH LOCATION=1.0 SPACING=0.25

QTY.MESH LOCATION=0.99 SPACING=0.0005
QTY.MESH LOCATION=1.01 SPACING=0.0005
```

will set up an area bounded by the sides $X=0.0$, $X=1.0$, $Y=0.99$, and $Y=1.01$. By additionally setting the `QTUNN.DIR` parameter on the `MODELS` statement to be 0, you define the tunneling direction to be in the y-direction. Therefore, we have 5 parallel tunneling slices at a uniform separation of 0.25 microns, each with $0.02/0.0005 + 1 = 41$ mesh points along them. This region is consistent with a p-n junction parallel to the x-direction, and having a y-position of close to 1.0 microns. Notice that the mesh is very fine in the direction of tunneling.

It is recommended to have as fine mesh as possible in the tunneling direction, both for the physical mesh and this tunneling mesh, so that values can be accurately interpolated between the two meshes. If the tunneling direction is the x-direction, then set `QTUNN.DIR` to 1 on the `MODELS` statement.

The second method of setting up a mesh for tunneling can be applied to either planar or non-planar junctions. It can be used instead of, or in addition to, the first method.

To use the second method, create one or more `QREGION` statements. These must be located after any `X.MESH`, `Y.MESH`, `ELECTRODE`, and `REGION` statements and before any `MODELS` statements that specify `BBT.NONLOCAL`. The parameters for `QREGION` include the position coordinates of the four corners of a general quadrilateral. These parameters are `X1`, `Y1`, `X2`, `Y2`, `X3`, `Y3`, `X4`, `Y4`, and should describe the quadrilateral in a counter-clockwise sense as illustrated in Figure 3-7. The pair (x_1, y_1) describe the coordinates of point 1. The other pairs (e.g., (x_2, y_2)) describe the coordinates of the other points (e.g., 2).

The tunneling is calculated between points 1 and 4, and between points 2 and 3, and along all the slices in between. The tunneling slices do not need to be parallel to one another as shown in Figure 3-7 for the special case where the spacing between tunneling slices is regular along side 3-4 and also along side 1-2. The tunneling direction changes gradually as the quadrilateral is traversed (see Figure 3-7).

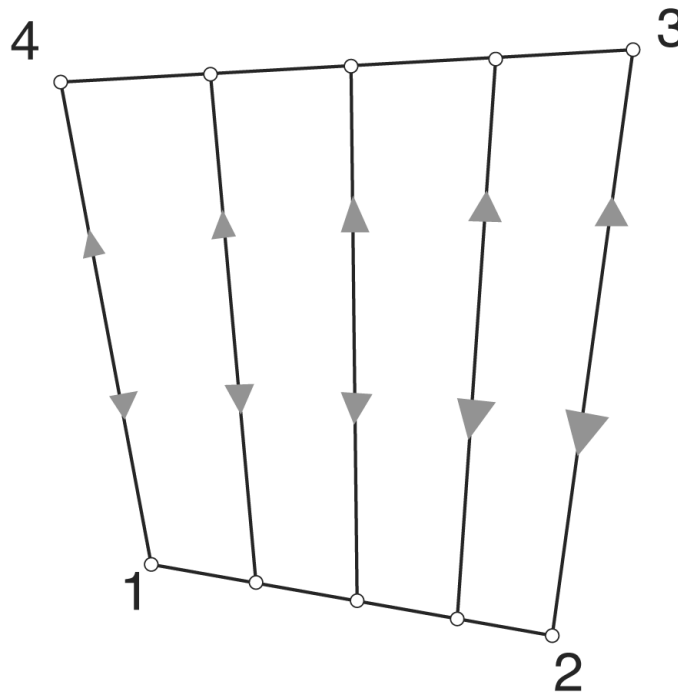


Figure 3-7: Quadrilateral region example arising from a `QREGION` statement. `PTS.NORMAL=5` has been specified, modeling tunneling along 5 rays, which are not quite parallel. The spacing between the lines is regular along edge 1->2 and along edge 4->3. The tunneling direction is indicated by the arrows.

For tunneling through non-planar junctions, it is preferable to construct a complicated polygonal region to use the `BBT.NONLOCAL` method.

You can achieve this by using several joined QTREGION's: all with a common value of the NUMBER parameter. The simple rule that must be followed to join the quadrilaterals is to ensure that point (X2, Y2) on the first matches (X1, Y1) on the other, and that point (X3, Y3) on the first matches point (X4, Y4) on the next. If (X1, Y1) or (X4, Y4) or both are not specified, then they default to the values of (X2, Y2) and (X3, Y3) respectively from the previous QTREGION statement. The first QTREGION must have all 4 corner points described. In this way, you can build up a tunneling mesh to cover quite complicated p-n junction shapes. An example is given in Figure 3-8.

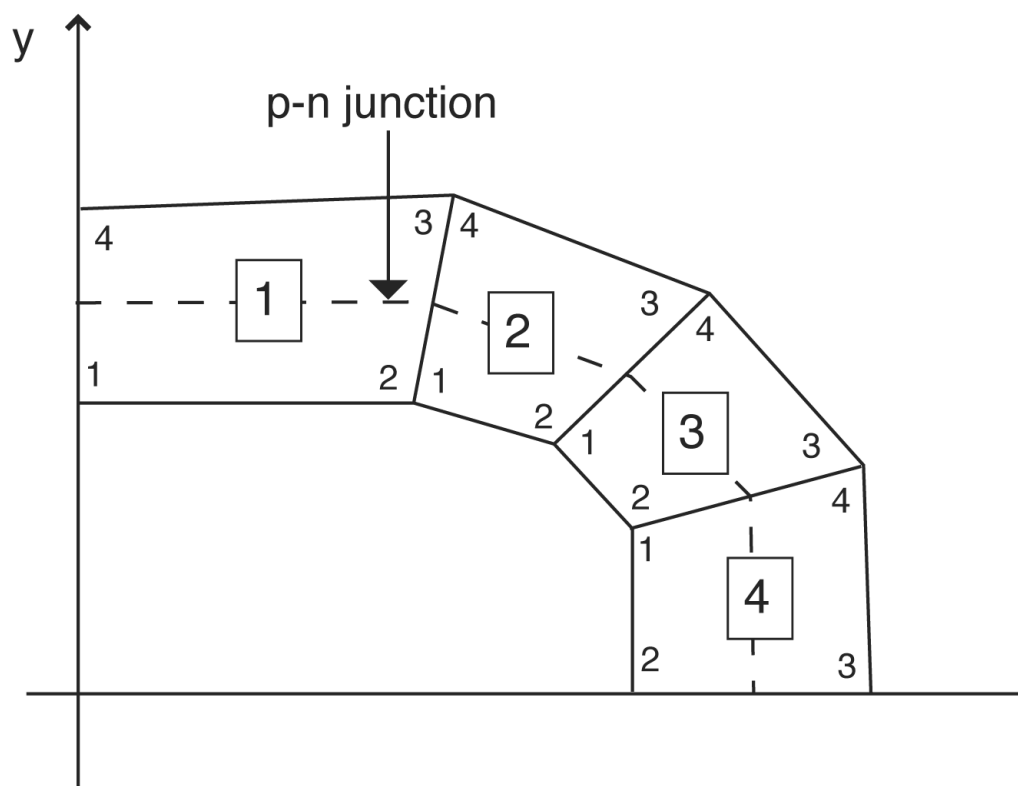


Figure 3-8: Example of a polygonal region made by joining 4 quadrilaterals. The region encloses the p-n junction, which is geometrically curved and ensures the BBT current calculation occurs along lines that are approximately locally normal to the junction. Quadrilateral 1 must have (X1,Y1), (X2,Y2), (X3,Y3), and (X4,Y4) specified. For quadrilaterals 2,3 and 4, specifying (X1,Y1) and (X4, Y4) is optional. If they are specified, they must be equal to the values of (X2,Y2) and (X3,Y3) on the adjacent quadrilateral.

You must set up the number of mesh points you require in the tunneling direction and the simplest way to do this is to use the PTS.TUNNEL parameter. The value of PTS.TUNNEL applies to all slices in a region of one or more joined quadrilaterals. You can also set the number of slices in each quadrilateral using the PTS.NORMAL parameter. You may have a different value of PTS.NORMAL for each quadrilateral in the same region. If there is more than one value of PTS.TUNNEL specified for a particular region, then the one specified by the last QTREGION statement will be used.

To allow some flexibility, there are two alternatives for specifying non-uniform mesh spacing in the tunneling direction. You can use the parameters STNL.BEG and STNL.END to give the mesh spacing at the beginning and end of the slice. Otherwise, you can use the F.RESOLUTION parameter to specify the name of an ASCII-format datafile. This data file must contain a single column of ascending values, in the range [0,1]. The density of mesh points in the tunneling direction is obtained from linearly mapping from the [0,1] range in the datafile to the start and end position of each tunneling slice for each quadrilateral having the same NUMBER parameter.

If you wish to specify non-uniform separations of the tunnel slices in a quadrilateral, then you can achieve this using the `SNRM.BEG` and `SNRM.END` parameters. The spacing at the left hand side of the quadrilateral is given by `SNRM.BEG` and that at the end by `SNRM.END`. This functionality is useful because it allows you to match the interpolated tunneling mesh to the underlying device mesh. Each quadrilateral may have its own unique values of `SNRM.BEG` and `SNRM.END`.

In summary, you can set up one or more quantum band-to-band tunneling regions, each comprised of one or more `QTREGION`'s. All `QTREGION`'s having the same value of the `NUMBER` parameter are treated as part of the same region, and they must be joined together. Additionally, one region set up by `QTX.MESH` and `QTY.MESH` can also be set up. The number of slices in each region, and the density of points along those slices can be set up in several ways. Quantities from the underlying device mesh are obtained from interpolation, and it is imperative that the device mesh resolves the rapid changes in potential near to a highly doped p-n junction.

The resolution of the tunneling slices in the tunneling direction should also be fine enough to capture these rapid changes. Each tunneling slice must include exactly one p-n junction for the model to work. The start and end points of the tunnel slices should ideally be in the flat band regions on either side of the junction.

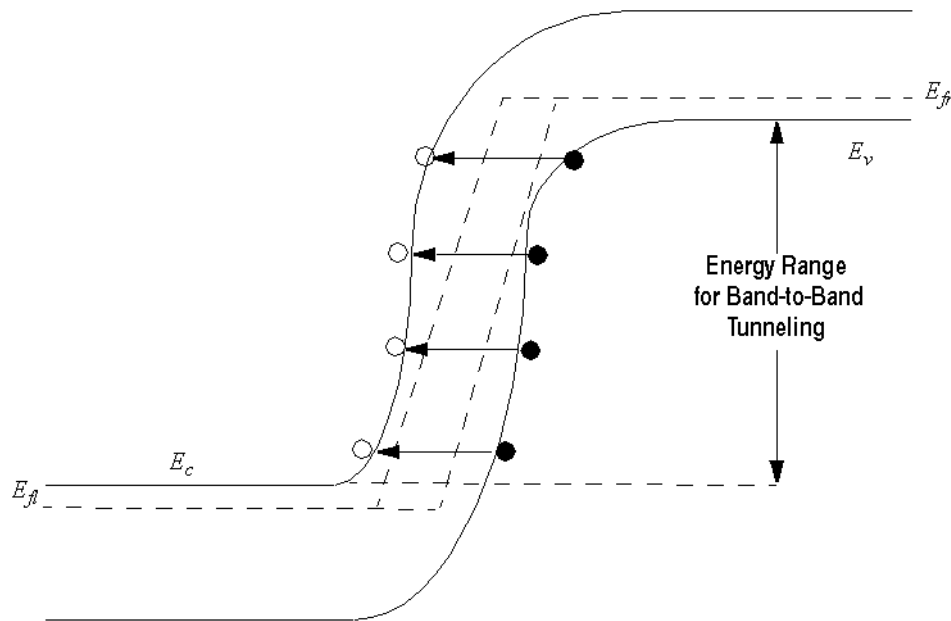


Figure 3-9: Schematic of non-local band to band tunneling in reverse bias

In order to explain how the tunneling current is calculated, let us consider the energy band profile along each tunneling slice with reverse bias applied across the junction. The range of valence band electron energies for which tunneling is permitted is shown in the schematic of the energy band profile in Figure 3-9. The highest energy at which an electron can tunnel is E_{upper} and the lowest is E_{lower} . The tunneling can be thought of being either the transfer of electrons or the transfer of holes across the junction. The rates for electrons and holes are equal and opposite because the tunneling results in the generation or recombination of electron-hole pairs.

Considering the tunneling process as a transfer of an electron across the junction the net current per unit area for an electron with longitudinal energy E and transverse energy E_T is

$$J(E) = \frac{q}{\pi \hbar} \int T(E) [f_l(E + E_T) - f_r(E + E_T)] \rho(E_T) dE dE_T \quad 3-423$$

where $T(E)$ is the tunneling probability for an electron with longitudinal energy E . $\rho(E_T)$ is the 2-dimensional density of states corresponding to the 2 transverse wavevector components and

$$f_l = (1 + \exp[(E + E_T - E_{Fl})/KT])^{-1} \quad 3-424$$

is the Fermi-Dirac function using the quasi Fermi-level on the left hand side of the junction. Similarly

$$f_r = (1 + \exp[(E + E_T - E_{Fr})/KT])^{-1} \quad 3-425$$

uses the quasi-Fermi level on the right hand side of the junction. This assumes that the transverse energy is conserved in the tunneling transition. Because we are using a 2-band model to give the evanescent wavevector, the transverse electron effective mass and the transverse hole effective mass are combined in the 2D density of states

$$\rho(E_T) = \frac{\sqrt{m_e m_h}}{2\pi \hbar^2} \quad 3-426$$

By integrating over transverse carrier energies, we obtain the contribution to the current from the longitudinal energy range $E - \Delta E/2$ to $E + \Delta E/2$ as follows:

$$J(E)\Delta E = \frac{qKT\sqrt{m_e m_h}}{2\pi^2 \hbar^3} T(E) \left[\frac{\log(1 + \exp[(E_{Fl} - E - E_T)/KT])}{\log(1 + \exp[(E_{Fr} - E - E_T)/KT])} \right]_0^{E_{max}} \Delta E \quad 3-427$$

where the upper limit of integration, E_{max} is smaller of $E - E_{lower}$ and $E_{upper} - E$. This is consistent with the 2-band model of the tunneling and the restriction on total carrier energy for tunneling $E_{lower} \leq E + E_T \leq E_{upper}$. Putting the above integration limits into Equation 3-427 we obtain

$$J(E)\Delta E = \frac{qKT\sqrt{m_e m_h}}{2\pi^2 \hbar^3} T(E) \frac{\log(1 + \exp[(E_{Fl} - E)/KT]) \log(1 + \exp[(E_{Fr} - E - E_{max})/KT])}{\log(1 + \exp[(E_{Fr} - E)/KT]) \log(1 + \exp[(E_{Fl} - E - E_{max})/KT])} \Delta E \quad 3-428$$

The Fermi levels used in Equation 3-428 are the quasi-Fermi levels belonging to the majority carrier at the relevant side of the junction. In Figure 3-9 for example, E_{Fl} would be the Electron quasi-Fermi level and E_{Fr} would be the hole quasi-Fermi level. In equilibrium, $E_{Fl} = E_{Fr}$ and the current contributions are all zero. As also seen in Figure 3-9, the start and end points of the tunneling paths, x_{start} and x_{end} , depend on Energy. ATLAS calculates these start and end points for each value of E and calculates the evanescent wavevector at points in between as

$$k(x) = \frac{k_e k_h}{\sqrt{k_e^2 + k_h^2}} \quad 3-429$$

where

$$k_e(x) = \frac{1}{i \hbar} \sqrt{2m_o m_e(x)(E - E_c(x))} \quad 3-430$$

and

$$k_h(x) = \frac{1}{i\hbar} \sqrt{2m_o m_e(x)(E_v(x) - E)} \quad 3-431$$

This ensures that the energy dispersion relationship is electron-like near the conduction band and hole-like near the valence band, and approximately mixed in between. The tunneling probability, $T(E)$, is then calculated using the WKB approximation

$$T(E) = \exp\left(-2 \int_{x_{start}}^{x_{end}} k(x) dx\right) \quad 3-432$$

This value is put into Equation 3-428 to give the tunneling current density at a given perpendicular energy, E , and the resulting current is injected into the simulation at x_{start} and x_{end} . This is repeated for all values of E between E_{lower} and E_{upper} and is done for every tunneling slice in the tunneling regions.

To calibrate the BBT.NONLOCAL model, you can specify the values of effective mass used in Equations 3-428, 3-430, and 3-431. Set the values of effective mass used in Equations 3-430 and 3-431 using ME.TUNNEL and MH.TUNNEL on the MATERIAL statement respectively. If ME.TUNNEL (MH.TUNNEL) is not specified, then the value specified for MC (MV) on the MATERIAL statement is used. For the transverse effective masses as used in Equation 3-428, a suitable value will be calculated by ATLAS, unless MC or MV or both have been specified on the MATERIAL statement, in which case these are used. The tunneling current is most sensitive to the effective masses used in Equations 3-430 and 3-431 because the tunneling probability depends exponentially on them.

Across very highly doped junctions, the Band-To-Band tunneling current can be very high and depends very strongly on the band edge profile throughout the junction. In turn, the injected tunnel current creates a charge dipole and strongly affects the potential, and consequently the band energies, at and near the junction. This strong coupling can cause convergence problems in some situations. ATLAS has two features to try to mitigate this problem. First, you can specify BBT.NLDERIVS on the MODELS statement to include non-local coupling. This puts the derivatives of $J(E)$ with respect to all potential values along its path into the Jacobian matrix. Generally, this improves the convergence properties. But, this increases the solution time per iteration because of the consequent increase in the size of the Jacobian matrix.

Second, the position at which the tunnel current is injected into the simulation can affect convergence. The default described above is the most physically accurate. As an alternative, use the parameter BBT.FORWARD on the MODELS statement. This causes the tunnel current to be injected at the start and end positions of each tunnel slice, further from the junction than with the default model. The parameter BBT.REVERSE on the MODELS statement causes the tunnel current to be injected in a locally charge neutral manner across the width of the junction, thus avoiding the creation of a charge dipole. The injected currents can be viewed as recombination rates in the structure file. They are automatically output whenever the BBT.NONLOCAL model is used. They will be negative for a reverse biased junction and positive for a forward biased junction.

Because the BBT.NONLOCAL model is unsuitable for all band-to-band tunneling, you can use the local Band-To-Band tunneling models (e.g., BBT.STD and BBT.KLA) simultaneously with BBT.NONLOCAL. These local models are not applied inside any of the Quantum Tunneling regions set up by the QTREGION statement or QTX.MESH/PTY.MESH statements.

Table 3-88. Non-Local Band-to-Band Tunneling Parameters for the MODELS Statement

| Parameter | Type | Default |
|--------------|---------|---------|
| BBT.NONLOCAL | Logical | False |
| BBT.NLDERIVS | Logical | False |
| BBT.FORWARD | Logical | False |
| BBT.REVERSE | Logical | False |

Table 3-89. Non-Local Band-to-Band Tunneling Parameters for the MATERIAL Statement

| Parameter | Type | Units |
|-----------|------|-------|
| ME | Real | None |
| MV | Real | None |
| ME.TUNNEL | Real | None |
| MH.TUNNEL | Real | None |

Table 3-90. Parameters for the QTREGION Statement

| Statement | Parameter | Type | Units |
|-----------|--------------|-----------|---------|
| QTREGION | F.RESOLUTION | Character | |
| QTREGION | NUMBER | Real | |
| QTREGION | PTS.NORMAL | Real | |
| QTREGION | PTS.TUNNEL | Real | |
| QTREGION | SNRM.BEG | Real | Microns |
| QTREGION | SNRM.END | Real | Microns |
| QTREGION | STNL.BEG | Real | Microns |
| QTREGION | STNL.END | Real | Microns |
| QTREGION | X1 | Real | Microns |
| QTREGION | X2 | Real | Microns |
| QTREGION | X3 | Real | Microns |
| QTREGION | X4 | Real | Microns |
| QTREGION | Y1 | Real | Microns |
| QTREGION | Y2 | Real | Microns |
| QTREGION | Y3 | Real | Microns |
| QTREGION | Y4 | Real | Microns |

Note: QREGION must be specified after any X.MESH,Y.MESH,ELECTRODE and REGION statements, but before any DOPING statements.

Note: If you want to fine tune the Band to Band tunneling, we recommend you use ME.TUNNEL and MH.TUNNEL parameters because they will only modify the effective masses used in tunneling.

3.6.6: Gate Current Models

In devices that have a metal-insulator-semiconductor (MIS) formation, the conductance of the insulating film would ideally be considered as zero. But, for the sub 0.5um generation of MOS devices there is now considerable conductance being measured on the gate contacts. This gate current has resulted in two major consequences, one negative and one positive.

On the negative side, the gate current is responsible for the degradation in device operating characteristics with time. This reliability issue is important because the lifetime of electronic parts has to be guaranteed. You can simulate reliability within the Silvaco suite of tools for device level reliability which are described in a later chapter.

On the positive side, the existence of this gate current has caused the proliferation of the non-volatile memory market. These devices use the existence of gate current to program and erase the charge on a “floating” contact. This concept has resulted in a variety of different devices such as FLASH, FLOTOX, and EEPROM. All such devices rely on the physics of the gate current process for their existence.

There are a variety of different conduction mechanisms within an insulating layer [223], but in the case of nonvolatile memory, only two mechanism are relevant: Fowler-Nordheim tunneling and hot carrier injection. Models for these two injection processes are described in the following sections. In the case of hot electron injection, two models are available: the lucky electron model and the Concannon gate current model.

Fowler-Nordheim Tunneling

If the electric field across an insulator is sufficiently high, then it may cause tunneling of electrons from the semiconductor (or metal) Fermi level into the insulator conduction band. This process is strongly dependent on the applied electric field but is independent of the ambient temperature.

The Fowler-Nordheim Equation [113] expresses tunnel current density through the oxide as:

$$J_{FN} = F.AE E^2 \exp\left(-\frac{F.BE}{E}\right) \quad 3-433$$

$$J_{FP} = F.AH E^2 \exp\left(-\frac{F.BH}{E}\right) \quad 3-434$$

where E specifies the magnitude of the electric field in the oxide. The model parameters: F.AE, F.AH, F.BE, and F.BH can be defined on the MODELS statement. The default values for these parameters, obtained from Keeney, Piccini, and Morelli [113], are shown in Table 3-91.

Table 3-91. User-Specifiable Parameters for Equations 3-433 and 3-434

| Symbol | Statement | Parameter | Default Values |
|----------|-----------|-----------|-----------------------|
| A_{FN} | MODELS | F.AE | 1.82×10^{-7} |
| B_{FN} | MODELS | F.BE | 1.90×10^8 |
| A_{FH} | MODELS | F.AH | 1.82×10^{-7} |
| B_{FH} | MODELS | F.BH | 1.90×10^8 |

The Fowler-Nordheim model in ATLAS has been implemented in two ways. In the post-processing implementation, the tunneling current is calculated from the solution to the device equations at each bias step. In the self-consistent implementation, the tunneling current is included directly in the current-continuity equations. Thus, it is part of the solution to the equations and gives accurate current continuity for the device.

To enable the post processing version, use the MODELS statement parameters FNPP for electron current and FNHPP for hole current. To enable the self-consistent solution, use the MODELS statement parameters FNORD for electrons and FNHOLES for holes. Setting the parameter FN.CUR is the same as specifying FNORD and FNHOLES.

For either model, the implementation scheme is the same. Each electrode-insulator and insulator-semiconductor interface is divided into discrete segments which are based upon the mesh. For each insulator-semiconductor segment, the Fowler-Nordheim current is calculated as described above. This current is then added to a segment on the electrode-insulator boundary. Two schemes have been implemented to find out to which segment this current should be added.

The default model that calculates which electrode segment receives the Fowler-Nordheim current follows the path of the electric field vector at the semiconductor-insulator interface. The first electrode-insulator segment that is found along this trajectory, provided no other semiconductors or metals are found along the trajectory, receives the Fowler-Nordheim current.

A second model may be chosen using the NEARFLG parameter of the MODEL statement. In this case, the electrode-insulator segment found closest to the semiconductor-insulator segment receives the Fowler-Nordheim current.

The total current on the gate electrode is then the sum of the currents from all the individual segments around the electrode boundary. To include the tunneling current in the logfile, specify J.TUN on the LOG statement.

By default, the Fowler-Nordheim model, when enabled, is applied to all relevant interfaces in the device structure. To localize the model, use one or more INTERFACE statements with one or more of the parameters X.MIN, X.MAX, Y.MIN, and Y.MAX specified. This restricts the application of Fowler-Nordheim tunneling to interfaces contained in the union of the rectangular areas defined by the INTERFACE statements. The parameter S.I. must also be set on the INTERFACE statement but is enabled by default.

In the special situation of an insulator layer between two semiconductor regions, the FN.SIS parameter can be specified on the REGION statement. This precludes the Fowler-Nordheim current generated on the interfaces of the region from being added to any terminal current. The current is instead added to current continuity equations at one side of the region and subtracted on the other side. This simulates tunneling through an insulator placed between two semiconductors.

Note: Since Fowler-Nordheim tunneling current is responsible for EPROM and EEPROM cell erasure, this model should always be specified when performing erasure simulation. We also recommend that you model the band-to-band tunneling model if you model Fowler-Norheim tunneling.

Note: When simulating EPROM erasure in a transient analysis with this model, the floating contact charge becomes a function of the gate current. In this case, the total current flowing into the floating electrode is multiplied by the time step to calculate the charge added to the electrode during that time step. The new value of the charge is then used as the boundary condition for the next time step.

Lucky Electron Hot Carrier Injection Model

In the Lucky-Electron Hot Carrier Injection Model it is proposed that an electron is emitted into the oxide by first gaining enough energy from the electric field in the channel to surmount the insulator/semiconductor barrier. Once the required energy to surmount the barrier has been obtained the electrons are redirected towards the insulator/semiconductor interface by some form of phonon scattering. When these conditions are met, the carrier travelling towards the interface will then have an additional probability that it will not suffer any additional collision through which energy could be lost.

The model implemented into ATLAS is a modified version of the model proposed by Tam [227] and is activated by the parameters HEI and HHI, for electron and hole injection respectively, on the MODELS statement. The gate electrode-insulator interface is subdivided into a number of discrete segments which are defined by the mesh. For each segment the lucky electron model is used to calculate the injected current into that segment. The total gate current is then the sum of all of the discrete values.

If we consider a discrete point on the gate electrode-insulator boundary we can write a mathematical formula for the current injected from the semiconductor. The formula calculates the injected gate current contribution from every node point within the semiconductor according to:

$$I_{inj} = \iint P_n(x, y) |\vec{J}_n(x, y)| dx dy + \iint P_p(x, y) |\vec{J}_p(x, y)| dx dy \quad 3-435$$

where $J_{n,p}(x, y)$ are the electron and hole current densities at a point (x, y) within the semiconductor, and $P_{n,p}(x, y)$ are the probabilities that a fraction of this current reaches the gate oxide and is injected across into the gate electrode. The total probability $P_{n,p}(x, y)$ is defined by:

$$P_n(x, y) = P_{\phi B, n} P_{1, n} P_{2, n}^{IG.ELINR} \quad 3-436$$

$$P_p(x, y) = P_{\phi B, p} P_{1, p} P_{2, p}^{IG.HLINR} \quad 3-437$$

where E is the electric field parallel to the current flow, IG.ELINR and IG.HLINR are the electron and hole mean free path lengths between redirecting collisions. The three probability factors will now be described.

The probability $P_{\phi B}$ is the probability of a carrier gaining the energy ϕ_B by moving in, and parallel to, an electric field E, without suffering energy loss by optical phonon scattering and is given by:

$$P_{\phi B, n} = 0.25 \left(\frac{E \cdot IG.ELINF}{\phi_{B, n}} \right) \exp \left(-\frac{\phi_{B, n}}{E \cdot IG.ELINF} \right) \quad 3-438$$

$$P_{\phi_{B,p}} = 0.25 \left(\frac{E_{IG.HLINF}}{\phi_{B,p}} \right) \exp \left(-\frac{\phi_{B,p}}{E_{IG.HLINF}} \right) \quad 3-439$$

where $IG.ELINF$ and $IG.HLINF$ are the mean free path lengths of electrons and holes for scattering by optical phonons. The barrier heights $\phi_{Bn,p}$ are defined according to:

$$\phi_{B,n} = IG.EB0 - IG.EBETA \sqrt{E_{\perp}} - IG.EETA E_{\perp}^{2/3} - \Delta\psi(x, y) \quad 3-440$$

$$\phi_{B,p} = IG.HB0 - IG.HBETA \sqrt{E_{\perp}} - IG.HETA E_{\perp}^{2/3} - \Delta\psi(x, y) \quad 3-441$$

where E_{\perp} is the electric field perpendicular to the semiconductor-insulator interface. The traditional barrier heights, $IG.EB0$ and $IG.HB0$, are reduced to take account of three effects. The first effect is due to Schottky barrier lowering which depends on the perpendicular electric field at the semiconductor-insulator interface. The second effect takes account of tunneling through the gate oxide by reducing the barrier height. The third effect takes into account that a potential difference exists between the semiconductor-insulator interface and the starting position of the hot carrier. By default, this last effect is disabled. But you can enable it by specifying the $E.BENDING$ and $H.BENDING$ parameters for electrons and holes respectively.

The second probability P_1 is the probability that no energy is lost by optical phonon scattering as the hot carrier travels towards the semiconductor-insulator interface after being redirected, and is given by:

$$P_{1,n} \sim \exp \left(-\frac{r}{IG.ELINF} \right) \quad 3-442$$

$$P_{1,p} \sim \exp \left(-\frac{r}{IG.HLINF} \right) \quad 3-443$$

where r is the distance from point of redirection to the semiconductor-insulator interface.

The final probability P_2 accounts for the probability of scattering in the image force potential well in the gate oxide and is given by:

$$P_{2,n} = \exp \left(-\frac{\sqrt{\frac{q}{16\pi\epsilon_{ox} E_{ox}}}}{PATH.N} \right) \quad \text{for } \theta > THETA.N \quad 3-444$$

$$P_{2,n} = 0 \quad \text{for } \theta < THETA.N \quad 3-445$$

$$P_{2,p} = \exp \left(-\frac{\sqrt{\frac{q}{16\pi\epsilon_{ox} E_{ox}}}}{PATH.P} \right) \quad \text{for } \theta > THETA.P \quad 3-446$$

$$P_{2,p} = 0 \quad \text{for } \theta < THETA.P \quad 3-447$$

Here, $PATH.N$ and $PATH.P$ are the electron and hole mean free path lengths within the oxide, ϵ_{ox} is the oxide permittivity and E_{ox} is the electric field in the oxide. The angle θ introduces an angle dependence which is based upon the work of Wada [243]. His experiments indicate a critical rejection angle, $THETA.N$ and $THETA.P$, between the angle θ formed between the semiconductor-insulator interface and the electric field in the oxide. If the angle θ is less than the rejection angle then the electrons are repelled back to the substrate.

Table 3-92 lists the user-definable model parameters that can be set in the `MODELS` statement, their default values, and their units.

| Table 3-92. User-Definable Parameters in Concannon's Gate Current Model | | | |
|---|-----------|-----------------------|--------------------|
| Statement | Parameter | Default | Units |
| MODELS | IG.EB0 | 3.2 | eV |
| MODELS | IG.ELINR | 6.16×10^{-6} | cm |
| MODELS | IG.HLINR | 6.16×10^{-6} | cm |
| MODELS | IG.ELINF | 9.2×10^{-7} | cm |
| MODELS | IG.HB0 | 4.0 | eV |
| MODELS | IG.HLINF | 9.2×10^{-7} | cm |
| MODELS | IG.EBETA | 2.59×10^{-4} | $(Vcm)^{1/2}$ |
| MODELS | IG.HBETA | 2.59×10^{-4} | $(Vcm)^{1/2}$ |
| MODELS | IG.EETA | 2.0×10^{-5} | $V^{1/3} cm^{2/3}$ |
| MODELS | IG.HETA | 2.0×10^{-5} | $V^{1/3} cm^{2/3}$ |
| MODELS | IG.LRELE | 3.0×10^{-6} | [Q=1] cm |
| MODELS | IG.LRELH | 2.0×10^{-6} | [Q=1] cm |
| MODELS | PATH.N | 3.4×10^{-7} | cm |
| MODELS | PATH.P | 2.38×10^{-7} | cm |
| MODELS | THETA.N | 60 | degrees |
| MODELS | THETA.P | 60 | degrees |

The implementation of this model is similar to that for Fowler-Nordheim tunneling. Each electrode-insulator and insulator-semiconductor interface is divided into discrete segments, which are based upon the mesh. For each insulator-semiconductor segment the Fowler-Nordheim current is calculated as described above. This current will then be added to a segment on the electrode-insulator boundary. Two schemes have been implemented to find out to which segment this current should be added.

The default model that calculates which electrode segment receives the hot carrier injected current follows the path of the electric field vector at the semiconductor-insulator interface. The first electrode-insulator segment that is found along this trajectory, provided no other semiconductors or metals are found along the trajectory, will receive the current.

A second model may be chosen using the `NEARFLG` parameter of the `MODELS` statement. In this case, the electrode-insulator segment found closest to the semiconductor-insulator segment will receive the hot carrier injected current.

The total current on the gate electrode is then the sum of the currents from all the individual segments around the electrode boundary.

The lucky electron hot carrier injection model can be used to include the electron or hole carrier temperature in the solution because the carrier temperature does not directly enter the equations.

The one exception is in `ATLAS2D` where the electric field parallel to the current flow is calculated as

$$E = 1.5 K_B T_n / IG.LRELE$$

for electrons if `HCTE.EL` is specified and

$$E = 1.5 K_B T_p / IG.LRELH$$

for holes if `HCTE.HO` is specified. K_B is Boltzmann's constant in units of eV/Kelvin. If `IG.LRELE` is set to zero then E will be calculated the same way as if `HCTE.EL` is unspecified. The same is true for `IG.LRELH` and `HCTE.HO`. In `ATLAS3D`, this model is unavailable and E is calculated the same way regardless if `HCTE` is specified.

Note: When simulating EPROM programming with this model, the floating contact charging is simulated in the transient mode. In this case, the total current flowing into the floating electrode is multiplied by the time step to calculate the charge added to the electrode during that time step. The new value of charge is then used as the boundary condition for the next time step.

The hot electron and hot hole currents can be output separately to a logfile by specifying the parameters `J.HEI` and `J.HHI` on the `LOG` statement. They are also automatically included in the electron and hole currents which are output to a logfile. The value of hot carrier current density associated with each interface node can be output to any standard structure file by specifying the `HEI` and `HHI` parameters on the `OUTPUT` statement.

Concannon's Injection Model

The implicit assumption in the lucky electron approach is a Maxwellian shape for the energy distribution of the hot carriers. Recent work by Fiegna [69] using Monte Carlo simulations suggests a non-Maxwellian high energy tail to the distribution function. To accurately model these effects, a non-Maxwellian based model from Concannon [50] has been implemented. This model requires the solution to the energy balance equation for the carrier temperatures but has been implemented in a similar manner to the lucky electron model. The Concannon gate injection model may be specified with the parameters `N.CONCANNON` and `P.CONCANNON` on the `MODELS` statement. This choice of parameters automatically activates the Energy Balance Transport Model.

The Concannon injection model has a similar form to the lucky electron model. The injected current is calculated according to:

$$I_{inj} = \iint P_n(x, y) n(x, y) dx dy + \iint P_p(x, y) p(x, y) dx dy \quad 3-448$$

where $n(x, y)$ and $p(x, y)$ are the carrier concentrations within the semiconductor. The probability functions $P_n(x, y)$ and $P_p(x, y)$ are now defined by:

$$P_n(x, y) = -q CGATE.N P_{\phi_{B,n}} P_{1,n} P_{2,n} \quad 3-449$$

$$P_p(x, y) = q CGATE.P P_{\phi_{B,p}} P_{1,p} P_{2,p} \quad 3-450$$

where q is the electronic charge and the parameters `CGATE.N` and `CGATE.P` are user-definable on the `MODEL` statement. The three probability functions in Equations 3-449 and 3-450 shall now be described.

The probability that a carrier has sufficient energy to surmount the insulator-semiconductor barrier of height ϕ_B is now defined as a function of energy. The probability has the form:

$$P_{\phi_{B,n}} = \int_{\phi_{B,n}}^{\infty} v_{\perp}(\varepsilon) F(\varepsilon, T_n(x, y)) d\varepsilon \quad 3-451$$

$$P_{\phi_{B,p}} = \int_{\phi_{B,p}}^{\infty} v_{\perp}(\varepsilon) F(\varepsilon, T_p(x, y)) d\varepsilon \quad 3-452$$

Here, $v_{\perp}(\varepsilon)$ is the perpendicular velocity of a hot carrier and defines the probability of a hot carrier with an energy ε travelling in the direction of the insulator-semiconductor. The barrier heights $\phi_{Bn,p}$ are defined according to:

$$\phi_{B,n} = \text{IG.EB0} - \text{IG.EBETA} \sqrt{E_{\perp}} - \text{IG.EETA} E_{\perp}^{2/3} - \Delta\psi(x, y) \quad 3-453$$

$$\phi_{B,p} = \text{IG.HB0} - \text{IG.HBETA} \sqrt{E_{\perp}} - \text{IG.HETA} E_{\perp}^{2/3} - \Delta\psi(x, y) \quad 3-454$$

where E_{\perp} is the electric field perpendicular to the semiconductor-insulator interface. The traditional barrier heights, `IG.EB0` and `IG.HB0`, are reduced to take account of three effects. The first effect is due to Schottky barrier lowering which depends on the perpendicular electric field at the semiconductor-insulator interface. The second effect takes account of tunneling through the gate oxide by reducing the barrier height. The third effect takes into account that a potential difference exists between the semiconductor-insulator interface and the starting position of the hot carrier. By default, this last effect is disabled. But you can enable it by specifying the `E.BENDING` and `H.BENDING` parameters for electrons and holes respectively.

The carrier velocity model follows the approach of Fiegna et. al. [69] where velocity is proportional to energy according to:

$$v_{\perp} \sim \varepsilon^{0.25} \quad 3-455$$

The function, $F(\varepsilon, T_{n,p}(x, y))$, is determined by the density of states and the energy distribution function according to:

$$F(\varepsilon, T_n(x, y)) \sim \frac{g(\varepsilon)f(\varepsilon)}{\int_0^{\infty} g(\varepsilon)f(\varepsilon)d\varepsilon} \quad 3-456$$

The density of states $g(\varepsilon)$ follows the analysis of Cassi [38] where:

$$g(\varepsilon) \sim \varepsilon^{1.25} \quad 3-457$$

Finally, the energy distribution functions for electrons and holes are defined by:

$$f_n(\varepsilon) \sim \left[\exp\left(\frac{-\text{CHIA} \varepsilon^3}{T_n^{1.5}}\right) + \text{CO} \exp\left(\frac{-\text{CHIB} \varepsilon^3}{T_n^{1.5}}\right) \right] \quad 3-458$$

$$f_p(\varepsilon) \sim \exp\left(\frac{-\text{CHI.HOLES } \varepsilon^3}{T_p^{1.5}}\right) \quad 3-459$$

where CHIA, CHIB, CHI.HOLES, and C0 are user-definable constants found from fitting to measured data. The terms: T_n and T_p are the mean carrier temperatures for electrons and holes, which are calculated from the Energy Balance Transport Model.

Normalization in all of the above equations is accounted for in the combined constants of proportionality, CGATE.N and CGATE.P.

The second probability P_1 is the probability that no energy is lost by optical phonon scattering as the hot carrier travels towards the semiconductor-insulator interface after being redirected and is given by:

$$P_{1,n} \sim \exp\left(-\frac{r}{\text{IG.ELINF}}\right) \quad 3-460$$

$$P_{1,p} \sim \exp\left(-\frac{r}{\text{IG.HLINF}}\right) \quad 3-461$$

where r is the distance from point of redirection to the semiconductor-insulator interface.

The final probability P_2 accounts for the probability of scattering in the image force potential well in the gate oxide and is given by:

$$P_{2,n} = \exp\left(-\frac{\sqrt{\frac{q}{16\pi\varepsilon_{ox}E_{ox}}}}{\text{PATH.N}}\right) \quad \text{for } \theta > \text{THETA.N} \quad 3-462$$

$$P_{2,n} = 0 \quad \text{for } \theta > \text{THETA.N} \quad 3-463$$

$$P_{2,p} = \exp\left(-\frac{\sqrt{\frac{q}{16\pi\varepsilon_{ox}E_{ox}}}}{\text{PATH.P}}\right) \quad \text{for } \theta > \text{THETA.P} \quad 3-464$$

$$P_{2,p} = 0 \quad \text{for } \theta < \text{THETA.P} \quad 3-465$$

Here, PATH.N and PATH.P are the electron and hole mean free path lengths within the oxide, ε_{ox} is the oxide permittivity and E_{ox} is the electric field in the oxide. The angle θ introduces an angle dependence which is based upon the work of Wada [243]. His experiments indicate a critical rejection angle, THETA.N and THETA.P between the angle θ formed between the semiconductor-insulator interface and the electric field in the oxide. If the angle θ is less than the rejection angle, then the electrons are repelled back to the substrate.

Note: The current implementation of the Concannon model for hot carrier injection is that only carriers along the semiconductor-insulator interface are significant and as a result the probability P_1 is assumed unity. This also means that the integration is only applied to those node points along the semiconductor-insulator interface.

Two other parameters of the `MODELS` statement that may affect the result of the numeric integration are user-definable. The `ENERGY.STEP` parameter specifies the energy step size in eV used during the numeric integration. The default step size is 25 meV. The `INFINITY` parameter sets the upper limit of the integration and specifies ratio of the increment added to the integral divided by the current value of the integral. The default value of the `INFINITY` parameter is 0.001.

The implementation of this model is similar to that for Fowler-Nordheim tunneling. Each electrode-insulator and insulator-semiconductor interface is divided into discrete segments which are based upon the mesh. For each insulator-semiconductor segment the Fowler-Nordheim current is calculated as described above. This current will then be added to a segment on the electrode-insulator boundary. Two schemes have been implemented to find out to which segment this current should be added.

The default model that calculates which electrode segment receives the hot carrier injected current follows the path of the electric field vector at the semiconductor-insulator interface. The first electrode-insulator segment that is found along this trajectory, provided no other semiconductors or metals are found along the trajectory, will receive the current.

A second model may be chosen using the `NEARFLG` parameter of the `MODELS` statement. In this case the electrode-insulator segment found closest to the semiconductor-insulator segment will receive the hot carrier injected current.

The total current on the gate electrode is then the sum of the currents from all the individual segments around the electrode boundary.

Note: To maintain self-consistent results, it's important that this model is implemented if the Concannon model is being used for the simulation of substrate current.

The Concannon hot electron and hole currents may be output separately to a logfile using the parameters `J.HEI` and `J.HHI` on the `LOG` statement respectively. They are also automatically included in the electron and hole currents that are output to a logfile. The value of Concannon hot carrier current density associated with each interface node can be output to any standard structure file by specifying the `HEI` and `HHI` parameters on the `OUTPUT` statement.

Direct Quantum Tunneling Model

For deep submicron devices, the thickness of the insulating layers can be very small. For example, gate oxide thicknesses in MOS devices can be as low as several nanometers. In this case, the main assumptions of the Fowler-Nordheim approximation are generally invalid and you need a more accurate expression for tunneling current. The one ATLAS uses is based on a formula, which was introduced by Price and Radcliffe [185] and developed by later authors. It formulates the Schrodinger equation in the effective mass approximation and solves it to calculate the transmission probability, $T(E)$, of an electron or hole through the potential barrier formed by the oxide layer. The incident (perpendicular) energy of the charge carrier, E , is a parameter. It is assumed that the tunneling process is elastic. After taking into account carrier statistics and integrating over lateral energy, the formula

$$J = \frac{qkT}{2\pi^2\hbar^3} \sqrt{m_y m_z} \int T(E) \ln \left\{ \frac{1 + \exp[(E_{Fr} - E)/kT]}{1 + \exp[(E_{Fl} - E)/kT]} \right\} dE \quad 3-466$$

is obtained, which gives the current density J (A/m^2) through the barrier. The effective masses m_y and m_z are the effective masses in the lateral direction in the semiconductor. For example, for a direct bandgap material, where the Γ valley is isotropic, both m_y and m_z are the same as the density of states effective mass. The logarithmic term includes the carrier statistics and E_{fl} and E_{fr} are the quasi-Fermi levels on either side of the barrier (see Figure 3-10). The range of integration is determined according to the band edge shape at any given contact bias.

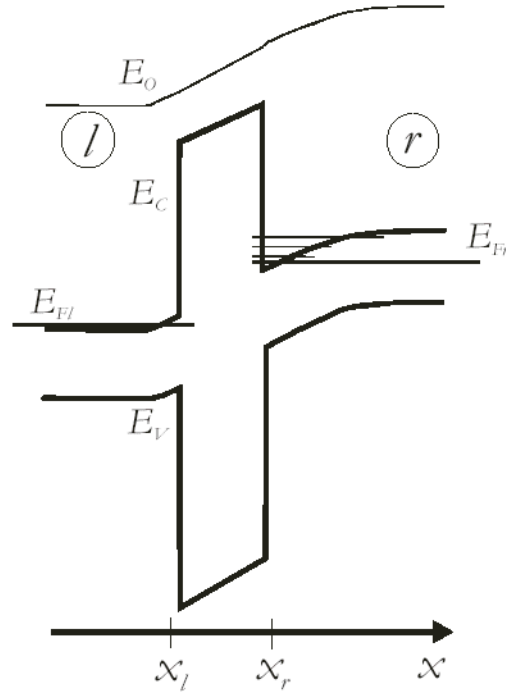


Figure 3-10: Typical conduction and valence band profiles of a MOS capacitor. The right region represents the MOS bulk, the left region represents the gate.

For indirect bandgap materials, Equation 3-467 is applied to each valley and the resulting sum gives the tunneling current. For the conduction band of silicon, for example, summing over the 6 valleys gives

$$J = \frac{qkT}{2\pi^2\hbar^3} (2m_t + 4\sqrt{m_l m_t}) \int T(E) \ln \left\{ \frac{1 + \exp[(E_{Fr} - E)/kT]}{1 + \exp[(E_{Fl} - E)/kT]} \right\} dE \quad 3-467$$

where m_t is the transverse effective mass and m_l the longitudinal mass. For a valence band, you need to sum the light hole and heavy hole contributions separately. For the valence band, the light hole and heavy contributions are summed to give

$$J = \frac{qkT}{2\pi^2\hbar^3} (m_{lh} + m_{hh}) \int T(E) \ln \left\{ \frac{1 + \exp[(E_{Fr} - E)/kT]}{1 + \exp[(E_{Fl} - E)/kT]} \right\} dE \quad 3-468$$

In equilibrium, $E_{fl} = E_{fr}$ and the logarithmic term and consequently J is identically zero.

Tunneling Types

ATLAS can account for several types of tunneling. For clarity, we assume the material on the left hand side of Figure 3-10 is polysilicon. Electron tunneling occurs when electrons tunnel through the insulator energy barrier from one conduction band to the other. Hole tunneling occurs when holes tunnel from one valence band to the other. If the bias applied to the contact is sufficiently large, then the situation illustrated in Figure 3-11 can occur. In this case, an electron in the Silicon valence band tunnels through the insulator to the polysilicon conduction band.

If the bias is reversed, then the opposite occurs in which an electron in the polysilicon valence band tunnels to the Silicon conduction band. Both of these cases are referred to as band-to-band Tunneling. These should not be confused, however, with the other band-to-band tunneling models implemented in ATLAS, which apply to regions of high electric field within a semiconductor. All these types of tunneling can be used as post-processing calculations or self-consistent calculations. In the former case, the tunneling currents are calculated after ATLAS has found a converged solution at a given bias. ATLAS then outputs the calculated tunneling currents to the logfile. In the latter case, the tunneling currents are coupled with the solution of the current continuity equations in the semiconductor. Therefore, the terminal currents are self-consistent.

In situations where there is a strong quantum confinement in the semiconductor, ATLAS can include charge quantization effects. To do this, use the Schrodinger-Poisson solver in the Silicon, which causes the tunneling current to be calculated as a sum over eigenstates. The relevant formulae are

$$J = \frac{qkT}{\pi\hbar^2} \sqrt{m_y m_z} \sum_i v_r(E_i) T(E_i) \ln \left\{ \frac{1 + \exp[(E_{Fl} - E_i)/kT]}{1 + \exp[(E_{Fr} - E_i)/kT]} \right\} dE \quad 3-469$$

where the sum is over all bound state energies, E_i , for a particular band minimum.

For electrons in silicon, with 6 conduction band minima, we obtain

$$J = \frac{2qkT}{\pi\hbar^2} m_t \sum_i v_{ril} T(E_{il}) \ln \left\{ \frac{1 + \exp[(E_{Fl} - E_{il})/kT]}{1 + \exp[(E_{Fr} - E_{il})/kT]} \right\} \\ + \frac{4qkT}{\pi\hbar^2} \sqrt{m_t m_l} \sum_i v_{rit} T(E_{it}) \ln \left\{ \frac{1 + \exp[(E_{Fl} - E_{it})/kT]}{1 + \exp[(E_{Fr} - E_{it})/kT]} \right\} \quad 3-470$$

where the sums over longitudinal bound eigenstates and transverse bound eigenstates are done separately. For holes, the current is calculated using the equation

$$J = \frac{qkT}{\pi\hbar^2} m_{lh} \sum_i v_{ri_lh} T(E_{i_lh}) \ln \left\{ \frac{1 + \exp[(E_{i_lh} - E_{Fl})/kT]}{1 + \exp[(E_{i_lh} - E_{Fr})/kT]} \right\} \\ + \frac{qkT}{\pi\hbar^2} m_{hh} \sum_i v_{ri_hh} T(E_{i_hh}) \ln \left\{ \frac{1 + \exp[(E_{i_hh} - E_{Fl})/kT]}{1 + \exp[(E_{i_hh} - E_{Fr})/kT]} \right\} \quad 3-471$$

where the sums over light hole and heavy hole bound eigenstates are done separately.

The expression v is called the attempt frequency and is given by

$$v_r = \frac{\hbar k}{4m} \left[|\Psi(x_r)|^2 + \left| \frac{d\Psi}{dx}(x_r) \right|^2 \frac{1}{k^2} \right] \quad 3-472$$

It is evaluated at the semiconductor-oxide interface if quantum confinement occurs there. This quantum confined modification of the tunneling will be applied when you set the `SCHRODINGER` parameter and set quantum tunneling. This requires you to set `CARRIERS=0` on the `METHOD` statement. Therefore, this model cannot be used if it is required to solve the current continuity equations.

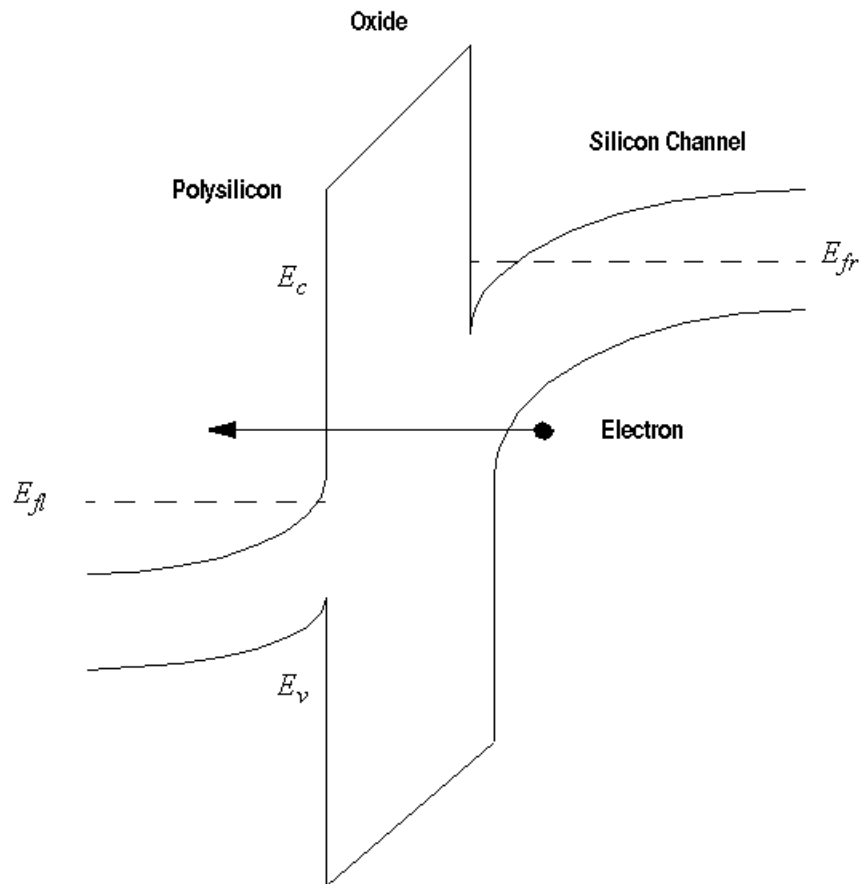


Figure 3-11: Schematic of band-to-band tunneling across a gate insulator with a polysilicon gate.

Enabling the Models

To enable the quantum tunneling model for electrons, specify `QTUNN.EL` in the `MODELS` statement. To enable the quantum tunneling model for holes, specify `QTUNN.HO` in the `MODELS` statement. To enable Band-to-Band tunneling, specify `QTUNN.BBT` in the `MODELS` statement. In order to enable all three options, specify `QTUNN` in the `MODELS` statement.

| Table 3-93. MODELS Statement: Quantum Tunneling Parameters | | |
|--|---------|---------|
| Parameter | Type | Default |
| QTUNN | Logical | False |
| QTUNN.BBT | Logical | False |
| QTUNN.EL | Logical | False |
| QTUNN.HO | Logical | False |

QTUNN.EL and QTUNN.HO are available with the CARRIERS=0, CARRIERS=1, and CARRIERS=2 options on the METHOD statement. With CARRIERS=0, the semi-classical and quantum-confined variants are available. QTUNN.BBT is only available as part of a semi-classical calculation with either CARRIERS=0, CARRIERS=1 or CARRIERS=2.

To enable the self-consistent versions of the quantum tunneling models, specify the QTNLSC.EL and QTNLSC.HO parameters on the MODELS statement for electron and hole tunneling respectively. The Band-to-Band tunneling option is enabled using QTNLSC.BBT. You can enable all three models using the QTUNNSC parameter on the MODELS statement.

| Table 3-94. MODELS Statement: Self-consistent quantum tunneling parameters. | | |
|---|---------|---------|
| Parameter | Type | Default |
| QTNL.DERIVS | Logical | false |
| QTNLSC.EL | Logical | false |
| QTNLSC.HO | Logical | false |
| QTNLSC.BBT | Logical | false |
| QTUNNSC | Logical | false |

For the self-consistent implementations, convergence can be somewhat poor in some circumstances, particularly for high values of tunneling current. In this case, you can set the QTNL.DERIVS parameter on the MODELS statement. This will include extra terms in the Jacobian matrix, which should improve convergence. It will also increase the time needed to solve each iteration.

Mesh Considerations

The tunneling current model is quasi one-dimensional and the tunneling current is evaluated on a series of parallel or nearly parallel slices through the insulator. Implementation details therefore depend on the type of mesh. If the mesh was generated by ATLAS meshing commands, then everything including the direction of tunneling is determined automatically. If the mesh was created by another Silvaco product, for example ATHENA or DEVEDIT, then there are two options.

The first option is to use the QTX.MESH and QTY.MESH commands to create a rectangular mesh on which all quantum tunneling is calculated. Interpolation is used to couple between this supplementary mesh and the device mesh. By default, the tunneling will be assumed to be in the Y direction. You can change this by setting the QTUNN.DIR parameter on the MODELS statement to 1 instead of its default value of 0. Place the QT mesh to enclose the insulator and to not overextend into the conductor or semiconductor. The second option is to allow ATLAS to automatically generate slices through the oxide layer. This is to be preferred if the oxide geometry is non-planar.

There are a choice of two algorithms for determining the slices. The default is to calculate the currents on slices constructed as being locally perpendicular to each semiconductor-oxide segment on the interface. To enable the alternative algorithm, use the SHAPEOX parameter on the MODELS statement. In this case, slices giving the shortest distance to the contact are constructed from each node on the semiconductor-insulator interface.

If you specified the Schrodinger equation using the NEW.SCHRODINGER parameter and solved on a rectangular mesh specified by the SPX.MESH and SPY.MESH commands, then the Quantum tunneling current must also be calculated on the rectangular mesh defined by the QTX.MESH and QTY.MESH commands. Best results will be obtained if the mesh lines in the direction of tunneling are roughly coincident and if the SP mesh ends at the semiconductor-insulator interface.

Table 3-95. QTX.MESH and QTY.MESH Statements

| Parameter | Type | Units | Default |
|-----------|------|---------|---------|
| NODE | Int | | -999 |
| LOCATION | Real | microns | -999 |
| X | Real | microns | -999 |
| RATIO | Real | microns | 1.0 |
| SPACING | Real | microns | -999 |

Table 3-96. MODELS Statement

| Parameter | Type | Default |
|-----------|---------|---------|
| QTUNN.DIR | Real | 0 |
| SHAPEOX | Logical | False |

Contact Specifications

Carriers that tunnel through an oxide are added to the current of the electrode into or from which they flow. If they tunnel into a polysilicon region with several contacts attached, then the tunnel current is added to the electrode that is nearest to the segment of the oxide/polysilicon interface across which the current is being calculated. The NEARFLG parameter in the MODELS statement is automatically set for quantum tunneling. Therefore, the algorithm used to obtain the nearest electrode is the same as when you set NEARFLG. To exclude any electrode from this algorithm, set the EXCLUDE_NEAR flag in the CONTACTS statement.

You can also set the effective mass to use inside each contact for the tunneling current calculation using the QTUNN.CMASS (electrons) and QTUNN.VMASS (holes) parameters in the CONTACTS statement. If the contact is polysilicon, then the default effective mass is either the conduction band or valence band density of states effective mass depending on its dopant specification.

Table 3-97. CONTACTS Statement

| Parameter | Type | Units | Default |
|--------------|---------|-------|---------|
| EXCLUDE_NEAR | Logical | | False |
| QTUNN.CMASS | Real | | 1.0 |
| QTUNN.VMASS | Real | | 1.0 |

To calibrate the tunneling current, use the effective mass in the oxide region. You can set this by using either the MC or ME.TUNNEL parameters on the MATERIAL statement for electrons and the MV or MH.TUNNEL parameters on the MATERIAL statement for holes.

For example:

```
MATERIAL MATERIAL=OXIDE MC=0.6 MV=0.2
```

In addition to this direct tunneling model and Fowler Nordheim model, there are several quantum tunneling models included in ATLAS for compatibility with other products. These are mutually exclusive and the tunneling current outputs to a variable I_{tnt} (A) or J_{tnt} (A/um) regardless of model chosen.

The direct quantum tunneling current density associated with each interface node can be output to any standard structure file using the parameters QTUNN.EL, QTUNN.HO, and QTUNN.BBT on the OUTPUT statement. This applies to both post-processing and self-consistent versions of the direct quantum tunneling model.

When using the direct quantum tunnelling model in conjunction with the Bohm Quantum Potential or Density Gradient models, some correction is made for the quantum confinement effects introduced by these models. In Equations 3-366 and 3-367, the lower limit of energy integration is usually the band edge in the semiconductor at the interface with the insulator. It is changed to be the ground state of the confining potential well formed by the band edge. This is modeled as a triangular potential well. The ground state of the potential well is approximated as

$$\left[\frac{9}{8}\pi\right]^{2/3} \left(\frac{(qF\hbar)^2}{2m_0m^*}\right)^{1/3} \quad 3-473$$

relative to the minimum of the well. The quantity F is the local electric field at the interface. If the potential is not confining, then the Field will be zero or negative, and the ground state is set to zero. By integrating over a continuous energy range beginning at the ground state energy, quantization effects in the channel are introduced into the gate tunnel current model for a drift-diffusion solution.

Schenk Oxide Tunneling model

Another approximate tunneling model is based on the Gundlach model [83] and includes the effects of barrier lowering due to the image force potentials [201]. As such, it is especially suited for tunneling through ultra-thin gate oxides. It involves mapping from the energy barrier arising from the actual barrier profile plus the correction due to the image force to an effective trapezoidal barrier. The exact Transmission Coefficient for a trapezoidal barrier can then be obtained from

$$T(E) = \frac{2}{1 + g(E)} \quad 3-474$$

where

$$g(E) = \frac{\pi}{2} \left[\frac{m_s k_c}{m_c k_s} (Bi'_d Ai'_o - Ai'_d Bi'_o)^2 + \frac{m_c k_s}{m_s k_c} (Bi_d Ai'_o - Ai_d Bi'_o)^2 \right. \\ \left. + \frac{m_c m_s}{\lambda_o^2 m_{ox}^2 k_c k_s} (Bi'_d Ai'_o - Ai'_d Bi'_o)^2 + \frac{\lambda_o^2 m_{ox}^2 k_c k_s}{m_c m_s} (Bi_d Ai'_o - Ai_d Bi'_o)^2 \right] \quad 3-475$$

where k_c is the wavevector in the contact, k_s is the wavevector in the semiconductor, m_c is the effective mass in the contact, m_{ox} is the effective mass in the oxide and m_s is the effective mass in the semiconductor.

Complication arises because the image potential is not of a simple functional form, it is given by

$$E_{im}(x) = \frac{q^2}{16\pi\epsilon_{ox}} \sum_{n=0}^{\infty} (k_1 k_2)^n \times \left[\frac{k_1}{nd+x} + \frac{k_2}{d(n+1)-x} + \frac{2k_1 k_2}{d(n+1)} \right] \quad 3-476$$

with

$$k_1 = \frac{\epsilon_{ox} - \epsilon_M}{\epsilon_{ox} + \epsilon_M} = -1, \quad k_2 = \frac{\epsilon_{ox} - \epsilon_s}{\epsilon_{ox} + \epsilon_s} \quad 3-477$$

where ϵ is the relative dielectric permittivity (of the material indicated by the subscript), d is the oxide thickness and x is the position in the barrier. The sum can be evaluated numerically and the potential added to the barrier potential. This allows one to evaluate the action of an electron of incident energy E when moving through this barrier by numerically integrating the barrier energy minus the electron energy as a function of distance between the classical turning points of the motion.

This can be equated with the action of the carrier moving through a trapezoidal barrier with the barrier height as a fitting parameter.

$$S_{eff}(E) = S_{im+actual}(E) \quad 3-478$$

This results in an effective trapezoidal barrier height as a function of electron incident energy E . This is evaluated at three different energies and these values are used to calculate the effective barrier height as a function of electron energy. The interpolation formula used is

$$\begin{aligned} \Phi_B(E) = & \Phi_B(E_0) + \frac{\Phi_B(E_2) - \Phi_B(E_0)}{(E_2 - E_0)(E_1 - E_2)}(E - E_0)(E_1 - E) \\ & - \frac{\Phi_B(E_1) - \Phi_B(E_0)}{(E_1 - E_0)(E_1 - E_2)}(E - E_0)(E_2 - E) \end{aligned} \quad 3-479$$

For a given electron incident energy, you use Equation 3-479 to calculate the effective barrier height and then use Equation 3-475 to calculate the Transmission Probability, $T(E)$. This is placed in an equation like Equation 3-466 and the integration over the range of tunneling energies is carried out to give the tunneling current.

The model has been implemented as both a post-processing step and alternatively, as being solved self-consistently with the current continuity equations. To enable the post-processing option, specify SCHENK on the MODELS statement. To enable the self-consistent version, use SCHKSC with the MODELS statement. You can enable them separately for electrons and holes if required using the parameters SCHENK.EL, SHENCK.HO (post-processing) and SCHKSC.EL, SCHKSC.HO (self-consistent) on the MODELS statement. The values of effective mass and permittivity will affect the quantity of tunneling current as will the electron affinities and work functions of the materials involved.

| Table 3-98. Schenk Oxide Tunneling Flags | | | |
|--|---------|---------|-------|
| Parameter | Type | Default | Units |
| SCHENK.EL | Logical | False | |
| SCHENK.HO | Logical | False | |
| SCHENK | Logical | False | |
| SCHKSC.EL | Logical | False | |

Table 3-98. Schenk Oxide Tunneling Flags

| Parameter | Type | Default | Units |
|------------|---------|---------|-------|
| SCHKSC.HO | Logical | False | |
| SCHKSC | Logical | False | |
| SCHENK.BBT | Logical | False | |

Gate Tunneling Models for SONOS Type Structures

One approach to obtaining Non-Volatile Memories with low operating Voltages is to use a SONOS structure. The (S)emiconducting channel has a thin layer of tunnel (O)xide grown on it, followed by a thin layer of silicon (N)itride, and then followed by a thicker blocking or capping layer of (O)xide, and finally a (S)emiconducting polysilicon gate. The nitride has trapping levels located within it and the nitride-oxide band offset allows charge to be accumulated in the nitride layer.

The use of a charge-trapping Silicon nitride layer as a basis for a Non-Volatile memory device goes back to 1967 [244]. There has recently been a lot of interest in SONOS devices because of the continuing trend to smaller device dimensions.

To achieve low-voltage, low-power operation, you need to have an ultrathin tunneling layer so that charging by direct tunneling is possible. The presence of a defect in an ultrathin oxide tunneling layer can cause the complete failure of a floating gate device because it will fully discharge. In a SONOS device, the charge is stored in traps in the Silicon Nitride and consequently a defect will have only a localized effect. Thus, the SONOS structure is potentially more reliable [254].

ATLAS has three different SONOS models for attempting to model the behavior of these devices.

The first is the FNONOS model that relies on using embedded floating gates in the Nitride layer but can model capture efficiency and trap saturation.

The second is the SONOS model that assumes that the trapping of charge in the Silicon Nitride occurs at the interface with the tunneling oxide.

The third, and most complete, is the DYNASONOS model. This model includes several tunneling mechanisms, carrier transport and trap dynamics in the Silicon Nitride layer. It assumes that the traps are evenly distributed throughout the Silicon Nitride layer. It is the most complete model for SONOS devices in ATLAS.

All three models are described below.

FNONOS Model

To enable this model, specify FNONOS on the MODELS statement. To use the FNONOS model, you must either set the whole Silicon Nitride layer as a floating contact or embed floating contacts in the Silicon Nitride layer. Use the FLOATING flag on the CONTACT statement to make an electrode into a floating contact. For each point in the channel-oxide interface, ATLAS calculates the distance to the nearest point in the Silicon Nitride layer. The tunneling current for this point is then calculated as'

$$J_n = F_{AE} E^2 / factor1 \exp(-F_{BE} factor2 / E) \quad 3-480$$

where

$$factor1 = \left[1 - (1 - DV/BH_{FNONOS})^{\frac{1}{2}} \right]^2 \quad 3-481$$

and

$$factor2 = \left[1 - (1 - DV/BH.FNONOS)^{\frac{3}{2}} \right] \quad 3-482$$

DV is the potential drop across the tunnel oxide layer and is calculated automatically by ATLAS. The value BH.FNONOS is the Barrier height and if not specified directly ATLAS will calculate it. This formula is calculated using WKB theory for the tunneling co-efficient through a trapezoidal barrier.

If $DV > BH.FNONOS$, then *factor1* and *factor2* are both set to be unity. In this case, Equation 3-480 is the same as the Fowler-Nordheim Expression (Equation 3-433).

ETA.FNONOS times the tunneling current is added to the nearest floating electrode, where ETA.FNONOS is the capture efficiency. A factor $(1 - ETA.FNONOS)$ times the tunneling current is added to the next nearest (gate) electrode. The efficiency can depend on the Charge state of the floating electrode itself. To enable this, set the NT.FNONOS parameter on the MODELS statement to a positive value. The efficiency is modified by an extra term

$$1.0 - Q_{floating}/(q_{NT.FNONOS}) \quad 3-483$$

where $Q_{floating}$ is the Floating gate charge density in C/micron. NT.FNONOS is the integrated trap density /micron. If this term is negative, then zero is used instead. This allows you to model the phenomenon of trap saturation.

| Table 3-99. MODELS Statement | | | |
|------------------------------|---------|---------|------------------|
| Parameter | Type | Default | Units |
| FNONOS | Logical | False | |
| ETA.FNONOS | Real | 1.0 | |
| BH.FNONOS | Real | 3.07 | eV |
| NT.FNONOS | Real | 0.0 | um ⁻¹ |

SONOS Model

This is a model of intermediate complexity for modeling SONOS devices. It assumes that the trapped charge in the Silicon Nitride is at the interface of the Silicon Nitride and the surrounding insulator materials. The traps can be charged up and discharged by direct tunneling through the tunnel oxide, or by hot carrier injection (lucky electron or concannon models).

To enable this model, you include an INTERFACE statement with the parameter N.I specified. You must also explicitly suppress the DYNASONOS flag by specifying ^DYNASONOS. This is because the DYNASONOS model (see below) is the default. The gate stack materials must all be insulators. If they are changed to wide bandgap semiconductors, then the model will not work correctly.

You can view the trapped carrier density as a sheet charge density under the **Insulator Charge** field in TONYPLOT.

The tunneling current is calculated using the direct quantum tunneling Equation 3-466 with the tunneling probability $T(E)$ obtained using the WKB approximation. The quasi-Fermi energy E_{fi} in the Silicon Nitride is obtained from the energy level at the gate contact. This value is then clipped to ensure that it lies within the Silicon Nitride bandgap. The value of E_{fr} is the usual value of quasi-

Fermi level near the interface of the channel and the oxide. The shortest paths between each point on the interface and the Silicon Nitride are used as the tunneling paths.

The value of $T(E)$ is strongly dependent on the values of effective mass in the tunnel oxide. You can use the MC and MV parameters on the MATERIAL statement as fitting parameters.

If a hot carrier gate current model is selected (HEI, HEI, N.CONCANNON, or P.CONCANNON on the MODELS statement), then the hot carrier current charges points on the Silicon Nitride interface in a way, which is consistent with the motion of the hot carriers in the local electric field.

The limitations of this model are that:

- The trapped charge is constrained to be negative (holes can only erase).
- The trapped charge is localized at the Silicon Nitride boundary.
- Trap dynamics are not included.
- Charge transport in the Silicon Nitride is not included.

Its advantage is that it is a robust model and can model spatial variations in the trapped charge density.

DYNASONOS Model

To address some of the limitations of the SONOS model, the DYNASONOS model was developed by adapting features of various published models [186], [75], [44], [57], [76], [45].

To enable this model, you specify the N.I parameter on the INTERFACE statement. You can also specify the DYNASONOS parameter, although this is enabled by default (it has no effect unless you also specify N.I).

You must also change all of the insulator materials in the gate stack to wide bandgap semiconductors using the SEMICONDUCTOR parameter on the MATERIAL statement. You also need to specify effective masses, mobilities, and effective densities of states in the gate stack materials with the MATERIAL statement.

The properties of the traps in the Silicon Nitride must be set using the NITRIDECHARGE statement. These parameters are now introduced. ATLAS models the trap states in the Nitride as being either acceptor-like (for storing electrons) or donor-like (for storing holes), at a single discrete energy level below the Nitride conduction band (acceptor-like) or above the valence band (donor-like). The number of available trap states is assumed to be spatially uniform, with the number density of acceptor-like traps being set by the NT.N parameter in units of cm^{-3} and the number density of donor-like states being set by NT.P in the same units.

By default, the traps are initialized to be empty (uncharged) and are charged using a transient SOLVE statement. It is possible, however, to set up an initial distribution of charged traps by using the NIT.N and NIT.P parameters on the SOLVE statement. These set the trapped electron and trapped hole densities respectively to the specified value within the limits specified by the optional parameters: NIT.XMIN, NIT.XMAX, NIT.YMIN, and NIT.YMAX. The default values of these parameters are the maximum extents of the Nitride region. The effect of consecutive SOLVE statements with NIT.N or NIT.P is cumulative, allowing you to create a complicated profile of trapped charge density. This is useful for studying known trapped charge distributions.

To simulate the charging of the Nitride layer, you use a transient SOLVE statement. The Silicon Nitride layer can be charged by quantum mechanical tunneling or by hot carrier injection. Two types of tunneling are modeled. The first is tunneling to the Silicon Nitride conduction band and valence band. The second is direct tunneling to and from the trap levels. In the former case, some of the free carriers are captured by the trapping centers. For acceptor traps, the rate of capture of electron density is

$$\text{SIGMAT} \cdot N_{v_{th,n}} n(\text{NT.N} - n_t)$$

3-484

where SIGMAT.N is a capture cross-section in cm^2 , $v_{th,n}$ is the electron thermal velocity in cm/s , n is the free electron density in cm^{-3} and n_t is the trapped electron density in cm^{-3} . Trapped electrons can be re-emitted to the conduction band, the rate for this process being

$$n_t e_n \quad 3-485$$

where e_n is an emission rate in s^{-1} . There are also rates for hole capture from the valence band

$$\text{SIGMAN.P} v_{th,p} p n_t \quad 3-486$$

where p is the free hole density in cm^{-3} and $v_{th,p}$ is the hole thermal velocity in cm/s . To get an equilibrium solution, you need to include an hole emission term

$$(\text{NT.N} - n_t) e_{eq,p} \quad 3-487$$

where the hole emission rate $e_{eq,p}$ is calculated from the other parameters and the equilibrium carrier densities and cannot be independently specified. The rate of direct trap charging due to tunneling is given by

$$P(s\text{NT.N} - n_t) \quad 3-488$$

where s is the Fermi-Dirac factor in the conduction band, and the tunneling rate per trap is P in units of per second (see Equation 3-491).

Putting these terms together we obtain an expression for the rate of the change of the local trapped electron density.

$$\frac{dn_t}{dt} = \text{SIGMAT.N} v_{th,n} n (\text{NT.N} - n_t) - \text{SIGMAN.P} v_{th,p} p n_t + (\text{NT.N} - n_t) \quad 3-489$$

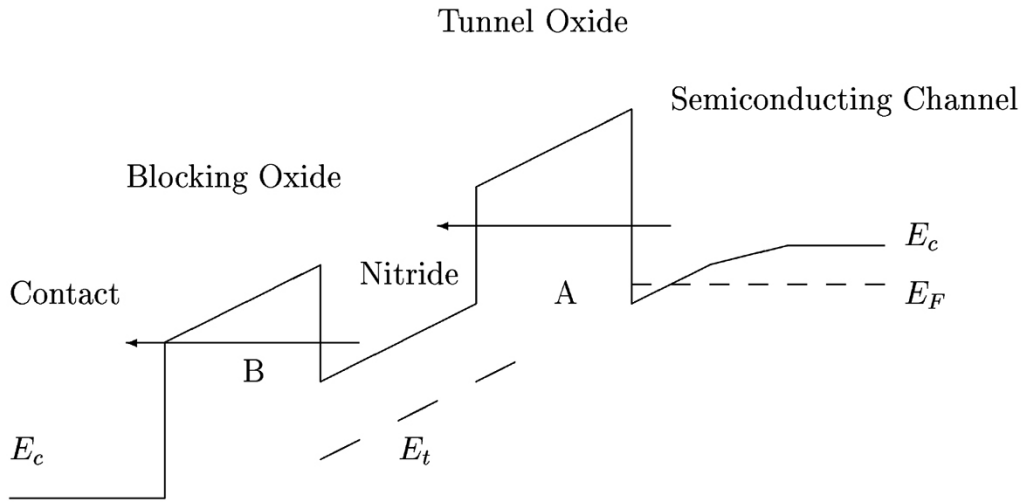
$$e_{eq,p} - n_t e_n + P(s\text{NT.N} - n_t)$$

The equivalent expression for the rate of change of trapped hole density is

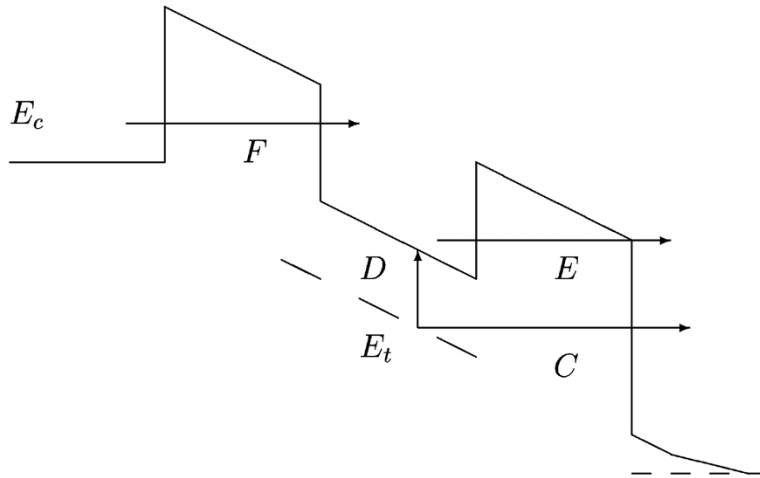
$$\frac{dp_t}{dt} = \text{SIGMAT.P} v_{th,p} p (\text{NT.P} - p_t) - \text{SIGMAP.N} v_{th,n} n p_t + (\text{NT.P} - p_t) \quad 3-490$$

$$e_{eq,n} - p_t e_p + P(s\text{NT.P} - p_t)$$

The tunneling terms are zero for any tunneling processes, which start or end in the band gap of the channel material. We now consider electron trapping. To charge the traps, there must be electrons in the Silicon Nitride and these are generated by direct quantum tunneling, shown schematically as process A in part a) of Figure 3-12, where the tunnelling transitions are allowed at energies greater than the conduction band energy in the channel. Any excess electrons in the Silicon Nitride may tunnel to the contact as shown schematically as process B. Clearly tunneling directly into the Silicon Nitride traps is not possible in this band lineup. For a band lineup during a typical erase operation, as in part b) of Figure 3-12, direct trap-to-channel tunneling is possible (process C). In process D, trapped electrons are emitted to the Silicon Nitride conduction band, drift to the interface with the tunnel oxide and then tunnel out of the Silicon Nitride in process E. Some electrons may be injected from the contact as shown in process F. There are analogous process for hole traps.



a. Conduction band configuration for trap charging



b. Conduction band configuration for trap erasing

Figure 3-12: Schematic of band structure and processes for SONOS model

For trap-to-channel tunneling, the range of states in the channel corresponding to the tunneling to or from a specific trap energy are such that the total energy must add up to the energy at the trap level. This means that we do an integral over transverse wavevector $k_{||}$, with the constraint that the transverse and perpendicular energies sum to the value of the trap energy. The electron band-to-trap tunneling rate in units of s^{-1} is

$$P = \frac{4\hbar m_{nitride}}{m_{oxide}^2} \int_0^\infty \frac{Hk_{\perp}}{\kappa_1^2 + k_{\perp}^2} WKB(E, k_{||}) \frac{\kappa_2^2}{(\kappa_2 + \kappa_3)^2} k_{||} dk_{||} \quad 3-491$$

where $H^2 = \frac{2m_{\text{nitride}}}{\hbar^2} \text{ELEC.DEPTH}$, k_{\perp} is the perpendicular wavevector at the channel side of the Channel/Oxide interface and κ_1 is the evanescent wavevector at the Oxide side of the Channel/Oxide interface. Similarly, κ_2 and κ_3 are evanescent wavevectors evaluated at the Nitride/Oxide interface and $WKB(E, k_{\parallel})$ is the product of the WKB tunneling probabilities through the oxide and through part of the Nitride to the trap position. This is derived by extending the result of Lundst rm et al. [145] to a realistic bandstructure.

The electron emission rate (for acceptor traps) and hole emission rate (for donor traps) are important in determining the trapped carrier density after charging, and also the importance of process D in Figure 3-12. These rates are either set using the `TAU.N` and `TAU.P` parameters on the `NITRIDECHARGE` statement, or by enabling the Poole-Frenkel detrapping model by specifying the `PF.NITRIDE` flag on the `MODELS` statement. In the former case, the emission rates are constants $e_n = 1/\text{TAU.N}$ and $e_p = 1/\text{TAU.P}$. In the latter case, the emission rates depend on the local value of field in the device. For electrons

$$e_n = \text{PF.B} \exp\left(-\left[\frac{\text{ELEC.DEPTH} - q\sqrt{qF/\pi\epsilon}}{K_{BT}}\right]\right) \quad 3-492$$

where `ELEC.DEPTH` is the depth of the electron traps below the conduction band, F is the local electric field in V/m and ϵ is the dielectric permittivity of the Silicon Nitride in F/m. The overall rate is proportional to `PF.B`, which has a default value of $10^{13}/\text{s}$.

If you want to use the Poole-Frenkel model without modifying `ELEC.DEPTH`, then you can use `PF.BARRIER`. If `PF.BARRIER` is specified, then it is used in place of `ELEC.DEPTH` in Equation 3-492.

The parameters that are set on the `NITRIDECHARGE` statement are summarized in Table 3-100, along with their default values. Parameters that are relevant to electron traps (acceptor-like) are only used if `NT.N` is greater than zero, and parameters that are relevant to hole traps (donor-like) are only used if `NT.P` is greater than zero.

| Table 3-100. NITRIDECHARGE Statement | | | |
|--------------------------------------|------|---------|-----------------|
| Parameter | Type | Default | Units |
| <code>NT.N</code> | Real | 0.0 | cm ³ |
| <code>NT.P</code> | Real | 0.0 | cm ³ |
| <code>TAU.N</code> | Real | 1.0e300 | s |
| <code>TAU.P</code> | Real | 1.0e300 | s |
| <code>ELEC.DEPTH</code> | Real | -999.0 | eV |
| <code>HOLE.DEPTH</code> | Real | -999.0 | eV |
| <code>SIGMAN.P</code> | Real | 1.0e-15 | cm ² |
| <code>SIGMAP.N</code> | Real | 1.0e-14 | cm ² |
| <code>SIGMAT.N</code> | Real | 1.0e-16 | cm ² |
| <code>SIGMAT.P</code> | Real | 1.0e-14 | cm ² |
| <code>PF.BARRIER</code> | Real | | eV |
| <code>PF.B</code> | Real | 1.0e13 | Hertz |

In the Silicon Nitride, the fully transient current continuity equations are solved, self-consistently along with the Equations 3-489 (if `NT.N` is non-zero) and 3-490 (if `NT.P` is non-zero) for the trap occupancies. The Poisson Equation is also solved to self-consistently include the effect of nitride trap charging. There are two algorithms available for solving the trap equations. The default method uses an approximate analytical solution for each timestep. The other method, chosen by specifying `ICDE.ELEC`, `ICDE.HOLE`, or `ICDE` on the `METHOD` statement, ensures that the trap equations are solved implicitly using the TR-BDF2 method. The second method can only be used with Drift-Diffusion simulations. It cannot be used with Energy Balance simulations. In practice, the second method is seldom required.

In order to simulate hot carrier injection into the Silicon Nitride, you may enable the existing hot carrier models `HEI/HHI` for drift diffusion simulations or `N.CONCANNON/P.CONCANNON` with Energy balance simulations. In general, `N.CONCANNON` and `P.CONCANNON` should give physically more reasonable results. An additional model is available to use in drift-diffusion simulations. It is enabled by specifying `N.HOTSONOS` (for electrons) and `P.HOTSONOS` (for holes) on the `MODELS` statement. It uses the parallel field along the channel/insulator interface to obtain an effective carrier temperature using the formulae:

$$\begin{aligned}T_n &= F_{IG.LRELE}/(1.5K_B) \\T_p &= F_{IG.LRELH}/(1.5K_B)\end{aligned}\tag{3-493}$$

where F is the parallel field along the interface.

It then uses these effective carrier temperatures in the Concannon expressions for Hot carrier gate current.

The final distribution of trapped charge depends on the distribution of carrier generation and recombination, the parameters of the trap equation and the simulation time. The trapped carrier concentrations are output automatically to any structure file as Trapped Insulator e- Concentration and Trapped Insulator h+ Concentration. The instantaneous rates of carrier generation in the Silicon Nitride layer can be output to any structure file by specifying `SONOS.RATES` on the `OUTPUT` statement. Both through barrier direct tunneling and trap-to-channel tunneling are included and are given as a generation term in units of $\text{cm}^{-3} \text{s}^{-1}$. The net rate of electron capture from the conduction band and hole capture from the valence band are calculated from Equations 3-489 and 3-490 and output as recombination rates in units of $\text{cm}^{-3} \text{s}^{-1}$ if `SONOS.RATES` is specified.

You can obtain the net trapped charge density (electron density - hole density) by specifying the `SONOS.CHARGE` statement on the `PROBE` statement. Furthermore, you can view the overall tunneling current injected into the Nitride layer from the channel as a function of time by specifying `SONOS.CURR` on the `LOG` statement. Choosing this option will also output the tunnel current entering the external contact from the Nitride layer. They are referred to as the SONOS Tunneling Insulator Current and SONOS Blocking Insulator Current respectively and are given in units of $\text{A}/\mu\text{m}$.

In steady state, the trapped charge in the Silicon Nitride layer remains fixed at its charged value, allowing you to do threshold voltage shift calculations. If the gate stack materials remain as wide bandgap semiconductors, the large stored fixed charge combined with weakly coupled quasi-Fermi levels mean that `SOLVE INIT` may wrongly introduce a compensating free carrier charge. To avoid this, either revert the gate stack materials to insulators or specify the `SONOS` flag on the `SOLVE` statement when you also specify `INITIAL`.

The BESONOS model is an extension of the DYNASONOS model to SONOS devices with Band-Engineered tunnel layers. It is enabled by setting the parameter `BESONOS` on the `INTERFACE` statement together with the `DYNASONOS` parameter. The BESONOS model uses the direct quantum tunneling model for calculating the tunneling current through the layered insulator tunnel stack. This model is described in Section 3.6.6: "Gate Current Models" and can calculate tunnel current through a stack of materials with different band offsets and effective masses.

Some Band-Engineered tunnel layers may contain ultra-thin Nitride layers, which do not trap charge. In order to specify which Silicon Nitride regions to charge in the BESONOS model, you must use the TRAPPY parameter on the REGION statement. Only Silicon Nitride regions that have the TRAPPY parameter set will be able to have trapped charge stored in them. The TRAPPY parameter is only active for the BESONOS model.

| Table 3-101. Parameters Relevant to the SONOS MODEL | | | |
|---|--------------|---------|---------|
| Statement | Parameter | Type | Default |
| INTERFACE | BESONOS | Logical | False |
| INTERFACE | N.I | Logical | False |
| INTERFACE | DYNASONOS | Logical | True |
| LOG | SONOS.CURR | Logical | False |
| METHOD | ICDE.ELEC | Logical | False |
| METHOD | ICDE.HOLE | Logical | False |
| METHOD | ICDE | Logical | False |
| MODELS | N.HOTSONOS | Logical | False |
| MODELS | P.HOTSONOS | Logical | False |
| OUTPUT | SONOS.RATES | Logical | False |
| PROBE | SONOS.CHARGE | Logical | False |
| REGION | TRAPPY | Logical | False |
| SOLVE | NIT.N | Real | 0.0 |
| SOLVE | NIT.P | Real | 0.0 |
| SOLVE | NIT.XMAX | Real | 0.0 |
| SOLVE | NIT.XMIN | Real | 0.0 |
| SOLVE | NIT.YMAX | Real | 0.0 |
| SOLVE | NIT.YMIN | Real | 0.0 |
| SOLVE | SONOS | Logical | False |

Floating Gate to Control Gate (FGCG) Current

In a conventional Flash memory device structure, it is usual to neglect the tunneling current between the control gate and the floating gate. This is because the insulating layer separating the floating gate from the channel (tunnel oxide) is much thinner than that separating the floating gate from the control gate (barrier oxide). This will typically result in the dominance of the channel to floating gate tunneling current, at least under normal operating conditions.

As flash memory technology develops, it may be necessary to quantify the floating gate to control gate tunneling currents [57]. ATLAS incorporates this capability with a new model called the FGCG model. This model calculates the tunneling currents between the floating gate and the semiconducting channel and between the floating gate and the control gate. Both of these currents can be taken into account when calculating the charge state of the floating gate. The model also applies to more complicated geometries where there are several floating gates and/or several control gates.

The tunneling currents are calculated using the direct tunneling formula, Equation 3-466, with the Transmission co-efficient being obtained using the WKB approximation.

This formula includes the carrier statistics and automatically determines the sign of the currents using the Fermi levels in the gates and quasi-Fermi in the channel.

To enable the model for electron tunneling, use the parameter `E.FGCGTUN` on the `MODELS` statement. To enable the model for hole tunneling, use the parameter `H.FGCGTUN` on the `MODELS` statement.

It is also important to specify how the floating gate to control gate current is output and how it affects the charge state of the floating gate. This is controlled by the `CGTUNN` parameter on the `CONTACT` statement. This only has an effect on a floating gate. If it is set (default), then the tunneling current attributed to the floating gate is obtained by calculating the current from that floating gate to every control gate.

This is then subtracted from the channel to floating gate current to give a net current. This net current is the one output. It is also the one used in the calculation of the amount of charging during a transient simulation.

If `CGTUNN` is explicitly cleared for a floating gate, then only the channel to floating gate current is used for the charging calculation and output.

Note: The tunneling current at a control gate is the sum of channel to control gate current, plus the floating gate to control gate current from all floating gates in the device. This is not affected by the `CGTUNN` parameter because the `CGTUNN` parameter is only effective for floating contacts.

A specific example is shown in Figure 3-13, where there are 3 control gates and 2 floating gates. The following `CONTACT` statements are issued:

```
CONTACT NAME=fgate1 FLOATING WORKF=4.28 CGTUNN
CONTACT NAME=fgate2 FLOATING WORKF=4.28 ^CGTUNN
```

so that `CGTUNN` is set for `fgate1` and explicitly cleared for `fgate2`. The currents attributed to each electrode are calculated by ATLAS as follows:

```
jfgate1 = jchannel1 - jcg1fg1 - jcg2fg1 - jcg3fg1
jfgate2 = jchannel3
jcgate1 = jcg1fg1 + jcg1fg2
jcgate2 = jchannel2 + jcg2fg1 + jcg2fg2
jcgate3 = jcg3fg1 + jcg3fg2
```

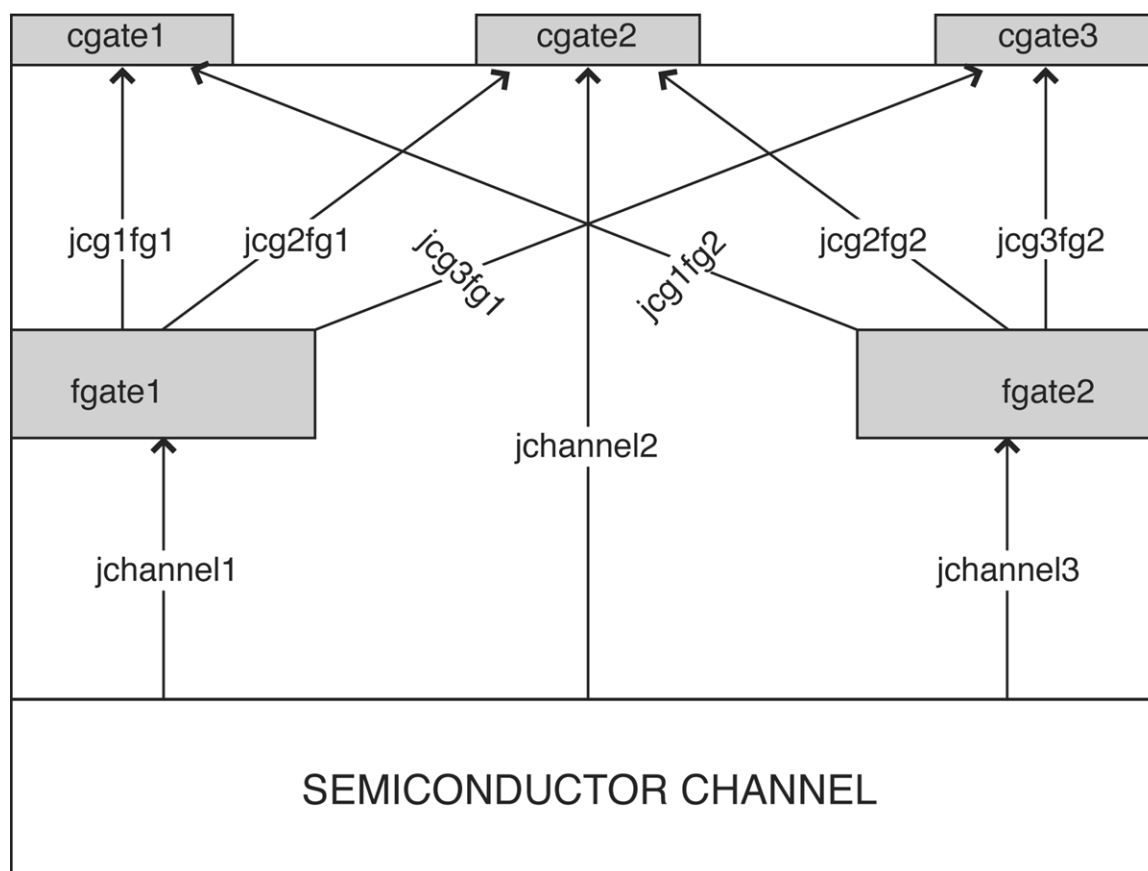


Figure 3-13: Example Structure that can be modeled with FGCG model, showing the current components.

The intention is that the model is used with `CGTUNN` set on every floating gate. You are, however, given the ability to see the effect of leaving out the control gate components of the floating gate current by clearing `CGTUNN`.

When used in transient mode, the floating gate tunneling currents are integrated over time to give the charges on the floating gates. Because the floating gate charge affects the floating gate voltage, which in turn affects the floating gate to control gate current, there is strong coupling between floating gate to control gate current and floating gate charge. For large timesteps this can cause numerical instability.

One approach to avoid this problem is to control the maximum timestep allowed using the `DT.MAX` parameter on the `METHOD` statement. The recommended alternative, however, is to specify `FGCNTRL` on the `METHOD` statement, which invokes an algorithm to control step size based on the relative size of the charging current. There are two parameters that can be used to control the behavior of this stabilization algorithm. One is `QMAX.FGCNTRL`, which is in units of electronic charge. If the charge on the floating gate is less than `QMAX.FGCNTRL`, then the algorithm will not be applied. The other parameter is `RAT.FGCNTRL`. This controls how much the timestep is reduced by the algorithm. Reduce it from the default value of 1.0 to give better control, but longer runtime.

For example, the following statement will enable the stability algorithm for those floating gates having an absolute charge of more than 8.01×10^{-17} Coulombs, and give a high level of stability due to the low value of `RAT.FGCNTRL`.

```
METHOD FGCNTRL RAT.FGCNTRL=0.05 QMAX.FGCNTRL=500
```

The parameters `E.FGCGTUN` and `H.FGCGTUN` enable the FGCG model. This will not include the current tunneling from the semiconducting channel into the current continuity equations in the semiconductor. The parameters `E.SC.FGCGTUN` and `H.SC.FGCGTUN` enable the FGCG model. This will include this current in the current continuity equations. If you set also `CGTUNN` is for every floating gate in the device, then overall current continuity for the device will be attained when you set the `E.SC.FGCGTUN` and `H.SC.FGCGTUN` parameters.

Table 3-102 shows the parameters used in the FGCG model.

| Table 3-102. FGCG Model Parameters | | | |
|------------------------------------|---------------------------|---------|-------|
| Statement | Parameter | Default | Units |
| MODELS | <code>E.FGCGTUN</code> | FALSE | |
| MODELS | <code>H.FGCGTUN</code> | FALSE | |
| MODELS | <code>E.SC.FGCGTUN</code> | FALSE | |
| MODELS | <code>H.SC.FGCGTUN</code> | FALSE | |
| CONTACT | <code>CGTUNN</code> | TRUE | |
| METHOD | <code>FGCNTRL</code> | TRUE | |
| METHOD | <code>RAT.FGCNTRL</code> | 1.0 | |
| METHOD | <code>QMAX.FGCNTRL</code> | 100 | |

Metal-Insulator-Metal Tunneling

The simulation of some classes of device, for example Metal-Insulator-Metal tunnel diodes, requires the calculation of the tunneling current between electrodes. ATLAS has the MIMTUN model for this class of device. The MIMTUN model calculates the tunneling paths between electrodes and obtains the tunnel currents using the Direct Quantum Tunneling model of Equation 3-466.

The quasi-Fermi levels are defined by the biases on the electrodes. The tunneling current can be calculated through a single or multi-layer insulator stack. The insulator materials can also be modeled as wide bandgap semiconductors using the `SEMICONDUCTOR` parameter on the `MATERIAL` statement. It is possible to model electrodes having different workfunctions by using the `WORKF` parameter on the `CONTACT` statement.

To enable this MODEL, specify MIMTUN on the MODELS statement.

It is recommended that the effective masses of the insulator materials are explicitly assigned using the `MC` and `MV` parameters on the `MATERIAL` statement.

3.6.7: Device Level Reliability Modeling

Hansch MOS Reliability Model

The Hansch Reliability Model [88,4,195] can be used to simulate MOS transistor degradation under stress conditions. The causes of device characteristic degradation are the hot electron (hole) injection into gate oxide, and the trapping of electron (hole) charge on the effective interface acceptor (donor) like traps.

The model calculates hot electron (hole) injection current according to the lucky electron model. The arbitrary position-dependent distributions of acceptor and donor-like traps are specified on the oxide-semiconductor interface with corresponding capture cross sections. The device degradation is calculated as a function of stress time by performing transient calculations. The trap rate equation is solved on every time-step and thus the trapped electron (hole) concentration is calculated. The rate of electron trapping can be described by the equations:

$$\frac{dN_n(x,t)}{dt} = \frac{\text{SIGMAE}}{q} \cdot J_{inj,n}(x,t) \cdot (\text{NTA}(x) - N(x,t)) \quad 3-494$$

$$\frac{dN_p(x,t)}{dt} = \frac{\text{SIGMAH}}{q} \cdot J_{inj,p}(x,t) \cdot (\text{NTD}(x) - N(x,t)) \quad 3-495$$

where $N(x,t)$ represents the trapped electron (hole) density, at the interface point x , at time= t during a transient simulation. The NTA and NTD parameters represent the acceptor and donor-like trap densities at time=0. The $J_{inj,n}(x,t)$ and $J_{inj,p}(x,t)$ parameters are the injected electron and hole current densities, SIGMAE and SIGMAH are the capture cross section of electrons and holes.

To activate this model, use the DEVDEG, DEVDEG.E, and DEVDEG.H parameters in the MODELS statement (to account for both hot electron and hole injection, hot electron or hot hole injection, respectively). The model parameters are user-definable on the DEGRADATION statement.

Table 3-103. User-Definable Parameters for Equations 3-494 and 3-495

| Statement | Parameter | Units |
|-------------|-----------|-----------------|
| DEGRADATION | SIGMAE | cm ² |
| DEGRADATION | SIGMAH | cm ² |
| DEGRADATION | NTA/F.NTA | cm ² |
| DEGRADATION | NTD/F.NTD | cm ² |

The results of stress simulation can be used to calculate the characteristics of the degraded device (the shift of the threshold voltage, transconductance degradation, and so on). You can view the distribution of traps, hot electron (hole) current density, and trapped electron (hole) distribution by using TONYPLOT.

The model parameters: NTA, NTD, SIGMAE, and SIGMAH can also be defined through the C-INTERPRETER functions: F.NTA, F.NTD, F.SIGMAE, and F.SIGMAH. This allows you to define these values as functions of their position (x,y) along the insulator-semiconductor interface. These C-function libraries are also defined on the DEGRADATION statement. More information on the C-INTERPRETER functions can be found in Appendix A: “C-Interpreter Functions”.

3.6.8: The Ferroelectric Permittivity Model

Ferroelectric materials exhibit high dielectric constants, polarization and hysteresis. Such materials are finding more and more applications in integrated memory devices. To simulate these effects, a modified version of the ferroelectric model from Miller [158] has been implemented.

To enable the Ferroelectric Model, set the `FERRO` parameter in the `MODELS` statement. In this model the permittivity used in Poisson's Equation (Equation 3-1) is given the following functional form:

$$\varepsilon(E) = \text{FERRO.EPSF} + \text{FERRO.PS} \cdot 2\delta \cdot \text{sech}^2 \left[\frac{E - \text{FERRO.EC}}{2\delta} \right] \quad 3-496$$

where `FERRO.EPSF` is the permittivity, E is the electric field and δ is given as follows:

$$\delta = \text{FERRO.EC} \left[\log \frac{1 + \text{FERRO.PR}/\text{FERRO.PS}}{1 - \text{FERRO.PR}/\text{FERRO.PS}} \right]^{-1} \quad 3-497$$

The `FERRO.EPSF`, `FERRO.PS`, `FERRO.PR`, and `FERRO.EC` parameters can be modified in the `MATERIAL` statement (see Table 3-104).

The permittivity in Equation 3-496 can be replaced with a user-defined expression with the `C-INTERPRETER`. The `F.FERRO` parameter of the `MATERIAL` statement (see Chapter 21: "Statements", Section 21.29: "MATERIAL") defines the file that contains the C-function. This function allows the permittivity to be position and field dependent.

For more information about C-Interpreter, see Appendix A: "C-Interpreter Functions".

The derivative of the dipole polarization with respect to electric field is given by:

$$\frac{dP_d}{dE} = \Gamma \frac{dP_{sat}}{dE} \quad 3-498$$

where P_d is the position dependent dipole polarization. A numeric integration of this function is carried out in ATLAS to determine the position dependent dipole polarization.

For saturated loop polarization, the Γ function is equal to unity, which corresponds to the default model. If you specify the `UNSAT.FERRO` parameter in the `MODELS` statement, the Γ function will take on a more general form suitable for simulation of unsaturated loops. In this case, the Γ function is given by:

$$\Gamma = 1 - \tanh \left[\left(\frac{P_d - P_{sat}}{\xi P_s - P_d} \right)^{1/2} \right] \quad 3-499$$

where $\xi = 1$ for increasing fields and $\xi = -1$ for decreasing fields.

| Table 3-104. User-Specifiable Parameters for Equations 3-496 to 3-497 | | | |
|---|-----------|---------|--------|
| Statement | Parameter | Default | Units |
| MATERIAL | FERRO.EC | 0.0 | V/cm |
| MATERIAL | FERRO.EPS | 1.0 | |
| MATERIAL | FERRO.PS | 0.0 | C/sqcm |
| MATERIAL | FERRO.PR | 0.0 | C/sqcm |

3.6.9: Epitaxial Strain Tensor Calculations in Zincblende

The strain tensor in epitaxial layers is used in the calculation of the zincblende gain and spontaneous recombination models discussed in Section 3.9.8: “Strained Zincblende Gain and Radiative Recombination Models”. In epitaxial layers, the strain tensor can be represented by ε_{xx} , ε_{yy} , ε_{zz} , ε_{xy} , ε_{yz} and ε_{zx} . The relationship between the various components of the strain tensor are given as follows:

$$\varepsilon_{xx} = \varepsilon_{yy} = \frac{a_s - a_0}{a_0} \quad 3-500$$

$$\varepsilon_{zz} = -2 \frac{C_{12}}{C_{11}} \varepsilon_{xx} \quad 3-501$$

$$\varepsilon_{xy} = \varepsilon_{yz} = \varepsilon_{zx} = 0 \quad 3-502$$

where C_{12} and C_{11} are the elastic constants, which can be specified by the parameters C12 and C11 on the MATERIAL statement. The default values for C_{12} and C_{11} are given for various binary zincblende materials in Table B-28. Values for ternary and quaternary materials are linearly interpolated from the binary values.

The principal value of strain, ε_{xx} , can be specified or calculated. To specify the value of ε_{xx} , assign the desired value to the STRAIN parameter of the REGION statement.

In Equation 3-500 a_s is the lattice constant in the layer in question. The parameter a_0 is the lattice constant in the “substrate”. You can specify the lattice constant in the given layer by the ALATTICE parameter of the MATERIAL statement.

Default values for ALATTICE are taken from Table B-28. Temperature coefficients are included in the default calculation.

There are several ways to un-ambiguously specify the substrate or the substrate lattice constant. You can specify a region as the substrate for all strain calculations by specifying the logical parameter SUBSTRATE on the REGION statement of the substrate. Alternatively, you can directly specify the substrate lattice constant “local” REGION statement using the ASUB parameter.

If the substrate lattice constant is not otherwise specified through the use of the ASUB or SUBSTRATE parameters, the substrate lattice constant is taken as the average of the lattice constants of the two adjacent epitaxial layers (regions above and below the local region). If there is only one adjacent region, the lattice constant of that region is used as the substrate lattice constant.

3.6.10: Epitaxial Strain Tensor Calculation in Wurtzite

The strain tensor in epitaxial layers is used to calculate piezoelectric polarization (Section 3.6.11: “Polarization in Wurtzite Materials [26]”) or in gain modeling (Section 3.9.9: “Strained Wurtzite Three-Band Model for Gain and Radiative Recombination”) or both. In epitaxial layers, the strain tensor can be represented by ε_{xx} , ε_{yy} , ε_{zz} , ε_{xy} , ε_{yz} and ε_{zx} . The relationship between the various components of the strain tensor are given as follows:

$$\varepsilon_{xx} = \varepsilon_{yy} = \frac{a_s - a_0}{a_0} \quad 3-503$$

$$\varepsilon_{zz} = -2 \frac{C_{13}}{C_{33}} \varepsilon_{xx} \quad 3-504$$

$$\varepsilon_{xy} = \varepsilon_{yz} = \varepsilon_{zx} = 0 \quad 3-505$$

where C_{13} and C_{33} are elastic constants, which can be specified by the parameters C13 and C33 on the MATERIAL statement. The default values for C_{13} and C_{33} are given for the GaN system in Section B.8: “Material Defaults for GaN/InN/AlN System”.

The principal value of strain, ε_{xx} , can be specified or calculated. To specify ε_{xx} , assign the desired value to the STRAIN parameter of the REGION statement.

In Equation 3-503 a_s is the lattice constant in the layer in question. The parameter a_0 is the lattice constant in the “substrate”. You can specify the lattice constant in the given layer by the ALATTICE parameter of the MATERIAL statement.

Default values for ALATTICE can be found for the GaN/AlN/InN system in Section B.8: “Material Defaults for GaN/InN/AlN System”.

The substrate is more ambiguously defined so there are several ways to specify the substrate or the substrate lattice constant. First, you can specify a region as the substrate for strain calculations by specifying the logical parameter SUBSTRATE on the associated REGION statement. You can then specify the lattice constant for that region using the ALATTICE parameter of the corresponding MATERIAL statement. Alternatively, you can directly specify the substrate lattice constant in the REGION statement, which make the strain calculations, using the ASUB parameter.

If the substrate lattice constant is not otherwise specified through the ASUB or SUBSTRATE parameters, the substrate lattice constant is taken as the average of the lattice constants of the two adjacent epitaxial layers (region above and below the region in question). If there is only one adjacent region, the lattice constant of that region is used as the substrate lattice constant.

3.6.11: Polarization in Wurtzite Materials [26]

Polarization in wurtzite materials is characterized by two components, spontaneous polarization, P_{sp} , and piezoelectric polarization, P_{pi} . Therefore, the total polarization, P_t , is given by:

$$P_t = P_{sp} + P_{pi} \quad 3-506$$

where P_{sp} is specified on the MATERIAL statement and specifies the total spontaneous polarization, P_{sp} , for the given material(s). The piezoelectric polarization, P_{pi} , is given by:

$$P_{pi} = 2 \frac{a_s - a_0}{a_0} \left(E_{31} - \frac{C_{13}}{C_{33}} E_{33} \right) \quad 3-507$$

where E_{31} and E_{33} are piezoelectric constants, and C_{13} and C_{33} are elastic constants all specified in the MATERIAL statement. The a_0 parameter is the lattice constant of the material layer in question, which can be specified by the ALATTICE parameter of the MATERIAL statement. The a_s parameter is the average value of the lattice constants of the layers directly above and below the layer in question.

To enable the polarization model, specify POLARIZATION in the REGION statement for the region for which you wish to characterize polarization effects. Typically, this will be a quantum well layer or active layer.

The polarization enters into the simulation as a positive and negative fixed charges appearing at the top (most negative Y coordinate) and bottom (most positive Y coordinate) of the layer in question. By default, the positive charge is added at the bottom and the negative charge is added at the top. You can modify the sign and magnitude of this charge by specifying POLAR.SCALE in the REGION statement. This parameter is multiplied by the polarization determined by Equation 3-506 to obtain the applied charge. The default value for POLAR.SCALE is 1.0.

In some cases, the introduction of polarization charges may introduce difficulties with convergence due to problems with initial guess. If these problems arise, you can use the PIEZSCALE parameter of the SOLVE statement to gradually introduce the effects of polarization. This parameter defaults to 1.0 and is multiplied by the net charge given by the product of the results of Equation 3-507 and the POLAR.SCALE parameter.

Table 3-105 shows the parameters of the wurtzite polarization model.

| Table 3-105. User Specifiable Parameters of the Wurtzite Polarization Model | | | |
|---|-----------|----------------------|------------------|
| Statement | Parameter | Default | Units |
| MATERIAL | PSP | see Tables B-17-B-23 | cm^{-2} |
| MATERIAL | ALATTICE | see Tables B-17-B-23 | Å |
| MATERIAL | E13 | see Tables B-17-B-23 | cm^{-2} |
| MATERIAL | E33 | see Tables B-17-B-23 | cm^{-2} |
| MATERIAL | C13 | see Tables B-17-B-23 | GPa |
| MATERIAL | C33 | see Tables B-17-B-23 | GPa |

Note: You should carefully consider the effects of polarization especially in FET devices. Although, polarization effects in the top AlGaIn layer of GaN FET devices are expected, the model presented in this section predicts the formation of positive and negative sheet charges at the top surface and the AlGaIn-GaN interface. In simulation, the surface charge induces a channel at the surface of the device, which leads to unphysical results. For various physical reasons, the surface is conditioned to negate the surface charge. For this reason, it is suggested when simulating FET devices to add the charge predicted by the above equations using the CHARGE parameter of the INTERFACE statement to only add charge at the AlGaIn-GaN interface and not to use the polarization model per se.

3.6.12: Stress Effects on Bandgap in Si

Mechanical stress causes change in the band edges in silicon. These band edge shifts are given by the deformation potential theory [80]. The shifts for the conduction band edges are given by:

$$\Delta E_c^{(i)} = D \cdot \text{DEFPOT}(\varepsilon_{xx} + \varepsilon_{yy} + \varepsilon_{zz}) + U \cdot \text{DEFPOT} \cdot \varepsilon_{ii} \quad 3-508$$

where $\Delta E_c^{(i)}$ is the shift in the band edge of the i th ellipsoidal conduction band minima. The parameters $U \cdot \text{DEFPOT}$ and $D \cdot \text{DEFPOT}$ are the user-definable dilation and shear deformation potentials for the conduction band.

The ε_{xx} , ε_{yy} , and ε_{zz} parameters are the diagonal components of the strain tensor.

The shifts in the valence band edges are calculated by:

$$\Delta E_v^{(hl)} = A \cdot \text{DEFPOT}(\varepsilon_{xx} + \varepsilon_{yy} + \varepsilon_{zz}) \pm \sqrt{\xi} \quad 3-509$$

where $\Delta E_v^{(hl)}$ are the band edge shifts in the light and heavy hole valence band maxima. The ξ parameter is given by:

$$\xi = \frac{B \cdot \text{DEFPOT}^2}{2} \left\{ (\varepsilon_{xx} - \varepsilon_{yy})^2 + (\varepsilon_{yy} - \varepsilon_{zz})^2 + (\varepsilon_{zz} - \varepsilon_{xx})^2 \right\} + C \cdot \text{DEFPOT}^2 (\varepsilon_{xy}^2 + \varepsilon_{yz}^2 + \varepsilon_{zx}^2) \quad 3-510$$

where ε_{xy} , ε_{yz} , and ε_{zx} are the off diagonal components of the strain tensor.

The strain components are calculated from the stress components stored in the input structure file if included (typically imported from ATHENA). The conversion between stress and strain is given by Equations 3-511, 3-512, and 3-513.

$$\varepsilon_{xx} = \sigma_{xx}s_{11} + \sigma_{yy}s_{12} \quad 3-511$$

$$\varepsilon_{yy} = \sigma_{xx}s_{12} + \sigma_{yy}s_{11} \quad 3-512$$

$$\varepsilon_{zz} = 2\sigma_{zz}s_{44} \quad 3-513$$

Here, σ_{xx} , σ_{yy} , and σ_{zz} are the diagonal components of the stress tensor and s_{11} , s_{12} , and s_{44} are the material compliance coefficients.

The compliance coefficients are given by:

$$s_{11} = \frac{c_{11} + c_{12}}{c_{11}^2 + c_{11}c_{12} - 2c_{12}^2} \quad 3-514$$

$$s_{12} = \frac{-c_{12}}{c_{11}^2 + c_{11}c_{12} - 2c_{12}^2} \quad 3-515$$

$$s_{44} = \frac{1}{c_{44}} \quad 3-516$$

where c_{11} , c_{12} , and c_{44} are the elastic stiffness coefficients. The stiffness coefficients for silicon and germanium are given by [103]:

$$\left. \begin{aligned} c_{11} &= 163.8 - T \times 0.0128 \\ c_{12} &= 59.2 - T \times 0.0048 \\ c_{44} &= 81.7 - T \times 0.0059 \end{aligned} \right\} Si \quad 3-517$$

$$\left. \begin{aligned} c_{11} &= 126.0 \\ c_{12} &= 44.0 \\ c_{44} &= 67.7 \end{aligned} \right\} Ge \quad 3-518$$

where T is the temperature. The stiffness coefficients for SiGe at composition are given by linear interpolation.

If the stress tensor is not loaded from a structure file, you can specify the values of the strain tensor as described in Table 3-106. If the stress tensor is not loaded from a structure file and the strain tensor is not specified, then the strain tensor is calculated as [148]:

$$\varepsilon_{xx} = \varepsilon_{yy} = \frac{(1 + \nu) a_{SiGe} - a_{Si}}{(1 - \nu) a_{SiGe}} \quad 3-519$$

where ν is Poisson's ratio, a_{SiGe} is the lattice constant of SiGe, and a_{Si} is the lattice constant of Ge. The lattice constants and Poisson's ratio for Si and Ge are given by:

$$a_{Si} = 5.43102 + 1.41 \times 10^{-5} (T - 300) \quad 3-520$$

$$a_{Ge} = 5.6579 + 3.34 \times 10^{-5} (T - 300) \quad 3-521$$

$$\nu_{Si} = 0.28 \quad 3-522$$

$$\nu_{Ge} = 0.273 \quad 3-523$$

The lattice constant and Poisson's ratio for $Si_{1-x}Ge_x$ is calculated by linear interpolation.

In Equations 3-508 through 3-509, A.DEFPOT, B.DEFPOT, and C.DEFPOT are user-definable valence band deformation potential constants.

The user-definable parameters are shown in Table 3-106.

| Table 3-106. User Definable Parameters for Strained Silicon Band Gap | | | |
|--|-----------|---------|-------|
| Statement | Parameter | Default | Units |
| MATERIAL | A.DEFPOT | 2.1 | eV |
| MATERIAL | B.DEFPOT | -2.33 | eV |
| MATERIAL | C.DEFPOT | -4.75 | eV |
| MATERIAL | D.DEFPOT | 1.1 | eV |
| MATERIAL | U.DEFPOT | 10.5 | eV |
| MATERIAL | EPS11 | * | |
| MATERIAL | EPS22 | * | |
| MATERIAL | EPS33 | * | |
| MATERIAL | EPS12 | * | |
| MATERIAL | EPS13 | * | |
| MATERIAL | EPS23 | * | |

Note: * If unspecified, Equations 3-511, 3-512, and 3-513 calculate these parameters.

The net changes in the band edges, under Boltzman's statistics, are given by Equations 3-524 and 3-525.

$$\Delta E_c = kT \ln \left[\sum_{i=1}^3 \frac{\exp\left(-\frac{\Delta E_c^{(i)}}{kT}\right)}{3} \right] \quad 3-524$$

$$\Delta E_v = kT \ln \left[\frac{r}{1+r} \exp\left(-\frac{\Delta E_v^{(1)}}{kT}\right) + \frac{1}{1+r} \exp\left(-\frac{\Delta E_v^{(h)}}{kT}\right) \right] \quad 3-525$$

Here, the parameter r is given by Equation 3-526.

$$r = (m_l/m_h)^{3/2} \quad 3-526$$

In Equation 3-526, m_l and m_h are the effective masses of light and heavy holes as described in other places in this manual.

To enable the model for stress dependent band gap in silicon, specify the `STRESS` parameter of the `MODELS` statement.

3.6.13: Low-Field Mobility in Strained Silicon

For Boltzman's statistics, the following expressions can be used for strain dependent electron and hole low-field mobilities in silicon [64]:

$$\mu_n = \mu_{n0} \left\{ 1 + \frac{1 - ML/MT1}{1 + 2(ML/MT1)} \left[\exp \left(\frac{\Delta E_c - \Delta E_c^{(i)}}{kT} \right) - 1 \right] \right\} \quad 3-527$$

$$\mu_p = \mu_{p0} \left\{ 1 + (\text{EGLEY.R} - 1) \frac{(MLH/MHH)^{1.5}}{1 + (MLH/MHH)^{1.5}} \left[\exp \left(\frac{\Delta E_v^l - \Delta E_v^h}{kT} \right) - 1 \right] \right\} \quad 3-528$$

where μ_{n0} and μ_{p0} are the concentration dependent low field mobilities for electrons and holes, and $\Delta E_c^{(i)}$, ΔE_c , $\Delta E_v^{(l)}$, and $\Delta E_v^{(h)}$ are given by Equations 3-508, 3-524, and 3-509 respectively. Table 3-107 shows user-definable parameters for this model.

| Table 3-107. User Definable Parameters for the Strained Silicon Low-Field Mobility Model | | | |
|--|-----------|---------|-------|
| Statement | Parameter | Default | Units |
| MATERIAL | ML | 0.916 | |
| MATERIAL | MT1 | 0.191 | |
| MATERIAL | MLH | 0.16 | |
| MATERIAL | MHH | 0.49 | |
| MOBILITY | EGLEY.R | 2.79 | |

To enable the strained silicon low-field mobility model, specify EGLEY.N for electrons and EGLEY.P for holes on the MOBILITY statement.

3.6.14: Light Absorption in Strained Silicon

The effects of strain on the optical absorption in silicon can be modeled by modifications [174] made to a model suggested by Rajkanan [188]. The Rajkanan model can be described by:

$$\alpha(T) = \sum_{\substack{i=1,2 \\ j=1,2}} C_i A_j \left[\frac{\{\hbar\omega - E_{gj}(T) + E_{pi}\}^2}{\{\exp(E_{pi}/kT) - 1\}} - \frac{\{\hbar\omega - E_{gj}(T) + E_{pi}\}^2}{\{1 - \exp(E_{pi}/kT)\}} \right] + A_d [\hbar\omega - E_{gd}(T)]^{1/2} \quad 3-529$$

where:

- $\alpha(T)$ is the temperature dependent absorption coefficient.
- ω is the optical frequency.
- $E_{gi}(T)$ are the indirect energy band gaps given by Equations 3-530 and 3-531.
- $E_{gd}(T)$ is the direct energy band gap given by Equation 3-532.
- T is the temperature in Kelvin.
- A_d, A_j, C_i , and E_{pi} are empirical constants given in Table 3-108.

The temperature dependent E_g in Equation 3-529 are given by Equations 3-530 through 3-532.

$$E_{g1}(T) = EG1.RAJ - (BETA.RAJ \cdot T^2 / [T + GAMMA.RAJ]) \quad 3-530$$

$$E_{g2}(T) = EG2.RAJ - (BETA.RAJ \cdot T^2 / [T + GAMMA.RAJ]) \quad 3-531$$

$$E_{gD}(T) = EGD.RAJ - (BETA.RAJ \cdot T^2 / [T + GAMMA.RAJ]) \quad 3-532$$

To enable the model given in Equation 3-529, enable the RAJKANAN parameter of the MODELS statement.

Table 3-108. User Modifiable Parameters of Equation 3-529.

| Symbol | Parameter | Statement | Default | Units |
|----------|-----------|-----------|------------------------|-------|
| E_{p1} | EP1.RAJ | MATERIAL | 1.827×10^{-2} | |
| E_{p2} | EP2.RAJ | MATERIAL | 5.773×10^{-2} | |
| C_1 | C1.RAJ | MATERIAL | 5.5 | |
| C_2 | C2.RAJ | MATERIAL | 4.0 | |
| A_1 | A1.RAJ | MATERIAL | 3.231×10^2 | |
| A_2 | A2.RAJ | MATERIAL | 7.237×10^3 | |
| A_d | AD.RAJ | MATERIAL | 1.052×10^6 | |
| | BETA.RAJ | MATERIAL | 7.021×10^{-4} | eV/K |
| | GAMMA.RAJ | MATERIAL | 1108.0 | K |

Table 3-108. User Modifiable Parameters of Equation 3-529.

| Symbol | Parameter | Statement | Default | Units |
|--------|-----------|-----------|---------|-------|
| | EG1 .RAJ | MATERIAL | 1 .1557 | eV |
| | EG2 .RAJ | MATERIAL | 2 .5 | eV |
| | EGD .RAJ | MATERIAL | 3 .2 | eV |

To account for strain effects, the expressions in Equations 3-530 through 3-532 are modified by the changes in band edges induced by strain as given in Equations 3-508 and 3-509. To enable these modifications, set the `PATRIN` parameter of the `MODELS` statement.

3.7: Quasistatic Capacitance - Voltage Profiles

Quasistatic Capacitance is calculated by specifying the `QSCV` parameter in the `SOLVE` statement. The quasistatic capacitance is obtained for the electrode (whose bias is being ramped) by subtracting the electrode charge on the electrode at one bias from that at the adjacent bias and dividing by the Voltage increment. The charge density is calculated by applying Gauss' Flux Theorem to the electrode. This gives the capacitance at the midpoint between the two bias points. ATLAS does not correct the output for this because the voltage increment should be sufficient fine. Therefore, this small shift is negligible. A fine voltage increment will also give a good approximation to the continuous derivative.

`QSCV` will work with `CARRIERS=0, 1 or 2` specified in the `METHOD` statement. If you link electrodes using the `COMMON` parameter of the `CONTACT` statement, then the capacitance for each one and the sum of capacitances will be calculated. If you specify `MULT` and `FACTOR` for a linked electrode, then the capacitance will be calculated for the appropriate bias points, but will be stored as a function of the bias applied to the `COMMON` electrode. In this case, scaling or shifting of the C-V curve may be necessary.

3.8: Conductive Materials

In certain cases, it may be advantageous to simulate metal conductivity directly rather than handling electrodes as boundaries. You can define metal regions as “conductive” by specifying the `CONDUCTOR` parameter of the `REGION` statement. This might be useful, for example in simulating self-heating in metal regions.

When the metal is treated as a conductor, the conduction equation for all points in the region are solved as follows:

$$J = E / \text{RESISTIVITY} \quad 3-533$$

where J is the current density, E is the electric field, and `RESISTIVITY` is the metal resistivity in metal resistivity in $\mu\Omega\cdot\text{cm}$. To specify the metal resistivity, use the `RESISTIVITY` parameter from the `MATERIAL` statement. To specify the thermal coefficient of resistivity, use the `DRHODT` parameter from the `MATERIAL` statement.

3.8.1: Conductors with Interface Resistance

You can add interface contact resistance at interfaces between conductor and semiconductor regions. To do this, assign a positive value to the `INT.RESIST` parameter of the `INTERFACE` statement. This value corresponds to the interface resistivity in units of Ωcm^2 . To achieve the desired effect, also specify `S.C` on the `INTERFACE` statement. The interface resistance is completely analogous to using contact resistance (the `CON.RESIST` parameter of the `CONTACT` statement) only for conductor-semiconductor interfaces.

3.8.2: Importing Conductors from ATHENA

By default, all imported metals are treated as electrodes. To override this functionality, specify the `CONDUCTOR` parameter on the `MESH` statement. Also, for regions that you would like to simulate at PCM materials, you should make them into conductors by specifying `CONDUCTOR` and `MODIFY` on the `REGION` statement.

3.9: Optoelectronic Models

This section discusses various physical models used to simulate optoelectronic devices. These models predict fundamental optoelectronic processes, such as absorption and gain and radiative recombination rates versus material composition, temperature and optical wavelength.

These models are based on various band theories and account for the following:

- the existence of multiple valence bands supporting multiple optical transitions,
- asymmetry in conduction band effective masses,
- the effects of strain on the band parameters,
- the effects of quantum confinement on allowable transitions.

In the following paragraphs, we will discuss four-band structure dependent optoelectronic models.

The first two gain and spontaneous recombination models are for one- and two-band unstrained zincblende materials and are discussed in Section 3.9.7: “Unstrained Zincblende Models for Gain and Radiative Recombination”. The second band structure dependent gain and spontaneous recombination model includes the effects of strain in zincblende is discussed in [section 3.9.8](#). Finally, Section 3.9.9: “Strained Wurtzite Three-Band Model for Gain and Radiative Recombination” describes a strained dependent three band gain and recombination model for wurtzite.

In addition to the band structure based models, there are certain, more general but less physical models that are also mentioned. All of these models are used in the following applications:

- General drift-diffusion to account for radiative recombination for any semiconductor device,
- Laser and VCSEL simulation in both stimulated emission gain and spontaneous emission (see Chapters 8: “Laser: Edge Emitting Simulator” and 9: “VCSEL Simulator”),
- LED light emission (see Chapter 11: “LED: Light Emitting Diode Simulator”).

3.9.1: The General Radiative Recombination Model

At the most fundamental level the radiative recombination model described in Equation 3-534 describes all the most salient features of radiative recombination except spectral content. You can, however, use this model in all three applications mentioned above. It has the advantages of being fast, simple and easily calibrated.

To enable the general model, specify `OPTR` in the `MODEL` statement. This will enable radiative recombination using the general model in the drift diffusion part of the simulation. To enable this model in `LASER` or `VCSEL`, disable the default model for `LASER` and `VCSEL` by specifying `^SPONTANEOUS` in the `LASER` statement. To use the general model for `LED`, make sure no other competing mechanisms are enabled. The disadvantage of using this model for any light emission application is that it lacks spectral information.

When used in `LASER` and `VCSEL` the spontaneous recombination rate is given by:

$$r(r, z) = \frac{\text{EMISSION_FACTOR} \cdot \text{COPT} \cdot (n \cdot p - n_i^2)}{N_l} \quad 3-534$$

where n and p are the electron and hole concentrations, n_i is the intrinsic concentration, N_l is the number of longitudinal modes, `EMISSION_FACTOR` and `COPT` are user-defined parameters on the `MATERIAL` statement. `COPT` accounts for the radiative rate in all directions and energies. `EMISSION_FACTOR` represents the fraction of energy coupled into the direction of interest and in the energy range of interest. Note that Equation 3-534 contains no spectral information.

3.9.2: The Default Radiative Recombination Model

The default spontaneous radiative recombination model is given by

$$r_{sp_m}(x, y) = \text{ESEP} \cdot \text{EMISSION_FACTOR} \frac{c}{\text{NEFF}} \cdot D(E) \cdot \text{GAIN0} \cdot \sqrt{\frac{\hbar\omega - E_g}{kT}} \cdot f\left(\frac{E_c - E_{fn} + \text{GAMMA}(\hbar\omega - E_g)}{kT}\right) \cdot \left[1 - f\left(\frac{E_v - E_{fp} - (1 - \text{GAMMA})(\hbar\omega - E_g)}{kT}\right)\right] \quad 3-535$$

where:

- c is the speed of light,
- \hbar Planck's constant,
- k Boltzman's constant,
- E_g is the energy bandgap,
- E_c and E_v are the conduction and valence band edge energies,
- T is the lattice temperature,
- E_{fn} and E_{fp} are the electron and hole quasi-Fermi energies,
- ω is the emission frequency that corresponds to the transition energy E ,
- $D(E)$ is the optical mode density,
- `EMISSION.FACTOR`, `GAIN0` and `GAMMA` are user defined parameters from the `MATERIAL` statement,
- `ESEP` and `NEFF` are user-defined parameters specified from the `LASER` statement.

The optical mode density $D(E)$ is given by

$$D(E) = \frac{n^3 E^2}{\pi^2 \hbar^3 c^3} \quad 3-536$$

where n is the index of refraction.

The function $f(x)$ is given by

$$f(x) = \frac{1}{1 + \exp(x)}. \quad 3-537$$

3.9.3: The Standard Gain Model

The standard gain model [165] is enabled by specifying `G.STANDARD` in the `MODELS` statement. The standard gain model is given by

$$g(x, y) = \text{GAIN0} \sqrt{\frac{\hbar\omega - E_g}{kT}} \left[f\left(\frac{E_c - E_{fn} + \text{GAMMA}(\hbar\omega - E_g)}{kT}\right) - f\left(\frac{E_v - E_{fp} - (1 - \text{GAMMA})(\hbar\omega - E_g)}{kT}\right) \right] \quad 3-538$$

where:

- \hbar is Planck's constant,
- E_g is the energy bandgap,
- k is Boltzman's constant,
- T is the lattice temperature,
- E_{fn} and E_{fp} are the electron and hole quasi-Fermi energies,

- ω is the emission frequency,
- E_v and E_c are the valence and conduction band edge energies,
- the function f is defined in Equation 3-537,
- GAMMA and GAIN0 user-definable parameters specified on the MATERIAL statement.

Table 3-109 describes the user defined parameters of Equation 3-538.

| Table 3-109. User-Specifiable Parameters for Equation 3-538 | | | |
|---|-----------|---------|------------------|
| Statement | Parameter | Default | Units |
| MATERIAL | GAIN0 | 2000.0 | cm^{-1} |
| MATERIAL | GAMMA | | |

If GAMMA in Equation 3-538 is not specified, it is automatically calculated from the following expression:

$$\text{GAMMA} = \frac{1}{\frac{2}{3} \left(\frac{N_c}{N_v} \right) + 1} \quad 3-539$$

where N_c and N_v are the conduction and valence band densities of states.

3.9.4: The Empirical Gain Model

The empirical gain model is enabled by specifying G.EMPIRICAL in the MODELS statement. The model is described by the following expression [256]:

$$g(x, y) = \text{GAIN00} + \text{GAIN1N} \cdot n + \text{GAIN1P} \cdot p + \text{GAIN2NP} \cdot np + \text{GAIN1MIN} \cdot \min(n, p) \quad 3-540$$

where n and p are the electron and hole concentrations, and GAIN00, GAIN1N, GAIN1P, GAIN2NP and GAIN1MIN are user-specified parameters from the MATERIAL statement. Note that the empirical model contains no spectral dependency and should not be used for LASER or VCSEL simulations with multiple longitudinal modes. Table 3-110 shows the user-definable parameters for Equation 3-540.

| Table 3-110. User-Specifiable Parameters for Equation 3-540 | | | |
|---|-----------|-----------------------|------------------|
| Statement | Parameter | Default | Units |
| MATERIAL | GAIN00 | -200.0 | cm^{-1} |
| MATERIAL | GAIN1P | 0 | cm^2 |
| MATERIAL | GAIN1N | 0 | cm^2 |
| MATERIAL | GAIN2NP | 0 | cm^5 |
| MATERIAL | GAIN1MIN | 3.0×10^{-16} | cm^2 |

3.9.5: Takayama's Gain Model

Takayama's gain model [226] is enabled by specifying `TAYAMAYA` in the `MODELS` statement. Takayama's model is described by the following expression:

$$\begin{aligned} g(x, y) &= \text{GN1}(n(x, y) - \text{NTRANSPARENT}) & n > \text{NTRANSPARENT} \\ g(x, y) &= \text{GN2}(n(x, y) - \text{NTRANSPARENT}) & n \leq \text{NTRANSPARENT} \end{aligned} \quad 3-541$$

where n is the electron concentration and `GN1`, `GN2` and `NTRANSPARENT` are user-specified parameters from the `MATERIAL` statement. As in the empirical gain model, this model contains no spectral dependency and should not be used to simulate multiple longitudinal modes in `LASER` or `VCSEL`. Table 3-111 shows the user definable parameters for Equation 3-541.

| Table 3-111. User-specified values for Equation 3-541 | | | |
|---|---------------------------|-----------------------|------------------|
| Statement | Parameter | Default | Units |
| <code>MATERIAL</code> | <code>GN1</code> | 3.0×10^{-16} | cm^2 |
| <code>MATERIAL</code> | <code>GN2</code> | 4.0×10^{-15} | cm^2 |
| <code>MATERIAL</code> | <code>NTRANSPARENT</code> | 2.0×10^{18} | cm^{-3} |

3.9.6: Band Structure Dependent Optoelectronic Models

Although the simple models described in Sections 3.9.1: “The General Radiative Recombination Model” through 3.9.5: “Takayama's Gain Model” are useful for modeling the principal effects, they suffer from one or more of the following drawbacks:

- they lack spectral dependencies,
- they are not generally calibrated to all tools,
- they do not account for effects of strain,
- they do not account for the effects of quantum confinement,
- the lack physical basis.

The following sections will describe more physically based models. Figure 3-14 illustrates the simulation flow for these models.

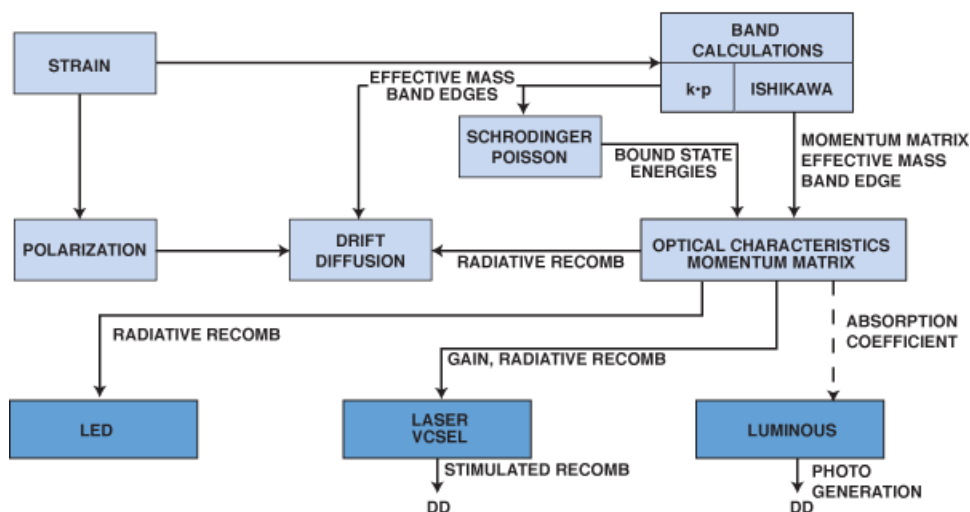


Figure 3-14: Simulation Flow For Physically Based Optoelectronic Models

First, strain is introduced either directly or calculated from lattice mismatch and used to calculate the strain effects on band calculations. The strain is also introduced to polarization calculations that enter directly into the drift diffusion calculations as polarization fields.

Next, the band parameters (band edges and effective masses) are used directly in the drift diffusion simulations as well as feeding into the solutions of Schrodinger's equations to calculate the bound state energies. The band parameters and bound state energies are then used to calculate gain, radiative recombination rate and optical absorption.

3.9.7: Unstrained Zincblende Models for Gain and Radiative Recombination

For zincblende materials, you can select one of two models for optical gain and spontaneous recombination. If the `LI` parameter is specified on the `MODELS` statement, the model by Li [140] will be used. If the `YAN` parameter is specified on the `MODELS` statement, the model by Yan [266] will be used. The difference between the models is that in the `YAN` model only one valence band is accounted for, whereas the `LI` model accounts for both light and heavy holes in the valence band.

If simulating quantum wells, the first step in calculating the gain and radiative recombination is to calculate the bound state energies and wavefunctions. The band edge energies and effective masses are used to calculate the quantum well bound state energies and wavefunctions through the Schrodinger's Equation (See Chapter 13: "Quantum: Quantum Effect Simulator", Equations 13-1 and 13-3). This calculation is performed in the same manner as the self-consistent coupled Schrodinger Poisson model. The calculation of the bound state energies is performed over a discrete domain that isn't the same as the device simulation mesh. The discrete domain is specified by the `WELL.NX` and `WELL.NY` parameters in the `REGION` statement.

The `WELL.NX` and `WELL.NY` parameters specify the number of uniform mesh locations in the bounding box where the solution of Schrodinger's Equation is performed to extract bound state energies. Typically, `WELL.NY` should be set to a large number so that there will be several samples per well. `WELL.NX` should be comparable to the number of grid lines in the device mesh over the same extent in the X direction.

Next, the bulk momentum matrix element is calculated as shown in Equation 3-542.

$$|M_{avg}|^2 = \text{MBULKSQ} = \frac{m_0}{6} \text{EP.MBULK} = \frac{m_0}{6} \left(\frac{m_0}{m^*} - 1 - 2\text{FB.MBULK} \right) \frac{E_g(E_g + \text{SO.DELTA})}{\left(E_g + \frac{2}{3}\text{SO.DELTA} \right)} \quad 3-542$$

In Equation 3-542, you can specify the bulk momentum matrix element directly using the `MBULKSQ` parameter of the `MATERIAL` statement. You can also calculate it using either the energy parameter `EP.MBULK` of the `MATERIAL` statement, or the band gap E_g , correction factor `FB.MBULK` and split-off energy, or `SO.DELTA` parameters of the `MATERIAL` statement. Table 3-112 shows the default values for the `EP.MBULK`, `FB.MBULK`, and `SO.DELTA` parameters for several materials.

| Table 3-112. Default Values for User Specifiable Parameters of Equation 3-542 [179] | | | |
|---|------------------------------|----------------------|------------------------------|
| Parameter Statement Units | EP.MBULK MATERIAL (eV) | FB.MBULK MATERIAL | SO.DELTA MATERIAL (eV) |
| AlAs | 21.1 | -0.48 | 0.28 |
| AlP | 17.7 | -0.65 | 0.07 |
| AlSb | 18.7 | -0.56 | 0.676 |
| GaAs | 28.8 | -1.94 | 0.341 |
| GaP | 31.4 | -2.04 | 0.08 |
| GaSb | 27.0 | -1.63 | 0.76 |
| InAs | 21.5 | -2.9 | 0.39 |
| InP | 20.7 | -1.31 | 0.108 |
| InSb | 23.3 | -0.23 | 0.81 |

In Equation 3-490, m_* is by default equal to the conduction band effective mass, m_c . You may, however, specify the value of m_* using the `MSTAR` parameter of the `MATERIAL` statement. Yan et. al. [266] recommend a value of 0.053 for GaAs.

For materials not listed in Table 3-112, `SO.DELTA` has a default value of 0.341 and `EP.MBULK` and `FB.MBULK` are 0.

For quantum wells, the matrix elements are asymmetric and for light and heavy holes are given by Equations 3-543 and 3-544.

$$M_{hh} = A_{hh} M_{avg} O_{hh} \quad 3-543$$

$$M_{lh} = A_{lh} M_{avg} O_{lh} \quad 3-544$$

where A_{hh} and A_{lh} are anisotropy factors for heavy and light holes. O_{hh} and O_{lh} are overlap integrals. You can specify the overlap using the `WELL.OVERLAP` parameter of the `MODELS` statement. If not specified, O_{hh} and O_{lh} are calculated from the wavefunctions.

The anisotropy factors depend upon whether TM or TE modes are the dominant modes [140]. The dominant mode is user-specifiable by using the `TE.MODES` parameter of the `MATERIAL` statement. When this parameter is `true` (default), the TE mode models are used and when `false` the TM mode model is used.

For TE modes, the values of the anisotropy factors are given by Equation 3-545.

$$\begin{aligned} A_{hh} &= \frac{3 + 3E_{ij}/E}{4}, & A_{lh} &= \frac{5 - 3E_{ij}/E}{4} & \text{for}(E > E_{ij}) \\ A_{hh} &= 3/2, & A_{lh} &= 1/2 & \text{for}(E \leq E_{ij}) \end{aligned} \quad 3-545$$

For TM modes, the values of the anisotropy factors are given by Equation 3-546.

$$\begin{aligned} A_{hh} &= \frac{3 - 3E_{ij}/E}{2} & A_{hh} &= \frac{1 + 3E_{ij}/E}{2} & \text{for}(E > E_{ij}) \\ A_{hh} &= 0 & A_{lh} &= 2 & \text{for}(E < E_{ij}) \end{aligned} \quad 3-546$$

Here, E is the transition energy and E_{ij} is the energy difference between the i th valence bound state and the j th conduction band state.

The bound state energies and effective masses are then used to calculate the Fermi functions given in Equation 3-547.

$$\begin{aligned} f_i^v &= \left\{ 1 + \exp \left[\left(E_i - \frac{m_{ij}}{m_i} (E - E_{ij}) - E_{fp} \right) / kT \right] \right\}^{-1} \\ f_j^c &= \left\{ 1 + \exp \left[\left(E_j - \frac{m_{ij}}{m_j} (E - E_{ij}) - E_{fn} \right) / kT \right] \right\}^{-1} \end{aligned} \quad 3-547$$

Here, E_{fp} is the hole Fermi level, E_{fn} is the electron Fermi level, E_i is the valence band energy, E_j is the conduction band energy, m_i is the valence band effective mass, m_j is the conduction band effective mass, and m_{ij} is the reduced mass given in by Equation 3-548.

$$m_{ij} = \left(\frac{1}{m_i} + \frac{1}{m_j} \right)^{-1} \quad 3-548$$

Next, use the effective masses to calculate the density of states. In bulk semiconductors, the density of states is given by Equation 3-549.

$$\rho = \frac{1}{2\pi} \left(\frac{2m_{ij}}{\hbar} \right)^{3/2} \sqrt{E - E_g} \quad 3-549$$

E is the energy and E_g is the band gap.

For quantum wells, we calculate the 2D density of states as given in Equation 3-550.

$$\rho = \frac{m_{ij}}{\pi \hbar^2 t} \quad 3-550$$

t is the quantum well thickness.

Next, the optical mode density is calculated as given by Equation 3-551.

$$D(E) = \frac{n^3 E^2}{\pi^2 \hbar^3 c^3} \quad 3-551$$

Optical Gain Models

For the LI and YAN Models, the optical gain is given by Equation 3-552.

$$g(E) = \left(\frac{\pi q^2 \hbar}{\epsilon_0 n c m_0^2 E} \right) |M(E)|^2 \rho(E) \cdot D(E) (f_j' - f_i') \quad 3-552$$

Spontaneous Recombination Models

For the LI and YAN Models, the spontaneous recombination is given by Equation 3-553.

$$r_{sp}(E) = \left(\frac{q}{m_0} \right)^2 \frac{\pi \hbar}{\epsilon E} |M(E)|^2 \rho \cdot D(E) \cdot f_j' (1 - f_i') \quad 3-553$$

3.9.8: Strained Zincblende Gain and Radiative Recombination Models

The zincblende two band model is a k·p model assuming parabolic bands accounting for light and heavy holes and the effects of strain. This model is enabled by specifying ZB.KP on the MODELS statement.

In the zincblende two band model we first calculate P_ε and Q_ε as given by Equations 3-554 and 3-555.

$$P_\varepsilon = -a_v(\varepsilon_{xx} + \varepsilon_{yy} + \varepsilon_{zz}) \quad 3-554$$

$$Q_\varepsilon = -\frac{b}{2}(\varepsilon_{xx} + \varepsilon_{yy} + \varepsilon_{zz}) \quad 3-555$$

Here, a_v and b are the valence band hydrostatic deformation potentials and ε_{xx} , ε_{yy} , and ε_{zz} are the strain tensor as calculated in Section 3.6.9: “Epitaxial Strain Tensor Calculations in Zincblende”. The default values of a_v and b for various binary materials are given in Table B-28. Values for ternary and quaternary materials are linearly interpolated from the binary values.

Next, we can calculate the conduction, heavy hole and light hole band edge energies from Equations 3-556, 3-557, and 3-558.

$$E_c = E_v + E_g + a_c(\varepsilon_{xx} + \varepsilon_{yy} + \varepsilon_{zz}) \quad 3-556$$

$$E_{hh} = E_v - P_\varepsilon - \text{sgn}(Q_\varepsilon)\sqrt{Q_\varepsilon^2} \quad 3-557$$

$$E_{lh} = E_v - P_\varepsilon + \text{sgn}(Q_\varepsilon)\sqrt{Q_\varepsilon^2} \quad 3-558$$

Here, a_c is the conduction band hydrostatic deformation potential, E_c , E_v , and E_g are the unstrained conduction band edge energy, valence band edge energy, and band gap. These are calculated from the material specific affinity and bandgap.

The default values of a_c for various binary materials are given in Table B-28. Values for ternary and quaternary materials are linearly interpolated from the binary values.

The function $\text{sgn}()$ is the “sign” function (i.e., +1 for positive arguments and -1 for negative arguments).

Next, we calculate the effective masses for the various bands using Equations 3-559 through 3-562.

$$m_{hh}^z = m_0/(\gamma_1 - 2\gamma_2) \quad 3-559$$

$$m_{lh}^z = m_0/(\gamma_1 + 2\gamma_2) \quad 3-560$$

$$m_{hh}^t = m_0/(\gamma_1 + \gamma_2) \quad 3-561$$

$$m_{lh}^t = m_0/(\gamma_1 - \gamma_2) \quad 3-562$$

Here, m_0 is the rest mass of an electron, and γ_1 and γ_2 are the Luttinger parameters. The default values of the luttinger parameters for various binary materials are given in Table B-29. Values for ternary and quaternary materials are linearly interpolated from the binary values.

Finally, the band edges and effective masses are placed into the gain and spontaneous recombination models described in Section 3.9.7: “Unstrained Zincblende Models for Gain and Radiative Recombination”.

3.9.9: Strained Wurtzite Three-Band Model for Gain and Radiative Recombination

The strained wurtzite three-band model [41, 42, 127] is derived from the k·p method for three valence bands in wurtzite crystalline structure. Given the assumptions of parabolic bands, no valence band mixing and momentum approaching zero, the following approach can be used. First, we calculate the parameters from Equations 3-563 and 3-564.

$$\theta_{\varepsilon} = D_3 \varepsilon_{zz} + D_4 (\varepsilon_{xx} + \varepsilon_{yy}) \quad 3-563$$

$$\lambda_{\varepsilon} = D_1 \varepsilon_{zz} + D_2 (\varepsilon_{xx} + \varepsilon_{yy}) \quad 3-564$$

Here, D_1 , D_2 , D_3 , and D_4 are shear deformation potentials and ε_{xx} , ε_{yy} , and ε_{zz} are taken from the strain tensor calculations described in Section 3.6.10: “Epitaxial Strain Tensor Calculation in Wurtzite”. Next, we can calculate the valence band energies from Equations 3-565 through 3-567.

$$E_{hh}^0 = E_v^0 + \Delta_1 + \Delta_2 + \theta_{\varepsilon} + \lambda_{\varepsilon} \quad 3-565$$

$$E_{lh}^0 = E_v^0 + \frac{\Delta_1 - \Delta_2 + \theta_{\varepsilon}}{2} + \lambda_{\varepsilon} + \sqrt{\left(\frac{\Delta_1 - \Delta_2 + \theta_{\varepsilon}}{2}\right)^2 + 2\Delta_3^2} \quad 3-566$$

$$E_{ch}^0 = E_v^0 + \frac{\Delta_1 - \Delta_2 + \theta_{\varepsilon}}{2} + \lambda_{\varepsilon} - \sqrt{\left(\frac{\Delta_1 - \Delta_2 + \theta_{\varepsilon}}{2}\right)^2 + 2\Delta_3^2} \quad 3-567$$

Here, Δ_1 , Δ_2 and Δ_3 are split energies and E_v is the valence band reference level. Next, we can calculate the hydrostatic energy shift from Equation 3-568.

$$P_{c\varepsilon} = a_{cz} \varepsilon_{zz} + a_{ct} (\varepsilon_{xx} + \varepsilon_{yy}) \quad 3-568$$

Here, a_{cz} and a_{ct} are hydrostatic deformation potentials. From which we can calculate the conduction band energy as given in Equation 3-569.

$$E_c^0 = E_v^0 + \Delta_1 + \Delta_2 + E_g + P_{c\varepsilon} \quad 3-569$$

Here, E_g is the energy bandgap.

Next, we can calculate the effective masses in the various bands using the expressions in Equations 3-570 through 3-575.

$$m_{hh}^z = -m_0 (A_1 + A_3)^{-1} \quad 3-570$$

$$m_{hh}^t = -m_0 (A_2 + A_4)^{-1} \quad 3-571$$

$$m_{lh}^z = -m_0 \left[A_1 + \left(\frac{E_{lh}^0 - \lambda_\varepsilon}{E_{lh}^0 - E_{ch}^0} \right) A_3 \right]^{-1} \quad 3-572$$

$$m_{lh}^t = -m_0 \left[A_2 + \left(\frac{E_{lh}^0 - \lambda_\varepsilon}{E_{lh}^0 - E_{ch}^0} \right) A_4 \right]^{-1} \quad 3-573$$

$$m_{ch}^z = -m_0 \left[A_1 + \left(\frac{E_{ch}^0 - \lambda_\varepsilon}{E_{ch}^0 - E_{lh}^0} \right) A_3 \right]^{-1} \quad 3-574$$

$$m_{ch}^t = -m_0 \left[A_2 + \left(\frac{E_{ch}^0 - \lambda_\varepsilon}{E_{ch}^0 - E_{lh}^0} \right) A_4 \right]^{-1} \quad 3-575$$

Here, m_ϕ is the free space mass of an electron, m_{hh}^z , m_{hh}^t , m_{lh}^z , m_{lh}^t , m_{ch}^z and m_{ch}^t are the effective masses for heavy holes, light holes and crystal split off holes in the axial and transverse directions and A_1, A_2, A_3 and A_4 are hole effective mass parameters.

The momentum matrix elements for the various transitions can be calculated by Equations 3-576 through 3-581.

$$M_{hh}^{11} = 0 \quad 3-576$$

$$M_{hh}^{11} = b^2 \left(\frac{m_0}{2} E_{pz} \right) \quad 3-577$$

$$M_{ch}^{11} = a^2 \left(\frac{m_0}{2} E_{pz} \right) \quad 3-578$$

$$M_{hh}^\perp = \frac{m_0}{4} E_{px} \quad 3-579$$

$$M_{lh}^\perp = a^2 \left(\frac{m_0}{4} \right) E_{px} \quad 3-580$$

$$M_{ch}^\perp = b^2 \left(\frac{m_0}{4} \right) E_{px} \quad 3-581$$

Here, E_{px} and E_{pz} are given by Equations 3-582 and 3-583, a^2 and b^2 are given by Equations 3-586 and 3-587. The values of P_1^2 and P_2^2 are given by Equations 3-584 and 3-585.

$$E_{px} = \left(2m_0/\hbar^2 \right) P_2^2 \quad 3-582$$

$$E_{pz} = \left(2m_0/\hbar^2 \right) P_1^2 \quad 3-583$$

$$P_1^2 = \frac{\hbar^2}{2m_0} \left(\frac{m_0}{m_e^z} - 1 \right) \frac{(E_g + \Delta_2 + \Delta_2)(E_g + 2\Delta_2) - 2\Delta_3^2}{(E_g + 2\Delta_2)} \quad 3-584$$

$$P_2^2 = \frac{\hbar^2}{2m_0} \left(\frac{m_0}{m_e^t} - 1 \right) \frac{E_g [(E_g + \Delta_1 + \Delta_2)(E_g + 2\Delta_2) - 2\Delta_3^2]}{(E_g + \Delta_1 + \Delta_2)(E_g + \Delta_2) - \Delta_3^2} \quad 3-585$$

$$a^2 = \left(\frac{E_{lh}^0 - \lambda_\varepsilon}{E_{lh}^0 - E_{ch}^0} \right) \quad 3-586$$

$$b^2 = \left(\frac{E_{ch}^0 - \lambda_\varepsilon}{E_{ch}^0 - E_{lh}^0} \right) \quad 3-587$$

In Equations 3-582 through 3-587, m_e^t and m_e^z are the transverse and axial conduction band effective masses.

The default values for the parameters of Equations 3-563 through 3-587 are shown in Appendix B: “Material Systems”, Section B.8: “Material Defaults for GaN/InN/AlN System”.

3.9.10: Lorentzian Gain Broadening

Gain broadening due to intra-band scattering can be introduced by specifying `LORENTZ` in the `MODEL` statement. The following equation describes gain broadening when it's applied.

$$g(E) = \int_{E_{ij}}^{\infty} g(E') L(E' - E) dE' \quad 3-588$$

The Lorentzian shape function is given by Equation 3-589.

$$L(E' - E) = \frac{1}{\pi} \cdot \frac{\text{WELL.GAMMA0}}{(E' - E)^2 + \text{WELL.GAMMA0}^2} \quad 3-589$$

where `WELL.GAMMA0` is user-specifiable in the `MATERIAL` statement.

3.9.11: Ishikawa's Strain Effects Model

The strained layer InGaAsP and InGaAlAs quantum well material models from [104] are implemented in the ATLAS simulator. To enable these models, specify the `ISHIKAWA` parameter in the `MODELS` statement. Strain percentages are specified by the `STRAIN` parameter in the `MQW` statement. `STRAIN` between a substrate material with lattice constant, d_s , and an epitaxial material without `STRAIN`, with lattice constant, d_e , is $(d_e - d_s) / d_s$.

When you enable this model, the band edge parameters for materials in the InGaAsP and InGaAlAs systems are calculated using Equations 3-590, 3-591, and 3-592.

InGaAs

$$\begin{aligned}
 E_c &= 1.040 - 0.0474 \text{STRAIN} + 0.003303 \text{STRAIN}^2 \\
 E_{v, hh} &= 0.3331 + 0.05503 \text{STRAIN} - 0.002212 \text{STRAIN}^2 \\
 E_{v, lh} &= 0.331 - 0.01503 \varepsilon - 0.003695 \text{STRAIN}^2
 \end{aligned}
 \tag{3-590}$$

InGaAsP

$$\begin{aligned}
 &a) \text{STRAIN} < 0 \\
 E_c &= (0.6958 + 0.4836 E_g) - 0.03031 \text{STRAIN} \\
 E_{v, lh} &= (0.5766 - 0.3439 E_g) - 0.3031 \text{STRAIN} \\
 &b) \text{STRAIN} > 0 \\
 E_c &= (0.6958 + 0.4836 E_g) + 0.003382 \text{STRAIN} \\
 E_{v, hh} &= (0.6958 - 0.5164 E_g) + 0.003382 \text{STRAIN}
 \end{aligned}
 \tag{3-591}$$

InGaAlAs

$$\begin{aligned}
 &a) \text{STRAIN} < 0 \\
 E_c &= (0.5766 + 0.6561 E_g) - 0.02307 \text{STRAIN} \\
 E_{v, lh} &= (0.5766 - 0.3439 E_g) - 0.2307 \text{STRAIN} \\
 &b) \text{STRAIN} > 0 \\
 E_c &= (0.5766 + 0.6561 E_g) + 0.01888 \text{STRAIN} \\
 E_{v, hh} &= (0.5766 - 0.3439 E_g) + 0.01888 \text{STRAIN}
 \end{aligned}
 \tag{3-592}$$

A `STRAIN` parameter has also been added to the `REGION` statement to account for strain in the bulk materials. Note that for the InGaAs material system, the equations ignore composition fraction and variation in the parameters is accounted strictly through strain (see Equation 3-590).

These band edge parameters are used through all subsequent calculations. Most importantly, the band edges are used in solving the Schrodinger's Equation (See Chapter 13: "Quantum: Quantum Effect Simulator", Equations 13-1 and 13-3) to obtain the bound state energies in multiple quantum wells.

If you enable the Ishikawa Model, this would include the effects of strain in the valence and conduction band effective masses as described in [104]. The effects of strain are introduced in Equation 3-593.

$$\frac{1}{m_{lh}} = \text{ASTR} + \text{BSTRSTRAIN} + \text{CSTRSTRAIN}^2$$

$$\frac{1}{m_{hh}} = \text{DSTR} + \text{ESTRSTRAIN} + \text{FSTRSTRAIN}^2$$

3-593

The ASTR, BSTR, CSTR, DSTR, ESTR, and FSTR parameters are user-definable in the MATERIAL statement. You can also choose the appropriate values for these parameters from Tables 3-113 or 3-114.

Table 3-113. In-Plane Effective Mass of InGaAsP Barrier (1.2μm)/InGaAs(P) Well and InGaAlAs Barrier (1.2μm)/InGa(Al)As Well System for 1.55μm Operation [104]

| −2.0<Strain($\%$$-0.5$ | | | | 0<Strain($\%$$2.0$ | | |
|---|--------|---------|--------|--|-------|--------|
| | ASTR | BSTR | CSTR | DSTR | ESTR | FSTR |
| Lattice-matched InGaAsP barrier/InGaAs well | −4.238 | −6.913 | −1.687 | 4.260 | 2.253 | −0.584 |
| InGaAsP (1.6-μm) well | −0.936 | −4.825 | −1.754 | 2.986 | 5.505 | −1.736 |
| Strain-compensated InGaAsP barrier/InGaAs well | −7.761 | −13.601 | −5.100 | 4.166 | 1.933 | −0.558 |
| Lattice-matched InGaAlAs barrier/InGaAs well | −3.469 | −6.133 | −1.481 | 3.9134 | 2.336 | −0.633 |
| InGaAlAs(1.6-μm) well | −1.297 | −5.598 | −2.104 | 2.725 | 6.317 | −1.766 |
| Strain-compensated InGaAlAs barrier/InGaAs well | −5.889 | −9.467 | −2.730 | 4.193 | 1.075 | −0.155 |

Table 3-114. In-Plane Effective Mass of InGaAsP Barrier (1.1μm)/InGaAs(P) Well and InGaAlAs Barrier (1.1μm)/InGa(Al)As Well System for 1.30μm Operation [104]

| −2.0<Strain($\%$$-0.5$ | | | | −0.5<Strain($\%$$2.0$ | | |
|---|--------|--------|--------|---|-------|---------|
| | ASTR | BSTR | CSTR | DSTR | ESTR | FSTR |
| Lattice-matched InGaAsP barrier/InGaAs well | −9.558 | −8.634 | −1.847 | 4.631 | 1.249 | −0.313 |
| InGaAsP (1.4-μm) well | −2.453 | −4.432 | −1.222 | 3.327 | 3.425 | −1.542 |
| Strain-compensated InGaAsP barrier/InGaAs well | | | | 4.720 | 0.421 | −0.014 |
| Lattice-matched InGaAlAs barrier/InGaAs well | −8.332 | −8.582 | −2.031 | 3.931 | 1.760 | −0.543 |
| InGaAlAs(1.4-μm) well | −3.269 | −5.559 | −1.594 | 3.164 | 4.065 | −1.321 |
| Strain-compensated InGaAlAs barrier/InGaAs well | | | | 4.078 | 0.516 | −0.0621 |

To choose these values, use the `STABLE` parameter in the `MATERIAL` statement. You can set this parameter to the row number in the tables. The rows are numbered sequentially. For example, the first row in Table 3-113 is selected by specifying `STABLE=1`. The first row of Table 3-114 is selected by specifying `STABLE=7`.

You can also choose to specify the effective masses directly. The conduction band effective mass is specified by the `MC` parameter in the `MATERIAL` statement. There are two ways to specify the valence band. One way, is to use the `MV` parameter to specify a net effective mass. The other way, is to use the `MLH` and `MHH` parameters to specify the light and heavy hole effective masses individually.

If you don't specify the effective masses by using one of these methods, then the masses will be calculated from the default density of states for the given material as described in Section 3.4.2: "Density of States".

The effective masses described are also used to solve the Schrodinger Equation (see Chapter 13: "Quantum: Quantum Effect Simulator", Equations and 13-3).

3.10: Optical Index Models

The index of refraction of materials are used in several places in the ATLAS simulation environment. For LUMINOUS and LUMINOUS3D, the index is used to calculate reflections during raytrace. For LASER and VCSEL, the index is key to determining optical confinement. For LED, the index is used to calculate reflections for reverse raytrace.

In the ATLAS environment there are a variety of ways the optical index of refraction can be introduced as well as reasonable energy dependent defaults for many material systems. For some these defaults are tabular (see Table B-36). For others there exist analytic functions. Here we describe some of those analytic models.

3.10.1: The Sellmeier Dispersion Model

To enable the Sellmeier dispersion model, specify `NDX.SELLMIEIER` on the `MATERIAL` statement. The Sellmeier dispersion model is given in Equation 3-594.

$$n_r(\lambda) = \sqrt{S0SELL + \frac{S1SELL\lambda^2}{\lambda^2 - L1SELL^2} + \frac{S2SELL\lambda^2}{\lambda^2 - L2SELL^2}} \quad 3-594$$

In this equation, λ is the wavelength in microns, and `S0SELL`, `S1SELL`, `S2SELL`, `L1SELL` and `L2SELL` are all user-definable parameters on the `MATERIAL` statement. Default values for these parameters of various materials are given in Table B-37.

3.10.2: Adachi's Dispersion Model

To enable a model by Adachi [1], specify `NDX.ADACHI` on the `MATERIAL` statement. This model is given by Equations 3-350, 3-351, and 3-352.

$$n_r(w)^2 = AADACHI \left[f(x_1) + 0.5 \left(\frac{E_g}{E_g + DADACHI} \right)^{1.5} f(x_2) \right] + BADACHI \quad 3-595$$

$$f(x_1) = \frac{1}{x_1} (2 - \sqrt{1+x_1} - \sqrt{1-x_1}) \quad , x_1 = \frac{\hbar\omega}{E_g} \quad 3-596$$

$$f(x_2) = \frac{1}{x_2} (2 - \sqrt{1+x_2} - \sqrt{1-x_2}) \quad , x_2 = \frac{\hbar\omega}{E_g + DADACHI} \quad 3-597$$

In these equations, E_g is the band gap, \hbar is plank's constant, ω is the optical frequency, and `AADACHI`, `BADACHI` and `DADACHI` are user-specifiable parameters on the `MATERIAL` statement. Default values for these parameters for various binary III-V materials are given in Table B-38. The compositionally dependent default values for the ternary combinations listed in Table B-38 are linearly interpolated from the binary values listed in the same table.

For nitride compounds, you can use a modified version of this model, which is described in Chapter 5: “Blaze: Compound Material 2D Simulator”, Section 5.3.7: “GaN, InN, AlN, Al(x)Ga(1-x)N, In(x)Ga(1-x)N, Al(x)In(1-x)N, and Al(x)In(y)Ga(1-x-y)N”.

3.10.3: Tauc-Lorentz Dielectric Function with Optional Urbach Tail Model for Complex Index of Refraction

A parameterization of the Tauc-Lorentz dielectric function was proposed by Foldyna et.al. [71], which includes Urbach tails. The imaginary part of the dielectric function is given by Equation 3-598.

$$\epsilon_2(E) = \begin{cases} \frac{1}{E} \frac{TLU.A \cdot TLU.E0 \cdot TLU.C(E - TLU.EG)^2}{(E^2 - TLU.E0^2)^2 + TLU.C^2 E^2} & E \geq TLU.EC \\ \frac{A_u}{E} \exp\left(\frac{E}{E_u}\right) & E < TLU.EC \end{cases} \quad 3-598$$

Here, for energies greater than $TLU.EC$, the standard Tauc-Lorentz form is used while for energies less than $TLU.EC$, Urbach tails are parameterized as a function of energy and two matching parameters A_u and E_u that are calculated by Equations 3-599 and 3-600 to give a continuous function and first derivative at $E=TLU.EC$.

$$\epsilon_u = \frac{(TLU.EC - TLU.EG)}{2 - 2TLU.EC(TLU.EC - TLU.EG) - \frac{TLU.EC^2 + 2(TLU.EC^2 - TLU.E0^2)}{TLU.C^2 TLU.EC^2 + (TLU.EC^2 - TLU.E0^2)^2}} \quad 3-599$$

$$\epsilon_u = \exp\left(\frac{TLU.EC}{E_u}\right) \frac{TLU.A \cdot TLU.E0 \cdot TLU.C(TLU.EC - TLU.EG)^2}{(TLU.EC^2 - TLU.E0^2)^2 + TLU.C^2 TLU.EC^2} \quad 3-600$$

In our implementation, if you do not specify $TLU.EC$, then the standard form of the Tauc-Lorentz dielectric function is used. For energies less than $TLU.EG$, the imaginary part is zero.

The real part of the dielectric function is obtained from the imaginary part using the Kramers-Krönig relation as given in Equation 3-601:

$$\epsilon_1(E) = TLU.EPS + \frac{2}{\pi} (C.P.) \int_0^\infty \frac{\xi \epsilon_2(\xi)}{\xi^2 - E^2} d\xi \quad 3-601$$

where (C.P.) denotes the Cauchy principal value of the integral. The integral itself is resolved using some analytic forms the details of which are given in [71].

The complex index of refraction is calculated from the complex dielectric function using Equations 3-602 and 3-603.

$$n = \sqrt{\frac{\sqrt{\epsilon_1^2 + \epsilon_2^2} + \epsilon_1}{2}} \quad 3-602$$

$$k = \sqrt{\frac{\sqrt{\epsilon_1^2 + \epsilon_2^2} - \epsilon_1}{2}} \quad 3-603$$

You can enable the model by specifying `TLU.INDEX` on the `MODELS` statement. Table 3-115 gives a summary of the relevant model parameters.

| Table 3-115. Parameters for the Tauc-Lorentz-Urbach Dielectric Model | | | |
|--|-----------------------|---------|-------|
| Parameter | Statement | Default | Units |
| <code>TLU.A</code> | <code>MATERIAL</code> | | eV |
| <code>TLU.C</code> | <code>MATERIAL</code> | | eV |
| <code>TLU.E0</code> | <code>MATERIAL</code> | | eV |
| <code>TLU.EG</code> | <code>MATERIAL</code> | | eV |
| <code>TLU.EC</code> | <code>MATERIAL</code> | | eV |
| <code>TLU.EPS</code> | <code>MATERIAL</code> | 1.0 | |

3.11: Carrier Transport in an Applied Magnetic Field

Magnetic field effects have been used in semiconductor characterization measurements and exploited in semiconductor device applications. ATLAS can model the effect of applied magnetic fields on the behavior of a semiconductor device.

The basic property, which is measured is the Hall coefficient R_H . For a uniformly doped device with a current flowing in the X direction and a magnetic field in the Z direction, an electric field (the Hall field) is set up in the Y direction. The Hall coefficient is then obtained by combining these measured quantities in the ratio:

$$R_H = \frac{E_y}{J_x B_z} \quad 3-604$$

The Hall co-efficient also has a theoretical value:

$$R_H = \frac{r(p - s^2 n)}{q(p + sn)^2} \quad 3-605$$

where s is the electron mobility divided by hole mobility. The Hall scattering factor, r , can be obtained from the mean free time between carrier collisions and is typically not very different from unity.

Another quantity that is measured experimentally is the Hall mobility:

$$\mu^* = |R_H \sigma| \quad 3-606$$

where σ is the electrical conductivity. We will consider the electron and hole currents separately. Therefore, taking the limits ($n \gg p$) and then ($p \gg n$) in Equation 3-606, we obtain the Hall mobilities for electrons and holes respectively as:

$$\begin{aligned} \mu_n^* &= r \mu_n \\ \mu_p^* &= r \mu_p \end{aligned} \quad 3-607$$

where μ_n and μ_p are the carrier mobilities. The Hall scattering factor for electrons can be different to that for holes in general. Published values for silicon are 1.2 and 1.2 [7] and 1.1 and 0.7 [194] for electrons and holes respectively. The default in ATLAS is the latter. You can set the values on the MODELS statement using the R.ELEC and R.HOLE parameters.

The effect of the magnetic field on a carrier travelling with velocity v is to add a term called the Lorentz force:

$$q(\underline{v} \times \underline{B}) \quad 3-608$$

to the force it feels. The magnetic field density B is a vector (B_x, B_y, B_z) and is in units of Tesla ($V \cdot s/m^2$) in ATLAS.

The consequence of this extra force in a semiconductor can be calculated by including it in a relaxation time based transport equation and making a low-field approximation [7]. You can relate the current density vector obtained with a magnetic field applied to that obtained with no magnetic field using a linear equation:

$$\underline{J}_B = \underline{M} \underline{J}_0 \quad 3-609$$

The Matrix M can be written as:

$$M = \frac{1}{1 + a^2 + b^2 + c^2} \begin{pmatrix} 1 + a^2 & ab - c & ca + b \\ c + ab & 1 + b^2 & bc - a \\ ca - b & a + bc & 1 + c^2 \end{pmatrix} \quad 3-610$$

where $a = \mu^* B_x$, $b = \mu^* B_y$, $c = \mu^* B_z$. The matrix takes this form for both electrons and holes. Using this form, you can include the magnetic field effects in ATLAS. The model is derived from an expansion in powers of Magnetic field and is only accurate if the weak field condition:

$$\mu^* |B| \ll 1 \quad 3-611$$

is satisfied. Therefore, for example, a field of 1 Tesla in Silicon with a typical mobility of $0.1 \text{ m}^2/(\text{V} \cdot \text{s})$, the product is 0.1 so that the condition is satisfied.

To invoke this model in ATLAS2D, simply supply a value for BZ on the MODELS statement. Nonzero values of BX and BY are not permitted because they would generally result in current in the Z direction, thereby voiding the assumption of two-dimensionality. In ATLAS3D, any combination of BX, BY or BZ can be specified as long as condition (Equation 3-611) is satisfied.

Table 3-116 shows the parameters used for the carrier transport in a magnetic field.

| Table 3-116. MODELS Statement Parameters | | | |
|--|------|---------|-------|
| Parameter | Type | Default | Units |
| BX | Real | 0.0 | Tesla |
| BY | Real | 0.0 | Tesla |
| BZ | Real | 0.0 | Tesla |
| R.ELEC | Real | 1.1 | |
| R.HOLE | Real | 0.7 | |

3.12: Anisotropic Relative Dielectric Permittivity

In the general case, the relationship between the electric displacement vector and the electric field is given by:

$$\vec{D} = \epsilon_0 \vec{\epsilon} \vec{E} \quad 3-612$$

where ϵ , the relative dielectric permittivity, is a symmetric second order tensor represented by a 3×3 matrix. Since it is symmetric, it can be written as:

$$\vec{\epsilon} = \begin{pmatrix} \epsilon_{xx} & \epsilon_{xy} & \epsilon_{xz} \\ \epsilon_{xy} & \epsilon_{yy} & \epsilon_{yx} \\ \epsilon_{xz} & \epsilon_{yz} & \epsilon_{zz} \end{pmatrix} \quad 3-613$$

In the isotropic case, the off-diagonal terms are zero and the diagonal terms all have the same value as each other. In the anisotropic case, you can always set the off-diagonal elements to zero by a suitable transformation of coordinates. This coordinate system may not match the coordinate system used by ATLAS for the simulation. Therefore, it is necessary to allow ATLAS to model anisotropic permittivity for the relationship Equation 3-613 where the off-diagonal elements are non-zero.

The discretization of the flux term in the Poisson equation:

$$\epsilon_0 \nabla \cdot (\vec{\epsilon} \vec{E}) \quad 3-614$$

requires a more general treatment in the anisotropic case. For example, the x-component of the electric displacement vector will now contain a contribution from all the components of the electric field:

$$D_x = \epsilon_{xx} E_x + \epsilon_{xy} E_y + \epsilon_{xz} E_z \quad 3-615$$

and so the discretization is more complicated and uses more CPU time. A simplification can be made when:

- the permittivity matrix is diagonal.
- the mesh used in modeling the device is rectangular.

In this case, discretization will occur only in the directions of the coordinate axes and simply using a scalar permittivity for each direction is correct. This retains the simplicity and speed of the discretization for isotropic materials.

ATLAS allows you to specify a value of anisotropic relative dielectric permittivity using the PERM.ANISO parameter on the MATERIAL statement. By default, this is the value of (ϵ_{yy}) if the simulation is in 2D and (ϵ_{zz}) if it is in 3D. The off-diagonal elements are assumed to be zero. In the case of a 3D simulation, you can apply the value of PERM.ANISO to the Y direction instead of the Z direction by specifying YDIR.ANISO or ^ZDIR.ANISO on the MATERIAL statement. You can specify the value of (ϵ_{xx}) by using the PERMITTIVITY parameter on the MATERIAL statement. The simpler version of discretization will be used in this case by default.

If the coordinate system in which the permittivity tensor is diagonal and the ATLAS coordinate system are non-coincident, then the coordinate transformation can be specified as a set of vectors

$$X = (X.X, X.Y, X.Z)$$

$$Y = (Y.X, Y.Y, Y.Z)$$

$$Z = (Z.X, Z.Y, Z.Z)$$

where the vector components can be specified on the MATERIAL statement.

The default is that

$X = (1.0, 0.0, 0.0)$

$Y = (0.0, 1.0, 0.0)$

$Z = (0.0, 0.0, 1.0)$

and you should specify all necessary components. You do not need to normalize the vectors to unit length. ATLAS will normalize them and transform the relative dielectric tensor according to the usual rules. If you specify any component of X, Y or Z, then the more complete form of discretization will be used. You can also enable the more complete form of electric displacement vector discretization by using the E.FULL.ANISO parameter on the MATERIAL statement.

Table 3-117 shows the parameters used in the Anisotropic Relative Dielectric Permittivity.

| Table 3-117. MATERIAL Statement Parameters | | |
|--|---------|---------|
| Parameter | Type | Default |
| PERM.ANISO | Real | -999.0 |
| YDIR.ANISO | Logical | False |
| ZDIR.ANISO | Logical | True |
| E.FULL.ANISO | Logical | False |
| X.X | Real | 1.0 |
| X.Y | Real | 0.0 |
| X.Z | Real | 0.0 |
| Y.X | Real | 0.0 |
| Y.Y | Real | 1.0 |
| Y.Z | Real | 0.0 |
| Z.X | Real | 0.0 |
| Z.Y | Real | 0.0 |
| Z.Z | Real | 1.0 |

3.13: Single Event Upset Simulation

The capability of single event upset/photogeneration transient simulation is included in 2D and 3D using the `SINGLEEVENTUPSET` statement (see Chapter 21: “Statements”, Section 21.51: “`SINGLEEVENTUPSET`” for more information). It allows you to specify the radial, length, and time dependence of generated charge along tracks. There can be a single particle strike or multiple strikes. Each track is specified by an Entry Point Location (x0,y0,z0) and an Exit Point Location (x1,y1,z1). This is assumed to be a cylinder with the radius defined with the `RADIUS` parameter. In 2D, z0 and z1 should be neglected.

The entry and exit points are specified by the `ENTRYPOINT` and `EXITPOINT` parameters of the `SINGLEEVENTUPSET` statement. These are character parameters that represent the ordered triplet coordinates of the entry and exit points of the particle track.

The electron/hole pairs generated at any point is a function of the radial distance, r , from the center of the track to the point, the distance l along the track and the time, t . The implementation into ATLAS allows you to define the generation rate as the number of electron-hole pairs per cm^3 along the track according to the equation:

$$G(r, l, t) = (\text{DENSITY} * L1(l) + S * \text{B.DENSITY} * L2(l)) * R(r) * T(t) \quad 3-616$$

where `DENSITY` and `B.DENSITY` are defined as the number of generated electron/hole pairs per cm^3 .

In radiation studies, the ionizing particle is typically described by the linear charge deposition (LCD) value, which defines the actual charge deposited in units of $\text{pC}/\mu\text{m}$. You can use this definition within ATLAS by specifying the `PCUNITS` parameter in the `SINGLEEVENTUPSET` statement. If the user-defined parameter, `PCUNITS`, is set in the `SINGLEEVENTUPSET` statement, then `B.DENSITY` is the generated charge, in $\text{pC}/\mu\text{m}$, and the scaling factor S is:

$$S = \frac{1}{q\pi \text{RADIUS}^2} \quad 3-617$$

where `RADIUS` is defined on the `SINGLEEVENTUPSET` statement. If the `PCUNITS` parameter isn't set, then `B.DENSITY` is the number of generated electron/hole pairs in cm^{-3} and the scaling parameter, S , is unity.

Another common measure of the loss of energy of the SEU particle, as it suffers collisions in a material, is the linear energy transfer (LET) value, which is given in units of $\text{MeV}/\text{mg}/\text{cm}^2$ (or $\text{MeV}\cdot\text{cm}^2/\text{mg}$). In silicon, you can convert energy to charge by considering you need approximately 3.6 eV of energy to generate an electron-hole pair. The conversion factor from the LET value to the LCD value is then approximately 0.01 for silicon. So for instance, a LET value of $25 \text{ MeV}\cdot\text{cm}^2/\text{mg}$ is equivalent to $0.25 \text{ pC}/\mu\text{m}$, which can then be defined with the `B.DENSITY` and `PCUNITS` parameters.

The factors, $L1$ and $L2$, in Equation 3-616 define the variation of charge or carrier generation along the path of the SEU track. These variations are defined by the equations:

$$L1(l) = A1 + A2 \cdot l + A3 \exp(A4 \cdot l) \quad 3-618$$

$$L2(l) = B1(B2 + l \cdot B3)^{B4} \quad 3-619$$

where the $A1$, $A2$, $A3$, $A4$, $B1$, $B2$, $B3$ and $B4$ parameters are user-definable as shown in Table 3-118.

Table 3-118. User-Specifiable Parameters for Equations 3-618 and 3-619

| Statement | Parameter | Default | Units |
|------------------|-----------|---------|------------------|
| SINGLEEVENTUPSET | A1 | 1 | |
| SINGLEEVENTUPSET | A2 | 0 | cm ⁻¹ |
| SINGLEEVENTUPSET | A3 | 0 | |
| SINGLEEVENTUPSET | A4 | 0 | cm ⁻¹ |
| SINGLEEVENTUPSET | B1 | 1 | |
| SINGLEEVENTUPSET | B2 | 1 | |
| SINGLEEVENTUPSET | B3 | 0 | cm ⁻¹ |
| SINGLEEVENTUPSET | B4 | 0 | |

Note: The default parameters in Table 3-118 were chosen to result in constant carrier or charge generation as a function of distance along the particle track.

The factor $R(r)$ is the radial parameter, which is defined by one of two equations. The default is:

$$R(r) = \exp\left(-\frac{r}{\text{RADIUS}}\right) \quad 3-620$$

where r is the radial distance from the center of the track to the point and RADIUS is a user-definable parameter as shown in Table 3-119. You can choose an alternative expression if you specify the RADIALGAUSS parameter on the SINGLEEVENTUPSET statement. In this case, $R(r)$ is given by:

$$R(r) = \exp\left(-\frac{r}{\text{RADIUS}}\right)^2 \quad 3-621$$

The time dependency of the charge generation $T(t)$ is controlled with the TC parameter through two functions.

For TC=0:

$$T(t) = \text{deltafunction}(t - T0) \quad 3-622$$

For TC>0:

$$T(t) = \frac{2e^{-\left(\frac{t - T0}{TC}\right)^2}}{TC\sqrt{\pi}\text{erfc}\left(\frac{-T0}{TC}\right)} \quad 3-623$$

where T0 and TC are parameters of the SINGLEEVENTUPSET statement.

Table 3-119. User-Specifiable Parameters for Equations 3-616, 3-617, 3-622, and 3-623

| Statement | Parameter | Default | Units |
|------------------|-----------|---------|---------------------------|
| SINGLEEVENTUPSET | DENSITY | 0.0 | cm ⁻³ |
| SINGLEEVENTUPSET | B.DENSITY | 0.0 | cm ⁻³ or pC/μm |
| SINGLEEVENTUPSET | TO | 0.0 | s |
| SINGLEEVENTUPSET | TC | 0.0 | s |
| SINGLEEVENTUPSET | RADIUS | 0.05 | μm |

The following example shows a particle strike that is perpendicular to the surface along the Z plane. Therefore, only the Z coordinates change has a radius of 0.1 μm and a LET value of 20 MeV-cm²/mg (B.DENSITY=0.2). The strike has a delay time of 60 ps and the Gaussian profile has a characteristic time of 10 ps. The generation track for this striking particle is from z=0 to z=10 μm and carrier generation occurs along its entire length.

```
single    entry="5.5,0.0,0.0" exit="5.5,0.0,10" radius=0.1 \
pcunits b.density=0.2 t0=60.e-12 tc=10.e-12
```

User-Defined SEU

In addition to the model described above, you can use the C-Interpreter to specify an arbitrary generation profile as a function of position and time. This is specified using the F.SEU parameter of the SINGLEEVENTUPSET statement.

```
SINGLEEVENTUPSET F.SEU=myseu.c
.
SOLVE DT=1e-14 TSTOP=1e-7
```

The F.SEU parameter indicates an external C-language sub-routine conforming to the template supplied. The file, *myseu.c*, returns a time and position dependent value of carrier generation. For more information about the C-Interpreter, see Appendix A: “C-Interpreter Functions”.

3.14: Field Emission from Semiconductor Surfaces

Vacuum microelectronic devices often utilize field emission from the sharp tips of emitters made from semiconductor materials [58][161]. The current emitted can be modeled using a tunneling model, usually a variant of the Fowler-Nordheim model. ATLAS implements one such model, which we refer to as the Zaidman model [273]. In this model, the tunneling current is calculated at each segment of a semiconductor/vacuum interface. The current density in A/cm² is given by

$$J = \frac{F \cdot AE F^2}{\phi TSQ \cdot ZAIDMAN} \exp\left(\frac{-F \cdot BE(0.95 - 1.43641 \times 10^{-7} F/\phi^2) \phi^{3/2}}{F}\right) \quad 3-624$$

Here, ϕ is the semiconductor-vacuum barrier height in eV. F is the electric field strength normal to the surface in units of V/cm and $TSQ \cdot ZAIDMAN$ is a fitting parameter. The parameters $F \cdot AE$ and $F \cdot BE$ are also fitting parameters.

The current produced in each segment then follows the field lines until it either reaches a contact or exits the device boundary. To enable the model, use the `ZAIDMAN` parameter on the `MODELS` statement. It should not be used concurrently with the `FNORD` model.

It presently omits self-consistent evaluation with respect to the carrier continuity equations. It also neglects any modification of the current in the vacuum arising from the space charge present there.

| Table 3-120. Zaidmann Model Parameters | | | |
|--|-------------|-------------------------|---|
| Statement | Parameter | Default | Units |
| MODELS | ZAIDMAN | False | |
| MODELS | TSQ.ZAIDMAN | 1.1 | |
| MODELS | F.AE | 1.5414×10 ⁻⁶ | Q ² /Vs |
| MODELS | F.BE | 6.8308×10 ⁷ | cm ⁻¹ V ^{1/2} Q ^{-3/2} |

3.15: Conduction in Silicon Nitride

It is known that at high fields and for temperatures above 325 Kelvin, the conduction in Silicon Nitride is dominated by Poole-Frenkel emission. ATLAS can model this by adding an electron generation term to the electron continuity equation. To use this model, you define a trap density, `NT.N`, using the `NITRIDECHARGE` statement. You also change the Silicon Nitride layer into a semiconductor using the `SEMICONDUCTOR` parameter on the `MATERIAL` statement.

The electron generation term is proportional to

$$PF.A \exp\left(-\frac{PF.BARRIER}{K_B T_L}\right) + PF.B \exp\left(-\frac{PF.BARRIER}{K_B T_L} + \frac{Beta \sqrt{F}}{K_B T_L}\right) \quad 3-625$$

where `PF.A`, `PF.B`, and `PF.BARRIER` can be specified on the `NITRIDECHARGE` statement. The first term is an ohmic term that will dominate at low fields. The local electric field is F , the lattice temperature is T_L , K_B is the Boltzmann constant, and $Beta$ is a factor obtained from the equation:

$$Beta = Q \sqrt{Q / (\pi \epsilon)} \quad 3-626$$

where Q is the electronic charge, and ϵ is the dielectric permittivity of Silicon Nitride. This model only applies to steady state simulations. The traps should first be charged using the `NIT.N` parameter on the `SOLVE` statement. The value `MUN` on the `MOBILITY` statement can also be used to calibrate the resulting I-V curves.

4.1: Overview

S-PISCES is a powerful and accurate two-dimensional device modeling program that simulates the electrical characteristics of silicon based semiconductor devices including MOS, bipolar, SOI, EEPROM, and power device technologies.

S-PISCES calculates the internal distributions of physical parameters and predicts the electrical behavior of devices under either steady-state, transient, or small signal AC conditions. This is performed by solving Poisson's Equation (see Chapter 3: "Physics", Section 3.1.1: "Poisson's Equation") and the electron and hole carrier continuity equations in two dimensions (see Chapter 3: "Physics", Section 3.1.2: "Carrier Continuity Equations").

S-PISCES solves basic semiconductor equations on non-uniform triangular grids. The structure of the simulated device can be completely arbitrary. Doping profiles and the structure of the device may be obtained from analytical functions, experimentally measured data, or from process modeling programs SSUPREM3 and ATHENA.

For more information on semiconductor equations, see Chapter 3: "Physics", Section 3.1: "Basic Semiconductor Equations".

You should be familiar with ATLAS before reading this chapter any further. If not, read Chapter 2: "Getting Started with ATLAS".

4.2: Simulating Silicon Devices Using S-PISCES

4.2.1: Simulating MOS Technologies

Physical Models for MOSFETs

S-PISCES provides special physical models tuned for simulating MOS devices. Most of these models are accessed from the `MODEL` statement. The `MOS` parameter of the `MODEL` statement can be specified to turn on a default set of physical models that are most useful for MOS simulation. The `MOS` parameter enables Shockley-Read-Hall (`SRH`), Fermi Statistics (`FERMI`), and the Lombardi Mobility model (`CVT`) for transverse field dependence. To set the default MOS simulation models, use:

```
MODEL MOS PRINT
```

The transverse field dependent mobility models are of particular importance for simulating MOS devices. S-PISCES currently supports several different transverse field dependent mobility models. The `CVT` parameter selects the Lombardi CVT model. The `YAMA` parameter selects the Yamaguchi model. The `TASCH` parameter selects the Tasch model. The `WATT` parameter selects the Watt Surface Model, which can be operated in a more accurate mode with the extra parameter, `MOD.WATT`, on the `MOBILITY` statement.

You will find that the `MOBILITY` statement can be used to modify some of the parameters of the various models, to apply different models to different regions, or to apply different models to electrons and holes.

Meshing for MOS Devices

In device simulation of MOS devices, the key areas for a tight mesh are:

- very small vertical mesh spacing in the channel under the gate. The exact size of mesh required depends on the transverse field or surface mobility model chosen. See Figure 4-1 for an example of the effect of mesh size on drain current.
- lateral mesh spacing along the length of the channel for deep sub-micron devices. This is required to get the correct source-drain resistance and to resolve the channel pinch-off point.
- lateral mesh at the drain/channel junction for breakdown simulations. This is required to resolve the peak of electric field, carrier temperature and impact ionization.
- several vertical grid spacings inside the gate oxide when simulating gate field effects such as gate induced drain leakage (GIDL) or using any hot electron or tunneling gate current models

Figures 4-1 and 4-2 show the effect of mesh size in the MOS channel on IV curves. In Figure 4-1, the mesh density in the vertical direction is increased. As the mesh density increases, the resolution of the electric field and carrier concentration is improved. This example uses the `CVT` mobility model. Improvements in transverse electric field resolution lead to a reduced mobility in the channel and a stronger IV roll-off.

But Figure 4-2 shows the effect of surface channel mesh in MOSFETs is model dependent. This result shows the current at $V_{ds}=3.0V$ and $V_{gs}=0.1V$ versus the size of the first grid division into the silicon. Results vary for each model but note that for all models, a very fine grid is required to reduce the grid dependence to acceptable levels.

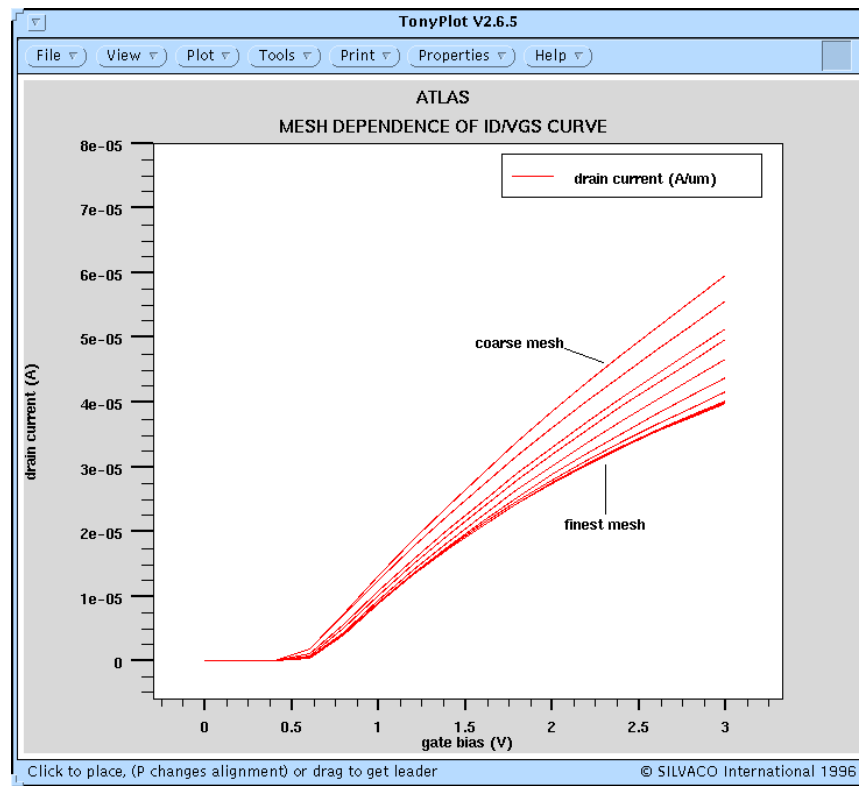


Figure 4-1: Effect on MOS IV curve of progressive refinement of the vertical mesh spacing at the surface of the MOS channel

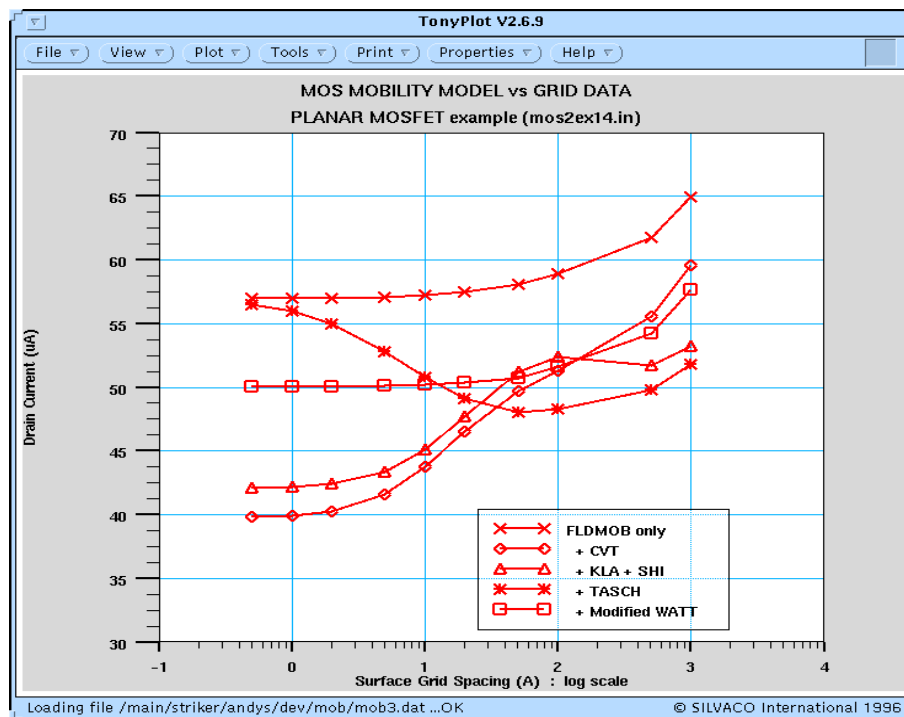


Figure 4-2: Effect of surface mesh spacing on simulated current for several MOS Mobility Models

MOS Electrode Naming

For MOS simulation, S-PISCES allows you to use standard electrode names to reduce confusion with the use of electrode indices. These names include: source, drain, gate, and substrate. Electrode names can be defined in ATHENA or DEVEDIT or in the ELECTRODE statement in ATLAS. These names can be used in the SOLVE statements for setting bias voltages such as:

```
SOLVE VGATE=1.0 VSTEP=1.0 VFINAL=5.0 NAME=GATE
```

Gate Workfunction

In MOS simulations, the workfunction of the gate is an important parameter. This must be set in each input deck using the WORK parameter of the CONTACT statement. For example:

```
CONTACT NAME=GATE WORK=4.17
```

would set the workfunction on the gate at 4.17 eV.

Certain material names can also be used to set the workfunction of common gate materials. For example:

```
CONTACT NAME=GATE N.POLY
```

would set the workfunction on the gate to that of n type polysilicon.

Note: The gate workfunction should be set on a CONTACT statement even though the material or workfunction might be set from ATHENA or DEVEDIT.

Interface Charge

For accurate simulation of MOS devices, the interface charge at the oxide, specify semiconductor interface. To do this, set the QF parameters for the INTERFACE statement. Typically, a value of $3 \times 10^{10} \text{ cm}^{-2}$ is representative for the interface charge found in silicon MOS devices. The proper syntax for setting the value for this interface fixed charge is:

```
INTERFACE QF=3e10
```

You can also try to model the fixed charge more directly by using interface traps to simulate the surface states. To do this, use the INTTRAP statement. But this is rarely done in practice.

Single Carrier Solutions

Frequently for MOS simulation, you can choose to simulate only the majority carrier. This will significantly speed up simulations where minority carrier effects can be neglected. This can be done by turning off the minority carrier. To do this, use the ATLAS negation character, ^, and one of the carrier parameters (ELECTRONS or HOLES) in the METHOD statement. For example, to simulate electrons only, you can specify one of the following:

```
METHOD CARRIERS=1 ELECTRONS  
METHOD ^HOLES
```

Single carrier solutions should not be performed where impact ionization, any recombination mechanism, lumped element boundaries, or small signal AC analysis are involved.

Energy Balance Solutions

As MOS devices become smaller and smaller, non-local carrier heating effects becomes important. You can perform accurate simulation of non-local carrier heating effects using the energy balance model (EBM). As a general rule, you can use the gate length as a gauge to predict when non-local effects are important. Generally, for drain currents, energy balance should be applied for gate lengths less than 0.5 microns. For substrate currents, energy balance should be applied for gate lengths less than 1.0 micron.

To enable energy balance for electrons/holes, set either the `HCTE.EL` or `HCTE.HO` parameters on the `MODEL` statement. For example:

```
MODEL HCTE.EL
```

enables the energy balance model for electrons.

ESD Simulation

In some cases, lattice heating may be important to MOS simulation. This typically occurs in cases with very high currents, just like the case with ESD simulation. In these cases, GIGA should be used to simulate the heat-flow in the device. To enable heat flow simulation, set the `LAT.TEMP` parameter of the `MODEL` statement (a license for GIGA is required). For example, the statement:

```
MODEL LAT.TEMP
```

enables heat-flow simulation.

4.2.2: Simulating Silicon Bipolar Devices

Physical Models for BJTs

S-PISCES provides special physical models for bipolar device simulation. You can select these models using the `MODEL` statement. The `BIPOLAR` parameter of the `MODEL` statement enables a reasonable default set of bipolar models. These include: concentration dependent mobility (`CONMOB`), field dependent mobility (`FLDMOB`), bandgap narrowing (`BGN`), concentration-dependent lifetime (`CONSRH`) and Auger recombination (`AUGER`).

For the most accurate bipolar simulations, the recommended mobility model is the Klaassen model (`KLA`). This includes doping, temperature and carrier dependence. It applies separate mobility expressions for majority and minority carriers. You should also use this model with Klaassen's Auger model (`KLAAUG`) and Klaassen's concentration dependent SRH model (`KLASRH`). Combine the mobility model with `FLDMOB` to model velocity saturation. For surface (or lateral) bipolar devices, you can use the Shirahata model (`SHI`) to extend the Klaassen model with a transverse electric field dependence. The most accurate and appropriate model statement for bipolar devices is therefore:

```
MODELS KLA FLDMOB KLASRH KLAAUG BGN FERMI PRINT
```

You can choose this set of models by using the `BIPOLAR2` parameter from the `MODEL` statement.

Note: For a complete syntax including description of models and method for simulating polysilicon emitter bipolar devices, see the BJT directory in the on-line examples.

Meshing Issues for BJTs

The most important areas to resolve in bipolar transistors are the emitter/base and base/collector junctions. Typically, a very fine mesh throughout the base region is required. The gain of the bipolar device is determined primarily by the recombination at the emitter/base junction or inside the emitter. Therefore, these regions need to be resolved with a fine mesh.

BJT Electrode Naming

S-PISCES also provides special electrode names for bipolar simulation that can be used to ease confusion over electrode indices. These electrode names include: “emitter”, “base”, “collector”, “anode”, and “cathode”. Electrode names can be defined in ATHENA or DEVEDIT or in the ELECTRODE statement in ATLAS. The electrode names are used on SOLVE statement. For example:

```
SOLVE VBASE=1.0 VSTEP=1.0 VFINAL=5.0 NAME=BASE
```

Dual Base BJTs

It is possible in S-PISCES to tie two or more contacts together so that voltages on both contacts are equal. This is useful for many technologies for example dual base bipolar transistors. There are several methods for achieving this depending on how the structure was initially defined.

If the structure is defined using ATLAS syntax, it is possible to have multiple ELECTRODE statements with the same NAME parameter defining separate locations within the device structure. In this case, the areas defined to be electrodes will be considered as having the same applied voltage. A single current will appear combining the current through both ELECTRODE areas.

Similarly, if two separate metal regions in ATHENA are defined using the ATHENA ELECTRODE statement to have the same name, then in ATLAS these two electrodes will be considered as shorted together.

If the electrodes are defined with different names, the following syntax can be used to link the voltages applied to the two electrodes.

```
CONTACT NAME=base1 COMMON=base
.
SOLVE VBASE=0.1
```

Here, the electrode, base1, will be linked to the electrode, base. Then, the applied 0.1V on base will also appear on base1. But ATLAS will calculate and store separate currents for both base and base1. This can be a useful feature. In some cases, however, such as where functions of the currents are required in EXTRACT or TONYPLOT, it is undesirable. You can add the SHORT parameter to the CONTACT statement above to specify that only a single base current will appear combining the currents from base and base1.

When loading a structure from ATHENA or DEVEDIT where two defined electrode regions are touching, ATLAS will automatically short these and use the first defined electrode name.

Creating an Open Circuit Electrode

It is often required to perform a simulation with an open circuit, such as for an open-base breakdown voltage simulation, on one of the defined electrodes. There are three different methods that will accomplish this. The first method is to delete an electrode from the structure file. The second method is to add an extremely large lumped resistance, for example $10^{20}\Omega$, onto the contact to be made open circuited. The third method is to first switch the boundary conditions on the contact to be made open circuited from voltage controlled to current controlled. Then, specify a very small current through that electrode.

Each of these methods are feasible. But if a floating region is created within the structure while using these methods, then numerical convergence may be affected. As a result, it is normally recommended to use the second method to ensure that no floating region is created.

Solution Techniques for BJTs

To obtain bipolar solutions, you almost always need to simulate using two carriers. This is due to the importance of minority carriers to device operation.

In certain cases, non-local carrier heating may be important to accurately simulate bipolar devices. In these cases, use the energy balance model. To model non-local carrier heating for electrons/holes, set the `HCTE.EL` and `HCTE.HO` parameters in the `MODEL` statement. For example, the statement:

```
MODEL HCTE.EL
```

invokes the carrier heating equation for electrons.

4.2.3: Simulating Non-Volatile Memory Technologies (EEPROMs, FLASH Memories)

To simulate non-volatile memory devices, you must become familiar with the basics of MOSFET simulation (see Section 4.2.1: “Simulating MOS Technologies”).

Defining Floating Gates

To simulate non-volatile memory technologies, such as EEPROMs or FLASH EEPROMs, specify one or more electrodes as floating gates. To do this, set the `FLOATING` parameter of the `CONTACT` statement. For example:

```
CONTACT NAME=fgate FLOATING
```

This specifies that the electrode named `fgate` is simulated as a floating gate. This means that the charge on the floating gate is calculated as the integral of the gate current at that gate during a transient simulation.

Modeling the correct coupling capacitance ratio between the floating gate and control gate often requires adding an extra lumped capacitor from the floating gate to the control gate or one of the other device terminals. This is often required since S-PISCES is performing a 2D simulation whereas the coupling of the gates is often determined by their 3D geometry. Parameters on the `CONTACT` statement are used to apply these extra lumped capacitances. For example, to add a capacitor of 1fF/mm between the control and floating gates the syntax is:

```
CONTACT NAME=fgate FLOATING FG1.CAP=1.0e-15 EL1.CAP=cgate
```

Gate Current Models

You can supply the gate currents for the floating gate structure by one of three sources: hot electron injection (`HEI` or `N.CONCAN`), hot hole injection (`HHI` or `P.CONCAN`) and Fowler-Nordheim tunneling current (`FNORD`).

These currents are of importance, depending on whether electrons are being moved onto the gate or off the floating gate. In the case of placing electrons on the floating gate, use hot electron injection and Fowler-Nordheim tunneling. In the case of removing electrons from the floating gate, set hot hole injection and Fowler-Nordheim tunneling.

In drift diffusion simulations, perform hot electron injection by setting the `HEI` parameter of the `MODELS` statement. To simulate hot hole injection, use the `HHI` parameter of the `MODELS` statement. To enable Fowler-Nordheim tunneling, set the `FNORD` parameter of the `MODELS` statement. The following example demonstrated the proper setting for Flash EPROM programming.

```
MODELS MOS HEI PRINT
```

This next example is appropriate for EEPROM erasure.

```
MODELS MOS HHI FNORD PRINT
```

With energy balance simulations, use the Concannon Models for EPROM programming and erasing. For more information about these models, see Chapter 3: “Physics”, the “Concannon’s Injection Model” section on page 3-131.

Note: Writing and erasure of floating gate devices should be done using transient simulation.

Gate Current Assignment (NEARFLG)

The actual calculation of floating gate current magnitude is done at the silicon-oxide interface. The question of distribution of oxide currents to the various electrodes near the interface is resolved using one of two models. The actual flow of carriers in oxides is not well known. Accepted physical models of carrier flow in oxides are still under research. As such, S-PISCES provides two heuristic models to choose from. The default is to distribute currents calculated at points along the interface to the electrode in the direction of highest contributing field. This model is somewhat analogous to a purely drift model of oxide carrier transport. The alternative is to set the NEARFLG parameter of the MODEL statement. In this case, the currents calculated at points along the interface are distributed to the geometrically closest electrode. This model is analogous to a purely diffusion model of carrier transport in oxide.

4.2.4: Simulating SOI Technologies

Silicon substrates are now being produced that contain an oxide layer buried below the surface of the silicon at some predefined depth. The existence of this buried oxide layer has resulted in a change not only in the fabrication process used to manufacture a device in the surface silicon but also in the challenges facing device simulation.

All of the issues raised previously about MOS device simulation should be considered with some extra SOI specific problems.

The most common device technology that uses these SOI substrates is the SOI MOSFET. This section summarizes the simulation requirements for SOI using this particular technology as a reference.

Meshing in SOI devices

The mesh requirements for SOI MOSFETs is very similar to that described in the previous section for bulk MOS transistors. In addition to these requirements, there are some additional points to meshing these devices. These are:

- Two channel regions may exist: one underneath the top (front) gate oxide and the other above the buried (back gate) oxide.
- Inside the buried oxide layer, the mesh constraints can be relaxed considerably compared with the top gate oxide.
- The active silicon underneath the top gate can act as the base region of a bipolar transistor and as such may require a finer mesh when compared to bulk MOS transistors.

Physical Models for SOI

SOI MOSFET simulations are based upon the physical operation of the device, which exhibits both MOS and bipolar phenomena. As a result a more complex set of physical models will be required than for either MOS or bipolar technologies. Table 4-1 shows these models.

| Table 4-1: SOI Physical Models | |
|--------------------------------|--|
| Model | Description |
| Mobility | Klaassen's Model (KLA) is recommended to account for lattice scattering, impurity scattering, carrier-carrier scattering and impurity clustering effects at high concentration. The Shirahata mobility model (SHI) is needed to take into account surface scattering effects at the silicon/oxide interface, which is a function of the transverse electric field. High electric field velocity saturation is modelled through the field dependent mobility model (FLDMOB). You can tune model parameters using the MOBILITY statement syntax. |
| Interface Charge | In SOI transistors, there exist two active silicon to oxide interfaces on the wafer. The top interface, under the top gate, is similar to MOS technology. The bottom interface is quite different and typically contains significantly more charge. You can set different interface charges in SPISCES using the INTERFACE statement with region specific parameters. |
| Recombination | To take account of recombination effects, we recommend the use of the Shockley-Read-Hall (SRH) model. This simulates the leakage currents that exist due to thermal generation. You may also need to simulate the presence of interface traps at the silicon/oxide interface. Then, turn on the direct recombination model (AUGER). The parameters for both models can be tuned in the MOBILITY statement. |
| Bandgap Narrowing | This model (BGN) is necessary to correctly model the bipolar current gain when the SOI MOSFET behaves like a bipolar transistor. Specify the parameters for this model in the MODELS statement. |

Table 4-1: SOI Physical Models

| Model | Description |
|---------------------------|--|
| Carrier Generation | Impact ionization significantly modifies the operation of SOI MOSFETs. To account for this phenomena, switch on the impact ionization model (IMPACT) and calibrate for SOI technology. The calibration parameters are set in the IMPACT statement. |
| Lattice Heating | When you switch a device on, there can be significant current density within the silicon. This could generate a significant amount of heat. In bulk MOS devices, the silicon substrates behaves like a good heat conductor. This generated heat is then quickly removed. But this isn't the case with SOI substrates as the buried oxide layer allows this generated heat to be retained. For SOI MOSFETs, this can be a significant amount and can drastically affect the operation of the device. In such cases, take account of this by using the GIGA module. Note that when you switch on lattice heating by using the LAT.TEMP parameter in the MODELS statement, you also need to specify a thermal boundary condition with the THERMCONTACT statement. See Chapter 7: "Giga: Self-Heating Simulator" for more details. |
| Carrier Heating | <p>In deep submicron designs, you may need to switch on the additional energy balance equations. These take into account the exchange of energy between carriers and between the carriers and the lattice. See Section 4.2.1: "Simulating MOS Technologies" for more information.</p> <p>An example of a set of typical models for a partially depleted SOI MOSFET could be:</p> <pre> MODEL KLA SHI FLDMOB SRH AUGER BGN LAT.TEMP INTERFACE QF=1e10 Y.MAX=0.05 INTERFACE QF=1e11 Y.MIN=0.05 THERMCONTACT NUM=1 ELEC.NUM=4 EXT.TEMP=300 IMPACT SELB </pre> |

Numerical Methods for SOI

One important issue with SOI device simulation is the choice of numerical methods. In SOI technology, the potential in the channel (or body) region is commonly referred to as "floating". This occurs because there exists no direct contact to it by any electrode. As a result, when a bias is applied, or increased, on a contact there may be some convergence problem. This occurs because the guess used in the numerical solution scheme for (ψ, n, p) may be poor, particularly in the "floating" region. This is particularly true if impact ionization is used. To overcome the problem of poor initial guess, use the following numerical methods syntax in isothermal drift-diffusion simulations.

```
METHOD GUMMEL NEWTON
```

This method initially performs a GUMMEL iteration to obtain an improved initial guess for the NEWTON solution scheme. Although this method is more robust, this is slower than using the NEWTON scheme alone. For more information on the numerical schemes available, see Chapter 20: "Numerical Techniques".

SOI Physical Phenomena

The physical models and the numerical schemes described above should allow S-PISCES to study all the important SOI phenomena. These include:

- full or partial depletion effects
- threshold voltage
- subthreshold slopes
- front to back gate coupling effects
- leakage current analysis
- high frequency analysis
- device breakdown
- snapback effects
- the kink effect in the output I_{ds} - V_{ds} characteristics
- negative differential resistance

This page is intentionally left blank.

5.1: Overview

If you are unfamiliar with the general operation of the ATLAS framework, read Chapter 2: “Getting Started with ATLAS” before reading this chapter.

BLAZE is a general purpose 2D device simulator for III-V, II-VI materials, and devices with position dependent band structure (e.g., heterojunctions). BLAZE accounts for the effects of positionally dependent band structure by modifications to the charge transport equations and Poisson’s equation. BLAZE is applicable to a broad range of devices such as: HBTs, HEMTs, LEDs, lasers, heterojunction photodetectors (e.g., APDs, solar cells) and heterojunction diodes.

This chapter is composed of several sections. Section 5.1.1: “Basic Heterojunction Definitions” gives an overview of the basic heterojunction band parameters. Section 5.1.2: “Alignment” explains heterojunction alignment. Heterojunction charge transport is covered in Section 5.1.3: “The Drift Diffusion Transport Model”. This section includes the details of how BLAZE modifies the basic transport models to simulate heterodevices. Section 5.2: “The Physical Models” covers the BLAZE models specific to compositionally dependent materials. Detailed information about the material systems encountered in heterojunction simulation is covered in Section 5.3: “Material Dependent Physical Models”. This includes the relationships between the compound elemental concentrations and bandgap, dielectric constant, low field mobility, and other important material and transport parameters. Finally, Section 5.4: “Simulating Heterojunction Devices with Blaze” covers how to define materials and models for heterojunction devices with BLAZE.

See Appendix B: “Material Systems” for the defaults parameters and for some of the materials discussed in this chapter.

5.1.1: Basic Heterojunction Definitions

Figure 5-1 shows the band diagrams and band parameters for a basic p-n heterojunction device under equilibrium conditions. This diagram illustrates two materials with different bandgaps and electron affinities and a Schottky barrier in contact to the n-type material.

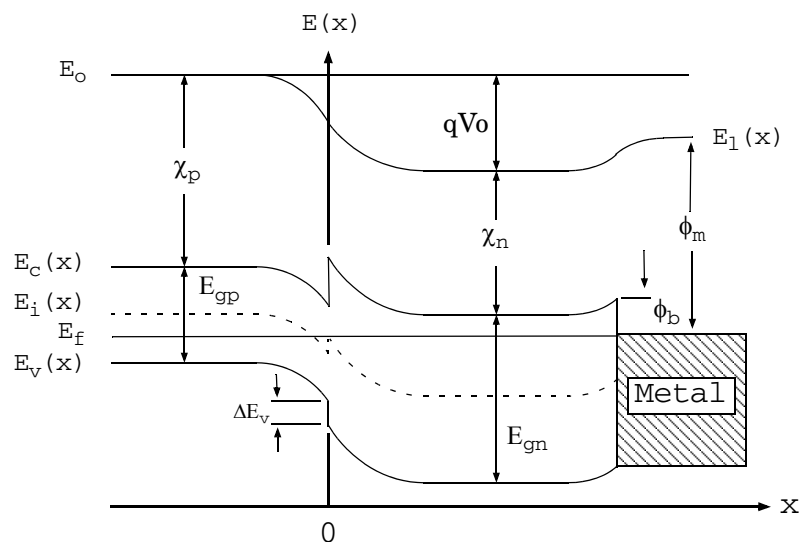


Figure 5-1: Band Diagram of p-n Heterojunction

Referring to Figure 5-1:

- $E_c(x)$, $E_v(x)$ and $E_i(x)$ are the spatially dependent conduction band, valence band and intrinsic energy levels respectively.
- E_f and E_o are the Fermi and Vacuum level energies.
- E_{gp} and E_{gn} are the p-type and n-type material bandgaps.
- ΔE_v is the fraction of the difference between E_{gp} and E_{gn} that appears in the valence band at the heterojunction interface.
- ΔE_c (not labelled) is the fraction of the difference between E_{gp} and E_{gn} that appears in the conduction band at the heterojunction interface.
- qV_o is the built-in potential of the heterojunction.
- χ_p and χ_n are the electron affinities of the p-type and n-type materials.
- ϕ_m is the work function of the metal.
- ϕ_b is the barrier height between the metal and the semiconductor.

The basic band parameters for defining heterojunctions in BLAZE are bandgap parameter, EG300, AFFINITY, and the conduction and valence band density of states, NC300 and NV300. To define these parameters for each material, use the MATERIAL statement. Other transport parameters relating these basic definitions to compound elemental concentrations (X.COMPOSITION and Y.COMPOSITION) can also be defined.

See Section 5.3: “Material Dependent Physical Models” for a description of these relationships for each material system and the Section 5.4: “Simulating Heterojunction Devices with Blaze” for their usage.

The work function of metals is defined using the CONTACT statement.

Note: In the following, the affinities are defined by the vacuum energy minus the lowest conduction band edge energy.

5.1.2: Alignment

As shown from Figure 5-1, the difference between the two materials bandgaps creates conduction and valence band discontinuities. The distribution of bandgap between the conduction and valence bands has a large impact on the charge transport in these heterodevices. There are two methods for defining the conduction band alignment for a heterointerface. The first method is the Affinity Rule, which uses the ALIGN parameter on the MATERIAL statement. The second method is to adjust the material affinities using the AFFINITY parameter on the MATERIAL statement.

The Affinity Rule

This is the default method in BLAZE for assigning how much of the bandgap difference appears as the conduction band discontinuity. The affinity rule assigns the conduction band discontinuity equal to the difference between the two materials electron affinities (AFFINITY on the MATERIAL statement). The affinity rule method is used by default for all materials where the ALIGN parameter has not been defined on the MATERIAL statement.

Using the ALIGN parameter in the MATERIAL statement

Experimental measurements of band discontinuities can differ from what is assigned using the affinity rule with the standard material electron affinities. Therefore, BLAZE allows ΔE_c to be calculated by specifying the ALIGN parameter on the MATERIAL statement. ALIGN specifies the fraction of the bandgap difference, which will appear as the conduction band discontinuity. This bandgap difference is between the material, which is specified by the ALIGN parameter, and the smallest bandgap material in the overall structure (the reference material). Use the ALIGN parameter to modify the electron affinity of the material and BLAZE will create the desired conduction band offset.

In many applications, a Schottky barrier or more than two different semiconductor materials are present. Keep the reference material bandgap and these assigned affinities in mind when defining offsets for multiple materials or Schottky barrier heights. Examples for multiple materials and Schottky barriers are given in the following section. In the following examples, ΔE_g , ΔX , ΔE_c , and E_v are positive.

Manually Adjusting Material Affinity

You can use the AFFINITY parameter on the MATERIAL statement to adjust the conduction band offset. The following examples describe the procedure for aligning heterojunctions using this method in BLAZE.

EXAMPLE 1

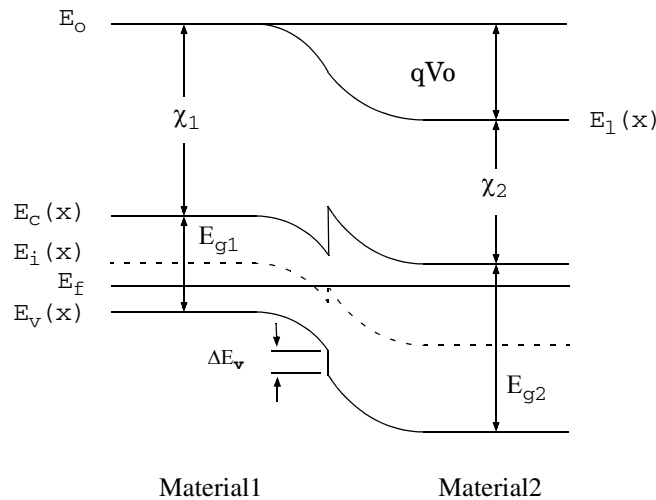


Figure 5-2: Band diagram of heterojunction with band offset.

Figure 5-2 shows a heterojunction consisting of two semiconductors with different bandgaps E_{g1} and E_{g2} and electron affinities χ_1 and χ_2 . This example is similar to the bandstructure of a HFET or HEMT. For this example, $E_{g1} < E_{g2}$ and $\chi_2 < \chi_1$.

Allocating the conduction band offsets using the affinity rule:

$$\Delta E_c = \chi_1 - \chi_2 \quad 5-1$$

$$\Delta E_g = E_{g2} - E_{g1} \quad 5-2$$

and

$$\Delta E_v = \Delta E_g - \Delta E_c \quad 5-3$$

ΔE_c is the amount of the conduction band discontinuity at the heterointerface. ΔE_v is the amount of the valence band discontinuity.

Note: The Affinity Rule is used to calculate the conduction band offset for a material if the `ALIGN` parameter is not specified on the `MATERIAL` statement for that material.

Using the `ALIGN` parameter on the `MATERIAL` statement

Let's assign 80% of the bandgap difference between `Material1` and `Material2` to the conduction band offset. Then, define the `ALIGN` parameter on the `MATERIAL` statement for `Material2` using

```
MATERIAL NAME=Material2 ALIGN=0.80
```

Then:

$$\Delta E_c = (E_{g2} - E_{g1}) \cdot 0.80 \quad 5-4$$

Internally, the affinity of `Material2` is adjusted so that ΔE_c equals this value. This value of electron affinity will override any electron affinity specification for `Material2`. This has an impact on any calculation where this material's electron affinity is used and considered when specifying Schottky barriers contacted to this materials. See "EXAMPLE 4" on page 5-10 for more details on Schottky barrier considerations.

Manually Adjusting Material Affinity

```
MATERIAL NAME=Material2 AFFINITY=VALUE
```

where `VALUE` is adjusted to provide for the desired conduction band offset as calculated by the affinity rule, that is, relative to all other assigned affinities. This value of electron affinity will override any prior specification of electron affinity for `Material2`. This has an impact on any calculation where this material's electron affinity is used and must be considered when specifying Schottky barriers contacted to this materials. See "EXAMPLE 4" on page 5-10 for more details on Schottky barrier considerations

Note: If you do not specify the `ALIGN` parameter on the `MATERIAL` statement, `BLAZE` will use the Affinity Rule and either the default electron affinity or the affinity assigned using the `AFFINITY` parameter on the `MATERIAL` statement to calculate the conduction band offsets.

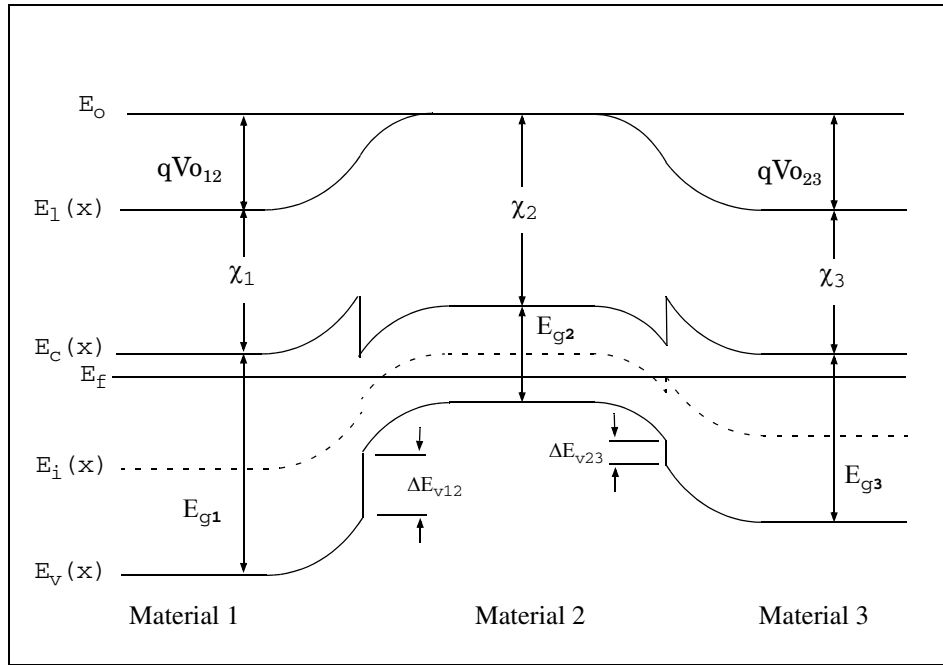
EXAMPLE 2**Figure 5-3: Band diagram of three material system (lowest E_g in center)**

Figure 5-3 details a heterostructure device consisting of three semiconductors with different bandgaps E_{g1} , E_{g2} and E_{g3} and electron affinities χ_1 , χ_2 and χ_3 . This is similar to the band diagram of a Double Heterojunction Bipolar Transistor. For this example, $E_{g1} > E_{g2} < E_{g3}$ and $\chi_1 < \chi_2 > \chi_3$.

Allocating the conduction band offsets using the affinity rule:

$$\Delta E_{c12} = \chi_2 - \chi_1 \quad 5-5$$

$$\Delta E_{g12} = E_{g1} - E_{g2} \quad 5-6$$

and

$$\Delta E_{v12} = \Delta E_{g12} - \Delta E_{c12} \quad 5-7$$

for the heterojunction between Material1 and Material2 and:

$$\Delta E_{c23} = \chi_2 - \chi_3 \quad 5-8$$

$$\Delta E_{g23} = E_{g2} - E_{g3} \quad 5-9$$

and

$$\Delta E_{v23} = \Delta E_{g23} - \Delta E_{c23} \quad 5-10$$

for the heterojunction between Material2 and Material3.

Notice the reference material (i.e., material) with the smallest bandgap. In this case, Material2, is located between the two larger bandgap materials, Material1, and Material3.

Let's assign 80% of the bandgap difference between Material1 and Material2 to the conduction band offset for this heterojunction. Then, define the ALIGN parameter on the MATERIAL statement for Material 1 using:

```
MATERIAL NAME=Material1 ALIGN=0.8
```

then:

$$\Delta E_{c12} = (E_{g1} - E_{g2}) \cdot 0.80 \quad 5-11$$

Internally, the affinity of Material1 is adjusted so that ΔE_{c12} equals this value.

Let's assign 70% of the bandgap difference between Material3 and Material2 to the conduction band offset for this heterojunction. Defining the ALIGN parameter on the MATERIAL statement for Material3 using:

```
MATERIAL NAME=Material3 ALIGN=0.70
```

then:

$$\Delta E_{c23} = (E_{g3} - E_{g2}) \cdot 0.70 \quad 5-12$$

Internally, the affinity of Material3 is adjusted so that ΔE_{c23} equals this value.

These new values of electron affinity for Material1 and Material3 will override any electron affinity specification for these materials. This has an impact on any calculation where these materials's electron affinity is used and must be considered when specifying Schottky barriers contacted to these materials. See "EXAMPLE 4" on page 5-10 for more details on Schottky barrier considerations.

Manually Adjusting Material Affinity

You can assign the conduction band offsets for each heterojunction by setting the electron affinities for Material1 and Material3 using the AFFINITY parameter on the MATERIAL statement.

Let's assume an electron affinity for Material2 of 4eV (~ that of GaAs). Let's decide that between Material1 and Material2, the conduction band offset is 0.3eV and that between Material3 and Material2, the conduction band offset is 0.2eV. Then, for Material1:

```
MATERIAL NAME=Material1 AFFINITY=3.7
```

and for Material3:

```
MATERIAL NAME=Material3 AFFINITY=3.8
```

This is the easiest method to define the conduction band offsets for multiple materials. This value of electron affinity will override any electron affinity specification. This has an impact on any calculation where this material's electron affinity is used and must be considered when specifying Schottky barriers contacted to this materials. See "EXAMPLE 4" on page 5-10 for more details on Schottky barrier considerations.

Note: The band offsets are always defined with reference to the conduction band. Therefore, if a specific valence band offset is required, the appropriate conduction band offset should be calculated from the desired valence band offset and the materials bandgap.

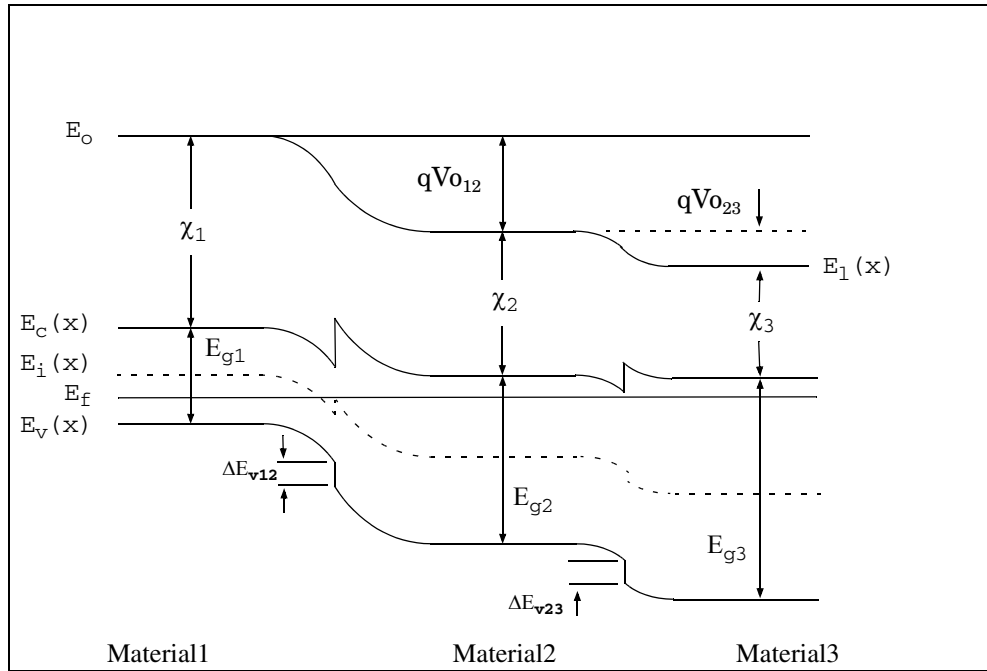
EXAMPLE 3**Figure 5-4: Band diagram of three material system (lowest E_g not in center)**

Figure 5-4 details a heterostructure device consisting of three semiconductors with different bandgaps E_{g1} , E_{g2} and E_{g3} and electron affinities χ_1 , χ_2 and χ_3 . This is similar to the “EXAMPLE 2” on page 5-5, except that the narrow bandgap material is not located in between the other larger bandgap materials. This will add extra complexity to the conduction and valence band offset calculations. For this example, $E_{g1} < E_{g2} < E_{g3}$ and $\chi_3 < \chi_2 < \chi_1$.

Allocating the conduction band offsets using the affinity rule:

$$\Delta E_{c12} = \chi_1 - \chi_2 \quad 5-13$$

$$\Delta E_{g12} = E_{g2} - E_{g1} \quad 5-14$$

and

$$\Delta E_{v12} = \Delta E_{g12} - \Delta E_{c12} \quad 5-15$$

for the heterojunction between Material1 and Material2 and:

$$\Delta E_{c23} = \chi_2 - \chi_3 \quad 5-16$$

$$\Delta E_{g23} = E_{g3} - E_{g2} \quad 5-17$$

and

$$\Delta E_{v23} = \Delta E_{g23} - \Delta E_{c23} \quad 5-18$$

for the heterojunction between Material2 and Material3.

Using the ALIGN parameter on the MATERIAL statement

Notice that the reference material (i.e., the material with the smallest bandgap), Material1, is not shared between the two larger bandgap materials, Material2, and Material3. This will be important in calculating the conduction band offsets for the heterojunction formed by Material2 and Material3.

Let's assign 80% of the bandgap difference between Material1 and Material2 to the conduction band offset for this heterojunction. Since the reference material is one of the materials of this heterojunction, we can proceed as before. Define the ALIGN parameter in the MATERIAL statement for Material2 using:

```
MATERIAL NAME=Material2 ALIGN=0.8
```

then

$$\Delta E_{c12} = (E_{g2} - E_{g1}) \cdot 0.80 \quad 5-19$$

Let's assign 70% of the bandgap difference between Material3 and Material2 to the conduction band offset for this heterojunction. Since the reference material is not one of the materials in this heterojunction, another procedure will be used. Since BLAZE always uses the bandgap of the reference material (the smallest bandgap material in overall structure) when calculating the conduction band offset using the ALIGN parameter on the MATERIAL statement, the actual value for the ALIGN parameter needs to be calculated as follows:

$$\text{ALIGN} = (\Delta E_{g32} / \Delta E_{g31}) \cdot (\Delta E_{c32} / \Delta E_{g32}) \quad 5-20$$

Once calculated, you can use this value for the ALIGN parameter on the MATERIAL statement for Material3. For this example, let's assume that

$$\Delta E_{g32} = 0.2 \quad 5-21$$

$$\Delta E_g = E_{g2} - E_{g1} \quad 5-22$$

and

$$\Delta E_{g31} = 0.4 \quad 5-23$$

then for a desired conduction band offset fraction of 0.70:

$$\text{ALIGN} = (\Delta E_{g32} / \Delta E_{g31}) \cdot (\Delta E_{c32} / \Delta E_{g32}) = (0.2 / 0.4) \times 0.70 = 0.35 \quad 5-24$$

You can assign the proper value of the ALIGN parameter reflecting the desired conduction band offset as:

```
MATERIAL NAME=Material3 ALIGN=0.35
```

This assigns 70% of the bandgap difference between Material3 and Material2 as the conduction band offset.

Note: Calculating ALIGN in this manner is only necessary when the reference material is not in contact with the material where the ALIGN parameter will be specified.

These new values of electron affinity for Material2 (from the first heterojunction band offset calculation) and Material3 (from the second heterojunction band offset calculation) will override any electron affinity specification for these materials. This has an impact on any calculation where these materials's electron affinity is used and must be considered when specifying Schottky barriers contacted to these materials. See “EXAMPLE 4” on page 5-10 for more details on Schottky barrier considerations.

Manually Adjusting Material Affinity

You can assign the conduction band offsets for each heterojunction by setting the electron affinities for Material2 and Material3 using the AFFINITY parameter on the MATERIAL statement. The electron affinity for Material2 is adjusted relative to Material1 and Material3 is adjusted relative to Material2 by the amount of the desired conduction band offset for each heterojunction. Since Material1 affinity is larger than that for Material2 and Material2 affinity is larger than that for Material3, the affinities for Material2 and Material3 are reduced to provide the desired conduction band offsets.

Let's assume an electron affinity for Material1 of 4eV (~ that of GaAs). Let's decide that between Material1 and Material2, the conduction band offset is 0.3eV and that between Material2 and Material 3, the conduction band offset is 0.2eV. Then, for Material2:

```
MATERIAL NAME=Material2 AFFINITY=3.7
```

and for Material3:

```
MATERIAL NAME=Material3 AFFINITY=3.5
```

This is the easiest method to define the conduction band offsets for multiple materials. This has an impact on any calculation where this materials electron affinity is used and must be considered when specifying Schottky barriers contacted to this materials. See “EXAMPLE 4” on page 5-10 for more details on Schottky barrier considerations.

Note: The band offsets are always defined with reference to the conduction band. Therefore, if a specific valence band offset is required, the appropriate conduction band offset should be calculated from the desired valence band offset and the materials bandgap.

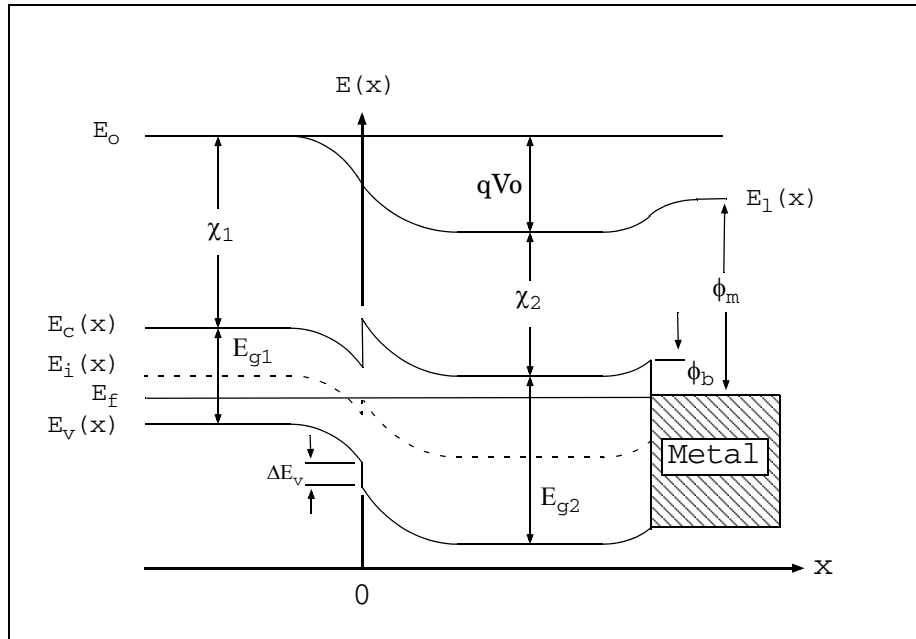
EXAMPLE 4**Figure 5-5: Schematic band diagram for an abrupt heterojunction**

Figure 5-5 details a heterostructure device consisting of two semiconductors with different bandgaps E_{g1} and E_{g2} and electron affinities χ_1 and χ_2 and a Schottky barrier. For this example, $E_{g1} < E_{g2}$ and $\chi_2 < \chi_1$.

This example will first define the heterojunction band offsets and then the Schottky barrier height. Schottky contact barrier heights are calculated by BLAZE using the metal work function and the semiconductor electron affinity as:

$$\phi_b = \phi_m - \chi_s \quad 5-25$$

where ϕ_b is the Schottky barrier height, ϕ_m is the work function of the metal, and χ_s is the semiconductor electron affinity. ϕ_m is set using the `WORKFUN` parameter in the `CONTACT` statement. Therefore, the semiconductor electron affinity as modified or defined during the heterojunction alignment process plays an important role in determining the value of the metal workfunction needed to provide the desired barrier height. Let's assume for this example that a Schottky barrier height of 0.2eV is desired and calculate the appropriate metal workfunction for each case.

Using the Affinity rule for the heterojunction

$$\Delta E_c = \chi_1 - \chi_2 \quad 5-26$$

and

$$\Delta E_v = \Delta E_g - \Delta E_c \quad 5-27$$

ΔE_c is the amount of the conduction band discontinuity at the heterointerface. ΔE_v is the amount of the valence band discontinuity.

Note: The Affinity Rule is used for a material if the `ALIGN` parameter is not specified on the `MATERIAL` statement for that material.

Let's use an electron affinity for `Material1` of 4eV and for `Material2` of 3.5eV. Since the affinity of the material on which the Schottky barrier is formed was not modified with this method of alignment, the metal work function needed to provide for a Schottky barrier height of 0.2eV is:

$$\phi_m = 3.5 + 0.2 = 3.7 \quad 5-28$$

You can now assign this value to the `WORKFUN` parameter on the `CONTACT` statement as:

```
CONTACT NUMBER=1 WORKFUN=3.7
```

This produces a Schottky barrier height of 0.2eV between the metal and `Material 2` using the `ALIGN` parameter on the `MATERIAL` statement:

Let's assign 80% of the bandgap difference between `Material1` and `Material2` to the conduction band offset, an electron affinity for `Material1` of 4eV, and ΔE_g of 0.2eV. Then, define the `ALIGN` parameter on the `MATERIAL` statement for `Material2` using:

```
MATERIAL NAME=Material2 ALIGN=0.80
```

Then:

$$\Delta E_c = (E_{g2} - E_{g1}) \cdot 0.80 = 0.2 \cdot 0.80 = 0.16 \quad 5-29$$

Internally, the affinity of `Material2` is reduced by 0.16eV so:

$$\chi_2 = \chi_1 - \Delta E_c = (4 - 0.16) = 3.84 \quad 5-30$$

You can use this value of electron affinity to assign the proper value of `WORKFUN` on the `CONTACT` statement to provide for a Schottky barrier height of 0.2eV.

$$\phi_m = 3.84 + 0.2 = 4.04 \quad 5-31$$

You can now assign this value to the `WORKFUN` parameter on the `CONTACT` statement as:

```
CONTACT NUMBER=1 WORKFUN=4.04
```

producing a Schottky barrier height of 0.2eV between the metal and `Material2`.

Manually Adjusting Material Affinity

Let's assign a conduction band offset between `Material1` and `Material2` of 0.15eV, an electron affinity for `Material1` of 4eV, and the desired Schottky barrier height of 0.2eV. The affinity for `Material2` is calculated from the affinity of `Material1` and the desired conduction band offset as:

$$\chi_2 = \chi_1 - 0.15 = 4 - 0.15 = 3.85 \quad 5-32$$

This is then used to assign the value of `AFFINITY` using:

```
MATERIAL NAME=Material2 AFFINITY=3.85
```

You can now use this value of electron affinity to calculate the metal workfunction necessary to produce a Schottky barrier height of 0.2eV as:

$$\phi_m = 3.85 + 0.2 = 4.05 \quad 5-33$$

You can now assign this value to the WORKFUN parameter on the CONTACT statement as:

```
CONTACT NUMBER=1 WORKFUN=4.05
```

This produces a Schottky barrier height of 0.2eV between the metal and Material2.

5.1.3: The Drift Diffusion Transport Model

Drift-Diffusion with Position Dependent Band Structure

The current continuity equations for electrons and holes, and the Poisson Equation (see Chapter 3: "Physics", Equation 3-1) are the same as for the homogeneous case. Although the changing dielectric constant is taken into account. The current density expressions, however, must be modified to take into account the nonuniform band structure [146]. This procedure starts with the current density expressions:

$$\vec{J}_n = -\mu_n n \nabla \phi_n \quad 5-34$$

$$\vec{J}_p = -\mu_p p \nabla \phi_p \quad 5-35$$

where ϕ_n and ϕ_p are quasi-Fermi potentials.

$$\phi_n = \frac{1}{q} E_{FN} \quad 5-36$$

$$\phi_p = \frac{1}{q} E_{FP} \quad 5-37$$

The conduction and valence band edge energies can be written as:

$$E_c = q(\psi_0 - \psi) - \chi \quad 5-38$$

$$E_v = q(\psi_0 - \psi) - \chi - E_g \quad 5-39$$

where:

- ψ_0 is some reference potential.
- χ is the position-dependent electron affinity.
- E_g is the position-dependent bandgap.
- ψ_0 can be selected in the form:

$$\psi_0 = \frac{\chi_r}{q} + \frac{kT_L}{q} \ln \frac{N_{cr}}{n_{ir}} = \frac{\chi_r + E_g}{q} - \frac{kT_L}{q} \ln \frac{N_{vr}}{n_{ir}} \quad 5-40$$

where n_{ir} is the intrinsic carrier concentration of the arbitrarily selected reference material, and r is the index that indicates all of the parameters are taken from reference material.

Fermi energies are expressed in the form:

$$E_{FN} = E_c + kT_L \ln \frac{n}{N_c} - kT_L \ln \gamma_n \quad 5-41$$

$$E_{FP} = E_v + kT_L \ln \frac{n}{N_v} - kT_L \ln \gamma_p \quad 5-42$$

The final terms in Equations 5-41 and 5-42 are due to the influence of Fermi-Dirac statistics. These final terms are defined as follows:

$$\gamma_n = \frac{F_{1/2}(\eta_n)}{\eta_n}, \quad \eta_n = \frac{E_{FN} - E_c}{kT_L} = F_{1/2}^{-1}\left(\frac{n}{N_c}\right) \quad 5-43$$

$$\gamma_p = \frac{F_{1/2}(\eta_p)}{\eta_p}, \quad \eta_p = \frac{E_v - E_{FP}}{kT_L} = F_{1/2}^{-1}\left(\frac{p}{N_v}\right) \quad 5-44$$

where N_c and N_v are position-dependent and $\gamma_n = \gamma_p = 1$ for Boltzmann statistics.

By combining Equations 5-34 to 5-44, you can obtain the following expressions for current densities.

$$\vec{J}_n = kT_L \mu_n \nabla n - q \mu_n n \nabla \left(\psi + \frac{kT_L}{q} \ln \gamma_n + \frac{\chi}{q} + \frac{kT_L}{q} \ln \frac{N_c}{n_{ir}} \right) \quad 5-45$$

$$\vec{J}_p = kT_L \mu_p \nabla p - q \mu_p p \nabla \left(\psi + \frac{kT_L}{q} \ln \gamma_p + \frac{\chi + E_g}{q} + \frac{kT_L}{q} \ln \frac{N_v}{n_{ir}} \right) \quad 5-46$$

5.1.4: The Thermionic Emission and Field Emission Transport Model

You can activate alternative current density expressions for electron and hole current [261,267], which take into account thermionic emission dominated current in abrupt heterojunctions. These equation applies only at the node points along the interface of the heterojunction and take the form:

$$\vec{J}_n = q v_n (1 + \delta) \left(n^+ - n^- \exp\left(\frac{-\Delta E_C}{kT_L}\right) \right) \quad 5-47$$

$$\vec{J}_p = (-q) v_p (1 + \delta) \left(p^+ - p^- \exp\left(\frac{-\Delta E_V}{kT_L}\right) \right) \quad 5-48$$

where J_n and J_p are the electron and hole current densities from the "-" region to the "+" region. v_n and v_p are the electron and hole thermal velocities. ΔE_c is conduction band energy change going from the "-" region to the "+" region. ΔE_v is the valence band energy change going from the "-" region to the "+" region. The δ parameter represents the contribution due to thermionic field emission (tunneling).

The thermal velocities v_n and v_p are given by:

$$v_n = \frac{A_n^* T_L^2}{q N_C} \quad 5-49$$

$$\nu_p = \frac{A_p^* T_L^2}{q N_V} \quad 5-50$$

where T_L is the lattice temperature, N_C is the conduction band density of states, N_V is the valence band density of states and A_n^* and A_p^* are the electron and hole Richardson constants.

The minimum valued Richardson constants from the “-” region or “+” region are used for the calculation of the thermal velocities [267]. You can specify the Richardson constants with the `ARICHN` and `ARICHP` parameters of the `MATERIAL` statement. If the Richardson constants aren't specified, the following expressions will be used:

$$A_n^* = \frac{4\pi q k^2 m_n^*}{h^3} \quad 5-51$$

$$A_p^* = \frac{4\pi q k^2 m_p^*}{h^3} \quad 5-52$$

where m_n^* and m_p^* are the electron and hole effective masses. The electron and hole effective masses can be specified with the `M.VTHN` and `M.VTHP` parameters of the `MATERIAL` statement. If the effective masses aren't specified, then they will be calculated from the conduction and valence band densities of states using Equations 3-31 and 3-32 in Chapter 3: “Physics”. To enable the thermionic transport model, you must specify `THERMIONIC` on the `INTERFACE` statement. You must also set the `S.S` parameter on the `INTERFACE` statement to indicate that the model applies to semiconductor-semiconductor interfaces.

The tunneling factor δ in Equation 5-47 is zero when the tunneling mechanism is neglected. When you account for tunneling by specifying the `TUNNEL` parameter in the `INTERFACE` statement, the tunneling factor, δ , is calculated by using the expression:

$$\delta = \frac{1}{kT} \int_{E_{min}}^{E_C^+} \exp\left(\frac{E_C^+ - E_x}{kT}\right) \exp\left(\frac{-4\pi}{h} \int_0^{X_E} \left[2m_n^*(E_C - E_x)\right]^{0.5} dx\right) dE_x \quad 5-53$$

where E_x is the energy component in the X direction and $E_{min} = \max[E_c(0^-), E_c(W)]$ as described in Figure 5-6.

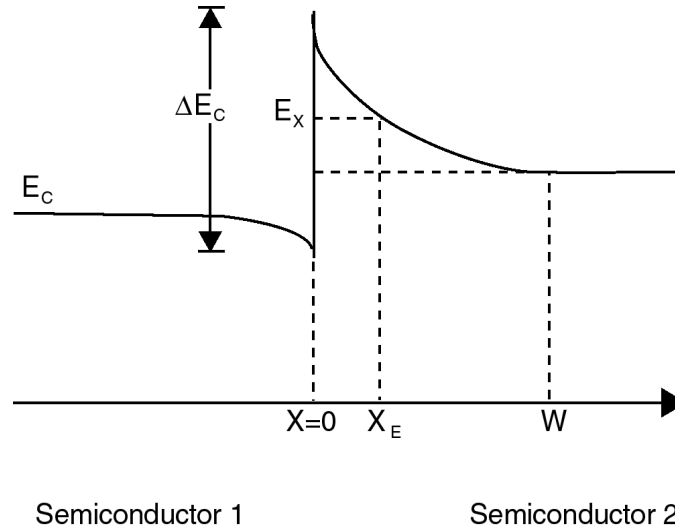


Figure 5-6: Band Diagram of p-n heterojunction

5.1.5: Temperature Dependence of Electron Affinity

The electron affinity of a semiconductor is generally a function of lattice temperature. This temperature dependence is usually modelled implicitly in ATLAS by making it a fraction of the temperature dependence of the bandgap. The default value of the fraction is 0.5 but you can assign it a value in the range [0,1] using the `CHI. EG. TDEP`.

If you specify the `ALIGN` parameter, then `CHI. EG. TDEP` will be ignored. In that case, the affinity is adjusted to keep the conduction band offset at the specified ratio of the bandgap differences at the heterojunction at the particular temperature required.

Example 1

For a material where the affinity is given only at 300 K (e.g., GaAs) the electron affinity at temperature T would be

$$\chi(T) = \chi(300) - \text{CHI. EG. TDEP} \times (E_g(T_L) - E_g(300)) \quad 5-54$$

Example 2

For HgCdTe, the affinity depends on bandgap and consequently temperature (see Equation 5-153). In this case, you must include the following statement.

```
MATERIAL MATERIAL=HGCDTE CHI. EG. TDEP=0
```

Example 3

If you are using `F.BANDCOMP` to specify the electron affinity and your function includes its full temperature dependence, then specify `CHI. EG. TDEP = 0` on the `MATERIAL` statement.

If your function excludes temperature dependence of affinity, then you can use the value of `CHI. EG. TDEP` to adjust this.

Note: The `ASYMMETRY` parameter on the `MATERIAL` statement will be used to assign a fraction of bandgap narrowing to the affinity. See Section 3.2.9: "Bandgap Narrowing" for more information.

5.2: The Physical Models

Chapter 3: “Physics”, Section 3.6: “Physical Models” already describes a comprehensive set of physical models for silicon. It is known, however, that for III-V, II-VI, and ternary compounds that special consideration are required such as for mole fraction dependence and material properties. The following sections describe the material dependent physical models that have been implemented into BLAZE to account for these effects.

First, a description of the common mobility model equations is given. These equations are applicable to all materials unless stated in the following material sections. Following this are sections describing the physical models on a material-per-material basis. For each material, there are descriptions of the models for bandgap narrowing, electron affinity, density of states, dielectric permittivity, and low field mobility.

5.2.1: Common Physical Models

Low Field Mobility Models

The default low field mobility models used for most materials in BLAZE are given by the following:

$$\mu_{n0}(T_L) = \text{MUN} \left(\frac{T_L}{300} \right)^{-\text{TMUN}} \quad 5-55$$

$$\mu_{p0}(T_L) = \text{MUP} \left(\frac{T_L}{300} \right)^{-\text{TMUP}} \quad 5-56$$

where T_L is the temperature in degrees Kelvin and the MUN, MUP, TMUN and TMUP parameters are user-definable as shown in Table 5-1.

Note: All the mobility models described in Chapter 3: “Physics”, except for the TASCH model, can be used in BLAZE. But all default coefficients exist only for Silicon and therefore are not suitable for compound materials.

Table 5-1. User-Specifiable Parameters for Equations 5-55 and 5-56

| Statement | Parameter | Units |
|-----------|-----------|-------------------------|
| MOBILITY | MUN | cm ² / V · s |
| MOBILITY | TMUN | |
| MOBILITY | MUP | cm ² / V · s |
| MOBILITY | TMUP | |

Parallel Electric Field-Dependent Mobility Models

There are two types of electric field-dependent mobility models used in ATLAS/BLAZE. These models are called Standard Mobility Model and Negative Differential Mobility Model. Both of these models contain appropriate default values of parameters for different materials. You need to specify which type of mobility will be used for each material and which material parameters you want to alter.

The Standard Mobility Model that takes account of velocity saturation is defined according to:

$$\mu_n(E) = \mu_{n0} \left[\frac{1}{1 + \left(\frac{\mu_{n0} E}{VSATN} \right)^{BETAN}} \right]^{1/BETAN} \quad 5-57$$

$$\mu_p(E) = \mu_{p0} \left[\frac{1}{1 + \left(\frac{\mu_{p0} E}{VSATP} \right)^{BETAP}} \right]^{1/BETAP} \quad 5-58$$

where VSATN and VSATP are the saturation velocities for electrons and holes, BETAN and BETAP are constants given in Table 5-2, and $\mu_{n0,p0}$ are the electron and hole low field mobilities. This model is activated by specifying the FLDMOB and the EVSATMOD=0 parameter in the MODEL statement.

| Table 5-2. User-Specifiable Parameters for Equations 5-57 and 5-58 | | |
|--|-----------|-------|
| Statement | Parameter | Units |
| MOBILITY | BETAN | |
| MOBILITY | BETAP | |
| MOBILITY | VSATN | cm/s |
| MOBILITY | VSATP | cm/s |

The Negative Differential Mobility Model of Barnes et. al. [21] has been implemented to account for certain devices where the carrier drift velocity peaks at some electric field before reducing as the electric field increases. This model takes account of this through the carrier mobility with equations of the form:

$$\mu_n(E) = \frac{\mu_{n0} + \frac{VSATN}{E} \left(\frac{E}{ECRITN} \right)^{GAMMAN}}{1 + \left(\frac{E}{ECRITN} \right)^{GAMMAN}} \quad 5-59$$

$$\mu_p(E) = \frac{\mu_{p0} + \frac{VSATP}{E} \left(\frac{E}{ECRITP} \right)^{GAMMAP}}{1 + \left(\frac{E}{ECRITP} \right)^{GAMMAP}} \quad 5-60$$

where VSATN and VSATP are the electron and hole saturation velocities, E_0 is a constant, and $\mu_{n0,p0}$ are the low-field electron and hole mobilities. To activate this mobility model, specify EVSATMOD=1 in the MODEL statement.

| Table 5-3. User-Specifiable Parameters for Equations 5-59 and 5-60 | | | |
|--|-----------|-------------------|-------|
| Statement | Parameter | Default | Units |
| MOBILITY | ECRITN | 4.0×10^3 | V/cm |
| MOBILITY | ECRITP | 4.0×10^3 | V/cm |
| MOBILITY | GAMMAN | 4.0 | |
| MOBILITY | GAMMAP | 1.0 | |

Note: The Negative Differential Mobility Model introduces an instability in the solution process and is not recommended for general use. Only activate this model in cases where the device operation directly depends on negative differential mobility (e.g., a Gunn diode).

For both the standard and negative differential models, an empirical temperature-dependent model for saturation velocity in GaAs [142] is implemented according to:

$$VSATN = VSATN.T0 - VSATN.T1 T_L \quad 5-61$$

$$VSATP = VSATP.T0 - VSATP.T1 T_L \quad 5-62$$

where $VSATN$ and $VSATP$ are expressed in cm/sec and T_L is the temperature in degrees Kelvin.

Alternatively, you can set the saturation velocities to constant values using the $VSATN$ and $VSATP$ parameters of the `MATERIAL` statement.

| Table 5-4. User-Specifiable Parameters for Equations 5-61 and 5-62 | | | |
|--|-----------|--------------------|--------|
| Statement | Parameter | Default | Units |
| MOBILITY | VSATN.T0 | 1.13×10^7 | cm/s |
| MOBILITY | VSATN.T1 | 1.2×10^6 | cm/s·K |
| MOBILITY | VSATP.T0 | 1.13×10^7 | cm/s |
| MOBILITY | VSATP.T1 | 1.2×10^4 | cm/s·K |

Velocity Saturation with Energy Balance Transport Model

When the Energy Balance Transport Model is activated, the mobility can be made a function of carrier energy. In Chapter 3: “Physics”, Section 3.6.1: “Mobility Modeling”, physical models for the dependence of carrier mobility on carrier energy were introduced. The same models are applicable for use within BLAZE with one additional model, which applies when the negative differential mobility model is used.

The carrier temperature dependence is activated when the `EVSATMOD=1` parameter is on the `MODEL` statement. This model can be derived in a similar fashion as in the case of `EVSATMOD=0` described in Chapter 3: “Physics”, “Parallel Electric Field-Dependent Mobility” on page 3-77. These expressions, however, require several piecewise approximations, which are too in-depth to show in this manual. To say that these piecewise expressions provide a continuous velocity saturation model for mobility versus carrier temperature are completely like the expressions for drift diffusion given in Equations 3-288 and 3-289 from Chapter 3: “Physics”.

5.2.2: Recombination and Generation Models

The recombination and generation models for compound semiconductors are the same as the models previously described in Chapter 3: “Physics”, Section 3.6.3: “Carrier Generation-Recombination Models”. The default parameters for different materials are automatically used, unless new values are specified. The default parameter values are listed in Appendix B: “Material Systems”.

5.3: Material Dependent Physical Models

5.3.1: Cubic III-V Semiconductors

The basic band parameters (E_g , χ , ϵ , N_c , and N_v) of most III-V cubic can be modeled using composition dependent interpolation schemes from the parameters of the constituent binary semiconductors. Table 5-5 lists the compound semiconductors you can model using this approach. The first column of this table gives the material name used on the REGION, DOPING, ELECTRODE, PRINT, MODELS, MATERIAL, INTERFACE, IMPACT, MOBILITY, TRAP, DEFECT, PROBE, LASER, and ODEFECTS statements. The second column of Table 5-5 shows the association of composition fractions with the constituent elements. The third column indicates whether this model is used by default (see Section 3.2.5: “Rules for Evaluation of Energy Bandgap”). If this model is not used, then there is another default model for that material described in the section listed in the last column of the table.

You can apply the Cubic III-V model to materials, which use an alternative model described in the **Section** column of Table 5-5, by setting the CUBIC35 parameter of the MODELS statement.

In specifying a material name, ATLAS will recognize alternate spellings switching the order of cations or anions as long as you remember to maintain the associations of elements with composition fractions as given in Table 5-5 (e.g., $\text{Al}(x)\text{Ga}(1-x)\text{As} = \text{Ga}(1-x)\text{Al}(x)\text{As}$).

| Table 5-5. Cubic III-V Interpolation Model Applicability Chart | | | |
|--|---------------------------------------|---------|---------|
| ATLAS Name | Composition | Default | Section |
| GaAs | | No | 5.3.2 |
| AlP | | Yes | |
| AlAs | | No | 5.3.3 |
| AlSb | | Yes | |
| GaSb | | Yes | |
| GaP | | No | 5.3.4 |
| InP | | No | 5.3.4 |
| InSb | | Yes | |
| InAs | | No | 5.3.4 |
| AlGaAs | $\text{Al}(x)\text{Ga}(1-x)\text{As}$ | No | 5.3.3 |
| InAlP | $\text{In}(1-x)\text{Al}(x)\text{P}$ | Yes | |
| InGaAs | $\text{In}(1-x)\text{Ga}(x)\text{As}$ | No | 5.3.4 |
| InGaP | $\text{In}(1-x)\text{Ga}(x)\text{P}$ | No | 5.3.4 |
| GaSbP | $\text{GaSb}(1-y)\text{P}(y)$ | Yes | |
| InAlAs | $\text{In}(1-x)\text{Al}(x)\text{As}$ | Yes | |
| InAsP | $\text{InAs}(1-y)\text{P}(y)$ | No | 5.3.4 |
| GaAsP | $\text{GaAs}(1-y)\text{P}(y)$ | No | 5.3.4 |
| InGaSb | $\text{In}(1-x)\text{Ga}(x)\text{Sb}$ | Yes | |

| Table 5-5. Cubic III-V Interpolation Model Applicability Chart | | | |
|--|--|-----|-------|
| InAlSb | $\text{In}(1-x)\text{Al}(x)\text{Sb}$ | Yes | |
| AlGaSb | $\text{Al}(x)\text{Ga}(1-x)\text{Sb}$ | Yes | |
| InAsSb | $\text{InAs}(y)\text{Sb}(1-y)$ | Yes | |
| GaAsSb | $\text{GaAs}(y)\text{Sb}(1-y)$ | Yes | |
| AlAsSb | $\text{AlAs}(y)\text{Sb}(1-y)$ | Yes | |
| InPSb | $\text{InSb}(1-y)\text{P}(y)$ | Yes | |
| AlPSb | $\text{AlP}(y)\text{Sb}(1-y)$ | Yes | |
| AlPAs | $\text{AlP}(y)\text{As}(1-y)$ | Yes | |
| AlGaP | $\text{Al}(x)\text{Ga}(1-x)\text{P}$ | Yes | |
| InPAsSb | $\text{InP}(x)\text{As}(y)\text{Sb}(1-x-y)$ | Yes | |
| InGaAsP | $\text{In}(1-x)\text{Ga}(x)\text{As}(1-y)\text{P}(y)$ | No | 5.3.4 |
| AlGaAsP | $\text{Al}(x)\text{Ga}(1-x)\text{As}(1-y)\text{P}(y)$ | Yes | |
| AlGaAsSb | $\text{Al}(x)\text{Ga}(1-x)\text{As}(y)\text{Sb}(1-y)$ | Yes | |
| InAlGaAs | $\text{In}(1-x-y)\text{Al}(x)\text{Ga}(y)\text{As}$ | Yes | |
| InAlGaP | $\text{In}(1-x-y)\text{Al}(x)\text{Ga}(y)\text{P}$ | Yes | |
| InAlAsP | $\text{In}(1-x)\text{Al}(x)\text{As}(1-y)\text{P}(y)$ | Yes | |
| InGaAsSb | $\text{In}(1-x)\text{Ga}(x)\text{As}(y)\text{Sb}(1-y)$ | Yes | |
| InAlAsSb | $\text{In}(1-x)\text{Al}(x)\text{As}(y)\text{Sb}(1-y)$ | Yes | |

Energy Bandgap

The energy bandgaps of the binary compounds are calculated for transitions in each of the Γ , X and L directions using the universal formula for temperature dependent bandgap (see Equation 3-38). Table 5-7 shows the default parameters for Equation 3-38 for the binary compounds.

| Table 5-6. Default Bandgap Parameters for Cubic III-V Binary Compounds [179] | | | | | | | | | |
|--|-------------------------|----------------------------|-----------------------|--------------------|-----------------------|------------------|--------------------|-----------------------|------------------|
| Binary | $E_g^\Gamma(0)$ (eV) | α^Γ (meV/K) | β^Γ (K) | $E_g^X(0)$ (eV) | α^X (meV/K) | β^X (K) | $E_g^L(0)$ (eV) | α^L (meV/K) | β^L (K) |
| GaAs | 1.519 | 0.5405 | 204.0 | 1.981 | 0.4600 | 204.0 | 1.815 | 0.6050 | 204 |
| AlP | 3.63 | 0.5771 | 372.0 | 2.52 | 0.3180 | 588.0 | 3.57 | 0.3180 | 588 |
| AlAs | 3.099 | 0.885 | 530.0 | 2.240 | 0.700 | 530.0 | 2.460 | 0.605 | 240 |
| AlSb | 2.386 | 0.42 | 140.0 | 1.696 | 0.39 | 140.0 | 2.329 | 0.58 | 140 |
| GaSb | 0.812 | 0.417 | 140.0 | 1.141 | 0.475 | 94.00 | 0.875 | 0.597 | 140 |
| GaP | 2.886 | 0.0 | 0.0 | 2.350 | 0.5771 | 372.0 | 2.720 | 0.5771 | 372 |

Table 5-6. Default Bandgap Parameters for Cubic III-V Binary Compounds [179]

| | | | | | | | | | |
|------|--------|-------|-------|--------|-------|------|--------|-------|-----|
| InP | 1.4236 | 0.363 | 162.0 | 2.3840 | 0.0 | 0.0 | 2.0140 | 0.363 | 162 |
| InSb | 0.235 | 0.32 | 170.0 | 0.630 | 0.00 | 0.0 | 0.930 | 0.00 | 0.0 |
| InAs | 0.417 | 0.276 | 93.0 | 1.433 | 0.276 | 93.0 | 1.133 | 0.276 | 93 |

For the ternary materials the bandgap in each principal direction is approximated by the function [2]:

$$Tabc(x) = xTac + (1-x)Tbc - x(1-x)Cabc \quad 5-63$$

where $Tabc$ is the ternary bandgap, Tac and Tbc are the binary bandgaps, x is the composition fraction and $Cabc$ is the bowing factor as given for each of the ternary compounds in each of the principal directions in Table 5-6.

Table 5-7. Bowing Factors and Alignment for Cubic III-V Ternary Compounds [179]

| Ternary | $C(Eg^{\Gamma})$ (eV) | $C(Eg^X)$ (eV) | $C(Eg^L)$ (eV) | dEc/dEg |
|---------|--------------------------|-------------------|-------------------|---------|
| AlGaAs | $1.31*x-0.127$ | 0.055 | 0.0 | 0.65 |
| InAlP | -0.48 | 0.38 | 0.0 | 0.5 |
| InGaAs | 0.477 | 1.4 | 0.33 | 0.4 |
| InGaP | 0.65 | 0.2 | 1.3 | 0.4 |
| GaSbP | 2.558 | 2.7 | 2.7 | 0.5 |
| GaSbAs | 1.43 | 1.2 | 1.2 | 0.5 |
| InAlAs | 0.7 | 0.0 | 0.0 | 0.7 |
| InAsP | 0.1 | 0.27 | 0.27 | 0.4 |
| GaAsP | 0.19 | 0.24 | 0.16 | 0.4 |
| InGaSb | 0.415 | 0.330 | 0.4 | 0.5 |
| InAlSb | 0.43 | 0.0 | 0.0 | 0.5 |
| AlGaSb | $1.22*x-0.044$ | 0.0 | 0.0 | 0.5 |
| InAsSb | 0.67 | 0.6 | 0.6 | 0.5 |
| GaAsSb | 1.43 | 1.2 | 1.2 | 0.5 |
| AlAsSb | 0.84 | 0.28 | 0.28 | 0.5 |
| InPSb | 1.9 | 1.9 | 1.9 | 0.5 |
| AlPSb | 3.56 | 2.7 | 2.7 | 0.5 |
| AlPAs | 0.22 | 0.22 | 0.22 | 0.5 |
| AlGaP | 0.0 | 0.13 | 0.0 | 0.5 |

For the quaternary compounds, the bandgap in each principal direction is approximated by the function [2]:

$$Q_{abcd}(x, y) = \frac{x(1-x)[yTabc(x) + (1-y)Tabd(x)] + y(1-y)[xTacd(y) + (1-x)Tbcd(y)]}{x(1-x) + y(1-y)} \quad 5-64$$

or for compounds with three anions [2]:

$$Q_{abcd}(x, y) = \frac{xyTabc(u) + y(1-x-y)Tacd(v) + (1-x-y)xTabd(w)}{xy + y(1-x-y) + (1-x-y)x} \quad 5-65$$

where $Tabc$, $Tabd$, $Tacd$, and $Tbcd$ are the ternary bandgaps, x and y are the composition fractions and u , v and w are given as follows:

$$u = (1-x+y)/2 \quad 5-66$$

$$v = (2-x-2y)/2 \quad 5-67$$

and

$$w = (2-2x-y)/2 \quad 5-68$$

For any case (binary, ternary or quaternary), the bandgap used in the drift-diffusion calculations is taken as the minimum of E_g^Γ , E_g^X or E_g^L .

Electron Affinity

Table 5-8 shows the electron affinities for the binary compounds in the given direction in k space.

| Table 5-8. Default Electron Affinities and Alignments for Cubic III-V Binary Compounds [179] | | | |
|--|---------------|-----------|---------|
| Binary | Affinity (eV) | Direction | dEc/dEg |
| GaAs | 4.07 | Γ | 0.65 |
| AlP | 3.98 | X | 0.7 |
| AlAs | 3.85 | X | 0.65 |
| AlSb | 3.60 | X | 0.5 |
| GaSb | 4.06 | Γ | 0.5 |
| GaP | 4.0 | X | 0.4 |
| InP | 4.4 | Γ | 0.4 |
| InSb | 4.59 | Γ | 0.5 |
| InAs | 4.90 | Γ | 0.65 |

The affinities for the other directions in k space not given in Table 5-8 are calculated by the following:

$$\chi^{\Gamma} = \chi^X - (Eg^X - Eg^{\Gamma})(dEc/dEg) \quad 5-69$$

$$\chi^X = \chi^{\Gamma} - (Eg^{\Gamma} - Eg^X)(dEc/dEg) \quad 5-70$$

$$\chi^L = \chi^{X/\Gamma} - (Eg^{X/\Gamma} - Eg^L)(dEc/dEg) \quad 5-71$$

where X^{Γ} , X^X and X^L are the affinities in each of the principal directions, Eg^{Γ} , Eg^X and Eg^L are the energy bandgaps in each of the principal directions as calculated above and dEc/dEg is an alignment parameter describing the proportion of change in bandgap that can be associated with the conduction band edge. Table 5-8 lists the default values of dEc/dEg . You can define the value of dEc/dEg by using the `DEC.DEG` parameter of the `MATERIAL` statement.

For ternary compounds, the affinities are calculated from the binary values using Equation 5-63 except $Tabc$ is the ternary affinity, Tac and Tbc are the binary affinities and $Cabc$ is the bowing factor for affinity which is given by:

$$Cabc(\chi) = -Cabc(Eg)dEc/dEg \quad 5-72$$

where $Cabc(\chi)$ is the bowing factor for affinity, $Cabc(Eg)$ is the bowing factor for bandgap as given in Table 5-7 and dEc/dEg is the alignment parameter as given in Table 5-7.

For quaternaries, the affinities are approximated by the Equations 5-64 and 5-65 with affinities replacing energy bandgaps.

Finally for all cases (binary, ternary and quaternary), the affinity used in the drift-diffusion calculation is chosen as the one in the same direction (Γ , X or L) as chosen for energy bandgap.

Density of States

For the III-V cubic semiconductor model, the density of states (Nc and Nv) are each calculated from the effective masses using Equations 3-31 and 3-32. For binary materials, the density of states effective masses are given in Table 5-10.

Table 5-9. Default Cubic III-V Effective Masses and Permittivities

| Binary | m_c^{Γ} ($\times mo$) | m_{ct}^X ($\times mo$) | m_{cl}^X ($\times mo$) | m_{ct}^{Γ} ($\times mo$) | m_{cl}^{Γ} ($\times mo$) | m_{hh} ($\times mo$) | m_{lh} ($\times mo$) | ϵ_r |
|--------|-----------------------------------|-------------------------------|-------------------------------|--------------------------------------|--------------------------------------|-----------------------------|-----------------------------|--------------|
| GaAs | 0.067 | 0.23 | 1.3 | 0.0754 | 1.9 | 0.49 | 0.16 | 12.91 |
| AlP | 0.22 | 0.155 | 2.68 | 0.0 | 0.0 | 0.63 | 0.20 | 9.8 |
| AlAs | 0.15 | 0.22 | 0.97 | 0.15 | 1.32 | 0.76 | 0.15 | 10.06 |
| AlSb | 0.14 | 0.123 | 1.357 | 0.23 | 1.64 | 0.94 | 0.14 | 12.04 |
| GaSb | 0.039 | 0.22 | 1.51 | 0.10 | 1.3 | 0.28 | 0.05 | 15.69 |
| GaP | 0.13 | 0.253 | 2.0 | 0.15 | 1.2 | 0.79 | 0.14 | 11.10 |
| InP | 0.0795 | 0.88 | 0.0 | 0.47 | 0.0 | 0.56 | 0.12 | 12.61 |
| InSb | 0.0135 | 0.0 | 0.0 | 0.25 | 0.0 | 0.43 | 0.015 | 17.70 |
| InAs | 0.026 | 0.16 | 1.13 | 0.05 | 0.64 | 0.57 | 0.025 | 15.15 |

For ternary materials, the effective masses are interpolated using the following expression[2]:

$$M_{abc} = xM_{ac} + (1-x)M_{bc} \quad 5-73$$

where M_{abc} is the ternary effective mass, M_{ac} and M_{bc} are the binary effective masses and x is the composition fraction.

For quaternary compounds the effective masses are interpolated using the following expression[2]:

$$M_{abcd} = xyM_{ac} + x(1-y)M_{ad} + (1-x)yM_{bc} + (1-x)(1-y)M_{bd} \quad 5-74$$

or for compounds with 3 anions [2]:

$$M_{abcd} = xM_{ab} + yM_{ab} + (1-x-y)M_{ad} \quad 5-75$$

where M_{abcd} is the quaternary effective mass, M_{ac} , M_{ad} , M_{bc} and M_{bd} are the binary effective masses and x and y are the composition fractions.

For the calculation of conduction band density of states, the conduction band density of states mass is calculated for the same direction (Γ , X or L) as is used for energy bandgap as follows:

$$m_c = m_c^{\Gamma} \quad 5-76$$

$$m_c = \left[(m_{ct}^X)^2 \cdot (m_{cl}^X) \right]^{1/3} \quad 5-77$$

or

$$m_c = \left[(m_{ct}^L)^2 \cdot (m_{cl}^L) \right]^{1/3} \quad 5-78$$

For the calculation of valence band density of states, the valence band density of states mass is calculated as follows:

$$m_v = \left(m_{hh}^{3/2} + m_{lh}^{3/2} \right)^{2/3} \quad 5-79$$

Static Permittivity

Table 5-9 shows the permittivities of the binary compounds. The ternary and quaternary permittivities are approximated by the interpolation formulas analogous to those used for effective mass (Equations 5-73, 5-74 and 5-75) replacing masses by permittivities.

5.3.2: Gallium Arsenide (GaAs) Physical Models

Bandgap Narrowing

Following Klausmeier-Brown [123], the bandgap narrowing effects are important only for p-type regions. By default, BLAZE uses the bandgap narrowing values shown in Table 5-10.

| Table 5-10. Default Bandgap Narrowing Values | |
|--|-------------------------|
| Concentration (cm ⁻³) | Bandgap Narrowing (meV) |
| 1.0×10 ¹⁸ | 31.0 |
| 2.0×10 ¹⁸ | 36.0 |
| 4.0×10 ¹⁸ | 44.2 |
| 6.0×10 ¹⁸ | 48.5 |
| 8.0×10 ¹⁸ | 51.7 |
| 1.0×10 ¹⁹ | 54.3 |
| 2.0×10 ¹⁹ | 61.1 |
| 4.0×10 ¹⁹ | 64.4 |
| 6.0×10 ¹⁹ | 61.9 |
| 8.0×10 ¹⁹ | 56.9 |
| 1.0×10 ²⁰ | 53.2 |
| 2.0×10 ²⁰ | 18.0 |

Note: This table is only used for GaAs. No data is available at present for other materials. The C-INTERPRETER function for bandgap narrowing, however, allows a user-defined model for bandgap narrowing to be applied for these materials. See Appendix A: "C-Interpreter Functions" for more information about on these functions.

Low Field Mobility

You can make the mobility in GaAs concentration dependent by setting the CONMOB parameter of the MODEL statement. In this model, mobility is interpolated from the values in Table 5-11.

| Table 5-11. Default Concentration Dependent Mobility for GaAs | | |
|---|---|-------|
| Concentration (cm ⁻³) | Mobility in GaAs (cm ² /v-s) | |
| | Electrons | Holes |
| 1.0×10 ¹⁴ | 8000.0 | 390.0 |
| 2.0×10 ¹⁴ | 7718.0 | 380.0 |
| 4.0×10 ¹⁴ | 7445.0 | 375.0 |
| 6.0×10 ¹⁴ | 7290.0 | 360.0 |
| 8.0×10 ¹⁴ | 7182.0 | 350.0 |
| 1.0×10 ¹⁵ | 7300.0 | 340.0 |
| 2.0×10 ¹⁵ | 6847.0 | 335.0 |
| 4.0×10 ¹⁵ | 6422.0 | 320.0 |
| 6.0×10 ¹⁵ | 6185.0 | 315.0 |
| 8.0×10 ¹⁵ | 6023.0 | 305.0 |
| 1.0×10 ¹⁶ | 5900.0 | 302.0 |
| 2.0×10 ¹⁶ | 5474.0 | 300.0 |
| 4.0×10 ¹⁶ | 5079.0 | 285.0 |
| 6.0×10 ¹⁶ | 4861.0 | 270.0 |
| 8.0×10 ¹⁶ | 4712.0 | 245.0 |
| 1.0×10 ¹⁷ | 4600.0 | 240.0 |
| 2.0×10 ¹⁷ | 3874.0 | 210.0 |
| 4.0×10 ¹⁷ | 3263.0 | 205.0 |
| 6.0×10 ¹⁷ | 2950.0 | 200.0 |
| 8.0×10 ¹⁷ | 2747.0 | 186.9 |
| 1.0×10 ¹⁸ | 2600.0 | 170.0 |
| 2.0×10 ¹⁸ | 2060.0 | 130.0 |
| 4.0×10 ¹⁸ | 1632.0 | 90.0 |

| Table 5-11. Default Concentration Dependent Mobility for GaAs | | |
|---|---|-------|
| Concentration (cm ⁻³) | Mobility in GaAs (cm ² /v-s) | |
| | Electrons | Holes |
| 6.0×10 ¹⁸ | 1424.0 | 74.5 |
| 8.0×10 ¹⁸ | 1293.0 | 66.6 |
| 1.0×10 ²⁰ | 1200.0 | 61.0 |

If MODEL ANALYTIC is specified, the program will use [123]:

$$\mu_{n,p} = 940 + \frac{8000 - 940}{1 + \left(\frac{Nt}{2.8 \times 10^{16}} \right)^{0.75}} \quad 5-80$$

where Nt is the total impurity concentration.

5.3.3: Al(x)Ga(1-x)As System

The Al(x)Ga(1-x)As material system is commonly used for the fabrication of heterojunction devices. These materials are available in BLAZE by specifying the material name GaAs, AlGaAs, or AlAs. As a ternary material system, different material properties are obtained by adjusting the molar fraction of Aluminum and Gallium. This mole fraction is represented by the x as written in Al(x)Ga(1-x)As. GaAs material parameters are identical to the those of AlGaAs with the mole fraction x set equal to zero. AlAs material parameters are identical to the those of AlGaAs with mole the fraction x set equal to one. Fundamental in the proper simulation with the AlGaAs material system is the relationship between this mole fraction x , and the material parameters for that composition. In the following sections, the relationship between mole fraction and material parameters for the AlGaAs material system will be described. You can specify the x-composition fraction of a material in the REGION statement with the X.COMP parameter.

Bandgap

There are three primary conduction bands in the AlGaAs system, depending on mole fraction, that determine the bandgap. These are named Gamma, L, and X. The default bandgaps for each of these conduction band valleys are as follows:

$$E_{g\Gamma} = EG300 + x.comp \cdot (1.155 + 0.37 \cdot X.COMP) \quad 5-81$$

$$E_{gL} = 1.734 + x.comp \cdot (0.574 + 0.055 \cdot X.COMP) \quad 5-82$$

$$E_{gX} = 1.911 + x.comp \cdot (0.005 + 0.245 \cdot X.COMP) \quad 5-83$$

The bandgap used for any given Al concentration is the minimum as calculated from these equations. EG300 is the bandgap at 300K and specified on the material statement. x.composition is the Aluminum mole fraction and can be user-defined in the REGION statement.

The temperature dependence of the bandgap is calculated according to:

$$E_g(T_L) = E_g(300) + \text{EGALPHA} \cdot \left[\frac{300^2}{300 + \text{EGBETA}} - \frac{T_L^2}{T_L + \text{EGBETA}} \right] \quad 5-84$$

The value of $E_g(300)$ is taken as the minimum of E_{gI} , E_{gx} , and E_{gL} . The default temperature dependent bandgap parameters for AlGaAs are listed in Table 5-12.

| Table 5-12. Default Bandgap Parameters for Al(x)Ga(1-x)As | | | |
|---|-----------|------------------------|-------|
| Statement | Parameter | Default | Units |
| MATERIAL | EG300 | 1.59 | eV |
| MATERIAL | EGALPHA | 5.405×10^{-4} | eV/K |
| MATERIAL | EGBETA | 204 | K |

Electron Affinity

As indicated in the introduction, the semiconductor electron affinity χ is a key parameter for determining the alignment of heterojunctions. For AlGaAs, χ is a function of E_{gI} and is given by:

$$\chi_{AlGaAs} = 4.07 - 0.85 \cdot (E_{gI}(\text{X.COMP}) - E_{gGaAs}) \quad 5-85$$

Density of States and Effective Mass

The valence and conduction band densities of states, N_C and N_V , are calculated from the effective masses according to the following equations:

$$N_c = 2 \left(\frac{2\pi m_e^* k T_L}{h^2} \right)^{\frac{3}{2}} \quad 5-86$$

$$N_v = 2 \left(\frac{2\pi m_h^* k T_L}{h^2} \right)^{\frac{3}{2}} \quad 5-87$$

For the AlGaAs system the conduction band and valence band effective masses, for electrons and holes, are given by [146]:

$$m_e = \begin{cases} 0.067 + 0.083x & (0 < x < 0.45) \\ 0.85 - 0.14x & (x > 0.45) \end{cases} \quad 5-88$$

$$m_{lh} = 0.087 + 0.063x \quad 5-89$$

$$m_{hh} = 0.62 + 0.14x \quad 5-90$$

$$m_h = (m_{lh}^{3/2} + m_{hh}^{3/2})^{2/3} \quad 5-91$$

Dielectric Permittivity

The default static dielectric constant for AlGaAs is given by:

$$\varepsilon_{AlGaAs} = 13.18 - 2.9 \cdot X.COMP \quad 5-92$$

Low Field Mobility

The default low field electron mobility for AlGaAs is a function of the composition fraction, x, within the system. The following equations outline this relationship.

| Table 5-13. Low Field Mobility Equations | |
|---|---------------------------|
| AlGaAs Low Field Mobility | Mole Fraction Range |
| $\mu_n = 8000 - (1.818 \times 10^4 \cdot X.COMP)$ | $(0 < X.COMP < 0.429)$ |
| $\mu_n = 90 + 1.1435 \times 10^4 \cdot (X.COMP - 0.46)^2$ | $(0.429 < X.COMP < 0.46)$ |
| $\mu_n = 90 + 3.75 \times 10^4 \cdot (X.COMP - 0.46)^2$ | $(0.46 < X.COMP < 0.5)$ |
| $\mu_n = 200 - (2 / (X.COMP - 0.46))$ | $(0.5 < X.COMP < 1.0)$ |

5.3.4: In(1-x)Ga(x)As(y)P(1-y) System

The In(1-x)Ga(x)As(y)P(1-y) material system is commonly used for the fabrication of heterojunction devices. These include laser diodes, photodiodes, Gunn diodes, and high speed heterostructure transistors. As a quaternary material, two different mole fraction parameters, x and y, are necessary to specify any particular combination. This produces a wide array of InGaAsP materials and characteristics. Of particular interest in this system are materials that are lattice matched to InP.

The default material characteristics in BLAZE for the InGaAsP system correspond to composition fractions x and y that yield InGaAsP material that is lattice matched to InP. The xcomposition and ycomposition are specified in the REGION statement with the X.COMP and Y.COMP parameters. The relationship between x and y that satisfy this condition is given by:

$$x = \frac{0.1896 \cdot Y.COMP}{0.4176 - (0.0125 \cdot Y.COMP)} \quad 0 < Y.COMP < 1 \quad 5-93$$

Many of the parameter models for the In(1-x)Ga(x)As(y)P(1-y) system are functions of the composition fraction Y.COMP only. The composition fraction, X.COMP, can be deduced from the preceding relationship. Again, the default material characteristics in BLAZE for the InGaAsP system correspond to composition fractions x and y that yield InGaAsP material that is lattice matched to InP.

Note: Don't use this material system to form GaAs by setting x=1 and y=1, specify GaAs as the material instead.

Bandgap

The default energy bandgap for the InP lattice matched In(1-x)Ga(x)As(y)P(1-y) system used in BLAZE is given by:

$$E_g(\text{InGaAsP}) = 1.35 + X \cdot \text{COMP} \cdot (0.642 + (0.758 \cdot X \cdot \text{COMP})) + (0.101 \cdot Y \cdot \text{COMP} - 1.101) \cdot Y \cdot \text{COMP} - (0.28 \cdot X \cdot \text{COMP} - 0.109 \cdot Y \cdot \text{COMP} + 0.159) \cdot X \cdot \text{COMP} \cdot Y \cdot \text{COMP} \quad 5-94$$

Electron Affinity

The electron affinities for materials in the InP lattice matched InGaAsP system are derived from conduction band offsets and from the assumption that the affinity of InP is 4.4eV. The default conduction band edge offset between lattice matched InGaAsP and InP is then:

$$\Delta E_c = 0.268 \cdot Y \cdot \text{COMP} + 0.003 \cdot (Y \cdot \text{COMP})^2 \quad 5-95$$

Density of States and Effective Mass

The density of states is defined, as before, as a function of the effective masses of electrons and holes according to Chapter 3: "Physics", Equation 3-31. For the InGaAsP system, the default conduction and valence band effective masses, for electrons and holes, are given by the following.

For the conduction band:

$$m_e^* = 0.08 - (0.116 \cdot Y \cdot \text{COMP}) + (0.026 \cdot X \cdot \text{COMP}) - 0.059 \cdot (X \cdot \text{COMP} \cdot Y \cdot \text{COMP}) + (0.064 - 0.02 \cdot Y \cdot \text{COMP}) \cdot (X \cdot \text{COMP})^2 + (0.06 + 0.032 \cdot X \cdot \text{COMP}) \cdot (Y \cdot \text{COMP})^2 \quad 5-96$$

For the valence band the hole effective mass is defined by:

$$m_h^* = \left(m_{lh}^{1.5} + m_{hh}^{1.5} \right)^{\frac{2}{3}} \quad 5-97$$

where the default light hole effective mass is given by:

$$m_{lh} = 0.120 - (0.116 \cdot Y \cdot \text{COMP}) + 0.03 \cdot (X \cdot \text{COMP})^2 \quad 5-98$$

and the default heavy hole effective mass is a constant and is given by:

$$m_{hh} = 0.46 \quad 5-99$$

Dielectric Permittivity

The default static dielectric constant for lattice matched InGaAsP to InP is given by

$$\epsilon_{\text{InGaAsP}} = (14.6 \cdot (1 - X \cdot \text{COMP}) \cdot Y \cdot \text{COMP}) + 12.5 \cdot (1 - X \cdot \text{COMP}) \cdot (1 - Y \cdot \text{COMP}) + 13.18 \cdot X \cdot \text{COMP} \cdot Y \cdot \text{COMP} + 11.11 \cdot X \cdot \text{COMP} \cdot (1 - Y \cdot \text{COMP}) \quad 5-100$$

Low Field Mobility

The default low field mobility parameters for electrons and holes for lattice matched InGaAs are given by linear interpolations from the binary compounds GaAs and InP. The following formulas are used:

$$\mu_{n1} = 33000 + (8500 - 33000) \cdot X \cdot \text{COMP} \quad 5-101$$

$$\mu_{p1} = 460 + (400 - 460) \cdot X \cdot \text{COMP} \quad 5-102$$

$$\mu_{n2} = 4600 + (300 - 4600) \cdot X \cdot \text{COMP} \quad 5-103$$

$$\mu_{p2} = 150 + (100 - 150) \cdot X \cdot \text{COMP} \quad 5-104$$

$$\mu_{n0} = \mu_{n1} + (1 - Y \cdot \text{COMP})(\mu_{n2} - \mu_{n1}) \quad 5-105$$

$$\mu_{p0} = \mu_{p1} + (1 - Y \cdot \text{COMP})(\mu_{p2} - \mu_{p1}) \quad 5-106$$

5.3.5: The Si(1-x)Ge(x) System

Advances in the growth of Silicon and Si(1-x)Ge(x) alloys have allowed the potential for using bandgap engineering to construct heterojunction devices such as HBTs and HEMTs using these materials. BLAZE supports the SiGe material system by providing composition dependent material parameters. These parameters are accessed by specifying the material name SiGe.

The following sections describe the functional relationship between Ge mole fraction x , and the SiGe material characteristics necessary for device simulation.

Bandgap [132]

Bandgap is one of the most fundamental parameters for any material. For SiGe, the dependence of the bandgap on the Ge mole fraction, $x \cdot \text{composition}$, is divided into ranges as follows:

$$E_g = 1.08 + X \cdot \text{COMP} \cdot (0.945 - 1.08) / 0.245; \quad 5-107$$

for $x \leq 0.245$

$$E_g = 0.945 + (X \cdot \text{COMP} - 0.245) \cdot (0.87 - 0.945) / (0.35 - 0.245); \quad 5-108$$

for $0.245 < x \leq 0.35$

$$E_g = 0.87 + (X \cdot \text{COMP} - 0.35) \cdot (0.78 - 0.87) / (0.5 - 0.35); \quad 5-109$$

for $0.35 < x \leq 0.5$

$$E_g = 0.78 + (X \cdot \text{COMP} - 0.5) \cdot (0.72 - 0.78) / (0.6 - 0.5); \quad 5-110$$

for $0.5 < x \leq 0.6$

$$E_g = 0.72 + (X \cdot \text{COMP} - 0.6) \cdot (0.69 - 0.72) / (0.675 - 0.6); \quad 5-111$$

for $0.6 < x \leq 0.675$

$$E_g = 0.69 + (X.COMP - 0.675) \cdot (0.67 - 0.69) / (0.735 - 0.675); \quad 5-112$$

for $0.675 < x \leq 0.735$

$$E_g = 0.67; \quad 5-113$$

for $0.735 < x \leq 1$

The temperature dependence of the bandgap of SiGe is calculated the same as for Silicon except that EGALPHA and EGBETA are a function of Ge mole fraction x as follows:

$$E_g(T_L) = E_g + EGALPHA \left[\frac{300^2}{300 + EGBETA} - \frac{T_L^2}{T_L + EGBETA} \right] \quad 5-114$$

$$EGALPHA = (4.73 + X.COMP \cdot (4.77 - 4.73)) \times 10^4 \quad 5-115$$

$$EGBETA = 626 + X.COMP \cdot (235 - 636) \quad 5-116$$

where E_g is dependent upon the mole fraction as above.

Electron Affinity

The electron affinity χ of SiGe is taken to be constant (4.17) with respect to composition.

Density of States

The density of states for SiGe is defined differently compared to the previous materials by not being a function of the effective masses. Instead the density of states have been made to depend upon the Ge mole fraction, *x.composition*, according to:

$$N_c = 2.8 \times 10^{19} + X.COMP \cdot (1.04 \times 10^{19} - 2.8 \times 10^{19}) \quad 5-117$$

$$N_v = 1.04 \times 10^{19} + X.COMP \cdot (6.0 \times 10^{18} - 1.04 \times 10^{19}) \quad 5-118$$

Dielectric Function

The compositional dependence of the static dielectric constant of SiGe is given by

$$\epsilon = 11.8 + 4.2 \cdot X.COMP \quad 5-119$$

Low Field Mobility

No specific SiGe low field mobility models have been implemented into BLAZE.

Velocity Saturation

In SiGe, the temperature dependent velocity saturation, used in the field dependent mobility model is defined by the following equations.

$$VSATN = 1.38 \times 10^7 \cdot \sqrt{\tanh\left(\frac{175}{T_L}\right)} \quad 5-120$$

$$VSATP = 9.05 \times 10^6 \cdot \sqrt{\tanh\left(\frac{312}{T_L}\right)} \quad 5-121$$

Note: All other defaults used for SiGe are taken from Silicon

5.3.6: Silicon Carbide (SiC)

Silicon carbide materials are of interest for high power, high temperature applications. The main characteristics of silicon carbide are that they have a very wide bandgap, high thermal conductivity, high saturation velocity, and high breakdown strength. Silicon carbide is commercially available in three polytypes called 6H-SiC, 3H-SiC, and 4H-SiC. ATLAS supports all three these polytypes. The following paragraphs describe the material defaults for these materials.

Band Parameters for SiC

SiC band parameter equations are identical to those used for Silicon but with the values adjusted for 3C-SiC, 4H-SiC, and 6H-SiC. The physical band parameter values are shown in Tables B-15 and B-16 of Appendix B: "Material Systems".

SiC Mobility Parameters

Isotropic Mobility

By default, mobility is assumed to be entirely isotropic in nature. That is, there is no directional component. The default low field mobilities of electrons and holes for 3C-SiC, 4H-SiC, and 6H-SiC are shown in Table 5-14.

| Table 5-14. Silicon Carbide Low Field Mobility Defaults | | | | | |
|---|-----------|--------|--------|--------|-------------------------------------|
| Statement | Parameter | 6H-SiC | 3C-SiC | 4H-SiC | Units |
| MOBILITY | MUN | 330 | 1000 | 460 | $\text{cm}^2/\text{V}\cdot\text{s}$ |
| MOBILITY | MUP | 60 | 50 | 124 | $\text{cm}^2/\text{V}\cdot\text{s}$ |

Anisotropic Mobility

The mobility behavior within SiC is now known to be anisotropic in nature, which dramatically alters the electrical performance of a device. A anisotropic model has been implemented into ATLAS to correctly model this behavior. Following the ideas of Lindefelt [141] and Lades [130], the mobility within the drift diffusion equations has been made a tensor property. As a result the mobility has become:

$$\mu = \begin{bmatrix} \mu_1 & 0 & 0 \\ 0 & \mu_1 & 0 \\ 0 & 0 & \mu_2 \end{bmatrix} \quad 5-122$$

where μ_1 represents the mobility defined in one plane and μ_2 the mobility defined in a second plane. In the case of SiC, μ_1 represents the mobility of the direction $\langle 1100 \rangle$ while μ_2 represents the mobility of the direction $\langle 1000 \rangle$. These mobilities are defined for both holes and electrons.

Anisotropy is handled by allowing you to specify mobility parameters in two directions normal to each other. To enable the model, specify the N.ANGLE or P.ANGLE or both parameters of the MOBILITY statement. When you specify the parameter(s), it signifies that the mobility parameter values and model flags in the enclosing MOBILITY statement apply along the specified angle, with respect to the X

axis, for electrons (N.ANGLE) and holes (P.ANGLE). The parameter values and model flags specified in a second MOBILITY statement (without the N.ANGLE or P.ANGLE specification) apply to all normal directions (in the x-y plane) to the angle specified in the other statement.

When calculating the current along an element edge, the direction vector of the edge is used to calculate the weighting of the two mobilities specified by the two MOBILITY statements. The weights (w_1 and w_2) are taken to be the dot product of the current direction vector with the angle specified on the N.ANGLE or P.ANGLE parameter for the associated parameters and models, the dot product of the current direction vector, and the normal to the specified angle for the models and parameters not associated with the N.ANGLE or P.ANGLE parameter specification.

The net weighted mobility is calculated by a weighted application of Mattheissen's rule as given by Equation 5-123.

$$\mu = \frac{1}{\frac{w_1}{\mu_1} + \frac{w_2}{\mu_2}} \quad 5-123$$

Defining Anisotropic Mobility in ATLAS

To define a material with anisotropic mobility, specify two MOBILITY statements. In each statement, the N.ANGLE and P.ANGLE parameters are used to specify the direction where that particular mobility is to apply. The following example shows how this is done.

```
# FIRST DEFINE MOBILITY IN PLANE <1100>
#
MOBILITY MATERIAL=3C-SiC VSATN=2E7 VSATP=2E7 BETAN=2 BETAP=2 \
    MU1N.CAUG=10 MU2N.CAUG=410 NCRITN.CAUG=13E17 \
    DELTAN.CAUG=0.6 GAMMAN.CAUG=0.0 \
    ALPHAN.CAUG=-3 BETAN.CAUG=-3 \
    MU1P.CAUG=20 MU2P.CAUG=95 NCRITP.CAUG=1E19 \
    DELTAP.CAUG=0.5 GAMMAP.CAUG=0.0 \
    ALPHAP.CAUG=-3 BETAP.CAUG=-3
#
# NOW DEFINE MOBILITY IN PLANE <1000>
#
MOBILITY MATERIAL=3C-SiC N.ANGLE=90.0 P.ANGLE=90.0 VSATN=2E7 VSATP=2E7 \
    BETAN=2 BETAP=2 MU1N.CAUG=5 MU2N.CAUG=80 NCRITN.CAUG=13E17 \
    DELTAN.CAUG=0.6 GAMMAN.CAUG=0.0 \
    ALPHAN.CAUG=-3 BETAN.CAUG=-3 \
    MU1P.CAUG=2.5 MU2P.CAUG=20 NCRITP.CAUG=1E19 \
    DELTAP.CAUG=0.5 GAMMAP.CAUG=0.0 \
    ALPHAP.CAUG=-3 BETAP.CAUG=-3
```

In this example, the second MOBILITY statement applies to the direction 90° with respect to the X axis (or along the Y axis). The first MOBILITY statement without the N.ANGLE and P.ANGLE parameter assignments applies along the X axis.

Anisotropic Impact Ionization of 4H-SiC

To enable a model [91] for the anisotropic impact ionization rate of 4H-SiC, specify the `ANISO` parameter of the `IMPACT` statement. In this model, the following equations describe the ionization rate:

$$\alpha(E_x E_y) = a \exp \left(-c \sqrt{1 - A^2 c^2 \left(\frac{E_x E_y}{b_x b_y} \right)^2} \right) \quad 5-124$$

$$A = \ln(a_y/a_x) \quad 5-125$$

$$c = \frac{b}{E} = \left(\frac{E_x^2}{b_x^2} + \frac{E_y^2}{b_y^2} \right)^{-1/2} \quad 5-126$$

$$a = a_x \frac{c^2 E_x^2}{b_x^2} a_y \frac{c^2 E_y^2}{b_y^2} \quad 5-127$$

Here, E_x and E_y are the electric field magnitude in the x and y directions. The values parameters a_x , a_y , b_x , and b_y depend upon the crystal orientation. The crystal orientation can be either 0001 or 1120 as specified by either the `SIC4H0001` or the `SIC4H1120` flag of the `IMPACT` statement. By default, `SIC4H0001` is selected.

The values associated with the y coordinates (a_y and b_y) correspond to the selected orientation. The values of the unselected orientation are then associated with the x coordinates (a_x and b_x). Table 5-15 shows the default values of a_x , b_x , a_y , and b_y , where AE^* and BE^* are for electrons and AH^* and BH^* are for holes.

| Table 5-15. Anisotropic Impact Ionization Model Defaults | | | |
|--|-----------|--------------------|------------------|
| Parameter | Statement | Default | Units |
| AE0001 | IMPACT | 1.76×10^8 | cm^{-1} |
| BE0001 | IMPACT | 3.30×10^7 | V/cm |
| AH0001 | IMPACT | 3.41×10^8 | cm^{-1} |
| BH0001 | IMPACT | 2.50×10^7 | V/cm |
| AE1120 | IMPACT | 2.10×10^7 | cm^{-1} |
| BE1120 | IMPACT | 1.70×10^7 | V/cm |
| AH1120 | IMPACT | 2.96×10^7 | cm^{-1} |
| BH1120 | IMPACT | 1.60×10^7 | V/cm |

Thermal Parameters

The equations governing these effects are identical to those for Silicon but with adjusted coefficients. See Appendix B: “Material Systems” for a list of all these parameters.

5.3.7: GaN, InN, AlN, Al(x)Ga(1-x)N, In(x)Ga(1-x)N, Al(x)In(1-x)N, and Al(x)In(y)Ga(1-x-y)N

The following sections describe the relationship between mole fraction, X_{COMP} , and the material parameters and various physical models specific to the Al/In/GaN system.

Bandgap

By default, the bandgap for the nitrides is calculated in a two step process. First, the bandgap(s) of the relevant binary compounds are computed as a function of temperature, T , using Equations 5-128 through 5-130 [241].

$$Eg(GaN) = 3.507 - \frac{0.909 \times 10^{-3} T^2}{T + 830.0} \quad 5-128$$

$$Eg(InN) = 1.994 - \frac{0.245 \times 10^{-3} T^2}{T + 624.0} \quad 5-129$$

$$Eg(AlN) = 6.23 - \frac{1.799 \times 10^{-3} T^2}{T + 1462.0} \quad 5-130$$

Note: The bandgap for InN contradicts recent observations [246,55,262] of a bandgap of less than 1.0 eV. Despite these observations, we keep the above specified value to maintain consistency with ternary and quaternary blends. You should carefully consider whether to use the default values, or supply your own values using one of the standard methods of user specification. The simplest method is to specify EG300 on the MATERIAL statement.

Then, the dependence on composition fraction, x , is described by Equations 5-131 and 5-132 [179].

$$Eg(In_xGa_{1-x}N) = Eg(InN)x + Eg(GaN)(1-x) - 3.8x(1-x) \quad 5-131$$

$$Eg(Al_xGa_{1-x}N) = Eg(AlN)x + Eg(GaN)(1-x) - 1.3x(1-x) \quad 5-132$$

$$Eg(Al_xIn_{1-x}N) = Eg(AlN)x + Eg(InN)(1-x)$$

Electron Affinity

The electron affinity is calculated such that the band edge offset ratio is given by [179].

$$\frac{\Delta Ec}{\Delta Ev} = \frac{0.7}{0.3} \quad 5-133$$

You can override this ratio by specifying the ALIGN parameter of the MATERIAL statement.

Permittivity

The permittivity of the nitrides as a function of composition fraction, x , is given by linear interpolations of the values for the binary compounds as in Equations 5-134 and 5-135 [8].

$$\varepsilon(In_xGa_{1-x}N) = 15.3x + 8.9(1-x) \quad 5-134$$

$$\varepsilon(Al_xGa_{1-x}N) = 85x + 8.9(1-x) \quad 5-135$$

Density of States Masses

The nitride density of states masses as a function of composition fraction, x , is given by linear interpolations of the values for the binary compounds as in Equations 5-136 through 5-139 [241].

$$m_e(In_xGa_{1-x}N) = 0.12x + 0.2(1-x) \quad 5-136$$

$$m_h(In_xGa_{1-x}N) = 0.17x + 1.0(1-x) \quad 5-137$$

$$m_e(Al_xGa_{1-x}N) = 0.314x + 0.2(1-x) \quad 5-138$$

$$m_h(Al_xGa_{1-x}N) = 0.417x + 1.0(1-x) \quad 5-139$$

Low Field Mobility

The Albrecht Model

You can choose to model low field mobility following the work of Albrecht et.al [6] by specifying ALBRCT on the MODEL statement or ALBRCT.N or ALBRCT.P or both on the MOBILITY statement for separate control over electrons and holes. This model is described as follows:

$$\begin{aligned} \frac{1}{\mu(N, T_L)} &= \frac{AN \cdot ALBRCT \cdot N}{N0N \cdot ALBRCT} \left(\frac{T_L}{T0N \cdot ALBRCT} \right)^{-3/2} \\ &\ln \left[1 + 3 \left(\frac{T_L}{T0N \cdot ALBRCT} \right)^2 \left(\frac{N}{N0N \cdot ALBRCT} \right)^{-2/3} \right] \\ &+ BN \cdot ALBRCT \times \left(\frac{T_L}{T0N \cdot ALBRCT} \right)^{3/2} + \\ &\frac{CN \cdot ALBRCT}{\exp(T1N \cdot ALBRCT / T_L) - 1} \end{aligned} \quad 5-140$$

where $\mu(N, T)$ is the mobility as a function of doping and lattice temperature, N is the total doping concentration, and T_L is the lattice temperature. AN.ALBRCT, BN.ALBRCT, CN.ALBRCT, N0N.ALBRCT, T0N.ALBRCT and T1N.ALBRCT are user-specifiable parameters on the MOBILITY statement. You can use a similar expression for holes with the user-defined parameters AP.ALBRCT, BP.ALBRCT, CP.ALBRCT, N0P.ALBRCT, T0P.ALBRCT and T1P.ALBRCT.

Table 5-16 shows the default values for the parameters of the Albrecht Model.

| Table 5-16. Default Parameter Values for the Albrecht Model | | | | |
|---|------------------------|------------|------------------------|----------------------|
| Parameter | Default | Parameter | Default | Units |
| AN.ALBRCT | 2.61×10^{-4} | AP.ALBRCT | 2.61×10^{-4} | $V \cdot s / (cm^2)$ |
| BN.ALBRCT | 2.9×10^{-4} | BP.ALBRCT | 2.9×10^{-4} | $V \cdot s / (cm^2)$ |
| CN.ALBRCT | 170.0×10^{-4} | CP.ALBRCT | 170.0×10^{-4} | $V \cdot s / (cm^2)$ |
| NON.ALBRCT | 1.0×10^{-17} | N0P.ALBRCT | 1.0×10^{-17} | cm^{-3} |
| T0N.ALBRCT | 300.0 | T0P.ALBRCT | 300.0 | K |
| T1N.ALBRCT | 1065.0 | T1P.ALBRCT | 1065.0 | K |

Farahmand Modified Caughey Thomas

You can use a composition and temperature dependent low field model by specifying the FMCT.N and FMCT.P in the MOBILITY statement. FMCT stands for Farahmand Modified Caughey Thomas. This model [68] was the result of fitting a Caughey Thomas like model to Monte Carlo data. The model is similar to the analytic model described by Equations 3-174 and 3-175 in Chapter 3: “Physics”. This modified model is described by Equations 5-141 and 5-142 for electrons and holes.

$$\mu_n(T, N) = MU1N.FMCT \left(\frac{T}{300} \right)^{BETAN.FMCT} + \quad 5-141$$

$$I + \frac{(MU2N.FMCT - MU1N.FMCT) \left(\frac{T}{300} \right)^{DELTAN.FMCT}}{\left[\frac{N}{NCRITN.FMCT \left(\frac{T}{300} \right)^{GAMMAN.FMCT}} \right]^{ALPHAN.FMCT} (T/300)^{EPSP.FMCT}}$$

$$\mu_p(T, N) = \text{MU1P.FMCT} \left(\frac{T}{300} \right)^{\text{BETAP.FMCT}} +$$

5-142

$$\frac{(\text{MU2P.FMCT} - \text{MU1P.FMCT}) \left(\frac{T}{300} \right)^{\text{DELTAP.FMCT}}}{1 + \left[\frac{N}{\text{NCRITP.FMCT} \left(\frac{T}{300} \right)^{\text{GAMMAP.FMCT}}} \right]^{\text{ALPHAP.FMCT} (T/300)^{\text{EPSP.FMCT}}}}$$

In these equations, T is the lattice temperature and N is the total doping. Table 5-17a shows the user-definable parameters.

| Table 5-17a. User-specifiable parameters for the Faramand modified Caughey Thomas model for Nitrides. | | | |
|--|------------------|-------------|-------------------------|
| Parameter | Statement | Type | Units |
| MU1N.FMCT | MOBILITY | Real | cm ² / (V*s) |
| MU1P.FMCT | MOBILITY | Real | cm ² / (V*s) |
| MU2N.FMCT | MOBILITY | Real | cm ² / (V*s) |
| MU2P.FMCT | MOBILITY | Real | cm ² / (V*s) |
| ALPHAN.FMCT | MOBILITY | Real | |
| ALPHAP.FMCT | MOBILITY | Real | |
| BETAN.FMCT | MOBILITY | Real | |
| BETAP.FMCT | MOBILITY | Real | |
| GAMMAN.FMCT | MOBILITY | Real | |
| GAMMAP.FMCT | MOBILITY | Real | |
| DELTAN.FMCT | MOBILITY | Real | |
| DELTAP.FMCT | MOBILITY | Real | |
| EPSN.FMCT | MOBILITY | Real | |
| EPSP.FMCT | MOBILITY | Real | |
| NCRITN.FMCT | MOBILITY | Real | cm ⁻³ |
| NCRITP.FMCT | MOBILITY | Real | cm ⁻³ |

Tables 5-16b and 5-16c show the default parameters as taken from the Monte Carlo fits for various nitride compositions.

| Table 5-16b. Default Nitride Low Field Mobility Model Parameter Values [68] | | | | |
|--|-------------------------------------|-------------------------------------|-------------|------------|
| MATERIAL | MU1N.FMCT (cm ² /V.s) | MU2N.FMCT (cm ² /V.s) | ALPHAN.FMCT | BETAN.FMCT |
| InN | 774 | 3138.4 | 0.68 | -6.39 |
| In _{0.8} Ga _{0.2} N | 644.3 | 1252.7 | 0.82 | -1.81 |
| In _{0.5} Ga _{0.5} N | 456.4 | 758.1 | 1.04 | -1.16 |
| In _{0.2} Ga _{0.8} N | 386.4 | 684.2 | 1.37 | -1.36 |
| GaN | 295.0 | 1460.7 | 0.66 | -1.02 |
| Al _{0.2} Ga _{0.8} N | 132.0 | 306.1 | 0.29 | -1.33 |
| Al _{0.5} Ga _{0.5} N | 41.7 | 208.3 | 0.12 | -0.6 |
| Al _{0.8} Ga _{0.2} N | 47.8 | 199.6 | 0.17 | -0.74 |
| AlN | 297.8 | 683.8 | 1.16 | -1.82 |

| Table 5-16c. Default Nitride Low Field Mobility Model Parameter Values [68] | | | | |
|--|-------------|-------------|-----------|------------------|
| MATERIAL | GAMMAN.FMCT | DELTAN.FMCT | EPSN.FMCT | NCRITN.FMCT |
| InN | -1.81 | 8.05 | -0.94 | 10 ¹⁷ |
| In _{0.8} Ga _{0.2} N | -1.30 | 4.84 | -0.41 | 10 ¹⁷ |
| In _{0.5} Ga _{0.5} N | -1.74 | 2.21 | -0.22 | 10 ¹⁷ |
| In _{0.2} Ga _{0.8} N | -1.95 | 2.12 | -0.99 | 10 ¹⁷ |
| GaN | -3.84 | 3.02 | 0.81 | 10 ¹⁷ |
| Al _{0.2} Ga _{0.8} N | -1.75 | 6.02 | 1.44 | 10 ¹⁷ |
| Al _{0.5} Ga _{0.5} N | -2.08 | 10.45 | 2.00 | 10 ¹⁷ |
| Al _{0.8} Ga _{0.2} N | -2.04 | 20.65 | 0.01 | 10 ¹⁷ |
| AlN | -3.43 | 3.78 | 0.86 | 10 ¹⁷ |

For composition fractions not listed in Tables 5-16b and 5-16c, the default parameters are linearly interpolated from the nearest composition fractions on the table. You can override these defaults by specifying any of the parameters listed in Table 5-17a on the MOBILITY statement. Currently, this model has only been calibrated for electrons. We only recommend that you use this model for holes when you define a set of real default parameters.

High Field Mobility

You can select nitride specific field dependent mobility model by specifying `GANSAT.N` and `GANSAT.P` on the `MOBILITY` statement. This model [68] is based on a fit to Monte Carlo data for bulk nitride, which is described in Equations 5-143 and 5-144.

$$\mu_n = \frac{\mu_{n0}(T, N) + VSATN \frac{E^{N1N \cdot GANSAT - 1}}{ECN \cdot GANSAT^{N1N \cdot GANSAT}}}{1 + ANN \cdot GANSAT \left(\frac{E}{ECN \cdot GANSAT} \right)^{N2N \cdot GANSAT} + \left(\frac{E}{ECN \cdot GANSAT} \right)^{N1N \cdot GANSAT}} \quad 5-143$$

$$\mu_p = \frac{\mu_{p0}(T, N) + VSATP \frac{E^{N1P \cdot GANSAT - 1}}{ECP \cdot GANSAT^{N1P \cdot GANSAT}}}{1 + ANP \cdot GANSAT \left(\frac{E}{ECP \cdot GANSAT} \right)^{N2P \cdot GANSAT} + \left(\frac{E}{ECP \cdot GANSAT} \right)^{N1P \cdot GANSAT}} \quad 5-144$$

In these equations, $\mu_0(T, N)$ is the low field mobility and E is the electric field. Table 5-17 lists the user-definable parameters.

| Table 5-17. User Definable Low Field Nitride Mobility Model Parameters | | | |
|--|-----------|------|-------|
| Parameter | Statement | Type | Units |
| N1N.GANSAT | MOBILITY | Real | |
| N1P.GANSAT | MOBILITY | Real | |
| N2N.GANSAT | MOBILITY | Real | |
| N2P.GANSAT | MOBILITY | Real | |
| ANN.GANSAT | MOBILITY | Real | |
| ANP.GANSAT | MOBILITY | Real | |
| ECN.GANSAT | MOBILITY | Real | V/cm |
| ECP.GANSAT | MOBILITY | Real | V/cm |

Table 5-18 shows the default parameters as taken from the Monte Carlo fits for various nitride compositions.

| Table 5-18. Default Nitride Field Dependent Mobility Model Parameter Values [68] | | | | | |
|--|----------------------|-----------------------|------------|------------|------------|
| MATERIAL | VSATN | ECN.GANSAT (kV/cm) | N1N.GANSAT | N2N.GANSAT | ANN.GANSAT |
| InN | 1.3595×10^7 | 52.4242 | 3.8501 | 0.6078 | 2.2623 |
| In _{0.8} Ga _{0.2} N | 0.8714×10^7 | 103.4550 | 4.2379 | 1.1227 | 3.0295 |

Table 5-18. Default Nitride Field Dependent Mobility Model Parameter Values [68]

| | | | | | |
|---------------------------------------|------------------------|----------|---------|--------|--------|
| In _{0.5} Ga _{0.5} N | 0.7973×10 ⁷ | 148.9098 | 4.0635 | 1.0849 | 3.0052 |
| In _{0.2} Ga _{0.8} N | 1.0428×10 ⁷ | 207.5922 | 4.7193 | 1.0239 | 3.6204 |
| GaN | 1.9064×10 ⁷ | 220.8936 | 7.2044 | 0.7857 | 6.1973 |
| Al _{0.2} Ga _{0.8} N | 1.1219×10 ⁷ | 365.5529 | 5.3193 | 1.0396 | 3.2332 |
| Al _{0.5} Ga _{0.5} N | 1.1459×10 ⁷ | 455.4437 | 5.0264 | 1.0016 | 2.6055 |
| Al _{0.8} Ga _{0.2} N | 1.5804×10 ⁷ | 428.1290 | 7.8166 | 1.0196 | 2.4359 |
| AlN | 2.1670×10 ⁷ | 447.0339 | 17.3681 | 0.8554 | 8.7253 |

For composition fractions not listed in Table 5-18, the default parameters are linearly interpolated from the nearest composition fractions on the table.

You can override these defaults by specifying any of the parameters listed in Table 5-17 in the MOBILITY statement. Currently, this model has only been calibrated for electrons. We only recommend that you use this model for holes when you define a set of real default parameters. Also note that these models exhibit negative differential mobility and may exhibit poor convergence. In such cases, you may do well to use the simpler model given in Equations 3-274 and 3-275 with a reasonable value of saturation velocity.

Impact Ionization Parameters

Table 5-19 shows the extracted default values for the Selberherr impact ionization model from [164] for GaN.

Table 5-19. Default Impact Ionization Parameters (IMPACT statement)

| Parameter | Units | GaN | InN | AlN | InGaN | AlGaIn |
|-----------|------------------|----------------------|----------------------|----------------------|----------------------|----------------------|
| AN1 | cm ⁻¹ | 2.52×10 ⁸ | 2.52×10 ⁸ | 2.52×10 ⁸ | 2.52×10 ⁸ | 2.52×10 ⁸ |
| AN2 | cm ⁻¹ | 2.52×10 ⁸ | 2.52×10 ⁸ | 2.52×10 ⁸ | 2.52×10 ⁸ | 2.52×10 ⁸ |
| BN1 | V/cm | 3.41×10 ⁷ | 3.41×10 ⁷ | 3.41×10 ⁷ | 3.41×10 ⁷ | 3.41×10 ⁷ |
| BN2 | V/cm | 3.41×10 ⁷ | 3.41×10 ⁷ | 3.41×10 ⁷ | 3.41×10 ⁷ | 3.41×10 ⁷ |
| AP1 | cm ⁻¹ | 5.37×10 ⁶ | 5.37×10 ⁶ | 5.37×10 ⁶ | 5.37×10 ⁶ | 5.37×10 ⁶ |
| AP2 | cm ⁻¹ | 5.37×10 ⁶ | 5.37×10 ⁶ | 5.37×10 ⁶ | 5.37×10 ⁶ | 5.37×10 ⁶ |
| BP1 | V/cm | 1.96×10 ⁷ | 1.96×10 ⁷ | 1.96×10 ⁷ | 1.96×10 ⁷ | 1.96×10 ⁷ |
| BP2 | V/cm | 1.96×10 ⁷ | 1.96×10 ⁷ | 1.96×10 ⁷ | 1.96×10 ⁷ | 1.96×10 ⁷ |
| BETAN | | 1.0 | 1.0 | 1.0 | 1.0 | 1.0 |
| BETAP | | 1.0 | 1.0 | 1.0 | 1.0 | 1.0 |
| EGRAN | V/cm | 0.0 | 0.0 | 0.0 | 0.0 | 0.0 |

Recombination Parameters

Table 5-20 shows the default values for radiative rates for the the binary wurtzite nitride compounds.

| Table 5-20. Default Radiative Rates for Nitrides (MATERIAL COPT) | | | |
|--|-----------------------|------------------------|-----------|
| Material | COPT | Units | Reference |
| GaN | 1.1×10^{-8} | cm^3/s | [159] |
| InN | 2.0×10^{-10} | cm^3/s | [277] |
| AlN | 0.4×10^{-10} | cm^3/s | [245] |

Note: Currently, no default formula have been implemented for ternary and quaternary compounds for COPT.

Default Models for Heat Capacity and Thermal Conductivity

By default, the heat capacity and thermal conductivities used in self-consistent heat flow simulations (GIGA and GIGA3D) for the GaN/AlGaIn/InGaIn system are given by the following equations [179].

$$C_L(T) = C_L(300K) \frac{20 - (\Theta_D/T)^2}{20 - (\Theta_D/300K)^2} \rho_L \quad 5-145$$

$$\kappa_L(T) = \kappa_L(300K) \left(\frac{T}{300K} \right)^{\delta_\kappa} \quad 5-146$$

Here, T is the local temperature and the other parameters are given in Table 5-21 [179].

| Table 5-21. Default Heat Capacity and Thermal Conductivity Parameters for GaN | | | | | |
|---|--------------------|---------------|-------------------------------|----------------|-----------------|
| Parameter Unit | κ_L (W/Kcm) | C_L (Ws/gK) | ρ_L (g/cm ³) | Θ_D (K) | δ_κ |
| GaN | 1.30 | 0.49 | 6.15 | 600 | -0.28 |
| AlN | 2.85 | 0.6 | 3.23 | 1150 | -1.64 |
| InN | 0.45 | 0.32 | 6.81 | 660 | 0.0 |

Values for ternary and quaternary compositions are obtained by linear interpolation as a function of composition.

Adachi's Refractive Index Model [179]

For the III-V nitride compounds, Adachi's refractive index model is expressed by Equation 5-147.

$$n_r(\omega) = \sqrt{A \left(\frac{\hbar\omega}{E_g} \right)^{-2} \left\{ 2 - \sqrt{1 + \frac{\hbar\omega}{E_g}} - \sqrt{1 - \frac{\hbar\omega}{E_g}} \right\} + B} \quad 5-147$$

where E_g is the bandgap, ω is the optical frequency and A and B are material composition dependent parameters. For $Al_xGa_{1-x}N$, the compositional dependence of the A and B parameters are given by the expressions in Equations 5-148 and 5-149.

$$A(x) = 9.827 - 8.216X - 31.59X^2 \quad 5-148$$

$$B(x) = 2.736 + 0.842X - 6.293X^2 \quad 5-149$$

For $In_xGa_{1-x}N$, the compositional dependence of the A and B parameters are given by the expressions in Equations 5-150 and 5-151.

$$A(x) = 9.827_{(1-X)} - 53.57X \quad 5-150$$

$$B(x) = 2.736(1-X) - 9.19X. \quad 5-151$$

5.3.8: The Hg(1-x)Cd(x)Te System

The following sections describe the relationship between mole fraction, X_{COMP} , and the material parameters of the of the Hg(1-x)Cd(x)Te system. This data has been taken from [251].

Bandgap

Equation 5-152 is used in the calculation of bandgap as a function of composition fraction.

$$E_g = -0.302 + 1.93 * X_{COMP} - 0.810 * X_{COMP}^2 \quad 5-152$$

$$+ 0.832 * X_{COMP}^3 + 5.354 \times 10^{-4} * \left(1 - 2 * X_{COMP} \right) T_L$$

Here, T_L is lattice temperature.

Electron Affinity

Equation 5-153 is used in the calculation of electron affinity as a function of composition fraction.

$$\chi = 4.23 - 0.813 * (E_g(T_L) - 0.083) \quad 5-153$$

Permittivity

Equation 5-154 is used in the calculation of relative permittivity as a function of composition fraction.

$$\varepsilon = 20.5 - 15.5 * X_{COMP} + 5.7 * X_{COMP}^2 \quad 5-154$$

Density of States Masses

Equations 5-155 and 5-156 are used to calculate the density of states effective masses of electrons and holes.

$$\frac{m_e}{m_0} = \left[-0.6 + 6.333 \left(\frac{2}{E_g(T_L)} + \frac{1}{E_g(T_L) + 1} \right) \right]^{-1} \quad 5-155$$

$$\frac{m_e}{m_0} = 0.55 \quad 5-156$$

Mobility

Equations 5-157 and 5-158 are used to calculate the electron and hole mobilities as functions of composition fraction.

$$\mu_e = 9 \times 10^8 \left(\frac{0.2}{X.COMP} \right)^{7.5} T_L^{-2} \left(\frac{0.2}{X.COMP} \right)^{0.6} \quad 5-157$$

$$\mu_h = 0.01 * \mu_e \quad 5-158$$

5.3.9: CIGS (CuIn(1-x)Ga(x)Se₂), CdS, and ZnO

The following table gives the default material parameter values for CIGS, CdS, and ZnO [62, 133, 211].

| Table 5-22. Default Parameters ofr CIGS, CdS, and ZnO | | | |
|---|----------------------|-----------------------|----------------------|
| Parameter | ZnO | CdS | CIGS |
| ϵ_r | 9 | 10 | 13.6 |
| μ_n | 100 | 100 | 100 |
| μ_p | 25 | 25 | 25 |
| E_g | 3.3 | 2.48 | Equation 5-159 |
| χ | 4.5 | 4.18 | 4.58 |
| N_c | 2.2×10^{18} | 2.41×10^{18} | 2.2×10^{18} |
| N_v | 1.8×10^{19} | 2.57×10^{19} | 1.8×10^{19} |

$$E_g = (1.036 + 4.238 \times 10^{-5} * T_L - 8.875 \times 10^{-5} * 170.0 / (\tanh(170.0 * 0.5 / T_L) - 1.0) (1 - X.COMP) + (1.691 + 8.820 \times 10^{-5} * T_L - 16.0 \times 10^{-5} * 189.0 / \tanh(189.8 * 0.5 / T_L) - 1.0) X.COMP - 0.02 * X.COMP * (1 - X.COMP) \quad 5-159$$

5.4: Simulating Heterojunction Devices with Blaze

5.4.1: Defining Material Regions with Positionally-Dependent Band Structure

Step Junctions

The easiest way to define a device with positionally dependent band structure is to specify two adjacent semiconductor regions with dissimilar bandgap. In this case, BLAZE would simulate an abrupt heterojunction between the two materials.

For example, you want to simulate an abrupt heterojunction parallel to the X axis at a location of $y=0.1$ microns. For values of y greater than 0.1 specify, GaAs. For values of y less than 0.1, specify AlGaAs with a composition fraction of 0.3. The following statements would specify this situation.

```
REGION Y.MIN=0.1 MATERIAL=GaAs
REGION Y.MAX=0.1 MATERIAL=AlGaAs x.COMP=0.3
```

This fragment specifies that the two regions form an abrupt heterojunction at $Y=0.1$. The first region is composed of GaAs while the second is composed of AlGaAs.

These two material names are used by BLAZE to choose default material models for the two regions. For a complete list of the materials available in ATLAS/BLAZE, see Appendix B: “Material Systems”. For the AlGaAs region a composition fraction of 0.3 is specified.

Graded Junctions

A grading can be applied to this heterojunction with a simple modification. For example:

```
REGION Y.MIN=0.1 MATERIAL=GaAs
REGION Y.MAX=0.1 MATERIAL=AlGaAs x.COMP=0.3 GRAD.34=0.01
```

specifies that the composition fraction of the AlGaAs region decreases from 0.3 at $y=0.1$ microns to 0.0 at $y=0.11$ microns. The GRAD parameter specifies the distance over which the mole fraction reduces to zero. The GRAD parameter is indexed such that GRAD.12 corresponds to the Y.MIN side of the region, GRAD.23 corresponds to the x.MAX side of the region, GRAD.34 corresponds to the Y.MAX side of the region, and GRAD.41 corresponds to the x.MIN side of the region. In most cases, the GRAD.n parameter acts to increase the size of the region. By default, the GRAD.n parameters are set to zero and all heterojunctions are abrupt. Note that the GRAD parameter acts just like the other region geometry parameters in that later defined regions overlapping the graded part of the region will overlap the grading. If in the previous example the grading had been applied to the GaAs region, it would be overlapped by the AlGaAs region. This would have produced an abrupt interface. A solution would be to limit Y.MAX in the AlGaAs region to 0.09. Make sure you specify regions in the proper order to avoid such problems.

Along similar lines, you can use the overlapping of regions to an advantage in forming graded heterojunctions between two materials in the same system with different non-zero composition fractions. For example:

```
REGION Y.MIN=0.1 MATERIAL=AlGaAs x.COMP=0.3 GRAD.12=0.02
REGION Y.MAX=0.11 MATERIAL=AlGaAs x.COMP=0.1
```

specifies a graded heterojunction with a composition of 0.3 at $y = 0.1$ falling to 0.1 at $y = 0.11$.

5.4.2: Defining Materials and Models

Materials

For example to set the bandgap for the material, InP, use the following syntax.

```
MATERIAL MATERIAL=InP EG300=1.35
```

Models

BLAZE has two ways of simulating the physical effects of variations in semiconductor composition. For relatively gradual variations in composition, the standard modifications to the drift-diffusion equations can be considered adequate for simulation purposes. For abrupt heterojunctions, it has been suggested that thermionic emission may be the dominant factor in the behavior of heterojunction behavior.

Individual material parameters and models can be defined for each material or region. These models are set in the MATERIAL, MODEL, and IMPACT statements.

This statement uses the MATERIAL parameter to select all regions composed of the material "InP". The bandgap in these regions will be set to 1.35. There are two ways to set the parameters of a particular region. The first is to use the region index. For example:

```
MODEL REGION=1 BGN
```

In this case, the bandgap narrowing model is enabled in the region indexed number 1.

The second is to use the region name. For example:

```
IMPACT NAME=substrate SELB
```

This example turns on the Selberherr Impact Ionization Model in the region named substrate. You can then set the parameters for all regions and materials by omitting the MATERIAL, REGION, or NAME parameters, as in the following:

```
MODEL BGN
```

This statement sets the bandgap narrowing model for all regions and materials

Parser Functions

To use the C-INTERPRETER functions, you need to know the C programming language. See Appendix A: "C-Interpreter Functions" for a description of the parser functions.

To specify a completely arbitrary spatial variation of varying composition fraction, use a parser function. To define the parser function for composition fraction, write a C function describing the composition fraction as a function of position. A template for the function called COMPOSITION is provided with this release of ATLAS. Once you define the COMPOSITION function, store it in a file. To use the function for composition, set the F.COMPOSIT parameter to the file name of the function.

6.1: 3D Device Simulation Programs

This chapter aims to highlight the extra information required for 3D simulation as compared to 2D. You should be familiar with the equivalent 2D models before reading this chapter.

This chapter describes the set of ATLAS products that extends 2D simulation models and techniques and applies them to general non-planar 3D structures. The structural definition, models and material parameters settings and solution techniques are similar to 2D. You should be familiar with the simulation techniques described in Chapter 2: “Getting Started with ATLAS” and the equivalent 2D product chapters before reading the sections that follow. The products that form 3D device simulation in ATLAS are:

- **DEVICE3D** – silicon compound material and heterojunction simulation
- **GIGA3D** – non-isothermal simulation
- **MIXEDMODE3D** – mixed device-circuit simulation
- **TFT3D** – thin film transistor simulation
- **QUANTUM3D** – quantum effects simulation
- **LUMINOUS3D** – photodetection simulation

The 3D modules, **THERMAL3D**, are described in Chapter 17: “Thermal 3D: Thermal Packaging Simulator”.

In a similar manner to the 2D products, **GIGA3D**, **MIXEDMODE3D**, **LUMINOUS3D** and **QUANTUM3D** should be combined with both **DEVICE3D** or **BLAZE3D** depending on the semiconductor materials used.

6.1.1: DEVICE3D

DEVICE3D provides semiconductor device in 3D. Its use is analogous to the 2D simulations in **S-PISCES** and **BLAZE**. See Chapter 4: “S-Piscis: Silicon Based 2D Simulator” for more information on **S-PISCES**. See Chapter 5: “Blaze: Compound Material 2D Simulator” for more information on **BLAZE**.

6.1.2: GIGA3D

GIGA3D is an extension of **DEVICE3D** that accounts for lattice heat flow in 3D devices. **GIGA3D** has all the functionality of **GIGA** (see Chapter 7: “Giga: Self-Heating Simulator”) with a few exceptions. One exception is that additional syntax has been added to account for the three dimensional nature of thermal contacts. You can specify the **Z.MIN** and **Z.MAX** parameters on the **THERMCONTACT** statement to describe the extent of the contact in the **Z** direction. Another exception is that there is no **BLOCK** method available in the 3D version.

6.1.3: TFT3D

TFT3D is an extension of **DEVICE3D** that allows you to simulate amorphous and polycrystalline semiconductor materials in three dimensions. **TFT3D** is completely analogous to the **TFT** simulator described in Chapter 14: “TFT: Thin-Film Transistor Simulator”. The complete functionality of the **TFT** simulator is available in **TFT3D** for three dimensional devices.

6.1.4: MIXEDMODE3D

MIXEDMODE3D is an extension of **DEVICE3D** or **BLAZE3D** that allows you to simulate physical devices embedded in lumped element circuits (**SPICE** circuits). **MIXEDMODE3D** is completely analogous to the **MIXEDMODE** simulator, which is described in Chapter 12: “MixedMode: Mixed Circuit and Device Simulator”. The complete functionality of the **MIXEDMODE** simulator is available in **MIXEDMODE3D** for three dimensional devices.

6.1.5: QUANTUM3D

QUANTUM3D is an extension of DEVICE3D or BLAZE3D, which allows you to simulate the effects of quantum confinement using the Quantum Transport Model (Quantum Moments Model). QUANTUM3D is completely analogous to the QUANTUM model but applies to three dimensional devices. See Chapter 13: “Quantum: Quantum Effect Simulator” for more information on QUANTUM.

6.1.6: LUMINOUS3D

LUMINOUS3D is an extension of DEVICE3D that allows you to simulate photodetection in three dimensions. LUMINOUS3D is analogous to the LUMINOUS simulator, which is described in Chapter 10: “Luminous: Optoelectronic Simulator” with a few significant differences described in Section 6.3.11: “LUMINOUS3D Models”.

6.2: 3D Structure Generation

All 3D programs in ATLAS supports structures defined on 3D prismatic meshes. Structures may have arbitrary geometries in two dimensions and consist of multiple slices in the third dimension.

There are two methods for creating a 3D structure that can be used with ATLAS. One way is through the command syntax of ATLAS. Another way is through an interface to DEVEDIT3D.

A direct interface from ATHENA to 3D ATLAS impossible. But DEVEDIT3D provides the ability to read in 2D structures from ATHENA and extend them non-uniformly to create 3D structures for ATLAS.

ATLAS Syntax For 3D Structure Generation

Mesh generation

Chapter 2: “Getting Started with ATLAS”, Section 2.6.3: “Using The Command Language To Define A Structure” covers the generation of 2D and 3D mesh structures using the ATLAS command language. The Z.MESH statement and the NZ and THREE.D parameters of the MESH statement are required to extend a 2D mesh into 3D.

Conventionally, slices are made perpendicular to the Z axis. The mesh is triangular in XY but rectangular in XZ or YZ planes.

Region, Electrode, and Doping definition

Chapter 2: “Getting Started with ATLAS”, Section 2.6.3: “Using The Command Language To Define A Structure” also covers the definition of 2D regions, electrodes and doping profiles. To extend the regions into 3D, use the Z.MIN and Z.MAX parameters. For example:

```
REGION NUM=2 MATERIAL=Silicon X.MIN=0 X.MAX=1 Y.MIN=0 Y.MAX=1 Z.MIN=0 Z.MAX=1
ELECTRODE NAME=gate X.MIN=0 X.MAX=1 Y.MIN=0 Y.MAX=1 Z.MIN=0 Z.MAX=1
DOPING GAUSS N.TYPE CONC=1E20 JUNC=0.2 Z.MIN=0.0 Z.MAX=1.0
```

For 2D regions or electrodes defined with the command language, geometry is limited to rectangular shapes. Similarly, in 3D regions and electrodes are composed of rectangular parallelopeds.

DevEdit3D Interface

DEVEDIT3D is a graphical tool that allows you to draw 3D device structures and create 3D meshes. It can also read 2D structures from ATHENA and extend them into 3D. These structures can be saved from DEVEDIT3D as structure files for ATLAS. Also, save a command file when using DEVEDIT3D. This file is used to recreate the 3D structure inside DEVEDIT3D, which is important, since DEVEDIT3D doesn't read in 3D structure files.

ATLAS can read structures generated by DEVEDIT3D using the command:

```
MESH INF=<filename>
```

The program is able to distinguish automatically between 2D and 3D meshes read in using this command.

Defining Devices with Circular Masks

DEVEDIT3D makes a triangular mesh in the XY plane and uses Z plane slices. This means, that normally the Y direction is vertically down into the substrate. But in the case of using circular masks, you need to rotate the device.

With defining devices using circular masks in DEVEDIT3D, the XY plane should be the surface of the device and the Z direction should be into the substrate.

6.3: Model And Material Parameter Selection in 3D

Models and material parameters are chosen in 3D in common with other 2D modules using the `MODELS`, `IMPACT`, `MATERIAL`, `MOBILITY`, `INTERFACE`, and `CONTACT` statements. The following models are available in 3D device simulation programs. All of these models are documented in Chapter 3: “Physics” or in the 2D product chapters.

6.3.1: Mobility

- Table for 300K (`CONMOB`)
- Thomas’s model (`ANALYTIC`)
- Arora’s model (`ARORA`)
- Klaassen’s model (`KLAASSEN`)
- Lombardi’s model (`CVT`)
- Yamaguchi’s model (`YAMA`)
- Parallel field dependence (`FLDMOB`)
- Parallel field dependence with negative differential mobility (`FLDMOB EVSATMOD=1`)

6.3.2: Recombination

- Shockley Read Hall (`SRH`)
- Concentration dependent lifetime `SRH` (`CONSRH`)
- Klaassen’s concentration dependent lifetime `SRH` (`KLASRH`)
- Auger (`AUGER`)
- Klaassen’s concentration dependent Auger recombination model (`KLAAUG`)
- Optical recombination (`OPTR`)
- Bulk and interface traps (`TRAP`, `INTTRAP`)
- Continuous defect states (`DEFECT`)

6.3.3: Generation

- Selberherr’s impact ionization (`IMPACT SELB`)
- Crowell’s impact ionization (`IMPACT CROWELL`)
- Hot electron injection (`HEI`)
- Fowler Nordheim tunneling (`FNORD`)

6.3.4: Carrier Statistics

- Boltzmann (default)
- Fermi (`FERMI`)
- Band gap narrowing (`BGN`)
- Incomplete ionization (`INCOMPLETE`)
- Quantum mechanical effects (`QUANTUM`)
- Heterojunction thermionic field emission

6.3.5: Boundary Conditions

- Ohmic and Schottky
- Current boundary conditions
- Lumped element boundary conditions
- Distributed contact resistance

6.3.6: Optical

- Photogeneration with ray tracing (LUMINOUS3D).

6.3.7: Single Event Upset Simulation

- Single event upset simulation.

All these models, with the exception of `SINGLEEVENTUPSET`, are documented in the Chapter 3: “Physics” or in the 2D product chapters of this manual.

6.3.8: Boundary Conditions in 3D

External Passive Elements

You can attach external lumped resistors, capacitors and inductors to any contact. The syntax is the same as for the 2D products, which is:

```
CONTACT NAME=drain RES=1e3 CAP=1e-12 L=1e-6
```

You can also apply distributed resistances to contacts. The algorithm used for estimating contact area for 3D distributed contact resistance multiplies the contact perimeter in a given Z plane by the displacement in the Z direction. This algorithm will only work properly for planar contacts that do not vary in the Z direction. They may however abruptly terminate or start in the Z direction.

The units of lumped external passive elements are ohms for resistors, Farads for capacitors and Henrys for inductors. Distributed contact resistance is defined in ohms.cm³.

Thermal Contacts for GIGA3D

Thermal contacts for non-isothermal simulation in GIGA3D are defined in an analogous manner to the 2D thermal contacts in GIGA. The `Z.MIN` and `Z.MAX` parameters are used to define the extent of the thermal contact in the Z plane. The units of the thermal resistance parameter `ALPHA` are scaled in 3D to W/(cm.K). For more information about GIGA3D, see Chapter 7: “Giga: Self-Heating Simulator”.

6.3.9: TFT3D Models

Models for simulating thin-film transistors made from amorphous or polycrystalline semiconductors are supported in TFT3D. The definition of the continuous defect states in the bandgap is performed using the same parameters as in 2D simulations with TFT. The models for continuous defect (or trap) densities are documented in Chapter 14: “TFT: Thin-Film Transistor Simulator”.

6.3.10: QUANTUM3D Models

Models for simulating quantum effects semiconductors are supported in QUANTUM3D. The definition of the quantum moments solver is the same as in 2D simulations with QUANTUM. The models for simulating quantum effects and the parameters to control the model are shown in Chapter 13: “Quantum: Quantum Effect Simulator”.

6.3.11: LUMINOUS3D Models

Many of the models for simulating photodetection in LUMINOUS3D are similar to those for simulating photodetection in LUMINOUS. For more information about LUMINOUS, see Chapter 10: “Luminous: Optoelectronic Simulator”. This section, however, shows several important differences between LUMINOUS and LUMINOUS3D.

6.4: Numerical Methods for 3D

6.4.1: DC Solutions

There are several differences between the default numerical methods applied in 2D ATLAS and those applied in 3D ATLAS. For example, with respect to non-linear iteration strategies, the current version of the 3D simulator does not support the `BLOCK` method. The `NEWTON` and `GUMMEL` iteration strategies are supported for 3D simulations, whereas `NEWTON`, `GUMMEL` and `BLOCK` are all supported for 2D simulations.

In solving the linear subproblem, the default approach in 3D is to use an iterative solver. This is believed to be the most efficient method for general 3D problems. In 2D, the direct solver is used by default. You may find it desirable to use direct methods in 3D problems due to improved convergence of computational efficiency. You can select the direct method by specifying `DIRECT` in the `METHOD` statement. Also, in 3D there are two linear iterative solution methods available. The defaults are `ILUCGS` (incomplete lower-upper decomposition conjugate gradient system) and `BICGST` (bi-conjugate gradient stabilized). Historically, tests have shown that the current implementation of `ILUCGS` is slightly more stable than `BICGST` and is the default iterative solver in 3D. You can define the `BICGST` solver by specifying `BICGST` in the `METHOD` statement.

Note: Iterative solvers are recommended for large problems, typically greater than 5000 node points, due to lower solution times and memory usage.

6.4.2: Transient Solutions

In transient mode, a semi-implicit scheme is used in addition to the default TR-BDF algorithm [3]. This algorithm is recommended for complex simulations such as Single Event Upset. To select this method, use:

```
METHOD HALFIMPLICIT
```

It is available for solving the drift-diffusion equations and if `LAT.TEMP` is specified on the `MODELS` statement. If a carrier temperature solution is requested (`HCTE.EL` or `HCTE.HO` or both), then `HALFIMPLICIT` cannot be used.

6.4.3: Obtaining Solutions In 3D

ATLAS3D programs can perform DC and transient analysis in an equivalent manner to 2D. The `SOLVE` statement is used to define the solution procedure. The syntax used is described in Chapter 2: "Getting Started with ATLAS", Section 2.9: "Obtaining Solutions".

6.4.4: Interpreting the Results From 3D

The log files produced by 3D ATLAS can be plotted in `TONYPLOT` exactly as those that result from `S-PISCES` or `BLAZE`. The only difference is the units of the currents produced. Log files from 3D simulations save current in Amperes, whereas the 2D simulations use Amperes/micron.

The solution files produced by 3D ATLAS should be plotted using `TONYPLOT3D`. These files cannot be read directly into the 2D `TONYPLOT` program. `TONYPLOT3D` contains features that allows you to make slices of the 3D structure, which can be plotted in 2D `TONYPLOT`. For more information about `TONYPLOT3D`, see the `TONYPLOT3D USER'S MANUAL`.

6.4.5: More Information

Many examples using 3D ATLAS have been installed on your distribution tape or CD. You can find more information about 3D ATLAS by reading the text associated with each example. You can also find find some more information at www.silvaco.com.

7.1: Overview

GIGA extends ATLAS to account for lattice heat flow and general thermal environments. GIGA implements Wachutka's thermodynamically rigorous model of lattice heating [242], which accounts for Joule heating, heating, and cooling due to carrier generation and recombination, and the Peltier and Thomson effects. GIGA accounts for the dependence of material and transport parameters on the lattice temperature. GIGA also supports the specification of general thermal environments using a combination of realistic heat-sink structures, thermal impedances, and specified ambient temperatures. GIGA works with both S-PISCES and BLAZE and with both the drift-diffusion and energy balance transport models. See Chapter 3: "Physics", the "Drift-Diffusion Transport Model" section on page 3-2 and the "Energy Balance Transport Model" section on page 3-4 for more information on these models.

Before continuing with this chapter, you should be familiar with ATLAS. If not, read Chapter 2: "Getting Started with ATLAS", along with Chapter 4: "S-Piscis: Silicon Based 2D Simulator" or Chapter 5: "Blaze: Compound Material 2D Simulator".

7.1.1: Applications

A major application of GIGA is the simulation of high-power structures including bipolar, MOS, IGBT, and thyristor devices. Another important application is the simulation of electrostatic discharge (ESD) protection devices. Thermal effects are also important in SOI device operation due to the low thermal conductivity of the buried oxide, and in devices fabricated in III-V material systems due to the relatively low thermal conductivity of these materials.

Recent studies have demonstrated that accounting self-consistently for lattice heating is necessary for accurate simulation of bipolar VLSI devices. This is due to the sensitive temperature dependence of the carrier injection process. Since bipolar devices are key components of CMOS technologies and many devices can be impacted by parasitic bipolar effects, the applications of GIGA are very general.

For other more information on GIGA's application, see Section 7.3: "Applications of GIGA".

7.1.2: Numerics

GIGA supplies numerical techniques that provide efficient and robust solution of the complicated systems of equations that result when lattice heating is accounted for. These numerical techniques include fully-coupled and block iteration methods. When GIGA is used with the energy balance equations, the result is a "six equation solver", which defines the state-of-the-art for general purpose device simulation.

For more information on numerical techniques, see Chapter 20: "Numerical Techniques".

7.2: Physical Models

7.2.1: The Lattice Heat Flow Equation

GIGA adds the heat flow equation to the primary equations that are solved by ATLAS. The heat flow equation has the form:

$$C \frac{\partial T_L}{\partial t} = \nabla(\kappa \nabla T_L) + H \quad 7-1$$

where:

- C is the heat capacitance per unit volume.
- κ is the thermal conductivity.
- H is the heat generation
- T_L is the local lattice temperature.

The heat capacitance can be expressed as $C = \rho C_p$, where C_p is the specific heat and ρ is the density of the material.

Specifying the `LAT.TEMP` parameter in the `MODELS` statement includes the lattice heat flow equation in ATLAS simulations.

GIGA supports different combinations of models. For example, if the `HCTE` and `LAT.TEMP` parameters are specified in the `MODELS` statement and both particle continuity equations are solved, all six equations are solved. If `HCTE.EL` is specified instead of `HCTE`, only five equations are solved and the hole temperature T_p is set equal to lattice temperature T_L .

7.2.2: Specifying Thermal Conductivity

Standard Model

The value of thermal conductivity, k , for each region should be specified in the `MATERIAL` statement. Because thermal conductivity is generally temperature dependent, the following four models are available.

| Table 7-1. Standard Thermal Conductivity Models | | |
|---|------------------|-------------------------|
| Equation | Units | MATERIAL Flag |
| $k(T) = \text{TC.CONST}$ | $(W/cm \cdot K)$ | <code>TCON.CONST</code> |
| $k(T) = (\text{TC.CONST}) / (T_L / 300)^{\text{TC.NPOW}}$ | $(W/cm \cdot K)$ | <code>TCON.POWER</code> |
| $k(T) = 1 / \left(\text{TC.A} + (\text{TC.B}) * T_L + (\text{TC.C}) * T_L^2 \right)$ | $(W/cm \cdot K)$ | <code>TCON.POLYN</code> |
| $k(T) = (\text{TC.E}) / (T_L - \text{TC.D})$ | $(W/cm \cdot K)$ | <code>TCON.RECIP</code> |

The TC.CONST, TC.NPOW, TC.A, TC.B, TC.C, TC.D and TC.E parameters are all user-specifiable in the MATERIAL statement. As described in Table 7-1, the choice of models is also user-specified in the MATERIAL statement.

To clarify model selection and parameter value definition, the following syntax examples are given.

Enabling TCON.POWER:

```
material mat=Diamond TCON.POWER TC.NPOW=2 TC.CONST=1.4
```

Enabling TCON.POLYN:

```
material mat=GaN TCON.POLYN TC.A=1 TC.B=2 TC.C=4
```

Enabling TCON.RECIP:

```
material mat=silicon TCON.RECIP TC.B=2 TC.D=4
```

The thermal model and parameter selection can also be completed through REGION statements as follows:

```
MATERIAL REGION=5 TC.A=<n> TC.B=<n> TC.C=<n>
```

```
MATERIAL REGION=6 TC.A=<n> TC.B=<n> TC.C=<n>
```

It is also advised that you include PRINT on the MODELS statement to verify model selection and parameter values used.

Compositionally Dependent Thermal Conductivity (TCON.COMP) [170]

The key material dependent parameters in Equation 7-1 are the thermal conductivity and the heat capacity. In general, both thermal conductivity and heat capacity are both composition and temperature dependent. In later sections, we will show how you have a great deal of flexibility in specifying these model dependencies.

For most materials, we provide reasonable default values for these material parameters, which you can examine by specifying PRINT on the MODELS statement. These models allow user specification but are not material composition dependent. As such, we have provided default models for some of the more popular materials that are both composition and temperature dependent. These models described here apply to the following materials: Si, Ge, GaAs, AlAs, InAs, InP, GaP, SiGe, AlGaAs, InGaAs, InAlAs, InAsP, GaAsP and InGaP.

The default built-in model derives temperature dependency in a manner very similar to the user specifiable models discussed later in this section.

The composition dependencies of the ternary compounds and the binary, SiGe, are derived from interpolation from the binary compounds (or the values for Si and Ge in the case of SiGe).

The basic model for thermal conductivity is given by:

$$\kappa(T_L) = K_{300} \cdot \left(\frac{T_L}{300}\right)^\alpha \quad 7-2$$

where $\kappa(T_L)$ is the temperature dependent thermal conductivity, T_L is the lattice temperature and K_{300} and α are material dependent parameters.

Table 7-2 shows the default values for K_{300} and α for Si, Ge and the binary III-V compounds .

| Table 7-2. Default Parameter Values for Thermal Conductivity | | |
|--|-------------------|----------|
| Material | K_{300} (W/Kcm) | α |
| Si | 1.48 | -1.65 |
| Ge | 0.60 | -1.25 |
| GaAs | 0.46 | -1.25 |
| AlAs | 0.80 | -1.37 |
| InAs | 0.273 | -1.1 |
| InP | 0.68 | -1.4 |
| GaP | 0.77 | -1.4 |

The parameters K_{300} and α are interpolated as a function of composition fraction x using Equations 7-3 and 7-4.

$$K_{300}^{AB} = \frac{1}{\left(\frac{1-x}{K_{300}^A} + \frac{x}{K_{300}^B} + \frac{(1-x)x}{C} \right)} \quad 7-3$$

$$\alpha^{AB} = (1-x)\alpha^A + x\alpha^B \quad 7-4$$

The C parameter in Equation 7-3 is a bowing factor used to account for the non-linear aspects of the variation of thermal conductivity with composition. Table 7-3 shows the default values of the bowing factor, C , for the various ternary compounds and SiGe.

| Table 7-3. Default Bowing Parameter Values for Thermal Conductivity | |
|---|--------------|
| Material | C (W/K cm) |
| SiGe | 0.028 |
| AlGaAs | 0.033 |
| InGaAs | 0.014 |
| InAlAs | 0.033 |
| InAsP | 0.033 |
| GaAsP | 0.014 |
| InGaP | 0.014 |

C-Interpreter Defined Thermal Conductivity

You can use the C-INTERPRETER to define the thermal conductivity, κ , as a function of the lattice temperature, position, doping and fraction composition. This is defined using the syntax:

```
MATERIAL REGION=<n> F.TCOND=<filename>
```

where the <filename> parameter is an ASCII file containing the C-INTERPRETER function. For more information about the C-INTERPRETER, see Appendix A: “C-Interpreter Functions”.

Anisotropic Thermal Conductivity

The flux term in Equation 7-1 models the thermal conductivity κ as being isotropic by default. You can specify an anisotropic thermal conductivity κ_{aniso} . In GIGA2D, the anisotropic value is applied in the Y direction. In GIGA3D, it is applied in the Z direction by default. In this case, the thermal conductivity tensor is

$$\kappa = \begin{bmatrix} \kappa_1 & 0 & 0 \\ 0 & \kappa_1 & 0 \\ 0 & 0 & \kappa_2 \end{bmatrix} \quad 7-5$$

You can also change the anisotropic direction to be the Y direction instead of the Z direction by specifying the YDIR.ANISO parameter or by specifying ^ZDIR.ANISO.

The thermal conductivity is temperature dependent, and the anisotropic thermal conductivity must have a model selected for its dependence on temperature. To do this, select TANI.CONST, TANI.POWER, TANI.POLYNOM or TANI.RECIP. These are analogous to TCON.CONST, TCON.POWER, TCON.POLYNOM and TCON.RECIP respectively. You can specify different temperature dependency models for the $\kappa(T)$ and $\kappa_{\text{aniso}}(T)$. The parameters for the chosen model for $\kappa_{\text{aniso}}(T)$ are specified by using the relevant parameters from A.TC.CONST, A.TC.A, A.TC.B, A.TC.C, A.TC.D, A.TC.E and A.TC.NPOW. These are equivalent to the isotropic parameters but with a prefix of A. to distinguish them. No built-in models are available for the anisotropic component of thermal conductivity. To give the anisotropic component the same temperature dependence as for the built-in model (Equation 7-2), specify the TANI.POWER.

As in the case of anisotropic permittivity, the discretization of the flux term is modified. For the simple cases of a rectangular mesh and a diagonal thermal conductivity tensor, the discretization chooses the value of thermal conductivity appropriate to the direction.

If the coordinate system where the thermal conductivity tensor is diagonal and the ATLAS coordinate system are non-coincident, then the coordinate transformation can be specified as a set of vectors

$$\begin{aligned} X &= (X.X, X.Y, X.Z) \\ Y &= (Y.X, Y.Y, Y.Z) \\ Z &= (Z.X, Z.Y, Z.Z) \end{aligned}$$

where the vector components can be specified on the MATERIAL statement. The default is that

$$\begin{aligned} X &= (1.0, 0.0, 0.0) \\ Y &= (0.0, 1.0, 0.0) \\ Z &= (0.0, 0.0, 1.0) \end{aligned}$$

and you should specify all necessary components. You do not need to normalize the vectors to unit length. ATLAS will normalize them and transform the thermal conductivity tensor according to the usual rules. If you specify any component of X, Y or Z, then a more complete form of discretization will be used.

This is similar to the complete discretization carried out for the case of a generally anisotropic dielectric permittivity described in Section 3.12: “Anisotropic Relative Dielectric Permittivity”.

To enable the more complete form of discretization, use the `TC.FULL.ANISO` parameter on the `MATERIAL` statement.

Table 7-4 shows the parameters used in Anisotropic Thermal Conductivity.

| Table 7-4. MATERIAL Statement Parameters | | | |
|--|---------|---------|-----------|
| Parameter | Type | Default | Units |
| A.TC.CONST | Real | 0.0 | (W/cm/K) |
| A.TC.A | Real | 0.0 | cm K /W |
| A.TC.B | Real | 0.0 | cm /W |
| A.TC.C | Real | 0.0 | cm / W /K |
| A.TC.D | Real | 0.0 | K |
| A.TC.E | Real | 0.0 | W/cm |
| A.TC.NPOW | Real | 0.0 | – |
| TANI.CONST | Logical | False | |
| TANI.POWER | Logical | False | |
| TANI.POLYNOM | Logical | False | |
| TANI.RECIP | Logical | False | |
| TC.FULL.ANISO | Logical | False | |
| YDIR.ANISO | Logical | False | |
| ZDIR.ANISO | Logical | True | |
| X.X | Real | 1.0 | |
| X.Y | Real | 0.0 | |
| X.Z | Real | 0.0 | |
| Y.X | Real | 0.0 | |
| Y.Y | Real | 1.0 | |
| Y.Z | Real | 0.0 | |
| Z.X | Real | 0.0 | |
| Z.Y | Real | 0.0 | |
| Z.Z | Real | 1.0 | |

7.2.3: Specifying Heat Capacity

Standard Model

For transient calculations, specify heat capacities for every region in the structure. These are also functions of the lattice temperature and are modeled as:

$$C = HC.A + HC.B T_L + HC.C T_L^2 + \frac{HC.D}{T_L^2} \quad (J/cm^3/K) \quad 7-6$$

Default values of HC.A, HC.B, HC.C, and HC.D are provided for common materials. You can specify these values in the MATERIAL statement.

The following statements will be used to specify the temperature dependent heat capacities of the regions previously defined.

```
MATERIAL REGION=5 HC.A=<n> HC.B=<n> HC.C=<n> HC.D=<n>
```

```
MATERIAL REGION=6 HC.A=<n> HC.B=<n> HC.C=<n> HC.D=<n>
```

| Table 7-5. User Specifiable Parameters for Equation 7-6 | | |
|---|-----------|-----------------------------------|
| Statement | Parameter | Units |
| MATERIAL | HC.A | J/cm ³ /K |
| MATERIAL | HC.B | J/cm ³ ·K ² |
| MATERIAL | HC.C | J/cm ³ ·K ³ |
| MATERIAL | HC.D | JK/cm ³ |

To select the standard model for heat capacity, specify HC.STD on the MATERIAL statement.

Compositionally Dependent Heat Capacity [170]

The temperature dependence of heat capacity can be expressed by:

$$C(T_L) = \rho \left[C_{300} + C_1 \frac{\left(\frac{T_L}{300}\right)^\beta - 1}{\left(\frac{T_L}{300}\right)^\beta + \frac{C_1}{C_{300}}} \right] \quad 7-7$$

where $C(T_L)$ is the temperature dependent heat capacity, ρ is the mass density, C_{300} , C_1 and β are material dependent parameters. Table 7-6 shows the default values of ρ , C_{300} , C_1 and β for the binary compounds and Si and Ge.

Table 7-6. Default Parameter Values for Heat Capacity

| Material | ρ (g/cm ³) | C_{300} (J/K/kg) | C_1 (J/K/kg) | β |
|----------|--------------------------------|-----------------------|-------------------|---------|
| Si | 2.33 | 711 | 255 | 1.85 |
| Ge | 5.327 | 360 | 130 | 1.3 |
| GaAs | 5.32 | 322 | 50 | 1.6 |
| AlAs | 3.76 | 441 | 50 | 1.2 |
| InAs | 5.667 | 394 | 50 | 1.95 |
| InP | 4.81 | 410 | 50 | 2.05 |
| GaP | 4.138 | 519 | 50 | 2.6 |

For the ternary compounds and SiGe, the parameters ρ , C_{300} , C_1 and β are interpolated versus composition using a simple linear form as in Equation 7-8.

$$P_{ab} = (1-x)P_a + xP_b \quad 7-8$$

When the lattice heat flow equation is solved, the global device temperature parameter is the maximum temperature at any mesh point in the device.

To select the compositionally dependent heat capacity, specify `HC.COMP` on the `MATERIAL` statement.

C-Interpreter Defined Thermal Capacity

You can use the C-INTERPRETER to define the thermal capacity, `TCAP`, as a function of the lattice temperature, position, doping and fraction composition. This is defined using the syntax:

```
MATERIAL REGION=<n.region> F.TCAP=<filename>
```

where the `<filename>` parameter is an ASCII file containing the C-INTERPRETER function. For more information about the C-INTERPRETER, see Appendix A: "C-Interpreter Functions".

You can override the default values for ρ , C_{300} , C_1 , and β by specifying `HC.RHO`, `HC.C300`, `HC.C1`, `HC.BETA` respectively on the `MATERIAL` statement.

7.2.4: Specifying Heat Sink Layers

You can define regions to only include thermal calculations. These regions will typically consist of layers associated with heat sinks. They are defined using the `REGION` statement. Even though in reality the heat sink materials are typically metal conductors, it is easier to specify these layers with the material type, `INSULATOR`. This is because as insulators the program will only solve heat flow and not attempt to solve current continuity in these layers. The region number is subsequently used as an identifier when thermal conductivities and heat capacities are assigned to these regions.

The following statements specify two layers of a heat sink for inclusion in the thermal calculation.

```
REGION NUM=5 Y.MIN=0.5 Y.MAX=2.0 INSULATOR
REGION NUM=6 Y.MIN=2.0 Y.MAX=3.0 INSULATOR
```

7.2.5: Non-Isothermal Models

Effective Density Of States

When lattice heating is specified with the drift-diffusion transport model, the effective density of states for electrons and holes are modeled as functions of the local lattice temperature as defined by Equations 3-31 and 3-32 in Chapter 3: “Physics”.

When lattice heating is specified with the energy balance model, the effective densities of states are modeled as functions of the local carrier temperatures, T_n and T_p , as defined by Equations 3-126 and 3-127 in Chapter 3: “Physics”.

Non-isothermal Current Densities

When GIGA is used, the electron and hole current densities are modified to account for spatially varying lattice temperatures:

$$\vec{J}_n = -q\mu_n n(\nabla\phi_n + P_n \nabla T_L) \quad 7-9$$

$$\vec{J}_p = -q\mu_p p(\nabla\phi_p + P_p \nabla T_L) \quad 7-10$$

where:

P_n and P_p are the absolute thermoelectric powers for electrons and holes. P_n and P_p are modeled as follows:

$$P_n = -\frac{k_B}{Q} \left(\frac{5}{2} + \ln \frac{N_c}{n} + K_{SN} + \zeta_n \right) \quad 7-11$$

$$P_p = \frac{k_B}{Q} \left(\frac{5}{2} + \ln \frac{N_v}{p} + K_{SP} + \zeta_p \right) \quad 7-12$$

Here, k_B is Boltzmann’s constant. K_{SN} and K_{SP} are the exponents in the power law relationship between relaxation time (or mobility) and carrier temperature. They are also used in the energy balance model. Their values typically range between -1 and 2 in Silicon and they are set on the `MODELS` statement.

You can also model them using the C-Interpreter functions `F.KSN` and `F.KSP` if a more complicated dependence is required.

The quantities ζ_n and ζ_p are the phonon drag contribution to the thermopower. These are only significant in low doped material and at low temperatures. `ATLAS` has a built in model for this phonon drag contribution, which you enable by specifying the `PHONONDRAG` parameter on the `MODELS` statement. The built-in model is

$$\zeta_n = \left(\frac{k_B}{Q} \right)^{PDA_N} \left(\frac{T_L}{300} \right)^{PDEXP_N} \quad 7-13$$

for electrons and

$$\zeta_p = \left(\frac{k_B}{Q} \right)^{PDA_P} \left(\frac{T_L}{300} \right)^{PDEXP_P} \quad 7-14$$

for holes. A theoretically derived value for `PDEXP.N` and `PDEXP.P` is $-7/2$ [94] but experimentally obtained results generally give a value of around $-5/2$ [78]. The values of `PDA.N` and `PDA.P` depend on doping level and can also depend on sample size. Therefore, it is recommended that you choose values to fit to your sample. Alternatively, empirical data or more complicated formulae can be incorporated by using the C-Interpreter functions `F.PDN` and `F.PDP` on the `MATERIAL` or `MODELS` statements [23], [89], [235].

The thermopower can be thought of as having 3 components. The first is the derivative of the Fermi Potential with respect to temperature. For Maxwell-Boltzmann statistics, this is

$$-\frac{k_B}{Q}\left(\frac{3}{2} + \ln \frac{Nc}{n}\right) \quad 7-15$$

for electrons and

$$\frac{k_B}{Q}\left(\frac{3}{2} + \ln \frac{Nv}{p}\right) \quad 7-16$$

for holes.

ATLAS incorporates this effect indirectly through the boundary conditions. It does not contribute directly to the temperature gradient term in the expressions for current, see Equations 7-9 and 7-10.

The second term is due to carrier scattering and is

$$-\frac{k_B}{Q}(1 + KSN) \quad 7-17$$

for electrons and

$$\frac{k_B}{Q}(1 + KSP) \quad 7-18$$

for holes. The third term is the phonon drag contribution $-\zeta_n$ and ζ_p , and the second and third terms are included directly into the temperature gradient term in the expressions for current.

Seebeck Effect

This is the phenomenon in which an open circuited voltage is generated across a semiconductor having a temperature gradient. To observe this in practice, you need two materials each with a different thermopower. In simulation, you can directly observe the Seebeck effect because you can measure the open circuit voltage between two contacts at different temperatures. Current boundary conditions are applied to one contact and solved for zero current.

This will result in a voltage difference between the two contacts.

The Seebeck coefficient is given as the ratio of the Voltage difference between the contacts to the temperature difference, and the most convenient units for expressing it are mV/K. To theoretically calculate the Voltage difference generated by the temperature gradient, integrate the thermopower as a function of temperature between the temperatures on the contact

$$V_1 - V_0 = - \int_{T_0}^{T_1} \frac{\mu_n N_D P_n(T) + \mu_p N_A P_p(T) dT}{\mu_n N_D + \mu_p N_A} \quad 7-19$$

for a compensated material, where T_0 and T_1 are the temperatures on the contacts and V_0 and V_1 are the voltages. The effective Seebeck coefficient for the device is obtained by dividing the voltage difference so obtained by the temperature difference ($T_1 - T_0$).

Table 7-7 shows the default values for Equations 7-11 and 7-12.

| Table 7-7. User-Specifiable Parameters for Equations 7-11 and 7-12 | | | |
|--|-----------|---------|-------|
| Statement | Parameter | Default | Units |
| MODELS | F.KSN | | |
| MODELS | F.KSP | | |
| MODELS | KSN | -1 | None |
| MODELS | KSP | -1 | None |
| MODELS | PHONONDRA | False | |
| MODELS | F.PDN | | |
| MODELS | F.PDP | | |
| MATERIAL | F.PDN | | |
| MATERIAL | F.PDP | | |
| MATERIAL | PDA.N | 0.2 | |
| MATERIAL | PDA.P | 0.2 | |
| MATERIAL | PDEXP.N | -2.5 | |
| MATERIAL | PDEXP.P | -2.5 | |

7.2.6: Heat Generation

When carrier transport is handled in the drift-diffusion approximation the heat generation term, H , used in Equation 7-1 has the form:

$$\begin{aligned}
 H = & \frac{|\vec{J}_n|^2}{q\mu_n n} + \frac{|\vec{J}_p|^2}{q\mu_p p} - T_L(\vec{J}_n \nabla P_n) - T_L(\vec{J}_p \nabla P_p) \\
 & + q(R - G) \left[T_L\left(\frac{\partial \phi_n}{\partial T}\right)_{n,p} - \phi_n - T_L\left(\frac{\partial \phi_p}{\partial T}\right)_{n,p} + \phi_p \right] \\
 & - T_L \left[\left(\frac{\partial \phi_n}{\partial T}\right)_{n,p} + P_n \right] \text{div} J_n - T_L \left[\left(\frac{\partial \phi_p}{\partial T}\right)_{n,p} + P_p \right] \text{div} J_p
 \end{aligned} \tag{7-20}$$

In the steady-state case, the current divergence can be replaced with the net recombination. Equation 7-20 then simplifies to:

$$H = \left[\frac{|\vec{J}_n|^2}{q\mu_n n} + \frac{|\vec{J}_p|^2}{q\mu_p p} \right] + q(R - G)[\phi_p - \phi_n + T_L(P_p - P_n)] - T_L(\vec{J}_n \nabla P_n + \vec{J}_p \nabla P_p) \tag{7-21}$$

where:

$$\left[\frac{|\vec{J}_n|^2}{q\mu_n n} + \frac{|\vec{J}_p|^2}{q\mu_p p} \right] \text{ is the Joule heating term,}$$

$q(R - G)[\phi_p - \phi_n + T_L(P_p - P_n)]$ is the recombination and generation heating and cooling term,

$-T_L(\vec{J}_n \nabla P_n + \vec{J}_p \nabla P_p)$ accounts for the Peltier and Joule-Thomson effects.

A simple and intuitive form of H that has been widely used in the past is:

$$H = (\vec{J}_n + \vec{J}_p) \cdot \vec{E} \tag{7-22}$$

GIGA can use either Equations 7-21 or 7-22 for steady-state calculations. By default, Equation 7-22 is used. Equation 7-21 is used if the `HEAT.FULL` parameter is specified in the `MODELS` statement. To enable/disable the individual terms of Equation 7-21, use the `JOULE.HEAT`, `GR.HEAT`, and `PT.HEAT` parameters of the `MODEL` statement.

If the general expression shown in Equation 7-20 is used for the non-stationary case, the derivatives

$\left(\frac{\partial \phi_n}{\partial T}\right)_{n,p}$ and $\left(\frac{\partial \phi_p}{\partial T}\right)_{n,p}$ are evaluated for the case of an idealized non-degenerate semiconductor and complete ionization.

The heat generation term, H , is always set equal to 0 in insulators.

For conductors $H = \frac{(\nabla V)^2}{\rho}$.

When electron and hole transport are modeled in the energy balance approximation (by specifying HCTE on the MODELS statement), the following expression is used for H :

$$H = W_n + W_p + E_g U, \quad 7-23$$

where U , W_n and W_p are defined by Equations 3-128 through 3-130 in Chapter 3: “Physics”.

If the energy balance model is enabled for only electrons or only holes, then a hybrid of Equations 7-23 and 7-21 or 7-22 is used. For example if the energy balance equation is solved for electrons, but not for holes, then H is evaluated as follows if HEAT.FULL is specified.

$$H = W_n + E_g U + \frac{|\vec{J}_p|^2}{q\mu_p p} - T_L \vec{J}_p \cdot \nabla P_p \quad 7-24$$

A simpler form for the heating will be used if HEAT.FULL is not specified.

$$H = W_n + E_g U + \vec{J}_p \cdot \vec{E} \quad 7-25$$

If the energy balance equation is solved for holes, but drift-diffusion is solved for holes, then the heating term is analogous to Equations 7-24 and 7-25 with hole terms swapped for electron terms and vice versa.

The first terms of W_n and W_p are output to structure files as Joule heating. The last term in Equation 7-24 is output as Peltier Thomson Heat power. The remaining terms are output as recombination heat power.

7.2.7: Thermal Boundary Conditions

At least one thermal boundary condition must be specified when the lattice heat flow equation is solved. The thermal boundary conditions used have the following general form:

$$\sigma(\vec{J}_{tot}^u \cdot \vec{s}) = \alpha(T_L - T_{ext}) \quad 7-26$$

where σ is either 0 or 1, \vec{J}_{tot}^u is the total energy flux and \vec{s} is the unit external normal of the boundary.

The projection of the energy flux onto \vec{s} is:

$$(\vec{J}_{tot}^u \cdot \vec{s}) = -\kappa \frac{\partial T_L}{\partial n} + (T_L P_n + \phi_n) \vec{J}_n \cdot \vec{s} + (T_L P_p + \phi_p) \vec{J}_p \cdot \vec{s} \quad 7-27$$

When $\sigma = 0$, Equation 7-26 specifies a Dirichlet (fixed temperature) boundary condition:

$$T_L = \text{TEMPER}. \quad 7-28$$

where you define TEMPER in the THERMCONTACT statement as shown in the next section. You can specify dirichlet boundary conditions for an external boundary (which may coincide with an electrode) or for an electrode inside the device.

When $\sigma = 1$, Equation 7-26 takes the form:

$$\left(\overrightarrow{J_{tot}^u} \cdot \hat{s} \right) = \frac{1}{R_{th}} (T_L - \text{TEMPER}) \quad 7-29$$

where the thermal resistance, R_{th} , is given by:

$$R_{th} = \frac{1}{\text{ALPHA}} \quad 7-30$$

and ALPHA is user-definable on the THERMCONTACT statement.

Specifying Thermal Boundary Conditions

Setting thermal boundary conditions is similar to setting electrical boundary conditions. The THERMCONTACT statement is used to specify the position of the thermal contact and any optional properties of the contact. You can place thermal contacts anywhere in the device (including sidewalls). Equation 7-29 is used if a value is specified for α . Otherwise, Equation 7-28 is used.

The following command specifies that thermal contact number 1 is located between $x=0 \mu\text{m}$ and $x=2 \mu\text{m}$ at $y=0 \mu\text{m}$, and that the temperature at the contact is 300K.

```
THERMCONTACT NUM=1 X.MIN=0 X.MAX=2 Y.MIN=0 Y.MAX=0 TEMP=300
```

You can use simpler statement if the coordinates of a thermal contact coincide with the coordinates of an electrical contact. In this case, it is permissible to specify the location of the thermal contact by referring to the electrode number of the electrical contact. For example, the statement:

```
THERMCONTACT NUM=1 ELEC.NUM=3 TEMP=400
```

specifies that thermal contact number 1 is located in the same position as electrode number 3 and that the contact temperature is 400K.

Specifying the BOUNDARY parameter gives you flexibility in applying thermal boundary conditions. This parameter is set by default and means that the thermal boundary condition will only be set on the outside surface of the thermal contact, where it forms the exterior of the device. If the parameter is cleared by specifying ^BOUNDARY in the THERMCONTACT statement, the boundary conditions will be applied to the interior of the thermal contact and to the part of the surface of the thermal contact that forms an interface with the interior of the device. In a 2D model, you may have a thermal contact that is internal to the device and in this case you would need to specify ^BOUNDARY. Otherwise, the contact will be ignored.

For example:

```
THERMCONTACT ELEC.NUM=1 ^BOUNDARY TEMPER=450 ALPHA=2.5
```

where the ELECTRODE extends into the device and will set the interior points of the thermalcontact to 450K and will apply the flux boundary condition on all faces of the thermal contact that interface with the interior of the device.

Table 7-8. User Specifiable Parameters for Equations 7-28 and 7-29

| Statement | Parameter | Units | Default |
|--------------|-----------|------------------------|----------|
| THERMCONTACT | ALPHA | W/ (cm ² K) | ∞ |
| THERMCONTACT | BOUNDARY | - | True |
| THERMCONTACT | TEMPER | K | 300 |

Representing a thermal environment, in terms of thermal impedances, leads to efficient solutions. But, thermal impedance representations are typically only approximations. Detailed thermal modeling (e.g., the effect of heat sink design changes) typically requires using detailed modeling of thermal regions with specified external ambient temperatures.

Note: You can't alter the value of a thermal resistor within a sequence of SOLVE statements. Rerun the input file whenever a thermal resistor is changed.

7.2.8: Temperature Dependent Material Parameters

GIGA automatically uses the built-in temperature dependence of the physical models that are specified. When lattice heating is specified, temperature dependent values are evaluated locally at each point in the device. When lattice heating is not solved, the models only provide global temperature dependence. In other words, all points in the device are assumed to be at the specified temperature.

The non-isothermal energy balance model uses the same carrier temperature dependencies of the mobility and impact ionization models as in the pure energy balance case, but with coefficients that depend on the local lattice temperature. Impact ionization coefficients depend on lattice temperature. Almost all other models and coefficients depend on lattice temperature.

When lattice heating is used, there is no point in specifying models that do not include temperature dependence. For mobilities, don't specify CONMOB. Instead, specify ANALYTIC or ARORA. For impact ionization coefficients, specify the SELBERHERR model.

GIGA can account for the temperature dependence of the minority carrier lifetimes for electrons or holes or both. The LT.TAUN (electrons) and LT.TAUP (holes) parameters of the MATERIAL statement are used to select this model. This model is turned on whenever the value of LT.TAUN or LT.TAUP is greater than 0, which is the default.

The temperature dependence of electron and hole lifetimes in the SRH recombination model have the forms:

$$\tau_n = \text{TAUN0} \left(\frac{T_L}{300} \right)^{\text{LT.TAUN}} \quad 7-31$$

$$\tau_p = \text{TAUP0} \left(\frac{T_L}{300} \right)^{\text{LT.TAUP}} \quad 7-32$$

Table 7-9. User-Specifiable Parameters for Equations 7-31 and 7-32

| Statement | Parameter | Default | Units |
|-----------|-----------|--------------------|-------|
| MATERIAL | TAUN0 | 1×10^{-7} | s |
| MATERIAL | TAUP0 | 1×10^{-7} | s |
| MATERIAL | LT.TAUN | 0 | |
| MATERIAL | LT.TAUP | 0 | |

See Equations 3-299 and 3-300 in Chapter 3: “Physics” for information regarding concentration dependent lifetimes.

There is an alternative model for the temperature dependence of the recombination lifetimes. This is

$$\tau_n(T_L) = \text{TAUN0} \exp(\text{TCOEFF.N}(T_L/300 - 1.0)) \quad 7-33$$

$$\tau_p(T_L) = \text{TAUP0} \exp(\text{TCOEFF.P}(T_L/300 - 1.0)) \quad 7-34$$

To enable this model, use `SRH.EXPTEMP` on the `MODELS` statement along with `SRH` or `CONSRH`. You can set the parameters `TCOEFF.N` and `TCOEFF.P` on the `MATERIAL` statement (see Table 7-10).

| Table 7-10. Material Parameters for Exponential Temperature Dependence Model. | | | |
|---|-----------|------|---------|
| Statement | Parameter | Type | Default |
| MATERIAL | TCOEFF.N | Real | 2.55 |
| MATERIAL | TCOEFF.P | Real | 2.55 |

7.2.9: Phase Change Materials (PCMs)

Phase Change Materials, PCMs, are materials that display a change in resistivity with temperature that can be associated with a phase change in the material between crystalline and amorphous states. Typically, the material exhibits a low resistivity in the crystalline state and a relatively higher resistivity in the amorphous state. Once a state (crystalline/amorphous or low/high resistivity) is obtained, it can be "frozen" into the material by rapidly lowering the temperature. This characteristic enables PCM materials to exhibit hysteresis under such conditions and makes them suitable to store information. Although this model was designed for PCM materials, it is also applicable to other materials exhibiting similar characteristics.

To enable the PCM model, specify `PCM` in the `MODEL` statement. When you enable this model, the resistivity as a function of lattice temperature will be described (see Figure 7-1).

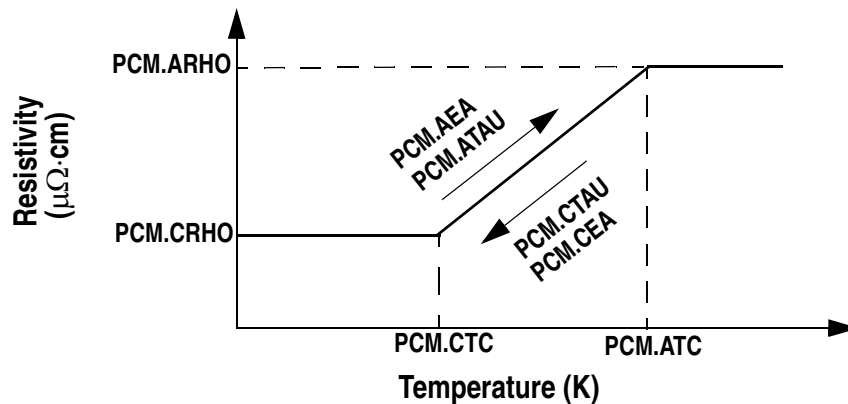


Figure 7-1: PCM Temperature Dependent Resistivity Model

Here at low temperatures, less than or equal to PCM.CTC. The resistivity is constant and equal to the value specified by PCM.CRHO. At high temperatures above PCM.ATC, the resistivity is constant and equal to the value of PCM.ARHO. Between the temperatures PCM.CTC and PCM.ATC, the resistivity varies either linearly or logarithmically with temperature depending on the value of the PCM.LOG parameter of the MODEL statement.

The resistivity as a function of temperature is as given in Equations 7-35 through 7-37 for the case where PCM.LOG is not true.

$$\rho = \text{PCM_CRHO} \quad (T < \text{PCM_CTC}) \quad 7-35$$

$$\rho = \text{PCM_ARHO} \quad (T > \text{PCM_ATC}) \quad 7-36$$

$$\rho = \frac{(T - \text{PCM_CTC})(\text{PCM_ARHO} - \text{PCM_CRHO})}{(\text{PCM_ATC} - \text{PCM_CTC})} + \text{PCM_CRHO} \quad (\text{PCM_CTC} < T < \text{PCM_ATC}) \quad 7-37$$

For the case where PCM.LOG is true, the resistivity between the critical temperatures is given by Equations 7-38 and 7-39.

$$\rho = 10^x \quad 7-38$$

$$x = \left(\frac{T - \text{PCM_CTC}}{\text{PCM_ATC} - \text{PCM_CTC}} \right) (\log_{10}(\text{PCM_ARHO}) - \log_{10}(\text{PCM_CRHO})) \\ + \log_{10}(\text{PCM_CRHO}) \quad (\text{PCM_CTC} < T < \text{PCM_ATC}) \quad 7-39$$

Hysteresis is built into the model in two ways. In static simulations, the resistivity is updated according to Figure 7-1 only for increasing temperature. This is suitable since phase changes in memory devices are generally made during increasing temperature ramps.

For time domain simulations, the hysteresis is described using the Johnson-Mehl-Avrami model as given in Equations 7-40 and 7-41. Here, t is the time at the last time step, dt is the size of the time step, T is the lattice temperature, $\hat{\rho}(T)$ is the temperature dependent static resistivity given by Equations 7-35 through 7-39, $\rho(t, T)$ is the resistivity at the last time step, and $\rho(t+dt, T)$ is the resistivity at the new time step.

Equation 7-40 applies to increasing temperature. Equation 7-41 applies to decreasing temperature.

$$\rho(t + \Delta t, T) = \rho(t, T) + [\hat{\rho}(T) - \rho(t, T)] \cdot \quad 7-40$$

$$\left\{ 1 - \exp \left[(-dt / \text{PCM_ATAU})^{\text{PCM_AP}} \exp \left(\frac{-\text{PCM_AEA}}{kT} \right) \right] \right\}$$

$$\rho(t + \Delta t, T) = \rho(t, T) + [\hat{\rho}(T) - \rho(t, T)] \cdot \quad 7-41$$

$$\left\{ 1 - \exp \left[(-dt / \text{PCM.CTAU})^{\text{PCM.CP}} \exp \left(\frac{-\text{PCM.CEA}}{kT} \right) \right] \right\}$$

Table 7-11 shows the parameters of Equations 7-35 through 7-41.

| Table 7-11. Material Parameters for PCM Materials | | | | |
|---|-------------|------|---------------------|-------|
| Statement | Parameter | Type | Default | Units |
| MATERIAL | PCM.AEA | Real | 3.2 | eV |
| MATERIAL | PCM.AP | Real | 1.0 | |
| MATERIAL | PCM.ARHO | Real | 10 ⁸ | μΩcm |
| MATERIAL | PCM.ATAU | Real | 2×10 ⁻³⁶ | s |
| MATERIAL | PCM.ATC | Real | 620 | K |
| MATERIAL | PCM.CEA | Real | 3.7 | eV |
| MATERIAL | PCM.CP | Real | 1.0 | |
| MATERIAL | PCM.CRHO | Real | 10 ⁸ | μΩcm |
| MATERIAL | PCM.CTAU | Real | 2×10 ⁻³⁶ | s |
| MATERIAL | PCM.CTC | Real | 600 | K |
| MATERIAL | PCM.LATHEAT | Real | 622 | J |

Latent heat can be also be introduced into the source term of the heatflow equation (Equation 7-1) by specifying PCM.LATHEAT on the MATERIAL statement. The latent heat is introduced as described in Equation 7-42 for increasing temperatures and Equation 7-43 for decreasing temperatures where $H(t+dt, T)$ is the the latent heat at the current time step and $H(t, T)$ is the latent heat at the previous time step. $\hat{H}(T)$ is the temperature dependent static latent heat given by Equation 7-44 for increasing temperature and Equation 7-46 for decreasing temperature.

Note: The time integration performed in Equations 7-40 and 7-41 above and Equations 7-42 and 7-43 below critically depends on the choice of the parameters PCM.AEA, PCM.CEA, PCM.ATAU, and PCM.CTAU relative to the operating temperatures and time steps. In some cases, you may find that the simulator produces no discernable changes in resistivity. In this case, you should carefully reconsider the specifications of these parameters.

$$H(t + \Delta t, T) = H(t, T) + [\hat{H}(T) - H(t, T)] \cdot \quad 7-42$$

$$\left\{ 1 - \exp \left[(-dt / \text{PCM.ATAU})^{\text{PCM.AP}} \exp \left(\frac{-\text{PCM.AEA}}{kT} \right) \right] \right\}$$

$$H(t + \Delta t, T) = H(t, T) + [\hat{H}(T) - H(t, T)] \cdot \quad 7-43$$

$$\left\{ 1 - \exp \left[(-dt / \text{PCM} . \text{CTAU})^{\text{PCM} . \text{CP}} \exp \left(\frac{-\text{PCM} . \text{CEA}}{kT} \right) \right] \right\}$$

$$\hat{H}(T) = \left(\frac{T - \text{PCM} . \text{CTC}}{\text{PCM} . \text{ATC} - \text{PCM} . \text{CTC}} \right) \text{PCM} . \text{LATHEAT} \quad (\text{PCM} . \text{CTC} < T < \text{PCM} . \text{ATC}) \quad 7-44$$

$$\hat{H}(T) = - \left(\frac{\text{PCM} . \text{ATC} - T}{\text{PCM} . \text{ATC} - \text{PCM} . \text{CTC}} \right) \text{PCM} . \text{LATHEAT} \quad (\text{PCM} . \text{CTC} < T < \text{PCM} . \text{ATC}) \quad 7-45$$

You can initialize the resistivity of a PCM material to a user-specified value by setting the `RESISTIVITY` parameter of the `MATERIAL` statement. If unspecified, the initial resistivity will be set to the value of `PCM.CRHO`.

To simplify the numerics of PCM simulation, set the `PCM` parameter of the `METHOD` statement. This parameter effectively sets the `METHOD` parameters as described in Table 7-12.

| Table 7-12. PCM Method Settings | |
|---------------------------------|---------|
| Parameter | Setting |
| <code>MIN.TEMP</code> | 1e-9 |
| <code>MAX.TEMP</code> | 1e9 |
| <code>DVMAX</code> | 1e9 |
| <code>DIRECT</code> | TRUE |
| <code>CARRIERS</code> | 0 |
| <code>NEWTON</code> | TRUE |
| <code>TAUTO</code> | FALSE |

If you want to simulate a mixture of semiconductors and PCM materials, then set both `PCM` and `CARRIERS=2` on the `METHOD` statement.

You can redefine the resistivity relations given by Equations 7-35 through 7-44 with a user-specified function using the C-interpreter. You can assign the `F.PCM` parameter of the `MATERIAL` statement to the file name of a valid C interpreter function expressing the variation of resistivity with temperature and history.

7.2.10: C-Interpreter Defined Scattering Law Exponents

KSN and KSP are exponents in the relationship between relaxation time and carrier energy. In the case for electrons:

$$\tau_n \sim (E - E_c)^{KSN} \quad 7-46$$

They are generally calculated from the dependence of mobility on carrier temperature, see Equations 3-123 and 3-124 in Section 3.4.1: “The Energy Balance Equations”.

The value of KSN and KSP therefore depend on the scattering mechanisms, which are determining the relaxation time. Generally, KSN and KSP will themselves depend on Carrier Energy. The C-Interpreter functions F.KSN and F.KSP are available in ATLAS to model this dependence. The Energy input is $1.5 k_B T_{n,p}$ if HCTE is specified, or $1.5 k_B T_L$ if only LAT.TEMP is specified. To use these C-Interpreter functions, the syntax is

```
MODELS F.KSN=<filename> F.KSP=<filename>
```

where the <filename> parameter is an ASCII file containing the C-INTERPRETER function. See Appendix A: “C-Interpreter Functions” for more information regarding the C-INTERPRETER and its functions.

7.3: Applications of GIGA

7.3.1: Power Device Simulation Techniques

This section contains a series of techniques, which you may find useful when simulating typical power device structures. Not all of the features described below are specific to GIGA and are common to the ATLAS framework.

Floating Guard Rings

No special syntax is needed for the simulation of uncontacted doping areas used in floating guard rings. The program is able to simulate guard ring breakdown with the standard impact ionization models. In some extreme cases, convergence may be slow due to poor initial guesses. If convergence is slow, both GUMMEL and NEWTON should be used in the METHOD statement.

Floating Field Plates

You should use the ELECTRODE statement to specify the field plate regions as electrodes. If these plates do not contact any semiconductor, then you can set these electrodes to float in the same manner as EEPROM floating gates. The following statement line specifies that the field plate region PLATE1 is a floating field plate.

```
CONTACT NAME=PLATE1 FLOATING
```

If the plates do contact the semiconductor, then do not use this syntax. Instead, current boundary conditions are used at the electrode with zero current. See Chapter 2: “Getting Started with ATLAS”, the “Floating Contacts” section on page 2-37 for more information about floating electrodes.

External Inductors

Inductors are commonly used in the external circuits of power devices. You can use the CONTACT statement to set an inductor on any electrode. The following statement sets an inductance on the drain electrode of 3 $\mu\text{H}/\mu\text{m}$.

```
CONTACT NAME=DRAIN L=3E-3
```

The next statement is used to specify a non-ideal inductor with a resistance of 100 $\Omega/\mu\text{m}$.

```
CONTACT NAME=DRAIN L=3E-3 R=100
```

7.3.2: More Information

Many examples using GIGA have been installed on your distribution tape or CD. These include power device examples but also SOI and III-V technologies. You can find more information about the use of GIGA by reading the text associated with each example.

This page is intentionally left blank.

8.1: Overview

LASER performs coupled electrical and optical simulation of semiconductor lasers. LASER works with BLAZE and allows you to:

- Solve the Helmholtz Equation (see Equation 8-1) to calculate the optical field and photon densities.
- Calculate the carrier recombination due to light emission (i.e., stimulated emission).
- Calculate optical gain, depending on the photon energy and the quasi-Fermi levels.
- Calculate laser light output power.
- Calculate the light intensity profile corresponding to the multiple transverse modes.
- Calculate light output and modal gain spectra for several longitudinal modes.

To perform a LASER simulation, you need to know ATLAS and BLAZE first. If you don't, read Chapter 2: "Getting Started" and Chapter 5: "BLAZE".

8.2: Physical Models

To simulate semiconductor lasers, the basic semiconductor equations (see Equations 3-1 to 3-4 in Chapter 3: “Physics”) are solved self-consistently with an optical equation that determines the optical field intensity distribution. LASER uses the following coordinate system:

- The X axis is perpendicular to the laser cavity and goes along the surface (from left to right).
- The Y axis is perpendicular to the laser cavity and goes down from the surface.
- The Z axis goes along the laser cavity.

The X and Y axes are the same as in other ATLAS products. The electrical and optical equations are solved in the X and Y plane (i.e., perpendicular to the laser cavity).

8.2.1: Scalar Helmholtz Equation

LASER solves a two-dimensional Helmholtz equation to determine the transverse optical field profile $E_k(x,y)$ [256]:

$$\nabla_{xy}^2 E_k(x,y) + \left(\frac{\omega_m^2}{c^2} \varepsilon(x,y) - \beta_k^2 \right) E_k(x,y) = 0 \quad 8-1$$

where:

$\nabla_{xy}^2 = \left(\frac{\partial^2}{\partial x^2} + \frac{\partial^2}{\partial y^2} \right)$ is the two-dimensional Laplace operator, ω_m is the frequency corresponding to

longitudinal mode m (ω_m corresponds to OMEGA on the LASER statement for single frequency simulations), c is the velocity of light in vacuum, and $\varepsilon(x,y)$ is the high frequency dielectric permittivity.

Equation 8-1 is a complex eigenvalue problem. LASER solves this equation to determine the set of complex eigenvalues (β_k) and corresponding eigenfunctions $E_k(x,y)$. LASER takes into account only the fundamental transverse mode solution. Therefore, the index (k) will be dropped from subsequent equations.

In principle, Equation 8-1 should be solved for each longitudinal mode that is taken into account. Since very few longitudinal modes are actually lasing, LASER solves Equation 8-1 only once for the longitudinal mode with the greatest power and subsequently assumes:

$$E_m(x,y) = E_o(x,y) \quad 8-2$$

where $E_o(x,y)$ is the optical field corresponding to the most powerful longitudinal mode. This assumption is reasonable, since the shape of the solution is almost independent of the frequency within the range of interest.

For dielectric permittivity, LASER uses the following model [110]:

$$\varepsilon(r,z) = \varepsilon_0 + (-\text{ALPHAR} + j) \frac{\sqrt{\varepsilon_0} g(x,y)}{k_\omega} - j \frac{\sqrt{\varepsilon_0} (\text{ALPHA} + \text{FCN} \cdot n + \text{FCP} \cdot p)}{k_\omega} \quad 8-3$$

where:

- ϵ_0 is the bulk high frequency permittivity. You can specify the bulk high frequency permittivity using the EPSINF parameter of the MATERIAL statement. If unspecified, the rule hierarchy in Table 8-2 will be used to define the high frequency permittivity.
- ALPHAR is a line width broadening factor.
- $j = \sqrt{-1}$
- $k_\omega = \omega/c$
- $g(x,y)$ is the local optical gain.
- ALPHAA is the bulk absorption loss and is specified in the MATERIAL statement.
- FCN and FCP are the coefficients of the free-carrier loss and are set through the MATERIAL statement. FCARRIER must be specified on the LASER to include this loss mechanism.

Table 8-1: User-Specifiable Parameters for Equation 8-3

| Statement | Parameter | Default | Units |
|-----------|------------|-----------------------|------------------|
| MATERIAL | ALPHAR | 4.0 | |
| MATERIAL | ALPHAA | 0.0 | cm^{-1} |
| MATERIAL | EPSINF | | |
| MATERIAL | FCN | 3.0×10^{-18} | cm^2 |
| MATERIAL | FCP | 7.0×10^{-18} | cm^2 |
| LASER | ABSORPTION | FALSE | |
| LASER | FCARRIER | FALSE | |

To enable absorption loss, set the ABSORPTION parameter on the LASER statement.

Table 8-2: Rule Hierarchy for Determination of High Frequency Bulk Permittivity

| |
|--|
| If EPSINF is defined in the MATERIAL statement, that value is used. |
| If F.INDEX defined in the MATERIAL statement, then the bulk permittivity is calculated from the square of the index returned from the C-Interpreter function defined in the file specified by F.INDEX. |
| If INDEX.FILE is defined in the MATERIAL statement, the bulk permittivity is calculated as the square of the index interpolated from the table specified in the file pointed to by INDEX.FILE. |
| If the material is listed in Section B.13: “Optical Properties”, Table B-30, the permittivity is calculated as the square of index interpolated from the built-in tables for that material. |
| If PERMITTI is defined in the MATERIAL statement, that value is used. If it’s not defined, the default material permittivity is used. |

8.2.2: Vector Helmholtz Equation

Scalar Helmholtz equation is an approximation for the case of isotropic and homogeneous dielectric constant. In a more general case of a device with different materials, non-homogeneous gain or optical anisotropy, x- and y-components of optical electric or magnetic field will be coupled together into a system of equations, which are represent vector Helmholtz equation. Starting from Maxwell equations and assuming that laser waveguide is homogeneous in z-direction, dielectric permittivity tensor is diagonal and magnetic permeability is homogeneous. This system for magnetic field can be written as follows:

$$\begin{cases} \varepsilon_{yy} \left[\frac{\partial}{\partial x} (L_x / \varepsilon_{yy}) + \frac{\partial}{\partial y} (L_y / \varepsilon_{zz}) \right] + \left(\frac{\partial \varepsilon_{yy}}{\partial x} \right) \frac{L_x}{\varepsilon_{yy}} + \frac{\omega^2}{c^2} \varepsilon_{yy} H_x = \beta^2 H_x \\ \varepsilon_{xx} \left[\frac{\partial}{\partial x} (-L_y / \varepsilon_{zz}) + \frac{\partial}{\partial y} (L_x / \varepsilon_{xx}) \right] + \left(\frac{\partial \varepsilon_{xx}}{\partial y} \right) \frac{L_x}{\varepsilon_{xx}} + \frac{\omega^2}{c^2} \varepsilon_{xx} H_y = \beta^2 H_y \end{cases} \quad 8-4$$

where

$$L_x \equiv \frac{\partial H_x}{\partial x} + \frac{\partial H_y}{\partial y} \quad L_y \equiv \frac{\partial H_x}{\partial y} - \frac{\partial H_y}{\partial x} \quad 8-5$$

This is a non-Hermitian complex eigenvalue problem for the square of propagation constant β and eigenvector $\xi = (H_x, H_y)$. The system is discretized with finite volume integration method and solved with a sparse iterative eigenvalue solver, using frequency ω as a parameter. To launch vector Helmholtz solver for laser simulation, set V.HELM parameter on the LASER or MODELS statements. Dielectric constant is still given by Equation 8-3, but the material dielectric constant ε_0 can be made anisotropic using parameters EPS.XX, EPS.YY, and EPS.ZZ on the MATERIAL statement. After the eigenvalue problem is solved, all other components of optical field can be found:

$$H_z = \frac{i}{\beta} \left(\frac{\partial H_x}{\partial x} + \frac{\partial H_y}{\partial y} \right) \quad 8-6$$

$$E_x = \frac{i}{\omega \varepsilon_{xx} \varepsilon_0} \left(\frac{\partial H_z}{\partial y} - \frac{\partial H_y}{\partial z} \right) \quad 8-7$$

$$E_y = -\frac{i}{\omega \varepsilon_{yy} \varepsilon_0} \left(\frac{\partial H_z}{\partial x} - \frac{\partial H_x}{\partial z} \right) \quad 8-8$$

$$E_z = \frac{i}{\beta \varepsilon_{zz}} \left(\varepsilon_{xx} \frac{\partial E_x}{\partial x} + \varepsilon_{yy} \frac{\partial E_y}{\partial y} \right) \quad 8-9$$

The intensity pattern for each transverse optical mode is then computed using

$$I_m(x, y) = ([\vec{E}_m \times \vec{H}_m^*] + [\vec{E}_m^* \times \vec{H}_m]) \cdot \hat{z} \quad 8-10$$

and normalized by area:

$$\int I_m(x, y) ds = 1 \quad 8-11$$

In the following expressions for stimulated recombination and modal gain, a special care is taken to account for anisotropy of gain (e.g., in quantum well gain model) and optical electric field.

8.2.3: Local Optical Gain

For a discussion of gain models, see Chapter 3: “Physics”, Sections 3.9.3: “The Standard Gain Model” through 3.9.5: “Takayama's Gain Model”.

8.2.4: Stimulated Emission

Carrier recombination due to stimulated light emission is modeled as follows:

$$R_{st}(x, y) = \sum_m \frac{c}{NEFF} g(x, y) |E(x, y)|^2 \cdot S_m \quad 8-12$$

where R_{st} is the recombination rate due to stimulated light emission, $NEFF$ is the group effective refractive index, and S is the linear photon density. The m subscript in this equation and all subsequent equations refer to a modal quantity. For example, S_m in Equation 8-12 is the photon linear density for mode m . The $NEFF$ parameter is user-specifiable but has a default value of 3.57 (see Table 8-3).

| Table 8-3: User-Specifiable Parameters for Equation 8-12 | | | |
|--|-----------|---------|-------|
| Statement | Parameter | Default | Units |
| LASER | NEFF | 3.57 | |

8.2.5: Photon Rate Equations

Optical gain provides a link between optical and electrical models. The optical gain depends on the quasi-Fermi levels and in turn impacts dielectric permittivity (see Equation 8-3), and by the coupling between the stimulated carrier recombination rate (R_{st}) and the density of photons (S) as described by Equation 8-12.

To determine S_m , LASER solves the system of photon rate equations:

$$\frac{dS_m}{dt} = \left(\frac{c}{NEFF} G_m - \frac{1}{\tau_p h_m} - \frac{c \text{ LOSSES}}{NEFF} \right) S_m + R_{sp_m} \quad 8-13$$

where the modal gain G_m is given by:

$$G_m = \iint g_m(x, y) \cdot |E(x, y)|^2 \cdot dx \, dy \quad 8-14$$

and the modal spontaneous emission rate R_{sp_m} is given by:

$$R_{sp_m} = \iint (r_{sp}(x, y))_m \cdot dx \, dy \quad 8-15$$

LOSSES is the internal losses and can be specified in the MODEL statement (see Table 8-4). $E(x,y)$ is the normalized optical field.

| Table 8-4: User Specifiable Parameters for Equation 8-13 | | | |
|--|-----------|---------|------------------|
| Statement | Parameter | Default | Units |
| LASER | LOSSES | 0 | cm ⁻¹ |

The modal photon lifetime, τ_{ph_m} , in Equation 8-16 represents the losses in the laser. The losses per mode are given by [165,206]:

$$\frac{1}{\tau_{ph}} = \frac{c}{NEFF}(\alpha_a + \alpha_{fc} + \alpha_{mir}) \quad 8-16$$

α_a is the bulk absorption loss, α_{fc} is the free-carrier loss, and α_{mir} is the mirror loss. The models for absorption and free carrier loss are switched on with the ABSORPTION and FCARRIER parameters on the LASER statement. The mirror loss is always on. These are defined as:

$$\alpha_a = \iint \text{ALPHAA} \cdot |E(x,y)|^2 dx dy \quad 8-17$$

$$\alpha_{fc} = \iint (\text{FCN } n + \text{FCP } p) \cdot |E(x,y)|^2 \cdot dx dy \quad 8-18$$

The mirror loss, α_{mir} , can be defined in two ways. One way is to define the percentage reflectivity of both mirrors. The other way is to define the individual facet mirror reflectivities. If the former is chosen, then set the MIRROR.LOSS parameter on the LASER statement to the percentage reflectivity for the facet cavity mirrors. This assumes that both front and back mirrors are identical and gives a mirror loss calculated by:

$$\alpha_{mir} = \frac{1}{2 \text{ CAVITY.LENGTH}} \ln \left(\frac{1}{\text{MIRROR.LOSS}^2} \right) \quad 8-19$$

where CAVITY.LENGTH is set to the length of the laser cavity on the LASER statement.

If you choose the latter model for α_{mir} , set the RR and RF parameters on the LASER statement instead. These parameters are the rear and front facet reflectivities respectively. The mirror loss is then calculated by:

$$\alpha_{mir} = \frac{1}{2 \cdot \text{CAVITY.LENGTH}} \ln \frac{1}{\text{RF} \cdot \text{RR}} \quad 8-20$$

The user-specified parameters for the loss models in Equations 8-16 to 8-20 are given in Tables 8-1, 8-3, 8-4, and 8-5.

Table 8-5: User-Specifiable Parameters for LASER Loss Models

| Statement | Parameter | Default | Units |
|-----------|---------------|---------|-------|
| LASER | MIRROR.LOSS | 90.0 | % |
| LASER | CAVITY.LENGTH | 100.0 | μm |

Note: Absorption loss and free carrier loss are switched off by default. These are switched on by specifying the ABSORPTION and FCARRIER parameters in the LASER statement. Mirror loss is switched on by default to 90%.

8.2.6: Spontaneous Recombination Model

For a discussion of spontaneous recombination models, see Chapter 3: “Physics”, Sections 3.9.1: “The General Radiative Recombination Model” and 3.9.2: “The Default Radiative Recombination Model”.

8.2.7: Optical Power

The optical power emitted from the front mirror is calculated by [165, 228]

$$P_f = \frac{h \omega S_m c}{2 N_{EFF}} \frac{\ln(1/(R_f R_r))}{1 + \sqrt{R_f/R_r(1-R_r)/(1-R_f)}} \quad 8-21$$

where S_m is the photon density of mode m , w is the frequency of emitted light, R_f and R_r are the front and rear mirror reflectivities, and N_{EFF} is a user-defined in the LASER statement.

The total optical intensity emitted from the front mirror is given by

$$I(x, y) = \sum_m P_{fm} I_m(x, y) \quad 8-22$$

8.2.8: Gain Saturation

To simulate non-linear gain saturation in LASER, use the simple model described by [32]

$$g'(x, y) = \frac{g(x, y)}{1 + I(x, y)/GAIN_SAT} \quad 8-23$$

where $GAIN_SAT$ is a user-specifiable parameter on the MATERIAL statement, $g'(x, y)$ is the local gain.

To enable this model, specify $GAIN_SAT$ on the LASER statement. Non-linear, absorption loss is similarly modeled using the following expression.

$$\alpha'(x, y) = \frac{\alpha(x, y)}{1 + I(x, y)/ABSORPTION_SAT} \quad 8-24$$

where $\alpha'(x, y)$ is the local absorption and $ABSORPTION_SAT$ is a user-definable parameter on the MATERIAL statement. To enable this model, specify $ABSOR_SAT$ on the LASER statment.

8.3: WAVEGUIDE Statement

It is often useful to know and to be able to optimize the optical intensity patterns in a laser waveguide before doing a full-scale laser simulation. For that reason, vector Helmholtz solver can also be used as a standalone optical solver. To find optical modes at any point during a device simulation, use `WAVEGUIDE` statement and specify the `V.HELM`, `OMEGA`, or `PHOTON.ENERGY` parameters and the number of transverse modes `NMODE`. If any of the regions has a gain model turned on, it will be included in the imaginary part of the dielectric constant. Thus, you can check how the optical modes are modified by the increase of gain in the system or by changing temperature profile. `WAVEGUIDE` statement as well as its parameters is completely independent of the `LASER` statement. Therefore, it can be used by itself or simultaneously with the laser simulation.

In addition, `WAVEGUIDE` statement also allows you to get a dispersion of the propagation constant $\beta(\omega)$. To run a dispersion calculation, specify `DISPERSION`, the range of photon frequencies `OMEGA.INIT` (or `E.INIT`) and `OMEGA.FINAL` (or `E.FINAL`), the number of samples `NDISP` and the log file name `DISP.NAME`, where dispersion will be stored.

8.4: Solution Techniques

LASER solves the electrical and optical equations self consistently. LASER solves the Helmholtz equation in a rectangular region, which is a subdomain of the general ATLAS simulation region. An eigenvalue solver provides a set of eigenfunctions and corresponding eigenvectors.

LASER uses boundary conditions in the form, $E(x,y)=0$, on the boundaries of the solution region. This region should be large enough to cover the entire active region of the laser diode with some inclusion of the passive regions. When the single frequency model is used, the lasing frequency used in Equation 8-1 is an external parameter that is fixed during the calculation and either model can be then used for optical gain.

The multiple longitudinal mode model requires you to use a physically-based optical gain model. Specify an initial estimate of the lasing frequency. This is adjusted during calculations. You can also specify a frequency range or photon energy range, which LASER will then calculate multiple longitudinal modes.

LASER may also simulate multiple transverse modes.

8.5: Specifying Laser Simulation Problems

The structure of the laser diode and the mesh used to simulate it are specified in the normal way using the capabilities provided by ATLAS and BLAZE. To enable LASER simulation, use the parameters and do the following:

1. Activate LASER by specifying a LASER statement.
2. Define a mesh for solution of the Helmholtz equation. The Helmholtz Equation is solved on a rectangular mesh. The rectangular mesh can be independent of the triangular mesh, which is used for device simulation. This rectangular mesh is specified by the LX.MESH and LY.MESH statements. The area specified by the laser mesh must be completely inside the ATLAS simulation domain and should completely cover the active lasing region.
3. For single-frequency calculations, you can select different gain models for different regions/materials using the REGION or MATERIAL parameters of the MODELS statement.

Note: If multiple longitudinal modes are to be accounted for, then specify GAINMOD equal to 1 or 5 for the active lasing region.

8.5.1: LASER Statement Parameters

You can simulate multiple transverse modes by setting the NMODE parameter in the LASER statement. Set it to the desired number of modes you want to simulate.

There are several kinds of parameters that appear in the LASER statement. There are parameters that deal with the numerical solution to the photon rate equation, parameters that deal with loss mechanisms, and parameters that deal with specifying energies to look for longitudinal solutions.

Specify laser physical parameters and models and do the following:

1. Specify the CAVITY.LENGTH parameter, which is the length of the laser cavity in the Z direction.
2. Specify the PHOTON.ENERGY or OMEGA parameters for (initial) photon energy or laser frequency.
3. Specify laser loss mechanisms (MIRROR, FCARRIER, ABSORPTION parameters in the LASER statement) and any associated constants (FCN, FCP, ALPHAA in the MATERIAL statement).
4. Specify any additional laser losses (LOSSES parameter).

If you want to calculate the laser spectrum, specify the multiple longitudinal modes model and additional parameters. Then, do the following:

1. Specify the LMODES in the statement. This enables the multiple longitudinal mode model.
2. Specify the EINIT and EFINAL parameters. These parameters set the photon energy range within, which LASER will take into account multiple longitudinal modes. Make sure that initial photon energy is within this range and is specified for the active lasing region.
3. Specify the photon energy separation (ESEP parameter). If this isn't specified, LASER will automatically calculate the number of longitudinal modes based on the cavity length and the energy range. We recommend that you allow LASER to choose the photon energy separation.
4. Specify the spectrum file name (SPEC.NAME). LASER will produce a structure file containing spectrum data after calculation of each bias point. LASER will automatically append *_dcN.log* to the specified file name (where *N* is the number of the bias point) for steady-state solutions or *_trN.log* for a transient simulation. The first bias point where LASER is active will have *N=1*. This is often not the first bias point during simulation. You can examine these files using TONYPLOT. If you specify the SPECSAVE parameter, the spectrum files will only be saved on every LAS.SPECSAVE solution.

Note: The index in the spectrum file name will still increase by one each time. The spectrum data can be stored in a single file for the transient simulation, only if `MULTISAVE – LASER` statement is set to `FALSE`.

You can save near and far field patterns by specifying a value for the `PATTERNS` parameter in the `SAVE` statement. The value of the `PATTERNS` parameter is a character string representing the root name of a file for saving the near and far field patterns. The near field pattern is saved to a file with the string `".nfp"` appended to the root. The far field pattern is saved to a file with the string `".ffp"` appended to the root name. You can examine these files using `TONYPLOT`.

You can also use the numeric parameters. These parameters are `TOLER`, `ITMAX`, `SIN`, `TAUSS`, and `MAXCH`. The default values of these parameters have been selected to give a good exchange between accuracy, efficiency, and robustness for most applications. You can adjust the calculation by specifying different values. These parameters are discussed in the next section.

8.5.2: Numerical Parameters

The following numerical parameters control the performance of the `LASER` simulation. All of these parameters have reasonable default values, but you can specify them in the `LASER` statement.

- `ITMAX` sets maximum number of external `LASER` iterations during photon density calculation. The default value is 30.
- `MAXCH` is the maximum allowed relative change of the photon density between `LASER` iterations. Using a larger value of this parameter can speed up the calculation but may cause convergence problems.
- `SIN` is the initial photon density used only with simple `LASER` models. `LASER` starts the iteration process for photon density calculation from this value. This parameter influences only the calculation time for the first bias point after the laser threshold is reached.
- `TAUSS` is the relaxation parameter for the solution of the photon rate equation(s). Larger values of `TAUSS` tends to reduce the calculation time required to achieve convergence but leads to less stability. In other words, increasing `TAUSS` reduces calculation time while decreasing `TAUSS` improve convergence.
- `TOLER` sets the desired relative tolerance of the photon density calculation. The default value is 0.01. Setting this parameter to a lower value may slow down the calculation significantly. Using a larger value will result in a faster but less accurate calculations.
- `TRAP` specifies that a cutback scheme for the photon rate equation(s) should be used if convergence is not obtained. In this case, the value of `TAUSS` is reduced by multiplying it by `ATRAP` and the solution for the rate equations is repeated. The value of `MAXTRAP` specifies the maximum number of cut-backs attempts before the simulation ends.

8.6: Semiconductor Laser Simulation Techniques

The most common technique for simulating laser diodes is to simulate forward characteristics with a gradually increasing bias. The forward voltage is usually specified, but current boundary conditions can be used, and external elements can be included.

To save computational time, we recommend that you don't enable LASER models at the start of the simulation. Ramp the device bias first. Then, enable LASER simulation by using the LASER parameter in an additional MODELS statement.

Generally, the single frequency LASER model, which doesn't take into account the longitudinal mode spectrum, is faster. This model provides accurate results. We recommend that you use it if the lasing spectrum isn't the subject of interest. If you use the multiple longitudinal mode model, computational time will longer depend on the number of longitudinal modes involved in the calculation.

Although ATLAS is a two-dimensional device simulator, the laser spectrum and all other laser results strongly depend on cavity length, which is effectively the device length of the Z direction. For example, you can scale terminal currents to apply a different length in the third dimension by using simple multiplication. This isn't the case for LASER, since the cavity length determines energy spacing between longitudinal modes and influences all other laser characteristics.

Be sure to specify the CAVITY.LENGTH parameter in the MODELS statement when the longitudinal mode spectrum is to be calculated.

For symmetric devices, you can improve computational efficiency by simulating half of the device. To do this, define the device so that the center of the device is located at $X=0$ and only half of the device is defined at coordinate values at $X \geq 0$.

For device simulation, the default boundary condition is a mirror boundary, which means symmetry is implied.

For laser simulation, (see Section 8.2.1: "Scalar Helmholtz Equation") specify that the laser mesh starts at $X=0$. Also, specify the REFLECT parameter in the LASER statement. This tells the Helmholtz Equation that a mirror boundary condition is to be used at $X=0$.

8.6.1: Generation of Near-Field and Far-Field Patterns

The intensity profile of the laser at the cleaved surface can be examined in the standard structure file using TONYPLOT. To generate a structure file, use the OUTFILE parameter on either the SOLVE or SAVE statements. The intensity far from the laser surface, in the Fraunhofer region, is important for designing the optical coupling to the laser.

LASER can generate the far-field pattern if you specify the PATTERNS parameter of the SAVE statement. The PATTERNS parameter specifies the file name prefix of two output files. The first of these files, with the *.nfp* suffix, contains the near-field pattern. This is essentially a copy of the near field pattern contained in the structure file output. The second of these files, with the *.ffp* suffix, contains the far-field pattern.

The far-field pattern is essentially a 2D fast Fourier transform (FFT) of the near-field pattern. The sampling for this transform is set by the minimum spacing in the laser mesh and the overall size of the laser mesh. The output samplings for the near-field and far-field patterns are controlled by the NEAR.NX, NEAR.NY, FAR.NX, and FAR.NY parameters of the LASER statement. These specify the numbers of samples in the X and Y directions in the near and far field. By default, the values are set to 100.

9.1: Overview

VCSEL (Vertical Cavity Surface Emitting Lasers) performs electrical, thermal, and optical simulation of vertical cavity surface emitting lasers using accurate, robust, and reliable fully numerical methods and non-uniform meshes. With VCSEL, you can simulate advanced structures containing multiple quantum wells and oxide apertures including the effects, such as gain guiding, lattice heating, current crowding, and spatial hole burning. VCSEL works with BLAZE and GIGA and allows you to do the following:

- Test whether the structure complies to general VCSEL device requirements by simulating cold cavity reflectivity experiments. Calculate the reflectivity of a VCSEL cavity as a function of the incident light wavelength in a user-specified range. Then, determine the resonant frequency of the cold cavity.
- Solve the Helmholtz equation (see Equation 9-1) in cylindrical coordinates to calculate optical intensities of the multiple transverse modes for index guiding and gain guiding structures.
- Calculate the optical gain in multiple quantum well systems depending on the photon energies, quasi-Fermi levels, temperature, and optical intensity distribution. Calculate the carrier recombination due to the spontaneous and stimulated emission.
- Solve the photon rate equations (see Section 9.2.4: “Photon Rate Equations”) for multiple transverse modes to calculate the photon density in each mode and the total photon density.
- Calculate the light output power and the wavelength for each transverse mode.
- Speed up solution of the Helmholtz equation by using perturbational treatment.
- Simulate more general cavities that support multiple longitudinal modes. This obtains modal gain spectra and determines the dominant mode with maximum gain.

To perform a VCSEL simulation, you need be familiar with ATLAS and BLAZE first. Please see Chapter 2: “Getting Started” and Chapter 5: “BLAZE” for more information.

Note: To avoid the confusion in terms, we refer to a VCSEL device as VCSEL and to a VCSEL simulator as VCSEL:ATLAS in this chapter.

9.2: Physical Models

When modeling VCSELs, it is essential to take into account interaction of optical, electrical, and thermal phenomena that occur during the VCSEL operation. Modeling only optical properties is already an involved task. Different methods developed recently to improve the accuracy of optical solution produce results that vary from method to method [24]. The variation is especially strong between vectorial models that tend to produce a spread in results much larger than simpler scalar models.

On the other hand, the complexity of the vectorial methods makes the self-consistent electro-thermo-optical simulation impractical from the point of view of the calculation time required. For VCSEL simulation in VCSEL:ATLAS, we adopted an approach that can account for mutual dependence of electrical, optical, and thermal phenomena.

Basic semiconductor equations (See Equations 3-1 to 3-4 in Chapter 3: “Physics”) are solved self-consistently with the Helmholtz Equation, Lattice Heat Flow Equation (See Chapter 7: “Giga: Self-Heating Simulator”, Equation 7-1), and the Photon Rate Equation (see Equation 9-12). Since we are using a scalar method, we neglect polarization effects and reduce Maxwell equations to scalar Helmholtz equation. The method used for the solution of Helmholtz equation is based on a well developed effective index model, which showed its validity for a much wider range of problems than originally expected [252]. This method fine tuned for simulation of various VCSEL structures is often referred to as Effective Frequency Method (EFM). EFM is a fast and flexible method that allows further development to include dispersion, diffraction losses, and graded interfaces.

VCSEL:ATLAS uses a cylindrical coordinate system to take advantage of the cylindrical symmetry of the VCSEL devices. Figure 9-1 shows the relationship between ATLAS's XY coordinate system and the r- θ -z cylindrical system used in VCSEL:ATLAS. Note that the X coordinate axis is equivalent to the radius r, and the Y coordinate axis is equivalent to the Z axis in the cylindrical system.

9.2.1: Reflectivity Test Simulation

Reflectivity experiment is an important test conducted to evaluate the quality of a VCSEL device. In this experiment, the light is normally incident on a VCSEL device and its reflectivity is measured as a function of wavelength. Most manufactured VCSEL resonators are tested this way to ensure adequate optical performance. Numerical simulation of this experiment enables you to calibrate the material parameters used in the optical model and eliminate possible specification errors at the early stage of numerical analysis of a VCSEL device.

Another purpose of the numerical reflectivity test is to ensure that the analyzed device complies with general VCSEL requirements. These requirements include the following:

1. Presence of a high reflectivity band in the reflectivity spectrum of a VCSEL cavity.
2. The reflectivity over 99% in the high reflectivity band.
3. Presence of a drop in reflectivity within the high reflectivity band. The drop in reflectivity (increase in absorptance) occurs at the resonant wavelength of the cavity.

VCSEL:ATLAS calculates reflectivity and absorptance using transfer matrix approach (Chapter 10: “Luminous: Optoelectronic Simulator”, Section 10.3: “Matrix Method”). In the simulation, the incident light propagates along the axis of symmetry of the device.

The `VCSEL.INCIDENTCE` parameter specifies the position of the light origin with respect to the device (top or bottom). Specific output associated with the reflectivity test includes reflectivity and absorptance spectra plotted in the corresponding files, `reflectivity(absorption)_top.log` and `reflectivity(absorption)_bottom.log`.

To run the reflectivity test simulation, specify the `VCSEL.CHECK` parameter and other parameters in Table 9-1 on a `VCSEL` statement. Section 9.3.3: “Enabling VCSEL Solution” will discuss parameter specification in detail.

| Table 9-1: User-Specifiable Parameters for the Reflectivity Test | | | |
|--|-----------------|---------|----------|
| Statement | Parameter | Default | Units |
| VCSEL | VCSEL.CHECK | False | |
| VCSEL | VCSEL.INCIDENCE | 1 | |
| VCSEL | OMEGA | | s^{-1} |
| VCSEL | EINIT | | eV |
| VCSEL | EFINAL | | eV |
| VCSEL | PHOTON.ENERGY | | eV |
| VCSEL | INDEX.TOP | 1.0 | |
| VCSEL | INDEX.BOTTOM | 1.0 | |
| VCSEL | NSPEC | 100 | |

If the structure does not meet requirements 1-3, VCSEL:ATLAS will close with an error. Otherwise, VCSEL:ATLAS uses Brent's minimization procedure to find the resonant frequency of the cold cavity. VCSEL:ATLAS uses the obtained value as a reference frequency in the solution of the Helmholtz equation.

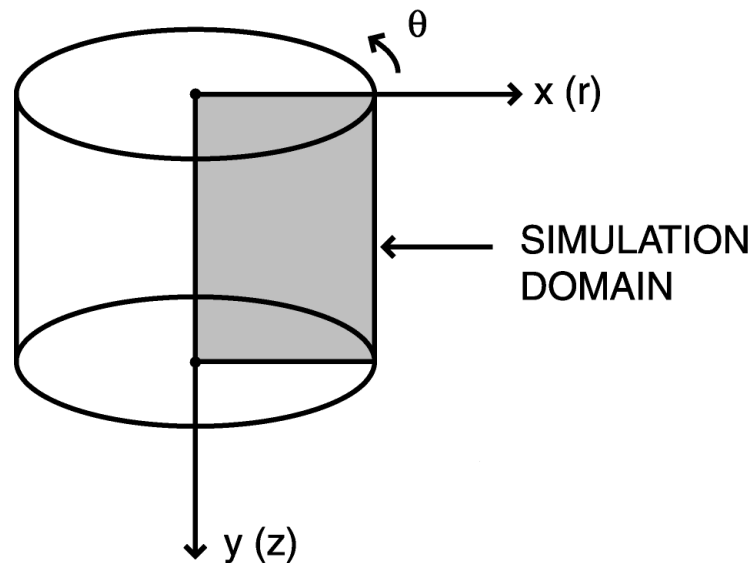


Figure 9-1: The relationship between rectangular and cylindrical coordinate systems used by VCSEL

9.2.2: Helmholtz Equation

VCSEL:ATLAS solves the Helmholtz Equation in cylindrical coordinates r , z , and ϕ using effective frequency method [252].

$$\nabla^2 E(r, z, \phi) + \frac{\omega^2}{c^2} \varepsilon(r, z, \phi, \omega) E(r, z, \phi) = 0 \quad 9-1$$

where ω is frequency, $\varepsilon(r, z, \phi, \omega)$ is the complex dielectric permittivity, $E(r, z, \phi)$ is the optical electric field, and c is the speed of light in vacuum.

Using the expansion around a reference frequency ω_0 :

$$\frac{\omega^2}{c^2} \varepsilon(r, z, \phi, \omega) \approx \frac{\omega_0^2}{c^2} \varepsilon(r, z, \phi, \omega_0) + 2 \frac{\omega_0}{c^2} \varepsilon(r, z, \phi, \omega_0) (\omega - \omega_0) \quad 9-2$$

we transform the Helmholtz equation into:

$$\left[\nabla^2 + k_0^2 \varepsilon(r, z, \phi) \right] E(r, z, \phi) = \nu k_0^2 \varepsilon(r, z, \phi) E(r, z, \phi) \quad 9-3$$

where $k_0 = \omega_0/c$ and ν is a dimensionless frequency parameter given by:

$$\nu = 2 \frac{\omega_0 - \omega}{\omega_0} = 2 \frac{\lambda - \lambda_0}{\lambda} - j 2 \frac{\text{Im}(\omega)}{\omega_0} \quad 9-4$$

We assume that the field is separable:

$$E(r, z, \phi) = f(r, z, \phi) \Phi(r, \phi) \quad 9-5$$

This assumption of separability is the main approximation of the method. The applicability of the method can be extended beyond this approximation by adding a non-separable component of the field on the right hand side of Equation 9-5. For dispersive materials, you can make another modification of the effective frequency method by taking into account material dispersion in Equation 9-2. For separable fields, we obtain the longitudinal wave equation for function f :

$$\left[\frac{\partial^2}{\partial z^2} + k_0^2 \varepsilon(r, z, \phi) \right] f(r, z, \phi) = \nu_{eff}(r, \phi) k_0^2 \varepsilon(r, z, \phi) f(r, z, \phi) \quad 9-6$$

at each lateral position (r, ϕ) . Due to the cylindrical symmetry, we can ignore the azimuthal variations. In this case, we only need to solve Equation 9-6 for each cylindrically symmetric region characterized by a particular distribution of ε in the vertical direction z . Complex Newton method combined with the characteristic matrix approach (Chapter 10: “Luminous: Optoelectronic Simulator”, Section 10.3: “Matrix Method”) yields eigenvalues ν_{eff} and eigenfunctions $f(z)$ of the longitudinal wave equation.

The transverse wave equation takes the form:

$$\left[\frac{1}{r} \frac{d}{dr} \left(r \frac{d}{dr} \right) - \frac{l^2}{r^2} + \nu_{eff}(r) k_0^2 \langle \varepsilon \rangle_r \right] \Phi_{lm}(r) = n_{lm} K_0 \langle \varepsilon \rangle_r \Phi_{lm}(r) \quad 9-7$$

where

$$\langle \varepsilon \rangle_r = \int_0^L \varepsilon(r, z) f^2(r, z) dz \quad 9-8$$

VCSEL:ATLAS uses standard eigentechniques to solve an ordinary differential Equation 9-7. Solutions of this equation are LP_{lm} modes.

For each mode, the imaginary part of the eigenvalue determines the overall mode gain(loss) factor, which is negative below the lasing threshold. The lasing occurs when:

$$Im(n_{lm})|_{th} = 0 \quad 9-9$$

The dielectric permittivity is given by:

$$\varepsilon(r, z) = \varepsilon_0 + (-ALPHAR + j) \frac{\sqrt{\varepsilon_0} g(r, z)}{k_0} - j \frac{\sqrt{\varepsilon_0} (ALPHAA + FCN \cdot n + FCP \cdot p)}{k_0} \quad 9-10$$

where:

- ε_0 is the bulk high frequency permittivity. You can specify the bulk high frequency permittivity using the EPSINF parameter of the MATERIAL statement. If unspecified, the rule hierarchy in Table 8-2 will be used to define the high frequency permittivity.
- ALPHAR is a line width broadening factor.
- $k_0 = \omega/c$
- $g(r, z)$ is the local optical gain.
- ALPHAA is the bulk absorption loss and is specified in the MATERIAL statement (specify ABSORPTION in the VCSEL statement to include absorption loss).
- FCN and FCP are the coefficients of the free-carrier loss and are set using the MATERIAL statement (specify FCARRIER in the VCSEL statement to include this loss mechanism).

Table 9-2: User-Specifiable Parameters for Equation 9-10

| Statement | Parameter | Default | Units |
|-----------|------------|-----------------------|------------------|
| MATERIAL | ALPHAR | 4.0 | |
| MATERIAL | ALPHAA | 0.0 | cm ⁻¹ |
| MATERIAL | EPSINF | | |
| MATERIAL | FCN | 3.0×10 ⁻¹⁸ | cm ² |
| MATERIAL | FCP | 7.0×10 ⁻¹⁸ | cm ² |
| VCSEL | ABSORPTION | FALSE | |
| VCSEL | FCARRIER | FALSE | |

9.2.3: Local Optical Gain

For a discussion of gain models, see Chapter 3: “Physics”, Sections 3.9.3: “The Standard Gain Model” through 3.9.5: “Takayama's Gain Model”.

Stimulated Emission

Carrier recombination due to stimulated light emission is modeled as follows:

$$R_{st}(r, z) = \sum_m \frac{c}{n_{\text{NEFF}}} g_m(r, z) |E_m(r, z)|^2 \cdot S_m \quad 9-11$$

where R_{st} is the recombination rate due to stimulated light emission, n_{NEFF} is the group effective refractive index, and S_m is the photon number. The m subscript in this equation and all subsequent equations refers to a modal quantity. For example, S_m in Equation 9-11 is the photon number for mode m . The n_{NEFF} parameter is user-defined but has a default value of 3.57 (see Table 9-3).

| Table 9-3: User-Specifiable Parameters for Equation 9-11 | | | |
|--|-----------|---------|-------|
| Statement | Parameter | Default | Units |
| VCSEL | NEFF | 3.57 | |

9.2.4: Photon Rate Equations

Optical gain provides the link between optical and electrical models. The optical gain depends on the quasi-Fermi levels and in turn impacts dielectric permittivity (see Equation 9-12), and by the coupling between the stimulated carrier recombination rate (R_{st}) and the density of photons (S) as described by Equation 9-11.

To determine S_m , VCSEL solves the system of photon rate equations:

$$\frac{dS_m}{dt} = \left(\frac{c}{n_{\text{NEFF}}} G_m - \frac{1}{\tau_p h_m} - \frac{c \text{ LOSSES}}{n_{\text{NEFF}}} \right) S_m + R_{sp_m} \quad 9-12$$

where the modal gain G_m is given by

$$G_m = \iiint g_m(r, z) \cdot |E_m(r, z)|^2 r d\theta dr dz \quad 9-13$$

and the modal spontaneous emission rate R_{sp_m} is given by

$$R_{sp_m} = \iiint r_{sp}(r, z)_m r d\theta dr dz. \quad 9-14$$

$E_m(r, z)$ is the normalized optical field.

| Table 9-4: User Specifiable Parameters for Equation 9-12 | | | |
|--|-----------|---------|------------------|
| Statement | Parameter | Default | Units |
| VCSEL | LOSSES | 0 | cm ⁻¹ |

The modal photon lifetime, τ_{ph_m} , in Equation 9-12 represents the losses in the laser. The losses per mode are given by

$$\frac{1}{\tau_{ph_m}} = \frac{c}{NEFF} (\alpha_{a_m} + \alpha_{fc_m} + \alpha_{mir}) = \frac{c}{NEFF} G_m - \omega_0 \cdot \nu_{lm} \quad 9-15$$

α_a is the bulk absorption loss, α_{fc} is the free-carrier loss, α_{mir} is the mirror loss, and ν_{lm} is a dimensionless frequency parameter. These are defined as:

$$\alpha_{a_m} = \iiint \text{ALPHA}_{AA} \cdot |E_m(r, z)|^2 \times r d\theta dr dz \quad 9-16$$

$$\alpha_{fc_m} = \iiint (\text{FCN}_n + \text{FCP}_p) \cdot |E_m(r, z)|^2 r d\theta dr dz \quad 9-17$$

$$\alpha_{mir} = G_m - \alpha_{a_m} - \alpha_{fc_m} - \omega_0 \cdot \nu_{lm} \frac{NEFF}{c} \quad 9-18$$

Spontaneous Recombination Model

For a discussion of spontaneous recombination models, see Chapter 3: “Physics”, Sections 3.9.1: “The General Radiative Recombination Model” and 3.9.2: “The Default Radiative Recombination Model”.

Optical Power

The optical power emitted by the front facet is given by Equation 9-19.

$$P_f = \frac{\hbar \omega S_m c}{NEFF} \frac{\alpha_{mir}}{1 + \sqrt{R_f R_r (1 - R_r) / (1 - R_f)}} \quad 9-19$$

9.3: Simulating Vertical Cavity Surface Emitting Lasers

The key to simulating a Vertical Cavity Surface Emitting Laser is the input deck. The input deck describes the physical device structure, the physical models to be used, and the specific measurements to be performed. The deck itself can be roughly divided into three sections: structure specification, model definition, and obtaining solutions. The following sections will describe these concepts in detail.

9.3.1: Specifying the Device Structure

VCSEL devices are the most complicated devices to be addressed by device simulation. This is due to the many layers involved in making distributed Bragg reflectors (See “Specifying Distributed Bragg Reflectors” section on page 9-10) and the possible quantum well (See “Specifying Quantum Wells” section on page 9-10) active layers. This complexity is mitigated by the fact that these devices are mostly epitaxial. Also, many of the layers are periodic. Recognizing these simplifications, we’ve designed a custom syntax for defining VCSEL devices.

This syntax makes specification of periodic structures (e.g., super-lattices) simple, which completely avoids problems of aligning various layers to each other. This new syntax also simplifies meshing the structure.

Despite this simplification, specifying a VCSEL device can still be complex. We recommend that you look at the standard examples. See Chapter 2: “Getting Started with ATLAS”, Section 2.4: “Accessing The Examples” for more information about these examples.

The order of statements is important when specifying the device structure. The following order of statements should be strictly followed.

1. Specify the `MESH` statement. This initializes the structure definition and allows specification of cylindrical symmetry.
2. Set up the mesh in the X direction by using the `X.MESH` statements. The mesh in the Y direction is usually specified along with the device layers in the `REGION` statements. You can, however, introduce the Y mesh lines by using the `Y.MESH` statements after the `X.MESH` statements.
3. Specify the device regions using `REGION` and `DBR` statements. These statements specify the layer thickness, composition, doping, order of placement, and meshing information in the Y direction. The order of `REGION` and `DBR` statements is up to you and is usually defined by the order the layers appear through the structure.
4. You can use quantum well models for the gain and spontaneous recombination (see Sections 3.9.7: “Unstrained Zincblende Models for Gain and Radiative Recombination” and 3.9.9: “Strained Wurtzite Three-Band Model for Gain and Radiative Recombination”) by specifying `QWELL` on the `REGION` statement for the appropriate regions (see Section 13.6: “General Quantum Well Model”).
5. Specify the locations of the electrodes using `ELECTRODE` statements.
6. Use `DOPING` statements to specify additional doping or composition fraction information. This usually isn’t necessary since most, if not all doping and composition information can be specified during the specification of regions.

Setting Up Cylindrical Symmetry

VCSELs use cylindrical symmetry to account for the 3D nature of VCSEL devices. To specify cylindrical symmetry in the MESH statement, use the CYLINDRICAL parameter. An example of specifying cylindrical symmetry is down below.

Example

```
MESH CYLINDRICAL
```

The axis of symmetry for cylindrical is the Y axis at X=0. When using cylindrical symmetry, no X coordinates should be specified with negative values since X represents radius.

The usual abbreviation rules for parameter names can be used. See Chapter 2: “Getting Started with ATLAS”, Section 2.5: “The ATLAS Syntax” for more information.

Specifying the Mesh

To specify the mesh in the X direction, use the X.MESH statement. Each X.MESH statement specifies the location of one mesh line in the X direction and the spacing between mesh lines at that location.

The location is specified by the LOCATION parameter in microns. The spacing is specified by the SPACING parameter, which is also in microns. The number of mesh lines specified is limited to built-in limits in the overall size of the mesh. There should be, however, at least two X.MESH statements. There shouldn't be X.MESH specifications with negative values in the LOCATION parameter. Such specification would be ill-defined due to the cylindrical symmetry.

You should also specify mesh lines at any defining edges of regions, electrodes, or other geometrical aspects in the X direction. Also for similar reasons, use the Y.MESH statements to specify mesh lines in the Y direction.

To have mesh lines inserted automatically at defined region edges, use the REGION and DBR statements. To enable this feature, specify AUTO in the MESH statements. See Chapter 21: “Statements”, Section 21.31: “MESH” for information about the MESH statement.

Specifying Regions

A region is a volume (in cylindrical coordinates a disk or annulus) that has a uniform material composition. The region is specified by a REGION statement. In the REGION statement, the material composition is specified by the MATERIAL parameter.

The MATERIAL parameter can take on values of any material name as described in Appendix B: “Material Systems”. For Ternary and Quaternary materials, you can also specify composition fractions X or Y or both, using the X.COMPOSE or Y.COMPOSE parameters or both. You can use both the DONORS and ACCEPTORS parameters to specify uniform densities of ionized donors or acceptors or both.

The thickness of the region in the Y direction in microns is specified by the THICKNESS parameter. You can also use the X.MIN, X.MAX, Y.MIN, and Y.MAX parameters to specify the location and extent of the region. Except in special cases, we don't recommend this because of the difficulties aligning the numerous layers involved.

Unless it's specified, the region will encompass the entire range of mesh in the X direction as specified in the X.MESH statements. Mesh lines in the Y direction will then be added at the upper and lower edges of the region. The mesh spacing at the edges is specified in microns by the SY parameter.

The TOP/BOTTOM parameters specifies the relative ordering of regions in the Y direction. Specifying TOP indicates that the region starts at the top of all previously specified regions (i.e., at the minimum previously specified Y coordinate) and extends to the thickness in the negative Y direction. Remember for device simulation, the Y axis conventionally extends down into the wafer for increasing values of Y. If no previous regions are specified, TOP indicates the region starts at Y=0 and extends to the thickness

in the negative Y direction. `BOTTOM` indicates that the region starts at the bottom of all previously specified regions (i.e., at the maximum previously specified Y coordinate) and extends to the thickness in the positive Y direction. If no previous regions are specified, `BOTTOM` indicates the region starts at `Y=0` and extends to the thickness in the positive Y direction.

Conventionally, we have found it convenient to start the active layers at the `Y=0` location (as done in the standard examples). In ordering, `REGION` statements:

1. Start with the upper DBR by using the `TOP` parameter.
2. Use the `TOP` parameter on the top side contact layers.
3. Use the `BOTTOM` parameter on the active layers.
4. Use the `BOTTOM` parameter on the lower DBR.
5. Use the `BOTTOM` parameter on the substrate/lower contact regions.

Specifying Distributed Bragg Reflectors

A Distributed Bragg Reflector (DBR) is a periodic structure composed of regions of two alternating material compositions. A DBR can be specified by a series of `REGION` statements alternating between two different material composition. DBRs, however, typically consist of many of such layers and specifying them with `REGION` statements can be tedious, which could be prone to errors. You can use the `DBR` statement to simplify the specification instead. Generally, the `DBR` statement (alias `SUPERLATTICE`) can be used to specify any superlattice composed of layers of two alternating material compositions. For more information about this statement, see Chapter 21: “Statements”, Section 21.7: “DBR”.

The `MAT1` and `MAT2` parameters specify the material names of the two materials, which is used the same way the `MATERIAL` parameter of the `REGION` statement is used to specify a single material.

The `X1.COMP`, `Y1.COMP`, `X2.COMP`, and `Y2.COMP` parameters are used to specify the X and Y composition fractions of the two materials for ternary and quaternary materials.

The thicknesses of the two layers are specified by the `THICK1` and `THICK2` parameters of the `DBR` statement. The doping for the layers are specified by the `NA1` and `NA2` parameters for acceptors. The `ND1` and `ND2` parameters for donors.

The mesh spacing for the DBR can be specified using the `SPA1` and `SPA2` parameters, just like the `SY` parameter of the `REGION` statement. You can also use the `N1` and `N2` parameters to specify the integer number of the mesh divisions in the introduction of Y direction for each of the layers.

The total number of layers is specified by the integer `HALF.CYCLE` parameter. The `HALF.CYCLE` parameter specifies the total number of layers. Thus, an odd values specifies that one more layer of the material 1 is to be used than of material 2.

The `TOP` and `BOTTOM` parameters of the `DBR` statement are used just like the `REGION` statement, except the first material to be added to the top/bottom of the device is always of material 1.

`DBR` and `REGION` statements can be intermingled indiscriminately.

Specifying Oxide Apertures

Once you specify all the epitaxial layers of the VCSEL, you can then specify an oxide aperture by using a `REGION` statement with the `MATERIAL` parameter assigned to an insulator and specify the geometry by using the `X.MIN`, `X.MAX`, `Y.MIN`, and `Y.MAX` parameters.

Specifying Quantum Wells

You can implement single and multiple quantum wells as described in Section 13.6: “General Quantum Well Model”.

Specifying Electrodes

Device electrodes are specified using the `ELECTRODE` statement. Note that electrodes in device simulation are treated as boundary conditions. Therefore, there's no advantage to resolve the full outline of the electrode. Usually, the easiest way is to place electrodes at the top and bottom of the structure. To do this, specify the `TOP` or `BOTTOM` parameters of the `ELECTRODE` statement. The extent along the top or bottom of the device can be described by the `X.MIN` or `X.MAX` or both parameters. If you omit these parameters the electrode will extend all the way along the corresponding surface of the device.

Use the `NUMBER` parameter to assign electrodes to a number. Electrodes should be assigned consecutive numbers starting at 1. They can also be given a name by using the `NAME` parameter. They can also be addressed later by their name or number when modifying the electrode characteristics, using the `CONTACT` statement or assigning biasing information in the `SOLVE` statements.

9.3.2: Specifying VCSEL Physical Models and Material Parameters

Much of the simulation results depend on how the physical models are described. For more information about physical models, see Chapter 3: "Physics", Section 3.6: "Physical Models".

Selecting Device Models

For most laser devices including VCSELs, we advise that you at least enable predominant recombination mechanisms, since these usually define the threshold characteristics and compete with stimulated emission for carrier recombination. Thus, directly impact the efficiency of the device.

Typically, three bulk recombination mechanisms should be addressed: Shockley-Read-Hall (SRH), Auger, and radiative recombination. You can enable these mechanisms by specifying `SRH`, `AUGER`, and `OPTR` parameters on a `MODEL` statement.

The parameters of these models are specified on `MATERIAL` statements. These include `TAUN` and `TAUP`, which specify the SRH lifetimes. `AUGN` and `AUGP`, which specify the Auger coefficients. And `COPT`, which specifies the radiative recombination rate coefficient.

These models and associated parameters are discussed in more detail in Chapter 3: "Physics", Section 3.6.3: "Carrier Generation-Recombination Models".

Specifying Material Parameters

For `LASER` or `VCSEL` simulation there are several other material parameters that should be considered. First and foremost, specify the high frequency dielectric relative permittivity of each material region. This can be specified as given by Table 8-2.

The high frequency dielectric enters in the Helmholtz equation and directly affects which laser mode may be present. In particular, try to consider the design of the DBRs carefully. Typically, the objective of the design of the DBRs is to choose the layer thicknesses so that they are one quarter wavelength thick relative to the local dielectric. During this design process, you need to also carefully consider the band-gap of the active region, since this affects the energy and wavelength of the maximal gain. A good design will try to operate near the peak gain, while satisfying the conditions for oscillation between the DBR mirrors.

Another important consideration for choosing material parameters is the selection of band edge parameters such as band gap and electron affinity. Although defaults do exist for many material systems it is almost always better for you to specify the best estimate. Also, consider the mobilities since they directly affect series resistance.

Chapter 3: "Physics", Section 3.6.1: "Mobility Modeling" has more information about these parameters. For more about `MATERIAL` statements, see Chapter 21: "Statements", Section 21.29: "MATERIAL".

9.3.3: Enabling VCSEL Solution

VCSEL Solution Mesh

The solution to Helmholtz equation is performed on a spatially discrete domain or mesh. Use of matrix method for the solution of the longitudinal wave equation allows the reduction in the number of mesh points in y (z in VCSEL) to the number of material boundaries. This significantly improves calculation time while maintaining the accuracy. The mesh points in the transverse direction x (r in VCSEL) coincide with the device mesh.

Specifying VCSEL Parameters

Specify the `VCSEL` statement to enable the VCSEL simulator. Once you enable it, the semiconductor device equations are solved self-consistently with the photon rate equations and the Helmholtz equation.

To enable reflectivity test simulation, do the following:

1. Specify the `VCSEL.CHECK` parameter in a `VCSEL` statement.
2. Specify the `VCSEL.INCIDENT` parameter to monitor cold cavity reflectivity for light incident on a structure from either top or bottom of the structure.
 - `VCSEL.INCIDENT = 1` - The light incident from the top.
 - `VCSEL.INCIDENT = 0` - The light incident from the bottom.
 - `VCSEL.INCIDENT = 2` or `>2` - Both directions of light incidence are considered. The program compares cavity resonant frequencies obtained for each direction of incidence. If results do not agree within a certain tolerance, `VCSEL:ATLAS` will close with an error.

By default, light is incident from the top of the structure.

3. Specify `INDEX.TOP` for the refractive index of the medium above the structure.
4. Specify `INDEX.BOTTOM` for the refractive index of the medium below the structure. Default medium above and below the structure is air.
5. Specify the `PHOTON.ENERGY` or `OMEGA` parameters for (initial) photon energy or frequency.
6. Specify the `EINIT` and `EFINAL` parameters. These parameters set the photon energy range in reflectivity test. If not specified, they take the following default values: `EINIT=0.8 PHOTON.ENERGY` and `EFINAL=1.2 PHOTON.ENERGY`.
7. Specify `NSPEC` for the number of sampling points between `EINIT` and `EFINAL`. The default value is `NSPEC=100`.

You can specify the following optional parameters in the `VCSEL` simulation:

- `NMODE` specifies the number of transverse modes of interest. Default value is `NMODE=1`.
- `PROJ` enables faster solution of the photon rate equations below threshold. You should disable this solution scheme when the bias reaches lasing threshold. Specify `^PROJ` in a `VCSEL` statement to do that.
- `PERTURB` enables faster solution of the Helmholtz equation. When specified, the program solves the longitudinal wave equation only once. Perturbational approach is used to account for the refractive index changes [252].
- `LOSSES` specifies any additional laser losses.

9.3.4: Numerical Parameters

The following numerical parameters control the performance of the VCSEL simulation.

- `TOLER` sets the desired relative tolerance of the photon density calculation. The default value is 0.01. Setting this parameter to a lower value may slow down the calculation significantly. Using a larger value will result in a faster but less accurate calculations.
- `ITMAX` sets maximum number of external VCSEL iterations during photon density calculation. The default value is 30.
- `TAUSS` is an iteration parameter used in the calculation of photon densities. Using a larger value of this parameter can speed up the calculation but may cause convergence problems.
- `MAXCH` is the maximum allowed relative change of the photon density between VCSEL iterations. Using a larger value of this parameter can speed up the calculation but may cause convergence problems.

9.3.5: Alternative VCSEL Simulator

If you need to model a vertical cavity laser that supports multiple longitudinal modes, use the `LASER` statement to enable VCSEL solution.

Specify the `LASER` statement to enable the laser simulator. Once you enable it, the semiconductor device equations are solved self-consistently with the laser rate equations. The major difference between this simulator and the one discussed above is in the approach to the solution of the Helmholtz equation.

The solver used in this case allows multiple longitudinal modes, but it is not as efficient in dealing with structural variations in the transverse direction.

There are several kinds of parameters that appear in the `LASER` statement. Most of the parameters available are discussed above with respect to `VCSEL` statement.

Specify laser physical parameters and models, and specify the `DBR1 . START`, `DBR1 . FINAL`, `DBR2 . START`, and `DBR2 . FINAL` parameters in the `LASER` statement.

The mirror loss is defined as:

$$\alpha_{mir} = \frac{1}{2L} \ln\left(\frac{1}{R_f R_r}\right) \quad 9-20$$

where L is the cavity length given as:

$$L = \text{DBR2 . START} - \text{DBR1 . FINAL}$$

R_f and R_r are the front and rear mirror reflectivities and are calculated from the solution of Helmholtz equation in the range specified by `DBR1 . START`, `DBR2 . START`, and `DBR2 . FINAL`.

`LASER` simulates single or multiple longitudinal modes as well as single or multiple transverse modes. Also with `LASER`, you can simulate index guiding only or gain guiding. Simulation of gain guiding takes more computation time but should be considered when spatially varying gain effects are anticipated.

If you to calculate the laser spectrum, specify the multiple longitudinal modes model and additional parameters. Do the following:

1. Specify the `LMODES` parameter in the statement. This enables the multiple longitudinal mode model.
2. Specify the `EINIT` and `EFINAL` parameters. These parameters set the photon energy range within, which `LASER` will take into account multiple longitudinal modes. Make sure initial photon energy is within this range and is specified for the active lasing region.

3. Specify the photon energy separation (ESEP parameter). If this isn't specified, LASER will automatically calculate the number of longitudinal modes based on the cavity length and the energy range. We recommend that you allow LASER to choose the photon energy separation.
4. Specify the spectrum file name (SPEC.SAVE). LASER will produce a structure file containing spectrum data after calculation of each bias point. LASER will automatically append `_dcN.log` to the specified file name (where N is the number of the bias point) for steady-state solutions or `_trN.log` for a transient simulation. The first bias point where LASER is active will have N=1. This is rarely the first bias point during simulation. Use TONYPLOT to examine these files. If you specify the SPECSAVE parameter, it will only save the spectrum files on every `las.SPECSAVE` solution.

The index in the spectrum file name will still increase by one each time. The spectrum data can be stored in a single file for the transient simulation, only if the MULTISAVE-LASER statement is set to FALSE. To enable multiple transverse mode solutions, specify the number of transverse modes by using the NMODE parameter from the LASER statement.

By default, VCSELs simulate using the index guiding model. To simulate using the gain guiding, specify `INDEX.MODEL=1`.

9.3.6: Far Field Patterns

Sometimes it is convenient to describe the beam as a diffraction free beam [61, 230]. We first model the near field pattern as a Gaussian by fitting to the near-field pattern calculated by VCSEL as described above. The equation for the Gaussian pattern is given in Equation 9-21.

$$E(r) = \exp\left[-\left(\frac{r}{w}\right)^2\right] \quad 9-21$$

Here r is the radial coordinate and w is the fitting parameter. You can model the far-field pattern as a Gaussian by specifying GAUSS on the VCSEL statement. The Bessel beam far-field pattern described by Equation 9-22 can be selected by specifying BESSEL on the VCSEL statement.

$$E(r) = J_0(A \cdot \text{BESSEL} \times r) \exp\left[-\left(\frac{r}{w}\right)^2\right] \quad 9-22$$

Here J_0 is the zero order Bessel function and $A \cdot \text{BESSEL}$ is a user specifiable parameter with units of $1/\mu$ on the VCSEL statement.

You can choose a combination Gaussian/Bessel function by specifying GBESSEL on the VCSEL statement. This function is described by Equation 9-23.

$$E(r) = J_0(A \cdot \text{BESSEL} \times r) \quad 9-23$$

You can save near and far field patterns by specifying a value for the PATTERNS parameter in the SAVE statement. The value of the PATTERNS parameter is a character string representing the root name of a file for saving the near and far field patterns. The near field pattern is saved to a file with the string `.nfp` appended to the root name. The far field pattern is saved to a file with the string `.ffp` appended to the root name. Use TONYPLOT to examine these files.

9.4: Semiconductor Laser Simulation Techniques

The most common technique for simulating laser diodes is to simulate forward characteristics with a gradually increasing bias. The forward voltage is usually specified. You can use, however, current boundary conditions and include external elements.

To save computational time, we recommend that you use the `VCSEL` statement. The effective frequency method employed for the solution of the Helmholtz equation in this case allows you to consider structures with oxide apertures or other structural variations in transverse direction. We also recommend that you test the structure using reflectivity experiment simulation prior to applying the bias.

If you use the multiple longitudinal mode model, computational time will be longer and strongly dependent on the number of longitudinal modes involved in the calculation.

Simulating multiple transverse modes takes more computation time and should only be preformed when the higher order modes are of interest.

This page is intentionally left blank.

10.1: Overview

LUMINOUS is a general purpose light propagation and absorption program integrated into the ATLAS framework. When used with S-PISCES or BLAZE, or DEVICE3D simulators, LUMINOUS and LUMINOUS3D calculate optical intensity profiles within the semiconductor device. They will then convert these profiles into photogeneration rates. This unique coupling of tools allows you to simulate electronic responses to optical signals for a broad range of optical detectors. These devices include but are not limited to pn and pin photodiodes, avalanche photodiodes, Schottky photodetectors, MSMs, photoconductors, optical FETs, optical transistors, solar cells, and CCDs.

The following sections address various types of optoelectronic devices. Go to the sections that are most relevant to your application. We strongly recommend, however, that you read the other sections too.

Note: You should be familiar with ATLAS and either S-PISCES or BLAZE before you can use LUMINOUS. If not, read Chapter 2: “Getting Started with ATLAS” and either Chapter 4: “S-Piscis: Silicon Based 2D Simulator” or Chapter 5: “Blaze: Compound Material 2D Simulator”.

The propagation of light can be described by any one of 4 physical models or several user-defined approaches. The physical models for light propagation include the following.

- Ray tracing (RT), which is described in Section 10.2: “Ray Tracing”. Ray tracing is a general method of resolving 2D and 3D non-planar geometries but ignores coherence and diffraction effects.
- The transfer matrix method (TMM), which is described in Section 10.3: “Matrix Method”. The matrix method is a 1D method that includes interference effects. This method is recommended for large area devices such as thin film solar cells.
- The beam propagation method (BPM), which is described in Section 10.4: “Beam Propagation Method in 2D”. BPM is a general 2D method that includes diffraction effects at an increased computational expense.
- Finite difference time domain (FDTD) methods, which are described in Section 10.5: “Finite Difference Time Domain Analysis [269]”. FDTD is the most general 2D and 3D method and accounts for both diffraction and coherence by direct solution of Maxwell’s equations. This is the most computationally expensive approach.

The user-definable methods are described in Section 10.6: “User-Defined Photogeneration”. The remaining sections in this chapter discuss the various other common topics in photodetector simulation.

10.2: Ray Tracing

Optoelectronic device simulation is split into two distinct models that are calculated simultaneously at each DC bias point or transient timestep.

1. Optical ray trace using real component of refractive index to calculate the optical intensity at each grid point
2. Absorption or photogeneration model using the imaginary component of refractive index to calculate a new carrier concentration at each grid point.

This is followed by an electrical simulation using S-PISCES or BLAZE to calculate terminal currents.

Note: LUMINOUS assumes that the refractive indices, both real and imaginary, are constant within a particular region.

10.2.1: Ray Tracing in 2D

Defining The Incident Beam

An optical beam is modeled as a collimated source using the BEAM statement. The origin of the beam is defined by parameters X.ORIGIN and Y.ORIGIN (see Figure 10-1). The ANGLE parameter specifies the direction of propagation of the beam relative to the X axis. ANGLE=90 is vertical illumination from the top. MIN.WINDOW/MAX.WINDOW parameters specify the illumination window. As shown in Figure 10-1, the Illumination Window is “clipped” against the device domain so that none of the beam bypasses the device.

The beam is automatically split into a series of rays so that the sum of the rays covers the entire width of the illumination window. When the beam is split, ATLAS automatically resolves discontinuities along the region boundaries of the device.

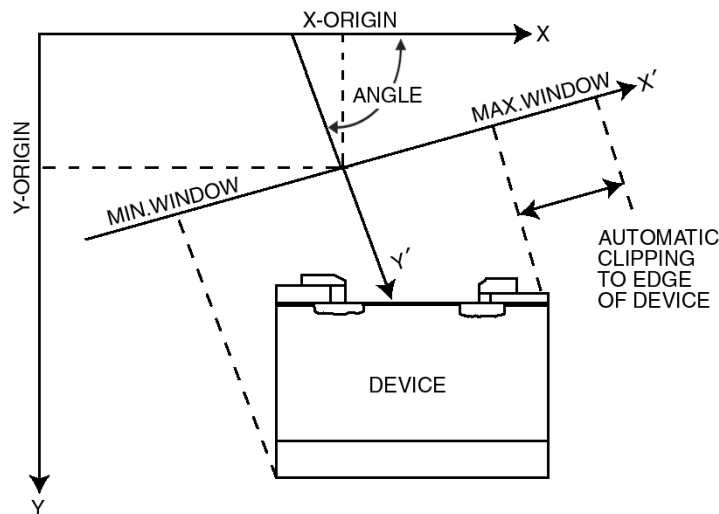


Figure 10-1: Optical Beam Geometry

Although the automatic algorithm is usually sufficient, you can also split the beam up into a number of rays using the RAYS parameter. Each ray will then have the same width at the beam origin and the sum of the rays will cover the illumination window. Even when you specify the RAYS parameter, ATLAS will automatically split the rays to resolve the device geometry.

Ray Splitting At Interfaces

Rays are also split at interfaces between regions into a transmitted ray and a reflected ray. Figure 10-2 illustrates the difference between rays that are split to resolve the geometry and transmitted/reflected rays split at a region interfaces.

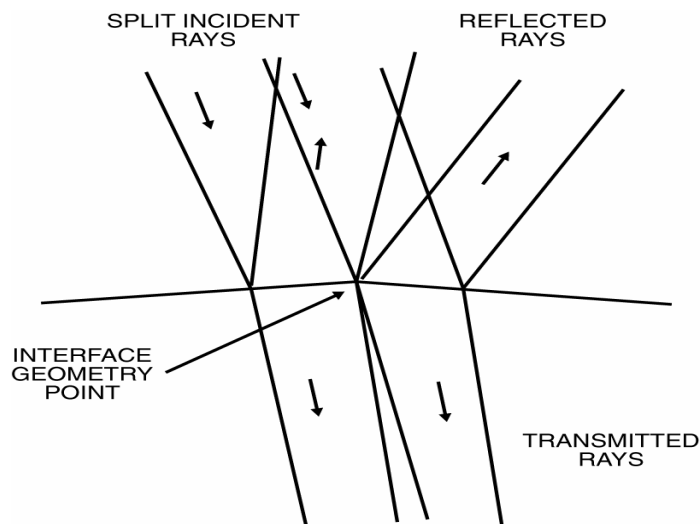


Figure 10-2: Reflected and Transmitted Rays

In Figure 10-2, the incident rays come in from the top left. They intersect a interface between two material regions with differing refractive indices. Within this interface lies a geometric point where the normal to the interface changes. This implies that the angles of reflection and transmission will be different for light incident to the left of the point from light incident on the right. Thus, the incident rays are split to resolve the interface point. The second level of splitting occurs at the interface itself. Here, the incident rays are split into reflected and transmitted rays.

10.2.2: Ray Tracing in 3D

In 3D, a simpler algorithm is used for ray tracing because the 2D algorithms become intractable in 3D. Therefore, the algorithm doesn't automatically split rays to resolve topological features of the device. You should specify enough rays to resolve such features to the desired accuracy. But there's a trade off between the computation time and accuracy in specifying the number of rays.

The 3D source geometry is very similar to the geometry shown in Figure 10-1. In 3D, the source origin is specified by three coordinates: X.ORIGIN, Y.ORIGIN, and Z.ORIGIN. Unlike Figure 10-1, there are two angles that describe the direction of propagation.

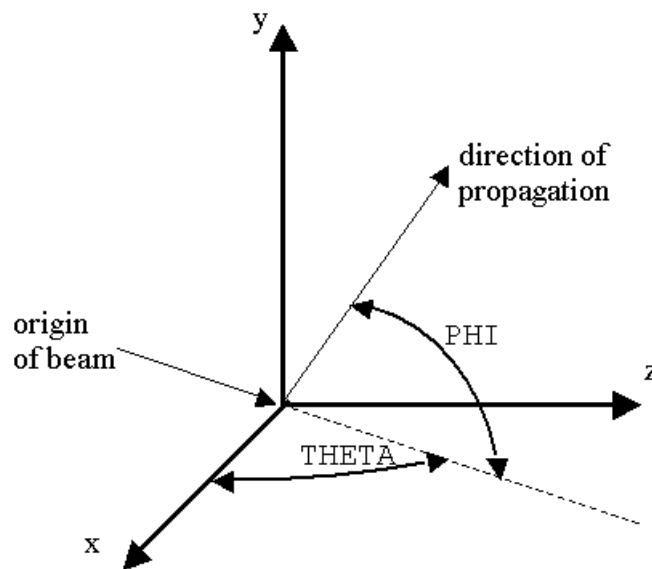


Figure 10-3: Propagation in 3D

Here, the angle PHI (aliased to ANGLE) describes the angle of propagation with respect to the XZ plane. The angle THETA describes the angle of rotation specified about the Y axis. These angles are on the BEAM statement.

In 3D, the clipping of the window of propagation is done in two directions. In the X direction, this is described by XMIN and XMAX. XMIN and XMAX are aliases of MIN.WINDOW and MAX.WINDOW. In the Z direction, the window is described by ZMIN and ZMAX.

The numbers of rays in the X and Z directions are described by NX and NZ. Ray samples are taken at regular intervals over the source window.

The discrete sampling of the source beam into rays in LUMINOUS3D is unlike that done in LUMINOUS. In LUMINOUS, the source beam is automatically broken up into a set of rays that resolve the device topology and variations in the interior of the device. In LUMINOUS3D, this process is more complex and is a computationally intractable. As such in LUMINOUS3D, specify a discrete sampling of the source beam (see Figure 10-4).

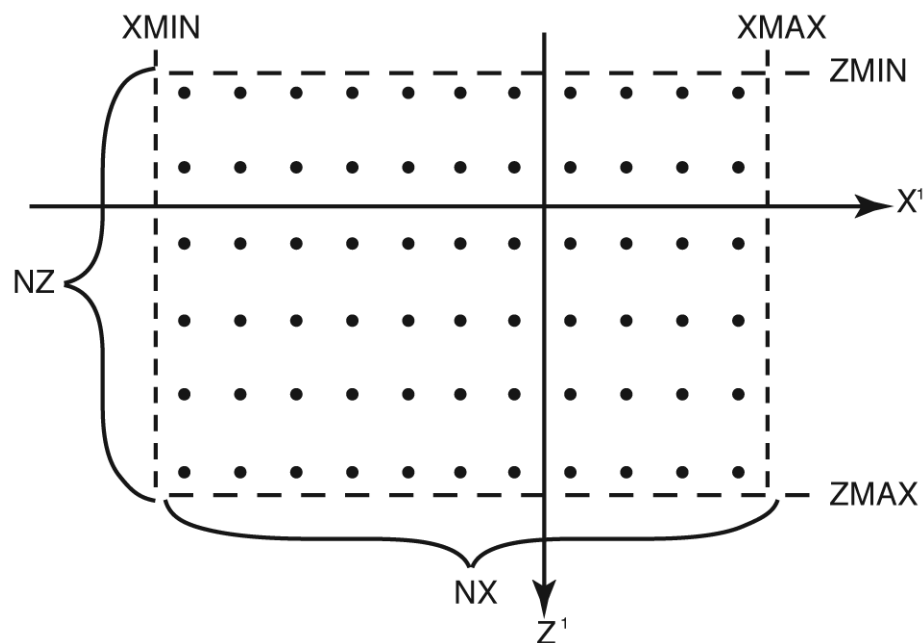


Figure 10-4: Source beam sampling

In Figure 10-4, the extent of the source sampling is specified by the $XMIN$, $XMAX$, $ZMIN$ and $ZMAX$ parameters of the `BEAM` statement. Even samples are taken along each of the beam front principal axes. The number of samples in the X and Z directions are given by the NX and NZ parameters of the `BEAM` statement.

10.2.3: Reflection and Transmission

Figure 10-5 shows the relationship between the angles of incidence (θ_i), reflection (θ_r), and transmission (θ_t) at the interface between two media. These coefficients are calculated as a function of the refractive indices in the two media.

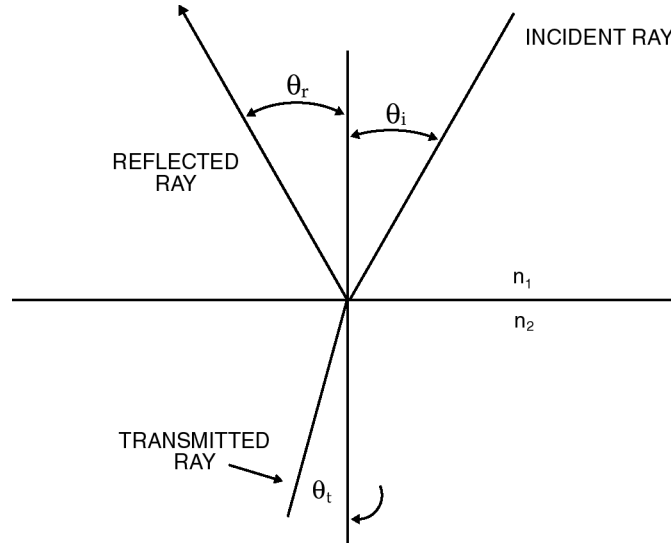


Figure 10-5: Angles of incidence, reflection and transmission

The reflection and transmission coefficients of the light for parallel and perpendicular polarization are calculated as shown in Equations 10-1 to 10-6.

$$E_r = \frac{n_2 \cos \theta_i - n_1 \cos \theta_t}{n_1 \cos \theta_t + n_2 \cos \theta_i} E_i \quad (\text{parallel p or TE polarization}) \quad 10-1$$

$$E_t = \frac{2n_1 \cos \theta_i}{n_1 \cos \theta_t + n_2 \cos \theta_i} E_i \quad (\text{parallel p or TE polarization}) \quad 10-2$$

$$E_r = \frac{n_1 \cos \theta_i - n_2 \cos \theta_t}{n_1 \cos \theta_i + n_2 \cos \theta_t} E_i \quad (\text{perpendicular s or TM polarization}) \quad 10-3$$

$$E_t = \frac{2n_1 \cos \theta_i}{n_1 \cos \theta_i + n_2 \cos \theta_t} E_i \quad (\text{perpendicular s or TM polarization}) \quad 10-4$$

$$R = \left(\frac{E_r}{E_i} \right)^2 \quad (\text{perpendicular s or TM polarization}) \quad 10-5$$

$$T = \left(\frac{E_t}{E_i} \right)^2 \frac{n_2}{n_1} \frac{\cos \theta_t}{\cos \theta_i} \quad (\text{perpendicular s or TM polarization}) \quad 10-6$$

where E_i is electric field of the incident wave, E_r is the field of the reflected wave, E_t is the field of the transmitted wave. R is the reflection coefficient, T is the transmission coefficient, n_1 is the refractive index on the incident side and n_2 is the refractive index on the transmission side.

Note: Here, we have adopted Yee's notation for TM (Transverse Magnetic) and TE (Transverse Electric) fields [269].

The angles of reflection and transmission are given in Equations 10-7 and 10-8.

$$\theta_r = \theta_i \quad 10-7$$

$$n_1 \sin \theta_i = n_2 \sin \theta_t \quad 10-8$$

where θ_i is the angle of incidence, θ_t is the angle of transmission and θ_r is the angle of reflection.

Specifying Reflections

By default, no reflected rays are traced. The transmission coefficients are properly calculated for the transmitted rays. The `REFLECTS=<i>` parameter is used to set an integer number of reflections to consider. Note that setting a very large number of reflections can lead to extremely long simulation times for the ray trace.

One convenient way to overcome the long CPU times is to use the `MIN.POWER` parameter. This terminates each ray when the optical power falls to the fraction of the original power defined by this parameter.

Front Reflection

By default, reflection and refraction at the first interface (the initial interface with the device) are ignored. The first reflection coefficient is zero and the transmission coefficient is one. The polarization and angle of the transmitted ray at the first interface is identical to the polarization and angle of the incident beam.

If the `FRONT.REFL` parameter of the `BEAM` statement is specified, the transmission coefficient is calculated using Equations 10-1 to 10-6. When the transmission coefficient is calculated, it's assumed that the material outside the device domain is a vacuum. The transmitted rays are attenuated by the transmission coefficient but the reflected ray is not traced.

Back Reflection

By default, the reflection at the back of the device are ignored. No reflected ray is traced once the back of the device is reached. If the `BACK.REFL` parameter is specified, the backside reflection coefficient is calculated (again assuming a vacuum outside the device) and the back-side reflected ray is traced.

Sidewall Reflection

By default, the reflection from the sides of the device are ignored. No reflected ray is traced back into the structure. As above, `BACK.REFL` is used to enable the sidewall reflections assuming a vacuum outside the device.

User Specified Reflection

You can specify the value of the reflection coefficient at an interfaces by specifying the `REFLECT` parameter of the `INTERFACE` statement. The value of `REFLECT` must be between 0.0 and 1.0 inclusive, and the `OPTICAL` parameter must also be specified on the statement. You should also specify the values of `P1.X`, `P1.Y`, `P2.X`, and `P2.Y`.

Discontinuous Regions

You can simulate devices electrically where a single region is defined as two or more separated areas. The ray tracing algorithm, however, doesn't support such structures. If a structure has two separate areas with the same region number, we recommend you using DEVEDIT to renumber the regions, perhaps even creating a new region number for each area.

Note: This limitation is only for two separated areas with the same region number and not for two regions with different region numbers of the same material. This latter case can be simulated.

10.2.4: Diffusive Reflection [272]

For optical ray-tracing semiconductor interfaces may be modelled as having diffusive reflections. To enable this model, specify the `DIFFUSIVE` parameter on the `INTERFACE` statement. When using this model, you must also specify the region of incidence. To do this, use the `REGION` parameter of the `INTERFACE` statement.

You can also specify the fraction of the incident power that experiences specular reflection using the `SPECULAR` parameter of the `INTERFACE` statement. The fraction of the incident power that is lost to absorption can be specified using the `ABSORPTION` parameter of the `INTERFACE` statement.

By default, the diffusive reflection has a Lambertian distribution (having constant luminance with respect to angle). You can also choose a Gaussian or Lorenz distribution by specifying either `GAUSS` or `LORENZ` respectively on the `INTERFACE` statement. The Gaussian function is described by Equation 10-9.

$$F(\phi) = \frac{I}{\text{DISPERSION}} e^{-\left(\frac{\phi^2}{2\text{DISPERSION}^2}\right)} \quad 10-9$$

Here, $F(\phi)$ is the scattering function. ϕ is the dispersion angle and `DISPERSION` is a user definable parameter on the `INTERFACE` statement specifying the relative spread of the dispersion.

The Lorenz function is described by Equation 10-10.

$$F(\phi) = \frac{\text{DISPERSION}}{\phi^2 + \text{DISPERSION}^2} \quad 10-10$$

When the `DISPERSION` parameter is set to zero no dispersion takes place.

The `SCATTERED` parameter on the `INTERFACE` statement specifies the number of rays per scattering event.

10.2.5: Light Absorption and Photogeneration

The cumulative effects of the reflection coefficients, transmission coefficients, and the integrated loss due to absorption over the ray path are saved for each ray. The generation associated with each grid point can be calculated by integration of the Generation Rate Formula (Equation 10-11) over the area of intersection between the ray and the polygon associated with the grid point.

$$G = \eta_0 \frac{P\lambda}{hc} e^{-\alpha y} \quad 10-11$$

where:

- P is the ray intensity factor, which contains the cumulative effects of reflections, transmissions, and loss due to absorption over the ray path.
- η_0 is the internal quantum efficiency, which represents the number of carrier pairs generated per photon observed.
- y is a relative distance for the ray in question.
- h is Planck's constant
- λ is the wavelength.
- c is the speed of light.
- α is the absorption coefficient given by Equation 10-12.

$$\alpha = \frac{4\pi k}{\lambda} \quad 10-12$$

where k is the imaginary part of the optical index of refraction.

Photogeneration on a Non-uniform Mesh

The photogeneration algorithm used integrates the optical intensity around each node point. This is done to ensure that the total photogeneration rate isn't grid sensitive. A uniform photogeneration rate is defined as a constant value of (photogeneration rate at any node)*(element area around the node). In TONYPLOT, a uniform photogeneration rate may appear to vary across a non-uniform mesh density.

Photogeneration at Contacts

The photogeneration associated with nodes that are also defined as electrodes is a special case. The electrical boundary conditions require that the carrier concentration at electrode nodes equals the doping level. This means that photogeneration at nodes that are electrodes must be zero. But just setting these nodes to zero photogeneration will typically cause an apparent drop in quantum efficiency.

The photogeneration rate at the contact nodes is calculated as usual. This photogeneration rate, however, is applied to the neighboring node inside the semiconductor. This means for a uniform mesh and photogeneration rate, if the photogeneration rate is 1.0×10^{17} pairs/cm³s, then the nodes at the contacts will have zero photogeneration and the next node into the semiconductor will have 2.0×10^{17} pairs/cm³s.

10.2.6: Outputting the Ray Trace

For example, in LUMINOUS the rays generated during ray tracing are stored in all subsequent structure files. In LUMINOUS3D, this isn't the case. To save the rays in LUMINOUS3D, set the RAYTRACE parameter of the BEAM statement to the name of a file where the results of the ray trace are to be stored.

10.3: Matrix Method

Matrix method presents a fast and accurate way to simulate electromagnetic wave propagation through a layered medium. Among a variety of approaches to matrix theory, the most commonly used are the characteristic matrix and the transfer matrix descriptions.

Using the matrix method is not limited to LUMINOUS only. It also finds its application in VCSEL and LED modules. ATLAS uses the characteristic matrix approach that relates total tangential components of the electric and magnetic fields at the multilayer boundaries. More often used transfer matrix, which relates tangential components of the electric field of left-travelling and right-travelling waves, has several disadvantages that limit its applicability.

The structure of a multilayer completely determines the characteristic matrix of this multilayer. The transfer matrix also contains information about the media on both sides of the multilayer. The characteristic matrix approach is more general and can be expanded to deal with graded interfaces, in which case, the transfer matrix method is inappropriate to use.

10.3.1: Characteristic Matrix

First, we describe the characteristic matrix of a single layer. As mentioned earlier, the matrix relates tangential components of the electric $E(z)$ and magnetic $H(z)$ fields at the layer boundaries $z=0$ and $z=d$.

$$\begin{bmatrix} E(0) \\ H(0) \end{bmatrix} = M \begin{bmatrix} E(d) \\ H(d) \end{bmatrix} \quad 10-13$$

The matrix itself is

$$M = \begin{bmatrix} \cos \varphi & j \sin \varphi / Y \\ j Y \sin \varphi & \cos \varphi \end{bmatrix} \quad 10-14$$

where

$$\varphi = \frac{2\pi}{\lambda} n d \cos \Theta \quad 10-15$$

is the phase shift for the wave propagating through the layer, n is the complex refractive index, and Θ is the angle of wave propagation in the layer (Figure 10-6). Y is the optical admittance of the layer, which is for parallel (p or TE) and perpendicular (s or TM) polarizations, is given by:

$$Y^{(s)} = \sqrt{\frac{\varepsilon_0}{\mu_0}} n \cos \Theta \quad 10-16$$

$$Y^{(p)} = \sqrt{\frac{\varepsilon_0}{\mu_0}} n / \cos \Theta \quad 10-17$$

where ε_0 and μ_0 are permittivity and permeability of free space.

The characteristic matrix of a multilayer is a product of corresponding single layer matrices. If m is the number of layers, then the field at the first ($z=z_0$) and the last ($z=z_m$) boundaries are related as follows:

$$\begin{bmatrix} E(Z_0) \\ H(Z_0) \end{bmatrix} = M_1 M_2 \dots M_m \begin{bmatrix} E(Z_m) \\ H(Z_m) \end{bmatrix}, M_i = \begin{bmatrix} \cos \varphi_i & j \sin \varphi_i / Y_i \\ j Y_i \sin \varphi_i & \cos \varphi_i \end{bmatrix} \quad 10-18$$

10.3.2: Reflectivity, Transmissivity, and Absorptance

The detailed derivation of amplitude reflection (r) and transmission (t) coefficients is given in [189]. The resulting expressions are shown in Equations 10-19 and 10-20.

$$r = \frac{Y_0 M_{11} + Y_0 Y_s M_{12} + M_{21} - Y_s M_{22}}{Y_0 M_{11} + Y_0 Y_s M_{12} + M_{21} + Y_s M_{22}} \quad 10-19$$

$$t = \frac{2Y_0}{Y_0 M_{11} + Y_0 Y_s M_{12} + M_{21} + Y_s M_{22}} \quad 10-20$$

where Y_0 and Y_s are the characteristic admittances of the media on both sides of the multilayer. M_{ij} are the elements of the characteristic matrix of the multilayer. Light is incident from the medium with admittance Y_0 . The energy coefficients (reflectivity, transmissivity, and absorptance) are given by:

$$R = |r|^2 \quad 10-21$$

$$T = \frac{\text{Re}(Y_s)}{\text{Re}(Y_0)} |t|^2 \quad 10-22$$

$$A = (1 - R) \left[1 - \frac{\text{Re}(Y_s)}{\text{Re}[(M_{11} + Y_s M_{12})(M_{21} + Y_s M_{22})^*]} \right] \quad 10-23$$

These expressions take into account imaginary part of refractive index. Therefore, they are more general than Fresnel formulae (Equations 10-1 through 10-6). LUMINOUS automatically uses these expressions when appropriate.

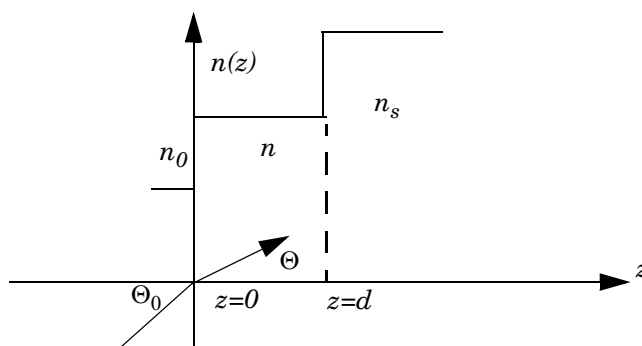


Figure 10-6: Refractive index profile of a single-layer coating

10.3.3: Transfer Matrix and Standing Wave Pattern

The characteristic matrix of a multilayer structure fully describes the optical properties of the multilayer. It is not completely, however, independent of external parameters. If the angle of incidence of light on a multilayer structure changes, the characteristic matrix changes too. Equations 10-15, 10-16, and 10-17 show the dependence of the single layer matrix elements on the angle of wave propagation in the layer. This implicit dependence on the angle of light incidence makes the characteristic matrix approach similar to the transfer matrix method for most practical purposes. In fact, when the multilayer structure does not contain any graded layers, the two methods are equivalent.

The transfer matrix directly relates the electric field amplitudes of transmitted and reflected waves to the amplitude of the incident wave. This property of the transfer matrix makes it the method of choice in many optics applications.

The transfer matrix elements are related to the characteristic matrix elements by the following expressions:

$$Q_{11} = (M_{11} + M_{21}/Y_i + Y_o M_{12} + Y_o/Y_i M_{22})/2 \quad 10-24$$

$$Q_{12} = (M_{11} + M_{21}/Y_i - Y_o M_{12} - Y_o/Y_i M_{22})/2 \quad 10-25$$

$$Q_{21} = (M_{11} - M_{21}/Y_i + Y_o M_{12} - Y_o/Y_i M_{22})/2 \quad 10-26$$

$$Q_{22} = (M_{11} - M_{21}/Y_i - Y_o M_{12} + Y_o/Y_i M_{22})/2 \quad 10-27$$

where Y_i and Y_o are the admittances of the input and output media defined according to Equations 10-16 and 10-17 for (s) and (p) polarization components respectively.

The amplitude reflection and transmission coefficients are:

$$r = Q_{21}/Q_{11} \quad 10-28$$

$$t = 1/Q_{11} \quad 10-29$$

In some devices that use multilayer structures, it is sufficient to know the transmittance and reflectance of the structure in order to fully characterize the device response to incident light. Other devices, however, such as thin film detectors, require the knowledge of light intensity distribution within the multilayer structure. Therefore in addition to the light transfer properties of such a structure, you need to be able to calculate the standing wave pattern formed by interference of traveling wave components in each layer. Standard intensity based ray-tracing calculations do not account for coherent effects and are unable to simulate standing wave patterns. Beam Propagation Method and full-wave Maxwell solvers are computationally expensive and are not useful for structures containing large number of layers. In this case, the numerical solution of the Helmholtz equation using the transfer matrix method is an attractive alternative.

Although this approach is inherently one-dimensional, it is known to produce highly accurate results for practical devices in two dimensions. Important requirements are:

- Lateral feature sizes in the device are much larger than typical layer thicknesses in a multilayer.
- Incident light is normal to the surface or is at small angles to the surface normal. When these requirements are met, the device can be divided into several lateral regions in which the structural variations occur in vertical direction z only.

For each lateral region, the one-dimensional Helmholtz equation is solved using the transfer matrix method.

First, we find reflected component of electrical field at $z=0$:

$$E_r = rE_i$$

where E_i and E_r are the amplitudes of incident and reflected waves respectively. The electric field and magnetic field at $z=0$ are:

$$E(0) = E_i + E_r \quad 10-30$$

$$H(0) = (E_r - E_i)Y_i \quad 10-31$$

Then, the fields at layer interfaces can be found step by step using one layer characteristic matrices. The electric field at any point within a certain layer is given by:

$$E(z) = E(z_j)\cos(\phi) - iH(z_j)\sin(\phi)/Y(j) \quad 10-32$$

$$H(z) = H(z_j)\cos(\phi) - iE(z_j)\sin(\phi)/Y(i) \quad 10-33$$

where $E(z_j)$ and $H(z_j)$ are electric and magnetic fields at layer interface between layers (j) and ($j-1$), $Y(j)$ is the optical admittance of the layer (j) and phase is given by:

$$\phi = 2\pi n \cos(\theta)(z - z_j)/\lambda \quad 10-34$$

This way, intensity profile is generated throughout the device structure. The photogeneration rate is given by:

$$G(z) = \frac{\lambda}{hc} \alpha \frac{|E(z)|^2}{2\eta} \quad 10-35$$

To enable transfer matrix method for calculation of intensity distribution and photogeneration profiles in thin film detectors, specify `TR.MATRIX` parameter on a `BEAM` statement.

For convenience, the parameters are shown in Table 10-1. The `SUB.INDEX` and `SUB.EXTINCT` parameters allow specification of the complex index of refraction at the exit side of the layer stack. Similarly, you can use the `AMBIENT.INDEX` parameter of the `BEAM` statement to specify the real index on the input side of the layer stack.

| Table 10-1. External Index Parameters | | |
|---------------------------------------|---------------|---------|
| Statement | Parameter | Default |
| BEAM | AMBIENT.INDEX | 1.0 |
| BEAM | SUB.INDEX | 1.0 |
| BEAM | SUB.EXTINCT | 0.0 |

10.3.4: Transfer Matrix with Diffusive Interfaces

Frequently, thin-film detectors are constructed with rough or irregularly textured interfaces between materials. These interfaces exhibit partly specular and partly diffused reflection and transmission characteristics.

An approach has been proposed [124, 125, 276] that models both coherent (specular) and incoherent (diffused) light propagation and absorption. With this approach, the specular light is modeled using the transfer matrix method while the diffuse light is modeled using ray tracing.

The connection between the specular and diffused portions of the light is described by haze functions defined at each irregular interface as shown in Figure 10-14.

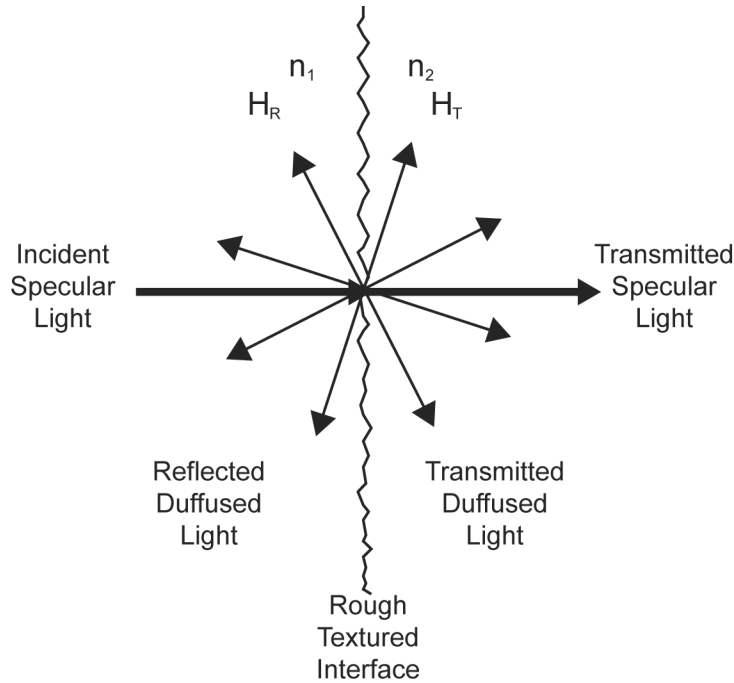


Figure 10-7: Relationship between the haze functions and the specular and diffused light at a textured interface

Equations 10-38 and 10-39 give the transmissive haze function H_T and the reflective haze function H_R .

$$H_T = 1 - \exp \left[- \left(\frac{4\pi \text{SIGMA} \cdot \text{CT} \cdot |n_1 \cos \phi_1 - n_2 \cos \phi_2|}{\lambda} \right)^{\text{NT}} \right] \quad 10-36$$

$$H_R = 1 - \exp \left[- \left(\frac{4\pi \text{SIGMA} \cdot \text{CR} \cdot \cos(\phi) n_1}{\lambda} \right)^{\text{NR}} \right] \quad 10-37$$

Here:

- λ is the optical wavelength.
- ϕ is the angle of incidence.
- n_1 is the index of refraction on the incident side of the interface.
- n_2 is the index of refraction on the transmitted side of the interface.
- CR, CT, NR, NT, and SIGMA are user-defined parameters described in Table 10-2.

Here, CR, CT, NR, and NT can be considered tuning parameters. SIGMA characterizes the mean variation of rough features on the interface.

| Table 10-2. Default Values for User Specifiable Parameters of Equations 10-47 and 10-48 | | | |
|---|-----------|---------|-------|
| Parameter | Statement | Default | Units |
| CR | INTERFACE | 1.0 | |
| CT | INTERFACE | 0.5 | |
| NR | INTERFACE | 2.0 | |
| NT | INTERFACE | 3.0 | |
| SIGMA | INTERFACE | 20.0 | nm |

You can describe the CT and CR parameters as a wavelength function in tabular form using the TCT.TABLE and TCR.TABLE parameters of the INTERFACE statement. These parameters can be names of the files containing ASCII descriptions of the dependencies. The first row of each file is a single number describing the number of samples. Subsequent rows contain pairs of numbers containing specifying the wavelength in microns and the value of CT or CR at that wavelength.

The hazefunctions, H_T and H_R , give the fraction of transmitted or reflected light that is diffused as given in Equations 10-38 and 10-39.

$$H_T = \frac{I_{dT}}{I_{dT} + I_{sT}} \quad 10-38$$

$$H_R = \frac{I_{dR}}{I_{dR} + I_{sR}} \quad 10-39$$

Here:

- I_{dT} is the transmitted diffused intensity.
- I_{sT} is the transmitted specular intensity.
- I_{dR} is the reflected diffused intensity.
- I_{sR} is the reflected specular intensity.

The transmissive haze function, H_T , gives the ratio of the transmitted diffused light intensity to the specular light intensity. The reflective haze function, H_R , gives the ratio of the reflected diffused light intensity to the specular light intensity. Figure 10-8 shows some example evaluations of the haze functions.

The transmissive and reflective hazefunctions can be written to log files by assigning the OUT.HT and OUT.HR parameters of the INTERFACE statement to the desired output file names. When outputting the haze functions, you should also specify the range of wavelengths and number of samples using the LAM1, LAM2, and NLAM parameters on the INTERFACE statement.

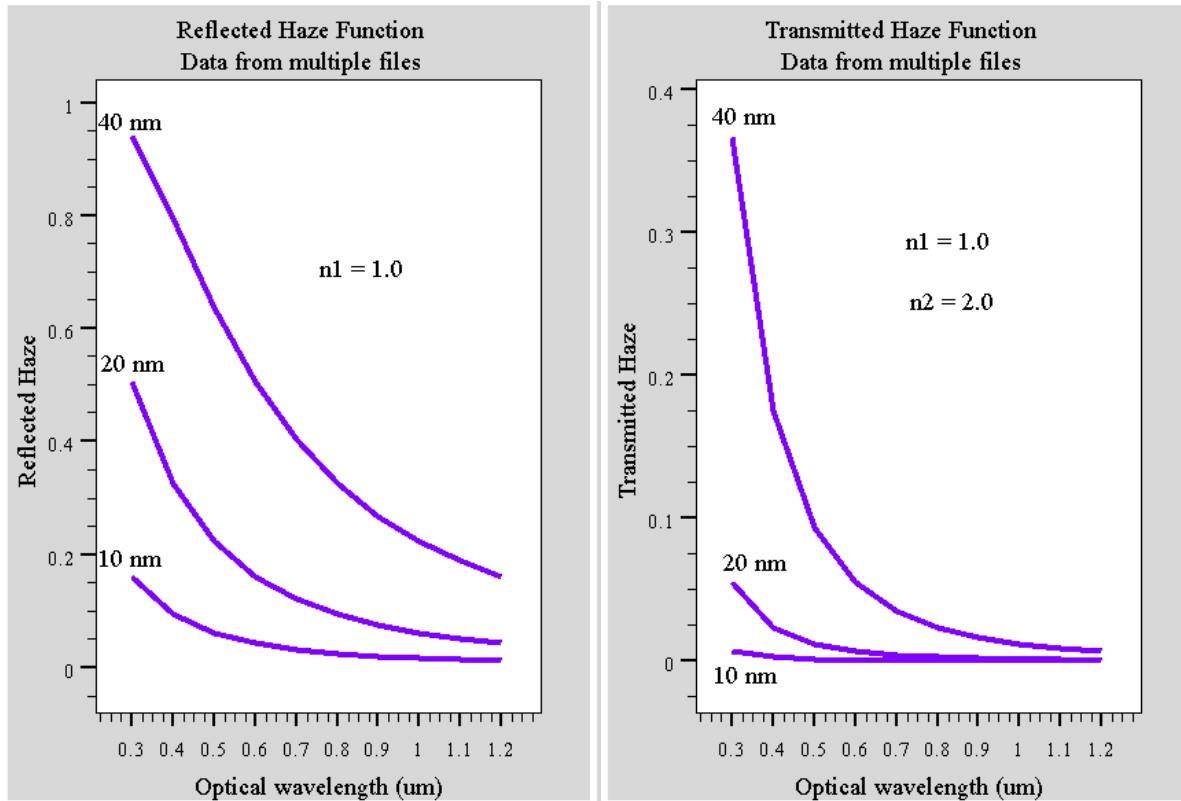


Figure 10-8: Haze Functions as a Function of Wavelength Example

The transmitted and reflected incoherent (diffused) light is also described by an Angular Distribution Function (ADF). The ADF is specified on the INTERFACE statement as either CONSTANT, TRIANGLE, GAUSS, LORENZ, LAMBERT, or ELLIPSE. Equations 10-40 through 10-45 show the functional forms for the various ADFs.

$$\text{CONSTANT:} \quad \text{ADF}(\phi) = 1 \quad 10-40$$

$$\text{TRIANGLE:} \quad \text{ADF}(\phi) = 1 - 2\phi/\pi \quad 10-41$$

$$\text{GAUSS:} \quad \text{ADF}(\phi) = \exp\left(\frac{-\phi^2}{2\text{DISPERSION}}\right) \quad 10-42$$

$$\text{LORENZ:} \quad \text{ADF}(\phi) = \exp\frac{1}{\phi^2 + \text{DISPERSION}^2} \quad 10-43$$

$$\text{LAMBERT:} \quad \text{ADF}(\phi) = \cos(\phi) \quad 10-44$$

$$\text{LORENZ:} \quad \text{ADF}(\phi) = \frac{\cos(\phi)}{\cos^2(\phi) + \left(\frac{0.5}{\text{SEMIMINOR}}\right)^2 \sin^2\phi} \quad 10-45$$

Here, the angles are in radians and the DISPERSION and SEMIMINOR parameters are specified on the INTERFACE statements.

You can also specify the ADFs in tabular form. You can assign the `ADF.TABLE` parameter to the file name of the file containing an ASCII description of the angular dependence of ADF. The first row of this table contains the number of samples. Subsequent rows contains two numbers. The first number is the angle in degrees from 0° to 90°, and the second number is the optional unnormalized value of the ADF at that angle.

To enable the diffusive transfer matrix model, specify `DIFFUSE` on the `BEAM` statement.

The ADFs are normalized in each case for evaluation of diffusive generation by photoabsorption as given in Equation 10-46.

$$G(y) = 2 \int_0^{\pi/2} P_o \text{ADF}(\phi) \alpha e^{\frac{-\alpha y}{\cos \phi}} d\phi \quad 10-46$$

Here:

α is the absorption coefficient.

P_o is the intensity at the interface (either I_{dT} or I_{dR}).

y is the distance from the interface.

To enable the model specify `DIFFUSIVE` on the `BEAM` statement and specify the diffusive characteristics of each interface as appropriate using `INTERFACE` statements.

The ADFs can be output by assigning the `OUTADF` parameter of the `INTERFACE` statement to the name of the output file. When you output the ADF, you should also specify the range of wavelengths and number of samples using the `LAM1`, `LAM2`, and `NLAM` parameters of the `INTERFACE` statement.

10.4: Beam Propagation Method in 2D

You can simulate most optoelectronic devices using ray tracing based on geometrical optic principles. But when diffraction or coherent effects are important, ray tracing methods are no longer sufficient. In this case, you need a method that takes into account the wave nature of light.

A method that does this is called the Beam Propagation Method (BPM). BPMs such as [237] rely on paraxial approximation. The BPM in LUMINOUS, however, has been extended to solve a more general Helmholtz Wave Equation (Equation 10-47).

$$\nabla^2 E(\vec{r}, t) - \frac{n^2}{c^2} \frac{\partial^2 E(\vec{r}, t)}{\partial t^2} = 0 \quad 10-47$$

Here, E is the electric field of an optical wave, n is the complex refractive index of the material, and c is the speed of light in vacuum.

The Helmholtz Wave Equation is consistent with the Rayleigh-Sommerfeld formulation of scalar diffraction theory [90]. It can also be derived from Maxwell's equations assuming homogeneous and isotropic media and neglecting non-linear effects.

These assumptions put certain restrictions on the applicability of BPM. For example, material regions with gradual change in refractive index or photodetector saturation modeling aren't supported.

10.4.1: Using BPM

The BPM in LUMINOUS isn't designed to completely replace the fast and robust ray tracing algorithm. In fact, we recommend you start the analysis of your particular application using the ray tracing method (see Sections 10.2.1: "Ray Tracing in 2D" to 10.2.3: "Reflection and Transmission").

Only use BPM when you think light diffraction or coherent effects are important. Here are the following guidelines when to use it:

- The source is monochromatic (no coherent effects are observed for multispectral sources).
- The application is 2D (currently, a 3D BPM isn't implemented due to calculation time considerations).
- Spatial distribution of irradiance or photogenerated carrier density is important.

Note: Carrier diffusion lengths should be considered.

- The structure isn't periodic in the X direction.

BPM should be useful for:

- Multilayer structures with layer thicknesses comparable to wavelength.
- Narrow incident beams (when transverse beam size is comparable to wavelength).

Currently, BPM doesn't support either user-specified reflection coefficient models (`F.REFLECT`) or photogeneration rate vs. position or time. The `SCAN.SPOT` parameter of `SOLVE` statement (see Chapter 21: "Statements", Section 21.53: "SOLVE") and anti-reflection coatings (see "Anti-Reflective (AR) Coatings for Ray Tracing and Matrix Method" on page 10-38) are also not included.

If you need to use BPM, include the `BPM` parameter in the `BEAM` statement (see Chapter 21: "Statements", Section 21.3: "BEAM"). `BEAM` parameters related specifically to ray tracing (such as `RAYTRACE`, `RAYS`, `THINEST`, `MAX.WINDOW`, and `MIN.WINDOW`) are ignored when BPM is specified.

Unlike ray tracing, the incident beam is specified on the top of the device. The origin of the beam is then assumed to be at the `X.ORIGIN` in the `BEAM` statement, where `Y.ORIGIN` parameter is ignored. This is done to avoid unnecessary beam propagation in the material surrounding the device.

You can specify additional parameters (`LONGIT.STEP` and `TRANSV.STEP`) in the `BEAM` statement to set respective step sizes for the internal BPM grid. If you don't define these step sizes, the default values are used. The default step size in both directions is equal to $\lambda/16.0$, where λ is the wavelength of light in vacuum. Don't use step sizes larger than $\lambda/2.0$, especially if coherent effects are of interest. Also, we don't recommend extremely small step sizes because it can result in unnecessarily long computation times. The default values are adequate for most cases.

10.4.2: Light Propagation In A Multiple Region Device

Since Equation 10-47 doesn't describe light propagation through the region's boundary, each region has to be considered separately. Each region's boundary is composed of straight line segments (edges) that form a polygon. Light propagating from one of the segments could be reflected back into the region from other segments of the boundary, while transmitted light enters other regions. Reflected and transmitted optical fields are calculated using Fresnel formulae described in Equations 10-1 to 10-6 in Section 10.2.3: "Reflection and Transmission".

Once the field reflected from a certain boundary is known, it then propagates back into the region. The light then reaches all edges of the polygon. At this point, the field incident upon each boundary is saved (i.e., added to the total field incident on each boundary). Once all polygon edges are addressed like this, the algorithm then proceeds to the next region.

When the pass through the device is complete, one reflection of light on each boundary has been accounted. The `REFLECTS` parameter specifies the number of passes to be done.

Like in ray tracing, if the `REFLECTS` parameter is large (e.g., 10), the optical part of the simulation might take considerable amount of time. To limit the number of propagation routines, use the `MIN.POWER` parameter. But unlike in ray tracing, where the default value of this parameter is zero, the default is `MIN.POWER=1e-6`. This limit helps avoid unnecessary computations.

Since only propagation through convex polygons can be properly addressed, concave polygons are automatically split to form two convex regions. If necessary, air polygons are added at the top of the device structure to fill the empty regions, where the propagation of light also needs to be considered.

10.4.3: Fast Fourier Transform (FFT) Based Beam Propagation Algorithm

Field propagation from a boundary segment through a region is considered in the coordinate system of that segment. The `X` axis is along the boundary and `Z` axis is along the normal (i.e., the `Z` axis corresponds to the usual `ATLAS Y` axis, see Figure 10-9).

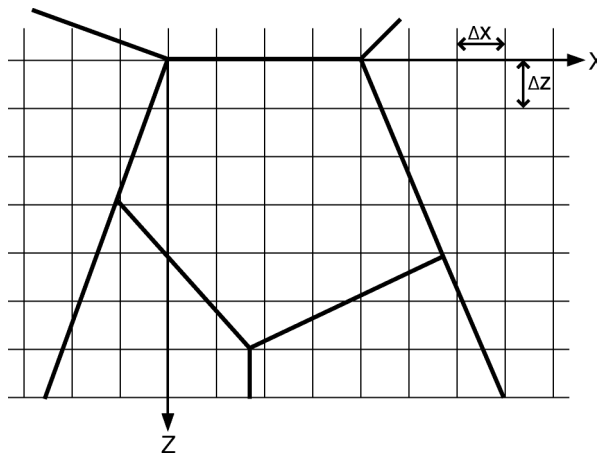


Figure 10-9: Internal Coordinate System

We assume the optical field and the device structure are uniform in the Y direction (perpendicular to the plane of the Figure 10-9). The rectangular grid covering the whole region is chosen according to the step sizes defined by LONGIT.STEP (ΔZ) and TRANSV.STEP (ΔX) parameters. The Helmholtz Equation in a 2D cartesian coordinate system (see Equation 10-48) describes field propagation through the region.

$$\frac{\partial^2 E(x, z)}{\partial z^2} + \frac{\partial^2 E(x, z)}{\partial x^2} + k^2 E(x, z) = 0 \quad 10-48$$

Provided that the field on the input plane $Z=0$ is known, Equation 10-48 allows you to find the field on any subsequent plane $Z=\Delta Z$. The numerical solution of Equation 10-48 is based on the transformation of input complex field into superposition of plane waves. This superposition represents the direction cosine spectrum of plane waves, which is obtained by the FFT of the original field (see Equation 10-49).

$$F(k_x, z=0) = \int_{-\infty}^{\infty} E(x, z=0) \exp(-ik_x X) dx \quad 10-49$$

Each plane wave propagates at a certain angle to the Z axis. The phase accumulated by each plane wave component before reaching the plane $Z=\Delta Z$ is given by:

$$F(k_x, z=\Delta Z) = F(k_x, z=0) \exp\left(i\sqrt{k^2 - k_x^2} \Delta Z\right) \quad 10-50$$

where $K=2\pi n/\lambda$, n is the complex refractive index. We then can include diffraction and absorption upon propagation simultaneously. The direction cosine spectrum given by Equation 10-50 at $Z=\Delta Z$ is transformed back into the spatial domain by applying an inverse FFT.

$$E(x, z=\Delta Z) = \frac{1}{2\pi} \int_{-\infty}^{\infty} F(k_x, Z=\Delta Z) \exp(ik_x X) dk_x \quad 10-51$$

The field distribution at $Z=\Delta Z$ is then found.

These steps are repeated until the field in the whole region is found. The field incident on each boundary segment and the field at each node within the region are obtained using bi-linear interpolation.

When the propagation through the same region is considered, the resulting field values at each node are added to the values saved upon the previous propagation. Since the phase information is retained in our propagation scheme, adding the field ensures the coherent effects are taken into account.

The numerical scheme to solve Equation 10-48 requires the rectangular grid in the transverse direction (X) to cover an area significantly larger than the region of interest.

Zero-padding of the input field distribution is done automatically to specify the input field on the grid. Super-gaussian filters are used in the spatial domain to suppress possible reflections from numerical boundary.

Evanescent waves are included in the propagation scheme to avoid discontinuities in the spectral domain [90].

10.5: Finite Difference Time Domain Analysis [269]

The finite-difference time-domain (FDTD) method can be used to model optical interactions between a directed optical source and a semiconductor device in much the same way as in geometric ray tracing. The difference is that the FDTD solves for the electric and magnetic field propagation directly from the fundamental wave equations. The FDTD approach correctly models the wave propagation with reflection, diffraction, and interference effects at relatively high computational expense.

Note: It is important to remember that in these applications, the carrier diffusion lengths are usually much greater than the wavelength of the light stimulus. Therefore, ray tracing is usually an adequate description. But in certain applications, the physical scale of details of the semiconductor device are too small for ray tracing to describe the optical interaction. One such case would be a nonplanar antireflective structure. In such cases, you should consider the FDTD approach.

10.5.1: Physical Model

Maxwell's equations of light propagation are given by:

$$\frac{\partial H}{\partial t} = \frac{-1}{\mu} \nabla \times E - \frac{1}{\mu} (M_{source} + \sigma^* H) \quad 10-52$$

$$\frac{\partial E}{\partial t} = \frac{-1}{\varepsilon} \nabla \times H - \frac{1}{\varepsilon} (J_{source} + \sigma E) \quad 10-53$$

Here, E is the electric field, H is the magnetic field, ε is the permittivity, μ is the permeability, M_{source} is the equivalent magnetic current density, J_{source} is the electric current density, σ is the electric conductivity, and σ^* is the equivalent magnetic loss.

In two dimensions Equations 10-52 and 10-53 can be rewritten for transverse electric (TE) polarization as:

$$H_x = H_y = E_z = 0 \quad 10-54$$

$$\frac{\partial H_z}{\partial t} = \frac{1}{\mu} \left[\frac{\partial E_x}{\partial y} - \frac{\partial E_y}{\partial x} - (M_s + \sigma^* H_z) \right] \quad 10-55$$

$$\frac{\partial E_x}{\partial t} = \frac{1}{\varepsilon} \left[\frac{\partial H_z}{\partial y} - (J_s + \sigma E_x) \right] \quad 10-56$$

$$\frac{\partial E_y}{\partial t} = \frac{1}{\varepsilon} \left[\frac{\partial H_z}{\partial x} - (J_s + \sigma E_y) \right] \quad 10-57$$

For transverse magnetic (TM), Equations 10-52 and 10-53 can be written as:

$$E_x = E_y = H_z = 0 \quad 10-58$$

$$\frac{\partial H_x}{\partial t} = \frac{1}{\mu} \left[\frac{\partial E_z}{\partial y} - (M_s + \sigma^* H_x) \right] \quad 10-59$$

$$\frac{\partial H_y}{\partial t} = \frac{1}{\mu} \left[\frac{\partial E_z}{\partial x} - (M_s + \sigma^* H_y) \right] \quad 10-60$$

$$\frac{\partial E_z}{\partial t} = \frac{1}{\varepsilon} \left[\frac{\partial H_y}{\partial x} - \frac{\partial H_x}{\partial y} - (J_s + \sigma E_z) \right] \quad 10-61$$

For three dimensions, Equations 10-52 and 10-53 can be written as:

$$\frac{\partial E_x}{\partial t} = \frac{1}{\varepsilon} \left[\frac{\partial H_z}{\partial y} - \frac{\partial H_y}{\partial z} - \sigma E_x \right] \quad 10-62$$

$$\frac{\partial E_y}{\partial t} = \frac{1}{\varepsilon} \left[\frac{\partial H_x}{\partial z} - \frac{\partial H_z}{\partial x} - \sigma E_y \right] \quad 10-63$$

$$\frac{\partial E_z}{\partial t} = \frac{1}{\varepsilon} \left[\frac{\partial H_y}{\partial x} - \frac{\partial H_x}{\partial y} - \sigma E_z \right] \quad 10-64$$

$$\frac{\partial H_x}{\partial t} = \frac{1}{\mu} \left[\frac{\partial E_y}{\partial z} - \frac{\partial E_z}{\partial y} - \sigma^* H_x \right] \quad 10-65$$

$$\frac{\partial H_y}{\partial t} = \frac{1}{\mu} \left[\frac{\partial E_z}{\partial x} - \frac{\partial E_x}{\partial z} - \sigma^* H_y \right] \quad 10-66$$

$$\frac{\partial H_z}{\partial t} = \frac{1}{\mu} \left[\frac{\partial E_x}{\partial y} - \frac{\partial E_y}{\partial x} - \sigma^* H_z \right] \quad 10-67$$

You can specify the parameters of these equations as described in Table 10-3.

| Table 10-3. User Specifiable FDTD Material Parameters | | | |
|---|--------------|---------|--------------------|
| Statement | Parameter | Default | Units |
| MATERIAL | MAG. LOSS | 0.0 | mho/cm |
| MATERIAL | E. CONDUCT | 0.0 | Ω/cm |
| MATERIAL | PERMITTIVITY | 1.0 | |
| MATERIAL | PERMEABILITY | 1.0 | |
| MATERIAL | J. ELECT | 0.0 | A/cm ² |
| MATERIAL | J. MAGNET | 0.0 | V/cm ² |

Rather than using the parameters listed in Table 10-3, it is usually more convenient to use the complex index of refraction. The implementation of FDTD allows you to use the complex index of refraction exactly as it is used in ray tracing and the appropriate conversions to the parameters of Table 10-3 are done automatically.

In FDTD analysis, Equations 10-54 through 10-61 are solved using a finite-difference approximation in space and finite-difference in time with suitable boundary conditions to obtain static predictions of optical intensity and photogeneration rate as a function of optical source.

10.5.2: Beam and Mesh

To initiate FDTD analysis in LUMINOUS2D and LUMINOUS3D, you should specify FDTD on the BEAM statement. The X.ORIGIN, Y.ORIGIN, Z.ORIGIN, ANGLE, X.MIN, Y.MIN, Z.MIN, and Z.MAX of the BEAM statement are defined for FDTD exactly as for ray tracing (see Figure 10-1). In FDTD, an auxiliary mesh is set up to solve the electro-magnetic equations (see Equations 10-54 through 10-61). The FDTD mesh, as we will refer to it, is defined in the primed coordinate system (x' , y' , z') as shown in Figure 10-1. We will refer to the primed coordinate system as the FDTD coordinate system. The FDTD mesh is a tensor product (rectangular) mesh that is not necessarily uniform in the x' , y' , and z' directions.

Note: For the remainder of this section, we will refer to the FDTD coordinate system using the unprimed x , y , and z .

There are several ways of specifying the FDTD mesh. You can specify the FDTD mesh using the mesh line statements: FDX.MESH and FDY.MESH. These statements are similar to the X.MESH, Y.MESH, and Z.MESH statements and allow you to specify location and spacing using the LOCATION and SPACING parameters. When using FDX.MESH, FDY.MESH, and FDZ.MESH, the locations and spacings are relative to the FDTD mesh and are specified in microns. This method offers the advantage of non-uniform meshing and allows for local mesh refinement. In this approach, all FDX.MESH, FDY.MESH, and FDZ.MESH lines must be stated before the associated BEAM statement.

You may specify a uniform mesh using the SX, SY, and SZ, or SPACING parameters of the BEAM statement. The limits of the FDTD mesh are chosen by the minimum and maximum device coordinates relative to the FDTD coordinate system or XMIN, XMAX, ZMIN, and ZMAX parameters (if specified) depending on coordinate clipping. The actual spacings in x and y will be adjusted to fit an integer number of uniform mesh lines within the FDTD mesh domain.

You can also define a rectangular uniform mesh in x , y , and z by specifying the desired number of mesh lines in the x' , y' , and z' directions using the NX, NY, and NZ parameters on the BEAM statement. TM polarization is the default.

You can specify the polarization of the beam by using the POLARIZATION parameter on the BEAM statement (POLARIZATION=0.0 implies TE polarization, POLARIZATION not equal to 0.0 implies TM polarization). Conversely, you can specify TM or TE directly on the BEAM statement.

To initiate FDTD analysis, specify the FDTD parameter on the BEAM statement.

10.5.3: Boundary Conditions [224]

As mentioned previously, Equations 10-54 through 10-61 are solved in a 2D rectangular domain. You must specify boundary conditions to complete the problem description. In LUMINOUS2D and LUMINOUS3D, FDTD has 3 types of boundary conditions: Perfect Electrical Conductor (PEC) boundaries, Perfectly Matched Layer (PML) boundaries, and source boundaries (plane and point)

Perfect Electrical Conductor (PEC) Boundary

Currently, all boundaries other than the source boundary are by default perfect electrical conductor (PEC) boundary conditions. This implies that field values vanish at the boundaries and incident waves are completely reflected. This is convenient when simulating periodic problems, however, it may present difficulties when simulating non-periodic domains. In such cases, the perfectly matched layer boundary is preferred.

Perfectly Matched Layer (PML) Boundary [27]

The perfectly matched layer boundary is used to absorb outgoing light. This is useful when we want to simulate an unbounded domain. In other words, we try to absorb (rather than reflect) all outward bound waves. There are several main concepts for PMLs you should know.

- PMLs are not really boundary conditions in the conventional sense. These boundary conditions have a thickness associated with them and are included in the mesh. We hope to select the absorption coefficient of the layer to allow absorption of the outgoing light to a specified minimum.
- A PMLs is terminated by a PEC. Thus, all light passing through the PML, after accounting for absorption, is reflected back into the simulation domain after making two trips through the PML.
- PMLs are designed to be impedance matched to the simulation domain so that there is no reflection at the interface between the PML and the simulation domain.
- PMLs absorb only in one direction x or y depending on their location. Therefore, light propagating parallel to a PML is not affected by the PML.

The absorption coefficient normal to the PML is specified by Equation 10-68.

$$\alpha(x) = \text{ALPHA} \left| \frac{x - x_0}{\text{WIDTH}} \right|^{\text{DEGREE}} \quad 10-68$$

Here, x_0 is the coordinate of the interface between the PML and the simulation domain, and $x - x_0$ represents the depth into the PML. The ALPHA parameter is user-definable on the PML statement and specifies the maximum absorption coefficient in the layer. The WIDTH parameter specifies the width of the layer

Note: The PML is added to the simulation domain. WIDTH should be chosen appropriate to the relative dimensions of the simulation domain.

The DEGREE parameter allows absorption to be increased with the depth into the PML. Theoretically, DEGREE=0 should produce no reflection at the interface between the PML and the simulation domain. In practice, however, it is found that such abrupt transitions produce reflections due to discretization. Experience has shown that a value of 2 or more for DEGREE produces a smooth reflectionless interface.

Table 10-4 shows the default values for the PML statement.

| Table 10-4. PML Definition Parameters | | | |
|---------------------------------------|-----------|---------|-------|
| Statement | Parameter | Default | Units |
| PML | ALL | False | |
| PML | ALPHA | 0.0 | 1/cm |
| PML | BACK | False | |
| PML | BEAM | (all) | |
| PML | BOTTOM | True | |
| PML | DEGREE | 2 | |
| PML | FRONT | False | |

Table 10-4. PML Definition Parameters

| | | | |
|-----|--------------|-------|---------|
| PML | LEFT | False | |
| PML | NSAMP | 10 | |
| PML | PERMEABILITY | 1.0 | |
| PML | PERMITTIVITY | 1.0 | |
| PML | R90 | 0.0 | |
| PML | SIGMAX | 0.0 | mho/cm |
| PML | TOP | False | |
| PML | RIGHT | False | |
| PML | WIDTH | 0.0 | microns |
| PML | XDIR | False | |
| PML | YDIR | False | |

As mentioned, the PML is terminated by a PEC. Therefore, the reflection coefficient can be calculated by Equation 10-69.

$$R(\Theta) = \exp\left(\frac{2 - \text{ALPHA} \cdot \text{WIDTH} \cos \Theta}{\text{DEGREE} + 1}\right) \quad 10-69$$

Here, $R(\Theta)$ is the reflection coefficient of the PML as a function of Θ , the angle of incidence. For convenience, you can specify the reflection coefficient at normal incidence using the R90 parameter of the PML statement. Given a selected value of DEGREE, LUMINOUS2D calculates the value of one of R90, WIDTH, and ALPHA if the remaining two parameters are specified.

The placement of PMLs using the PML statement is described in Figure 10-10.

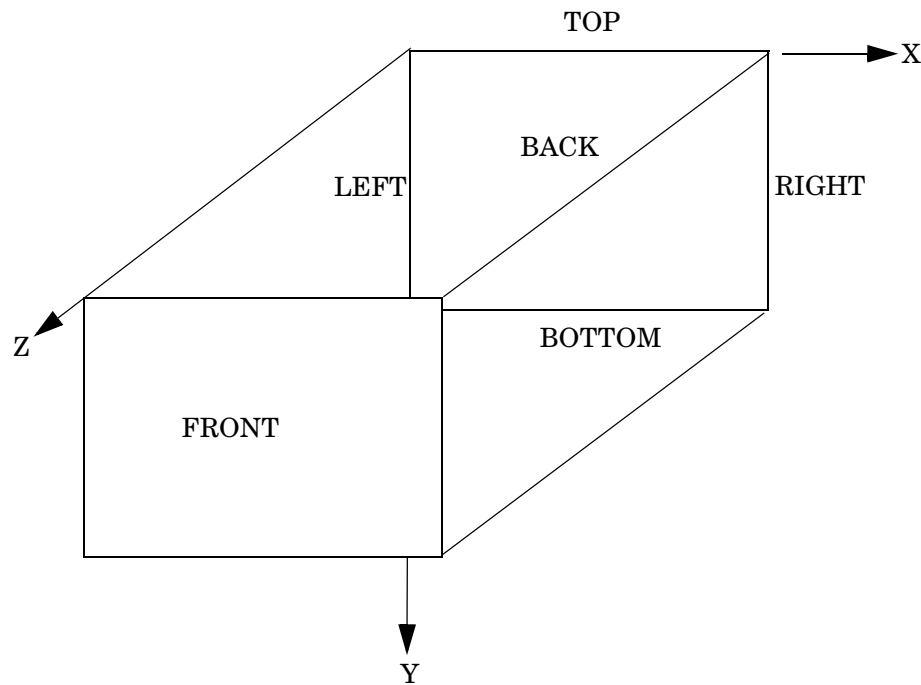


Figure 10-10: PML Placement

The **ALL** parameter specifies that the PML will apply to **TOP**, **BOTTOM**, **RIGHT**, **LEFT**, **FRONT**, and **BACK**.

You must also specify the number of grid points used to resolve the PML with the **NSAMP** parameter of the **PML** statement. As usual, the number of grid points used to represent the PML directly impacts computation time.

You can use the **BEAM** parameter of the **PML** statement to associate the PML with a previously defined optical source by beam number. This means that the **BEAM** statement must precede any associated **PML** statements. If the **BEAM** parameter is not specified, the PML will apply to all previously defined **BEAMs**.

Plane Source Boundary

The planar sources in **LUMINOUS FDTD** use the transmitted field scattered field (TFSF) formulation. In this formulation, fields scattered from the target in the direction of the source are allowed to pass through the source. This enables absorbing boundaries, such as PMLs, behind the source to absorb the scattered fields. Thus, preventing them from further interaction with the target. This is important to avoid secondary interactions with re-scattered fields reflecting from the source that might occur if only a PEC boundary (default) is used. Therefore, it is strongly recommended that you always define a PML on the same edge as a plane source to avoid difficult to interpret results, such as "available photocurrents" exceeding the "source photocurrent".

By default, the source boundary is located along the **X** axis (see Figure 10-1). The source is simulated as a plane sinusoidal wave. Since the source originates at one of the edges of the simulation domain, the source is a **TE** wave if **TE** is specified on the **BEAM** statement and **TM** otherwise.

You can define the stimulus as a cosine or a sine wave by specifying **COSINE** or **SINE** on the **BEAM** statement. In addition, you can specify an offset phase angle on the **PHASE** parameter of the **BEAM** statement.

Outside of the context of the beam propagation from the FDTD coordinate system origin in the positive **Y** direction, the plane wave may originate from any edge of the FDTD domain. The origin of the plane source is located using the **S.TOP**, **S.BOTTOM**, **S.LEFT**, **S.RIGHT**, **S.FRONT**, and **S.BACK** parameters of the **BEAM** statement.

By default, the `S.TOP` is true and the beam propagates in the same direction as for ray tracing. The alternate origins are not suggested for general usage but may be useful for optimizing PML boundaries.

Point Source Boundary

Another convenience that is usually not suggested for general usage is a point source. To enable a point source, specify `POINT` on the `BEAM` statement.

The location of the point source is defined by the `X.POINT`, `Y.POINT`, and `Z.POINT` parameters of the `BEAM` statement relative to the X, Y coordinate system in units of microns.

10.5.4: Static Solutions and Error Estimation

The FDTD method is frequently used to analyze problems that are inherently transient. In the context of `LUMINOUS2D` and `LUMINOUS3D` the problems are usually static.

To approximate static solutions, we allow the optical source to propagate from a static source until all transients are settled out. To help automate the detection of this "steady-state", the error estimator given by equation 10-71 is defined.

$$Error = \sqrt{\frac{\sum_{in} \left(\frac{E_x'' - E_x' + E_y'' - E_y' + E_z'' - E_z'}{n_x n_y n_z} \right)^2}{\frac{E_x' + E_x' + E_z'}{n_x n_y n_z}}} \quad 10-70$$

Here, E_x' , E_y' , and E_z' represent the field envelope over the last full cycle of the source. E_x'' , E_y'' , and E_z'' represent the field envelope over the previous full cycle. If you specify the parameter `TD.ERRMAX` on the `BEAM` statement, you can use this parameter to terminate the time domain simulation when "steady-state" is achieved.

Run-Time Output

To enable the run-time output, specify the `VERBOSE` parameter on either the `BEAM` or the `OPTIONS` statements. The output first prints out the coordinates of the FDTD mesh and a mesh summary. Next, the run-time output prints out the specified time step, the time step limit for Courant-Friedrich-Levy stability, the time corresponding to the reciprocal of the optical frequency, and the transition time for the minimum space step. Then, the run-time output contains a summary of the optical constants for each region. Region 0 is outside the device mesh domain. This table includes regions corresponding to electrodes.

Finally, the run-time output contains iteration values. The first column is the iteration number. The second is the simulation time in seconds. The third is the number of wavelengths of the source. The fourth is the percent of the current wavelength. The fifth is the current error estimate, and the last is the estimated time to complete (if `TD.LIMIT` is specified).

Time Domain Output

Output structure file "snapshots" can be saved by assigning a root file name to the `TD.FILE` parameter of the `BEAM` statement. This specifies that outfiles will be written periodically with incremented names to a file with the specified root name. These files can be examined by `TONYPLOT` to view the field distributions as a function of time. `TD.MANY` specifies how many file names will be used in total before files are written over. `TD.EVERY` specifies how many time domain solutions are calculated between each output file.

Typically, the FDTD mesh is much larger/denser than the typical ATLAS device simulation mesh. This implies that saving the "snapshots" and loading them into `TONYPLOT` can be lengthy. To improve the efficiency of visualization, you can subsample the domain on output. To do this, specify the parameters `SUBNX`, `SUBNY`, and `SUBNZ` or `SUBDX`, `SUBDY`, and `SUBDZ` on the `BEAM` statement. The parameters `SUBNX`, `SUBNY`, and `SUBNZ` specify the numbers of evenly spaced samples output in the X, Y, and Z directions. You can use the parameters `SUBDX`, `SUBDY`, and `SUBDZ` to specify the sample spacing in X, Y, and Z.

Photogeneration

Once "steady-state" is achieved, the FDTD simulation is stopped and the resultant intensities are exported (interpolated) back onto the device simulation mesh. These intensities are used to calculate photogeneration rates used directly in the drift-diffusion equations exactly as it is done in ray tracing. The photogeneration rate is given by:

$$G = \frac{\lambda}{hc} \alpha \frac{|E|^2}{2\eta} \quad 10-71$$

Energy Dissipation and Interference

To close the discussion of FDTD, we will mention a couple of things about energy dissipation and interference effects.

Suppose we illuminate a layer 1 micron thick with a TE sine wave of wavelength 1 micron. Further assume the wave propagates from the left of the layer against a PEC at the right of the layer. Figure 10-11 shows the resultant envelope of the light intensity after 1, 2, 3 and 4 wavelengths. The effects of the coherent reflection should be obvious. It is also notable, however, that the peak of the envelope increases as the square of the number of wavelengths. This is because there is no power dissipation in the system. The wave amplitude increases as the number of wavelengths and the power increases as the square of the amplitude. This illustrates an important consideration in FDTD analysis. That is that if projected waves are not completely absorbed by the test structure and the PML boundary conditions, the envelope of intensity increases with time. This has an important impact on the error estimation. The error estimate that is proportional to the change in intensity envelope divided by the value of the intensity envelope will be bounded by the square of the simulation time.

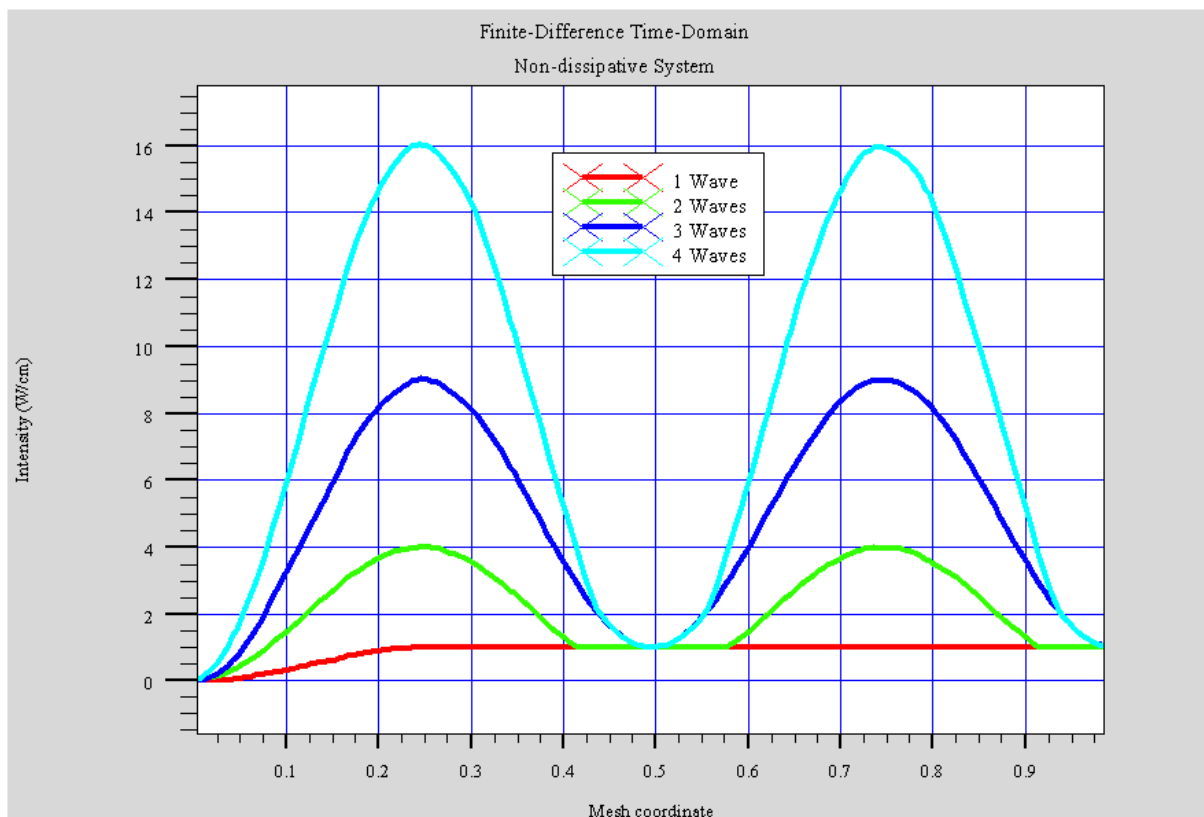


Figure 10-11: Finite-Difference Time Domain Non-Dissipative System

Another interesting aspect of Figure 10-11 is that the minimum of the envelope is not at 0 as expected for such interference but 1. This is because the initial wave does not experience interference and thus contributes a unit offset to the minimum.

10.6: User-Defined Photogeneration

10.6.1: User-Defined Beams

Standard beam input syntax in LUMINOUS and LUMINOUS3D allows specification of plane waves with Gaussian or flat-top (top-hat) irradiance profiles. Although many practical applications require only plane wave illumination, some optoelectronic devices rely on certain focusing or collimating optical systems that collect incident light. Some of these optical systems are implemented as lens arrays deposited on top of the device structure, which can be directly included in LUMINOUS3D. Still, a number of applications that require complex collimating or focusing optics cannot be approached in this way. To accommodate these applications, we enabled input of incident beams with complex wavefronts. Currently, the ray-tracing is not restricted to particular beam properties and allows specification of an arbitrary collection of rays as an input beam.

Theoretically, a number of ways to specify a beam of arbitrary shape exists. The one chosen in ATLAS aims to allow you an easy interface with optical system design software. Thus, collimators or focusing optics designed with conventional optical system tools can be represented in ATLAS by a ray bundle obtained on the output of the optics tool. ATLAS treats the ray bundle specified in a file as one beam. You need to set the input file name on the BEAM statement as a value of INPUTRAYS parameter.

The file INPUTRAYS must have the following format.

```
NUMBER OF RAYS
NUMBER OF CHANGING PARAMETERS
PARAMETER1 PARAMETER2 PARAMETER3 ...
RAY NUMBER      PARAMETER1 VALUE      PARAMETER2 VALUE      PARAMETER3 VALUE ...
RAY NUMBER      PARAMETER1 VALUE      PARAMETER2 VALUE      PARAMETER3 VALUE ...
...
RAY NUMBER      ...                    ...                    ...
```

NUMBER OF RAYS stands for the total number of rays specified in the file. It should be the same as the last RAY NUMBER in the table.

NUMBER OF CHANGING PARAMETERS gives the total number of ray parameters given in the table. Most often, some parameters are the same for all the rays. For example, wavelength or ray power can be the same. In this case, there is no need to keep the table column for this constant parameter. Instead, you can set this parameter directly in the BEAM statement. NUMBER OF CHANGING PARAMETERS is equal to the number of columns in the table (not counting the first column of ray numbers).

PARAMETER1, PARAMETER2, PARAMETER3, and so on are numerical codes of parameters. Their order specifies the order of columns in the table. Numerical codes correspond to the following parameters.

- 1 - X coordinate of ray origin (in device coordinate system).
- 2 - Y coordinate of ray origin (in device coordinate system).
- 3 - Z coordinate of ray origin (in device coordinate system).
- 4 - ray angle phi in XY plane (0 - along X and 90 - along Y).
- 5 - ray angle theta in XZ plane (in 3D only, 0 - along X and 90 - along Z).
- 6 - ray polarization angle (relative to the plane of incidence, 0 - TE, and 90 - TM).
- 7 - ray relative power.
- 8 - ray wavelength.
- 9 - ray area (μm^2 in 3D) or thickness (μm in 2D).

The first column of the table where ray parameters are specified lists ray numbers (integer values) in ascending order. The first ray number should be 1. The last ray number should be equal to the NUMBER OF RAYS. Often, it is the case that ray parameters change continuously from ray to ray (at least in parts of the table). The INPUTRAYS file in ATLAS allows a shorthand input for these parts. You can omit ray numbers where possible to allow for automatic fitting of parameter values for these rays.

Linear approximation is used for the omitted rays based on the values of parameters given in the table. This is better illustrated in the following example.

```

21
3
1 4 7
1 0.0 60.0 0.2
11 300.0 90.0 1.0
21 600.0 120.0 0.2

```

Here, NUMBER OF RAYS=21, NUMBER OF PARAMETERS=3, and the order of parameter columns: X coordinate (1), angle phi (4), and relative ray power (7).

The rays from 2 to 10 are specified using linear interpolation with end values given by rays 1 and 11. The rays from 12 to 20 are also defined similarly. This shorthand input is equivalent to the following.

```

21
3
1 4 7
1 0.0 60.0 0.2
2 30.0 63.0 0.28
3 60.0 66.0 0.36
4 90.0 69.0 0.44
5 120.0 72.0 0.52
6 150.0 75.0 0.6
7 180.0 78.0 0.68
8 210.0 81.0 0.76
9 240.0 84.0 0.84
10 270.0 87.0 0.92
11 300.0 90.0 1.0
12 330.0 93.0 0.92
13 360.0 96.0 0.84
14 390.0 99.0 0.76
15 420.0 102.0 0.68
16 450.0 105.0 0.6
17 480.0 108.0 0.52
18 510.0 111.0 0.44
19 540.0 114.0 0.36
20 570.0 117.0 0.28
21 600.0 120.0 0.2

```

When you use the INPUTRAYS file to define the beam, some of the parameters on the BEAM statements are disabled because they become incompatible with the user-defined beam. The parameters that are ignored in this case are CIRCULAR, ELLIPTICAL, GAUSSIAN, all LENS.* parameters, MAX.WINDOW, MIN.WINDOW, MEAN, RAYS, SIGMA, X.CENTER, X.GAUSSIAN, X.MEAN, X.RADIUS, X.SIGMA, X.SEMIAxis, XMAX, XMIN, Y.SEMIAxis, Z.CENTER, Z.GAUSSIAN, Z.MEAN, Z.RADIUS, Z.SIGMA, Z.SEMIAxis, ZMAX, and ZMIN.

The X.ORIGIN, Y.ORIGIN, Z.ORIGIN, PHI, THETA, POLARIZE, REL.POWER, WAVELENGTH, RAYAREA parameters in the BEAM statement specify values for all rays if the corresponding parameters are not defined explicitly in the INPUTRAYS file. The parameters Z.ORIGIN and THETA and the corresponding parameters in INPUTRAYS are for LUMINOUS3D applications only. They are ignored in LUMINOUS2D.

RAYAREA is a parameter that specifies area in μm^2 (thickness in 2D in μm) of each ray in the BEAM statement. This parameter is used when the specified INPUTRAYS file does not contain ray area information.

One difficulty that arises when dealing with arbitrary beams has to do with specification of beam intensity (W/cm^2) in the `SOLVE` statement. For a general ray bundle, illuminating the device the intensity distribution is not uniform. Thus, intensity cannot be specified by a single number. There are two ways to avoid this problem. Instead of setting intensity for a ray bundle obtained on the output of an optical system (collimator or focusing system), you can go back to the original beam that produced this ray bundle. According to the intensity law of geometrical optics [31], you can define ray area (thickness) and overall beam intensity for that input beam. Alternatively, if power (W) carried by each ray is known, you can treat beam intensity parameter `B<n>` in the `SOLVE` statement as a scaling factor. Then, set all ray power values using the ray relative power parameter in the `INPUTRAYS` file (or `REL.POWER` on the `BEAM` statement if it is the same for all rays). In this case, you can treat `RAYAREA` as another scaling parameter for unit conversions. In any case, make sure you define the ray area because it's important for obtaining correct values of photogeneration rates. If you don't specify ray area, ATLAS uses an estimate based of coordinate values of ray origins. You should not rely, however, on the accuracy of such an estimate.

You can use `INPUTRAYS` with `POWER.FILE` to define multi-spectral complex beams. In this case, ATLAS ignores ray wavelength specified in `INPUTRAYS` and uses the wavelength values from `POWER.FILE` for each ray. Ray power is then a product of relative ray power from `INPUTRAYS` and spectral power density defined in `POWER.FILE`.

10.6.2: User-Defined Arbitrary Photogeneration

An option exists for you to define the photogeneration rate. A `C-INTERPRETER` function written into a text file can be supplied to the program using the `F.RADIATE` parameter of the `BEAM` statement. For example, if a file, `myoptics.c`, was developed using the template `C-INTERPRETER` functions supplied, it can be referenced by using:

```
BEAM NUM=1 F.RADIATE=myoptics.c
.
.
SOLVE B1=1.0
SOLVE B1=2.0
```

The file, `myoptics.c`, returns a time and position dependent photogeneration rate to the program. This returned value is multiplied at every node point by the value of `B1`. With this option, you override all other parameters of the `BEAM` statement and all the material refractive indices.

10.6.3: Exponential Photogeneration

Another option is available if distribution of photo-injected carriers is uniform, linear, or has an exponential dependence on depth. Use the PHOTOGENERATE statement to specify the desired dependence on depth along a line segment.

The X.ORIGIN, Y.ORIGIN and X.END, Y.END parameters set the coordinates of the beginning and the end of the line segment. The default values correspond to the top left and bottom left corners of the device. Other parameters CONSTANT, EXPONENT, FACTOR, LINEAR, and RADIAL specify the photogeneration rate according to the following formula:

$$G(l, r) = (\text{CONSTANT} + \text{LINEAR} \cdot l + \text{FACTOR} \exp(-\text{EXPONENT} \cdot l)) \exp\left(-\left(\frac{r^2}{\text{RADIAL}^2}\right)\right) \quad 10-72$$

where l is the distance along the line segment from the origin point and r is the radial distance from the line segment (Figure 10-12). PHOTOGENERATE statement ensures TMA compatibility with PHOTOGEN statement. See Chapter 21: “Statements”, Section 21.41: “PHOTOGENERATE” for the list of TMA compatible parameter names.

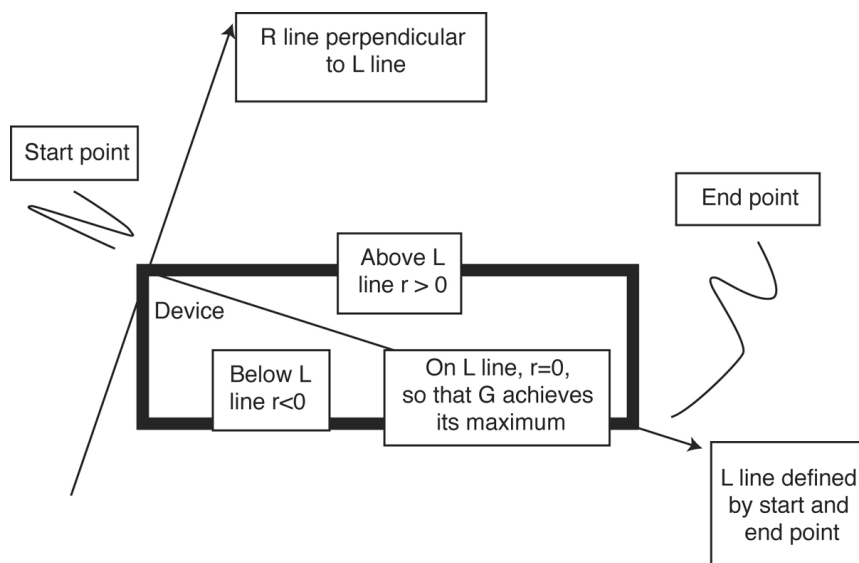


Figure 10-12: Specification of the Photogeneration Rate

10.6.4: Tabular Photogeneration (Luminous2D only)

You may also specify the photogeneration rate as a function of location through a simple tabular interface. This is often useful to importing data from some other generic optical propagation tool. The values of photogeneration rate are contained in a file. You specify the file name on the `FILE.PHOTOGEN` parameter of the `BEAM` statement.

The file contains ASCII values of the photogeneration rate in units of per second per cubic cm. These samples are made on a regular mesh in X and Y rastered in increasing values of X and then Y (i.e., row - column order). The values are space separated in X (along each row) and separated by carriage returns in Y (between rows along each column).

The spacings in X and Y in microns are specified in the `DX.PHOTOGEN` and `DY.PHOTOGEN` parameters of the `BEAM` statement. You can specify the origin of the photogeneration in microns using the `X0.PHOTOGEN` and `Y0.PHOTOGEN` parameters of the `BEAM` statement. If you do not specify `X0.PHOTOGEN` and `Y0.PHOTOGEN`, then the origin will be assumed to coincide with the minimum X and Y coordinates in the device structure.

For example, the `BEAM` statement might read:

```
BEAM X0.PHOTOGEN=0 Y0.PHOTOGEN=0 DX.PHOTOGEN=1 DY.PHOTOGEN=1 \  
      FILE.PHOTOGEN=generation.table
```

The contents of the file named "generation.table" might be simply:

```
1e22 1e22  
1e20 1e20
```

In this case, the photogeneration rate is uniform in the X direction range of X=0 to X=1 micron but varies linearly between 1e22 to 1e20 in the Y direction.

10.7: Photocurrent and Quantum Efficiency

One of the important figures of merit of a photodetector is quantum efficiency. Here, quantum efficiency is defined as the ratio of the number of carriers detected at a given photodetector electrode divided by the number of incident photons on the detector. Ideally, this ratio should be 1.0 in detectors without any positive feedback mechanisms, such as avalanche gain. LUMINOUS doesn't directly calculate quantum efficiency. It does, however, calculate two useful quantities printed to the run-time output and saved to the log file. These quantities are source photocurrent and available photocurrent, which can be viewed in TONYPLOT from log files produced by LUMINOUS.

Definition of Source Photocurrent

The source photocurrent for a monochromatic source is given in Equation 10-73. Here, B_n is the intensity of the beam number n , which is user-definable in the SOLVE statement. λ is the source wavelength specified by the WAVELENGTH parameter in the BEAM statement. \hbar is Planck's constant. c is the speed of light. W_t is the width of the beam including the effects of clipping (see Section 10.2.1: "Ray Tracing in 2D"). This can be considered as a measure of the rate of photons incident on the device expressed as a current density.

$$I_s = q \frac{B_n \lambda}{\hbar c} W_t \quad 10-73$$

Definition of Available Photocurrent

The available photocurrent for a monochromatic source is given by Equation 10-74. Here, all the terms in front of the summation have the same definitions as for the source photocurrent. The sum is taken over the number of rays traced, N_R . W_R is the width associated with the ray. The integral is taken over the length, Y_i , associated with the ray. P_i accounts for the attenuation before the start of the ray due to non-unity transmission coefficients and absorption prior to the ray start. α_i is the absorption coefficient in the material that the ray is traversing.

The available photocurrent can be thought of as a measure of the photo absorption rate in the device expressed as a current density. This should be similar but somewhat less than the source photocurrent. The losses are due to reflection and transmission of light out of the device structure.

$$I_A = q \frac{B_n \lambda}{\hbar c} \sum_{i=1}^{N_R} W_R \int_0^{Y_i} P_i \alpha_i e^{-\alpha_i y} dy \quad 10-74$$

Depending how you define it, you can calculate quantum efficiency by dividing the current from one of the device electrodes by either the source photocurrent or the available photocurrent.

10.8: Defining Optical Properties of Materials

For ray tracing, the complex index of refraction of the various material regions in the structure must be specified. For many of the more common semiconductors and insulators, there are built-in tables of index versus wavelength. You can specify the index for the materials lacking reasonable default complex index of refraction.

Note: You can add the `INDEX.CHECK` parameter to any `SOLVE` statement to print out the refractive indices being used for that bias step. The indices are only printed when you perform the ray trace at the first reference to a given beam on the `SOLVE` statement.

10.8.1: Setting Single Values For The Refractive Index

The `REAL.INDEX` and `IMAG.INDEX` parameters of the `MATERIAL` statement can be used to set the real and imaginary indices of a specified material, region or regions. For example, the statement:

```
MATERIAL MATERIAL=Air REAL.INDEX=1.0 IMAG.INDEX=0.0
```

would set the index for all material regions composed of "Air"

The statement:

```
MATERIAL REGION=1 REAL.INDEX=1.0 IMAG.INDEX=0.0
```

would set the index for region number 1.

The statement:

```
MATERIAL REAL.INDEX=1.0 IMAG.INDEX=0.0
```

would set the index for all regions.

10.8.2: Setting A Wavelength Dependent Refractive Index

The preceding examples set the complex index of refraction for a material regardless of wavelength. This is probably adequate for monochromatic sources. For multispectral simulations, the index of refraction should be modeled as having a dependence on wavelength. There are two ways to do this.

ASCII File Input

The first way is to specify index versus wavelength in a file. This is a text file that contains ordered triplets of wavelength, real index, and imaginary index. The first entry in the table is the number of samples. If you set the `INDEX.FILE` parameter of the `MATERIAL` statement to the name of the index file, the linear interpolation from this table will complete to obtain the index of refraction as a function of wavelength.

A valid index file is shown below.

```
2
0.5 2.0 0.0
0.6 3.0 0.02
```

In this example, a real index of 2.5 and an imaginary index of 0.015 would be used for a wavelength of 0.55 microns.

You may also use ASCII file inputs to input real index and complex index independently. You can assign `INDX.REAL` to the name of an index file containing ordered pairs representing the wavelength and real index of refraction. Similarly, you can assign `INDX.IMAG` to the name of an index file containing ordered pairs representing the wavelength and the imaginary index. In all cases the table is preceded by the integer number of samples.

In each case, you may also choose to imbed comment lines delimited by a "#" character at the beginning of the line that will not be processed when read in.

By default, the units of wavelength are microns and the index is represented by real and imaginary parts. You can change this interpretation by including two character codes as the first non-comment line in the file. The following table explains these interpretations.

| Table 10-5. ASCII Index File Interpretation Codes. | |
|--|--|
| Code | Interpretation |
| none | Wavelength in microns, real index, and imaginary index |
| "ae" | Energy in eV, real index, and absorption coefficient in cm^{-1} |
| "an" | Wavelength in nm, real index, and absorption coefficient in cm^{-1} |
| "am" | Wavelength in μm , real index, and absorption coefficient in cm^{-1} |
| "nm" | Wavelength in nm, real index, and imaginary index |
| "ev" | Energy in eV, real index, and imaginary index |

C-Interpreter Function

The second way to specify index versus wavelength is by using the C-INTERPRETER function. The syntax is:

```
MATERIAL NAME=Silicon F.INDEX=myindex.c
```

The file myindex.c is an external file conforming to the template supplied with the program. It returns wavelength dependent real and imaginary indices. Instructions for using the C-INTERPRETER and finding the template functions are described in Appendix A: "C-Interpreter Functions".

SOPRA Database

You can choose to use refractive index data from the SOPRA database. To do this, you must specify the appropriate index file from Table B-39 on the SOPRA parameter of the MATERIAL statement (see Section B.13.1: "SOPRA Database").

Outputting Wavelength Dependent Complex Index for TonyPlot

The complex indices of refraction can be written to files suitable for display in TONYPLOT by specifying the file name root without extension on the OUT.INDEX parameter of the MATERIAL statement. The files created will use this root appended by "n.log" for real indices and "k.log" for imaginary indices. For indices input by the SOPRA database, the root will be appended by "N-n.log" and "N-k.log" where N is a sequence number (e.g., 1, 2, 3 . . .) to accommodate the capability of the SOPRA format to allow dependence on composition fraction and temperature.

10.9: Anti-Reflective (AR) Coatings for Ray Tracing and Matrix Method

It's a popular strategy to place Anti-Reflective (AR) coatings on light detecting devices to improve device quantum efficiency. Such coatings rely on destructive interference of reflected waves to reduce overall reflection coefficient of light incident on the detecting device.

Simple AR coatings are typically composed of one layer of a transparent insulating material that is one quarter optical wavelength thick. Such coatings significantly reduce reflectivity of light at the design wavelength. Far from the wavelength in question, however, their performance is poor. Currently, more sophisticated multilayer AR coatings are used for improved detection of broad-band light.

LUMINOUS enables you to model and design complicated AR coatings optimized for your specific application. AR coatings are simulated in LUMINOUS using an efficient transfer matrix method. This method enables you to deal with multilayer AR coatings with virtually no overhead in computation time. Section 10.2.4: "Matrix Method" discusses matrix method and its application to wave propagation in a stratified medium. AR coatings can be modeled using this approach for Matrix Method analysis (see Section 10.3: "Matrix Method") or ray tracing (see Section 10.2: "Ray Tracing").

Typically, AR coatings affect only optical properties of the device. Therefore, specifying the coating as a part of the device structure will unnecessarily increase the complexity of the electrical simulation. In ATLAS, coatings are associated with the interfaces of the device instead. This allows you to specify certain optical properties of any material boundary while not affecting electrical properties of the structure.

To define optical properties of a coating associated with that interface, use the `INTERFACE` statement and include the `OPTICAL` parameter. Using this statement, you can define an AR coating, a dielectric mirror, or an ideally reflecting surface. Note that the coating is absent in the structure defined for ATLAS.

The `AR.THICK` parameter defines the thickness of the coating layer. The `AR.INDEX` parameter defines the refractive index of the layer. For a single-layer coating or for the first layer of a multilayer coating, specify the coordinates of the points defining the coated surface `P1.X`, `P1.Y`, `P2.X`, and `P2.Y`.

Note: These coordinates should define a line, not a rectangular box of thickness (`AR.THICK`).

Figure 10-13 shows an example of a single-layer coating. The following shows the syntax used for a single-layer coating.

```
INTERFACE OPTICAL AR.INDEX=2.05 AR.THICK=0.0634 P1.X=0.0 P1.Y=0.0 P2.X=10.0
P2.Y=0.0
```

This defines a 63.4 μ m layer of real refractive index 2.05 at $Y=0.0\ \mu$ m in a structure.

For a single-layer coating or for the first layer of a multilayer coating, you can also specify coordinates of the bounding box `XMIN`, `XMAX`, `YMIN`, `YMAX`. All interfaces within the bounding box obtain optical properties of the coating. If you don't set the bounding box coordinates, the default bounding box containing the whole device will be used.

The `REGION` parameter gives you additional flexibility in the description of an AR coating. `REGION` specifies the number of a region adjacent to the coating. `REGION=0` is the default value, corresponding to the ambient region outside the device boundaries.

When you define a bounding box for an interface, it could contain other interfaces, which you do not intend to be AR coated. When you use `REGION`, you can select only those interfaces adjacent to that region to have AR coating properties.

You can specify any number of coatings for each device. The COATING parameter in the INTERFACE statement refers to the number of the coating. If COATING parameter is not set, the first coating will be used. Coatings should be specified in order (i.e., COATING=3 cannot be set before COATING=2 is defined).

Different coatings should not overlap. If this occurs, the later coating will be used in the overlapping part.

Typically, the purpose of a single-layer AR coating is to minimize reflectivity of normally incident monochromatic light at the design wavelength λ .

Equations 10-75 and 10-76 define the parameters of choice for a single-layer AR coating between materials with refractive indexes n_1 and n_2 :

$$\text{AR.INDEX} = \sqrt{n_1 n_2} \quad 10-75$$

$$\text{AR.THICK} = \frac{\lambda}{4 \cdot \text{AR.INDEX}} \quad 10-76$$

According to Equations 10-75 and 10-76, the coating in the example considered above has optimal properties for light at 520nm normally incident from air on a silicon detector.

You need several INTERFACE statements to specify a coating composed of multiple layers. Each statement defines only one layer of a coating. The syntax of the first INTERFACE statement for a multilayer coating is identical to the specification of a single-layer coating. Each subsequent layer must have the number of the coating and the number of the layer specified by COATING and LAYER parameters. Specify the same COATING parameter for all INTERFACE statements that refer to the layers of the same AR coating. For example, the following statements specify a two-layer coating:

```
INTERFACE OPTICAL AR.INDEX=1.5 AR.THICK=0.06 P1.X=0.0 P1.Y=0.0 P2.X=10.0 \
P2.Y=0.0 REGION =2
INTERFACE OPTICAL AR.INDEX=2.05 AR.THICK=0.06 COATING=1 LAYER=2
```

Here, COATING=1 and LAYER=2 show the second INTERFACE statement describing a second layer of a two-layer coating number one. Use the LAYER parameter to describe the order of layers in a coating. If LAYER is not specified, the first (top) layer will be used. Again, you cannot specify LAYER=3 before LAYER=2. You only need to specify the coordinates of the interface for the first layer of each coating.

In this example, the first coating layer with refractive index 1.5 is adjacent to the region number 2 on all boundaries within the specified bounding box. The second layer is outside of the first layer relative to region number 2, along the same boundaries. You only need to specify the bounding box and REGION only for the first layer of each coating.

Note: You also should also the COATING parameter to a unique index for each device in a MIXEDMODE simulation.

If a coating is made out of an absorbing material, you can use AR.ABSORB parameter to take into account absorption. You can also use totally reflective coatings. The coating will behave as an ideal reflector if you set the AR.INDEX parameter to a value > 1000.

Another way to specify the refractive index of the coating is to use the MATERIAL parameter on the INTERFACE statement. This enables you to apply any refractive index model supported by MATERIAL statement in ATLAS. This includes default wavelength dependent refractive index for supported materials, user-specified index in INDEX.FILE, C-interpreter function in F.INDEX, or the REAL.INDEX and IMAG.INDEX parameters on the corresponding MATERIAL statement. When you use the MATERIAL parameter on the INTERFACE statement, the AR.INDEX and AR.ABSORB parameters will be disabled.

An alternative way to set the properties of the top interface is to use C-INTERPRETER function with F.REFLECT specified in the BEAM statement. Using this function, you can specify the reflection coefficient, angle of transmission, and transmitted polarization as a function of position, wavelength, angle of incidence, and incident polarization.

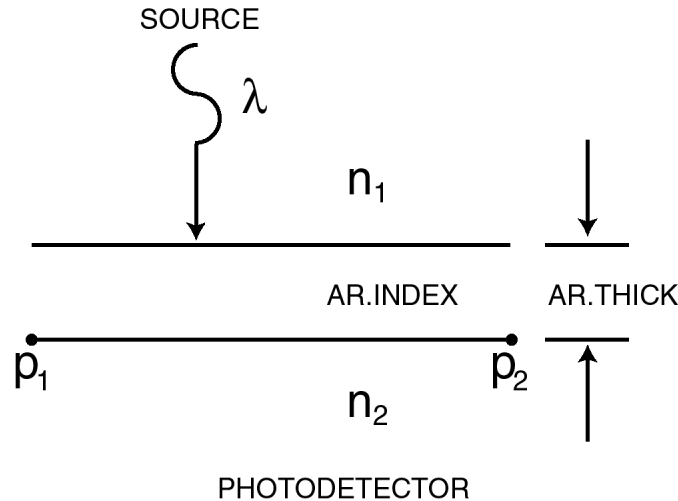


Figure 10-13: Single Layer AR Coating Under Normal Incidence

10.9.1: Anti-Reflective Coatings in LUMINOUS3D

LUMINOUS3D enables you to model and design multilayer AR coatings optimized for your specific 3D application.

As in LUMINOUS, you can define properties of an AR coating using the INTERFACE statement with OPTICAL parameter in LUMINOUS3D. The AR.THICK, AR.INDEX, AR.ABSORB, LAYER, REGION, and COATING parameters retain their meaning and functionality in 3D. The only difference in description of an AR coating in 3D pertains to specification of the coating location. The coating location cannot be set by specifying point coordinates. For a single-layer 3D coating or for the first layer of a multilayer 3D coating, you need to specify coordinates of the bounding box XMIN, XMAX, YMIN, YMAX, ZMIN, and ZMAX.

The following example

```
INTERFACE OPTICAL AR.INDEX=2.05 AR.THICK=0.0634 REGION=0
```

specifies that a 63.4nm layer of real refractive index 2.05 covers the entire outside boundary of a 3D device. All possible internal boundaries (heterojunctions) are not coated.

In a multilayer coating, the first layer is assumed to be adjacent to the region specified by REGION.

```
INTERFACE OPTICAL AR.INDEX=1.5 AR.THICK=0.06 XMIN=0.0 XMAX=2.0 YMIN=0.0 \
    YMAX=1.0 ZMIN=0.0 ZMAX=6.0 REGION=2
INTERFACE OPTICAL AR.INDEX=2.05 AR.THICK=0.06 COATING=1 LAYER=2
```

Here, COATING=1 and LAYER=2 show the second INTERFACE statement describing a second layer of a two-layer coating number one. Use the LAYER parameter to describe the order of layers in a coating. If LAYER is not specified, the first (top) layer will be used. Again, you cannot specify LAYER=3 before LAYER=2. You only need to specify the coordinates of the interface for the first layer of each coating.

In this example, the first coating layer with refractive index 1.5 is adjacent to the region number 2 on all boundaries within the specified bounding box. The second layer is outside of the first layer relative to region number 2, along the same boundaries. You only need to specify the bounding box and REGION only for the first layer of each coating.

10.10: Specifying Lenslets

You can specify one of four lenslets to focus the light into the device. The lenslet has no direct effect on the device simulation mesh. It is only used in the ray trace. Lenslets are described by user defined parameters of the LENS statement. All lenslet specifications apply to the last previously specified beam.

Spherical Lenslets

The spherical lenslet is described by the intersection of a plane (perpendicular to the Y axis and a sphere). See Figure 10-14. The Y coordinate of the plane is given by PLANE. The origin of the sphere is described by X.LOC, Y.LOC, and Z.LOC. The sphere radius is described by RADIUS.

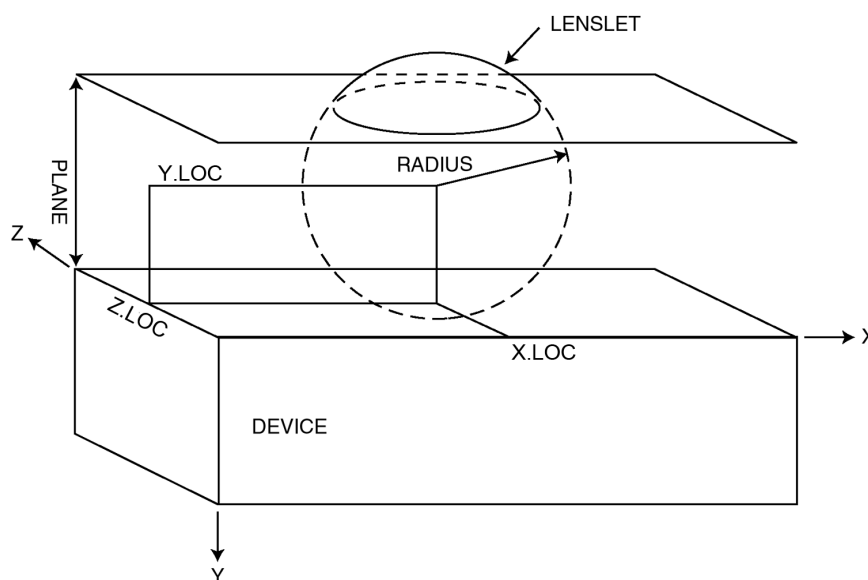


Figure 10-14: Luminous3D Lenslet Specification

For ray tracing purposes, the space between the plane and the device surface is uniformly of a single index of refraction specified by INDEX. The spherical section projecting above the plane in the negative Y direction is also considered to consist of the same index of refraction. The plane and the spherical section form the lenslet.

Ellipsoidal Lenslets

To specify an ellipsoidal lenslet, define the axial half lengths using the X.SEMI, Y.SEMI and Z.SEMI parameters of the LENS statement. The ellipsoidal lenslet center is specified by the X.LOC, Y.LOC, and Z.LOC parameters. The PLANE parameter defines the location of the lens plane. The INDEX parameter gives the lens real index of refraction. Equation 10-77 gives the lenslet surface above the lens plane.

$$\frac{(x - X_LOC)^2}{X_SEMI^2} + \frac{(y - Y_LOC)^2}{Y_SEMI^2} + \frac{(z - Z_LOC)^2}{Z_SEMI^2} = 1 \quad 10-77$$

Composite Lenslets

You can also specify a composite lenslet. The composite lenslet is composed of a central planar section, four cylinder sections and four sphere sections, which is shown in Figure 10-15. The composite lenslet is defined by the XMIN, XMAX, ZMIN, ZMAX, WIDTH, HEIGHT, PLANE and INDEX parameters. Figure 10-15 shows the meanings of these parameters.

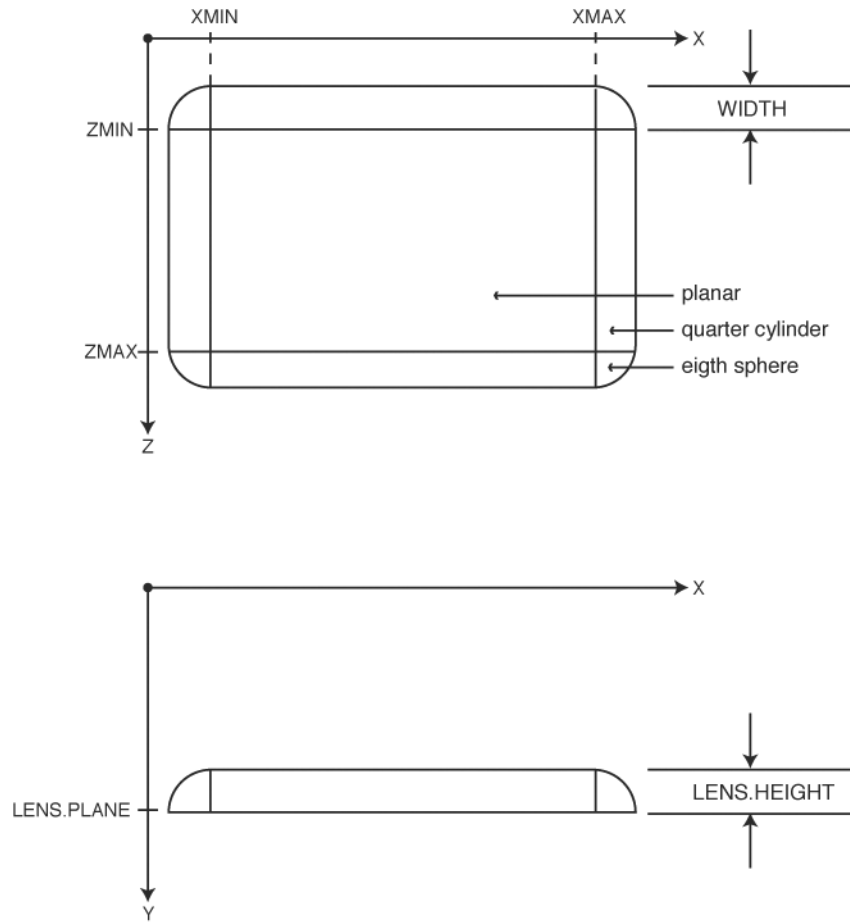


Figure 10-15: Composite Lenslet

Aspheric Lenslets

Aspheric lenslets are characterized in the normal directions x and z by the following two equations:

$$Y_x = \frac{X^2}{R_x + (R_x^2 - X^2)^{1/2}} + C_{4_x} X^4 + C_{6_x} X^6 + C_{8_x} X^8 + C_{10_x} X^{10} \quad 10-78$$

$$Y_z = \frac{Z^2}{R_z + (R_z^2 - Z^2)^{1/2}} + C_{4_z} Z^4 + C_{6_z} Z^6 + C_{8_z} Z^8 + C_{10_z} Z^{10} \quad 10-79$$

To arrive at these equations, you must provide tabulated data in the form of Sag-h pairs describing the surface of the lenslet in the x and the Z direction. You should specify the name of the file containing the data for the X direction in the `X.SAGS` parameter in the `BEAM` statement. You should also specify the name of the file containing the data for the Z direction in the `Z.SAGS` parameter in the `LENS` statement.

These files should first contain one line with the integer number of samples. The file should then contain a number (equal to the number of samples) of additional lines each containing a pair of real numbers representing the ordered pair of Sag-h data. These pairs must be arranged by increasing h . A sample at $h=0$ is implicit and corresponds to $Sag=1$.

From this data, a Levenberg-Marquardt non-linear least squares algorithm is applied to obtain the constants r , c_4 , c_6 , c_8 and c_{10} . This algorithm is iterative. You can specify the number of iterations used in the `SAGITS` parameter on the `LENS` statement with a default value of 10.

To have the results of the least squares fit written to files to be displayed in TONYPLOT, specify the file names using the `X.SOUT` and `Z.SOUT` parameters of the `LENS` statement.

Other parameters on the `LENS` statement describing the aspheric lenslet that should be specified include: `X.LOC`, `Z.LOC`, `INDEX`, and `PLANE`.

Pyramid Lenslets

To enable a pyramid shaped lenslet, specify `PYRAMID` on the `LENS` statement. The remainder of the specification is described in Figure 10-16. The level of the lenslet is specified by the `PLANE` parameter. The perimeter is specified by the `X.MIN`, `X.MAX`, `Z.MIN`, and `Z.MAX` parameters. The peak of the pyramid is located by the `X.LOC` and `Z.LOC` parameters. The height of the pyramid is given by the `APEX` parameter.

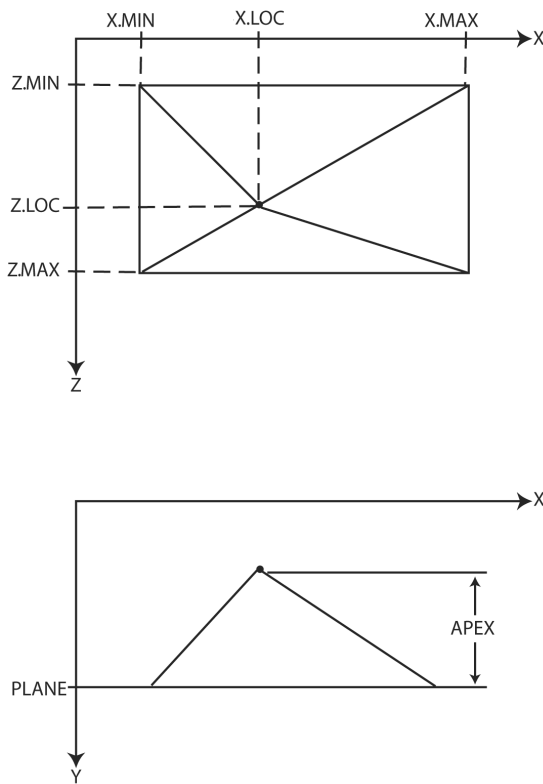


Figure 10-16: Pyramid Lenslet

Random Textured Lenslets

Random textured lenslets provide the capability to simulate random textured surfaces. The texturing can be best described by its algorithm.

First, a set of random steps are generated across the device domain in the Z direction. These random steps start at the minimum Z coordinate and progress until the maximum Z coordinate is reached. Each random step is made by first generating a Gaussian distributed random number with mean given by the value of the Z.MEAN parameter and a standard deviation given by the Z.SIGMA parameter of the LENS statement. This random step size is added to the previous Z location to yield the next Z location. Step sizes are restricted to positive numbers. This process is repeated until the Z location reaches the maximum Z coordinate.

Next, for each Z location the same process is applied in the X direction, where the mean step size is given by the X.MEAN parameter and the standard deviation X.SIGMA. This being done, we now have a complete set of X, Z locations. At each X, Z location, we next generate a Gaussian distributed random number. This number has a mean given by the value of the PLANE parameter and a standard deviation given by the Y.SIGMA parameter of the LENS statement. This random number gives the locations of the lenslet surface in the Y direction.

For convenience, the parameter MEAN can be used to specify a single value of both X.MEAN and Z.MEAN. Similarly, the parameter SIGMA can be used to specify a single value for X.SIGMA, Y.SIGMA, and Z.SIGMA.

Figure 10-17 shows an example surface generated using a value of MEAN=0.1 and SIGMA=0.1.

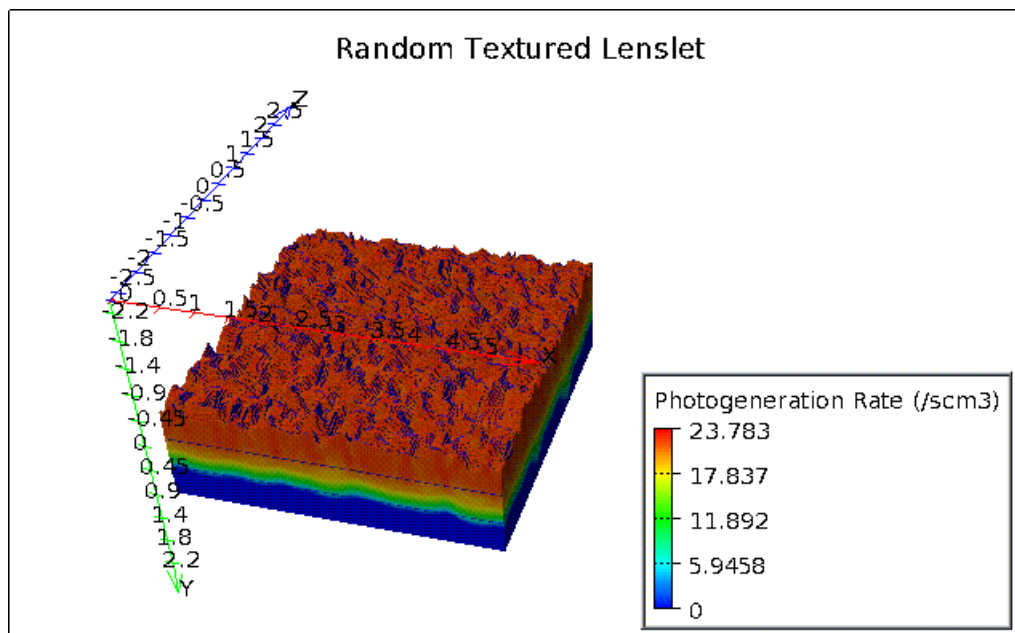


Figure 10-17: An Example Random Textured Lenslet (MEAN=0.1, SIGMA=0.1)

You can enable the user of a random textured lenslet by specifying the RANDOM parameter on the LENS statement. You can vary the seed value of the random number generation using the SEED parameter of the LENS statement. For a fixed value of the SEED parameter, the same random surface will be generated.

The random lenslet can also be used for 2D ray tracing.

User-Definable Lenslets

User-definable lenslets allow you to define the lenslet surface in a C-Interpreter function (see Appendix A: “C-Interpreter Functions”). The function has a simple interface where given the X and Z coordinates, you define the y coordinate of the lens surface. To enable the user-definable lenslet, you need to specify the `USER` parameter of the `LENS` statement. You also need to assign the `F.LENS` parameter of the `LENS` statement to the name of the file containing the C interpreter function. Finally, you will need to specify the index of refraction of the lenslet using the `N` and `K` parameters or the `MATERIAL` parameter of the `LENS` statement.

Lenslet Anti-reflective Coatings

It is sometimes useful to specify anti-reflective coatings on lenslets. For FDTD, this is simple to accomplish by nesting two lenslet specifications a small distance apart. For ray tracing, this is ineffectual since ray tracing does not directly account for the coherence effects necessary for proper modeling of reflective properties for thin coatings. In these cases, you should use the lenslet built-in AR coating capability. This works much like the AR coating capability described in Section 10.9: “Anti-Reflective (AR) Coatings for Ray Tracing and Matrix Method”.

To specify an AR coating on a lenslet for ray tracing, you need to specify the `AR.INDEX` and `AR.THICKNESS` parameters of the `LENS` statement. The `AR.INDEX` parameter is set to the real index of refraction of the coating. The `AR.THICKNESS` parameter is set to the coating thickness in microns.

10.11: Frequency Conversion Materials (2D Only)

Frequency conversion materials have the property that light absorbed in the material can be re-emitted at a single wavelength. This property can be used to either up or down convert light to improve spectral response of photodetectors, for example in solar cells.

In LUMINOUS, these materials are modeled electrically as insulators. The light conversion capability is enabled by specifying `FREQ.CONV` on the `MODELS` statement.

The re-emission process is modeled at discrete locations in the frequency conversion material. These locations are described by even sampling in the X and Y directions. You can specify the numbers of samples in the respective directions using the `EMISS.NX` and `EMISS.NY` parameters of the `MATERIAL` statement. The sampling of emission centers is described in Figure 10-18.

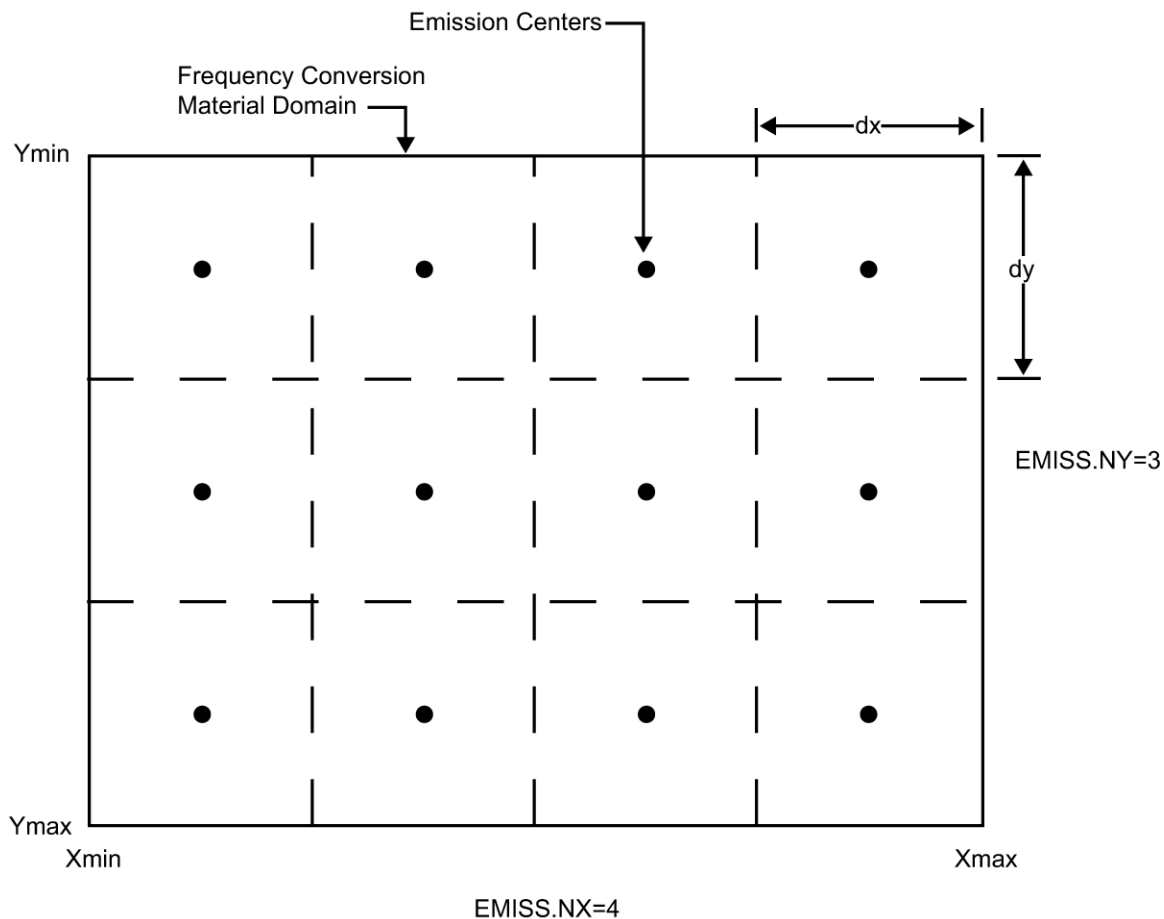


Figure 10-18: Frequency Conversion Material Emission Center Sampling

Physically, the remission process occurs in random directions. This process is modeled by performing ray traces from the emission centers in all directions 0 to 360° over an even sampling. You can specify the number of samples in angle space by the parameter `EMISS.NANG` on the `MATERIAL` statement. The angular sampling is described in Figure 10-19.

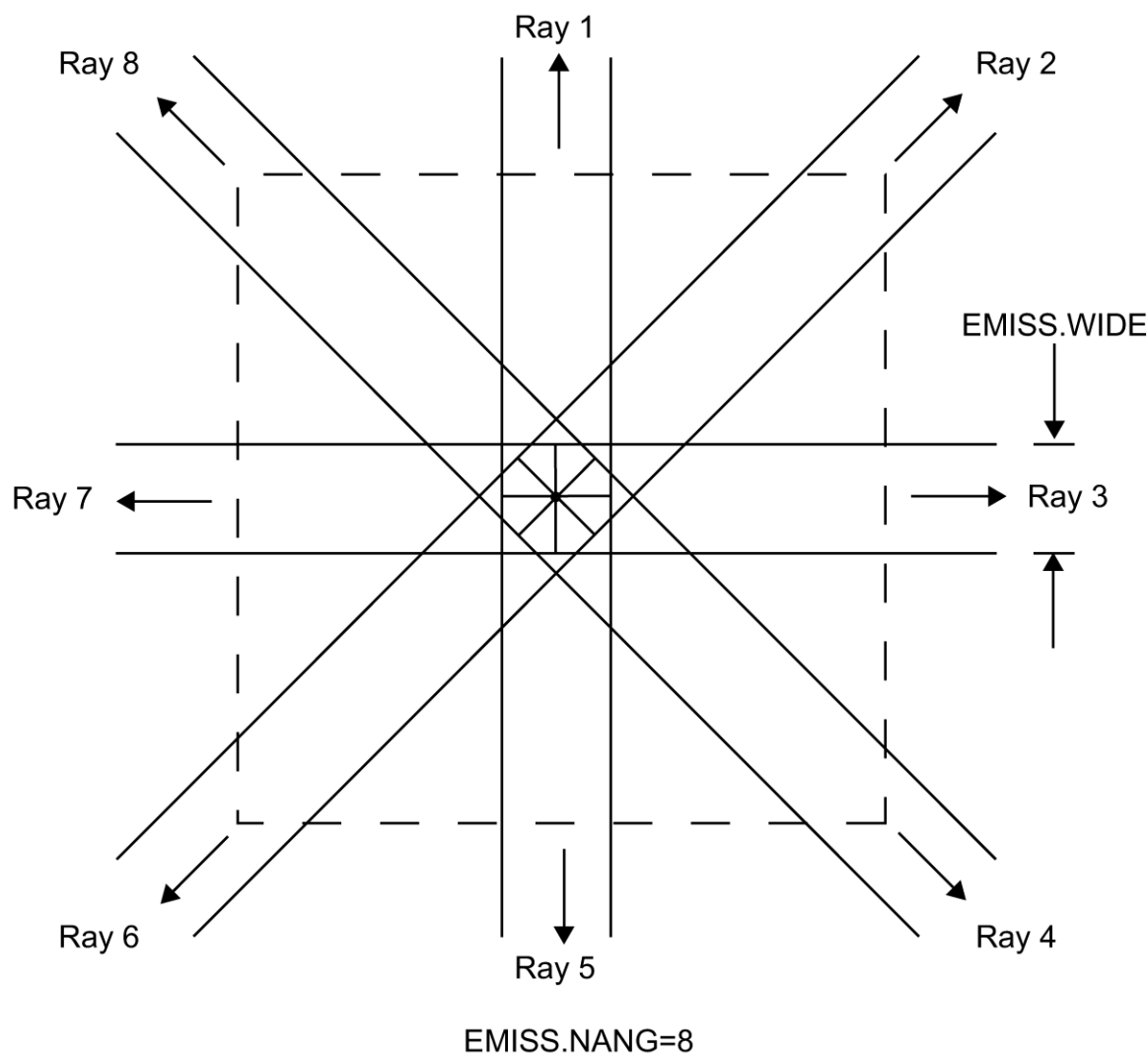


Figure 10-19: Frequency Conversion Material Angular Sampling

The rays are traced using the 2D trapezoidal ray tracing described in Section 10.2: “Ray Tracing”. The ray tracing automatically resolves internal and surface topologies. You can specify that the device domain will be treated as periodic with respect to the re-emitted rays by specifying `PFREQ.CONV` on the `MODELS` statement. By default, the value of `PFREQ.CONV` is `TRUE`, so the periodicity can be turned off by specifying `^PFREQ.CONV` on the `MODELS` statement.

You can specify the width of each trapezoid as described in Figure 10-19 using the `EMISS.WIDE` parameter of the `MATERIAL` statement. The width of the trapezoids is limited, however, by the minimum of the spacing between emission centers (the minimum of dx and dy in Figure 10-18).

The rays are emitted in monochromatic light at a wavelength specified by the `EMISS.LAMB` parameter of the `MATERIAL` statement.

The intensity of each ray is calculated by integrating the photogeneration rate due to absorption of primary and re-emitted light in the frequency conversion material. The emission rate is given by Equation 10-80.

$$P_{ray} = \int_{\substack{\text{Emission} \\ \text{Center} \\ \text{Area}}} G(x,y) dA \frac{hc}{\text{EMISS.LAMB}} \frac{\text{EMISS.EFFI}}{\text{EMISS.LAMB} \cdot \text{EMISS.NANG}} \quad 10-80$$

where:

- P_{ray} is the initial intensity of each ray.
- $G(x,y)$ is the photogeneration due to absorption in the area of the emission center.
- `EMISS.LAMB` is the user-specified emission wavelength.
- `EMISS.WIDE` is the user-specified emission ray width.
- `EMISS.NANG` is the user specified number of angles for emission.
- `EMISS.EFFI` is the user specified emission efficiency (number of photons emitted per electron hole pair generated by absorption).

The emission rate per ray is recalculated iteratively since the generation rate includes the generation due to re-emitted rays. Convergence of this iterative sequence is controlled by the `FC.ACCURACY` parameter of the `MODELS` statement, which specifies the maximum change in emission intensity as a divided by the most recently calculated emission intensity.

The user-controllable parameters of the frequency conversion model are given in Table 10-6.

| Table 10-6. Frequency Conversion Material Parameter Summary | | | |
|---|-----------------------|---------|---------|
| Parameter | Statement | Default | Units |
| <code>FREQ.CONV</code> | <code>MODELS</code> | False | |
| <code>PFREQ.CONV</code> | <code>MODELS</code> | True | |
| <code>FC.ACCURACY</code> | <code>MODELS</code> | 1.0e-6 | |
| <code>EMISS.LAMB</code> | <code>MATERIAL</code> | 0.5 | microns |
| <code>EMISS.EFFI</code> | <code>MATERIAL</code> | 1.0 | |
| <code>EMISS.NX</code> | <code>MATERIAL</code> | 1 | |
| <code>EMISS.NY</code> | <code>MATERIAL</code> | 1 | |
| <code>EMISS.NANG</code> | <code>MATERIAL</code> | 1 | |
| <code>EMISS.WIDE</code> | <code>MATERIAL</code> | 1.0 | microns |

10.12: Simulating Photodetectors

This section describes techniques simulate photodetectors. This section applies to the simulation of any of the following devices: p-n and p-i-n photodiodes, avalanche photodiodes, Schottky photodetectors, CCDs, MSMs, photoconductors, optical FETs and optically triggered power devices.

10.12.1: Defining Optical Sources

Identifying an Optical Beam

You can define up to ten optical sources. Optical sources are described by using the BEAM statement. All BEAM statements must appear somewhere after the MESH, REGION, DOPING, and ELECTRODE statements and before any SOLVE statement. The parameters in the BEAM statement describe a single optical source.

The NUM parameter is used to uniquely identify one optical source. Values between 1 and 10 are valid for the NUM parameter. Optical sources are subsequently referred to by the value of their NUM parameter. The power of the optical beam is set by using the B<n> parameter of the SOLVE statement, where n is the beam number defined by NUM.

Origin Plane of the Beam for 2D Optical Sources

To specify the origin of the optical source, use the X.ORIGIN and Y.ORIGIN parameters. These parameters describe the origin of the optical beam relative to the device coordinate system. Currently, it is required that the origin lie outside any device region. The ANGLE parameter specifies the angle of the direction of propagation of the beam with respect to the device coordinate system. ANGLE=90 specifies vertical (normal) illumination from above.

The width of the optical beam is specified using the MIN.WINDOW and MAX.WINDOW parameters. These parameters specify the limits of the source beam relative to the beam origin. If you omit either of the limits, that limit will be clipped to the edge of the device domain.

Note: It's extremely important that no section of the origin plane of the beam intersects or is inside the simulation grid. Otherwise, you'll get incorrect results. This is important to check in cases where the ANGLE isn't 90° or 270°.

Origin Plane of the Beam for 3D Optical Sources

To specify the origin of a 3D source, use the X.ORIGIN, Y.ORIGIN, and Z.ORIGIN parameters. These parameters describe the location of the origin relative to the device coordinate system. The THETA and PHI parameters describe the direction of propagation relative to the beam origin. The THETA parameter describes rotation of the X axis about the Z axis. The PHI parameter describes rotation of the Z axis about the Y axis. As with the 2D for normal illumination, specify a negative Y.ORIGIN and THETA=90.

Specify the window of illumination using the XMIN, XMAX, ZMIN, and ZMAX parameters. Then, specify the numbers of samples in the X and Z directions using the NX and NZ parameters. These values should be set to numbers large enough to resolve any salient features of the topology.

To save the rays into a file for visualization, specify the RAYTRACE=<filename> parameter. The components (u_x , u_y and u_z) of the direction vector representing the direction of the beam propagation are given by the following:

$$u_y = \cos(\text{PHI} - 90) \quad 10-81$$

$$r = -\sin(\text{PHI} - 90) \quad 10-82$$

$$u_x = r \cos(\text{THETA}) \quad 10-83$$

$$u_z = r \sin(\text{THETA}) \quad 10-84$$

Reflections

You can also specify whether to ignore the first reflection using the `FRONT.REFL` or the backside and sidewall reflection using the `BACK.REFL`. You should activate the backside reflections for devices, which use a back side reflector to improve collection efficiency. To set the number of reflections solved, use the `REFLECTS` parameter.

Typically, `BACK.REFL` should be used if the structure simulated is equivalent to the complete photodetector geometry as in a discrete device. If the simulation structure is a section of a larger substrate as in CCD simulation then don't use `BACK.REFL`.

Since the ray trace for arbitrary angles of incidence uses reflection and transmission coefficients, specify the polarization by using the `POLARIZATION` parameter.

In complex structures, you should limit the ray tracing to trace only those rays with significant optical power. The `MIN.POWER` parameter is used to terminate ray traces that drop below `MIN.POWER*` (optical source power).

10.12.2: Specifying Periodicity in the Ray Trace

By default, the unspecified boundary conditions for device simulation are mirror or periodic boundary conditions. For ray tracing, by default, the edges of the device are considered interfaces with a vacuum. Thus, at the edges of the device, by default, reflections are calculated. In some cases, it is convenient to consider the edges of the device to be periodic with respect to ray tracing. This is particularly true when the beam is not normal to the plane. You should specify `PERIODIC` in the `BEAM` statement to obtain such boundaries for ray tracing.

10.12.3: Defining Luminous Beam Intensity in 2D

When a beam is defined in `LUMINOUS`, it is, by default, assumed to have a uniform light intensity across the width of the beam. The intensity is defined in the `SOLVE` statement with the `B<n>` parameter and is in the units of W/cm^2 .

The beam intensity distribution can also be defined with a Gaussian profile.

$$f(x) = \frac{1}{\text{SIGMA} \sqrt{2\pi}} \exp\left(-\frac{(x - \text{MEAN})^2}{2(\text{SIGMA})^2}\right) \quad 10-85$$

The location of the peak of the Gaussian distribution with respect to the beam coordinates is specified by the `MEAN` parameter of the `BEAM` statement. The standard deviation of the distribution is specified with the `SIGMA` parameter.

x is the cumulative distance over the beam width where the distribution will be formed. Define the `RAYS` parameter to get smooth distribution of intensity profile. This determines the increment of x . Therefore, the `RAYS` parameter should be set to a large number as the spacing between rays is always a constant (width of the beam / `RAYS`).

The resultant distribution has a unity peak value, which is then scaled by the $B_{<n>}$ value specified on the SOLVE statement. For example, the following BEAM statement will define a beam window 2 μm wide centered at X.ORIGIN and Y.ORIGIN, which has a Gaussian peak of 0.01 W/cm^2 and a standard deviation of 0.05 μm .

```
beam  num=1 x.origin=5.0 y.origin=-1.0 angle=90.0 wavelength=0.6 \
xmin=-1 xmax=1 GAUSSIAN MEAN=0 SIGMA=0.05 RAYS=200 \
SOLVE B1=1E-2
```

10.12.4: Defining Luminous3D Beam Intensity

A beam defined in LUMINOUS3D is assumed by default to have a uniform light intensity across the width of the beam. The intensity is defined in the SOLVE statement with the B_n parameter and is in the units of W/cm^2 .

In LUMINOUS3D, you can also specify a circular or elliptical source. To specify an elliptical source, specify the appropriate origin location using X.ORIGIN, Y.ORIGIN, and Z.ORIGIN. This will specify the center of the elliptical source. The major and minor axes of the ellipse are specified by the XRADIUS and ZRADIUS parameters. Remember, you must also specify the NX and NZ parameters. These will sample uniformly across the diameters of the ellipse.

You may also specify Gaussian profiles in LUMINOUS3D. To do this, specify the location of the beam origin. You can specify the Gaussian(s) in the X and Z direction. These can be done independently or together. These Gaussians are specified by the XMEAN, XSIGMA, ZMEAN, and ZSIGMA parameters of the BEAM statement.

10.12.5: Monochromatic or Multispectral Sources

The optical source can be either monochromatic or multispectral. For monochromatic sources, you can use the WAVELENGTH parameter to assign the optical wavelength. WAVELENGTH uses the units microns to be more consistent with the rest of ATLAS. Note this if you're accustomed to the optoelectronic engineering preference for nanometers.

For multispectral sources, spectral intensity is described in an external ASCII file indicated by the POWER.FILE parameter. This is a text file that contains a list of pairs defining wavelength and spectral intensity. The first line of the file gives the integer number of wavelength-intensity pairs in the file. An example of such a file is shown below.

```
4
0.4 0.5
0.5 1.0
0.6 1.2
0.7 1.1
```

This example specifies that there are four samples and that at a wavelength of 0.4 μm , the intensity is 0.5 Watts per square cm per μm of wavelength, and so on. With multispectral sources, specify a discretization of the interpolated information. Values must be specified for the WAVEL.START, WAVEL.END, and WAVEL.NUM parameters. These values specify the starting and ending wavelengths and the number of wavelengths to sample. LUMINOUS uses wavelengths at equal intervals over a specified range of wavelengths.

If you don't specify the values of WAVEL.START, WAVEL.END, and WAVEL.NUM, these parameters take on the corresponding values from the specified POWER.FILE. For the example file shown above, LUMINOUS uses the following default values of these parameters: WAVEL.START=0.4, WAVEL.END=0.7, and WAVEL.NUM=4.

LUMINOUS performs an independent ray trace at each of the sample wavelengths. For example:

WAVEL.START=0.4 WAVEL.END=0.6 WAVEL.NUM=2

causes ray traces at wavelengths of 0.45 and 0.55. LUMINOUS obtains the intensity associated with each sample by integrating the values of the spectral intensity file using a piece wise linear approximation. Each integral is performed over the range between successive midpoints. In the preceding example, the integration for the sample at 0.45 would be performed over the range of 0.4 to 0.5.

For a multispectral source, the generation rate (like Equation 10-11) is given by:

$$G = \eta_0 \int_{\text{WAVEL.START}}^{\text{WAVEL.END}} \frac{P(\lambda)L\lambda}{hc} \alpha e^{-\alpha y} d\lambda \quad 10-86$$

where:

- η_0 is the internal quantum efficiency.
- $P(\lambda)$ is the power spectral density of the source.
- L is a factor representing the cumulative loss due to reflections, transmissions, and absorption over the ray path.
- λ is the wavelength.
- h is Planck's constant.
- c is the speed of light.
- α is the absorption coefficient given by Equation 10-12.
- y is the depth of the device, where x,y forms the two-dimensional mesh.

WAVEL.START and WAVEL.END are the spectral limits specified on the BEAM statement.

Note: The integral in Equation 10-86 may be inexact due to the discrete sampling in conjunction with wavelength dependence of the absorption coefficient. For constant absorption coefficient, the integral is exact of the number of discrete wavelength samples specified by WAVEL.NUM on the BEAM statement.

The source photocurrent (like Equation 10-73) is given by:

$$I_s = q \frac{B_n}{hc} W_t \int_{\text{WAVEL.START}}^{\text{WAVEL.END}} P(\lambda) \lambda d\lambda \quad 10-87$$

where $P(\lambda)$ is the power spectral density of the source. The other parameters have the same definition as in Equation 10-73.

The available photo current (like Equation 10-74) is given by:

$$I_A = q \frac{B_n}{hc} \sum_{i=1}^{N_R} X_i \int_{\text{WAVEL.START}}^{\text{WAVEL.END}} P(\lambda) \alpha_i e^{-\alpha_i y} P_i \lambda dy d\lambda \quad 10-88$$

where $P(\lambda)$ is the power spectral density of the source. The other parameters have the same definition as in Equation 10-74.

LUMINOUS allows you to choose the units of spectral intensity in an input spectrum file. By default, the units of spectral intensity in the `POWER.FILE` are $\text{W}/(\text{cm}^2 \mu\text{m})$. In this case, LUMINOUS carries out the integration according to Equations 10-86, 10-87, 10-88. If the units of spectral intensity in the `POWER.FILE` are W/cm^2 , then you need to use the flag `^INTEGRATE` on the `BEAM` statement. In this case, each value $P(\lambda)$ in the second column of the file is a total intensity for a corresponding spectral interval. Integrals over spectrum in Equations 10-86, 10-87, 10-88 are reduced to summations of $P(\lambda)$ values. In both cases, LUMINOUS treats the subsequently specified value of `B<n>` on the `SOLVE` statement as a unitless multiplier or scale factor for intensity.

This is different from monochromatic case where this parameter has units of W/cm^2 . To preserve consistency with monochromatic case, you can also do the same in the multispectral applications. If you specify the total beam intensity for multispectral sources using `B<n>` parameter on the `SOLVE` statement, you need to set `NORMALIZE` flag on the `BEAM` statements. This ensures that the intensity spectrum is normalized and `B<n>` has units of W/cm^2 .

For either the monochromatic or multispectral sources, you can uniformly scale the wavelength(s) and intensities by using the `WAVEL.SCALE` parameter and the `POWER.SCALE` parameter respectively. These parameters are useful if the intensities or wavelengths are specified in units other than the default units. To output the samples from the input spectrum file to a file suitable for display in TONYPLOT, specify the output file name on the `OUT.POWER` parameter of the `BEAM` statement.

Remember that these are built-in tabular spectra and include many samples. You are therefore advised to use subsample using the `WAVEL.START`, `WAVEL.END`, and `WAVEL.NUM` parameters as described in Section 10.12.5: “Monochromatic or Multispectral Sources”.

The run-time output includes a couple of headings to represent the integrated intensity as input and as subsampled. “`Iinput`” is the integrated input spectrum. This is the integral over the samples contained in the file specified by the `POWER.FILE` parameter (or contained in the built-in AM0 or AM1.5 spectra). “`Isampled`” is the integral of the sub-sampled spectrum. You sub-sample the input spectrum when you specify `WAVEL.START`, `WAVEL.END`, and `WAVEL.NUM`. If you do not specify this sub-sampling, the raw input samples are used and “`Isampled`” is identical to “`Iinput`”.

If you sub-sample, “`Isample`” is always less than or equal to “`Iinput`”. If you chose the start and end samples to match those contained in the input spectrum, you will get “`Iinput`” equal to “`Isampled`” due to the way we integrate power when we sub-sample.

You can look at the input spectrum in TONYPLOT by specifying a log file name in the value of the `OUT.POWER` parameter of the `BEAM` statement and loading that file into TONYPLOT.

Sub-sampling has advantages to save on time computing optical propagation, such as ray tracing or FDTD solutions for each specified wavelength. Usually, sub-sampling introduces only moderate quantization error if the index of refraction does not vary too quickly.

10.12.6: Solar Sources

LUMINOUS and LUMINOUS3D provide built-in definitions of solar spectra for AM0 [191] and AM1.5 [192] conditions. To specify these spectra, define AM0 or AM1.5 on the appropriate `BEAM` statement.

10.12.7: Extracting Dark Characteristics

One of the first tasks in analyzing a new detector design is to examine dark current, device capacitance, and possibly other unilluminated characteristics. This can normally be done without using LUMINOUS. Extraction of the characteristics is adequately covered in the chapters on S-PISCES or BLAZE.

The extraction of reverse bias leakage currents for diodes presents some difficult numerical problems for device simulators. These problems are associated with limitations on numerical precision. ATLAS, as well as most other available device simulators, use double precision arithmetic to evaluate terminal currents. Double precision arithmetic provides roughly 16 decimal digits of precision. Internal scaling allows the measurement of currents down to a level of between about 10^{-12} A/micron to 10^{-16} A/micron. Unfortunately, photodiode leakage currents are often around or below this level. This means that the currents printed are subject to significant numerical noise and don't provide an accurate estimate of the device leakage currents. There are two ways to estimate reverse leakage current.

Integrated Recombination

From a theoretical standpoint, the reverse behavior of diodes can be dominated by one of two effects: diffusion currents in the neutral regions or recombination currents inside the depletion region [223]. ATLAS can provide insight into both of these contributing mechanisms. To estimate recombination current, use the MEASURE statement to calculate the integrated recombination rate. The following statement can be used:

```
MEASURE U.TOTAL
```

When this statement is executed, it prints out the total integrated recombination rate. Multiply this value by the electron charge (1.6023×10^{-19} coulombs) to obtain an estimate of the recombination current contribution to the reverse diode leakage current.

Extrapolation from High Temperatures

The diffusion current contribution can be estimated by taking advantage of the non-linear relationship between the diffusion current and temperature. Referring to the expression for the "Ideal Diode" current given by Equation 10-89, the dominant temperature dependency arises from the variation of the intrinsic concentration.

$$J = \left(\frac{qD_p p_{n0}}{L_p} + \frac{qD_n n_{p0}}{L_n} \right) \left(\exp\left(\frac{qV}{kT_L}\right) - 1 \right) \quad 10-89$$

where n_{p0} and p_{n0} are thermal-equilibrium minority carrier densities on either side of the junction. This gives an exponential variation of the diffusion current with temperature given in Equation 10-90.

$$J \approx \exp\left(\frac{-E_g}{kT_L}\right) \cdot \left(\exp\left(\frac{qV}{kT_L}\right) - 1 \right) \quad 10-90$$

This relation can be used to estimate the diffusion current contribution at the operating temperature. The basic idea is to calculate the current at a high temperature where the problem of numerical precision does not arise. Then, scale the current to the operating temperature using Equation 10-90. For example, if the device is to operate at 300K, you can set the temperature to 450K using the TEMPERATURE parameter of the MODEL statement. Disable any temperature dependence of the energy gap by specifying the band gap using the EG300 parameter and setting EGALPHA and EGBETA parameters to zero, which are all on the MATERIAL statement. The following statement illustrates this approach as it might apply to a silicon diode:

```
MODEL TEMPERATURE=450
MATERIAL EG300=1.12 EGALPHA=0.0 EGBETA=0.0
```

ATLAS can then be used to obtain the reverse bias current at the elevated temperature. Equation 10-91 can be applied to obtain the depletion current contribution at the operating temperature:

$$J = J_e \cdot \exp\left(\frac{E_g}{kT_e} - \frac{E_g}{kT_L}\right) \cdot \left(\frac{\exp\left(\frac{qV}{kT_L}\right) - 1}{\exp\left(\frac{qV}{kT_e}\right) - 1}\right) \quad 10-91$$

where J_e is the current measured at the elevated temperature, E_g is the bandgap, T_e is the elevated temperature, T_L is the operating temperature, V is the operating bias voltage, and J is the current estimate at the operating temperature. Once you've obtained estimates of the recombination and diffusion contributions, you can obtain the total leakage current by summing the two contributions.

Numerical Solution Parameters

ATLAS uses a cut-off value of carrier concentration below, which solutions are not required to converge. This limit is set by the CLIM.DD. parameter. See Chapter 20: "Numerical Techniques" for more details on CLIM.DD. For photodetectors, you often need to reduce CLIM.DD to 10^5 in order to resolve carrier concentrations in depleted regions before illumination.

10.12.8: Extracting Detection Efficiency

One of the simpler tasks in characterizing a photodetector design is to measure DC detection efficiency. This will be done typically as a function of bias voltage, optical intensity, or wavelength. Each of these analyses can be performed using the SOLVE statement. The Bn parameter can be used to set the optical intensity of the optical sources described in the previous section. The following example illustrates obtaining a solution with a specified optical intensity:

```
SOLVE B1=1.0
```

This specifies that a solution is to be obtained for an optical intensity in the beam numbered "1" of 1.0 Watt/cm². If this were the first SOLVE statement specified, the ray trace in LUMINOUS would be initiated. At the start of the solution, the optical intensities of each optical source with a positive intensity is printed. In addition, the available photocurrent and source photocurrent are printed. See the prior section on Photocurrent for a definition of these two quantities.

Internal and External Quantum Efficiency

The available photocurrent divided by the source photocurrent is a measure of the external quantum efficiency of the detector. The calculated terminal current can be divided by the source or available photocurrents is used to evaluate the internal quantum efficiency of the device.

10.12.9: Obtaining Quantum Efficiency versus Bias

The intensities specified in the SOLVE statement apply until another SOLVE statement changes the intensity of the beam. Sequences of SOLVE statements can be used to vary the optical intensity at arbitrary intervals. The simple linear ramps of optical intensity can be abbreviated using the LIT.STEP and NSTEP parameters of the SOLVE statement. The LIT.STEP parameter specifies the size of the DC step and NSTEP specifies how many steps are desired.

Another option for analyzing DC quantum efficiency is to fix the optical intensity and vary bias voltages. The bias voltages can be varied in arbitrary discrete steps using several SOLVE statements, or in a linear ramp using individual SOLVE statements. This is useful for determining the optimum operating bias of devices such as avalanche detectors and photo transistors.

10.12.10: Obtaining Transient Response to Optical Sources

It is sometimes desirable to examine the time domain response of a detector to time-dependent (e.g., ramped or pulsed) optical sources. LUMINOUS provides this capability with the `RAMP.LIT` parameter. When the `RAMP.LIT` parameter is specified in a `SOLVE` statement, the optical intensity is changed linearly from the most recently set intensity to the intensity set in the `B` parameter. If a particular source intensity is not set using the corresponding `B` parameter, its intensity is not varied during the transient.

The period of the linear ramp is specified by the `RAMPTIME` parameter. The transient simulation stops after the time specified by the `TSTOP` parameter. If the time given by `TSTOP` is greater than that given by `RAMPTIME`, the source intensities remain constant until the time given by `TSTOP`. For transient ramps, the `TSTEP` parameter should also be set. `TSTEP` is typically set to allow several samples within the `RAMPTIME`. After the first time step, subsequent time step sizes will be chosen automatically based on estimates of truncation error. The following is an example of the specification of an optical impulse transient:

```
SOLVE B1=1.0 RAMPTIME=1E-9 TSTOP=1E-9 TSTEP=1E-11
SOLVE B1=0.0 RAMPTIME=1E-9 TSTOP=20E-9 TSTEP=1E-11
```

In this example, a triangular impulse in the intensity of the optical source is simulated. The peak intensity is 1.0 and the impulse width is 2 ns. The response of the device is simulated for an additional 18 ns. An initial time step of 10 ps is chosen for both parts of the impulse.

10.12.11: Obtaining Frequency Response to Optical Sources

You can also simulate small signal response to optical sources. To obtain a solution for small signal response, set the `SS.PHOT` parameter in the `SOLVE` statement. The `BEAM` parameter must also be assigned to the specific optical source index for small signal response of that source. A single source small signal frequency can be specified using the `FREQUENCY` parameter. You can vary the frequency within a single `SOLVE` statement by using the `NFSTEP` and `FSTEP` parameters. The `NFSTEP` indicates how many frequency steps are to be simulated, while the `FSTEP` indicates the step size. If the `MULT.F` parameter is specified, the start frequency is multiplied by the step size for the specified number of steps. If not, the step size will be added to the start frequency for the specified number of steps. For example:

```
SOLVE SS.PHOT BEAM=1 FREQUENCY=1e6 NFSTEP=5 FSTEP=10 MULT.F
```

will invoke solutions as optical frequencies at every decade from 1MHz to 100 GHz.

If the small signal parameters are specified in the same `SOLVE` statement as a DC bias ramp, the small signal response is extracted for each bias voltage for each small signal frequency. This is a useful strategy for analyzing the frequency response of the device as a function of bias voltage.

Note: When simulating spectral response you should try to sample enough to resolve variations in complex index of refraction, variations in input spectrum (e.g., AM1.5), and variations due to coherence effects in layers with thicknesses on the order of the wavelength. Such coherence effects are of no consequence in ray tracing but may be important in the transfer matrix or finite difference time domain methods.

10.12.12: Obtaining Spatial Response

To obtain spatial response, move an optical spot along a line segment perpendicular to the direction of propagation of the source. Each incremental step is equal to the width of the spot. The total distance over which the source is scanned is defined by the `MIN.WINDOW` and `MAX.WINDOW` parameters of the `BEAM` statement. The number of steps is defined by the `RAYS` parameter of the `BEAM` statement. The spot width is defined by the ratio:

$$(\text{MAX.WINDOW} - \text{MIN.WINDOW}) / \text{RAYS}$$

The spot scan is started by the `SCAN.SPOT` parameter of the `SOLVE` statement. This parameter is set to the beam index of the optical source to be scanned. In other words, the beam defined by the `BEAM` statement whose `NUMBER` parameter is set to the beam index. During the spot scan, `ATLAS` obtains solutions and outputs, such as terminal currents, as well as the relative beam location at each incremental spot location. This information can be used by `TONYPLOT` to produce plots of photoresponse as a function of position.

In `LUMINOUS3D`, the `SCAN.SPOT` parameter will cause the simulator to power each ray defined by the `NX` and `NZ` parameters sequentially.

10.12.13: Obtaining Spectral Response

The spectral response, defined as device current as a function of the wavelength of the optical source wavelength, can be obtained. The `LAMBDA` parameter of the `SOLVE` statement sets the source wavelength of the beam in microns. Since the wavelength can be set in each `SOLVE` statement, successive solutions can be obtained as a function of wavelength. Each time the `LAMBDA` parameter is specified, a new ray trace is run for that new wavelength and the electrical solution recalculated.

The following statements could be used to extract terminal currents at a series of discrete wavelengths:

```
SOLVE B1=1 LAMBDA=0.2
SOLVE B1=1 LAMBDA=0.3
SOLVE B1=1 LAMBDA=0.4
SOLVE B1=1 LAMBDA=0.5
SOLVE B1=1 LAMBDA=0.6
SOLVE B1=1 LAMBDA=0.7
SOLVE B1=1 LAMBDA=0.8
```

In this example, the spectral response is obtained for wavelengths from 0.2 microns to 0.8 microns. When using `LAMBDA`, the `WAVELENGTH` parameter of the `BEAM` statement will be overridden.

Equivalently, you may find it more convenient to specify a spectral ramp. To specify a ramp of wavelength, you should assign the `BEAM` parameter to the beam index of the optical source to be ramped. Also, you should specify the initial wavelength with the `LAMBDA` parameter, the final wavelength with the `WFINAL` parameter, and the wavelength step size with the `WSTEP` parameter as illustrated in the following.

```
SOLVE B1=1 BEAM=1 LAMBDA=0.2 WSTEP=0.1 WFINAL=0.8
```

This is completely analogous to the seven statements described above.

Note: If you specify `POWER.FILE` on the `BEAM` statement, the spectral intensities will be scaled by the value interpolated from the power file.

10.12.14: Obtaining Angular Response

The response of photodetectors to angle of incidence can be obtained in a manner analogous to the method used to obtain spectral response.

In this case, the `ANGLE` parameter of the `SOLVE` statement specifies an angle added to the value of the `BEAM` parameter `PHI` (`ANGLE`). This allows collection of response versus angle. The following examples statements demonstrate the syntax.

```
SOLVE B1=1 ANGLE=0
SOLVE B1=1 ANGLE=10
SOLVE B1=1 ANGLE=20
SOLVE B1=1 ANGLE=30
SOLVE B1=1 ANGLE=40
SOLVE B1=1 ANGLE=50
SOLVE B1=1 ANGLE=60
```

Equivalently, you may find it more convenient to specify a angle ramp. To specify a ramp of angle, you should assign the `BEAM` parameter to the beam index of the optical source to be ramped. Also, you should specify the initial angle with the `ANGLE` parameter, the final angle with the `AFINAL` parameter, and the angle step size with the `ASTEP` parameter as illustrated in the following.

```
SOLVE B1=1 BEAM=1 ANGLE=0.0 ASTEP=10.0 AFINAL=60.0
```

This is completely analogous to the seven statements described above.

10.13: Simulating Solar Cells

The LUMINOUS simulators are well suited to the simulation of solar cells. Particularly, the variety of robust optical propagation models in combination of the capabilities of the device simulators in the ATLAS framework makes accurate solar cell simulation a possibility. The following paragraphs focus on problems and solutions specific to the simulation of solar cells.

10.13.1: Solar Spectra

As discussed in Section 10.12.5: “Monochromatic or Multispectral Sources”, LUMINOUS2D and LUMINOUS3D provide flexible means for defining multispectral sources. In addition, you can directly access built-in public domain [191, 192] solar spectra for am0 and am1.5 conditions by specifying AM0 or AM1.5 on the BEAM statement. These spectra consist of numerous samples and we therefore suggest you carefully consider subsampling as discussed in Section 10.12.5: “Monochromatic or Multispectral Sources”.

The following is an example of how you might define the BEAM statement for analysis of am1.5 conditions with subsampling.

```
BEAM NUM=1 AM1.5 WAVEL.START=0.3 WAVEL.END=1.2 WAVEL.NUM=50
```

Here, we are choosing to simulate am1.5 conditions sampled between 0.3 microns and 1.2 microns at 50 samples. We do not have to worry about sampling the many peaks and valleys in the solar spectrum as it is automatically integrated into each subsample. The subsampling effects only the number of wavelengths for which the propagation model is calculated not the integrated intensity.

10.13.2: Solar Optical Propagation Models

The choice of optical propagation model for your purposes depends largely on the nature of your solar cell devices. In some cases, you may want to apply several of the different models to compare the results against measurement for your particular analysis.

In all cases, accurate knowledge of the complex index of refraction of the materials comprising the solar cell versus wavelength is key in accurate light propagation modeling. LUMINOUS2D and LUMINOUS3D provide built-in defaults for most materials of importance to solar cell technology (see Section B.13: “Optical Properties” for more details). Additionally, LUMINOUS2D and LUMINOUS3D provide flexible means for you to introduce user-supplied data in the form of ASCII tables or C-Interpreter functions as discussed in Section 10.8: “Defining Optical Properties of Materials”.

If you have little knowledge of the optical properties of the materials in your solar cell, or if you are less interested in the propagation problem, you may choose to simply define the photogeneration rate using the C-Interpreter function F.RADIATE. This function allows you to directly specify the photogeneration rate as a function of position in the device. The following illustrates the use of the F.RADIATE C-Interpreter function for constant generation rate.

First, you need to identify the C function defining the generation rate to the simulator. This is done in the input deck on the BEAM statement using the F.RADIATE parameter as follows:

```
BEAM NUM=1 F.RADIATE=solar.lib
```

Here, the C-Interpreter function is contained in a separate file named "solar.lib". For example, the contents of the file "solar.lib" may be as follows:

```
#include <stdio.h>
#include <stdlib.h>
#include <math.h>
#include <ctype.h>
#include <malloc.h>
#include <string.h>
#include <template.h>
```

```
/*
 * Generation rate as a function of position
 * Statement: BEAM
 * Parameter: F.RADIATE
 * Arguments:
 * x          location x (microns)
 * y          location y (microns)
 * z          location z (microns)
 * t          time (seconds )
 * *rat       generation rate per cc per sec.
 */
int radiate(double x, double y, double z, double t, double *rat)
{
  *rat = 1e21;
  return(0);          /* 0 - ok */
}
```

Here, we simply define a constant photogeneration rate everywhere in the semiconductor of $1e21$ carrier pairs per second per cubic centimeter.

You can easily define this function to specify any arbitrary generation rate as a function of position and time. You should refer to Appendix A: “C-Interpreter Functions” for more information on the C-Interpreter.

Ray tracing is the principal propagation model for cases where we are not concerned about interference or diffraction effects in the bulk of the device. This is most useful for relatively thick bulk devices, such as crystalline silicon devices. It is useful for planar or textured devices. For textured devices, the texturing must be described explicitly in the device structure. Details of the ray tracing models are given in Section 10.2: “Ray Tracing”.

The following gives an example of the specification of ray tracing for the optical propagation model for LUMINOUS2D.

```
BEAM NUM=1 AM1.5 WAVEL.START=0.3 WAVEL.END=1.2 WAVEL.NUM=50
```

In this case, we will perform 50 ray traces. The omission of other model keywords, such as TR.MATRIX, FDTD, or BPM, signifies that ray tracing will be performed.

For LUMINOUS2D, the algorithm automatically traces exactly the right number of rays to completely resolve all discontinuities at the surface and deep into the device. In 3D, you must specify enough rays to resolve the geometry in the NX and NZ parameters.

With ray tracing, you can also specify anti-reflection coatings using the INTERFACE statement as discussed in Section 10.9: “Anti-Reflective (AR) Coatings for Ray Tracing and Matrix Method”.

We recommend the transfer matrix method, as discussed in Section 10.3: “Matrix Method”, for simulation planar or (1D) devices where bulk interference effects may be of consequence. In these cases, the transfer matrix method provides fast accurate solutions for 1D analysis problems only.

To enable transfer matrix analysis, you need to add the TR.MATRIX parameter to the BEAM statement as in:

```
BEAM NUM=1 AM1.5 WAVEL.START=0.3 WAVEL.END=1.2 WAVEL.NUM=50 TR.MATRIX
```

We stress that the transfer matrix method is a one dimensional method and can only address variations in the Y direction. This should be adequate for much of the simulation problems addressed for planar thin film devices.

In the same way, you define anti-reflection coatings in ray tracing, you can also use the INTERFACE statement to define anti-reflection coatings (see Section 10.9: “Anti-Reflective (AR) Coatings for Ray Tracing and Matrix Method”) for the transfer matrix method.

For textured thin film devices, we have implemented a hybrid transfer matrix– 1D ray tracing method. In this case, interfaces can be characterized by haze functions defining the proportion of light transmitted and reflected as diffuse versus specular light and angular distribution functions describing the angular intensity of diffuse light. These are bulk characteristics and you should define the device as a planar structure as if you were applying the 1D transfer matrix method. These haze and angular distribution functions are described in the `INTERFACE` statement as illustrated in the following example:

```
INTERFACE OPTI P1.X=0 P2.X=1 P1.Y=0 P2.Y=0 DIFF ELLIPSE SEM=.31 SIG=20
```

Here, the optical interface, `OPTI`, defined along two points `P1.X`, `P1.Y` and `P2.X`, `P2.Y`– is treated as a diffusive (textured) interface as signified by the `DIFF` parameter. The angular distribution function is elliptical as indicated by the `ELLIPSE` parameter with a semi-major axis of 0.31.

The interface haze function is characterized by a mean roughness length of 20 nm as specified by the `SIG` parameter. This parameter can be correlated to measured surface variations from SEM photomicrographs.

To enable the diffusive transfer matrix model, you should specify `DIFFUSE` on the `BEAM` statement as in the following:

```
BEAM NUM=1 AM1.5 WAVEL.START=0.3 WAVEL.END=1.2 WAVEL.NUM=50 TR.MAT DIFFUSE
```

The diffusive transfer matrix method is discussed in detail in Section 10.3.4: “Transfer Matrix with Diffusive Interfaces”.

For cases requiring full 2D or 3D analysis of coherence or diffraction effects, the finite difference time domain (FDTD) analysis should be used. This method provides the most accurate solutions for optical propagation problems but at the greatest computational expense. The FDTD method performs direct solutions to the electromagnetic equations of light propagation. To enable the FDTD model, you need to specify `FDTD` on the `BEAM` statement as in the following example:

```
BEAM NUM=1 AM1.5 WAVEL.START=0.3 WAVEL.END=1.2 WAVEL.NUM=50 FDTD
```

There are many additional parameters which should be set for FDTD analysis. These parameters are described in detail in Section 10.5: “Finite Difference Time Domain Analysis [269]”.

10.13.3: Solar Cell Extraction

Here, we will describe how to extract the most common figures of merit for solar cells. These extraction methods are solution strategies placed in your input deck after defining the device structure, physical models, and the optical source as described in the previous section.

Typically, the first step in solar analysis is to illuminate the device. You can turn on the illumination by assigning the beam intensity on a SOLVE statement as follows:

```
SOLVE B1=1.0
```

Here, we assign a value of one "sun" to the intensity of the optical source indexed as number "1" (B1).

As we had assigned AM1.5 on the BEAM statement, this corresponds to standard test conditions. In some cases, we may encounter convergence difficulties and may need to ramp the light intensity as shown in the following:

```
SOLVE B1=0.01
SOLVE B1=0.1
SOLVE B1=1.0
```

You may also choose to assign the beam intensity to a value greater than one to simulate solar concentrator effects. Since we have not yet assigned any bias voltages, the current in the run time output corresponds to the short circuit current (I_{sc}).

The next step is to extract the illuminated, forward current-voltage characteristic. First, we should define an output file for capturing the data. For example:

```
LOG OUTFILE="IV.LOG"
```

This specifies that all current voltage characteristics extracted from any following SOLVE statement will be captured in the file IV.LOG in the current working directory. To capture the I-V characteristic, you need to ramp the voltage past the open circuit voltage (V_{oc}) as in the following:

```
SOLVE VANODE=0 NAME=ANODE VSTEP=0.1 VFINAL=0.5
SOLVE NAME=ANODE VSTEP=0.01 VFINAL=0.7
```

Here we assume that the anode is P type and the characteristic is extracted on positive anode voltages. First, we ramp from 0 to 0.5 volts in 0.1 volt steps. Then, we ramp from 0.51 to 0.7 volts in 0.01 volt steps. We assume that the open circuit voltage is near to 0.7 volts. We chose the shorter voltage step in the second SOLVE statement to improve accuracy in obtaining V_{oc} . Essentially, we will resolve V_{oc} to an accuracy comparable to the final voltage step size.

The current-voltage characteristic is observable in TONYPLOT using the following:

```
TONYPLOT IV.LOG
```

We can now use the DECKBUILD Extract capability to capture the various solar cell figures of merit. We first initialize the Extract capability with the captured input file as in the following:

```
EXTRACT INIT INFILE="IV.LOG"
```

The following lines demonstrate the extraction of short circuit current (I_{sc}), open circuit voltage (V_{oc}), maximum power (P_m), voltage at maximum power (V_m), current at maximum power (I_m), and fill factor (FF).

```
EXTRACT NAME="Isc" Y.VAL FROM CURVE(V."anode", I."cathode") WHERE X.VAL=0.0
EXTRACT NAME="Voc" X.VAL FROM CURVE(V."anode", I."cathode") WHERE Y.VAL=0.0
EXTRACT NAME="Pm" MAX(CURVE(V."anode", (V."anode" * I."cathode")))
EXTRACT NAME="Vm" X.VAL FROM CURVE(V."anode", (V."anode"*I."cathode") ) \
    WHERE Y.VAL=$"Pm"
EXTRACT NAME="Im" $"Pm"/$"Vm"
EXTRACT NAME="FF" $"Pm"/($"Jsc"*$"Voc")
```

Given that we know the area of the device in square cm, we can assign it to a variable and extract power efficiency as follows:

```
SET area=1e4
EXTRACT NAME="OPT_INT"    MAX(BEAM."1")
EXTRACT NAME="POWER_EFF"  (ABS("$Pm")/($OPT_INT*$area))
```

Here, OPT_INT is the optical intensity in W/sqcm.

It is also common to extract spectral response of solar cells. In this case, the source is monochromatic so we can omit the inclusion of a source spectrum, such as AM1.5, and instead define a single wavelength as in the following:

```
BEAM NUM=1 WAVELENGTH=0.3
```

Here, the wavelength of choice is not important since we will define the extraction wavelength on the SOLVE statement. Again, we should open an output file to capture the data as in the following:

```
LOG OUTFILE="SPECTRUM.LOG"
```

Then, we can simply capture the spectral response using a wavelength ramp defined on the SOLVE statement as follows:

```
SOLVE B1=0.001 BEAM=1 LAMBDA=0.3 WSTEP=0.02 WFINAL=1.2
```

Here, the B1 parameter sets the intensity to 1 mW. The BEAM parameter identifies the index of the optical source that is going to be involved in the wavelength ramp. LAMBDA specifies the initial wavelength in microns, WFINAL specifies the final wavelength in microns, and WSTEP specifies the wavelength step in microns.

We can then observe the spectral response file using TONYPLOT as follows:

```
TONYPLOT SPECTRUM.LOG
```

If you had specified a spectrum file (or AM0 or AM1.5) on the BEAM statement, then the value of the B1 parameter is multiplied by the intensity interpolated from the spectrum file at the specified wavelengths.

This page is intentionally left blank.

11.1: Overview

LED is a simulator within the ATLAS framework that provides general capabilities for simulation of light emitting diode (LED) devices. When used with the BLAZE simulator, LED supports the simulation of DC and transient electrical and light emitting characteristics of LEDs. When used with the GIGA simulator, LED permits the self-consistent analysis of thermal effects on both electrical and optical emission characteristics. You can also use the LED simulator with the MIXEDMODE simulator to analyze the circuit level performance of LED devices.

The LED simulator supports simulation of both zincblende (e.g., AlGaAs/GaAs, InGaAsP/InP) as well as wurtzite (e.g., GaN/AlGaN/InGaN) material systems. It can also account polarization effects and the effects of strain on both emission spectra and piezoelectric polarization.

Extraction of electrical characteristics, such as DC, transient and small signal response, is augmented by the capability to extract light emitting characteristics, such as emission power versus current, emission spectra, emission wavelength, efficiency and output coupling (a function of emission angle).

The following sections describe how to specify LED devices, how to select and specify physical models including most importantly the optical models and how to extract the most pertinent device characteristics for device performance optimization.

11.2: Defining Light Emitting Devices (LEDs)

There are several ways to define an LED device structures in ATLAS/LED. First, you can define a structure using the ATHENA process simulator. ATHENA simulates the "construction" of devices by simulating the process flow and the physical process steps. Second, you can define the device structure using the DEVEDIT device builder tool. The DEVEDIT tool allows you to specify the device structure in a simple visual point and click environment. Finally, you can define device structures using ATLAS framework commands (statements). For LED devices, the ATLAS command language approach is probably the most convenient since the device structures are somewhat simple due to their epitaxial nature.

In the following sections, we will concentrate on definition of the device structure using the ATLAS command syntax. We recommend that you read Chapter 2: "Getting Started with ATLAS" where we describe general features of the ATLAS simulator, commands and structure definition before you proceed. Chapter 3: "Physics" also provides insight into the details of the electrical and optical physical models used by ATLAS/LED. Chapter 5: "Blaze: Compound Material 2D Simulator" describes some general physics of simulation of compound semiconductors and heterojunctions.

Within the ATLAS command syntax, there are two approaches for defining device structures. The general purpose structure definition approach (see Chapter 2: "Getting Started with ATLAS", Section 2.6.3: "Using The Command Language To Define A Structure") requires more user-specification and requires that you describe the entire mesh. The auto-mesh approach (see Chapter 2: "Getting Started with ATLAS", Section 2.6.4: "Automatic Meshing (Auto-meshing) Using The Command Language") is simpler to use, requires less user-specification and is particularly well-suited to specification of epitaxial (especially multiple-quantum well or super-lattice) devices. It is for these reasons that we recommend the auto-mesh approach when defining LED devices .

In the following sections, we will focus mainly on this approach. We will point out important differences with the other methods: ATHENA, DEVEDIT or manual-mesh as these differences may arise.

The first command in any ATLAS input deck is the MESH command. When loading a structure from ATHENA, DEVEDIT or a previous ATLAS simulation, you should assign the INFILE parameter of the MESH statement to the name of the file containing the device structure. For example:

```
MESH INFILE=led.in
```

would cause the simulator to load a device structure from the file named led.in in the current working directory. When defining the device structure in the ATLAS auto-meshing syntax, the first statement should contain the AUTO parameter as shown in the following statement:

```
MESH AUTO
```

This will invoke the auto meshing capability.

Note: The INFILE parameter is not specified since this would indicate that the device was both being loaded as well as constructed in the ATLAS synta.x Therefore, would produce an ambiguity or conflict.

When using auto-meshing, you must only specify the mesh in the X direction using X.MESH statements. The mesh spacing in the Y direction is specified in the REGION statements as described later. The following example shows how you would specify an X mesh 1 μm long with a uniform mesh spacing of 0.1 μm .

```
X.MESH LOCATION=0      SPACING=100
X.MESH LOCATION=1000   SPACING=100
```

Using auto-meshing, you should next specify the device regions using `REGION` statements. The `REGION` statement can be used to specify the material types of individual "regions", as characterized by a spatial extent in the X and Y directions, and their composition, doping, strain and certain other characteristics describing how the region is to be modeled.

In the following example, we will describe a simple GaN/InGaN diode structure suitable for LED device simulation.

```
REGION MATERIAL=GaN    THICKNESS=0.25  ACCEPTOR=1e19  BOTTOM NY=20
REGION MATERIAL=InGaN  THICKNESS=0.003  DONOR=2e14   X.COMP=0.2  BOTTOM NY=20  LED
REGION MATERIAL=GaN    THICKNESS=0.25  DONOR=1e18   BOTTOM NY=20
```

In this example, we describe a three layer LED. The top layer is composed of GaN (`MATERIAL=GaN`), it has a thickness of 0.25 microns (`THICKNESS=0.25`) and has an acceptor concentration of $1e19$ (`ACCEPTOR=1e19`). The middle layer is composed of InGaN (`MATERIAL=InGaN`), it has a thickness of 0.003 microns (`THICKNESS=0.003`) cm^{-3} , has an In composition fraction of 0.2 (`X.COMP=0.2`), and has a donor concentration of $2e14$ (`DONOR=2e14`) cm^{-3} . The bottom layer is also composed of GaN (`MATERIAL=GaN`), it has a thickness of 0.25 microns (`THICKNESS=0.25`), and has a donor concentration of $1e18$ (`DONOR=1e18`) cm^{-3} .

The `BOTTOM` parameter in each of the `REGION` statements specifies that each region resides directly below the preceeding region. `NY` specifies the minimum number of Y grid lines used to resolve the region. The `LED` parameter in the second `REGION` statement specifies that region will be treated as a light emitting region during the post-processing stages of the simulation, and certain light emitting characteristics of that region will be extracted.

The final step in defining the LED using auto-meshing is to specify the electrodes. To specify electrodes, use the `ELECTRODE` statement. The following example specifies two electrodes extending all the way across the top and the bottom of the device.

```
ELECTRODE NUMBER=1 NAME=anode TOP
ELECTRODE NUMBER=2 NAME=cathode BOTTOM
```

Here, the `NUMBER` parameter is used to give the electrodes numerical tags they can be referred to in subsequent operations. Similarly, the `NAME` parameter is used for future references (see Chapter 21: "Statements", Section 21.53: "SOLVE").

11.3: Specifying Light Emitting Diode Models

11.3.1: Specifying Polarization and Piezoelectric Effects

In some material systems (such as the GaN/InGaN system), the built-in fields due to polarization and strain (piezoelectric effect) can play significant roles in the LED emission characteristics. ATLAS introduces these polarization fields as sheet charges at the top and bottom edges of regions. To include the effects of polarization on a region, you should specify the `POLARIZATION` parameter on the corresponding `REGION` statement.

This will only include spontaneous polarization. If you want to also include piezoelectric polarization, you can also specify the `CALC.STRAIN` parameter. If you specify `CALC.STRAIN`, the simulator will automatically calculate strain from the lattice mismatch and will calculate the piezoelectric polarization and apply it to the region. You can also specify the value of the `STRAIN` parameter, which specifies the axial strain in the region.

With `STRAIN` and `POLARIZATION` set, the simulator will apply a piezoelectric polarization calculated using the strain value assigned by the `STRAIN` parameter.

11.3.2: Choosing Radiative Models

The next step in simulating LED devices is the selection of appropriate radiative models. For LED devices, the most relevant radiative model is the model for spontaneous (radiative) recombination. For radiative recombination, ATLAS/LED offers several options. Chapter 3: “Physics”, Section 3.9: “Optoelectronic Models” discusses these options in more detail.

First, is the general radiative model (see Chapter 3: “Physics”, Equation). To enable this equation, specify `OPTR` in a `MODELS` statement associated with the active region(s) of the LED device (i.e., those regions with the `LED` parameter specified in the `REGION` statement). For our example, the LED discussed is shown in the following statement:

```
MODELS MATERIAL=InGaN OPTR
```

will enable the standard radiative recombination model. The disadvantage of using the standard model is that it provides no information about the spectral content of the LED light emission. In fact to properly specify emission intensity, you must specify the emission wavelength in the `SOLVE` statement for extraction of LED luminous intensity. To specify the emission wavelength for the general radiative recombination model given by Equation 3-327 in Chapter 3: “Physics”, assign the value of the wavelength to the `L.WAVE` parameter as shown in the following `SOLVE` statement, where `L.WAVE` is in units of microns.

```
SOLVE L.WAVE=0.51
```

The `COPT` parameter of the `MATERIAL` statement assigns the rate constant for the general radiative recombination model. For example:

```
MATERIAL COPT=1.25e-10
```

`COPT` assigned a value of $1.25 \times 10^{-10} \text{ cm}^3/\text{s}$ to the radiative rate constant. You can calibrate the value of this constant using the more physical radiative models discussed next. This calibration will be discussed at the end of this section.

Beyond the basic model just described, ATLAS/LED provides three more physical models for radiative rates. For zincblende materials, ATLAS provides a one band model [266] and a two band [140] model. For wurtzite materials, ATLAS/LED provides a three band model [43].

The one band zincblende model by Yan *et.al.* [266] accounts for optical transitions between a single valence band and the conduction band. To activate this model, specify `YAN` in the `MODELS` statement. See Chapter 3: “Physics”, Section 3.9.7: “Unstrained Zincblende Models for Gain and Radiative Recombination” for a discussion of the Yan model.

The two band zincblende model by [140] accounts for optical transitions between light and heavy hole valence bands and the conduction band. To activate this model, specify `LI` in the `MODELS` statement. See Chapter 3: “Physics”, Section 3.9.7: “Unstrained Zincblende Models for Gain and Radiative Recombination” for a discussion of the `LI` model.

The three band wurtzite model [43] is based on k.p modeling and accounts for optical transitions between the conduction band and heavy and light hole and the crystal field split-off valence bands. See Chapter 3: “Physics”, Section 3.9.9: “Strained Wurtzite Three-Band Model for Gain and Radiative Recombination” for a discussion of the Chuang model. To activate this model, specify `CHUANG` in the `MODELS` statement. For the on-going example, we chose the following `CHUANG` model (since InGaN is a wurtzite material).

```
MODEL MATERIAL=InGaN CHUANG
```

You should note that any of the `YAN`, `LI` or `CHUANG` model can be used to analyze spectral characteristics, such as emission wavelength and emission spectra.

You can also choose to analyze LED efficiency degradation due to competing recombination mechanisms by enabling these other non-radiative mechanisms. Particularly, you can enable Shockley-Read-Hall or Auger mechanisms. To activate these models, specify `SRH` and `AUGER` in the `MODELS` statement as follows:

```
MODELS SRH AUGER
```

Make sure you do not enable two radiative mechanisms for the same region, such as `OPTR` and one or more of the `YAN`, `LI` or `CHUANG` models. If you do, you may over account for the same radiative recombination. For more information about recombination models, see Chapter 3: “Physics” Section 3.6.3: “Carrier Generation-Recombination Models”.

As mentioned before, you can calibrate the radiative rate constant (using `COPT` of the `MATERIAL` statement) of the basic radiative recombination model (enabled by the `OPTR` parameter of the `MODELS` statement) to the more physical models (`YAN`, `LI` or `CHUANG`). To do this, first prepare a simulation with the activated physical model. In this simulation, save a structure file around the device operating conditions. You can then extract the proper value of `COPT` to use with the `OPTR` model by dividing the radiative recombination rate at any point by the product of the electron and hole concentrations.

11.3.3: Using k.p Band Parameter Models in Drift Diffusion

For the Chuang model, the band calculations performed in Equations 3-565, 3-566, 3-567 and 3-569 can be used in the drift diffusion part of the simulation. To use this capability, specify the `K.P` parameter on the `MODELS` statement as follows:

```
MODELS CHUANG K.P
```

11.4: Data Extraction

11.4.1: Extracting Luminous Intensity

When the LED parameter is specified on any REGION statement, the luminous intensity emitted by the LED device is automatically calculated and written to the log file. The file that this information is output to is specified by the OUTFILE parameter of the LOG statement. The following example outputs the log file to the file led.log.

```
LOG OUTFILE=led.log
```

You can then load led.log into TONYPLOT for post-processing visualization, where you can plot characteristics, such as luminous intensity versus current (see Figure 11-1).

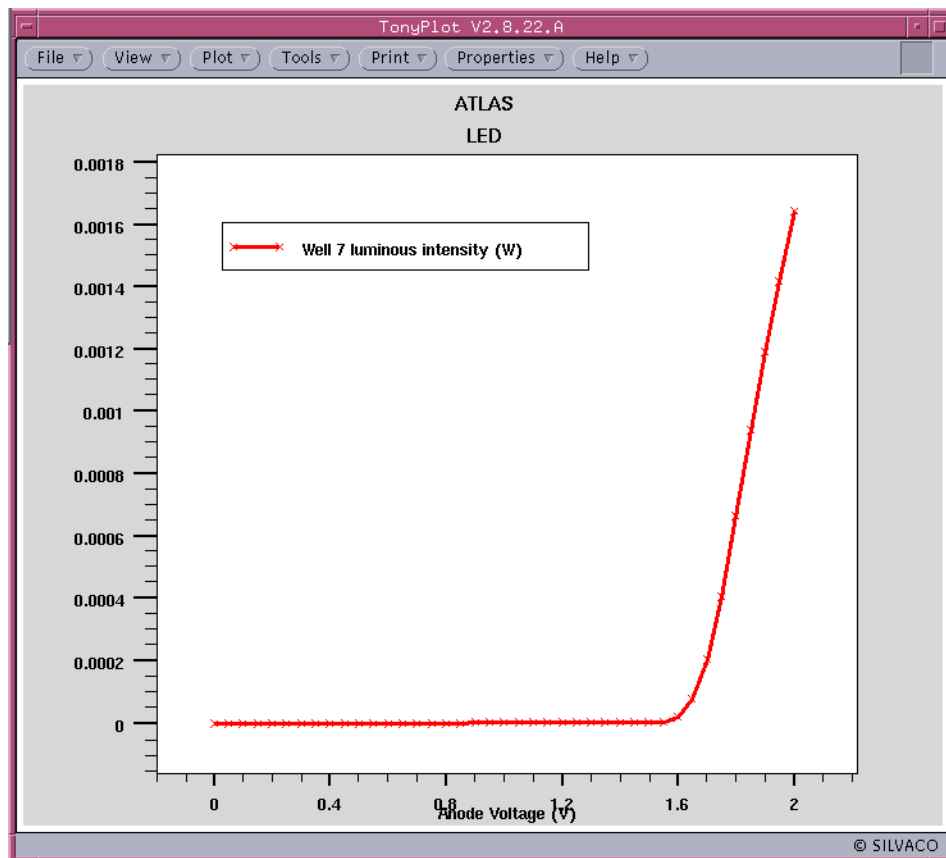


Figure 11-1: Example Luminous Intensity Plot

Note: Luminous intensity is calculated by integrating the luminous spectrum obtained by models containing spectral content (e.g., MODELS CHUANG SPONT). This does not include other non-spectral models (e.g., MODELS OPTR).

11.4.2: Extracting Emission Spectra

The LED simulator can save multiple spectrum files from the SOLVE statement. To save a spectrum file, specify the SPECTRUM parameter after each solution. SPECTRUM is assigned to the file name prefix. Each subsequent file will be written to a file named by SPECTRUM and appended with a version number starting at 0.

The LED simulator can output spectral intensity as a function of energy and wavelength integrated over all wells specified as LEDs. To output spectral intensity, specify the SPECTRUM parameter of the SAVE statement. SPECTRUM is assigned to the name of a file that the LED spectrum is written.

You must also specify either LMIN and LMAX or EMIN and EMAX. LMIN and LMAX specify the minimum and maximum values of wavelength in microns to be captured. EMIN and EMAX specify the minimum and maximum values of energy in eV to be captured. Specify either energy range or wavelength range but not both. To capture the number of discrete samples, specify the NSAMP parameter of the SAVE statement.

Figure 11-2 shows an example spectrum file plotted in TONYPLOT.

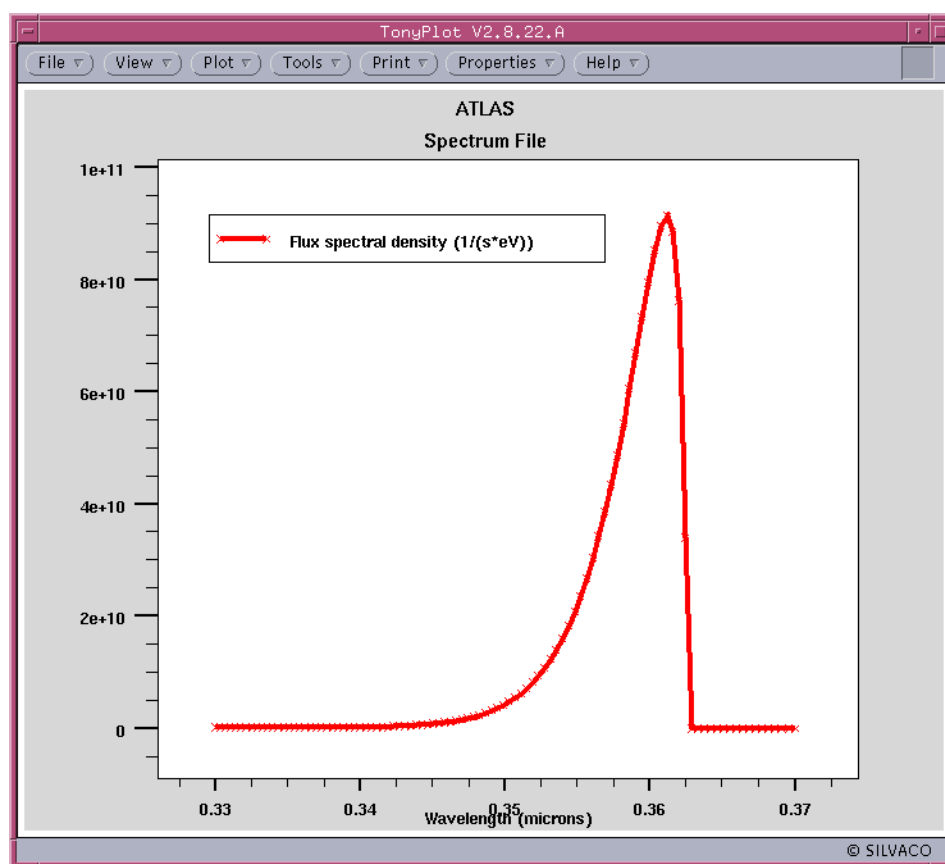


Figure 11-2: Plot of Spectrum File for LED

Note: Emission spectra can only be obtained using a spectral model (e.g., MODELS CHUANG SPONT).

11.4.3: Extracting Emission Wavelength

In the LED simulator, you can use the probe to measure wavelength for LED devices. This will extract the wavelength from the peak of the spectral response over a specified range. To use this capability, specify `WAVELENGTH` in the `PROBE` statement. Use either `EMIN` and `EMAX` or `LMIN` and `LMAX` in the `PROBE` statement to specify the search range. `EMIN` and `EMAX` specify the range in terms of energy in eV, while `LMIN` and `LMAX` specify the range in terms of wavelength in microns.

11.5: Reverse Ray-Tracing

Reverse ray-tracing is a technique that allows you to obtain optical output characteristics of an active optoelectronic device based on material properties and device geometry. Direct ray-tracing is commonly used for modeling of passive optoelectronic components, such as photo-detectors.

In direct ray-tracing, rays originating at the external light source are traced into the device and are absorbed to form electron/hole pairs, which are subsequently detected (using the ray-tracing method in LUMINOUS is described in Chapter 10: “Luminous: Optoelectronic Simulator”, Sections 10.2.1: “Ray Tracing in 2D” and 10.2.2: “Ray Tracing in 3D”). Unlike direct ray-tracing, the rays in the reverse method originate inside the active region and are traced until they exit the device. One or multiple origin points (user specified) for rays are considered, and interference effects for rays originating at the common source point can be taken into account. When you enable interference, you can analyze the spectral selectivity of the device structure by performing ray-tracing at multiple wavelengths.

You can assess light extraction from the device by using the `SAVE` statement (after biasing). Five different sets of parameters for reverse ray-tracing are used in the examples throughout the section to demonstrate the features available for modeling LEDs. The parameter sets are given in the order of increasing complexity of simulation. Computation times also vary. It takes approximately 200 times longer to run the last `SAVE` line compared to the first one.

Set the `ANGPOWER` parameter in the `SAVE` statement to start the reverse ray-tracing algorithm. The name of the output file containing the angular power density vs. output angle dependence is specified as a value for `ANGPOWER`. The information in the `angpower` file includes the angular power density for TE- and TM- polarized light and total angular power density and total flux angular density vs. output angle.

Note: In TonyPlot, polar charts show the Y axis directed upward (in the opposite direction to the internal coordinate system used in ATLAS). Therefore, the plots will appear to be flipped around X axis (top of the structure is at the bottom of the chart).

The `RAYPLOT` parameter specifies the name of the output file containing the information on each ray exiting the device. This file is only created when single origin for all rays is assumed. The information includes ray output angle, relative ray power (TE-, TM-polarization, and total), and initial internal angle at the origin (only if `INTERFERE` parameter is not specified). 0° angle corresponds to the rays in the X axis direction. 90° angle corresponds to the rays in the Y axis direction.

To start ray-tracing from one point of origin, specify the origin's coordinates for rays X and Y and the wavelength `L.WAVE`. It is important to choose the origin in the active region of the device. Rays are not traced if the radiative recombination is zero at the ray origin. All remaining parameters outlined below are optional and their default values are assumed if the parameters are not specified.

`REFLECTS` specifies a number of reflections to be traced for each ray originating at the point (X,Y) (similar to `REFLECTS` parameter in the `BEAM` statement). The default value (`REFLECTS=0`) provides for a quick estimate of the coupling efficiency. To obtain a more accurate result, use `REFLECTS>0`, especially if you specify `MIR.TOP` or `MIR.BOTTOM`. The choice of this parameter is based on a compromise between calculation time and accuracy. The maximum allowed value is `REFLECTS=10`. Number of reflections set to 3 or 4 is often a good choice. Example 1 produces a simple ray-tracing analysis of an LED. Figure 11-3 shows the resulting angular distribution of the emitted light intensity.

Example 1

```
SAVE    ANGPOWER=OPTOEX18ANG_1.LOG    RAYPLOT=OPTOEX18RAY_1.LOG    X=2.0    Y=1.01
L.WAVE=0.9  REFLECTS=4
```

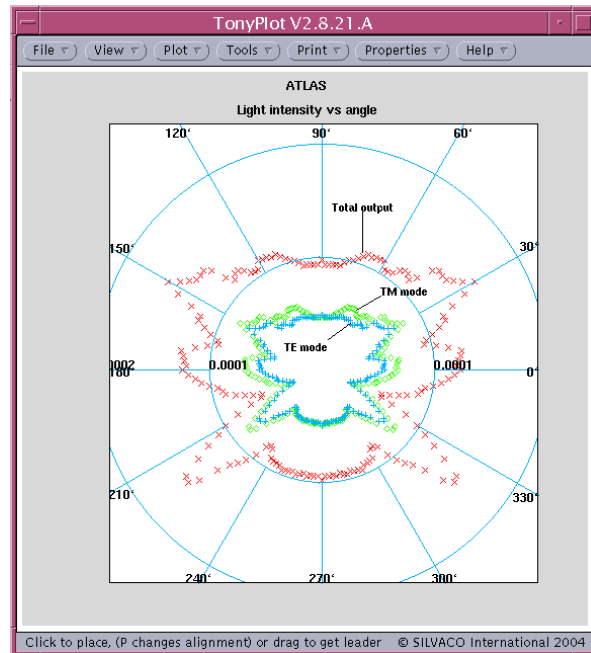


Figure 11-3: Emitted Light Intensity vs Angle for Example 1

Specify the `DIPOLE` parameter to turn on a particular angular distribution of the internal radiating field that corresponds to a preferred in-plane orientation of dipoles. This orientation is often found in polymer based OLEDs and results in higher optical output coupling. The default setting (`DIPOLE=false`) corresponds to isotropic distribution of emitting dipoles and spherically symmetric radiation pattern.

`MIR.TOP` specifies that the top surface of the device be treated as an ideal mirror.

`MIR.BOTTOM` specifies that the bottom surface of the device be treated as an ideal mirror.

`SIDE` specifies that the rays reaching the sides of the device terminate there and do not contribute to the total light output. This is often a good assumption for realistic LEDs as these rays tend to be either absorbed internally or blocked by the casing of the device.

`TEMPER` is the temperature (needed for using appropriate refractive indexes of the materials). The default setting of 300 K will be used if `TEMPER` is not specified.

`POLAR` specifies polarization of the emitted photons in degrees (linearly polarized light is assumed). Parallel (TM-mode, `POLAR=0.0`) and perpendicular (TE-mode, `POLAR=90.0`) polarizations result in significantly different output coupling values.

You should use the default value (`POLAR=45.0`) if there is no preferred direction of polarization of emitted photons (unpolarized light emission).

`MIN.POWER` specifies the minimum relative power of a ray (similar to `MIN.POWER` parameter in the `BEAM` statement). The ray is not traced after its power falls below `MIN.POWER` value. This is useful for limiting the number of rays traced. The default value is `MIN.POWER=1e-4`.

`NUMRAYS` specifies the number of rays starting from the origin. The default is 180. The acceptable range 36–3600.

Example 2 shows how some of the parameters described above are used for modeling of a realistic LED. The angular distribution of light power in Figure 11-4 exhibits almost a Lambertian pattern for this simple planar LED geometry. Note that optical coupling coefficient produced in this calculation reflects a 2D nature of the example (the light origin is not a point but rather an infinite line in Z direction).

Simultaneously, you can calculate the optical coupling efficiency for an axially symmetric 3D device. Normally, this is the value to be compared with experimental results. To do this, specify the COUPLING3D parameter (while SIDE is set). For this calculation, the light source is assumed to be a point located on the axis of symmetry.

Example 2

```
SAVE    ANGPOWER=OPTOEX18ANG_2.LOG    RAYPLOT=OPTOEX18RAY_2.LOG    X=2.0    Y=1.01
L.WAVE=0.9 SIDE MIR.BOTTOM NUMRAYS=360 REFLECTS=4
```

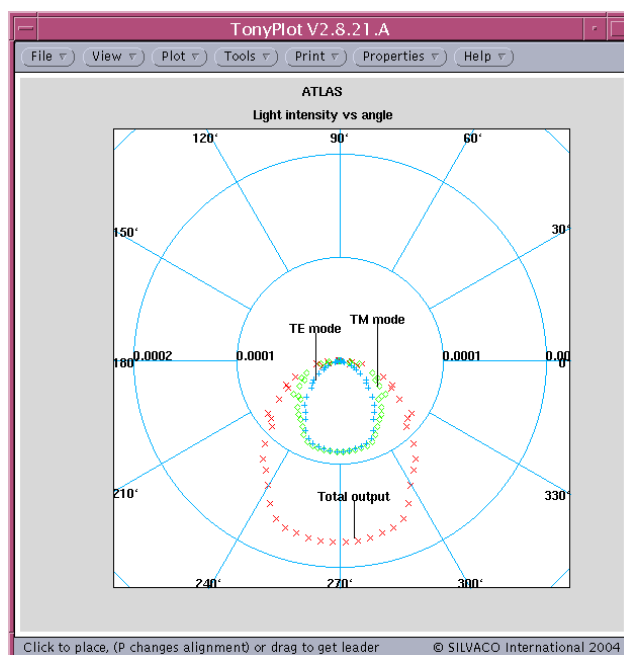


Figure 11-4: Emitted Light Intensity vs Angle for Example 2

The rays are assumed to be incoherent by default. This is a good approximation if the thickness of the active layer of the device is on the order of a wavelength/index. For layer thicknesses, smaller than the wavelength coherent effects might be important. When INTERFERE is set, the rays originating at the common source point are taken to be 100% coherent. In this case, the phase information upon propagation is preserved. Phase change upon reflection is also considered. Thus, interference of rays exiting the device at the same angle is taken into account. In this case, the internal angle information is not written to the output rayfile.

Example 3 takes into account interference. Figure 11-5 shows the result. You can take absorption of rays into account by setting the ABSORB parameter. The absorption is assumed to be specified for each material by the imaginary part of the refractive index. Carrier density dependent absorption and photon-recycling are not considered at this point.

Example 3

```
SAVE    ANGPOWER=OPTOEX18ANG_3.LOG    RAYPLOT=OPTOEX18RAY_3.LOG    X=2.0    Y=1.01
L.WAVE=0.9    INTERFERE SIDE MIR.BOTTOM REFLECTS=4
```

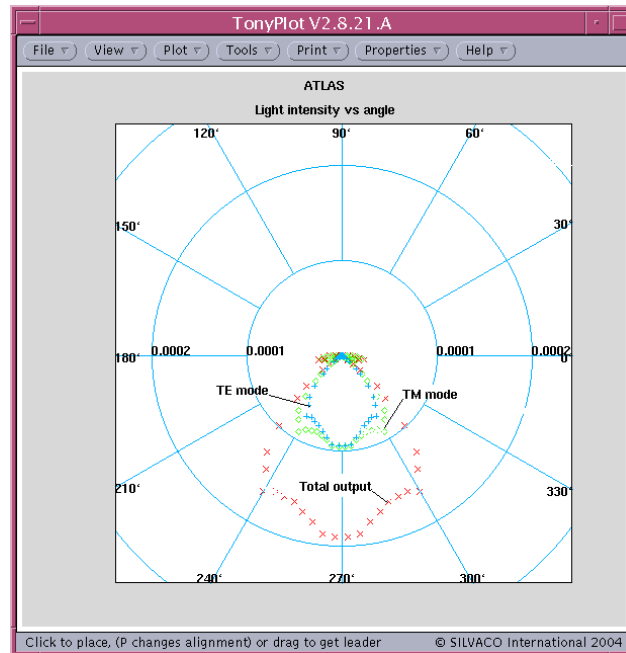


Figure 11-5: Emitted Light Intensity vs Angle for Example 3

Although ray-tracing from one point of origin can give a reasonable estimate of optical output coupling and angular distribution of light power, it is often desirable to consider multiple points within the active layer of the device to obtain more accurate results. To set multiple origin points, use the following parameters.

- XMIN, XMAX, YMIN, and YMAX define a rectangular area containing all origin points.
- XNUM and YNUM specify the number of points along x and y axes within the rectangular area. If XNUM=1, the X coordinate of all origin points will be set to XMIN so that the points are chosen along the line X=XMIN. Similarly, you can choose points along the specific y-line.

Ray-tracing from multiple origins is realized by repeating single origin algorithm for each point and by adding up the normalized angular power density values thus obtained. The luminous power assigned to each source (origin) is proportional to the radiative recombination at that point. The luminous power of all sources adds up to the value obtained by integration of radiative recombination over the entire device. Rays originating at different source points are completely incoherent (even when INTERFERE is set), which is consistent with the spontaneous character of the radiation produced by an LED. The rayplot file is not written for multiple origins (even if RAYPLOT parameter is set). Example 4 shows how multiple origin simulation can be done. Figure 11-6 shows angular distribution of light obtained in this case.

Example 4

```
SAVE  ANGPOWER=OPTOEX18ANG_4.LOG  XMIN=1.0  XMAX=3.0  XNUM=3  YMIN=1.01  YMAX=1.09
YNUM=9  INTERFERE  SIDE  L.WAVE=0.9  MIR.BOTTOM  REFLECTS=4
```

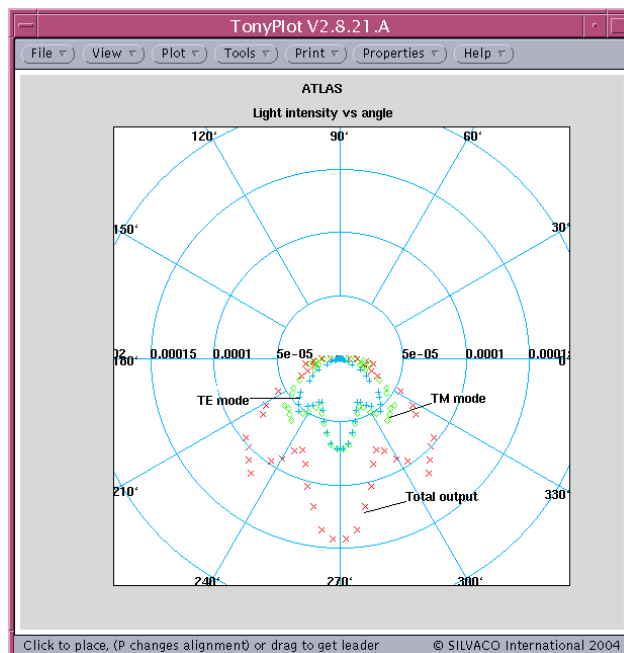


Figure 11-6: Emitted Light Intensity vs Angle for Example 4

You can also take spectral selectivity of optical output coupling for LEDs into account. Reverse ray-tracing at multiple wavelengths is considered if the `SPECTRUM` parameter specifies a filename for spectral selectivity output while the `ANGPOWER` parameter is set.

`EMIN` and `EMAX`, or `LMIN` and `LMAX` specify the energy or wavelength range respectively.

`NSAMP` specifies the number of spectral components to be considered. We suggest that you specify the `SPECTRUM` file only when `INTERFERE` is set. Otherwise, a warning will be issued during ray-tracing. When `ANGPOWER` and `SPECTRUM` are set in the `SAVE` statement, the resulting optical output coupling is averaged over the entire energy (wavelength) range from `EMIN` to `EMAX` (from `LMIN` to `LMAX`). The same applies to the quantities in the output angular distribution file. The spectrum file only shows how output coupling changes with wavelength. Currently, the shape of the gain curve is not taken into account (flat gain).

Example 5 shows how to use multiple spectral components. Figure 11-7 shows that the results obtained after averaging over spectral components and multiple origin points while taking interference into account are similar to the single point source model, where interference and multiple spectral content are ignored (Example 2). This demonstrates the applicability of a simpler model in this case.

Example 5

```
SAVE  ANGPOWER=OPTOEX18ANG_5.LOG  SPECTRUM=OPTOEX18SP_5.LOG  XMIN=1.0  XMAX=3.0  
XNUM=3  YMIN=1.01  YMAX=1.09  YNUM=5  INTERFERE  SIDE  LMIN=0.86  LMAX=0.94  NSAMP=15  
MIR.BOTTOM  REFLECTS=4
```

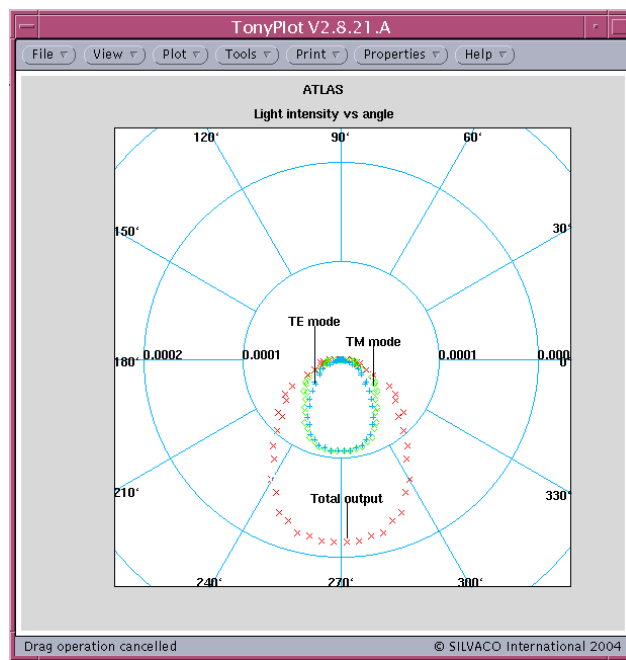


Figure 11-7: Emitted Light Intensity vs Angle for Parameter Set 5

11.6: The LED Statement

The LED statement can be used as a convenient method to perform all of the above mentioned SAVE operations automatically after each solution step.

The parameter names are the same as the individual SAVE statements. By default, the files named by the SPECTRUM, ANGPOWER and SPECT.ANGLE parameters of the LED statement will given unique incremented names at each save. This may generate many files. If you want to save only the last version of each file, specify the ONEFILE parameter of the LED statement.

11.6.1: User-Definable Emission Spectra

For some materials (particularly organics), the radiative models for emission spectra may be inadequate. In these cases, you can specify up to two user-definable emission spectra. These emission spectra are defined using a simple tabular description and is stored in a file separate from the input deck. The file contains first a line containing one number representing the number of wavelength-intensity pairs to follow. The wavelength-intensity pairs are lines with two numbers in them, the wavelength in microns and the relative intensity in Watts. The absolute intensity is not important since the intensity values are normalized.

The following file fragment demonstrates the format:

```
12
0.4 .00142
0.42 0.00222
0.44 0.013
.
.
.
```

Here, the first line contains the number of samples, in this case 12. Then next line specifies that at 0.4 microns wavelength the relative intensity is 0.00142 Watts etc.

To use the user-defined spectra, assign the values of USER.SPECT or DOPE.SPECT or both to the appropriate file name. To output the user and dopant spectra to TONYPLOT compatible log files, specify OUT.USPEC and OUT.DSPEC.

This page is intentionally left blank.

12.1: Overview

MIXEDMODE is a circuit simulator that can include elements simulated using device simulation and compact circuit models. It combines different levels of abstraction to simulate relatively small circuits where compact models for single devices are unavailable or sufficiently accurate. MIXEDMODE also allows you to also do multi-device simulations. MIXEDMODE uses advanced numerical algorithms that are efficient and robust for DC, transient, small signal AC and small signal network analysis.

MIXEDMODE is typically used to simulate circuits that contain semiconductor devices for accurate compact models that don't exist or circuits where devices play a critical role must be modeled accurately. Applications of MIXEDMODE include: power circuits that may include diodes, power transistors, IGBTs, and GTOs, optoelectronic circuits, circuits subject to single event upset, thin film transistor circuits, high-frequency circuits, precision analog circuits, and high performance digital circuits.

MIXEDMODE circuits can include up to 200 nodes, 300 elements, and up to ten numerical simulated ATLAS devices. These limits are reasonable for most applications. But, they can be increased in custom versions on request to Silvaco. The circuit elements that are supported include dependent and independent voltage and current sources as well as resistors, capacitors, inductors, coupled inductors, MOSFETs, BJTs, diodes, and switches. Commonly used SPICE compact models are available. The SPICE input language is used for circuit specification.

This chapter describes circuit simulation capabilities rather than device simulation capabilities. The first part of the chapter contains introductory and background information. Then, describes presents and explains MIXEDMODE syntax. This is followed by some sample input decks. The final sections contain a statement reference and a detailed description of the provided electrical compact models for diodes, BJTs, and MOSFETs.

12.1.1: Background

Circuit simulators such as SPICE [11] solve systems of equations that describe the behavior of electrical circuits. The devices that are of interest to circuit designers are normally well characterized. Compact or circuit models are analytic formulae that approximate measured terminal characteristics. Advanced compact models provide high accuracy with minimum computational complexity. Device modeling, device characterization and parameter extraction are concerned with the development and use of accurate and efficient compact models.

Physically based device simulation solves systems of equations that describe the physics of device operation. This approach provides predictive capabilities and information about the conditions inside a device. It can, however, require significant amounts of CPU time. Information is usually transferred from device simulation to circuit simulation as follows: electrical characteristics are calculated using a physically-based device simulator. These calculated electrical characteristics are then used as input by a device modeling and parameter extraction package such as UTMOST [231]. The extracted parameters are used to characterize a compact model used by the circuit simulator.

This approach is adequate for many purposes but has limitations. It requires that satisfactory compact models already exist. The use of compact models always introduces some error. Models that are adequate for digital circuit simulation may be inadequate for other applications. Applications and devices for which compact modeling is not always satisfactory include: precision low power, high power, high frequency circuit simulation, SOI, IGBT, GTO, TFT, and optoelectronic devices.

12.1.2: Advantages of MixedMode Simulation

The limitations of compact models can be overcome by using physically-based device simulation to predict the behavior of some of the devices contained in a circuit. The rest of the circuit is modeled using conventional circuit simulation techniques. This approach is referred to as mixed-mode simulation, since some circuit elements are described by compact models, and some by physically-based numerical models.

MIXEDMODE simulation provides several worthwhile advantages. No compact model need be specified for a numerical physically-based device. The approximation errors introduced by compact models can be avoided particularly for large signal transient performance. You can also examine the internal device conditions within a numerical physically-based device at any point during the circuit simulation. But the cost is increased CPU time over SPICE as CPU time is comparable to a device simulation excluding the external circuit nodes. MIXEDMODE simulation normally uses numerical simulated devices typically only for critical devices. Non-critical devices are modeled using compact models.

12.2: Using MixedMode

Input file specification for MIXEDMODE is different in many respects to the rest of ATLAS. But if you're familiar with SPICE and ATLAS syntax, you should have little difficulty understanding how these two syntax styles are joined in MIXEDMODE.

Each input file is split in two parts. The first part is SPICE-like and describes the circuit netlist and analysis. The second part is ATLAS-like and describes the device simulation model parameters. These two sections of an input file are separated as described in the next section.

The circuit description includes the circuit topology (called the netlist) and the electrical models and parameters of the circuit components. The simulation conditions specify the types of analysis to be performed. These items are described using syntax based on SPICE.

The ATLAS device descriptions provide information about device geometry, doping distribution, and meshes. Device descriptions can be prepared using the built-in ATLAS syntax, the ATHENA process simulator, or the DEVEDIT structure specification and meshing tool. You can also read-in previously calculated device solutions. The device data is read-in from standard structure format files.

When a simulation has finished, the following information is available:

- I-V data (voltages in all circuit nodes and currents in all circuit branches).
- Internal distributions of solution variables (such as electron, hole, and potential distributions) within the numerical devices.

The results of previous runs of MIXEDMODE can be used as initial guesses for future simulations. This is particularly helpful when multiple simulations must be performed from the same starting point.

The accessing and running of examples for ATLAS are documented in the DECKBUILD USER'S MANUAL. We recommend that you run at least one MIXEDMODE example provided on the distribution tape before trying their own simulations.

12.2.1: General Syntax Rules

The SPICE-like part of any MIXEDMODE input file starts with the `.BEGIN` statement. The SPICE-like part of the input file ends with `.END`. All parameters related to the device simulation models appear after the `.END` statement. To start MIXEDMODE3D, specify the `3D` parameter in the `BEGIN` statement.

The first non-comment statement after initializing ATLAS (`go atlas`) has to be `.BEGIN`. The order of the following netlist and control statements is arbitrary. The last SPICE-like statement has to be `.END`.

Unlike the rest of ATLAS, for SPICE-like statements the exact command has to be used, unique abbreviations are not accepted. Statements are not case sensitive.

There has to be at least one numerical ATLAS device ("A" device) within the netlist.

Comment characters are `#` and `$`, but not `*`.

All ATLAS statements specifying the parameters for the numerical device simulation have to be specified after `.END`

After all ATLAS statements, the simulation has to be explicitly terminated (`quit`, `go <simulator>`).

These rules do not apply to the `SET` statement for parameterization of the input file, since it is interpreted by DECKBUILD only.

EXTRACT statements are also an exception similar to `SET`. Since MIXEDMODE input files are parsed completely before execution (see Section 12.2.4: "Recommendations" for more information), extractions can only be done after completion of the simulation. To extract results from a MIXEDMODE simulation, `EXTRACT` should be specified after re-initialization of ATLAS (`go atlas`).

12.2.2: Circuit and Analysis Specification

The SPICE-like MIXEDMODE statements can be divided into three categories:

- Element Statements: These statements define the circuit netlist.
- Simulation Control Statements: These statements specify the analysis to be performed.
- Special Statements: These statements typically related to numerics and output (first character being a dot ".").

The specification of the circuit and analysis part has to be bracketed by a .BEGIN and an .END statements. In other words, all MIXEDMODE statements before .BEGIN or after .END will be ignored or regarded as an error. The order is between .BEGIN and .END is arbitrary.

Netlist Statements

Each device in the circuit is described by an element statement. The element statement contains the element name, the circuit nodes to which the element is connected and the values of the element parameters. The first letter of an element name specifies the type of element to be simulated. For example, a resistor name must begin with the letter, R, and can contain one or more characters. This means that R1, RSE, ROUT, and R3AC2ZY are all valid resistor names. Some elements, such as diodes and transistors, must always refer to a model. A set of elements can refer to the same model. For some elements, such as resistors and capacitors, model referencing is optional. Each element type has its own set of parameters. For example, a resistor statement can specify a resistance value after the optional model name. The bipolar transistor statement (Q) can specify an area parameter. All parameters have corresponding default values. Independent voltage and current sources have different specifications for transient, DC, and AC phases of simulation. Transient specifications use the keywords: EXP, PULSE, GAUSS, SFFM, SIN, and TABLE. AC parameters start with the keyword, AC.

Elements to be simulated numerically are defined as "A" devices (ATLAS devices). At least one ATLAS device in a circuit is mandatory.

MIXEDMODE supports the use of the following circuit elements:

- Numerically simulated ATLAS devices ("A" devices)
- User-defined two-terminal elements ("B" devices)
- Capacitors ("C" devices)
- Diodes ("D" devices)
- Voltage controlled voltage source ("E" devices)
- Current controlled current source ("F" devices)
- Voltage controlled current source ("G" devices)
- Current controlled voltage source ("H" devices)
- Independent current sources ("I" devices, may be time dependent)
- JFETs ("J" devices)
- Coupled (mutual) inductors ("K" devices)
- Inductors ("L" devices)
- MOSFETs ("M" devices)
- Optical sources ("O" devices)
- Bipolar junction transistors ("Q" devices)
- Resistors ("R" devices, may be time dependent)
- Lossless transmission lines ("T" devices)
- Independent voltage sources ("V" devices, may be time dependent)
- MESFETs ("Z" devices)

The physical models for linear elements (resistors, capacitors, sources, and so on) are described Section 12.4.1: “Circuit Element Statements”. The models for diodes: BJTs, JFETs, MESFETs and MOSFETs are described in Section 12.4.2: “Control and Analysis Statements”. You can find more extensive documentation, however, in the SMARTSPICE/UTMOST MODELING MANUALS Volumes 1, 2, and 3.

A node is a point in the circuit where two or more elements are connected. A node can be described either in terms of a node name or as a node number. The node names and numbers are arbitrary with the exception of the ground node. The ground node is set either by specifying “0” as the node number or using the name GND. All voltages at the nodes are calculated with respect to the voltage at the ground node.

Example

The netlist for the circuit shown in Figure 12-1 is represented by the following MIXEDMODE input deck fragment.

```
# independent voltage source, 0.1V, connected to node 0 (GND) and 1:
V0      1          0          0.1

# 1kOhm resistor, connected to node 1 and 2
R1      1          2          1K

# ATLAS device, connected to node 2 (anode) and 0 (cathode),
# current scaled by 5e7, mesh from file dio.str
ADIO    2=anode    0=cathode  WIDTH=5e7  INFILE=dio.str
```

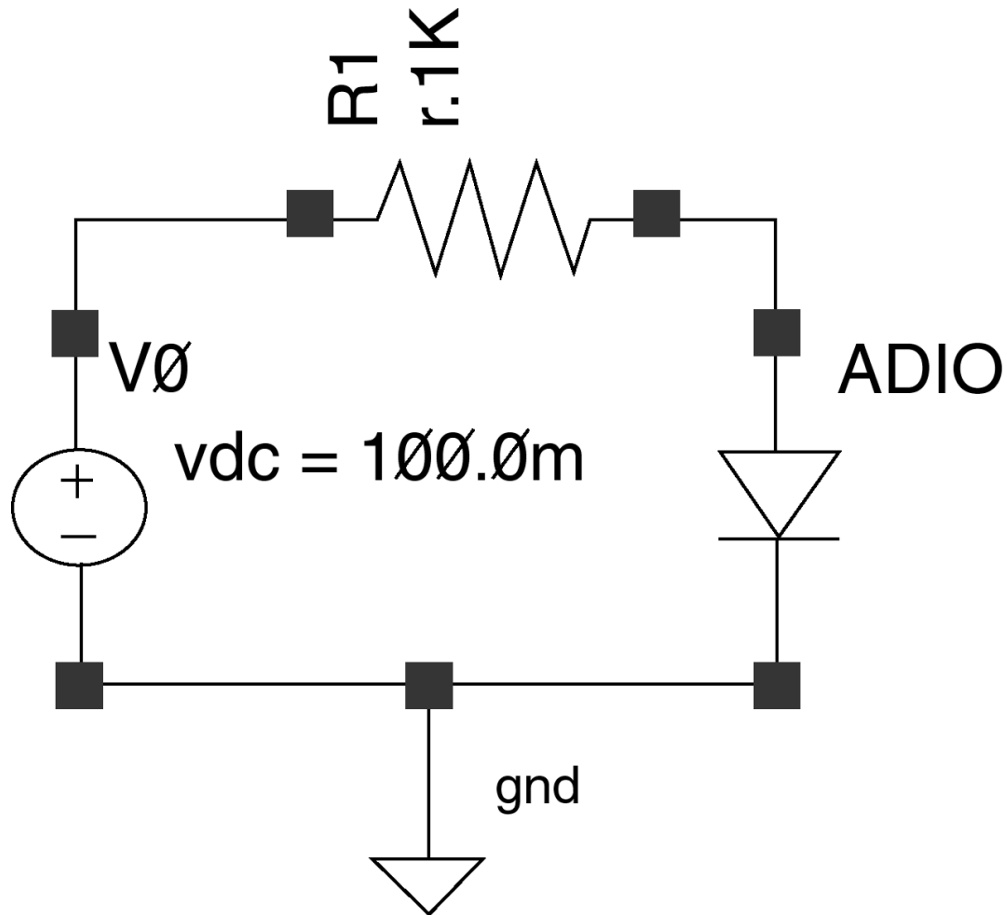


Figure 12-1: Schematic of Primitive Example Circuit

Control Statements

Control statements are used to specify the analysis to be performed in MIXEDMODE. These take the place of the SOLVE statements in a regular ATLAS input file. At least one of these statements must appear in each MIXEDMODE input file. These statements are:

- **.DC:** steady state analysis including loops
- **.TRAN:** transient analysis
- **.AC:** small signal AC analysis
- **.NET:** small signal parameter extraction (e.g., s-parameters)

If you wish to perform a DC analysis, you should have an associated DC source to relate the DC analysis to. Likewise, for an AC analysis you should have an associated AC source that you relate the AC analysis to. For a transient analysis, you should have an associated source with transient properties that you relate the transient analysis to. Failing to correctly run an analysis on the same sort of source could yield simulation problems, such as running an AC analysis on an independent voltage source where no AC magnitude for the source has been specified.

For more information about these statements, see Section 12.4.2: “Control and Analysis Statements”.

Special statements

Other statements beginning with a dot “.” specify special parameters for the circuit simulation. These include numerical options, file input and output, and device parameter output. These statements are listed below.

- compact device models (.MODEL)
- the output files (.LOG, .SAVE)
- initial conditions settings (.NODESET, .IC)
- initial conditions from a file (.LOAD)
- numerics (.NUMERIC, .OPTIONS)
- device parameter output (.PRINT)
- miscellaneous (.OPTIONS)

Full descriptions of each statement and associated parameters are found in Section 12.4.2: “Control and Analysis Statements”.

12.2.3: Device Simulation Syntax

The second part of a MIXEDMODE command file (after .END) is used to define physical models, material parameters, and numerical methods for ATLAS devices referenced in the “A”-element statements. The following statements may appear in this part of the command file: BEAM, CONTACT, DEFECT, IMPACT, INTERFACE, INTTRAP, MATERIAL, MOBILITY, METHOD, MODELS, OUTPUT, PROBE, TRAP, and THERMCONTACT.

You always need to include an indicator to the circuit element name in each device simulation statement even if there is only one A-device in the circuit. All statements specifying the device properties and models are just supplemented by the DEVICE=name parameter, where name is the circuit element in the netlist, and name will always begin with the letter “A”. This makes it possible to define different material properties and model settings for different devices within the circuit.

We recommended that you specify the REGION parameter referring to only one region in IMPACT, MATERIAL, and MODELS statements. If the device consists of more than one region, several statements with the same device parameters and different region parameters are recommended.

For example to specify the bipolar set of models to a device the syntax used might be:

```
MODEL DEVICE=AGTO REGION=2 BIPOLAR PRINT
```

12.2.4: Recommendations

Input Parsing

In regular ATLAS (non-MIXEDMODE) simulations, the input is interpreted line by line and each statement is executed immediately. This is very useful and nicely supported by DECKBUILD for the interactive development of the input. Circuit simulations, however, require the complete input before any simulation can be performed. Consequently, the following occur:

- The complete input is read and parsed before any simulation is initiated.
- An explicit termination of a simulation is required (quit).
- All post processing (extraction and plotting) has to be done after re-initializing ATLAS again.

No simulation is started until either a QUIT statement or a GO statement is seen in the input file. Post-processing can be done by restarting ATLAS.

Scale and Suffixes

In the MIXEDMODE part of the input, numerical values of parameters are represented in standard floating-point notation. The scale suffix may be followed by a unit suffix (e.g., A for Ampere, V for Volt, and so on). Using a unit suffix can increase the clarity of a command file. The unit suffix is ignored by the program. The scale suffixes are shown in Table 12-1.

| Table 12-1. Scale Suffixes | | |
|----------------------------|--------|--------|
| Factor | Name | Suffix |
| 10^{-15} | femto- | F |
| 10^{-12} | pico- | P |
| 10^{-9} | nano- | N |
| 10^{-6} | micro- | U |
| 10^{-3} | milli- | M |
| 10^3 | kilo- | K |
| 10^6 | mega- | MG |
| 10^9 | giga- | G |
| 10^{12} | tera- | T |

Numerics

MIXEDMODE solves circuit and device equations simultaneously using fully coupled algorithms. This provides better convergence and requires less CPU time than alternative approaches. The number of circuit variables is often small in comparison with the number of device variables. In this case, the CPU time required for simulation performed using MIXEDMODE does not increase drastically compared to the sum of the simulation times required for the individual numerical physically based devices. MIXEDMODE uses the Newton algorithm for each bias point during steady-state analysis and for each time step during transient analysis. Different variants of the Newton algorithm are used depending on the circumstances [153, 154]. The full Newton method [.OPTIONS FULLN] and a modified two-level Newton method [.OPTIONS M2LN] are available for steady-state simulation. The full Newton method provides rapid convergence when a good initial guess is available. The modified two-level Newton algorithm is less sensitive to the initial guess. For transient simulation, a good initial guess always exists. The full Newton method therefore works very well. Therefore, it is always used for transient simulation.

When using MIXEDMODE3D, it is recommended that you specify the DIRECT or GMRES solver in the ATLAS part of the MIXEDMODE input deck on the METHOD statement. Also, use the NOPROJ parameter in the .OPTIONS statement in the MIXEDMODE of the input deck.

Multi-Device Structure Representation

If more than one ATLAS device is defined in a MIXEDMODE simulation, the structures are merged together internally. The output solution file is a single file which contains both structures. The first structure referenced will be on top, all other structures will be attached below.

Example

A diode and a bipolar transistor are specified as numerical devices with the following element statements:

```
ABJT 1=BASE 2=EMITTER 4=COLLECTOR WIDTH=1E4 INFILE=bjt.str
ADIO 3=ANODE 4=CATHODE WIDTH=1.5E5 INFILE=dio.str
```


After outputting the solution with:

```
.SAVE MASTER=mas
```

The solution file for the first DC-point, mas_dc_1, contains both structures with the second ATLAS device (diode) shifted downwards (see Figure 12-2).

This coordinate shift has to be accounted for eventually when extracting position dependent solution quantities or when defining spatially dependent properties with the C-INTERPRETER (See Appendix A: “C-Interpreter Functions” for more information).

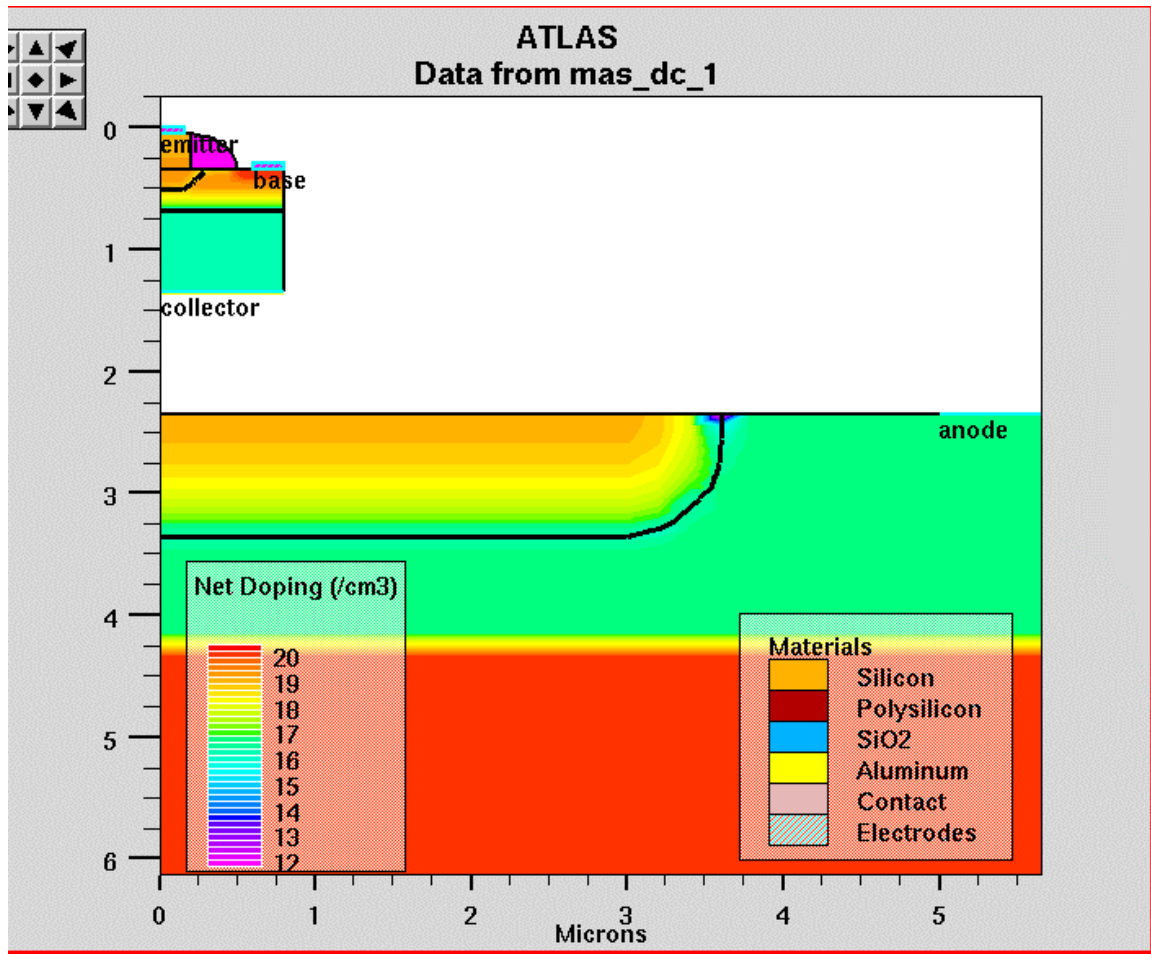


Figure 12-2: Display of a MixedMode solution with two Numerical Devices

Extraction of Results

By default, `EXTRACT` reads its data from the currently opened log-file when executed along with `ATLAS`. Since the extraction of `MIXEDMODE` log-files require a re-initialization of `ATLAS` (see “Input Parsing” section on page 12-7), `EXTRACT` has to be initialized explicitly with the correct name of the `MIXEDMODE` log file. To extract voltages at specific nodes, use the syntax `vcct.node."circuit node"`. To extract circuit elements, use `icct.node."circuit element"`.

Example

Specify the log file:

```
.LOG OUTFILE=hallo
```

Subsequent extraction from the transient log-file is done with:

```
go atlas

extract init inf="hallo_tr.log"

extract name="t0" x.val from curve(time,icct.node."Adio_anode") \
    where y.val=0
```

It extracts the time, `t0`, when the transient of the current from the anode electrode of the `adio` device in the circuit crosses zero. For more details for the `EXTRACT` syntax, see the `DECKBUILD USER'S MANUAL`.

Using MixedMode inside the VWF Automation Tools

Like all other Silvaco products, `MIXEDMODE` is fully integrated into the VWF framework and can be used for automated experiments. There are, however, some factors to take into account.

One factor is that the **auto-interface** feature doesn't work with `MIXEDMODE`. All structures have to be explicitly saved in unique files previous to the `MIXEDMODE` runs and referred to in the `A-` element statements. Another factor is that splits within `MIXEDMODE` runs are impossible. To overcome this problem, use the `SET` statement to define a variable in a process simulator or in the “dummy” internal run. This variable is used to parameterize the input file.

Example

Capacitance as an independent split variable in a VWF experiment.

```
go internal

# define the independent split variable in a re-entrant simulator:

set cap=5e-9

go atlas

.BEGIN

# use the variable as parameter in MixedMode:

C1    2    3    $cap
```

Another factor is that the automation tools only store files opened by the normal `ATLAS LOG` statement in the VWF database but ignore those defined by `.LOG`. To overcome this, re-initialize `ATLAS` and open the relevant log file of the previous `MIXEDMODE` run with `.log` as the append option (so that the file is not reset).

Example

MIXEDMODE log-file definition.

```
.LOG OUTFILE=hallo
```

Re-opening the second DC-log file and the transient log file to get them stored in the VWF database.

```
go atlas
```

```
log outfile=hallo_dc_2.log append
```

```
log outfile=hallo_tr.log append
```

Initial Settings

Initial convergence is critically dependent on the initial settings of the node voltages (i.e., `.IC` and `.NODESET`). There should not be any problem starting from the zero bias case. Just like starting from a preceding MIXEDMODE solution is simple, since the complete solution of the circuit and the ATLAS devices is directly available (i.e., `.LOAD` and `.SAVE`). But when loading solutions for the numerical devices from ATLAS, using `.OPTIONS LOADSOLUTIONS`, sometimes precise matching of the initial circuit condition is required. In this case, it is practical to extract the relevant properties in the preceding ATLAS run and use them to parameterize the MIXEDMODE input.

In the following example, the voltages and current of an ATLAS solution is extracted, and the results are used for the initial definition of the circuit.

The end of the first part is the stand-alone ATLAS simulation:

```
# extract the final voltage drop on the anode:
extract name="Von" max(vint."anode")

# extract the gate current:
extract name="I_gate" y.val from curve(vint."anode",i."gate") \
where x.val = $"Von"
extract name="V_gate" y.val from curve(vint."anode",vint."gate") \
where x.val = $"Von"

# now the MIXEDMODE part

go atlas

.BEGIN

# define the gate current source, use extracted value as parameter
I1 0 7 $"I_gate"

#

# use extracted gate bias and other expressions to calculate
# the node settings:
set Rgl = 10.5
set v7= $V_gate + $I_gate * $Rgl

.NODESET V(1)=2000 V(2)=$"Von" V(3)=$"V_gate" V(4)=$"V_gate" V(5)=-25 \
V(6)=-15 V(7)=$"v7"
```

12.3: A Sample Command File

A sample MIXEDMODE command file is shown below. This file is used to simulate the reverse recovery of a power diode. Several MIXEDMODE examples are provided with the product which can be accessed using DECKBUILD.

```
1. go atlas
2. .BEGIN
3. V1 1 0 1000.
4. R1 1 2 1m
5. L1 2 3 2nH
6. R2 4 0 1MG EXP 1MG 1E-3 0. 20NS 10 200
7. IL 0 4 300
8. ADIODE 3=cathode 4=anode WIDTH=5.E7 INFILE=pd.str
9. .NUMERIC LTE=0.3 TOLTR=1.E-5 VCHANGE=10.
10. .OPTIONS PRINT RELPOT WRITE=10
11. $
12. .LOAD INFILE=pdsave
13. .LOG OUTFILE=pd
14. .SAVE MASTER=pd
15. $
16. .TRAN 0.1NS 2US
17. $
18. .END
19. $
20. MODELS    DEVICE=ADIODE REG=1 CONMOB FLDMOB CONSRH AUGER BGN
21. MATERIAL  DEVICE=ADIODE REG=1 TAUN0=5E-6 TAUP=2E-6
22. IMPACT    DEVICE=ADIODE REG=1 SELB
23. $
24. METHOD     CLIM.DD=1.E8 DVMAX=1.E6
25. $
26. go atlas
27. tonyplot pd_tr.log
```

Description

Line 1: All ATLAS input files should begin with `go atlas`

Line 2: The `.BEGIN` and `.END` statements indicate the beginning and end of the circuit simulation syntax. These commands are similar to those used in SPICE.

Lines 3-7: Circuit components, topology, and analysis are defined within. Generally, the circuit component definition consists of three parts: the type of component, the lead or terminal mode assignments, and the component value or model name. For example, if the first component definition in this simulation is a DC voltage source, then `V1` defines the component as voltage source number one, 1 and 0 are the two circuit modes for this component, and 1000 indicates that the voltage source value is 1000 volts. The remaining circuit components are resistors (`R1`, `R2`) inductor (`L1`) and independent current source (`IL`).

The reverse recovery of the diode is simulated by dropping the value of output resistor `R2` over a small increment of time. The `R2` statement contains additional syntax to perform this task. Here, the resistor is treated as a source whose resistance decreases exponentially from 1 mOhm to 1 mOhm over the specified time step. This action essentially shorts out the parallel current source `IL`, which is also connected to the base of the diode.

Line 8: The `ADIODE` statement specifies a device to be analyzed by `ATLAS`. The `A` part of the `ADIODE` command specifies that this is a device statement. The `DIODE` portion simply defines the device name. The option `INFILE=` indicates which device structure file is to be used.

Lines 9-10: These set numerical options for the circuit simulation. `WRITE=10` specifies that every tenth timestep will be saved into the solution file specified on the `.SAVE` statement.

Line 12: Specifies a file generated by a previous `MIXEDMODE` simulation to be used as an initial guess to the voltage.

Line 13-14: Specifies the output log and solution filenames. These names are root names and extensions will be added automatically by the program.

Line 16: Indicates the type of analysis required. In this case, it is a transient simulation lasting 2 microseconds with an initial timestep of 0.1 nanoseconds.

Line 18: Indicates the end of the circuit description. All following statements will be related to the `ATLAS` device.

Lines 20-22: To completely specify the simulation, the physical models used by `ATLAS` must be identified. Note that `DEVICE=ADIODE` must be specified for each line. The `MODEL` statement is used to turn on the appropriate transport models. This set includes:

- `conmob`: the concentration dependent mobility mode,
- `fldmob`: the lateral electric field-dependent mobility model,
- `consrh`: Shockley-Read-Hall recombination using concentration dependent lifetimes,
- `auger`: recombination accounting for high level injection effects,
- `bgn`: band gap narrowing.

The `MATERIAL` statement is used to override default material parameters. In this case, the carrier recombination fixed lifetimes are set. Finally, the Selberherr impact ionization model is enabled using the `IMPACT` statement with the `SELB` option.

Line 24: The `METHOD` statement specifies numerical options for the device simulation. The `METHOD` statement must come after all other device simulation statements.

Line 26: The command `GO ATLAS` or a `QUIT` statement is needed to initiate simulation. Since a plot of the final log file is desired, the `GO ATLAS` option is used to restart `ATLAS` after the end of the `MIXEDMODE` simulation.

Line 27: The `TONYPLOT` command is used to plot the resulting log file.

12.4: MixedMode Syntax

This section is split into two parts. The first part describes circuit element statements, which describe the netlist. The second part describe the control and analysis statements.

12.4.1: Circuit Element Statements

A – ATLAS device to be simulated using device simulation

Syntax

```
Axxx n1=name1 n2=name2 [n3=name3 ...] infile=filename [width=val]
```

Description

This statement defines a device to be represented by a numerical ATLAS model. The device description with all necessary information (geometry, mesh, doping, models, electrode names, and so on) must be available in a standard structure file prior to starting a MIXEDMODE simulation.

| | |
|---------------|--|
| Axxx | Name of the element. It must begin with A. |
| n1 | Circuit node to which the ATLAS device electrode with the name, name1, is connected. The ATLAS device must have at least two electrodes. The maximum number of electrodes allowed in ATLAS is 50. This means that up to 25 ATLAS devices can be specified. For example, 25 devices with 2 electrodes each, or 10 devices with 5 electrodes each can be specified. The ATLAS device models should be used sparingly, because it can be very time consuming. Circuit models should be used for less important circuit components to conserve CPU time. If an ATLAS device electrode has been defined as FLOATING on the CONTACT statement, then this electrode should be connected to a circuit node with a negative node number. MIXEDMODE treats all circuit nodes with negative node numbers as dummy connection nodes and will not apply a voltage to these nodes. |
| infile | Name of standard structure format file with device geometry, mesh, doping, electrodes names, and so on. The number of electrodes and their names should match those mentioned in this statement. Optionally, this file can contain a solution, which MIXEDMODE will use as an initial guess (see the .OPTIONS statement for more details). |
| width | Device width. This is an optional parameter (default=1). All currents through ATLAS device terminals calculated using the 2D ATLAS model will be multiplied by this parameter to account for the third dimension of the device. width can still be used as a multiplier to the ATLAS current if a 3D ATLAS structure is used in MIXEDMODE3D. |

Example

```
ABJT1 3=EMITTER 4=BASE 6=COLLECTOR INFILE=BJT1.STR WIDTH=10
```

Note: Optional parameters for a statement are shown with square brackets (e.g., [n3=name3]).

B – User-Defined Two-terminal Elements

Syntax

```
Bxxx n+ n- INFILE=file_name FUNCTION=function_name
```

Description

| | |
|----------------------|---|
| Bxxx | User-defined two terminal element name. It must begin with B. |
| n+, n- | Positive and negative terminal nodes. |
| INFILE | Name of the text file (<i>file_name</i>) that contains C source code for a user-defined function that describes element behavior. This file can contain more than one function description. |
| function_name | Name of the function (" <i>function_name</i> ") from the file. |

Example

```
B1 2 3 infile=ud.c function=rc
```

MIXEDMODE users who are familiar with C-INTERPRETER can define their own two-terminal elements using the B statement and a function written in C that defines the behavior of the element.

User-Defined Model

A user-defined model is specified by defining the following:

- The dependencies of the device terminal current on the terminal voltages
- The derivatives of the terminal current with respect to the terminal voltages
- The device current (I) is described by Equation 12-1.

$$I = F1(U, t) + F2(U, t) \cdot \left(\frac{dU}{dt} \right) \quad 12-1$$

where:

U is the device voltage, t is time, and $F1$ and $F2$ are functions that determine the behavior of the device. The first term on the right hand side describes the “DC” current and the second term describes “capacitive” current.

The following four functions are user-specified:

- **F1(U,t):** the DC current.
- **F2(U,t):** the capacitance.
- **dF1(U,t)/dU:** the DC differential conductance.
- **Q:** the charge associated with F2(U,t).

To define the element, prepare a text file that contains an appropriate function written in C. A template for this user-defined function is shown below:

```
int udef(double v, double temp, double ktq, double time, double *curr,
double *didv, double *cap, double *charge)
{
/* user-supplied code here */
return(0);
}
```

Input Parameters

Four input parameters are supplied to the function and can be used in the user-defined code. The input parameters are:

- **v**: the voltage across the element (V)
- **temp**: the temperature (K)
- **ktq**: the thermal voltage kT/q (V)
- **time**: transient time (sec); a value of 0 is supplied during DC calculations.

Output Parameters

The four output parameters that must be returned by the function are:

- **curr**: the value of $F1$ (Amps)
- **didv**: the value of $dF1(v, time)/dU$ (A/V)
- **cap**: the value of $F2(v, time)$
- **charge**: the value of the charge (Q)

Example

Consider an element that consists of a resistor R and a capacitor C connected in parallel. The equation for the total current through this combination is:

$$I(U, t) = \frac{U}{R} + C \cdot \left(\frac{dU}{dt} \right) \quad 12-2$$

The quantities that must be user-defined are:

$$F1(U, t) = \frac{U}{R} \quad 12-3$$

$$F2(U, t) = C \quad 12-4$$

$$\frac{dF(U, t)}{dU} = \frac{1}{R} \quad 12-5$$

$$Q = C \cdot U \quad 12-6$$

When $R=2k\Omega$ and $C=100pF$, a user-defined function could have the following form:

```
intrc(double v, double temp, double ktq, double time, double *curr, double
*didv, double *cap, double *charge)
{
    *curr = v/2000.0;
    *didv = 1.0/2000.0
    *cap = 1.0e-10;
    *charge=1.0e-10*v;
    return(0);          /* 0 - ok */
}
```


C – Capacitor

Syntax

```
Cxxx n+ n- value
```

Description

| | |
|---------------|--|
| Cxxx | Name of a capacitor element. It must begin with “C”. |
| n+, n- | Positive and negative terminal nodes. |
| value | Capacitance in farads. |

Example

```
Cload 3 0 1pF
```

D – Diode

Syntax

```
Dxxx n+ n- mname [area] [L=val] [W=val] [PJ=val] [WP=val] [LP=val]
[WM=val]

[LM=val] [OFF] [IC=val] [M=val] [TEMP=val] [DTEMP=val]
```

Description

| | |
|---------------|---|
| Dxxx | Name of the diode element. It must begin with D. |
| n+, n- | Positive (anode) and negative (cathode) terminal nodes. |
| mname | Diode model name. It must refer to a diode model. |
| area | Area factor. The default is 1.0. |
| L | Length of the diode in meters. Used for LEVEL 3 diode model only. |
| W | Width of the diode in meters. Used for LEVEL 3 diode model only. |
| PJ | Periphery of the diode junction. Calculated from W and L if they are specified (in the LEVEL 3 diode model). The ISW and CJSW model parameters are affected by the value of PJ. |
| WP | Width of the polysilicon capacitor in meters. Used for LEVEL 3 diode model only. Default is 0m. |
| LP | Length of the polysilicon capacitor in meters. Used for LEVEL 3 diode model only. Default is 0m. |
| WM | Width of the metal capacitor in meters. Used for LEVEL 3 diode model only. Default is 0m. |
| LM | Length of the metal capacitor in meters. Used for LEVEL 3 diode model only. Default is 0m. |
| OFF | Sets ON/OFF startup condition for DC analysis. Default is ON. |
| IC | Initial voltage across the diode. |
| M | Multiplier used to describe multiple parallel diodes. |
| TEMP | Device operating temperature (°C). |
| DTEMP | Difference (in °C) between the device operating temperature and the circuit temperature. Default value is 0. |

Example

```
D1 2 3 dmodel1
Dclmp 3 7 Diol 3.0 IC=0.3
```

Note: See the SMARTSPICE/UTMOST MODELING MANUAL VOLUME 2 for a complete description of the diode models.

E – Linear voltage controlled source

Syntax

```
Exxx n+ n- nc+ nc- gain
```

Description

| | |
|-----------------|---|
| Exxx | Name of the linear voltage controlled voltage source. It must begin with E. |
| n+, n- | Positive and negative terminal nodes. A positive current flows from the node, n+, through the source to the node, n-. |
| nc+, nc- | Positive and negative controlling node numbers. |
| gain | Voltage gain. |

The linear voltage-controlled voltage source is characterized by Equation 12-7.

$$v(v+, n-) = gain * v(nc+, nc-)$$

12-7

Example

```
ER 4 5 6 7 55
```

F – Linear current controlled current source

Syntax

```
Fxxx n+ n- vcontrolname gain
```

Description

| | |
|---------------------|---|
| Fxxx | Name of the linear current controlled current source. It must begin with F. |
| n+, n- | Positive and negative terminal nodes. A positive current flows from the node, n+, through the source to the node, n-. |
| vcontrolname | Name of the voltage source through which the controlling current flows. The direction of positive controlling current flow is from the positive node, through the source, to the negative node of vcontrolname. |
| gain | Current gain. |

The linear current-controlled current source is characterized by Equation 12-8.

$$i(n+, n-) = gain * i(vcontrolname)$$

12-8

Example

```
F12 4 5 VIN 0.1
```

G – Linear voltage controlled current source

Syntax

Gxxx n+ n- nc+ nc- transconductance

Description

| | |
|-------------------------|---|
| Gxxx | Name of the linear voltage controlled current source. It must begin with G. |
| n+, n- | Positive and negative terminal nodes. A positive current flows from the node, n+, through the source to the node, n-. |
| nc+, nc- | Positive and negative controlling node numbers. |
| transconductance | Transconductance (in 1/Ohms). |

The linear voltage controlled current source is characterized by Equation 12-9.

$$i(n+, n-) = \text{transconductance} * v(nc+, nc-) \quad 12-9$$

Example

G2 4 5 6 7 5.5

H – Linear current controlled voltage source

Syntax

Hxxx n+ n- vcontrolname transresistance

Description

| | |
|------------------------|---|
| Hxxx | Name of the linear current controlled voltage source. Must begin from H. |
| n+, n- | Positive and negative terminal nodes. A positive current flows from the node, n+, through the source to the node, n-. |
| vcontrolname | Name of voltage source through which the controlling current flows. The direction of positive controlling current flow is from the positive node, through the source, to the negative node of vcontrolname. |
| transresistance | Transresistance (in Ohms). |

The linear current controlled voltage source is characterized by Equation 12-10.

$$v(n+, n-) = \text{transresistance} * i(vcontrolname) \quad 12-10$$

Example

H12 4 5 V1 0.1K

I – Independent current source

Syntax

```
Ixxx n+ n- value [AC acmag] [transient_parameters]
```

Description

| | |
|-----------------------------|---|
| Ixxx | Name of the independent current source. It must begin with I. |
| n+, n- | Positive and negative terminal nodes. |
| value | DC value of the source (amperes). |
| AC | Keyword for the AC source value. |
| acmag | AC magnitude. |
| transient_parameters | The transient parameters are described in Section 12.4.3: “Transient Parameters”. |

Example

```
I1 2 8 0. PULSE 0 200 0 20ns 20ns 100ns 10 100
```

```
I2 1 5 1u AC 2u
```

J – Junction Field-Effect Transistor (JFET)

Syntax

```
Jxxx nd ng ns [nb] mname [area] [M=val] [L=val] [W=val] [OFF]
[IC=vds,vgs]
[TEMP=val] [DTEMP=val]
```

Description

| | |
|-----------------------|---|
| Jxxx | Name of the JFET element. It must begin with J. |
| nd, ng, ns, nb | Drain, gate, source and bulk terminal nodes. The bulk node doesn't need to be specified. If the bulk node is not specified, then the bulk is connected to the source node |
| mname | Model name. It must refer to a JFET model. |
| area | Area factor. The default is 1.0. |
| M | Multiplier used to describe multiple parallel JFETs. |
| L | Length of the gate in meters. |
| W | Width of the gate in meters. |
| OFF | Sets ON/OFF startup condition for DC analysis. Default is ON. |
| IC | Initial condition specification for <i>vds</i> and <i>vgs</i> . |
| TEMP | Device operating temperature (°C). |
| DTEMP | Difference (in °C) between the device operating temperature and the circuit temperature. Default value is 0. |

Example

```
J44 1 4 6 jmodel
```

Note: See SMARTSPICE/UTMOST MODELING MANUAL, VOLUME 2 for a complete description of the JFET models.

K – Coupling between two inductors**Syntax**

```
Kxxx Lyyy Lzzz kval
```

Description

This is not a real circuit element. This statement defines only the coupling between two inductors.

| | |
|-------------|---|
| Kxxx | Name. This parameter is not important and is used only to distinguish the statement. It must begin with K. |
| Lyyy | First inductor element name. It must begin with an L and match one of the inductor names from the circuit. |
| Lzzz | Second inductor element name. It must begin with an L and match one of the inductor names from the circuit. |
| kval | Coefficient of mutual coupling, which must be in the range $0 < kval < 1$. |

The mutual inductance M will be determined from Equation 12-11.

$$M = kval * L1 * L2 \quad 12-11$$

Example

```
K1 L22 LLOAD 0.99
```

L – Inductor**Syntax**

```
Lxxx n+ n- value
```

Description

| | |
|---------------|---|
| Lxxx | Name of the inductor. It must begin with L. |
| n+, n- | Positive and negative terminal nodes. |
| value | Inductance in henries. |

Example

```
L2 2 3 2.5nH
```

M – MOSFET

Syntax

```
Mxxx nd ng ns [nb] mname [L=val] [W=val] [AD=val] [AS=val]
[PD=val] [PS=val] [NRD=val] [NRS=val] [OFF] [IC=vds,vgs,vbs] [M=val]
[TEMP=val] [DTEMP=val] [GEO=val] [DELVTO=val]
```

Description

| | |
|-----------------------|---|
| Mxxx | MOSFET element name. It must begin with M . |
| nd, ng, ns, nb | Drain, gate, source, and bulk terminal nodes. The bulk terminal node name is optional. If it is unspecified, ground is used. |
| mname | Model name. It must refer to a MOSFET model. |
| L=val | Channel length in meters. |
| W=val | Channel width in meters. |
| AD | Drain diffusion junction area (meters ²). This default is 0. |
| AS | Source diffusion junction area (meters ²). This default is 0. |
| PD | Drain diffusion junction perimeter (meters). This default is 0. |
| PS | Source diffusion junction perimeter (meters). This default is 0. |
| NRD | The Number of squares of drain diffusion for resistance calculations. The default is 0. |
| NRS | The Number of squares of source diffusion for resistance calculations. The default is 0. |
| OFF | Sets ON/OFF startup condition for DC analysis. Default is ON. |
| IC | Initial voltage condition specification for <i>vds</i> , <i>vgs</i> , and <i>vbs</i> . |
| M | Multiplier used to describe multiple parallel MOSFETs. The default is 1. |
| TEMP | Device operating temperature (°C). |
| DTEMP | Difference (in °C) between the device operating temperature and the circuit temperature. Default value is 0. |
| DELVTO | Threshold-voltage shift. When specified on the device line, the value overrides the value of the model parameter, DELVTO. If not specified, the value of the model parameter is used. |

Example

```
M1 2 4 8 9 mod1
Mout2 19 20 21 0 nmos L=5u W=2u TEMP=50
M22 3 5 7 8 mosmod1 L=10u W=5u AD=150p AS=150p PD=50u
PS=50u NRD=10 NRS=20
```

Note: See SMARTSPICE/UTMOST MODELING MANUAL, VOLUME 1 for a complete description of the MOSFET models.

O – Optical source

Syntax

```
Oxxx beam value [transient_parameters]
```

Description

| | |
|-----------------------------|--|
| Oxxx | Name of an independent optical source. It must begin with O. |
| beam | Beam number. The beam with this number should be described in the ATLAS section of the command file. See Chapter 10: “Luminous: Optoelectronic Simulator” for a complete description of optoelectronic simulation. |
| value | DC optical intensity value (W/cm ²). |
| transient_parameters | The transient parameters are described in Section 12.4.3: “Transient Parameters”. |

Note: The treatment of optical sources is fully similar to the treatment of independent voltage/current sources. In other words you can use, .DC statements to simulated DC light responses of the circuit and transient parameters in order to describe the transient behavior of the optical sources.

Example

```
O1 1 0.001 pulse 0.001 0.002 0 2ns 2ns 100ns 10 100
```

Q – Bipolar junction transistor

Syntax

```
Qxxx nc nb ne [ns] mname [area] [OFF] [IC=vbe,vce] [M=val] [TEMP=val]  
[DTEMP=val]
```

or

```
Qxxx nc nb ne [ns] mname [area=val] [areab=val] [areac=val] [OFF] [IC=vbe,vce]  
[M=val] [TEMP=val] [DTEMP=val]
```

Description

| | |
|-----------------------|--|
| Qxxx | Name of a bipolar junction transistor. It must begin with Q. |
| nc, nb, ne, ns | Collector, base, emitter, and substrate nodes. The substrate terminal node name is optional. If it is unspecified, ground is used. |
| mname | Model name. It must refer to a BJT model. |
| area | Emitter area factor. The default value is 1.0. |
| areab | Base area factor. The default is area. |

| | |
|--------------|--|
| areac | Collector area factor. The default is area. |
| OFF | Sets ON/OFF startup condition for DC analysis. Default is ON. |
| IC | Initial voltage condition specification for v_{be} , v_{ce} . |
| M | Multiplier used to describe multiple parallel BJTs. The default is 1. |
| TEMP | Device operating temperature (°C). |
| DTEMP | Difference (in °C) between the device operating temperature and the circuit temperature. Default value is 0. |

Example

```
Q1 2 3 9 npnmod 1.5 IC=0.6,5.0
Q9 10 11 12 20 mod22 OFF TEMP=50
```

Note: See SMARTSPICE MODELING MANUAL, VOLUME 2 for a complete description of the BJT models.

R – Resistor**Syntax**

```
Rxxx n+ n- value [transient_parameters]
```

Description

| | |
|-----------------------------|---|
| Rxxx | Name of the resistor element. It must begin with "R". |
| n+, n- | Positive and negative terminal nodes. |
| value | Resistance in ohms. |
| transient_parameters | The transient parameters are described in Section 12.4.3: "Transient Parameters". |

Note: Unlike the traditional SPICE program, transient parameters are acceptable for resistor elements. This allows simulation of different kinds of time-dependent resistors and switches in a simple way.

Example

```
R12 4 5 100k
```

T – Lossless transmission line

Syntax

```
Txxx n1 n2 n3 n4 Z0= val TD=val
```

Description

| | |
|---------------|--|
| Txxx | Name of the transmission line element. It must begin with T. |
| n1, n2 | Nodes at port 1. |
| n3, n4 | Nodes at port 2. |
| Z0 | Characteristic impedance. |
| TD | Transmission delay. |

Example

```
T1 1 0 2 0 Z0=50 TD=10ns
```

V – Independent voltage source

Syntax

```
Vxxx n+ n- value [AC acmag] [transient_parameters]
```

Description

| | |
|-----------------------------|---|
| Vxxx | Name of the independent voltage source. It must begin with V. |
| n+, n- | Positive and negative terminal nodes. |
| value | DC value of the source in units of volts. |
| AC | Keyword for the AC source value. |
| acmag | AC magnitude. |
| transient_parameters | The transient parameters are described in Section 12.4.3: “Transient Parameters”. |

Example

```
VCC 5 0 10.5  
VIN 2 4 5.5 AC 1
```

X - Subcircuit Call

Syntax

```
Xxxx n1 <n2 n3 ...> subcktname <<PARAMS:> parname=val ...>
```

Description

| | |
|--------------------|---|
| Xxxx | Subcircuit names must begin with x. |
| n1, n2, ... | Node names for external reference. |
| subcktname | Subcircuit definition. |
| PARAMS | The optional parameter preceding the list of parameters and their values. |
| parname | <p>The parameter name whose value is set to val, which will be local to the subcircuit. val is either a numerical value, an expression enclosed in single quotes containing previously defined parameters, or a string, which defines a model's name, that can be transmitted in subcircuit. If the same parameter is assigned a value on more than one statement in the input deck (.PARAM, .SUBCKT, and X statements), then will be one of the following:</p> <ul style="list-style-type: none"> • a value assigned in a global .PARAM statement (outside subcircuits) is used if it exists. • a value assigned in a corresponding X statement is used if it exists. • a value assigned in a corresponding .SUBCKT statement is used if it exists. • a value assigned in a local .PARAM statement (inside the subcircuit) is used if it exists. |

This statement creates instance **Xxxx** of subcircuit **subcktname**. There must be the same number of nodes **n1 ...** as in the subcircuit definition (see **.SUBCKT** statement). These nodes replace the formal node names in the **.SUBCKT** statement.

Subcircuits can be nested. The number of nesting levels is not limited but nesting must not be recursive. When the circuit is loaded, all subcircuit device names are expanded to the form **devtype.subcktname.devname**, where **devtype** is the first letter of **devname**. All local node names in the subcircuit are expanded to the form **subcktname.nodename**.

For nested subcircuits, expanded names have multiple dot-separated qualifiers. For example, if a circuit has a call to subcircuit **subcktname1** and the **subcktname1** definition contains a call to subcircuit **subcktname2**, then expanded names will have the following format:

```
devtype.subcktname1.subcktname2.devname
```

```
subcktname1.subcktname2.nodename
```

```
subcktname1.subcktname2.modelname
```

Z – MESFET

Syntax

```
Zxxx nd ng ns [nb] mname [area] [M=val] [L=val] [W=val] [OFF]
[IC=vds,vgs]
[TEMP=val] [DTEMP=val]
```

Description

| | |
|-----------------------|--|
| Jxxx | Name of the MESFET element. It must begin with Z. |
| nd, ng, ns, nb | Drain, gate, source and bulk terminal nodes. The bulk node doesn't need to be specified. If the bulk node is not specified, then the bulk is connected to the source node. |
| mname | Model name. It must refer to a MESFET model. |
| area | Area factor. The default is 1.0. |
| M | Multiplier used to describe multiple parallel MESFETs. |
| L | Length of the gate in meters. |
| W | Width of the gate in meters. |
| OFF | Sets ON/OFF startup condition for DC analysis. Default is ON. |
| IC | Initial condition specification for <i>vds</i> and <i>vgs</i> . |
| TEMP | Device operating temperature (°C). |
| DTEMP | Difference (in °C) between the device operating temperature and the circuit temperature. Default value is 0. |

Example

```
Z44 1 4 6 jmodel
```

Note: See SMARTSPICE MODELING MANUAL, VOLUME 2 for a complete description of the MESFET models.

12.4.2: Control and Analysis Statements

.AC

.AC performs an AC linear small-signal analysis on the circuit. MIXEDMODE first creates a linearized small-signal model at the operating point of the circuit and then computes the frequency response over a user-specified range of frequencies.

Syntax

```
.AC DEC|OCT|LIN nump fstart fstop/ sweep source_name start stop step
```

Description

| | |
|---------------|---|
| DEC | Sweep frequency by decades. |
| OCT | Sweep frequency by octaves. |
| LIN | Linear frequency sweep. This is default. |
| nump | Total number of points per decade or per octave, or the total number of points of the linear sweep. |
| fstart | Starting frequency (Hz). |
| fstop | Final frequency (Hz). |

Several .AC statements can be specified in the same command file. In this case, they will be executed sequentially. Before executing the first .AC statement, the program will execute all .DC statements (if any), regardless of the order of the .AC and .DC statements in the command file. At least one independent voltage or current source must have a AC specification.

| | |
|--------------------|--|
| source_name | Name of the independent voltage, current, or optical source to be swept. |
| start | Starting value of the sweep. |
| step | Increment value of the sweep. |
| stop | Final value of the sweep. |
| sweep | Performs a DC sweep at every frequency point. |

Example

```
.AC DEC 3 1.e3 1.e12
```

```
.AC LIN 20 1.e5 2.e6
```

.BEGIN

.BEGIN indicates the start of the circuit part of a MIXEDMODE command file. The synonym for this parameter is START.

```
.BEGIN 3D
```

Description

| | |
|-----------|---|
| 3D | Specifies that MIXEDMODE3D will be used instead of MIXEDMODE. |
|-----------|---|

.DC

.DC causes a DC transfer curve to be computed for the circuit with all capacitors opened and all inductors shorted.

Syntax

```
.DC DEC|OCT|LIN source_name start stop increment/numbers_steps  
source_name2 DEC|OCT|LIN start2 stop2 number_steps2
```

Description

| | |
|----------------------|--|
| DEC | Sweep DC bias (voltage or current) by decades. |
| OCT | Sweep DC bias by octaves. |
| LIN | Linear DC bias sweep. This is the default. |
| source_name | Name of the independent voltage, current, or optical source to be swept. |
| start | Starting value of the sweep argument. |
| stop | Final value of the sweep argument. |
| number_steps | Number of steps of the inner sweep |
| source_name2 | Name of the secondary sweep source. |
| start2 | start value of the secondary sweep source |
| stop2 | Final value of the secondary sweep source |
| number_steps2 | Number of steps of the secondary sweep. |

Several .DC statements can be specified in a command file. In this case, they will be executed sequentially. Before executing the first .DC statement, the program will simulate the circuit with the independent source values given in the description of those sources.

The .DC statement is also often used to increment the values of independent voltage and current sources in a circuit to avoid convergence problems.

Examples

```
.DC VIN 0. 5. 0.25  
.DC IE 50 500 50
```

.END

.END indicates the end of the circuit part of a MIXEDMODE command file. The synonym for this parameter is FINISH.

.ENDL

.ENDL specifies the end of a library definition.

Syntax

```
.ENDL [library_name]
```

Description

| | |
|---------------------|---------------------------------------|
| library_name | Name of the library being terminated. |
|---------------------|---------------------------------------|

.GLOBAL

.GLOBAL allows globally accessible nodes to be defined for use in subcircuits.

Syntax

```
.GLOBAL node1 <node2 ...>
```

Description

| | |
|--------------|--|
| node1 | Node name that is to be declared global. Any internal subcircuit nodes that have the same name as global node will be assumed to refer to the global node. |
|--------------|--|

Example

```
.GLOBAL V1
```

.IC

.IC sets specified node voltages during the steady-state simulation.

Syntax

```
.IC [V(I)=val_I...]
```

Description

This statement forces the specified node voltages to be set to specified values during the steady-state simulation. These voltages are released when the transient simulation begins.

Example

```
.IC V(1)=10
```

```
.IC V(node1)=-0.5
```

.INCLUDE

`.INCLUDE` includes a file into the input file.

Syntax

```
.INCLUDE filename
```

Description

| | |
|-----------------|---|
| filename | Name of the file to be inserted into the input deck at the point where the <code>.INCLUDE</code> statement appears. |
|-----------------|---|

Example

```
.INCLUDE inverter.in
```

.LIB

Syntax

```
.LIB filename [entryname]
```

Description

| | |
|------------------|--|
| filename | Name of the library file. |
| entryname | The entry name of the section of the library name to be included in the input deck. If <code>entryname</code> is not specified, then the entire library file will be included. |

Examples

```
.LIB lib1  
.LIB lib1 mos1
```

Library File Structure

Each section of the library file should start with a `.LIB` followed by `entryname` and ends with `.ENDL` followed by an optional entry name:

```
.LIB entryname  
....  
.ENDL [entryname]
```


.LOAD

.LOAD loads a solution file.

Syntax

```
.LOAD INFILE=filename
```

Description

| | |
|---------------|--|
| INFILE | Name of a file (<i>filename</i>) to be loaded as an initial guess for further simulation. This file must have been saved during a previous run of MIXEDMODE using the .SAVE statement. |
|---------------|--|

Example

```
.LOAD INFILE=pdsave
```

Note: This statement is not used to load SSF format solution files from ATLAS (see.OPTIONS LOADSOLUTIONS).

.LOG

.LOG specifies the filename for the circuit voltages and currents that will be saved.

Syntax

```
.LOG OUTFILE=filename CSVFILE=filename
```

Description

| | |
|----------------|--|
| OUTFILE | Name of a file (<i>filename</i>) for the circuit voltages and currents to be saved in standard structure format files. |
|----------------|--|

These files will have the following names:

For steady-state analysis:

```
"filename"_dc_1.log
```

```
"filename"_dc_2.log
```

```
"filename"_dc_3.log
```

```
..
```

(new file will be created for each .DC statement).

For AC analysis:

```
"filename"_ac_1.log
```

```
..
```

For network parameter extraction:

```
"filename"_net_1.log
```

```
..
```

For transient analysis:

```
"filename"_tr.log
```

```
..
```

To plot results of and entire steady-state analysis simultaneously, load all files related to steady-state analysis into TONYPLOT.

| | |
|----------------|---|
| CSVFILE | Name of a file for the circuit voltages and currents to be saved in Comma Separated Value (CSV) format. |
|----------------|---|

Example

```
.LOG OUTFILE=pd
```

.MODEL

.MODEL specifies the circuit element model to be used for diodes, BJTs, or MOSFETs, and the numerical values of parameters associated with the model.

Syntax

```
.MODEL name type <parameters>
```

Description

| | |
|-------------------|--|
| name | This is the model name. Circuit element definition statements refer to this name to link elements to models. |
| type | This is the model type. This type must be consistent with the type of the circuit elements that uses the model. The type can be one of the following: <ul style="list-style-type: none">• D - Diode model• NMOS - n-channel MOSFET model.• PMOS - p-channel MOSFET model.• NPN - npn BJT model• PNP - pnp BJT model• NJF - n-channel JFET/MESFET model• PJF - p-channel JFET/MESFET model |
| parameters | Model parameters. The parameters are described in the SMARTSPICE/UTMOST MODELING MANUALS VOLUMES 1, 2 and 3. |

Example

```
.MODEL MODBJT NPN IS=1.E-17 BF=100 CJE=1F TF=5PS \  
CJC=0.3F RB=100 RBM=20
```

.NET

.NET specifies that a network parameter extraction is to be performed.

Syntax

```
.NET INPORT OUTPUT DEC|OCT|LIN nump fstart fstop [Z0] [INDIN] [RSIN] [INDOUT]]
[RSOUT] [CIN] [COUT]
```

Description

| | |
|---------------|--|
| INPORT | <p>Input port description. It should be in one of the following formats.</p> <ul style="list-style-type: none"> • V(n+,n-): two nodes (positive (n+) and negative (n-)). • Vxxxx: where Vxxxx is the name of an existing voltage source. The positive terminal of the source becomes the positive input port node and the negative terminal becomes the negative input node. • Ixxxx: where Ixxxx is the name of an existing current source. The positive terminal of the source becomes the positive input port node and the negative terminal becomes the negative input node. |
|---------------|--|

Note: If the nodes specified as the input port are the same nodes as an existing current or voltage source, then the name of the source must be specified as `inport`. Also, remove all AC parameters from voltage or current sources before using the .NET statement.

| | |
|---------------|---|
| OUTPUT | <p>Output port description. It should be in one of the following formats.</p> <ul style="list-style-type: none"> • V(n+,n-): two nodes (positive (n+) and negative (n-)). • Vxxxx: where Vxxxx is the name of an existing voltage source. The positive terminal of the source becomes the positive output port node and the negative terminal becomes the negative output node. • Ixxxx: where Ixxxx is the name of an existing current source. The positive terminal of the source becomes the positive output port node and the negative terminal becomes the negative output node. |
|---------------|---|

Note: If the nodes specified as the output port are the same nodes as an existing current or voltage source, then the name of the source must be specified as `outport`.

| | |
|---------------|---|
| DEC | Sweep frequency by decades. |
| OCT | Sweep frequency by octaves. |
| LIN | Linear frequency sweep. This is default. |
| nump | Total number of points per decade or per octave, or the total number of points of the linear sweep. |
| fstart | Starting frequency (Hz). |
| fstop | Final frequency (Hz). |

Additional optional parameters may also be specified on the .NET statement.

| | |
|---------------|---|
| Z0 | Matching Impedance (default = 50 Ohms). |
| INDIN | Inductance through which the DC voltage source is connected to the input source (only if INPORT is given as Vxxxx). |
| RSIN | Series resistance of INDIN. |
| INDOUT | Inductance through which the DC voltage source is connected to the output source (only if OUTPORT is given as Vxxxx). |
| RSOUT | Series resistance of INDOUT. |
| CIN | Capacitance through which the S-parameter test circuit is connected to the input port. |
| COUT | Capacitance through which the S-parameter test circuit is connected to the output port. |

Note: The S-parameters will be automatically saved to the log file. The Z, Y, H, ABCD, and gain small-signal parameters can also be written to the log file. These are selected through the .OPTIONS statement. You can also view the default values if PRINT is specified in the .OPTIONS statement

Examples

```
.NET V1 V2 DEC 10 1e6 1e10
.NET I1 V2 DEC 10 1e6 1e10 Z0=75 RSOUT=100
.NET V(1,0) V(2,3) DEC 10 1e6 1e10
```

.NODESET

.NODESET sets initial values for circuit node voltages.

Syntax

```
.NODESET [V(I)=VAL_I ...]
```

Description

This statement specifies the initial values for circuit node voltages. If a node voltage is not specified, the program will try to find a solution using zero as an initial guess for this node. This statement can significantly reduce the CPU time needed to calculate the initial condition.

Example

```
.NODESET V(1)=50 V(2)=49.4 V(3)=10 V(5)=-1.5
.NODESET V(in1)=0 V(2)=2 V(out1)=-1
```

.NUMERIC

.NUMERIC specifies special numeric parameters for the circuit analysis.

Syntax

```
.NUMERIC [parameters]
```

| Parameter | Type | Default | Units |
|-----------|---------|---------------------|-------|
| IMAXDC | Integer | 25 | |
| IMAXTR | Integer | 15 | |
| DTMIN | Real | 1×10^{-12} | s |
| LTE | Real | 0.1 | |
| TOLDC | Real | 1×10^{-4} | |
| TOLTR | Real | 1×10^{-4} | |
| VCHANGE | Real | 5×10^7 | V |
| VMAX | Real | 5×10^7 | V |
| VMIN | Real | -5×10^7 | V |

Description

| | |
|----------------|---|
| IMAXDC | Maximum number of mixed circuit-device iterations to be performed during steady-state analysis. |
| IMAXTR | Maximum number of mixed circuit-device iterations to be performed during transient analysis. |
| DTMIN | Minimum time step value for transient analysis. |
| LTE | Local truncation error for transient analysis. |
| TOLDC | Relative accuracy to be achieved during steady-state analysis for the calculation of voltages in circuit nodes. |
| TOLTR | Relative accuracy to be achieved during transient analysis for the calculation of voltages in circuit nodes. |
| VCHANGE | Maximum allowable change in circuit node voltages between two mixed circuit-device iterations. This parameter can be useful for reaching steady-state convergence with a bad initial guess. |
| VMAX | Maximum value for circuit node voltages. |
| VMIN | Minimum value for circuit node voltages. |

Example

```
.NUMERIC LTE=0.05 TOLDC=1.*10-8 DTMIN=1ns
```

.OPTIONS

.OPTIONS specifies various circuit simulation options.

Syntax

.OPTIONS [parameters]

| Parameter | Type | Default | Units |
|---------------|---------|---------------------|---------------|
| ABCD.PARAM | Logical | False | |
| CNODE | Real | 1×10^{-16} | F |
| CYLINDR | Logical | False | |
| DC.WRITE | Real | 1 | |
| DT.NOCHECK | Logical | False | |
| FULLLN | Logical | True | |
| GAINS | Logical | False | |
| H.PARAM | Logical | False | |
| LOADFLOATING | Logical | False | |
| LOADSOLUTIONS | Logical | False | |
| M2LN | Logical | False | |
| M2LN.TR | Logical | False | |
| NOPROJ | Logical | False | |
| NOSHIFT | Logical | False | |
| PRINT | Logical | False | |
| REL POT | Logical | False | |
| RV | Real | 1×10^{-4} | W |
| STR.XOFFSET | Real | 1 | μm |
| STR.XSHIFT | Logical | | |
| STR.YOFFSET | Real | 1 | μm |
| STR.YSHIFT | Logical | | |
| STR.ZOFFSET | Real | 1 | μm |
| STR.ZSHIFT | Logical | | |
| TEMP | Real | 300 | K |
| TNOM | Real | 300 | K |
| WRITE | Integer | 1 | |

| Parameter | Type | Default | Units |
|------------|---------|---------|-------|
| Y.PARAM | Logical | False | |
| Z.PARAM | Logical | False | |
| ZIP.SOLVER | Logical | False | |

Description

| | |
|----------------------|--|
| ABCD.PARAM | ABCD parameters will be written to the log file. This is used in conjunction with the .NET statement. |
| CNODE | A very small capacitance, which for algorithmic reasons automatically connected from each circuit node to ground. This value can be set to 0. |
| CYLINDR | Cylindrical coordinate system for all ATLAS devices. |
| DC.WRITE | Specifies how often a structure file (as specified by the MASTER parameter on the .SAVE statement) will be written during .DC solutions. If this parameter is set to 0, then no .DC structure files will be written. |
| DT.NOCHECK | Specifies that the transient pulse and table definitions will not be taken into account when calculating the time step. |
| FULLN | Full Newton solution method is used during steady-state simulation. |
| GAIN | Stability factor (K), unilateral power gain (GU), maximum unilateral transducer power gain (GTUmax) and $ H_{21} ^2$ are written to the LOG file. This is used in conjunction with the .NET statement. |
| H.PARAM | H-parameters will be written to the LOG file. This is used in conjunction with the .NET statement. |
| LOADFLOATING | Specifies that the charge bias value for floating electrodes will be loaded. |
| LOADSOLUTIONS | <p>Solutions, structures, doping distributions, and meshes, are to be loaded from standard structure files. The solutions are used as the initial guess or initial conditions for subsequent MIXEDMODE simulation. To use this feature, you must:</p> <ul style="list-style-type: none"> • Calculate a solution for each ATLAS device and save each solution in a separate standard structure format file using SAVE or SOLVE... MASTER. • For each ATLAS device, use the A statement in the MIXEDMODE command file to specify the associated standard structure format file • Set node voltages to appropriate values with the .NODESET statement • Specify LOADSOLUTIONS in the .OPTIONS statement |

Note: If using this feature, specify solutions for all ATLAS devices.

The .NODESET statement must always be used when LOADSOLUTIONS is used. The .NODESET statement is used to make the initial circuit voltages match those device solutions that were obtained. You may also need to specify the NOSHIFT parameter of the OPTIONS statement. By default, MIXEDMODE shifts

device terminal voltages with respect to the voltage on the first terminal that is specified in the A statement. You must either prepare initial solutions with this terminal grounded, or specify NOSHIFT in the OPTIONS statement.

| | |
|--------------------|---|
| M2LN | Uses the modified two-level Newton solution method during steady-state simulation. The full NEWTON method provides faster solution than the modified two-level Newton method when a good initial guess is available. The modified two-level method is more reliable when the initial guess is far from the solution. The default is the full NEWTON method. |
| M2LN.TR | Uses the modified two-level Newton solution method during transient simulations. |
| NOPROJ | Disables the initial guess project method for the ATLAS iterations. MIXEDMODE attempts to extrapolate the values of the ATLAS device variables (such as potential and carrier concentration) for the each iteration. Specifying NOPROJ disables the extrapolation and the previous values of potential and carrier concentration are used instead. |
| NOSHIFT | Disables the shift of voltages for ATLAS device models. MIXEDMODE normally shifts the voltages on ATLAS device terminals to be referenced to the voltage on the first terminal. From the physical point of view, the state of the p-n diode is the same for voltages of 0V and 0.5V on the diode terminals with 1000V and 1000.5V, but the first situation is better for numerical simulation. |
| PRINT | Enables printing of circuit nodes voltages after the calculation for each bias point (DC analysis) or time step (transient the analysis). |
| RELPO | Enables the use of relative convergence criteria for potential for ATLAS models. By default, ALTAS models use absolute convergence criteria for potential. When bias voltages are large (a common situation for power devices), then absolute convergence criteria are not appropriate and this parameter should be specified. |
| RV | Defines the ohmic resistance that MIXEDMODE associates with all voltage sources and all inductances. This value should never be set to 0. The default value is small enough to avoid errors due to the influence of the internal resistance. Usually, extremely small values of this parameters can cause convergence problems. It is usually acceptable to decrease this parameter to the range of $1 \cdot 10^{-6}$ - $1 \cdot 10^{-7}$. This parameter should not be varied unless there is a compelling reason to do so. |
| STR.XOFFSET | Specifies the X direction shift offset for multiple ATLAS devices. |
| STR.XSHIFT | Specifies that multiple ATLAS device will be shifted in the X direction. |
| STR.YOFFSET | Specifies the Y direction shift offset for multiple ATLAS devices. |
| STR.YSHIFT | Specifies that multiple ATLAS device will be shifted in the Y direction. |
| STR.ZOFFSET | Specifies the Z direction shift offset for multiple ATLAS devices. |
| STR.ZSHIFT | Specifies that multiple ATLAS device will be shifted in the Z direction. |
| TEMP | Device temperature to be use during the simulation. |
| TNOM | Circuit temperature to be use during the simulation. |
| WRITE | How often the solution is to be saved in standard structure files during the simulation. For example, write=3 specifies that the solution will be saved at every third timestep. Specifying this parameter can help avoid disk overflow. |

| | |
|-------------------|--|
| Y.PARAM | Y-parameters should be written to the log file. This is used in conjunction with the .NET statement. |
| Z.PARAM | Z-parameters should be written to the log file. This is used in conjunction with the .NET statement. |
| ZIP.SOLVER | Specifies that the ZIP library version of BICGST iterative solver will be used to calculate the device conduction matrix instead of the CGS or BICGST solver. If you specify the DIRECT parameter in the METHOD statement, then the direct solver will be used for both the device conduction matrix calculation and the ATLAS solution. |

Example

```
.OPTIONS TNOM=293 FULLN
```

.PRINT

.PRINT specifies which device output parameters will be printed to the log files.

Syntax

```
.PRINT [antype] parameter(device_name) [parameter2(device_name) ...]
```

Description

| | |
|---------------|---|
| antype | <p>Type of analysis for which the outputs are desired. If antype is unspecified, the outputs of all simulation types will be printed. antype must be one of the following keywords:</p> <ul style="list-style-type: none"> • AC: AC analysis outputs • DC: DC analysis outputs • NET: Network analysis outputs • TRAN: Transient analysis outputs • parameter: Output variables or expressions to be printed. • device_name: The device name. |
|---------------|---|

Example

```
.PRINT ic(q1) ib(q1) is(q1)
.PRINT AC ic(q1) ib(q2)
.PRINT DC ic(q1) ib(q2) i(d1)
.PRINT TRAN cd(m1) cg(m1) cs(m1) cb(m1)
```

.PARAM

.PARAM specifies a parameter definition.

Syntax

```
.PARAM parname1=val1 [parname2=val2 ...]
```

The .PARAM statement defines one or more parameter labels by assigning the names parname1, parname2 to constant values val1, val2. Parameter labels must begin with alphabetic character(s) or the underscore character(s).

The .PARAM statement can be globally and locally (i.e., inside a subcircuit definition) specified. Once defined, a global parameter label or an expression containing global parameter labels can be used in the input deck when a numerical value is expected. A local parameter label can be used only inside the subcircuit.

.SAVE

.SAVE saves simulation results into files for visualization or for future use as an initial guess.

Syntax

```
.SAVE OUTFILE=name [MASTER=mname] [TSAVE=timepts]
```

Description

| | |
|---------------|---|
| MASTER | <p>This will cause MIXEDMODE to output standard structure files for visualization in TONYPLOT. These files, with the base name, mname, will be written after the calculation of each bias point during DC simulation, and after of each time step during transient simulation. For example, if you wish to save a structure file for each DC bias solution, you would write:</p> <pre>.save master=my_structure.str</pre> <p>MIXEDMODE will then output structure files at each DC bias point. MIXEDMODE will also automatically append a number to the end of the file name indicating which bias point the file is for.</p> |
|---------------|---|

Example

```
.SAVE MASTER=my_filename.str
```

| | |
|----------------|--|
| OUTFILE | <p>Specifies that after the simulation is finished the solution is to be written to a file called my_filename.str. In other words, only one structure file will output after the simulation has finished. Even if you have several .dc solutions, MIXEDMODE will only output one structure file if for example:</p> <pre>.save outfile=filename.str</pre> <p>has been used. The ATLAS model solutions will be written to the file (name) and the circuit solution will be written to the file, name.cir. These files can be used later for loading solutions to be used as an initial guess (see .LOAD statement).</p> |
|----------------|--|

Example

```
.save outfile=my_filename.str
```

| | |
|--------------|--|
| TSAVE | Specifies the transient time points at which a MASTER file will be written. The time points should be specified as a comma separated list. |
|--------------|--|

The program will automatically add the following suffixes to `mname`:

- During DC simulation: `_dc_number`, where `number` is the number of the DC point.
- During transient simulation: `_tr_number`, where `number` is the number of the time step.

Example

```
.SAVE OUTFILE=pdsave MASTER=pd
```

.SUBCKT

`.SUBCKT` specifies a subcircuit definition.

Syntax

```
.SUBCKT subcktname <n1 n2 ...>
+ <OPTIONAL: optn1=defval1 <optn2=defval2 ...>>
+ <<PARAMS|PARAM:> parname1=val1 <parname2=val2 ...>>
```

Description

| | |
|--------------------------------|--|
| subcktname | The subcircuit name. It is used by an X element statement to reference the subcircuit. |
| n1 ... | The optional list of external nodes. Ground nodes (zero) are not allowed. |
| PARAMS PARAM | The parameter preceding the list of parameters and their values. |
| parname1, parname2, ... | The name of a parameter with value set to <code>val1</code> , <code>val2</code> , ... that will be local to the subcircuit. <code>val</code> is a numerical value. If the same parameter is assigned, a value on more than one statement in the input deck (<code>.PARAM</code> , <code>.SUBCKT</code> , and <code>X</code> statements) will be one of the following: <ul style="list-style-type: none"> • a value assigned in a global <code>.PARAM</code> statement (outside subcircuits) is used if it exists. • a value assigned in a corresponding <code>X</code> statement is used if it exists. • a value assigned in a corresponding <code>.SUBCKT</code> statement is used if it exists. • a value assigned in a local <code>.PARAM</code> statement (inside the subcircuit) is used if it exists. |

A subcircuit definition is initiated by a `.SUBCKT` statement. The group of element statements, which immediately follow the `.SUBCKT` statement define the subcircuit. The last statement in a subcircuit definition is the `.ENDS` statement. Control statements cannot appear within a subcircuit definition; however, subcircuit definitions may contain anything else, including other subcircuit definitions, device models, and subcircuit calls.

All internal nodes (if not included on the `.SUBCKT` statement) are local with the exception of the global node 0.

.TRAN

.TRAN specifies that a transient analysis is to be performed.

Syntax

```
.TRAN tstep tstop
```

Description

| | |
|--------------|---|
| tstep | Time interval in seconds. |
| tstop | Final time value for which the simulation is to be performed. |

Transient analysis is performed only after the execution of all .DC statements. If no DC statements are used, the transient starts after the calculation of the initial circuit state with the values of the independent sources given in the descriptions of those sources.

Multiple .TRAN statements are supported. The TSTOP parameter is not reset between each .TRAN statement.

Example

```
.TRAN 1ns 100ns
```

12.4.3: Transient Parameters

MIXEDMODE allows you to specify transient parameters for voltage sources (Vxxx), current sources (Ixxx), and resistors (Rxxx). These parameters describe the time development behavior of the source.

EXP

EXP is used to define an exponential waveform. The waveform is specified as follows:

```
EXP i1 i2 td1 tau1 td2 tau2
```

where:

- **i1** is the initial value.
- **i2** is the pulsed value.
- **td1** is the rise delay time.
- **td2** is the fall delay time.
- **tau1** is the rise time constant.
- **tau2** is the fall time constant.

The transient behavior is shown in Table 12-2.

| Table 12-2. Transient behavior for EXP | |
|--|--|
| Time | Value |
| $0 < t < td1$ | i1 |
| $td1 \leq t < td2$ | $i1 + (i2 - i1) \cdot (1 - \exp[-(t - td1)/\tau1])$ |
| $td2 \leq t$ | $i1 + (i2 - i1) \cdot (1 - \exp[-(t - td1)/\tau1]) + (i1 - i2) \cdot (1 - \exp[-(t - td2)/\tau2])$ |

GAUSS

GAUSS is used to define a Gaussian waveform. The waveform is specified as follows:

```
GAUSS i1 i2 td1 tau1 td2 tau2
```

where:

- **i1** is the initial value.
- **i2** is the pulsed value.
- **td1** is the rise delay time.
- **td2** is the fall delay time.
- **tau1** is the rise time constant.
- **tau2** is the fall time constant.

The transient behavior is shown in Table 12-3.

| Table 12-3. The Transient behavior for GAUSS | |
|--|--|
| Time | Value |
| $0 < t < td1$ | $i1$ |
| $td1 \leq t < td2$ | $i1 + (i2 - i1) \cdot (1 - \exp[-((t - td1) / \tau_{1})^2])$ |
| $td2 \leq t$ | $i1 + (i2 - i1) \cdot (1 - \exp[-((t - td1) / \tau_{1})^2]) + (i1 - i2) \cdot (1 - \exp[-((t - td2) / \tau_{2})^2])$ |

PULSE

PULSE is used to define a pulse waveform. The waveform is specified as follows:

```
PULSE i1 i2 td tr tf pw per
```

where:

- **i1** is the initial value.
- **i2** is the pulsed value.
- **td** is the delay time before the pulse is started.
- **tr** is the rise time of the pulse.
- **tf** is the fall time of the pulse.
- **pw** is the pulse length per period
- **per** is the period.

The transient behavior is described in Table 12-4. Intermediate points are found by linear interpolation.

Table 12-4. Transient behavior for PULSE

| Time | Value |
|---|--------------------|
| 0 | i1 |
| t _d | i1 |
| t _d + t _r | i2 |
| t _d + t _r + p _w | i2 |
| t _d + t _r + p _w + t _f | i1 |
| t _d + p _{er} | i1 |
| t _d + p _{er} + t _r | i2 (second period) |

PWL

PWL is used to define a piece-wise linear waveform. The waveform is specified as a list of time and value point with the time values in ascending order. The waveform is specified as follows:

```
PWL t1, v1 [t2,v2 ....] [R=tval]
```

where:

- **t1** is the first time value.
- **v1** is the bias value at time=t1.
- **t2** is the second time value (t2>t1).
- **v2** is the bias value at time=t2.\
- **R** is the repeat time point. This specifies the time point from which the PWL waveform should be repeated. The section of the waveform between tval and the end of the PWL will be repeated until the transient analysis is completed.

PWLFILE

PWLFILE is used to define a file name containing a piece-wise linear waveform. The waveform is specified as a list of time and value points with time values in ascending order. The file is specified as follows:

```
PWLFILE filename [R=tval]
```

where:

- **filename** is the PWL file.
- **R** is the repeat time point. This specifies the time point from which the PWLFILE waveform should be repeated. The section of the waveform between tval and the end of the PWL will be repeated until the transient analysis is completed.

SFFM

SFFM is used to define a modulated sinusoidal waveform. The waveform is specified as follows:

```
SFFM io ia fc mdi fs
```

where:

- **io** is the DC offset.
- **ia** is the amplitude.
- **fc** is the carrier frequency.
- **mdi** is the modulation index.
- **fs** is the signal frequency.

The transient behavior will be:

$$\text{value}(t) = \text{io} + \text{ia} \cdot \sin[\pi \cdot \text{fc} \cdot t + \text{mdi} \cdot \sin(2\pi \cdot \text{fs} \cdot t)]$$

SIN

SIN is used to define a sinusoidal waveform. The waveform is specified as follows:

```
SIN io ia freq td theta
```

where:

- **io** is the offset.
- **ia** is the amplitude.
- **freq** is the frequency.
- **td** is the delay.
- **theta** is the damping factor.

The transient behavior is shown in Table 12-5.

| Table 12-5. Transient Behavior for SIN | |
|--|--|
| Time | Value |
| $t < t_d$ | $\text{value}(t) = \text{io}$ |
| $t \geq t_d$ | $\text{value}(t) = \text{io} + \text{ia} \cdot \exp[-(t - t_d) / \text{THETA}] \cdot \sin[2\pi \cdot \text{freq} \cdot (t - t_d)]$ |

TABLE

TABLE is used to define a waveform using a table of values. This parameter is used as follows:

```
TABLE infile=<table_file_name>[R=tval]
```

where `table_file_name` is an ASCII text file that contains the tabulated time-dependence of a variable in the following format:

```
t1 v1
t2 v2
t3 v3
...
tN vN
end
```

Each line contains two numbers. The first number is the time in seconds. The second number is the time-dependent variable) voltage in volts, the current in amps, or the resistance in ohms). Up to 1000 lines can be used. Input is terminated by the word `end`.

If during the simulation the transient time becomes larger than the last value in the table, then the last value will be used for the remainder of the simulation.

R is the repeat time point. This specifies the time point from which the TABLE waveform should be repeated. The section of the waveform between `tval` and the end of the PWL will be repeated until the transient analysis is completed.

12.4.4: Expressions

Expressions can be used at input deck statements to specify (by means of calculations) the value of a parameter.

Functions

MIXEDMODE supports the functions listed in Table 12-6. The table gives the definition for each function, and shows the types of function arguments.

| Table 12-6: Functions | | | | |
|-------------------------|--------|--------|--|-------|
| Function | Scalar | Vector | Description | Notes |
| abs (x) | + | + | Absolute value x | |
| acos (x) | + | + | Arc cosine x | |
| acosh (x) | + | + | Hyperbolic arc cosine x | |
| asin (x) | + | + | Arc sine x | |
| asinh (x) | + | + | Hyperbolic arc sine x | |
| arctan (x) | + | - | Arc tangent x | |
| atan (x) | + | + | Arc tangent x | |
| atanh (x) | + | + | Hyperbolic arc tangent x | |
| cos (x) | + | + | Cosine of x | |
| cosh (x) | + | + | Hyperbolic cosine of x | |
| db (x) | - | + | Magnitude of the complex vector in decibels: $db(x) = 20 \times \log(mag(x))$ | |
| erf (x) | + | + | Error function $erf(x) = \frac{2}{\sqrt{\pi}} \times \int_0^x e^{-t^2} dt$ | |
| erfc (x) | + | + | Error function complement $erfc(x) = 1 - erf(x)$ | |
| exp (x) | + | + | Exponential: <i>e</i> raised to power <i>x</i> | |
| int (x) or trunc (x) | + | + | Returns the integer part of x | |
| log10 (x) | + | + | Logarithm (base 10) of x | |
| log (x) or ln (x) | + | + | Natural logarithm (base <i>e</i>) of x | |
| max (x, y) | + | + | Maximum of two values, if $x > y$ then $max(x,y)=x$; otherwise $=y$ | |

Table 12-6: Functions

| Function | Scalar | Vector | Description | Notes |
|--|--------|--------|--|---|
| <code>min(x, y)</code> | + | + | Minimum of two values, if $x < y$ then $\min(x, y) = x$; otherwise $= y$ | |
| <code>pow(x, y)</code> | + | - | Absolute power: absolute value of x raised to integer part of y: $\text{pow}(x, y) = \text{abs}(x)^{\text{int}(y)}$ | |
| <code>rnd(x)</code> | + | + | Returns a random integer number (or the vector with each component a random integer number) between 0 and absolute value x (absolute value of the vector x components) | |
| <code>sgn(x)</code> | + | + | Sign of value, if $x < 0$ then $\text{sgn}(x) = -1$; if $x = 0$ then $\text{sgn}(x) = 0$; if $x > 0$ then $\text{sgn}(x) = 1$ | |
| <code>sin(x)</code> | + | + | Sine of x | |
| <code>sinh(x)</code> | + | + | Hyperbolic sine of x | |
| <code>sqrt(x)</code> | + | + | Square root of x | |
| <code>tan(x)</code> | + | + | Tangent of x | |
| <code>tanh(x)</code> | + | + | Hyperbolic tangent of x | |
| <code>valif(log_cond, x, y)</code> or <code>if(log_cond, x, y)</code> - in '-pspice' mode | + | - | Logical expression: <i>if(log_cond) then x else y</i> | <i>log_cond</i> is the a logical condition, which consist of two expressions compared using operators: <code>==</code> ; <code>!=</code> ; <code><</code> ; <code>></code> ; <code><=</code> ; <code>>=</code> or their alphabetical equivalents: <code>eq</code> , <code>ne</code> , <code>lt</code> , <code>gt</code> , <code>le</code> , <code>ge</code> . |

Operators

Table 12-7 lists the operations supported by MIXEDMODE.

The results of the modulo operation is the remainder when the first number is divided by the second number. Both modulo operation arguments are rounded down to the nearest integer before the operation is performed.

| Table 12-7: Operations | | | | | |
|------------------------|-----------------|--------------------------------|----------|---------|-------------------|
| Operation Type | Operator | Meaning | Example | Synonym | Notes |
| Algebraic | + | Plus | $a + b$ | | |
| | + | Unary Plus | $+a$ | | |
| | - | Minus | $a - b$ | | |
| | - | Unary Minus | $-a$ | | |
| | * | Multiply | $a*b$ | | |
| | / | Divide | a/b | | |
| | ^ | Power | a^b | | |
| | % | Modulo | $a\%b$ | | |
| | , | Comma | a,b | | |
| Logical | & | And | $a\&b$ | and | |
| | | Or | $a b$ | or | |
| | && | And | $a\&\&b$ | and | |
| | | Or | $a b$ | or | |
| | ! | Unary negation | $!a$ | not | |
| | [cond] ? x:y | Ternary conditional expression | | | See Example below |
| Relational | < | Less than | $a<b$ | lt | |
| | > | Greater than | $a>b$ | gt | |
| | <= | Less than or equal | $a<=b$ | le | |
| | >= | Greater than or equal | $a>=b$ | ge | |
| | == | Equal | $a==b$ | eq | |
| | != | Not equal | $a!=b$ | ne | |

Example

```
.param Param1=5 Param2=10
+ Test='(Param>Param2) ? 1 : 2'
+ Test2='5*((Param1<Param2) ? (Param+1) : (Param2+2))'
```

This page is intentionally left blank.

13.1: Quantum Effects Modeling

There are several quantum effects models that work with ATLAS to simulate various effects of quantum mechanical confinement. These models are generally independent and should not be used simultaneously in any given simulation. These models are described in the following sections.

In Section 13.2: “Self-Consistent Coupled Schrodinger Poisson Model”, we discuss the self-consistent Schrodinger-Poisson model. This model self-consistently solves Poisson's equation (for potential) and Schrodinger's equation (for bound state energies and carrier wavefunctions). This model should not be used to look at carrier transport problems.

In Section 13.3: “Density Gradient (Quantum Moments Model)”, we describe the density gradient model. This model is based on the moments of the Wigner function equations of motion and calculates a quantum correction to the carrier temperatures in the transport equations. This model can accurately reproduce the carrier concentration predicted by the Schrodinger-Poisson model but can also predict transport properties. This model cannot, however, predict the bound state energies or wave functions given by the Schrodinger-Poisson model.

In Section 13.4: “Bohm Quantum Potential (BQP)”, we describe the Bohm quantum potential model. This model can be used to address a similar set of problems as the density gradient model. The Bohm quantum potential model has two advantages over the density gradient model: 1) better convergence and 2) better calibration to the Schrodinger-Poisson model.

In Section 13.5: “Quantum Correction Models”, we describe two quantum correction models. These models by Van Dort and Hansch are both phenomenological models that give corrections for the effects of quantum confinement in the inversion layer under the gate of MOSFET devices.

In Section 13.6: “General Quantum Well Model”, we describe a general quantum well model used to predict the gain and spontaneous recombination in quantum well light emitting devices. This model is based on Schrodinger-Poisson modelling and is used to calculate the bound state energies and wave functions. The bound state energies are used to predict the gain and spontaneous recombination rates and the wave functions can be used to predict the overlap integral.

In Section 13.7: “Quantum Transport: Non-Equilibrium Green's Function Approach”, we describe a fully quantum non-equilibrium Green's function approach to modeling transport in nanoscale devices with strong transverse confinement. This model predicts eigen energies and eigen functions, quantum electron and current density, and ballistic current-voltage characteristics.

In Section 13.8: “Drift-Diffusion Mode-Space Method (DD_MS)”, we describe a semiclassical approach to modeling transport in nanoscale devices with strong transverse confinement. This model is coupled to ATLAS models for mobility, generation, and recombination. It also predicts eigen energies and eigen functions, quantum electron and current density, and drift-diffusion current-voltage characteristics.

13.2: Self-Consistent Coupled Schrodinger Poisson Model

The solution of Schrodinger's equation gives a quantized description of the density of states in the presence of quantum mechanical confining potential variations.

The SCHRO parameter of the MODEL statement enables the self-consistent coupled Schrodinger-Poisson model for electrons. Set the P.SCHRO parameter in the MODEL statement to enable the Schrodinger-Poisson model for holes. You can specify both SCHRO and P.SCHRO on the same statement to model two carrier types simultaneously. ATLAS2D can solve Schrodinger equation in 1D slices or 2D plane. In the case of cylindrical coordinates, Schrodinger equation is solved in radial direction for different orbital quantum numbers and for all slices perpendicular to the axis. ATLAS3D solves a 1D Schrodinger equation along one of the axes at all in-plane nodes or 2D Schrodinger equation in plane slices. To set up dimensionality and direction of the solver, use the SP.GEOM parameter on the MODELS statement. Table 13-1 shows the possible values of the SP.GEOM parameter. If the parameter is not specified, ATLAS will use a default value, depending on the situation. Note that the 2DXY option in cylindrical coordinates corresponds to a case of a 3D quantum confinement in radial, axial, and azimuthal directions.

Table 13-1. Geometry of Schrodinger solver

| SP.GEOM | Geometry | Comments |
|---------|-------------------|---|
| 1DX | 1D in X direction | default for cylindrical mesh in Atlas2D |
| 1DY | 1D in Y direction | default for non-cylindrical mesh in Atlas2D. |
| 1DZ | 1D in Z direction | Unavailable in Atlas2D |
| 2DXY | 2D in XY plane | Default in Atlas2D if option 2DXY.SCHRO is on Default in Atlas3D for cylindrical or non Atlas mesh or if option 2DXY.SCHRO is on |
| 2DXZ | 2D in XZ plane | Unavailable in Atlas2D |
| 2DYZ | 2D in YZ plane | Default for Atlas mesh in Atlas3D Unavailable in Atlas2D |

When the quantum confinement is in one dimension (along Y axis), the calculation of the quantum electron density relies upon a solution of a 1D Schrodinger equation solved for eigen state energies $E_{iv}(x)$ and wavefunctions $\Psi_{iv}(x,y)$ at each slice perpendicular to the X axis and for each electron valley (or hole band) v .

$$-\frac{\hbar^2}{2} \frac{\partial}{\partial y} \left(\frac{1}{m_y^v(x,y)} \frac{\partial \Psi_{iv}}{\partial y} \right) + E_C(x,y) \Psi_{iv} = E_{iv} \Psi_{iv} \quad 13-1$$

Here, $m_y^v(x,y)$ is a spatially dependent effective mass in Y direction for the v -th valley and $E_C(x,y)$ is a conduction band edge. The equation for holes is obtained by substituting hole effective masses instead of electron ones and valence band edge $-E_V(x,y)$ instead of $E_C(x,y)$. Analogously, in cylindrical coordinates, the equation for the radial part of the wavefunction $R_{imv}(r)$ for each orbital quantum number m reads

$$-\frac{\hbar^2}{2} \left[\frac{1}{r} \frac{\partial}{\partial r} \left(\frac{1}{m_r^v(r,z)} r \frac{\partial R_{imv}}{\partial r} \right) - \frac{1}{m_r^v(r,z)} \frac{m^2}{r^2} \right] + E_C(r,z) R_{imv} = E_{imv} R_{imv} \quad 13-2$$

Finally, a 2D Schrodinger equation reads:

$$-\frac{\hbar^2}{2} \left[\frac{\partial}{\partial x} \left(\frac{1}{m_x^v(x, y)} \frac{\partial \Psi_{iv}}{\partial x} \right) + \frac{\partial}{\partial y} \left(\frac{1}{m_y^v(x, y)} \frac{\partial \Psi_{iv}}{\partial y} \right) \right] + E_C(x, y) \Psi_{iv} = E_{iv} \Psi_{iv} \quad 13-3$$

In order to take into account exchange-correlation effects, you can specify the `SP.EXCORR` parameter on the `MODELS` statement. The exchange-correlation, treated within local density approximation, is an additional negative potential energy term in the Hamiltonian, which depends on the local carrier density and is given by

$$V_{exc} = -\frac{q^2}{4\pi^2 \epsilon \epsilon_0} [3\pi^2 n(x, y, z)]^{1/3} \quad 13-4$$

The electron valleys denoted in TONYPLOT as **Longitudinal**, **Transverse1** and **Transverse2** correspond to the effective mass along the Y axis being respectively `ML`, `MT1`, and `MT2` on the `MATERIAL` statement. Table 13-2 shows the effective mass for each valley along all the axes. In cylindrical coordinates, ATLAS makes an approximation to the effective mass in the radial direction as shown in Table 13-3.

| Table 13-2. Effective Mass | | | |
|----------------------------|-----|-----|-----|
| Valley | mx | my | mz |
| Longitudinal | MT1 | ML | MT2 |
| Transverse1 | MT2 | MT1 | ML |
| Transverse2 | ML | MT2 | MT1 |

| Table 13-3. Effective Mass in cylindrical case | | |
|--|-------------------|-----|
| Valley | mr | mz |
| Longitudinal | MT1 | ML |
| Transverse1 | 2*MT1*ML/(MT1+ML) | MT1 |

To choose the number of electron valleys and anisotropy of effective mass, specify the `NUM.DIRECT` and `SP.DIR` parameters on the `MODELS` statement. If `NUM.DIRECT` is set to 1 and `SP.DIR=0` (default), a solution for one valley with isotropic effective mass `MC` (on the `MATERIAL` statement) is obtained. An additional flexibility in case of `NUM.DIRECT=1` can be gained by changing `SP.DIR` parameter. If `SP.DIR` is set to 1, 2 or 3, only one valley is assumed, but with anisotropic effective mass, corresponding to **Longitudinal**, **Transverse1** or **Transverse2** respectively from Tables 13-2 or 13-3. If `NUM.DIRECT` is set to 3, `SP.DIR` is ignored and three valleys are assumed, each with anisotropic effective mass given by Tables 13-2 or 13-3. In ATLAS2D, in a special case of a 1D confinement and equivalent transverse masses or in a cylindrical mesh, you can set `NUM.DIRECT` to 2 and only two solutions will be obtained (`ML` and `MT1`) with appropriate degeneracy factors. To specify how many valence bands to consider, use the `NUM.BAND` parameter. If `NUM.BAND` is set to 1, a solution for only one valence band `MV` (on the `MATERIAL` statement) is obtained. If `NUM.BAND` is set to 3, a solution for heavy

holes, light holes, and split-off band holes (MHH, MLH, and MSO on the MATERIAL statement) is obtained. If NUM.BAND is set to 2, only heavy holes and light holes are taken into account. SP.DIR is ignored in case of holes.

Schrodinger equation uses a conduction or valence band edge of the bulk material. You have an option to set an additional band off-set manually without getting into details of its origin. To do so, use the following parameters from the MODELS or REGION or MATERIAL statements.

| Table 13-4. Band off-set | |
|--------------------------|-----------------------------|
| Valley/Band | Band off-set |
| Longitudinal | DEC.C1 |
| Transverse1 | DEC.C2 |
| Transverse2 | DEC.C3 |
| Isotropic Electron Band | DEC.ISO (when NUM.DIRECT=1) |
| Heavy Holes | DEV.HH |
| Light Holes | DEV.LH |
| Split-off Holes | DEV.SO |
| Isotropic Hole band | DEV.ISO (when NUM.BAND=1) |

The expression for the electron concentration is obtained by using Fermi statistics and eigen energies and wave functions:

$$n(x, y) = 2 \frac{k_B T}{\pi \hbar^2} \sum_v \sqrt{m_x^v(x, y) m_z^v(x, y)} \sum_{i=0}^{\infty} |\Psi_{iv}(x, y)|^2 \ln \left[1 + \exp \left(-\frac{E_{iv} - E_F}{k_B T} \right) \right] \quad 13-5$$

for 1D confinement and

$$n(x, y) = 2 \frac{\sqrt{2k_B T}}{\hbar} \sum_v \sqrt{m_z^v(x, y)} \sum_{i=0}^{\infty} |\Psi_{iv}(x, y)|^2 F_{-1/2} \left(-\frac{E_{iv} - E_F}{k_B T} \right) \quad 13-6$$

for a 2D confinement case and cylindrical case, where $F_{-1/2}$ is the Fermi-Dirac integral of order $-1/2$.

ATLAS will search for a minimum number of filled eigen states in the range between $(-\infty; 20kT]$. You can also use EIGEN=X when a certain fixed number X of eigen states is required. In the case of cylindrical mesh in ATLAS2D, Schrodinger equation has two quantum numbers: radial number n_r and orbital number m . All states with non zero m are doubly degenerate, which corresponds to $+m$ and $-m$ or to clockwise and counter-clockwise polarization of electron wave function. Therefore, when you set the EIGEN parameter to X, ATLAS will store X states for $m=0$ and X states for each of $2*(X-1)$ orbital numbers $m = \pm 1, \pm 2, \dots \pm X$. This will add up to a total of $X*(2X-1)$ states. In TONYPLOT, the states are sorted in ascending order with respect to their eigen energies, while the information about values of radial and orbital numbers (n_r, m) is not stored. You can still determine n_r and m of a state, using a general property of wave functions $R_{n_r, m}(r)$. n_r is always equal to the number of times the wave function changes sign $+1$. For $m=0$, $R_{n_r, m}(r)$ is always non zero and has zero first derivative at $r=0$. For $m=1$,

$R_{nr,m}(r)$ is always zero and has zero second derivative at $r=0$. For $m>1$, $R_{nr,m}(r)$ is always zero and has zero first derivative at $r=0$.

By default, electron penetration into insulator regions is not allowed. Use the `OX.SCHRO` parameter on the `MODELS` statement to allow electron penetration and `OX.MARGIN=` to specify the maximum penetration distance (default is 0.0003 microns). By default, ATLAS attempts to find a solution in all semiconducting regions. If a solution is unnecessary in a particular region, switch off `SCHRO` parameter on the `REGION` statement for that particular region.

When Schrodinger equation is solved in 1D or 2D slices, it is required that all nodes are aligned (1D) or lie in one plane (2D). In case of unstructured or non-ATLAS mesh, ATLAS can find a solution on an additional rectangular mesh and then interpolate results onto original mesh. To set an additional rectangular mesh, use `SPX.MESH`, `SPY.MESH`, and `SPZ.MESH` statements in a way similar to `X.MESH`, `Y.MESH`, and `Z.MESH`. In ATLAS3D, if `Z.MESH` is not specified, Z planes of original mesh will be used.

Note that 2D Schrodinger does not require rectangular mesh within the 2D slice and can handle meshes created outside of ATLAS (e.g., `DEVEDIT` or `ATHENA`). In devices with crosssection close to rectangular, ATLAS gives an option to speed up a solution by using the `SP.FAST` parameter on the `MODELS` statement. When this parameter is on, a 2D solution is sought in the form of linear combination of products on 1D solutions in the middle of the solution domain along perpendicular axes. The solution will be exact for rectangular structure and deviate slightly for non rectangular. `SP.FAST` parameter requires a rectangular mesh. If it is unavailable, use `SPX.MESH`, `SPY.MESH`, and `SPZ.MESH` to set up an additional rectangular mesh.

Since the wavefunctions diminish rapidly from the confining potential barriers in the Schrodinger solutions, the carrier concentrations become small and noisy. You can refine these carrier concentrations by setting a minimum carrier concentration using the `QMINCONC` parameter on the `MODELS` statement. This parameter sets the minimum carrier concentration passed along to the Poisson solver and the output to the structure files. The transition between the Schrodinger solution and the minimum concentration is refined between $10 \times \text{QMINCONC}$ and `QMINCONC` so that it is continuous in the first derivative.

Once the carrier concentration is calculated using Equation 13-5 and Equation 13-6, it is substituted into the charge part of Poisson's Equation. The potential derived from solution of Poisson's equation is substituted back into Schrodinger's equation. This solution process (alternating between Schrodinger's and Poisson's equations) continues until convergence and a self-consistent solution of Schrodinger's and Poisson's equations is reached. A default predictor-corrector scheme is used to avoid instability and oscillations of Poisson convergence. In this scheme, after wave functions are found and fixed, eigen energies are changed locally and plugged into Poisson equation (predictor). After several predictor iterations, a new set of wave functions and eigen energies is computed (corrector). You can control the number of Predictor iterations by a parameter `NPRED.NEGF=` (default is 7) on the `MODELS` statement.

The convergence criterion for potential for Schrodinger-Poisson as well as for `NEGF` and `DDMS` models is given by the `QCRIT.NEGF` parameter on the `MODELS` statement with a default of 0.001 eV. Maximum number of iterations after which Schrodinger-Poisson proceeds to the next bias is set by `SP.NUMITER` with a default of 30. ATLAS also checks for oscillatory convergence behavior for the last `SP.NUMOSC` (default 30) iterations starting from iteration number `SP.STAOSC` (default 3). If logarithm of potential update or residual is smaller than `SP.MINDIF` (default 0.001), then ATLAS will proceed to the next bias point.

For modeling of devices with transverse confinement, it is sometimes more preferable to set von Neumann Boundary Conditions (BC) for potential in a contact. Von Neumann BC will be applied if you set the `REFLECT` parameter on the `CONTACT` statement and if `SCHRO` or `P.SCHRO` parameter is present on the `MODELS` statement.

To set number of eigen states stored in a structure file, use the `EIGENS` parameter on the `OUTPUT` statement. Use the `SAVE` statement or the `OUTFILE` parameter on the `SOLVE` statement to write the solutions of the self-consistent system into a structure file.

In obtaining self-consistent solutions for the Schrodinger's Equation, an assumption is made about the location of the electron or hole quasi-fermi level. Normally, ATLAS tries to set the quasi-fermi to that of a contact attached to the region where solution is obtained. To ensure that the fermi level is zero, set `FIXED.FERMI` parameter on the `MODELS` statement.

If you want to solve Schrodinger equation as a postprocessing step under non-equilibrium, specify `CARRIERS=2` or `CARRIERS=1 HOLES` or `CARRIERS=1 ELECTRONS` on the `METHOD` statement. In this case, a classical quasi Fermi level will be computed by solving drift-diffusion equations. It is then used to find quantum electron density self-consistently with Poisson equation. Flag `FIXED.FERMI` will be ignored. In case of bias sweep, ATLAS will solve Schrodinger for each bias point. The `SP.LAST` parameter on the `SOLVE` statement allows to solve the Schrodinger equation with classically computed Fermi levels only for the last bias point.

13.3: Density Gradient (Quantum Moments Model)

The quantum models apply to several different types of problems. These problems are HEMT channel confinement simulation, thin gate oxide MOS capacitors and transistors, and other problems such as small geometry MESFETs and heterojunction diodes.

The effects due to confinement of carriers associated with variations of local potential on the scale of the electron wave functions (i.e., quantum effects) can be modeled in ATLAS using a density gradient. This model is based on the moments of the Wigner function equations-of-motion [278, 279, 264, 253], which consists of quantum correction to the carrier temperatures in the carrier current and energy flux equations (see Chapter 3: “Physics”, Equations 3-20 to 3-23).

In the density gradient model, the expression for electron current given in Chapter 3: “Physics”, Equation 3-11 is replaced by the expression given in Equation 13-7.

$$\vec{J}_n = qD_n \nabla n - qn\mu_n \nabla(\psi - \Lambda) - \mu_n n(kT_L \nabla(\ln n_{ie})) \quad 13-7$$

Here, Λ is a quantum correction potential.

Equation 13-8 is the density gradient model for holes.

$$\vec{J}_p = -qD_p \nabla p - qp\mu_p \nabla(\psi - \Lambda) + \mu_p p(kT_L \nabla(\ln n_{ie})) \quad 13-8$$

The quantum potential can be calculated using either of the two expressions given in Equations 13-9 and 13-10.

$$\Lambda = -\frac{\gamma\hbar^2}{12m} \left[\nabla^2 \log n + \frac{1}{2} (\nabla \log n)^2 \right] \quad 13-9$$

$$\Lambda = -\frac{\gamma\hbar^2}{6m} \frac{\nabla^2 \sqrt{n}}{\sqrt{n}} \quad 13-10$$

where γ is a fit factor, m is the carrier effective mass, and n represents electron or hole concentration as appropriate. To choose between these expressions, specify DGLOG for Equation 13-9 or DGROOT for Equation 13-10 in the MODELS statement. By default, DGLOG is used. The fit factors for electrons and holes can be specified independently using the DGN.GAMMA or the DGP.GAMMA parameters of the MODELS statement respectively.

These expressions and particularly their derivatives can be seen to be sensitive to low carrier concentrations. You can specify a minimum concentration to use in these calculations using the QMINCONC parameter in the MODELS statement. This parameter specifies the minimum concentration used in the calculations of Equations 13-9 and 13-10 in cm^{-3} .

You can activate the model for electrons and holes independently. To activate the quantum model with the quantum moments equation for electrons, use the quantum switch, MODELS QUANTUM, in the MODELS statement. To activate the quantum moments equation for holes, use the quantum switch, MODELS P.QUANTUM.

Specify T.QUANTUM in the OUTPUT statement to write the quantum temperatures in the standard structure file. Once written you can examine the quantum temperature distribution using TONYPLOT.

Since the distributions of carriers given by the density gradient can vary greatly from the distributions predicted by the standard drift-diffusion or energy-balance models, the standard initial guess strategies (e.g., INIT) aren't usually suitable for obtaining solutions for quantum moments. Until more suitable initial guess strategies can be devised, we've included a damping factor to gradually apply to the density gradient.

This damping factor is specified by the QFACTOR parameter in the SOLVE statement. The QFACTOR is implemented as a pre-factor to the expression for the quantum correction potential, Λ , in Equations 13-9 and 13-10. As such, a value of QFACTOR of 0.0 implies that the density gradient is either turned off or not applied. A value of QFACTOR of 1.0 implies that the Quantum Moment Model is turned on and applied.

You can vary the value of QFACTOR between 0.0 and 1.0 to overcome the problems of initial guess. During this ramping of QFACTOR, PREVIOUS should be used as an initial guess. Also, while varying the QFACTOR, trapping is available if a given solution doesn't converge. In such cases, the QFACTOR is reduced and solutions proceed until convergence is obtained or the maximum number of trap steps is exceeded.

The following is a typical fragment from an input file that ramps the QFACTOR parameter from 0 to 1:

```
MODEL NUMCARR=1 QUANTUM FLDMOB CONMOB SRH PRINT
OUTPUT CON.BAND VAL.BAND BAND.PARAM T.QUANTUM
SOLVE INIT
SOLVE QFACTOR=0.0
SOLVE QFACTOR=0.0001
SOLVE QFACTOR=0.001
SOLVE QFACTOR=0.01
SOLVE QFACTOR=0.1
SOLVE QFACTOR=1.0
LOG OUTF=test.log
SOLVE VDRAIN=0.01
```

13.4: Bohm Quantum Potential (BQP)

This model was developed for SILVACO by the University of Pisa and has been implemented into ATLAS with the collaboration of the University of Pisa. This is an alternative to the Density Gradient method and can be applied to a similar range of problems. There are two advantages to using Bohm Quantum Potential (BQP) over the density gradient method. First, it has better convergence properties in many situations. Second, you can calibrate it against results from the Schrodinger-Poisson equation under conditions of negligible current flow.

The model introduces a position dependent quantum potential, Q , which is added to the Potential Energy of a given carrier type. This quantum potential is derived using the Bohm interpretation of quantum mechanics [101] and takes the following form

$$Q = \frac{-\hbar^2}{2} \frac{\gamma \nabla(M^{-1} \nabla(n^\alpha))}{n^\alpha} \quad 13-11$$

where γ and α are two adjustable parameters, M^{-1} is the inverse effective mass tensor and n is the electron (or hole) density. This result is similar to the expression for the quantum potential in the density gradient model with $\alpha = 0.5$, but there are some differences about how they are implemented. Q is added to the continuity equations the same way Λ is for the density gradient method as shown in Equations 13-7 and 13-8.

The Bohm Quantum Potential (BQP) method can also be used for the Energy balance and hydrodynamic models, where the semi-classical potential is modified by the quantum potential the same way as for the continuity equations.

The iterative scheme used to solve the non-linear BQP equation along with a set of semi-classical equations is as follows. After an initial semi-classical solution has been obtained, the BQP equation is solved on its own Gummel iteration to give Q at every node in the device. The semi-classical potential is modified by the value of Q at every node and the set of semi-classical equations is then solved to convergence as usual (using a Newton or block iterative scheme). Then, the BQP equation is solved to convergence again and the process is repeated until self-consistency is achieved between the solution of the BQP equation and the set of semi-classical equations. The set of semi-classical equations solved can be any of the combinations usually permitted by ATLAS.

To use the BQP model for electrons (or holes), specify `BQP.N` (`BQP.P`) in the `MODELS` statement. You can also set the parameter values (α and γ) and the direction of the quantization (confinement). Tables 13-5 and 13-6 show the parameters to use for the `MODEL` statement.

Table 13-5. MODEL Statement Parameters for Electrons

| Parameter | Type | Default | Units |
|------------|---------|---------|-------|
| BQP.N | Logical | false | |
| BQP.NGAMMA | Real | 1.2 | -- |
| BQP.NALPHA | Real | 0.5 | -- |
| BQP.QDIR | Integer | 2 | -- |

Table 13-6. MODEL Statement Parameters for Holes

| Parameter | Type | Default | Units |
|------------|---------|---------|-------|
| BQP.P | Logical | false | |
| BQP.PGAMMA | Real | 1.0 | -- |
| BQP.PALPHA | Real | 0.5 | -- |
| BQP.QDIR | Integer | 2 | -- |

BQP.N switches on the model for electrons. BQP.P switches it on for holes. The BQP.NGAMMA and BQP.PGAMMA allow you to set the γ parameter for electrons and holes respectively. BQP.NALPHA and BQP.PALPHA allow you to set the α parameter for electrons and holes respectively.

You can specify BQP.N and BQP.P separately. But if quantum effects for electrons and holes occur in the same device, then you can specify them together in the same MODELS statement.

The BQP.QDIR parameter specifies the principal quantization direction.

BQP.QDIR = 1 means the X direction

BQP.QDIR = 2 means the Y direction

BQP.QDIR = 3 means the Z direction

For example, if a MOSFET channel is in the XY plane, the direction of quantization (quantum confinement) is the Z direction you would set BQP.QDIR=3. For semiconductors with spherical bands, BQP.QDIR will have no effect.

13.4.1: Calibration against Schrodinger-Poisson Model

You can obtain close agreement between BQP and the results of Schrodinger-Poisson (S-P) calculations for any given class of device. To obtain comparisons with S-P results, we recommend to use either the new quasistatic capacitance-voltage profile feature or compare charge-voltage curves. This will ensure similar charge control properties between the two models.

The first part of the calibration is to choose a suitable biasing for the device. There should be negligible current flow and quantum confinement effects that manifest at the chosen biases. The second part of the calibration is to set the appropriate BQP parameters in the MATERIAL or MODELS statements, and to set CARRIERS=0 in the METHOD statement.

This will cause the BQP equation to be coupled with Poisson's equation using the charge density terms.

$$n = N_c \exp\left(-\frac{(E_c + qQ)}{kT_L}\right) \quad 13-12$$

$$p = N_v \exp\left(-\frac{(qQ - E_v)}{kT_L}\right) \quad 13-13$$

This gives the same results as solving the current continuity equations with the constraint of zero current density.

The third part of calibration is to choose the quantity to compare with S-P results.

For example, for a MOSFET holding the drain and source voltages at the same bias and ramping the gate bias will give us a bias dependent capacitance with negligible current flow. So for an NMOS, you may have the statement

```
SOLVE VGATE=0.0 NAME=GATE VSTEP=0.01 VFINAL=2.0 QSCV
```

to give us the quasi-static C-V curve as it is biased into inversion. It is best to use a fine voltage step with QSCV to give good resolution. The process can be repeated by setting the S-P model in the MODELS statement instead of BQP to obtain the same set of curves for the S-P model.

The BQP model is then rerun with different sets of parameters until an acceptable agreement with the curves produced by the S-P model is achieved.

13.4.2: Post Calibration runs

After obtaining the parameters for BQP, either the Drift-Diffusion or energy balance (hydrodynamic) equations can be solved as usual. For cases where Lattice Heating is important then LAT.TEMP can be enabled at the same time.

The iteration scheme uses a modified version of BLOCK. Set BLOCK in the METHOD statement (although NEWTON and GUMMEL are ignored, BLOCK is always used if the BQP model is set). If an energy balance model is chosen (HCTE.EL or HCTE.HO on the MODELS statement), then an alternative iteration scheme will become available by specifying BQP.ALTEB in the METHOD statement. This method is slower and is only available in ATLAS2D but may have better convergence properties.

By using BQP.NOFERMI, the BQP equation will only use its Boltzmann statistics form. Without this parameter, the statistics used are those specified for the other equations. With fermi statistics, the convergence can be poor for very high carrier densities, and this parameter can circumvent some convergence properties.

Re-calibrate the BQP parameters if you set BQP.NOFERMI.

| Table 13-7. METHOD Statement Parameter | | | |
|--|---------|---------|-------|
| Parameter | Type | Default | Units |
| BQP.ALTEB | Logical | false | |
| BQP.NOFERMI | Logical | false | |

To speed up convergence, specify the NOCURRENT parameter on the first SOLVE statement after SOLVE INIT. It should prevent the need to use the QFACTOR parameter as was necessary for the density gradient method. QSCV enables the quasistatic capacitance calculation and output.

| Table 13-8. SOLVE Statement Parameters | | | |
|--|---------|---------|-------|
| Parameter | Type | Default | Units |
| NOCURRENT | Logical | false | |
| QSCV | Logical | false | |
| QFACTOR | Real | 1.0 | |

Use the parameters in Table 13-9 to control solution convergence behavior.

Table 13-9. METHOD Statement Parameters

| Parameter | Type | Default |
|-----------|---------|--|
| BQPX.TOL | Real | 2.5×10^{-7} |
| BQPR.TOL | Real | 1.0×10^{-26} (2D) 1.0×10^{-18} (3D) |
| BQP.NMIX | Real | 1 |
| BQP.PMIX | Real | 1 |
| NBLOCKIT | Integer | 15 |
| ITLIMIT | Integer | 25 |
| GUMITS | Integer | 100 |

The solution comprises of OUTER iterations (which end when self-consistency occurs) and within these are solutions of groups of equations or single equations. The BQP equation is implemented so that both LHS and RHS convergence are required. You cannot override this default behavior. Tests carried out have shown it gives the best performance. ITLIMIT controls how many iterations can occur for the BQP equation in SOLVE INIT. This is $10 * ITLIMIT$. For CARRIERS=0 solutions, the maximum number of iterations for the individual equation solvers is GUMITS. The maximum number of OUTER iterations is ITLIMIT. NBLOCKIT controls the number of OUTER cycles in the drift-diffusion and energy-balance cases. the maximum number of drift-diffusion solution and carrier-energy solution iterations is ITLIMIT, and the maximum number of BQP solutions is GUMITS. The convergence may become unsteady when the carrier density is very high and Fermi statistics is used. In this case, you may decrease BQP.NMIX or BQP.PMIX parameters or both to a value between 0 and 1. This will cause relaxation of Fermi factors between two consecutive iterations and result in steadier convergence.

Note: The Bohm Quantum potential is stored in ATLAS as an energy and so the convergence criteria are actually of order KT less than those for scaled electrostatic potential. In ATLAS 3D, the BQP equation had an extra scaling factor applied and so the RHS norms are larger than in 2D. LHS norms, however, are the same.

The Bohm Quantum Potential is automatically calculated in insulators. If you specify the SEMICONDUCTOR parameter in the MATERIAL statement for the insulator, the drift-diffusion equations will be solved in the insulator and will include the BQP corrections. It is also recommended to set the densities of states of the insulator to be the same as the semiconductor to which they interface. For example for Silicon/SiO₂ system, set

```
MATERIAL REGION=N NC300=2.8E19 NV300=1.04E19
```

where N is region number of SiO₂.

You can also set the BQP parameters on a material by material basis, which may be necessary for heterojunction based devices. The BQP model is applied globally and cannot be set on a region by region basis.

Table 13-10 shows the material parameters that have a direct impact on the BQP equation.

| Table 13-10. MATERIAL Statement | | |
|---------------------------------|---------|---------|
| Parameter | Type | Default |
| SEMICONDUCTOR | Logical | false |
| EG300 | Real | |
| AFFINITY | Real | |
| NC300 | Real | |
| NV300 | Real | |
| BQP.NALPHA | Real | 0.5 |
| BQP.NGAMMA | Real | 1.2 |
| BQP.PALPHA | Real | 0.5 |
| BQP.PGAMMA | Real | 1.0 |

There is one more pertinent parameter, BQP.NEUMANN, which can be set on the MODELS statement.

BQP.NEUMANN sets the normal gradient of classical+quantum potential explicitly to zero on non-contact boundaries. If cleared using MODELS ^BQP.NEUMANN, the Neumann conditions will then be applied implicitly. Clearing this flag may give a slight speed increase and slight differences in solution.

| Table 13-11. OUTPUT Statement Parameters | | |
|--|---------|---------|
| Parameter | Type | Default |
| P.QUANTUM | Logical | False |

Setting the P.Quantum parameter in the OUTPUT statement will cause the Bohm Quantum Potential to output to a structure file. The Electron Quantum Potential and Hole Quantum Potential will both output.

13.5: Quantum Correction Models

In deep submicron MOS devices, quantum effects in the channel can have significant effects on the device characteristics. These effects are directly due to the increased doping levels and thinner gate oxide. In the channel of such devices, the potential well formed during inversion where the effects of quantum confinement must be considered. The direct effect of such quantum confinement is that the peak of the carrier concentration is shifted away from the interface and the thinner gate oxide can cause a marked difference in gate capacitance. Consideration of the effects may be essential for accurate prediction of the device turn-on voltage.

To fully treat quantum effects, solving the Schrodinger's equation, isn't always desirable or necessary.

13.5.1: Hansch's Model

The quantum mechanical correction given by Hansch [87] is suitable for accurate simulation of the effects of quantum mechanical confinement near the gate oxide interface in MOSFETs. To enable the model, specify the `HANSCHQM` parameter of the `MODEL` statement. This correction model is a modification of the density of states as a function of depth below the Si/SiO₂ interface, which is given by Equation 13-14.

$$N_C^* = N_C \left[1 - \exp\left(-\left(\frac{z}{\text{LAMBDA}}\right)^2\right) \right] . \quad 13-14$$

Here, N_C is the standard density of states, z is the depth below the interface. `LAMBDA` is a user-definable parameter in the `MODEL` statement.

Table 13-12. User-definable parameter for Equation 13-14

| Statement | Parameter | Default | Units |
|-----------|-----------|----------------------|---------------|
| MODELS | LAMBDA | 1.0×10^{-3} | μm |

13.5.2: Van Dort's Model

In the Van Dort's model [234], the effects of the quantum confinement are modeled by broadening the bandgap near the surface, which makes a function of a perpendicular electric field and distance from the surface. In Van Dort's model, the change in bandgap is given by the expression in Equation 13-15.

$$\Delta E_g = (\text{B_DORT}) \beta \frac{13}{9} \left(\frac{\epsilon_{Si}}{4 q k_B T_L} \right)^{1/3} (E_{\perp})^{2/3} g(y) . \quad 13-15$$

Here, `B_DORT` is a user-definable parameter in the `MODEL` statement, β is equal to 6.1×10^{-8} eV cm, E_{\perp} is the perpendicular electric field, and $g(y)$ is a function to restrict the application of the model to the channel region, given by Equation 13-16.

$$g(y) = \frac{2e^{-(Y/(\text{D_DORT}))^2}}{1 + e^{-2(Y/(\text{D_DORT}))^2}} . \quad 13-16$$

The Van Dort's model for N channel devices is enabled by specifying `N_DORT` in the `MODELS` statement. For P channel devices, the Van Dort's model is enabled by specifying `P_DORT` in the `MODELS` statement.

Table 13-13. User-definable parameters for Equation 13-16

| Statement | Parameter | Default | Units |
|-----------|-----------|----------------------|-------|
| MODELS | D.DORT | 2.5×10^{-6} | cm |
| MODELS | B.DORT | 1.0 | cm |

13.6: General Quantum Well Model

The general quantum well model is used to predict bound state energies in a region for subsequent use in modelling optoelectronic gain, radiative recombination and absorption. Figure 13-1 shows the simulation flow for such modelling.

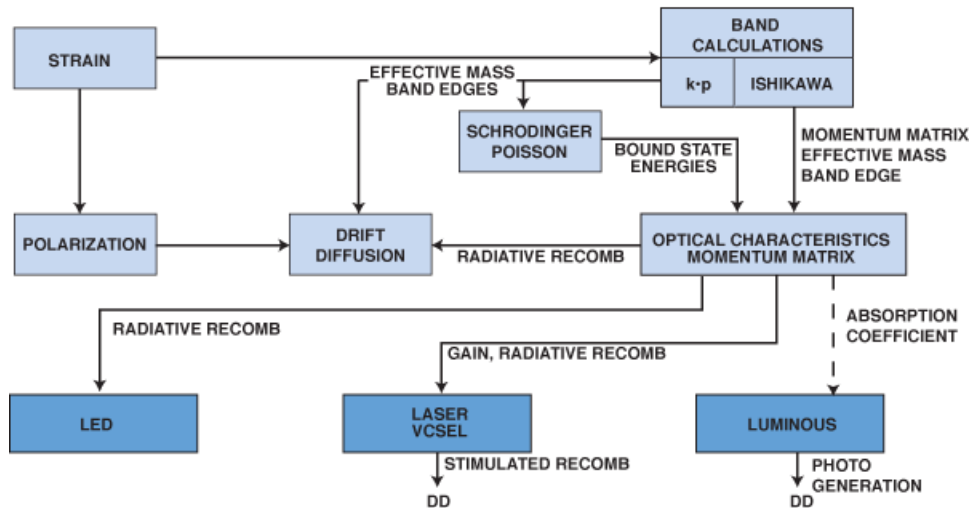


Figure 13-1: Simulation Flow For Physically Based Optoelectronic Models

The solution for of bound state energies is done by solving Schrodinger equation (see Equation 13-1) along discrete slices in the quantization direction. Effective masses and band-edge parameters are taken from multi-band k.p-based models, set by YAN, LI, ZB.KP, or CHUANG parameters on the MODELS statement.

You can enable the quantum well model by specifying QWELL in the REGION or MODELS statement. The orientation and dimensionality of Schrodinger solver is set by SP.GEOMETRY parameter on the MODELS statement with a default of 1DY. Alternatively, you may solve 1DX and 1DZ cases. Regions with QWELL parameter are treated as independent quantum wells, unless they are adjacent to each other and have the same orientation, in which case they are merged into one quantum well region. This means that a single quantum well region can include different materials. Merging of adjacent regions into a single quantum well can be overridden by assigning different numbers to different wells, using QWNUM parameter on the REGION or the MODELS statement.

Whenever a quantum well region is specified, the solution domain for Schrodinger equation will actually be expanded into neighboring regions to account for wavefunction penetration into the barriers. The maximum penetration length is set by WELL.MARGIN parameter on the MODELS statement with a default value of 0.01 micron. It is perfectly admissible to have wavefunctions of two different wells to overlap.

By default, ATLAS mesh is used for discretization. If the ATLAS mesh too coarse, you can specify WELL.NX or WELL.NY or WELL.NZ or all three in the REGION or the MODELS statement to use an auxiliary quantum well mesh. If an auxiliary mesh is used, the sampling is uniform and bound state energy values are interpolated back onto the device mesh for the optical modelling. Generally, you should select WELL.NX, WELL.NY, and WELL.NZ to adequately resolve the geometry but there is a trade-off between computational accuracy and speed.

The `WELL.CNBS` and `WELL.VNBS` parameters of the `REGION` or the `MODELS` statement specify the maximum number of bound state energies to resolve for each conduction and valence band with default values of 1. An output structure file of the `QWELL` model contains bound state energies and wavefunctions for each well, band, and subband. The actual number of bound states found may be less than or equal to the value specified by `WELL.CNBS` and `WELL.VNBS`. Additionally, the output contains band edge energies for each band and bound carrier densities.

You can also specify regions for quantum well simulation in the `SUPERLATTICE (DBR)` statement. To enable the model, specify the `QWELL1` and `QWELL2` parameters. These enable quantum modeling for the first and second superlattice cycles respectively. The sampling of the quantum wells are controlled by the `WELL1.NX`, `WELL2.NX`, `WELL1.NY` and `WELL2.NY` parameters. The numbers of bound states are controlled by the `WELL1.CNBS`, `WELL2.CNBS`, `WELL1.VNBS` and `WELL2.VNBS` parameters.

13.7: Quantum Transport: Non-Equilibrium Green's Function Approach

This section describes a Non Equilibrium Green's Function approach (NEGF). This fully quantum method treats such effects as source-to-drain tunneling, ballistic transport, quantum confinement on equal footing. In the first part, we discuss a mode space approach, where NEGF formalism in transport direction is coupled with Schrodinger equation in transverse plane. This situation is common to double gate transistors, FinFETs, nanowire FETS, and so on. In the second part, we discuss a planar NEGF approach, where the transverse plane is assumed to be infinite. This approach is more applicable to multiple barrier structures, such a resonant tunneling diode (RTD).

13.7.1: Mode Space NEGF Approach

By specifying the NEGF_MS and SCHRODINGER options on the MODELS statement, you can launch an NEGF solver to model ballistic quantum transport in such devices as double gate or surround gate MOSFET in ATLAS2D or ATLAS3D. All the parameters described in Section 13.2: "Self-Consistent Coupled Schrodinger Poisson Model" have the same meaning in the context of NEGF.

An effective-mass Hamiltonian H_o of a two-dimensional device, given by

$$H_o = -\frac{\hbar^2}{2} \left[\frac{\partial}{\partial x} \left(\frac{1}{m_x^v(x, y)} \frac{\partial}{\partial x} \right) + \frac{\partial}{\partial y} \left(\frac{1}{m_y^v(x, y)} \frac{\partial}{\partial y} \right) \right] \quad 13-17$$

is discretized in real space using a finite volume method. A corresponding expression in cylindrical coordinates is

$$H_o = -\frac{\hbar^2}{2} \left[\frac{1}{r} \frac{\partial}{\partial r} \left(\frac{1}{m_r^v(r, z)} r \frac{\partial}{\partial r} \right) - \frac{1}{m_r^v(r, z)} \frac{m^2}{r^2} + \frac{\partial}{\partial z} \left(\frac{1}{m_z^v(r, z)} \frac{\partial}{\partial z} \right) \right] \quad 13-18$$

Instead of solving a 2D or 3D problem, which may take too much computational time, a Mode Space (MS) approach is used. A Schrodinger equation is first solved in each slice of the device to find eigen energies and eigen functions. Then, a transport equation of electrons moving in the sub-bands is solved. Because only a few lowest eigen sub-bands are occupied and the upper subbands can be safely neglected, the size of the problem is reduced. Moreover, in the devices where the cross-section does not change (e.g., a nanowire transistor), the sub-bands are not quantum-mechanically coupled to each other and the transport equations become essentially 1D for each sub-band. Therefore, you can further divide the method into Coupled (CMS) or Uncoupled Mode Space (UMS) approaches. ATLAS will automatically decide on the minimum number of sub-bands required and the method to be used. It is possible, however, to set the number of sub-bands by using the EIGEN parameter on the MODELS statement. To enforce either CMS or UMS approaches, you can use NEGF_CMS or NEGF_UMS instead of NEGF_MS on the MODELS statement. The transformation of a real space Hamiltonian H_o to a mode space is done by taking a matrix element between m-th and n-th wave functions of k-th and l-th slices:

$$H^{MS}_{mnkl} = \langle \psi_m^k(y) | H_o | \psi_n^l(y) \rangle \quad 13-19$$

Note, that in cylindrical geometry, different orbital quantum numbers will result in zero matrix element and are therefore uncoupled. The quantum transport equations in the mode space read:

$$\left(E - H^{MS}_{mnkl} - \Sigma_S^R - \Sigma_D^R \right) G^R = I \quad 13-20$$

$$\left(E - H^{MS}_{mnkl} - \Sigma_S^R - \Sigma_D^R \right) G^< = \left(\Sigma_S^< + \Sigma_D^< \right) G^A \quad 13-21$$

Here, E is an electron (hole) energy. $\Sigma_{S,D}^R$ are retarded self-energies, carrying information about the density of states of source and drain semi-infinite contacts. $\Sigma_{S,D}^<$ are less-than self-energies, carrying information about the Fermi distribution function in contacts.

The solution of these equations are a retarded Green's function $G^R(E)$, whose diagonal elements have a meaning of the local density of states as a function of energy and a less-than Green's function $G^<(E)$, whose diagonal elements have a meaning of carrier density as a function of energy. $G^A(E) = (G^R(E))^\dagger$ is an advanced Green's function. A non-uniform energy grid will be generated internally, while you can control the number of energy grid points using a parameter `ESIZE.NEGF=` on the `MODELS` statement. After solving the above equations at each energy, following quantities of interest are computed by ATLAS and stored in a structure file (expressions are given for rectangular grid):

- carrier density

$$n(x_i, y_j) = -\frac{i}{L_z} \sum_{k_z} \sum_{\sigma m n} \int G_{mnii}^<(E) \psi_m^j(y_j) \psi_n^{*i}(y_j) \frac{dE}{2\pi} \quad 13-22$$

- x-component of current density

$$J_x(x_i, y_j) = -\frac{2e}{\hbar L_z \Delta x} \sum_{k_z} \sum_{\sigma m n} \int \Re(t_{i+1jj} G_{mnii+1}^<(E)) \psi_m^j(y_j) \psi_n^{*i+1}(y_j) \frac{dE}{2\pi} \quad 13-23$$

- y-component of current density

$$J_y(x_i, y_j) = -\frac{2e}{\hbar L_z \Delta y} \sum_{k_z} \sum_{\sigma m n} \int \Re(t_{iijj+1} G_{mnii}^<(E)) \psi_m^j(y_j) \psi_n^{*i}(y_{j+1}) \frac{dE}{2\pi} \quad 13-24$$

- total current density

$$J = (J_x^2 + J_y^2)^{1/2} \quad 13-25$$

Here, t_{ijkl} is an off-diagonal element of real space Hamiltonian H_o , which couples nodes (x_i, y_k) and (x_j, y_l) . The summation over k_z is absent in the cylindrical geometry. Instead, a summation over orbital quantum numbers is performed. Additionally, you can probe the following energy dependent quantities (a new log file will be created at each bias point).

Additionally, you can probe the following energy dependent quantities. A new log file will be created every time you set `NEGF.LOG` on the `SAVE` statement.

Transmission coefficient for m-th sub-band

$$T_m(E) = \text{tr} \left\{ G^R \Gamma_S G^A \Gamma_D \right\}, \quad \Gamma_{S,D} = 2 \Im m \left\{ \Sigma_{S,D}^R \right\} \quad 13-26$$

You must set a `TRANSMISSION` parameter on the `PROBE` statement. It is followed by `BAND=` and `STATE=` parameters to specify the effective mass band (valley) and the number of sub-band respectively. In addition, a log file name is a specified `FILENAME=` parameter. At each bias, point a “k” will be added to the log file name, where k is the number of the bias point. If `BAND=` or `STATE=` is missing, a summation over this index is performed.

Density of states in the m-th subband

$$DOS_m(E, x_i) = 2 \Im \left\{ G_{mmii}^R(E) \right\} \quad 13-27$$

You must set a parameter DOSVSE on the PROBE statement. It is followed by BAND= , STATE= , and X= parameters to specify the effective mass band (valley), the number of subband, and the location along transport direction respectively. If BAND= or STATE= is missing, a summation over this index is performed.

Electron density per energy in m-th subband

$$N_m(E, x_i) = \Im \left\{ G_{mmii}^<(E) \right\} \quad 13-28$$

You must set a parameter DENSUSE on the PROBE statement. It is followed by BAND= , STATE= , and X= parameters to specify the effective mass band (valley), the number of subband, and the location along transport direction respectively. If BAND= or STATE= is missing, a summation over this index is performed.

Current density per energy in the m-th subband

$$J_m(E, x_i) = \frac{2e}{h} \Re \left\{ h_{mmi} + i G_{mmii+1}^<(E) \right\} \quad 13-29$$

You must set a parameter CURDSUSE on the PROBE statement. It is followed by BAND= , STATE= , and X= parameters to specify the effective mass band (valley), the number of subband, and the location along transport direction respectively.

The energy dependent quantities are stored on a uniform energy grid. You can specify the size of the grid by setting a parameter ESIZEOUT.NEGF= on OUTPUT statement. If it is not specified, the size will be the same as ESIZE.NEGF on the MODELS statement

A solution of NEGF equations is performed self-consistently with Poisson equation using a predictor-corrector scheme. You can specify the number of predictor iterations using a NPRED.NEGF= parameter on the MODELS statement. The criterion for convergence of Poisson iterations is set by a QCRIT.NEGF= parameter on the MODELS statement.

By default, Dirichlet boundary conditions (BC) for potential and open-boundary condition for electrons are used in the contacts. You can also use von Neumann boundary conditions for potential by specifying REFLECT parameter on the CONTACT statement. This type of BC is useful because ballistic carriers do not create voltage drop near the source and drain contacts. Moreover, the potential in the source and drain must be allowed to float because the number of electrons reflected backward and thus total carrier concentration in contacts can change with bias. The third type of BC is applicable to Schottky contacts, where potential is fixed by Dirichlet BC, but carriers are injected at all energies, mimicking a near-constant density of states of metal contact near the Fermi level. To set Schottky BC, set NEGF.TUNNEL on the CONTACT statement and also specify metal density of states by DOS.NEGF with the default of 0.1 1/eV. In the case of Schottky contacts, contact self-energy is given by

$$\Sigma_c^R = i \cdot t^2 \cdot DOS.NEGF \quad 13-30$$

Finally, a few comments has to be made about NEGF model:

- NEGF is a fully quantum approach to electron transport, which takes into account the wave nature of electron in both transport and transverse directions. This is the main difference of this method and drift-diffusion or Boltzmann Transport equation, which treat electron classically.
- In the present version, the transport is ballistic (i.e., no scattering occurs). Currently, this model gives an upper limit of current. In future versions, electron-phonon scattering may be added.
- The model is robust to predict subthreshold current, threshold voltage. The Poisson convergence, however, may be unstable when a device is completely open because the assumption of equilibrium contacts breaks down. In the long run, adding scattering will mitigate this problem.
- A discretized effective-mass Hamiltonian has a finite bandwidth, which depends on the mesh spacing in the transport direction and is given by $\hbar^2/(2m\Delta_x^2)$. A spacing in the transport direction should be fine enough, so that a half-bandwidth of discretized effective mass Hamiltonian is larger than applied bias. ATLAS will give a warning if the grid is not fine enough.

13.7.2: Planar NEGF approach

Most of the equations and syntax of the mode-space approach are also applicable to planar devices. Here, we discuss only a few new parameters specific to planar approach. Planar NEGF solver is based on 1D NEGF with effective mass Hamiltonian discretized in real space. Current and carrier density are obtained by analytically integrating Green's function over 2D transverse k-space. The solution is done for each electron or hole band independently of all other bands. Ballistic transport is assumed. In real devices, such as resonant tunneling diodes (RTD), injection into the double barrier structure occurs from emitter quasi-bound states. To model this effect without including inelastic phonon scattering, we treat emitter and collector as quasi-equilibrium regions, while the central region with double barrier structure is treated as non-equilibrium.

To launch the model, specify `N.NEGF_PL1D` or `P.NEGF_PL1D` or both on the `MODELS` statement for electrons and holes respectively. This will tell ATLAS to solve 1D NEGF equation in the first slice in transport direction and copy carrier and current density to all other slices. If the slices are not equivalent, use `N.NEGF_PL` or `P.NEGF_PL` or both instead to solve 1D NEGF equation for each slice separately.

To specify a region as quasi-equilibrium, use `EQUIL.NEGF` on the `MODELS` or the `REGION` statements. It is a good idea to specify all regions in front of the first barrier and behind the last barrier as quasi-equilibrium, so that all possible quasi-bound states are filled. Quasi-equilibrium regions are characterized by a broadening, which can be set by `ETA.NEGF` parameter on the `MODELS` or the `REGION` statements, with a default of 0.0066 eV.

The output quantities of interest are the IV characteristics, spectrum of transmission, DOS, density and current, and also spatial profiles of carrier density and conduction or valence band edge.

The solution of 1D NEGF equations starts with resonance finding in the whole device using Quantum Transmitting Boundary Method (QTBM) and a construction of the energy grid. It is the resolution of these resonances that is critical for correct simulation. The resonances can be seen as extremely narrow peaks in the transmission vs. energy plot. Use log scale in `TONYPLOT` to get a better understanding of the position of the transmission and DOS resonances.

In case of poor convergence, energy grid size (`ESIZE.NEGF` on the `MODELS` statement) and magnitude of the broadening in quasi-equilibrium regions have to be increased.

13.8: Drift-Diffusion Mode-Space Method (DD_MS)

This model is a semiclassical approach to transport in devices with strong transverse confinement and is a simpler alternative to mode-space NEGF approach (NEGF_MS) as described earlier. Similar to NEGF_MS, the solution is decoupled into Schrodinger equation in transverse direction and 1D transport equations in each subband. In this model, however, a classical drift-diffusion equation is solved instead of a quantum transport equation. Thus, the model captures quantum effects in transverse direction and yet inherits all familiar ATLAS models for mobility, recombination, impact ionization, and band-to-band tunneling. Unlike NEGF_MS, the model can handle only devices with uniform cross-section because quantum mechanical coupling between electron subbands is neglected. To activate the model, use DD_MS together with SCHRO or P.SCHRO parameters or both on the MODELS statement. Note that CARRIERS parameter on the METHOD statement should be set to 0 because multi-dimensional ATLAS continuity equation solvers are not used in this method.

One-dimensional drift-diffusion transport in each subband, characterized by subband index v and effective mass index b is described by

$$\frac{1}{q} \frac{\partial J_{vb}}{\partial x} = R_{vb} - G_{vb} \quad 13-31$$

$$J_{vb} = q \mu_{vb} n_{vb} \frac{\partial E_{vb}}{\partial x} - q D_{vb} \frac{\partial n_{vb}}{\partial x} \quad 13-32$$

where $J_{vb}(x)$ is subband current, $n_{vb}(x)$ is subband carrier density to be found, and $E_{vb}(x)$ is subband eigen energy as found by Schrodinger solver in transverse direction. The 1D transport equation is discretized using Scharfetter-Gummel scheme. Mobility $\mu_{vb}(x)$ is defined by ATLAS mobility models and is in general dependent on material, doping, local longitudinal electric field, and temperature. Diffusion coefficient $D_{vb}(x)$ is related to mobility by

$$D_{vb} = \mu_{vb} \left(\frac{\partial n_{vb}}{\partial E_{vb}} \right)^{-1} \quad 13-33$$

As Fermi-Dirac statistics is always assumed, the relation between subband carrier densities (cm^{-3}), quasi-fermi levels and eigen energies is given by the following relations:

$$n_{vb} = 2 \frac{k_B T}{A \pi h} \sum_v \sqrt{m_x^{vb} m_z^{vb}} \ln \left[1 + \exp \left(-\frac{E_{vb} - E_{F, vb}}{k_B T} \right) \right] \quad 13-34$$

in case of 1D confinement in y direction and

$$n_{vb} = 2 \frac{\sqrt{2k_B T}}{A h} \sum_v \sqrt{m_x^{vb}} F_{-1/2} \left(-\frac{E_{vb} - E_{F, vb}}{k_B T} \right) \quad 13-35$$

in case of 2D confinement in y-z plane, where A is a normalizing area.

Recombination rates $R_{vb}(x)$ are computed by taking into account recombination of a particular electron (hole) subband with all hole (electron) subbands:

$$R_{vb} = \sum_{\lambda b'} R_{vb \lambda b'} = \sum_{\lambda b'} \frac{n_{vb} p_{\lambda b'} - n_i^2}{\tau_{vb \lambda b'}} \quad 13-36$$

Here, $R_{vb\lambda b'}(x)$ are computed using ATLAS bulk recombination models with a substitution of subband carrier densities for bulk densities, subband eigen energies for conduction and valence bands, and subband fermi levels for bulk fermi levels. Unlike the rest of ATLAS, recombination rates are set to 0 when only one carrier type is solved for.

Total impact ionization generation rates are computed by taking a sum over all electron and hole subbands:

$$G_{total} = \sum_{vb\lambda b'} \left(\alpha_n^{vb} |J_{vb}| + \alpha_p^{\lambda b'} |J_{\lambda b'}| \right) \quad 13-37$$

Impact ionization coefficients α_n and α_p are computed using ATLAS bulk impact ionization models. Then, the generation rate in each subband is given by G_{total} , weighted by the carrier population in the subband:

$$G_{vb} = G_{total} \cdot \frac{n_{vb}}{n_{total}} \quad 13-38$$

$$G_{\lambda b'} = G_{total} \cdot \frac{p_{\lambda b'}}{p_{total}} \quad 13-39$$

Unlike the rest of ATLAS, it is allowed to use impact ionization model with only one carrier type. While one carrier type calculation may give incorrect answer, it is sometimes very useful to understand the effect of electrons and holes separately.

When generation-recombination mechanisms are present, you can iterate between carrier density and G-R rates before solving the Poisson equation. The self-consistency between carrier density and G-R rates, achieved in this inner iteration procedure, will result in a more stable Poisson convergence. To control the number of inner iterations, use the `RGITER.DDMS=N` and the `RGCONV.DDMS=X` parameters on the `METHOD` statement. Here, N is the maximum number of inner iterations (default is 0) and X is minimum error between 0 and 1 (default is 1e-5).

After 1D transport equations are solved in each subband and quasi-fermi levels are extracted, bulk (3D) carrier densities and currents are computed by summing over all subbands and weighting with corresponding wave function squared as done in Equation 13-5 or Equation 13-6. The same procedure is used to compute total generation and recombination rates, which are stored in output structure file.

A usual predictor-corrector scheme is used to solve Poisson equation self-consistently. Similar to `NEGF_MS`, Dirichlet boundary conditions for potential in contacts are default. Von Neumann boundary conditions can be used by specifying `REFLECT` on the `CONTACT` statement. Schottky contacts boundary conditions can be set by `DDMS.TUNNEL` parameter on the `CONTACT` statement. In the case of Schottky contacts, potential is fixed but new generation terms will be added to the drift-diffusion equations. The local tunneling generation rate is given by

$$G_{TUN}(x) = \frac{A^* T}{k} \vec{F}(x) \Gamma_v(x) \ln \left(\frac{1 + \exp(E_v(x) - E_{F,v}(x))}{1 + \exp(E_v(x) - E_{F,contact})} \right) \quad 13-40$$

where A^* is Richardson constant, $F(x)$ is the local electric field, and $\Gamma(x)$ is the tunneling probability, computed within WKB approximation:

$$\Gamma_v(x) = \exp \left(-\frac{4\pi}{h} \int_0^x \sqrt{2m(E_v(0) - E_v(x'))} dx' \right) \quad 13-41$$

An output structure file contains quantities summed over all subbands. If you want detailed information about 1D subband-resolved eigen energies, carrier densities, currents, quasi fermi levels or generation-recombination rates, you can save an additional log file along with master structure file by specifying the `DDMS.LOG` option on the `SAVE` or `SOLVE` statements. If you specify `DDMS.LOG` on the `SOLVE` statement, then you must also set `MASTER` and `OUTF`. The name of the extra file is the same as the corresponding structure file but ending with `"_ddms.log"`.

14.1: Polycrystalline and Amorphous Semiconductor Models

TFT is an ATLAS module that simulates disordered material systems. TFT doesn't contain material models so you need to combine either S-PISCES or BLAZE with TFT to simulate these material systems.

TFT enables you to define an energy distribution of defect states in the bandgap of semiconductor materials. This is necessary for the accurate treatment of the electrical properties of such materials as polysilicon and amorphous silicon.

The syntax used by TFT is a part of the ATLAS syntax so there's no need for you to learn how to use a new simulator to run TFT simulations.

Before continuing with this chapter, you should be familiar with ATLAS physics. If not, read Chapters 2: "Getting Started with ATLAS" and 3: "Physics" before proceeding further. For more information on S-PISCES and BLAZE, see Chapters 4: "S-Piscs: Silicon Based 2D Simulator" and 5: "Blaze: Compound Material 2D Simulator".

14.2: Simulating TFT Devices

This section is intended to illustrate the basic building blocks for a thin-film transistor simulation.

To use TFT, specify the addition of defect states into the bandgap of a previously defined crystalline material. Throughout this section the example of polysilicon is used. Amorphous silicon and other disordered materials are handled in a similar manner.

14.2.1: Defining The Materials

Use the ATLAS command syntax to define a simple polysilicon thin-film transistor structure. The MESH, X.MESH, and Y.MESH statements can be used to construct a mesh as described in Chapter 2: “Getting Started with ATLAS”, Section 2.6: “Defining A Structure”. For more information on MESH statements, Chapter 21: “Statements,” Sections 21.31: “MESH” and 21.2: “A.MESH, R.MESH, X.MESH, Y.MESH, Z.MESH”.

When defining the material regions, use the following syntax.

```
REGION Y.MIN=-0.05 Y.MAX=0    OXIDE
REGION Y.MIN=0      Y.MAX=0.2 SILICON
REGION Y.MIN=0.2    Y.MAX=2    OXIDE
```

Note that the region is defined as silicon. You can also define the material as polysilicon. But note that it is the defect distribution rather than this initial material definition that will determine the electrical characteristics.

14.2.2: Defining The Defect States

Disordered materials contain a large number of defect states within the band gap of the material. To accurately model devices made of polycrystalline or amorphous materials, use a continuous density of states. The DEFECT statement is used to specify the density of defect states (DOS) as a combination of exponentially decaying band tail states and Gaussian distributions of mid-gap states [114, 84]. In addition, you may need to model the grain-grain boundary interface as a thermionic field emission boundary [117].

Note: The INTDEFECTS, INTERFACE S.S and TRAP.COULOMBIC models are available for grain-grain boundary interface modeling. These models have been developed in collaboration with Epsom and Cambridge University. For more information, see Chapter 21: “Statements,” Sections 21.20: “INTDEFECTS”, 21.21: “INTERFACE”, and 21.34: “MODELS”.

14.2.3: Density of States Model

It is assumed that the total density of states (DOS) and $g(E)$, is composed of four bands: two tail bands (a donor-like valence band and an acceptor-like conduction band) and two deep level bands (one acceptor-like and the other donor-like) which are modeled using a Gaussian distribution.

$$g(E) = g_{TA}(E) + g_{TD}(E) + g_{GA}(E) + g_{GD}(E) \quad 14-1$$

Here, E is the trap energy, E_C is the conduction band energy, E_V is the valence band energy and the subscripts (T, G, A, D) stand for tail, Gaussian (deep level), acceptor and donor states respectively.

$$g_{TA}(E) = N_{TA} \exp\left[\frac{E - E_C}{W_{TA}}\right] \quad 14-2$$

$$g_{TD}(E) = \text{NTD} \exp\left[\frac{E_v - E}{\text{WTD}}\right] \quad 14-3$$

$$g_{GA}(E) = \text{NGA} \exp\left[-\left[\frac{\text{EGA} - E}{\text{WGA}}\right]^2\right] \quad 14-4$$

$$g_{GD}(E) = \text{NGD} \exp\left[-\left[\frac{E - \text{EGD}}{\text{WGD}}\right]^2\right] \quad 14-5$$

For an exponential tail distribution, the DOS is described by its conduction and valence band edge intercept densities (NTA and NTD), and by its characteristic decay energy (WTA and WTD).

For Gaussian distributions, the DOS is described by its total density of states (NGA and NGD), its characteristic decay energy (WGA and WGD), and its peak energy/peak distribution (EGA and EGD). Table 14-1 shows the user-specifiable parameters for the density of defect states.

| Table 14-1. User-Specifiable Parameters for Equations 14-2 to 14-5 | | | |
|--|-----------|-----------------------|----------------------------|
| Statement | Parameter | Default | Units |
| DEFECTS | NTA | 1.12×10^{21} | cm^{-3}/eV |
| DEFECTS | NTD | 4.0×10^{20} | cm^{-3}/eV |
| DEFECTS | NGA | 5.0×10^{17} | cm^{-3}/eV |
| DEFECTS | NGD | 1.5×10^{18} | cm^{-3}/eV |
| DEFECTS | EGA | 0.4 | eV |
| DEFECTS | EGD | 0.4 | eV |
| DEFECTS | WTA | 0.025 | eV |
| DEFECTS | WTD | 0.05 | eV |
| DEFECTS | WGA | 0.1 | eV |
| DEFECTS | WGD | 0.1 | eV |

14.2.4: Trapped Carrier Density

The ionized densities of acceptor and donor like states (n_T and p_T respectively) are given by:

$$p_T = p_{TA} + p_{GA} \quad 14-6$$

$$n_T = n_{TD} + n_{GD} \quad 14-7$$

where n_{TA} , n_{GA} , p_{TD} and p_{GD} are given below.

$$p_{TA} = \int_{E_V}^{E_C} g_{TA}(E) \cdot f_{t_{TA}}(E, n, p) dE \quad 14-8$$

$$p_{GA} = \int_{E_V}^{E_C} g_{GA}(E) \cdot f_{t_{GA}}(E, n, p) dE \quad 14-9$$

$$n_{TD} = \int_{E_V}^{E_C} g_{TD}(E) \cdot f_{t_{TD}}(E, n, p) dE \quad 14-10$$

$$n_{GD} = \int_{E_V}^{E_C} g_{GD}(E) \cdot f_{t_{GD}}(E, n, p) dE \quad 14-11$$

$f_{t_{TA}}(E, n, p)$ and $f_{t_{GA}}(E, n, p)$ are the ionization probabilities for the tail and Gaussian acceptor DOS, while $f_{t_{TD}}(E, n, p)$ and $f_{t_{GD}}(E, n, p)$ are the ionization probabilities for the donors.

In the steady-state case, the probability of occupation of a trap level at energy E for the tail and Gaussian acceptor and donor states are given by Equations 14-12 through 14-15.

$$f_{t_{TA}}(E, n, p) = \frac{v_n \text{SIGTAE } n + v_p \text{SIGTAH } n_i \exp\left[\frac{E_i - E}{kT}\right]}{v_n \text{SIGTAE} \left(n + n_i \exp\left[\frac{E - E_i}{kT}\right] \right) + v_p \text{SIGTAH} \left(p + n_i \exp\left[\frac{E_i - E}{kT}\right] \right)} \quad 14-12$$

$$f_{t_{GA}}(E, n, p) = \frac{v_n \text{SIGGAE } n + v_p \text{SIGGAH } n_i \exp\left[\frac{E_i - E}{kT}\right]}{v_n \text{SIGGAE} \left(n + n_i \exp\left[\frac{E - E_i}{kT}\right] \right) + v_p \text{SIGGAH} \left(p + n_i \exp\left[\frac{E_i - E}{kT}\right] \right)} \quad 14-13$$

$$f_{tTD}(E, n, p) = \frac{v_p \text{SIGTDH } p + v_n \text{SIGTDE } n_i \exp\left[\frac{E - E_i}{kT}\right]}{v_n \text{SIGTDE} \left(n + n_i \exp\left[\frac{E - E_i}{kT}\right] \right) + v_p \text{SIGTDH} \left(p + n_i \exp\left[\frac{E_i - E}{kT}\right] \right)} \quad 14-14$$

$$f_{tGD}(E, n, p) = \frac{v_p \text{SIGGDH } p + v_n \text{SIGGDE } n_i \exp\left[\frac{E - E_i}{kT}\right]}{v_n \text{SIGGDE} \left(n + n_i \exp\left[\frac{E - E_i}{kT}\right] \right) + v_p \text{SIGGDH} \left(p + n_i \exp\left[\frac{E_i - E}{kT}\right] \right)} \quad 14-15$$

where v_n is the electron thermal velocity and v_p is the hole thermal velocity, n_i is the intrinsic carrier concentration. SIGTAE and SIGGAE are the electron capture cross-section for the acceptor tail and Gaussian states respectively. SIGTAH and SIGGAH are the hole capture cross-sections for the acceptor tail and Gaussian states respectively and SIGTDE, SIGGDE, SIGGDH, and SIGGDH are the equivalents for donors states.

Table 14-2. User-Specifiable Parameters for Equations 14-12 to 14-15

| Statement | Parameter | Default | Units |
|-----------|-----------|-----------------------|---------------|
| DEFECT | SIGTAE | 1.0×10^{-16} | cm^2 |
| DEFECT | SIGTDE | 1.0×10^{-14} | cm^2 |
| DEFECT | SIGGAE | 1.0×10^{-16} | cm^2 |
| DEFECT | SIGGDE | 1.0×10^{-14} | cm^2 |
| DEFECT | SIGTAH | 1.0×10^{-14} | cm^2 |
| DEFECT | SIGTDH | 1.0×10^{-16} | cm^2 |
| DEFECT | SIGGAH | 1.0×10^{-14} | cm^2 |
| DEFECT | SIGGDH | 1.0×10^{-16} | cm^2 |

14.2.5: Steady-State Trap Recombination

For steady-state conditions, the net recombination/generation rate is identical for electrons (R_n) and holes (R_p) (i.e., instantaneous equilibrium). Using Equations 14-12 through 14-15 to give the values of f_t and following the derivation by Shockley and Read [215] and Hall [86], the Shockley-Read-Hall recombination/generation rate due to the defect states is given by:

$$r_{sp} = \int_{E_V}^{E_C} \left(\frac{v_n v_p \text{SIGTAE} \text{SIGTAH} (n p - n_i^2) g_{TA}(E)}{v_n \text{SIGTAE} \left(n + n_i \exp \left[\frac{E - E_i}{k T} \right] \right) + v_p \text{SIGTAH} \left(p + n_i \exp \left[\frac{E_i - E}{k T} \right] \right)} + \frac{v_n v_p \text{SIGTGAE} \text{SIGGAH} (n p - n_i^2) g_{GA}(E)}{v_n \text{SIGGAE} \left(n + n_i \exp \left[\frac{E - E_i}{k T} \right] \right) + v_p \text{SIGGAH} \left(p + n_i \exp \left[\frac{E_i - E}{k T} \right] \right)} + \frac{v_n v_p \text{SIGTDE} \text{SIGTDH} (n p - n_i^2) g_{TD}(E)}{v_n \text{SIGTDE} \left(n + n_i \exp \left[\frac{E - E_i}{k T} \right] \right) + v_p \text{SIGTDH} \left(p + n_i \exp \left[\frac{E_i - E}{k T} \right] \right)} + \frac{v_n v_p \text{SIGGDE} \text{SIGGDH} (n p - n_i^2) g_{GD}(E)}{v_n \text{SIGGDE} \left(n + n_i \exp \left[\frac{E - E_i}{k T} \right] \right) + v_p \text{SIGGDH} \left(p + n_i \exp \left[\frac{E_i - E}{k T} \right] \right)} \right) dE \quad 14-16$$

14.2.6: Transient Traps

For the transient case, time is required for carriers to be emitted or captured and therefore instantaneous equilibrium cannot be assumed. This means that Equation 14-16 is no longer valid for transient simulations. Instead, the total recombination/generation rate for electrons (which is equal to electron recombination rate minus the generation rate for electrons) is calculated using the transient probabilities of occupation for acceptors (f_{tTA} and f_{tGA}). These are calculated by solving additional rate equations (Equations 14-17 and 14-18).

$$\frac{d}{dt}(p_{TA}) = \int_{E_V}^{E_C} g_{TA}(E) \left[v_n \text{SIGTAE} \left(n (1 - f_{tTA}(E)) - f_{tTA}(E) n_i \exp \left[\frac{E - E_i}{k T} \right] \right) - v_p \text{SIGTAH} \left(p f_{tTA}(E) - (1 - f_{tTA}(E)) n_i \exp \left[\frac{E_i - E}{k T} \right] \right) \right] dE \quad 14-17$$

$$\begin{aligned}
\frac{d}{dt}(p_{GA}) = & \int_{E_V}^{E_C} g_{GA}(E) \left[v_n \text{SIGGAE} \left(n \left(1 - f_{t_{GA}}(E) \right) - f_{t_{GA}}(E) n_i \exp \left[\frac{E - E_i}{k T} \right] \right) \right. \\
& \left. - v_p \text{SIGGAH} \left(p f_{t_{GA}}(E) - \left(1 - f_{t_{GA}}(E) \right) n_i \exp \left[\frac{E_i - E}{k T} \right] \right) \right] dE
\end{aligned} \tag{14-18}$$

The total hole recombination/generation rate can also be determined from the transient values of f_{tTD} and f_{tGD} (see Equations 14-19 and 14-20).

$$\begin{aligned}
\frac{d}{dt}(n_{TD}) = & \int_{E_V}^{E_C} g_{TD}(E) \left[v_n \text{SIGTDH} \left(p \left(1 - f_{t_{TD}}(E) \right) - f_{t_{TD}}(E) n_i \exp \left[\frac{E_i - E}{k T} \right] \right) \right. \\
& \left. - v_n \text{SIGTDE} \left(n f_{t_{TD}}(E) - \left(1 - f_{t_{TD}}(E) \right) n_i \exp \left[\frac{E - E_i}{k T} \right] \right) \right] dE
\end{aligned} \tag{14-19}$$

$$\begin{aligned}
\frac{d}{dt}(n_{GD}) = & \int_{E_V}^{E_C} g_{GD}(E) \left[v_p \text{SIGGDH} \left(p \left(1 - f_{t_{GD}}(E) \right) - f_{t_{GD}}(E) n_i \exp \left[\frac{E_i - E}{k T} \right] \right) \right. \\
& \left. - v_n \text{SIGGDE} \left(n f_{t_{GD}}(E) - \left(1 - f_{t_{GD}}(E) \right) n_i \exp \left[\frac{E - E_i}{k T} \right] \right) \right] dE
\end{aligned} \tag{14-20}$$

A transient trap simulation using this model is more time consuming than using the static model but gives a much more accurate description of the device physics. It may sometimes be acceptable to perform transient calculations using the static trap distribution and assume that traps reach equilibrium instantaneously. Specifying `FAST` on the `DEFECTS` statement will neglect the trap rate equation from the simulation.

Trap-Assisted Tunneling

Trap-Assisted Tunneling models the trap-to-band phonon-assisted tunneling effects for Dirac wells. At high electric fields, tunneling of electrons from the valence band to the conduction band through trap or defect states can have an important effect on the current.

Trap-assisted tunneling is modeled by including field-effect enhancement terms [99] (Γ_n^{DIRAC} and Γ_p^{DIRAC}) in the trap lifetimes in capture cross-sections. This model is enabled by specifying `TRAP.TUNNEL` in the `MODELS` statement.

The electron capture cross-section (`SIGTAE`, `SIGGAE`, and `SIGTDE`, and `SIGGDE`) are modified by including the electron field-effect term (Γ_n^{DIRAC}). For example, the electron capture cross-section for acceptor tail states (`SIGTAE`) becomes:

The field-effect enhancement term for electrons is given by:

$$SIGTAE \times \left(1 + \Gamma_n^{DIRAC}\right) \quad 14-21$$

`SIGGAE`, `SIGTDE`, and `SIGGDE` are also modified this way.

$$\Gamma_n^{DIRAC} = \frac{1}{kT_L} \int_0^{\Delta E_n} \exp\left(\frac{\Delta E_n}{kT_L} u - k_n u^{3/2}\right) du \quad 14-22$$

While the field-effect enhancement term for hole is:

$$\Gamma_p^{DIRAC} = \frac{1}{kT_L} \int_0^{\Delta E_p} \exp\left(\frac{\Delta E_n}{kT_L} u - k_p u^{3/2}\right) du \quad 14-23$$

The hole capture cross-sections (`SIGTAH`, `SIGGAH`, `SIGTDH`, and `SIGGDH`) are modified by including the hole field effect term (Γ_n^{DIRAC}). For example, `SIGTAH` now becomes:

$$SIGTAH \times \left(1 + \Gamma_n^{DIRAC}\right) \quad 14-24$$

`SIGGAH`, `SIGTDH`, and `SIGGDH` are also modified this way.

where u is the integration variable, ΔE_n is the energy range where tunneling can occur for electrons, ΔE_p is the tunneling energy range for holes, and k_n and k_p are given by:

$$k_n = \frac{4}{3} \sqrt{\frac{2m_0^{MASS.TUNNEL} \Delta E_n^3}{3q\hbar|E|}} \quad 14-25$$

$$k_p = \frac{4}{3} \sqrt{\frac{2m_0^{MASS.TUNNEL} \Delta E_p^3}{3q\hbar|E|}} \quad 14-26$$

\hbar is the reduced Planck's constant, m_0 is the rest mass of an electron, and `MASS.TUNNEL` is the relative effective mass (You can specify `MASS.TUNNEL` by setting the `MASS.TUNNEL` parameter in the `MODELS` statement).

Poole-Frenkel Barrier Lowering

The Poole Frenkel barrier lowering effect enhances the emission rate for trap-to-band phonon-assisted tunneling and pure thermal emissions at low electric fields. The Poole Frenkel effect occurs when the Coulombic potential barrier is lowered due to the electric field and only occurs in traps with a Coulombic potential (such as traps that are neutral when filled).

The Poole-Frenkel effect is modeled by including field-effect enhancement terms for Coulombic wells (Γ_n^{COUL} and Γ_p^{COUL}) and thermal emission (χ_F) [144] in the capture cross-sections. The model also includes the trap-assisted tunneling effects in the Dirac well. To enable this model, specify `TRAP.COULOMBIC` in the `MODELS` statement.

In the electron recombination/generation term (R_N), the Coulombic barrier lowering term (cF), and the electron Coulombic field-effect enhancement term (Γ_n^{COUL}) are applied to the electron capture cross-sections.

For example, `SIGTAE` now becomes:

$$\text{SIGTAE} \times \left(\chi_F + \Gamma_n^{COUL} \right) \quad 14-27$$

`SIGGAE`, `SIGTDE`, and `SIGGDE` are modified in the same manner.

The hole capture cross-section are modified by including the Dirac field-effect enhancement term for holes (Γ_n^{DIRAC}).

For example, `SIGTAH` now becomes:

$$\text{SIGTAE} \times \left(\chi_F + \Gamma_n^{COUL} \right) \quad 14-28$$

`SIGGAH`, `SIGTDH`, and `SIGGDH` are modified in the same manner.

In the hole recombination/generation term (R_p), the Coulombic terms are applied to the hole capture cross-sections and the Dirac terms applied to the electron capture cross-sections.

The Poole-Frenkel thermal emission enhancement factor, χ_F , is defined as:

$$\chi_F = \text{A.TRAPCOULOMBIC} \exp\left(\frac{\Delta E_{fp}}{kT_L}\right) \quad 14-29$$

ΔE_{fp} is the barrier lowering term for a Coulombic well (see Equation 14-30).

$$\Delta E_{fp} = \sqrt{\frac{\text{B.TRAPCOULOMBIC} q^3 |E|}{\pi \epsilon}} \quad 14-30$$

The Coulombic field-enhancement terms, Γ_n^{COUL} and Γ_p^{COUL} , are defined as:

$$\Gamma_n^{COUL} = \frac{\Delta E_n}{kT_L} \int_{\frac{\Delta E_{fp}}{\Delta E_n}}^1 \exp\left(\frac{\Delta E_n}{KT_L} u - k_p u^{3/2} \left[1 - \left(\frac{\Delta E_{fp}}{u \Delta E_n}\right)^{5/3}\right]\right) du \quad 14-31$$

$$\Gamma_p^{COUL} = \frac{\Delta E_p}{kT_L} \int_{\frac{\Delta E_{fp}}{\Delta E_n}}^1 \exp\left(\frac{\Delta E_p}{KT_L} u - k_p u^{3/2} \left[1 - \left(\frac{\Delta E_{fp}}{u \Delta E_p}\right)^{5/3}\right]\right) du \quad 14-32$$

Table 14-3. User-Specificable Parameters for Equations 14-29 and 14-30

| Statement | Parameter | Default | Units |
|-----------|-----------------|---------|-------|
| MATERIAL | A.TRAPCOULOMBIC | 1.0 | |
| MATERIAL | B.TRAPCOULOMBIC | 1.0 | |

14.2.7: Continuous Defects

If CONTINUOUS is specified in the DEFECTS statement, then the integral equations for the charge and recombination are evaluated using a numerical integral scheme [209]. In this case, the NUMA and NUMD (DEFECTS statement) parameters correspond to the number of acceptor and donor energy level intervals used in the integral.

14.2.8: Discrete Defects

If CONTINUOUS is not specified on the DEFECTS statement, the equation is modeled with discrete energy levels. The integrals terms in Equations 14-8 to 14-11 are replaced by summations, which run over the number of discrete energy levels (NUMA and NUMD). The acceptor and donor density of states terms are integrated separately. For example, the equation for the electron trap concentration (Equation 14-6) is replaced by:

$$n_T = \sum_{i=0}^{NUMA} \left(f_{t_{TA}}(E_i, n, p) \cdot \int_{-\infty}^{+\infty} g_{TA}(E) dE + f_{t_{GA}}(E_i, n, p) \cdot \int_{-\infty}^{+\infty} g_{GA}(E) dE \right) \quad 14-33$$

Table 14-4. Additional Parameters for the DEFECTS Statement

| Statement | Parameter | Default | Units |
|-----------|-----------|---------|-------|
| DEFECT | FAST | FALSE | |

Table 14-4. Additional Parameters for the DEFECTS Statement

| Statement | Parameter | Default | Units |
|-----------|------------|---------|-------|
| DEFECT | CONTINUOUS | FALSE | |
| DEFECT | NUMA | 12 | |
| DEFECT | NUMD | 12 | |

Syntax for a typical defect states definition is given below.

```
DEFECTS NTA=1.12E21 NTD=4.E20 WTA=0.025 WTD=0.05 \
      NGA=5.E17 NGD=1.5E18 EGA=0.4 EGD=0.4 \
      GA=0.1 WGD=0.1 SIGTAE=1.E-16 \
      SIGTAH=1.E-14 SIGTDE=1.E-14 \
      SIGTDH=1.E-16 SIGGAE=1.E-16 SIGGAH=1.E-14 \
      SIGGDE=1.E-14 SIGGDH=1.E-16
```

Figure 14-1 shows how the syntax is used to define the peak density of states and distribution widths for the two tail states and two Gaussian distributions.

14.2.9: Amphoteric Defects

In hydrogenated amorphous silicon (a-Si:H), the effect of dangling-bonds states on recombination can be significant. The dangling-bond states are amphoteric and located around the middle of the bandgap. If you specify the AMPHOTERIC parameter on the DEFECTS or INTDEFECTS statements, the dangling-bond density of states for a-Si:H will be calculated using the defect-pool model [182, 183] as will the amphoteric defect density and recombination [232].

The amphoteric defects are given by:

$$n_{AMP}^{+} = D(E)f_{AMP}^{+}(E) \quad 14-34$$

$$n_{AMP}^{0} = D(E)f_{AMP}^{0}(E) \quad 14-35$$

$$n_{AMP}^{-} = D(E)f_{AMP}^{-}(E) \quad 14-36$$

where:

- $n_{AMP}^{+}(E)$ is the occupied density of the positive amphoteric traps.
- $n_{AMP}^{0}(E)$ is the occupied density of the neutral amphoteric traps.
- $n_{AMP}^{-}(E)$ is the occupied density of the negative amphoteric traps.
- $f_{AMP}^{+}(E)$ is the probability of occupation of the positive amphoteric traps,

- $f_{AMP}^0(E)$ is the probability of occupation of the neutral amphoteric traps,
- $f_{AMP}^-(E)$ is the probability of occupation of the negative amphoteric traps.
- $D(E)$ is the dangling-bond density of states given by Equation 14-38.

The total charge caused by the presence of amphoteric traps is subtracted from the right hand side of Poisson's equation. The total charge value is defined by:

$$Q_{TAMP} = q \int_{E_V}^{E_C} (n_{AMP}^+(E) - n_{AMP}^-(E)) dE \quad 14-37$$

$$D(E) = NV0.AMPHOTERIC \left(\frac{HCONC.AMPHOTERIC}{NSISI.AMPHOTERIC} \right)^{\frac{kT0.AMPHOTERIC}{4EV0.AMPHOTERIC}} \quad 14-38$$

$$\cdot \left(\frac{2EV0.AMPHOTERIC^2}{2EV0.AMPHOTERIC - kT0.AMPHOTERIC} \right)$$

$$\exp \left[-\frac{I}{2EV0.AMPHOTERIC} \left(EP.AMPHOTERIC - E_v - \frac{SIGMA.AMPHOTERIC^2}{4EV0.AMPHOTERIC} \right) \right]$$

$$\cdot \left(\frac{2}{f_{AMP0}^0(E)} \right)^{\frac{kT0.AMPHOTERIC}{2EV0.AMPHOTERIC}} \cdot \frac{I}{\sqrt{2\pi SIGMA.AMPHOTERIC^2}}$$

$$\cdot \exp \left[-\left(\frac{E + \frac{SIGMA.AMPHOTERIC^2}{2EV0.AMPHOTERIC} - EP.AMPHOTERIC}{2SIGMA.AMPHOTERIC^2} \right)^2 \right]$$

where:

- EP.AMPHOTERIC is the most probable potential defect energy.
- E_V is the valence band edge.
- EV0.AMPHOTERIC is the characteristic energy.
- HCONC.AMPHOTERIC is the density of hydrogen.
- NSISI.AMPHOTERIC is the density of Si-Si bonds.
- NV0.AMPHOTERIC is the density of states of the valence-band tail exponential region extrapolated to the valence-band edge.
- SIGMA.AMPHOTERIC is the defect pool width.
- T0.AMPHOTERIC is the freeze-in temperature.

- $f_{AMP_0}^0(E)$ is the equilibrium probability of occupation of the neutral amphoteric traps.

The probabilities of occupation can be calculated from the equilibrium probabilities of occupation ($f_{AMP_0}^+(E)$, $f_{AMP_0}^0(E)$, and $f_{AMP_0}^-(E)$) and the capture and emission rates:

$$f_{AMP}^+(E) = \frac{1}{1 + \left[\frac{e_p^+ + n v_n \text{SIGNP.AMPHOTERIC}}{e_n^0 + p v_p \text{SIGP0.AMPHOTERIC}} \right] \left[1 + \frac{e_p^0 + n v_n \text{SIGN0.AMPHOTERIC}}{e_n^- + p v_p \text{SIGPN.AMPHOTERIC}} \right]} \quad 14-39$$

$$f_{AMP}^0(E) = \frac{1}{1 + \left[\frac{e_n^0 + p v_p \text{SIGP0.AMPHOTERIC}}{e_p^+ + n v_n \text{SIGNP.AMPHOTERIC}} \right] + \left[\frac{e_p^0 + n v_n \text{SIGN0.AMPHOTERIC}}{e_n^- + p v_p \text{SIGPN.AMPHOTERIC}} \right]} \quad 14-40$$

$$f_{AMP}^-(E) = 1 - f_{AMP}^0(E) - f_{AMP}^+(E) \quad 14-41$$

where:

- SIGN0.AMPHOTERIC is the electron capture cross-section for neutral defects.
- SIGNP.AMPHOTERIC is the electron capture cross-section for positive defects.
- SIGP0.AMPHOTERIC is the hole capture cross-section for neutral defects.
- SIGPN.AMPHOTERIC is the hole capture cross-section for negative defects.
- e_n^0 is the electron emission coefficient for neutral defects.
- e_n^- is the electron emission coefficient for negative defects.
- e_p^+ is the hole emission coefficient for positive defects.
- e_p^0 is the hole emission coefficient for neutral defects.

$$e_n^0 = \frac{n_0 f_{AMP_0}^+(E) v_n \text{SIGNP.AMPHOTERIC}}{f_{AMP_0}^0(E)} \quad 14-42$$

$$e_n^- = \frac{n_0 f_{AMP_0}^0(E) v_n \text{SIGN0.AMPHOTERIC}}{f_{AMP_0}^-(E)} \quad 14-43$$

$$e_p^0 = \frac{p_0 f_{AMP_0}^-(E) v_p \text{SIGPN.AMPHOTERIC}}{f_{AMP_0}^0(E)} \quad 14-44$$

$$e_p^+ = \frac{p_0 f_{AMP_0}^0(E) v_p^{\text{SIGP0.AMPHOTERIC}}}{f_{AMP_0}^+(E)} \quad 14-45$$

$$f_{AMP_0}^+(E) = \frac{1}{1 + 2 \exp\left[\frac{E_F - E_T}{kT}\right] + \exp\left[\frac{2E_F - 2E_T - \text{EU.AMPHOTERIC}}{kT}\right]} \quad 14-46$$

$$f_{AMP_0}^0(E) = \frac{2 \exp\left[\frac{E_F - E_T}{kT}\right]}{1 + 2 \exp\left[\frac{E_F - E_T}{kT}\right] + \exp\left[\frac{2E_F - 2E_T - \text{EU.AMPHOTERIC}}{kT}\right]} \quad 14-47$$

$$f_{AMP_0}^-(E) = 1 - f_{AMP_0}^+(E) - f_{AMP_0}^0(E) \quad 14-48$$

where:

- n_0 is the equilibrium electron concentration.
- p_0 is the equilibrium hole0 concentration.
- E_F is the Fermi energy.
- E_T is the trap energy.
- EU.AMPHOTERIC is the defect electron correlation energy.

The recombination terms are given by:

$$R_{AMP}^+ = D(E) [n v_n^{\text{SIGNP.AMPHOTERIC}} f_{AMP}^+(E) - e_n^0 f_{AMP}^0(E)] \quad 14-49$$

$$R_{AMP}^- = D(E) [n v_n^{\text{SIGN0.AMPHOTERIC}} f_{AMP}^0(E) - e_n^- f_{AMP}^-(E)] \quad 14-50$$

Table 14-5. User-Specifiable Parameters for Equations 14-34-14-50

| Statement | Parameter | Default | Units |
|----------------------|------------------|---|---------------------------------------|
| DEFECTS (INTDEFECTS) | EP.AMPHOTERIC | 1.27 | eV |
| DEFECTS (INTDEFECTS) | EU.AMPHOTERIC | 0.2 | eV |
| DEFECTS (INTDEFECTS) | EV0.AMPHOTERIC | 0.056 | eV |
| DEFECTS (INTDEFECTS) | HCONC.AMPHOTERIC | 5×10^{21} (5×10^{17}) | cm^{-3} (cm^{-2}) |
| DEFECTS (INTDEFECTS) | NSISI.AMPHOTERIC | 2×10^{23} (2×10^{19}) | cm^{-3} (cm^{-2}) |
| DEFECTS (INTDEFECTS) | NV0.AMPHOTERIC | NV300 | cm^{-3} (cm^{-2}) |
| DEFECTS (INTDEFECTS) | SIGMA.AMPHOTERIC | 0.19 | eV |
| DEFECTS (INTDEFECTS) | SIGN0.AMPHOTERIC | 1e-16 | cm^2 |
| DEFECTS (INTDEFECTS) | SIGNP.AMPHOTERIC | 1e-16 | cm^2 |

Table 14-5. User-Specifiable Parameters for Equations 14-34-14-50

| | | | |
|----------------------|------------------|-------|-----------------|
| DEFECTS (INTDEFECTS) | SIGP0.AMPHOTERIC | 1e-16 | cm ² |
| DEFECTS (INTDEFECTS) | SIGPN.AMPHOTERIC | 1e-16 | cm ² |
| DEFECTS (INTDEFECTS) | T0.AMPHOTERIC | 300 | K |

14.2.10: Amphoteric Defect Generation

This model calculates the dangling bond density of amphoteric defects as a function of bias stress time. If the parameter `TIME.EP` on the `MODELS` statement is specified, then the value of `EP.AMPHOTERIC` in the amphoteric defect model will be replaced by E_p :

$$E_p = EP.AMPHOTERIC \exp\left(-\left(\frac{TIME.EP}{EPT0.AMPHOTERIC}\right)^{EPBETA.AMPHOTERIC}\right) \quad 14-51$$

where E_p is the stress time dependent most probable potential defect energy.

Table 14-6. User-Specifiable Parameters for Equation 14-51

| Statement | Parameter | Type | Default | Units |
|-----------|-------------------|------|---------|-------|
| MODELS | TIME.EP | Real | 0 | s |
| DEFECTS | EPT0.AMPHOTERIC | Real | 1.3e6 | s |
| DEFECTS | EPBETA.AMPHOTERIC | Real | 0.5 | |

14.2.11: Light Induced Defect Generation

This model calculates the dangling bond density of amphoteric defects as a function of light [157]. The model is enabled by specifying `TRAP.LID` on the `MODELS` statement. The total dangling bond density of amphoteric defects (N_{AMP}) is given by:

$$N_{AMP} = \left[3G^2_{TIME.LID} \left(\frac{KD.LID - 2KH.LID}{SIG.LID^2} \right) + N_{AMP0} \right] \quad 14-52$$

where

- N_{AMP0} is the initial total dangling bond density.
- G is the photogeneration rate.
- `KD.LID` is the light induced SiHD creation constant.
- `KH.LID` is the dissociation constant of a hydrogen atom from a SiHD defect.
- `SIG.LID` is the capture coefficient of free carriers by dangling bonds.
- `TIME.LID` is the time values used in the light induced defect generation model.

By default, the photogeneration rate (G) is calculated from all active `BEAM` statements. If you specify the `BEAM.LID` parameter on the `MODELS` statement, then only active `BEAM` statements that were defined with the parameter `BEAM.LID` will be used in the photogeneration rate calculation. If you specify the parameter `GENRATE.LID` parameter on the `MODELS` statement, then this value will be used as the photogeneration rate in Equation 14-52.

Table 14-7. User-Specifiable Parameters for Equation 14-52

| Statement | Parameter | Type | Default | Units |
|-----------|-----------|------|---------|---------------------------------|
| MODELS | TIME.LID | Real | 0 | s |
| MATERIAL | KD.LID | Real | 5.0e-15 | cm ³ s ⁻¹ |
| MATERIAL | KH.LID | Real | 1.0e-18 | cm ³ s ⁻¹ |
| MATERIAL | SIG.LID | Real | 1.0e-8 | cm ³ s ⁻¹ |

14.2.12: Plotting The Density Of States Versus Energy

The DFILE and AFILE parameters were used to allow you to specify output file names for capture of defect densities as a function of energy for donor states and acceptor states, respectively. For example, if you want to look at the donor and acceptor defect distributions, specify the following line:

```
DEFECTS DFILE=donors AFILE=acceptors
```

The files, *donors* and *acceptors*, could then be loaded into TONYPLOT to look at the distributions of donor and acceptor defects as a function of energy.

14.2.13: Using the C-Interpreter to define DEFECTS

The C-INTERPRETER can be used to define the defect states in the bandgap. The F.TFTDON and F.TFTACC parameters of the DEFECT statement indicate the filenames containing the C functions. For more information on using the C-INTERPRETER, See Appendix A: "C-Interpreter Functions".

```
DEFECTS F.TFTDON=mydefects.c F.TFTACC=mydefects.c
```

The file, *mydefects.c*, will contain C functions for donor and acceptor defect densities as a function of energy. These user defined defects are added to the existing defect distribution. If you want to use only your own function, set the gaussian and tail functions to zero. The following example defect states are defined in the file, *tft.lib*. These are added to a zero background set using the tail and gaussian state syntax. The resultant distribution of defects versus energy can be plotted in the files, *don.dat* and *acc.dat*.

```
DEFECTS F.TFTDON=tft.lib F.TFTACC=tft.lib DFILE=don.dat AFILE=acc.dat \
NTA=0 NTD=0 WTA=1.0 WTD=1.0 \
NGA=0 NGD=0 EGA=0.6 EGD=0.6 WGA=1 WGD=1 \
SIGTAE=1.E-16 SIGTAH=1.E-14 SIGTDE=1.E-14 SIGTDH=1.E-16
SIGGAE=1.E-16 SIGGAH=1.E-14 SIGGDE=1.E-14 SIGGDH=1.E-16
```

14.2.14: Setting Mobility and Other Models

TFT uses adaptations of the standard models of S-PISCES or BLAZE. The example below shows how to select the models and material parameters for polysilicon.

```
MATERIAL MUN=300 MUP=30
```

```
MODELS SRH
```

Typical mobility values for amorphous silicon can be set by:

```
MATERIAL MUN=20 MUP=1.5
```

Other models are also available in TFT. These include impact ionization and tunneling. Set them by using:

```
MODELS BBT.STD IMPACT
```

Note: Don't use concentration dependent mobility models (CONMOB, ANALYTIC, ARORA, KLA) because they overwrite the low field mobilities set in the MATERIAL statement.

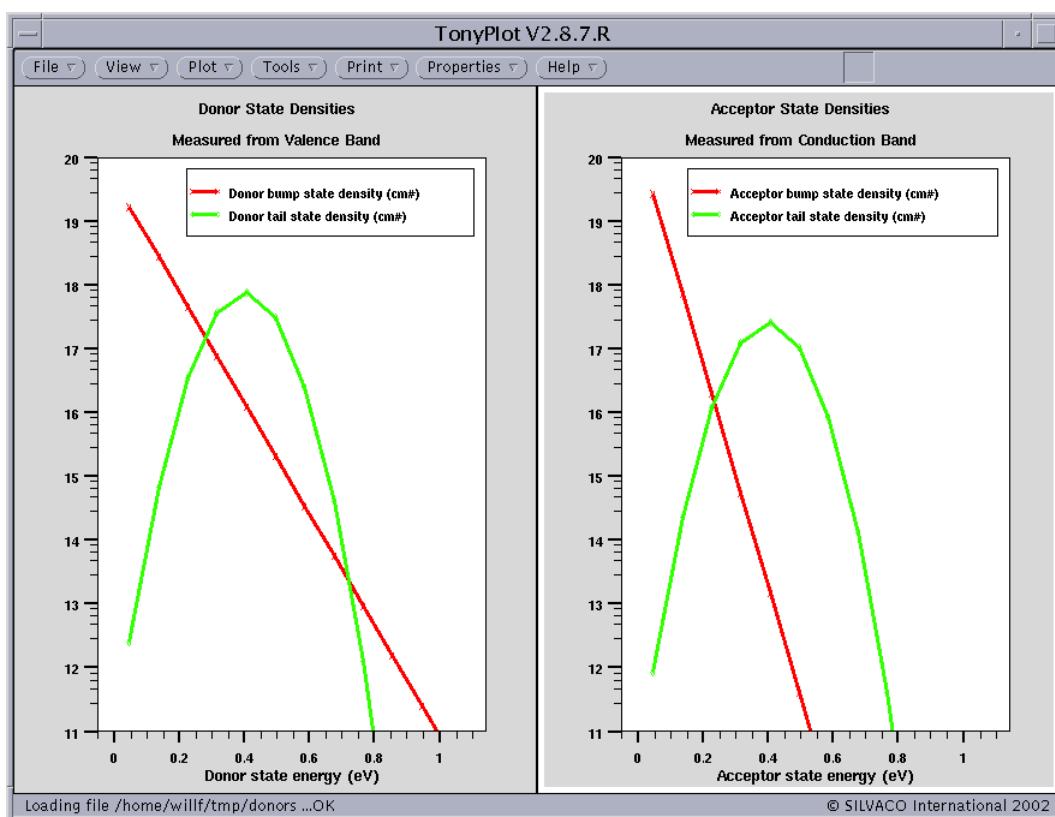


Figure 14-1: Syntax Guide to Define Two Tail States and Two Gaussian Distributions. NGA and NDG are the integrated values of the Gaussian distributions. Gaussians are entered on energies EGA and EGD respectively.

This page is intentionally left blank.

Chapter 15:

Organic Display and Organic Solar: Organic Simulators

15.1: Organic Device Simulation

Organic device simulation in the ATLAS framework is supported by two products: ORGANIC DISPLAY and ORGANIC SOLAR. As implied by the names, these simulators are targeted at specific applications requiring specific physical features. In the case of ORGANIC DISPLAY, the simulator is set up to perform analysis of organic based active displays. This entails simulation of principally organic FET devices, OFETs, and organic light emitting devices, OLEDs. The ORGANIC SOLAR simulator is specific to light sensitive devices, particularly solar cells. Organic based imaging sensors and the like may also be simulated using Organic Solar.

The following sections describe each of the simulators in more detail. This is followed by details of the physical models used in each case.

15.1.1: Organic Display

ORGANIC DISPLAY allows simulation of complex organic light emitting devices and circuits. Much of this capability is discussed elsewhere in this manual. Before reading this section, you should already be familiar with the general concepts discussed in Chapters 2: “Getting Started with ATLAS” and 3: “Physics”. Chapter 2: “Getting Started with ATLAS” gives an overview of the general concepts of building a simulation deck and using the simulator. Chapter 3: “Physics” gives a fairly detailed discussion of the basic physical concepts and models that define device modeling.

If you are interested in simulation of organic thin film transistors, OTFTs, then also read Chapter 14: “TFT: Thin-Film Transistor Simulator”. The drift diffusion concepts discussed in that chapter are completely analogous to those involved in simulation of OTFTs. Also if you are interested in embedding physical devices in lumped element (SPICE) circuits, then read Chapter 12: “MixedMode: Mixed Circuit and Device Simulator”. If you are interested in simulating organic light emitting devices, OLEDs, then also read Chapter 11: “LED: Light Emitting Diode Simulator”. This chapter discusses the physical concepts for simulation of light emitting devices in general including OLEDs. Finally, those interested may also want to look over Chapter 20: “Numerical Techniques” where they will be given a description of the workings of the numerics of the simulator including information on convergence.

In this section, we will lead you through the important differences that you will need to know about when simulating organic display devices. We will do this in a sequential manner similar to the description of deck construction presented in Chapter 2: “Getting Started with ATLAS”.

First, with respect to definition of the device structure, there is little difference with what is described in Chapter 2: “Getting Started with ATLAS”. The main thing you should be aware of is that there are several default material names that are recognized by ORGANIC DISPLAY. These materials are Organic, Pentacene, Alq3, TPD, PPV, Tetracene, and NPB. For insulating dielectrics and conductive materials, see Appendix B: “Material Systems”.

If you want to simulate a material not included in the default set recognized by ORGANIC DISPLAY, you should follow the steps described in Section B.2.5: “Specifying Unknown or User-Defined Materials in ATLAS”.

After you have specified the device structure, you may decide how to handle interfaces between homogenous layers. These interfaces are analogous to heterojunctions in the drift diffusion formulation where the band edges are replaced by the HOMO and LUMO.

You may choose to make the interfaces obey the physics of thermionic emission and tunneling. To do this, specify the INTERFACE statement with the parameters THERMIONIC and TUNNEL set. There are various ways in which characteristics may be assigned to a particular interface geometrically using

principally the `X.MIN`, `X.MAX`, `Y.MIN`, and `Y.MAX` parameters. These types of interfaces are discussed in more detail in Section 5.1.4: “The Thermionic Emission and Field Emission Transport Model”.

Next, you may want to fix the workfunction of electrodes to a certain value relative to the LUMO and HOMO. To do this, use the `CONTACT` statement where the workfunction is specified with the `WORKF` parameter. A particular `CONTACT` statement is associated with an electrode using the `NAME` or `NUMBER` parameters. Also, you can assign various Schottky characteristics to the electrode using, for example, the `SURF.REC` parameter to enable surface recombination or `BARRIER` to enable barrier lowering. For more details, see Section 21.5: “CONTACT”.

Key parameters in the simulation of organic devices are the energies of the LUMO and HOMO. In `ORGANIC DISPLAY`, these are set (indirectly) on the `MATERIAL` statement using the `EG300` and `AFFINITY` parameters. The LUMO energy corresponds to the negative of the value specified by the `AFFINITY` parameter. The HOMO energy corresponds to the negative of the sum of the values of the `AFFINITY` and `EG300` parameters.

Defect states can be specified in organic materials using the `ODEFECT` and `OINTDEFECT` statements. These statements are described in Section 15.2.1: “Organic Defects Model”. The organic defects are important to correctly model defect recombination (Equation 15-13), hopping mobility (Equations 15-16 and 15-17), and dopant light emission rates (see Section 15.3.1: “Dopants”).

You should also enable Poole-Frenkel mobility modeling in organic devices by specifying `PFMOB` on the `MODEL` statement. This should be done in conjunction with the Langevin recombination model enabled by the `LANGEVIN` parameter of the `MODEL` statement. Langevin recombination is needed to enable exchange between charged carriers and singlet and triplet excitons as described in Equations 15-33 and 15-34. To enable the singlet and triplet exciton rate equations, specify `SINGLET` and `TRIPLET` on the `MODELS` statement.

Radiative emission can come from two sources: the host material singlets and the dopants. The dopant rate equation is given in Equation 15-37 and is enabled by specifying `DOPANT` on the `ODEFECT` statement. `ORGANIC DISPLAY` cannot predict the output spectra so you must supply it. These are in the form of tabular descriptions of intensity vs. wavelength as described in Section 11.6.1: “User-Definable Emission Spectra”. To connect materials and their emission spectra, assign the `USER.SPECT` and `DOPE.SPECT` parameters of the `MATERIAL` statement to the file names containing the appropriate tables. The spectra need not be normalized as this is done automatically. To output the spectra to TONYPLOT compatible log files, specify `OUT.USPEC` and `OUT.DSPEC`.

The normalized emission spectra are scaled by the radiative emission rates given in Equations 15-33 and 15-37. The `PHEFF.EXCITON` and `DPHEFF.EXCITON` parameters are quantum efficiencies for host and dopant emission and act to scale the emission rates. The emission spectra are critical in calculation through reverse ray tracing (see Section 11.5: “Reverse Ray-Tracing”) of output coupling and output emission spectrum. Also for reverse ray tracing, you should accurately specify the complex indices of refraction for the various materials. This can be done as described in Section 10.8: “Defining Optical Properties of Materials”.

Finally, a variety of useful information can be output after each solution using the `LED` statement (see Section 11.5: “Reverse Ray-Tracing” and Section 21.24: “LED”). These information include the angular distribution of emission spectra and output coupling.

15.1.2: Organic Solar

ORGANIC SOLAR allows simulation of complex organic light sensitive devices such as solar cells and imaging sensors. Much of this capability is discussed elsewhere in this manual. Before reading this section, you should already be familiar with the general concepts discussed in Chapters 2: “Getting Started with ATLAS” and 3: “Physics”. Chapter 2: “Getting Started with ATLAS” gives an overview of the general concepts of building a simulation deck and using the simulator. Chapter 3: “Physics” gives a fairly detailed discussion of the base physical concepts and models that define device modeling.

To understand the general concepts of photodetection, read Chapter 10: “Luminous: Optoelectronic Simulator”. If you are interested in embedding physical devices in lumped element (SPICE) circuits, then read Chapter 12: “MixedMode: Mixed Circuit and Device Simulator”. Those interested may also want to look over Chapter 20: “Numerical Techniques” where they will be given a description of the workings of the numerics of the simulator including information on convergence.

In this section, we will lead you through the important differences you will need to know about when simulating organic display devices. We will do this in a sequential manner similar to the description of deck construction presented in Chapter 2: “Getting Started with ATLAS”.

First with respect to definition of the device structure, there is little difference with what is described in Chapter 2: “Getting Started with ATLAS”. You should be aware of is that there are several default material names that are recognized by ORGANIC DISPLAY. These materials are Organic, Pentacene, Alq3, TPD, PPV, Tetracene, and NPB. For insulating dielectrics and conductive materials, see Appendix B: “Material Systems”.

If you want to simulate a material not included in the default set recognized by ORGANIC SOLAR, you should follow the steps described in Section B.2.5: “Specifying Unknown or User-Defined Materials in ATLAS”.

After you have specified the device structure, you may decide how to handle interfaces between homogenous layers. These interfaces are analogous to heterojunctions in the drift diffusion formulation where the band edges are replaced by HOMO and LUMO.

As such, you may choose to make the interfaces obey the physics of thermionic emission and tunneling. To do this, specify the INTERFACE statement with the parameters THERMIONIC and TUNNEL set. There are various ways in which interfaces may be specified to a particular interface using principally the X.MIN, X.MAX, Y.MIN, and Y.MAX parameters. These types of interfaces are discussed in more detail in Section 5.1.4: “The Thermionic Emission and Field Emission Transport Model”.

Next, you may want to fix the workfunction of electrodes to a certain value relative to the LUMO and HOMO. To do this, use the CONTACT statement where the workfunction is specified with the WORKF parameter. A particular CONTACT statement is associated with an electrode using the NAME or NUMBER parameters. Also, you can assign various Schottky characteristics to the electrode using, for example, the SURF.REC parameter to enable surface recombination or BARRIER to enable barrier lowering. For more details, see Section 21.5: “CONTACT”.

Key parameters in the simulation of organic devices are the energies of the LUMO and HOMO. In ORGANIC SOLAR, these are set (indirectly) on the MATERIAL statement using the EG300 and AFFINITY parameters. The LUMO energy corresponds to the negative of the value specified by the AFFINITY parameter. The HOMO energy corresponds to the negative of the sum of the values of the AFFINITY and EG300 parameters.

Defect states can be specified in organic materials using the ODEFECT and OINTDEFECT statements. These statements are described in Section 15.2.1: “Organic Defects Model”. The organic defects are important to correctly model defect recombination (Equation 15-13), hopping mobility (Equations 15-16 and 15-17), and dopant light emission rates (see Section 15.3.1: “Dopants”).

You should also enable Poole-Frenkel mobility modeling in organic devices by specifying `PFMOB` on the `MODEL` statement. This should be done in conjunction with the Langevin recombination model enabled by the `LANGEVIN` parameter of the `MODEL` statement. Langevin recombination is needed to enable exchange between charged carriers and singlet and triplet excitons as described in Equations 15-33 and 15-34. To enable the singlet and triplet exciton rate equations, specify `SINGLET` and `TRIPLET` on the `MODELS` statement.

Photodetection in organic photo detectors is a two part process. First, absorbed photons generate singlet excitons. The `QE.EXCITON` parameter of the `MATERIAL` statement (see Section 15.3.2: “Light Generation of Excitons”) specifies the efficiency of this conversion. Then, excitons are generated and they diffuse to interfaces in the "blend" material where they experience dissociation as described in Section 15.3.3: “Exciton Dissociation”. Once electrons and holes dissociate from the singlets, they experience built-in electric fields. They are then separated and detected at the electrodes. To enable dissociation, specify `S.DISSOC` on the `MODELS` statement.

15.2: Organic Materials Physical Models

This section describes the model definition required for the simulation of organic devices.

15.2.1: Organic Defects Model

Density of States

The ODEFECTS statement is used to specify the energy distribution of defect states. The total density of states (DOS) is composed of an acceptor-like conduction band DOS ($g_A(E)$) and a donor-like valence band DOS ($g_D(E)$). There are two defect distribution models available. The first model defines the defects based on a characteristic temperature and density [210].

$$g_A(E) = \frac{HA}{kTCA} \exp\left(\frac{E-E_c}{kTCA}\right) \quad 15-1$$

$$g_D(E) = \frac{HD}{kTCD} \exp\left(\frac{E_v-E}{kTCD}\right) \quad 15-2$$

HA is the acceptor traps density of states, HD is the donor traps density of states, TCA is the acceptor traps characteristic temperature, TCD is the donor traps characteristic temperature, and E is the energy.

| Table 15-1. User-Specifiable Parameters for Equations 15-1 and 15-2 | | | |
|---|-----------|---------|------------------|
| Statement | Parameter | Default | Units |
| ODEFECTS | HA | 0 | cm^{-3} |
| ODEFECTS | HD | 0 | cm^{-3} |
| ODEFECTS | TCA | 0 | K |
| ODEFECTS | TCD | 0 | K |

The trapped state concentrations for electrons (n_A) and holes (p_D) are given by:

$$n_A = \int_{E_v}^{E_c} g_A(E) \cdot f_{tA}(E, n, p) dE \quad 15-3$$

$$p_D = \int_{E_v}^{E_c} g_D(E) \cdot f_{tD}(E, n, p) dE \quad 15-4$$

where $f_{tA}(E, n, p)$ is the acceptor probability of occupation and $f_{tD}(E, n, p)$ is the donor probability of occupation.

The second model is the effective transport hopping energy model and defines the defects using a double peak Gaussian distribution [14],[15].

$$g_A(E) = \frac{NIA}{\sqrt{2\pi} \text{SIGMAIA}} \exp\left(\frac{(E - E_c)^2}{2\text{SIGMAIA}^2}\right) + \frac{NA}{\sqrt{2\pi} \text{SIGMAA}} \exp\left(\frac{(E - E_c + EA)^2}{2\text{SIGMAA}^2}\right) \quad 15-5$$

$$g_D(E) = \frac{NID}{\sqrt{2\pi} \text{SIGMAID}} \exp\left(\frac{(E_v - E)^2}{2\text{SIGMAID}^2}\right) + \frac{ND}{\sqrt{2\pi} \text{SIGMAD}} \exp\left(\frac{(E_v - E + ED)^2}{2\text{SIGMAD}^2}\right) \quad 15-6$$

NIA is the total intrinsic density for acceptor-like traps. NID is the total intrinsic density for donor-like traps. SIGMAIA is the Gaussian width for the intrinsic acceptor-like traps. SIGMAID is the Gaussian width for the intrinsic donor-like traps. NA is the total doping density for acceptor-like traps. ND is the total doping density for donor-like traps. SIGMAA is the Gaussian width for the doping acceptor-like traps. SIGMAD specifies the Gaussian width for the doping donor-like traps. EA is the energy shift between the intrinsic and doping states for acceptor-like traps. ED is the energy shift between the intrinsic and doping states for donor-like traps.

The trapped state concentrations are given by:

$$n_A = \int_{E_c}^{E_{tr_n}} g_A(E) F_{tA}(E, n, p) dE \quad 15-7$$

$$p_D = \int_{E_{tr_p}}^{E_v} g_D(E) F_{tD}(E, n, p) dE \quad 15-8$$

where E_{tr_n} is the effective transport energy for electrons and E_{tr_p} is the effective transport energy for holes. You must specify the HOPPING parameter on the ODEFECTS statement to use the effective transport hopping energy model. The effective transport energy for electrons and holes is calculate by solving Equations 15-5 and 15-6 along with Equations 15-7 and 15-8.

$$\int_{-\infty}^{E_{tr_n}} g_A(E) (E_{tr_n} - E)^3 dE = \frac{6\text{HOPN.BETA}}{\pi} (\text{HOPN.GAMMA} kT)^3 \quad 15-9$$

$$\int_{-\infty}^{E_{tr_p}} g_D(E) (E_{tr_p} - E)^3 dE = \frac{6\text{HOPP.BETA}}{\pi} (\text{HOPP.GAMMA} kT)^3 \quad 15-10$$

where HOPN.BETA is the electron percolation constant, HOPP.BETA is the hole percolation constant, HOPN.GAMMA is 1/carrier localization radius for electrons and HOPP.GAMMA is 1/carrier localization radius for holes.

Table 15-2. User-Specifiable Parameters for Equations 15-5-15-10

| Statement | Parameter | Value | Units |
|-----------|-----------|-------|-------|
| ODEFECTS | EA | 0.0 | eV |
| ODEFECTS | ED | 0.0 | eV |
| MATERIAL | HOPN.BETA | 1.5 | |

| Table 15-2. User-Specifiable Parameters for Equations 15-5-15-10 | | | |
|--|------------|-------------------|------------------|
| MATERIAL | HOPN.GAMMA | 5.0×10^7 | cm^{-1} |
| MATERIAL | HOPP.BETA | 1.5 | |
| MATERIAL | HOPP.GAMMA | 5.0×10^7 | cm^{-1} |
| ODEFFECTS | HOPPING | False | |
| ODEFFECTS | NA | 0.0 | cm^{-3} |
| ODEFFECTS | ND | 0.0 | cm^{-3} |
| ODEFFECTS | NIA | 0.0 | cm^{-3} |
| ODEFFECTS | NID | 0.0 | cm^{-3} |
| ODEFFECTS | SIGMAA | 0.0 | eV |
| ODEFFECTS | SIGMAD | 0.0 | eV |
| ODEFFECTS | SIGMAIA | 0.0 | eV |
| ODEFFECTS | SIGMAID | 0.0 | eV |

In steady-state, the probabilities of occupation are given by:

$$f_{tA} = \frac{v_n \text{SIGAE}n + v_p \text{SIGAH}n_i \exp\left[\frac{E_i - E}{kT_L}\right]}{v_n \text{SIGAE}\left(n + n_i \exp\left[\frac{E - E_i}{kT_L}\right]\right) + v_p \text{SIGAH}\left(p + n_i \exp\left[\frac{E_i - E}{kT_L}\right]\right)} \quad 15-11$$

$$f_{tD} = \frac{v_n \text{SIGDEN} + v_p \text{SIGDHN}_i \exp\left[\frac{E_i - E}{kT_L}\right]}{v_n \text{SIGDE}\left(n + n_i \exp\left[\frac{E - E_i}{kT_L}\right]\right) + v_p \text{SIGDH}\left(p + n_i \exp\left[\frac{E_i - E}{kT_L}\right]\right)} \quad 15-12$$

where v_n is the electron thermal velocity, v_p is the hole thermal velocity, n_i is the intrinsic carrier concentration, SIGAE and SIGAH are the acceptor electron and hole capture cross-sections respectively and SIGDE and SIGDH are the donor electron and hole capture cross-sections respectively.

| Table 15-3. User-Specifiable Parameters for Equations 15-11 and 15-12 | | | |
|---|-----------|------------|---------------|
| Statement | Parameter | Default | Units |
| ODEFFECTS | SIGAE | 10^{-16} | cm^2 |

Table 15-3. User-Specifiable Parameters for Equations 15-11 and 15-12

| | | | |
|-----------|-------|------------|---------------|
| ODEFFECTS | SIGAH | 10^{-14} | cm^2 |
| ODEFFECTS | SIGDE | 10^{-14} | cm^2 |
| ODEFFECTS | SIGDH | 10^{-16} | cm^2 |

Steady-State and Transient Recombination

The steady-state net recombination/generation rate is identical for electrons (R_n) and holes (R_p) as equilibrium is assumed to be instantaneous. The Shockley-Read-Hall recombination/generation rate due to the defect states is given by:

$$R_{n,p} = \int_{Ev}^{Ec} \left[\frac{v_n v_p \text{SIGAE} \text{SIGAH} (np - n_i^2) g_A(E)}{v_n \text{SIGAE} \left(n + n_i \exp \left[\frac{E - E_i}{kT_L} \right] \right) + v_p \text{SIGAH} \left(p + n_i \exp \left[\frac{E_i - E}{kT_L} \right] \right)} + \frac{v_n v_p \text{SIGDE} \text{SIGDH} (np - n_i^2) g_D(E)}{v_n \text{SIGDE} \left(n + n_i \exp \left[\frac{E - E_i}{kT} \right] \right) + v_p \text{SIGDH} \left(p + n_i \exp \left[\frac{E_i - E}{kT} \right] \right)} \right] dE \quad 15-13$$

In transient simulations, the instantaneous equilibrium can no longer be assumed. Instead, the recombination/generation rate is calculated using the transient acceptor and donor probabilities of occupation. These are calculated by solving additional rate equations:

$$\frac{d}{dt}(n_A) = \int_{Ev}^{Ec} g_A(E) \left[v_n \text{SIGAE} \left(n(1 - f_{tA}(E)) - f_{tA}(E) n_i \exp \left[\frac{E - E_i}{kT_L} \right] \right) - v_p \text{SIGAH} \left(p f_{tA}(E) - (1 - f_{tA}(E)) n_i \exp \left[\frac{E - E_i}{kT_L} \right] \right) \right] dE \quad 15-14$$

$$\frac{d}{dt}(p_D) = \int_{Ev}^{Ec} g_D(E) \left[v_n \text{SIGDE} \left(n(1 - f_{tD}(E)) - f_{tD}(E) n_i \exp \left[\frac{E - E_i}{kT_L} \right] \right) - v_p \text{SIGDH} \left(p f_{tD}(E) - (1 - f_{tD}(E)) n_i \exp \left[\frac{E - E_i}{kT_L} \right] \right) \right] dE \quad 15-15$$

Additional Parameters

If the parameter FAST is specified in the ODEFFECTS statement, then the traps are assumed to reach equilibrium instantaneously. Therefore, Equations 15-14 and 15-15 will not be solved. In this case, the steady-state probabilities of a occupation will be used in transient simulations.

You can use the C-Interpreter to define the defect states in the bandgap. The F.OTFTDON and F.OTFTACC parameters of the ODEFECTS statement indicate the filenames containing the C functions. For more information on using the C-Interpreter, see Appendix A: “C-Interpreter Functions”.

```
ODEFECTS F.OTFTDON=mydefects.c F.OTFTACC=mydefects.c
```

The file, *mydefects.c*, will contain C functions for donor and acceptor defect densities as a function of energy. The following example defect states are defined in the file, *otft.lib*. The resultant distribution of defects versus energy can be plotted in the files, *odon.dat* and *oacc.dat*.

```
ODEFECTS F.OTFTDON=otft.lib F.OTFTACC=otft.lib DFILE=odon.dat AFILE=oacc.dat \
SIGAE=1.E-16 SIGAH=1.E-14 SIGDE=1.E-14 SIGDH=1.E-16
```

If you specify the CONTINUOUS parameter in the ODEFECTS statement, then a numerical integral will be used to calculate the charge and recombination integrals. In this case, you can use the parameters NUMA and NUMD to specify the number of acceptor and donor energy levels intervals used in the integral. If CONTINUOUS is not specified, then the integrals will be modelled with discrete energy levels. The integral terms are replaced by summations, which run over the number of discrete energy levels (NUMA for acceptors and NUMD for donors).

| Table 15-4. Additional Parameters for the ODEFECTS statement | | | |
|--|------------|---------|-------|
| Statement | Parameter | Default | Units |
| ODEFECTS | AFILE | | |
| ODEFECTS | CONTINUOUS | False | |
| ODEFECTS | DFILE | | |
| ODEFECTS | F.OTFTACC | | |
| ODEFECTS | F.OTFTDON | | |
| ODEFECTS | FAST | False | |
| ODEFECTS | NUMA | 12 | |
| ODEFECTS | NUMD | 12 | |

15.2.2: Hopping Mobility Model

If the effective transport hopping energy model is specified (HOPPING on the ODEFECTS statement), then the field-independent hopping mobility can be used (HOPMOB on the MODELS statement). This is given by [15]:

$$\mu_{n0} = \frac{q \text{HOPN.V0}}{kT} \left[\int_{-\infty}^{E_{tr_n}} g_A(E) dE \right]^{-2/3} \exp \left[-2 \left(\frac{3 \text{HOPN.BETA}}{4\pi} \right)^{1/3} \text{HOPN.GAMMA} \left[\int_{-\infty}^{E_{tr_n}} g_A(E) dE \right]^{-1/3} \right] \quad 15-16$$

$$\mu_{p0} = \frac{q \text{HOPP.V0}}{kT} \left[\int_{-\infty}^{E_{tr_p}} g_D(E) dE \right]^{-2/3} \exp \left[-2 \left(\frac{3 \text{HOPP.BETA}}{4\pi} \right)^{1/3} \text{HOPP.GAMMA} \left[\int_{-\infty}^{E_{tr_p}} g_D(E) dE \right]^{-1/3} \right] \quad 15-17$$

where HOPN.V0 is the attempt-to-jump frequency for electrons and HOPP.V0 is the attempt-to-jump frequency for holes.

Table 15-5. User-Specifiable Parameters for Equations 15-16 and 15-17

| Statement | Parameter | Value | Units |
|-----------|-----------|--------|-------|
| MODEL | HOPMOB | False | |
| MOBILITY | HOPMOB.N | False | |
| MOBILITY | HOPMOB.P | False | |
| MATERIAL | HOPN.V0 | 1.0e11 | Hz |
| MATERIAL | HOPP.V0 | 1.0e11 | Hz |

15.2.3: Poole-Frenkel Mobility Model

The Poole-Frenkel mobility model is given by [79][96]:

$$\mu_{n_{PF}}(E) = \mu_{n0} \exp \left(-\frac{\text{DELTAEN.PFMOB}}{kT_{neff}} + \left(\frac{\text{BETAN.PFMOB}}{kT_{neff}} - \text{GAMMAN.PFMOB} \right) \sqrt{|E|} \right) \quad 15-18$$

$$\mu_{p_{PF}}(E) = \mu_{p0} \exp \left(-\frac{\text{DELTAEP.PFMOB}}{kT_{peff}} + \left(\frac{\text{BETAP.PFMOB}}{kT_{peff}} - \text{GAMMAP.PFMOB} \right) \sqrt{|E|} \right) \quad 15-19$$

where $\mu_{n_{PF}}(E)$ and $\mu_{p_{PF}}(E)$ are the Poole-Frenkel mobilities for electrons and holes respectively, μ_{n0} and μ_{p0} are the zero field mobilities for electrons and holes respectively, and E is the electric field. DELTAEN.PFMOB and DELTAEP.PFMOB are the activation energy at zero electric field for electrons and holes respectively. BETAN.PFMOB is the electron Poole-Frenkel factor, and BETAP.PFMOB is the hole Poole-Frenkel factor.

T_{neff} is the effective temperature for electrons and is defined as:

$$T_{neff} = \frac{\text{T0N.PFMOB} \cdot T_L}{\text{T0N.PFMOB} - T_L} \quad 15-20$$

T_{peff} is the effective temperature for holes and is defined as:

$$T_{peff} = \frac{\text{T0P.PFMOB} \cdot T_L}{\text{T0P.PFMOB} - T_L} \quad 15-21$$

If you specify the BETANAUTO.PFMOB parameter on the MOBILITY statement, then BETAN.PFMOB in Equation 15-18 will be calculated from the permittivity:

$$\text{BETAN.PFMOB} = q \sqrt{\frac{q}{\pi \epsilon \epsilon_0}} \quad 15-22$$

Similarly, if you specify BETAPAUTO.PFMOB, then BETAP.PFMOB in Equation 15-19 will be calculated from the permittivity.

If you use EON.PFMOB, EOP.PFMOB, EONAUTO.PFMOB or EOPAUTO.PFMOB instead of BETAN.PFMOB, BETAP.PFMOB, BETANAUTO.PFMOB and BETAPAUTO.PFMOB, you will then use a simplified form of the Poole-Frenkel mobility [96][198]:

$$\mu_{nPF}(E) = \mu_{n0} \exp\left(-\frac{\text{DELTAEN.PFMOB}}{kT_{neff}} + \sqrt{\frac{|E|}{\text{EON.PFMOB}}}\right) \quad 15-23$$

$$\mu_{pPF}(E) = \mu_{p0} \exp\left(-\frac{\text{DELTAEP.PFMOB}}{kT_{peff}} + \sqrt{\frac{|E|}{\text{EOP.PFMOB}}}\right) \quad 15-24$$

where $E0$ is the characteristic field. You can use the parameters EONAUTO.PFMOB and EOPAUTO.PFMOB in the MOBILITY statement to calculate the electron and hole characteristic field values from the permittivity:

$$E0 = \left(\frac{kT_L}{q}\right)^2 \left(\frac{\pi\epsilon\epsilon0}{q}\right) \quad 15-25$$

If you specify the PFMOB parameter on the MODELS statement, the Poole-Frenkel mobility model will be used for both electrons and holes. You can specify this model individually for electrons and holes by using the PFMOB.N and PFMOD.P parameters in the MOBILITY statement.

Table 15-6. User-Specifiable Parameters for Poole-Frenkel Mobility Model

| Statement | Parameter | Default | Units |
|-----------|-----------------|---------|--------------------------|
| MOBILITY | BETAN.PFMOB | 0 | eV (cm/V) ^{1/2} |
| MOBILITY | BETAP.PFMOB | 0 | eV (cm/V) ^{1/2} |
| MOBILITY | BETANAUTO.PFMOB | False | |
| MOBILITY | BETAPAUTO.PFMOB | False | |
| MOBILITY | DELTAEN.PFMOB | 0 | eV |
| MOBILITY | DELTAEP.PFMOB | 0 | eV |
| MOBILITY | EON.PFMOB | 1956 | V/cm |
| MOBILITY | EOP.PFMOB | 1956 | V/cm |
| MOBILITY | EONAUTO.PFMOB | False | |
| MOBILITY | EOPAUTO.PFMOB | False | |
| MOBILITY | GAMMAN.PFMOB | 0 | (cm/V) ^{1/2} |
| MOBILITY | GAMMAP.PFMOB | 0 | (cm/V) ^{1/2} |
| MOBILITY | PFMOB | False | |
| MOBILITY | PFMOB.N | False | |
| MOBILITY | PFMOB.P | False | |
| MOBILITY | TON.PFMOB | 0 | K |

Table 15-6. User-Specifiable Parameters for Poole-Frenkel Mobility Model

| | | | |
|----------|--------------|---|------|
| MOBILITY | TOP . PFMOB | 0 | K |
| MOBILITY | VTHN . PFMOB | | cm/s |
| MOBILITY | VTHP . PFMOB | | cm/s |

Due to the strong dependence on the electric field, the Poole-Frenkel mobility model can cause convergence problems. To increase the stability of the Poole-Frenkel mobility model, it is combined with a limiting mobility ($\mu_{n_{lim}}(E)$ and $\mu_{p_{lim}}(E)$) calculated from the thermal velocities (v_n and v_p).

$$\mu_n(E) = \frac{I}{\frac{I}{\mu_{n_{PF}}(E)} + \frac{I}{\mu_{n_{lim}}(E)}} \quad 15-26$$

$$\mu_p(E) = \frac{I}{\frac{I}{\mu_{p_{PF}}(E)} + \frac{I}{\mu_{p_{lim}}(E)}} \quad 15-27$$

where:

$$\mu_{n_{lim}}(E) = \frac{v_n}{E} \quad 15-28$$

$$\mu_{p_{lim}}(E) = \frac{v_p}{E} \quad 15-29$$

If you specify VTHN . PFMOB on the MOBILITY statement, then Equation 15-29 becomes:

$$\mu_{n_{lim}}(E) = \frac{VTHN . PFMOB}{E} \quad 15-30$$

Similarly, if you specify VTHP . PFMOB on the MOBILITY statement, then Equation 15-30 becomes:

$$\mu_{p_{lim}}(E) = \frac{VTHP . PFMOB}{E} \quad 15-31$$

15.2.4: Bimolecular Langevin Recombination Model

To enable this model, specify the parameter `LANGEVIN` in the `MODELS` statement. The Langevin recombination rate coefficient is given by [28][205]:

$$r_L(x, y, t) = A_LANGEVIN \frac{q[\mu_n(E) + \mu_p(E)]}{\epsilon_r \epsilon_0} \quad 15-32$$

Table 15-7. User-Specifiable Parameters for Poole-Frenkel Mobility Model

| Statement | Parameter | Default | Units |
|-----------|------------|---------|-------|
| MATERIAL | A.LANGEVIN | 1 | |

The Langevin recombination rate is given by:

$$R_{L,n,p} = r_L(x, y, t)(np - n_i^2) \quad 15-33$$

When enabled, the Langevin recombination rate is included in recombination terms in the carrier continuity equations (Equations 3-3 and 3-4). This rate is also included in the exciton singlet and triplet continuity equations described in Section 15.3: “Singlet and Triplet Excitons”.

15.3: Singlet and Triplet Excitons

The distribution of singlet or triplet excitons can be used to infer the radiative rates for luminescence or phosphorescence in organic material LEDs. In ATLAS, you can self-consistently solve the singlet and triplet exciton continuity equations along with the electron and hole drift diffusion equations. The singlet exciton continuity equation is given by [198] and [240]:

$$\begin{aligned} \frac{dS(x, y, t)}{dt} = & \text{RST} \cdot \text{EXCITON} R_{Ln, p} + \frac{\text{RST} \cdot \text{EXCITON}}{1 + \text{RST} \cdot \text{EXCITON}} \text{KTT} \cdot \text{EXCITON} T^2(x, y, t) \\ & - \text{KISC} \cdot \text{EXCITON} S(x, y, t) - \text{KST} \cdot \text{EXCITON} S(x, y, t) T(x, y, t) - \text{KDD} \cdot \text{EXCITON} S(x, y, t) \\ & - \text{KSP} \cdot \text{EXCITON} S(x, y, t)(n(x, y, t) + p(x, y, t)) - \frac{\text{KSS} \cdot \text{EXCITON}}{2} S^2(x, y, t) \\ & - \text{KNRS} \cdot \text{EXCITON} S(x, y, t) - \frac{\text{PHEFF} \cdot \text{EXCITON}}{\text{TAUS} \cdot \text{EXCITON}} S(x, y, t) + \nabla D_s \nabla S(x, y, t) - Q(x, y) S(x, y, z) \\ & - R_{Dn, p} S(x, y, t) + G_{ph} \text{QE} \cdot \text{EXCITON} \end{aligned} \quad 15-34$$

while the triplet exciton continuity equation is given by:

$$\begin{aligned} \frac{dT(x, y, t)}{dt} = & (1 - \text{RST} \cdot \text{EXCITON}) R_{Ln, p} + \text{KISC} \cdot \text{EXCITON} S(x, y, t) \\ & - \text{KTP} \cdot \text{EXCITON} T(x, y, t)(n(x, y, t) + p(x, y, t)) - \text{KTT} \cdot \text{EXCITON} T^2(x, y, t) \\ & - \text{KNRT} \cdot \text{EXCITON} T(x, y, t) - \frac{T(x, y, t)}{\text{TAUT} \cdot \text{EXCITON}} + \nabla(D_T \nabla T(x, y, t)) \end{aligned} \quad 15-35$$

where:

- $S(x, y, t)$ is the spatial and temporal singlet exciton density,
- $T(x, y, t)$ is the spatial and temporal triplet exciton density,
- $\text{RST} \cdot \text{EXCITON}$ is the fraction of singlets formed,
- $R_{Ln, p}$ is the Langevin recombination rate,
- $n(x, y, t)$ is the electron concentration,
- $p(x, y, t)$ is the hole concentration,
- $\text{TAUS} \cdot \text{EXCITON}$ is the singlet radiative decay lifetime,
- $\text{TAUT} \cdot \text{EXCITON}$ is the triplet radiative decay lifetime,
- $\text{KISC} \cdot \text{EXCITON}$ is the intersystem crossing constant,
- $\text{KST} \cdot \text{EXCITON}$ is the singlet-triplet constant,
- $\text{KSP} \cdot \text{EXCITON}$ is the singlet-polaron constant,
- $\text{KTP} \cdot \text{EXCITON}$ is the triplet-polaron constant,
- $\text{KSS} \cdot \text{EXCITON}$ is the singlet-singlet constant,
- $\text{KTT} \cdot \text{EXCITON}$ is the triplet-triplet constant,
- $\text{KNRS} \cdot \text{EXCITON}$ is the singlet non-radiative decay constant
- $\text{KNRT} \cdot \text{EXCITON}$ is the triplet non-radiative decay constant.
- $\text{KDD} \cdot \text{EXCITON}$ is the dipole-dipole exciton transfer rate (Forster).
- $Q(x, y)$ is the metal quenching rate.
- $\text{PHEFF} \cdot \text{EXCITON}$ is the host photoluminescence quantum efficiency.
- $R_{Dn, p}$ is the excitation dissociation rate described in Section 15.3.3: "Exciton Dissociation".

- G_{ph} is the photoabsorption rate.
- `QE.EXCITON` is the proportion of absorbed photons that is responsible for generating singlets.

The singlet diffusion constant, D_S , can be expressed as:

$$D_S = \frac{LDS.EXCITON^2}{TAUS.EXCITON} \quad 15-36$$

where `LDS.EXCITON` is the singlet diffusion length.

The triplet diffusion constant, D_T , can be expressed as:

$$D_T = \frac{LDT.EXCITON^2}{TAUT.EXCITON} \quad 15-37$$

where `LDT.EXCITON` is the triplet diffusion length.

Table 15-8. User-Specifiable Parameters for Equations 15-34, 15-35, 15-36, and 15-37

| Statement | Parameter | Default | Units |
|-----------|---------------|--------------------|---------------|
| MATERIAL | KISC.EXCITON | 0 | s^{-1} |
| MATERIAL | KNRS.EXCITON | 0 | s^{-1} |
| MATERIAL | KNRT.EXCITON | 0 | s^{-1} |
| MATERIAL | KSP.EXCITON | 0 | $cm^3 s^{-1}$ |
| MATERIAL | KST.EXCITON | 0 | $cm^3 s^{-1}$ |
| MATERIAL | KTP.EXCITON | 0 | $cm^3 s^{-1}$ |
| MATERIAL | KSS.EXCITON | 0 | $cm^3 s^{-1}$ |
| MATERIAL | KTt.EXCITON | 0 | $cm^3 s^{-1}$ |
| MATERIAL | LDS.EXCITON | 0.01 | microns |
| MATERIAL | LDT.EXCITON | 0.0632 | microns |
| MATERIAL | RST.EXCITON | 0.25 | |
| MATERIAL | TAUS.EXCITON | 1×10^{-9} | s |
| MATERIAL | TAUT.EXCITON | 1×10^{-4} | s |
| MATERIAL | KDD.EXCITON | 0 | s^{-1} |
| MATERIAL | PHEFF.EXCITON | 1.0 | |

Table 15-9. User-Specifiable Parameters for Tetracene

| Statement | Parameter | Default | Units |
|-----------|--------------|--------------------|---------------|
| MATERIAL | KISC.EXCITON | 0 | s^{-1} |
| MATERIAL | KNRS.EXCITON | 0 | s^{-1} |
| MATERIAL | KNRT.EXCITON | 0 | s^{-1} |
| MATERIAL | KSP.EXCITON | 4×10^{-8} | $cm^3 s^{-1}$ |
| MATERIAL | KST.EXCITON | 2×10^{-7} | $cm^3 s^{-1}$ |
| MATERIAL | KTP.EXCITON | 2×10^{-9} | $cm^3 s^{-1}$ |
| MATERIAL | KSS.EXCITON | 5×10^{-8} | $cm^3 s^{-1}$ |
| MATERIAL | KTT.EXCITON | 1×10^{-9} | $cm^3 s^{-1}$ |
| MATERIAL | LDS.EXCITON | 0.01 | microns |
| MATERIAL | LDT.EXCITON | 0.0632 | microns |
| MATERIAL | RST.EXCITON | 0.25 | |
| MATERIAL | TAUS.EXCITON | 1×10^{-7} | s |
| MATERIAL | TAUT.EXCITON | 1×10^{-4} | s |

To enable the self-constant simulation of both singlet and triplet excitons, specify EXCITONS in the MODEL statement. Specifying SINGLET instead of EXCITONS will enable the solution of the singlet exciton equations, while specifying TRIPLET will enable the triplet exciton equation.

Table 15-10. Exciton Model Flags

| Statement | Parameter | Default |
|-----------|-----------|---------|
| MODELS | EXCITONS | False |
| MODELS | SINGLET | False |
| MODELS | TRIPLET | False |

When solving for excitons, you can examine the density distribution of the singlet and triplet excitons in TONYPLOT in files saved in the standard structure file format. You can also specify EXCITON in the PROBE statement to save the singlet exciton density to log files. For further analysis of LED devices, see Chapter 11: “LED: Light Emitting Diode Simulator”.

15.3.1: Dopants

The singlet exciton density for dopants [138] can also be calculated. If you specify the parameter DOPANT on the ODEFECTS statement, then the trap densities defined using the NA, SIGMAA, EA, ND, SIGMAD, and ED parameters will be used in dopant singlet exciton calculation.

Note: Only one dopant is allowed per region.

The equation for dopant singlet excitons [138] is given by:

$$\frac{dS_d(x, y, t)}{dt} = G_d + \text{KDD} . \text{EXCITON} S(x, y, t) - \frac{1}{2} \text{DKSS} . \text{EXCITON} S_d^2(x, y, t) - \left(\text{DKNRS} . \text{EXCITON} + \frac{\text{DPHEFF} . \text{EXCITON}}{\text{DTAUS} . \text{EXCITON}} + \text{DKCQ} . \text{EXCITON} N_{dTOT} + Q(x, y) \right) S_d(x, y, t) \quad 15-38$$

where:

- $S_d(x, y, t)$ is the spatial and temporal singlet exciton density for dopants.
- $\text{DKNRS} . \text{EXCITON}$ is the dopant nonradiative decay rate.
- $\text{DTAUS} . \text{EXCITON}$ is the dopant radiative decay lifetime.
- $\text{DKCQ} . \text{EXCITON}$ is the dopant concentration quenching rate.
- N_d is the dopant concentration as calculated from the ODEFECTS statement.
- $\text{DKSS} . \text{EXCITON}$ is the bimolecular annihilation constant.
- $\text{KDD} . \text{EXCITON}$ is the dipole-dipole exciton transfer rate (Forster).
- $Q(x, y)$ is the metal quenching rate.
- $\text{DPHEFF} . \text{EXCITON}$ is the dopant photoluminescent quantum efficiency.
- G_d is the dopant Langevin recombination rate given by:

$$G_d = \frac{q \text{DRST} . \text{EXCITON}}{\varepsilon \varepsilon_o} (n N_{dd}^{\mu} (E) + p N_{da}^{\mu} (E)) \quad 15-39$$

where:

- $\text{DRST} . \text{EXCITON}$ is the fraction of singlets formed.
- N_{dd} is the density of occupied dopant donor traps.
- N_{da} is the density of occupied dopant acceptor traps.

An additional Langevin recombination term [138] is also added to the electron (R_{dn}) and hole (R_{dp}) current continuity equations:

$$R_{dn} = \frac{n N_{dd}^{\mu} (E)}{\varepsilon \varepsilon_o} \quad 15-40$$

$$R_{dp} = \frac{p N_{da}^{\mu} (E)}{\varepsilon \varepsilon_o} \quad 15-41$$

Table 15-11. User-Specifiable Parameters for Equations 15-38, 15-39, 15-40, and 15-41

| Statement | Parameter | Default | Units |
|-----------|----------------|----------------------|------------------------------|
| MATERIAL | DRST.EXCITON | 0.25 | |
| MATERIAL | DTAUS.EXCITON | 5.0×10^{-9} | s |
| MATERIAL | DKSS.EXCITON | 3.0×10^{-8} | $\text{cm}^3 \text{ s}^{-1}$ |
| MATERIAL | DKCQ.EXCITON | 1.1×10^{-8} | s^{-1} |
| MATERIAL | DKNRS.EXCITON | 0.0 | s^{-1} |
| MATERIAL | KDD.EXCITON | 0.0 | s^{-1} |
| MATERIAL | DPHEFF.EXCITON | 1.0 | |

15.3.2: Light Generation of Excitons

Optical generation of excitons is available in ORGANIC SOLAR. All of the capabilities available in LUMINOUS2D are also available in ORGANIC SOLAR for the description of the propagation and absorption of light. If you are interested in photogeneration in organic materials, then read Chapter 10: “Luminous: Optoelectronic Simulator”.

The additional parameter QE.EXCITON of the MATERIAL statement specifies the fraction of the absorbed photons that generate singlet excitons.

The fraction $1 - \text{QE.EXCITON}$ of the absorbed photons leads to the generation of electron hole pairs. By default, the value of QE.EXCITON is 0. For ORGANIC SOLAR analysis, a value of one is more recommended. The actual detection mechanism requires exciton dissociation as described in the next section.

15.3.3: Exciton Dissociation

Another source of carrier generation in the carrier continuity equations (Equations 3-3 and 3-4) is due to exciton dissociation. Exciton dissociation is the dissociation of a neutral singlet exciton into a free electron hole pair. Dissociation rate is given by:

$$R_{D,n,p} = \frac{3r_L(x,y,t)}{4\pi A_{\text{SINGLET}}^3} \exp\left(-\frac{S_{\text{BINDING}}}{kT}\right) \frac{J_1(2\sqrt{-2b})}{\sqrt{-2b}} S(x,y,t) \quad 15-42$$

Here, r_L is the Langevin recombination rate constant (Equation 15-32). A_{SINGLET} and S_{BINDING} are user-specified parameters as described in Table 15-12 representing the electron and hole separation distance and the singlet exciton binding energy. J_1 is the first order Bessel function and $S(x,y,t)$ is the local density of singlet excitons.

The parameter b is given by:

$$b = \frac{q^3 |E|}{8\pi\epsilon_r\epsilon_0 k^2 T^2} \quad 15-43$$

where E is the local electric field and ϵ_r is the relative permittivity.

The dissociation rate is also included in the singlet continuity equation described in Section 15.3: “Singlet and Triplet Excitons”. To include the singlet dissociation rate, you must specify `S.DISSOC` on the `MODELS` statement and also enable Langevin recombination.

| Table 15-12. User Specifiable Parameters of the Singlet Dissociation Model and Metal Quenching | | | |
|--|------------|---------|--------------------|
| Statement | Parameter | Default | Units |
| MATERIAL | A.SINGLET | 1.8 | nm |
| MATERIAL | S.BINDING | 0.1 | eV |
| MATERIAL | QR.EXCITON | 0 | cm ³ /s |

15.3.4: Metal Quenching

The metal quenching rate is given by:

$$Q(x, y) = QR_EXCITON \cdot M(x, y) \quad 15-44$$

where $M(x, y)$ is the metal atomic density. `QR.EXCITON` is the quenching constant specifiable on the `MATERIAL` statement. To specify the metal atomic density, use the `METAL` parameter on the `DOPING` statement. The defaults for `QR.EXCITON` are given in Table 15-12.

This page is intentionally left blank.

16.1: Introduction

NOISE is an ATLAS based product that simulates the small-signal noise generated by devices. Electronic noise results in an unavoidable degradation of a circuit's performance. It is important to understand the properties of noise to minimize its effect.

You should already be familiar with ATLAS before using NOISE. If not, see Chapter 2: "Getting Started with ATLAS".

16.2: Simulating Noise in ATLAS

ATLAS models the noise of a device by calculating the statistical behavior of equivalent random voltage sources at its ports. You can use the results of this calculation in a circuit simulator (e.g., SMARTSPICE) to minimize the disruption caused by the (inevitable) presence of noise. The following shows the minimum needed to simulate noise in ATLAS.

1. Add the noise parameter to a log command. For example:

```
log outfile=noise.log inport=gate outport=drain noise
```

2. Use the noise parameter on the subsequent solve command. For example:

```
solve noise frequency=100.0
```

NOISE is an extension of the AC analysis of a device (see Chapter 2: “Getting Started with ATLAS”, Section 2.9.3: “Small-Signal AC Solutions” for more information on AC analysis). You can perform a noise simulation on any device (one-port or two-port) where small-signal AC analysis can be performed.

A direct AC analysis is automatically performed on the device before the noise simulation (i.e., you don’t need to perform the analysis).

For more information about the LOG and SOLVE commands, see Chapter 21: “Statements”, Sections 21.27: “LOG” and 21.53: “SOLVE”.

16.3: Circuit Level Description of Noise

Noise is the name given to the random fluctuations in the currents and voltages of real devices.

The simple Drude model of an n-type resistor gives

$$\langle J \rangle = \langle \sigma \rangle \cdot E = q \cdot \langle n \rangle \cdot \langle v \rangle \quad 16-1$$

where $\langle J \rangle$ is the mean current density, q is the electronic charge, $\langle n \rangle$ is the mean electron density, and $\langle v \rangle$ is the mean electron drift velocity. Time dependent fluctuations in the instantaneous electron density and drift velocity will cause fluctuations in the resultant current density.

The current at a contact of the resistor would be

$$i(t) = \langle i \rangle + \delta i(t) \quad 16-2$$

where the $\delta i(t)$ term is the noise generated by the resistor.

A noisy device can be represented by external current sources added to the terminals of an ideal (noiseless) device (see Figure 16-1).

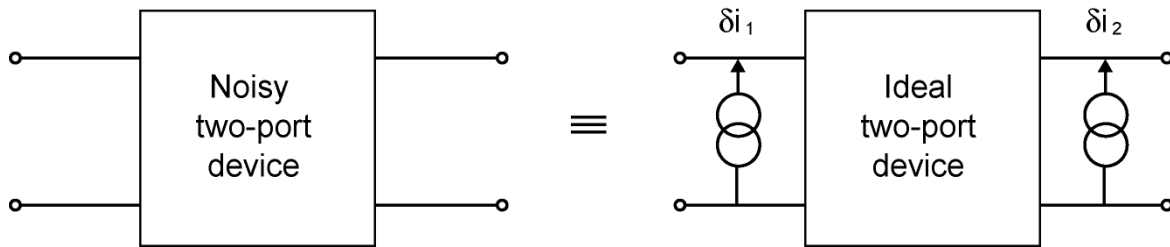


Figure 16-1: A real (noisy) device is modelled as an ideal (noiseless) device with random current sources attached to the ports.

These current sources are small and random. The description of noise is the statistical properties of these current sources. Normally, you describe the behavior of the frequency domain representation of the current sources.

The means of the current sources are zero. For example:

$$\langle \delta i_1(\omega) \rangle = 0 \text{ and } \langle \delta i_2(\omega) \rangle = 0 \quad 16-3$$

The noise is described by the auto-correlation:

$$\langle \delta i_1^2(\omega) \rangle \text{ and } \langle \delta i_2^2(\omega) \rangle \quad 16-4$$

and the cross-correlation:

$$\langle \delta i_1(\omega) \cdot \delta i_2(\omega)^* \rangle \text{ and } \langle \delta i_2(\omega) \cdot \delta i_1(\omega)^* \rangle \quad 16-5$$

It may be more convenient to describe the noise in terms of the behavior of voltage sources instead of current sources. The noise current can be easily translated into a noise voltage. For example:

$$\begin{pmatrix} \delta v_1(\omega) \\ \delta v_2(\omega) \end{pmatrix} = \begin{pmatrix} Z_{11}(\omega) & Z_{12}(\omega) \\ Z_{21}(\omega) & Z_{22}(\omega) \end{pmatrix} \cdot \begin{pmatrix} \delta i_1(\omega) \\ \delta i_2(\omega) \end{pmatrix} \quad 16-6$$

Figure 16-2 shows that both representations are the same.

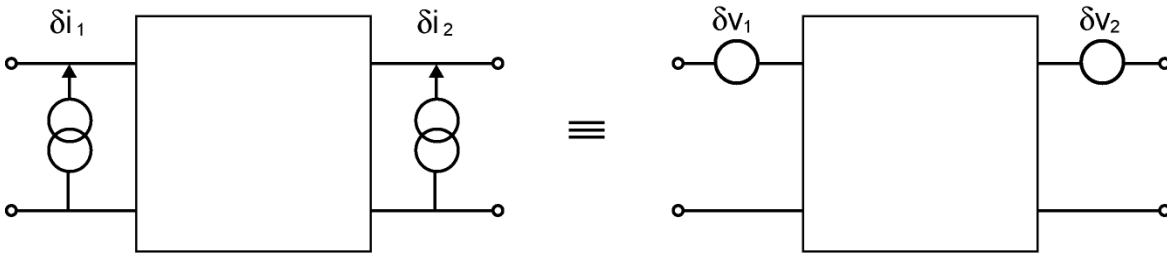


Figure 16-2: The noise can be modelled with random current sources or random voltage sources.

16.3.1: Noise “Figures of Merit” for a Two-Port Device

Figure 16-3 shows a simple two-port circuit.

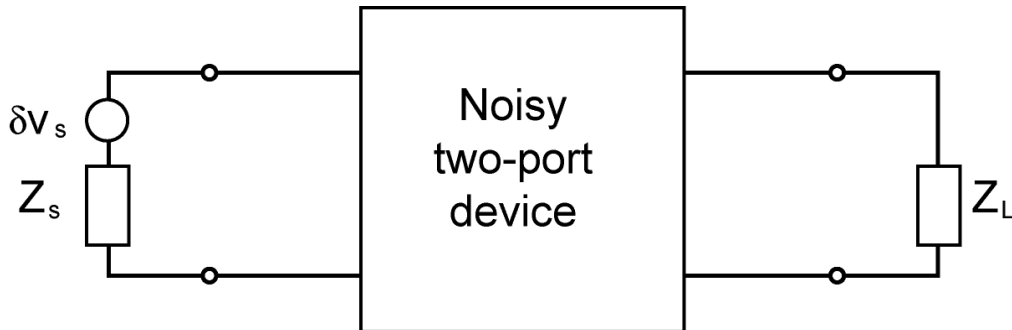


Figure 16-3: A block diagram of a simple circuit. We are interested in how much noise reaches the load.

The noise figure, F , is a measure of the increased amount of noise power delivered to the load because of the device's noise.

$$F = \frac{P_{S,D}}{P_S} \quad 16-7$$

Here:

- P_S is the noise power that would be delivered to the load if the device was noiseless (i.e., only the noise from the source is transferred to the load).
- $P_{S,D}$ is the noise power that is delivered to the load from both the source and the device.

The standard definition of noise figure assumes the source is generating thermal noise at the temperature of the device:

$$\langle v_s^2 \rangle = 4kTR_s \quad 16-8$$

Here, we have for the two-port circuit:

$$F = F_{min} + \frac{g_n}{R_s} |Z_S - Z_0|^2 \quad 16-9$$

where the traditional two-port figures of merit for noise are as follows:

- the minimum noise figure, F_{min} ;
- the best source impedance, Z_0 ;
- the noise conductance, g_n .

The best source impedance gives the minimum noise figure (i.e., $F=F_{min}$ when $Z_S=Z_0$). The noise conductance is a measure of how much the noise figure increases as the source impedance moves away from Z_0 .

16.4: Noise Calculation

ATLAS does the following to calculate the noise of a device.

1. Takes a small volume of a device and calculates the random current fluctuations in that volume.
2. Uses the impedance field to calculate the resultant voltage on a contact.
3. Repeats the above steps until the noise from each part of the device has been calculated, which is then the total noise of a device.

16.4.1: The Impedance Field

The impedance field is a transfer function relating current (injected at some point in the device) to the resultant contact voltage.

Suppose a current is injected into a point \mathbf{r} of a device (see Figure 16-4).

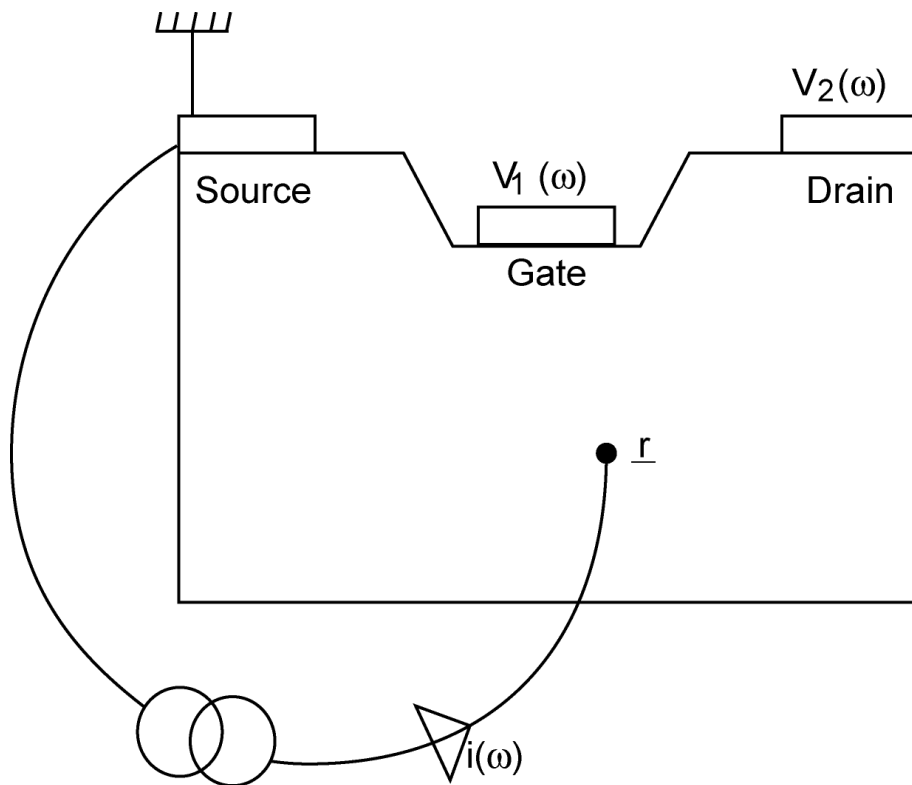


Figure 16-4: We calculate the impedance field at point \mathbf{r} by injecting a unit current at the point getting the resultant voltages V_1 and V_2 . (This is impossible to do in practice but is easy for ATLAS to simulate.)

This will generate a voltage on the open circuit contacts. The device is assumed to be linear so that the voltage will be at the same frequency as the input current. Here, we get

$$v_1(\omega) = Z_1(\mathbf{r}; \omega) \cdot i(\omega) \quad 16-10$$

and

$$v_2(\omega) = Z_2(\mathbf{r}; \omega) \cdot i(\omega) \quad 16-11$$

The $Z_i(r;\omega)$ parameters, when taken over the whole device, are called the impedance fields.

There are separate impedance fields for when the injected current is electrons or holes. In other words, a two-port device has four associated impedance fields: $Z_1^n(r;\omega)$, $Z_2^n(r;\omega)$, $Z_1^p(r;\omega)$, and $Z_2^p(r;\omega)$.

16.4.2: Microscopic Noise Source

We assume the statistical behavior of the noise from one point in the device is totally uncorrelated with the statistical behavior of the noise at all other points. So we describe the correlation of a parameter, x , as:

$$\langle \delta x \cdot \delta x \rangle(r, r'; \omega) = k_{\delta x, \delta x}(r; \omega) \cdot \delta(r - r') \quad 16-12$$

where the term $k_{\delta x, \delta x}(r; \omega)$ is called the microscopic noise source.

The theory of Generation-Recombination noise gives the auto-correlation of the current:

$$k_{\delta i, \delta i}(r; \omega) \quad 16-13$$

The theory of Diffusion noise gives the auto-correlation of the current density:

$$k_{\delta J, \delta J}(r; \omega) \quad 16-14$$

16.4.3: Local Noise Source

The local noise source is the effect that a microscopic noise source has on the noise behavior of the device.

For $k_{\delta i, \delta i}(r; \omega)$ we have

$$\langle \delta v_\alpha \delta v_\beta^* \rangle(\omega) = \int_{\Omega} Z_\alpha(r; \omega) k_{\delta i, \delta i}(r; \omega) \cdot Z_\beta^*(r; \omega) \cdot dr \quad 16-15$$

where the integral is over the device volume. The integrand function is called the local noise source.

For $k_{\delta J, \delta J}(r; \omega)$ we have

$$\langle \delta v_\alpha \delta v_\beta^* \rangle(\omega) = \int_{\Omega} Z_\alpha(r; \omega) k_{\delta J, \delta J}(r; \omega) \cdot Z_\beta^*(r; \omega) \cdot dr \quad 16-16$$

Again, the integral is over the device volume and the integrand function is called the local noise source.

The vector impedance field is defined as

$$\mathbf{Z}(r; \omega) = \nabla Z(r; \omega) \quad 16-17$$

16.5: ATLAS Models

ATLAS has models for three types of microscopic noise source: Diffusion Noise, Generation-Recombination Noise, and Flicker Noise.

If noise is being calculated then diffusion noise is on by default. Generation-recombination noise is on if any Generation-Recombination (GR) or Impact Ionization (II) models are defined. Flicker noise is off by default.

The default noise models for diffusion and GR/II have no user-definable parameters. They get all the needed information from the simulation.

16.5.1: Diffusion Noise

Diffusion noise is caused by variations in the velocity of the carriers.

Einstein Diffusion Equation

There are no independent user-definable parameters for this model. You can set the mobility model in a MATERIAL statement (See Chapter 21: “Statements”, Section 21.29: “MATERIAL”) but that will affect the whole simulation not just the noise calculation. It is on by default and can only be turned off by choosing a different model for diffusion noise.

The equation for the microscopic noise source is

$$k_{\delta \mathbf{J}, \delta \mathbf{J}}(\mathbf{r}; \omega) = 4q^2 n(\mathbf{r}) D(\omega) \quad 16-18$$

where:

- q is the fundamental electronic charge.
- $n(\mathbf{r})$ is the carrier concentration.
- $D(\omega)$ is the diffusion coefficient.

The diffusion coefficient is given by Einstein's relationship, which is:

$$D(\omega) = \frac{kT}{q} \mu \quad 16-19$$

where:

- k is Boltzmann's constant.
- T is the temperature.
- μ is the carrier mobility.

C-Interpreter

You can define a C-Interpreter function to calculate the microscopic noise source for diffusion noise. If a C-Interpreter function is defined, then the default model is turned off.

For a C-Interpreter function to calculate the electron microscopic noise source, use the MATERIAL statement:

```
material F.MNSNDIFF=<filename>
```

The header for this C-Interpreter function is

```
/*
 * Microscopic Noise Source for electron diffusion noise.
 * Statement: MATERIAL
 * Parameter: F.MNSNDIFF
 * Arguments:
```

```

* xcomp      composition fraction x
* ycomp      composition fraction y
* temp       lattice temperature (K)
* n          electron concentration ( $\text{cm}^{-3}$ )
* mun        electron mobility ( $\text{cm}^2/\text{V s}$ )
* e          electric field (V/cm)
* *mns       microscopic noise source ( $\text{s A}^2 / \text{cm}$ )
*/
int mnsndiff(double xcomp, double ycomp, double temp, double n,
double mun, double e, double *mns);

```

For a C-Interpreter function to calculate the hole microscopic noise source, use the MATERIAL statement:

```
material F.MNSPDIFF=<filename>
```

The header for this C-Interpreter function is

```

/*
* Microscopic Noise Source for hole diffusion noise.
* Statement: MATERIAL
* Parameter: F.MNSPDIFF
* Arguments:
* xcomp      composition fraction x
* ycomp      composition fraction y
* temp       lattice temperature (K)
* p          hole concentration ( $\text{cm}^{-3}$ )
* mup        hole mobility ( $\text{cm}^2 / \text{V s}$ )
* e          electric field (V / cm)
* *mns       microscopic noise source ( $\text{s A}^2 / \text{cm}$ )
*/
int mnspsdiff(double xcomp, double ycomp, double temp, double p,
double mup, double e, double *mns);

```

16.5.2: Generation-Recombination Noise

Generation-Recombination noise is caused by variations in the number of the carriers.

There are no user-definable parameters for GR noise. You can, however, set the parameters for the various GR models in the MATERIAL statement (see Chapter 21: “Statements”, Section 21.29: “MATERIAL”) and the various II models in the IMPACT statement (Chapter 21: “Statements”, Section 21.19: “IMPACT”). Setting these parameters will affect the whole simulation, not just the noise calculation.

There are two families of GR in ATLAS: direct and trap assisted. Direct GR is when the electron travels directly from the conduction band to the valence band (or vice versa). Trap assisted GR is when the electron travels from a band to a trap level. If more than one trap level is defined, then they are treated as independent trap assisted GR sites (i.e., electrons are not assumed to move between different trap levels).

Generation-Recombination is defined by four parameters:

- G_n
- G_p
- R_n
- R_p

G is the generation rate, R is the recombination rate, n is for electrons, and p is for holes. The generation rate of electrons is the number of electrons that appears (per unit time, per unit volume) in the conduction band. The recombination rate is the number of electrons that disappears from the conduction band.

Direct GR

Since there are no trap levels, all electrons leaving the conduction band end up in the valence band. All electrons leaving the valence band end up in the conduction band.

Therefore:

$$G_n = G_p \text{ and } R_n = R_p \quad 16-20$$

The GR parameters are calculated with

$$\begin{aligned} G &= C \cdot n_i^2 \\ R &= C \cdot np \end{aligned} \quad 16-21$$

For optical GR (OPTR in the MODELS statement), the C parameter is COPT in the MATERIALS statement. For Auger GR (AUGER in the MODELS statement), the C parameter is a function of the carrier density.

The microscopic noise sources are

$$k_{\delta n, \delta n} = k_{\delta p, \delta p} = k_{\delta n, \delta p} = 2(G + R) \quad 16-22$$

Trap Assisted GR

There are assumed to be no direct transitions in trap assisted GR. Therefore, an electron leaving the conduction band ends up at the trap level. An electron entering the conduction band comes from the trap level. Unlike direct GR, the following four parameters are independent.

$$\begin{aligned} G_n &= \frac{n_1 n_t}{\tau_n N_t} \\ G_p &= \frac{p_1}{\tau_p} \left(1 - \frac{n_t}{N_t}\right) \\ R_n &= \frac{n}{\tau_n} \left(1 - \frac{n_t}{N_t}\right) \\ R_p &= \frac{p}{\tau_p} \frac{n_t}{N_t} \end{aligned} \quad 16-23$$

The ratio n_t/N_t is the fraction of ionized traps. The concentration n_1 is the electron concentration if the Fermi level were at the trap level. p_1 is the hole concentration if the Fermi level were at the trap level.

You can define the lifetimes τ_n and τ_p using the TAUN0 and TAUP0 parameters from the MATERIALS statement.

The microscopic noise sources are

$$k_{\delta n, \delta n} = 2(G_n + R_n) \quad 16-24$$

There are no direct transitions between the conduction and valence band. Therefore:

$$k_{\delta p, \delta p} = 2(G_p + R_p) \quad 16-25$$

Impact Ionization

Impact ionization is a pure generation term. For each electron created in the conduction band, a corresponding hole is also created in the valence band. This is similar to direct GR without a recombination term.

The microscopic noise sources are

$$k_{\delta n, \delta n} = k_{\delta p, \delta p} = k_{\delta p} = 2G \quad 16-26$$

16.5.3: Flicker Noise

Flicker noise is observed experimentally, however, a complete theory about what causes flicker noise isn't known [30].

Hooge

The Hooge model, which is shown below, is a phenomenological microscopic noise source.

$$K_{\delta J_n, \delta J_n}(\mathbf{r}; \omega) = \frac{\alpha_{Hn} |J_n(\mathbf{r})|^2}{f n(\mathbf{r})} \text{ and } K_{\delta J_p, \delta J_p}(\mathbf{r}; \omega) = \frac{\alpha_{Hp} |J_p(\mathbf{r})|^2}{f p(\mathbf{r})} \quad 16-27$$

In this model:

- α_{Hn} is the electron Hooge constant.
- α_{Hp} is the hole Hooge constant.
- f is the frequency.
- $J_n(\mathbf{r})$ is the electron current density.
- $J_p(\mathbf{r})$ is the hole current density.
- $n(\mathbf{r})$ is the electron concentration.
- $p(\mathbf{r})$ is the hole concentration.

The Hooge constants are defined in the MATERIAL statement:

```
material HOOGEN=<value> HOOGE=<value>
```

The default values for these parameters is zero (which means the flicker noise is turned off).

C-Interpreter

You can define a C-Interpreter function to calculate the microscopic noise source for flicker noise. If a C-Interpreter function is defined, then the default model is turned off.

For a C-Interpreter function to calculate the electron microscopic noise source, use the MATERIAL statement:

```
material F.MNSNFLICKER=<filename>
```

The header for this C-Interpreter function is:

```
/*
 * Microscopic Noise Source for electron flicker (1/f) noise.
 * Statement: MATERIAL
 * Parameter: F.MNSNFLICKER
```

```
* Arguments:
* x          location x (microns)
* y          location y (microns)
* temp       lattice temperature (K)
* n          electron concentration (cm-3)
* jn         electron current density (A / cm2)
* f          frequency (Hz)
* e          electric field (V / cm)
* *mns       microscopic noise source (s A2 / cm)
*/
int mnsnflicker(double x, double y, double temp, double n,
double jn, double f, double e, double *mns);
```

For a C-Interpreter function to calculate the hole microscopic noise source, use the MATERIAL statement:

```
material F.MNSPFLICKER=<filename>
```

The header for this C-Interpreter function is

```
/*
* Microscopic Noise Source for hole flicker (1/f) noise.
* Statement: MATERIAL
* Parameter: F.MNSPFLICKER
* Arguments:
* x          location x (microns)
* y          location y (microns)
* temp       lattice temperature (K)
* p          hole concentration (cm-3)
* jp         hole current density (A / cm2)
* f          frequency (Hz)
* e          electric field (V/cm)
* *mns       microscopic noise source (s A2/cm)
*/
int mnspflicker(double x, double y, double temp, double p,
double jp, double f, double e, double *mns);
```

16.6: Output

The noise simulation results can output to the log file. The intermediate values in the calculation can output to the structure file.

16.6.1: Log Files

There are five groups of data that can output to a log file. They are as follows:

- The two-port figures of merit (FOM): F_{min} , Z_{opt} , g_n .
- The correlation of the total noise voltage sources.
- The correlation of the total noise current sources.
- The correlation of the individual noise voltage sources (GR, II, electron and hole diffusion; electron and hole flicker).
- The correlation of the individual noise current sources (GR, II, electron and hole diffusion; electron and hole flicker).

Table 16-1 shows the logical parameters in the LOG command (see Chapter 21: “Statements”, Section 21.27: “LOG” for more information) that cause these groups to output. The columns in this table correspond to the groups above.

| Table 16-1. Logical Parameters in the LOG command | | | | | |
|---|--------------------------------|------------------------|------------------------|-----------------------------|-----------------------------|
| | two-port FOM ^(a) | Total V correlation | Total I correlation | Individual V correlation | Individual I correlation |
| NOISE | X | _ (b) | – | – | – |
| NOISE.V | X | X | – | – | – |
| NOISE.I | X | – | X | – | – |
| NOISE.IV | X | X | X | – | – |
| NOISE.VI | X | X | X | – | – |
| NOISE.V.ALL | X | X | – | X | – |
| NOISE.I.ALL | X | – | X | – | X |
| NOISE.ALL | X | X | X | X | X |

Note a: If the device is a one-port, then this data will not be output: the two-port figures of merit have no meaning for a one-port device.

Note b: If the device is a one-port and NOISE is the only noise output in the LOG command, then the total noise voltage sources will output.

16.6.2: Structure Files

There are five groups of data that can output to a structure file. They are as follows:

- Total Local Noise Source (LNS)
- Impedance fields
- Short-circuit Green's function
- Individual Microscopic Noise Sources (MNS)
- Individual local noise sources

Table 16-2 shows the logical parameters from the `OUTPUT` command (see Chapter 21: “Statements”, Section 21.40: “OUTPUT” for more information) that cause these groups to output. The columns in this table correspond to the groups above.

| Table 16-2. Logical Parameters in the OUTPUT command | | | | | |
|--|-----------|------------------|--------------------------------|----------------|----------------|
| | Total LNS | Impedance Fields | Short-circuit Green's function | Individual MNS | Individual LNS |
| NOISE | X | – | – | – | – |
| NOISE.IMP | – | X | – | – | – |
| NOISE.ALL | X | X | X | X | X |

17.1: Overview

THERMAL3D solves the steady-state heat equation to find the equilibrium temperature distribution in planar and non-planar three-dimensional structures. Specify the heat sinks and sources and choose from several temperature-dependent models for thermal conductivity within each region. A typical application for THERMAL3D is a package simulation for a power circuit or III-V ICs.

If you're unfamiliar with THERMAL3D, see also Chapter 6: "3D Device Simulator". If you're unfamiliar with ATLAS, see Chapter 2: "Getting Started with ATLAS".

17.1.1: 3D Structure Generation

THERMAL3D supports structure defined on 3D prismatic meshes. Structures may have arbitrary geometries in two dimensions and consist of multiple slices in the third dimension. There are two methods for creating a 3D structure that can be used with THERMAL3D. One method is through the command syntax of ATLAS. The other method is through an interface to DEVEDIT. See Chapter 6: "3D Device Simulator", Section 6.2: "3D Structure Generation" for more information on both methods.

Defining Heat Sources

Heat sources are identified with regions in the 3D structure. Regions are defined in the manner documented in Chapter 2: "Getting Started with ATLAS", the "Specifying Regions And Materials" section on page 2-12 and Chapter 6: "3D Device Simulator", the "ATLAS Syntax For 3D Structure Generation" section on page 6-3. A region has a unique number, which is used to identify the region on the MATERIAL statement. The POWER parameter of the MATERIAL statement is used to set the power of the heat source in watts.

```
MATERIAL REGION=2 POWER=0.35
```

Set the POWER parameter in the SOLVE statement if you want to step the power through a range of values. See Section 17.4: "Obtaining Solutions In THERMAL3D" for the proper syntax.

Defining Heat Sinks

Heat sinks are identified as electrodes in the 3D structure. Heat sink areas should be defined as electrodes in the manner documented in Chapter 2: "Getting Started with ATLAS", the "Specifying Electrodes" section on page 2-13 and Chapter 6: "3D Device Simulator", the "ATLAS Syntax For 3D Structure Generation" section on page 6-3.

Each electrode (heat sink) has a unique number, which is used to set the temperature on the heat sink during simulation. For more information on setting the temperature of the heat sink, see Section 17.4: "Obtaining Solutions In THERMAL3D".

17.2: Model and Material Parameter Selection

17.2.1: Thermal Simulation Model

To obtain steady-state solutions for the temperature distribution, THERMAL3D solves Poisson's equation for temperature:

$$\nabla(k(T) \nabla T) = q \quad 17-1$$

where T represents the steady state temperature, k the temperature-dependent thermal conductivity, and q the power generation per unit volume in the medium (heat sources).

The prescribed temperatures at the heat sinks form boundary conditions for Equation 17-1.

The solution of the heat equation by THERMAL3D is invoked by the following syntax:

```
MODELS THERMAL
```

17.2.2: Setting Thermal Conductivity

To set the thermal conductivities, see Section 7.2.2: "Specifying Thermal Conductivity".

17.3: Numerical Methods

No special numerical methods are required for thermal simulation. A `METHOD` statement with no parameters is assumed by default.

17.4: Obtaining Solutions In THERMAL3D

The SOLVE statement is used in THERMAL3D for heat-flow solutions much the same as it is used in other ATLAS simulations involving electrical biases. The temperature in kelvin on each heat sink is used to prescribe the boundary condition temperatures. For example:

```
SOLVE T1=300 T2=500
```

sets the temperature at 300 K and 500 K on heat sink #1 and #2 respectively.

Multiple SOLVE statements are allowed in THERMAL3D. This is useful for obtaining solutions for several combinations of heat sinks and thermal power sources. A range of solutions can also be obtained by stepping the value of a heat sink or power source. For example:

```
SOLVE T1=300 POWER2=0.35 POWER3=0.4 NSTEPS=5 STEPREGION=3 \  
POWERFINAL=0.8 OUTFILE=thermal_out0
```

increments the thermal power source in region #3 from 0.4 watts to 0.8 watts in 5 steps and:

```
SOLVE T1=300 POWER2=0.35 NSTEPS=3 ELECTRODE=1 \  
TEMPFINAL=600 OUTFILE=thermal_out0
```

increments the temperature on electrode #1 from 300 K to 600 K in 3 steps. Thermal power and temperature can be simultaneously sweep.

If more than one region power is specified during a sweep, the region to be stepped must be specified by STEPREGION=# as shown in the first example above. If the STEPREGION parameter is not specified, the smallest numerical value of POWER# is stepped.

During temperature and power sweeps, the output filename is modified according to the following rule. The rightmost character is incremented using the sequence: 0-9, A-Z, a-z. When a character is incremented beyond z, the character is set to 0> and the character to the left (smaller than 'z') is incremented.

Complete syntax information for the SOLVE statement can be found in Chapter 21: "Statements", Section 21.53: "SOLVE".

The SOLVE statement is used in THERMAL3D for heat flow solutions much as it is used in other ATLAS simulations for electrical biases. The temperature in Kelvin on each heat sink in the device must be set in the SOLVE statement. The T_n parameter, where n is the number of the heat sink, is used to set the temperature. For example:

```
SOLVE T1=300 T2=500
```

This sets 300K on heat sink #1 and 500K on heat sink #2. Only one SOLVE statement is allowed in any THERMAL3D input file.

17.5: Interpreting The Results From THERMAL3D

The output of thermal simulation consists of the minimum and maximum calculated temperature of each region and its location. The three-dimensional temperature distribution can be saved in an output structure file by setting the `OUTFILE` parameter in the `SOLVE` statement and visualized using `TONYPLOT3D`.

17.6: More Information

Many examples using THERMAL3D have been installed on your distribution tape or CDROM. More information about the use of THERMAL3D can be found by reading the text associated with each example.

You can also find some information at www.silvaco.com.

18.1: Introduction

MERCURY is an ATLAS module for the fast simulation of FET devices. The MERCURY command syntax is similar to the ATLAS command syntax. See Chapter 2: "Getting Started with ATLAS" if you are unfamiliar with the ATLAS command syntax.

18.1.1: Accessing Mercury

To access the MERCURY module, use the MERCURY command or the MERCURY parameter on the MESH command. This command must be specified immediately after the GO ATLAS command, so you can activate the MERCURY module either with

```
GO ATLAS
MERCURY
MESH WIDTH=100
```

or with

```
GO ATLAS
MESH MERCURY WIDTH=100
```

18.2: External Circuit

The MERCURY module can use a Harmonic Balance simulation to calculate the large signal behavior of a FET. As the large signal behavior of a device depends upon the circuit around the device, the MERCURY module always embeds the FET under simulation in an external circuit. The system that MERCURY simulates is shown in Figure 18-1.

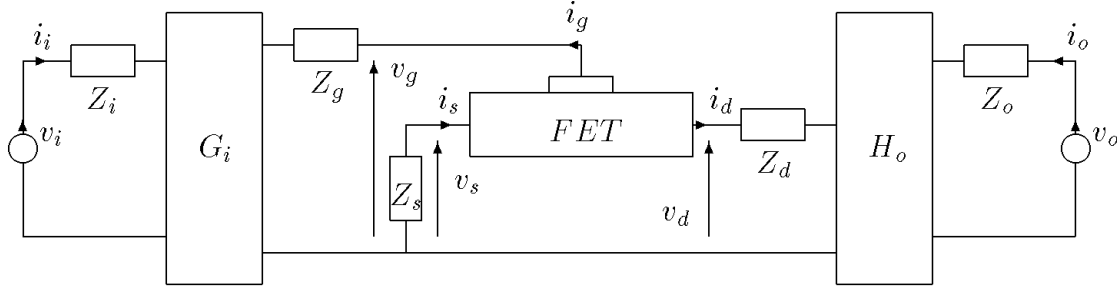


Figure 18-1: FET Embedded In An External Circuit

The input matching network is described by a set of G two-port parameters

$$\begin{pmatrix} I_i \\ V_g \end{pmatrix} = \begin{pmatrix} G_{11} & G_{12} \\ G_{21} & G_{22} \end{pmatrix} \cdot \begin{pmatrix} V_i \\ I_g \end{pmatrix} \quad 18-1$$

The output matching network is described by a set of H two-port parameters

$$\begin{pmatrix} V_d \\ I_o \end{pmatrix} = \begin{pmatrix} H_{11} & H_{12} \\ H_{21} & H_{22} \end{pmatrix} \cdot \begin{pmatrix} I_d \\ V_o \end{pmatrix} \quad 18-2$$

The contact elements Z_i , Z_o , Z_s , Z_g , and Z_d are simple impedances. The input and output matching circuits, G_i and H_o , are defined as two-port networks. At DC, all elements are assumed to be real. At RF, all elements can be complex.

The NETWORK command is used to define the characteristics of the external circuit.

For a DC or small-signal AC simulation, the external circuit is usually not wanted so the CLEAR parameter will remove the external circuit. This will set all the contact impedances to 0. The input matching network becomes

$$\begin{pmatrix} I_i \\ V_g \end{pmatrix} = \begin{pmatrix} 0 & -1 \\ 1 & 0 \end{pmatrix} \cdot \begin{pmatrix} V_i \\ I_g \end{pmatrix} \quad 18-3$$

which just applies the input voltage to the gate and passes the gate current to the output. The output matching network becomes

$$\begin{pmatrix} V_d \\ I_o \end{pmatrix} = \begin{pmatrix} 0 & 1 \\ -1 & 0 \end{pmatrix} \cdot \begin{pmatrix} I_d \\ V_o \end{pmatrix} \quad 18-4$$

which just applies the output voltage to the drain and passes the drain current directly to the output.

For a harmonic balance simulation, you must define the external circuit. The circuit should be defined at DC, the fundamental frequency, and at all the harmonics that are being modeled.

At DC, the contact impedances are set as resistances. You can define the input matching network as a set of G-parameters, S-parameters, or Z-parameters. You can define the output matching network as a set of H-parameters, S-parameters, or Z-parameters.

The RF circuits must be defined at a range of frequencies. There are several ways to do this. The first way is to define the impedance as an RLC triplet. This calculates the impedance as

$$Z = R + j \cdot \omega \cdot L - j / (\omega \cdot C) \quad 18-5$$

The default capacitance is infinite, so the $1/(\omega \cdot C)$ term goes to zero if the capacitance is not set. The second way is to set an explicit value that is the same for all frequencies. The third way is to use the HARMONIC=<n> parameter and set a value for a single frequency (where HARMONIC=1 is the fundamental, f , HARMONIC=2 is $2 \cdot f$, HARMONIC=3 is $3 \cdot f$, and so on).

The RF contact impedances can be defined as RLC triplets, as admittances, or as impedances.

The RF input matching network can be defined as a G-parameter network, an S-parameter network, or as a Z-parameter network. If it is defined as a Z-parameter network, then you can set the z-parameters or you can define them as an RLC triplet.

The RF output matching network can be defined as a H-parameter network, an S-parameter network, or a Z-parameter network. If it is defined as a Z-parameter network, then you can set the Z-parameters or you can define them as an RLC triplet.

Example

```
NETWORK CLEAR
```

This removes the network and provides a clean slate to work with

```
NETWORK ZI.RE.RF=50.0 ZI.IM.RF=0.0 ZO.RE.RF=50.0 ZO.IM.RF=0.0
```

This sets the input and output impedance to 50 Ohms at all frequencies.

```
NETWORK RG.RF=0.01 LG.RF=1e-13
```

This sets a resistance and inductance on the gate contact, the impedance will be calculated at each frequency.

```
NETWORK GI.11.RE.RF=10.0 GI.11.IM.RF=5.0 GI.12.RE.RF=7.0 ...
```

```
NETWORK HARMONIC=1 ZI.11.RE.RF=...
```

This sets an input network at all harmonics and then changes the network at the fundamental.

18.3: Device

The FET in Figure 18-1 consists of an intrinsic FET and some parasitics as shown in Figure 18-2.

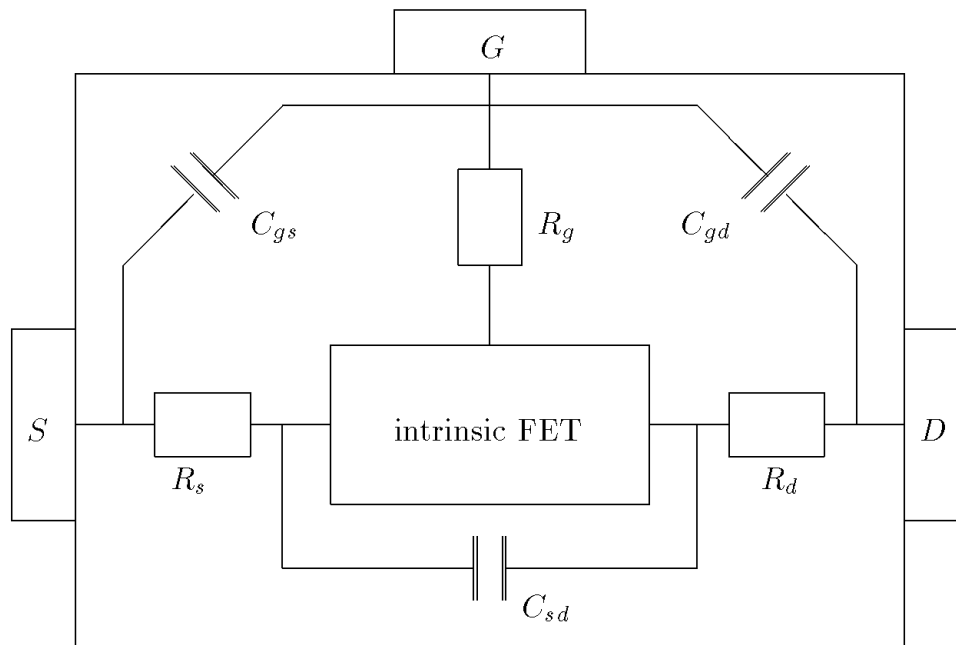


Figure 18-2: Intrinsic FET With Parasitics

The MERCURY module imposes some restrictions on device structures and requires some assumptions of device geometry to use the quasi-2D method to speed up the simulation (see Figure 18-3). All material layers and doping profiles are planar: they have no variation in the x-direction. The only exceptions to this rule are the gate and a possible recess in the surface. The source and drain contacts are not considered part of the intrinsic device and are modeled as perfectly ohmic contacts to the channel on the left and right of the device.

The method for defining a device in the MERCURY module is similar to the method used in ATLAS. First, the MESH statements are used to set the z-depth of the device and to define the physical extent of the device in the xy-plane

```
MESH WIDTH=100
X.MESH LOCATION=0.0 SPACING=0.1
X.MESH LOCATION=1.1 SPACING=0.2
X.MESH LOCATION=2.5 SPACING=0.1
Y.MESH LOCATION=0.0 SPACING=0.01
Y.MESH LOCATION=3.0 SPACING=0.01
```

But the MERCURY module only uses the extreme values of x and y to define the extent of the device, any locations between these two extremes (such as the "X.MESH LOCATION=1.1" command) are ignored.

Then **REGION** commands are used to define the epilayers. Only the y-extent of the regions are recognized by **MERCURY**: each layer must cover the whole x-range of the device

```
REGION MATERIAL=GaAs THICKNESS=0.2
REGION MATERIAL=AlAs THICKNESS=0.3
REGION MATERIAL=GaAs THICKNESS=2.0
```

Then, **DOPING** commands are used to define the doping. Again, these commands can only have a y-variation. Any x-variation in the doping will be ignored.

```
DOPING UNIFORM N.TYPE CONCENTRATION=1e17 Y.MIN=0.0 Y.MAX=0.2
```

The only non-uniformity in the X direction is a recess in the surface of the device

```
SURFACE X=0.50 Y=0.00
SURFACE X=0.65 Y=0.15
SURFACE X=1.35 Y=0.15
SURFACE Y=1.50 Y=0.00
```

and the position of the gate

```
ELECTRODE NAME=gate X.MIN=0.7 X.MAX=1.3
```

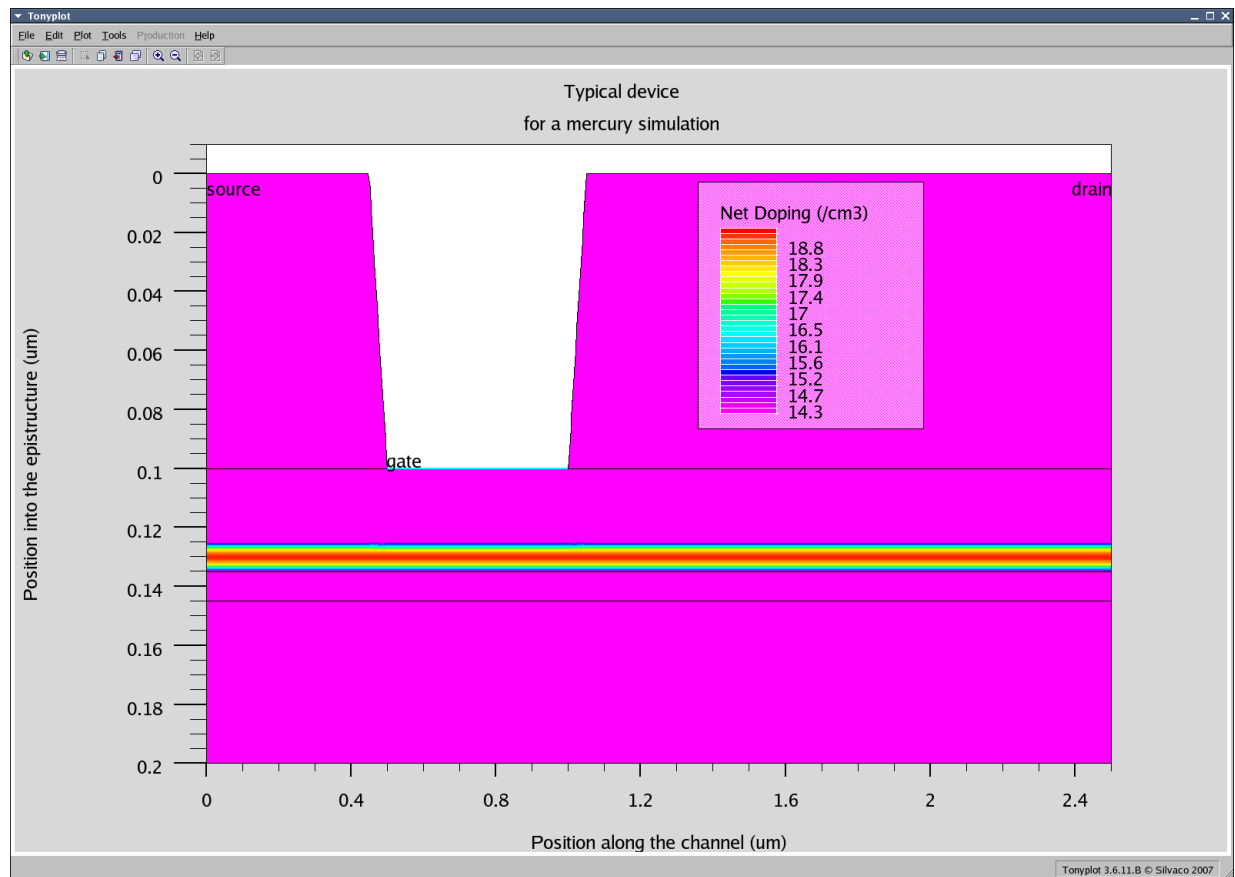


Figure 18-3: Typical Planar Device for a MERCURY Simulation

18.4: Quasi-2D Simulation

The quasi-2D method has two parts. The first calculates Poisson's equation in the Y direction. The second calculates the transport equations in the X direction.

18.4.1: Poisson Equation

The first part of the simulation calculates Poisson's equation in the Y direction of the device over a range of surface conditions. This calculates the carrier density as a function of depth into the device (see Figure 18-4). The program then converts this profile into a "channel" with a width and a constant 3D density (see Figure 18-5).

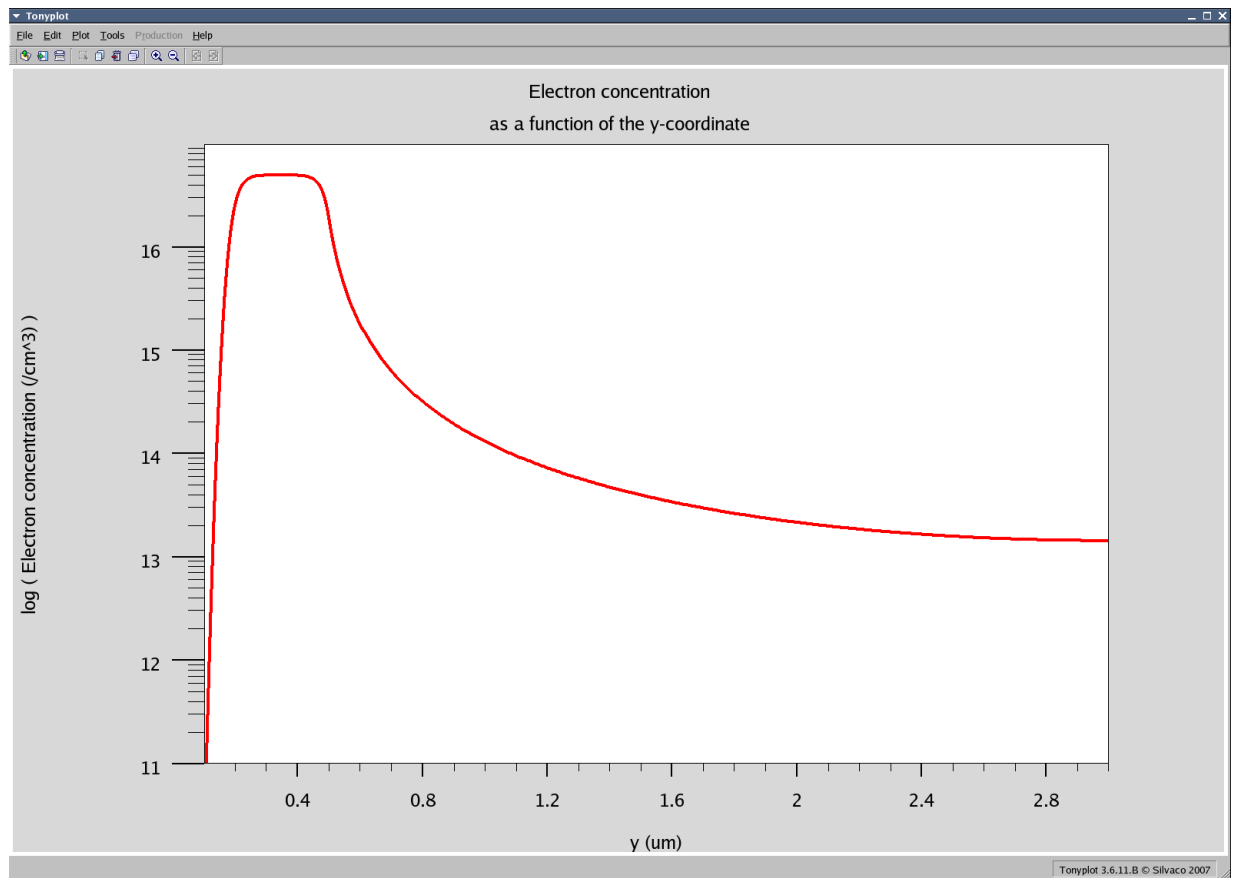


Figure 18-4: Carrier Density as a Function of Depth

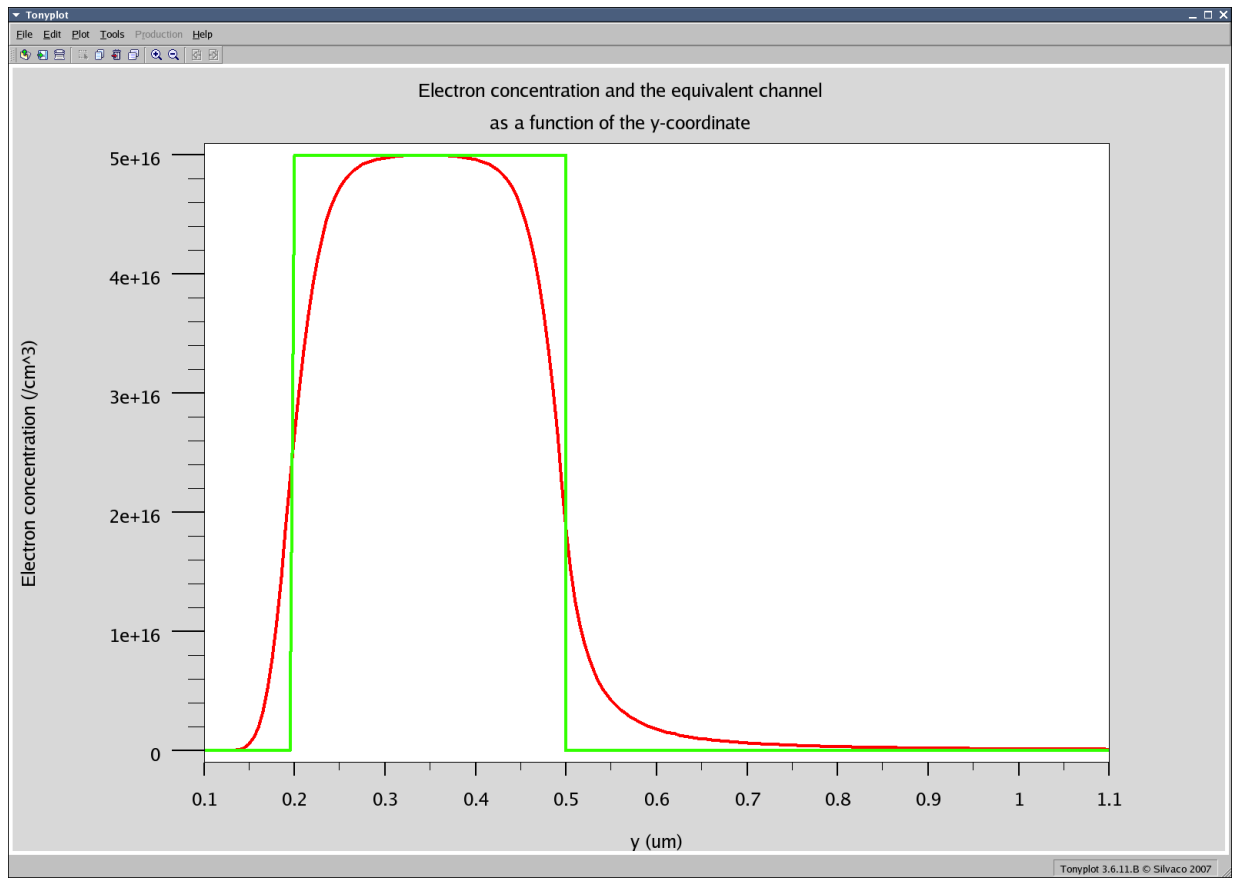


Figure 18-5: Channel with a Width and a Constant 3D Density

Two look-up tables are generated. One from the results of Poisson's equation for an ungated slice over the range of recess depths of the device (if the device is planar this is a single point). The other from the results of Poisson's equation for a gated slice over the range of contact voltages expected in the simulation, see Figure 18-6.

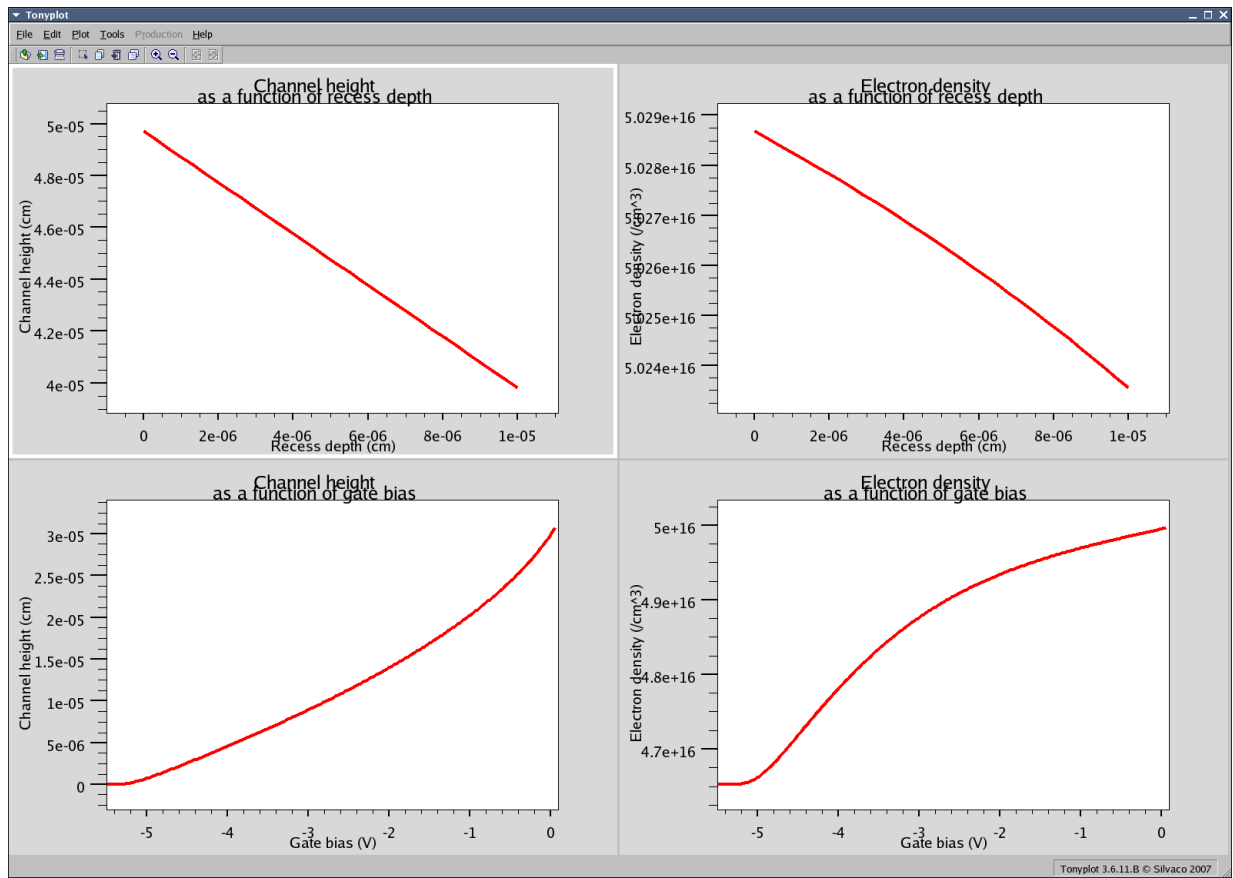


Figure 18-6: Channel Height and Electron Volume Density

The look-up tables are generated with the command

```
POISSON LOOK_UP VG_MIN=-2.5 VG_MAX=0.0 VD_MIN=0.0 VD_MAX=1.0
```

The parameters `VG_MIN` and `VG_MAX` are used to define the range of gate voltages. The parameters `VD_MIN` and `VD_MAX` are used to define the range of drain voltages. These ranges are needed to ensure that the gate look-up table is calculated over a sufficient range.

18.4.2: Channel Simulation

The main channel simulation is essentially one-dimensional. The device is divided into slices from the source to the drain. The transport equations are derived around the parallelogram surrounding a grid point (see Figure 18-7).

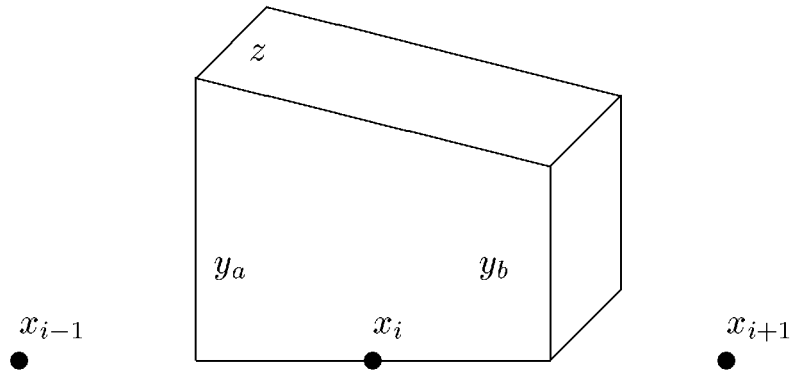


Figure 18-7: The section of the channel around the grid point x_i .

Here, y_a and y_b are the heights of the channel (rather than the device). The volume of this parallelogram is

$$V = \frac{(x_{i+1} - x_{i-1})}{2} \cdot \frac{(y_a + y_b)}{2} \cdot z = 0.25 \cdot (x_{i+1} - x_{i-1}) \cdot (y_a + y_b) \cdot z \quad 18-6$$

The resultant equations are similar to the standard set of equations used in the drift diffusion model.

Poisson's Equation

MERCURY's version of Poisson's equation is derived by analyzing the electric fields on the surface of a section of the channel.

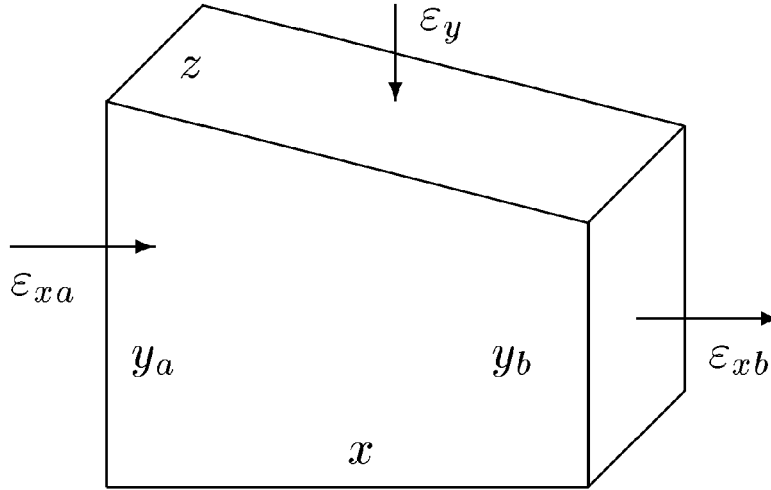


Figure 18-8: The electric fields around a section of the channel.

Start with Gauss's law

$$\int \epsilon \cdot dA = \frac{Q}{\epsilon} \quad 18-7$$

Q is the total charge contained within the surface. Initially, $\epsilon_{xa}=0$ and $\epsilon_{xb}=0$.

Therefore

$$-\epsilon_y \cdot x \cdot z = \frac{Q_0}{\epsilon} \quad 18-8$$

The relationship between Q_0 and ϵ_y is calculated in the charge-control simulation. Therefore, when you add the X direction electric fields you have

$$\epsilon_{xb} \cdot y_b \cdot z - \epsilon_{xa} \cdot y_a \cdot z - \epsilon_y \cdot x \cdot z = \frac{Q}{\epsilon} \quad 18-9$$

Replace the ϵ_y term with the values from the charge control

$$\epsilon_{xb} \cdot y_b \cdot z - \epsilon_{xa} \cdot y_a \cdot z = \frac{Q - Q_0}{\epsilon} \quad 18-10$$

Write the charge in terms of the carrier density (where q is the charge on a hole, V is the volume of the parallelogram, and ρ is the density of carriers).

$$Q = q \cdot V \cdot \rho \quad 18-11$$

Therefore, p is the density of holes, n is the density of electrons, N_D^+ is the density of ionized donors, and N_A^- is the density of ionized acceptors.

$$\rho = p - n + N_D^+ - N_A^- \quad 18-12$$

If the ionization density is a constant, then

$$\rho - \rho_0 = (p - p_0) - (n - n_0) \quad 18-13$$

Therefore

$$\varepsilon_{xb} \cdot y_b \cdot z - \varepsilon_{xa} \cdot y_a \cdot z = \left(\frac{q \cdot V}{\varepsilon} \cdot [(p - p_0) - (n - n_0)] \right) \quad 18-14$$

In the limit $x \rightarrow 0$ ($y_a = y_b$), this becomes Poisson's equation. MERCURY, however, implements the discrete version.

Continuity Equation

MERCURY's version of the continuity equation is derived by analyzing the currents on the surface of a section of the channel.

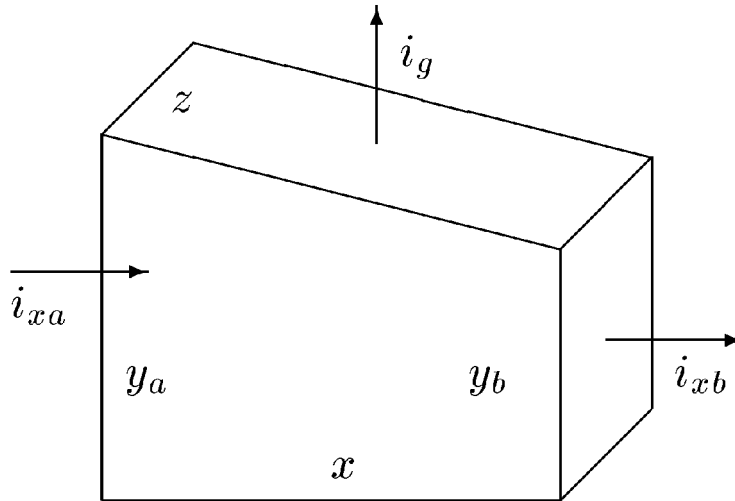


Figure 18-9: The currents around a section of the channel.

A current is a flow of positive charge. Therefore, the change in the number of carriers in a small time δt due to a current i is (s is the sign of the carriers)

$$\delta C = s \cdot \frac{1}{q} \cdot i \cdot \delta t \quad 18-15$$

So in a small time δt , the change in the number of carriers in the parallelogram is

$$\delta C = s \cdot \frac{1}{q} \cdot i_{xa} \cdot \delta t - s \cdot \frac{1}{q} \cdot i_{xb} \cdot \delta t - s \cdot \frac{1}{q} \cdot i_g \cdot \delta t + genTerm \quad 18-16$$

Here, $genTerm$ is the number of carriers generated in the volume in the small time δt . Dividing through by δt

$$\frac{\delta C}{\delta t} = \frac{s}{q} \cdot i_{xa} - \frac{s}{q} \cdot i_{xb} - \frac{s}{q} \cdot i_g + \frac{genTerm}{\delta t} \quad 18-17$$

Writing in terms of the current density rather than the current and dividing by the volume

$$\frac{\delta C}{V \cdot \delta t} = \frac{s}{V \cdot q} \cdot J_{xa} \cdot y_a \cdot z - \frac{s}{V \cdot q} \cdot J_{xb} \cdot y_b \cdot z - \frac{s}{V \cdot q} \cdot J_g \cdot \frac{x_i + 1 - x_x - 1}{2} \cdot z + \frac{genTerm}{V \cdot \delta t} \quad 18-18$$

Take the limit as $\delta t \rightarrow 0$ and get

$$\frac{dc}{dt} = \frac{s}{V \cdot q} \cdot J_{xa} \cdot y_a \cdot z - \frac{s}{V \cdot q} \cdot J_{xb} \cdot y_b \cdot z - \frac{s}{V \cdot q} \cdot J_g \cdot \frac{x_i + 1 - x_i - 1}{2} \cdot z + U_c \quad 18-19$$

Here, c is now the density of the carriers and U_c is the generation rate of the carrier. In the limit as $x \rightarrow 0$, this becomes the standard continuity equation.

Channel Current

The channel current is described by the standard drift diffusion model written using the Bernoulli function

$$J = \frac{s \cdot k \cdot T \cdot \mu_c}{x_{i+1} - x_i} \cdot (B(-\Phi_{i,i+1}) \cdot c_i - B(-\Phi_{i,i+1}) \cdot c_{i+1}) \quad 18-20$$

with

$$\Phi_{i,i+1} = \frac{s \cdot q}{k \cdot T} \cdot (v_i - v_{v+1}) \quad 18-21$$

18.5: DC and Small-Signal AC

As mentioned in Section 18.2: “External Circuit”, the FET under simulation is embedded in an external circuit. But when investigating the DC or small-signal AC behavior, you will normally be interested in the characteristics of the bare FET. The `NETWORK CLEAR` command sets the external circuit so that the input voltage is applied directly to the gate and the output voltage is applied directly to the drain.

To calculate a set of DC-IV curves, you need to issue a set of commands like this (the DC-IV data would be saved to the file `DC.LOG`).

```
LOG OUTFILE=DC.LOG

SOLVE VINPUT=-0.0 VOUTPUT=0.0 VSTEP=0.5 VFINAL=5.0 NAME=output
SOLVE VINPUT=-0.5 VOUTPUT=0.0 VSTEP=0.5 VFINAL=5.0 NAME=output
SOLVE VINPUT=-1.0 VOUTPUT=0.0 VSTEP=0.5 VFINAL=5.0 NAME=output
SOLVE VINPUT=-1.5 VOUTPUT=0.0 VSTEP=0.5 VFINAL=5.0 NAME=output
SOLVE VINPUT=-2.0 VOUTPUT=0.0 VSTEP=0.5 VFINAL=5.0 NAME=output
```

In order to make a MERCURY input deck as close to an ATLAS input deck as possible, `GATE` is recognized as an alias for `INPUT` and `DRAIN` is recognized as an alias for `OUTPUT`. So the previous set of commands can be written as:

```
LOG OUTFILE=DC.LOG

SOLVE VGATE=-0.0 VDRAIN=0.0 VSTEP=0.5 VFINAL=5.0 NAME=drain
SOLVE VGATE=-0.5 VDRAIN=0.0 VSTEP=0.5 VFINAL=5.0 NAME=drain
SOLVE VGATE=-1.0 VDRAIN=0.0 VSTEP=0.5 VFINAL=5.0 NAME=drain
SOLVE VGATE=-1.5 VDRAIN=0.0 VSTEP=0.5 VFINAL=5.0 NAME=drain
SOLVE VGATE=-2.0 VDRAIN=0.0 VSTEP=0.5 VFINAL=5.0 NAME=drain
```

But be careful, `VGATE` is just an alias for `VINPUT` and `VDRAIN` is just an alias for `VOUTPUT`. Therefore, the command `VGATE` sets the voltage V_i (rather than the voltage V_g). The command `VDRAIN` sets the voltage V_o (rather than the voltage V_d). But if the external network has been cleared (as it usually will during a DC or small-signal AC simulation), setting V_i is equivalent to setting V_g and setting V_o is equivalent to setting V_d .

18.5.1: Small-Signal AC

In MERCURY, the FET is always arranged in a common source configuration, port 1 is always the gate-source port, and port 2 is always the drain-source port. A typical set of commands for a small-signal AC simulation will be

```
SOLVE VGATE=-1.0 VDRAIN=3.0

LOG S.PARAM GAINS NOISE.V OUTFILE=AC.LOG

SOLVE AC NOISE FREQUENCY=1.0E6 FSTEP=1.2589 NFSTEP=40 MULT.FREQ
```

MERCURY can calculate the small-signal noise of the device in addition to the small-signal AC behavior.

18.6: Harmonic Balance

Harmonic Balance simulates the behavior of a device when its input is large enough to cause a non-linear response.

The following shows the minimum needed to simulate the large-signal response in MERCURY.

1. Solve at a dc bias point

```
SOLVE vinput=-0.5 voutput=2.0
```

2. Open a file to store the results.

```
log num.harmonic=3 outfile=hb.log
```

The harmonic balance simulation is slow so it's a good idea to record a result when it calculates.

3. Use the SOLVE command to simulate the large-signal behavior. You define the frequency and the range of the size of the input signal at this frequency.

```
SOLVE hb vinput=1e-4 vfinal=1.0 nvstep=20 name=input mult.v
```

For more information about the LOG and SOLVE commands see Chapter 19: "Statements".

The SOLVE Command

The NUM_HARMONICS parameter on the SOLVE command defines the number of harmonics used in the harmonic balance simulation. That is, the number of frequency components used to describe the time domain signal. The number of harmonics should be high enough to model the time domain signal with sufficient fidelity. But there should be no more harmonics than necessary: the more harmonics the slower the simulation.

The LOG Command

The following data is stored in the harmonic balance log file:

- the DC bias point,
- a list of the frequency components of the input and output voltages and currents,
- the input power at the fundamental,
- the output power at the fundamental and each harmonic.

The NUM_HARMONICS parameter on the LOG command defines how many harmonics to output the data for. The complex numbers can output as a real/imaginary pair or a magnitude/phase pair.

18.6.1: Non-Linearity

Figure 18-10 shows a schematic of a two-port circuit.

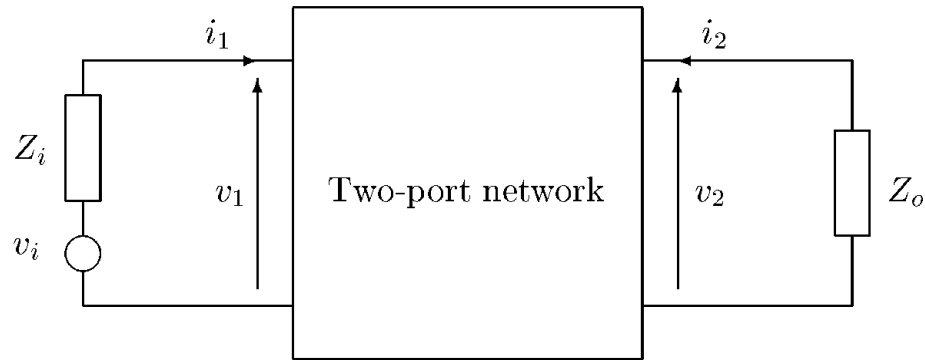


Figure 18-10: Two-Port Circuit

A signal is input into port 1 of the circuit. It is then transmitted through the two-port to the output impedance on port 2. In reality, the input signal will be irregular. But for analysis, the input signal is usually assumed to be sinusoidal at a frequency of ω . The frequency ω is called the fundamental frequency.

This section focuses on the steady-state output from the circuit to a periodic input signal. It does not focus on the transient response of the circuit to non-periodic changes to the input.

A Linear Circuit

In a linear circuit, the shape of the output signal is a perfect reproduction of the shape of the input signal. (The amplitude of the output signal is likely to be different from the input: almost all circuits amplify or attenuate. And there may be a delay between a signal appearing at the input and being transmitted to the output.)

If the input is a sinusoid at a frequency of ω , then the output will be a sinusoid at a frequency of ω . But probably with a different amplitude and phase than the amplitude and phase of the input sinusoid.

The behavior of this circuit can be summarized by a set of two-port parameters.

$$\begin{pmatrix} v_1(\omega) \\ v_2(\omega) \end{pmatrix} = \begin{pmatrix} Z_{11}(\omega) & Z_{12}(\omega) \\ Z_{21}(\omega) & Z_{22}(\omega) \end{pmatrix} \cdot \begin{pmatrix} i_1(\omega) \\ i_2(\omega) \end{pmatrix} \quad 18-22$$

The Z-parameters depend only upon the frequency of the input signal. They don't depend upon the magnitude of the input signal.

A Non-linear Circuit

In a non-linear circuit, the shape of the output signal is not the same as the shape of the input signal.

If the input is a sinusoid at a fundamental frequency of ω , then the output is a signal that is a sum of a component at the fundamental frequency and additional components at the integer harmonics of this fundamental frequency.

$$v_0 \equiv v_{0,1}(\omega) + v_{0,2}(2 \cdot \omega) + v_{0,3}(3 \cdot \omega) + \dots \quad 18-23$$

In principle, this series is infinite but in practice we need only the first few terms. The bigger the magnitude of the input signal the more terms you need to include in the calculation of the output signal.

Real Devices

In reality, all devices and components are non-linear. If the input signal is small enough, only the first term in the expansion of the output is required and the circuit will be effectively linear.

18.6.2: Harmonic Balance

Time Domain and Frequency Domain

Any measured signal is real (rather than complex). A periodic real signal that is described by n harmonics can be written as

$$v(t) = V_0 + V_1 \cdot \exp(j \cdot \omega \cdot t) + V_2 \cdot \exp(2 \cdot j \cdot \omega \cdot t) + \dots + V_n \cdot \exp(n \cdot j \cdot \omega \cdot t) \\ + V_1^* \cdot \exp(-j \cdot \omega \cdot t) + V_2^* \cdot \exp(-2 \cdot j \cdot \omega \cdot t) + V_n^* \cdot \exp(-n \cdot j \cdot \omega \cdot t) \quad 18-24$$

The "positive frequencies" correspond to sinusoidal waves moving in the negative direction. The "negative frequencies" correspond to sinusoidal waves moving in the positive direction.

The signal $v(t)$ is completely described by the set of coefficients V_0 to V_n . This is $2 \cdot n + 1$ real numbers (V_0 is real and the coefficients V_1 to V_n are complex). This representation of $v(t)$ is called the frequency domain description.

Correspondingly, the signal $v(t)$ is completely described by a set of $2 \cdot n + 1$ values equally spaced over one period. The period of $v(t)$ is dictated by the period of the fundamental. The period T is such that

$$v(t) = v(t + T) \quad 18-25$$

Therefore

$$T = \frac{2 \cdot \pi}{\omega} \quad 18-26$$

We define the time step t_s as

$$t_s = \frac{T}{2 \cdot n + 1} \quad 18-27$$

The time domain representation of $v(t)$ is the set of points

$$v_0 = v(0), v_1 = v(t_s), v_2 = v(2 \cdot t_s), \dots, v_{2 \cdot n} = v(2 \cdot n \cdot t_s) \quad 18-28$$

These two representations of the signal $v(t)$ are equivalent. The discrete Fourier transform is used to translate between them.

The Problem With Large-Signal Simulation

The equations that describe the behavior of non-linear components are mostly written in the time domain. Therefore, they must be solved in the time domain. The time domain behavior must be solved at $2.n+1$ points over one period of the signal.

A linear circuit almost certainly contains resistance, capacitance, and inductance and has an RCL time constant. The output from a time domain simulation of a linear circuit will initially contain a transient part in addition to the steady state part. For the transient part of the result to decay and leave only the steady state part, the simulation must continue for several multiples of the RCL time constant. If the time constant is longer than the period of the input signal, a time domain simulation may have to run for many hundreds of periods before reaching the steady state solution.

This is a problem when trying to solve a circuit that contains both linear and non-linear elements. The non-linear elements must be solved in the time domain. Solving the linear elements, however, in the time domain is very inefficient.

Harmonic Balance Method

While the steady state response of a linear circuit is difficult to calculate in the time domain, this response can be directly calculated in the frequency domain. This is the key to the Harmonic Balance method.

The circuit is divided into the linear parts and the non-linear parts (see Figure 18-11). Attention is focused on the ports where the two circuits connect.

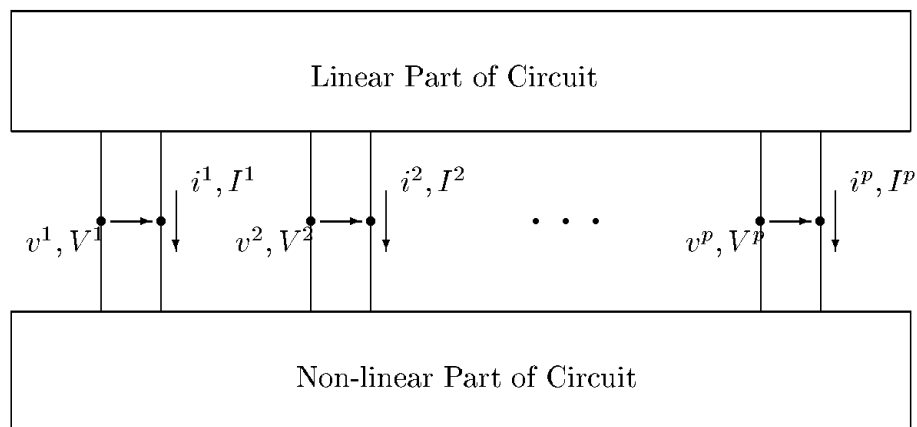


Figure 18-11: A Circuit divided into Linear and Non-linear Parts

The Harmonic Balance algorithm is as follows:

1. MERCURY makes an initial guess of the time domain voltage at the ports.
2. MERCURY uses the non-linear circuit to calculate the resultant time domain current at the ports.
3. MERCURY uses the Fourier transform to translate each time domain current into a frequency domain current.
4. MERCURY uses the linear circuit to calculate the resultant frequency domain voltage at the ports.

5. MERCURY uses the Fourier transform to translate each frequency domain voltage into a time domain voltage.
6. If the new time domain voltage is close enough to the time domain voltage from the previous iteration, MERCURY has solved the response of the circuit. If the new time domain voltage is significantly different from the time domain voltage in the previous iteration, MERCURY returns to step 2 and performs another iteration.

18.7: NETWORK

NETWORK allows you to define the external network surrounding the FET in a MERCURY simulation. This command is valid only when using the MERCURY module.

Syntax

```
NETWORK [CLEAR] [HARMONIC=<n>] [dc_circuit] [rf_circuit]
```

| Parameter | Type | Default | Units |
|-------------|---------|---------|-------|
| CLEAR | Logical | False | |
| HARMONIC | Integer | | |
| CD.RF | Real | 0.0 | F |
| CG.RF | Real | 0.0 | F |
| CI.11.RF | Real | 0.0 | F |
| CI.12.RF | Real | 0.0 | F |
| CI.21.RF | Real | 0.0 | F |
| CI.22.RF | Real | 0.0 | F |
| CI.RF | Real | 0.0 | F |
| CO.11.RF | Real | 0.0 | F |
| CO.12.RF | Real | 0.0 | F |
| CO.21.RF | Real | 0.0 | F |
| CO.22.RF | Real | 0.0 | F |
| CO.RF | Real | 0.0 | F |
| CS.RF | Real | 0.0 | F |
| GI.11.DC | Real | 0.0 | Mho |
| GI.11.IM.RF | Real | 0.0 | Mho |
| GI.11.RE.RF | Real | 0.0 | Mho |
| GI.12.DC | Real | 0.0 | Mho |
| GI.12.IM.RF | Real | 0.0 | |
| GI.12.RE.RF | Real | 0.0 | |
| GI.21.DC | Real | 0.0 | |
| GI.21.IM.RF | Real | 0.0 | |
| GI.21.RE.RF | Real | 0.0 | |
| GI.22.DC | Real | 0.0 | Ohm |

| | | | |
|-------------|------|-----|-----|
| GI.22.IM.RF | Real | 0.0 | Ohm |
| GI.22.RE.RF | Real | 0.0 | Ohm |
| HO.11.DC | Real | 0.0 | Ohm |
| HO.11.IM.RF | Real | 0.0 | Ohm |
| HO.11.RE.RF | Real | 0.0 | Ohm |
| HO.12.DC | Real | 0.0 | |
| HO.12.IM.RF | Real | 0.0 | |
| HO.12.RE.RF | Real | 0.0 | |
| HO.21.DC | Real | 0.0 | |
| HO.21.IM.RF | Real | 0.0 | |
| HO.21.RE.RF | Real | 0.0 | |
| HO.22.DC | Real | 0.0 | Mho |
| HO.22.IM.RF | Real | 0.0 | Mho |
| HO.22.RE.RF | Real | 0.0 | Mho |
| LD.RF | Real | 0.0 | H |
| LG.RF | Real | 0.0 | H |
| LI.11.RF | Real | 0.0 | H |
| LI.12.RF | Real | 0.0 | H |
| LI.21.RF | Real | 0.0 | H |
| LI.22.RF | Real | 0.0 | H |
| LI.RF | Real | 0.0 | H |
| LO.11.RF | Real | 0.0 | H |
| LO.12.RF | Real | 0.0 | H |
| LO.21.RF | Real | 0.0 | H |
| LO.22.RF | Real | 0.0 | H |
| LO.RF | Real | 0.0 | H |
| LS.RF | Real | 0.0 | H |
| RD.DC | Real | 0.0 | Ohm |
| RD.RF | Real | 0.0 | Ohm |
| RG.DC | Real | 0.0 | Ohm |
| RG.RF | Real | 0.0 | Ohm |
| RI.11.RF | Real | 0.0 | Ohm |

| | | | |
|-------------|------|-----|-----|
| RI.12.RF | Real | 0.0 | Ohm |
| RI.21.RF | Real | 0.0 | Ohm |
| RI.22.RF | Real | 0.0 | Ohm |
| RI.DC | Real | 0.0 | Ohm |
| RI.RF | Real | 0.0 | Ohm |
| RO.11.RF | Real | 0.0 | Ohm |
| RO.12.RF | Real | 0.0 | Ohm |
| RO.21.RF | Real | 0.0 | Ohm |
| RO.22.RF | Real | 0.0 | Ohm |
| RO.DC | Real | 0.0 | Ohm |
| RO.RF | Real | 0.0 | Ohm |
| RS.DC | Real | 0.0 | Ohm |
| RS.RF | Real | 0.0 | Ohm |
| SI.11.DC | Real | 0.0 | |
| SI.11.IM.RF | Real | 0.0 | |
| SI.11.RE.RF | Real | 0.0 | |
| SI.12.DC | Real | 0.0 | |
| SI.12.IM.RF | Real | 0.0 | |
| SI.12.RE.RF | Real | 0.0 | |
| SI.21.DC | Real | 0.0 | |
| SI.21.IM.RF | Real | 0.0 | |
| SI.21.RE.RF | Real | 0.0 | |
| SI.22.DC | Real | 0.0 | |
| SI.22.IM.RF | Real | 0.0 | |
| SI.22.RE.RF | Real | 0.0 | |
| SO.11.DC | Real | 0.0 | |
| SO.11.IM.RF | Real | 0.0 | |
| SO.11.RE.RF | Real | 0.0 | |
| SO.12.DC | Real | 0.0 | |
| SO.12.IM.RF | Real | 0.0 | |
| SO.12.RE.RF | Real | 0.0 | |
| SO.21.DC | Real | 0.0 | |

| | | | |
|-------------|------|-----|-----|
| SO.21.IM.RF | Real | 0.0 | |
| SO.21.RE.RF | Real | 0.0 | |
| SO.22.DC | Real | 0.0 | |
| SO.22.IM.RF | Real | 0.0 | |
| SO.22.RE.RF | Real | 0.0 | |
| YD.IM.RF | Real | 0.0 | Mho |
| YD.RE.RF | Real | 0.0 | Mho |
| YG.IM.RF | Real | 0.0 | Mho |
| YG.RE.RF | Real | 0.0 | Mho |
| YI.IM.RF | Real | 0.0 | Mho |
| YI.RE.RF | Real | 0.0 | Mho |
| YO.IM.RF | Real | 0.0 | Mho |
| YO.RE.RF | Real | 0.0 | Mho |
| YS.IM.RF | Real | 0.0 | Mho |
| YS.RE.RF | Real | 0.0 | Mho |
| ZD.IM.RF | Real | 0.0 | Ohm |
| ZD.RE.RF | Real | 0.0 | Ohm |
| ZG.IM.RF | Real | 0.0 | Ohm |
| ZG.RE.RF | Real | 0.0 | Ohm |
| ZI.11.DC | Real | 0.0 | Ohm |
| ZI.11.IM.RF | Real | 0.0 | Ohm |
| ZI.11.RE.RF | Real | 0.0 | Ohm |
| ZI.12.DC | Real | 0.0 | Ohm |
| ZI.12.IM.RF | Real | 0.0 | Ohm |
| ZI.12.RE.RF | Real | 0.0 | Ohm |
| ZI.21.DC | Real | 0.0 | Ohm |
| ZI.21.IM.RF | Real | 0.0 | Ohm |
| ZI.21.RE.RF | Real | 0.0 | Ohm |
| ZI.22.DC | Real | 0.0 | Ohm |
| ZI.22.IM.RF | Real | 0.0 | Ohm |
| ZI.22.RE.RF | Real | 0.0 | Ohm |
| ZI.IM.RF | Real | 0.0 | Ohm |

| | | | |
|-------------|------|-----|-----|
| ZI.RE.RF | Real | 0.0 | Ohm |
| ZO.11.DC | Real | 0.0 | Ohm |
| ZO.11.IM.RF | Real | 0.0 | Ohm |
| ZO.11.RE.RF | Real | 0.0 | Ohm |
| ZO.12.DC | Real | 0.0 | Ohm |
| ZO.12.IM.RF | Real | 0.0 | Ohm |
| ZO.12.RE.RF | Real | 0.0 | Ohm |
| ZO.21.DC | Real | 0.0 | Ohm |
| ZO.21.IM.RF | Real | 0.0 | Ohm |
| ZO.21.RE.RF | Real | 0.0 | Ohm |
| ZO.22.DC | Real | 0.0 | Ohm |
| ZO.22.IM.RF | Real | 0.0 | Ohm |
| ZO.22.RE.RF | Real | 0.0 | Ohm |
| ZO.IM.RF | Real | 0.0 | Ohm |
| ZO.RE.RF | Real | 0.0 | Ohm |
| ZS.IM.RF | Real | 0.0 | Ohm |
| ZS.RE.RF | Real | 0.0 | Ohm |

Description

| | |
|-----------------|--|
| CLEAR | Sets all contact impedances to 0, sets the input matching network to G11=0, G12=-1, G21=1, and G22=0, and sets the output matching network to H11=0, H12=1, H21=-1, and H22=0. |
| HARMONIC | Specifies which harmonic, in a harmonic balance simulation, the RF circuit is applied to. If HARMONIC is not set, then the RF circuit will be applied to all harmonics. |

DC Contact Resistances

Note: At DC all circuits are assumed to be real.

| | |
|--------------|-----------------------------------|
| RD.DC | Defines the DC drain resistance. |
| RG.DC | Defines the DC gate resistance. |
| RI.DC | Defines the DC input resistance. |
| RO.DC | Defines the DC output resistance. |
| RS.DC | Defines the DC source resistance. |

DC Input Matching Network

| | |
|---|---|
| GI.11.DC, GI.12.DC, GI.21.DC, GI.22.DC | Defines the DC input matching network as a set of g-parameters. |
| SI.11.DC, SI.12.DC, SI.21.DC, SI.22.DC | Defines the DC input matching network as a set of s-parameters. |
| ZI.11.DC, ZI.12.DC, ZI.21.DC, ZI.22.DC | Defined the DC input matching network as a set of z-parameters. |

DC Output Matching Network

| | |
|---|--|
| HO.11.DC, HO.12.DC, HO.21.DC, HO.22.DC | Defines the DC output matching network as a set of h-parameters. |
| SO.11.DC, SO.12.DC, SO.21.DC, SO.22.DC | Defines the DC output matching network as a set of s-parameters. |
| ZO.11.DC, ZO.12.DC, ZO.21.DC, ZO.22.DC | Defines the DC output matching network as a set of z-parameters. |

RF Contact Impedances

| | |
|----------------------------|--|
| RD.RF, CD.RF, LD.RF | Defines the RF drain impedance as a series RCL circuit. |
| RG.RF, CG.RF, LG.RF | Defines the RF gate impedance as a series RCL circuit. |
| RI.RF, CI.RF, LI.RF | Defines the RF input impedance as a series RCL circuit. |
| RO.RF, CO.RF, LO.RF | Defines the RF output impedance as a series RCL circuit. |
| RS.RF, CS.RF, LS.RF | Defines the RF source impedance as a series RCL circuit. |
| YD.RE.RF, YD.IM.RF | Defines the RF drain impedance as an admittance. |
| YG.RE.RF, YG.IM.RF | Defines the RF gate impedance as an admittance. |
| YI.RE.RF, YI.IM.RF | Defines the RF input impedance as an admittance. |
| YO.RE.RF, YO.IM.RF | Defines the RF output impedance as an admittance. |
| YS.RE.RF, YS.IM.RF | Defines the RF source impedance as an admittance. |
| ZD.RE.RF, ZD.IM.RF | Defines the RF drain impedance as an impedance. |
| ZG.RE.RF, ZG.IM.RF | Defines the RF gate impedance as an impedance. |
| ZI.RE.RF, ZI.IM.RF | Defines the RF input impedance as an impedance. |
| ZO.RE.RF, ZO.IM.RF | Defines the RF output impedance as an impedance. |
| ZS.RE.RF, ZS.IM.RF | Defines the RF source impedance as an impedance. |

RF Input Matching Network

| | |
|---|---|
| RI.11.RF, CI.11.RF, LI.11.RF, RI.12.RF, CI.12.RF, LI.12.RF, RI.21.RF, CI.21.RF, LI.21.RF, RI.22.RF, CI.22.RF, LI.22.RF | Defines the RF input matching network, each parameter of the z-parameter two-port is defined as a series RCL circuit. |
| GI.11.RE.RF, GI.11.IM.RF, GI.12.RE.RF, GI.12.IM.RF, GI.21.RE.RF, GI.21.IM.RF, GI.22.RE.RF, GI.22.IM.RF | Defines the RF input matching network as a set of g-parameters. |
| SI.11.RE.RF, SI.11.IM.RF, SI.12.RE.RF, SI.12.IM.RF, SI.21.RE.RF, SI.21.IM.RF, SI.22.RE.RF, SI.22.IM.RF | Defines the RF input matching network as a set of s-parameters. |
| ZI.11.RE.RF, ZI.11.IM.RF, ZI.12.RE.RF, ZI.12.IM.RF, ZI.21.RE.RF, ZI.21.IM.RF, ZI.22.RE.RF, ZI.22.IM.RF | Defines the RF input matching network as a set of z-parameters. |

RF Output Matching Network

| | |
|--|--|
| RO.11.RF, CO.11.RF, LO.11.RF, RO.12.RF, CO.12.RF, LO.12.RF, RO.21.RF, CO.21.RF, LO.21.RF, RO.22.RF, CO.22.RF, LO.22.RF, | Defines the RF output matching network, each parameter of the z-parameter two-port is defined as a series RCL circuit. |
| HO.11.RE.RF, HO.11.IM.RF, HO.12.RE.RF, HO.12.IM.RF, HO.21.RE.RF, HO.21.IM.RF, HO.22.RE.RF, HO.22.IM.RF | Defines the RF output matching network as a set of h-parameters. |
| SO.11.RE.RF, SO.11.IM.RF, SO.12.RE.RF, SO.12.IM.RF, SO.21.RE.RF, SO.21.IM.RF, SO.22.RE.RF, SO.22.IM.RF | Defines the RF output matching network as a set of s-parameters. |
| ZO.11.RE.RF, ZO.11.IM.RF, ZO.12.RE.RF, ZO.12.IM.RF, ZO.21.RE.RF, ZO.21.IM.RF, ZO.22.RE.RF, ZO.22.IM.RF | Defines the RF output matching network as a set of z-parameters. |

Examples

NETWORK CLEAR

Do this before DC and small-signal AC simulations to remove the input and output matching networks.

```
network zi.re.rf=50.0 zi.im.rf=0.0 zo.re.rf=50.0 zo.im.rf=0.0
```

This sets the input and output impedance to 50 Ohms at all harmonics.

18.8: POISSON

POISSON allows you to solve Poisson's equation in the Y direction of a FET in a MERCURY simulation. This command is valid only when using the MERCURY module.

Syntax

POISSON <cap simulation> <gate simulation> <look-up table calculation>

| Parameter | Type | Default | Units |
|-------------------|-----------|---------|-------|
| ASCII | Logical | False | |
| BINARY | Logical | False | |
| CAP | Logical | False | |
| COMPRESSED | Logical | False | |
| DE.DX | Real | 0.0 | V/cm2 |
| DEBUG.CAP | Character | | |
| DEBUG.GATE | Character | | |
| E.SURF | Real | 0.0 | V/cm |
| GATE | Logical | False | |
| IN.FILE | Character | | |
| LOOK.UP.TABLE | Logical | False | |
| NUM.RECESS.POINTS | Integer | | |
| OUT.FILE | Character | | |
| QUICK | Logical | False | |
| RECESS | Real | 0.0 | um |
| SAFE | Logical | False | |
| STANDARD | Logical | True | |
| V.GATE | Real | V | |
| V.SUBSTRATE | Real | | V |
| V.TYPICAL | Real | 0.0 | V |
| VD.MAX | Real | 0.0 | V |
| VD.MIN | Real | 0.0 | V |
| VG.MAX | Real | 0.0 | V |
| VG.MIN | Real | 0.0 | V |
| VG.NUM | Real | | |

| | | | |
|------------|------|-----|---|
| VG.START | Real | | V |
| VG.STOP | Real | | V |
| VG.TYPICAL | Real | 0.0 | V |
| VI.MAX | Real | 0.0 | V |
| VI.MIN | Real | 0.0 | V |
| VO.MAX | Real | 0.0 | V |
| VO.MIN | Real | 0.0 | V |

Description

| | |
|--------------------|---|
| ASCII | Saves the data file in a standard, uncompressed format. |
| BINARY | Saves the data file in a binary format. |
| COMPRESSED | Saves the data file in a compressed ASCII format. |
| OUT.FILE | Specifies the name of the output file. |
| V.SUBSTRATE | Specifies the potential on the substrate contact. |

Cap Poisson Solution

| | |
|---------------|--|
| CAP | Defines that Poisson's equation is solved once, over an ungated slice of the device. |
| DE.DX | Specifies the gradient of the X direction electric field. |
| E.SURF | Specifies the Y direction electric field at the surface of the slice. |
| RECESS | Specifies the position of the surface of the slice. |

Gate Poisson Solution

| | |
|---------------|---|
| DE.DX | Specifies the gradient of the X direction electric field. |
| GATE | Defines that Poisson's equation is solved once, over a gated slice of the device. The recess depth is automatically set to the position of the gate specified in the device construction. |
| V.GATE | Specifies the potential on the gate contact. |

Poisson Look-Up Table Calculation

| | |
|--------------------------|--|
| DEBUG.CAP | Specifies a file to save the results of the cap look-up table calculation. This file is suitable for viewing in TONYPLOT but has no other purpose in a device simulation. |
| DEBUG.GATE | Specifies a file to save the results of the gate look-up table calculation. This file is suitable for viewing in TONYPLOT but has no other purpose in a device simulation. |
| IN.FILE | Specifies the file name of a previously calculated Poisson look-up table. If a table cannot be read, then you must calculate it. |
| LOOK.UP.TABLE | Defines that the Poisson look-up table must be calculated. |
| NUM.RECESS.POINTS | Specifies the number of points to use when calculating the cap look-up table. |
| QUICK | Specifies that a sparse look-up table should be calculated (16 points in the cap look-up table and 128 points in the gate look-up table). |
| SAFE | Specifies that a dense look-up table should be calculated (48 points in the cap look-up table and 384 points in the gate look-up table). |
| STANDARD | Specifies that a normal look-up table should be calculated (32 points in the cap look-up table and 256 points in the gate look-up table) |
| V.TYPICAL | Specifies a typical voltage that is used to initialize the Poisson solution. This should be a gate voltage that generates a noticable 2D sheet carrier density. But it doesn't generate too much additional charge at the surface. |
| VD.MAX | Specifies the maximum expected bias on the drain contact. This is used to calculate the range over which to solve the gate look-up table. |
| VD.MIN | Specifies the minimum expected bias on the drain contact. This is used to calculate the range over which to solve the gate look-up table. |
| VG.MAX | Specifies the maximum expected bias on the gate contact. This is used to calculate the range over which to solve the gate look-up table. |
| VG.MIN | Specifies the maximum expected bias on the drain contact. This is used to calculate the range over which to solve the gate look-up table. |
| VG.NUM | Specifies the number of points to use when calculating the gate look-up table. |
| VG.START | Sets the lower value of gate bias to use when calculating the gate look-up table. |
| VG.STOP | Sets the upper value of gate bias to use when calculating the gate look-up table. |
| VG.TYPICAL | This is a synonym for V.TYPICAL. |
| VI.MAX | This is a synonym for VG.MAX. |

| | |
|---------------|-------------------------------|
| VI.MIN | This is a synonym for VG.MIN. |
| VO.MAX | This is a synonym for VD.MAX. |
| VO.MIN | This is a synonym for VD.MIN. |

Examples

```
poisson cap recess=0.0 out.file=cap.str
```

This solves Poisson's equation for an ungated slice with the surface at $y=0$. The results are stored in a file `cap.str`.

```
poisson gate v.gate=0.0 out.file=gate.str
```

This solves Poisson's equation for a gated slice with a bias of $V_g=0$. The results are stored in a file `gate.str`.

```
poisson look.up vg.min=-1.5 vd.max=5.0 out.file=look_up.dat
```

The Poisson look-up table must be calculated before a channel simulation is attempted (basically before a `SOLVE` command). The simulation is going to have gate biases in the range of 0 to -1.5 V and drain biases in the range of 0 to 5 V.

18.9: SURFACE

SURFACE allows you to define the surface topography of a FET in a MERCURY simulation. This command is valid only when using the MERCURY module.

Syntax

```
SURFACE X=<x> Y=<y>
```

| Parameter | Type | Default | Units |
|-----------|------|---------|-------|
| X | Real | 0.0 | um |
| Y | Real | 0.0 | um |

Description

| | |
|----------|--|
| x | Gives the X coordinate of the point being defined. |
| y | Gives the Y coordinate of the point being defined. |

Examples

```
surface x=0.5 y=0.0
surface x=0.6 y=0.1
surface x=1.4 y=0.1
surface x=1.5 y=0.0
```

These commands define a 0.1 um deep recess on the surface of the device. The bottom of the recess is 0.8 um long and centered around x=1 um. The sides of the recess slope at 45°.

This page is intentionally left blank.

19.1: What is MC Device

MC DEVICE is a module for performing full-band Monte Carlo simulation of silicon and strained silicon devices. MC DEVICE is based on MOCA. The MOCA software was developed by the Department of Electrical and Computer Engineering at the University of Illinois at Urbana-Champaign.

MC DEVICE has two operating modes:

- A bulk mode, which is for fitting material parameters to experimental data. This mode provides a unipolar, space-homogeneous transport model that can be used to investigate femtosecond transients, impact-ionization coefficients, doping, field or stress-dependent mobilities, and many other bulk transport properties. This mode is intrinsically unipolar (i.e., only the behavior of electrons or holes can be simulated).
- A 2D mode, which is for performing device MC simulation with regions of different materials, ohmic and blocking contacts, and so on. A non-linear Poisson solver and Schroedinger solver are included. This mode shares the band structure and scattering models with the bulk mode.

Providing the two modes above in a single module has advantages of maintainability and consistency. For example, a scattering mechanism added to the bulk mode is available in the 2D mode. The complication of sharing some models but not other models between modes is tolerable. For example, position-dependent impurity scattering is necessary in the 2D mode because the impurity concentration is not uniform over the device. A different model that considers only one doping level is used for the bulk mode.

19.2: Using MC Device

The MC DEVICE module can be used in all modes of operations of ATLAS (see Section 2.3: “Modes of Operation”). We recommend that you run MC DEVICE in the DECKBUILD’s run-time environment as described in Sections 2.3.1: “Interactive Mode With DeckBuild” through 2.3.4: “Running ATLAS inside Deckbuild”.

The MC DEVICE module can also be used in batch mode without DECKBUILD, although this is not recommended by Silvaco. Running in batch mode without DECKBUILD can be used for reading input files in MOCA input format (see Section 19.3.3: “Migrating From MOCA Input Format”). If you don’t want the overhead of a DeckBuild window, then use DECKBUILD with the no-windows mode (see Section 2.3.3: “No Windows Batch Mode With DeckBuild”). Many important features such as variable substitution, automatic interfacing to process simulation, and parameter extraction are only available inside the DECKBUILD run-time environment.

To use the MC DEVICE module in batch mode without DECKBUILD, use the statement:

```
atlas <input file>
```

<input file> is the name of an input file that contains the simulation parameters. The input file can have any extension. Here, we will use *.in*. The following statement line runs MC DEVICE using the input file *mcdeviceex01.in*:

```
atlas mcdeviceex01.in
```

The file *defaults.in* contains default values for all parameters; the input file overrides those values that need to be changed. For example, the default lattice temperature for the material is 300 K. So you do not need to set the *TEMP* parameter to run a room-temperature simulation. Section 19.3: “Input Language and Syntax” describes the format of the input file. Appendix D: “MC Device Files” gives the complete default configuration file.

At startup, MC DEVICE reads the *defaults.in* file (i.e., `$<S_INSTALL>/lib/atlas/<version>/common/mcdevice/defaults.in`). Next, MC DEVICE reads your input file (i.e., *mcdeviceex01.in*). Simulation parameters defined in your input file override those in the *defaults.in* file. Next, upon processing a *SOLVE* statement, MC DEVICE loads database files (i.e., band structure or scattering rate data or both) from a database directory (i.e., `$<INSTALL>/lib/mcdevice_db/<version>`).

You can modify the file MC DEVICE *defaults.in* file in the directory where this file is installed (namely, `$<S_INSTALL>/lib/atlas/<version>/common/mcdevice`). But, we do not recommend this. Instead, if you need to modify the *defaults.in* file, we recommend that you set the *MCDEVICEDEFDIR* environment variable to a new directory. Copy `$<S_INSTALL>/lib/atlas/<version>/common/mcdevice/defaults.in` to that new directory. Then, make whatever changes you want to the copied *defaults.in* file. If the *MCDEVICEDEFDIR* environment variable is unset, it is automatically set in the start-up ATLAS script to `$<S_INSTALL>/lib/atlas/<version>/common/mcdevice`. On Windows platforms, *MCDEVICEDEFDIR* begins with the driver letter and a colon (i.e., *C:/*).

You can modify the MC DEVICE database files in the directory where they are installed (namely, `$<S_INSTALL>/lib/mcdevice_db/<version>`). But, we do not recommend this. Instead, if you need to modify the database files, we recommend that you set the *MCDEVICEDIR* environment variable to a new directory. Copy `$<S_INSTALL>/lib/mcdevice_db/<version>` to that new directory. Then, make whatever changes you want to the copied database files. If the *MCDEVICEDIR* environment variable is unset, it is automatically set in the start-up ATLAS script to `$<S_INSTALL>/lib/mcdevice_db/<version>`. On Windows platforms, *MCDEVICEDIR* begins with the driver letter and a colon (i.e., *C:/*).

Upon processing `SOLVE` statements, MC DEVICE writes a summary file that reports all the user-definable parameters that have been used for the solve. The name of this file is by default `summary.out`. You can change this name in the input file. See the description of the `OUTPUT` statement in Section 19.3.4: “Commonly-Used Statements”. You can permanently change this name by editing `defaults.in`. Most of the simulation parameters affect the physical models (e.g., optical-phonon energies) and will not be changed often. Others, like the number of iterations or the simulation mode, will be redefined at every run. There are also some numerical parameters that cannot be changed (e.g., \hbar , π , and the unstrained lattice constant of silicon).

19.3: Input Language and Syntax

19.3.1: The Input Language

MC DEVICE reads input files in MC DEVICE input format with data grouped on to statements. Each statement can have parameter settings or no parameter settings.

For example, the BULK statement initializes the bulk simulation parameters and looks like this:

```
BULK FIELD=(100e3,5e3) DOPING=1e17 \  
      CONC=0.0
```

The body of the statement follows its name and is continued by using the backslash (\) at end of each line except the last line of the statement. The body of the statement may be empty or it may contain one or more settings of simulation parameters. For example, the (electric) field, the doping, and the (carrier) concentration are parameters on the BULK statement.

A parameter setting has the form:

```
<parameter>=value
```

The value can be an integer, a floating-point number, a string, or a vector of one of the three simple types. A vector is a list of values separated by commas and enclosed in parentheses. For example, the FIELD parameter on the bulk statement has a list of two floating-point numbers as its value: the first is the value for $\text{TIME} < 0$; the second is the value for $\text{TIME} \geq 0$. In the example input above, we are simulating the sudden reduction of the electric field from 100e3 V/cm to 5e3 V/cm. Normally, you should provide the value in cgs units although lengths are given in um by default (see the UNITS statement in Section 19.5.1: “Device Geometry”).

Note: Field values for $\text{TIME} < 0$ and $\text{TIME} \geq 0$ field may be set equal. In this case, $\text{TIME} < 0$ is used to improve the quality of the initial conditions used at $\text{TIME} = 0$. Output averaging in MC DEVICE is done for $\text{TIME} \geq 0$.

A vector should include values of the same type. MC DEVICE can make conversions between real and integer types. For clarity, we recommend you use values with the same type as the parameter. All example input files and the defaults.in files demonstrate this approach. MC DEVICE stops if you set a parameter using an incompatible type (e.g., a string for a floating-point parameter).

19.3.2: Statement allocation and usage

Memory associated with MC DEVICE statements is either allocated once or is allocated for each occurrence. The allocation behavior of each statement relates to its usage. For example, memory associated with the BULK statement, shown above, is allocated once. This means that if the BULK statement occurs more than once in the input file before a SOLVE statement, then each occurrence of the BULK statement changes parameter settings associated with prior BULK statements beginning with the BULK statement in the defaults.in file. All MC DEVICE statements that appear in the defaults.in file (except for the MATDEF statement) are allocated once. The SOLVE statement is also allocated once, although it does not appear in the defaults.in file.

The MC DEVICE statements associated with mesh, regions, materials, and doping (see Section 19.5.1: “Device Geometry”) are allocated for each occurrence. All statements involving other types of regions (e.g., current regions and Schrödinger regions) are also allocated for each occurrence. The parameters on statements that are allocated for each occurrence are initialized to zero (or null). Therefore, non-zero settings from prior occurrences are not retained. All MC DEVICE statements that are allocated for each occurrence (except the MATDEF) do not appear in the defaults.in file.

19.3.3: Migrating From MOCA Input Format

Although MC DEVICE can read input files in MOCA input format as an aid to users migrating from MOCA to MC DEVICE (e-mail support@silvaco.com for details), Silvaco strongly recommends that MOCA users transform their input files to MC DEVICE input format.

Files in MOCA input format look like this:

```
bulk {
    field = {100e3,5e3};
    doping = 1e17;
    conc =0.0;
}
```

If you compare this bulk statement to the same statement definition (in MC DEVICE input format) in Section 19.3.1: “The Input Language”, you can see the differences. Semicolons terminate parameter assignments rather than white space. Curly braces enclose statement bodies rather than using continuation characters. Curly braces enclose vectors rather than using parentheses.

To transform a file from MOCA input format into MC DEVICE input format, you will need to make the following changes:

1. Add the line “MCDEVICE” as the first uncommented line of the input file.
2. Delete any semicolons.
3. Delete any curly braces that surround the body of a statement.
4. Use a continuation character (\) to continue statements to the next line. Move any comments that were inside a statement to outside of that statement.
5. Replace curly braces that surround parameter vectors with parentheses.
6. Remove any braces that surround the value of the `n` parameter on the `PARTICLE` statement. For example, `particle {n={10000}};` becomes `PARTICLE N=10000`. Do likewise, for any other scalar parameter which unnecessarily used braces surrounding its value. Using array syntax on scalar parameters is allowed in the MOCA input format but is not allowed in the MC DEVICE input format.
7. Replace any MOCA’s `1d` statements with MC DEVICE’s `oned` statements. In MC DEVICE input format, statements names and parameter names may not begin with a number, so the `1d` statement has been changed to `ONED`.
8. Replace any use of the `p` parameter on an `IMPACT` statement with the `PARAM` parameter. Both MC DEVICE input format and MOCA input format have changed from using the `p` parameter to using the `PARAM` parameter to distinguish it from the symbol for phosphorus, `P`.
9. Insert the contents of the `$MCDEVEDIR/“bands2d.hole.in”` file into an input file that uses `carrier=h` (for MC holes) on the `ALGO` statement. (The “bands2d.*.in” files are not used by MC DEVICE, so this input must now reside in your input file.)
10. Insert the contents of the `$MCDEVEDIR/“bands2d.elec.ssi.in”` file into an input file that uses `TYPE=1` (for MC electrons in strained silicon) on the `mmat` statement. (The “bands2d.*.in” files are not used by MC DEVICE, so this input must now reside in your input file.)
11. If you used the `IMPORT` statement, change the `TYPE` and `filename` parameters as needed. (See Section 19.5.8: “Importing Data”.) The default in MC DEVICE is `TYPE=8` for Silvaco structure files.
12. If you have meshing or boundary specifications in centimeters in your input file, add the statement `units length=cm`. By default, MC DEVICE uses `units length=um`. Alternatively, you may want to change values in cm to um by multiplying them by `1e4`.
13. Add a `SOLVE` statement at the end of your input file. The `SOLVE` statement is not required in MOCA input format. In MOCA input format, all explicit `SOLVE` statements are ignored and a single implicit `SOLVE` statement is performed after processing all input. The `SOLVE` statement is required in MC DEVICE input format. In MC DEVICE input format, `SOLVE` statements are processed explicitly at the point at which they appear in the input file.

You can add the `GO ATLAS` and `QUIT` statements to the start and end of your input file. These statements tell `DECKBUILD` to start and stop `ATLAS`. These statements are ignored when you use them outside `DECKBUILD`.

You not required to convert statement and parameter keywords to uppercase when converting an input file in `MOCA` input format to `MC DEVICE` input format. Our convention in the body of this manual is to use uppercase for statement and parameter keywords to make these stand out in the input file. (Our defaults and examples are provided, however, using lowercase keywords.) Our convention is to use lowercase for keywords in `MOCA` input format, since `UIUC MOCA` only supported lowercase keywords. Uppercase, lowercase, and even mixedcase keywords are supported in `MC DEVICE`. In `MC DEVICE`, arbitrarily mixedcase keywords are supported in both the `MC DEVICE` input format and the `MOCA` input format. Abbreviated keywords are supported in exclusively in `MC DEVICE` input format.

19.3.4: Commonly-Used Statements

Many input statements are used to establish `MC DEVICE`'s default configuration and are not commonly used in input files. As mentioned in Section 19.2: "Using MC Device", the default values of most parameters are set in the `defaults.in` file. Any parameters that do not appear in the `defaults` file take the value `0` | `FALSE` | `NO`, `0.0`, or a null string, depending on the type of the parameter.

Note: `MC DEVICE` uses `0`, `FALSE`, and `NO` interchangeably. `MC DEVICE` also uses `1`, `TRUE`, and `YES` interchangeably. As part of `MC DEVICE` input format, `MC DEVICE` also supports the use of bare parameter names (i.e. `ALGO RESTART`) to set a boolean variable to true, and bare parameter names preceded by the negation symbol, `^`, (i.e. `ALGO ^RESTART`) to set a boolean variable to false.

The following is a description of the most commonly used input statements and their parameters. For a more complete list of input statements, see Section 19.3.5: "List of Statements".

The `MCDEVICE` statement below must be included at the start of every `MC DEVICE` input file or interactive input session.

```
MCDEVICE
```

The statement above must be the first non-comment line and indicates that the input that follows pertains to the `MC DEVICE` module.

The `ALGO` statement contains the fundamental Monte Carlo algorithm parameters:

```
ALGO MODE=2 CARRIER=E DT=1e-15 ITER=6000 TRANS=4000 \  
RESTART=YES SEED=65428
```

The `MODE` parameter controls the type of simulation to be run. Set `MODE=0` perform a bulk simulation. Set `MODE=2` to perform a 2D simulation. `CARRIER` is the Monte Carlo carrier type, Set `CARRIER=E` to simulate electrons with an MC transport model. Set `CARRIER=H` to simulate holes with an MC transport model. When `MODE=0` (bulk simulation), only one carrier type is possible and it is set by the `CARRIER` parameter. When `MODE=2` (2D), both carrier types are possible. The carrier type not specified by the carrier parameter will be treated with the constant quasi-Fermi level model (see "Regions" on page 19-17 and Section 19.7.1: "Self-Consistent Simulation"). The `DT` parameter is the time step for the free-flights. The default is 2×10^{-15} s. Use a lower value for high fields (100 kV/cm and up) or for relatively more accurate free-flight calculations. The `ITER` parameter is the number of iteration steps in a simulation and relates to the simulation time as `TIME=ITER*DT`. The `TRANS` parameter is the number of time steps (`DT`) taken as an initial transient. During the initial transient, no estimator averaging and estimator output is performed.

Note: MC DEVICE uses parameters which begin with the letter D (DT, DX, and DE) to denote differential intervals of quantities (here time, space, and energy). Similarly, MC DEVICE uses parameters, which end with the word STEP (TSTEP, XSTEP, and ESTEP) to denote integer multiples of the corresponding differential intervals. For example, TSTEP is an integer parameter, DT is a floating-point parameter (in seconds), TSTEP denotes an integer multiple of DT, and a time of TSTEP*DT seconds.

If RESTART is 0, as it is by default, a new simulation will be started. Otherwise, the carrier states (positions and momenta) are read from the "status.in" file.

SEED is the initial seed for the random-number generator. Since the outcome of the MC simulation depends on a sequence of random numbers, you can use the variable SEED to perform different simulations of the same physical system.

```
PARTICLE N=20000 NNORM=10000 CONC=0 DZ=-1.0
```

The PARTICLE statement defines parameters for the particle (electron or hole) ensemble. N is the maximum number of particles. If NNORM>0, then NNORM sets the number of particles to use at the beginning of the simulation to normalize the charge. NNORM must be less than or equal to N. If NNORM=0 (as it is by default), then NNORM=N is assumed.

If the device width, DZ, is greater than 0.0, then DZ is the device width in cm. If CONC>Ntot, where Ntot is the internally-calculated initial integrated particle concentration (cm^{-1}) and where CONC is a user-specified initial integrated particle concentration (cm^{-1}), then the device width is NNORM/CONC. (Ntot and CONC have the units cm^{-1} since they are volumetric concentrations integrated over x and y .) If neither of the two previous conditions are true, then the device width is determined as $N/1.5/N_{\text{tot}}$. If NNORM, CONC, and DZ are left at their default values of 0, 0.0, and -1.0 respectively, then the choice above for the device width means that the initial particle number is $(2/3)*N$. This is normally the case. The fraction of 2/3 represents the fraction of initially-used particle memory compared to allocated particle memory. This choice allows the particle number to vary during the simulation.

Note: For the mcdeviceex02.in example (Section D.3.2: "A 25-nm n-MOSFET: mcdeviceex02"), the device width and initial particle number are determined as they normally are where NNORM, CONC, and DZ are left at their default values of 0. In this example, the device width is $N/1.5/N_{\text{tot}}=40,000/1.5/(1.76182\text{E}+09 \text{ cm}^{-1})=1.51359\text{E}-05 \text{ cm}$ and the initial particle number is $(2/3)*N=(2/3)(40,000)=26,666$.

You can use CONC to set a total charge in the device. This is useful for strong-inversion devices, where you need to help MC DEVICE establish the amount of stored charge in the device. This may be necessary because the transient time of the charging is much longer than can realistically be simulated with MC DEVICE.

```
MAT TEMP=77.0 CUT=(1.0,0.0,0.0)
```

This MAT statement defines material parameters (i.e., temperature and wafer cut or crystal orientation). TEMP is the lattice temperature in Kelvin. CUT is a triplet of real numbers that give the orientation of k -space with respect to real space. When properly normalized, they are the direction cosines of the X in the (k_x, k_y, k_z) space. For example, 1.0, 1.0, 0.0 means that the X -axis of real space (i.e., the direction of the electric field) is in the (110) direction of the crystal.

```
OUTPUT SUMMARYOUTFILE="summary.out" DIFFLOGFILE="diff.log" \
CURRENTLOGFILE="current.log" SOLSTRFILE="sol.str" SCATOUTFILE="scat.out" \
TSTEP=100 XSTEP=(1,1,1) ESTEP=50 RESTART=500 \
WPSTEP=PINF INIT=NO HYDRO=NO HIST=YES QETA=NO OUTFILES=NO
```

The `OUTPUT` statement has parameter settings associated with output. The `SUMMARYOUTFILE` parameter sets the name of a file written for each `SOLVE` statement, which holds the input related to each solve statement. If you don't change the value of `SUMMARYOUTFILE` from its default value of `summary.out`, then after your simulation is complete, `summary.out` will hold the input used for your last solve statement. The `DIFFLOGFILE` parameter sets the name of the file used to hold time-averaged quantities for a bulk simulation (see `diff.log` in Appendix D.2.1: "Silvaco Output Files"). The `CURRENTLOGFILE` parameter sets the name of the file used to hold currents for a 2D simulation (see `current.log` in Appendix D.2.1: "Silvaco Output Files"). The `SOLSTRFILE` parameter sets name of the file used to hold the time-averaged and instantaneous quantities related to a 2D solution (see `sol.str` in Appendix D.2.1: "Silvaco Output Files").

The `SCATOUTFILE` parameter sets the name of the file used to hold the scattering rates that were calculated and used during your simulation (see `scat.out` in Appendix D.2.4: "Scattering Output Files").

Note: The aliases `SUMMARYFILE` (for `SUMMARYOUTFILE`) and `SCATFILE` (for `SCATOUTFILE`) have been provided on the `OUTPUT` statement for backward compatibility with MOCA.

The `TSTEP` parameter is the number of time steps (`DT` on the `ALGO` statement) between output of observables (or estimators). The `XSTEP` parameter is the size of spatial bins (`DX`, `DY`, `DZ`) in units of mesh cells used for output. The `ESTEP` parameter is the size of energy bins in meV used for output. The `RESTART` parameter is the number of time steps between dumps of the particle status to the `restart.out` file. The `WPSTEP` parameter is the number of time steps between successive writes of the instantaneous electric potential (voltage) and the instantaneous MC carrier concentration. The `init` parameter indicates MC DEVICE will write out the initial electrostatic potential (voltage) and initial MC carrier concentration at 5 points during the initialization process. The `HYDRO` parameter indicates MC DEVICE should write out 2D estimators for hydrodynamic parameter extraction. The `HIST` parameter indicates that MC DEVICE should write the energy histograms. The `QETA` parameter indicates that MC DEVICE should write the quantum potential.

Note: The `OUTFILES` parameter on the `OUTPUT` statement is an important control variable in MC DEVICE. The `OUTFILES` parameter enables/disables the writing of almost all `*.out` files generated by MC DEVICE. By default, the `outfiles` parameter is set to `0 | FALSE | NO` so that `*.out` files are not written. (The `summaryfile` is treated as an exception and is always created.) Setting `OUTFILES=FALSE` results in no `*.out` files in the directory where the test is run and makes it easy to see the output files that can be used with other Silvaco tools, especially `TONYPLOT`. To enable the generation of all `*.out` files, set the `OUTFILES` parameter to `1 | TRUE | YES`. If other boolean parameters are specifically associated with a `*.out` file (like the `init` parameter above), then you must also set this parameter to `1 | TRUE | YES` if it is not true by default.

`DEBUG NPICK=0`

The `DEBUG` statement defines debugging parameters like a particle to track and holds the output parameter, which controls the generation of virtually all non-Silvaco-standard file formats.

If `NPICK>0`, MC DEVICE tracks the corresponding particle index, dumping debugging data to various files. If `NPICK<0`, a large amount of debugging data is stored for the entire simulation (enough to fill up a 1 GB disk in a few hours). Also when `NPICK≠0`, many internal self-consistency checks are performed to catch bugs. The status of subroutine calls are then printed out at the console for each iteration.

`SOLVE`

If the `SOLVE` statement includes no parameters settings, it indicates that an MC solve should be performed for the biases specified by the input that precedes it (see "Biasing" on page 19-21).

`SOLVE VGATE=1.0 VDRAIN=1.0`

The SOLVE statement can also include one or more parameter settings of the form: `V<NAME>=#`. For these settings, # is the applied voltage in V. <NAME> must be from the list: GATE, GG, DRAIN, DD, SOURCE, BULK, SUBSTRATE, EMITTER, EE, COLLECTOR, CC, BASE, BB, ANODE, CATHODE, FGATE, CGATE, NGATE, PGATE, WELL, NWELL, PWELL, CHANNEL, and GROUND. Multiple SOLVE statements may be used in an input file. The `V<NAME>` settings are preserved from one SOLVE statement to the next. The `V<NAME>` settings are updated after the ramping SOLVE (see example below) so that they can be used in subsequent solves. The `V<NAME>` parameters default to 0 on the first SOLVE, so you only have to set non-zero biases. You can generate all output files when MC DEVICE processes the SOLVE statement. To retain output files from one SOLVE after executing a second SOLVE, change the output files using an OUTPUT statement between the SOLVE statements.

```
SOLVE NAME="drain" VSTEP=1.0 VFINAL=2.0
```

If you set `VSTEP!=0` or `NSTEPS>0` on the SOLVE statement, then MC DEVICE performs a voltage ramp in 2D simulations. The voltage ramp is done on the contact specified by the NAME parameter. The voltage ramp completes after solving at a voltage of VFINAL. When `USELOG=0|false|no` (as it is by default), MC DEVICE will use VSTEP for uniform spacing on a linear scale. When `USELOG=1|true|yes`, MC DEVICE will use VSTEP for uniform spacing on a logarithmic scale. The USELOG parameter defaults to 0 on each SOLVE statement. Transient solves are performed for each bias condition beginning with those specified on the same or prior SOLVE statements.

The `*current.log` and `*sol.str` files produced during each voltage ramp step are saved by inserting the contact voltage after the base file name. For example, if the voltage on the drain were 1.0 V prior to the solve above, then `current_vdrain=1.log` will pertain to the first ramp step. In this case, only one step is performed. The currents after this voltage step are saved in `current_vdrain=2.log`. Correspondingly, for this example, the solution structure files are saved as `sol_vdrain=1.str` and `sol_vdrain=2.str`. The NAME parameter must match a contact name as specified by the NAME parameter on a REGION statement (with `TYPE=CONTACT`). After the ramping SOLVE is complete, the corresponding `V<GATE>` parameter is automatically set to VFINAL so that this value will be used in subsequent solves. The VSTEP and VFINAL parameters are in V. The values of the voltage included in the filenames are also in V. The VSTEP, VFINAL, NAME, and NSTEPS parameters default to 0 or null on each SOLVE statement.

Note: MC DEVICE checks that VSTEP takes the voltage evenly to VFINAL. It stops with an error if it does not. Please choose VSTEP and VFINAL consistently or use NSTEPS instead of VFINAL or VSTEP.

The results in `*current.log` pertaining to the last simulation time for each voltage in the ramp are saved into the `*current_ramp.log` file. To specify the file name, use `CURRENTRAMPLOGFILE` parameter on the OUTPUT statement. Since this file contains both the voltage at the contact and the currents, you may use it to plot a current-voltage (I-V) curve.

```
SOLVE NSTEPS=3 VFINAL=1e6 USELOG=yes
```

If you set `FSTEP!=0` or `NSTEPS>0` on the SOLVE statement, then MC DEVICE performs an electric field ramp in bulk simulations. The field ramp completes after solving with the field at FFINAL. When `USELOG=0|false|no` (as it is by default), MC DEVICE will use FSTEP for uniform spacing on a linear scale. When `USELOG=1|true|yes`, MC DEVICE will use FSTEP for uniform spacing on a logarithmic scale. The USELOG parameter defaults to 0 on each SOLVE statement. Transient solves are performed for each ramp step beginning with those specified by the FIELD parameter on the BULK statements (see Section 19.5.1: “Device Geometry”). To simplify solves during field ramping, FSTEP is added to both components of the FIELD vector (namely both the value for `time<0` and the value for `time>=0`). If you want to control each component of the FIELD parameter on the BULK statement separately, perform the ramp steps as a sequence of separate solves by setting the FIELD parameter on the ALGO statement as desired. Then, change the DIFFLOG file parameter on the OUTPUT statement between the SOLVE statements.

Note: MC DEVICE checks that FSTEP takes the field evenly to FFINAL. It stops with an error if it does not. Please choose FSTEP and FFINAL consistently or use NSTEPS instead of FFINAL or FSTEP.

The results in *diff.log files produced during each field ramp step are saved by inserting the field after the base file name. For example, if the field were 1000 V/cm prior to the solve above, then diff_field=1000.log will pertain to the first ramp step. In this case, then only two more iterations are performed at 1e4 V/cm and 1e5 V/cm. The results for these iterations are saved in diff_field=1e4.log and diff_field=1e5.log respectively. The FSTEP and FFINAL parameters are fields in V/cm. The values of the fields included in the filenames are also in V/cm. The FSTEP, FFINAL, and NSTEPS parameters default to 0 on each SOLVE statement.

The results in the *diff.log file pertaining to the last simulation time for each field ramp step will be saved into the the *diff_ramp.log file. To specify the file name, use the DIFFRAMPLOGFILE parameter on the OUTPUT statement. Since this file contains both the field and the bulk results (like mobilities), you may use this file to plot a mobility-field curve.

When you use the drift diffusion transport model to obtain the solution for a particular DC bias point, it is reasonable to think that you get the same solution for the same bias conditions even when the DC bias points that precede the final point differ. This is normally not true (because normally each solution uses the prior solution as an initial conditions), but the solutions are close enough to each other that you can think of them as being the same.

When you use the Monte Carlo transport model (MC DEVICE), small variations in the initial conditions can have a relatively larger effect on the solutions than they do for the drift diffusion model. To keep this behavior similar to what you are accustomed to with drift diffusion, we have implemented the SOLVE statement in MC DEVICE to exactly reproduce the results (on a particular hardware platform) whenever the bias conditions are exactly the same regardless what the preceding bias point was. For example, this means that the solution you obtain as the last step of a ramp will be identical to the solution you obtain by a single solve for the final condition of the ramp. This means that you can add solution points to your results without re-running the entire ramp. The results you obtain for the additional single solves are identical to those you would obtain by re-running the entire ramp.

The QUIT statement stops execution at the point in the input where the QUIT statement appears. All input lines after the QUIT statement are ignored. The QUIT statement should be the last statement in your input file. The QUIT statement must be included when you run DECKBUILD in batch mode and use DECKBUILD's outfile command-line option. Otherwise, your output file will finish with an ATLAS> prompt and the END-OF-RUN message of MC DEVICE will be omitted.

19.3.5: List of Statements

| Table 19-1. Lists of Statements | |
|---------------------------------|---|
| Statement | Description |
| AC | Acoustic phonon scattering. See Section 19.7.5: “Phonon Scattering”. |
| ALGO | Simulation mode parameters. See Section 19.3: “Input Language and Syntax”. |
| BANDS | Band structure information. See Section 19.7.2: “Band Structure”. |
| BIPOLAR | Pipe for interprocess communication. See Section 19.5.5: “Bipolar”. |
| BULK | Bulk simulation parameters. See Section 19.4: “Bulk Simulation”. |
| CREGION | Current estimation region. See Section 19.5.3: “Estimators”. |
| CROSSEST | Boundary crossing estimators. See Section 19.5.6: “Track Boundary Crossings”. |
| DEBUG | Toggle debugging on/off. See Section 19.3: “Input Language and Syntax”. |
| DEVICE | Device applied voltages. See Section 19.5.1: “Device Geometry”. |
| DOPING | Doping profile definition. See Section 19.5.1: “Device Geometry”. |
| DTREGION | Fine time-step region. See Section 19.5.7: “Time Step Regions”. |
| EBREGION | Eta barrier region definition. See Section 19.7.8: “Size Quantization”. |
| EEREGION | Energy estimator region definition. See “Energy Regions” on page 19-25. |
| ENHAN | Statistical enhancement. See Section 19.6: “Statistical Enhancement”. |
| EREGION | Statistical enhancement region. See Section 19.6: “Statistical Enhancement”. |
| ESTIM1D | 1D averaging. See Section 19.6.6: “Statistical Enhancement Statements”. |
| FIELD | Initial field definition. See “Biasing” on page 19-21. |
| FFREGION | Fixed-field region definition. See Section 19.5.4: “Initial Conditions”. |
| FINAL | Final state selection. See Section 19.7.4: “Coulomb Interaction”. |
| GO | DECKBUILD control. See Section 19.3.3: “Migrating From MOCA Input Format”. |
| ICLREGION | Initial concentration limit region. See Section 19.5.4: “Initial Conditions”. |
| IMPACT | Impact ionization parameters. See Section 19.7.6: “Impurity Scattering”. |
| IMPORT | Import initial guess. See Section 19.5.8: “Importing Data”. |
| INJECT | 2D injection parameters. See Section 19.5.2: “Ohmic Contacts”. |
| LINBIAS | Additional linear biasing. See “Biasing” on page 19-21. |
| MAT | Material parameters. See Section 19.3: “Input Language and Syntax”. |
| MATDEF | Material definition. See Section 19.5.1: “Device Geometry”. |
| MCDEVICE | Module specification. See Section 19.3.4: “Commonly-Used Statements”. |
| OUTPUT | File outputs. See Section 19.3: “Input Language and Syntax”. |

Table 19-1. Lists of Statements

| Statement | Description |
|--------------------|---|
| PARTICLE | Number of particles. See Section 19.3: “Input Language and Syntax”. |
| PHON | High-energy phonon scattering. See Section 19.7.5: “Phonon Scattering”. |
| POISSON | Poisson solver parameters. See Section 19.7.1: “Self-Consistent Simulation”. |
| QREGION | Quantum region definition. See Section 19.7.8: “Size Quantization”. |
| QUANTUM | Quantum correction parameters. See Section 19.7.8: “Size Quantization”. |
| QUIT | Stop execution. Section 19.3.4: “Commonly-Used Statements”. |
| QSS | Surface charge parameters. See Section 19.5.4: “Initial Conditions”. |
| REFLECT | Properties for reflection. See Section 19.5.2: “Ohmic Contacts”. |
| REGION | Region definition. See Section 19.5.1: “Device Geometry”. |
| RESIST | Contact resistance information. See Section 19.5.2: “Ohmic Contacts”. |
| RIDLEY | Ridley model for impurity scattering. See Section 19.7.6: “Impurity Scattering”. |
| SCHRMESH | Schrödinger solver mesh definition. See Section 19.7.8: “Size Quantization”. |
| SCHRRREGION | Schrödinger region definition. See Section 19.7.8: “Size Quantization”. |
| SEREGION | Scattering estimation region. See Section 19.7.4: “Coulomb Interaction”. |
| SMREGION | Smoothing region definition. See Section 19.6: “Statistical Enhancement”. |
| SOLVE | Perform MC solve. See Section 19.3.4: “Commonly-Used Statements”. |
| SSPARAM | Surface scattering parameters. See Section 19.7.6: “Impurity Scattering”. |
| SSREGION | Surface scattering region. See Section 19.7.6: “Impurity Scattering”. |
| TRACKSCAT | Track scattering region definition. See Section 19.7.6: “Impurity Scattering”. |
| TRAJ | Track particle trajectories. See Section 19.7.6: “Impurity Scattering”. |
| TTEMP | Transverse temperature calculation region. See Section 19.7.8: “Size Quantization”. |
| TUNEL | Gate tunneling current calculator. See Section 19.7.7: “Tunneling”. |
| UNITS | Set units used in other statements. See Section 19.5.1: “Device Geometry”. |
| XL | X-L phonon scattering. See Section 19.7.5: “Phonon Scattering”. |
| XMESH | X-mesh definition. See Section 19.5.1: “Device Geometry”. |
| XXF | X-X f-type phonon scattering. See Section 19.7.5: “Phonon Scattering”. |
| XXG | X-X g-type phonon scattering. See Section 19.7.5: “Phonon Scattering”. |
| YMESH | Y-mesh definition. See Section 19.5.1: “Device Geometry”. |
| ZSREGION | Zero-scattering region definition. See Section 19.7.6: “Impurity Scattering”. |

19.3.6: Accessing The Examples

MC DEVICE is supplied with standard examples that demonstrate the tool. We recommended that new users study the examples and use them as a starting point for creating their own simulations. Please learn how to access, load, plot, and run these examples by following the procedure below.

The examples are accessed from the menu system in DECKBUILD.

1. Start DECKBUILD with ATLAS as the simulator as described in Section 19.2: “Using MC Device”.
2. Click the **MainControl** button to open this pull-down menu.
3. Click **Examples...** button to open the DECKBUILD: Examples window (see Figure 19-1).

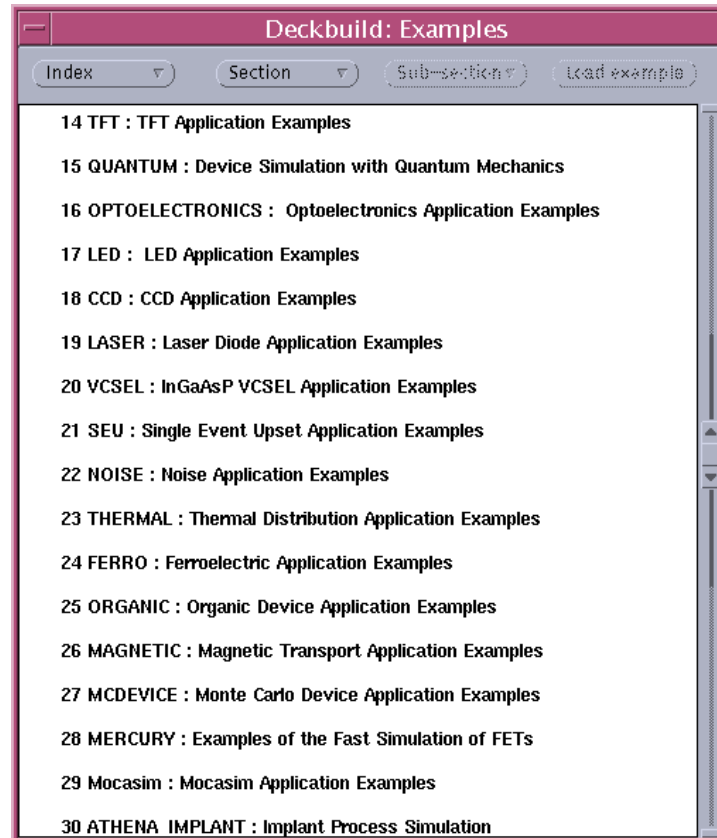


Figure 19-1: DeckBuild: Examples Window

4. Scroll down to show **MCDEVICE: Monte Carlo Appliation Examples** by clicking on the bottom arrow of the slider at the right of the window.
5. Choose MC DEVICE by double clicking the MC DEVICE line of the index. A list of examples will appear (see Figure 19-2). These examples illustrate different types of devices or different applications of MC DEVICE.

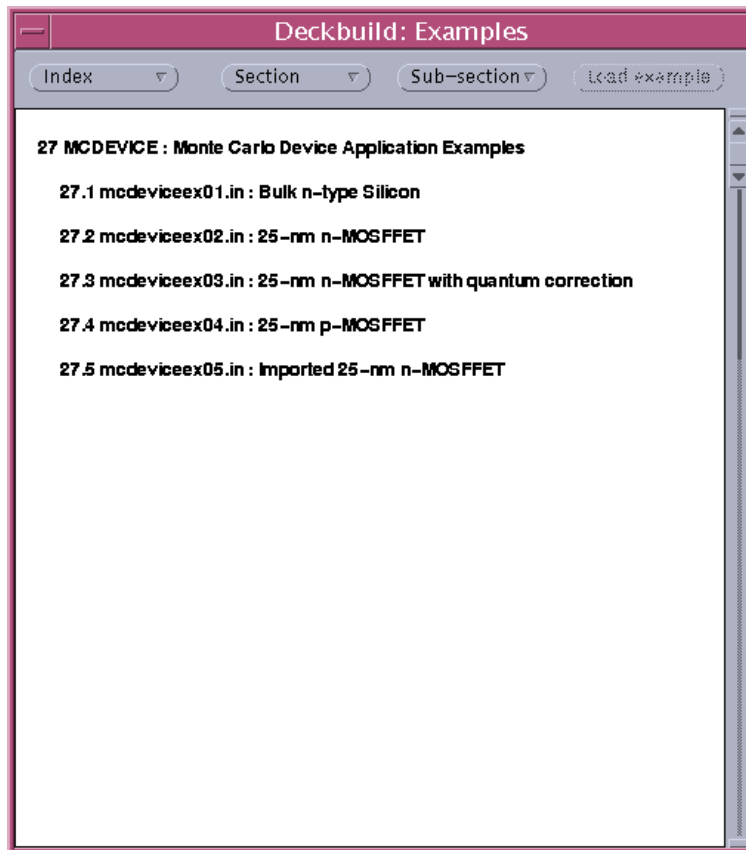


Figure 19-2: MC Device Examples Window

6. Choose each example by double clicking that item in the list. A description of the example will appear in the window. This description gives important details about how to use MC DEVICE. Please read this before proceeding. We recommend that you begin with example 1 and go in order since important concepts and statements are described only in the first example in which they appear.
7. Click on the **Load example** button. All files associated with that example are copied into the current working directory. The input command (*.in) file is loaded into DECKBUILD. The sample output (*_diff.log or *_current.log and *_sol.str) files produced on x86-64-linux are copied to the working directory. TONYPLOT set (*.set) files associated with each output file are also copied into the local working directory. DECKBUILD will overwrite existing files with fresh copies when you click the **load** button and click to confirm.
8. Look over the input file in DECKBUILD. One or more `tonyplot` statements are included near the end of the file to plot some of the simulation results. You may view the sample results without running the example. To do this, highlighting the first `tonyplot` statement and click the **line** button to have DECKBUILD to prepare to start at this line. Then, click the **next** button to execute the next line or click the **cont** button to continue with all remaining lines (to generate all the plots).
9. To run the entire example, click on the **run** button. The examples will finish by generating the plots in Tonyplot. Each `tonyplot` statement near the end of the input file will produce a separate TONYPLOT window.

19.4: Bulk Simulation

Bulk simulation parameters are specified on the BULK statement.

```
BULK FIELD=(10e3,200e3) DOPING=1e18 CONC=4e17 MEMORY=NO MMFRAC=0.0
```

As mentioned in Section 19.3.1: “The Input Language”, the FIELD parameter sets the values of the electric field for $\text{TIME} < 0$ and $\text{TIME} \geq 0$ in V/cm. Splitting the simulation into two parts serves two purposes. First, waiting for a transient time before computing time averages. Second, allowing the time-dependent study of carrier dynamics on the femtosecond or picosecond scale. The first case obviously applies only when the electric field before and after $\text{TIME} = 0$ is the same. The second case applies when the field changes abruptly.

The DOPING parameter is the background doping level in cm^{-3} .

The CONC parameter allows you to specify the carrier concentration. This is relevant for a bulk simulation since it affects the screening of impurities and the scattering of carrier with ionized-impurities.

If you set the MEMORY parameter to 1 | TRUE | YES, the status of the carrier ensemble will be maintained during the simulation. The energy and other quantities associated with MC carriers are recorded at time steps determined by the step field of the OUTPUT statement. This slows down MC DEVICE but allows the time-dependent study of the microscopic histories of the particles. The file memory.out is printed out at the end of the run with statistics on impact ionization events.

For modeling the bulk behavior of strained silicon, the MMFRAC parameter sets the effective strain level in the bulk from 0.0 to 1.0. When modeling the bulk behavior of strained silicon layers on a relaxed $\text{Si}_{1-x}\text{Ge}_x$ substrate, MMFRAC refers to x , the fraction of Germanium in the substrate. When modeling the bulk behavior of strain silicon on a silicon substrate, MMFRAC refers to an effective strain which can vary from 0.0 (unstrained) to 1.0 (max strain of the fitting). For a full description of the strain model in MC DEVICE, see Section 19.7.13: “Strain”.

19.5: Device Simulation

19.5.1: Device Geometry

Grid

MC DEVICE solves the device equations on a rectangular non-uniform grid. Grid points are conventionally labeled by a pair of integers ranging from 1 to N_i , where $i=x,y$. The rectangular grid comprises $(N_x+1)(N_y+1)$ nodes and N_xN_y rectangular domains, or mesh cells. Cell (i,j) is bounded by the rectangle whose two opposite vertices are (i,j) and $(i+1,j+1)$.

The grid is specified using XMESH and YMESH statements in the input file in a manner similar to that used in ATLAS. Each statement gives the coordinate of a node in the sequence of X or Y -coordinates. Node positions in between specified nodes are interpolated by geometric growth. The specification for a node layer in the X -direction is

XMESH (NODE= n LOC= l RATIO= r)

where NODE, LOC and RATIO are respectively the node index, the X -position, and the growth ratio. The format for the corresponding ymesh is the same.

Here, we will use the following terms:

- Grid lines: The loci $x=X_i$ or $y=Y_j$, where X_i and Y_j are grid coordinates.
- Grid point: The intersection of two grid lines. In other words, a point (X_i, Y_j) .
- Grid segment: The segment joining two adjacent grid points in the X - or Y -direction. For example:

$$(X_i, Y_j) - (X_{i+1}, Y_j) \quad 19-1$$

or

$$(X_i, Y_j) - (X_i, Y_{j+1}) \quad 19-2$$

- Box: The rectangle surrounding a grid point, delimited by the lines bisecting grid segments.
- Mesh cell: The rectangle delimited by two pairs of adjacent grid lines. One pair in the X -direction and the other pair in the Y -direction.

The units of the values specified by the LOC parameter on the XMESH and YMESH statements are determined by the LENGTH parameter on the UNITS statement. The LENGTH parameter is set to UM for micrometers by default. You can change to LENGTH=CM for centimeters for backward compatibility with UIUC MOCA. The LENGTH parameter on the UNITS statement also defines the length units for all positional bound parameters (including all BOUNDP parameters) and the CHAR parameter on the DOPING statement.

Regions

A region is a rectangular area whose boundaries lie on mesh points. A region is geometrically defined by four integer numbers specifying the discrete indices of the first and last mesh nodes in the X- and Y-directions. (For your convenience, we recommend you define the boundaries using minimum and maximum positions along the X and Y axes, see the `BOUNDP` parameter on the `REGION` statement described below.) Regions are identified by number using the `N` parameter on the `REGION` statement. The `N` parameter should be set to a positive integer starting with 1. We recommend you additionally give each region a name which identifies its function in your device, see the `NAME` parameter on the `REGION` statement described below.

A region is assigned a material. Silicon (`SI`), polysilicon (`POLY`), silicon dioxide (`SIO2`), silicon nitride (`SI3N4`), aluminum (`AL`), gold (`AU`), platinum (`PT`), tungsten (`W`), and air (`AIR`) are supported.

The behavior of each region is specified by its type. Possible types are `MC`, `CONTACT`, `BLOCK`, and `OUT`. A `MC` region is assigned particles and its time-dependent behavior is determined during a solve. A `CONTACT` region is assumed to behave like a sample of the specified material at thermal equilibrium. It also functions as a boundary condition for other regions forcing a constant quasi-Fermi level during unipolar solves and a space-dependent electric potential. For example, if a silicon `MC` region neighbors a `CONTACT`, the equilibrium carrier concentration is computed for each point along the region boundary based on the doping concentration. Particles are then injected into `MC` regions to maintain that concentration. Also, spatially dependent boundary conditions for the Poisson equation are used, where the boundary conditions depends on the variations of the quasi-Fermi level. For a non-semiconducting material, such as SiO_2 or aluminum, the boundary concentration is computed from the known barrier height with respect to a `MC` region material and the uniform boundary condition for the electrostatic potential. Finally, regions of type `BLOCK` and `OUT` are insulator regions. These enters the simulation as part of the Poisson solve. The simulation depends on the dielectric constant of these regions as well as their size and location.

The definition of a device proceeds by successive definitions of regions, each overriding previous definitions. For example, to create a mesh structure, define a rectangular silicon region and then etching out two regions at the sides by defining additional regions. This will effectively define a T-shaped `MC` region. Insulator regions can be of two types: `BLOCK` and `OUT`. `BLOCK` and `OUT` regions are distinguished in order to simplify the handling of `MC` carrier reflections. `BLOCK` regions reflect particles towards the outside of their rectangular boundaries. `OUT` regions do not reflect particles. Instead, `OUT` regions are used to define insulating regions with boundaries defined implicitly by the boundaries of other regions. Usually, a large `OUT` region is defined as a global container for the entire device and regions that define the device structure are defined inside it. This allows complicated insulator shapes to be defined as multiple insulating `BLOCK` regions. At the same time, reflection of particles is ensured by the boundaries of the remaining regions. `BLOCK` regions are used in turn to make insulating parts out of the `MC` and contact regions. This scheme allows an arbitrary device structure without requiring the CPU-intensive algorithm of reflecting carriers along non-rectangular boundaries. Figure 19-3 shows an example.

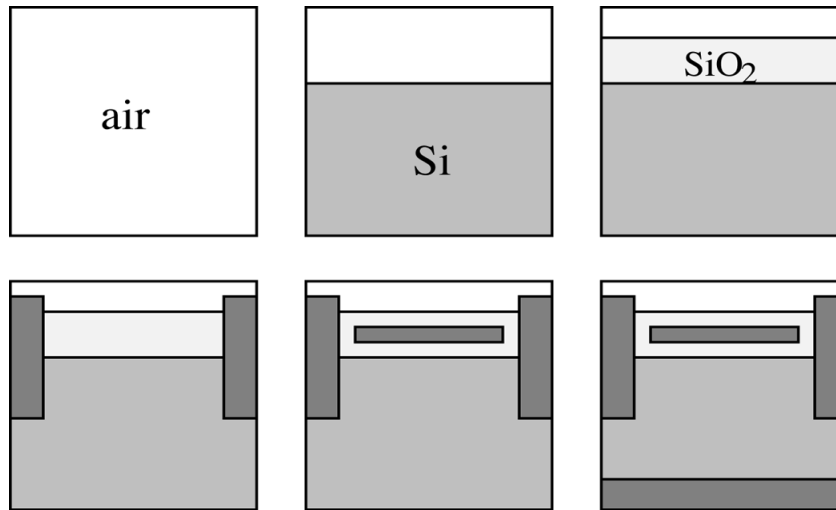


Figure 19-3: Example of device structure definition for a simple MOSFET. The successive steps define the simulation region (out), silicon substrate (MC), oxide (block), source/drain contacts (contact), gate (contact), and substrate contact (contact), respectively.

All combinations of material and type are allowed in principle, even though they may be unphysical (e.g., an aluminum insulator region). MC DEVICE will complain about combinations for which it has no knowledge (e.g., a Si_3N_4 MC region). Otherwise, the material is independent of the way the region is simulated. For example, you can simulate a silicon region with the Monte Carlo method or treat it as a contact. Thus, assuming assigned potential and concentration along its edges. Similarly, you can directly simulate a polysilicon region using MC. It can also simply be a boundary condition for Poisson's equation.

You must apply a bias voltage to each contact region. MC DEVICE does not allow you to have “floating shorts” in the device, which equalize potential along the edges without being connected to a voltage source. Also, non-MC, non-fixed charges in MC regions will be modeled assuming an uniform quasi-Fermi level propagating from the nearest contact region. The propagation algorithm is explained in Section 19.7.1: “Self-Consistent Simulation”.

A region is specified by a REGION statement:

```
REGION N=n NAME="Region Name" MAT=AIR|SI|POLY|SIO2|SIN4|AL|PT|W|AU \
      TYPE=MC|CONTACT|BLOCK|OUT BOUNDP=(x1,x2,y1,y2) VBIAS=1.0 \
      USEFERMI=NO FERMI=0.0
```

N is an integer (≥ 1) and represents the region number.

NAME is the name of the region. You can see the name of regions in TONYPLOT by selecting **Color by: Region** in the Tonyplot: Regions window. When using the IMPORT statement to import regions from a structure file, you can set the NAME parameter to the name of an imported region to redefine properties of that region. For example, you may need to specify a different spatial boundary for a contact region using the BOUNDP parameter. When using the import statement to import regions from a structure file, if the name of a contact region does not match a contact region in the import structure file, then a new contact region will be added to the imported structure. In the last case, the region number, N, is automatically set as the highest region number in the device (at the time that region is processed).

MAT is the material type. The appropriate electrical and transport parameters are taken from a library of materials provided in the defaults.in file. TYPE is the region type.

BOUNDP provides the positions of the rectangular region bounds using units specified by the LENGTH parameter on the UNITS statement (see Section 19.5.1: “Device Geometry”). $x1$ is the minimum position along x . $x2$ is the maximum position along x . $y1$ is the minimum position along y . $y2$ is the maximum position along y . The BOUND=($ix1\ ix2\ iy1\ iy2$) (not shown above) provides the rectangular region bounds in terms of integral mesh indices rather than positions.

The BOUND parameter is provided for backward compatibility with MOCA. We recommend using BOUNDP rather than BOUND since it enables you to change the mesh with little effect on your device geometry. BOUNDP is also more convenient to use when you import the device structure or mesh or both. See Section 19.5.8: “Importing Data” on using the IMPORT statement. If BOUND=(0 0 0 0) as it is by default, then BOUNDP is used.

VBIAS enables you to set the applied bias voltage on regions with TYPE=CONTACT. If the bias on a contact is set to a non-zero value using the VBIAS parameter on the REGION statement, then it will not be set by the VBIAS parameter on the DEVICE statement. But if the VBIAS parameter on the REGION statement is left at its default value of zero, then the VBIAS parameter on the REGION statement will be used to set the applied bias at the contact (see “Biasing” on page 19-21). When you are importing regions from a structure file, you must use the VBIAS parameter on the REGION statement rather than the VBIAS parameter on the DEVICE statement. Since the VBIAS parameter on the REGION statement can be used in all cases (including when you are importing regions), it is recommended over the VBIAS parameter on the DEVICE statement.

The USEFERMI and FERMI parameters enable you to obtain improved results for quantities related to the non-MC quasi-Fermi potential and a small correction to the terminal currents. By default, USEFERMI=0. As a result, the non-MC quasi-Fermi potential is set using the default method to the voltage applied at the contact within the doping well associated with the contact. If you set USEFERMI=1 on a REGION statement with TYPE=CONTACT, then MC DEVICE will set the non-MC quasi-Fermi potential (V_n or V_p in Section 19.7.1: “Self-Consistent Simulation” for CARRIER=H and CARRIER=E on the ALGO statement, respectively) using the FERMI parameter within the doping well associated with that contact.

For example, let’s consider the common case of simulating an n -MOSFET using CARRIER=E on the ALGO statement, a positive voltage on the drain, 0.0 V on the source, and a gate high voltage enough to create an inversion layer. In this common case, you can use USEFERMI=1 on the REGION statement associated with the drain contact to obtain an improved estimate for the hole quasi-Fermi potential in the drain’s doping well (see examples of the USEFERMI=1 setting in the standard examples). USEFERMI=1 means that the hole quasi-Fermi potential within the drain’s doping well will be set using the FERMI parameter (which is 0.0 V by default). Since we’ve assumed in this example that the source voltage is 0.0 V, the default of FERMI=0.0 correctly sets the hole quasi-Fermi level within the drain doping well to the applied bias at the source (0.0 V). You can then omit the setting FERMI=0.0 from your input since it matches the default setting. Since equilibrium is assumed within each contact region, the electron and hole quasi-Fermi potentials are always equal to each other and equal to the voltage applied within a particular contact region. Therefore, the USEFERMI and FERMI parameter have no effect within contact regions themselves. In this example, the USEFERMI and FERMI parameters provide improved estimates for the hole quasi-Fermi level and the hole concentration within the drain’s doping well (neighboring the drain contact) and a small correction to the terminal currents.

Materials

The materials in listed in the description of the `mat` parameter on the region statement are predefined. You can override their default values and, thereby, create new materials using `MATDEF` statements. For example:

```
MATDEF N=n NAME="Material Name" EPS=e_r BARRIER=phi_B ROUGH=r
```

The barrier height is defined with respect to n-type silicon. It is used for determining the boundary conditions for the potential for a given applied bias. The `ROUGH` parameter specifies the probability of diffuse scattering due to surface roughness.

Note: Any parameters not explicitly listed in a `MATDEF` section will be set to 0 | 0.0 | null. You cannot split settings for one material onto two separate statements (although, normally, this can be done). Instead, only the last statement for that material type in the input file is considered and all non-null settings must appear on that statement.

Doping

You can assign any part of the device a doping concentration and profile. Though, the simulator will complain if you try to dope a material, such as Aluminum. By default, there is no doping define for any material. Doping is assigned using the `DOPING` statement as follows:

```
DOPING DOPANT=B CONC=1e19 \  
      BOUNDP=(0.0,0.095,0.0019,0.002) \  
      CHAR=(0.0172,0.0172,0.016,0.016)
```

The `DOPANT` parameter can be either B (Boron), P (Phosphorus), In (Indium), or As (Arsenic). The `CONC` is concentration in atoms/cm³ for the box defined by `BOUNDP` parameter. The `BOUNDP` parameter defines the coordinates of the box for the `DOPING` statement in units specified by the `LENGTH` parameter on the `UNITS` statement (see “Grid” on page 19-16). Again, a `BOUND` parameter for mesh indices rather than positions is provided for backward compatibility with UIUC MOCA. `BOUNDP` is used if `BOUND=(0 0 0 0)` as it is by default. Finally, the `CHAR` parameter provides the Gaussian distribution parameters in units specified by the `LENGTH` on the `UNITS` statement (see “Grid” on page 19-16). It works very similar to the Gaussian doping statement used by ATLAS. The values specified are standard deviations in the directions respectively.

–x, +x, –y, +y

19-3

Biasing

Assign any non-zero applied voltage biases using the SOLVE statement (see “Commonly-Used Statements” on page 19-6).

For backward compatibility with MOCA, you may assign the voltage for every contact defined using the VBIAS parameter on the DEVICE statement as follows:

```
DEVICE VBIAS=(Vi,Vj,Vk,Vl)
```

where each value of the VBIAS parameter is specified in Volts. The subscripts i, j, k, and l refer to the contacts in the order they are defined. In this case, first suppose the source and drain contacts are defined, followed by the gate and finally a substrate contact. Then, the statement above will assign voltages as follows:

```
DEVICE VBIAS=(Vs=Vi Vd=Vj Vg=Vk Vsub=Vl)
```

The DEVICE statement supports up to 16 contact definitions or 16 values on the VBIAS parameter.

Defining contacts and then assigning each one a potential is essentially setting the boundary conditions for the simulation. There are some cases where you must be careful. For example, if you define a MOS device with a very shallow body, but in reality when the device is fabricated, then there is a much larger distance to the substrate grounding potential. The simulation results then may not be accurate.

The preferred method is to set the applied biases with the SOLVE statement. MC DEVICE will stop with an error if you use both the DEVICE statement and the SOLVE statement to set non-zero biases. Instead, you may only use the DEVICE statement or the SOLVE statement to do this.

MC DEVICE provides you ways to define fields over chosen regions. The FIELD statement lets you do this.

```
FIELD MAXFIELD=(start,end) RAMP=(start,end) NEGFIELD=0|1 USEBARR=0|1
```

MAXFIELD defines the starting and ending maximum electric fields in [V/cm]. The RAMP parameter sets the iteration (ITER) on which to start ramping the field and the iteration on which to end ramping the field. NEGFIELD sets whether to use the negative of the field. USEBARR sets whether to use the material-dependent band-offset barriers in the field calculation.

The material-dependent band-offset barriers are determined by the AFFINITY parameter (for the conduction band barriers) and the AFFINITY and EGAP parameters (for the valence band barriers) on the MATDEF statements, which appear at the end of the defaults.in file. The material-dependent band-offset barriers are only used when using the multi-material model (when TYPE=1 on the MMAT statement).

MC DEVICE also allows you to setup bias conditions that vary linearly between them. The LINBIAS statement allows you to choose a specific REGION and specify the boundary voltages of that region.

```
LINBIAS LBREGION=n LBX1=Vx1 LBX2=Vx2 LBY1=Vy LBY2=Vy2
```

The LBREGION parameter chooses which region this LINBIAS statement applies to. The remaining fields set the voltage for each of the 4 boundaries of the chosen region. LBX1 sets the potential at the left-hand x boundary. LBX2 sets the potential at the right-hand x boundary. LBY1 sets the potential at the top y boundary. LBY2 sets the potential at the bottom y boundary.

19.5.2: Ohmic Contacts

For metal-semiconductor contacts, the barrier height, ϕ_B , represents the difference between the metal work function and the electron affinity of the semiconductor, χ , namely

$$\phi_B = \Phi_m - \chi \quad 19-4$$

and is taken from the material library. For silicon contacts, the barrier height is found using the surface electron concentration, $n_s(x)$ (where x is the position along the boundary), and the conduction band density of states, N_c (where n_s is found by assuming charge neutrality at each node on the contact). For the non-degenerate case:

$$\phi_B(x) = \frac{k_B T_L}{q} \ln\left(\frac{N_c}{n_s(x)}\right) \quad 19-5$$

For the degenerate case, the logarithm above is replaced by an inverse Fermi-Dirac integral. In all cases, the surface potential, ϕ_s , is determined by the barrier height, ϕ_B , and the applied bias, V_a , as:

$$\phi_s(x) = V_a - \phi_B(x) \quad 19-6$$

Regarding the MC simulation, ohmic contacts must obviously force a quasi-equilibrium concentration. We adopt the same algorithm as used by DAMOCLES [95].

The total charge along a contact is computed, and particles are injected to the mesh nodes where the depletion is maximum. It must be observed that, for the case of non-uniform doping or mesh spacing or both, this method can easily lead to unphysical non-uniformities of concentration. The only solution to this problem is to use small, uniform contacts.

In MC DEVICE, the INJECT statement controls injection from the contacts and RESIST controls the resistance of the contact region.

```
INJECT DN=0.0 DP=0.0 HEMIMAX=NO OVERINJ=0.0 TSTEP=1
```

DN and DP allow the selection of the fraction of electron and holes injected. This is more useful in bipolar mode when both particle types are actually simulated simultaneously. HEMIMAX sets injection to be a hemi-Maxwellian distribution (or not). OVERINJ sets the allowed fraction of over-injection. So OVERINJ=0.01 allows 1% over-injection. TSTEP sets the injection time step relative to the simulation time step. The default in MOCA is to inject every time Poisson is solved.

```
RESIST OHM=0.0 CRNUM=-1 DIR=1 CONTNUM=-1 TSTEP=PINF
```

OHM defined the ohmic value of the contact in Omega-cm. CRNUM is the index of the region in the input file from which to take material properties. DIR is the direction primary injection direction for the contact, where 1 is for the x-direction and 2 is for the y-direction. CONTNUM is the index of the actual contact in the .in input file. TSTEP is the simulation step interval on which to update values.

You can also control reflection from boundaries and contacts in MOCA. The REFLECT statement is used to set the minimum distance travelled after reflection. By default, this value is set to -1 to turn off the function.

```
REFLECT MINDIST=-1E0
```

The value of MINDIST is given in cm.

Note: Unlike other regions, the information about a contact is not overwritten by subsequent regions. Once you specify a grid point to be a contact, it will remain that way regardless what follows in the input file.

19.5.3: Estimators

Current Regions

MC DEVICE allows you to define one or more rectangular current regions (C-Regions) where you can calculate the current. A CREGION statement takes the form:

```
CREGION BOUNDP=(0.0275 0.0675 0.0 0.08)
```

The BOUNDP parameter contains the boundaries of the region as on the REGION statement (see “Regions” on page 19-17). Again, a BOUND parameter is provided for backward compatibility.

The total current is the sum of the conduction current and the displacement current. The conduction current is computed by assuming that carriers flow either along the X or along the Y direction (or through two opposite sides of each rectangular region). The displacement current is computed by considering the current across all four edges of each rectangular region.

Consider the case of the X-oriented current, flowing in the negative X-direction (the normal case for an *n*-MOSFET). Case a in Figure 19-4 illustrates how to calculate the current exiting from the left-hand side of a rectangle, such as at the source of an *n*-MOSFET. Case b in Figure 19-4 illustrates how to calculate the current entering from the right-hand-side of a rectangle, such as at the drain of an *n*-MOSFET.

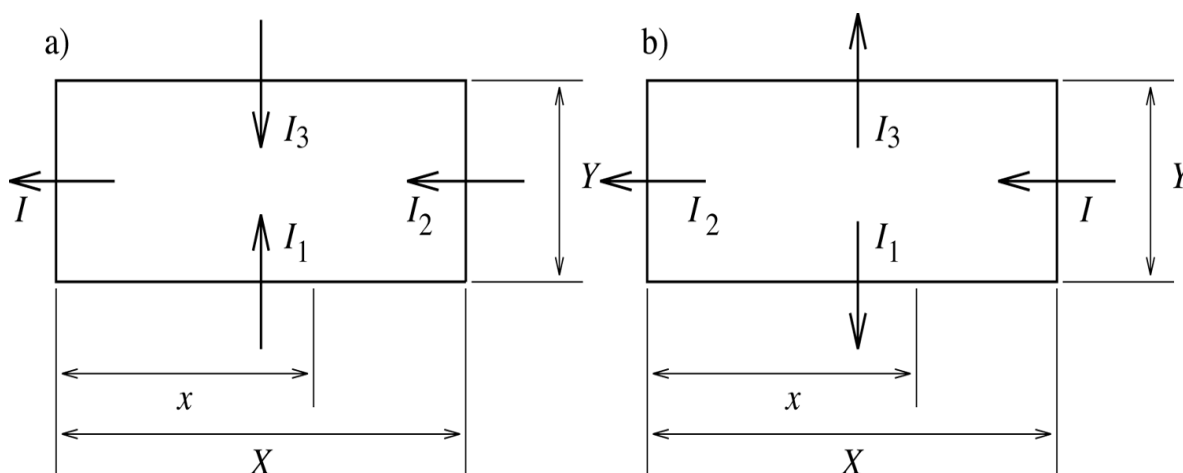


Figure 19-4: Rectangular regions are employed to compute the total current *I* for cases a and b, which pertain to the source and drain of an *n*-MOSFET.

Since the sum of the currents into any region is 0, the current *I* can be written, in both cases, as:

$$I = I_1 + I_2 + I_3 \quad 19-7$$

where *I*, *I*₁, *I*₂, and *I*₃ refer to either to case a or case b collectively.

We will use the equation

$$I = \int J_{tot} dl = \int_0^L [\dot{D} + J] dl = \int_0^L [\epsilon \dot{E} + J] dl \quad 19-8$$

where the total current density, *J*_{tot}, is written as the sum of the displacement current density, \dot{D} , and the conduction current density, *J*, and where *I* represents a current per unit length in a 2D domain.

The source current *I* in case a of Figure 19-4 is then:

$$I = \int_0^x \varepsilon \dot{E}_y(x', 0) dx' - \int_0^Y [\varepsilon \dot{E}_x(x, y) + J(x, y)] dy - \int_0^x \varepsilon \dot{E}_y(x', Y) dx' \quad 19-9$$

We now consider the average current within the C-Region by integrating the RHS of Equation 19-9 from $x=0$ to $x=X$ and by dividing by X , namely:

$$I = \frac{1}{X} \left[\varepsilon \int_0^X \int_0^Y [\dot{E}_y(x', 0) - \dot{E}_y(x', Y)] dx' dy - \int_0^X \int_0^Y J(x, y) dy dx - \varepsilon \int_0^X \int_0^Y \dot{E}_x(x, y) dy dx \right] \quad 19-10$$

The first integral in Equation 19-10 is evaluated as:

$$\int_0^X \left(\int_0^x \dot{E}_y(x', \eta) dx' \right) dx = \int_0^X \left(\int_0^X \dot{E}_y(x', \eta) H(x - x') dx' \right) dx \quad 19-11$$

$$= \int_0^X \dot{E}_y(x', \eta) dx' \int_0^X H(x - x') dx \quad 19-12$$

$$= \int_0^X \dot{E}_y(x, \eta) (X - x) dx \quad 19-13$$

where H is the Heaviside or unit step function.

The expression for the source current I in case a in Figure 19-4 is then:

$$I = \frac{1}{X} \left[- \int_0^X \left(\int_0^Y J(x, y) dy \right) dx + \varepsilon \int_0^Y [\dot{\phi}(X, y) - \dot{\phi}(0, y)] dy + \varepsilon \int_0^X (X - x) [\dot{E}_y(x, 0) - \dot{E}_y(x, Y)] dx \right] \quad 19-14$$

where the x component of the electric field, E_x , has been expressed in terms of the electrostatic potential, ϕ , using the fundamental theorem of calculus.

Similarly, the drain current I in case b in Figure 19-4 is:

$$I = - \int_0^X \varepsilon \dot{E}_y(x', 0) dx' - \int_0^Y [\varepsilon \dot{E}_x(x, y) + J(x, y)] dy + \int_x^X \varepsilon \dot{E}_y(x', Y) dx' \quad 19-15$$

Again, we consider the average current in the C-Region by integrating the RHS of Equation 19-15 from $x=0$ to $x=X$ and by dividing by X . The expression for the drain current I in case b in Figure 19-4 is then:

$$I = \frac{1}{X} \left[- \int_0^X \left(\int_0^Y J(x, y) dy \right) dx + \varepsilon \int_0^Y [\dot{\phi}(X, y) - \dot{\phi}(0, y)] dy + \varepsilon \int_0^X x [\dot{E}_y(x, Y) - \dot{E}_y(x, 0)] dx \right] \quad 19-16$$

In both Equations 19-14 and 19-16, the first term represents the conduction current. The second term represents the displacement current flowing through the left ($x=0$) and right ($x=X$) boundaries. The third term represents the displacement current flowing through the lower ($y=0$) and upper ($y=Y$) boundaries.

In steady state, all displacement currents average to zero, so the second and third terms in Equations 19-14 and 19-16 drop out. So in steady state, the current in both cases is negative the integral over y of the X -average of the conduction current density.

During the MC simulation, the current will be averaged over time to reduce the noise and increase the accuracy of the estimates. The time derivatives of the potentials and electric fields do not need to be

time-averaged. Instead, these can be directly calculated with a backward difference approximation to the derivatives. The conduction current density, however, is time averaged.

The sign convention for the current was adopted from MOCA where a net flow of electrons in the positive x direction (from source to drain in an n-MOSFET) was defined as positive current despite the fact this is contrary to the standard definition. Conversely, a net flow of holes in the positive x direction (from source to drain in a p-MOSFET) is defined as negative current. Since the currents calculated by a current regions is not necessarily associated with a terminal, the reference direction for the current is not related to the terminals. This means that the source and drain currents from current regions (normally the x-component of the current in each current region) will be positive for *n*-MOSFETs and negative for *p*-MOSFETs when these devices are biased in the linear or saturations regions.

Energy Regions

MC DEVICE also allows you to define one or more rectangular regions used for the calculating the energy estimator (EE-Regions). A EERECTION statement takes this form:

```
EERECTION BOUNDP=(0.0051,0.0102,-0.0015,0.0102)
```

The BOUNDP parameter contains the boundaries of the region as on the REGION statement (see “Regions” on page 19-17). Again, a BOUND parameter is provided for backward compatibility.

The energy estimator is calculated for each EERECTION in a way similar to how the total current is calculated (see “Current Regions” on page 19-23).

19.5.4: Initial Conditions

MC DEVICE allows you to customize many quantities used in the simulation. You can do the following:

- Defining regions over which the field is constant.
- Setting the initial particle concentration in a given region.
- Setting the particle injection rate.
- Setting a linear bias over a region.

FFREGION allows setting up a constant field region. The FFREGION statement has three parameters: FIELDX, FIELDY, and BOUNDP. FIELDX sets the x-directed field at the four edges of the region. FIELDY sets the y-directed field at the four edges of the region. BOUNDP defines the boundaries of the region (see “Regions” on page 19-17). Again, a BOUND parameter is provided for backward compatibility.

```
FFREGION \
  FIELDX=(Ex1,Ex2,Ey1,Ey2) \
  FIELDY=(Ex1,Ex2,Ey1,Ey2) \
  BOUNDP=(x1,x2,y1,y2)
```

You can use the ICLREGION statement to set the initial carrier concentration. This statement is useful for controlling the initial solution to Poisson’s equation.

```
ICLREGION CONC=conc BOUNDP=(x1,x2,y1,y2)
```

CONC sets the initial concentration. BOUNDP sets the boundary wherein this concentration is applied (see “Regions” on page 19-17). Again, a BOUND parameter is provided for backward compatibility.

You can use the QSS statement to set a fixed surface charge density. This statement is useful for studying trapped oxide charge in MOS devices.

```
QSS QSCHARGE=conc BOUNDP=(x1,x2,y1,y2)
```

QSCHARGE sets the fixed surface charge density. BOUNDP sets the boundary wherein this concentration is applied (see “Regions” on page 19-17). Again, a BOUND parameter is provided for backward compatibility.

If you need to define a line charge, then set y1 and y2 to be equal to one another.

19.5.5: Bipolar

For devices where impact ionization is important, you can run MC DEVICE in bipolar mode. The BIPOLAR statement sets the interprocess communication parameters.

```
BIPOLAR COMM=0|1|2 MSFILE="msfile" SMFILE="smfile" NSLAVE=n INITNLIN=conc \
NFRACII=0.0
```

The `comm` field sets the communication method, 0 is to turn bipolar mode off, 1 is for master, and 2 is for slave (unix pipe). If COMM is set to 1, the variable MSFILE is set to the master to slave pipe. If COMM is set to 2, then the variable SMFILE is set to the slave to master pipe. NSLAVE is the number of slave particles. INITNLIN is the initial slave concentration. NFRACII is the fraction at which to increase the number of particles.

19.5.6: Track Boundary Crossings

Along with using statements in the scattering section to track particles (see “Impact Ionization and other topics” on page 19-59), there is CROSSEST to track particles crossing boundary regions. The CROSSEST statement specifies where region you want to track particles. Multiple CROSSEST regions may be defined.

```
CROSSEST CROSSREG=n
```

19.5.7: Time Step Regions

To precisely simulate some areas of a device where carriers move quickly, you can use DTREGION to set a small time step. Conversely, to efficiently simulate areas of a device where carriers move slowly, you can use DTREGION statements to set a larger time step.

Use the DTREGION statement to define the area over which to use the fine time step.

```
DTREGION BOUNDP=(x1 x2 y1 y2)
```

The region defined by DTREGION will be simulated every flight time step while the rest of the device will only be updated every Poisson time step. This way you can accurately simulate, say, the channel region with a flight time step of 0.01 fs while still keeping the Poisson step around 0.1 fs. The BOUNDP parameter defined the rectangular boundary of the region (see “Regions” on page 19-17). Again, a BOUND parameter is provided for backward compatibility.

19.5.8: Importing Data

MC DEVICE allows you to import data from input data files. In particular, you can import the electric potential, the initial MC carrier concentration, doping profiles, regions and mesh. You can import all these data or any combination of them. All imports must be done from one file type, specified by the TYPE parameter on the IMPORT statement.

```
IMPORT TYPE=1 VOLT=FALSE AVGVOLT=FALSE \
NCONC=FALSE AVGNCONC=FALSE PCONC=FALSE AVGPCONC=FALSE DOP=TRUE \
MESH=FALSE REGIONS=FALSE \
DIPSH=0 OFFSET={x,y} BOUNDP=(x1,x2,y1,y2) \
DOPFILE="ref/dop.in"
```

The TYPE parameter allows you select from eight different file formats:

- TYPE=1 is for UIUC MOCA files.
- TYPE=2 is for PISCES version-2 files.
- TYPE=3 is for PISCES version-3 files.
- TYPE=4 is for ISE files.
- TYPE=5 is for rectangular grid files.
- TYPE=6 is for TIF files.
- TYPE=7 is for Well-Tempered MOSFET (WTM) files.

- TYPE=8 is for Silvaco structure files.

The TYPE parameter sets the file type for all imported files. The default value of TYPE=8 is for Silvaco Structure files.

VOLT, AVGVOLT, NCONC, AVGNCONC, PCONC, AVGPCONC, and DOP are boolean parameters that enable you to import the related quantities. By default, these parameters are FALSE so that no import occurs. Setting VOLT to 1|TRUE|YES will import the “Potential” as the electric potential. Setting AVGVOLT to 1|TRUE|YES will import the “Average Potential” as the electric potential. You may not set both VOLT=1 and AVGVOLT=1. When CARRIER=E on the ALGO statement, setting NCONC to 1|TRUE|YES will import the “Electrons” as the initial electron concentration and setting AVGNCONC to 1|TRUE|YES will import the “Average Electrons” as the initial electron concentration. You may not set both NCONC=1 and AVGNCONC=1. When CARRIER=H on the ALGO statement, setting PCONC to 1|TRUE|YES will import the “Holes” as the initial hole concentration and setting AVGPCONC to 1|TRUE|YES will import the “Average Holes” as the initial hole concentration. You may not set both PCONC=1 and AVGPCONC=1. Setting DOP=1|TRUE|YES will import the “Net Doping” if IONIZ=0|FALSE|NO on the POISSON statement (for complete ionization of dopants). Setting DOP=1|TRUE|YES will import “Boron”, “Arsenic”, “Indium”, and “Phosphorus” if IONIZ=0|FALSE|NO on the POISSON statement (for incomplete ionization of dopants).

MESH and REGIONS are boolean parameters that enable you to import these structure elements from a Silvaco structure files (TYPE=8). Setting MESH=1|TRUE|YES will import the mesh from STRFILE and ignore XMESH and YMESH statements in your input file. Since MC DEVICE supports only rectangular tensor product meshes, meshes of a type other than this are transformed to a rectangular tensor mesh which includes every x position and every y position in the imported mesh. Setting REGIONS=1|TRUE|YES will import regions from STRFILE. You must comment out any REGION statements in your input file unless you want to add additional regions or redefine regions which get imported. Since MC Device supports only rectangular regions, regions with a shape different than this are expanded to a rectangle which includes every mesh point in the imported region. You can not import contacts from a structure file using an IMPORT statement. Instead, when REGIONS=1|TRUE|YES, MC DEVICE will continue to process any uncommented REGION statements in your input file. Those with TYPE=CONTACT will represent the contact regions for the device and any contacts in the structure file will be ignored. Contacts in your input file are added to the imported structure in the order they appear in the input file. So when you import a structure from strfile using TYPE=8, you will still need to use REGION statements with TYPE=CONTACT in your input file to create contacts for the imported structure.

The DIPSH parameter is set to 0 (off) by default. You may set DIPSH to 1 (on) to use ISE DIPSH with the import.

The OFFSET parameter is an (X,Y) offset for importing quantities. The OFFSET parameter is (0,0) by default and (X,Y) are specified in cm.

The BOUNDP=(x1 x2 y1 y2) parameter sets a rectangular boundary over which doping imports are applied. If any of x1,x2,y1, or y2 are left as their default values of 0, then these are set to the xmin,xmax,ymin,ymax of the device structure respectively, so that doping imports are applied to the entire device by default. Alternatively, you can set x1,x2,y1, and y2 to set to defined a window for importing the doping. Imports for the voltage and concentration are always done over the whole device, so these are not affected by the BOUNDP parameter (see “Regions” on page 19-17). Again, a BOUND parameter is provided for backward compatibility.

The VOLTFILE, CONCFIL, DOPFILE, GRIDFILE, SOLFILE, VERFILE, TRIFILE, SDFILE, RETROFILE, and STRFILE parameters provide the filenames of the data to be imported. The particular parameters that are used depend on the TYPE parameter.

For TYPE=1, VOLTFILE, CONCFIL, and DOPFILE are used, where VOLTFILE is a 2D voltage file, CONCFIL is a 2D MC carrier concentration file, and DOPFILE is a 2D doping file.

For TYPE=2|3, GRIDFILE and SOLFILE are used, where GRIDFILE is a 2D grid file and SOLFILE is a 2D solution file.

For TYPE=4 | 5 | 6, VERFILE, TRIFILE, DOPFILE, and SOLFILE are used, where VERFILE is a 2D vertex file (a 2D grid file when DIPSH=1), TRIFILE is a 2D triangle file (a 2D data file when DIPSH=1), DOPFILE is a 2D doping file, and SOLFILE is a 2D solution file.

For TYPE=7, SDFILE, RETROFILE, and VOLTFIL are used, where SDFILE is a 2D source-drain doping file, RETROFILE is a 1D retrograde doping file, and VOLTFIL is a 2D voltage file.

For TYPE=8, STRFILE is used, where STRFILE is a 2D Silvaco structure file.

For example, if you set `volt=1|TRUE|YES` and TYPE=1 (for the UIUC MOCA file type), then MC DEVICE will import the electric potential (voltage) from the file specified by the VOLTFIL parameter (which is, by default, `'volt.in'`). Correspondingly, if you set `CONC=TRUE` and TYPE=1, then MC DEVICE will import the MC carrier concentration from the file specified by the CONCFIL parameter (which is, by default, `'conc.in'`). Finally, if you set `DOPING=TRUE` and TYPE=1, then MC DEVICE will import the doping profiles from the file specified by the DOPFILE parameter (which is, by default, `'dop.in'`).

19.6: Statistical Enhancement

The methods for statistical enhancement are controlled with the `ENHAN` statement.

```
ENHAN MODE=2 TSTEP=2 ESTEP=100 XSTEP=(0,0,0) \
      LOTHRE=1e-20 HITHRE=1e20 RELTHRE=0.05 RATIO=2. N=10
```

The default value of `MODE=0` indicates that statistical enhancement is turned off. `MODE=1` is deprecated and should not be used. `MODE=2` selects the non-local gathering algorithm also known as phase-space balancing [168, 169]. `MODE=3` selects the comb method (for bulk simulation only). In all cases, `TSTEP` is the interval in time steps between calls of the variance-reduction subroutine. This depends on a compromise between quality of the simulation (reduction of the noise) and CPU time spent in the balancing routine. Usually, a balancing step of less than 100 fs is needed to achieve significant reduction of the noise. `ESTEP` and `XSTEP` specify the partitioning of phase space in units of meV and mesh cells respectively. Time steps between application of the enhancement algorithm.

You can also specify only a sub-region of the device to perform the statistical enhancement. The `BOUND` parameter defines a rectangular boundary where to apply the statistical enhancement.

The non-local gathering method works by a two-phase process. First, the ensemble of particles will be scanned. A linked list is then created that contains all particles that do not contribute to the simulation or redundant particles. A particle is marked as redundant if its weight is less than `RELTHRE` times that of the largest particle in the same bin. Then, the average number of particles per bin is computed. Particles in under-populated bins are split until the occupation of phase space is balanced. Every splitting needs some storage for the newly-created particles. This storage is obtained by gathering particles. You can perform gathering on the redundant set if this is available. If more splittings are needed than redundant particles are available, some local gatherings will be performed in bins with higher particles.

The algorithm is completely controlled by only five variables:

- `LOTHRE`
- `HITHRE`
- `RELTHRE`
- `RATIO`
- `N`

These will be described in the following sections.

19.6.1: LOTHRE

The `LOTHRE` parameter is the single most important parameter in the non-local gathering method. It is the minimum weight allowed for particles in the simulation. That is, particles with weight below `LOTHRE` cannot be split further. This minimum threshold defines the accuracy of the simulation, since the weakest details will have to be resolved by very small particles. Usually, a minimum weight of 10^{-20} to 10^{-10} is adequate to resolve most important high-energy effects. Since this parameter is a double-precision number, you can specify a very small value. A small value for `LOTHRE` uses particles to populate a large number of bins. Therefore, it trades the overall accuracy of the simulation for a wider coverage of phase space.

19.6.2: HITHRE

The `HITHRE` parameter controls the maximum allowed size for particles in the simulation. It is used in two different ways. One way is to control the maximum total weight for particles in a gathering set if the redundant set is used. Another way is to control the maximum size of any particle in the gathering set if local gathering is used. A value of 1.0 will force a maximum unit weight for all particles, so that no particle will be larger than in the conventional situation. This will inhibit any gathering starting from a situation where all particles have unit weight. In this case, if you apply balancing to an initial status from a non-balanced simulation, then some extra particles will have to be allocated (`NREF` larger than the initial number of particles). Therefore, the algorithm will be able to expand the ensemble without gathering particles.

19.6.3: RELTHRE

The `RELTHRE` parameter defines the criterion for marking particles as redundant. A value of 10^{-3} means that a particle will be included in the redundant set only if there exists another particle in the same bin with a weight 1,000 times larger. While a value of 10^{-3} is safe because it only tries to “reuse” very small particles, it may be inefficient in cleaning the bins of particles that do not contribute to the simulation. A large value like 10^{-1} , however, may mark as redundant particles that actually contribute significantly to the estimators.

The optimum value of `RELTHRE` depends on the dynamic range of weights in any given bin. A simple rule of thumb can be derived from the exponential dependence of electron occupancy on energy. We can reasonably take the thermal-equilibrium distribution as the steepest possible distribution in a common device. If ΔE is the width of the energy bins, we have a possible dynamic range inside a bin of $\exp(\Delta E/k_B T_L) \approx 50$ for 0.1 eV bins and room temperature.

In this case, you can see a value of 10^{-2} for `RELTHRE` is safely low enough. Also for space dependence, you can apply the same criterion, where the energy range is simply the maximum voltage drop across a space bin. For a typical bin width of 10 nm and an electric field of 200 kV/cm, we have an energy difference of 0.2 eV, which yields a dynamic range of about 2500. For this case, a value for `RELTHRE` below 4×10^{-4} is suggested by our rule of thumb.

Note: In high-field regions, you cannot assume a thermal-equilibrium distribution. But in high-field regions, you should not use the guidelines described above.

19.6.4: RATIO, N

These `RATIO` and `N` parameters define the gathering process. `RATIO` is the maximum dynamic range of weights for any gathering. `n` is the maximum number of particles in the gathering set. Let us assume that `n` particles are being gathered and the `RATIO` of weights between the largest and the smallest particle is `RATIO`. This means that if the smallest particle is retained, its weight will increase by a factor between `RATIO` and `n`×`RATIO`. If there is a great increase in weight, it will worsen the numerical noise. To estimate the maximum tolerable increase of weight, consider the case of gathering of redundant particles. For each redundant particle, there is another particle in the same part of phase space with a weight `RELTHRE`⁻¹ times larger. The increase will be tolerable if the retained particle remains quite smaller than the dominant particles in the same bin. In other words, if:

$$ratio \times n \ll relthre^{-1} \quad 19-17$$

This gives us the rule of thumb:

$$ratio \ll \frac{relthre^{-1}}{n} \quad 19-18$$

For example, with $RELTHRE=10^{-2}$ and $n=10$, a dynamic range equal to 10 can be tolerated before an excessive increase of variance occurs. If you use a very aggressive criterion for marking redundant particles (e.g., $RELTHRE=10^{-1}$ or more) then rescale $RATIO$ accordingly. Otherwise, the sudden growth of the redundant particles will create large spikes in the estimated distribution function. The optimum value for $RATIO$ depends on the number of particles used. For a large number of particles (20,000 or more), a value as low as 2 allows a very small increase in variance without impairing the performance. For small number of particles, a value of 10 or more can be necessary to collect a sufficient number of redundant particles for the gathering to be effective. If the constraint becomes too strict, lower $RELTHRE$ instead of setting $RATIO$ to a very low value.

19.6.5: Particle Compression

MC DEVICE automatically sets a reference number of particles, N_{ref} , as slightly less than the number physically allocated in memory. In this way, it allows for some fluctuations of the number of computational number of particles. If the current number n of particles is larger than N_{ref} , MC DEVICE can perform some gatherings with no splittings to reduce the total number. This step is called compression. If $n < N_{ref}$, the extra storage available is used to perform some “free” splittings with no gatherings. Under normal conditions, at the exit of the variance-reduction procedure the number of particles will be equal to N_{ref} . The introduction of N_{ref} solves a problem intrinsic with the manipulation of the particle states. The total number of particles in the simulation is related to the transit time of carriers through the device. If no variance reduction is used, this will be the physical transit time, so that the number of particle will be easily estimated and controlled. The introduction of variance reduction algorithms changes the distribution of MC particles in phase space, so that the computational transit time can be higher or lower than the physical one. This leads to unpredictable drifts and fluctuations in the storage required by the program. You can only use the compression step by a many-particle variance-reduction scheme [169]. This solves this problem by forcing an almost-constant number N_{ref} of particles.

19.6.6: Statistical Enhancement Statements

The following statements don't specifically reduce the noise during the simulation. These are only statements that smooth the output. `ESTIM1D` allows you to select a region and make a 1D cut through it and study quantities of that cut. `SMREGION` sets a region to perform the smoothing of the outputs.

```
ESTIM1D DIR=X/Y BOUNDP=(x1,x2,y1,y2)
```

`DIR` sets what direction to make the cut in. `BOUNDP` defines the boundary where to run the 1D estimator (see “Regions” on page 19-17). Again, a `BOUND` parameter is provided for backward compatibility.

```
SMREGION BOUNDP=(x1,x2,y1,y2) TYPE=n
```

The `BOUNDP` parameter contains the boundaries of the region, as on the `REGION` statement (see “Regions” on page 19-17). Again, a `BOUND` parameter is provided for backward compatibility. `TYPE` sets the quantity to smooth. Setting `TYPE` to 1 smooths the potential, `ETA`. Setting it to 2 smooths the quantum potential, `QETA`.

19.7: Physical Models

19.7.1: Self-Consistent Simulation

Background

Poisson's equation is solved on the same grid used to define the device. Assuming CARRIER=E on the ALGO statement, the non-linear Poisson equation takes the form

$$-\nabla \cdot (\epsilon \nabla \phi) = e(- (n_{MC} + n(\phi)) + N_D^+(\phi) - N_A^-(\phi) + p(\phi)) . \quad 19-19$$

Here, ϵ is the permittivity. ϕ is the electrostatic potential. e is the fundamental electron charge. n_{MC} is the electron concentration computed using the Monte Carlo cloud-in-cell (CIC) scheme [95]. n_{MC} is zero in semiconductor contact regions and non-contact gate regions and non-zero in MC regions. $n(\phi)$ is the electron concentration computed using ϕ and N_c using Equation 19-23. N_c is the effective density of states of the conduction band. N_c and $n(\phi)$ are zero in MC regions. N_c and $n(\phi)$ are non-zero in semiconductor contact regions and non-contact gate regions and zero in MC regions. N_D^+ is the ionized donor concentration. N_A^- is the ionized acceptor concentrations. $p(\phi)$ is the hole concentration computed using ϕ and N_v using Equation 19-22. N_v and $p(\phi)$ are non-zero in all semiconducting regions.

All potential-dependent terms in the RHS of Equations 19-19 are determined self-consistently using the quasi-Fermi potentials in each mesh cell and the electrostatic potential, ϕ , at each grid point. For 1D simulation, the linear Poisson equation is solved and holes must be considered in the MC simulation.

For CARRIER=H on the ALGO statement, $-n$ and p are switched in Equation 19-19.

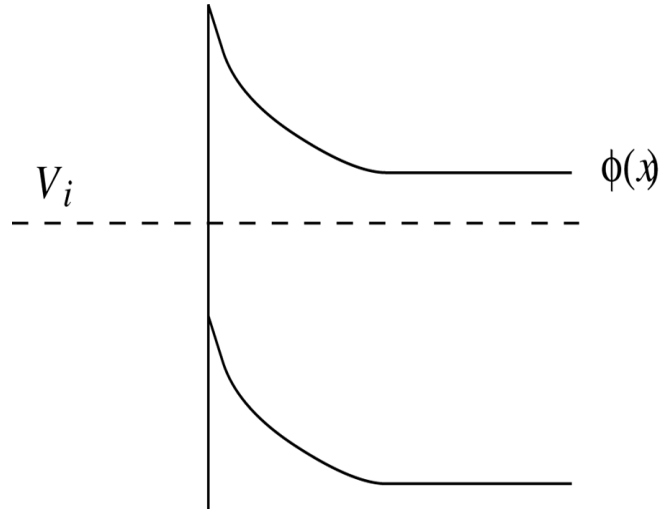


Figure 19-5: V_i is the contact bias at contact i . By default, $E_{fp} = -eV_i$ is the hole quasi-Fermi energy.

$\phi(x) = (E_g(Si)/2 - E_c(x))/e$ is the electrostatic potential.

Still assuming CARRIER=E on the ALGO statement, the hole density is computed as

$$p(\phi) = \int_0^\infty dE g_v(E) f_D((E - E_v + E_{fp})/k_B T_L) = \int_0^\infty dE g_v(E) f_D((E + e\phi(x) + E_g - eV_i)/k_B T_L) \quad 19-20$$

where $f_D(\xi) = f_D(\xi, g=1)$ is the Fermi-Dirac distribution and generalizes for a degeneracy g to

$$f_D(\xi, g) = \frac{1}{1 + g \cdot \exp(\xi)} \quad 19-21$$

This is the Fermi-Dirac distribution including degeneracy. ξ is a unitless factor proportional to the energy, E_g is the bandgap energy. $g_v(E)$ is the energy-dependent valence-band density of states. E_{fp} is the hole quasi-Fermi energy, and V_i is the applied voltage at contact i .

By default, within contact region i , $E_{fp} = -eV_i$. Also by default, within the doping well of contact i , $E_{fp} = -eV_i$, where each contact is assumed to reside in a doping well of one type (n or p). This is the default implementation of the constant quasi-Fermi level method in MC DEVICE.

The USEFERMI and FERMI parameters on the REGION statement provide you with a way to modify the default behavior of the constant quasi-Fermi level method. For example, for a n -MOSFET with an inversion channel and assuming Ohmic contacts, you can change the default choice for the hole quasi-Fermi energy of $E_{fp} = -eV_{drain}$ in the well adjacent to the drain contact by setting E_{fp} using USEFERMI=1 and FERMI=<value> on the REGION statement for the drain (see “Regions” on page 19-17). For example, you may wish to set $E_{fp} = -\min(V_{source}, V_{drain}) = -\min(0.0 \text{ eV}, eV_{drain} > 0 \text{ V}) = 0.0 \text{ eV}$. To do so, you can then use the default value of FERMI=0.0 eV by simply including USEFERMI=1 on the REGION statement for the drain contact. Similarly, for a p -MOSFET when $V_{source} = 0.0 \text{ V}$ and $V_{drain} < 0 \text{ V}$ and when using CARRIER=H on the ALGO statement, you can use USEFERMI=1 on the REGION statement for the drain contact to get $E_{fn} = -\max(V_{source}, V_{drain}) = \text{FERMI} = 0.0 \text{ eV}$ in the drain well instead of the default of $E_{fn} = -eV_i = -eV_{drain}$.

For non-MC carrier concentrations:

$$p(\phi) = N_v F_{1/2}((E_v - E_{fp})/k_B T_L) = N_v F_{1/2}((-e\phi(x) - E_g + eV_i)/k_B T_L) \quad 19-22$$

$$n(\phi) = N_c F_{1/2}((E_{fn} - E_c)/k_B T_L) = N_c F_{1/2}((-eV_i + e\phi(x))/k_B T_L) \quad 19-23$$

where

$$F_{1/2}(\xi) = \int_0^\infty \xi^{1/2} f_D(\eta - \xi) d\eta \quad 19-24$$

is the Fermi-Dirac integral of order 1/2 and where f_D is defined above. E_{fn} is the electron quasi-Fermi energy and is equal to negative the applied voltage at contact i , V_i , within each contact region i . For incomplete ionization of donors, E_{fn} is also assumed to be constant and equal to the contact value within each doping well surrounding contact i . E_{fn} is calculated from Equation 19-23 using the average electron concentration, $\langle n \rangle$, and the average conduction band edge, $\langle E_c \rangle$, and taking $E_{fn} = 0$ wherever $\langle n \rangle = 0$. Although MC DEVICE uses Equation 19-23 to calculate E_{fn} throughout semiconductor regions, MC DEVICE treats electrons to be in quasi-equilibrium (or to have thermalized to a distribution based on the lattice temperature). Instead, E_{fn} is simply an output quantity that you can plot in energy band diagrams. E_{fn} obtained with MC DEVICE compares closely with E_{fn} obtained with the drift diffusion model inside regions of your device where quasi-equilibrium holds. Conversely, E_{fn} obtained with MC DEVICE diverts from E_{fn} obtained with the drift-diffusion model in regions of your device where quasi-equilibrium does not hold.

For the fixed charge, if E_D and E_A are the donor and acceptor impurity energies (with respect to each corresponding band edge), we have for donors:

$$N_D^+(\phi) = N_D f_D(-E_c + E_D + E_{fn}, g_D) = N_D f_D(e\phi + E_D - eV_i, g_D) \quad 19-25$$

and for acceptors:

$$N_A^-(\phi) = N_A f_D(E_c + E_A - E_g - E_{fp}, g_A) = N_A f_D(-e\phi + E_A - E_g + eV_p, g_A) \quad 19-26$$

where $g_D=2$ is the donor degeneracy factor for phosphorus and arsenic. $g_A=4$ is the acceptor degeneracy factor for boron and indium.

The ionization energies of donors and acceptors are assumed constant. No heavy-doping effect, such as the donor deionization effect [128], are considered.

The 1D simulation has no specific input statement. The solver is actually controlled by the `MODE` variable on the `ONED` statement.

Most of the energies and concentrations used in the Equations 19-19 through 19-26 are saved in `*sol.str` (structure) files when performing a 2D simulation. See Section D.2: “File Formats”. You can perform 1D cuts of the 2D structures to plot energy-band diagrams relating to your solution.

The 2D Poisson solver is controlled through the `POISSON` statement

```
POISSON TSTEP=5 ITER=100 TOL=(2e-4,1e-6) IONIZ=NO \
START=1 FREEZE=PINF LINPOI=NO CUTOFF=1e25
```

`TSTEP` sets the number of flight time steps between each Poisson solution. `ITER` is the maximum number of Newton iterations. `TOL` is a vector of 2 values, which is the L_2 -norm tolerance for the Newton and conjugate-gradient methods respectively.

`IONIZ` is used to switch on and off incomplete ionization of dopants. Two reasons exist to disable incomplete ionization. First, the response time of dopant levels is much longer than the time scale used in the MC simulation. Therefore, it is unrealistic to treat dopants in the “adiabatic” approximation (i.e., with instantaneous response). Second, for very high doping levels (above $10E18 \text{ cm}^{-3}$), it is approximately correct to assume that all dopant atoms are ionized [176]. In any case, the program automatically switches off the `IONIZ` flag whenever the quasi-Fermi energies are not constant across a non-depleted region (e.g., in a JFET or MESFET simulation) where a finite voltage is applied across a non-depleted channel.

The fields `START` and `FREEZE` define the time window during which the solver actually works. The field is frozen outside that window, either using a result from a previous simulation, or an average from the same simulation. In the example above, the field is kept frozen during the first 1000 time steps. The Poisson solver is then used until the end of the simulation. The keyword `PINF` is internally defined as the largest positive integer. The keyword `NINF` is internally defined for the largest negative integer.

If the first field of `FREEZE` is greater than one, then an initial fixed field is needed to start the simulation. By default, MC DEVICE reads this field from the file `volt.in`. This file is also written at the end of each run for use in a subsequent simulation.

`LINPOI` selects whether the linear or non-linear Poisson equation is solved. If `LINPOI=1|TRUE|YES`, then a linear version of the Poisson equation is solved where complete ionization of dopants is assumed and where the opposite carrier type as set by the `CARRIER` parameter on the `ALGO` statement is assumed to be 0. If `LINPOI=0|FALSE|NO` (as it is by default), the non-linear poisson equation is solved. In this case, the `IONIZ` parameter may be used to include incomplete ionization and the Poisson equation includes a expression for the density of the opposite carrier type as set by the `CARRIER` parameter on the `ALGO` statement as a function of the unknown potential.

`CUTOFF` sets an upper limit for the complete ionization of dopants. The default value of `CUTOFF` is $1e25 \text{ cm}^{-3}$. Because the default value of `CUTOFF` is high compared to typical doping concentrations, the `CUTOFF` parameter typically has no effect when the default value is used. The `CUTOFF` parameter will only have an effect if it is reduced to below the peak of the net doping profile of your device and if `IONIZ=0|FALSE|NO` for complete ionization. Since using the `CUTOFF` parameter can change the net doping profile that will be used internally by MC DEVICE for solving Poisson's equation and for treating impurity scattering, the effects of using the `CUTOFF` parameter can be significant. The `CUTOFF` parameter should not be reduced below $3e19 \text{ cm}^{-3}$ since this may dramatically affect impurity

scattering. The CUTOFF parameter also affects the doping in the gate, so a value of the CUTOFF parameter below the net doping in the gate will change the threshold voltage. Since there are many restrictions associated with proper use of the CUTOFF parameter, we recommend that you not include the CUTOFF parameter in your input files. Instead, we encourage you to choose doping levels at or below the doping ionization limit when using complete ionization of dopants. Note that CUTOFF has no effect when IONIZ=1 | TRUE | YES for incomplete ionization of dopants.

In MOCA, the IPOLY parameter turned the model for the depletion of polysilicon on and off. In MC DEVICE, the IPOLY parameter is ignored and the depletion of polysilicon gates (or of any semiconducting region where the TYPE is not MC) is considered automatically whenever they appear in a device. For example, in MC DEVICE, you can define the entire gate as type CONTACT, and no depletion will occur on the gate. Instead, you can set the region immediately above the gate oxide to a MAT=POLY (or any semiconducting material) and TYPE=BLOCK, and you can define a contact above this semiconducting non-contact region. In this case, the non-linear Poisson equation including potential-dependent terms for both the electron and hole concentrations is solved within the non-contact portion of the gate to account for the depletion effect.

Microscopic Analysis of Noise

Here is a brief analysis of voltage fluctuations in a conductive medium under the hypothesis of weak screening. This amounts to assuming a non-collisional system because we compute the fluctuations within a screening sphere from the generating carriers. Since the result will be expressed as a power spectrum, the analysis is valid for frequencies above the plasma frequency. The result will be useful when the plasma frequency is low (i.e., for low-density regions).

Velocity Autocorrelation

We start with an elementary model of one-dimensional velocity autocorrelation in a non-interacting gas of classical particles:

$$C_v(t) = E\{v(t')v(t' + t)\} \approx v_{th}^2 e^{-|t|/\tau} \quad 19-27$$

where v_{th} is the thermal velocity and τ is the momentum-relaxation time. At thermal equilibrium:

$$v_{th}^2 = \frac{k_B T_L}{m^*} \quad 19-28$$

The corresponding power spectrum of the velocity is

$$S_v(f) = \int_0^\infty v_{th}^2 e^{-2\pi f t - |t|/\tau} dt = \frac{2v_{th}^2 \tau}{1 + (2\pi f \tau)^2} \quad 19-29$$

and is approximately white up to the frequency $1/(2\pi\tau)$, which is several THz. This frequency must be compared with the plasma frequency that characterizes the dynamic screening of the thermal oscillations by the electron gas.

In the following, we will assume a white spectrum with uniform power density $v_{th}^2 \tau$ for each of the three components of the particle velocity, truncated at the autocorrelation frequency. Although we consider the simple, constant-relaxation-time model at thermal equilibrium, the non-equilibrium case with variable scattering rate can be analyzed by replacing v_{th} with an average RMS group velocity and τ with an average relaxation time.

Current-Density Fluctuations

The current density at a point r in space is defined as the limit.

$$\mathbf{J}(r) = \lim_{\Omega \rightarrow 0} \frac{1}{\Omega} \sum_{x_i \in \Omega} e \mathbf{v}_i \quad 19-30$$

From this definition, the power spectrum of the fluctuations of the k -th component of the current density can be readily computed as

$$S_{J_k}(f) = \lim_{\Omega \rightarrow 0} \frac{e^2}{\Omega^2} \sum_{x_i \in \Omega} S_{v_i}(f) \quad 19-31$$

$$S_{J_k}(f) = \lim_{\Omega \rightarrow 0} \frac{2\tau n e^2 k_B T_L}{\Omega m^*} \quad 19-32$$

It is clear that, as Ω tends to zero, the fluctuation diverges. It follows that the fluctuation is not well defined for the current density but only for its average on a finite volume. This can be verified by a simple derivation, from Equations 19-21, of the familiar formula for the Johnson noise. Assuming for simplicity a cylindrical resistor of length L and area A , the total (conduction plus displacement) terminal current can be computed as

$$I = \frac{1}{L} \int_0^L \left(\int_0^A J \right) d^3 \mathbf{r} \quad 19-33$$

$$I = \frac{1}{L} \sum_{\mathbf{x}_i \in L \times A} e(v_i)_x \quad 19-34$$

The short-current noise power spectrum is therefore

$$S_I(f) = \frac{A}{L} \times \frac{2\tau n e^2 k_B T_L}{m^*} \quad 19-35$$

$$S_I(f) = \frac{2A\sigma k_B T_L}{L} = \frac{2k_B T_L}{R} \quad 19-36$$

This is the usual short-circuit thermal-noise current formula for a resistance R , in the relaxation time hypothesis where the conductivity σ is given by $ne^2\tau/m^*$.

Potential Fluctuations

The main reason for the divergence for the current-density fluctuation is the finite size of the charge carriers. Let us now analyze the power spectrum of the electrostatic potential. Each carrier of charge e generates a potential

$$V_i(\mathbf{r}) = \frac{e}{4\pi\epsilon|\mathbf{r} - \mathbf{r}_i|} \quad 19-37$$

In a given point \mathbf{r} of space, the total potential, V , will be given by the sum of all contributions from nearby carriers:

$$V = \frac{e}{4\pi\epsilon} \sum_i \frac{1}{r_i} \quad 19-38$$

where the origin has been conveniently chosen at \mathbf{r} . Deriving Equations 19-22 with respect to time and using Equations 19-20, we obtain the power spectrum of the time-derivative of the potential:

$$S_{\dot{V}}(f) = \frac{e^2 \tau k_B T_L}{8\pi^2 \epsilon^2 m^*} \sum_i \frac{1}{r_i^4} \quad 19-39$$

The summation, for a large number of particles, can be approximated with an integral:

$$S_{\dot{V}}(f) = \frac{e^2 \tau k_B T_L}{8\pi^2 \epsilon^2 m^*} \int_0^\infty 4\pi r^2 n \frac{1}{r^4} dr \quad 19-40$$

$$S_{\dot{V}}(f) = \frac{e^2 \tau k_B T_L n}{2\pi \epsilon^2 m^*} \int_0^\infty \frac{1}{r^2} dr \quad 19-41$$

Again, the integral presents a pole for vanishing distances, due to the $1/r$ dependence of the potential. We may remove the singularity by assuming a minimum characteristic distance, r_c . In a physical sense, that forces a discretization cutoff in Equations 19-25. With computer simulations, r_c is the size of the discretization mesh on which Poisson's equation is solved. Applying this minimum-distance cutoff, we have

$$S_{\dot{V}}(f) = \frac{e^2 \tau k_B T_L n}{2\pi \epsilon^2 m^* r_c} \quad 19-42$$

We have found the high-frequency behavior of the fluctuations of the potential can be useful for estimating the oscillations of potential barriers. Unfortunately, we have assumed no correlation between positions of the carriers, which results in a perfectly white spectrum of the time-derivative of the potential. This implies an infinite power of the potential fluctuations (i.e., a “random walk” of the potential). In reality, Coulomb interaction between carriers limits the possible oscillation of the potential. You can get a rough estimate of the total amplitude of the potential fluctuations by limiting the bandwidth of its derivative to some characteristic frequency f_c . It's usually the inverse of the dielectric-relaxation time. The power spectrum of the potential is then

$$S_V(f) = \frac{e^2 \tau k_B T_L n}{2\pi \epsilon^2 m^* r_c [(2\pi f)^2 + (2\pi f_c)^2]} \quad 19-43$$

Integrating over the entire spectrum, we have

$$P_V = \frac{e^2 \tau k_B T_L n}{8 \pi^2 \epsilon^2 m^* r_c f_c}.$$

It is evident that as $f_c \rightarrow \infty$, the fluctuations of the potential diverge without bound.

Even after removing the similarities, we see that the total power is proportional to the factor $e^2 n$. This means that the granularity of the charge carriers affect directly the noise. Only when the critical radius r_c is scaled along with the charge n , the limit remains finite. With computer simulations, this means the mesh size must decrease by the same factor as the weight of the particles. In a physical system, you can obtain a rough estimate of the microscopic noise using the dielectric relaxation frequency $\sigma/2\pi\epsilon$ as the cutoff frequency. If the conductivity is approximated as

$$\sigma = \frac{e^2 \tau n}{m} \quad 19-44$$

we have

$$P_V = \frac{e^2 \tau k_B T_L}{4 \pi \epsilon m^* r_c \sigma} = \frac{k_B T_L}{e} \times \frac{e}{4 \pi \epsilon r_c} \quad 19-45$$

The standard deviation of the electrostatic potential is the geometric mean between the thermal voltage and the potential at a distance r_c from a charge e .

In Equations 19-25, the volume integral converges within a radius of a few times r_c from the center point. This means that most of the potential noise is local and thus electrostatic screen. Entering Equations 19-25 as a convergence factor $\exp(-r/\beta_s)$ does not affect it as long as r_c is smaller than the screening length $1/\beta_s$.

You may want to estimate the fluctuations for the potential for the case of a two-dimensional system of particles with charge λ per unit length in the third dimension. The corresponding potential generated from the i -th particle is

$$V_i = \frac{\lambda \ln r_i}{2 \pi \epsilon} \quad 19-46$$

Along the lines of the derivation of Equations 19-26, we have

$$S_V(f) = \frac{\lambda^2 \tau k_B T_L}{2 \pi^2 \epsilon^2 m^*} \int_0^\infty 2 \pi r n (2 v_{th}^2 \tau) \frac{dr}{r^2} \quad 19-47$$

$$= \frac{\lambda^2 \tau k_B T_L n}{\pi \epsilon^2 m^*} \int_0^\infty \frac{dr}{r} \quad 19-48$$

This time there are two singularities. One arising from the short-range effect and another one from the very-long-range action of the two-dimensional Coulomb force. Again, you can remove the short-range singularity by assuming a finite size for the particles or a discretized solution of Poisson's equation. The long-range action will be effectively screened at low frequencies. Therefore, a convergence factor $\exp(-r\beta i)$ can be introduced into the integral of Equations 19-29. This, however, will remain largely unscreened for high frequencies (in the THz range). Therefore, in the high-frequency range, there is no upper bound on the potential fluctuations. Unlike the three-dimensional case, the fluctuations are mainly of a non-local nature and depend on the physical size of the two-dimensional system. We can conclude that a two-dimensional model of fundamental noise cannot account quantitatively for the microscopic fluctuation in the physical three-dimensional system.

19.7.2: Band Structure

Band Structure of Silicon

MC DEVICE models the band structure of silicon by using a numerical representation of 2 or 4 conduction bands and 3 valence bands. Figure 19-6 shows the silicon band structure as obtained from a local pseudopotential calculation [49].

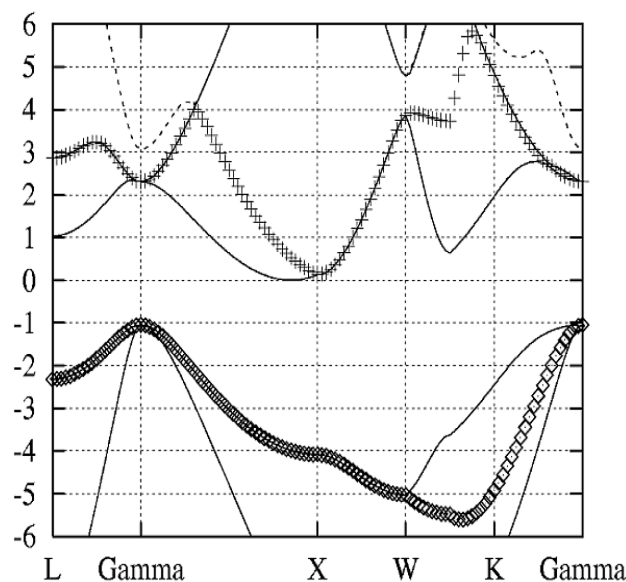


Figure 19-6: Silicon band structure.

The second and third conduction band of silicon are degenerate, or very close, from 2.3 eV to 4 eV over a large part of the Brillouin zone around Γ , so that electron kinematics at those energies is quite well described by the second band alone. Nevertheless, the third and fourth bands can affect energy gain through three “fast” Γ valleys, located at about 2.3 and 3.1 eV. Although these have a small density of states, they can work as effective “tunnels” to oxide-injection energies. Figures 19-7 and 19-8 show the density of states for the first 6 conduction bands and for the first 4 valence bands respectively.

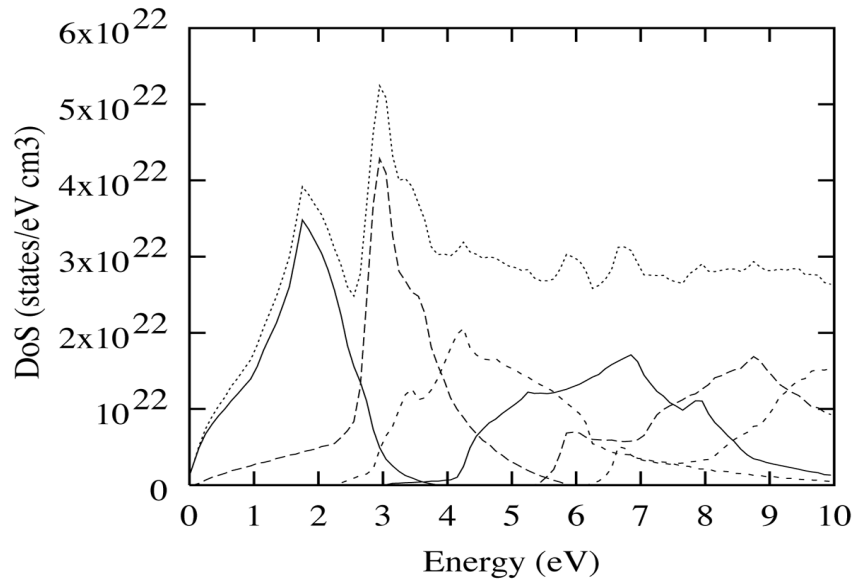


Figure 19-7: Density of states for the first 6 conduction bands of silicon.

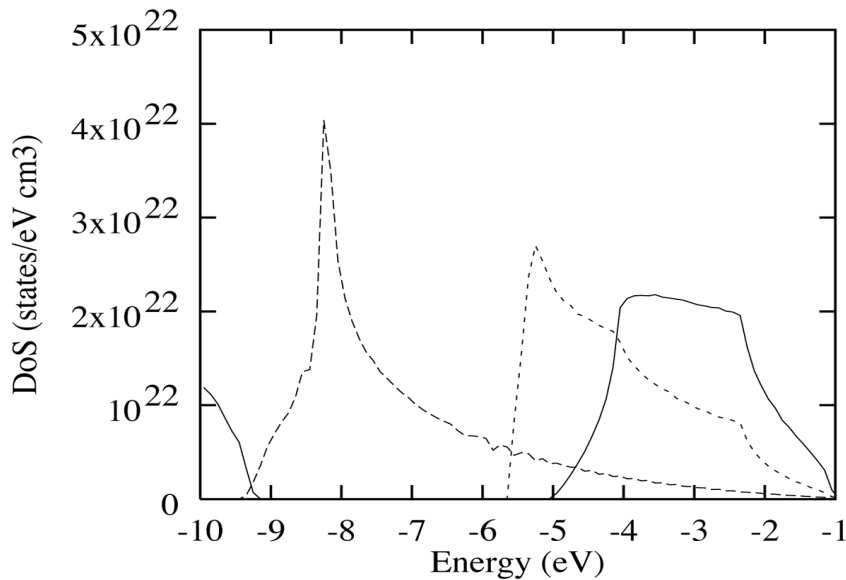


Figure 19-8: Density of states for the first 4 valence bands of silicon.

The BANDS statement controls the representation of the band structure:

```
BANDS N=2 NK=40 FILE="eder40_2.in" INTERP=0
```

Here, *N* is the total number of bands, *NK* is the number of points on Γ -*X*, and *file* is the ASCII file containing the band structure representation. These fields have two values each, one for the conduction bands and the second for the valence bands. Due to their different shapes, two independent representations are allowed for the conduction and valence bands. *FILE* is the file where the energies and velocities (as functions of the wave vector and band index) are stored (see Section D.2.7: “Band Structure Input Files”). *INTERP* is the interpolation algorithm (0 for tricubic, 1 for less-accurate (but faster) trilinear, 2 for more-accurate (but slower) trilinear). When using *INTERP*=0 on the *BANDS* statement and *TYPE*=1 on the *MMAT* statement (for the strain model), the energies and velocities are corrected using the full quadratic correction factors.

When using INTERP=1 or INTERP=2 on the BANDS statement and TYPE=1 on the MMAT statement (for the strain model), the energies and velocities are approximately corrected using fitting parameters that depend on the mole fraction (or effective strain).

Band Degeneracies

To most accurately model charge transport in more than one band, you should model the behavior of electrons at degeneracy points. Two types of degeneracy points may occur: symmetry-induced degeneracies and accidental degeneracies. At symmetry-induced degeneracies, Bragg reflection occurs. At accidental degeneracies, the carrier's group velocity should be continuous during a free flight. Early MC programs [34] and DAMOCLES [135] neglect symmetry-induced degeneracies. MC DEVICE neglects accidental degeneracies. This can be an important effect when transport occurs in more than one band since, for example, an electron can switch from the second to the third band around 3 eV, with a rapid increase in energy.

In research on this topic [167], the problem of ballistic interband transitions has been approached by assuming that the free flight of electrons can be described by a perturbation of the electron potential, leading to transitions between eigenstates of the total lattice potential. When an electron moves in k -space, its band index varies according to the overlap integral between nearby states, which describes the matrix element for smooth perturbations.

The overlap integrals have been computed between the midpoints of all neighboring domains in a 40-point cubic discretization of the irreducible wedge. Since during a 2-fs time step an electron covers only 10^6 cm^{-1} of k -space, the mesh step equal to about $2.9 \times 10^6 \text{ cm}^{-1}$ is large enough to ensure that transitions only occur between neighboring domains. For each cubic domain, the band-index transition with the largest overlap integral is stored in a look-up table. When an electron crosses the interface between domains the band-index changes accordingly. There is a discretization problem with this method that could lead to small violations of energy conservation. That is, if bands cross far from the boundary of the domain (Figure 19-9), there is an abrupt jump of energy when the particle crosses the boundary.

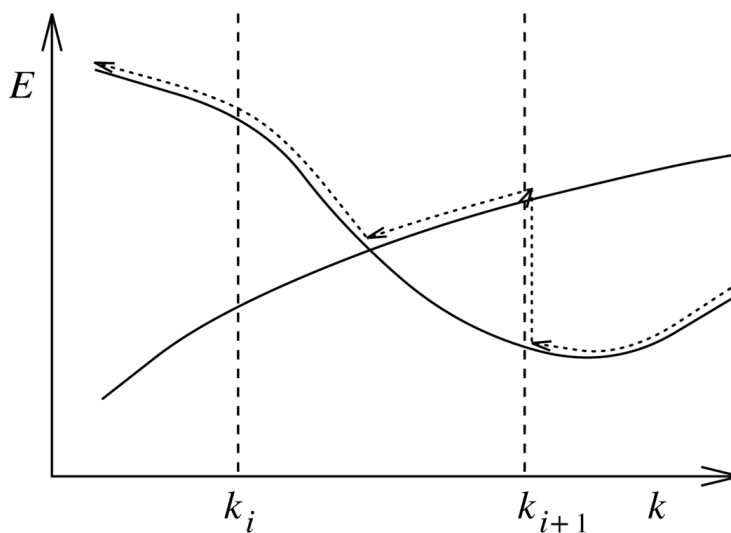


Figure 19-9: Lack of energy conservation during ballistic band switching.

Although the correct trajectory in k -space is recovered after the crossing, energy is not conserved because the finite difference in energy cannot be accounted for by the electric field. An approximate solution to this problem can be obtained by placing the particle right at the center of the cube to minimize the energy step. To obtain a better solution to this problem, re-order the bands globally to achieve continuity of the Bloch functions. A separate program has been written to search the

irreducible wedge for an optimal ordering of the bands [167]. This functionality, however, has not been integrated into MC DEVICE.

This topic has been presented to make you aware of the issue of band degeneracies, to explain what research has been done on this topic, and to clarify that MC device modeling programs, including MC DEVICE, are neglecting some aspects of band degeneracies. Particularly, MC DEVICE neglects accidental degeneracies.

19.7.3: Electron Dispersion and Equations of Motion

MC DEVICE can use either a tricubic or a trilinear interpolation of the electron dispersion in k -space. The tricubic interpolation yields a very good accuracy since it uses the “real” partial derivatives at mesh points to obtain continuity of the group velocity across cubic domains. On the other hand, the tricubic-interpolation subroutine takes a longer CPU time than the simpler trilinear formula. Such a high accuracy may not be necessary if a consistent method is used to integrate the equations of motion in real space.

Let us consider a sampling of the energy dispersion on a discrete set of points $\{(k_i, E_i)\}$. Any two interpolating functions $E'(k)$ and $E''(k)$. A particular case can be the true electron dispersion $E(k)$ (see Figure 19-10).

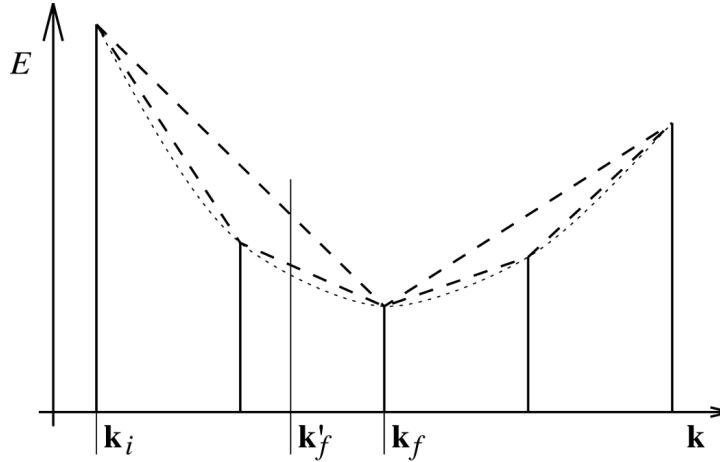


Figure 19-10: Different linear interpolations for the electron energy dispersion shown as a dotted line.

Let us assume that during a time T a given particle moves between two sampling points k_i and k_f for a constant electric field F . The trajectory in k -space is a straight line. Therefore, we know exactly the final point in k -space and the final energy $E(k_f)$. We now assume that the basic equations of motion are consistent with the chosen interpolating dispersion \tilde{E} . This means that for any \tilde{E} so that $\tilde{E}(k_i) = E_i$ and $\tilde{E}(k_f) = E_f$, the difference in real coordinate x_j is

$$\Delta x_j = \frac{1}{\hbar} \int_0^{\Delta t} \frac{\partial}{\partial k_j} \tilde{E}(k(t)) dt \quad 19-49$$

$$= \frac{1}{eF_j} \int_{(k_i)_j}^{(k_f)_j} \frac{\partial}{\partial k_j} \tilde{E}(k(k_j)) dk_j \quad 19-50$$

where we have used the linearity of the transformation between t and the components of k to express everything as an unambiguous function of k_j . Now we take our coordinates so that there is only the component F_j of the field is different from zero. In this case, the partial derivative with respect to k_j gives the total differential of energy, so that we can integrate and obtain

$$\Delta x_j = \frac{\tilde{E}_f - \tilde{E}_i}{eF_j} = \frac{E_f - E_i}{eF_j} \quad 19-51$$

Now, nothing changes replacing \tilde{E} with E' , or E' , or the true $E(k)$. Therefore, as long as the equations of motion are consistently solved, there will be conservation of energy and the final point in real space will remain. Only the interpolating trajectory in real and reciprocal space change, which should be irrelevant if you satisfy some basic accuracy requirements. If the starting or ending or both points of the trajectory are not sampling points for the electron dispersion, there will be an error, which is related to the accuracy of the interpolation scheme. The previous treatment, however, is valid for any (non-infinitesimal) trajectory. Therefore, the energy-conservation error is limited to the local error on energy. It does not grow as the particle moves. Instead, the error goes back to zero whenever the particle touches a sampling point. The maximum violation of energy conservation is in practice when the maximum value of the error in the interpolation scheme.

The real difference between different schemes is now that more accurate interpolation is more difficult to integrate in real space. For example, another final point k'_f in Figure 19-10. The two interpolations give different final energies, which the more finely spaced is certainly closer to the true dispersion. But, integration of the simpler trajectory is trivial, whereas the finer interpolation requires breaking the trajectory into two linear segments. Nevertheless, both schemes are consistent. That is, the difference between initial and final energy is exactly the energy taken by the electric field. The finer scheme yields a lower energy because the average group velocity is higher. Therefore, the energy loss is larger. This scheme fails if we assume a constant group velocity (as it is likely to happen if we want a fast real-space trajectory algorithm), while the more coarse interpolation gives no error in this respect.

Of course, these arguments do not allow us to say anything about what happens to the components of velocity *transverse* to the field. The analysis guarantees conservation of energy or invariance of the trajectory in the direction of field, which is important from a physical standpoint. Although transverse motion is critical for real-space transfer (coupling between carrier energy and diffusion properties), you only need a basic requirement of group-velocity accuracy to ensure an accurate modeling of such phenomena.

Summarizing, we can conclude that:

- Any interpolation scheme is consistent and physically sound as long as a consistent real-space trajectory is calculated.
- A lower-order interpolation allowing exact integration in real space can be more accurate than a higher-order, hard-to-integrate method.
- A coarse-mesh scheme can be more accurate than one based on a fine mesh if an approximate method for integrating the equations of motion is used.

Interpolation Scheme Comparisons

Figure 19-11 compares the average error achieved with the tricubic and the trilinear schemes.

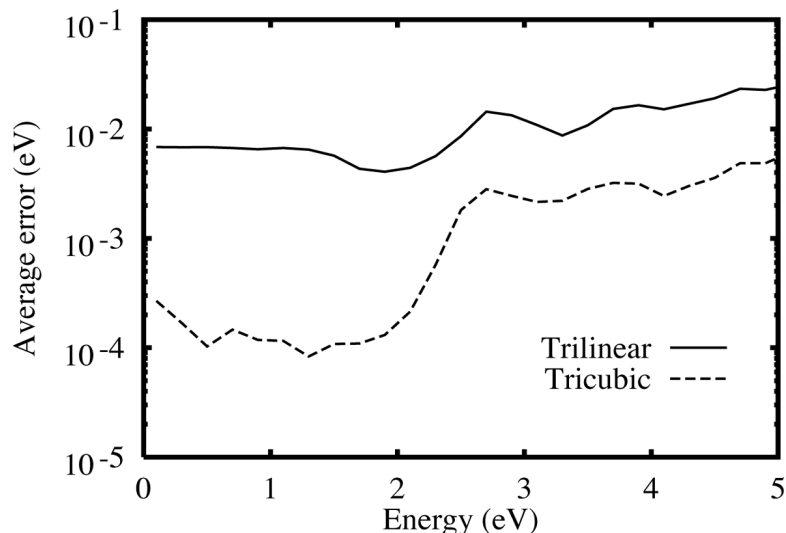


Figure 19-11: Tricubic vs. trilinear interpolation scheme, average error as a function of energy.

The averaging has been performed on the midpoints of all cubes making a 6281-point IW. The tricubic technique obviously performs much better than the simple trilinear scheme. The average error is often in the order of 0.1 meV vs. 5–10 meV for the trilinear interpolation. Figure 19-12 compares the maximum error instead of the average error.

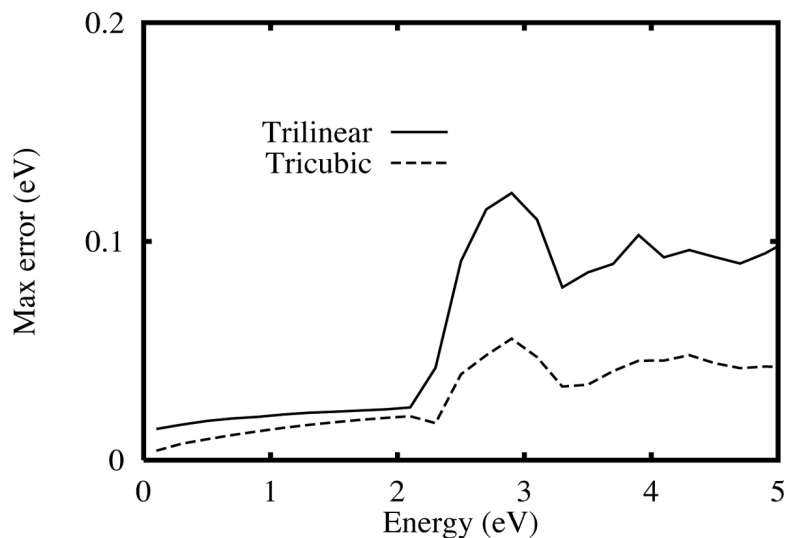


Figure 19-12: Tricubic vs. trilinear interpolation scheme, maximum error as a function of energy.

In the second case, the difference is not so marked. In fact, it may be argued, that a trilinear scheme with a finer mesh would give a smaller maximum error than the tricubic scheme. This fact is important since a Chebychev-norm constraint on the energy conservation is a good proof of physical robustness of the simulator. In any case, we see that the accuracy of both schemes drops dramatically at approximately 2.5 eV. This may be due to the presence of a sharp crossing between the second and third conduction band, which starts at about 2.3 eV. This crossing, however, occurs only on the Δ symmetry line. Therefore, it does not represent a serious limitation to either scheme.

To check the practical usefulness of the interpolation schemes, the same simulation has been performed in which carriers started at zero energy were accelerated by a field of 100 kV/cm. Acoustic inelastic scattering has been switched off, the temperature of intervalley phonons reduced to only 1 Kelvin, and collision broadening reduced by a factor of 20, so as to obtain a quasi-monoenergetic beam particles, but with a negligible probability of ballistic transport. Figure 19-13 shows the histogram of electrons at three points along this imaginary device (50, 100, and 150 nm). The deformation potential has been reduced accordingly to avoid an enormous scattering rate.

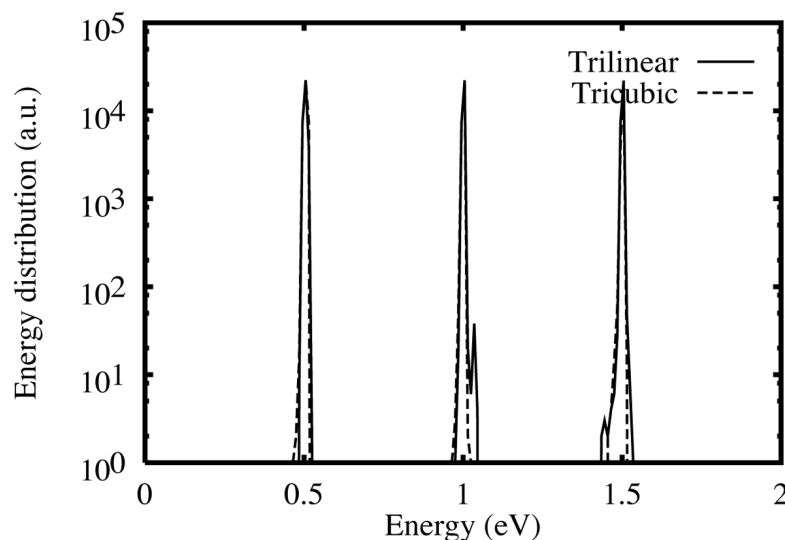


Figure 19-13: Monoenergetic beams of electrons simulated with both a trilinear and tricubic interpolation schemes.

The expected energies for the three beams are 0.5, 1.0, and 1.5 eV. It is evident that energy conservation is fully satisfied in both cases. Occasionally, only a few more electrons in the trilinear case are scattered to energies slightly above and below the expected value with respect to the tricubic case. This spread, however, is comparable with the “natural” spread due to collision broadening. In a real simulation, the broadening will be 20 times stronger and this effect will be irrelevant.

There are two problems that can occur with a simpler interpolation scheme. One, improper modeling of the transverse motion with respect to the electric field. Two, an error on the quantities which depend strictly on energy, notably the scattering rates. The first error is important for hot electrons when real-space transfer is a relevant phenomenon. The second error affects mostly regions of k -space where the scattering rate is a strong function of energy (i.e., the bottom of the conduction band). Figure 19-14 shows the various components of the room-temperature scattering rate at low energies (less than 100 meV).

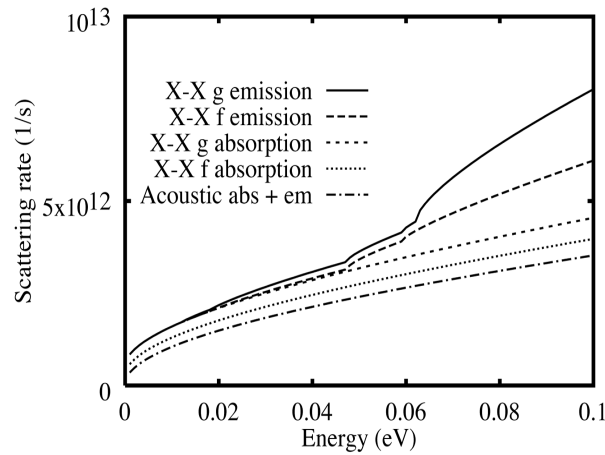


Figure 19-14: Low-energy scattering rate at 300 K.

The phonon-emission thresholds are clearly visible. At these critical points, we expect some inaccuracies of the trilinear scheme. But even for a smoothly varying scattering rate, a strictly linear interpolation for the energy can lead to some error in the time-dependent scattering rate. For example, if an electron starts a ballistic flight from the bottom of the first conduction band, its momentum increases linearly. Since the scattering rate is roughly proportional to the square root of the energy, which then is proportional to the absolute value of the momentum, we will expect the scattering rate also to increase linearly in time. But if in our linear interpolation scheme the electron energy is proportional to the wave vector, we have a linear increase in energy with time. Therefore, the scattering rate appears to grow as the square root of time. This was to be expected because we overestimated the energy during the flight and the scattering rate.

There is another class of problems that can arise with a linear interpolation for the electron dispersion. Since the algorithm for the choice of the final state uses a table of states sorted according to their energy, an electron after a scattering event will always have the exact energy as computed by the empirical-pseudopotential approximation. Generally, a tricubic scheme will give a very small error on the energy. Therefore, it can be considered as consistent with the final-state algorithm. The trilinear scheme, however, can lead to unphysical effects, such as the k -vector returned by the final-state routine can correspond, in the linear interpolation, to a very different energy. For example, an electron that moves after a scattering event under the effect of the electric field. After a first free flight, the interpolation routine is called to calculate the new energy to determine the next scattering event. In the linear scheme, though, the new k -vector can correspond to a very different energy from that assumed by the final-state algorithm. This can lead to an artificial gain or loss of energy because the final-state and the interpolation algorithms use two different energy dispersions. Therefore when using a trilinear interpolation, you want to use the same k -space discretization for the choice of the final state. That way, an electron will always be scattered to a node of the trilinear-interpolation mesh, where the interpolation error is zero.

In most MC DEVICE modeling tools including DAMOCLES [167] and MC DEVICE, an analytical approximation is used to increase the accuracy of the final-state selection at low energies, where the $k \cdot p$ nonparabolic expansion is valid. This unfortunately contrasts with the requirement of using the same grid for the selection of the final states and for interpolation of the dispersion relation. This problem can be overcome in two ways. One, by using a nonparabolic approximation for the E -to- k relation. Two, by using the discrete grid for the selection of final states.

Although the second way is simpler and more consistent, it reproduces the low-field transport parameters very poorly. If you adopt the second way, you cannot accurately model contact regions. Therefore, MC DEVICE uses the first way. Namely, MC DEVICE uses the non-parabolic approximation for the E -to- k relation.

The standard non-parabolic expression in the Herring-Vogt starred k -space is

$$E(1 + \alpha E) = \frac{h^2 (k^*)^2}{2m} = \beta \quad 19-52$$

$$E = \frac{\sqrt{1 + 4\alpha\beta} - 1}{2\alpha} \quad 19-53$$

and can be approximated to second order in β as

$$E = \beta - \alpha\beta^2 = \beta(1 - \alpha\beta) \quad 19-54$$

This approximation gives an error of less than 0.3 meV for all energies below 0.1 eV with respect to the full $k p$ formula and simultaneously it is very fast to compute. All the parameters (effective masses, non-parabolicity factor) have been derived directly from the pseudopotential calculation to avoid inconsistencies. Particularly, the non-parabolicity factor of 0.3 eV⁻¹ has been found to minimize the average error for all states below 0.1 eV instead of the more common value of 0.5 eV⁻¹. The average error is kept within 5 meV for all energies less than 0.1 eV and 1 meV for states below 0.05 eV. The minimum of the conduction band has been identified, for the form factors given in [49], exactly at 0.850031. This is particularly important because even a small asymmetry of the band causes large errors in the calculation of the effective masses. These have been determined as $m_c=0.194755$ and $m_v=0.912548$. Note that the perfect parabolic, symmetrical band is only valid for very small energies. For energies of the order of 1 meV, the asymmetry is such that an accurate estimate of the effective masses is impossible. In fact, the asymmetry effect has been found to be stronger than the non-parabolicity effect. The correction is applied to all particles below 0.1 eV after the trilinear interpolation has been performed. Execution profiles show that this method increases the total time spent on the interpolation by only 20%, still ensuring low-temperature and low-field accuracy. For example, the diffusion coefficients (a stringent test for low-field mobility) are correctly reproduced both at 300 Kelvin and at 77 Kelvin. Since the trilinear interpolation is used only as a rough check to separate high-energy from low-energy particles, the accuracy of the low-field behavior is semi-dependent on the k -space mesh step. A small error, of the order of 10% on the diffusion coefficient, is obtained for a very coarse mesh with just 40 points on Γ -X for both final states and interpolation.

19.7.4: Coulomb Interaction

Types of Coulomb Interaction

Modeling the intrinsically three-dimensional Coulomb interaction by a two-dimensional simulation requires some care to conserve the main physical features of the system. Screening must be accounted for first. In a non-degenerate situation, we can think of screening as an exponential decay of the effective interaction potential, according to the space-dependent screening factor:

$$\beta_s^{-2} = \frac{\varepsilon(k_B T_e / e)}{en} \quad 19-55$$

where T_e is the effective temperature of the carriers and n is their concentration. This picture holds up to plasma frequencies. For higher frequencies, the ensemble of carriers will not follow the perturbing potential quickly enough and anti-screening or no screening will occur.

To check the validity of the screening model from a thermodynamical point of view, the plasma frequency must be compared with the power spectrum of the carrier velocity. The auto-correlation of velocity extends up to about the frequency $S/2\pi$, where S is the scattering rate. For thermal carriers, this frequency is of the order of 10^{12} Hz. The plasma frequency ranges from 2×10^{12} Hz for $n=10^{17} \text{ cm}^{-3}$ to about 10^{14} Hz for $n=3 \times 10^{20} \text{ cm}^{-3}$. Within this range of concentrations, you can assume all interactions as screened. For lower concentrations, part of the power spectrum will remain unscreened. In these cases, however, the microscopic Coulomb interactions can usually be neglected when compared to the macroscopic electric field. Moreover, the screening length is so large (13 nm at $n=10^{17} \text{ cm}^{-3}$) that unscreened interaction will occur in any case over a significant distance.

The general idea is to separate Coulomb interaction into two classes:

- **Short-range Coulomb interaction:** This occurs within a screening length. Since the wave packets representing the electrons can be assumed as overlapping, a simple space-homogeneous theory based on Bloch functions can be used to estimate the scattering rate for a given electron concentration. Given the average electron density, you can compute the full three-dimensional scattering probability per unit time. Screening of the Coulomb perturbation potential is included in the calculation if necessary. Electron-electron scattering is applied to carriers within a screening length in the two-dimensional simulation. The effect of short-range interaction is an exchange of energy between carriers. The position of the particles is not changed. Therefore, the potential energy remains constant and ensemble modes are not affected.
- **Long-range Coulomb interaction:** We can assume that beyond a few screening lengths, no interaction between single carriers occurs. Carrier-carrier is ineffective on these length scales because screening attenuates exponentially the mutual force. But, the perturbation has a large effect on the entire ensemble of carriers. In other words, beyond a screening length the individual carrier no longer sees other isolated carriers but rather a plasma. The long-range interaction is thus basically an exchange of energy between a single carrier and the particle-field ensemble system.

You can model the cutoff between short-range and long-range interactions by choosing a Poisson-mesh spacing equal to the local screening length [136]. Assuming that the short-range interactions are correctly represented by a two-particle scattering rate, there remains the problem of representing the 3D electron-plasma interactions in a 2D model. The most physical approach that can be followed is the conservation of collisionality in the system.

Discretization and Collisionality

The long-range interaction can be pictured as exchange of energy between the single particles and the plasma modes. The latter are correctly modeled by a fine representation of the continuous plasma. Particularly, the mesh spacing must be fine enough to represent plasma modes that suffer Landau damping. The required maximum spacing is

$$h_{Landau} = \frac{v_{th} T_p}{2} \quad 19-56$$

where v_{th} is the thermal energy and T_p is the plasma period. For example, for $v_{th}=2 \times 10^7$ cm/s and $T_p=10^{-13}$ s, we have $h_{Landau}=1$ nm. But, the thermal agitation of the carriers depends on the granularity of the simulation (i.e., each computational particle represents a physical energy E_{3D} equal to its “computational energy” E_{2D}) times the number of carriers per unit length s that it represents. No perfect mapping is possible between a completely 2D model and a completely 3D physical system as the density of states for collective modes changes also with dimensionality. As a basic constraint, we can try to preserve the collisionality of the system. For systems of low collisionality, the kinetic energy of carriers dominates over the potential energy, and interaction with plasma modes does not change it very much. For systems at thermal equilibrium, the collisionality is given by the number of carriers within a Debye sphere. This quantity is roughly conserved in the transition between 2D and 3D if

$$s = \beta_s \quad 19-57$$

This condition ensures that if Coulomb interaction is negligible in the physical system, it will also be in the 2D model and vice versa. Coupling between single carriers and collective modes will thus be qualitatively modeled. This criterion also minimizes the difference in short-range Coulomb interaction with respect to the 3D case [136]. It must be observed that a higher weight implies a higher physical kinetic energy, so that large particles will heat the plasma sea more than small particles. If all particles have the same size, the system will reach thermal equilibrium. If particles of different weights are plasma-coupled, there will be a transfer of energy from the large particles to the small particles.

Collisionality in Silicon Devices

The critical carrier concentration above, which an uniform sample of silicon is collisional, can be obtained as:

$$n \frac{4}{3} \pi \beta_s^{-3} = \frac{4}{3} \pi \left(\frac{\epsilon k_L / e}{e} \right)^{3/2} \frac{1}{\sqrt{n}} = 1 \quad 19-58$$

$$n = \frac{16 \pi^2}{9} \left(\frac{\epsilon k_L}{e} \right)^3 = 8 \times 10^{16} \text{ cm}^{-3} \quad 19-59$$

You see that basically all electron concentrations with some significant conductivity (such as contact regions) give rise to collisional systems. Several remarks can be made on this result.

First, the collisionality criterion is correct for systems at thermal equilibrium. Hot carriers, of course, will be much less sensitive to plasma interactions. Some corrections, however, can be expected in the position of the high-energy tails, especially when the important effects are very sensitive with respect to energy (e.g., impact ionization, oxide injection). Therefore, the collisionality rule retains validity even for very high fields. In other terms, the comparison between kinetic and potential energy becomes a comparison between the lattice vibration energy and potential energy (i.e., marks the separation between dominant electron-phonon or electron-plasma (plasmon) interaction).

Talking about plasmons, for high carrier concentrations the plasmon energy becomes significant and quantization effects cannot be neglected. Since all plasma modes have the same frequency, this problem cannot be solved by removing some modes and Poisson-modeling the others.

For collisional systems there is less than one carrier within a screening sphere, which means that screening is statistical in nature and cannot be represented as a continuous distribution of carriers “filling up” the perturbing potential.

Another issue is the strict locality of the collisionality rule. Since the screening length is a function of position, no unique scaling factor will preserve collisionality for the entire system, and the transverse size of the device must be imagined as “shrinking” and “widening.” More importantly, it will be impossible to model correctly TRUE long-range effects between regions with different doping. For example, the plasma modes in the highly-collisional contacts might couple to the hot electrons in the channel more effectively than the weak, low-frequency channel modes. In this case, the same statistical weight should be used for channel and drain electrons. Finally, there remains an open question whether the transverse plasma modes can be qualitatively different from their projection on the simulation plane.

The Collisionality Criterion

We start from the Bogoliubov, Born, Green, Kirkwood, and Yvon (BBGKY) hierarchy of transport equations, which relates each n -particle distribution function f_n to itself and to f_{n+1} . The first equation is

$$\frac{\partial f}{\partial t} + (\mathbf{v}_g \cdot \nabla_{\mathbf{r}} f) + \frac{1}{\hbar} \int d\mathbf{x}' d\mathbf{k}' F_{12} \nabla_{\mathbf{k}} f_2 = \left(\frac{\partial f}{\partial t} \right)_{scat} \quad 19-60$$

The collision term can be written as follows:

$$f_2(\mathbf{x}, \mathbf{x}') = f_1(\mathbf{x})f_1(\mathbf{x}') + g(\mathbf{x}, \mathbf{x}') \quad 19-61$$

Of course, the problem is minimized if short-range correlations can be neglected. In other words, if g is small with respect to the average-interaction term and to the collision term. The low-collisionality criterion can be considered in the following ways:

- **Absence of short-range correlation:** This is obtained if short-range interaction is smoothed out by solving Poisson's equation on a very coarse mesh. Particles do jerk around but plasma modes are unaffected. Of course, if $g=0$, particles “see through” each other.
- **Competition between phonon bath and e-e coupling:** Controls all correlations if scattering term is very strong because it will dominate both kinetic energy (by absorption/emission) and potential energy (by momentum relaxation). This happens when the thermal agitation energy is much larger than the interaction potential energy.
- **Kinetic vs. Potential Energy:** Same as above. Leads to the classical Debye-sphere criterion.
- **Energy of plasma modes:** Kinetic energy scales with the mass. Equipartition assigns the same amount of energy to all degrees of freedom. If particles are small enough, plasma modes will receive (and store) very little energy, and plasma-mediated exchange will be small.

General Scattering Statements

There are two MC DEVICE statements that apply to all scattering events. FINAL sets parameters dealing with computation of final states. SEREGION defines the boundary for scattering estimation.

```
FINAL NK=40 FORMAT=0 N=100 FILE="name" CUTOFF=0.0
```

Final states are tabulated along with band structure in the \$MOCA/lib directory. The default final states file is eord100_*.in. The * represents the number of conduction bands chosen to be used in BANDS (4 by default). See Section D.2.7: "Band Structure Input Files" for a description of these files. NK sets the number of points on the Gamma-X line. The default is 40 and the pre-calculated tables use 40 points. To use another value, you need to calculate new bandstructure data. FORMAT selects ASCII or binary (0 or 1) as the format of the final states file. The default is 0 for ASCII. n sets the number of final states points. The default is 100. Again, the tabulated data is based on the default values and setting a new value will require recalculation of bandstructure data. CUTOFF is to set the cutoff used for Lorentzian broadening, the default value is 0.0. To turn scattering estimation ON, insert the statement SEREGION in your input file.

```
SEREGION BOUNDP=(x1,x2,y1,y2)
```

The SEREGION statement defines the region over which scattering estimators are turned on. Generally, you can set the boundaries as equal to the boundaries of the entire device using the BOUNDP parameter (see "Regions" on page 19-17). Again, a BOUND parameter is provided for backward compatibility.

19.7.5: Phonon Scattering

Phonon Modes

The scattering rates used in MC DEVICE are based on the energy dependent models first proposed by Jacoboni and Reggiani [107]. Both inelastic acoustic phonon modes and optical phonon modes are included to produce physical drift velocity versus field results. A wave vector dependent scattering was not implemented because the empirical models produced more physical results.

The derivation for the phonon scattering rates below is taken from [107]. The deformation potential method follows as

$$H' = E \frac{dy}{dr} \quad 19-62$$

where dy/dr is the deformation of the lattice due to phonons and E is the tensor that describes the shift in the electron band per unit deformation.

Let us define phonon absorption and emission vectors respectively.

$$q = k' - k + G \quad 19-63$$

$$q = k - k' + G \quad 19-64$$

This fact states the conservation of crystal momentum from the point of view of the crystal subsystem. For phonon creation (a_q) and annihilation (a_{-q}), the phonon densities for absorption and emission respectively are:

$$|\langle k' | a_q | k \rangle| = N_q \quad 19-65$$

$$|\langle k' | a_{-q} | k \rangle| = N_q + 1 \quad 19-66$$

where N_q is the phonon number.

Finally, Fermi's Golden Rule can be applied to obtain final transition probabilities that can be applied to all scattering mechanisms.

$$P(k, k') = \frac{\pi}{\rho V \omega_q} \binom{N_q}{N_q + 1} G |\mathfrak{I}_{ij} q_j \xi_i|^2 \delta[\varepsilon(k') - \varepsilon(k) \mp \hbar \omega_q] \quad 19-67$$

Acoustic Phonons

For a non-degenerate band at the center of the Brillouin zone, the deformation potential, \mathfrak{I} , is diagonal and can be treated as a scalar. This simple situation, energy, and momentum conservation imply

$$q = \mp 2 \left(k \cos \theta - \frac{m^* u_l}{\hbar} \right) \quad 19-68$$

where u_l is the longitudinal velocity of sound, m^* is the effective of an electron, θ is the angle between k and q , and the + and - are for emission and absorption respectively. The second term above is the correction for the phonon involved in the scattering event. Therefore, for an elastic event, the equation will just be

$$q = \mp 2 k \cos \theta \quad 19-69$$

One important observation to make when tying this into a simulation is that when collisions are assumed elastic, the energy distribution is also assumed to be Maxwellian. Generally, this assumption is FALSE and cannot be used in Monte Carlo simulation. But, the only case when this assumption does not hold is for low fields and temperature. At high fields and high temperature, acoustic phonon scattering can be assumed to be elastic and is the same as optical phonons.

For realistic band structures, there will be separate probabilities for longitudinal and transverse modes. But the anisotropy is small and can be neglected by averaging the velocity of sound over the two directions as

$$u = \frac{1}{3} (2u_t + u_l) \quad 19-70$$

The form of the final scattering probabilities are the same for inelastic acoustic phonon scattering. The main addition is that the δ function has phonon energy in it.

Keeping the same isotropic approximation for deformation potential coupling and using the Herring-Voigt transformation on k and q vectors, the magnitude of q becomes

$$q = q^* \left(\frac{m_l}{m_0} (\cos \theta^*)^2 + \frac{m_t}{m_0} (\sin \theta^*)^2 \right) \quad 19-71$$

$$q \left(\frac{m_l}{m_0} \right)^{1/2} \approx \left(\frac{m_l}{m_0} \right)^{1/2}, \quad 19-72$$

where θ^* is the angle between k^* and the principal axis of the valley. This approximation is sufficient for Silicon.

Optical Phonons

For optical modes, the perturbation Hamiltonian to the lowest value of approximation is assumed to be proportional to the atomic displacement cite [107]. The continuous medium approximation from long-wavelength acoustic phonons would be inconsistent for optical modes. The scattering probability can be written by substituting an optical coupling constant, D , for potential. The energy associated with intravalley transitions can be assumed to be constant and given by $\hbar\omega_{op} = k_B\theta_{op}$ where θ_{op} is the temperature of optical phonons. The resulting probability becomes

$$P(k, k') = \frac{\pi(D_t K)^2}{\rho V \omega_{op}} \left(\frac{N_{op}}{N_{op} + 1} \right) \delta[\varepsilon(k') - \varepsilon(k) \mp \hbar\omega_{op}] \quad 19-73$$

where N_{op} is replaced by $N_{op} + 1$ for emission. Note there is no angular dependence and therefore scattering is isotropic.

For the final state, it is random with constant probability over the energy-conserving sphere of k^* .

Intervalley Scattering

Electron transitions between states in two different equivalent valleys can be induced by both acoustic and optical phonons.

The phonon wave vector q involved in the transition remains close to the distance between initial and final minima, even for high electron energies. So the change in momentum and frequencies are approximately constant. Therefore, this scattering mechanism is treated exactly like intravalley scattering by optical phonons.

The coupling constant, $(D_t K)^2$, depends on the types of valleys involved in the scattering event and the branch of phonons involved.

In the case that electron energies are high and the particles can move up to bands of higher energy, the appropriate Δk in the first Brillouin zone must be considered along with the change in kinetic energy of the electron.

The integrated scattering probability for intervalley scattering is then

$$P_i(\varepsilon) = \frac{(D_t K)^2 m^{3/2} Z_f}{\sqrt{2} \pi \rho h^3 \omega_i} \left(\frac{N_i}{N_i + 1} \right) (\varepsilon \mp \hbar\omega_i - \Delta\varepsilon_{fi})^{1/2} \quad 19-74$$

where Z_f is the number of total number of final equivalent valleys for the scattering in consideration, N_i is the phonon number, and $\Delta\varepsilon_{fi}$ is the energy difference between the bottoms of the initial and final valleys.

Hole Intraband Scattering

There are both acoustic and optical types of this scattering for holes as there is for electrons. Due to the complexity of the valence band structure, use three deformation potential parameters. The characteristic wave function of holes also introduces an overlap factor.

To overcome analytical difficulties without losing the physics, use one coupling constant instead of the three deformation parameters. For a warped band, the resulting scattering probability is similarly to the electron acoustic scattering case.

$$P(k, k') = \frac{\pi q E^2}{\rho V u} \binom{N_q}{N_q + 1} \frac{1}{4} (1 + 3(\cos \theta)^2) \delta[\varepsilon(k') - \varepsilon(k) \mp \hbar q u] \quad 19-75$$

Here, E is the coupling constant, and θ is the angle between k and k' . A numerical method is used to solve this integral in MC DEVICE.

For optical hole intraband scattering, the rate can be described with one deformation potential parameter and has been found to be isotropic [107].

The integrated probability is then

$$P(k, k') = \frac{3\pi d_0^2}{2\rho V \omega_{op} a_0^2} \binom{N_q}{N_q + 1} \delta[\varepsilon(k') - \varepsilon(k) \mp \hbar \omega_{op}] \quad 19-76$$

where d_0 is the deformation potential parameter. The resulting energy dependence of the final equation is analogous to that for optical scattering of electrons.

Hole Interband Scattering

When a multi-band model is considered, scattering rates should be used to account for the scattering (transitions) between the bands. In MC DEVICE, only two bands (the heavy and light hole bands) of the three-bands hole scattering model are used. Since the calculations for the heavy-to-light and light-to-heavy interband scattering rates are somewhat complex, these rates are approximated by setting heavy-to-light rate equal to the light-to-light acoustic rate and by setting the light-to-heavy rate equal to the heavy-to-heavy acoustic rate. The file `scat.out` contains scattering rates for all possible processes. Any rates not calculated in MC DEVICE (such as those involving the split-off band) are set to 0.0.

Density-of-States Scaling

The calculation of density of states is a basic ingredient of any bulk-band Monte Carlo transport model to compute scattering rates and probabilities of final states. The density of states including both spin directions is

$$N(E) = \frac{1}{V_R} \left(\sum_{n, k' \in BZ} \delta[\varepsilon(k') - E] \right) \quad 19-77$$

where n is the band index. The sum is over all cubes/tetrahedra in all bands. It is assumed that the energy $\varepsilon(k)$ is known at the corners of whatever shape is used to discretize the Brillouin zone (BZ).

Final State Selection

In MC DEVICE, final state selection is based on the energy as opposed to being based on the momentum (or wave vector). To accomplish this, a relation for $k(E)$ is obtained. Since the bandstructure is stored in a table that is ordered by the wave vectors (k values). A final state table can be obtained by reordering the bandstructure table by energies, E .

The uncertainty principle is satisfied in MC DEVICE by broadening the energy using the imaginary part of the self-energy (i.e., $(\hbar/(2\tau))$) and not using a one-to-one relationship between k and E . For each final energy, there are a range of final energies (and a corresponding range of momenta) that may be selected. Therefore, there is uncertainty in the momentum of the electron after a scattering event in accordance with the uncertainty principle.

Using Scattering Parameters

At the beginning of the simulation, scattering rates are either calculated or are loaded from data files. In either case, the scattering rate table is written to `scat.out`. The manner of obtaining the scattering rates and the number and type of the mechanisms, depends on whether the strain model is on (`TYPE=1|TRUE|YES` on the `mmat` statement) and whether the `TYPE=ANALYTIC` or `TYPE=FULLBAND` is used on the `ESCAT` statement. Below is a description of its contents of the `scat.out` file. Table 19-2 is for electrons and holes when the strain model is off or when the strain model is on and `TYPE=ANALYTIC`. Table 12-2 is for electrons when the strain model is on and when `TYPE=FULLBAND` on the `escat` statement.

| Table 19-2. Form of scat.out (strain model off or TYPE=ANALYTIC) | | |
|--|-----------------------|-----------------------|
| Column | Format when CARRIER=E | Format when CARRIER=H |
| 1 | Energy | Energy |
| 2 | Total | Total |
| 3 | Ac abs | h-h AC abs |
| 4 | Ac emi | h-h AC emi |
| 5 | XX f abs (Tp=TF1) | l-l AC abs |
| 6 | XX f abs (Tp=TF2) | l-l AC emi |
| 7 | XX f abs (Tp=TF3) | s-s AC abs |
| 8 | XX g abs (Tp=TG1) | s-s AC emi |
| 9 | XX g abs (Tp=TG2) | h-h OP abs |
| 10 | XX g abs (Tp=TF3) | h-h OP emi |
| 11 | XX f emi (Tp=TF1) | l-l OP abs |
| 12 | XX f emi (Tp=TF2) | l-l OP emi |
| 13 | XX f emi (Tp=TF3) | s-s OP abs |
| 14 | XX g emi (Tp=TG1) | s-s OP emi |
| 15 | XX g emi (Tp=TG2) | h-l Interband |
| 16 | XX g emi (Tp=TG3) | l-h Interband |
| 17 | XL abs (Tp=TL1) | h-s Interband |

Table 19-2. Form of scat.out (strain model off or TYPE=ANALYTIC)

| | | |
|----|------------------|------------------|
| 18 | XL abs (Tp=TL2) | s-h Interband |
| 19 | XL abs (Tp=TL3) | l-s Interband |
| 20 | XL abs (Tp=TL4) | s-l Interband |
| 21 | XL emi (Tp=TL1) | Ionized impurity |
| 22 | XL emi (Tp=TL2) | Impact ioniz. |
| 23 | XL emi (Tp=TL3) | |
| 24 | XL emi (Tp=TL4) | |
| 25 | Ionized impurity | |
| 26 | Impact ioniz. | |

Table 19-3. Form of scat.out (strain model on and TYPE=FULLBAND)

| Column | Format when carrier=e |
|--------|-----------------------|
| 1 | Energy |
| 2 | Total |
| 3 | Longitudinal AC abs |
| 4 | Longitudinal AC emi |
| 5 | Transverse AC abs |
| 6 | Transverse AC emi |
| 7 | OP abs |
| 8 | OP emi |
| 9 | Impact ioniz. |

The statements relating to phonon scattering deal with both acoustic (AC) and optical (OP) types, X-L and X-X, and f and g types of scattering events. The abbreviations abs and emi refer to absorption and emission. The abbreviations h, l, and s refer to heavy, light, and split-off. Tp refers to the phonon temperature, which can be one of 3 values for f-type and g-type transitions and one of 4 values for X-L transitions.

Acoustic scattering parameters are set by the AC statement as

```
AC DEFO=0.0
```

where DEFO is the desired deformation potential in [eV]. The default value is 9.0 eV. Optical, or high energy, phonon scattering is characterized by the PHON statement as

```
PHON ETH=0.0 MODEL=0 FILE="name"
```

where ETH is the energy threshold, in [eV], to activate this type of scattering. MODEL chooses which scattering model to use.

Currently, the only model implemented in MC DEVICE is model=0 (Tang model). FILE chooses the density of states file. The default is dos_c.in, which is located in the \$MCDEVICEDIR directory.

The intervalley scattering statements XL, XXF, and XXG set phonon temperatures and deformation potentials. The default values have been determined experimentally for silicon. As shown above, 4 values are used for X-L transitions and 3 values are used for f and g-type X-X transitions.

```

XL   TEMP=(672.0,634.0,480.0,197.0)  DEFO=(2e8,2e8,2e8,2e8)
XXF  TEMP=(220.0,550.0,685.0)         DEFO=(3e7,2e8,2e8)
XXG  TEMP=(140.0,215.0,720.0)         DEFO=(5e7,8e7,11e8)

```

19.7.6: Impurity Scattering

For all materials, the lattice sites are many thousands of times heavier than electrons. Therefore, impurity scattering is essentially elastic in nature. Therefore, for the energy distribution to match reality, it must be accompanied by some dissipative mechanism.

The Brooks and Herring approach from [107] is described below.

For an ionized impurity, the scattering source is a screened Coulomb potential. The potential can be represented by a simple decaying exponential as

$$V(r) = \frac{Ze^2}{\kappa r} \exp(-\beta_s r) \quad 19-78$$

where β_s^{-1} is the screening length, κ the dielectric constant, and Z the number of charge units in the impurity. The Debye formulation for nondegenerate statistics gives

$$\beta_s = \left(\frac{4\pi e^2 n_0}{\kappa k_B T} \right)^{1/2} \quad 19-79$$

where n_0 is the free carrier density.

The Fourier transform of a screened Coulomb potential is given by

$$\begin{aligned} H(q) &= \frac{1}{(2\pi)^{3/2}} \int V(r) \exp(-iq \cdot r) dr \\ &= \frac{\sqrt{2}Ze^2}{\sqrt{\pi\kappa}} \frac{1}{\beta_s^2 + q^2} \end{aligned} \quad 19-80$$

and leads to a scattering probability per unit time of

$$P(k, k') = \frac{2^5 \pi^3 Z^2 n_{le}^4}{\hbar V \kappa^2} G \frac{1}{(\beta_s^2 + q^2)^2} \delta[\varepsilon(k') - \varepsilon(k)] \quad 19-81$$

where G is the overlap integral.

For electrons we can look at the case for spherical, parabolic bands or ellipsoidal, non-parabolic bands.

For the first case, G is 1, and multiplying by the density of states $V/(2\pi)^3$ we get

$$P_{e,l}(\varepsilon) = \frac{2^{5/2} \pi n_l Z^2 e^4}{\kappa^2 \varepsilon_\beta^{1/2} m^{1/2}} \frac{\varepsilon^{1/2}}{1 + 4\varepsilon/\varepsilon_\beta} \quad 19-82$$

where

$$\varepsilon_{\beta} = \frac{\hbar^2 \beta_2^2}{2m} \quad 19-83$$

For non-parabolic bands, The Herring-Voigt model is used. The results are given as

$$P_{e,I}(\varepsilon) = \frac{2^{5/2} \pi n_I Z^2 e^4}{\kappa^2 \varepsilon_{\beta}^{1/2} m_d^{1/2}} \frac{1 + 2\alpha\varepsilon}{1 + 4 \frac{\gamma(\varepsilon)}{\varepsilon_{\beta}'}} \quad 19-84$$

where

$$\varepsilon_{\beta}' = \frac{\hbar^2 \beta_2^2}{2m_d} \quad 19-85$$

There are also two cases to account for impurity scattering of holes. There is the spherical parabolic band case and the warped band case. For the parabolic band, we can adapt the general scattering probability given above by accounting for the overlap factor. This gives

$$P(k, k') = \frac{2^5 \pi^3 Z^2 n_I e^4}{\hbar V \kappa^2} \frac{0.25(1 + 3 \cos^2 \theta)}{(\beta_s^2 + q^2)^2} \times \delta[\varepsilon(k') - \varepsilon(k)] \quad 19-86$$

and finally integrating over the solid angle we arrive at

$$P_{h,I} = \frac{2^{5/2} \pi n_I Z^2 e^4}{\kappa^2 \varepsilon_{\beta}^2 m^{1/2}} \frac{\varepsilon^{1/2}}{1 + 4\varepsilon/\varepsilon_{\beta}} F_{ov} \quad 19-87$$

where F_{ov} is the overlap factor. The overlap factor essentially works to reduce the efficiency of the impurity scattering mechanism and can be found in [107].

We will neglect the warped band case because it can be neglected as long as the warping is small. For treatment of the case, see [107].

Implementation of Impurity Scattering

In MOCA, the Ridley impurity scattering model is implemented. The scattering rate is calculated as follows:

$$\frac{1}{\tau_{\text{imp}}} = \frac{\sqrt{\frac{2\gamma}{m^*A}}}{1 + 2\alpha E} \times 1 - \exp \left[-\frac{ae^2 m^* k_B T (1 + 2\alpha E)}{8\pi\epsilon\hbar^2 \gamma \left(1 + \frac{Ne^2 \hbar^2}{8\epsilon m^* k_B T \gamma} \right)} \right] \quad 19-88$$

Final state selection is for the Ridley model are calculated including the factor 2π from Chandrashekar.

$$\begin{aligned} F_1 &= \frac{e^2 m_d k_B T}{8\pi^2 \epsilon \hbar^2 N} \\ F_2 &= \frac{Ne^2 \hbar^2}{8m_d \epsilon k_B T} \\ F_3 &= \frac{-2\pi^2 N^2}{3} \end{aligned} \quad 19-89$$

These factors are used in density of states scaling. See Section “Impact Ionization and other topics” for more information.

MOCA includes the option to modify Ridley parameters using the RIDLEY statement.

```
RIDLEY SCALE=1.0 TSTEP=n
```

Here, SCALE is a scaling factor. TSTEP is the simulation time step where to update the concentration.

Impact Ionization and other topics

The other impurity-related scattering statements are: IMPACT, SSPARAM, SSREGION, TRACKSCAT, TRAJ, and ZSREGION. These are described below.

The IMPACT statement is for impact ionization.

```
IMPACT MODEL=0|1|2|3 PARAM=(i,j,k) ETH=(E1,E2,E3) \
  WEIGHT=NO FINAL=YES sec=NO CSEC=NO \
  START=1000 RANDSEC=NO RESPOS=(min,max)
```

The models for impact ionization that are available are KELDYDYSH (0), BUDE (1), KANE (2), and CARTIER (3). PARAM allows you to specify parameters for 3 terms in the rate. You can set three threshold energies with ETH corresponding to the three parameters in PARAM.

Here are the following parameters:

- 1 = eta
- 2 = e-field in x-direction
- 4 = carrier concentration
- 5 = carrier velocity
- 7 = energy
- 8 = impact ionization rate
- 9 = generation

WEIGHT either sets weighting off or doubles weighting. FINAL determines whether to set final energy of the initial particle to zero (NO) or 1/3 of its starting energy (YES). SEC toggles generation of secondary particles, and CSET does the same for complimentary secondary particles. START defines a transient period at the start of the simulation during which impact ionization is not to be calculated. RANDSEC chooses whether to randomly place secondary particles. RSPOS defines a range over which to place these particles (min and max from the location of the ionized impurity scattering event).

SSREGION and SSPARAM statements are for surface scattering.

```
SSPARAM SEXPL=i SEXPD=j SSFIELD=n FILE="name" SURPHON=(p,e)
```

SEXPL and SEXPD are factors used in calculating surface scattering. The default values are set for best fit with experimental mobility data.

SSFIELD is the global surface scattering field. You can choose the output file using FILE. Finally, SURPHON sets the prefactor and power for surface scattering calculations.

The TRACKSCAT statement is for outputting scattering estimators to a file called trackscat.out.

```
TRACKSCAT BOUNDP=(x1,x2,y1,y2) DIR=(x,1)
```

As with all statements, BOUNDP defines the boundaries over which to track scattering (see “Regions” on page 19-17). Again, a BOUND parameter is provided for backward compatibility. DIR sets the direction and the dimensionality of the tracking.

The TRAJ statement tracks the trajectories of particles.

```
TRAJ MODE=0 ZEROSCAT=NO BOUNDP=(x1,x2,y1,y2)
```

By including this statement, MOCA outputs a file called traj.out. MODE toggles this feature on and off. A value of 0 turns the feature OFF. Setting it to be 1 tracks particle trajectories and sets them to be initially evenly distributed in the bound box. Setting the value to 2 sets the feature ON and writes all the detailed information. ZEROSCAT chooses whether to zero the scattering rates in the simulation. Finally, BOUNDP determines the region where to track particle trajectories (see “Regions” on page 19-17). A BOUND parameter, which uncharacteristically takes arguments of position in cm is provided for backward compatibility.

The ZSREGION statement enables you to turn scattering off within more or more rectangular regions.

```
ZSREGION BOUNDP=(x1,x2,y1,y2)
```

The BOUNDP parameter contains the boundaries of the region, as on the REGION statement (see “Regions” on page 19-17). Again, a BOUND parameter is provided for backward compatibility.

19.7.7: Tunneling

No clear knowledge exists to date on the transmission mechanism from silicon into silicon dioxide. In principle, the full quantum problem should be approached, solving the Schrödinger equation for the given arrangement of silicon and oxygen atoms. The large number of unknown parameters in this problem has so far made this approach unfeasible. We will briefly illustrate two possible approaches to an analysis of the phenomenon, which rely on simple relationships between the silicon and silicon dioxide band structures.

Conservation of Parallel Momentum

The first approach, widely used in the literature, relies on all the following assumptions:

- **Conservation of parallel momentum:** The in-plane (or parallel) component, $k_{||}$, of the wave vector remains unchanged in the transition from Si to SiO₂ [126]. This corresponds to assuming that the band structure remains consistent in the transition, so that the interface can only supply an out-of-plane (normal) momentum. This hypothesis is sensible if a 10–20 Angstrom epi-oxide layer exists and if no significant image-force lowering of the potential barrier occurs. Thus, the epi-oxide layer can be thought as an extension of the Si lattice with a thin, abrupt dipole causing a discontinuity in the band edge.

Since the band structure of the epi-oxide is unknown, carrier tunneling through the epi-oxide must be analyzed by considering only the single, direct conduction band of amorphous SiO₂.

- **Conservation of energy:** We assume a sharp discontinuity of E_B in the potential energy between Si and SiO₂:

$$E_{ox}(0^+) = E_{Si}(0^-) - E_B \quad 19-90$$

In a sense, this hypothesis, combined with the previous one, implies a “disappearing” of all Si bands except the fourth conduction band, starting at 3.1 eV.

- **Isotropic dispersion in the oxide:** The dispersion relation in SiO₂ is assumed:

$$E_{ox} = \frac{\hbar^2}{2m_{ox}}(k_x^2 + k_y^2 + k_z^2) \quad 19-91$$

Again, this may not be a good approximation for the strained crystalline-oxide layer that we are considering. Since the parallel momentum is assigned, we obtain the normal momentum in the oxide as $k_{ox\perp}$:

$$k_{ox\perp}(x) = \sqrt{\frac{2m_{ox}E_{ox}(x)}{\hbar^2} - (k_{Si\parallel})^2} \quad 19-92$$

For simplicity, we assume a parabolic (non-Franz) dispersion with equal effective masses for both propagating and evanescent states. We note that for “true” tunneling states ($E_{ox} < 0$) both terms inside the square root are negative. The parallel-wavevector conservation can force some extent of tunneling even if the states have energies above the barrier ($E_{ox} > 0$).

- **WKB approximation:** The transmission coefficients should in principle take into account the discontinuity in the band structures (i.e., the overlap integrals between Tamm states in the silicon and the oxide). We do not have this information, however, we extend the consistent-lattice approach and we assume that no further reflection is due to the discontinuity in band structure. The error level is now so high that using the WKB approximation will do no harm to the results. Although for energies close to the top of an abrupt barrier, the WKB formula can lead to large errors. In any case, we use a modified version of the WKB formula that joins smoothly with a transmission coefficient of 1 for non-tunneling states:

$$T = \exp\left(2i \int_{x_1}^{x_2} k_{ox\perp}(x) dx\right) \quad 19-93$$

where x_1 and x_2 are the two classical inversion points where $k_{ox\perp} = 0$.

- **Constant field in the oxide:** This amounts to evaluating Equations 19-91 with $E_{ox}(x) = E_{Si}(0) - E_B + eF_{ox}x$.

This evaluation yields:

$$x_1 = 0 \quad 19-94$$

$$x_2 = \frac{1}{eF_{ox}} \left(E_B - E_{Si} + \frac{\hbar^2 (k_{Si\parallel})^2}{2m_{ox}} \right) \quad 19-95$$

$$k_{ox}^{\perp} = \sqrt{\frac{2m_{ox}^*}{2}(E_{Si} - E_B + eF_{ox}x) - (k_{Si}^{\parallel})^2} \quad 19-96$$

The result is

$$T_1 = \exp \left[-\frac{4}{3} \sqrt{\frac{2m_{ox}^*}{\hbar^2} \frac{1}{eF_{ox}}} \left(E_B - E_{Si} - \frac{\hbar^2 (k_{Si}^{\parallel})^2}{2m_{ox}^*} \right)^{3/2} \right] \quad 19-97$$

Band-Structure Approach

The second approach neglects totally momentum conservation in the transition from Si to SiO₂. But it assumes that the silicon band structure controls the amount of crystal momentum that can be used in the transition. We use the following assumptions:

- **Ballistic flight in silicon:** The entire difference in energy is assumed to be sustained within the silicon. From the initial state in k -space, a minimum-energy state is found in the same band that conserves parallel momentum. The energy $E_{si} - E_{min} - E_B$ is the difference between the minimum kinetic energy that the energy can achieve by ballistic emission and the barrier energy. It is taken as the kinetic energy of the emitted electron. An undetermined amount of parallel momentum is considered to be supplied by the heterojunction during the change of band structure to bring the electron to the Γ valley of the oxide.
- **Normal incidence in the oxide:** Since the silicon band structure has taken care of the kinetic aspects of the emission process, all remaining momentum is assumed to be available as normally-oriented kinetic energy in the oxide. Note that the energy not “used” for the ballistic emission is considered as “lost.” In other words, known in the silicon but unknown, and irrelevant, in the oxide. Therefore, the normal wavevector of the electron in the oxide is taken as

$$k_{ox}^{\perp}(x) = \sqrt{\frac{2m_{ox}^*}{\hbar^2}(E_{Si} - E_{min} - E_B + eF_{ox}x)} \quad 19-98$$

- **WKB approximation:** As before, the classical inversion points x_1 and x_2 are computed. The WKB formula (Equations 19-91) is used, where the dependence on k_{Si}^{\parallel} is neglected. The result is

$$T_2 = \exp \left[-\frac{4}{3} \sqrt{\frac{2m_{ox}^*}{\hbar^2} \frac{1}{eF_{ox}}} (E_B - E_{Si} + E_{min})^{3/2} \right] \quad 19-99$$

Comparison and Discussion

Figures 19-15 and 19-16 compare the results from the two approaches with the usual WKB approximation for parabolic bands.

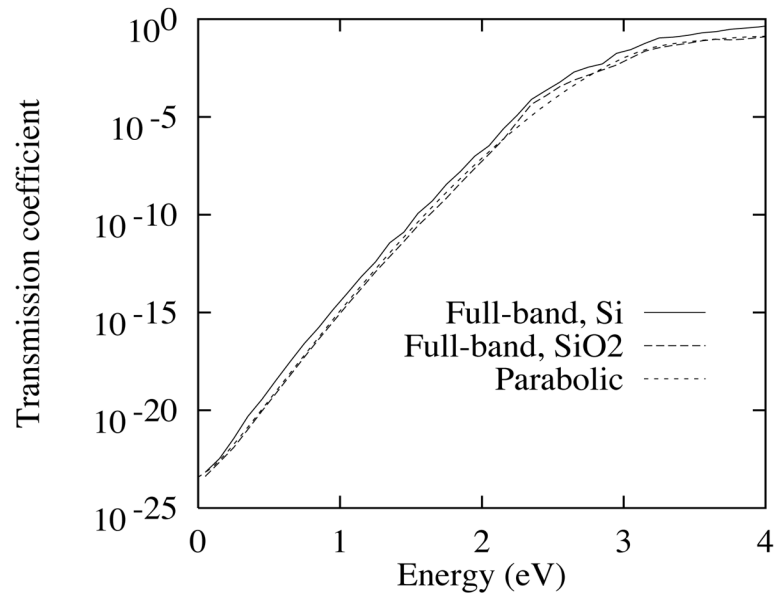


Figure 19-15: Comparison of formulae #1 and #2 with the parabolic WKB approximation.

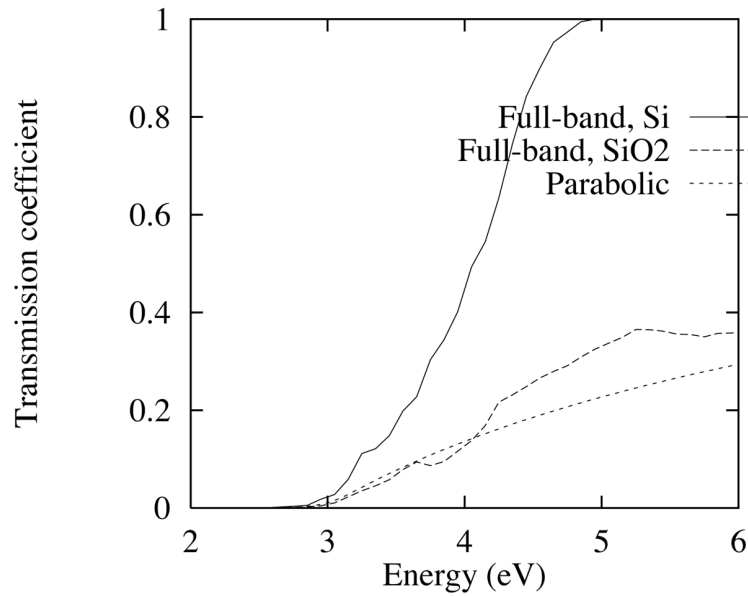


Figure 19-16: Comparison of formulae #1 and #2 with the parabolic WKB approximation for energies around the thermionic-emission threshold.

The transmission probabilities are plotted as a function of electron energy, assuming isotropic distribution of the incident particles. It is clear that the energy dependence of Equations 19-92 is very similar to a pure isotropic, parabolic electron dispersion. This is because the band structure of silicon is effectively neglected, and enters the calculation only through the density of states as a function of angle in k-space. But, the transmission coefficient obtained neglecting conservation of parallel momentum (Equations 19-95) is much higher. For low energies, the difference is on the order of a factor of 3, which is consistent with the arrangement of the conduction valleys in k-space.

Using the TUNNEL Statement

Oxide injection is calculated by default. The TUNNEL statement is used to calculate direct gate oxide tunneling on top of the carriers injected into the oxide.

```
TUNNEL MODE=0 | 1 | 2
```

MODE sets which calculation algorithm to use. MODE=0 turn off the calculation. MODE=1 chooses a simple triangular barrier. MODE=2 chooses a more accurate numerical integration with Schottky image force lowering.

19.7.8: Size Quantization

Background

In certain devices, such as inversion MOSFETs, as their dimensions become smaller, size quantization of charge layers occurs. The high fields in the device pull charge very strongly to the Si-oxide interface. Therefore, the depth of the charge layer becomes on the order of a deBroglie wavelength. Because the potential in the silicon changes by much more than k_{BT} over a carrier wavelength, the allowed energy levels become discrete and we must account for this effect.

The major effect of quantization is to alter the location of charge. In the MOSFET, destructive interference of the wave functions occurs at the Si-oxide interface because of the abrupt change in potential. This leads to a repulsion of carriers from the interface, which occurs both in accumulation and inversion. You can set the location of the charge density maximum back from the interface by 1 to 2nm, unlike the classical case where the maximum occurs directly at the interface. One of the important consequences of this is that the oxide thickness is effectively increased.

A secondary effect of charge quantization is an increase in phonon scattering. With quantization comes a sort of confinement, therefore the uncertainty in position is reduced. By the uncertainty principle, this implies an increase in momentum uncertainty. The delocalization in momentum space allows a range of phonon momenta to scatter between momentum eigenstates. Because conservation of momentum is relaxed, the density of final states for phonon scattering is increased. The consequence of this phenomenon is decreased mobility at medium field strengths (at high field strengths, surface scattering dominates).

The Schrödinger Equation

The 1D effective mass Schrödinger equation is [259]:

$$-\frac{\hbar^2}{2} \frac{\partial}{\partial z} \left(\frac{1}{m_z^*} \frac{\partial \phi}{\partial z} \right) + V(z) \phi = E \phi \quad 19-100$$

where $V(z)$ is the macroscopic potential, ψ the envelope wave function for the macroscopic potential, m_z^* is the effective mass in the direction of the quantization, and E is the eigenenergy. For silicon, this equation is solved twice to account for the two-fold degeneracy in longitudinal valleys and four-fold degeneracy in transverse valleys. The Schrödinger equation is solved for all eigenvalues by using a box-integration finite difference scheme [259].

Once the wave functions ψ_k and energies E_k are obtained, the particle concentration, n , is found by the following equations:

$$N_{\text{dos}}^{2D} = \frac{m_{xy}^* k_B T}{\pi \hbar^2} \quad 19-101$$

$$F_0(x) = \int_0^\infty (1 + \exp(x))^{-1} dx \quad 19-102$$

$$n(z) = N_{\text{dos}}^{2D} \sum_k F_0\left(\frac{E_F - E_k}{k_B T}\right) |\psi_k(z)|^2 \quad 19-103$$

where N^{2D} is the total density of states of the 2D gas that arises from applying a parabolic dispersion relation to the constant density of states in k -space. The density of states effective mass, m^* , is the mass in the plane perpendicular to the 1D solution. For example, in Si, the mass in longitudinal valleys is m_l^* and for transverse valleys is $\sqrt{m_l^* m_t^*}$. To find the density of occupied states in the conduction band, the density of states is multiplied by the Fermi factor and integrated over the entire band. In this procedure, F_0 is the Fermi integral of order zero. Finally, $n(z)$ is the quantum effect on the density.

Monte Carlo Schrödinger Formulation

The approach used in MC DEVICE is to periodically solve the Schrödinger equation during a simulation along the direction perpendicular to transport using the self-consistent electrostatic potential as input. The quantum potential in this method is found using the exact energies and wave functions. The correction to the Monte Carlo transport potential is found by linking the quantum density to the potential through

$$V_{\text{qc}}(z) = -k_B T \log(n_q(z)) - V_p(z) + V_0 \quad 19-104$$

Here, V_{qc} is the quantum correction. z is the direction normal to the interface. n_q is the quantum density from the Schrödinger equation or equivalently the converged Monte Carlo concentration. V_p is the potential from the solution of Poisson. V_0 is a reference potential determined by the fact that the correction should go to zero in a bulk-like region.

In Equation 19-104, the Schrödinger concentration profile goes in an arbitrary multiplicative constant. For the purpose of filling the energy levels, only the relative populations are significant. The particles simulated by Monte Carlo, once the potential correction has been added, move in a potential environment that shapes the space distribution as in the result of the Schrödinger equation. The non-equilibrium full band Monte Carlo model determine the magnitude of the particle distribution at different points along the transport path and momentum space trajectories.

MC DEVICE chooses the Fermi level to fill the energy levels according to the Maxwell-Boltzmann distribution. The setting of the Fermi level, E_F , also fixes the potential V_0 . Explicitly, this can be seen by

$$n_q(z) = \exp\left(-\frac{V_p(z) + V_{\text{qc}}(z)}{kT}\right) \exp\left(\frac{V_0}{kT}\right) \quad 19-105$$

$$\exp\left(-\frac{V_0(z) - V_p(z)}{kT}\right) \rightarrow N_{\text{eff}} \exp\left(-\frac{V_p(z) - E_F}{kT}\right) \quad 19-106$$

$$V_0 = kT \log(N_{\text{eff}}) + E_F \quad 19-107$$

N_{eff} is the effective density of states and E_F is the specified Fermi level. You can see that $n_q \rightarrow n_c$ as $V_{gc} \rightarrow 0$.

Using the Maxwell-Boltzmann relation in the formulation for the correction should be questioned since degeneracy is not explicitly taken into account. Degeneracy can be important for filling the levels in highly inverted MOS structures. But, despite using non-degenerate statistics to relate voltage and concentration in the correction, note that sufficient accuracy is retained even in the highly degenerate regime for all practical cases tested. This can be explained by the similar shape of the first three subbands in the region where the quantum correction is important. The correction only begins to break down at non-physical oxide fields where the higher subbands become degenerate.

Using the Quantum Correction

Using the quantum correction proceeds in a similar fashion to using the Monte Carlo simulation. First, quantum parameters are defined using the `QUANTUM` statement. Then, simulation regions are defined using `QREGION` and `SCHREGION`. Finally, you build a sub-mesh for the solution of the Schrödinger equation using `SCHRMESH`.

Default values for the quantum parameters are set in the default parameters file. These parameters have been optimized and you should not change them for simulation of practical devices. The defaults for the `QUANTUM` statement are

```
QUANTUM RESTART=NO OPTION=(NO,NO) DECAY=(100e-15,2000e-15) \
MINCONC=(1e10,1e10) MAXQV=-1.0 MAXQF=-1.0 \
STRENGTH=1.0 Q1D=(-1,-1,-1) FREEZE=PINF SIGMA=8e-8 \
RADIUS=3 LADDERS=(1,0,0) ENERGY=NO
```

In the example, quantum-corrected device input file is given in Appendix D.3: “Examples”. The `QUANTUM` statement is not included because the defaults are adequate. If you want to restart from an old quantum correction solution, change `RESTART` to `YES`. `DECAY` is the decay in time averaging. `MINCONC` is for setting the minimum Monte Carlo concentration and the minimum quantum concentration. `MAXQV` sets the maximum allowed correction to the potential. `MAXQF` does the same for the field. `STRENGTH` is only a multiplicative factor. `Q1D` is for 1D averaging and is turned off if the value is -1. `FREEZE` is to specify a freezing iteration. An option not included in the default configuration is `SMOOTH1D` and is for 1D smoothing. `SIGMA` is the smoothing standard deviation, and `RADIUS` is the integration radius for smoothing. `LADDERS` is the number of ladders to use, and `ENERGY` is whether quantum potential should contribute to carrier energy. One last option that is also not included in the defaults file is `NOBARR`. This is for choosing whether to perform barrier fitting.

The first statement you need in order to use the quantum correction is `QREGION`.

```
QREGION MODE=SCHROEDINGER RAMP=(0,0) \
BOUNDP=(x1,x2,y1,y2) ABOUNDP=(x1,x2,y1,y2) \
FIT=(-1,-1) FBOUNDP=(x1,x2,y1,y2) \
SHIFT=-1 SHIFTDIST=0 DIR=Y \
TSTEP=4000 XSTEP=1 ZERO=0
```


MODE is to choose the type of correction to use, such as FEYNMAN and WIGNER. RAMP is to specify a transient period where to ramp up the correction added to the Monte Carlo potential. BOUNDP is the region where to calculate the correction (see “Regions” on page 19-17). Again, a BOUND parameter is provided for backward compatibility. ABOUNDP is a region where to calculate attenuation. ABOUND is provided for backward compatibility. FIT is to specify a fitting function to fit the correction potential to. By setting the field to -1, it turns off the fitting function. FBOUNDP is the region where to fit the correction. FBOUND is provided for backward compatibility. SHIFT and SHIFTDIST are for specifying a grid to shift for interpolation and the distance to shift the grid respectively. DIR specifies the direction for the 1D correction, for a horizontal MOS device. This direction will be y. TSTEP is to specify the simulation step interval where Schrödinger is to be solved. XSTEP is the space step where to perform the calculation. Finally, the ZERO parameter specifies a grid line (≥ 1) where the quantum correction should go to zero. Leaving the ZERO parameter set to 0 (or -1 for backward compatibility with MOCA) lets MC DEVICE calculate this on its own positive integral value for the grid line at which the quantum correction will go to zero.

The SCHRREGION statement works very similar to the REGION statement. Any material chosen in SCHRREGION must have an entry in schroedinger.material.in. A quantum region is specified as follows.

```
SCHRREGION N=n MAT=AIR|SI|SiO2|Si3N4 BOUNDP=(x1,x2)
```

N is an integer (where $N \geq 1$) and represents the quantum region number. MAT is the material type. BOUNDP is the minimum and maximum position along the quantization axis (the y axis). A BOUND parameter, which uncharacteristically also uses positions rather than mesh indices, is provided for backward compatibility. The mesh for the quantum regions is defined using SCHRMesh. It is used in exactly as XMesh and YMesh. See the following.

```
SCHRMesh MODE=n LOC=x-pos RATIO=r
```

The definitions for SCHRMesh are the same as for the regular mesh statements. Because the correction is only calculated along a single direction, only a single grid needs to be defined.

To complete the quantum correction section of the input file, include the EBREGION statement for an energy barrier.

```
EBREGION BOUNDP=(x1,x2,y1,y2)
```

The BOUNDP parameter defines a boundary and is typically set to the boundaries of the whole device (see “Regions” on page 19-17). Again, a BOUND parameter is provided for backward compatibility.

The statement associated with the Schrödinger quantum correction is the calculation of transverse carrier temperature. You can calculate transverse temperature, T_t , with TTEMP.

```
TTEMP RESTART=NO SIGMA=0 SMOOTH=NO BOUNDP=(x1,x2,y1,y2)
```

The TTEMP statement allows you to define a region over which to calculate the transverse carrier temperature, T_t . The RESTART parameter, as with other statements, allows you to start using a previous solution file. SIGMA is set to 0 to run in normal mode or to 1 to run in best-fit mode. The SMOOTH parameter allows you to smooth the transverse temperature prior to writing it out. The BOUNDP parameter sets the boundary where to calculate the transverse temperature (see “Regions” on page 19-17). Again, a BOUND parameter is provided for backward compatibility.

19.7.9: Schottky Barrier Injection

Background

The Schottky barrier is a junction between a metal and semiconductor where the work function of the metal is greater than the electron affinity of the semiconductor. When in contact, these two materials then form a fixed energy barrier of constant height but varying width.

Although a MOSFET with Schottky source and drain regions looks similar to a bulk MOSFET, the behavior between the two is very different. Carrier flow from the source contact to the conduction channel takes place mainly by tunneling through the Schottky barrier at the silicon/silicide interface. The width of the barrier is spatially modulated by the gate voltage, and conduction occurs when the barrier is sufficiently thin [258]. When the gate voltage is small, the barrier between source and channel is sufficiently wide so that appreciable tunneling does not occur. A certain amount of leakage current due to thermionic emission from the metal may be present, originating from the tail of the quasi-equilibrium in the silicide. For higher gate voltages, the Schottky barrier just below the Si-oxide interface may become sufficiently thin to allow tunneling. A Schottky barrier is also present at the drain to channel interface and may impede the flow of carriers at low drain biases.

Transport in the channel remains semi-classical because scattering in silicon is strong enough to break quantum coherence. This justifies a coupled quantum injection – Monte Carlo particle transport approach.

The Airy Function Approach

The injection between contacts is handled by transmission probabilities, which are solutions of the Schrödinger equation along paths perpendicular to the silicon/silicide interface. The transmission probability is calculated using a standard Airy function approach based on the 1D Schrödinger equation. The Airy approach was chosen over WKB because of its accuracy with thermionic reflection and particles with energy near the top of the tunneling barrier.

For an equation of the form:

$$\frac{\partial^2 \psi}{\partial z^2} = z\psi \quad 19-108$$

the solution looks like

$$\psi(z) = a\text{Ai}(z) + b\text{Bi}(z) \quad 19-109$$

where $\text{Ai}(z)$ and $\text{Bi}(z)$ are the Airy functions given by

$$\text{Ai}(z) = \frac{1}{\pi} \int_0^\infty \cos\left(\frac{s^3}{3} + sz\right) ds \quad 19-110$$

$$\text{Bi}(z) = \frac{1}{\pi} \int_0^\infty \left[\exp\left(-\frac{s^3}{3} + sz\right) + \sin\left(\frac{s^3}{3} + sz\right) \right] ds \quad 19-111$$

The direct solution of the Schrödinger equation also has the added benefit of seamlessly treating thermionic emission and tunneling over the energy range.

To compute the current injected by the silicide contacts, a transmission coefficient $T(E_{\text{inc}}, k_{||})$ is defined as the ratio of the transmitted and incident probability current densities.

$$T(E_{\text{inc}}, k_{||}) = \frac{J_{\text{transmitted}}}{J_{\text{incident}}} = \frac{|\psi|^2 k_2}{m_2^*} \cdot \frac{m_1^*}{|\psi|^2 k_1} \quad 19-112$$

Here, the subscripts 1 and 2 refer to the silicide and silicon regions respectively. $|\psi|^2$ represents the wave function probability density for the carriers. At each iteration, a table of transmission probabilities is generated for each mesh location along the contact interface. Once the quasi-equilibrium distribution in the silicide is determined in terms of incident energy, the injected current density is obtained by integrating the product between carrier density and transmission probability.

Usage of Schottky Contacts

Compared to typical MOS devices, simulation of Schottky devices require few particles. Since the behavior of the silicide contacts can be shown by injection boundary conditions, depending on a quasi-equilibrium distribution, the entire ensemble of simulated particles is applied to transport in the conduction channel. This greatly improves performance and resolution of the method and allows you to easily probe the subthreshold regime.

For Schottky barrier devices, you can set the value for *N* on the `PARTICLE` statement to around 10000 without losing accuracy. To create a Schottky contact, you can use the `REGION` statement in the same way. Two silicides are provided, platinum silicide `PTSI`, and erbium silicide `ERSI`. To set the barrier height for your Schottky contact, use the `MATDEF` statement and modify the `BARRIER` field.

For simulation of Schottky barrier devices, there is also a secondary input file. The file `inj_2.in` is read in by MC DEVICE to interpret the Schottky-specific statements. The only thing is that the Poisson barrier height in the `inj_2.in` file must match the value for `BARRIER` set in the `MATDEF` statement for the Schottky material.

19.7.10: Gather/Scatter Algorithm

The identification of particles that need special handling in the simulation is performed as follows:

1. The predictor step is computed, yielding the k -vector and the position at the end of the time step. The first-order formula is used in k -space. The second-order formula in real space.
2. The time of the next scattering is computed for all particles as the ratio between the remaining normalized lifetime and the total scattering rate. This can be less than zero for particles that should have scattered in the previous time step, or greater than DT for particles that do not scatter.
3. The k and x -vectors at the end of the free flight are computed. The mesh and region indices are also computed. These state variables have the suffix `NEW`: `XNEW`, `KNEW`, `IXNEW`, and so on. A forward difference is used for the k -vector, assuming that the electric field doesn't change much during one time step. A second-order formula is used to compute the final position, in case the velocity varies during the free flight (e.g., for very strong electric fields, or long time steps).
4. If a particle changes region during the predicted time step, the time of boundary crossing is computed. A straight-line approximation is used for the flight trajectory. This reduces the calculation to a simple geometrical problem, speeding up the calculation considerably. Since region crossings are relatively rare events, this approximation does not affect accuracy very much. If the time of crossing is less than the scattering time, the particle is added to the appropriate reflection-handling list. The time of crossing and the side of the rectangular region where the crossing occurs are stored.
5. Particles that scatter are moved to their scattering position `XNEW`. A final state is selected and used as a new initial state for the remainder of the time step. The new predictor step is computed.
6. For each scattered particle, the region index is recomputed at the end of the time step, and compared with that at the beginning of the time step. The intermediate region index is not used in case the particle touches the corner of a region while scattering. If they differ, the particle is added to the reflection list.
7. For each rectangular region, the reflection is performed for all particles in the associated list. Boundary check is performed again and particles are added to the reflection lists. The step is repeated until all particles maintain the same region index during the last subflight in the time step.

19.7.11: Interpolation Schemes

Trilinear Interpolation

Consider a trilinear function in the form:

$$f(x, y, z) = a_0 + a_1x + a_2y + a_3z + a_4yz + a_5xz + a_6xy + a_7xyz \quad 19-113$$

where the following definitions are made:

$$f(0, 0, 0) = f_{000} \quad 19-114$$

$$f(1, 0, 0) = f_{100} \quad 19-115$$

$$f(0, 1, 0) = f_{010} \quad 19-116$$

$$f(1, 1, 0) = f_{110} \quad 19-117$$

$$f(0, 0, 1) = f_{001} \quad 19-118$$

$$f(1, 0, 1) = f_{101} \quad 19-119$$

$$f(0, 1, 1) = f_{011} \quad 19-120$$

$$f(1, 1, 1) = f_{111} \quad 19-121$$

Equations 19-113, 19-114, 19-115, 19-116, and 19-118 give:

$$a_0 = f_{000} \quad 19-122$$

$$a_1 = f_{100} - a_0 \quad 19-123$$

$$a_2 = f_{010} - a_0 \quad 19-124$$

$$a_3 = f_{001} - a_0 \quad 19-125$$

Equations 19-113, 19-116, and 19-120 yield:

$$f_{011} = a_0 + a_2 + a_3 + a_4 = f_{010} + a_3 + a_4 \quad 19-126$$

Therefore, by symmetry:

$$a_4 = f_{011} - f_{010} - a_3 \quad 19-127$$

$$a_5 = f_{101} - f_{001} - a_1 \quad 19-128$$

$$a_6 = f_{110} - f_{100} - a_2 \quad 19-129$$

Equations 19-113 and 19-121 yield:

$$f_{111} = \sum_{j=0}^7 a_j = f_{011} + a_1 + a_5 + a_6 + a_7 \quad 19-130$$

and therefore:

$$a_7 = f_{111} - f_{011} - a_1 - a_5 - a_6 \quad 19-131$$

An efficient implementation of the interpolation algorithm can be achieved by factoring Equation 19-113.

$$f(x, y, z) = a_0 + x(a_1 + a_5z + y(a_6 + a_7z)) + y(a_2 + a_4z) + a_3z \quad 19-132$$

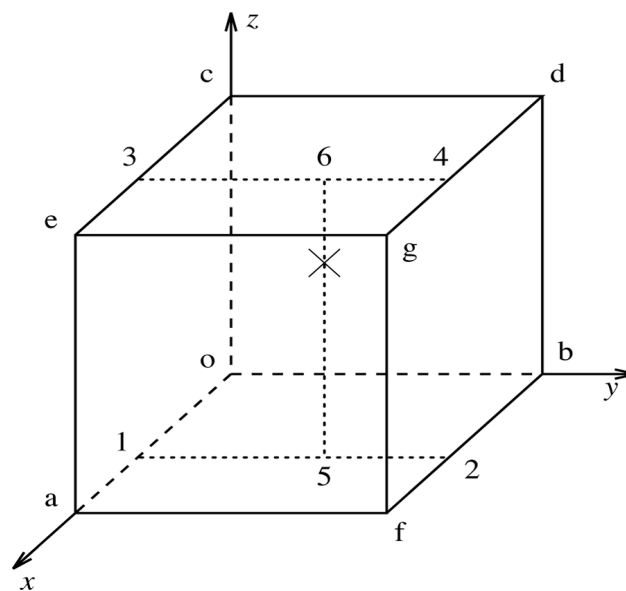


Figure 19-17: Tricubic interpolation scheme. The letters denote the vertices of the cube and lower-order interpolation points. The numbers denote the edges of the cube and higher-order (cubic) interpolation points.

Tricubic Interpolation

The tricubic interpolation is achieved by a sequence of 7 simple cubic interpolations (see Figure 19-17). The 1D cubic interpolation consists in finding a function of the form:

$$f(x) = a_0 + a_1x + a_2x^2 + a_3x^3 \quad 19-133$$

where the following definitions are made:

$$f(0) = f_0 \quad 19-134$$

$$f'(0) = f'_0 \quad 19-135$$

$$f(1) = f_1 \quad 19-136$$

$$f'(1) = f'_1 \quad 19-137$$

Substituting them, we have:

$$a_0 = f_0 \quad 19-138$$

$$a_1 = f'_0 \quad 19-139$$

$$a_3 = f'_1 - 2f'_0 + f'_0 + 2f'_0 \quad 19-140$$

$$a_2 = f_1 - a_3 - a_1 - a_0 \quad 19-141$$

The complete evaluation of one tricubic point requires $7 \times 3 = 21$ multiplications.

19.7.12: WKB Formula

The Schottky-lowered barrier can be described by the formula:

$$E(x) = W - Fx - \frac{e}{16\pi\epsilon x} \quad 19-142$$

Here, W is an effective barrier (i.e., the ideal (non-lowered) band-edge discontinuity, minus the normal component of the kinetic inside the oxide). F is the electric field and ϵ is the effective image-force dielectric constant [70]. We consider lowering at one of the ends of the barrier (Figure 19-18).

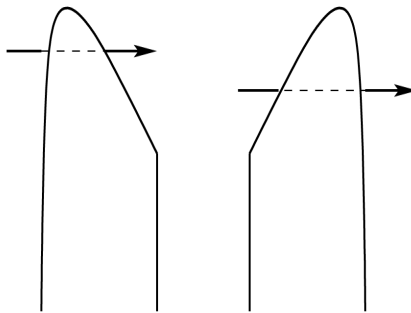


Figure 19-18: Schottky Lowering.

The entry and exit points x_{in} and x_{out} are found for $E(x)=0$.

$$x_{in, out} = \frac{W}{2F} \left(1 \pm \sqrt{1 - \frac{eF}{4\pi\epsilon W^2}} \right) \quad 19-143$$

For very low fields or very high barriers or both, the second term within the square root can be much smaller than one. In such cases, a much more accurate expression for $x_{in,out}$ is obtained by a series expansion of the square root:

$$x_{in} = \frac{e}{16\pi\epsilon W} \quad 19-144$$

$$x_{out} = \frac{W}{F} \quad 19-145$$

Finally, the WKB integral is performed numerically on a very fine mesh. Since a typical barrier is at most of the order of 1 Ry and the effective mass in the oxide is about $0.5m_0$, the attenuation factor is the order of a fraction of a_0^{-1} , where a_0 is the Bohr radius. A mesh step of $a_0/2$ has been chosen.

19.7.13: Strain

You can use the strain model in MC DEVICE to account for the effect of strains on the transport of electrons and holes in bulk and 2D simulations. This model can be applied to different materials and is also known as the multi-material model [259]. In its present form, the model can treat semiconductors that have 16-fold degeneracy in their band structures and where the irreducible wedge (IW) falls in the domain where $k_x \geq 0$, $k_y \geq 0$, $k_z \geq 0$, and $k_y \geq k_x$. In this version of MC DEVICE, fittings are provided for electron transport in silicon under biaxial tensile strain. When used in 2D, you may define any number of rectangular strain regions. In each strain region, the strain varies linearly from the value of the effective strain (or the effective mole fraction) you provide at the corners of the rectangle.

Band Structure

When you perform a bulk simulation, you need to consider just one value of the strain that pertains to the bulk. But when you perform device simulations, you often need to consider strain that varies over the device. For either type of simulation, it is convenient if your strain model uses one set of strain fittings that pertain to a wide range of strain levels so that these cases can be modeled with little change in your input. This is the case with the strain model in MC DEVICE. To test different bulk cases for a given strain type, you change the effective strain for each case. To test different strain levels within a device, you define the strain over your device structure. For supported strain types, you can simply set the level of strain to use the model. In such cases, you do not need to characterize the effect of strain on the band structure and on carrier scattering since it has already been set.

In Monte Carlo electronic transport modeling, two operations related to the semiconductor band structure are performed repeatedly. The first operation is called the forward (or direct) evaluation. In the forward evaluation, the modeling tool determines the carrier energy, E , and carrier velocity, v , of each MC carrier based on its band index, n , and its wave vector, \mathbf{k} . The second operation is call the reverse (or indirect) evaluation. In the reverse evaluation, the modeling tool determines the band index, n , and the wave vector, \mathbf{k} , after each MC carrier has scattered. Figure 19-4 shows a flowchart that depicts the forward and reverse evaluations done in MC DEVICE when the strain model is active. (The evaluations done in MC DEVICE when the strain model is not active amount to the top two-thirds of Figure 19-4.) Although not shown in Figure 19-4, the strain model also provides strain corrections for each component of the carrier velocity. Like the strain correction for the energy, the strain correction for each velocity component depends quadratically on the effective strain, m . For example, the strain correction for the x -component of the velocity involves a term that depends linearly with the effective strain (and uses the coefficients a_x) and a term that depends quadratically on the effective strain (and uses the coefficient b_x).

For the forward evaluation, the strain model uses the unstrained band structure along with fitting coefficients of the quadratic correction terms, $a(n, \mathbf{k})$ and $b(n, \mathbf{k})$. A quadratic correction was found to be reasonably accurate for modeling the band structure of strained silicon on relaxed SiGe over the entire Brillouin zone for both valence and conduction bands and for both the carrier energy and for the carrier velocity components [259]. Since two coefficients are needed for the correction for every point in the irreducible wedge and for every band, the amount of data needed to characterize a strain-dependent band structure is three times that of the unstrained band structure.

For the reverse evaluation, the strain model performs a search to obtain the strained band index, n_m , and strained wave vector, \mathbf{k}_m , of each MC carrier. In this case, the reverse lookup table that is used to obtain the final states based on the energy is extended to include the two quadratic fit parameters, $a(n, \mathbf{k})$ and $b(n, \mathbf{k})$. First, the final energy of the carrier is searched in the energy-ordered lookup table based on the energy of that state in unstrained silicon. This search yields an unstrained state (n_0, \mathbf{k}_0) . The location of the strain-dependent final state (n_m, \mathbf{k}_m) can be reduced to a small local region in the table around the unstrained state (n_0, \mathbf{k}_0) . The local region is small because the modification of the energy of the strained state is small relative to the energy range of the table. The size of the local region is chosen so that it will always contain the strained state.

Second, the strained state (n_m, \mathbf{k}_m) is determined by randomly choosing a state within the local region and checking if the strained energy, E_m , at the randomly chosen state matches the known final energy of the carrier, E_f .

Note: This search will correctly sample the states within the local region according to the density of states (DOS).

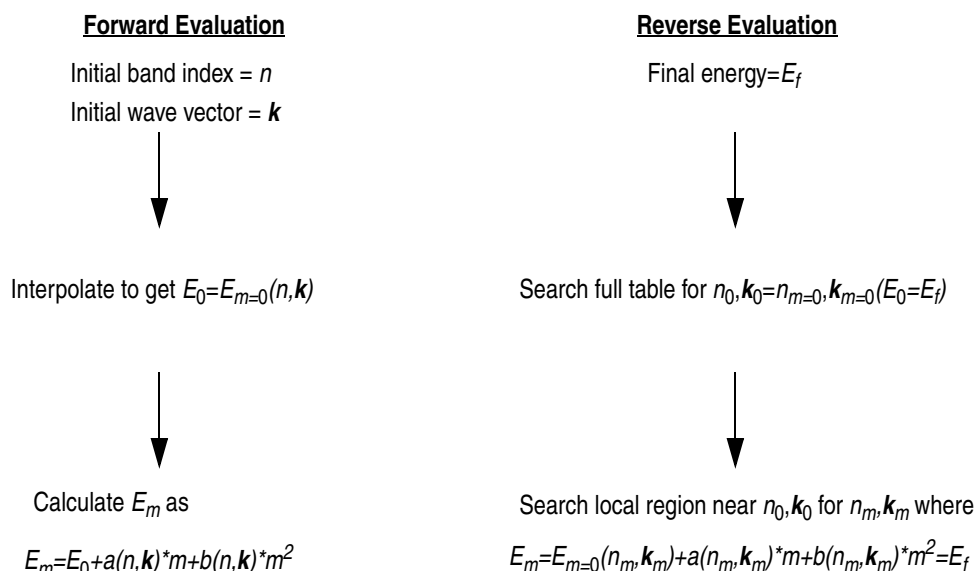


Figure 19-19: Forward and reverse evaluations for the strain model. m pertains to the effective strain (or to the effective mole fraction). When the strain model is inactive, the last step of the evaluation is skipped.

Phonon Scattering

MC DEVICE models the transport of charge carriers but not the transport of phonons. In this context, the term phonon scattering refers to carrier-phonon scattering or the scattering of charge carriers with phonons. The phonon scattering rates in MC DEVICE are determined at the start of the simulation by one of two methods. The first method is to calculate the rates using analytic formulas and is selected by setting `TYPE=ANALYTIC` on the `ESCAT` statement. The second method is to load the rates from data files and is selected by setting `TYPE=FULLBAND` on the `ESCAT` statement.

The first method (`TYPE=ANALYTIC`) is more flexible and supports a more complete set of mechanisms in MC DEVICE. For this method, the phonon scattering mechanisms include: intravalley acoustic, intervalley X-X f-type (at 3 phonon temperatures), intervalley X-X g-type (at 3 phonon temperatures), and intervalley X-L (at 4 phonon temperatures). Both absorption and emission of phonons are considered for all carrier phonon scattering mechanisms. Therefore, there are a total of $(1+3+3+4)*2=22$ carrier-phonon scattering mechanisms. Anisotropy in the final state selection is included by having different mechanisms (e.g., f and g-types) and through the density of states (DOS). The formulas for these rates are scaled by the full-band DOS at high energies to obtain accurate values for the rates at high energies. The rates for these mechanisms are described in Section 19.7.5: “Phonon Scattering”. The format of the `scat.out` file produced when `TYPE=ANALYTIC` is given in Table 19-2.

The second method (TYPE=FULLBAND) enables you to calculate the scattering rates using full band structure although it must be done outside of MC DEVICE. For this method, the phonon scattering mechanisms include: longitudinal and transverse acoustic scattering and one type of optical scattering. Both absorption and emission of phonons are considered for all carrier-phonon scattering mechanisms. Therefore, there are a total of $3 \times 2 = 6$ carrier-phonon scattering mechanisms. In this case, carrier phonon scattering is anisotropic only through the density of states. In this case, the rates do not need to be scaled by the full-band DOS at high energies, since they were calculated with full band structure. Table 19-3 shows the format of the `scat.out` file produced when TYPE=FULLBAND.

Bulk Simulations

Bulk simulations were performed with MC DEVICE and compared with experimental data to verify the model. The model was originally developed to treat transport in silicon under biaxial tensile strain, so much of the testing has been performed for this type of strain. For this case, the low-field electron mobility versus effective mole fraction is shown in Figure 19-20. Here, the TYPE=FULLBAND is used on the ESCAT statement and FIELD=(1e3 1e3) on the BULK statement. The plot of the field-based electron mobility estimate shows that the strain model in MC DEVICE obtains good agreement with the experimental results obtained by Welser [250] and with the experimental results obtained by Ismail at $x=0.3$ [105].

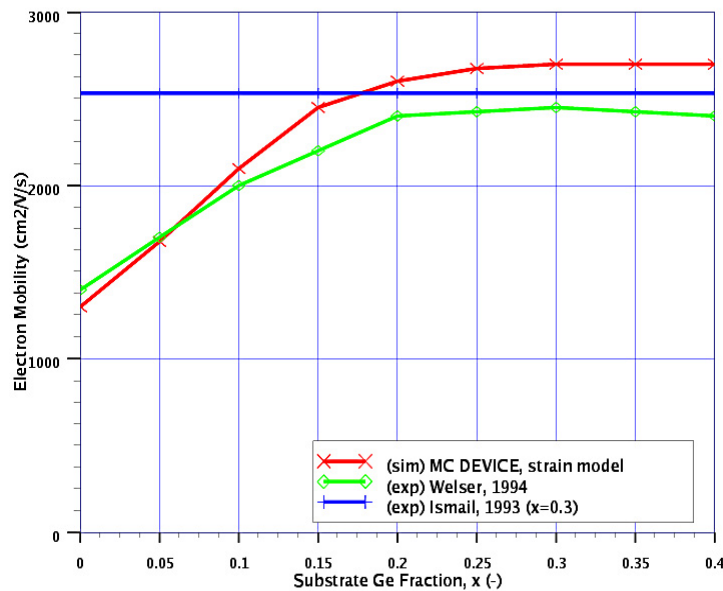


Figure 19-20: Electron mobility versus Substrate Ge fraction, x .

The mobility enhancement saturates at approximately $x=0.2$ (20% Ge in the substrate). This indicates that the splitting of the X valleys of the conduction band is sufficiently large at this mole fraction (strain level) that the entire population of electrons occupies the lower-lying X valleys where the effective mass is lower. Further splitting of the X valleys provides little increase in the electron mobility, since all electrons already reside in the lower-lying X valleys at $x=0.2$.

Note: The strain model in MC DEVICE predicts the impact of strain on band structure and carrier scattering. The strain model in MC DEVICE does not predict the impact of defects that can occur at high strain levels and the corresponding impact on carrier transport.

To use the strain model in MC DEVICE for bulk modeling, you must use some or all of the following input statements: MMAT, ESCAT, and BULK.

The MMAT statement is used to turn on the strain model.

```
MMAT TYPE=1
```

If the TYPE parameter is set to 1 | TRUE | YES, the strain mode is active. By default, the TYPE parameter is set to 0 | FALSE | NO, so the strain model is off.

The ESCAT statement is used to control carrier-phonon scattering (see “Phonon Scattering” on page 19-75).

```
ESCAT TYPE=ANALYTIC FBPROC=7 FBBAND=4 ANPROC=24 ANBAND=1 \
  FPNCPFILE="phcpl_c.in" PHNFACFILE="phon_fac_c_uni_300k.in" \
  PLOTFILE="scatfl_c_uni.in"
```

If the TYPE=ANALYTIC (as it is by default), then the scattering rates are calculated inside MC DEVICE using analytic formulas. If the TYPE=FULLBAND, then scattering rates are loaded from files in the \$MCDEVEDIR directory as specified by the PHNCPLFILE, PHNFACFILE, and PLOTFILE parameters.

FBPROC sets the number of scattering processes used for TYPE=FULLBAND. FBBAND sets the number of bands used for TYPE=FULLBAND. anproc sets the number of scattering processes used for TYPE=ANALYTIC. anband sets the number of bands used for TYPE=analytic.

PHNCPLFILE and PHNFACFILE set two filenames related to the phonon scattering rates when TYPE=FULLBAND. PHNCPLFILE sets the file which contains the phonon coupling parameters. PHNFACFILE sets the file which contains the sum prefactor in the phonon scattering formulas.

PLOTFILE sets the file from which the phonon scattering rates will be loaded when TYPE=FULLBAND. Column 1 in PLOTFILE is the carrier energy in eV. Columns 2-7 are the 6 phonon scattering rates. The 6 phonon scattering rates pertain to columns 3-8 of scat.out produced for this case (see Table 19-3). The rates must be scaled by the squared phonon coupling parameters (in "phcpl_c.in") and scaled by the sum prefactors (in "phon_c_uni_300k.in") in order to get units of 1/s. This calculation is done inside MC DEVICE after the data are loaded and the results can be written to "scat.out" (see Table 19-3).

Note: Fittings for TYPE=FULLBAND are only provided for simulating MC electrons in strained silicon (CARRIER=E on the ALGO statement). These are not provided for simulating MC holes (CARRIER=H on the ALGO statement).

The BULK statement is used to set parameters associated with a bulk simulation (see Section 19.4: “Bulk Simulation”).

```
BULK MMFRAC=0.05
```

The MMFRAC parameter sets an effective strain (or effective mole fraction) that pertains to the bulk. In the case of biaxial tensile strained silicon, this pertains to the mole fraction, x , of an assumed underlying substrate of relaxed $\text{Si}_{1-x}\text{Ge}_x$. For other types of strain, MMFRAC pertains to an effective strain.

Device Simulations

The strain model was tested in 2D by simulating a 50 nm well-tempered *n*-MOSFET in saturation with and without strain. The strained *n*-MOSFET was based on a relaxed $\text{Si}_{1-x}\text{Ge}_x=\text{Si}_{0.7}\text{Ge}_{0.3}$ substrate, while the unstrained (relaxed) *n*-MOSFET was based on a pure silicon substrate. Although no attempt was made to fit the surface scattering or the threshold voltage shift, relative comparisons of the results can be used to analyze the qualitative effects of strain. The strained channel device showed a 60% increase in the drive current relative to the unstrained case. This result agrees with the low-field mobility enhancement expected at low drain bias. A large velocity enhancement is seen in the strained *n*-MOSFET, which reflects the increased low-field mobility [259].

To use the strain model in MC DEVICE in device simulations, you must use some or all of the following input statements: MMAT, ESCAT, and MMREGION.

The MMAT and the ESCAT statements are described in Section 19.4: “Bulk Simulation”. The MMAT and ESCAT statements are used the same in 2D device simulations as they are in bulk simulations.

The MMREGION statements are used to define the effective strain (or effective mole fraction) in rectangular regions.

```
MMREGION BOUNDP=(0.025,0.175,-0.062,0.12) FRAC=(0.3,0.3,0.3,0.3)
```

The BOUNDP parameter gives the boundary of the region within which the strain model will be applied (see “Regions” on page 19-17). A BOUND parameter is provided for backward compatibility. The FRAC parameter gives a list of four values for the effective strain to be used at the corners of each rectangular region. These four values pertain to the values in the lower-left, the lower-right, the upper-right, and the upper-left corners, respectively. (These directions are based on the directions of the axes in TONYPLOT where \hat{x} is to the right and where \hat{y} is up.) The effective strain inside the rectangle is linearly interpolated based on the values at the corners.

19.8: Tips

1. Use the RESTART parameter when performing a series of simulations:

There is a switch for using RESTART option on the algo statement. If you set `RESTART = 1|TRUE|YES`, the simulator reads in the particle states from the `status.in` file. A corresponding `status.out` file can be written at the end of a simulation and you may copy `status.out` to `status.in`. The way it helps when performing a series of simulations is as follows. MC DEVICE initially places particles with the aim of achieving charge neutrality everywhere. Therefore, for any new simulation the bulk of the particles are placed in the source and the drain region initially. These particles are then redistributed in the channel region. Therefore, when the restart option is used, the particles are already in the channel satisfying the boundary conditions of the previous bias conditions and the time that is needed for achieving this steady state is reduced or eliminated.

2. Try changing the error bound for the inner loop for Poisson solver (see `TOL=(2e-4,1e-5)` parameter on the POISSON statement):

The TOL parameter takes two values which correspond to the two tolerances used by the Poisson solver in MC DEVICE. Since it is an iterative solver, it uses a preconditioner (inner loop) and then a linear search routine (outer loop) to get the solution. The two values for the TOL parameter are for the maximum error in the linear search routine and the tolerance of the preconditioner. Making the tolerance of preconditioner (the second value) more smaller (more strict) may increase the number on inner loops but reduce the number of outer loops. Thus, reducing the overall time. There is a trade off here. Depending on the device, you may want to adjust the solver for the fastest execution time while you keep the tolerance of the result (tolerance of linear search routine) the same.

3. Real time between Poisson solutions:

It has been observed that solutions are not as accurate when the real time step between successive Poisson solutions is more than 0.2 fs. Therefore, it is advised that the real time step between any two Poisson solutions should be 0.2 fs or less. For example, if your transport time step (on the ALGO statement) is 0.02 fs, then the Poisson TSTEP (on the POISSON statement) should not be greater than 10.

This page is intentionally left blank

20.1: Overview

This chapter describes the overall process of obtaining a numerical solution, the subtasks involved, and the options and defaults available in ATLAS.

You don't need to master this material in order to use ATLAS. Chapter 2: "Getting Started with ATLAS", Section 2.8: "Choosing Numerical Methods" presents the information about numerical techniques that is needed. This chapter provides additional information that will mainly be of interest to advanced users.

20.2: Numerical Solution Procedures

Semiconductor device operation is modeled in ATLAS by a set of anywhere from one to six coupled, non-linear, partial differential equations (PDEs). ATLAS produces numerical solutions of these equations by calculating the values of unknowns on a mesh of points within the device. An internal discretization procedure converts the original, continuous model to a discrete non-linear algebraic system that has approximately the same behavior. The set of PDEs, the mesh and the discretization procedure determine the non-linear algebraic problem that must be solved.

The non-linear algebraic system is solved using an iterative procedure that refines successive estimates of the solution. Iteration continues until the corrections are small enough to satisfy convergence criteria, or until it is clear that the procedure is not going to converge. The non-linear iteration procedure starts from an initial guess. The corrections are calculated by solving linearized versions of the problem. The linear subproblems are solved by using direct techniques or iteratively.

Different solution procedures exhibit different behavior with respect to convergence, accuracy, efficiency, and robustness. The two main aspects of convergence are whether a solution is obtained and how rapidly it is approached. Accuracy is how closely the computed solution approximates the true solution. Efficiency is the time required to produce a solution. Robustness is the ability to converge for a wide range of structures, using meshes and initial guess strategies that are not optimum.

When solving general systems of non-linear equations, there are no guarantees that any particular method will always work. It is also the case that different methods can work better for different problems. Fortunately, there is now a lot of practical experience concerning the numerical techniques that are effective for device simulation. This practical experience has been captured in ATLAS in the form of default methods and parameters that work well in almost all circumstances. This chapter provides advanced information of interest to users who want to change the defaults.

20.3: Meshes

The specification of meshes involves a trade-off between the requirements of accuracy and numerical efficiency. Accuracy requires a fine mesh that can resolve all significant features of the solution. Numerical efficiency requires a coarse mesh that minimizes the total number of grid points. This trade-off between accuracy and numerical efficiency is frequently a source of problems for beginners. Fortunately, enough experience to define reasonable meshes is soon acquired.

ATLAS uses triangular meshes. Some triangulations yield much better results than others. Mesh generation is still an inexact science. Guidelines and heuristics, however, for defining satisfactory meshes exist. Good triangulations have the following features:

- They contain enough points to provide the required accuracy.
- They do not contain too many unnecessary points that impair efficiency.
- They avoid, or at least minimize, the number of obtuse triangles. Obtuse triangles tend to impair accuracy, convergence, and robustness.
- They avoid, or at least minimize, the number of long, thin triangles. These triangles also tend to impair accuracy, convergence, and robustness.
- They allow the average size of triangles to change smoothly in transition from a region where very small triangles must be used to a region where the use of much larger triangles is acceptable.

The error associated with a mesh can be investigated systematically by repeating a calculation using a sequence of finer meshes. This is very time consuming and is hardly ever done. The typical approach is to adequately resolve structural features, including doping, with an initial or base mesh, and then add nodes as required to resolve significant features of the solution. The insertion of additional nodes (regridding) is normally done by the program using user-specified criteria.

The initial mesh used by ATLAS can be specified in several ways. It can be inherited from ATHENA. It can be constructed using DEVEDIT. It can be specified using the ATLAS command language. Meshes can be refined using ATLAS commands, or using DEVEDIT. The remainder of this section will focus on the capabilities available using ATLAS commands. The capabilities provided by DEVEDIT are documented in the DEVEDIT USER'S MANUAL.

There are limits on the maximum number of nodes that can be specified. Two-dimensional ATLAS simulations may have up to 20,000 nodes. Three-dimensional simulations may have up to 200,000 nodes, 400,000 elements, with no more than 20,000 in a single plane and a maximum of 200 planes in the Z direction. Most devices can be adequately simulated in two dimensions using meshes that contain from several hundred to around 3000 nodes.

20.3.1: Mesh Regridding

The `REGRID` statement supports refinement of regions of the mesh according to specified criteria. Refinement can occur when a specified solution variable exceeds some value, or when the change in that variable across a triangle exceeds a value. The variable can be any of the key quantities in a problem, such as potential, carrier concentration, doping concentration, or electric field.

The regrid algorithm searches the initial grid for triangles that meet the criterion specified for refinement. Each triangle that is identified is divided into four congruent subtriangles. Grid quantities (doping, potential, carrier concentrations, and so forth) are interpolated onto the new nodes, using linear or logarithmic interpolation, as appropriate for that quantity. The initial grid is referred to as being "on level 0" and the new triangles are referred to as "on level 1". After all level 0 triangles have been examined, the same procedure is applied to level 1 triangles, and any subtriangles of level 1 become "level 2" triangles. The grid is checked for consistency at each level and is updated to avoid abrupt changes of size from one triangle to the next. The regrid process continues until no more triangles meet the refinement criteria, or until a specified maximum level of refinement is reached. Grids used in practice are often coarser than is required to meet desirable refinement criteria. Therefore, the maximum level is the key factor in determining the size of the grid after refinement.

The `MAX.LEVEL` parameter of the `REGRID` statement is used to limit the amount of refinement at each step. By default, ATLAS sets the maximum level equal to one more than the highest level in the existing mesh. To update a coarse region without regidding the finer regions, after a mesh has already been refined several times, set the maximum level below the level of the finer regions in the existing grid.

If several levels of regrid are performed in immediate succession, interpolated data is used to make the refinement decisions at higher levels. Since semiconductor problems are non-linear, this interpolation may not produce satisfactory results. It is often a good idea to calculate a new solution between regrid operations. In other words, to regrid only one level at a time and obtain a new solution after each regrid operation.

Two popular choices of quantities to be used for mesh refinement are potential and doping. Ideally, variations of electrostatic and quasi-Fermi potentials across an element would be limited to no more than kT/q , and variations in doping would be no more than a factor of 5 or so. In practice, the refinement criteria are often significantly coarser: around 10-20 kT/q for potential, and two to three orders of magnitude for doping. In high level injection situations, it is a good idea to regrid when the value of minority carrier concentration exceeds the local doping concentration.

20.3.2: Mesh Smoothing

Although every step of grid generation can introduce obtuse triangles, two steps in particular can cause problems. The first is that distorting a rectangular mesh introduces a very large number of obtuse elements. The second is that when regidding a rectangular grid that contains triangles with an aspect ratio of 4:1 or greater, very obtuse triangles are created in the transition region between high and low grid density. The `REGRID` statement allows several procedures to be used when dealing with poorly shaped elements such as obtuse triangles.

The two techniques are node smoothing and triangle smoothing. With node smoothing, several iterative passes are carried out during, which each node is moved to a position and improves the angles of the triangles surrounding it. Node smoothing should only be used for grids that are already irregular. If node smoothing is used for nearly rectangular grids, it may significantly degrade the quality of the mesh.

With triangle smoothing (which is also referred to as diagonal flipping), each adjoining pair of triangles is examined. If appropriate, the diagonal of the quadrilateral is flipped to stabilize the discretization. The diagonal is never flipped when two elements are composed of different materials. When elements are of the same material but have different region numbers, you can specify whether or not to flip the diagonals.

Triangle smoothing is desirable in almost all cases, and should be performed on both the initial grid and on subsequent regrids. The only exception to this rule arises from an undesirable interaction of three elements: regrid, high aspect ratio triangles, and smoothing. This situation frequently occurs in gate oxide regions that involve long, thin triangles. In these cases, smoothing may produce large triangles surrounded by many smaller triangles, giving the appearance of a hole in the mesh. To overcome this, use the smoothing command `SMOOTH=4` to limit the formation of the large triangles.

20.4: Discretization

20.4.1: The Discretization Process

The discretization process yields relationships between the variables defined at mesh points [184]. In order to be useful, a discretization must be consistent (i.e., it must limit to the underlying equation in the limit that the mesh size tends to zero). All of the discretizations used in ATLAS have this property. Different discretizations can have different properties with respect to accuracy. The most important measure of accuracy is the order of the scheme (i.e., how errors scaled as the difference between mesh points tends to zero). Discretization schemes used in device simulation are often second order. In other words, as the mesh becomes very fine the discretization error varies as the square of the separation between mesh points.

The discretizations implemented in ATLAS uses the Box Integration Method [238] to approximate differential operators on a general triangular grid. Each equation is integrated over a small polygon which encloses each node. The set of all polygons completely covers the solution domain. The integration procedure equates fluxes into a polygon with sources and sinks inside the polygon, which means that quantities that are conserved physically are also conserved by the numerical solution.

The fluxes must be discretized carefully for the carrier continuity and energy balance equations. Otherwise, nonphysical oscillations and negative carrier concentrations and temperatures may arise. Scharfetter and Gummel [200] introduced approximations for current densities that overcome this problem. Generalizations of this approach are used in ATLAS for the discretization of current densities and energy fluxes.

20.5: Non-Linear Iteration

The non-linear solution method, and associated parameters such as iteration and convergence criteria, are specified in the `METHOD` statement. Non-linear iteration solution methods are specified in the `METHOD` statement using the `NEWTON`, `GUMMEL`, or `BLOCK` parameters. Combinations of these parameters may also be specified. In order to understand the effect of these parameters, it is helpful to briefly review how numerical solutions are obtained.

The non-linear algebraic system that results from discretization on a mesh is solved iteratively starting from an initial guess [196,257,9,36,33]. Linearized subproblems are set up and solved. These provide corrections that are used to update the current estimate of the solution. Different sequences of linear subproblems correspond to different non-linear iteration strategies. Iteration continues until convergence criteria are met, in which case the solution is accepted. Iteration also continues until a preset maximum allowable number of iterations is reached, in which case a different technique is tried or the solution procedure is abandoned. When a solution fails to converge, a user normally tries a different grid, a different initial guess strategy, or a different non-linear iteration technique.

20.5.1: Newton Iteration

Each iteration of the Newton method solves a linearized version of the entire non-linear algebraic system. The size of the problem is relatively large, and each iteration takes a relatively long time. The iteration, however, will normally converge quickly (in about three to eight iterations) as long as the initial guess is sufficiently close to the final solution. Strategies that use automatic bias step reduction in the event of non-convergence loosen the requirement of a good initial guess. Newton's method is the default for drift-diffusion calculations in ATLAS. There are several calculations for which ATLAS requires that Newton's method is used. These are DC calculations that involve lumped elements, transient calculations, curve tracing, and when frequency-domain small-signal analysis is performed.

The Newton-Richardson Method is a variant of the Newton iteration that calculates a new version of the coefficient matrix only when slowing convergence demonstrates that this is necessary. An automated Newton-Richardson method is available in ATLAS, and improves performance significantly on most problems. To enable the automated Newton-Richardson Method, specify the `AUTONR` parameter of the `METHOD` statement.

If convergence is obtained only after many Newton iterations, the problem is almost certainly poorly defined. The grid may be very poor (i.e., it contains many obtuse or high aspect ratio triangles), a depletion region may have extended into a region defined as an ohmic contact, or the initial guess may be very poor.

20.5.2: Gummel Iteration

Each iteration of Gummel's method solves a sequence of relatively small linear subproblems. The subproblems are obtained by linearizing one equation of the set with respect to its primary solution variable, while holding other variables at their most recently computed values. Solving this linear subsystem provides corrections for one solution variable. One step of Gummel iteration is completed when the procedure has been performed for each independent variable. Gummel iteration typically converges relatively slowly, but the method will often tolerate relatively poor initial guesses. The Gummel algorithm cannot be used with lumped elements or current boundary conditions.

Two variants of Gummel's method can improve its performance slightly. These both limit the size of the potential correction that is applied during each Gummel loop. The first method, called damping, truncates corrections that exceed a maximum allowable magnitude. It is used to overcome numerical ringing in the calculated potential when bias steps are large (greater than 1V for room temperature calculations). The maximum allowable magnitude of the potential correction must be carefully specified: too small a value slows convergence, while too large a value can lead to overflow. The `DVLIMIT` parameter of the `METHOD` statement is used to specify the maximum allowable magnitude of the potential correction. By default, the value of this parameter is 0.1 V. Thus, by default Gummel

iterations are damped. To specify undamped Gummel iterations, specify `DVLIMIT` to be negative or zero.

The second method limits the number of linearized Poisson solutions per Gummel iteration, usually to one. This leads to under-relaxation of the potential update. This “single-Poisson” solution mode extends the usefulness of Gummel’s method to higher currents. It can be useful for performing low current bipolar simulations, and simulating MOS transistors in the saturation region. It is invoked by specifying the `SINGLEPOISSON` parameter of the `METHOD` statement.

20.5.3: Block Iteration

ATLAS offers several block iteration schemes that are very useful when lattice heating or energy balance equations are included. Block iterations involve solving subgroups of equations in various sequences. The subgroups of equations used in ATLAS have been established as a result of numerical experiments that established, which combinations are most effective in practice.

In non-isothermal drift-diffusion simulation, specifying the `BLOCK` method means that Newton’s method is used to update potential and carrier concentrations, after which the heat flow equation is solved in a decoupled step.

When the carrier temperature equations are solved for a constant lattice temperature, the `BLOCK` iteration algorithm uses Newton’s method to update potential and concentrations. The carrier temperature equation is solved simultaneously with the appropriate continuity equation to update the carrier temperature and again carrier concentration.

When both the heat flow equation and the carrier temperature equations are included, the `BLOCK` scheme proceeds as described previously for the carrier temperature case. It then performs one decoupled solution for lattice temperature as a third step of each iteration.

20.5.4: Combining The Iteration Methods

You can start with the `GUMMEL` scheme. Then switch to `BLOCK` or `NEWTON` if convergence has not occurred within a certain number of iterations. One circumstance where this can be very helpful is that Gummel iteration can refine initial guess to a point from which Newton iteration can converge. The number of initial `GUMMEL` iterations is limited by `GUM.INIT`.

You may want to use `BLOCK` iteration and switch to `NEWTON` if there is no convergence. This is the recommended strategy for calculations that include lattice heating or energy balance. The number of initial `BLOCK` iterations is limited by `NBLOCKIT`.

Any combination of the parameters: `GUMMEL`, `BLOCK`, and `NEWTON` can be specified on the `METHOD` statement. ATLAS will start with `GUMMEL` if it is specified. If convergence is not achieved within the specified number of iterations, it will then switch to `BLOCK` if `BLOCK` is specified. If convergence is still not achieved the program will then switch to `NEWTON`.

20.5.5: Solving Linear Subproblems

The linear subproblems generated by non-linear iteration can be solved by direct or iterative methods. Direct methods produce solutions in a predictable number of arithmetic operations. Solutions are affected by roundoff error but are otherwise exact. Iterative methods obtain solutions by making a series of corrections to an initial guess. Iteration proceeds until the calculated corrections satisfy specified convergence criteria. The results are not exact to within roundoff error, and convergence is not guaranteed for general problems. Iterative methods, however, can be more efficient than direct methods for large linear systems, and generally require less memory.

There are mathematical proofs regarding the types of linear system for which iterative techniques converge. All common iterative schemes converge for linear systems that are symmetric positive definite (SPD). The linearized form of Poisson’s equation is of this type. The continuity equations are not SPD. But they can be reliably solved by modern, advanced iterative methods.

The size and structure of the coefficient matrix of the linear system plays an important role in the choice of direct or iterative methods. The overall problem size is determined by the number of variables per node (m) and the number of nodes (n). The number of unknowns is $m \times n$. The linear subproblems associated with Newton iteration have a coefficient matrix with $(m \times n)^2$ elements. Each linearized subproblem, which is used in Gummel iteration has a coefficient matrix with n^2 elements.

For practical 2D device simulation problems, the number of elements in the coefficient matrix is typically between 10^5 and 10^8 . Fortunately, the matrices are sparse (i.e., most of the entries are zero, and you do not store them). The sparsity arises because the variables at each node are coupled to only a few neighboring nodes. Special direct techniques are available for solving sparse matrices.

Direct techniques are preferred for relatively small problems. They provide reliable solutions that are exact to within roundoff error in a time that is predictable. Iterative techniques are preferred for very large problems because they are faster and require less memory. Direct techniques for solving sparse matrices have a competitive performance for the problem sizes typically encountered in 2D device simulation, and are used by ATLAS to solve most of the linear subproblems that arise.

20.5.6: Convergence Criteria for Non-linear Iterations

After a few non-linear iterations, the errors will generally decrease at a characteristic rate as the iteration proceeds. Non-linear iteration techniques typically converge at a rate that is either linear or quadratic. The error decreases linearly when Gummel iteration is used (i.e., it is reduced by about the same factor at each iteration). For Newton iteration, the convergence is quadratic. In other words, small errors less than one are approximately squared at each iteration. The non-linear iteration is terminated when the errors are acceptably small. The conditions required for termination are called convergence criteria. Much effort has gone into developing reliable default convergence criteria for ATLAS. The default parameters work well for nearly all situations, and most will never need to change them.

The main technique in ATLAS is Gaussian Elimination (or LU Decomposition) with a minimum degree of reordering applied to the nodes [65].

20.5.7: Error Measures

A single positive number that characterizes error is obtained by taking a norm of the errors associated with each unknown. The quantity that ATLAS tries to reduce to zero is the difference between the left and right hand sides of the equation. It is natural to use this quantity as the measure of the error. The associated error norm is called the right hand side (RHS) norm. The units of the RHS norm are $C/\mu m$ for the Poisson equation, and $A/\mu m$ for the continuity equations.

Carrier Concentrations and CLIM.DD (CLIMIT)

Another measure of error is provided by the size of the calculated corrections for each unknown. Since the updates are the unknown "xs" at each step, this is called the X norm. Potential updates are measured in units of kT/q . Updates to carrier concentrations are measured relative to the previous value at the point. This relative error (ϵ_C) is defined as:

$$\epsilon_C = \max_m \frac{C_m^{K+1} - C_m^K}{\max(C_0, C_m^K)} \quad 20-1$$

where $C = n$ or p , for electrons and holes respectively. m is the node identifier. C_0 is a characteristic concentration. K is the iteration number. C_0 is specified as or as `CLIM.DD` or as `CLIM-c*` and

$$\text{CLIM.DD} = \text{CLIMIT} \cdot c^* \quad 20-2$$

where:

$$c^* = 4 \sqrt{N_c N_v} \quad 20-3$$

CLIM.DD (or CLIMIT) is specified in the METHOD statement.

It is difficult to specify a reasonable default value for the CLIM.DD parameter in all situations. In many difficult cases, the round-off numerical errors do not allow for the resolution of very low concentrations. The default value of CLIMIT is set at 10^4 (the corresponding default value for CLIM.DD in Silicon is $4.5 \cdot 10^{13} \text{cm}^{-3}$). In simulation of breakdown, a lower value of CLIM.DD ($\sim 10^8 \text{cm}^{-3}$ for Silicon diodes) should be specified. Otherwise, a “false” solution may be obtained.

Discussion of CLIM.EB

To estimate errors in the lattice temperature equation and the energy balance equations, corresponding RHS norms and X norms are calculated in ATLAS. Updates to temperature are measured relative to some characteristic value of temperature. The CLIM.EB parameter can be viewed as a regularization parameter for the case of very small electron or hole densities in the energy balance equations. The CLIM.EB parameter specifies the minimum value of concentration for which the relaxation term in the energy balance equation will be properly resolved. The temperatures for points where the concentration is much less than CLIM.EB are equal to the lattice temperature. The units of CLIM.EB are cm^{-3} and the default is 0.0.

20.5.8: Terminal Current Criteria

Another qualification for convergence is derived from the relative changes in terminal currents and the satisfaction of total current conservation. This qualification can be expressed as the simultaneous satisfaction of the following conditions:

$$\left| I_i^{K+1} - I_i^K \right| \leq E_1 \left| I_i^{K+1} \right| + E_2 \quad 20-4$$

and

$$\left| \Delta I_i^{K+1} \right| < 0.01 \max \left(\left| I_i^{K+1} \right|, E_2 \right) \quad 20-5$$

$I = 1, nc$

where

- I_i is the current through contact i
- K is the iteration number
- E_1 and E_2 are specified tolerances
- nc is the number of contacts

20.5.9: Convergence Criteria

A summary of the termination criteria that is enough for most purposes will now be given. Detailed reference information is provided in the next section.

The non-linear iteration is terminated when one of the following four criteria is satisfied.

1. The X norm for every equation falls below a specified tolerance. The specified tolerances for X norms are:
 - P_{tol}^x for potential equation.
 - C_{tol}^x for concentration equations.
 - TL_{tol}^x for lattice temperature equation.
 - TC_{tol}^x for carrier temperature equation.
2. The RHS for all equations and X norms for energy balance falls below a specified tolerance. The specific tolerances are:
 - P_{tol}^r for potential equations.
 - C_{tol}^r for concentration equations.
 - TL_{tol}^r for lattice temperature equations.
 - TC_{tol}^r for carrier temperature equations.
3. For every equation either the X norm or the RHS norm falls below a specified tolerance. In this case, both the XNORM and RHSNORM parameters must be specified true.
4. If either 1 or 2 or 3 criterion is fulfilled for weaker values of tolerances. In other words, for specified tolerances multiplied by the W parameter and current criteria 20-4 and 20-5 are satisfied.

To exclude the X-norm criterion, specify ^XNORM in the METHOD statement. To exclude RHS-norm criterion, specify ^RHSNORM. To exclude the current criterion, make E1 and E2 very small. You can change all the above mentioned tolerances simultaneously by specifying the relaxation factor TOL.RELAX in the METHOD statement.

| Table 20-1. User-Specifiable Parameters for Convergence Criteria | | | |
|--|-----------|-----------|---------------|
| Symbol | Statement | Parameter | Default |
| P_{tol}^x | METHOD | PX.TOL | 10^{-5} |
| C_{tol}^x | METHOD | CX.TOL | 10^{-5} |
| TL_{tol}^x | METHOD | TLX.TOL | 10^{-5} (a) |
| TL_{tol}^x | METHOD | TOL.TEMP | 10^{-3} (b) |

| Table 20-1. User-Specifiable Parameters for Convergence Criteria | | | |
|--|-----------|----------------|-----------------------|
| Symbol | Statement | Parameter | Default |
| TC_{tol}^x | METHOD | TCX.TOL | 10^{-5} |
| P_{tol}^r | METHOD | PR.TOL | 5.0×10^{-26} |
| C_{tol}^r | METHOD | CR.TOL | 5.0×10^{-18} |
| TL_{tol}^r | METHOD | TLR.TOL | 100 |
| TC_{tol}^r | METHOD | TCR.TOL | 100 |
| E ₁ | METHOD | IX.TOL | 2.0×10^{-5} |
| E ₂ | METHOD | IR.TOL | 5.0×10^{-15} |
| W | METHOD | WEAK | 200 |
| TOL.RELAX | METHOD | TOL.RELAX | 1 |
| XNORM | METHOD | XNORM | TRUE |
| RHSNORM | METHOD | RHSNORM | TRUE |
| CLIMIT | METHOD | CLIMIT | 10^4 |
| CLIM.DD | METHOD | C ₀ | 4.5×10^{13} |
| CLIM.EB | METHOD | CLIM.EB | 0 |

Notes

a) This refers to the NEWTON and GUMMEL method.

b) This refers to the BLOCK method.

20.5.10: Detailed Convergence Criteria

Only in very difficult situations is more detailed information concerning error estimation and the specification of convergence criteria needed. The material is organized by algorithm.

Convergence Criteria For Gummel's Algorithms

Relative update errors are defined as follows.

For potential:

$$\varepsilon_v = \frac{\max_m \left| \varphi_m^{K+1} - \varphi_m^K \right|}{\max(1, \varphi_{mmax}^{K+1})}, \quad 20-6$$

where $mmax$ is the node where $\left| \varphi_m^{K+1} - \varphi_m^K \right|$ has its maximum value.

For electrons:

$$\varepsilon_n = \frac{\max_m \left| n_m^{K+1} - n_m^K \right|}{\max(C_0, n_m^K)} \quad 20-7$$

For holes:

$$\varepsilon_p = \frac{\max_m \left| p_m^{K+1} - p_m^K \right|}{\max(C_0, p_m^K)} \quad 20-8$$

For lattice temperature:

$$\varepsilon_{T_L} = \frac{(T_L)_{nmax}^{K+1} - (T_L)_{nmax}^K}{(T_L)_{nmax}^{K+1}} \quad 20-9$$

where $nmax$ is the node where $(T_L)_i^{K+1}$ has its maximum value.

For carrier temperature:

$$\varepsilon_{T_c} = \max(\varepsilon_{T_n}, \varepsilon_{T_p}) \quad 20-10$$

where

$$\varepsilon_{T_n} = \frac{\max_m \left| (T_n)_m^{K+1} - (T_n)_m^K \right|}{\max_m (T_n)_m^{K+1}} \quad 20-11$$

$$\varepsilon_{T_p} = \frac{\max_m \left| (T_p)_m^{K+1} - (T_p)_m^K \right|}{\max_m (T_p)_m^{K+1}} \quad 20-12$$

For drift diffusion, iterations are terminated if the following criteria are satisfied:

$$\varepsilon_v \leq P_{tol}^x \quad 20-13$$

$$\varepsilon_n \leq c_{tol}^x \quad 20-14$$

$$\varepsilon_v \leq C_{tol}^x \quad 20-15$$

In non-isothermal drift diffusion, iterations are terminated if Equations 20-10 to 20-12 are satisfied, the current convergence criteria in Equations 20-4 and 20-5 are met and:

$$\varepsilon_{T_L} < TL_{tol}^x \quad 20-16$$

In Gummel's method with energy balance equations, NITGUMM iterations, which only the non-linear Poisson equation is solved, will always be done. Gummel's method with energy balance equations is terminated if Equation 20-16 is fulfilled, the carrier temperature convergence criteria

$$\varepsilon_{T_c} \leq TC_{tol}^x \quad 20-17$$

is achieved, and one of the following conditions is valid:

- NITGUMM < K+1 ≤ NITGUMM+NT1 and Equation 20-13 is fulfilled,
- NT1 + NITGUMM < K+1 ≤ NITGUMM + NT3 and

$$\varepsilon_n \leq P_{tol}^x \cdot w \quad m \quad 20-18$$

where w = 10

- NT1 + NITGUMM < K + 1 ≤ NITGUMM + NT3, the current convergence criteria (Equations 20-4 and 20-5) are satisfied, and inequality (Equation 20-18) is valid for w = 100,
- NT1 + NITGUMM < K+1 and (Equation 20-18) is valid for w = 100,
- NT1 + NITGUMM < K+1 the current convergence criteria (Equations 20-4 and 20-5) are satisfied, and (Equation 20-18) is valid for w = 500.

The default values of the iteration parameters are NITGUMM = 5, NT0 = 4, NT1 = 10, and NT3 = 100.

Convergence Criteria For Newton's Algorithm

Relative update errors are defined as follows.

For potential

$$\varepsilon_v = \max_m \left| \varphi_m^{K+1} - \varphi_m^K \right| \quad 20-19$$

For electron concentration:

$$\varepsilon_n = \frac{\max_m \left| n_m^{K+1} - n_m^K \right|}{\max(C_0, n_m^K)} \quad 20-20$$

For hole concentration:

$$\varepsilon_p = \frac{\max_m \left| p_m^{K+1} - p_m^K \right|}{\max(C_0, p_m^K)} \quad 20-21$$

For lattice temperature and carrier temperature:

$$\varepsilon_{T_L} = \frac{\max_m \left| (T_L)_m^{K+1} - (T_L)_m^K \right|}{T_{scale}}, \quad 20-22$$

$$\varepsilon_{T_n} = \frac{\max_m \left| (T_n)_m^{K+1} - (T_n)_m^K \right|}{T_{scale}}, \quad 20-23$$

$$\varepsilon_{T_p} = \frac{\max_m \left| (T_p)_m^{K+1} - (T_p)_m^K \right|}{T_{scale}}, \quad 20-24$$

where the scaling temperature, T_{scale} , is by default equal to 300K.

To define the RHS norms used in ATLAS, first represent the non-linear equations obtained after discretization at every node as

$$F_\alpha(\vec{\chi}) = 0 \quad 20-25$$

where α can be ψ , n , p , T_L , T_n and T_p for the potential equation, electron continuity equation, hole continuity equation, lattice temperature equation, electron temperature equation and hole temperature equation, respectively. $\vec{\chi}$ represents the vector of unknowns.

The RHS norms in ATLAS is then defined as follows:

For the potential equation:

$$\varepsilon_v^g = \max_m |F_\psi| \quad 20-26$$

For the electron and continuity equations:

$$\varepsilon_n^g = \max_m |F_n| \cdot C_T \quad 20-27$$

$$\varepsilon_p^g = \max_m |F_p| \cdot C_T \quad 20-28$$

$$\text{where } CT = 10^{-4} \sqrt{N_c N_v} \quad kT$$

For the lattice temperature and carrier temperature equations:

$$\varepsilon_{T_L}^g = \max_m |F_{T_L}| \quad 20-29$$

$$\varepsilon_{T_n}^g = \max_m |F_{T_n}|. \quad 20-30$$

$$\varepsilon_{T_p}^g = \max_m |F_{T_p}| \quad 20-31$$

Newton iterations are terminated if one of the following criteria is satisfied.

The `XNORM` parameter is true and:

$$\varepsilon_v \leq P_{tol}^x \cdot w, \quad 20-32$$

$$\varepsilon_n \leq c_{tol}^x \cdot w, \quad 20-33$$

$$\varepsilon_p \leq P_{tol}^x \cdot w, \quad 20-34$$

$$\varepsilon_{T_L} \leq TL_{tol}^x \cdot w, \quad 20-35$$

$$\varepsilon_{T_n} \leq TC_{tol}^x \cdot w, \quad 20-36$$

$$\varepsilon_{T_p} \leq TL_{tol}^x \cdot w, \quad 20-37$$

where $w = 1$.

The `RHSNORM` parameter is true, conditions for Equations 20-36 and 20-37 are satisfied for $w = 1$ and:

$$\varepsilon_v^g \leq P_{tol}^r \cdot w_1, \quad 20-38$$

$$\varepsilon_n^g \leq C_{tol}^r \cdot w_1, \quad 20-39$$

$$\varepsilon_p^g \leq P_{tol}^r \cdot w_1, \quad 20-40$$

$$\varepsilon_{T_L}^g \leq TL_{tol}^r \cdot w_1, \quad 20-41$$

$$\varepsilon_{T_n}^g \leq TC_{tol}^r \cdot w_1, \quad 20-42$$

$$\varepsilon_{T_p}^g \leq TL_{tol}^r \cdot w_1, \quad 20-43$$

Both the `XNORM` and `RHSNORM` parameters are true. The convergence criteria for Equations 20-36 and 20-37 for carrier temperature are fulfilled for the inequalities (Equations 20-32 and 20-38), (Equations 20-33 and 20-39), (Equations 20-34 and 20-40), (Equations 20-35 and 20-41), and one of the conditions for every pair.

If the current convergence criteria are satisfied, then condition a) or condition b) or condition c) is fulfilled for `w = w1 = WEAK`.

Convergence Criteria For Block Iteration

For the potential equation and the continuity equations, Equations 20-19 to 20-21 and Equations 20-26 to 20-28 define the X norms and RHS norms for the Newton method. With s as an index that denotes the number of block iterations, update errors between successive pairs of block iterations for lattice and carrier temperature are defined by the following expressions.

For lattice temperature:

$$\varepsilon_{T_L}^B = \frac{|(T_L)_{mmax}^{s+1} - (T_L)_{mmax}^s|}{(T_L)_{mmax}^{s+1}} \quad 20-44$$

where $mmax$ is the number of the node where $(TL)_m$ has its maximum value.

For electron temperature:

$$\varepsilon_{T_n}^B = \frac{|(T_n)_{mmax}^{s+1} - (T_n)_{mmax}^s|}{(T_n)_{mmax}^{s+1}} \quad 20-45$$

For hole temperature:

$$\varepsilon_{T_p}^B = \frac{|(T_p)_{mmax}^{s+1} - (T_p)_{mmax}^s|}{(T_p)_{mmax}^{s+1}} \quad 20-46$$

Block iterations are terminated if:

$$\varepsilon_{T_L}^B \leq TL_{tol}^x \quad 20-47$$

$$\varepsilon_{T_n}^B \leq TC_{tol}^x \quad 20-48$$

$$\varepsilon_{T_p}^B \leq TL_{tol}^x \quad 20-49$$

and one of the following criteria is fulfilled:

- the `XNORM` parameter is true and Equations 20-32, 20-33, and 20-34 are valid for $w = 1$.
- the `RHSNORM` parameter is true and Equations 20-38, 20-39, and 20-40 are valid for $w_1 = 1$.
- both `XNORM` and `RHSNORM` are true and for the pairs of inequalities (Equations 20-32 and 20-38), (Equations 20-33 and 20-39), (Equations 20-34 and 20-40) one of the conditions is satisfied for each pair.
- the current convergence criteria are satisfied and condition 1, condition 2, or condition 3 is fulfilled for $w = w1 = \text{WEAK}$.

20.6: Initial Guess Strategies

Non-linear iteration starts from an initial guess. The quality of the initial guess (i.e., how close it is to the final solution) affects how quickly the solution is obtained and whether convergence is achieved. ATLAS users aren't required to specify an initial guess strategy. If no strategy is defined, ATLAS follows certain rules that implement a sensible, although not necessarily optimum strategy.

There is some interaction between the choice of non-linear iteration scheme and the initial guess strategy. Decoupled iteration usually converges linearly, although perhaps slowly, even from a relatively poor initial guess. Newton iteration converges much faster for a good initial guess, but fails to converge if started from a poor initial guess.

One very simple initial guess strategy is to use the most recent solution as the initial guess. Of course, there is no previous solution for the first calculation in a series of bias points. In this case, an initial solution is obtained for equilibrium conditions. There is no need to solve the current continuity equations at equilibrium, and a solution of Poisson's equation is quickly obtained.

You can also modify the initial guess in a way that makes some allowance for the new bias conditions. Typical strategies include:

- Using two previous solutions and interpolation to project a new solution at each mesh point.
- Solving a form of current continuity equation with carrier concentrations held constant. This strategy yields an improved estimate of new potential distribution.
- Modifying the majority carrier quasi-Fermi levels by the same amount as the bias changes.

You can use the parameters on the SOLVE statement to specify an initial guess strategy. Six initial guess strategies are available.

- `INITIAL` starts from space charge neutrality throughout the device. This choice is normally used to calculate a solution with zero applied bias.
- `PREVIOUS` uses the currently loaded solution as the initial guess at the next bias point. The solution is modified by setting a different applied bias at the contacts.
- `PROJECTION` takes two previous solutions whose bias conditions differ at one contact and extrapolates a solution for a new applied bias at that contact. This method is often used when performing a voltage ramp.
- `LOCAL` sets the applied bias to the specified values, and changes the majority carrier quasi-Fermi levels in heavily doped regions to be equal to the bias applied to that region. This choice is effective with Gummel iteration, particularly in reverse bias. It is less effective with Newton iteration.
- `MLOCAL` starts from the currently loaded solution and solves a form of the total current continuity equation that provides an improved estimate of the new potential distribution. All other quantities remain unchanged. `MLOCAL` is more effective than `LOCAL` because it provides a smooth potential distribution in the vicinity of p-n junctions. It is usually more effective than `PREVIOUS` because `MLOCAL` provides a better estimate of potential. This is especially true for highly doped contact regions and resistor-like structures.
- `NOCURRENT` assumes there is negligible current flow in the device and solves the non-linear Poisson equation to arrive at the initial guess. If the assumption of negligible current density is indeed correct, then the initial guess should be the solution to the current continuity equations too. You can use `NOCURRENT` to avoid ramping a bias to attain the solution at high bias.

When a regrid is performed, the solution is interpolated from the original grid onto a finer grid. This provides an initial guess that can be used to start the solution of the same bias point on the new grid. Although the initial guess is an interpolation of an exact solution, this type of guess does not provide particularly fast convergence.

20.6.1: Recommendations And Defaults

It is not normally required to specify any initial guess parameter.

The `INITIAL` parameter is normally used only to obtain a thermal equilibrium solution. The `PREVIOUS`, `PROJECT`, `LOCAL`, and `MLOCAL` parameters are used for other bias points. `PREVIOUS` and `PROJECTION` are the most frequently used. `PROJECTION` is normally preferred to `PREVIOUS` when it is available (i.e., when there are two previous solutions differing in the bias applied to the appropriate terminal). `PREVIOUS` is required for transient simulations, and for simulations that use current boundary conditions. `LOCAL` and `MLOCAL` tend to work well for reverse-biased devices, and are especially efficient when trying to increase very large voltage increments. By default, `PROJECTION` is used whenever two appropriate solutions are available. Otherwise, the `PREVIOUS` guess is used, unless there is no previous solution, in which case `INITIAL` is used.

20.7: The DC Curve-Tracer Algorithm

Tracing I-V curves for complicated device phenomena, such as breakdown or latchup, can be very difficult using conventional methods. ATLAS includes a special purpose DC curve-tracing algorithm that overcomes these problems. This algorithm is based on a dynamic load-line technique that adapts the boundary conditions for each step. The approach implemented in ATLAS for curve tracing is based on the work describe in [81].

The key idea is that bias conditions can evolve smoothly between the limits of pure voltage control and pure current control. This is achieved using external resistors that adapt dynamically to the shape of the I-V curves to ensure that at each point the load line is perpendicular to the local tangent of the trace. With this value for the external resistor, the solution is projected to the next operating point by stepping the external voltage. Once the solution has converged, a new external resistance is calculated based on the new tangent information and the process repeats itself.

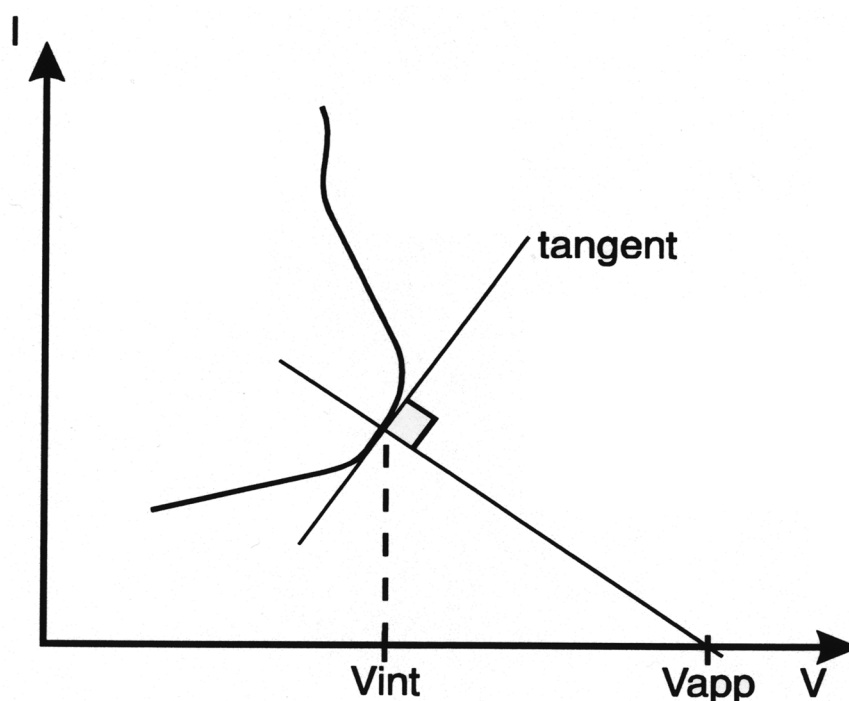


Figure 20-1: Load the algorithm used in the Curve Tracer

The curve tracing capability is activated by specifying the CURVETRACE parameter in the SOLVE statement. Prior to this, the CURVETRACE statement is used to set the parameters for the tracing algorithm. These parameters are the name CONTR.NAME of the ramped electrode (which will be referred to as a control electrode), the initial voltage increment STEP.INIT, the upper bound of the tracing curve, and additional parameters if they differ from the default values. The Upper bound parameter, END.VAL, is used to stop tracing. If the VOLT.CONT parameter is specified, END.VAL is a voltage. If the CURR.CONT parameter is specified, END.VAL is a current.

The applied voltage at each step is altered in accordance with the slope of the I-V curve. The resistor between the applied voltage and the semiconductor is also changed dynamically to ensure the voltage at the semiconductor (VINT) is smoothly varied along the I-V curve. If STEP.CONT is specified, the number of operational points on a trace will not exceed specified parameter STEPS.

20.8: Transient Simulation

When transient simulation is performed, the carrier continuity equations are integrated in the time domain. Time integration schemes differ in their accuracy, in the number of previous time levels they employ, and in their stability properties.

Accuracy is usually referred to as being “nth order”, where n is usually an integer between 1 and 4. In the limit of a small timestep, the magnitude of the local truncation error (LTE) introduced by the time integration scheme is proportional to the nth power of the timestep. Schemes that require the storage of solutions at timesteps previous to the most recent one are unattractive due to storage requirements. Single step integration schemes that use the solution at only one previous time level have a maximum order of 2.

The continuity equations are “stiff” (i.e., they are impacted by phenomena with very short timescales). Stiffness imposes stringent requirements on the stability of time integration schemes. Two forms of stability, A-stability and L-stability, are important. A-stability guarantees that errors introduced at one time step will not increase at the next timestep. L-stability guarantees that errors will decay even for large time step values. A-stability is a requirement for any practical scheme. L-stability is extremely desirable to avoid non-physical “ringing”.

Most device simulation codes use a simple first-order (implicit) backward difference formula for time integration [77,56,131]. This scheme, which is known as BDF1, is both A-stable and L-stable. Unfortunately, the scheme is inaccurate for typical timesteps of interest. Second order accuracy is obtained using the trapezoidal rule (TR) for time integration. This scheme is A-stable, but it is not L-stable. This means that solutions exhibit non-physical “ringing”, unless very small timesteps (much smaller than those dictated by LTE considerations) are used. The BDF2 scheme is second order, and is both A-stable and L-stable. The scheme, however, uses solutions from two previous time levels and is less accurate than TR.

For drift-diffusion calculations, ATLAS uses a composite TR-BDF2 scheme that was developed by Bank et. al.[19]. This method is one-step, second order, and both A-stable and L-stable. An estimate of the LTE is obtained at each timestep. This estimate is also used to automatically adapt the timestep.

Different schemes are available for transient solutions that include solving for lattice temperature or carrier temperatures or both. In ATLAS2D, the full TR-BDF2 is available as either full Newton or a block iteration scheme. To enable the block iteration scheme, use the `BLOCK.TRAN` keyword on the `METHOD` statement. In ATLAS3D, the TR-BDF2 is available as a full Newton scheme but the block iteration is unavailable. In ATLAS3D, the absolutely stable half-implicit scheme [181] is available (specify `HALFIMPLICIT` on the `METHOD` statement). It is only available if a lattice temperature solution is requested. It is not for carrier temperature solutions. Automatic timestep selection with local error control is implemented in this case. You can specify tolerance using the `TOL.TIME` parameter in the `METHOD` statement.

Note: You normally specify only the initial timestep with the `TSTEP` parameter of the `SOLVE` statement. After this, time steps are derived from the LTE and will typically increase.

20.9: Small Signal and Large Signal Analysis

There are several ways to predict the small-signal and large-signal high-frequency properties of semiconductor devices (review of these different techniques was presented by Laux [134]). Frequency domain perturbation analysis can be used to determine the small-signal characteristics. Fourier analysis of transient responses (FATR), however, can be used for both small-signal and large signal response.

You can also use charge partitioning models [106]. These methods, however, have been dropped because they can only be applied to insulated contacts, where there is only displacement current and are strictly quasi-static (low frequency).

20.9.1: Frequency Domain Perturbation Analysis

Frequency-domain perturbation analysis of a DC solution can be used to calculate small-signal characteristics at any user-specified frequency [134]. This scheme works for both 2D and 3D. The calculation proceeds in the following manner:

1. Variables are represented as the sum of the known DC component and a small unknown sinusoidal AC component.
2. All equations are expanded.
3. Differentiation in time becomes multiplication by the value of $j\omega$ ($\omega = 2\pi$ frequency).
4. Products of AC quantities are neglected since they are small with respect to other quantities
5. The DC solution is subtracted.

What remains is a complex linear system whose unknowns are the AC components of the solution. Solving this linear system with appropriate boundary conditions yields small-signal characteristics.

The coefficient matrix of the complex linear system is simply the Jacobian associated with the DC operating point with some terms on the leading diagonal supplemented by $j\omega$. The Jacobian is available 'for free' if the DC solution was calculated using Newton iteration. This is a very attractive feature of the Newton method. The resulting linear complex system can be solved by an iterative or a direct method. A form of successive over relaxation (SOR) works well for frequencies significantly below the cutoff frequency but fails at higher frequencies. More sophisticated iterative techniques can be used at higher frequencies. It is simpler and more reliable, however, to switch to direct sparse matrix methods if SOR fails to converge.

Frequency domain perturbation analysis is extremely attractive when the full Newton method is used to calculate a DC solution. The method works for all frequencies. It requires a predictable amount of computation, which is quite low with respect to other calculations, since only a single linear system is solved.

Frequency domain perturbation analysis is invoked in ATLAS by specifying the appropriate parameters in the SOLVE statement. The AC.ANALYSIS parameter specifies that this analysis is to be performed. TERMINAL specifies the contact whose terminal voltage is to be perturbed. A full characterization requires that all but one of the device terminals is perturbed. FREQUENCY, FSTEP, and NFSTEPS determine the frequencies for which solutions are obtained. FREQUENCY specifies the initial frequency. FSTEP and NFSTEPS define a loop on frequencies. If MULT.FREQ is specified, the frequency is multiplied by FSTEP at each increment. This is useful for characterizing the small-signal response over several decades of frequency. The solution method can be specified using the SOR, DIRECT, and AUTO parameters. AUTO starts out using SOR but switches to DIRECT if convergence problems are encountered.

You can specify the relaxation parameter by using the S.OMEGA parameter on the SOLVE statement. Its default value is unity, which usually suffices. If any of the contacts in the device has a lumped element, however, then the SOR method will probably fail to converge unless S.OMEGA is set to a value of less than 1. A value of 0.75 is recommended on a first attempt. For higher frequencies, you need to use the DIRECT method.

20.9.2: Fourier Analysis Of Transient Responses

FATR is a post-processing step that must be performed on a LOG file, which contains transient data. The FOURIER statement performs a Fast Fourier Transform (FFT) on the time domain data transforming it into the frequency domain. Table 20-2 shows the syntax of the FOURIER statement. For more information about the FOURIER statement, see Chapter 21: “Statements”, Section 21.17: “FOURIER”.

| Table 20-2. User-Specifiable Parameters for Fourier Statement | | |
|---|----------------|---------|
| Statement | Parameter | Default |
| FOURIER | INFILE | |
| FOURIER | OUTFILE | |
| FOURIER | T.START | |
| FOURIER | T.STOP | |
| FOURIER | FUNDAMENTAL | |
| FOURIER | MAX.HARMONIC | |
| FOURIER | NUM.SAMPLES | 64 |
| FOURIER | INTERPOLATE | FALSE |
| FOURIER | COMPLEX.VALUES | FALSE |

The explanation for the FOURIER parameters are as follows:

- INFILE – input log file. This should contain data from a transient simulation.
- OUTFILE – file output file for the Fourier transform.

The following parameters are optional:

- T.START – start of time data to be used for the FFT. The default value is the first time point in the input log file.
- T.STOP – end of time data to be used for the FFT. The default value is the last time point in the input log file.
- FUNDAMENTAL – fundamental frequency. If this is not specified, then the fundamental frequency is set to $1/(T.STOP - T.START)$. If the fundamental frequency is specified then T.STOP is set to $T.START + 1/FUNDAMENTAL$.
- MAX.HARMONIC – maximum harmonic frequency that the FFT should calculate. This will automatically calculate the correct number of samples (NUM.SAMPLES) required to generate this frequency. FUNDAMENTAL must be specified when MAX.HARMONIC is used.
- NUM.SAMPLES – number of samples. This should be an integer power of 2 (i.e., 2^n) where n is a positive integer. The default value is 64 unless the MAX.HARMONIC parameter is specified. In this case, the number of samples is set to the nearest integer power of 2, which will generate this frequency.
- INTERPOLATE – performs linear interpolation on input data with non-uniform timesteps. This interpolates the data on to uniform timesteps. Interpolation of data can introduce addition (inaccurate) harmonic values into the FFT, which would not occur if uniform time is taken. INTERPOLATE must be used if the log file contains non-uniform time steps.
- COMPLEX.VALUES – prints the real and imaginary components to file as well as the magnitude and phase.

Note: FFT works best with uniform time steps. Therefore, set `DT . MIN` and `DT . MAX` on the `METHOD` statement to the same value. The time step should be set to: $\text{time step} = 1/(\text{number of samples} * \text{fundamental frequency})$.

The FFT can then calculate harmonic frequencies up to:

$(\text{number of samples}/2 - 1) * \text{fundamental frequency}$.

You can obtain small-signal data at high frequencies by calculating the terminal current responses to terminal voltage perturbations. Then, Fourier analysis will be performed on currents and voltages. Their ratio at each frequency provides admittance data for that frequency. The voltage perturbations are normally selected to have an analytic form with a known Fourier transform. Care must be taken to self-consistently account for geometric capacitances when step function voltage perturbations are used. The advantages of this technique are that it can be used whenever transient calculations are possible. Each transient solution gives information over a broad range of frequencies. The main disadvantage is that transients become very long when low frequency effects are investigated.

20.9.3: Overall Recommendations

Use frequency-domain perturbation analysis when it is available. The method works for arbitrary frequencies and does not require transient calculations. Use Fourier analysis of transient responses for high frequencies when it is unavailable but transient calculations are possible.

20.10: Differences Between 2D and 3D Numerics

With respect to numerical techniques, there are several differences between 2D and 3D simulations.

First, with respect to the nonlinear iteration strategies, all three strategies, `NEWTON`, `GUMMEL` and `BLOCK` are supported in 2D simulation, whereas, only `NEWTON` and `GUMMEL` are supported for 3D simulations. Implementation of the `BLOCK` strategy is expected in a future release.

Second, solution of the linear subproblem is handled differently for 2D and 3D simulations. As previously noted, the computational burden of solving the linear subproblem increases with the size of the solution domain. For smaller problems, direct methods are quicker while for larger problems iterative methods are preferred. It turns out that the point at which the iterative methods become less burdensome roughly coincides with the transition between 2D and 3D domains. As such, the default method for 2D simulations is a direct solver. For 3D simulations, the default method is an iterative solver. By default, `ILUCGS` is applied to 3D simulations. `ILUCGS` is an acronym for incomplete lower upper decomposition conjugate gradient squared. Two alternative iterative solvers are also available for 3D simulations. `BICGST` (`BICGST` on the `METHOD` statement) is an acronym for biconjugate gradient squared stabilized. `GMRES` (`GMRES` on the `METHOD` statement) is an acronym for generalized minimum residual. Direct methods can be used for 3D simulation by specifying `DIRECT` on the `METHOD` statement. Practical experience shows that for 3D simulations either of the iterative methods are faster than the direct method. But in some cases, the accuracy produced by the iterative methods can prevent convergence in the nonlinear outer loop. For 2D simulations, only direct methods are supported.

This page is intentionally left blank.

21.1: Input Language

This chapter contains a complete description (in alphabetical order) of every statement and parameter used by any of the ATLAS products, except for MIXEDMODE. MIXEDMODE specific parameters are described in Chapter 12: “MixedMode: Mixed Circuit and Device Simulator”. MC DEVICE specific parameters are described in Chapter 19: “MC Device”. Descriptions for the statements in this chapter are as follows:

- The statement name.
- The product for which the statement is applicable.
- The syntax of the statement.
- A list of all statement parameters, their type, default value, and units.
- A description of each parameter.
- An example of the correct usage of each statement.

Note: An error message will be generated if you attempt to specify a statement for a simulator that you haven’t purchased. For example, the BEAM statement can only be used if you have purchased LUMINOUS or LUMINOUS 3D.

21.1.1: Syntax Rules

An input deck line is referred to as a statement (or statement line). Since statements and parameters are not case sensitive, they can be entered using either uppercase or lowercase letters.

A statement is specified in the general format:

`<STATEMENT> <PARAMETER>=<VALUE>`

where STATEMENT is the statement name, PARAMETER is the parameter name, and VALUE is the parameter value. The space character is used to separate the parameters in a statement.

The words and numbers, which follow a statement, are parameters of that statement. A word is an alphanumeric string, which is terminated either by a space or by a carriage return. A number is a numeric or alphanumeric string which is terminated either by a space or by a carriage return. Numerical values may range from 10^{-38} to 10^{38} . A number may contain the symbols + (positive), - (negative), and/or E (decimal notation). For example:

`+10 -1.234E5 .003 -.12E+10`

Four types of parameters are used by the ATLAS products. These are: real, integer, logical, and character. Table 21-1 explains these parameter types.

| Table 21-1. Types of Parameters | | | |
|---------------------------------|----------------------|----------------|-----------------|
| Parameter | Description | Value Required | Example |
| Character | Any character string | Yes | INFILE=NMOS.DOP |

| Table 21-1. Types of Parameters | | | |
|---------------------------------|---------------------------|----------------|------------|
| Parameter | Description | Value Required | Example |
| Integer | Any whole number | Yes | REGION=2 |
| Logical | A true or false condition | No | GAUSSIAN |
| Real | Any real number | Yes | X.MIN=0.52 |

Any parameter that doesn't have a logical value must be specified in the form: `PARAM=VAL`, where `PARAM` is the name of the parameter, and `VAL` is the value of the parameter. Logical parameters must be separated from other parameters or commands by a space.

For example, in the statement:

```
DOPING UNIFORM CONCENTRATION=1E16 P.TYPE
```

the `UNIFORM` and `P.TYPE` parameters have logical values and the `CONCENTRATION` parameter has a value of 1×10^{16} (real).

Logical parameters can be turned off (switched from true to false) by placing a caret (^) in front of the logical parameter. For example, in the statement:

```
DOPING UNIFORM CONCENTRATION=1E16 ^P.TYPE
```

the `P.TYPE` parameter has been set to false.

Mnemonics

It is not always necessary to input the entire statement or parameter name. ATLAS only requires that you input enough letters to distinguish that command or parameter from other commands or parameters. For example, `DOP` may be used to abbreviate the `DOPING` command. Excessive truncation is not recommended, since future ATLAS syntax might make short abbreviations become ambiguous.

Continuation Lines

Since it may be necessary for a statement line to contain more than 256 characters, ATLAS allows you to specify continuation lines. To continue a line, put a backslash (\) character at the end of the line that is to be continued. When ATLAS encounters the backslash, it will interpret the next line to be a continuation of the current line. The PISCES-II continuation of using a (+) at the start of the subsequent line is not supported in ATLAS.

Comments

Comments are indicated either by `COMMENT` command, or by a pound sign (#). All characters on a line, which follow a comment indicator (`COMMENT` or #) will not be analyzed by ATLAS.

Synonyms

Some parameters have synonyms. These are parameters that have a different name but the same functionality. A parameter's synonym is listed in the parameter descriptions of the statements.

Pseudonyms

Throughout the statement descriptions, pseudonyms are used either to indicate a group of parameters or to indicate the value of a particular parameter. A < symbol indicates the start of a pseudonym(s). A > symbol indicates the end of a pseudonym(s). Pseudonyms will be separated from one another by a space character (). For example, `LOC` might indicate a group of location parameters, and `FILENAME` might indicate the name of a file that must be specified.

Symbols

The following symbols are used in the statement descriptions:

- < Indicates the start of a list of pseudonyms.
- > Indicates the end of a list of pseudonyms.
- | Separates parameters or pseudonyms which are mutually exclusive. Only one of these parameters may be used in a statement.
- [Indicates the start of an optional command, parameter, or pseudonym.
-] Indicates the end of an optional command, parameter, or pseudonym.

Expressions

ATLAS does not support arithmetic expressions in the syntax. You can, however, evaluate and use expressions by using the `SET` or `EXTRACT` statements.

21.2: A.MESH, R.MESH, X.MESH, Y.MESH, Z.MESH

<n>.MESH specifies the location of grid lines along the <n>-axis in a rectangular mesh for 2D or 3D simulation. It also specifies radial and angular components for 3D cylindrical meshing (see Section 2.6.9: “Specifying 3D Cylindrical Structures”).

Note: The commands are equivalent in the X, Y, or Z directions.

Syntax

X.MESH LOCATION=<l> (NODE=<n> [RATIO=<r>]) | SPACING=<v>

| Parameter | Type | Default | Units |
|-----------|---------|---------|--------------|
| DEPTH | Real | | μm |
| H1 | Real | | μm |
| H2 | Real | | μm |
| H3 | Real | | μm |
| LOCATION | Real | | μm |
| N.SPACES | Integer | | |
| NODE | Integer | | |
| RATIO | Real | 1 | |
| SPACING | Real | | μm (degrees) |
| WIDTH | Real | | μm |
| X.MAX | Real | | μm |
| X.MIN | Real | 0.0 | μm |
| Y.MAX | Real | | μm |
| Y.MIN | Real | 0.0 | μm |

Description

| | |
|-----------------|--|
| DEPTH | Specifies the extent of a mesh section in the Y direction. |
| H1 | Specifies the spacing between consecutive mesh lines at the beginning of a mesh section. |
| H2 | Specifies the spacing between consecutive mesh lines at the end of a mesh section. |
| H3 | Specifies the spacing between consecutive mesh lines at the middle of a mesh section. |
| LOCATION | Specifies the location of the grid line. |

| | |
|--------------------|---|
| N.SPACES | Specifies the number of mesh spacings within a given mesh section. |
| NODE | Specifies mesh line index. There is a limit of 120 mesh lines. These mesh lines must be assigned in increasing order. |
| RATIO | Specifies the ratio to use when interpolating grid lines between given locations. Spacing between adjacent grid lines will increase or decrease by the factor assigned to the RATIO parameter. A RATIO value of between 0.667 and 1.5 is recommended. RATIO should not be used if SPACING is specified. |
| SPACING | Specifies the mesh spacing at the mesh locations specified by the LOCATION parameter. If the SPACING parameter is specified, the NODE and RATIO parameters should not be specified. If the SPACING parameter is used to specify mesh spacings, the NX, NY, and NZ parameters of the MESH statement should not be specified. When the mesh spacings are specified using the SPACING parameter, the mesh size will be calculated. |
| WIDTH | Specifies the extent of a mesh section in the X direction. |
| X.MAX/Y.MAX | Specify the location of the end of a given mesh section (should not be specified if DEPTH/WIDTH is specified). |
| X.MIN/Y.MIN | Specify the location of the beginning of a given mesh section (should only be specified for the first section). |

Setting Fine Grid at A Junction Example

This example shows how to space grid lines closely around a junction at y=0.85 microns.

```

Y.MESH  LOC=0.0  SPAC=0.2
Y.MESH  LOC=0.85 SPAC=0.01
Y.MESH  LOC=2    SPAC=0.35

```

21.3: BEAM

BEAM specifies an optical input signal in the form of a collimated beam of light. This statement is used with LUMINOUS or LUMINOUS 3D.

Syntax

BEAM <parameters>

| Parameter | Type | Default | Units |
|---------------|-----------|---------|---------|
| AM0 | Logical | False | |
| AM1.5 | Logical | False | |
| AMBIENT.INDEX | Real | 1.0 | |
| ANGLE | Real | 90.0 | Degrees |
| BACK.REFL | Logical | False | |
| BPM | Logical | False | |
| CIRCULAR | Logical | False | |
| CON.REFLECT | Logical | False | |
| COSINE | Logical | True | |
| DEVICE | Character | | |
| DIEL.FUNC | Logical | False | |
| DIFFUSIVE | Logical | False | |
| DT | Real | 0.0 | sec. |
| DX.PHOTOGEN | Real | | μm |
| DY.PHOTOGEN | Real | | μm |
| ELLIPTICAL | Logical | False | |
| F.RADIATE | Character | | |
| F.REFLECT | Character | | |
| F3.RADIATE | Character | | |
| FDTD | Logical | False | |
| FILE.PHOTOGEN | Character | | |
| FRONT.REFL | Logical | False | |
| GAUSSIAN | Logical | False | |
| INPUTRAYS | Character | | |
| INTEGRATE | Logical | True | |
| ITERATION | Integer | 0 | |

| Parameter | Type | Default | Units |
|---------------|-----------|-----------------------|------------------------|
| LENS.HEIGHT | Real | 0.0 | μm |
| LENS.INDEX | Real | 1.0 | |
| LENS.PLANE | Real | 0.0 | μm |
| LENS.RADIUS | Real | 0.0 | μm |
| LENS.WIDTH | Real | | μm |
| LENS.X | Real | 0.0 | μm |
| LENS.XMAX | Real | 0.0 | μm |
| LENS.XMIN | Real | 0.0 | μm |
| LENS.XSAGS | Character | | |
| LENS.Y | Real | 0.0 | μm |
| LENS.Z | Real | 0.0 | μm |
| LENS.ZMAX | Real | 0.0 | μm |
| LENS.ZMIN | Real | 0.0 | μm |
| LENS.ZSAGS | Character | | |
| LID | Logical | False | |
| LONGIT.STEP | Real | 0.0 | |
| MAX.WINDOW | Real | 1.0×10^{20} | μm |
| MEAN | Character | 0.0 | μm |
| METAL.REFLECT | Real | False | |
| MIN.POWER | Real | 0.0 | W/cm^2 |
| MIN.WINDOW | Real | -1.0×10^{20} | μm |
| NORMALIZE | Logical | False | |
| NOZLENS | Logical | False | |
| NSAMP | Integer | 25 | |
| NUMBER | Integer | 1 | |
| NX | Integer | 10 | |
| NY | Integer | 10 | |
| NZ | Integer | 10 | |
| OUT.POWER | Character | | |
| OUT.SAG | Character | | |
| OUT.XSAG | Character | | |

| Parameter | Type | Default | Units |
|-------------|-----------|---------|--|
| OUT.ZSAG | Character | | |
| PARALLEL | Logical | False | |
| PERIODIC | Logical | False | |
| PHASE | Real | 0.0 | Degrees |
| PHI | Real | 90.0 | Degrees |
| PLANE | Logical | True | |
| POINT | Logical | False | |
| POLARIZE | Real | 0.0 | Degrees |
| POWER.FILE | Character | | |
| POWER.SCAL | Real | 1.0 | |
| QUANTUM.EFF | Real | 1.0 | |
| RAY.CHECK | Logical | False | |
| RAYAREA | Real | 0.0 | μm (2D) μm^2 (3D) |
| RAYS | Integer | 1 | |
| RAYTRACE | Character | | |
| REFLECTS | Integer | 0 | |
| REL.POWER | Real | 1.0 | |
| S.BACK | Logical | False | |
| S.BOTTOM | Logical | False | |
| S.FRONT | Logical | False | |
| S.LEFT | Logical | False | |
| S.RIGHT | Logical | False | |
| S.TOP | Logical | False | |
| SAG.ITS | Integer | 10 | |
| SINE | Logical | False | |
| SIGMA | Real | 0.0 | μm |
| STRUCTURE | Character | | |
| SUB.EXTINCT | Real | 0.0 | |
| SUB.INDEX | Real | 1.0 | |
| SUBDX | Real | | μm |
| SUBDY | Real | | μm |

| Parameter | Type | Default | Units |
|---------------|-----------|---------|---------------|
| SUBDZ | Real | | μm |
| SUBNX | Integer | | |
| SUBNY | Integer | | |
| SUBNZ | Integer | | |
| SUBSTRATE | Logical | False | |
| SX | Real | 0.0 | μm |
| SY | Real | 0.0 | μm |
| SZ | Real | 0.0 | μm |
| TAUC.DOS | Logical | False | |
| TD.END | Logical | False | |
| TD.ERRMAX | Real | 0.0 | |
| TD.EVERY | Integer | 10 | |
| TD.FILE | Character | | |
| TD.LIMIT | Integer | | |
| TD.LOG | Character | | |
| TD.MANY | Integer | | |
| TD.ONE | Logical | False | |
| TD.PER | Integer | | |
| TD.SRATE | Integer | 20 | |
| TD.WAVES | Integer | | |
| TD.ZCUT | Real | 0.0 | μm |
| TE | Logical | False | |
| THETA | Real | 0.0 | Degrees |
| THINEST | Real | 0.0 | μm |
| TM | Logical | True | |
| TRANSV.STEP | Real | 0.0 | |
| TR.MATRIX | Logical | False | |
| USER.SPECTRUM | Logical | False | |
| VERBOSE | Logical | False | |
| WAVELENGTH | Real | 0.623 | μm |
| WAVEL.END | Real | 0.0 | μm |
| WAVEL.NUM | Integer | 1 | |

| Parameter | Type | Default | Units |
|-------------|---------|-----------------------|-------|
| WAVEL.SCAL | Real | 1.0 | |
| WAVEL.START | Real | 0.0 | μm |
| X0.PHOTOGEN | Real | | μm |
| X1 | Real | 0.0 | μm |
| X2 | Real | 0.0 | μm |
| X.CENTER | Real | 0.0 | μm |
| X.GAUSSIAN | Logical | False | |
| X.MEAN | Real | 0.0 | μm |
| X.ORIGIN | Real | 0.0 | μm |
| X.POINT | Real | 0.0 | μm |
| X.RADIUS | Real | 0.0 | μm |
| X.SEMIAxis | Real | 0.0 | μm |
| X.SIGMA | Real | 0.0 | μm |
| XCENTER | Real | 0.0 | μm |
| XGAUSSIAN | Logical | False | |
| XMAX | Real | 1.0×10^{20} | μm |
| XMEAN | Real | 0.0 | μm |
| XMIN | Real | -1.0×10^{20} | μm |
| XRADIUS | Real | 0.0 | μm |
| XSIGMA | Real | 0.0 | μm |
| Y0.PHOTOGEN | Real | | μm |
| Y.ORIGIN | Real | 0.0 | μm |
| Y.POINT | Real | 0.0 | μm |
| Y.SEMIAxis | Real | 0.0 | μm |
| Z1 | Real | 0.0 | μm |
| Z2 | Real | 0.0 | μm |
| Z.CENTER | Real | 0.0 | μm |
| Z.GAUSSIAN | Logical | False | |
| Z.MEAN | Real | 0.0 | μm |
| Z.ORIGIN | Real | 0.0 | μm |
| Z.POINT | Real | | μm |
| Z.RADIUS | Real | 0.0 | μm |

| Parameter | Type | Default | Units |
|------------|---------|-----------------------|---------------|
| Z.SEMIAxis | Real | 0.0 | μm |
| Z.SIGMA | Real | 0.0 | μm |
| ZCENTER | Real | 0.0 | μm |
| ZGAUSSIAN | Logical | False | |
| ZMEAN | Real | 0.0 | μm |
| ZMAX | Real | 1.0×10^{20} | μm |
| ZMIN | Real | -1.0×10^{20} | μm |
| ZRADIUS | Real | 0.0 | μm |
| ZSIGMA | Real | 0.0 | μm |

Description

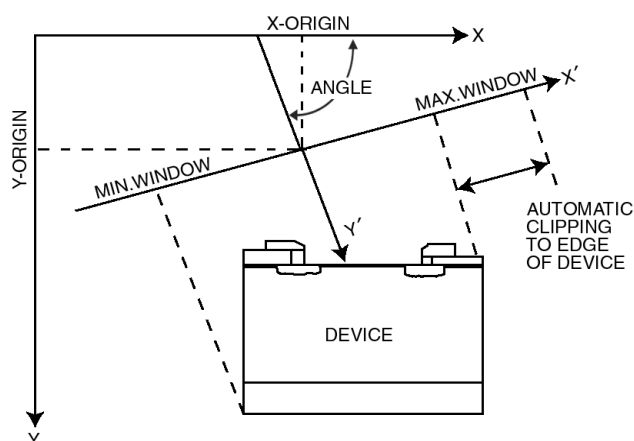


Figure 21-1: LUMINOUS Optical Source Coordinate System

| | |
|----------------------|--|
| AM0 | Enables the built-in AM0 solar spectrum. |
| AM1.5 | Enables the built-in AM1.5 solar spectrum. |
| AMBIENT.INDEX | Specifies the index of refraction of domain outside of all meshed regions. |
| ANGLE | This is the angle of propagation of the optical beam (see Figure 21-1). ANGLE=90 is vertical illumination from the top of the device. The synonym for this parameter is PHI. |
| BACK.REFL | Specifies that back side reflections are to be taken into account. When BACK.REFL is specified, the area outside the device domain is assumed to be a vacuum (i.e., $n = 1.0$, $k = 0.0$). |

| | |
|--------------------------------------|---|
| BPM (LUMINOUS2D) | Use the Beam Propagation Method instead of Ray-Tracing for analysis of light propagation in the device. Use BPM when diffraction of light or coherent effects are important (see Chapter 10: “Luminous: Optoelectronic Simulator”, Section 10.4: “Beam Propagation Method in 2D”). BEAM parameters related specifically to ray tracing (such as RAYTRACE, RAYS, THINEST, MAX.WINDOW, MIN.WINDOW) are ignored when BPM is specified. |
| CIRCULAR | This is the synonym for ELLIPTICAL. |
| CON.REFLECT | Specifies that all conductors are to be treated as perfect reflectors. |
| DEVICE | Specifies the name of a device in MIXEDMODE to identify to which device the beam is directed. The synonym for this parameter is STRUCTURE. |
| DIEL.FUNC | Enables the plotting of the dielectric function for the Tauc-Lorentz Model (see Section 3.10.3: “Tauc-Lorentz Dielectric Function with Optional Urbach Tail Model for Complex Index of Refraction”). To plot the model, you should also specify the energy range using the LAM1 and LAM2 parameters of the MATERIAL statement with the number of samples, NLAM and the output file name OUT.INDEX. |
| DIFFUSIVE | Enables the diffusive transfer matrix method. This method permits modeling of both coherent (specular) and incoherent (diffusive) interactions at material interfaces (see Section 10.3.4: “Transfer Matrix with Diffusive Interfaces”). |
| DX.PHOGEN DY.PHOGEN | Describe the spacings in the x and y directions for tabular photogeneration described in Section 10.6.4: “Tabular Photogeneration (Luminous2D only)”. |
| ELLIPTICAL | Specifies that an elliptical source is to be used in LUMINOUS 3D. When the ELLIPTICAL parameter is specified, the X.CENTER, Z.CENTER, X.RADIUS, and Z.RADIUS should also be specified. The synonym for this parameter is CIRCULAR. |
| F.RADIATE | Specifies the name of a file containing a C-Interpreter function for specifying generation rate as a function of position and optionally time. This function can be used to simulate single event upset (LUMINOUS2D only). |
| F.REFLECT | Specifies the name of a file containing a C-Interpreter function for specifying reflection coefficient models as a function of wavelength, position, and angle incidence (LUMINOUS only). |
| F3.RADIATE | This is the same as the F.RADIATE parameter but is applied in 3D. This is typically used for single event or photogeneration simulations with LUMINOUS 3D. |
| FILE.PHOGEN | Specifies the file name for tabular photogeneration described in Section 10.6.4: “Tabular Photogeneration (Luminous2D only)”. |
| FRONT.REFL | Specifies that front side reflections are to be taken into account. When FRONT.REFL is specified, the area outside the device domain is assumed to be a vacuum (i.e., $n=1.0$, $k=0.0$). |
| GAUSSIAN | This is the synonym for X.GAUSSIAN. |
| INPUTRAYS | Specifies the filename of a file containing user-defined beam information. The file format is described in Section 10.6.1: “User-Defined Beams”. |

| | |
|---|---|
| INTEGRATE | Specifies whether the user-specified spectrum (contained in the file identified by the <code>POWER.FILE</code> parameter) should be numerically integrated and averaged over the wavelength sampling or if the samples should be interpolated directly from the table. |
| ITERATION | Sets or resets the iteration number passed to the C-Interpreter function <code>F.CHARGING</code> . |
| LENS.HEIGHT | Specifies an attribute of the composite lenslet (see Chapter 10: “Luminous: Optoelectronic Simulator”, Figure 10-15). |
| LENS.INDEX | Specifies the index of refraction of a lenslet (LUMINOUS 3D only). |
| LENS.PLANE | Specifies the minimum y-coordinate of the lenslet sphere (LUMINOUS 3D only). |
| LENS.RADIUS | Specifies the radius of the sphere defining a lenslet (LUMINOUS 3D only). |
| LENS.WIDTH | Specifies an attribute of the composite lenslet (see Chapter 10: “Luminous: Optoelectronic Simulator”, Figure 10-15). |
| LENS.X | Specifies the X coordinate of the center of the sphere defining a lenslet (LUMINOUS 3D only). |
| LENS.Y | Specifies the Y coordinate of the center of the sphere defining a lenslet (LUMINOUS 3D only). |
| LENS.Z | Specifies the Z coordinate of the center of the sphere defining a lenslet (LUMINOUS 3D only). |
| LENS.XMIN, LENS.XMAX, LENS.ZMIN, LENS.ZMAX | Specify attributes of the composite lenslet (see Chapter 10: “Luminous: Optoelectronic Simulator”, Figure 10-15). |
| LENS.XSAGS, LENS.ZSAGS | <p>Specify the file names of aspheric lenslet Sag-h data files. These files must be in the following format.</p> <pre> number_of_pairs Sag_1 h_1 Sag_2 h_2 Sag_n h_n </pre> <p>Here, n is the number of pairs specified in the first line of the file. The pairs must be arranged in order of increasing h. The data modeling algorithm assumes that there is a sample with <code>Sag=0</code> at <code>h=0</code>. Therefore, such a sample must not be included in the file.</p> |
| LID | Specifies that the photogeneration rate of the beam will be applied only to the light induced defect generation model. It will not be included in the carrier continuity and temperature equations. |

| | |
|---------------------------|--|
| LONGIT.STEP | Sets the mesh size in the longitudinal direction when using BPM. The default value is <code>WAVELENGTH/16.0</code> . |
| MAX.WINDOW | Specifies the maximum x-value of the illumination window relative to the coordinate system of the optical beam (see Figure 21-1). The illumination window is always clipped to the device domain. The synonym for this parameter is <code>XMAX</code> . |
| MEAN | This is the synonym for <code>X.MEAN</code> . |
| METAL.REFLECT | Specifies that all metals are to be treated as perfect reflectors. |
| MIN.POWER | Specifies the minimum intensity relative to the source that a given ray will be traced. This is useful for limiting the numbers of rays traced. |
| MIN.WINDOW | specifies the minimum x-value of the illumination window relative to the coordinate system of the optical beam. The synonym for this parameter is <code>XMIN</code> . |
| NORMALIZE | Indicates that the <code>POWER.FILE</code> spectral intensity needs to be normalized (integral over spectrum equals 1). In this case, beam intensity is set by the <code>B<n></code> parameter on the <code>SOLVE</code> statement. |
| NSAMP | Specifies the number of samples used to represent the aspheric lenslet profile output using <code>OUT.SAG</code> . |
| NUMBER | Specifies the beam number (from 1 to 10). This number is used by the <code>SOLVE</code> statement to specify the relative intensity of different beams. You may specify beam numbers in any order that you desire. |
| NX | Specifies the number of rays traced along the source beam's X axis for <code>LUMINOUS 3D</code> . |
| NZ | Specifies the number of rays traced along the source beam's Z axis for <code>LUMINOUS 3D</code> . |
| OUT.POWER | Specifies the filename for output of multispectral samples, input using the <code>POWER.FILE</code> parameter, in a format suitable for display in <code>TONYPLOT</code> . |
| OUT.SAG | Specifies the name of a file used to output an aspheric lenslet profile for subsequent display in <code>TONYPLOT</code> . <code>OUT.SAG</code> allows a cutline along an arbitrary direction specified by two points in the XZ plane using the <code>X1</code> , <code>Z1</code> , <code>X2</code> , and <code>Z2</code> parameters. |
| OUT.XSAG, OUT.ZSAG | Specify the file names for output log files that can be displayed using <code>TONYPLOT</code> . These files contain the data input from the <code>LENS.XSAGS</code> and <code>LENS.ZSAGS</code> files and the results of the data modeling. |
| PARALLEL | Specifies that multiple processors can be used in parallel during ray trace calculation. |
| PERIODIC | Specifies that for ray tracing, the structure is to be treated as periodic in the X and Z directions. Rays exiting the sides of the device are wrapped around to the other side of the device. |
| PHI | This is the synonym for <code>ANGLE</code> . |

| | |
|-------------------|---|
| POLARIZE | Specifies the polarization of the optical beam at the origin. The polarization angle is the angle between the E vector and the incidence plane. |
| POWER.SCAL | Specifies a scale factor. This factor is multiplied by each of the relative powers in the spectrum file when multi-spectral simulations are performed. The POWER.SCAL parameter can be used to perform unit conversions. |
| POWER.FILE | Specifies the filename of a spectrum file. The spectrum file must be in the following format. <pre> number of pairs wavelength_1 power_1 wavelength_2 power_2 wavelength_n power_n </pre> |

Note: The power file must contain at least two power/wavelengths pairs.

| | |
|--------------------|--|
| QUANTUM.EFF | This is a quantum efficiency factor which specifies the number of carrier pairs generated per photon absorbed. |
| RAYTRACE | Specifies the name of a file where the results of a ray trace are saved. The ray trace may be viewed using TONYPLOT3D (LUMINOUS 3D only). |
| RAY.CHECK | Enables diagnostic printing during ray tracing. |
| RAYAREA | This is a parameter that specifies area in μm^2 (thickness in 2D in μm) of each ray in the BEAM statement. This parameter is used when the specified INPUTRAYS file does not contain ray area information. |
| RAYS | Specifies the number of rays you want to split the optical beam. LUMINOUS will automatically split the beam into enough rays to resolve the geometry. Use of the number parameter will cause further splitting of the optical beam (LUMINOUS only). |
| REFLECTS | Specifies the number of reflections that will be traced. When the value of the REFLECTS parameter is increased, the total number of rays traced increases non-linearly. We recommend that this parameter be used wisely. For example, a single ray incident on three material layers will produce 4 rays if REFLECTS=0 is specified, 10 rays if REFLECTS=1 is specified, and 24 rays if REFLECTS=2 is specified. |
| REL.POWER | Specifies the relative power in the beam when mono-spectral simulations are performed. This factor is multiplied by the power parameters specified in the SOLVE statement to give the total optical power in the beam. |
| SAG.ITS | Specifies the number of iterations used to model the aspherical lenslet Sagh data using non-linear least squares fitting. |
| SIGMA | This is the synonym for X.SIGMA. |

| | |
|------------------------------------|---|
| STRUCTURE | This is a synonym for <code>DEVICE</code> . |
| SUB.EXTINCT | Specifies the extinction coefficient used at the exit of a layer stack for analysis using the matrix method (see Section 10.3: “Matrix Method”). |
| SUB. INDEX | Specifies the index of refraction at the exit of a layer stack for analysis using the matrix method (see Section 10.3: “Matrix Method”). |
| SUBSTRATE | Indicates that the transfer matrix method in <code>LUMINOUS2D</code> will treat the final layer as the substrate (i.e., it is treated as being infinitely thick). |
| TAUC.DOS | Specifies that midgap density of states will be calculated from the absorption coefficient and output with absorption as specified by the <code>OUT. INDEX</code> parameter of the <code>MATERIAL</code> statement. |
| THETA | Specifies the angle of rotation for the source beam direction of propagation relative to the XY plane. |
| THINEST | Specifies the width of the thinnest ray to be traced (<code>LUMINOUS</code> only). |
| TR.MATRIX | Specifies that optical absorption and photogeneration analysis in <code>LUMINOUS 2D</code> will be done using the Matrix Method as described in Section 10.3: “Matrix Method”. |
| TRANSV. STEP | Sets the mesh size in the transverse direction when using BPM. The default value is <code>WAVELENGTH/16.0</code> . |
| USER.SPECTRUM | Specifies that sampling in wavelength used for simulation is the same as that contained in the <code>POWER.FILE</code> . |
| VERBOSE | Enables a higher level of diagnostic run-time printing. |
| WAVELENGTH | Specifies the optical wavelength of the source beam (in the vacuum) for mono-spectral simulations. |
| WAVEL.END | Specifies the maximum wavelength of the source beam (in the vacuum) when multi-spectral simulations are performed. |
| WAVEL.NUM | Specifies the number of wavelengths which will be used when multi-spectral simulations are performed. Spectral illumination is selected when the <code>WAVEL.NUM</code> parameter is greater than 1. Once multi-spectral simulations are selected, you must specify the <code>POWER.FILE</code> , <code>WAVEL.START</code> , and <code>WAVEL.END</code> parameters. |
| WAVEL.SCAL | Specifies the scale factor for the wavelengths which are used in multi-spectral simulations. Each of the wavelengths in the spectrum file is multiplied by this scale factor. |
| WAVEL.START | Specifies the minimum wavelength of the source beam (in the vacuum) when multi-spectral simulations are performed. |
| X0.PHOTOGEN Y0.PHOTOGEN | Describe the origin of the tabular photogeneration described in Section 10.6.4: “Tabular Photogeneration (<code>Luminous2D</code> only)”. |
| X1, X2, Z1, and Z2 | Specify the coordinates of two points in the XZ plane for extraction of an aspheric lenslet profile along the cutline defined by the two points. The profile is output to the file specified by the <code>OUT.SAG</code> parameter for subsequent display in <code>TONYLOT</code> . |

| | |
|---|---|
| X.CENTER | Specifies the X coordinate of the center of an elliptical source related to the beam coordinate system (which is centered at the beam origin) for LUMINOUS 3D. Note that to enable elliptical sources, the <code>ELLIPTICAL</code> parameter should also be specified. The synonym for this parameter is <code>XCENTER</code> . |
| X.GAUSSIAN | Specifies that a LUMINOUS 3D source is to have a Gaussian intensity profile in the X direction related to the beam coordinate system (which is centered at the beam origin). When <code>X.GAUSSIAN</code> is specified, <code>X.MEAN</code> and <code>X.SIGMA</code> should also be specified. The synonyms for this parameter are <code>XGAUSSIAN</code> and <code>GAUSSIAN</code> . |
| X.MEAN | Specifies the location of the mean value of a Gaussian source in the X direction related to the beam coordinate system (i.e., from the <code>X.CENTER</code> position). When <code>X.MEAN</code> is specified, <code>X.GAUSSIAN</code> and <code>X.SIGMA</code> should also be specified. The synonyms for this parameter are <code>XMEAN</code> and <code>MEAN</code> . |
| X.ORIGIN | Specifies the X coordinate of the optical beam origin (see Figure 21-1). The beam must originate outside all device regions. |
| X.RADIUS | Specifies the X axis radius of an elliptical source related to the beam coordinate system (which is centered at the beam origin) for LUMINOUS 3D. Note that to enable elliptical sources, the <code>ELLIPTICAL</code> should also be specified. The synonym for this parameter is <code>XRADIUS</code> . |
| X.SEMIAxis, Y.SEMIAxis, Z.SEMIAxis | Specify attributes of the elliptical lense (see Chapter 10: “Luminous: Opto-electronic Simulator”, Equation 10-77). |
| X.SIGMA | Specifies the standard deviation in the X direction of the beam coordinate system for a Gaussian source in LUMINOUS 3D. When <code>X.SIGMA</code> is specified, <code>X.GAUSSIAN</code> and <code>X.MEAN</code> should also be specified. The synonym for this parameter is <code>XSIGMA</code> . |
| XMAX | Specifies the maximum X coordinate in the source beam coordinate system for ray tracing in LUMINOUS 3D. |
| XMIN | Specifies the minimum X coordinate in the source beam coordinate system for ray tracing in LUMINOUS 3D. |
| Y.ORIGIN | Specifies the Y coordinate of the optical beam origin (see Figure 21-1). The beam must originate outside all device regions. |
| Z.CENTER | Specifies the Z coordinate of the center of an elliptical source related to the beam coordinate system (which is centered at the beam origin). Note that to enable elliptical sources, the <code>ELLIPTICAL</code> parameter should also be specified. The synonym for this parameter is <code>ZCENTER</code> . |
| Z.GAUSSIAN | Specifies that a LUMINOUS 3D source is to have a Gaussian intensity profile in the Z direction related to the beam coordinate system (which is centered at the beam origin). When <code>Z.GAUSSIAN</code> is specified, <code>Z.MEAN</code> and <code>Z.SIGMA</code> should also be specified. The synonym for this parameter is <code>ZGAUSSIAN</code> . |
| Z.MEAN | Specifies the location of the mean value of a Gaussian source in the Z direction related to the beam coordinate system. When <code>Z.MEAN</code> is specified, <code>Z.GAUSSIAN</code> and <code>Z.SIGMA</code> should also be specified. The synonym for this parameter is <code>ZMEAN</code> . |

| | |
|-----------------|--|
| Z.RADIUS | Specifies the X axis radius of an elliptical source related to the beam coordinate system. When Z.MEAN is specified, Z.GAUSSIAN and Z.SIGMA should also be specified. The synonym for this parameter is ZRADIUS. |
| Z.SIGMA | Specifies the standard deviation in the Z direction of the beam coordinate system for a Gaussian source in LUMINOUS 3D. When Z.SIGMA is specified, Z.GAUSSIAN and Z.MEAN should also be specified. The synonym for this parameter is ZSIGMA. |
| ZMAX | Specifies the maximum Z coordinate in the source beam coordinate system for ray tracing in LUMINOUS 3D. |
| ZMIN | Specifies the minimum Z coordinate in the source beam coordinate system for ray tracing in LUMINOUS 3D. |
| Z.ORIGIN | Specifies the Z coordinate of the optical beam origin. The beam must originate outside all device regions (LUMINOUS 3D only). |

FDTD Parameters

| | |
|-----------------|---|
| COSINE | Specifies that the FDTD source is modeled as a cosine wave. |
| DT | Specifies the uniform time step for FDTD analysis. |
| FDTD | Enables FDTD modeling of the beam propagation. |
| NOZLENS | Specifies that lens variation in the z direction is ignored. The x, y characteristics are taken at z=0. |
| NX | Specifies the number of uniformly spaced grid lines to be used in the FDTD mesh in the X direction. |
| NY | Specifies the number of uniformly spaced grid lines to be used in the FDTD mesh in the Y direction. |
| NZ | Specifies the number of uniformly spaced grid lines to be used in the FDTD mesh in the Z direction. |
| PHASE | Specifies the initial phase of the FDTD source. |
| PLANE | Specifies that the FDTD source is a plane wave located at $y' = 0.0$. |
| POINT | Specifies that the FDTD source is a point source. The location is specified by X.POINT, Y.POINT, and Z.POINT. |
| S.BOTTOM | Specifies that the plane source is located at the bottom (maximum Y coordinate) of the device. |
| S.BACK | Specifies that the plane source is located at the back (minimum Z coordinate) of the device. |
| S.FRONT | Specifies that the plane source is located at the front (maximum Z coordinate) of the device. |
| S.LEFT | Specifies that the plane source is located at the left (minimum X coordinate) of the device. |
| S.RIGHT | Specifies that the plane source is located at the right (maximum X coordinate) of the device. |

| | |
|----------------------------|--|
| S.TOP | Specifies that the plane source is located at the top (minimum Y coordinate) of the device. |
| SINE | Specifies that the FDTD source is modeled as a sine wave. |
| SUBDX, SUBDY, SUBDZ | Specify the spacing in microns that the FDTD mesh will be sampled at for subsampled output of FDTD meshes. |
| SUBNX, SUBNY, SUBNZ | Specify the number of uniform samples that the FDTD mesh will be sampled at for subsampled output of FDTD meshes. |
| SX | Specifies the spacing of uniformly spaced grid lines to be used in the FDTD mesh in the X direction. |
| SY | Specifies the spacing of uniformly spaced grid lines to be used in the FDTD mesh in the Y direction. |
| SZ | Specifies the spacing of uniformly spaced grid lines to be used in the FDTD mesh in the Z direction. |
| TE | Specifies that the FDTD source is a transverse electric wave. |
| TD.END | Specifies that a time-domain structure is written at the end of the number of specified iterations (TD.LIMIT or TD.WAVES) or when the estimated error is reduced below the specified maximum (TD.ERRMAX). This file will have a root name given by the parameter TD.FILE with a ".str" suffix. |
| TD.ERRMAX | Specifies the maximum residual (estimated) error for termination of FDTD time stepping. |
| TD.EVERY | Specifies how often FDTD time periodic saves are performed. A value of 1 indicates that files are saved during every time step. |
| TD.FILE | Specifies the root name of an output file saved periodically during the time domain simulation of FDTD. |
| TD.LIMIT | Specifies the maximum number of timesteps to simulate in FDTD analysis. If TD.LIMIT is unspecified, the time domain simulation will continue indefinitely. |
| TD.LOG | Specifies a log file for capture of time domain data for FDTD. |
| TD.MANY | Specifies how many FDTD files are saved during periodic time domain saves. |
| TD.ONE | Specifies that only one file name will be written for periodic FDTD saving. Each time a save is performed it is written over the previous save. |
| TD.PER | Specifies the number of structure files to output during a cycle at the source in FDTD time stepping. |
| TD.SRATE | Defines the spatial sampling rate in terms on the number of samples per wavelength (in vacuum). |
| TD.WAVES | Specifies the maximum number of cycles (wavelengths) at the source for FDTD time stepping. |

| | |
|-------------------------|---|
| TD.ZCUT | Specifies that structure files output by specification of TD.FILE in LUMINOUS3D will be output at 2D cutplanes. The z location of the 2D cutplane is specified by the value of TD.ZCUT. |
| TM | Specifies that the FDTD source is a transverse magnetic wave. |
| X.POINT, Y.POINT | Specify the location of a point source for FDTD. |

Monochromatic Beam Example

This beam has a monochromatic spectrum with a wavelength of 0.6 μm . The beam originates at $x=0.5$ and $y=-2.0$. It has a 90 degree propagation angle and a beam width of 0.2 μm which is centered at the beam origin. During the ray trace calculation the rays will be terminated when the power level along the ray falls to 5% of the original power.

```
BEAM NUM=1 WAVELENGTH=0.6 X=0.5 Y=-2.0 ANG=90.0 MIN=-0.1 MAX=0.1 \
MIN.POWER=0.05
```

Multi-spectral Beam Example

A multi-spectral beam (at a 45 degree angle) which originates at $x=0.0$ and $y=-1.0$. The multi-spectral source is imported from the spectrum file, *source.spc*. The spectrum is discretized into our wavelengths between 0.4 μm and 0.6 μm .

```
BEAM NUM=2 X=0.0 Y=-1.0 ANG=45.0 \
POWER.FILE=SOURCE.SPC WAVEL.START=0.4 \
WAVEL.END=0.6 WAVEL.NUM=4
```

LUMINOUS3D Lens Example

```
BEAM NUM=1 X.ORIGIN=2.5 Y.ORIGIN=-1.0 Z.ORIGIN = 2.5 ANG=90.0 WAVEL=0.6 \
NX=10 NZ=10 LENS.X=2.5 LENS.Y=-0.5 LENS.Z=2.5 \
LENS.INDEX=2.03 LENS.RADIUS=0.25 LENS.PLANE=-0.5
```

Gaussian Intensity Profile Example

The following beam statement will define a beam window 2 μm wide that is centred at (X.ORIGIN, Y.ORIGIN) with a Gaussian peak of 0.01 W/cm² with a standard deviation of 0.05 μm .

```
beam num=1 x.origin=5.0 y.origin=-1.0 angle=90.0 wavelength=0.6 \
xmin=-1 xmax=1 GAUSSIAN MEAN=0 SIGMA=0.05 RAYS=200
SOLVE B1=1E-2
```

Note: It is recommended that you use the RAYS parameter to define a large number of rays across the beam to ensure that the Gaussian profile is adequately reproduced. The rays are evenly spaced across the beam so it is necessary to use a large number of them.

21.4: COMMENT,

COMMENT allows comments to be placed in an ATLAS input file. ATLAS will print and display comment lines.

Syntax

```
COMMENT [<string>]
      # [<string>]
```

string is any alphabetic, numeric, or alphanumeric sequence of characters. The synonym for this parameter for #.

Example

```
COMMENT  ATLAS is a copyright of Silvaco International
      #   ATLAS is a copyright of Silvaco International
```

Note: The \$ was allowed as a comment character in previous versions of ATLAS. This should be avoided and replaced by the # or COMMENT statement.

21.5: CONTACT

CONTACT specifies the physical attributes of an electrode.

Note: If the CONTACT statement is not used for a given electrode, the electrode is assumed to be charge-neutral (Ohmic).

Syntax

CONTACT NUMBER=<n> | NAME=<ename> | ALL [<wfp>] [<bc>] [<lcr>] [<link>]

| Parameter | Type | Default | Units |
|--------------|-----------|---------|-----------------------|
| ALL | Logical | False | |
| ALPHA | Real | 0 | cm |
| ALUMINUM | Logical | False | |
| BARRIER | Logical | False | |
| BETA | Real | 1.0 | |
| CAPACITANCE | Real | 0 | F/μm |
| CGTUNN | Logical | True | |
| COMMON | Character | | |
| CON.RESIST | Real | 0 | Ω·cm ² |
| CURRENT | Logical | False | |
| DDMS.TUNNEL | Logical | False | |
| DEVICE | Character | | |
| DOS.NEGF | Real | 0.1 | 1/eV |
| E.TUNNEL | Logical | False | |
| ELE.CAP | Integer | | |
| EXCLUDE_NEAR | Logical | False | |
| EXT.ALPHA | Real | 0 | W/(cm ² K) |
| EXT.TEMP | Real | 300 | K |
| F.ETUNNEL | Character | | |
| F.WORKF | Character | | |
| FACTOR | Real | 0 | |
| FARADS | Logical | False | |
| FLOATING | Logical | False | |
| FG.CAP | Real | 0.0 | F/μm |

| Parameter | Type | Default | Units |
|---------------|-----------|---------|-------|
| GAMMA | Real | 1.0 | |
| H.TUNNEL | Logical | False | |
| HENRYS | Logical | False | |
| INDUCTANCE | Real | 0 | H·μm |
| ME.TUNNEL | Real | 1.0 | |
| MH.TUNNEL | Real | 1.0 | |
| MO.DISILICIDE | Logical | False | |
| MOLYBDENUM | Logical | False | |
| MULT | Logical | False | |
| NAME | Character | | |
| NEGF.TUNNEL | Logical | False | |
| NEUTRAL | Logical | True | |
| N.POLYSILICON | Logical | False | |
| NSURF.REC | Logical | False | |
| NUMBER | Integer | | |
| OHMS | Logical | False | |
| P.POLYSILICON | Logical | False | |
| PARABOLIC | Logical | False | |
| PIPINYS | Logical | False | |
| PSURF.REC | Logical | False | |
| REFLECT | Logical | False | |
| REFLECT | Real | | |
| RESISTANCE | Real | 0 | Ω·μm |
| RESONANT | Logical | False | |
| SHORT | Logical | False | |
| STRUCTURE | Character | | |
| SURF.REC | Logical | False | |
| QTUNN.CMASS | Real | 1.0 | |
| QTUNN.VMASS | Real | 1.0 | |
| TU.DISILICIDE | Logical | False | |
| TUNGSTEN | Logical | False | |

| Parameter | Type | Default | Units |
|-----------|------|-----------------|-------|
| VSURFN | Real | see description | cm/s |
| VSURFP | Real | see description | cm/s |
| WORKFUN | Real | 0 | V |

Description

| | |
|----------------------|--|
| ALL | Defines the same properties for all electrodes. |
| DDMS . TUNNEL | Specifies Schottky contact in DDMS model. |
| DEVICE | Specifies which device the CONTACT statement applies to in MIXEDMODE. The synonym for this parameter is STRUCTURE. |
| DOS . NEGF | Sets the value of metal density of states to be used in contact self-energy of Schottky contact. |
| NAME | Specifies the name of a previously defined electrode. See Section 21.12: "ELECTRODE" for more information. |
| NEGF . TUNNEL | Specifies Schottky contact in NEGF model. |
| NUMBER | Specifies the contact number to be defined. It must be the number of a previously defined electrode. It is recommended that electrode names be used rather than numbers. |
| STRUCTURE | This is a synonym for DEVICE. |
| wfp | This is one of the work function parameters described below. It is permitted to either specify the name of a material or a work function value (WORKFUN parameter). |
| bc | This is one or more of the boundary condition parameters. |
| lcr | This is one or more of the external parasitic element parameters. |
| link | This is one or more of a set of parameters that allow you to associate two or more electrodes electrically. |

Workfunction Parameters

| | |
|------------------------|--|
| ALUMINUM | Specifies aluminum as the contact material for the electrode. This sets the workfunction to 4.10V. Note that this parameter should not be set if an Ohmic contact is required. |
| F . WORKF | Specifies the name of a file containing a C-Interpreter function describing the workfunction as a function of the electric field. |
| MOLYBDENUM | Specifies molybdenum as the contact material for the electrode. This sets the work function of the electrode to 4.53V. |
| MO . DISILICIDE | Specifies molybdenum disilicide as the contact material for the electrode. This sets the work function of the electrode to 4.80V. |

| | |
|----------------------|--|
| NEUTRAL | Specifies that the electrode is Ohmic. This is the default characteristic of an electrode. |
| N.POLYSILICON | Specifies n+ doped polysilicon as the contact material for the electrode. This sets the work function to 4.17V. |
| NSURF.REC | Enables finite surface recombination velocity for electrons. |
| P.POLYSILICON | Specifies p+ polysilicon as the contact material for the electrode. This sets the work function to 4.17V + $E_g(\text{Si})$. |
| PARABOLIC | Enables the parabolic Schottky field emission model as given in Equation 3-153. |
| PSURF.REC | Enables finite surface recombination velocity for holes. |
| TU.DISILICIDE | Specifies tungsten disilicide as the contact material for the electrode. This sets the work function to 4.80V. |
| TUNGSTEN | Specifies tungsten as the contact material for the electrode. This sets the work function to 4.63V. |
| WORKFUN | Specifies the work function of the electrode in V. This parameter must be specified in the form <code>WORKFUN=n</code> where n is a real number. This specification is absolute workfunction and not workfunction difference to the semiconductor. |

Note: If no `WORKFUN` or material type parameter is specified, the electrode is assumed to be an Ohmic contact

Boundary Conditions

| | |
|-----------------|---|
| CURRENT | Specifies current boundary conditions. If specified, <code>CAPACITANCE</code> , <code>CON.RESIST</code> , <code>INDUCTANCE</code> , or <code>RESISTANCE</code> may not be specified. |
| FLOATING | Specifies a charge boundary condition. This parameter is used to specify the floating gate in EPROM devices. This parameter can only be used for insulated contacts. If specified, <code>CAPACITANCE</code> , <code>CON.RESIST</code> , <code>INDUCTANCE</code> , or <code>RESISTANCE</code> may not be specified, but special syntax exists for adding capacitances to a floating contact. See <code>EL<n>.CAP</code> and <code>FG<n>.CAP</code> . The synonym for this parameter is <code>CHARGE</code> . |
| ALPHA | Specifies the linear, dipole lowering coefficient. This parameter has no effect unless the <code>BARRIER</code> parameter has been specified (See Chapter 3: “Physics”, Equation 3-149). |
| BARRIER | Turns on the barrier lowering mechanism for Schottky contacts. |
| BETA | Specifies a prefactor in the barrier lowering (See Chapter 3: “Physics”, Equation 3-149). |
| CGTUNN | Includes Floating Gate to Control Gate Current (FGCG) in charging model. Only works on a <code>FLOATING</code> contact. |
| E.TUNNEL | Specifies that the Schottky tunneling model for electrons will be used. <code>E.TUNNEL</code> will also enable the <code>SURF.REC</code> boundary condition which models the thermionic emission in a Schottky contact. |

| | |
|--------------------------|--|
| H.TUNNEL | Specifies that the Schottky tunneling model for holes will be used. H.TUNNEL will also enable the SURF.REC boundary condition which models the thermionic emission in a Schottky contact. |
| EXCLUDE_NEAR | Specifies that the contact should be excluded from the algorithm that finds the nearest electrode to a given point in the direct quantum tunneling model (See Chapter 3: “Physics”, Section 3.6.6: “Gate Current Models”). |
| EXT.ALPHA | Specifies the inverse value of the thermal resistance that can be applied to a contact when performing energy balance simulations. Basically, the thermal resistance allows the carrier energy boundary condition at a contact to be a value other than the ambient temperature. |
| EXT.TEMP | Specifies the external temperature, or carrier energy, of an electrode when performing energy balance simulations. |
| F.ETUNNEL | Specifies the name of a file containing a C-Interpreter function that specifies electron tunneling at a Schottky contact. |
| GAMMA | Specifies a exponent in the linear barrier lowering term (See Chapter 3: “Physics”, Equation 3-149). |
| ME.TUNNEL | Specifies the relative effective mass for use in the electron tunneling mode (see E.TUNNEL). |
| MH.TUNNEL | Specifies the relative effective mass for use in the hole tunneling mode (see H.TUNNEL). |
| PIPINYS | Enables the reverse bias phonon-assisted tunneling model for GaN Schottky diodes. |
| REFLECT (Logical) | Specifies that for Energy Balance and Hydrodynamic simulation using a Neumann (reflective) boundary condition for carrier temperature equations. By default, contacts are handled as Dirichlet boundaries with carrier temperature equal to lattice temperature. In case of Schrodinger or NEGF solution, the parameter will enforce von Neumann boundary conditions for potential in the contact. |
| REFLECT (Real) | Specifies the reflection coefficient for all rays incident on the boundaries of the associated electrode for LUMINOUS2D. The alias for this parameter is L.REFLECT. |
| SURF.REC | Specifies that finite surface recombination velocities are used at the respective contact. This parameter must be specified in the form SURF.REC [VSURFN=<n>] [VSURFP=<p>], where n and p are real numbers. |
| VSURFN | <p>Specifies the actual surface recombination velocities for electrons (V_{sn}). If this parameter is not specified, its default value is calculated by Equation 21-1.</p> $V_{sn} = \frac{ARICHN \cdot T_L^2}{qN_C} \quad 21-1$ <p>where ARICHN is the effective Richardson constant for electrons. This constant accounts for quantum mechanical reflections and tunneling.</p> |

| | |
|--------------------|---|
| VSURFP | <p>Specifies the actual surface recombination velocities for holes (V_{sp}). If this parameter is not specified, its default value is calculated by Equation 21-2.</p> $V_{sp} = \frac{ARICHPT_L^2}{qN_V} \quad 21-2$ <p>where ARICHPT is the effective Richardson constants for holes. This constant accounts for quantum mechanical reflections and tunneling.</p> |
| QTUNN.CMASS | Specifies the electron effective mass to use in the contact for a direct quantum tunneling model (See Chapter 3: “Physics”, Section 3.6.6: “Gate Current Models”). |
| QTUNN.VMASS | Specifies the hole effective mass to use in the contact for a direct quantum tunneling model (See Chapter 3: “Physics”, Section 3.6.6: “Gate Current Models”). |

Contact Parasitics

| | |
|--------------------|---|
| CAPACITANCE | Specifies a lumped capacitance value to be attached to the contact. |
| CON.RESIST | Specifies a distributed contact resistance. You cannot specify both CON.RESIST and RESIST. |
| FARADS | Specifies that the CAPACITANCE value will be in the units of Farads. |
| HENRYS | Specifies that the INDUCTANCE value will be in the units of Henrys. |
| INDUCTANCE | Specifies an external inductance which is related to the specified electrode. A synonym is L. |
| OHMS | Specifies that the RESISTANCE value will be in the units of ohms. |
| RESISTANCE | Specifies a lumped resistance value. You may not specify both RESISTANCE and CON.RESIST. |

Note: There are restrictions on the allowed numerical methods and types of analysis possible when any form of parasitic element is attached to a contact. See Chapter 2: “Getting Started with ATLAS” for details.

| | |
|-----------------|---|
| RESONANT | Only applies to small signal AC analysis. If set, it models the lumped elements as forming a parallel resonant circuit. The resistor and inductor are joined in series, while the capacitor is in parallel with them. The driving voltage used in the perturbation analysis is then applied to the circuit. If you do not set RESONANT, then the capacitor will be connected to AC ground (see Figure 3-4). |
|-----------------|---|

Electrode Linking Parameters

These parameters allow one electrode to be biased as a function of another electrode. This allows separate regions of the same physical contact to be linked together. For example, in the statement:

```
CONTACT NAME=MYDRAIN COMMON=DRAIN FACTOR=4.6
```

The electrode, MYDRAIN, is linked to the electrode, DRAIN. The bias on MYDRAIN will always be equal to the bias on the drain plus 4.6. If the optional MULT parameter had been specified, the bias on MYDRAIN would be equal to the bias on the drain multiplied by 4.6.

| | |
|---------------|---|
| COMMON | Specifies the electrode name to which the contact referred to by NAME is linked. Although the electrodes are linked, separate currents will be saved for both electrodes unless SHORT is also specified. The electrode referred to in NAME should not appear on any SOLVE statements since its bias is now determined as a function of the electrode referred to by COMMON. |
| SHORT | Specifies that the electrode referred to by NAME is shorted to the electrode specified by the COMMON parameter. This implies that the two electrodes will be treated as one and only one value will be written to log files and in the run time output. |
| FACTOR | Specifies the constant offset voltage (or current) between the electrodes referred by NAME and COMMON. By default, FACTOR is added the defined voltage. |
| MULT | Specifies that FACTOR is a multiplier. |

Floating Gate Capacitance Parameters

In some cases, you may want to simulate floating gate structures, in 2D, which have control gates that are longer in the unsimulated dimension than the floating gate. In these cases, specify the following parameters to account for addition capacitance between the floating gate and the control gate and other electrodes. Up to four extra capacitances are allowed so in the following <n> is an integer number between 1 and 4.

| | |
|-------------------------|---|
| EL<n> .CAP | Specifies the name of the electrode to which the extra capacitance is linked. |
| FG<n> .CAP | Specifies the additional capacitance per unit length to be added between the floating gate and electrode specified in EL<n> .CAP. |

Schottky Barrier and Surface Recombination Example

This example defines all electrodes except number 2 (aluminum) to be neutral. Electrode number 2 also includes finite surface recombination velocities and barrier lowering. A definition in the second statement overrides that definition in the first statement.

```
CONTACT ALL NEUTRAL
CONTACT NUMBER=2 ALUMINUM SURF.REC BARRIER
```

Parasitic Resistance Example

This example attaches a lumped resistor with a value of $10^5 \Omega \mu\text{m}$ to the substrate. A distributed contact resistance of $10^{-6} \Omega \cdot \text{cm}^2$ is included on the drain.

```
CONTACT NAME=substrate RESISTANCE=1E5
CONTACT NAME=drain CON.RESIST=1E-6
```

Floating Gate Example

This syntax defines a floating contact with a workfunction equal to 4.17eV. An extra 1fF/um capacitance is added between this electrode and the electrode named cgate.

```
CONTACT NAME=fgate FLOATING N.POLY EL1.CAP=cgate FG1.CAP=1e-15
```

Note: The `MODELS PRINT` command can be used to echo the back contact workfunction and parasitic elements settings to the run-time output.

21.6: CURVETRACE

CURVETRACE sets the parameters for the automatic curve tracing routine.

Syntax

CURVETRACE <params>

| Parameter | Type | Default | Units |
|-----------------|-----------|-----------------------|----------|
| ANGLE1 | Real | 5 | Degree |
| ANGLE2 | Real | 10 | Degree |
| ANGLE3 | Real | 15 | Degree |
| BEG.VAL | Real | 0.0 | V |
| CONTROLRES | Real | 1.0×1.0^{10} | Ω |
| CONTR.ELEC | Integer | | |
| CONTR.NAME | Character | | |
| CURR.CONT | Logical | | |
| END.VAL | Real | | |
| MAXDV1 | Real | 0.1 | V |
| MAXDV2 | Real | 1.0 | V |
| MINCUR | Real | | |
| MINDL | Real | 0.1 | |
| NEXTST.RATIO | Real | 2.0 | |
| NO.BACKTRACE | Logical | False | |
| STEP.CONT | Logical | | |
| STEP.INIT | Real | 0.1 | V |
| STEPS | Real | 0.1 | |
| THETA.BACKTRACE | Real | 0.01 | Degree |
| TURNINGPOINT | Logical | False | |
| V.BACKTRACE | Real | 1 | V |
| VOLT.CONT | Logical | False | |

Description

| | |
|-----------------------------------|---|
| ANGLE1, ANGLE2, and ANGLE3 | These are the critical angles (in degrees) affecting the smoothness and step size of the trace. If the difference in slopes of the last two solution points is less than ANGLE1, the step size will be increased for the next projected solution. If the difference lies between ANGLE1 and ANGLE2, the step size remains the same. If the difference is greater than ANGLE2, the step size is reduced. ANGLE3 is the maximum difference allowed, unless overridden by the MINDL parameter. ANGLE2 should always be greater than ANGLE1 and less than ANGLE3. |
| BEG.VAL | This is the value of the voltage at the starting point of the curve trace for the controlling electrode. |
| CONTR.ELEC | This is the number of the electrode that is designated as a control electrode. |
| CONTR.NAME | This is the name of the control electrode. |
| CURR.CONT | Denotes that a maximum current on the control electrode, specified by END.VAL is used as the upper bound on the trace. |
| CONTROLRES | Specifies the control resistance value to be set at the control electrode after the current at the control electrode becomes greater than the value specified by the MINCUR parameter. Using a large value of the control resistance allows you to set the value of the current (instead of the internal voltage) on the control electrode. A large value of the control resistance is suitable for electron devices where the shape of the characteristic curve is vertical or exhibits the presence of turning points (where it is required to switch the electrode control from voltage to current). |
| END.VAL | This is used to stop tracing if the voltage or current of control electrode equals or exceeds END.VAL. |
| MAXDV1 | Specifies maximum value of the voltage bias step at the beginning of the CURVETRACER algorithm. This limitation is used until the current at the control electrode is greater than the value specified by the MINCUR parameter. |
| MAXDV2 | Specifies maximum value of the voltage bias step to be used after the current at the control electrode becomes greater than the value specified by the MINCUR parameter. |
| MAXDV1 and MAXDV2 | Control (together with NEXTST.RATIO) the maximum voltage step at each point of the IV curve. Using large values for them means that few points are used to trace the curve. This results in a faster simulation but can affect the stability of the tracing algorithm and decrease the accuracy of the IV curve. |
| MINCUR | This may be used to set a small current value in order to switch from internal control electrode bias ramping to external ramping with load resistor. This parameter is recommended for small current breakdown simulation. |

| | |
|----------------------|---|
| MINDL | This is the minimum normalized step size allowed in the trace. Usually, you don't need to adjust this parameter. Increasing MINDL will reduce the smoothness of the trace by overriding the angle criteria, resulting in more aggressive projection and fewer simulation points. Reducing MINDL will enhance the smoothness and increase the number of points in the trace. |
| NEXTST .RATIO | Specifies which factor to use to increase the voltage step on the smooth parts of the I-V curve. |
| NO .BACKTRACE | Stops curve tracing if it detects back tracing. |

Note: If you define the curvetrace using the CONTINUE parameter on the SOLVE statement and you specify _TMA on the command line, then the default value of NO .BACKTRACE is true.

| | |
|-------------------|--|
| STEPS | This is the number of operational points on a trace if STEP .CONT was specified. |
| STEP .CONT | Specifies that the trace will proceed for a certain number of simulation points. |
| STEP .INIT | Specifies initial voltage step size. |

Note: To set a sweep of increasingly negative voltage in CURVETRACE, you only need to set STEP .INIT to be negative. Since all parameters are multiplier of STEP .INIT, the whole voltage sweep will be negative.

| | |
|-------------------------|--|
| THETA .BACKTRACE | Specifies the angular difference at which the curve is considered to be backtracing. |
| TURNINGPOINT | Specifies that binary output solution files will be saved whenever the slope of the IV curve changes sign (i.e., there is a turning point). The name of the output file is <i>soln.num</i> , where <i>num</i> is the number of the current solution. |
| V .BACKTRACE | Specifies the (internal) voltage difference at which the curve is considered to be backtracing. |
| VOLT .CONT | Denotes that a maximum voltage on the control electrode, specified by END .VAL is used as the upper bound on the trace. |

Diode Breakdown Example

To trace a diode breakdown curve using current value as a termination criteria, the following statement may be used:

```
CURVETRACE CURR.CONT END.VAL=0.01 CONTR.NAME=anode \
MINCUR=5E-12 NEXTST.RATIO=1.1 STEP.INIT=0.1
SOLVE CURVETRACE
```


21.7: DBR

The DBR statement is used to define Distributed Bragg Reflectors (DBR). DBRs are periodic structures composed of alternating layers of two different materials. The alias for this parameter is SUPERLATTICE.

Syntax

DBR <parameters>

| Parameter | Type | Default | Units |
|--------------|-----------|---------|------------------|
| BOTTOM | Logical | False | |
| CALC1.STRAIN | Logical | False | |
| CALC2.STRAIN | Logical | False | |
| HALF.CYCLES | Real | 2 | |
| LAYERS | Real | 2 | |
| LED1 | Logical | False | |
| LED2 | Logical | False | |
| MAT1 | Character | | |
| MAT2 | Character | | |
| N1 | Real | 0 | |
| N2 | Real | 0 | |
| NA1 | Real | 0.0 | cm ⁻³ |
| NA2 | Real | 0.0 | cm ⁻³ |
| NAME1 | Character | | |
| NAME2 | Character | | |
| ND1 | Real | 0.0 | cm ⁻³ |
| ND2 | Real | 0.0 | cm ⁻³ |
| NU12 | Integer | 5 | |
| NU21 | Integer | 5 | |
| POLARIZ1 | Logical | False | |
| POLARIZ2 | Logical | False | |
| POLAR1.CHARG | Real | 0 | cm ⁻² |
| POLAR2.CHARG | Real | 0 | cm ⁻² |
| POLAR1.SCALE | Real | 1.0 | |
| POLAR2.SCALE | Real | 1.0 | |

| | | | |
|-------------|---------|-------|----|
| QWELL1 | Logical | False | |
| QWELL2 | Logical | False | |
| SPA1 | Real | 0.0 | μm |
| SPA2 | Real | 0.0 | μm |
| STRAIN1 | Real | 0.0 | |
| STRAIN2 | Real | 0.0 | |
| TH12 | Real | | |
| TH21 | Real | | |
| THICK1 | Real | 0.0 | μm |
| THICK2 | Real | 0.0 | μm |
| TOP | Logical | False | |
| WELL1.CNBS | Integer | 1 | |
| WELL2.CNBS | Integer | 1 | |
| WELL1.FIELD | Logical | True | |
| WELL2.FIELD | Logical | True | |
| WELL1.GAIN | Real | 1.0 | |
| WELL2.GAIN | Real | 1.0 | |
| WELL1.NX | Integer | 10 | |
| WELL2.NX | Integer | 10 | |
| WELL1.NY | Integer | 10 | |
| WELL2.NY | Integer | 10 | |
| WELL1.VNBS | Integer | 1 | |
| WELL2.VNBS | Integer | 1 | |
| Y.START | Real | 0.0 | μm |
| Y.FINISH | Real | 0.0 | μm |
| Y.FINAL | Real | 0.0 | μm |
| Y.END | Real | 0.0 | μm |
| Y1.COMP | Real | 0.0 | |
| Y2.COMP | Real | 0.0 | |
| X1.COMP | Real | 0.0 | |
| X2.COMP | Real | 0.0 | |

Description

The DBR statement is a short cut for specifying a set of REGION statements, which specifies a stack of alternating layers of two materials. The material compositions of the layers are specified by the MAT1, MAT2, NA1, NA2, ND1, ND2, STRAIN1, STRAIN2, X1.COMP, X2.COMP, Y1.COMP, and Y2.COMP parameters. The number of layers are specified by the HALF.CYCLES parameter. The locations of the layers are specified by the Y.START, Y.FINISH or the TOP/BOTTOM parameters. The meshing of the layers is specified by the N1, N2 or the SPA1, SPA2 parameters.

For more information about DBR, see Chapter 9: “VCSEL Simulator”, the “Specifying Distributed Bragg Reflectors” Section on page 9-10.

| | |
|-----------------------------------|---|
| BOTTOM | Specifies that the DBR is to be added at the bottom (starting at the maximum previously specified Y coordinate and extending in the positive Y direction) of the structure. |
| CALC1.STRAIN, CALC2.STRAIN | Specifies that the strain in the region/cycle is calculated from the lattice mismatch with adjacent regions. |
| HALF.CYCLES | Specifies the total number of layers. Note that if HALF.CYCLES is odd, there will be more layers of one material than the other. Its alias is LAYERS. |

Note: Don't confuse HALD.CYCLES with fractions of the optical emission wavelength. HALF.CYCLES relates to layers.

| | |
|---------------------|--|
| LAYERS | This is an alias for HALF.CYCLES. |
| LED1, LED2 | Specifies that the region/cycle is to be treated as a light emitting region and included in postprocessing for LED analysis. See Chapter 11: “LED: Light Emitting Diode Simulator”. |
| MAT1 | Specifies the material name for layers of material 1. |
| MAT2 | Specifies the material name for layers of material 2. |
| N1 | Specifies the integer number of mesh lines per layer of material 1. Note that if N1 is specified, then SPA1 shouldn't be specified. |
| N2 | Specifies the integer number of mesh lines per layer of material 2. Note that if N2 is specified, then SPA2 shouldn't be specified. |
| NAME1, NAME2 | Specify the names of the regions composed of material 1 and material 2. You can conveniently use these names to modify material parameters and models on the MATERIAL, MODEL, IMPACT, and MOBILITY statements. |
| NA1 | Specifies the ionized acceptor concentration in layers of material 1. |
| NA2 | Specifies the ionized acceptor concentration in layers of material 2. |
| ND1 | Specifies the ionized donor concentration in layers of material 1. |
| ND2 | Specifies the ionized donor concentration in layers of material 2. |
| NU12 | This is the number of grid lines in the graded region between the 1st and 2nd half cycle in the direction specified by the BOTTOM or TOP parameters. |
| NU21 | This is the number of grid lines in the graded region between the 2nd and 1st half cycle in the direction specified by the BOTTOM or TOP parameters. |

| | |
|---|---|
| POLARIZ1, POLARIZ2 | Enables the automatic calculation of added interface charge due to spontaneous and piezoelectric polarization. See Chapter 3: "Physics", Section 3.6.11: "Polarization in Wurtzite Materials [26]". |
| POLAR1.CHARG, POLAR2.CHARG | Specify polarization charge densities to replace those calculated using Equations 3-506 and 3-507. |
| POLAR1.SCALE, POLAR2.SCALE | Specifies a constant scale factor multiplied by the calculated spontaneous and piezoelectric polarization charges when you enable polarization by setting the POLARIZATION parameter of the DBR statement. See Chapter 3: "Physics", Section 3.6.11: "Polarization in Wurtzite Materials [26]". |
| QWELL1, QWELL2 | Specifies that the region/cycle is treated as a quantum well for calculation of radiative recombination or gain or both for certain optoelectronic models. |
| SPA1 | Specifies the spacing between mesh lines in layers of material 1. Note that this should be smaller than or equal to THICK1. |
| SPA2 | Specifies the spacing between mesh lines in layers of material 2. Note that this should be smaller than or equal to THICK2. |
| STRAIN1 | Specifies the strain in the layer of material 1. (Negative strain is compressive). |
| STRAIN2 | Specifies the strain in the layer of material 2. (Negative strain is compressive). |
| TOP | Specifies that the DBR is to be added at the top (starting at the minimum previously specified Y coordinate and extending in the negative Y direction) of the structure. |
| TH12 | This is the thickness of grading region between 1st half cycle and 2nd half cycle going in the direction specified by the BOTTOM or TOP parameters. |
| TH21 | This is the thickness of grading region between 2nd half cycle and 1st half cycle going in the direction specified by the BOTTOM or TOP parameters. |
| THICK1 | Specifies the thickness of each layer of material 1. |
| THICK2 | Specifies the thickness of each layer of material 2. |
| WELL1.CNBS, WELL2.CNBS, WELL1.VNBS, WELL2.VNBS | Specify the number of bound states retained for calculation of radiative recombination or gain if the region/cycle is treated as a quantum well as specified by the QWELL1, QWELL2 parameters. |
| WELL1.FIELD, WELL2.FIELD | When enabled, specify that the calculations of bound state energies should include the effects of the local field. |
| WELL1.GAIN, WELL2.GAIN | Specify a constant scale factor multiplied by the calculated gain to give the net gain used for certain optoelectronic calculations. |
| WELL1.NX, WELL2.NX, WELL1.NY, WELL2.NY | Specify the number of slices (WELL#.NX) and the number of samples per slice (WELL#.NY) are used in the solution of Schrodinger's equation to obtain the local bound state energies for calculation of radiative recombination or gain or both for certain optoelectronic models. |
| Y.START | Specifies the starting location of a DBR that begins with a layer of material 1 and alternates materials in an increasing Y direction. |

| | |
|---------------------------------|--|
| Y.FINISH | Specifies the starting location of a DBR that begins with a layer of material 1 and alternates materials in an decreasing Y direction. |
| Y.FINAL and Y.END | These are aliases for Y.FINISH. |
| Y1.COMP | Specifies the composition fraction y in layers of material 1. |
| Y2.COMP | Specifies the composition fraction y in layers of material 2. |
| X1.COMP | Specifies the composition fraction x in layers of material 1. |
| X2.COMP | Specifies the composition fraction x in layers of material 2. |

Note: DBR statements can be intermixed with X.MESH, Y.MESH, and REGION statements.

21.8: DEFECTS

DEFECTS activates the band gap defect model and sets the parameter values. This model can be used when thin-film transistor simulations are performed using the TFT product.

Syntax

DEFECTS [<parameters>]

| Parameter | Type | Default | Units |
|-------------------|-----------|----------------------|----------------------------|
| AFILE | Character | | |
| AMPHOTERIC | Logical | False | |
| CONTINUOUS | Logical | False | |
| DEVICE | Character | | |
| DFILE | Character | | |
| EGA | Real | 0.4 | eV |
| EGD | Real | 0.4 | eV |
| EP.AMPHOTERIC | Real | 1.27 | eV |
| EPT0.AMPHOTERIC | Real | 1.3×10^6 | s |
| EPBETA.AMPHOTERIC | Real | 0.5 | s |
| EU.AMPHOTERIC | Real | 0.2 | eV |
| EV0.AMPHOTERIC | Real | 0.056 | eV |
| F.TFTACC | Character | | |
| F.TFTDON | Character | | |
| FILE.AMPHOTERIC | Character | | |
| FILE.INT | Logical | False | |
| FILEX.AMPHOTERIC | Character | | |
| FILEY.AMPHOTERIC | Character | | |
| FILEZ.AMPHOTERIC | Character | | |
| HCONC.AMPHOTERIC | Real | 5×10^{21} | cm^{-3} |
| INT_LIM1 | Real | 0 | eV |
| INT_LIM2 | Real | 0 | eV |
| MATERIAL | Character | | |
| NA.MIN | Real | 1.0×10^{13} | cm^{-3} |
| ND.MIN | Real | 1.0×10^{13} | cm^{-3} |
| NGA | Real | 5.0×10^{17} | cm^{-3}/eV |

| Parameter | Type | Default | Units |
|------------------|-----------|-----------------------|----------------------------|
| NGD | Real | 1.5×10^{18} | cm^{-3}/eV |
| NSISI.AMPHOTERIC | Real | 2×10^{23} | cm^{-3} |
| NTA | Real | 1.12×10^{21} | cm^{-3}/eV |
| NTD | Real | 4.0×10^{20} | cm^{-3}/eV |
| NUM.AMPHOTERIC | Real | 20 | |
| NUMBER | Real | All | |
| NUMA | Real | 12 | |
| NUMD | Real | 12 | |
| NV0.AMPHOTERIC | Real | NV300 | cm^{-3} |
| REGION | Real | All | |
| SIGGAE | Real | 1.0×10^{-16} | cm^2 |
| SIGGAH | Real | 1.0×10^{-14} | cm^2 |
| SIGGDE | Real | 1.0×10^{-14} | cm^2 |
| SIGGDH | Real | 1.0×10^{-16} | cm^2 |
| SIGMA.AMPHOTERIC | Real | 0.19 | eV |
| SIGN0.AMPHOTERIC | Real | 1.0×10^{-16} | cm^2 |
| SIGNP.AMPHOTERIC | Real | 1.0×10^{-16} | cm^2 |
| SIGP0.AMPHOTERIC | Real | 1.0×10^{-16} | cm^2 |
| SIGPN.AMPHOTERIC | Real | 1.0×10^{-16} | cm^2 |
| SIGTAE | Real | 1.0×10^{-16} | cm^2 |
| SIGTAH | Real | 1.0×10^{-14} | cm^2 |
| SIGTDE | Real | 1.0×10^{-14} | cm^2 |
| SIGTDH | Real | 1.0×10^{-16} | cm^2 |
| STRUCTURE | Character | | |
| T0.AMPHOTERIC | Real | 300 | K |
| TFILE | Character | | |
| WGA | Real | 0.1 | eV |
| WGD | Real | 0.1 | eV |
| WTA | Real | 0.025 | eV |
| WTD | Real | 0.05 | ev |

| Parameter | Type | Default | Units |
|-----------|------|---------|---------------|
| X.MIN | Real | | μm |
| X.MAX | Real | | μm |
| Y.MIN | Real | | μm |
| Y.MAX | Real | | μm |
| Z.MIN | Real | | μm |
| Z.MAX | Real | | μm |

Description

The DEFECTS statement is used to describe the density of defect states in the band gap. You can specify up to four distributions, two for donor-like states and two for acceptor-like states. Each type of state may contain one exponential (tail) distribution and one Gaussian distribution.

| | |
|--------------------------|--|
| AFILE | Specifies the file name where the acceptor state density distribution, as a function of energy, will be stored. You can examine this file by using TONYPLOT. |
| AMPHOTERIC | Specifies the amphoteric defect model will be used. |
| CONTINUOUS | Specifies that the continuous defect integral model will be used. |
| DEVICE | Specifies which device the statement applies in mixed mode simulation. The synonym for this parameter is STRUCTURE. |
| DFILE | Specifies the file name where the donor state density distribution, as a function of energy, will be stored. You can examine this file by using TONYPLOT. |
| EGA | Specifies the energy that corresponds to the Gaussian distribution peak for acceptor-like states. This energy is measured from the conduction band edge. |
| EGD | Specifies the energy that corresponds to the Gaussian distribution peak for donor-like states. This energy is measured from the valence band edge. |
| EP.AMPHOTERIC | Specifies the most probable potential defect energy. |
| EPT0.AMPHOTERIC | Specifies the time constant used in time amphoteric reflect generation model. |
| EPBETA.AMPHOTERIC | Specifies the exponential constant used in the amphoteric defect generation model. |
| EU.AMPHOTERIC | Specifies the defect electron correlation energy. |
| EV0.AMPHOTERIC | Specifies the characteristic energy. |
| F.TFTACC | Specifies the name of a file containing a C-Interpreter function, describing the distribution of acceptor state densities as a function of energy. |

| | |
|--------------------------------|---|
| F.TFTDON | Specifies the name of a file containing a C-Interpreter function, describing the distribution of donor state densities as a function of energy. |
| FILE.AMPHOTERIC | Specifies the file name where the dangling bond density of states distribution, as a function of energy, will be stored. If you specify <code>FILEX.AMPHOTERIC</code> , <code>FILEY.AMPHOTERIC</code> , and <code>FILEZ.AMPHOTERIC</code> , then the file will be saved at the coordinate closest to the one specified by <code>FILEX.AMPHOTERIC</code> , <code>FILEY.AMPHOTERIC</code> , and <code>FILEZ.AMPHOTERIC</code> . |
| FILE.INT | Specifies the integrated density of states with respect to energy will be stored in the <code>AFILE</code> , <code>DFILE</code> , and <code>TFILE</code> files for discrete defects. |
| FILEX.AMPHOTERIC | Specifies the X coordinate used in <code>FILE.AMPHOTERIC</code> . |
| FILEY.AMPHOTERIC | Specifies the Y coordinate used in <code>FILE.AMPHOTERIC</code> . |
| FILEZ.AMPHOTERIC | Specifies the Z coordinate used in <code>FILE.AMPHOTERIC</code> . |
| HCONC.AMPHOTERIC | Specifies the density of hydrogen. |
| INT_LIM1 | Specifies the lower limit for the numerical integration of the CONTINUOUS method. |
| INT_LIM2 | Specifies the upper limit for the numerical integration of the CONTINUOUS method. |
| MATERIAL | Specifies which material from the table in Appendix B: “Material Systems” will apply to the DEFECT statements. If a material is specified, then the regions defined as being composed of that material will be affected. |
| NA.MIN | Specifies the minimum value of the acceptor trap DOS that will be used in the discrete DEFECTS model. |
| ND.MIN | Specifies the minimum value of the donor trap DOS that will be used in the discrete DEFECTS model. |
| NGA | Specifies the total density of acceptor-like states in a Gaussian distribution. |
| NGD | Specifies the total density of donor-like states in a Gaussian distribution. |
| NSISI.AMPHOTERIC | Specifies the density of Si-Si bonds. |
| NTA | Specifies the density of acceptor-like states in the tail distribution at the conduction band edge. |
| NTD | Specifies the density of donor-like states in the tail distribution at the valence band edge. |
| NUM.AMPHOTERIC | Specifies the number of energy levels used in the DOS integration for amphoteric defects. |
| NUMBER or REGION | Specifies the region index to which the DEFECT statement applies. |
| NUMA | Specifies the number of discrete levels that will be used to simulate the continuous distribution of acceptor states. |

| | |
|-------------------------|--|
| NUMD | Specifies the number of discrete levels that will be used to simulate the continuous distribution of donor states. |
| NV0.AMPHOTERIC | Specifies the density of states of the valance-band tail exponential region extrapolated to the valence-band edge. If this parameter is not specified, then the valence band density of states (NV300 on the MATERIAL statement) will be used instead. |
| SIGGAE | Specifies the capture cross-section for electrons in a Gaussian distribution of acceptor-like states. |
| SIGGAH | Specifies the capture cross-section for holes in a Gaussian distribution of acceptor-like states. |
| SIGGDE | Specifies the capture cross-section for electrons in a Gaussian distribution of donor-like states. |
| SIGGDH | Specifies the capture cross-section for holes in a Gaussian distribution of donor-like states. |
| SIGMA.AMPHOTERIC | Specifies the defect pool width. |
| SIGN0.AMPHOTERIC | Specifies the electron capture cross-section for neutral defects. |
| SIGNP.AMPHOTERIC | Specifies the electron capture cross-section for positive defects. |
| SIGP0.AMPHOTERIC | Specifies the hole capture cross-section for neutral defects. |
| SIGPN.AMPHOTERIC | Specifies the hole capture cross-section for negative defects. |
| SIGTAE | Specifies the capture cross-section for electrons in a tail distribution of acceptor-like states. |
| SIGTAH | Specifies the capture cross-section for holes in a tail distribution of acceptor-like states. |
| SIGTDE | Specifies the capture cross-section for electrons in a tail distribution of donor-like states. |
| SIGTDH | Specifies the capture cross-section for holes in a tail distribution of donor-like states. |
| STRUCTURE | This is a synonym for DEVICE. |
| TFILE | Specifies the file name where the acceptor and donor state density distributions, as a function of energy referenced from E_v , will be stored. You can examine this file by using TONYPLOT. |
| T0.AMPHOTERIC | Specifies the freeze-in temperature. |
| WGA | Specifies the characteristic decay energy for a Gaussian distribution of acceptor-like states. |
| WGD | Specifies the characteristic decay energy for a Gaussian distribution of donor-like states. |

| | |
|---|--|
| WTA | Specifies the characteristic decay energy for the tail distribution of acceptor-like states. |
| WTD | Specifies the characteristic decay energy for the tail distribution of donor-like states. |
| X.MIN, X.MAX, Y.MIN, Y.MAX, Z.MIN, and Z.MAX | Specify the bounding box for the DEFECT statement. |

TFT Example

The following statement lines specify distributed defect states which would typically be used for polysilicon.

```
DEFECTS NTA=1.E21 NTD=1.E21 WTA=0.033 WTD=0.049 \  
        NGA=1.5E15 NGD=1.5E15 EGA=0.62 EGD=0.78 \  
        WGA=0.15 WGD=0.15 SIGTAE=1.E-17 \  
        SIGTAH=1.E-15 SIGTDE=1.E-15 SIGTDH=1.E-17 \  
        SIGGAE=2.E-16 SIGGAH=2.E-15 SIGGDE=2.E-15 \  
        SIGGDH=2.E-16
```

21.9: DEGRADATION

DEGRADATION specifies parameters for MOS device degradation modeling.

Syntax

DEGRADATION <params>

| Parameter | Type | Default | Units |
|-----------|------|----------------------|------------------|
| F.NTA | Char | | |
| F.NTD | Char | | |
| F.NTD | Char | | |
| F.SIGMAE | Char | | |
| F.SIGMAH | Char | | |
| NTA | Real | 1.0×10^{11} | cm^{-2} |
| NTD | Real | 1.0×10^{10} | cm^{-2} |
| SIGMAE | Real | 1.0×10^{17} | cm^{-2} |
| SIGMAH | Real | 1.0×10^{17} | cm^{-2} |

Description

| | |
|-----------------|---|
| NTA | Specifies the uniform acceptor-like trap density on the interface. |
| NTD | Specifies the uniform donor-like trap density on the interface. |
| SIGMAE | Specifies the acceptor-like trap capture cross section. |
| SIGMAH | Specifies the donor-like trap capture cross section. |
| F.NTA | Specifies the file name for a C-Interpreter function that specifies arbitrary density distribution of the acceptor-like traps on the interface. |
| F.NTD | Specifies the file name for a C-Interpreter function that specifies arbitrary density distribution of the donor-like traps on the interface. |
| F.SIGMAE | Specifies the name of a file containing a C-Interpreter function specifying the distribution of acceptor trap cross-sections. |
| F.SIGMAH | Specifies the name of a file containing a C-Interpreter function specifying the distribution of donor trap cross-sections. |

MOS Interface State Example

```
DEGRADATION NTA=1.E-12 SIGMAE=5.E-18
```

This syntax defines a density of acceptor states uniformly distributed along the silicon-oxide interface. The trapping cross section is also defined. Traps will be filled by gate current in transient mode simulations leading to a shift in device parameters.

21.10: DOPING

DOPING specifies doping profiles either analytically or from an input file. The alias for this parameter is PROFILE.

Syntax

DOPING <prof> [<psp>] [<bound>] [<loc>] [<sprea>>] [OUTFILE= <fn>] [<trps>]

| Parameter | Type | Default | Units |
|----------------|-----------|---------|------------------|
| 1D.PROC | Logical | False | |
| 2D.ASCII | Logical | False | |
| A.MAX | Real | 360.0 | Degrees |
| A.MIN | Real | 0.0 | Degrees |
| ACCEPTOR | Logical | False | |
| ACTIVE | Logical | True | |
| ALUMINUM | Logical | False | |
| ANTIMONY | Logical | False | |
| ARSENIC | Logical | False | |
| ASCII | Logical | False | |
| ASPECT.RATIO | Logical | | |
| ATHENA | Logical | False | |
| ATHENA.1D | Logical | False | |
| BACKDOPE | Real | none | cm^{-3} |
| BORON | Logical | False | |
| C.MULT | Real | 1.0 | |
| CHARACTERISTIC | Real | | μm |
| CHEMICAL | Logical | False | |
| CONCENTRATION | Real | 0 | cm^{-3} |
| DEGEN.FAC | Real | | |
| DEVICE | Char | | 1 |
| DIRECTION | Character | y | |
| DONOR | Logical | False | |
| DOP.OFFSET | Real | 0 | cm^{-3} |
| DOP.SEED | Integer | -10 | |
| DOP.SIGMA | Real | 0.0 | cm^{-3} |

| Parameter | Type | Default | Units |
|--------------|-----------|---------|------------------|
| DOP.XMIN | Real | | |
| DOP.XMAX | Real | | |
| DOP.YMIN | Real | | |
| DOP.YMAX | Real | | |
| DOSE | Real | | cm^{-2} |
| ERFC | Logical | False | |
| ERFC.LATERAL | Logical | False | |
| E.LEVEL | Real | | eV |
| F.COMPOSIT | Character | | |
| F.DOPING | Character | | |
| F3.DOPING | Character | | |
| FILE | Character | | |
| GAUSSIAN | Logical | False | |
| IMATER | Character | None | |
| IN.FILE | Character | | |
| INDIUM | Logical | False | |
| INFILE | Character | | |
| INAME | Character | None | |
| INT.LIN | Logical | False | |
| INT.LOG | Logical | True | |
| INT.OPTM | Logical | False | |
| IREGION | Character | None | |
| JUNCTION | Real | | μm |
| LAT.CHAR | Real | | μm |
| MASTER | Logical | False | |
| MATERIAL | Character | | |
| METAL | Logical | False | |
| N.COLUMN | Integer | | |
| N.TYPE | Logical | False | |
| N-TYPE | Logical | False | |
| N.OFFSET | Real | 0.0 | cm^{-3} |

| Parameter | Type | Default | Units |
|---------------|-----------|---------------|--------------------------|
| N.PEAK | Real | 0 | cm^{-3} |
| NAME | Character | | |
| NET | Logical | False | |
| NOROLLOFF | Logical | False | |
| NOXROLLOFF | Logical | False | |
| NOYROLLOFF | Logical | False | |
| NOZROLLOFF | Logical | False | |
| OUTFILE | Character | | |
| OUTSIDE | Logical | False | |
| OX.CHARGE | Logical | False | |
| PEAK | Real | | |
| PHOSPHORUS | Logical | False | |
| P.COLUMN | Integer | | |
| P.TYPE | Logical | False | |
| P-TYPE | Logical | False | |
| R.MAX | Real | Device Radius | μm |
| R.MIN | Real | 0.0 | μm |
| RATIO.LATERAL | Real | 0.7 | |
| RESISTI | Real | | $\Omega \cdot \text{cm}$ |
| REGION | Integer | All | |
| SIGN | Real | | cm^2 |
| SIGP | Real | | cm^2 |
| SLICE.LAT | Real | | μm |
| START | Real | 0 | |
| STRUCTURE | Character | | |
| SUPREM3 | Logical | False | |
| TMA.SUPREM3 | Logical | False | |
| TAUN | Real | | |
| TAUP | Real | | |
| TRAP | Logical | False | |
| UNIFORM | Logical | False | |

| Parameter | Type | Default | Units |
|-----------|---------|---------------------|---------------|
| WIDTH | Real | width of structure | μm |
| X1 | Real | 0 | μm |
| X2 | Real | 0 | μm |
| XY | Logical | True | |
| XZ | Logical | False | |
| X.CHAR | Real | | μm |
| X.COLUMN | Integer | | |
| X.COMP | Logical | False | |
| X.DIR | Logical | False | |
| X.ERFC | Logical | False | |
| X.FLIP | Logical | False | |
| X.LEFT | Real | left of structure | μm |
| X.MAX | Real | | μm |
| X.MIN | Real | | μm |
| X.SCALE | Logical | True | |
| X.RIGHT | Real | right of structure | μm |
| XERFC.LAT | Logical | False | |
| XY.RATIO | Real | 0.7 | |
| Y.BOTTOM | Real | bottom of structure | μm |
| Y.CHAR | Real | | μm |
| Y.COLUMN | Integer | | |
| Y.FLIP | Logical | False | |
| Y.JUNCTI | Real | | μm |
| Y1 | Real | 0 | μm |
| Y2 | Real | 0 | μm |
| YX | Logical | True | |
| YZ | Logical | False | |
| Y.COMP | Logical | False | |
| Y.DIR | Logical | False | |
| Y.MAX | Real | | μm |
| Y.MIN | Real | | μm |
| Y.SCALE | Logical | True | |

| Parameter | Type | Default | Units |
|------------|---------|------------------|---------------|
| Y.TOP | Real | top of structure | |
| Z1 | Real | 0 | μm |
| Z2 | Real | 0 | μm |
| ZY | Logical | False | |
| ZX | Logical | False | |
| Z.BACK | Real | | |
| Z.DIR | Logical | False | |
| Z.FRONT | Real | | |
| Z.MAX | Real | | μm |
| Z.MIN | Real | | μm |
| Z.SCALE | Logical | True | |
| ZERFC.LAT | Logical | False | |
| ZLAT.CHAR | Real | | |
| ZRATIO.LAT | Real | 0.7 | |
| ZSLICE.LAT | Real | | |

Description

The DOPING statement is used to define doping profiles in the device structure. Typically a sequence of DOPING statements is given each building on the others.

| | |
|----------------|---|
| OUTFILE | Specifies the name of an output file for use with REGRID. The first DOPING statement should use this parameter to specify a filename. All doping information from the first DOPING statement and all subsequent DOPING statements in the input file are saved to this file. The REGRID statement can read this file and interpolate doping on the new grid. |
|----------------|---|

Note: The file from OUTFILE cannot be used in TONYPLOT or in the MESH statement. The SAVE command should be used after all of the DOPING commands required to save a file for plotting the doping profile.

Statement Applicability Parameters

| | |
|------------------|---|
| DEVICE | Specifies which device the statement applies to in the MIXEDMODE simulation. The synonym for this parameter is <i>STRUCTURE</i> . |
| MATERIAL | Restricts the applicability of the statement to regions of the specified material. |
| NAME | Restricts the applicability of the statement to regions with the specified name. |
| REGION | Restricts the applicability of the statement to regions with the specified region number. |
| STRUCTURE | This is a synonym for <i>DEVICE</i> . |

Note: If you don't specify the *DEVICE*, *MATERIAL*, *NAME* and *REGION* parameters, the *DOPING* statement will apply to all regions.

Interface Doping Profile Location Parameters

You can use these parameters with the parameters *NAME*, *MATER*, and *REGION* to describe interfaces between regions to be doped with an analytic profile. The *NAME*, *MATER*, and *REGION* parameters are used to describe the regions that receive the doping while the *INAME*, *IMATER*, and *IREGION* parameters describe regions incident on the regions receiving the doping where the doping is to be placed (i.e., along the interface).

The locations of of these interface profiles may also be restricted by the location parameters *X.MAX*, *X.MIN*, *Y.MAX*, and *Y.MIN*.

| | |
|----------------|---|
| IMATER | Specifies the material of all neighboring regions where an interface profile is placed. |
| INAME | Specifies the name of a neighboring region where an interface profile is placed. |
| IREGION | Specifies the region number of the a neighboring region where the interface profile is placed. |
| OUTSIDE | Specifies that interface regions will placed at all interfaces with the outside of the simulation domain. |

Analytical Profile Types

These parameters specify how ATLAS will generate a doping profile from analytical functions.

| | |
|-------------------|--|
| DOP.SIGMA | Specifies the variance for random gaussian dopant distribution. |
| DOP.SEED | Specifies a seed value for random gaussian dopant distribution. |
| ERFC | Specifies the use of a ERFC analytical function to generate the doping profile. If ERFC is specified, the following parameters must also be specified: <ul style="list-style-type: none"> • Polarity parameters N.TYPE or P.TYPE • One of the following groups of profile specifications: <ul style="list-style-type: none"> • Group 1:CONCENTRATION and JUNCTION • Group 2:DOSE and CHARACTERISTIC • Group 3:CONCENTRATION and CHARACTERISTIC |
| GAUSSIAN | Specifies the use of a gaussian analytical function to generate the doping profile. If GAUSSIAN is specified, the following parameters must also be specified: <ul style="list-style-type: none"> • Polarity parameters N.TYPE or P.TYPE • One of the following groups of profile specifications: <ul style="list-style-type: none"> • Group 1:CONCENTRATION and JUNCTION • Group 2:DOSE and CHARACTERISTIC • Group 3:CONCENTRATION and CHARACTERISTIC |
| UNIFORM | Specifies the use of uniform (constant) analytical functions to generate the doping profile. If UNIFORM is specified, the N.TYPE, P.TYPE, and CONCENTRATION parameters must be specified. Doping is introduced into a box defined by the boundary parameters (see the “Boundary Conditions” Section on page 21-25). The box by default includes the entire region. |
| F.COMPOSIT | Specifies the name of a file containing a C-Interpreter function specifying the spatial distribution of composition fractions. |
| F.DOPING | Specifies the name of a file containing a C-Interpreter function specifying the spatial distribution of dopants. |
| F3.DOPING | Specifies the name of a file containing a C-Interpreter function specifying the spatial distribution of dopants for a 3D device. |

File Import Profile Types

These parameters specify how ATLAS will generate a doping profile from a file. Files can be user-defined or from process simulation.

| | |
|------------------|--|
| 1D.PROC | Specifies is an alias for TMA.SUPREM3. |
| 2D.ASCII | Specifies that a 2D doping profile, which is defined on a rectangular Cartesian grid, should be loaded from a file specified by INFILE. 2D.ASCII must be specified along with either the N.TYPE, P.TYPE or NET parameters. This first column of the file should contain the X coordinates. The second column should contain the Y coordinates. The third column should contain the doping data. |
| ASCII | <p>There has two separate meanings. The first meaning is that it specifies the file type as ASCII when it's combined with other format parameters. The second meaning is when this parameter is used alone, it specifies ASCII data files containing concentration versus depth information. The alias for this parameter is 1D.PROC.</p> <p>In the second meaning, this parameter must be written in the form:</p> <pre>ASCII INFILE=<filename></pre> <p>where filename is the name of the ASCII input file. The data file must be in the following format:</p> <pre>depth concentration depth concentration depth concentration ...</pre> <p>where depth is specified in μm and concentration is specified in cm^{-3}. An input file name, a dopant type, and boundary parameters must be specified. Positive concentrations are assumed to be n-type and negative concentrations are assumed to be p-type unless the N.TYPE or P.TYPE parameters are used.</p> |
| ATHENA.1D | Specifies that the doping file is a ATHENA 1D export file. This parameter acts in a similar way to the SSUPREM3 parameter. |
| ATHENA | Reads 2D doping information from ATHENA standard structure file (SSF) or PISCES-II format files. The PISCES-II format is an obsolete file format. Doping information obtained from this file will be added to each point of the current ATLAS mesh. If points in the ATLAS mesh do not coincide with points in the ATHENA mesh, doping for ATLAS mesh points will be interpolated from ATHENA doping information. If this profile type is used, the INFILE parameter must also be specified. |

Note: The X.STRETCH function available in previous versions of ATLAS has been replaced by similar more powerful functions in DEVEDIT. This feature should no longer be used in ATLAS.

| | |
|--------------------|--|
| FILE | This is an alias for <code>INFILE</code> . |
| IN.FILE | This is a synonym for <code>INFILE</code> . The alias for this parameter is <code>FILE</code> . |
| INFILE | Specifies the name of the appropriate input file. The synonym for this parameter is <code>IN.FILE</code> . |
| MASTER | Specifies that the <code>INFILE</code> is written in the Silvaco standard structure file (SSF) format. This file format is the default output format of <code>ATHENA</code> and <code>SSUPREM3</code> . This parameter is typically combined with the <code>SSUPREM3</code> , <code>ATHENA 1D</code> , or <code>ATHENA</code> parameters. If neither of these are used the default is <code>SUPREM3</code> . |
| N.COLUMN | Specifies which column of an 2D ASCII table corresponds to the net donor concentration when <code>2D.ASCII</code> is specified. |
| P.COLUMN | Specifies which column of an 2D ASCII table corresponds to the net acceptor concentration when <code>2D.ASCII</code> is specified. |
| SUPREM3 | Specifies the <code>INFILE</code> was produced by <code>SSUPREM3</code> in standard structure file (SSF) format or binary or an ASCII export format. If this profile type is used, an input file name, a dopant, and boundary parameters must be specified. When <code>SSUPREM3</code> produces an output file, the doping profiles are stored by dopant. Therefore, a dopant parameter should be specified in order to import the correct doping profile into <code>ATLAS</code> . If a specific dopant is not specified the total donors and acceptor concentrations are loaded. |
| TMA.SUPREM3 | Specifies that the file specified by <code>INFILE</code> is in TMA <code>SUPREM3</code> binary format. The alias for this parameter is <code>1D.PROC</code> . |

Note: Files containing 1D doping profiles can be loaded into `BLAZE`, `BLAZE3D`, `DEVICE3D`, or `S-PISCES`. Files containing 2D doping profiles can only be loaded into `S-PISCES`.

| | |
|-----------------|--|
| X.COLUMN | Specifies which column of an 2D ASCII table corresponds to the X coordinate value when <code>2D.ASCII</code> is specified. |
| Y.COLUMN | Specifies which column of an 2D ASCII table corresponds to the Y coordinate value when <code>2D.ASCII</code> is specified. |

1D Profile Modifications

These parameters are used to modify the concentrations in 1D profiles.

| | |
|-------------------|---|
| C.MULT | Acts as a multiplier in 1D ASCII dopant profiles. |
| DOP.OFFSET | Subtracts a background doping value from the <code>ATHENA</code> or <code>SSUPREM3</code> doping. The alias for this parameter is <code>N.OFFSET</code> . |

Dopant Type Specification Parameters

These parameters give information about the dopant species or type to be used in the specified profile. Different profile types require different profile specifications.

| | |
|---------------------------------|---|
| ACTIVE | Specifies that for the dopant specified the active concentration as opposed to the chemical concentration is added. This is true by default. Files from ATHENA or SSUPREM3 contain both active and chemical concentrations for each dopant. |
| ALUMINUM | Specifies that aluminum dopant information be extracted from an imported file. |
| ANTIMONY | Specifies that antimony dopant information be extracted from an imported file. |
| ARSENIC | Specifies that arsenic dopant information be extracted from an imported file. |
| BORON | Specifies that boron dopant information be extracted from an imported file. |
| C.MULT | Acts as a multiplier in 1D ASCII dopant profiles. |
| CHEMICAL | Specifies that the chemical concentration (as opposed to the active concentration) will be read from the imported file. This is generally not advisable. |
| DOP.OFFSET | Subtracts a background doping value from the ATHENA or SSUPREM3 doping. The alias for this parameter is N.OFFSET. |
| E.LEVEL | Sets the energy of the discrete trap level. For acceptors, E.LEVEL is relative to the conduction band edge. For donors, it is relative to the valence band edge. |
| INDIUM | Specifies that indium dopant information be extracted from an imported file. |
| METAL | Specifies that the DOPING statement will define metal atomic concentration used in calculation of electrode quenching. |
| NET | Specifies that net doping information be extracted from an imported file. This is usually not advisable. It is better to use several DOPING statements to extract data dopant by dopant from a file. |
| N.OFFSET | This is an alias for DOP.OFFSET. |
| N.TYPE, N-TYPE, DONOR | Specifies an n-type or donor dopant. This parameter may be used with GAUSSIAN and UNIFORM profile types. |
| OX.CHARGE | Specifies a fixed oxide charge profile. Oxide charge can only be placed in any insulator region. The N.TYPE/P.TYPE parameters are not used hence a negative concentration implies a negative charge. |
| P.TYPE, P-TYPE, ACCEPTOR | Specifies a p-type or acceptor dopant. This parameter may be used with GAUSSIAN and UNIFORM profile types. |
| PHOSPHORUS | Specifies that phosphorus dopant information be extracted from an imported file. |

| | |
|----------------|--|
| RESISTI | This can be used to specify resistivity (in units of Ohm.cm) as an alternative to using the CONC parameter. Tabulated values are used to convert from the value of RESISTI to doping Concentration (in units of cm^{-3}). The tables are related to the ARORA mobility model at 300K and the result depends on whether the dopant has been specified as a donor or an acceptor. At high doping levels, the resistivity can also depend on the particular dopant species. But this is not taken into account in this model. |
| TRAP | Specifies that the dopant concentration is to be treated as a trap state density. |
| X.COMP | Specifies a profile of composition fraction x as defined in Appendix B: “Material Systems”. This profile can be used to change the composition fraction of cations in ternary and quaternary materials over a spatial distribution. |
| Y.COMP | Specifies a profile of composition fraction y as defined in Appendix B: “Material Systems”. This profile can be used to change the composition fraction of anions in ternary and quaternary materials over a spatial distribution. |

Vertical Distribution Parameters

| | |
|-----------------------|--|
| CHARACTERISTIC | <p>Specifies the principal characteristic length of the implant. For Gaussians, the characteristic length is equal to the square root of two times the standard deviation. If this parameter is left unspecified, the principal characteristic can be computed from the values of the</p> <ul style="list-style-type: none"> • Polarity Parameters • Boundary Parameters • Concentration and Junction parameters <p>The alias for this parameter is Y.CHAR.</p> |
| CONCENTRATION | <p>Specifies the peak concentration when a Gaussian profile is used. If this parameter is not specified, peak concentration may be computed from the values of the polarity, boundary, DOSE, or RESISTI, CHARACTERISTIC concentrations. When a uniform profile is specified, the CONCENTRATION parameter sets the value of the uniform doping level. Concentrations must be positive. The alias for this parameter is N.PEAK.</p> |
| DOSE | Specifies the total dose for a Gaussian profile. |
| JUNCTION | <p>Specifies the location of a p-n junction within the silicon region of a Gaussian profile. When JUNCTION is specified, the characteristic length is computed by examining the doping at a point halfway between the end of the constant box and the given depth. The JUNCTION location is evaluated considering all previous DOPING statements only. This means that in some cases the order of DOPING statements is important.</p> |
| N.PEAK | This is an alias for CONCENTRATION. |

| | |
|-----------------|--|
| PEAK | Specifies the depth location of the peak doping in a Gaussian profile. |
| Y.CHAR | This is an alias for CHARACTERISTIC. See Equation 21-3. |
| Y.JUNCTI | This is an alias for JUNCTION. See Equation 21-3. |

$$N(Y) = \text{PEAK} \cdot \exp \left[-\left(\frac{Y}{Y.CHAR} \right)^2 \right] \quad 21-3$$

Location Parameters

| | |
|------------------|---|
| DIRECTION | Specifies the axis along which a one-dimensional profile is directed in a two-dimensional device (x or y). DIR=y will typically be used for implanted profiles. |
| REGION | Specifies the region number where doping is to be added. |
| START | Specifies the depth in the Y direction where the profile should start. |

Lateral Extent Parameters

These parameters must be specified when a 1D doping profile type is used (MASTER, GAUSSIAN, ASCII, ERFC, or UNIFORM). These boundary parameters set the doping boundaries before applying lateral spreading. This is equivalent to setting implant mask edges.

| | |
|---|---|
| WIDTH | Specifies the extent of the profile in the X direction. Specifying WIDTH is equivalent to specifying X.MAX such that X.MAX=X.MIN+WIDTH. |
| R.MIN, R.MAX, A.MIN, and A.MAX | For an ATLAS3D device created using the MESH CYLINDRICAL option, these parameters restrict the radial and angular positions respectively of the analytical doping profile. The principal direction of the analytical doping profile is the Z direction in this case. |
| X.MIN, X.MAX, Y.MIN, Y.MAX, Z.MAX, and Z.MIN | Specify the x, y and z bounds of a rectangular shaped region or box in the device. The dopant profile within this box will be constant with a density equal to the value specified by the CONC parameter. Outside this box the profile decreases from the peak, CONC, with distance, from the box along the principal axes. The relationship between the concentration, outside the box, to distance will depend upon the profile type as specified by the GAUSSIAN, MASTER, ATHENA, ATLAS, and UNIFORM parameters. |
| X.LEFT, X.MIN | Specifies the left boundary of a vertical 1D profile. |
| X.RIGHT, X.MAX | Specifies the right boundary of a vertical 1D profile. |
| Y.BOTTOM, Y.MAX | Specifies the bottom boundary of a horizontal 1D profile. |
| Y.TOP, Y.MIN | Specifies the top boundary of a horizontal 1D profile. |
| Z.BACK, Z.MIN | Specifies the back boundary of a z directed 1D or 2D profile. |
| Z.FRONT, Z.MAX | Specifies the front boundary of a z directed 1D or 2D profile. |

Lateral Distribution Parameters

These parameters specify how a vertical 1D profile is extended outside the box defined by the lateral extent parameters.

| | |
|----------------------|---|
| BACKDOPE | Specifies the value to which the doping profile specified from the 1D profile will roll-off to outside its lateral and vertical extents. If this value is not specified, then the last doping value in the ASCII file is used as the background doping level, regardless of windowing in the Y direction. If NOXROLLOFF is used, then BACKDOPE will be ignored for the X direction. If NOYROLLOFF is used, then BACKDOPE will be ignored for the Y direction. If NOROLLOFF is used, then BACKDOPE will be completely ignored. |
| ERFC.LATERAL | Specifies that the complementary error function will be used to calculate the lateral falloff of doping level in the X direction. If you set the X.DIR flag, then this flag will apply to the Y direction instead. If you set ERFC for the analytical doping profile, then ERFC.LATERAL will be automatically enabled by default. If you set GAUSSIAN or UNIFORM, then ERFC.LATERAL will be disabled by default and the falloff will follow a Gaussian profile. The aliases for this parameter are X.ERFC and XERFC.LAT. |
| LAT.CHAR | Specifies the characteristic length of the lateral profile. If this parameter is not specified, the characteristic length is defined by: <div style="text-align: right;">21-4</div> $CL = RL \times OCL$ where: <ul style="list-style-type: none"> CL is the lateral characteristic length in the X direction. RL is the value of <code>RATIO.LATERAL</code>. OCL is the characteristic length of the original profile in the Y direction. The alias for this parameter is <code>X.CHAR</code> . |
| NOXROLLOFF | Causes the doping level to abruptly change to zero outside the x-limits. |
| NOYROLLOFF | Causes the doping level to abruptly change to zero outside the y-limits. |
| NOROLLOFF | This is the same as setting both NOXROLLOFF and NOYROLLOFF. |
| NOZROLLOFF | Causes the doping levels to abruptly change to zero outside the z-limits. |
| RATIO.LATERAL | This is the ratio of characteristic lengths in the X and Y directions. |
| SLICE.LAT | Specifies the point at which the doping is examined to compute the characteristic length of a Gaussian profile after JUNCTION has been specified. The default for this parameter is a point halfway between the end of the constant box and the given depth. |
| X.CHAR | This is an alias for <code>LAT.CHAR</code> . |
| X.ERFC | This is an alias for <code>ERFC.LAT</code> . |
| XERFC.LAT | This is an alias for <code>ERFC.LAT</code> . |
| XY.RATIO | This is an alias for <code>RATIO.LATERAL</code> . |
| ZLAT.CHAR | Specifies the characteristic length of the lateral profile in the Z direction. See also <code>LAT.CHAR</code> . |

| | |
|-------------------|---|
| ZERFC.LAT | Specifies that the complementary error function will be used to calculate the lateral falloff of doping level in the Z direction in ATLAS3D. If you specify ERFC as the analytical doping profile, then ZERFC.LAT will be enabled by default. The parameters ZLAT.CHAR and ZRATIO.LAT control the degree of lateral rolloff in the Z direction. |
| ZRATIO.LAT | This is used analogously to RATIO.LATERAL but applies to lateral spreading in the Z direction. See also LAT.CHAR. |
| ZSLICE.LAT | This is similar to SLICE.LAT but applies to profiles in the Z direction. |

Trap Parameters

| | |
|------------------|---|
| E.LEVEL | Sets the energy of the discrete trap level. For acceptors, E.LEVEL is relative to the conduction band edge, for donors it is relative to the valence band edge. |
| DEGEN.FAC | Specifies the degeneracy factor of the trap level used to calculate the density. |
| SIGN | Specifies the capture cross section of the trap for electrons. |
| SIGP | Specifies the capture cross section of the trap for holes. |
| TAUN | Specifies the lifetime of electrons in the trap level. |
| TAUP | Specifies the lifetime of holes in the trap level. |

Note: See Section 21.61: “TRAP” for more information on each of these parameters

Angled Distribution Parameters

| | |
|------------------------|--|
| X1, Y1, X2, Y2 | Specify the X and Y coordinates of the ends of the line segment describing the location of the specified angled profile. |
| X.DIR and Y.DIR | Specify the direction in which the angled profile is extended. |

In DEVICE3D, (see Chapter 6: “3D Device Simulator” for more information about this simulator), dopants can be added along angled segments in the XY plane. The start and ending coordinates of the line segment are defined by the X1, Y1, X2, and Y2 parameters. You can then specify whether a 2D profile is extended from the line segment in either the X or the Y direction. To specify it, set the X.DIR or Y.DIR parameter. You can then specify a 2D doping profile in the same DOPING statement. The profile can be an analytic, SUPREM, ASCII, or SUPREM4.

The dopants are placed relative to the defined line segment, according to the setting of X.DIR or Y.DIR. If X.DIR is specified, then the effective Y coordinate of the profile is the device Z coordinate and the effective X coordinate of the profile is the distance in the X direction from the center of the line segment. No dopants are added if the device Y coordinate is outside of the Y coordinates of the line segment. If Y.DIR is specified, then the effective Y coordinate of the profile is the device Z coordinate and the effective X coordinate of the profile is the distance in the Y direction from the of the line segment. No dopants are added if the device X coordinate is outside the X coordinates of the line segment.

Analytical Doping Definition Example

This example describes a 1.0 μ m n-channel MOSFET using Gaussian source and drain profiles. The lateral extent of the source is given by X.RIGHT=2. This corresponds to the mask edge for the implant. Sub-diffusion is determined by an error function based on the RATIO.LAT and JUNCTION parameters. For both source and drain, the n+ doping is added to the uniform p-well concentration to ensure a junction depth of 0.3 μ m.

```
DOP UNIF CONC=1E16 P.TYPE
DOP GAUSS CONC=9E19 N.TYPE X.RIGHT=2 JUNC=0.3 RATIO.LAT=0.6 ERFC.LAT
DOP GAUSS CONC=9E19 N.TYPE X.LEFT=3 JUNC=0.3 RATIO.LAT=0.6 ERFC.LAT
```

1D ATHENA or SSUPREM3 Interface Example

This example reads a 1D ATHENA bipolar profile and adds it to a uniform substrate concentration. The base and emitter doping are loaded from the same file by specifying the impurity required for each area (boron in the base and arsenic in the emitter).

The DOPOFF parameter is used to subtract the substrate arsenic dopant out of the 1D profile that is loaded since this dopant was already specified in the substrate doping line.

Versions of SSUPREM3 later than 5.0 use standard structure files as default when saving data. These can be loaded in ATLAS with the syntax below by replacing ATHENA.1D with SSUPREM3.

```
# SUBSTRATE
DOP REGION=1 UNIF CONC=1E16 N.TYPE
# BASE
DOP REGION=1 MASTER ATHENA.1D BORON RATIO.LAT=0.7 INF=bipolar.exp
# EMITTER
DOP REGION=1 MASTER ATHENA.1D ARSENIC RATIO.LAT=0.6 \
INF=bipolar.exp X.LEFT=12.0 X.RIGHT=13.0 DOPOFF=1e16
```

Athena Doping Interface Example

This example demonstrates how to use an SSF format ATHENA file to interpolate doping onto a ATLAS grid and save the doping information for subsequent regrid operations. This is an alternative to the ATHENA/ATLAS interface, which is described in Chapter 2: “Getting Started with ATLAS”, Section 2.6.1: “Interface From ATHENA”.

```
DOPING ATHENA MASTER INFILE=NMOS.DOP OUTFILE=NMOS.DOP
REGRID DOPING ABS LOG RATIO=4 OUTFILE=NMESH1.STR DOPFILE=NMOS.DOP
```

3D Doping Definition Example

The following example illustrates the formation of a Gaussian highly doped n-type area in a three-dimensional structure.

```
DOPING GAUSS N.TYPE CONC=1e20 PEAK=0.0 CHAR=0.2 X.LEFT=0.5 \
X.RIGHT=1.0 Z.LEFT=0.5 Z.RIGHT=1.0
```

For a cylindrical structure you can use the following syntax. In this case, it is for complementary error function doping.

```
doping erfc start=0.0 char=0.005 ratio.lat=0.1 conc=1.0e20 n.type r.min=0.01
a.min=45.0 a.max=225.0
```

3D Doping From ASCII 1D File

You can read a 1D doping profile from an ASCII file and apply it to the entire or part of a 3D device. The `X.DIR`, `Y.DIR`, or `Z.DIR` parameters specify the direction of the profile as applied in the 3D device. The starting position of the doping profile will be set by the relevant `X.MIN`, `Y.MIN`, or `Z.MIN` parameter. The ending position of the doping profile will be the minimum of the relevant `X.MIN`, `Y.MIN`, or `Z.MIN` plus the spatial extent of the doping profile in the ASCII file, or the `X.MAX`, `Y.MAX`, `Z.MAX` parameter or a physical boundary of the device. You can specify a general parallelogram in the plane perpendicular to the direction of doping direction. To specify it, use the appropriate combination of `X1`, `X2`, `Y1`, `Y2`, `Z1`, `Z2`, `X.MIN`, `X.MAX`, `Y.MIN`, `Y.MAX`, `Z.MIN`, `Z.MAX`. For example, we consider the `Y.DIR` parameter specified. We can then specify a parallelogram in the `XZ` plane as shown in Figure 21-2.

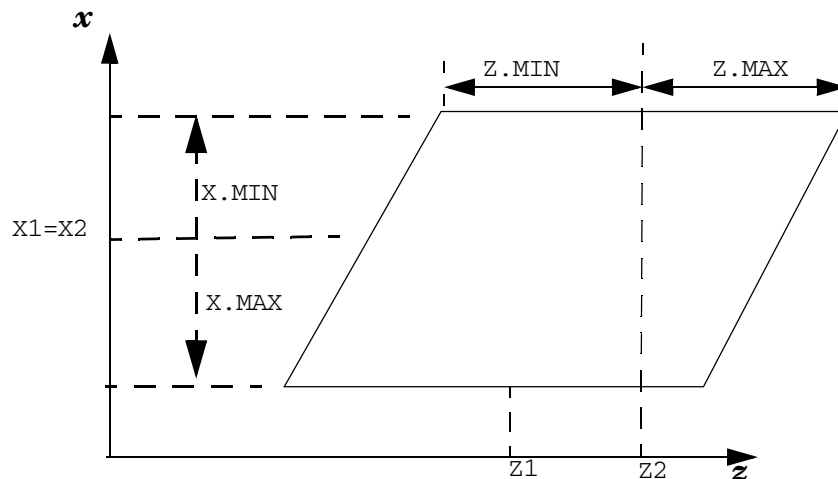


Figure 21-2: Parallelogram Geometry Example

In the figure, two sides are parallel to the `Z` axis. `Z1` and `Z2` specify the `Z` coordinate of the midpoints of these two sides. `Z.MIN` and `Z.MAX` together specify the lengths of the sides, and `Z.MIN` will be negative and equal to $-Z.MAX$. (In fact, the positions are evaluated as $Z1+Z.MIN$ and $Z1+Z.MAX$ for one side and $Z2+Z.MIN$ and $Z2+Z.MAX$ for the other. Therefore, having `Z1` and `Z2` and so on refer to the side midpoint is just a convenient convention.)

You must specify `X1` and `X2` as having the same value, and specify `X.MIN` and `X.MAX` the side lengths the same way as for `Z.MIN` and `Z.MAX`.

Setting `Z1` and `Z2` to the same value will result in a rectangle. By then changing `X1` and `X2` so they are not equal will result in a parallelogram with sides parallel to the `X` axis. If a different direction of doping variation is defined, then a parallelogram can be set up in the plane perpendicular to it in analogously to the above example.

Outside the specified parallelogram the doping level will be either the value of the last point in the ASCII file, or the value specified by the `BACKDOPE` parameter. A smooth transition of the doping from the value inside the parallelogram to the value outside can be applied elsewhere using the `LAT.CHAR` or `RATIO.LAT` parameters.

| | |
|-----------------------------------|---|
| X1, X2, Y1, Y2, Z1, Z2 | By convention, specify the midpoints of the sides making up the parallelogram. |
| X.MIN, X.MAX | Determine the X coordinate of the start and end points of the placement of the doping profile read in from an ASCII file (if you specify X.DIR). Otherwise, they specify the lateral extent of the parallelogram sides defining the location of the doping in a plane perpendicular to the specified direction of the doping variation. In this case, they are added to X1 and to X2 to determine the coordinates of the ends of sides. |
| Y.MIN, Y.MAX, Z.MIN, Z.MAX | These are the same as X.MIN and X.MAX except they apply to the y and Z directions respectively. |

Example:

```
doping ascii inf=ydop.dat y.dir n.type x1=6.0 x2=4.0 x.min=-2 x.max=2
z.min=3.0 z.max=7.0 y.min=2.0 y.max=10.0 lat.char=0.005 backdope=0.0
```

This will apply the doping profile specified in `ydop.dat` as n-type doping in the Y direction between the positions `y=2` microns and `y=10` microns (unless the length range in `ydop.dat` is less than this distance). In the XZ plane, it will be applied to a parallelogram with sides parallel to the X direction of length 4 microns. The Z coordinates of these sides are 3.0 microns and 7.0 microns. The doping will transition from the value inside the parallelogram to 0.0 outside on a length scale of 0.005 microns.

3D Doping From 2D ATHENA Master Files

In a 2D ATHENA master file, the doping profile is defined over a box in two dimensions. This doping is put over 2D-sections normal to the plane of a parallelogram to be defined in the doping statement. This parallelogram must lie in one of the XY, YZ, and XZ planes and have two edges parallel to one of the coordinate axes.

As the mesh in the ATHENA master file doesn't necessarily coincide with the three-dimensional mesh in ATLAS, an interpolation routine is required to import the doping in ATLAS. You can then choose between a linear and a logarithmic interpolation algorithm.

Here's a list of the parameters that are used for this kind of doping.

| | |
|---------------------|---|
| ASPECT.RATIO | Specifies the aspect ratio of the doping will be preserved when loaded into the doping parallelogram. |
| DOP.XMAX | Specifies the maximum X coordinate of the doping in the ATHENA file to be loaded into the doping parallelogram. |
| DOP.XMIN | Specifies the minimum X coordinate of the doping in the ATHENA file to be loaded into the doping parallelogram. |
| DOP.YMAX | Specifies the maximum Y coordinate of the doping in the ATHENA file to be loaded into the doping parallelogram. |
| DOP.YMIN | Specifies the minimum Y coordinate of the doping in the ATHENA file to be loaded into the doping parallelogram. |
| INT.LIN | Specifies that a linear interpolation is to be used to import doping from ATHENA into ATLAS. |
| INT.LOG | Specifies that the ATHENA doping is imported in ATLAS by using a logarithmic interpolation algorithm. |

| | |
|-------------------------------|---|
| INT.OPTM | Enables an optimized interpolation routine, which attempts to reduce CPU time due to the doping interpolation. |
| LAT.CHAR | Defines the characteristic length, CL, of the lateral spreading (in the $y > y_2$ and $y < y_1$ planes). If RATIO.LAT is used instead, then the characteristic length is assumed to come from this parameter by the height of the parallelogram (i.e., $CL = RL \times OCL$, OCL being the height of the parallelogram ($y_2 - y_1$ in this case). If both LAT.CHAR and RATIO.LAT aren't specified, then no lateral spreading is done. |
| XY | Specifies that the parallelogram containing doping in ATLAS3D is in the xy plane. |
| YX | This is a synonym for XY. |
| YZ | Specifies that a parallelogram containing doping in ATLAS3D is in the YZ plane. |
| ZY | This is a synonym for YZ. |
| XZ | Specifies that a parallelogram containing doping in ATLAS3D is in the XZ plane. |
| ZX | This is a synonym for ZX. |
| X1, X2, Y1, Y2, Z1, Z2 | Specify an average segment in one of the three coordinate planes defining the orientation of the parallelogram. |
| X.DIR, Y.DIR, Z.DIR | Specify that a parallelogram containing doping in ATLAS3D has two edges in the X direction, Y direction, and Z direction. |
| X.FLIP | Specifies that the orientation of the ATHENA file X axis will be flipped. |
| X.MIN, X.MAX | Define the minimum and maximum lateral extent of a parallelogram along the X direction lying in the xy or zx plane, starting from its average segment (they must be specified with X1 and X2). If a parallelogram is defined in the YZ plane, X.MIN can then be used to specify the initial coordinate to start the doping along the X direction. |
| X.SCALE | Specifies that the ATHENA file doping will be scaled in the X direction. |
| Y.FLIP | Specifies that the orientation of the ATHENA file Y axis will be flipped. |
| Y.MIN, Y.MAX | Define the minimum and maximum lateral extent of a parallelogram along the Y direction lying in the XY or YZ plane, starting from its average segment (they must be specified with Y1 and Y2). If a parallelogram is defined in the zx plane, Y.MIN can then be used to specify the initial coordinate to start the doping along the Y direction. |
| Y.SCALE | Specifies that the ATHENA file doping will be scaled in the Y direction. |
| Z.MIN, Z.MAX | Define the minimum and maximum lateral extent of a parallelogram along the Z direction lying in the yz or zx plane, starting from its average segment (they must be specified with Z1 and Z2). If a parallelogram is defined in the xy plane, Z.MIN can then be used to specify the initial coordinate to start the doping along the Z direction. |
| Z.SCALE | Specifies that the ATHENA file doping will be scaled in the Z direction. |

The following three cases, which correspond to the parallelograms in the xy, yz and zx planes, describe how the doping from the ATHENA master file is put into the ATLAS structure .

First Case: Parallelogram In The XY Plane

SUB-CASE A: Parallelogram along the X direction.

Sections of the ATLAS structure in zx planes are considered, which intersect for $y_1 < y < y_2$, the segment (x_a, x_b) inside the parallelogram. Each of these sections defines a box where the 2D doping is imported from ATHENA. Particularly, all the coordinates in ATHENA are scaled and translated so that the edge (x_c, x_d) of the ATHENA box containing the doping coincide with the segment (x_a, x_b) of the ATLAS box. This is done for all the sections inside the parallelogram. See Figure 21-3.

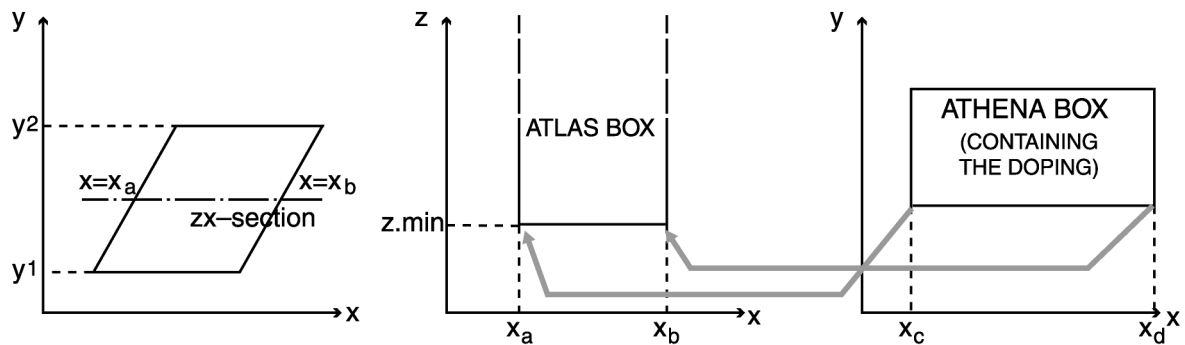


Figure 21-3: Parallelogram in the XY plane in the X direction and doping from the ATHENA2D master file

Examples:

```
doping athena master inf=athena.str boron xy \
x1=2.0 x2=3.0 y1=1.5 y2=4.0 x.dir \
x.min=-2.0 x.max=1.0 z.min=0.6 lat.char=0.05 int.log int.optm
```

For the Z coordinate, $z.min$ is used to specify the minimum value where to start putting the doping into the zx-sections (which properly defines the segment (x_a, x_b) in this plane).

In addition, a lateral spreading can be partially accomplished by extending the parallelogram into the planes, $y > y_2$ and $y < y_1$, where the doping is spread out according to a Gaussian law.

SUB-CASE B: Parallelogram along the Y direction

Sections of the ATLAS structure are considered in the YZ planes. A transformation of coordinates in ATHENA is accomplished in order to place the ATHENA segment (y_c, y_d) into the ATLAS one (y_a, y_b) . See Figure 21-4.

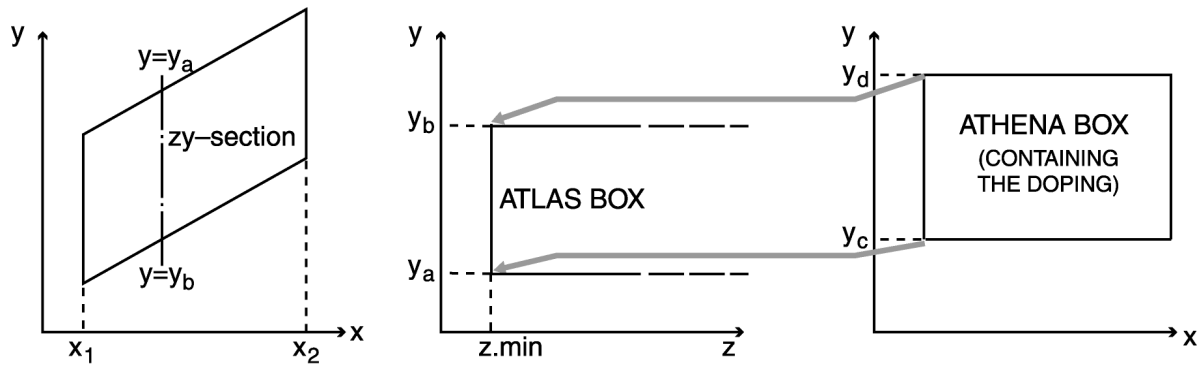


Figure 21-4: Parallelogram in the XY plane in the Y direction and doping from the ATHENA2D master file

Examples:

```
doping athena master inf=athena.str boron xy \
x1=2.0 x2=3.0 y1=1.5 y2=4.0 y.dir \
y.min=-2.0 y.max=1.0 z.min=0.6 lat.char=0.05 int.lin int.optm
```

Second Case: YZ Plane

The YZ plane containing the parallelogram is defined by the *yz* parameter (or *zy*) in the DOPING statement.

If parallelograms along the Z direction are defined (specify *Z.DIR* in doping statement), the doping from ATHENA is put over sections in the *zx* planes. If the parallelograms along the Y direction are defined (using *Y.DIR* in DOPING statement), the doping from ATHENA is put over sections in the *xy* planes.

The minimum X coordinate in ATLAS to start adding doping can be specified by *X.MIN* in DOPING statement.

Examples:

```
doping athena master inf=athena.str boron zy z.dir \
z1=0.3 z2=0.6 y1=0.35 y2=0.25 z.min=-0.2 z.max=0.6 \
x.min=0.2 ratio.lat=0.05
```

```
doping athena master inf=athena.str boron zy y.dir \
z1=0.3 z2=0.6 y1=0.35 y2=0.25 y.min=-0.2 y.max=0.6 \
x.min=0.2 ratio.lat=0.05
```

Third Case: ZX Plane

The ZX plane containing the parallelogram is defined by the *zx* parameter (or *xz*) in DOPING statement. If parallelograms along the Z direction are defined (using *Z.DIR* in the DOPING statement), the doping from ATHENA is placed over sections in the YZ planes.

If the parallelograms along the X direction are defined (using *X.DIR* in DOPING statement), the doping from ATHENA is placed over the sections in the XY planes.

The minimum Y coordinate in ATLAS to start adding doping can be specified by *Y.MIN* in doping statement.

Examples:

```
doping athena master inf=athena.str boron int.lin \  
xz z.dir z1=0.45 z2=0.55 x1=0.2 x2=0.7 x.min=-0.4 \  
x.max=0.2 y.min=0.0 lat.char=0.02  
doping athena master inf=athena.str boron int.lin \  
xz x.dir z1=0.4 z2=0.8 x1=0.2 x2=0.7 z.min=-0.4 \  
z.max=0.2 y.min=0.5 ratio.lat=0.5
```

21.11: DOSEXTRACT

DOSEXTRACT specifies the grain boundary and interface trap density of states as a function of energy [118] are to be extracted from IV and CV files and saved to log files.

Syntax

DOSEXTRACT [<parameters>]

| Parameter | Type | Default | Units |
|---------------|-----------|---------|-------------------------|
| ACCEPTOR | Logical | False | |
| CVFILE | Character | | |
| DONOR | Logical | False | |
| EG300 | Real | | eV |
| EI | Real | | eV |
| EMAX | Real | | eV |
| GRAIN.SIZE | Real | | μm |
| GRAINFILE | Character | | |
| INTFILE | Character | | |
| IVFILE | Character | | |
| LENGTH | Real | | μm |
| MIN.DENSITY | Real | 1 | cm^{-2} |
| MU | Real | | cm^2/Vs |
| NUM.DIVISIONS | Real | 25 | |
| NUM.GRAINS | Real | | |
| OUTFILE | Character | | |
| TEMPERATURE | Real | 300 | K |
| TOX | Real | | μm |
| TSI | Real | | μm |
| VDRAIN | Real | | V |
| WIDTH | Real | | μm |

Description

| | |
|----------------------|--|
| ACCEPTOR | Specifies that acceptor traps are to be extracted. |
| CVFILE | Specifies the file name which contains the capacitance/gate voltage data. |
| DONOR | Specifies that donor traps are to be extracted. |
| EG300 | Specifies the value of bandgap of the material. EMAX will be calculated from this value if it is specified along with EI . |
| EI | Specifies the intrinsic energy level of the material. |
| EMAX | Specifies the maximum energy separation from the intrinsic energy level (EI) that should be calculated. |
| GRAIN.SIZE | Specifies the size of the grains. |
| GRAINFILE | Specifies the file name where the grain boundary DOS distribution, as a function of energy, will be stored. |
| INTFILE | Specifies the file name where the interface DOS distribution, as a function of energy, will be stored. |
| IVFILE | Specifies the file name that contains the drain current/gate voltage data. |
| LENGTH | Specifies the x-direction length under the gate. |
| MIN.DENSITY | Specifies the minimum trap density to be used for the grain boundary traps. |
| MU | Specifies the majority carrier mobility. |
| NUM.DIVISIONS | Specifies the number of divisions used from the oxide-silicon interface to the substrate. |
| NUM.GRAINS | Specifies the number of grains in the device. |
| OUTFILE | Specifies the file name where the grain boundary and interface DOS distribution, as a function of energy, will be stored. |
| TEMPERATURE | Specifies the temperature used in the DOS extraction. |
| TOX | Specifies the oxide thickness. |
| TSI | Specifies the silicon thickness. |
| VDRAIN | Specifies the drain voltage used when the data in CVFILE and IVFILE were created. |
| WIDTH | Specifies the width of the device. |

Example

```
dosextract tox=0.1 tsi=0.05 width=25 length=5 vd=0.1 mu=50 num.grains=4 ei=0.54
eg=1.08 cvfile=cv.dat ivfile=iv.dat donor grainfile=grain.dat
intfile=int.dat
```

21.12: ELECTRODE

ELECTRODE specifies the locations and names of electrodes in a previously defined mesh.

Syntax

ELECTRODE NAME=<en> [NUMBER=<n>] [SUBSTRATE] <pos> <reg>

| Parameter | Type | Default | Units |
|-----------|-----------|--------------------------|---------|
| A.MAX | Real | | degrees |
| A.MIN | Real | | degrees |
| BOTTOM | Logical | False | |
| IX.HIGH | Integer | right side of structure | |
| IX.LOW | Integer | left side of structure | |
| IX.MAX | Integer | right side of structure | |
| IX.MIN | Integer | left side of structure | |
| IY.MAX | Integer | bottom side of structure | |
| IY.MIN | Integer | top side of structure | |
| IY.HIGH | Integer | bottom of structure | |
| IY.LOW | Integer | top of structure | |
| IZ.MAX | Integer | | |
| IZ.MIN | Integer | | |
| IZ.HIGH | Integer | | |
| IZ.LOW | Integer | | |
| LEFT | Logical | False | |
| LENGTH | Real | length of structure | μm |
| MATERIAL | Character | Contact | |
| NAME | Character | | |
| NUMBER | Integer | defined #(electrodes)+ 1 | |
| R.MAX | Real | | μm |
| R.MIN | Real | | μm |
| RIGHT | Logical | False | |
| SUBSTRATE | Logical | False | |
| THERMAL | Logical | False | |
| TOP | Logical | False | |
| X.MAX | Real | right side of structure | μm |
| X.MIN | Real | left side of structure | μm |

| Parameter | Type | Default | Units |
|-----------|------|----------------------|---------------|
| Y.MAX | Real | Y.MIN | μm |
| Y.MIN | Real | top of the structure | μm |
| Z.MIN | Real | | μm |
| Z.MAX | Real | | μm |

Description

| | |
|-----------------|---|
| MATERIAL | Specifies a material for the electrode (see Appendix B: “Material Systems”, Table B-1). This material will be displayed in TONYPLOT. The electrode material can also be used to define the electrode thermal characteristics (thermal conductivity) and optical characteristics (complex index of refraction). Setting the material here does not apply any electrical property such as workfunction to the terminal. All electrical properties of electrodes are set on the CONTACT statement. |
| NAME | <p>Specifies an electrode name. The electrode name can be referenced by other ATLAS statements to modify characteristics of the specified electrode. For reference by the CONTACT or THERMALCONTACT statements any valid character string can be used and properly cross-referenced. But when setting voltages, currents and charge from the SOLVE statement certain electrode names are recognized in a simplified syntax. By prepending the electrode name with "V" for voltage, "I" for current and "Q" for charge, you can directly and conveniently set the electrode bias, current or charge respectively. For example:</p> <pre>SOLVE VGATE=1.0</pre> <p>can be used to assign 1 volt bias to the electrode named "GATE". In such a manner, the following list of names can be used to set voltage, current or charge.</p> <ul style="list-style-type: none"> • GATE • FGATE • CGATE • NGATE • PGATE • VGG |

The following list of names can be used to assign only voltage or current.

- DRAIN
- SOURCE
- BULK
- SUBSTRATE
- EMITTER
- COLLECTOR
- BASE
- ANODE
- CATHODE
- WELL
- NWELL

- PWELL
- CHANNEL
- GROUND
- NSOURCE
- PSOURCE
- NDRAIN
- PDRAIN
- VDD
- VSS
- VEE
- VBB
- VCC

| | |
|------------------|---|
| NUMBER | Specifies an electrode number from 1 to 50. Electrode numbers may be specified in any order. If NUMBER is not specified, electrodes will be automatically numbered in sequential order. This parameter cannot re-number electrodes already defined in ATLAS or other programs. |
| pos | This is one of the position parameters described below. |
| reg | This is a set of the region parameters described on the next page. |
| SUBSTRATE | Places the specified electrode at the bottom of the device and names the electrode, substrate. |
| THERMAL | Specifies that the electrode is treated as a boundary condition for heatflow simulation using GIGA. |

Position Parameters

| | |
|-----------------------------------|--|
| BOTTOM or SUBSTRATE | Specifies that the electrode is positioned along the bottom of the device. |
| LEFT | Specifies that the electrode starts at the left-hand edge of the device. The electrode will be positioned from left to right along the top of the device. |
| RIGHT | Specifies that the electrode starts at the right-hand edge of the device. The electrode will be positioned from right to left along the top of the device. |
| TOP | Specifies that the electrode is positioned along the top of the device. |

Region Parameters

Device coordinates may be used to add regions to both rectangular and irregular meshes. In either case, boundaries must be specified with the `A.MAX`, `A.MIN`, `R.MAX`, `R.MIN`, `X.MAX`, `X.MIN`, `Y.MAX`, `Y.MIN`, `Z.MAX`, and `Z.MIN` parameters.

| | |
|---------------|---|
| LENGTH | Specifies the length of the electrode in the X direction. It is not necessary to specify <code>X.MIN</code> , <code>X.MAX</code> , and <code>LENGTH</code> . If two of these parameters are specified, the value of the third parameter will be calculated. |
| A.MAX | Specifies the maximum angle of a 3D cylindrical electrode. |
| A.MIN | Specifies the minimum angle of a 3D cylindrical electrode. |
| R.MAX | Specifies the maximum radius of a 3D cylindrical electrode. |
| R.MIN | Specifies the minimum radius of a 3D cylindrical electrode. |
| X.MAX | Specifies the maximum x-boundary of the electrode. |
| X.MIN | Specifies the minimum x-boundary of the electrode. |
| Y.MAX | Specifies the maximum y-boundary of the electrode. |
| Y.MIN | Specifies the minimum y-boundary of the electrode. |
| Z.MIN | Specifies the minimum z-boundary of the electrode. |
| Z.MAX | Specifies the maximum z-boundary of the electrode. |

Note: If an electrode has been shortened to fit the current mesh, a warning message will be generated by ATLAS. Electrode placement can only occur at previously defined mesh nodes.

Grid Indices

As an alternative to the region parameters, you can use grid indices to define a region only when the mesh is rectangular although these parameters are not recommended. To define a region with a rectangular mesh:

1. Use the `X.MESH` and `Y.MESH` statements to specify grid indices.
2. Use the `IX.HIGH`, `IX.LOW`, `IY.HIGH`, and `IY.LOW` parameters to specify x and y values.

| | |
|----------------|--|
| IX.HIGH | Specifies the maximum x-value of the grid index. The alias for this parameter is <code>IX.MAX</code> . |
| IX.LOW | Specifies the minimum x-value of the grid index. The alias for this parameter is <code>IX.MIN</code> . |
| IY.HIGH | Specifies the maximum y-value of the grid index. The alias for this parameter is <code>IY.MAX</code> . |
| IY.LOW | Specifies the minimum y-value of the grid index. The alias for this parameter is <code>IY.MIN</code> . Nodes, which have x and y grid indices, between <code>IX.LOW</code> and <code>IX.HIGH</code> and between <code>IY.LOW</code> and <code>IY.HIGH</code> are designated electrode nodes. Normally, horizontal planar electrodes will be used. In this case, <code>IY.LOW</code> equals <code>IY.HIGH</code> . |

| | |
|---|--|
| IZ.HIGH | Specifies the maximum z-value of the grid index. The alias for this parameter is IZ.MAX. |
| IZ.LOW | Specifies the minimum z-value of the grid index. The alias for this parameter is IZ.MIN. |
| IX.MAX, IX.MIN, IY.MIN, IZ.MAX, IZ.MIN | These are aliases for IX.HIGH, IX.LOW, IY.HIGH, IY.LOW, IZ.HIGH, and IZ.LOW. |

MOS Electrode Definition Example

This example defines electrodes for a typical MOS structure.

```

ELEC X.MIN=0.5 LENGTH=0.25 NAME=gate
ELEC LENGTH=0.25 Y.MIN=0 LEFT NAME=source
ELEC LENGTH=0.25 Y.MIN=0 RIGHT NAME=drain
ELEC SUBSTRATE

```

3D Electrode Definition Example

The following example illustrates electrode definition for a 3D structure.

```

ELECTRODE NAME=ANODE X.MIN=0.5 X.MAX=1.0 \
Z.MIN=0.5 Z.MAX=1.0

```

Note: In ATLAS, it is preferred to refer to `ELECTRODES` by name rather than number. Some functions, however, may require the electrode number. The syntax, `MODELS PRINT`, can be used to echo electrode numbers to the run-time output.

21.13: ELIMINATE

ELIMINATE terminates mesh points along lines in a rectangular grid defined within ATLAS in order to reduce the local mesh density.

Syntax

```
ELIMINATE X.DIRECTION|Y.DIRECTION [<boundary>]
```

| Parameter | Type | Default | Units |
|-----------|---------|---------|-------|
| COLUMNS | Logical | False | |
| IX.LOW | Integer | | |
| IX.HIGH | Integer | | |
| IY.LOW | Integer | | |
| IY.HIGH | Integer | | |
| ROWS | Logical | False | |
| X.MIN | Real | | μm |
| X.MAX | Real | | μm |
| Y.MIN | Real | | μm |
| Y.MAX | Real | | μm |

Description

The ELIMINATE statement is used to remove points along every other line within the chosen range. Successive eliminations of the same range remove points along every fourth line. For horizontal elimination, the vertical bounds should be decreased by one at each re-elimination of the same region. For vertical elimination, the horizontal bounds should be decreased by one at each re-elimination of the same region.

| | |
|--------------------------------|---|
| ROWS or X.DIR | Eliminates points along horizontal lines. |
| COLUMNS or Y.DIR | Eliminates points along vertical lines. |

Boundary Parameters

| | |
|---------------------------------------|---|
| X.MIN, X.MAX, Y.MIN, and Y.MAX | Specify the location of the boundaries of an area in coordinates, where the elimination is applied. |
|---------------------------------------|---|

The following are provided for backward compatibility only. Their use is not recommended.

| | |
|----------------|--|
| IX.HIGH | Specifies the mesh line number high boundary in the X direction. |
| IX.LOW | Specifies the mesh line number low boundary in the X direction. |
| IY.HIGH | Specifies the mesh line number high boundary in the Y direction. |
| IY.LOW | Specifies the mesh line number low boundary in the Y direction. |

Substrate Mesh Reduction Example

This example removes vertical points between the depth of 10 μ m and 20 μ m.

```
ELIM Y.DIR Y.MIN=10 Y.MAX=20 X.MIN=1 X.MAX=8
```

```
ELIM Y.DIR Y.MIN=10 Y.MAX=20 X.MIN=1 X.MAX=7
```

Note: In some cases, applications of the `ELIMINATE` statement can cause internal inconsistencies in the mesh. When this occurs, an error message will appear, warning you that there are triangles that are not associated with any region.

Note: The `ELIMINATE` statement only works on meshes defined using ATLAS syntax. You can eliminate mesh points on arbitrary meshes in `DEVEDIT`

21.14: EXTRACT

EXTRACT statements are used to measure parameters from both log and solution files.

Note: These commands are executed by DECKBUILD. This statement is documented in the DECKBUILD USER'S MANUAL.

Terminal Current Extraction Example

By default, EXTRACT works on the currently open log file. For example, to extract peak drain current from a run immediately after solution, type:

```
LOG OUTF=myfile.log
SOLVE .....
EXTRACT NAME="peak Id" max(i."drain")
```

Extraction Example from Previously Generated Results

To extract the same data from a previously run simulation, use the INIT parameter.

```
EXTRACT INIT INFILE="myfile.log"
EXTRACT NAME="peak Id" max(i."drain")
```

Solution Quantities Extraction Example

To use EXTRACT with solution files, use the INIT parameter. To find the integrated number of electrons in a 1D slice at X=1.0, use:

```
SAVE OUTF=mysolve.str    or    SOLVE ..... MASTER OUTF=mysolve.str
EXTRACT INIT INFILE="mysolve.str"
EXTRACT NAME="integrated e-" area from curve(depth,n.conc \
    material="Silicon" mat.occno=1 x.val=1.0)
```

Note: EXTRACT commands are generally case sensitive.

21.15: EYE.DIAGRAM

EYE.DIAGRAM specifies that an eye diagram should be generated from the specified log file. An eye diagram is created by dividing up transient data in periods of fixed size and then overlaying it.

Syntax

```
EYE.DIAGRAM INFILE OUTFILE PERIOD + [OPTIONAL PARAMETERS]
```

| Parameter | Type | Default | Units |
|-----------|-----------|---------|-------|
| INFILE | Character | | |
| OUTFILE | Character | | |
| PERIOD | Real | | s |
| T.START | Real | | s |
| T.STOP | Real | | s |

Description

| | |
|----------------|---|
| INFILE | Specifies the input log file. This should contain data from a transient simulation. |
| OUTFILE | Specifies the file output file for the eye diagram. |
| PERIOD | Specifies the window period. |
| T.START | Specifies the initial time value to be used. The default value is the first time point in the input log file. |
| T.STOP | Specifies the final time value to be used. The default value is the last time point in the input log file. |

Examples

```
EYE.DIAGRAM INFILE=laser.log OUTFILE=eye.log PERIOD=2e-10 T.START=1.5e-9
```

In this example, laser.log is a log file from the transient simulation of a buried heterostructure laser when it is biased using a pseudo-random bit sequence. The data values from time=1.5ns onwards are used to create the eye diagram with a data period of 0.2ns. The results are then saved to the log file, eye.log. Figure 21-5 shows the eye diagram in TONYPLOT.

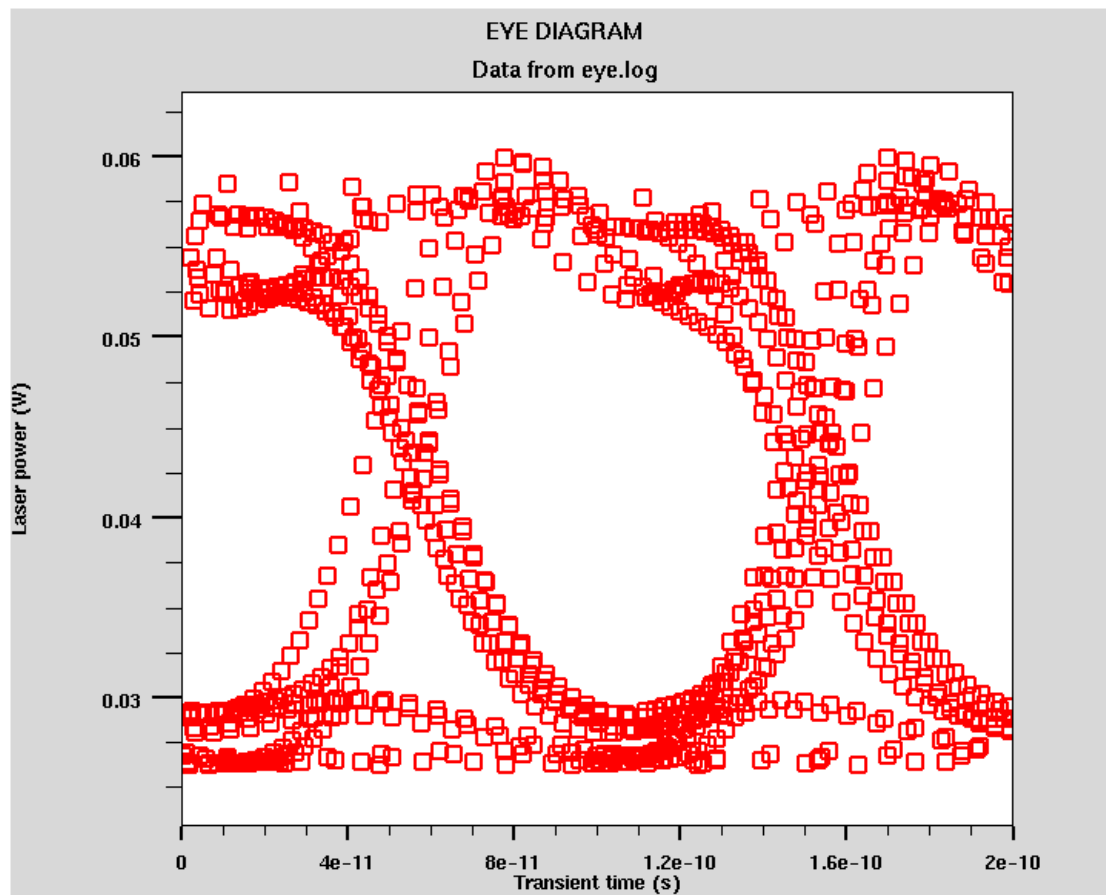


Figure 21-5: Eye diagram for BH Laser diode with a psuedo-random bit sequence input

21.16: FDX.MESH, FDY.MESH

FD<n>.MESH specifies the location of grid lines along the <n>-axis in a rectangular mesh used in FDTD simulation. The syntax is equivalent for X and Y directions.

Syntax

```
FDX.MESH NODE=<n> LOCATION=<n>
```

```
FDX.MESH SPACING=<n> LOCATION=<n>
```

```
FDY.MESH NODE=<n> LOCATION=<n>
```

```
FDY.MESH SPACING=<n> LOCATION=<n>
```

| Parameter | Type | Default | Units |
|-----------|---------|---------|-------|
| LOCATION | Real | | μm |
| NODE | Integer | | |
| SPACING | Real | | μm |

Description

| | |
|-----------------|---|
| NODE | Specifies the mesh line index. These mesh lines are assigned consecutively. |
| LOCATION | Specifies the location of the grid line. |
| SPACING | Specifies the mesh spacing at the mesh locations specified by the LOCATION parameter. If the SPACING parameter is specified, then the NODE parameter should not be specified. |

FDTD Mesh Example

This syntax defines a mesh of 33x33 covering the area bounded by (0.3,0.0) to (2.4,1.0).

```
FDX.M n=1 l=0.3
```

```
FDX.M n=33 l=2.4
```

```
FDY.M n=1 l=0.0
```

```
FDY.M n=33 l=1.0
```

Note: The mesh defined in these statements for the FDTD Solution is entirely separate from the electrical device simulation mesh defined on the MESH statement. The FDTD Mesh is defined in the coordinate system relative to the direction of beam propagation (see Figure 10-1).

Setting Locally Fine Grids Example

This example shows how to space grid lines closely around a topological feature such as a junction at y=0.85 microns.

```
LY.MESH LOC=0.0 SPAC=0.2
```

```
LY.MESH LOC=0.85 SPAC=0.01
```

```
LY.MESH LOC=2 SPAC=0.35
```

21.17: FOURIER

FOURIER enables you to do Fourier transformations.

Syntax

FOURIER INFILE OUTFILE + [OPTIONAL PARAMETERS]

| Parameter | Type | Default | Units |
|----------------|-----------|---------|-------|
| COMPLEX.VALUES | Logical | False | |
| FUNDAMENTAL | Real | | Hz |
| INFILE | Character | | |
| INTERPOLATE | Logical | False | |
| MAX.HARMONIC | Real | | Hz |
| NO.DC | Logical | False | |
| NUM.SAMPLES | Integer | 64 | |
| OUTFILE | Character | | |
| T.START | Real | | s |
| T.STOP | Real | | s |

Description

The FOURIER statement performs a Fast Fourier Transform on log file data.

| | |
|-----------------------|---|
| COMPLEX.VALUES | Specifies that the real and imaginary components are saved to file as well as the magnitude and phase values. The synonym for this parameter is REAL.VALUES. |
| FUNDAMENTAL | Specifies the fundamental frequency. If the fundamental frequency is specified, T.STOP is set to T.START+1/FUNDAMENTAL. If this is not specified, the fundamental frequency is set to (T.STOP-T.START)/NUM.SAMPLES. |
| INFILE | Specifies the input log file. This should contain data from a transient simulation. |
| INTERPOLATE | Specifies that the input data should be linearly interpolated such that data at uniform time steps are created. Interpolation of data can introduce addition (inaccurate) harmonic values into the Fourier transform. INTERPOLATE must be used if the log file contains non-uniform time steps. |
| MAX.HARMONIC | Specifies the maximum harmonic frequency that the Fourier transform should calculate. This will automatically calculate the correct number of samples (NUM.SAMPLES) required to generate this frequency. FUNDAMENTAL must be specified when MAX.HARMONIC is used. |
| NO.DC | Specifies that the DC component will not be saved to the log file. |

| | |
|---------------------|--|
| NUM. SAMPLES | Specifies the number of discrete samples. This should be an integer power of 2 (i.e., 2^n where n is a positive integer). The default value is 64 unless the MAX.HARMONIC parameter is specified. In this case the number of samples is set to the nearest integer power of 2 which will generate this frequency. |
| OUTFILE | Specifies the output file for the Fourier transform data. |
| T.START | Specifies the start of time data to be used for the Fourier transform. The default value is the first time point in the input log file. |
| T.STOP | Specifies the end of time data to be used for the Fourier transform. The default value is the last time point in the input log file. |

Example 1

In this example, the transient data previously written to log file, *hemt1.log*, is transformed from the time domain to the frequency domain. The fundamental frequency is set to 0.5 GHz, and harmonic frequencies up to 16 GHz are calculated. Since the data in *hemt1.log* has non-uniform time steps, the **INTERPOLATE** flag must be enabled. The complex values as well as the magnitude and phase values are stored in *fftout1.log*.

```
FOURIER INFILE=hemt1.log FUNDAMENTAL=5e8 MAX.HARMONIC=1.6E10 \
      OUTFILE=fftout1.log INTERPOLATE COMPLEX.VALUES
```

Example 2

In this example, the log file values between 31.25 ps and 2ns are transformed into the frequency domain. The fundamental frequency is automatically determined from the time period set by **T.START** and **T.STOP**. The data values from this time period are interpolated into 64 samples, giving a maximum harmonic frequency of 15.5 GHz. The magnitude and phase values are then stored in *fftout2.log*.

```
FOURIER INFILE=hemt1.log T.START=3.125e-11 T.STOP=2e-9 NUM.SAMPLES=64 \
      OUTFILE=fftout2.log INTERPOLATE
```


21.18: GO

GO quits and restarts ATLAS and also defines certain global parameters for ATLAS execution

Note: This command is executed by DECKBUILD. This statement is documented in the DECKBUILD USER'S MANUAL.

Example starting a given ATLAS Version

To start a given version of ATLAS the syntax is set by the `simflags` argument. To start version 5.12.0.R, type:

```
go atlas simflags="-V 5.12.0.R"
```

Parallel ATLAS Example

To define the number of processors to be used in parallel ATLAS, use the `P` flag. For example, to start parallel ATLAS use four processors. For example:

```
go atlas simflags="-V 5.12.0.R -P 4"
```

21.19: IMPACT

IMPACT specifies and set parameters for impact ionization models.

Syntax

IMPACT <model>

| Parameter | Type | Default | Units |
|-----------|---------|-------------------------|------------------|
| A.NT | Real | 0.588 | |
| A.PT | Real | 0.588 | |
| AE0001 | Real | 1.76×10^8 | cm^{-1} |
| AE1120 | Real | 3.30×10^7 | cm^{-1} |
| AH0001 | Real | 3.41×10^8 | cm^{-1} |
| AH1120 | Real | 2.50×10^7 | cm^{-1} |
| AN1 | Real | 7.03×10^5 | cm^{-1} |
| AN2 | Real | 7.03×10^5 | cm^{-1} |
| AN0.VALD | Real | 4.3383 | |
| AN1.VALD | Real | -2.42×10^{-12} | |
| AN2.VALD | Real | 4.1233 | |
| ANGLE | Real | 0.0 | Degrees |
| ANISO | Logical | False | |
| ANOKUTO | Real | 0.426 | V |
| ANLACKNER | Real | 1.316×10^6 | cm |
| AP0.VALD | Real | 2.376 | |
| AP1 | Real | 6.71×10^5 | cm^{-1} |
| AP2 | Real | 1.682×10^6 | cm^{-1} |
| AP1.VALD | Real | 0.01033 | |
| AP2.VALD | Real | 1.0 | |
| APOKUTO | Real | 0.243 | V |
| APLACKNER | Real | 1.818×10^6 | cm |
| B.NT | Real | 0.248 | |
| B.PT | Real | 0.248 | |
| BE0001 | Real | 2.10×10^7 | V/cm |

| Parameter | Type | Default | Units |
|-----------|------|-----------------------|-------------------------------|
| BE1120 | Real | 1.70×10^7 | V/cm |
| BETAN | Real | 1.0 | |
| BETAP | Real | 1.0 | |
| BH0001 | Real | 2.96×10^7 | V/cm |
| BH1120 | Real | 1.690×10^7 | V/cm |
| BN1 | Real | 1.231×10^6 | V/cm |
| BN2 | Real | 1.231×10^6 | V/cm |
| BN1.VALD | Real | 0.0 | |
| BN0.VALD | Real | 0.235 | |
| BNLACKNER | Real | 1.474×10^6 | V/cm |
| BNOKUTO | Real | 4.81×10^5 | V/cm |
| BP1 | Real | 1.231×10^6 | V/cm |
| BP2 | Real | 2.036×10^6 | V/cm |
| BP0.VALD | Real | 0.17714 | |
| BP1.VALD | Real | -0.002178 | |
| BPOKUTO | Real | 6.53×10^5 | V/cm |
| BPLACKNER | Real | 2.036×10^6 | V/cm |
| C0 | Real | 2.5×10^{-10} | |
| CHIA | Real | 3.0×10^5 | |
| CHIB | Real | 5.0×10^4 | |
| CHI.HOLES | Real | 4.6×10^4 | |
| CN2 | Real | 0.0 | $\text{cm}^{-1}\text{K}^{-1}$ |
| CN0.VALD | Real | 1.6831×10^4 | |
| CN1.VALD | Real | 4.3796 | |
| CN2.VALD | Real | 1.0 | |
| CN3.VALD | Real | 0.13005 | |
| CNOKUTO | Real | 3.05×10^{-4} | K |
| CP2 | Real | 0.0 | $\text{cm}^{-1}\text{K}^{-1}$ |
| CP0.VALD | Real | 0.0 | |

| Parameter | Type | Default | Units |
|-------------|-----------|------------------------|-------|
| CP1.VALD | Real | 0.00947 | |
| CP2.VALD | Real | 2.4929 | |
| CP3.VALD | Real | 0.0 | |
| CPOKUTO | Real | 5.35×10^{-4} | K |
| CROWELL | Logical | False | |
| CSUB.N | Real | 2.0×10^{14} | |
| CSUB.P | Real | 4.0×10^{12} | |
| DN0.VALD | Real | 1.233735×10^6 | |
| DN1.VALD | Real | 1.2039×10^3 | |
| DN2.VALD | Real | 0.56703 | |
| DNOKUTO | Real | 6.86×10^{-4} | K |
| DP0.VALD | Real | 1.4043×10^6 | |
| DP1.VALD | Real | 2.9744×10^3 | |
| DP2.VALD | Real | 1.4829 | |
| DPOKUTO | Real | 5.67×10^{-4} | K |
| DEVICE | Character | | |
| DIRECTED | Logical | False | |
| E.DIR | Logical | True | |
| E.SIDE | Logical | False | |
| E.VECTOR | Logical | False | |
| ECN.II | Real | 1.231×10^6 | |
| ECP.II | Real | 2.036×10^6 | |
| EGRAN | Real | 4.0×10^5 | V/cm |
| ENERGY.STEP | Real | 0.0025 | |
| ETH.N | Real | 1.8 | eV |
| ETH.P | Real | 3.5 | eV |
| EXN.II | Real | 1.0 | |
| EXP.II | Real | 1.0 | |
| F.EDIIN | Character | | |
| F.EDIIP | Character | | |

| Parameter | Type | Default | Units |
|------------|-----------|--|----------------------------------|
| GRADQFL | Logical | False | |
| GRANT | Logical | False | |
| ICRIT | Real | 4.0×10^{-3} | A/cm ² |
| INFINITY | Real | 0.001 | |
| LACKNER | Logical | False | |
| LAMDAE | Real | 6.2×10^{-7} | cm |
| LAMDAH | Real | 3.8×10^{-7} | cm |
| LAN300 | Real | 6.2×10^{-7} | cm |
| LAP300 | Real | 3.8×10^{-7} | cm |
| LENGTH.REL | Logical | False | |
| LREL.EL | Real | 3.35×10^{-2} | μm |
| LREL.HO | Real | 2.68×10^{-2} | μm |
| M.ANT | Real | 1.0 | |
| M.APT | Real | 1.0 | |
| M.BNT | Real | 1.0 | |
| M.BPT | Real | 1.0 | |
| MATERIAL | Character | | |
| NAME | Character | | |
| NEW | Logical | False | |
| NISEDELTA | Real | 1.5 | |
| N.ION.1 | Real | 0.0 | cm ⁻¹ K ⁻¹ |
| N.ION.2 | Real | 0.0 | cm ⁻¹ K ⁻² |
| N.IONIZA | Real | 7.03×10^5 | cm ⁻¹ |
| N.LACKHW | Real | 0.063 | eV |
| N.UPSILON | Logical | True/False (in silicon)/(otherwise) | |
| N.VANHW | Real | 0.063 | eV |
| NDELOKUTO | Real | 2.0 | |
| NGAMOKUTO | Real | 1.0 | |
| NISELAMBDA | Real | 1.0 | |
| OKUTO | Logical | False | |

| Parameter | Type | Default | Units |
|------------|-----------|--|-------------------------------|
| OLD | Logical | False | |
| OP.PH.EN | Real | 0.063 | eV |
| OPPHE | Real | 0.063 | eV |
| P.ION.1 | Real | 0.0 | $\text{cm}^{-1}\text{K}^{-1}$ |
| P.ION.2 | Real | 0.0 | $\text{cm}^{-1}\text{K}^{-2}$ |
| P.IONIZA | Real | 1.682×10^6 | cm^{-1} |
| P.LACKHW | Real | 0.063 | eV |
| P.UPSILON | Logical | True/False (in silicon)/(otherwise) | |
| P.VANHW | Real | 0.063 | eV |
| PDELOKUTO | Real | 2.0 | |
| PGAMOKUTO | Real | 1.0 | |
| PISEDELTA | Real | 1.5 | |
| PISELAMBDA | Real | 1.0 | |
| REGION | Integer | | |
| SIC4H0001 | Logical | False | |
| SIC4H1120 | Logical | False | |
| SELB | Logical | False | |
| STRUCTURE | Character | | |
| TAUSN | Real | 0.4×10^{-12} | s |
| TAUSP | Real | 0.4×10^{-12} | s |
| TOYABE | Logical | False | |
| VAL.AN0 | Real | 4.3383 | |
| VAL.AN1 | Real | -2.42×10^{-12} | |
| VAL.AN2 | Real | 4.1233 | |
| VAL.AP0 | Real | 2.376 | |
| VAL.AP1 | Real | 0.01033 | |
| VAL.AP2 | Real | 1.0 | |
| VAL.BN0 | Real | 0.235 | |
| VAL.BN1 | Real | 0.0 | |
| VAL.CN0 | Real | 1.6831×10^4 | |

| Parameter | Type | Default | Units |
|-----------|---------|------------------------|-----------|
| VAL.CN1 | Real | 4.3796 | |
| VAL.CN2 | Real | 1.0 | |
| VAL.CN3 | Real | 0.13005 | |
| VAL.DN0 | Real | 1.233735×10^6 | |
| VAL.DN1 | Real | 1.2039×10^3 | |
| VAL.DN2 | Real | 0.56703 | |
| VAL.BP0 | Real | 0.17714 | |
| VAL.BP1 | Real | -0.002178 | |
| VAL.CP0 | Real | 0.0 | |
| VAL.CP1 | Real | 0.00947 | |
| VAL.CP2 | Real | 2.4924 | |
| VAL.CP3 | Real | 0.0 | |
| VAL.DP0 | Real | 1.4043×10^6 | |
| VAL.DP1 | Real | 2.9744×10^3 | |
| VAL.DP2 | Real | 1.4829 | |
| VALDINOCI | Logical | False | |
| VANOVERS | Logical | False | |
| ZAPPA | Logical | False | |
| ZAP.AN | Real | 1.9 | eV |
| ZAP.BN | Real | 41.7 | angstroms |
| ZAP.CN | Real | 46.0 | meV |
| ZAP.DN | Real | 46.0 | meV |
| ZAP.EN | Real | 46.0 | meV |
| ZAP.AP | Real | 1.4 | eV |
| ZAP.BP | Real | 41.3 | angstroms |
| ZAP.CP | Real | 36.0 | meV |
| ZAP.DP | Real | 36.0 | meV |
| ZAP.EP | Real | 36.0 | meV |

Description

The impact ionization model for continuity equations allows the accurate prediction of avalanche breakdown for many devices. Since impact ionization is a two-carrier process, the following statement must be specified after setting impact ionization models.

```
METHOD CARRIERS=2
```

Model Selection Flags

| | |
|-------------------------------------|---|
| ANISO | Specifies the 4hSiC Model Equations 5-124 through 5-127. |
| CROWELL | Specifies the Crowell and Sze formulae [52]. |
| GRADQFL | Enables Gradient of Quasi-Fermi levels as drivers. |
| GRANT | Selects Grant's impact ionization model [63] (see Chapter 3: "Physics", Equations 3-368 through 3-384). |
| LACKNER | enables the Lackner model [129]. |
| SELB | Selects the impact ionization model described by Selberherr [207]. |
| OKUTO | Enables the Okuto-Crowell model [166]. |
| N.CONCANNON, P.CONCANNON | Set the Concannon substrate current model. |
| N.UPSILON | Enables non-linear dependence of effective field on electron temperature if you use the -ISE flag. |
| P.UPSILON | Enables non-linear dependence of effective field on hole temperature if you use the -ISE flag. |
| SIC4H0001 | Specifies that the y axis concides with the 0001 crystal orientation for the anisotropic impact ionization model. |
| SIC4H1120 | Specifies that the y axis concides with the 1120 crystal orientation for the anisotropic impact ionization model. |
| TOYABE | This is a synonym for SELB. |
| VANOVERS | Enables the VanOverstraeten de Man model [236]. |
| ZAPPA | Enables Zappa's model for ionization rates in InP. |

Note: If no model selection flag is set, the model parameters from Grant [63] are used. See Chapter 3: "Physics", "Grant's Impact Ionization Model" Section on page 3-108.

Okuto-Crowell Model Parameters

| | |
|------------------|--|
| ANOKUTO | See Section 3.6.4: “Impact Ionization Models”, Equation 3-396, Table 3-79. |
| APOKUTO | See Section 3.6.4: “Impact Ionization Models”, Equation 3-397, Table 3-79. |
| BNOKUTO | See Section 3.6.4: “Impact Ionization Models”, Equation 3-396, Table 3-79. |
| BPOKUTO | See Section 3.6.4: “Impact Ionization Models”, Equation 3-397, Table 3-79. |
| CNOKUTO | See Section 3.6.4: “Impact Ionization Models”, Equation 3-396, Table 3-79. |
| CPOKUTO | See Section 3.6.4: “Impact Ionization Models”, Equation 3-397, Table 3-79. |
| DNOKUTO | See Section 3.6.4: “Impact Ionization Models”, Equation 3-396, Table 3-79. |
| DPOKUTO | See Section 3.6.4: “Impact Ionization Models”, Equation 3-397, Table 3-79. |
| NGAMOKUTO | See Section 3.6.4: “Impact Ionization Models”, Equation 3-396, Table 3-79. |
| PGAMOKUTO | See Section 3.6.4: “Impact Ionization Models”, Equation 3-397, Table 3-79. |
| NDELOKUTO | See Section 3.6.4: “Impact Ionization Models”, Equation 3-396, Table 3-79. |
| PDELOKUTO | See Section 3.6.4: “Impact Ionization Models”, Equation 3-397, Table 3-79. |

van Overstraeten de Man Model Parameters

| | |
|------------------|--|
| N . VANHW | See Section 3.6.4: “Impact Ionization Models”, Equation 3-366, Table 3-75. |
| P . VANHW | See Section 3.6.4: “Impact Ionization Models”, Equation 3-367, Table 3-75. |

Note: You must also use the Selberherr model parameters with this model.

Lackner Model Parameters

| | |
|-------------------|--|
| ANLACKNER | See Section 3.6.4: “Impact Ionization Models”, Equation 3-399, Table 3-80. |
| APLACKNER | See Section 3.6.4: “Impact Ionization Models”, Equation 3-400, Table 3-80. |
| BNLACKNER | See Section 3.6.4: “Impact Ionization Models”, Equation 3-399, Table 3-80. |
| BPLACKNER | See Section 3.6.4: “Impact Ionization Models”, Equation 3-400, Table 3-80. |
| N . LACKHW | See Section 3.6.4: “Impact Ionization Models”, Equation 3-401, Table 3-80. |
| P . LACKHW | See Section 3.6.4: “Impact Ionization Models”, Equation 3-401, Table 3-80. |

Non-linear Hydrodynamic Model

To enable this model, use the command line flag `-ISE`.

| | |
|-------------------|--|
| N.UPSILON | See Section 3.6.4: “Impact Ionization Models”, Equation 3-414, Table 3-84. |
| P.UPSILON | See Section 3.6.4: “Impact Ionization Models”, Equation 3-415, Table 3-84. |
| NISELAMBDA | See Section 3.6.4: “Impact Ionization Models”, Equation 3-414, Table 3-84. |
| PISELAMBDA | See Section 3.6.4: “Impact Ionization Models”, Equation 3-415, Table 3-84. |
| NISEDELTA | See Section 3.6.4: “Impact Ionization Models”, Equation 3-414, Table 3-84. |
| PISEDELTA | See Section 3.6.4: “Impact Ionization Models”, Equation 3-415, Table 3-84. |

Electric Field Model Selection Flags

The default electric field to use for ionization rate calculations is calculated as the modulus of the electric field over a triangle. In ATLAS3D, this is combined with the z-component of the field at each corner of the prism to give an overall field modulus at each node. This corresponds to Equation 3-348 in Chapter 3: “Physics” for a triangle.

| | |
|-----------------|--|
| ANGLE | Specifies the direction along which field magnitude will be calculated for use in calculating ionization rate when you specify <code>DIRECTED</code> . |
| DIRECTED | Specifies that the field for ionization rate calculations will be calculated along a user-specified direction. That direction is specified by the <code>ANGLE</code> parameter. |
| E.DIR | Specifies that the impact ionization rate will be calculated as a function of the electric field in the direction of the current (see Equation 3-350 in Chapter 3: “Physics”). Its alias is <code>NEW</code> . |
| E.SIDE | Specifies that the impact ionization rate will be calculated as a function of the electric field along the side of the triangle (see Equation 3-349 in Chapter 3: “Physics”). This model is only supported in ATLAS2D. Its alias is <code>OLD</code> . |
| E.VECTOR | Specifies that the vector electric field will be used in the calculated of the impact ionization rate (see Equation 3-348 in Chapter 3: “Physics”). |
| OLD | This is the model that corresponds to Equation 3-349 in Chapter 3: “Physics” and is only supported in ATLAS2D. |
| NEW | This is the model that corresponds to Equation 3-350 in Chapter 3: “Physics”, where the component of the field in the direction of the current is used in the ionisation rate calculation. It is implemented in both ATLAS2D and ATLAS3D. If the dot product of E and J is negative, then the field component is taken as 0. Consequently, impact ionisation may only occur when a current is dominated by the drift term. |

Model Localization Parameters

| | |
|------------------|---|
| DEVICE | Specifies the device in MIXEDMODE simulation to which the statement should apply. The synonym for this parameter is STRUCTURE . |
| MATERIAL | Specifies what material from Appendix B: “Material Systems”, Table B-1 the statement should apply. If a material is specified then all regions defined as being composed of that material will be affected. |
| NAME | Specifies what region that the IMPACT statement should apply. Note that the name must match the name specified in the NAME parameter of the REGION statement or the region number. |
| REGION | Specifies that index of the region to which the impact parameters apply. |
| STRUCTURE | This is a synonym for DEVICE . |

Valdinoci Model Parameters

| | |
|-------------------|---|
| AN0 . VALD | This is an alias for VAL . AN0 . |
| AN1 . VALD | This is an alias for VAL . AN1 . |
| AN2 . VALD | This is an alias for VAL . AN2 . |
| AP0 . VALD | This is an alias for VAL . AP0 . |
| AP1 . VALD | This is an alias for VAL . AP1 . |
| AP2 . VALD | This is an alias for VAL . AP2 . |
| BN0 . VALD | This is an alias for VAL . BN0 . |
| BN1 . VALD | This is an alias for VAL . BN1 . |
| BP0 . VALD | This is an alias for VAL . BP0 . |
| BP1 . VALD | This is an alias for VAL . BP1 . |
| CN0 . VALD | This is an alias for VAL . CN0 . |
| CN1 . VALD | This is an alias for VAL . CN1 . |
| CN2 . VALD | This is an alias for VAL . CN2 . |
| CN3 . VALD | This is an alias for VAL . CN3 . |
| CP0 . VALD | This is an alias for VAL . CP0 . |
| CP1 . VALD | This is an alias for VAL . CP1 . |
| CP2 . VALD | This is an alias for VAL . CP2 . |
| CP3 . VALD | This is an alias for VAL . CP3 . |
| DN0 . VALD | This is an alias for VAL . DN0 . |
| DN1 . VALD | This is an alias for VAL . DN1 . |
| DN2 . VALD | This is an alias for VAL . DN2 . |

| | |
|-----------------|---|
| DP0.VALD | This is an alias for VAL.DP0. |
| DP1.VALD | This is an alias for VAL.DP1. |
| DP2.VALD | This is an alias for VAL.DP2. |
| VAL.AN0 | Specifies the value of a temperature dependent impact ionization parameter in Chapter 3: “Physics”, Equation 3-369. The alias for this parameter is AN0.VALD. |
| VAL.AN1 | Specifies the value of a temperature dependent impact ionization parameter in Chapter 3: “Physics”, Equation 3-369. The alias for this parameter is AN1.VALD. |
| VAL.AN2 | Specifies the value of a temperature dependent impact ionization parameter in Chapter 3: “Physics”, Equation 3-369. The alias for this parameter is AN2.VALD. |
| VAL.BN0 | Specifies the value of a temperature dependent impact ionization parameter in Chapter 3: “Physics”, Equation 3-370. The alias for this parameter is BN0.VALD. |
| VAL.BN1 | Specifies the value of a temperature dependent impact ionization parameter in Chapter 3: “Physics”, Equation 3-370. The alias for this parameter is BN1.VALD. |
| VAL.CN0 | Specifies the value of a temperature dependent impact ionization parameter in Chapter 3: “Physics”, Equation 3-371. The alias for this parameter is CN0.VALD. |
| VAL.CN1 | Specifies the value of a temperature dependent impact ionization parameter in Chapter 3: “Physics”, Equation 3-371. The alias for this parameter is CN1.VALD. |
| VAL.CN2 | Specifies the value of a temperature dependent impact ionization parameter in Chapter 3: “Physics”, Equation 3-371. The alias for this parameter is CN2.VALD. |
| VAL.CN3 | Specifies the value of a temperature dependent impact ionization parameter in Chapter 3: “Physics”, Equation 3-371. The alias for this parameter is CN3.VALD. |
| VAL.DN0 | Specifies the value of a temperature dependent impact ionization parameter in Chapter 3: “Physics”, Equation 3-372. The alias for this parameter is DN0.VALD. |
| VAL.DN1 | Specifies the value of a temperature dependent impact ionization parameter in Chapter 3: “Physics”, Equation 3-372. The alias for this parameter is DN1.VALD. |
| VAL.DN2 | Specifies the value of a temperature dependent impact ionization parameter in Chapter 3: “Physics”, Equation 3-372. The alias for this parameter is DN2.VALD. |
| VAL.AP0 | Specifies the value of a temperature dependent impact ionization parameter in Chapter 3: “Physics”, Equation 3-373. |
| VAL.AP1 | Specifies the value of a temperature dependent impact ionization parameter in Chapter 3: “Physics”, Equation 3-373. The alias for this parameter is AP1.VALD. |

| | |
|----------------|---|
| VAL.AP2 | Specifies the value of a temperature dependent impact ionization parameter in Chapter 3: “Physics”, Equation 3-373. The alias for this parameter is AP2.VALD. |
| VAL.BP0 | Specifies the value of a temperature dependent impact ionization parameter in Chapter 3: “Physics”, Equation 3-374. The alias for this parameter is BP0.VALD. |
| VAL.BP1 | Specifies the value of a temperature dependent impact ionization parameter in Chapter 3: “Physics”, Equation 3-374. The alias for this parameter is BP1.VALD. |
| VAL.CP0 | Specifies the value of a temperature dependent impact ionization parameter in Chapter 3: “Physics”, Equation 3-375. The alias for this parameter is CP0.VALD. |
| VAL.CP1 | Specifies the value of a temperature dependent impact ionization parameter in Chapter 3: “Physics”, Equation 3-375. The alias for this parameter is CP1.VALD. |
| VAL.CP2 | Specifies the value of a temperature dependent impact ionization parameter in Chapter 3: “Physics”, Equation 3-375. The alias for this parameter is CP2.VALD. |
| VAL.CP3 | Specifies the value of a temperature dependent impact ionization parameter in Chapter 3: “Physics”, Equation 3-375. The alias for this parameter is CP3.VALD. |
| VAL.DP0 | Specifies the value of a temperature dependent impact ionization parameter in Chapter 3: “Physics”, Equation 3-271. The alias for this parameter is DP0.VALD. |
| VAL.DP1 | Specifies the value of a temperature dependent impact ionization parameter in Chapter 3: “Physics”, Equation 3-376. The alias for this parameter is DP1.VALD. |
| VAL.DP2 | Specifies the value of a temperature dependent impact ionization parameter in Chapter 3: “Physics”, Equation 3-376. The alias for this parameter is DP2.VALD. |

Zappa Model Parameters

| | |
|---------------|--|
| ZAP.AN | Specifies the value of a temperature dependent ionization parameter in Chapter 3: “Physics”, Equation 3-377. |
| ZAP.BN | Specifies the value of a temperature dependent ionization parameter in Chapter 3: “Physics”, Equation 3-378. |
| ZAP.CN | Specifies the value of a temperature dependent ionization parameter in Chapter 3: “Physics”, Equation 3-378. |
| ZAP.DN | Specifies the value of a temperature dependent ionization parameter in Chapter 3: “Physics”, Equation 3-379. |
| ZAP.EN | Specifies the value of a temperature dependent ionization parameter in Chapter 3: “Physics”, Equation 3-379. |

| | |
|---------------|--|
| ZAP.AP | Specifies the value of a temperature dependent ionization parameter in Chapter 3: "Physics", Equation 3-380. |
| ZAP.BP | Specifies the value of a temperature dependent ionization parameter in Chapter 3: "Physics", Equation 3-381. |
| ZAP.CP | Specifies the value of a temperature dependent ionization parameter in Chapter 3: "Physics", Equation 3-381. |
| ZAP.DP | Specifies the value of a temperature dependent ionization parameter in Chapter 3: "Physics", Equation 3-382. |
| ZAP.EP | Specifies the value of a temperature dependent ionization parameter in Chapter 3: "Physics", Equation 3-382. |

Crowell Model Parameters

| | |
|-----------------|---|
| LAMDAE | Specifies the mean free path for electrons. The alias for this parameter is LAN300. |
| LAMDAH | Specifies the mean free path for holes. The alias for this parameter is LAP300. |
| LAN300 | This is an alias for LAMDAE. |
| LAP300 | This is an alias for LAMDAH. |
| OP.PH.EN | This is an alias for OPPHE. |
| OPPHE | Specifies the optical phonon energy. The alias for this parameter is OP.PH.EN. |

Selberherr Model Parameters

| | |
|----------------------------------|---|
| AN1, AN2, BN1, BN2, EGRAN | Specify the basic set of parameters for Selberherr's impact ionization model. Index 1 (AP1, BP1, AN1, and BN1) corresponds to field values less than EGRAN, and index 2 (AP2, BP2, AN2, and BN2) corresponds to field values greater than EGRAN. The aliases for these parameters are N.IONIZA, P.IONIZA, ECN.II, and ECP.II. |
| BETAN | This is for electrons and BETAP is for holes correspond to coefficients for the power of ECRIT/E. The aliases for these parameters are EXN.II and EXP.II. |
| EXN.II | This is an alias for BETAN. |
| EXP.II | This is an alias for BETAP. |

Temperature Dependence Parameters

| | |
|---|---|
| A.NT | Specifies the value of the temperature-dependent parameter in Chapter 3: “Physics”, Equation 3-354. |
| A.PT | Specifies the value of the temperature-dependent parameter in Chapter 3: “Physics”, Equation 3-355. |
| B.NT | Specifies the value of the temperature-dependent parameter in Chapter 3: “Physics”, Equation 3-356. |
| B.PT | Specifies the value of the temperature-dependent parameter in Chapter 3: “Physics”, Equation 3-357. |
| M.ANT | Specifies the value of the temperature-dependent parameter in Chapter 3: “Physics”, Equation 3-354. |
| M.APT | Specifies the value of the temperature-dependent parameter in Chapter 3: “Physics”, Equation 3-355. |
| M.BNT | Specifies the value of the temperature-dependent parameter in Chapter 3: “Physics”, Equation 3-356. |
| M.BPT | Specifies the value of the temperature-dependent parameter in Chapter 3: “Physics”, Equation 3-357. |
| CN2, CP2, DN2, and DP2 | These are specifiable coefficients in the temperature dependent models described in Chapter 3: “Physics”, Equations 3-355 and 3-356. The aliases for these parameters are N.ION.1 , P.ION.1 , N.ION.2 , and P.ION.2 . |
| N.ION.1, P.ION.1, N.ION.2, and P.ION.2 | These are the aliases for CN2, CP2, DN2, and DP2. |

Parameters for use with Energy Balance

| | |
|-------------------|--|
| F.EDIIN | Specifies the name of the file containing a C-Interpreter function describing the values of the parameters in Chapter 3: “Physics”, Equation 3-352 as a function of electron temperature. |
| F.EDIIP | Specifies the name of the file containing a C-Interpreter function describing the values of the parameters in Chapter 3: “Physics”, Equation 3-353 as a function of hole temperature. |
| LENGTH.REL | Specifies the use of energy relaxation length for the impact ionization model with the energy balance model. If LENGTH.REL is specified, TAUSN and TAUSP cannot be specified and have any affect. |
| LREL.EL | Specifies an energy relaxation length for electrons if LENGTH.REL is specified. |

| | |
|------------------|--|
| LREL . HO | Specifies an energy relaxation length for holes if LENGTH . REL is specified. |
| TAUSN | Specifies the relaxation time for electrons in the temperature dependent impact model. |
| TAUSP | Specifies the relaxation time for holes in the temperature dependent impact model. |

Note: When energy balance simulations are run, the Toyabe impact ionization model is used. This model is used regardless of the **SELB** or **CROWELL** settings. See Chapter 3: “Physics”, “Toyabe Impact Ionization Model” Section on page 3-112 for more information about this model.

Concannon Model Parameters

| | |
|----------------------|---|
| CSUB . N | This is an empirical tuning factor used in Concannon's Substrate Current Model (see Chapter 3: “Physics”, Equation 3-408) for electrons. |
| CSUB . P | This is an empirical tuning factor used in Concannon's Substrate Current Model (see Chapter 3: “Physics”, Equation 3-409) for holes. |
| ETH . N | Specifies the ionization threshold energy for electrons used in Concannon's Substrate Current Model (see Chapter 3: “Physics”, Equation 3-408). |
| ETH . P | Specifies the ionization threshold energy for holes used in Concannon's Substrate Current Model (see Chapter 3: “Physics”, Equation 3-409). |
| C0 | Specifies the electron distribution weight factor used in Concannon's Substrate Current Model (see Chapter 3: “Physics”, Equation 3-412). |
| CHIA | Specifies the electron distribution function constant used in Concannon's Substrate Current Model (see Chapter 3: “Physics”, Equation 3-412). |
| CHIB | Specifies the electron distribution function constant used in Concannon's Substrate Current Model (see Chapter 3: “Physics”, Equation 3-412). |
| CHI . HOLES | Specifies the hole distribution function constant used in Concannon's Substrate Current Model (see Chapter 3: “Physics”, Equation 3-413). |
| ENERGY . STEP | Specifies the energy step for numeric integration used in Concannon's Substrate Current Model |
| INFINITY | Specifies the limit for the highest energy in numeric integration used in Concannon's Substrate Current Model. |

Anisotropic Impact Ionization Parameters

| | |
|---------------|--|
| AE0001 | Anisotropic impact ionization parameter for Equations 5-124 through 5-127. |
| AE1120 | Anisotropic impact ionization parameter for Equations 5-124 through 5-127. |
| AH0001 | Anisotropic impact ionization parameter for Equations 5-124 through 5-127. |
| AH1120 | Anisotropic impact ionization parameter for Equations 5-124 through 5-127. |

| | |
|---------------|--|
| BE0001 | Anisotropic impact ionization parameter for Equations 5-124 through 5-127. |
| BE1120 | Anisotropic impact ionization parameter for Equations 5-124 through 5-127. |
| BH0001 | Anisotropic impact ionization parameter for Equations 5-124 through 5-127. |
| BH1120 | Anisotropic impact ionization parameter for Equations 5-124 through 5-127. |

Selberrherr Model Example

This example shows an `IMPACT` statement which specifies all parameters used by the model selected by the `SELB` parameter. In this case, only parameters for holes are field dependent. The `AP1` and `BP1` parameters correspond to parameters at field values more than `EGRAN`. The `AP2` and `BP2` parameters correspond to field values less than `EGRAN`. Coefficients for electrons should be repeated.

```
IMPACT SELB AN1=7.03E5 AN2=7.03E5 BN1=1.231E6 \
          BN2=1.231E6 AP1=6.71E5 AP2=1.58E6 BP1=1.693E6 \
          BP2=2.036E6 BETAN=1 BETAP=1 EGRAN=4.0E5
```

21.20: INTDEFECTS

INTDEFECTS activates the band gap interface defect model and sets the parameter values. This model can be used when thin-film transistor simulations are performed using the TFT product.

Syntax

INTDEFECTS [<parameters>]

| Parameter | Type | Default | Units |
|------------------|------------|-----------------------|----------------------------|
| AFILE | Character | | |
| AMPHOTERIC | Logical | False | |
| CONTINUOUS | Logical | True | |
| DEVICE | Character | | |
| DFILE | Characater | | |
| EGA | Real | 0.4 | eV |
| EGD | Real | 0.4 | eV |
| EP.AMPHOTERIC | Real | 1.27 | eV |
| EU.AMPHOTERIC | Real | 0.2 | eV |
| EV0.AMPHOTERIC | Real | 0.056 | eV |
| F.TFTACC | Character | | |
| F.TFTDON | Character | | |
| FILE.AMPHOTERIC | Character | | |
| FILEX.AMPHOTERIC | Character | | |
| FILEY.AMPHOTERIC | Character | | |
| FILEZ.AMPHOTERIC | Character | | |
| HCONC.AMPHOTERIC | Real | 5×10^{17} | cm^{-2} |
| INTMATERIAL | Character | | |
| INTNAME | Character | | |
| INTNUMBER | Character | | |
| INTREGION | Character | | |
| NGA | Real | 5.0×10^{17} | cm^{-2}/eV |
| NGD | Real | 1.5×10^{18} | cm^{-2}/eV |
| NSISI.AMPHOTERIC | Real | 2×10^{19} | cm^{-2} |
| NTA | Real | 1.12×10^{21} | cm^{-2}/eV |
| NTD | Real | 4.0×10^{20} | cm^{-2}/eV |

| Parameter | Type | Default | Units |
|------------------|-----------|-----------------------|------------------|
| NUM.AMPHOTERIC | Real | 20 | |
| NUMBER | Real | All | |
| NUMA | Real | 12 | |
| NUMD | Real | 12 | |
| NV0.AMPHOTERIC | Real | NV300 | cm ⁻² |
| R1MATERIAL | Character | | |
| R1NAME | Character | | |
| R1NUMBER | Integer | | |
| R1REGION | Character | | |
| R2MATERIAL | Character | | |
| R2NAME | Character | | |
| R2NUMBER | Integer | | |
| R2REGION | Character | | |
| S.I | Logical | True | |
| S.M | Logical | False | |
| S.S | Logical | False | |
| S.X | Logical | False | |
| SIGGAE | Real | 1.0×10 ⁻¹⁶ | cm ² |
| SIGGAH | Real | 1.0×10 ⁻¹⁴ | cm ² |
| SIGGDE | Real | 1.0×10 ⁻¹⁴ | cm ² |
| SIGGDH | Real | 1.0×10 ⁻¹⁶ | cm ² |
| SIGMA.AMPHOTERIC | Real | 0.19 | eV |
| SIGN0.AMPHOTERIC | Real | 1.0×10 ⁻¹⁶ | cm ² |
| SIGNP.AMPHOTERIC | Real | 1.0×10 ⁻¹⁶ | cm ² |
| SIGP0.AMPHOTERIC | Real | 1.0×10 ⁻¹⁶ | cm ² |
| SIGPN.AMPHOTERIC | Real | 1.0×10 ⁻¹⁶ | cm ² |
| SIGTAE | Real | 1.0×10 ⁻¹⁶ | cm ² |
| SIGTAH | Real | 1.0×10 ⁻¹⁴ | cm ² |
| SIGTDE | Real | 1.0×10 ⁻¹⁴ | cm ² |
| SIGTDH | Real | 1.0×10 ⁻¹⁶ | cm ² |

| Parameter | Type | Default | Units |
|---------------|-----------|---------------------|---------------|
| STRUCTURE | Character | | |
| TFILE | Character | | |
| T0.AMPHOTERIC | Real | 300 | K |
| WGA | Real | 0.1 | eV |
| WGD | Real | 0.1 | eV |
| WTA | Real | 0.025 | eV |
| WTD | Real | 0.05 | ev |
| X.MIN | Real | left of structure | μm |
| X.MAX | Real | right of structure | μm |
| Y.MIN | Real | top of structure | μm |
| Y.MAX | Real | bottom of structure | μm |
| Z.MIN | Real | back of structure | μm |
| Z.MAX | Real | front of structure | μm |

Description

The INTDEFECTS statement is used to describe the density of defect states in the band gap at semiconductor interfaces. You can specify up to four distributions, two for donor-like states and two for acceptor-like states. Each type of state may contain one exponential (tail) distribution and one Gaussian distribution.

| | |
|-----------------------|--|
| AFILE | Specifies the file name where the acceptor state density distribution, as a function of energy, will be stored. You can examine this file by using TONYPLOT. |
| AMPHOTERIC | Specifies the amphoteric defect model will be used. |
| CONTINUOUS | Specifies that the continuous defect integral model will be used. |
| DEVICE | Specifies which device the statement applies in mixed mode simulation. The synonym for this parameter is STRUCTURE. |
| DFILE | Specifies the file name where the donor state density distribution, as a function of energy, will be stored. You can examine this file by using TONYPLOT. |
| EGA | Specifies the energy that corresponds to the Gaussian distribution peak for acceptor-like states. This energy is measured from the conduction band edge. |
| EGD | Specifies the energy that corresponds to the Gaussian distribution peak for donor-like states. This energy is measured from the valence band edge. |
| EP.AMPHOTERIC | Specifies the most probable potential defect energy. |
| EU.AMPHOTERIC | Specifies the defect electron correlation energy. |
| EV0.AMPHOTERIC | Specifies the characteristic energy. |
| F.TFTACC | Specifies the name of a file containing a C-Interpreter function, describing the distribution of acceptor state densities as a function of energy. |

| | |
|-------------------------|---|
| F.TFTDON | Specifies the name of a file containing a C-Interpreter function, describing the distribution of donor state densities as a function of energy. |
| FILE.AMPHOTERIC | Specifies the file name where the dangling bond density of states distribution, as a function of energy, will be stored. If you specify <code>FILEX.AMPHOTERIC</code> , <code>FILEY.AMPHOTERIC</code> , and <code>FILEZ.AMPHOTERIC</code> , then the file will be saved at the coordinate closest to the one specified by <code>FILEX.AMPHOTERIC</code> , <code>FILEY.AMPHOTERIC</code> , and <code>FILEZ.AMPHOTERIC</code> . |
| FILEX.AMPHOTERIC | Specifies the X coordinate used in <code>FILE.AMPHOTERIC</code> . |
| FILEY.AMPHOTERIC | Specifies the Y coordinate used in <code>FILE.AMPHOTERIC</code> . |
| FILEZ.AMPHOTERIC | Specifies the Z coordinate used in <code>FILE.AMPHOTERIC</code> . |
| HCONC.AMPHOTERIC | Specifies the density of hydrogen. |
| INTMATERIAL | Specifies that the interface models defined on this command should be applied to every interface between the two given materials. For example, <code>INTMATERIAL="oxide/silicon"</code> . |
| INTNAME | Specifies that the interface models defined on this command should be applied to every interface between the two given regions (where the regions are defined by their region name). For example, <code>INTNAME="channel/substrate"</code> . |
| INTNUMBER | Specifies that the interface models defined on this command should be applied to every interface between the two given regions (where the regions are defined by their region number). For example, <code>INTNUMBER="2/3"</code> . |
| INTREGION | Specifies that the interface models defined on this command should be applied to every interface between the two given regions (where the regions are defined by either their region name or their region number). For example, <code>INTREGION="channel/substrate"</code> . |
| NGA | Specifies the total density of acceptor-like states in a Gaussian distribution. |
| NGD | Specifies the total density of donor-like states in a Gaussian distribution. |
| NSISI.AMPHOTERIC | Specifies the density of Si-Si bonds. |
| NTA | Specifies the density of acceptor-like states in the tail distribution at the conduction band edge. |
| NTD | Specifies the density of donor-like states in the tail distribution at the valence band edge. |
| NUM.AMPHOTERIC | Specifies the number of energy levels used in the DOS integration for amphoteric defects. |
| NV0.AMPHOTERIC | Specifies the density of states of the valence-band tail exponential region extrapolated to the valence-band edge. If this parameter is not specified, then the valence band density of states (<code>NV300</code> on the <code>MATERIAL</code> statement) will be used instead. |
| NUMBER or REGION | Specifies the region index to which the <code>DEFECT</code> statement applies. |
| NUMA | Specifies the number of discrete levels that will be used to simulate the continuous distribution of acceptor states. |

| | |
|---|---|
| NUMD | Specifies the number of discrete levels that will be used to simulate the continuous distribution of donor states. |
| R1MATERIAL and R2MATERIAL | Specifies that the interface models defined on this command should be applied to every interface between the two given materials. For example, R1MATERIAL=oxide R2MATERIAL=silicon. |
| R1NAME and R2NAME | Specifies that the interface models defined on this command should be applied to every interface between the two given regions (where the regions are defined by their region name). For example, R1NAME=channel R2NAME=substrate. |
| R1NUMBER and R2NUMBER | Specifies that the interface models defined on this command should be applied to every interface between the two given regions (where the regions are defined by their region number). For example, R1NUMBER=2 R2NUMBER=3. |
| R1REGION and R2REGION | Specifies that the interface models defined on this command should be applied to every interface between the two given regions (where the regions are defined by either their region name or their region number). For example, R1REGION=channel R2REGION=substrate. |
| S.I | Specifies that the INTDEFECTS statement should apply to semiconductor-insulator interfaces. |
| S.M | Specifies that the INTDEFECTS statement should apply to semiconductor-metal interfaces. |
| S.S | Specifies that the INTDEFECTS statement should apply to semiconductor-semiconductor interfaces. |
| S.X | Specifies that the INTDEFECTS statement should apply to all semiconductor-insulator interfaces, including those to the outside domain. |
| SIGGAE | Specifies the capture cross-section for electrons in a Gaussian distribution of acceptor-like states. |
| SIGGAH | Specifies the capture cross-section for holes in a Gaussian distribution of acceptor-like states. |
| SIGGDE | Specifies the capture cross-section for electrons in a Gaussian distribution of donor-like states. |
| SIGGDH | Specifies the capture cross-section for holes in a Gaussian distribution of donor-like states. |
| SIGMA.AMPHOTERIC | Specifies the defect pool width. |
| SIGN0.AMPHOTERIC | Specifies the electron capture cross-section for neutral defects. |
| SIGNP.AMPHOTERIC | Specifies the electron capture cross-section for positive defects. |
| SIGP0.AMPHOTERIC | Specifies the hole capture cross-section for neutral defects. |
| SIGPN.AMPHOTERIC | Specifies the hole capture cross-section for negative defects. |
| SIGTAE | Specifies the capture cross-section for electrons in a tail distribution of acceptor-like states. |
| SIGTAH | Specifies the capture cross-section for holes in a tail distribution of acceptor-like states. |

| | |
|----------------------|--|
| SIGTDE | Specifies the capture cross-section for electrons in a tail distribution of donor-like states. |
| SIGTDH | Specifies the capture cross-section for holes in a tail distribution of donor-like states. |
| STRUCTURE | This is a synonym for DEVICE. |
| TFILE | Specifies the file name where the acceptor and donor state density distributions, as a function of energy referenced from E_v , will be stored. You can examine this file by using TONYPLOT. |
| T0.AMPHOTERIC | Specifies the freeze-in temperature. |
| WGA | Specifies the characteristic decay energy for a Gaussian distribution of acceptor-like states. |
| WGD | Specifies the characteristic decay energy for a Gaussian distribution of donor-like states. |
| WTA | Specifies the characteristic decay energy for the tail distribution of acceptor-like states. |
| WTD | Specifies the characteristic decay energy for the tail distribution of donor-like states. |
| X.MIN | Specifies the left boundary of a box, where an interface must exist, where defects are to be applied. |
| X.MAX | Specifies the right boundary of a box, where an interface must exist, where defects are to be applied. |
| Y.MIN | Specifies the top boundary of a box, where an interface must exist, where defects are to be applied. |
| Y.MAX | Specifies the bottom boundary of a box, where an interface must exist, where defects are to be applied. |
| Z.MIN | Specifies the back boundary of a box, where an interface must exist, where defects are to be applied. |
| Z.MAX | Specifies the front boundary of a box, where an interface must exist, where defects are to be applied. |

21.21: INTERFACE

INTERFACE specifies interface parameters at semiconductor/insulator boundaries. All parameters apply only at the boundary nodes except where stated.

Syntax

INTERFACE [<params>]

| Parameter | Type | Default | Units |
|-------------|-----------|---------|---------------------|
| ABSORPTION | Real | 0.0 | |
| ADF.TABLE | Character | | |
| AR.ABSORB | Real | 0.0 | cm^{-1} |
| AR.INDEX | Real | 1 | |
| AR.THICK | Real | 0 | μm |
| BESONOS | Logical | False | |
| CHARGE | Real | 0.0 | cm^{-2} |
| COATING | Integer | 1 | |
| CONSTANT | Logical | False | |
| CR | Real | 1.0 | |
| CT | Real | 1.0 | |
| DEVICE | Character | | |
| DD.TUNNEL | Real | 0.1 | |
| DIFFUSIVE | Logical | False | |
| DISPERSION | Real | 0.0 | |
| DY.TUNNEL | Real | 0.1 | |
| DYNASONOS | Logical | True | |
| ELLIPSE | Logical | False | |
| F.QF | Character | | |
| GAUSS | Logical | False | |
| INT.RESIST | Real | 0.0 | Ωcm^2 |
| INTMATERIAL | Character | | |
| INTNAME | Character | | |
| INTNUMBER | Character | | |
| INTREGION | Character | | |
| LAM1 | Real | 0.0 | μm |

| Parameter | Type | Default | Units |
|------------|-----------|---------|------------------|
| LAM2 | Real | 0.0 | μm |
| LAMBERT | Logical | False | |
| LAYER | Integer | 1 | |
| LORENTZ | Logical | False | |
| MATERIAL | Character | | |
| N.I | Logical | False | |
| NLAM | Integer | 0 | |
| NR | Real | 2.0 | |
| NT | Real | 3.0 | |
| OPTICAL | Logical | False | |
| OUTADF | Character | | |
| OUT.HR | Character | | |
| OUT.HT | Character | | |
| QF | Real | 0.0 | cm^{-2} |
| P1.X | Real | | μm |
| P2.X | Real | | μm |
| P1.Y | Real | | μm |
| P2.Y | Real | | μm |
| R1MATERIAL | Character | | |
| R1NAME | Character | | |
| R1NUMBER | Integer | | |
| R1REGION | Character | | |
| R2MATERIAL | Character | | |
| R2NAME | Character | | |
| R2NUMBER | Integer | | |
| R2REGION | Character | | |
| REFLECT | Real | | |
| REGION | Integer | | |
| S.C | Logical | False | |
| S.I | Logical | True | |
| S.M | Logical | False | |

| Parameter | Type | Default | Units |
|------------|-----------|------------------------------|---------------|
| S.N | Real | 0.0 | cm/s |
| S.P | Real | 0.0 | cm/s |
| S.S | Logical | False | |
| S.X | Logical | False | |
| SCATTERED | Integer | 11 | |
| SIGMA | Real | 20.0 | nm |
| SEMIMINOR | Real | 0.31 | |
| SPECULAR | Real | 0.0 | |
| STRUCTURE | Character | | |
| TCR.TABLE | Character | | |
| TCT.TABLE | Character | | |
| THERMIONIC | Logical | False | |
| TRIANGLE | Logical | False | |
| TUNNEL | Logical | False | |
| X.MAX | Real | right hand side of structure | μm |
| X.MIN | Real | left hand side of structure | μm |
| Y.MAX | Real | bottom of structure | μm |
| Y.MIN | Real | top of structure | μm |
| Z.MIN | Real | | μm |
| Z.MAX | Real | | μm |

Description

The `INTERFACE` statement consists of a set of boundary condition parameters for the interface and a set of parameter to localize the effect of these parameters.

Boundary Condition Parameters

| | |
|-------------------|---|
| ABSORPTION | Specifies the fraction of the incident power lost to absorption in diffusive reflection. |
| ADF.TABLE | The name of the file containing a table describing the angular distribution function. The first entry is the number of samples. The following rows contain two numbers each. The first number is the angle in degrees, and the second number is the value of the ADF. |
| AR.ABSORB | Specifies the absorption coefficient of a anti-refractive coating layer. Default value is 0.0 cm^{-1} . |

| | |
|--------------------|---|
| AR . INDEX | Specifies the real component refractive index for the anti-reflective coating model in LUMINOUS. See Chapter 10: “Luminous: Optoelectronic Simulator”, “Anti-Reflective (AR) Coatings for Ray Tracing and Matrix Method” Section on page 10-38 for more information about the anti-reflective coating model. |
| AR . THICK | Specifies the thickness of an anti-reflective coating layer for the reflection model in LUMINOUS. This layer should generally not exist in the device mesh structure. See Chapter 10: “Luminous: Optoelectronic Simulator”, “Anti-Reflective (AR) Coatings for Ray Tracing and Matrix Method” Section on page 10-38 for more information about the anti-reflective coating model. |
| BESONOS | If DYNASONOS is enabled, this additionally enables the BESONOS model. This allows the use of a Band-Engineered tunnel insulator stack. |
| CHARGE | Specifies interface charge density (cm^{-2}) applied between two materials. The additional parameters (S.I, S.S, and S.X) allow this value to be applied at semiconductor-insulator, semiconductor-semiconductor, and semiconductor-domain edges respectively. A value of $1\text{e}10 \text{ cm}^{-2}$ represents $1\text{e}10$ electronic charges per cm^{-2} at the interface. A positive value will introduce a positive charge value and a negative value will introduce a negative charge value. |
| COATING | Specifies the number of a multilayer anti-reflective coating (ARC) referred to in the INTERFACE statement. If the COATING parameter is not set, the first coating is assumed. You must specify coatings in order (i.e., you must define COATING=2 before you define COATING=3). Different coatings should not overlap. If this occurs, the later coating is assumed in the overlapping part. For more information about ARC, see Chapter 10: “Luminous: Optoelectronic Simulator”, “Anti-Reflective (AR) Coatings for Ray Tracing and Matrix Method” Section on page 10-38. |
| CONSTANT | Specifies a constant angular distribution function as described in Equation 10-42. |
| CR | Specifies a user tuning parameter of the reflection haze function (see Equation 10-41). |
| CT | Specifies a user tuning parameter of the transmission haze function (see Equation 10-40). |
| DD . TUNNEL | Controls the numerical integration in Equation 5-53. The integral is considered converged when the argument of the outer integral is less than the value of DD . TUNNEL. |

Note: The numerical integral starts at the peak of the barrier where the argument should be equal to 1.0. Reducing this value increases simulation time but may improve accuracy.

| | |
|--------------------|--|
| DIFFUSIVE | Enables diffusive reflection and transmission at an interface. |
| DISPERSION | Specifies the spread of diffusive reflection. |
| DY . TUNNEL | Controls the step size in the numerical integration in Equation 5-53. The value of DY . TUNNEL specifies the size of the energy step, dE_x . The energy step is chosen as the product of the value for DY . TUNNEL and the energy change over the first triangle adjacent to the edge at the location in question. Reducing this value increases simulation time but may improve accuracy. |

| | |
|-----------------------------|---|
| DYNASONOS | Enables the DYNASONOS model unless explicitly cleared by using ^DYNASONOS. In this case, the SONOS model will be enabled. |
| ELLIPSE | Specifies a elliptical angular distribution function as described in Equation 10-47. |
| F.QF | Specifies the name of a file containing a C-INTERPRETER function describing the density of the interface fixed charge as a function of position. |
| GAUSS | Enables Gaussian distribution of diffusive reflection (see Equation 10-9). |
| LAYER | Describes the order of layers in a coating. If LAYER is not specified, the first (top) layer is assumed. You must specify the layers in order (i.e., you must define LAYER=2 before you define LAYER=3). Note that you only need to specify the coordinates of the interface for the first layer of each coating. |
| LAMBERT | Specifies a Lambertian angular distribution function as described in Equation 10-46. |
| LAM1 and LAM2 | Specify the beginning and ending wavelengths in microns for outputting haze functions. See OUT.HT and OUT.HR. |
| LORENZ | Enables Lorenz distribution of diffusive reflection (see Equation 10-10). |
| INT.RESIST | Specifies the value of a non-zero interface resistance between a conductor region and a semiconductor region. |

Note: When specifying INT.RESIST, you should also specify S.C on the INTERFACE statement.

| | |
|---------------------------------|---|
| MATERIAL | Specifies material name for the layer of a coating defined by the statement. Setting the material of a coating in this way enables you to apply any refractive index model supported by MATERIAL statement in ATLAS. See Chapter 10: “Luminous: Optoelectronic Simulator”, “Anti-Reflective (AR) Coatings for Ray Tracing and Matrix Method” Section on page 10-38 for more information about anti-reflective coatings. |
| N.I | Enables either the SONOS or DYNASONOS model. |
| NLAM | Specifies the number of samples to output haze functions. See OUT.HT and OUT.HR. |
| NR | Specifies a user tuning parameter of the reflection haze function (see Equation 10-41). |
| NT | Specifies a user tuning parameter of the transmission haze function (see Equation 10-40). |
| OPTICAL | Specifies the optical properties of the interface defined in the statement are modeled using Transfer Matrix Method. See Chapter 10: “Luminous: Optoelectronic Simulator”, Section 10.3: “Matrix Method” for more information. |
| OUTADF | Specifies the file name for outputting the angular distribution function. |
| OUT.HR and OUT.HT | Specify file names for outputting reflective and transmissive haze functions for display in TONYPLOT. See NLAM, LAM1, and LAM2. |

| | |
|---|---|
| RELECT | Specifies the reflection coefficient for ray tracing in LUMINOUS. The value should be between 0.0 and 1.0 inclusive. You should also specify OPTICAL and values for P1.X , P1.Y , and P2.Y . |
| QF | Specifies fixed oxide charge density (cm^{-2}) applied at a semiconductor to insulator interface. A value of $1\text{e}10 \text{ cm}^{-2}$ represents $1\text{e}10$ electronic charges per cm^{-2} at the interface. A positive value will introduce a positive charge value and a negative value will introduce a negative charge value. |
| S.C | Specifies that the application of interface models specified in this INTERFACE statement should include semiconductor-conductor interfaces. |
| S.I | Specifies that the application of interface models specified in this INTERFACE statement should include semiconductor-insulator interfaces. |
| S.M | Specifies that the application of interface models in this INTERFACE statement should include semiconductor-metal interfaces. |
| S.N | Specifies the electron surface recombination velocity. |
| S.P | Specifies the hole surface recombination velocity. |
| S.S | Specifies that the application of interface models specified in this INTERFACE statement should include semiconductor-semiconductor interfaces. |
| S.X | Specifies that the application of interface models specified in this INTERFACE statement should include any interfaces including interfaces with the outside domain. |
| SCATTERED | Specifies the number of rays scattering event for diffusive reflections. |
| SIGMA | Characterizes the mean feature size for rough interfaces as used in Equations 10-40 and 10-41. |
| SEMIMINOR | Specifies the semiminor axis of the elliptical angular distribution function described in Equation 10-47. |
| SPECULAR | Specifies the fraction of the incident power that experiences specular reflection. |
| TCR.TABLE and TCT.TABLE | Specify the names of files containing tables describing the wavelength dependent haze function parameters CR and CT . The first entry of the tables is the number of samples. The following rows contain pairs, where the first number is the wavelength in microns and the second number is the value for CR or CT . |
| THERMIONIC | Specifies that carrier transport across an interface is modeled by thermionic emission. This model will only be applied at semiconductor/semiconductor boundaries. See Chapter 5: “Blaze: Compound Material 2D Simulator”, Section 5.1.4: “The Thermionic Emission and Field Emission Transport Model” for more information on thermionic emission. |
| TRIANGLE | Specifies a triangular angular distribution function as described in Equation 10-43. |
| TUNNEL | Specifies that the carrier transport across the interface will account for thermionic field emission. When TUNNEL is specified, THERMIONIC should also be specified. See Chapter 5: “Blaze: Compound Material 2D Simulator”, Section 5.1.4: “The Thermionic Emission and Field Emission Transport Model” for more information on thermionic emission. |

Note: To use the `INTERFACE` statement to specify thermionic or tunneling interfaces, place the `INTERFACE` statement immediately after all `MESH`, `REGION`, `ELECTRODE` and `DOPING` statements and before any `CONTACT`, `MODEL`, `MATERIAL`, `MOBILITY` or `IMPACT` statements.

Position Parameters

| | |
|---|--|
| INTMATERIAL | Specifies that the interface models defined on this command should be applied to every interface between the two given materials. For example, <code>INTMATERIAL="oxide/silicon"</code> . |
| INTNAME | Specifies that the interface models defined on this command should be applied to every interface between the two given regions (where the regions are defined by their region name). For example, <code>INTNAME="channel/substrate"</code> . |
| INTNUMBER | Specifies that the interface models defined on this command should be applied to every interface between the two given regions (where the regions are defined by their region number). For example, <code>INTNUMBER="2/3"</code> . |
| INTREGION | Specifies that the interface models defined on this command should be applied to every interface between the two given regions (where the regions are defined by either their region name or their region number). For example, <code>INTREGION="channel/substrate"</code> . |
| R1MATERIAL and R2MATERIAL | Specifies that the interface models defined on this command should be applied to every interface between the two given materials. For example, <code>R1MATERIAL=oxide R2MATERIAL=silicon</code> . |
| R1NAME and R2NAME | Specifies that the interface models defined on this command should be applied to every interface between the two given regions (where the regions are defined by their region name). For example, <code>R1NAME=channel R2NAME=substrate</code> . |
| R1NUMBER and R2NUMBER | Specifies that the interface models defined on this command should be applied to every interface between the two given regions (where the regions are defined by their region number). For example, <code>R1NUMBER=2 R2NUMBER=3</code> . |
| R1REGION and R2REGION | Specifies that the interface models defined on this command should be applied to every interface between the two given regions (where the regions are defined by either their region name or their region number). For example, <code>R1REGION=channel R2REGION=substrate</code> . |
| X.MIN , X.MAX , Y.MIN , and Y.MAX | Define a bounding box. Any semiconductor/insulator interfaces found within this region are charged. If there is only one interface in a device, a non-planar surface may be defined using a box which contains the whole device. |
| X.MIN | Specifies the left X coordinate of the bounding box. |

| | |
|---|---|
| X . MAX | Specifies the right X coordinate of the bounding box. |
| Y . MIN | Specifies the bottom Y coordinate of the bounding box. |
| Y . MAX | Specifies the top Y coordinate of the bounding box. |
| Z . MIN | Specifies the front Z coordinate of the bounding box. It is used in 3D modules only. |
| Z . MAX | Specifies the back Z coordinate of the bounding box. It is used in 3D modules only. |
| P1 . X, P1 . Y, P2 . X, and P2 . Y | Define a bounding box. Within this box must lie the interface that is to be represented as the anti-reflective coating. See Chapter 10: “Luminous: Optoelectronic Simulator”, the “Anti-Reflective (AR) Coatings for Ray Tracing and Matrix Method” Section on page 10-38 for more information about the anti-reflective coating model. |

Note: For anti-reflective coatings in Luminous3D, use X . MIN, X . MAX, Y . MIN, Y . MAX, Z . MIN, and Z . MAX to define the bounding box.

| | |
|------------------|---|
| P1 . X | Specifies the left X coordinate of the bounding box. |
| P2 . X | Specifies the right X coordinate of the bounding box. |
| P1 . Y | Specifies the bottom Y coordinate of the bounding box. |
| P2 . Y | Specifies the top Y coordinate of the bounding box. |
| DEVICE | Specifies which device in a MIXEDMODE simulation applies to the statement. The synonym for this parameter is STRUCTURE. |
| REGION | Specifies which region number applies to the statement. |
| STRUCTURE | This is a synonym for DEVICE. |

MOS Example

This example defines an interface with both fixed charge and recombination velocities.

```
INTERFACE X.MIN=-4 X.MAX=4 Y.MIN=-0.5 Y.MAX=4 \
      QF=1E10 S.N=1E4 S.P=1E4
```

SOI Example

To define different fixed charge on the front and back interfaces of an SOI transistor, you need two INTERFACE statements.

In the syntax below, the first statement will apply $5 \cdot 10^{10} \text{ cm}^{-2}$ charge to any silicon/oxide interface above $Y=0.01\mu\text{m}$. The second statement applied a higher charge to any interface below $Y=0.01\mu\text{m}$. Note that charges are only applied at the material interfaces so the Y coordinate needs only to be somewhere within the silicon film.

```
INTERFACE Y.MAX=0.01 QF=5e10
INTERFACE Y.MIN=0.01 QF=2e11
```

Interface Charge for III-V Devices

By default, the `INTERFACE` statement is applied to semiconductor-insulator interfaces. Interface charge can, however, be added at the interfaces between two semiconductor regions or at the edges of semiconductor regions.

The `CHARGE` parameter defines the interface charge value in cm^{-2} . The `S.I`, `S.S`, and `S.X` parameters control whether the charge is placed between semiconductor-insulator regions, semiconductor-semiconductor regions, or at the semiconductor domain edges. You can control the location of the added charge by using the position parameters.

21.22: INTTRAP

INTTRAP activates interface defect traps at discrete energy levels within the bandgap of the semiconductor and sets their parameter values.

Syntax

```
INTTRAP <type> E.LEVEL=<r> DENSITY=<r> <capture parameters>
```

| Parameter | Type | Default | Units |
|-------------|-----------|---------|------------------|
| ACCEPTOR | Logical | False | |
| DEGEN.FAC | Real | 1 | |
| DENSITY | Real | | cm^{-2} |
| DEPTH | Real | 5.0e-3 | μm |
| DEVICE | Char | | |
| DONOR | Logical | False | |
| E.LEVEL | Real | | eV |
| F.DENSITY | Char | | |
| HEIMAN | Logical | False | |
| HPOINTS | Real | 10 | |
| INTMATERIAL | Character | | |
| INTNAME | Character | | |
| INTNUMBER | Character | | |
| INTREGION | Character | | |
| MIDGAP | Logical | False | |
| R1MATERIAL | Character | | |
| R1NAME | Character | | |
| R1NUMBER | Integer | | |
| R1REGION | Character | | |
| R2MATERIAL | Character | | |
| R2NAME | Character | | |
| R2NUMBER | Integer | | |
| R2REGION | Character | | |
| REGION | Integer | | |
| S.I | Logical | True | |
| S.M | Logical | False | |

| Parameter | Type | Default | Units |
|-----------|-----------|---------------------|---------------|
| S.S | Logical | False | |
| S.X | Logical | False | |
| SIGN | Real | | cm2 |
| SIGP | Real | | cm2 |
| STRUCTURE | Character | | |
| TAUN | Real | | s |
| TAUP | Real | | s |
| X.MIN | Real | left of structure | μm |
| X.MAX | Real | right of structure | μm |
| Y.MIN | Real | top of structure | μm |
| Y.MAX | Real | bottom of structure | μm |
| Z.MIN | Real | back of structure | μm |
| Z.MAX | Real | front of structure | μm |

Description

| | |
|--------------------|--|
| DEVICE | Specifies which device the statement applies to in MIXEDMODE simulation. The synonym for this parameter is STRUCTURE. |
| DONOR | Specifies a donor-type trap level. |
| ACCEPTOR | Specifies an acceptor-type trap level. |
| DEGEN.FAC | Specifies the degeneracy factor of the trap level used to calculate the density. |
| DENSITY | Sets the maximum density of states of the trap level. |
| DEPTH | The depth that the uniform interface trap density penetrates into the insulator. This requires the HEIMAN model. |
| E.LEVEL | Sets the energy of the discrete trap level. It is equal to the energy distance between conductance band and trap level for acceptor trap, and to energy distance between trap level and valence band for donor trap. |
| F.DENSITY | Specifies the name of a file containing a C-Interpreter function describing the density of donor/acceptor interface traps as a function of position. |
| HEIMAN | Enables the hysteresis interface traps model. |
| HPOINTS | Number of uniformly spaced points inside the insulator for which the interface trap density is calculated. This requires the HEIMAN model. |
| INTMATERIAL | Specifies that the interface models defined on this command should be applied to every interface between the two given materials. For example, INTMATERIAL="oxide/silicon". |

| | |
|---|---|
| INTNAME | Specifies that the interface models defined on this command should be applied to every interface between the two given regions (where the regions are defined by their region name). For example, INTNAME="channel/substrate". |
| INTNUMBER | Specifies that the interface models defined on this command should be applied to every interface between the two given regions (where the regions are defined by their region number). For example, INTNUMBER="2/3". |
| INTREGION | Specifies that the interface models defined on this command should be applied to every interface between the two given regions (where the regions are defined by either their region name or their region number). For example, INTREGION="channel/substrate". |
| MIDGAP | Specifies that the energy of the trap be set to the middle of the bandgap. |
| R1MATERIAL and R2MATERIAL | Specifies that the interface models defined on this command should be applied to every interface between the two given materials. For example, R1MATERIAL=oxide R2MATERIAL=silicon. |
| R1NAME and R2NAME | Specifies that the interface models defined on this command should be applied to every interface between the two given regions (where the regions are defined by their region name). For example, R1NAME=channel R2NAME=substrate. |
| R1NUMBER and R2NUMBER | Specifies that the interface models defined on this command should be applied to every interface between the two given regions (where the regions are defined by their region number). For example, R1NUMBER=2 R2NUMBER=3. |
| R1REGION and R2REGION | Specifies that the interface models defined on this command should be applied to every interface between the two given regions (where the regions are defined by either their region name or their region number). For example, R1REGION=channel R2REGION=substrate. |
| S.I | Specifies that the INTTRAP statement should apply to semiconductor-insulator interfaces. |
| S.M | Specifies that the INTTRAP statement should apply to semiconductor-metal interfaces. |
| S.S | Specifies that the INTTRAP statement should apply to semiconductor-semiconductor interfaces. |
| S.X | Specifies that the INTTRAP statement should apply to all semiconductor-insulator interfaces, including those to the outside domain. |
| STRUCTURE | This is a synonym for DEVICE. |
| X.MIN | Specifies the left boundary of a box, where an interface must exist and where traps are to be applied. |
| X.MAX | Specifies the right boundary of a box, where an interface must exist and where traps are to be applied. |
| Y.MIN | Specifies the top boundary of a box, where an interface must exist and where traps are to be applied. |

| | |
|--------------|--|
| Y.MAX | Specifies the bottom boundary of a box, where an interface must exist and where traps are to be applied. |
| Z.MIN | Specifies the back boundary of a box, where an interface must exist and where traps are to be applied. |
| Z.MAX | Specifies the front boundary of a box, where an interface must exist and where traps are to be applied. |

Capture Parameters

Either the cross section or lifetime parameters should be used to define the capture parameters.

| | |
|-------------|--|
| SIGN | Specifies the capture cross section of the trap for electrons. |
| SIGP | Specifies the capture cross section of the trap for holes. |
| TAUN | Specifies the lifetime of electrons in the trap level. |
| TAUP | Specifies the lifetime of holes in the trap level. |

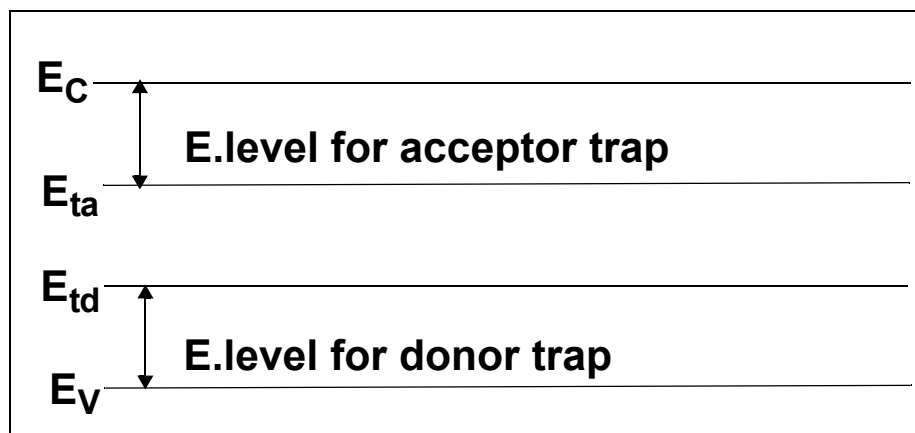


Figure 21-6: Acceptor and Donor Interface Trap Energy Levels

Multiple Interface Trap States Example

The following example sets three discrete interface trap levels within the silicon bandgap. These trap levels will capture carriers, which slows down the switching speed of any device. In this example, the capture cross sections are used to define the properties of each trap.

```
inttrap e.level=0.49 acceptor density=2.e10 degen=12 \
sign=2.84e-15 sigp=2.84e-14
inttrap e.level=0.41 acceptor density=1.e10 degen=12 \
sign=7.24e-16 sigp=7.24e-15
inttrap e.level=0.32 donor density=1.e10 degen=1 \
sign=1.00e-16 sigp=1.00e-17
```

Note: For semiconductor bulk trap levels, see Section 21.61: “TRAP”.

21.23: LASER

LASER defines physical models and model parameters for laser and Vertical Cavity Surface-Emitting Lasers (VCSEL) simulation. For more information about VCSEL, see Chapter 9: "VCSEL Simulator".

Syntax

LASER<parameters>

| Parameter | Type | Default | Units |
|---------------|-----------|---------|-------|
| ABSORPTION | Logical | False | |
| ATRAP | Real | 0.5 | |
| CAVITY.LENGTH | Real | 100.0 | cm |
| COUPLED | Logical | False | |
| DBR1.START | Real | 0.0 | μm |
| DBR1.FINAL | Real | 0.0 | μm |
| DBR2.START | Real | 0.0 | μm |
| DBR2.FINAL | Real | 0.0 | μm |
| DEVICE | Character | | |
| EFINAL | Real | 0.0 | eV |
| EINIT | Real | 0.0 | eV |
| ESEP | Real | 0.0 | eV |
| ETRANS | Logical | False | |
| F.MIRROR | Character | | |
| FAR.NX | Integer | 100 | |
| FAR.NY | Integer | 100 | |
| FCARRIER | Logical | False | |
| GAINMOD | Integer | -999 | |
| INDEX.BOTTOM | Real | 1.0 | |
| INDEX.MODEL | Integer | 0 | |
| INDEX.TOP | Real | 1.0 | |
| ITMAX | Integer | 30 | |
| LMODES | Logical | False | |
| LOSSES | Real | 0 | |
| LX.MAX | Real | 999 | μm |
| LX.MIN | Real | -999 | μm |

| | | | |
|---------------|-----------|-----------------------|-----------------|
| LY.MAX | Real | 999 | μm |
| LY.MIN | Real | -999 | μm |
| MATERIAL | Character | | |
| MAXCH | Real | 2.5 | |
| MAXTRAPS | Integer | 2 | |
| MIRROR | Real | 90.0 | % |
| MULTISAVE | Logical | True | |
| NAME | Character | | |
| NB.ITEREIG | Integer | 4 | |
| NEAR.NX | Integer | 100 | |
| NEAR.NY | Integer | 100 | |
| NEFF | Real | 3.57 | |
| NMOD.NEWTON | Integer | 50 | |
| NMODE | Integer | 1 | |
| NX | Integer | | |
| NSPEC | Integer | 100 | |
| NY | Integer | | |
| OMEGA | Real | 2.16×10^{15} | Hz |
| OMEGA.FINAL | Real | -999 | 1/s |
| OMEGA.INIT | Real | -999 | 1/s |
| PHOTON.ENERGY | Real | 0 | eV |
| PMINCONC | Real | 1.0×10^{-20} | 1/cm |
| PROJ | Logical | False | |
| PRT.ITEREIG | Logical | False | |
| REFLECT | Logical | False | |
| RF | Real | 0.0 | % |
| RF.FILE | Character | | |
| REGION | Integer | | |
| RR | Real | 0.0 | % |
| RR.FILE | Character | | |
| SIN | Real | 100000 | cm ² |
| SPEC.NAME | Character | | |
| SPECSAVE | Integer | 1 | |

| | | | |
|--------------------|-----------|--------|---------------|
| SPONTANEOUS | Integer | 1 | |
| START | Logical | False | |
| STRUCTURE | Character | | |
| TAUSS | Real | 0.05 | |
| TIMERATE | Logical | True | |
| TOLER | Real | 0.01 | |
| TRANS_ENERGY | Real | | eV |
| TRAP | Logical | False | |
| V.HELM | Logical | False | |
| VCSEL.CHECK | Integer | 1 | |
| VCSEL.INCIDENTENCE | Integer | False | |
| XMIN | Real | min. X | μm |
| XMAX | Real | max. X | μm |
| YMIN | Real | min. Y | μm |
| YMAX | Real | max. Y | μm |

Description

Localization Parameters

| | |
|------------------|---|
| DEVICE | Specifies which device the LASER statement should apply to in MIXEDMODE simulation. The synonym for this parameter is STRUCTURE. |
| LX.MAX | Sets the upper x boundary of solution domain for vector Helmholtz solver. |
| LX.MIN | Sets the lower x boundary of solution domain for vector Helmholtz solver. |
| LY.MAX | Sets the upper y boundary of solution domain for vector Helmholtz solver. |
| LY.MIN | Sets the lower y boundary of solution domain for vector Helmholtz solver. |
| MATERIAL | Specifies which material from the table in Appendix B: "Material Systems" that the LASER statement should apply. If a material is specified, then all regions defined as being composed of that material will be affected. |
| NAME | Specifies which region the LASER statement should apply. Note that the name must match the name specified in the NAME parameter of the REGION statement or the region number. |
| REGION | Specifies the region number to which these parameters apply. If there is more than one semiconductor region, specification of different parameters for each region is allowed. If LASER is not specified, all regions in the structure are changed. |
| STRUCTURE | This is a synonym for DEVICE. |

Laser Model Parameters

| | |
|---|--|
| ABSORPTION | Enables the absorption loss model in LASER. |
| ATRAP | Specifies the photon rate equation cutback ratio (see Chapter 8: “Laser: Edge Emitting Simulator”, Section 8.5.2: “Numerical Parameters”). |
| DBR1.START, DBR1.FINAL, DBR2.START, and DBR2.FINAL | These parameters specify the locations of the front and rear DBR mirrors for a VCSEL device (See Figure 21-7). The reflectivity of front and rear DBR mirrors will be calculated from the optical intensity profile. |
| CAVITY.LENGTH | Specifies the cavity length in the longitudinal direction (in μm). |
| COUPLED | Specifies that the solution process for the photon rate equation is fully coupled to the Jacobian of the drift-diffusion equations. |
| EINIT, EFINAL | Specify the lower and upper photon energies. LASER will calculate multiple longitudinal photon rates within this range. Using wide ranges can slow down simulation. |
| ESEP | Specifies the photon energy separation. If this isn’t specified, LASER will automatically calculate the number of longitudinal modes based on the cavity length and the energy range. |
| ETRANS | Enables the selection of a specific transverse mode. The selected transverse mode will be the mode with the closest energy to TRANS_ENERGY. |
| F.MIRROR | Specifies the name of a file containing a C-Interpreter function that defines the front and rear mirror reflectivities as a function of wavelength. |
| FAR.NX, FAR.NY | Describe the number of samples to output for the far-field pattern in the X and Y directions. For more information about the far-field pattern, see Chapter 8: “Laser: Edge Emitting Simulator”, Section 8.6.1: “Generation of Near-Field and Far-Field Patterns”. |
| FCARRIER | Enables the free carrier loss model in LASER. |
| GAINMOD | Sets the number of the gain model. |
| INDEX.BOTTOM | Specifies the refractive index of the medium below the structure. The default value is 1.0. |
| INDEX.MODEL | Specifies whether the simple refractive index model (INDEX.MODEL=0) or the more complex gain dependent refractive index (INDEX.MODEL=1) is used. |
| INDEX.TOP | Specifies the refractive index of the medium above the structure. The default value is 1.0. |

Note: When using `INDEX.MODEL=1`, a complex value Eigenvalue solver is used. This requires a refined X direction LASER mesh and a refined Y direction LASER mesh to ensure the accuracy of the solution. When the bulk refractive index model is used, only a refined Y direction LASER mesh is required for the Eigenvalue solver.

| | |
|-------------------------|--|
| ITMAX | Specifies the maximum number of iterations allowed for LASER simulation at each bias point. |
| LMODES | Specifies that multiple longitudinal models are to be accounted for during laser simulation. |
| LOSSES | Specifies the total losses in Chapter 8: “Laser: Edge Emitting Simulator”, Equation 8-13. |
| MAXCH | Specifies the maximum allowed relative change in photon densities between iterations. Rapid changes of the photon densities can cause convergence problems. |
| MAXTRAPS | Specifies the maximum number of cutbacks for the photon rate equation (see Chapter 8: “Laser: Edge Emitting Simulator”, Section 8.5.2: “Numerical Parameters”). |
| MIRROR | Specifies the percentage facet reflectivity for the mirror loss in LASER. 100% reflectivity is equivalent to no mirror loss. Both facets are assumed to have this value of reflectivity. |
| MULTISAVE | Specifies the whether to save the transient laser spectrum as one file or multiple files. |
| NB.ITEREIG | Sets the ratio of basis size for iterative Helmholtz eigensolver to the number of requested transverse modes, which is given by <code>NMODE</code> parameter. |
| NEAR.NX, NEAR.NY | Describe the number of samples to output for the near-field pattern in the X and Y directions. For more information about the near-field pattern, see Chapter 8: “Laser: Edge Emitting Simulator”, Section 8.6.1: “Generation of Near-Field and Far-Field Patterns”. |
| NEFF | Specifies the effective refractive index in Chapter 8: “Laser: Edge Emitting Simulator”, Equation 8-12. |
| NMOD.NEWTON | Sets the number of lasing modes, which enter Jacobian for Newton iterations. It can be smaller than the actual number of modes. It is decreased automatically, if it is larger than the actual number of modes. |
| NMODE | Specifies the number of transverse modes simulated. |
| NSPEC | Specifies the number of sampling points between <code>EINIT</code> and <code>EFINAL</code> in the reflectivity test. The default value is <code>NSPEC=100</code> . |
| NX | Defines the number of mesh divisions for the laser mesh in the X direction. |
| NY | Defines the number of mesh divisions for the laser mesh in the Y direction. |
| PHOTON.ENERGY | Specifies the energy of photons to be used in Chapter 8: “Laser: Edge Emitting Simulator”, Equation 8-1. If Chapter 8: “Laser: Edge Emitting Simulator”, Equation 8-2 is used for simulation, this parameter will only specify an initial estimate of the photon energy. If that's the case, use the <code>LAS.OMEGA</code> parameter instead to specify the lasing frequency. |

| | |
|-----------------------------------|---|
| PMINCONC | Sets the minimum photon concentration. |
| PROJ | Extrapolates that photon rates for the initial guess during bias ramp. |
| PRT.ITEREIG | Specifies that iterative Helmholtz eigensolver prints information about its internal parametrs and convergence. |
| OMEGA | Specifies the lasing frequency to be used in Chapter 8: “Laser: Edge Emitting Simulator”, Equation 8-1. If model 2 is used for simulation, then this parameter will estimate the lasing frequency. If that’s the case, use the PHOTON.ENERGY parameter to specify photon energy instead. |
| OMEGA.FINAL | Sets the upper boundary for frequencies of multiple longitudinal mode. |
| OMEGA.INIT | Sets the lower boundary for frequencies of multiple longitudinal mode. |
| REFLECT | Specifies that only half of the Laser structure is to be simulated. The axis of symmetry in this case is at x=0. Specify the laser mesh so that the minimum X coordinate is zero. |
| RF and RR | Specify the front and rear facet mirror reflectivities of Fabry-Perot type lasers. If these parameters aren’t specified, then they will be calculated from the average mirror loss parameter (MIRROR.LOSS parameter in the LASER or MODELS statements). If MIRROR.LOSS is used, then RF and RR shouldn’t be specified. |
| RF.FILE and RR.FILE | Specify the front and rear facet mirror reflectivity files. If RF.FILE is specified, the rear reflectivity will be read from the specified file. A linear interpolation algorithm will calculate value of the reflectivity from the tabulated values with the bounds given by the first and last wavelength value. The wavelength values in the file must be ascending order. The file format is as follows: <div style="text-align: center;"> number of samples wavelength (in microns) reflectivity (in %) </div> |

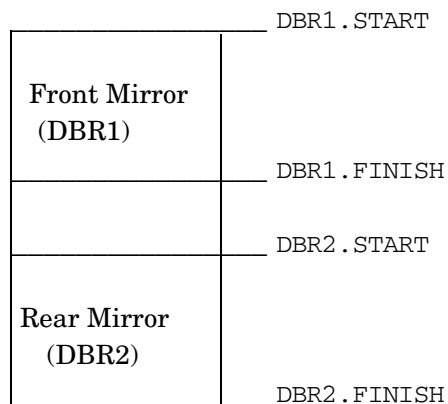


Figure 21-7: DBR Location Parameters

The cavity length used in the mirror loss calculation is given by `DBR2.START - DBR1.FINISH`. If both DBR mirrors are not defined, then the mirror loss will set to 0.

| | |
|-----------------------|--|
| SIN | Specifies an initial photon density in the fundamental lasing mode. This value provides an initial guess for subsequent iterations. This parameter is used only when the single frequency model has been selected. |
| SPEC.NAME | Specifies the name of a spectrum file, which LASER will produce for each bias point, if the <code>LMODES</code> parameter has been specified. |
| SPECSAVE | The spectrum file will be saved after every <code>LAS.SPECSAVE</code> laser solution step. |
| SPONTANEOUS | Enables the Spontaneous Recombination Model (see Chapter 3: “Physics”, Sections 3.9.1: “The General Radiative Recombination Model” and 3.9.2: “The Default Radiative Recombination Model”). |
| START | Specifies that laser simulation starts now. |
| TAUSS | Specifies the relaxation parameter to be used for the photon rate equation. See Chapter 8: “Laser: Edge Emitting Simulator”, Section 8.5.2: “Numerical Parameters” for more information. |
| TIMERATE | Specifies that the time dependent photon rate equation will be used in a transient laser simulation. |
| TOLER | Specifies the desired accuracy in photon areas. |
| TRANS_ENERGY | Specifies the energy for selective a single transverse mode (see also <code>ETRANS</code>). |
| TRAP | Specifies the photon rate equation cutback scheme (see Chapter 8: “Laser: Edge Emitting Simulator”, Section 8.5.2: “Numerical Parameters”). |
| V.HELM | Specifies that vector Helmholtz solver will be used for solution for transverse optical modes. |
| VCSEL.CHECK | Enables reflectivity test simulation of the VCSEL structure. |
| VCSEL.INCIDENT | Specifies the direction of light incident on the structure. <code>VCSEL.INCIDENT=1</code> is the light incident from the top. <code>VCSEL.INCIDENT=0</code> is the light incident from the bottom. <code>VCSEL.INCIDENT=2</code> or <code>>2</code> means both directions of light incidence are considered. By default, light is incident from the top of the structure. |
| XMIN | Defines the minimum X coordinate for the laser mesh. See also <code>LX.MESH</code> . |
| XMAX | Defines the maximum X coordinate for the laser mesh. See also <code>LX.MESH</code> . |
| YMIN | Defines the minimum Y coordinate for the laser mesh. See also <code>LY.MESH</code> . |
| YMAX | Defines the maximum Y coordinate for the laser mesh. See also <code>LY.MESH</code> . |

21.24: LED

LED saves LED output characteristics after each subsequent solution step.

Syntax

LED <parameters>

| Parameter | Type | Default | Units |
|--------------|-----------|--------------------|---------|
| AMBIEN.IMAG | Real | 0.0 | |
| AMBIEN.REAL | Real | 1.0 | |
| ANGLE.OUTPUT | Real | 30.0 | degrees |
| ANGPOWER | Character | | |
| DIPOLE | Logical | False | |
| EDGE_ONLY | Logical | False | |
| EDGE_REFLECT | Logical | False | |
| EMIN | Real | | eV |
| EMAX | Real | | eV |
| ESAMPLE | Logical | False | |
| HORIZONTAL | Real | 2/3 | |
| INCOHERENT | Logical | False | |
| INCOH.TOP | Logical | False | |
| L.WAVE | Real | 0.8 | μm |
| LMAX | Real | | μm |
| LMIN | Real | | μm |
| MIN.POWER | Real | 1×10^{-4} | |
| MIR.BOTTOM | Logical | False | |
| MIR.TOP | Logical | False | |
| NSAMP | Integer | 100 | |
| NUMRAYS | Integer | 180 | |
| ONEFILE | Logical | False | |
| POLAR | Real | 45.0 | |
| REFLECTS | Integer | 0 | |
| OUT.USPEC | Character | | |
| SIDE | Logical | False | |
| SMOOTHNESS | Real | 8.0 | |

| Parameter | Type | Default | Units |
|--------------|-----------|---------|---------------|
| SOURCE.TERM | Logical | False | |
| SOURCE_TERM | Logical | False | |
| SPECT.ANGLE | Character | | |
| SPECTRUM | Character | | |
| SURFACE_ONLY | Logical | False | |
| TEMPER | Real | 300.0 | |
| TR.MATRIX | Logical | False | |
| USER.SPECT | Character | | |
| X | Real | 0.0 | μm |
| XMAX | Real | 0.0 | μm |
| XMIN | Real | 0.0 | μm |
| XNUM | Integer | 0 | |
| Y | Real | 0.0 | μm |
| YMAX | Real | 0.0 | μm |
| Y.MAX | Real | 0.0 | μm |
| YMIN | Real | 0.0 | μm |
| Y.MIN | Real | 0.0 | μm |
| YNUM | Integer | 0 | |
| ZMAX | Real | 0.0 | μm |
| Z.MAX | Real | 0.0 | μm |
| ZMIN | Real | 0.0 | μm |
| Z.MIN | Real | 0.0 | μm |

Description

| | |
|---------------------|---|
| AMBIEN.IMAG | Specifies the imaginary index of refraction for the ambient outside the device domain for LED reverse ray tracing. |
| AMBIEN.REAL | Specifies the real index of refraction for the ambient outside the device domain for LED reverse ray tracing. |
| ANGLE.OUTPUT | Specifies the angular interval in degrees where spectrum versus angle are written to the file specified by the SPECT.ANGLE parameter. |

| | |
|---------------------|---|
| ANGPOWER | Enables the reverse ray-tracing algorithm (see Chapter 11: “LED: Light Emitting Diode Simulator”, Section 11.5: “Reverse Ray-Tracing”) for analysis of output coupling of light from the structure of a Light Emitting Diode. ANGPOWER specifies the name of the output file for the angular power density vs. output angle dependence. |
| DIPOLE | Specifies a particular angular distribution of the internal radiating field that corresponds to a preferred in-plane orientation of dipoles often relevant to OLED devices (see Chapter 11: “LED: Light Emitting Diode Simulator”, Section 11.5: “Reverse Ray-Tracing”). |
| EDGE_ONLY | Specifies that for LED reverse ray tracing only the rays exiting from the edges are considered. Rays exiting at the top and bottom surfaces are not shown. |
| EDGE_REFLECT | Specifies the rays in reverse ray tracing reaching the edges of the device are totally reflected. |
| EMAX, EMIN | Specify the energy range for saving a spectrum file. |
| ESAMPLE | Specifies that samples are taken evenly in energy unlike even sampling in wavelength. |
| HORIZONTAL | Specifies the proportion of horizontally oriented dipoles for the dipole emission model. |
| INCOHERENT | Specifies that an incoherent material in LED/OLED structure is used for the purpose of combined transfer matrix method/reverse ray tracing (TMM+RRT) optical analysis. |
| INCOH.TOP | When specified with the SOURCE.TERM parameter, it allows a combination of transfer matrix method in thin coherent layers and ray tracing in thick incoherent layers for LED reverse ray tracing. |
| LMAX, LMIN | Specify the range of wavelength for saving spectrum files. |
| L.WAVE | Specifies the wavelength for reverse ray-tracing (see Chapter 11: “LED: Light Emitting Diode Simulator”, Section 11.5: “Reverse Ray-Tracing”). |
| MIN.POWER | Specifies the minimum relative power of a ray (see Chapter 11: “LED: Light Emitting Diode Simulator”, Section 11.5: “Reverse Ray-Tracing”). The ray is not traced after its power falls below MIN.POWER value. This is useful to limit the number of rays traced. The default value is MIN.POWER=1e-4. |
| MIR.TOP | Specifies that the top surface of the device be treated as an ideal mirror in reverse ray-tracing (see Chapter 11: “LED: Light Emitting Diode Simulator”, Section 11.5: “Reverse Ray-Tracing”). |
| MIR.BOTTOM | Specifies that the bottom surface of the device be treated as an ideal mirror in reverse ray-tracing (see Chapter 11: “LED: Light Emitting Diode Simulator”, Section 11.5: “Reverse Ray-Tracing”). |
| NSAMP | Specifies the number of samples to use for a spectrum plot. |
| NUMRAYS | Specifies the number of rays starting from the origin in reverse ray-tracing (see Chapter 11: “LED: Light Emitting Diode Simulator”, Section 11.5: “Reverse Ray-Tracing”). The default is 180. Acceptable range is 36-3600. |
| ONEFILE | Specifies that successive files (output at each solution) will overwrite previous specified by SPECTRUM, ANGPOWER or SPECT.ANGLE or all three. By default, unique output files are written by incrementing the specified name. |

| | |
|---------------------|--|
| POLAR | Specifies polarization of the emitted photons in degrees while linearly polarized light is assumed (see Chapter 11: “LED: Light Emitting Diode Simulator”, Section 11.5: “Reverse Ray-Tracing”). Parallel (TM-mode, <code>POLAR=0.0</code>) and perpendicular (TE-mode, <code>POLAR=90.0</code>) polarizations result in significantly different output coupling values. Use the default value (<code>POLAR=45.0</code>) if there is no preferred direction of polarization of emitted photons (unpolarized light emission). |
| REFLECTS | Specifies a number of reflections to be traced for each ray in reverse ray-tracing (see Chapter 11: “LED: Light Emitting Diode Simulator”, Section 11.5: “Reverse Ray-Tracing”). The default value is <code>REFLECTS=0</code> . The maximum allowed value is <code>REFLECTS=10</code> . Setting the number of reflections to 3 or 4 is often a good choice. |
| SIDE | Specifies that the rays reaching the sides of the device are terminated there and do not contribute to the total light output (see Chapter 11: “LED: Light Emitting Diode Simulator”, Section 11.5: “Reverse Ray-Tracing”). |
| SOURCE_TERM | Indicates that dipole source terms are combined with transfer matrix calculation of light output for LEDs. The alias is <code>SOURCE_TERM</code> . |
| SPECT_ANGLE | Specifies the output file name where LED spectrum is written as a function of emission angle. |
| SPECTRUM | Specifies the name of a file for saving spectrum plots. |
| SURFACE_ONLY | Specifies that for LED reverse ray tracing only the rays exiting from the top and bottom surfaces are considered. Rays exiting at the edges are not shown. |
| TEMPER | This is the temperature (needed for using appropriate refractive indexes of the materials in reverse ray-tracing). The default setting of 300 K will be used if <code>TEMPER</code> is unspecified. |
| TR_MATRIX | Specifies that the transfer matrix method should be used to handle thin film LEDs. |
| OUT_USPEC | Specifies the TONYPLOT compatible file name associated with the <code>USER.SPECT</code> parameter. |
| X | This is the X coordinate of light origin for a single point reverse ray-tracing (see Chapter 11: “LED: Light Emitting Diode Simulator”, Section 11.5: “Reverse Ray-Tracing”). |
| XMAX | This is the maximum X coordinate of a rectangular area containing multiple origin points in reverse ray-tracing (see Chapter 11: “LED: Light Emitting Diode Simulator”, Section 11.5: “Reverse Ray-Tracing”). |
| XMIN | This is the minimum X coordinate of a rectangular area containing multiple origin points in reverse ray-tracing (see Chapter 11: “LED: Light Emitting Diode Simulator”, Section 11.5: “Reverse Ray-Tracing”). |
| XNUM | Specifies the number of points along X axis within a rectangular area in multiple origin reverse ray-tracing (see Chapter 11: “LED: Light Emitting Diode Simulator”, Section 11.5: “Reverse Ray-Tracing”). |
| Y | This is the Y coordinate of light origin for a single point reverse ray-tracing (see Chapter 11: “LED: Light Emitting Diode Simulator”, Section 11.5: “Reverse Ray-Tracing”). |

| | |
|-------------|---|
| YMAX | This is the maximum Y coordinate of a rectangular area containing multiple origin points in reverse ray-tracing (see Chapter 11: “LED: Light Emitting Diode Simulator”, Section 11.5: “Reverse Ray-Tracing”). |
| YMIN | This is the minimum Y coordinate of a rectangular area containing multiple origin points in reverse ray-tracing (see Chapter 11: “LED: Light Emitting Diode Simulator”, Section 11.5: “Reverse Ray-Tracing”). |
| YNUM | Specifies the number of points along Y axis within a rectangular area in multiple origin reverse ray-tracing (see Chapter 11: “LED: Light Emitting Diode Simulator”, Section 11.5: “Reverse Ray-Tracing”). |

21.25: LENS

The LENS statement is used to specify lenslet characteristics used for light propagation analysis in LUMINOUS.

Syntax

LENS <parameters>

| Parameter | Type | Default | Units |
|--------------|-----------|---------|-------|
| APEX | Real | | μm |
| AR.INDEX | Real | 1.0 | |
| AR.THICKNESS | Real | 0.0 | |
| ASPHERIC | Logical | False | |
| COMPOSITE | Logical | False | |
| ELLIPSE | Logical | False | |
| EXTINCT | Real | 0.0 | |
| F.LENS | Character | | |
| HEIGHT | Real | | μm |
| INDEX | Real | 1.0 | |
| K | Real | 0.0 | |
| MATERIAL | Character | | |
| MEAN | Real | 0.1 | μm |
| N | Real | 1.0 | |
| NEGATIVE | Logical | False | |
| NSAMP | Integer | | |
| PLANE | Real | | |
| PYRAMID | Logical | False | |
| RADIUS | Real | | μm |
| RANDOM | Logical | False | |
| SAG.OUT | Character | | |
| SAG.ITS | Integer | | |
| SEED | Integer | -10 | |
| SIGMA | Real | 0.1 | μm |
| SPHERIC | Logical | False | |
| TWODEE | Logical | False | |

| Parameter | Type | Default | Units |
|-----------|-----------|---------|-------|
| USER | Logical | False | |
| WIDTH | Real | | μm |
| X.LOC | Real | | μm |
| X.MAX | Real | | μm |
| X.MEAN | Real | 0.1 | μm |
| X.MIN | Real | | μm |
| X.SAGS | Character | | |
| X.SEMI | Real | | μm |
| X.SIGMA | Real | 0.1 | μm |
| X.SOUT | Character | | |
| Y.LOC | Real | | μm |
| Y.SEMI | Real | | μm |
| Y.SIGMA | Real | 0.1 | μm |
| Z.LOC | Character | | |
| Z.MAX | Real | | μm |
| Z.MEAN | Real | 0.1 | μm |
| Z.MIN | Real | | μm |
| Z.SAGS | Character | | |
| Z.SEMI | Real | | μm |
| Z.SIGMA | Real | 0.1 | μm |
| Z.SOUT | Character | | |

Description

| | |
|---------------------|---|
| APEX | Specifies the height of a pyramid lenslet. |
| AR.INDEX | Specifies the anti-reflective coating layer index of refraction for ray tracing. |
| AR.THICKNESS | Specifies the anti-reflective coating layer thickness in microns for ray tracing. |
| ASPHERIC | Specifies that the lenslet specification describes an aspheric lens. |
| COMPOSITE | Specifies that the lenslet specification describes a composite lens. |
| ELLIPSE | Specifies that the lenslet specification describes an elliptical lens. |
| EXTINCT | Specifies the extinction coefficient of the lenslet. |
| F.LENS | Specifies the file name of a C-Interpreter function for user-definable lenslets. |

| | |
|--|---|
| HEIGHT | Specifies the height of a composite lens. |
| INDEX | Specifies the real part of the index of refraction of the lenslet. |
| K | This is an alias for EXTINCT . |
| MATERIAL | Specifies the material name used to determine the complex index of refraction versus wavelength for the lens. |
| MEAN | Specifies the mean value of the random step size in the X and Z directions in microns for RANDOM lenslets. |
| N | This is an alias for INDEX . |
| NEGATIVE | Specifies that for spherical and elliptical lenses the concave surface is to be used rather than the convex side. |
| NSAMP | Specifies the number of samples for outputting aspheric lens data. |
| PLANE | Specifies the Y location of the planar background of the lenslet. |
| PYRAMID | Specifies that the lenslet specification describes a Pyramid lens. |
| RADIUS | Specifies the radius of a spherical lenslet. |
| RANDOM | Specifies that the lenslet is a random textured surface lenslet. |
| SAG.OUT | Specifies the file name for aspheric lens output. |
| SAG.ITS | Specifies the number of iterations to be used for the Levenberg-Marquardt non-linear least squares algorithm for aspheric lenslet specification. |
| SEED | Specifies the random number generator seed value for random textured surface lenslets. |
| SIGMA | Specifies the standard deviation of the Gaussian distributed random step size in the X, Y, and Z directions for RANDOM lenslets in microns. |
| SPHERIC | Specifies that the lenslet specification describes a spheric lens. |
| TWODEE | Specifies that there is no variation in the lens in the z direction (i.e., the z coordinate is set to 0 in the analytic formula describing the lens surface). |
| USER | Specifies that the lenslet will use the C-Interpreter function specified by the F.LENS parameter for a user-definable lenslet. |
| WIDTH | Specifies the periphery width of a composite lenslet. |
| X.LOC Y.LOC Z.LOC | Specify the center coordinates of a spheric or pyramid lenslet. |
| X.MEAN | Specifies the mean value of the random step size in the X direction in microns for RANDOM lenslets. |
| X.MIN X.MAX Z.MIN Z.MAX | Specify the perimeter of a composite or pyramid lenslet. |
| X.SAGS Z.SAGS | Specify the file names of the input sag data for an aspheric lenslet. |

| | |
|---|--|
| X.SEMI Y.SEMI Z.SEMI | Specify the semimajor axes of a elliptical lenslet. |
| X.SIGMA | Specifies the standard deviation of the Gaussian distributed random step size in the X direction for RANDOM lenslets in microns. |
| X.SOUT Z.SOUT | Specify the output file names for the X and Z aspheric lenslet. |
| Y.SIGMA | Specifies the standard deviation of the Gaussian distributed random step size in the Y direction for RANDOM lenslets in microns. |
| Z.MEAN | Specifies the mean value of the random step size in the Z direction in microns for RANDOM lenslets. |
| Z.SIGMA | Specifies the standard deviation of the Gaussian distributed random step size in the Z direction for RANDOM lenslets in microns. |

21.26: LOAD

LOAD loads previous solutions from files as initial guesses to other bias points.

Syntax

```
LOAD [ASCII|MASTER] [NO.CHECK] <files>
```

| Parameter | Type | Default | Units |
|--------------|-----------|---------|-------|
| ASCII | Logical | False | |
| IN.FILE | Character | | |
| INFILE | Character | | |
| IN1FILE | Character | | |
| IN2FILE | Character | | |
| LAS.SPECTRUM | Logical | False | |
| MASTER | Logical | False | |
| NO.CHECK | Logical | False | |
| TWOD | Logical | False | |

Description

| | |
|---------------------|---|
| ASCII | Specifies that any original PISCES format files read or written by this statement will be in an ASCII rather than in a binary format. |
| LAS.SPECTRUM | Loads the spectrum file (specified by the IN.FILE parameter) into LASER. |

Note: The number of longitudinal and transverse modes in the spectrum file must be the same as created by the LASER statement.

| | |
|-----------------|---|
| MASTER | Specifies that any files read by this statement will be in a standard structure file rather than the original PISCES format. Specify this parameter if you are using TONYPLOT to plot simulation results. |
| NO.CHECK | Prevents checking material parameter differences between loaded binary files and the values set in the current input file. |
| TWOD | Allows loading of a 2D solution into a 3D structure. Note that the values from the 2D solution are loaded uniformly in the Z direction. |

File Parameters

The LOAD statement requires that one of the following file parameter syntax be used.

```
LOAD INFILE=<filename>
```

or

```
LOAD IN1FILE=<filename> IN2FILE=<filename>
```

| | |
|----------------|--|
| IN.FILE | This is a synonym for <code>INFILE</code> . |
| INFILE | Specifies a single input filename for solution data. Use this parameter when you want to load only one solution, which is the most common case. The synonym for this parameter is <code>IN.FILE</code> . |
| IN1FILE | Specifies a filename for present solution data. Use this parameter if two input files are needed to perform an extrapolation for an initial approximation (i.e., the <code>PROJECT</code> parameter of the <code>SOLVE</code> statement). |
| IN2FILE | Specifies an input filename for previous solution data. Use this parameter if two input files are needed to perform an extrapolation for an initial approximation (i.e., the <code>PROJECT</code> parameter of the <code>SOLVE</code> statement). The solution specified by this parameter is the first to be overwritten when new solutions are obtained. |

Simple Save and Load Examples

This example saves and loads the master format solution file, `SOL.STR`.

```
SAVE OUTF=SOL.STR.
```

```
....
```

```
LOAD INFILE=SOL.STR MASTER
```

As before but using the `SOLVE` syntax.

```
SOLVE OUTF=SOL.STR MASTER
```

```
..
```

```
LOAD INF=SOL.STR MASTER
```

When the save and load operations are not done within the same `ATLAS` run see the note below.

Binary Format Example

Saving and loading using the binary format. This is quicker but these files cannot be plotted in `TONYPLOT`.

```
SOLVE OUTF=SOLVE_TMP
```

```
..
```

```
LOAD INF=SOLVE_TMP
```

Note: The function to calculate the difference between two files is now inside `TONYPLOT`. It has been discontinued from the `LOAD` statement

Note: The `LOAD` statement loads only the saved solution quantities into `ATLAS`. The mesh, electrodes, doping, regions, contact settings, material parameters, models, and numerical methods must all be specified in advance of any `LOAD` statement. See the Chapter 2: “Getting Started with `ATLAS`”, “Re-initializing `ATLAS` at a Given Bias Point” Section on page 2-63.

21.27: LOG

LOG allows all terminal characteristics of a run to be saved to a file. Any DC, transient, or AC data generated by SOLVE statements after the LOG statement is saved. Any parameters specified by the PROBE statement are also stored in the logfile. If a log file is already open, the open log file is closed and a new log file is opened.

Syntax

```
LOG [OUTFILE=<filename>] [MASTER] [acparams]
```

| Parameter | Type | Default | Units |
|------------|-----------|---------|----------|
| ABCD.PARAM | Logical | False | |
| APPEND | Logical | False | |
| CLOSE | Logical | False | |
| CSVFILE | Character | | |
| FILE | Character | | |
| GAINS | Logical | False | |
| H.PARAM | Logical | False | |
| IMPEDANCE | Real | 50 | Ω |
| INPORT | Character | | |
| IN2PORT | Character | | |
| J.DISP | Logical | False | |
| J.ELECTRON | Logical | False | |
| J.HEI | Logical | False | |
| J.HHI | Logical | False | |
| J.HOLE | Logical | False | |
| J.TUN | Logical | False | |
| LCOMMON | Real | 0 | H |
| LGROUND | Real | 0 | H |
| LIN | Real | 0 | H |
| LOUT | Real | 0 | H |
| MASTER | Logical | True | |
| NO.TRAP | Logical | False | |
| NOISE | Logical | False | |
| NOISE.ALL | Logical | False | |
| NOISE.I | Logical | False | |

| Parameter | Type | Default | Units |
|-------------|-----------|---------|---------------|
| NOISE.IV | Logical | False | |
| NOISE.I.ALL | Logical | False | |
| NOISE.V | Logical | False | |
| NOISE.VI | Logical | False | |
| NOISE.V.ALL | Logical | False | |
| OFF | Logical | False | |
| OLD | Logical | False | |
| OUTPORT | Character | | |
| OUT2PORT | Character | | |
| OUT.FILE | Character | | |
| OUTFILE | Character | | |
| RCOMMON | Real | 0 | Ω |
| RGROUND | Real | 0 | Ω |
| RIN | Real | 0 | Ω |
| ROUT | Real | 0 | Ω |
| S.PARAM | Logical | False | |
| SIM.TIME | Logical | False | s |
| SONOS.CURR | Logical | False | |
| WIDTH | Real | 1 | μm |
| Y.PARAM | Logical | False | |
| Z.PARAM | Logical | False | |

File Output Parameters

| | |
|-------------------|---|
| APPEND | Specifies that the output I-V information should be appended to an existing log file. Make sure that the existing log files contain the same type of data (e.g., DC, AC, transient) as the subsequent SOLVE statements. |
| CLOSE | This is an alias for OFF. |
| CSVFILE | Specifies the file name that will be used to store DC, AC, or transient IV information in Comma Separated Value (CSV) format. |
| FILE | This is an alias for OUTFILE. |
| J.DISPLAY | Specifies that displacement currents are written to the log file. |
| J.ELECTRON | Specifies that electron currents are to be written into the log file. |

| | |
|-------------------|--|
| J.HEI | Specifies that hot electron currents are written to the logfile. |
| J.HHI | Specifies that hot hole currents are written to the logfile. |
| J.HOLE | Specifies that hole currents are to be written into the log file. |
| J.TUN | Specifies that tunneling currents are to be written into the log file. |
| MASTER | Specifies that AC data and I-V information will be saved in a standard structure file format. This is the default format. |
| NO.TRAP | Specifies that no data will be written to the file for DC bias cut back steps. |
| OFF | Specifies that any currently open log file will be closed and log file output is discontinued. The alias for this parameter is CLOSE. |
| OLD | Specifies that AC data and IV information will be saved in the original PISCES-II file format. A synonym for this parameter is PISCES. |
| OUT.FILE | This is a synonym for OUTFILE. |
| OUTFILE | Specifies the log file that will be used to store DC, AC, or transient I-V information. The synonym for this parameter is OUT.FILE. |
| SONOS.CURR | Causes the output of SONOS Tunneling Insulator Current and SONOS Blocking Insulator Current from the DYNASONOS model. |

Note: The older ACFILE syntax is not supported and should not be used. AC results are stored in the file specified by OUTFILE as long as the first SOLVE statement after the LOG statement contains AC analysis.

RF Analysis Parameters

If S.PARAM, H.PARAM, Z.PARAM, GAINS, or ABCD.PARAM is specified, the capacitance and conductance data will be converted into the requested set of AC parameters. See Appendix C: “RF and Small Signal AC Parameter Extraction[239]” for more information.

| | |
|-------------------|---|
| S.PARAM | Elects s parameter analysis. For S-parameter analysis, you can also choose to set any of the parasitic element parameters. |
| H.PARAM | Selects H parameter analysis. |
| Y.PARAM | Selects Y parameter analysis |
| Z.PARAM | Selects Z parameter analysis. |
| ABCD.PARAM | selects ABCD parameter analysis. |
| GAINS | Selects the calculation of several types of gains used in RF analysis [184]. These are the stability factor, unilateral power gain (GUm _{ax}), maximum unilateral transducer power gain (GT _{max}), maximum available power gain (G _{ma}), and the maximum stable power gain (G _{ms}). The magnitude of H ₂₁ is also calculated. |
| IMPEDANCE | Specifies the matching impedance for s-parameter calculation. |

| | |
|-----------------|---|
| INPORT | Specifies the electrode name for the primary input port used when performing any AC parameter calculations. |
| IN2PORT | Specifies the electrode name of the secondary input port. |
| OUTPORT | Specifies the electrode name for the output ports used when performing any AC parameter calculations. |
| OUT2PORT | Specifies the electrode n of the secondary output port. |

NOISE Parameters

To perform noise analysis on a one-port device, define the **INPORT**. To perform noise analysis on a two-port device, define the **INPORT** and the **OUTPORT**.

| | |
|---------------------------------------|---|
| NOISE | Selects F_{min} , Z_O , and g_n (the two-port noise figures of merit, 2pNFOM) for output. |
| NOISE.ALL | Selects all noise results for output. These are 2pNFOM, total and individual noise voltage sources, and total and individual noise current sources. |
| NOISE.I | Selects the 2pNFOM and the correlation of the total noise current sources. |
| NOISE.I.ALL | Selects the 2pNFOM, the correlation of the total noise current sources, and the correlation of the noise current sources from the individual noise mechanisms (GR, II, electron and hole diffusion; electron and hole flicker). |
| NOISE.V | Selects the 2pNFOM and the correlation of the total noise voltage sources. |
| NOISE.VI or NOISE.IV | Selects the 2pNFOM and the correlations of both the total noise voltage sources and the total noise current sources. |
| NOISE.V.ALL | Selects the 2pNFOM, the correlation of the total noise voltage sources, and the correlation of the noise voltage sources from the individual noise mechanisms (GR, II, electron and hole diffusion; electron and hole flicker). |

Note: The 2pNFOM have no meaning for a one-port device and therefore don't output. If **NOISE** is the only parameter defined for a one-port device, then the correlation of the total noise voltage sources outputs (rather than outputting nothing).

Parasitic Element Parameters

For RF parameter extraction, you can also set any of the parasitic element parameters. By setting the parasitic element parameters, you can apply lumped parasitic resistances or inductances to the terminal of the two-port device during the RF parameter extraction. These parameters will not affect the capacitance or conductance matrices calculated by ATLAS.

| | |
|----------------|---|
| RIN | Specifies the lumped parasitic resistance on the input to the two port device for s-parameter extraction. The value of RIN is in Ohms. |
| ROUT | Specifies the lumped parasitic resistance on the output to the two port device for s-parameter extraction. The value of ROUT is in Ohms. |
| RCOMMON | This is an alias for RGROUND . |
| RGROUND | Specifies the lumped parasitic resistance on the ground or common side of the two port device for s-parameter extraction. The value of RGROUND is in Ohms. |

| | |
|-----------------|--|
| LIN | Specifies the lumped parasitic inductance on the input to the two port device for s-parameter extraction. The value of LIN is in Henrys. |
| LOUT | Specifies the lumped parasitic inductance on the output to the two port device for s-parameter extraction. The value of LOUT is in Henrys. |
| LCOMMON | This is an alias for LGROUND. |
| LGROUND | Specifies the lumped parasitic inductance on the ground or common side of the two port device for s-parameter extraction. The value of LGROUND is in Henrys. |
| SIM.TIME | Saves the time taken for a bias point into the log file and measured in seconds. Note that if multiple jobs are using the same CPU that this method may not be a true reflection of processor speed. |
| WIDTH | Specified an output width (in Z direction) to apply during the s-parameter calculation. Note that this parameter affects only the derived RF parameters and not currents, capacitances or conductances. The WIDTH parameter of the MESH statement can be used to scale these. Using both these WIDTH parameters will lead to a multiplication of the two widths for the RF parameters. |

Simple Logfile Definition Example

This example saves all I-V data in file, *myfile.log*.

```
LOG OUTF=myfile.log
```

Results should be plotted using TONYPLOT.

RF Analysis Example

To generate s-parameters, assume the input is gate/source and the output is drain/source. A width of 100 microns is also defined along with 100ohm resistance on the input. For example:

```
LOG OUTF=mysparams.log S.PARAM INPORT=gate OUTPORT=drain \
IN2PORT=source OUT2PORT=source WIDTH=100 RIN=100
```

Transient or AC Logfile Example

The contents of LOG files varies for different types of simulations (e.g., DC, transient, AC). The content is set by the first SOLVE statement after the LOG statement. Therefore, the following syntax is required.

```
SOLVE VDRAIN=0.5
LOG OUTF=myfile.log
SOLVE VDRAIN=3.0 RAMPTIME=1e-9 DT=1e-11 TSTOP=1e-7
```

Correct transient parameters would have not been stored, if the LOG statement had been placed before the first SOLVE statement, which is DC.

21.28: LX.MESH, LY.MESH

L<n>.MESH specifies the location of grid lines along the <n>-axis in a rectangular mesh used in LASER simulation. The syntax is equivalent for X and Y directions.

Syntax

```
LX.MESH NODE=<n> LOCATION=<n>
LX.MESH SPACING=<n> LOCATION=<n>
LY.MESH NODE=<n> LOCATION=<n>
LY.MESH SPACING=<n> LOCATION=<n>
```

| Parameter | Type | Default | Units |
|-----------|---------|---------|-------|
| LOCATION | Real | | μm |
| NODE | Integer | | |
| SPACING | Real | | μm |

Description

| | |
|-----------------|---|
| NODE | Specifies the mesh line index. These mesh lines are assigned consecutively. |
| LOCATION | Specifies the location of the grid line. |
| SPACING | Specifies the mesh spacing at the mesh locations specified by the LOCATION parameter. If the SPACING parameter is specified, then the NODE parameter should not be specified. |

LASER Mesh Example

This syntax defines a mesh of 33x33 covering the area bounded by (0.3,0.0) to (2.4,1.0).

```
LX.M n=1 l=0.3
LX.M n=33 l=2.4
LY.M n=1 l=0.0
LY.M n=33 l=1.0
```

Note: The mesh defined in these statements for the Laser Helmholtz Solver is entirely separate from the electrical device simulation mesh defined on the MESH statement.

Setting Locally Fine Grids Example

This example shows how to space grid lines closely around a topological feature such as a junction at y=0.85 microns.

```
LY.MESH LOC=0.0 SPAC=0.2
LY.MESH LOC=0.85 SPAC=0.01
LY.MESH LOC=2 SPAC=0.35
```

21.29: MATERIAL

MATERIAL associates physical parameters with materials in the mesh. The parameter default values for standard semiconductors are shown in Appendix B: “Material Systems”.

Syntax

```
MATERIAL <localization> <material_definition>
```

| Parameter | Type | Default | Units |
|-----------------|------|-----------------------|------------------|
| A.DEFPOT | Real | 2.1 | eV |
| A.LANGEVIN | Real | 1.0 | |
| A.PASSLER | Real | 3.18×10^{-4} | eV/K |
| A.SINGLET | Real | 1.8 | nm |
| A.TRAPCOULOMBIC | Real | 1.0 | |
| A1.RAJ | Real | 3.231×10^2 | cm^{-1} |
| A2.RAJ | Real | 7.237×10^3 | cm^{-1} |
| AD.RAJ | Real | 1.056×10^6 | cm^{-1} |
| A1 | Real | 0.0 | |
| A2 | Real | 0.0 | |
| A3 | Real | 0.0 | |
| A4 | Real | 0.0 | |
| A5 | Real | 0.0 | |
| A6 | Real | 0.0 | |
| AADACHI | Real | see Appendix B | |
| ABSORPTION.SAT | Real | 1.0×10^7 | |
| AC | Real | 0.0 | eV |
| AFFINITY | Real | see Appendix B | eV |
| ALATTICE | Real | 0.0 | Å |
| ALIGN | Real | use AFFINITY | |
| ALPHA A | Real | 0.0 | |
| ALPHA R | Real | 4.0 | |
| AN | Real | 1.0 | |
| AN2 | Real | 7.03×10^5 | cm^{-1} |
| AN0.VALD | Real | 4.3383 | |

| Parameter | Type | Default | Units |
|-----------------|------|-------------------------|-----------------------------------|
| AN1.VALD | Real | -2.42×10^{-12} | |
| AN2.VALD | Real | 4.1233 | |
| AP0.VALD | Real | 2.376 | |
| AP1.VALD | Real | 0.01033 | |
| AP2.VALD | Real | 1.0 | |
| AP | Real | 1.0 | |
| AP2 | Real | 1.682×10^6 | cm^{-1} |
| ARICHN | Real | see Appendix B | $\text{A}/\text{cm}^2/\text{K}^2$ |
| ARICHP | Real | see Appendix B | $\text{A}/\text{cm}^2/\text{K}^2$ |
| ASTR | Real | 0.0 | |
| ASYMMETRY | Real | 0.5 | |
| A.TC.A | Real | 0.0 | $\text{cm K} / \text{W}$ |
| A.TC.B | Real | 0.0 | cm / W |
| A.TC.C | Real | 0.0 | $\text{cm} / \text{W} / \text{K}$ |
| A.TC.CONST | Real | 0.0 | $(\text{W}/\text{cm}/\text{K})$ |
| A.TC.D | Real | 0.0 | K |
| A.TC.E | Real | 0.0 | W/cm |
| A.TC.NPOW | Real | 0.0 | – |
| AUG.CNL | Real | 2.2×10^{-31} | cm^6/s |
| AUG.CPL | Real | 9.2×10^{-32} | cm^6/s |
| AUG.CHI | Real | 1.66×10^{-80} | cm^6/s |
| AUGN | Real | see Appendix B | cm^6/s |
| AUGP | Real | see Appendix B | cm^6/s |
| AUGKN | Num | 0.0 | cm^3 |
| AUGKP | Num | 0.0 | cm^3 |
| AV | Real | 0.0 | eV |
| B.TRAPCOULOMBIC | Real | 1.0 | |
| B.DEFPOT | Real | -2.33 | eV |
| BADACHI | Real | see Appendix B | |
| BBB | Real | 0.0 | eV |

| Parameter | Type | Default | Units |
|------------|------|---|---|
| BB.A | Real | 4.0×10^{14} | $\text{eV}^{-2} \cdot \text{s}^{-1} \cdot \text{cm}^{-1}$ |
| BB.B | Real | 1.97×10^7 | V/cm |
| BB.GAMMA | Real | 2.5 | |
| BETAN | Real | 1.0 | |
| BETAP | Real | 1.0 | |
| BETA.RAJ | Real | 7.021×10^4 | eV/K |
| BGN.C | Real | 0.5 | |
| BGN.E | Real | 9.0×10^{-3} (Slotboom) 6.92×10^{-3} (Klaassen) 6.84×10^{-3} (Bennett) 1.87×10^{-2} (del Alamo) | eV |
| BGN.N | Real | 1.0×10^{17} (Slotboom) 1.3×10^{17} (Klaassen) 3.162×10^{18} (Bennett) 7.0×10^{17} (del Alamo) | cm^{-3} |
| BN | Real | 1.0 | |
| BN2 | Real | 1.231×10^6 | V/cm |
| BN1.VALD | Real | 0.0 | |
| BN0.VALD | Real | 0.235 | |
| BP | Real | 1.0 | |
| BP2 | Real | 2.036×10^6 | V/cm |
| BP0.VALD | Real | 0.17714 | |
| BP1.VALD | Real | -0.002178 | |
| BQP.NGAMMA | Real | 1.2 | |
| BQP.NALPHA | Real | 0.5 | |
| BQP.PGAMMA | Real | 1.0 | |
| BQP.PALPHA | Real | 0.5 | |
| BSTR | Real | 0.0 | |

| Parameter | Type | Default | Units |
|--------------|------|------------------------|----------------------------------|
| C.DEFPOT | Real | -4.75 | eV |
| C.DIRECT | Real | 0.0 | cm ³ /s |
| C1.RAJ | Real | 5.5 | |
| C2.RAJ | Real | 4.0 | |
| C11 | Real | 0.0 | GPa |
| C12 | Real | 0.0 | GPa |
| C13 | Real | 0.0 | GPa |
| C33 | Real | 0.0 | GPa |
| CDL.COUPLING | Real | 1.0 | s ⁻¹ cm ⁻³ |
| CDL.ETR1 | Real | 0.0 | eV |
| CDL.ETR2 | Real | 0.0 | eV |
| CDL.TN1 | Real | 1.0 | s |
| CDL.TN2 | Real | 1.0 | s |
| CDL.TP1 | Real | 1.0 | s |
| CDL.TP2 | Real | 1.0 | s |
| CHI.EG.TDEP | Real | 0.5 | |
| CON.BGN | Real | 0.5 | |
| CN | Real | 0.0 | |
| CN2 | Real | 0.0 | cm ⁻¹ K ⁻¹ |
| CN0.VALD | Real | 1.6831×10 ⁴ | |
| CN1.VALD | Real | 4.3796 | |
| CN2.VALD | Real | 1.0 | |
| CN3.VALD | Real | 0.13005 | |
| COPT | Real | 0.0 | cm ³ /s |
| CP | Real | 0.0 | |
| CP2 | Real | 0.0 | cm ⁻¹ K ⁻¹ |
| CP0.VALD | Real | 0.0 | |
| CP1.VALD | Real | 0.00947 | |
| CP2.VALD | Real | 2.4929 | |
| CP3.VALD | Real | 0.0 | |
| CSTR | Real | 0.0 | |

| Parameter | Type | Default | Units |
|---------------|-----------|----------------------|------------------|
| D.DEFPOT | Real | 1.1 | eV |
| D.TUNNEL | Real | 10^{-6} | cm |
| D1 | Real | 0.0 | eV |
| D2 | Real | 0.0 | eV |
| D3 | Real | 0.0 | eV |
| D4 | Real | 0.0 | eV |
| DADACHI | Real | see Appendix B | eV |
| DEC.DEG | Real | see Table 5-8 | |
| DEC.C1 | Real | 0.0 | eV |
| DEC.C2 | Real | 0.0 | eV |
| DEC.C3 | Real | 0.0 | eV |
| DEC.ISO | Real | 0.0 | eV |
| DEC.D2 | Real | 0.0 | eV |
| DEC.D4 | Real | 0.0 | eV |
| DEV.HH | Real | 0.0 | eV |
| DEV.LH | Real | 0.0 | eV |
| DEV.ISO | Real | 0.0 | eV |
| DEV.SO | Real | 0.0 | eV |
| DEGENERACY | Integer | 2 | |
| DELTA1 | Real | 0.0 | eV |
| DELTA2 | Real | 0.0 | eV |
| DELTA3 | Real | 0.0 | eV |
| DEVICE | Character | | |
| DGN.GAMMA | Real | 3.6 | |
| DGP.GAMMA | Real | 3.6 | |
| DINDEXDT | Real | 0.0 | 1/K |
| DIST.SBT | Real | 10^{-6} | cm |
| DKCQ.EXCITON | Real | 1.1×10^{-8} | s^{-1} |
| DKNRS.EXCITON | Real | 0 | s^{-1} |
| DKSS.EXCITON | Real | 3×10^{-8} | $cm^3 s^{-1}$ |
| DN2 | Real | 0.0 | $cm^{-1} K^{-1}$ |

| Parameter | Type | Default | Units |
|----------------|-----------|------------------------|--------------------------------------|
| DN0.VALD | Real | 1.233735×10^6 | |
| DN1.VALD | Real | 1.2039×10^3 | |
| DN2.VALD | Real | 0.56703 | |
| DOPE.SPECT | Character | | |
| DP2 | Real | 0.0 | $\text{cm}^{-1}\text{K}^{-1}$ |
| DP0.VALD | Real | 1.4043×10^6 | |
| DP1.VALD | Real | 2.9744×10^3 | |
| DP2.VALD | Real | 1.4829 | |
| DPHEFF.EXCITON | Real | 1 | |
| DRST.EXCITON | Real | 0.25 | |
| DTAUS.EXCITON | Real | 5×10^{-9} | s |
| DRHODT | Real | 0.0 | $\mu\Omega \cdot \text{cm}/\text{K}$ |
| DSTR | Real | 0.0 | |
| E.CONDUC | Real | 0.0 | Ω/cm |
| E.FULL.ANISO | Logical | False | E.FULL.ANISO |
| E31 | Real | 0.0 | cm^{-2} |
| E33 | Real | 0.0 | cm^{-2} |
| EAB | Real | 0.045 | eV |
| ECN.II | Real | 1.231×10^6 | |
| ECP.II | Real | 2.036×10^6 | |
| EDB | Real | 0.044 | eV |
| EG1.RAJ | Real | 1.1557 | eV |
| EG2.RAJ | Real | 2.5 | eV |
| EG3.RAJ | Real | 3.2 | eV |
| EG300 | Real | see Appendix B | eV |
| EG1300 | Real | 0.0 | eV |
| EG2300 | Real | 0.0 | eV |
| EG12BOW | Real | 0.0 | eV |
| EG1ALPH | Real | 0.0 | eV/K |
| EG2ALPH | Real | 0.0 | eV/K |

| Parameter | Type | Default | Units |
|-----------------|-----------|--------------------------|---------|
| EG1BETA | Real | 0.0 | K |
| EG2BETA | Real | 0.0 | K |
| EGALPHA | Real | see Appendix B | eV/K |
| EGBETA | Real | see Appendix B | K |
| EMISS.EFFI | Real | 1.0 | |
| EMISS.LAMB | Real | 0.5 | microns |
| EMISS.NX | Integer | 1 | |
| EMISS.NY | Integer | 1 | |
| EMISS.WIDE | Real | 1.0 | microns |
| EMISSION.FACTOR | Real | 27.1728×10^{-5} | |
| EN | Real | 0.0 | |
| EP | Real | 0.0 | |
| EP.MBULK | Real | see Table 3-112 | eV |
| EP1.RAJ | Real | 1.827×10^{-2} | eV |
| EP2.RAJ | Real | 5.773×10^{-2} | eV |
| EPS11 | Real | 0.0 | |
| EPS12 | Real | 0.0 | |
| EPS13 | Real | 0.0 | |
| EPS22 | Real | 0.0 | |
| EPS23 | Real | 0.0 | |
| EPS33 | Real | 0.0 | |
| EPS.XX | Real | 0.0 | |
| EPS.YY | Real | 0.0 | |
| EPS.ZZ | Real | 0.0 | |
| ESTR | Real | 0.0 | |
| ETRAP | Real | 0.0 | eV |
| EPSINF | Real | | |
| EXN.II | Real | 1.0 | |
| EXP.II | Real | 1.0 | |
| F.ALPHAA | Character | | |
| F.BANDCOMP | Character | | |

| Parameter | Type | Default | Units |
|---------------|-----------|-----------------|-------|
| F.BBT | Character | | |
| F.BGN | Character | | |
| F.CBDOSFN | Character | | |
| F.CONMUN | Character | | |
| F.CONMUP | Character | | |
| F.COPT | Character | | |
| F.EPSILON | Character | | |
| F.ENMUN | Character | | |
| F.ENMUP | Character | | |
| F.PDN | Character | | |
| F.PDP | Character | | |
| F.FERRO | Character | | |
| F.GAUN | Character | | |
| F.GAUP | Character | | |
| F.INDEX | Character | | |
| F.MNSNDIFF | Character | | |
| F.MNSPDIFF | Character | | |
| F.MNSNFLICKER | Character | | |
| F.MNSPFlicker | Character | | |
| F.MUNSAT | Character | | |
| F.MUPSAT | Character | | |
| F.RECOMB | Character | | |
| F.TAUN | Character | | |
| F.TAUP | Character | | |
| F.TAURN | Character | | |
| F.TAURP | Character | | |
| F.TCAP | Character | | |
| F.TCOND | Character | | |
| F.VBDOSFN | Character | | |
| F.VSATN | Character | | |
| F.VSATP | Character | | |
| FB.MBULK | Real | see Table 3-112 | |

| Parameter | Type | Default | Units |
|------------|------|-----------------------|----------------------------------|
| FCN | Real | 3.0×10^{-18} | cm^{-2} |
| FCP | Real | 7.0×10^{-18} | cm^{-2} |
| FERRO.EC | Real | 0.0 | V/cm |
| FERRO.EPSF | Real | 1.0 | |
| FERRO.PS | Real | 0.0 | C/cm^2 |
| FERRO.PR | Real | 0.0 | C/cm^2 |
| FSTR | Real | 0.0 | |
| GAIN.SAT | Real | 1.0×10^7 | |
| GAIN0 | Real | 2000.0 | cm^{-1} |
| GAIN00 | Real | -200.0 | cm^{-1} |
| GAIN1N | Real | 0 | cm^2 |
| GAIN1P | Real | 0 | cm^2 |
| GAIN1MIN | Real | 3.0×10^{-16} | cm^2 |
| GAIN2NP | Real | 0 | cm^5 |
| GAMMA | Real | | |
| GAMMA.RAJ | Real | 1108.0 | K |
| GCB | Real | 2.0 | |
| GN1 | Real | 3.0×10^{-16} | cm^{-2} |
| GN2 | Real | 4.0×10^{-15} | cm^{-2} |
| G.SURF | Real | 1.0 | cm^2 |
| GVB | Real | 4.0 | |
| HC.A | Real | See Appendix B | J/Kcm^3 |
| HC.B | Real | See Appendix B | $\text{J}/\text{K}^2\text{cm}^3$ |
| HC.BETA | Real | | |
| HC.C | Real | See Appendix B | $\text{J}/\text{K}^3\text{cm}^3$ |
| HC.C1 | Real | | $\text{J}/\text{K}/\text{kg}$ |
| HC.C300 | Real | | $\text{J}/\text{K}/\text{kg}$ |
| HC.D | Real | See Appendix B | JK/cm^3 |
| HC.RHO | Real | | g/cm^3 |

| Parameter | Type | Default | Units |
|------------|-----------|------------------------|------------------------|
| HOOGEN | Real | 0.0 | |
| HNS.AE | Real | 6.7×10^{-32} | cm^6/s |
| HNS.AH | Real | 7.2×10^{-32} | cm^6/s |
| HNS.BE | Real | 2.45×10^{-31} | cm^6/s |
| HNS.BH | Real | 4.5×10^{-33} | cm^6/s |
| HNS.CE | Real | -2.2×10^{-32} | cm^6/s |
| HNS.CH | Real | 2.63×10^{-32} | cm^6/s |
| HNS.HE | Real | 3.4667 | |
| HNS.HH | Real | 8.25688 | |
| HNS.NOE | Real | 1.0×10^{18} | cm^{-3} |
| HNS.NOH | Real | 1.0×10^{18} | cm^{-3} |
| HNU1 | Real | 1.0 | eV |
| HNU2 | Real | 1.0 | eV |
| HOOGEF | Real | 0.0 | |
| HOPN.BETA | Real | 1.5 | |
| HOPN.GAMMA | Real | 5×10^{-7} | cm^{-1} |
| HOPN.V0 | Real | 1×10^{11} | Hz |
| HOPP.BETA | Real | 1.5 | |
| HOPP.GAMMA | Real | 1×10^{11} | cm^{-1} |
| HOPP.V0 | Real | 1×10^{11} | Hz |
| HUANG.RHYS | Real | 3.5 | |
| IG.ELINR | Real | 6.16×10^{-6} | cm |
| IG.HLINR | Real | 6.16×10^{-6} | cm |
| IG.ELINF | Real | 9.2×10^{-7} | cm |
| IG.HLINF | Real | 9.2×10^{-7} | cm |
| IMAG.INDEX | Real | See Appendix B | |
| INDEX.FILE | Character | | |
| INDX.IMAG | Character | | |
| INDX.REAL | Character | | |
| INSULATOR | Logical | False | |

| Parameter | Type | Default | Units |
|--------------|------|-------------------------|----------------------------------|
| J.ELECT | Real | 0.0 | A/cm ² |
| J.MAGNET | Real | 0.0 | V/cm ² |
| K.SHIFT | Real | 0.0 | eV |
| KAUGCN | Real | 1.83×10^{-31} | cm ⁶ /s |
| KAUGCP | Real | 2.78×10^{-31} | cm ⁶ /s |
| KAUGDN | Real | 1.18 | |
| KAUGDP | Real | 0.72 | |
| KD.LID | Real | 5×10^{-15} | cm ³ s ⁻¹ |
| KH.LID | Real | 5×10^{-18} | cm ³ s ⁻¹ |
| KISC.EXCITON | Real | 0 | s ⁻¹ |
| KNRS.EXCITON | Real | 0 | s ⁻¹ |
| KNRT.EXCITON | Real | 0 | s ⁻¹ |
| KSP.EXCITON | Real | 0 | cm ⁻³ s ⁻¹ |
| KSRHCN | Real | 3.0×10^{-13} | cm ³ |
| KSRHCP | Real | 11.76×10^{-13} | cm ³ |
| KSRHGN | Real | 1.77 | |
| KSRHGP | Real | 0.57 | |
| KSRHTN | Real | 2.5×10^{-3} | s |
| KSRHTP | Real | 2.5×10^{-3} | s |
| KSS.EXCITON | Real | 0 | cm ⁻³ s ⁻¹ |
| KST.EXCITON | Real | 0 | cm ⁻³ s ⁻¹ |
| KTP.EXCITON | Real | 0 | cm ⁻³ s ⁻¹ |
| KT.T.EXCITON | Real | 0 | cm ⁻³ s ⁻¹ |
| L1SELL | Real | Appendix B | μm |
| L2SELL | Real | Appendix B | μm |
| LAM1 | Real | 0 | μm |
| LAM2 | Real | 0 | μm |
| LAMDAE | Real | 6.2×10^{-7} | cm |
| LAMDAH | Real | 3.8×10^{-7} | cm |

| Parameter | Type | Default | Units |
|-------------|-----------|-----------------------|---------------|
| LAMHN | Real | 9.2×10^{-7} | cm |
| LAMHP | Real | 9.2×10^{-7} | cm |
| LAMRN | Real | 6.16×10^{-6} | cm |
| LAMRP | Real | 6.16×10^{-6} | cm |
| LAN300 | Real | 6.2×10^{-7} | cm |
| LAP300 | Real | 3.8×10^{-7} | cm |
| LDS.EXCITON | Real | 0.01 | μm |
| LDT.EXCITON | Real | 0.632 | μm |
| LT.TAUN | Real | 0.0 | |
| LT.TAUP | Real | 0.0 | |
| LUTT1 | Real | 0.0 | |
| LUTT2 | Real | 0.0 | |
| LUTT3 | Real | 0.0 | |
| M.DSN | Real | See Appendix B | |
| M.DSP | Real | See Appendix B | |
| M.VTHN | Real | | |
| M.VTHP | Real | | |
| MATERIAL | Character | | |
| MAG.LOSS | Real | 0.0 | mho/cm |
| MBULKSQ | Real | | eV |
| MC | Real | 0.0 | |
| ME.TUNNEL | Real | | |
| MH.TUNNEL | Real | | |
| ME.SBT | Real | | |
| MH.SBT | Real | | |
| MHH | Real | 0.49 | |
| MINIMA | Real | 6 | |
| ML | Real | 0.916 | |
| MLH | Real | 0.16 | |
| MSO | Real | 0.23 | |
| MSTAR | Real | 0.0 | |

| Parameter | Type | Default | Units |
|---------------|-----------|----------------------|-------------------------------|
| MTT | Real | 0.0 | |
| MT1 | Real | 0.191 | |
| MT2 | Real | 0.191 | |
| MUN | Real | See Appendix B | |
| MUP | Real | See Appendix B | |
| MV | Real | 0.0 | |
| MZZ | Real | 0.0 | |
| N.ION.1 | Real | 0.0 | $\text{cm}^{-1}\text{K}^{-1}$ |
| N.ION.2 | Real | 0.0 | $\text{cm}^{-1}\text{K}^{-2}$ |
| N.IONIZA | Real | 7.03×10^5 | cm^{-1} |
| N.SHIFT | Real | 0.0 | eV |
| NK.SHIFT | Real | 0.0 | eV |
| N0.BGN | Real | 1.0×10^{17} | cm^{-3} |
| NAME | Character | | |
| NC.F | Real | 1.5 | |
| NC300 | Real | See Appendix B | cm^{-3} |
| NDX.ADACHI | Logical | False | |
| NDX.SELLMEIER | Logical | False | |
| NHNU | Integer | 0 | |
| NI.MIN | Real | 0.0 | cm^{-3} |
| NK.EV | Logical | False | |
| NK.NM | Logical | False | |
| NLAM | Integer | 0 | |
| N.SCH.GAMMA | Real | 1.0 | s |
| N.SCH.MAX | Real | 3.0×10^{-6} | s |
| N.SCH.MIN | Real | 0.0 | s |
| N.SCH.NREF | Real | 1.0×10^{16} | cm^{-3} |
| NSRHN | Real | See Appendix B | cm^{-3} |
| NSRHP | Real | See Appendix B | cm^{-3} |
| NTRANSPARENT | Real | 2.0×10^{18} | cm^{-3} |

| Parameter | Type | Default | Units |
|-------------|-----------|----------------------|-------------------------------|
| NUE.EXTR | Real | | |
| NUH.EXTR | Real | | |
| NV.F | Real | 1.5 | |
| NV300 | Real | See Appendix B | cm^{-3} |
| OP.PH.EN | Real | 0.063 | eV |
| OPPHE | Real | 0.063 | eV |
| OUT.DSPEC | Character | | |
| OUT.INDEX | Character | | |
| OUT.USPEC | Character | | |
| OXCH.ONLY | Logical | False | |
| P.ION.1 | Real | 0.0 | $\text{cm}^{-1}\text{K}^{-1}$ |
| P.ION.2 | Real | 0.0 | $\text{cm}^{-1}\text{K}^{-1}$ |
| P.IONIZA | Real | 1.682×10^6 | cm^{-1} |
| P.PASSLER | Real | 2.33 | |
| P.SCH.GAMMA | Real | 1.0 | s |
| P.SCH.MAX | Real | 3.0×10^{-6} | s |
| P.SCH.MIN | Real | 0.0 | s |
| P.SCH.NREF | Real | 1.0×10^{16} | cm^{-3} |
| PCM.AEA | Real | 3.2 | eV |
| PCM.AP | Real | 1.0 | |
| PCM.ARHO | Real | | $\mu\Omega\text{cm}$ |
| PCM.ATAU | Real | | S |
| PCM.ATC | Real | | K |
| PCM.CEA | Real | 3.7 | eV |
| PCM.CP | Real | 1.0 | |
| PCM.CRHO | Real | | $\mu\Omega\text{cm}$ |
| PCM.CTAU | Real | | S |
| PCM.CTC | Real | | K |
| PCM.LATHEAT | Real | 0.0 | J |
| PDA.N | Real | 0.2 | |
| PDA.P | Real | 0.2 | |

| Parameter | Type | Default | Units |
|---------------|-----------|----------------------|----------------------------------|
| PDEXP.N | Real | -2.5 | |
| PDEXP.P | Real | -2.5 | |
| PERM.ANISO | Real | -999.0 | |
| PERMEABILITY | Real | 1.0 | |
| PERMITTIVITY | Real | See Appendix B | |
| PHEFF.EXCITON | Real | 1 | |
| PHONON.ENERGY | Real | 0.068 | eV |
| PIP.ACC | Real | 2.0 | |
| PIP.ET | Real | 1.0 | eV |
| PIP.NT | Real | 0.0 | cm ² |
| PIP.OMEGA | Real | 0.07 | eV |
| POWER | Real | | |
| PSP | Real | 0.0 | cm ⁻² |
| QE.EXCITON | Real | 0.0 | |
| QR.EXCITON | Real | 0.0 | |
| REAL.INDEX | Real | See Appendix B | |
| REGION | | All regions | |
| RESISTIVITY | Real | | $\mu\Omega\cdot\text{cm}$ |
| RST.EXCITON | Real | 0.25 | |
| S.BINDING | Real | 0.1 | eV |
| S0SELL | Real | See Appendix B | |
| S1SELL | Real | See Appendix B | |
| S2SELL | Real | See Appendix B | |
| SIG.LID | Real | 1.0×10^{-8} | cm ⁻³ s ⁻¹ |
| SEMICONDUC | Logical | False | |
| SO.DELTA | Real | see Table 3-112 | eV |
| SOPRA | Character | | |
| STABLE | Integer | | |
| STRUCTURE | Character | | |
| T.PASSLER | Real | 406.0 | |
| TAA.CN | Real | 1.0×10^{-12} | cm ³ /s |

| Parameter | Type | Default | Units |
|---------------|---------|-----------------------|---|
| TAA.CP | Real | 1.0×10^{-12} | cm^3/s |
| TANI.CONST | Logical | False | |
| TANI.POWER | Logical | False | |
| TANI.POLYNOM | Logical | False | |
| TANI.RECIP | Logical | false | |
| TAUMOB.EL | Real | 0.4×10^{-12} | s |
| TAUMOB.HO | Real | 0.4×10^{-12} | s |
| TAUN0 | Real | See Appendix B | s |
| TAUP0 | Real | See Appendix B | s |
| TAUREL.EL | Real | 0.4×10^{-12} | s |
| TAUREL.HO | Real | 0.4×10^{-12} | s |
| TAUS.EXCITON | Real | 1×10^{-9} | s |
| TAUT.EXCITON | Real | 1×10^{-9} | s |
| TC.A | Real | See Appendix B | $\frac{\text{cm} \cdot \text{K}}{\text{W}}$ |
| TC.B | Real | See Appendix B | $\frac{\text{cm}}{\text{W}}$ |
| TC.C | Real | See Appendix B | $\frac{\text{cm}}{\text{W} \cdot \text{K}}$ |
| TC.CONST | Real | | W/cm·K |
| TC.NPOW | Real | | |
| TC.D | Real | | K |
| TC.E | Real | | W/cm |
| TC.FULL.ANISO | Logical | False | |
| TCOEFF.N | Real | 2.55 | |
| TCOEFF.P | Real | 2.55 | |
| TCON.CONST | Logical | | |
| TCON.POWER | Logical | | |
| TCON.POLYNOM | Logical | | |
| TCON.RECIPRO | Logical | | |
| TE.MODES | Logical | False | |

| Parameter | Type | Default | Units |
|--------------|-----------|-------------------------|-------|
| TLU.A | Real | 0 | eV |
| TLU.C | Real | 0 | eV |
| TLU.E0 | Real | 0 | eV |
| TLU.EC | Real | 0 | eV |
| TLU.EG | Real | 0 | eV |
| TLU.EPS | Real | 1.0 | |
| TMUN | Real | | |
| TMUP | Real | | |
| TRE.T1 | Real | | s |
| TRE.T2 | Real | | s |
| TRE.T3 | Real | | s |
| TRE.W1 | Real | | eV |
| TRE.W2 | Real | | eV |
| TRE.W3 | Real | | eV |
| TRH.T1 | Real | | s |
| TRH.T2 | Real | | s |
| TRH.T3 | Real | | s |
| TRH.W1 | Real | | eV |
| TRH.W2 | Real | | eV |
| TRH.W3 | Real | | eV |
| U.DEFPOT | Real | 10.5 | eV |
| UBGN.B | Real | 3.1×10^{12} | |
| UBGN.C | Real | -3.9×10^{-5} | |
| USER.DEFAULT | Character | | |
| USER.GROUP | Character | SEMICONDUCTOR | |
| USER.SPECT | Character | | |
| V0.BGN | Real | 9.0×10^{-3} | eV |
| VAL.AN0 | Real | 4.3383 | |
| VAL.AN1 | Real | -2.42×10^{-12} | |
| VAL.AN2 | Real | 4.1233 | |
| VAL.AP0 | Real | 2.376 | |

| Parameter | Type | Default | Units |
|-------------|------|------------------------|-------|
| VAL.AP1 | Real | 0.01033 | |
| VAL.AP2 | Real | 1.0 | |
| VAL.BN0 | Real | 0.235 | |
| VAL.BN1 | Real | 0.0 | |
| VAL.CN0 | Real | 1.6831×10^4 | |
| VAL.CN1 | Real | 4.3796 | |
| VAL.CN2 | Real | 1.0 | |
| VAL.CN3 | Real | 0.13005 | |
| VAL.DN0 | Real | 1.233735×10^6 | |
| VAL.DN1 | Real | 1.2039e3 | |
| VAL.DN2 | Real | 0.56703 | |
| VAL.BP0 | Real | 0.17714 | |
| VAL.BP1 | Real | -0.002178 | |
| VAL.CP0 | Real | 0.0 | |
| VAL.CP1 | Real | 0.00947 | |
| VAL.CP2 | Real | 2.4924 | |
| VAL.CP3 | Real | 0.0 | |
| VAL.DP0 | Real | 1.4043×10^6 | |
| VAL.DP1 | Real | 2.9744×10^3 | |
| VAL.DP2 | Real | 1.4829 | |
| VSAT | Real | | cm/s |
| VSATN | Real | | cm/s |
| VSATP | Real | | cm/s |
| WELL.DELTA | Real | see Table 3-112 | eV |
| WELL.EPS | Real | 0 | eV |
| WELL.GAMMA0 | Real | 2×10^{-3} | eV |
| WELL.TAUIN | Real | 3.3×10^{-13} | s |
| X.X | Real | 1.0 | |
| X.Y | Real | 0.0 | |
| X.Z | Real | 0.0 | |

| Parameter | Type | Default | Units |
|------------|---------|----------------------|-------|
| XDIR.ANISO | Logical | False | |
| Y.X | Real | 0.0 | |
| Y.Y | Real | 1.0 | |
| Y.Z | Real | 0.0 | |
| YDIR.ANISO | Logical | False | |
| ZDIR.ANISO | Logical | True | |
| Z.SCHENK | Real | 1.0 | |
| Z.X | Real | 0.0 | |
| Z.Y | Real | 0.0 | |
| Z.Z | Real | 1.0 | |
| ZAMDMEZ.Z0 | Real | 7.0×10^{-7} | cm |

Description

The **MATERIAL** statement is used set basic material parameters related to band structure and parameters for certain mobility, recombination or carrier statistics models. Parameters for temperature dependence are noted in a separate section below.

Localization of Material Parameters

| | |
|-----------------|--|
| DEVICE | Specifies which device the MATERIAL statement should apply to in MIXEDMODE simulation. The synonym for this parameter is STRUCTURE . |
| MATERIAL | Specifies which material from the table in Appendix B: “Material Systems” that the MATERIAL statement should apply. If a material is specified, then all regions defined as being composed of that material will be affected. |

Note: You can specify the following logical parameters to indicate the material instead of assigning the **MATERIAL** parameter: **SILICON**, **GAAS**, **POLYSILI**, **GERMANIU**, **SIC**, **SEMICON**, **SIGE**, **ALGAAS**, **A-SILICO**, **DIAMOND**, **HGCDTE**, **INAS**, **INGAAS**, **INP**, **S.OXIDE**, **ZNSE**, **ZNTE**, **ALINAS**, **GAASP**, **INGAP** and **MINASP**.

| | |
|------------------|---|
| NAME | Specifies which region the MATERIAL statement should apply. Note that the name must match the name specified in the NAME parameter of the REGION statement or the region number. |
| REGION | Specifies the region number to which these parameters apply. If there is more than one semiconductor region, specification of different parameters for each region is allowed. If REGION is not specified, all regions in the structure are changed. |
| STRUCTURE | This is a synonym for DEVICE . |

Band Structure Parameters

| | |
|---|--|
| A.DEFPOT, B.DEFPOT, C.DEFPOT, D.DEFPOT, and U.DEFPOT | Specify the deformation potentials used in calculating the effects of strains on the bandgap of silicon (see Section 3.6.12: “Stress Effects on Bandgap in Si”). |
| AFFINITY | Specifies the electron affinity. |
| ALIGN | Specifies the fraction of the bandgap difference that is applied to the conduction band edge, relative to the minimum bandgap material in the device. Note that specifying this parameter overrides any electron affinity specification. See the Chapter 5: “Blaze: Compound Material 2D Simulator”, Section 5.1.2: “Alignment” for information on setting the band alignment. |
| ARICHN | Specifies the effective Richardson constant for electrons. |
| ARICHP | Specifies the effective Richardson constant for holes. |
| CHI. EG. TDEP | This is a ratio that specifies what fraction of the change in bandgap due to temperature change ascribed to the electron affinity. CHI. EG. TDEP is not active when ALIGN is specified. |
| D. TUNNEL | Specifies the maximum tunneling distance for the universal Schottky tunneling model (see Chapter 3: “Physics”, Section 3.5.2: “Schottky Contacts”). The alias for this parameter is DIST. SBT. |
| DEC. DEG | Overrides the default values of dE_c/dE_v given in Table 5-8. |
| DEC. C1 | This is a conduction band shift for 1st pair of electron valleys. |
| DEC. C2 | This is a conduction band shift for 2nd pair of electron valleys. |
| DEC. C3 | This is a conduction band shift for 3rd pair of electron valleys. |
| DEC. D2 | This is a conduction band shift for $\Delta 2$ electron valleys if DEC. C1 is not set. |
| DEC. D4 | This is a conduction band shift for $\Delta 4$ electron valleys if DEC. C2 is not set. |
| DEC. ISO | This is a conduction band shift for isotropic electron band, when NUM. DIRECT=1. |
| DEV. HH | This is a valence band shift for heavy holes. |
| DEV. LH | This is a valence band shift for light holes. |
| DEV. ISO | This is a valence band shift for isotropic hole band, when NUM. BAND=1. |
| DEV. SO | This is a valence band shift for split-off holes. |
| DIST. SBT | This is an alias for D. TUNNEL. |

| | |
|--|---|
| EG300 | Specifies energy gap at 300K (see Chapter 3: "Physics", Equation 3-38). All semiconductor materials in ATLAS must have a defined EG300. |
| EG1300, EG2300, EG12BOW, EG1ALPH, EG2ALPH, EG1BETA, and EG2BETA | Specify parameters of the General Ternary bandgap model described in Chapter 3: "Physics", Equations 3-42 through 3-44. |
| EPS11, EPS12, EPS13, EPS22, EPS23, and EPS33 | Specify the strain tensor used in the calculation of the strain effects on bandgap of silicon (see Section 3.6.12: "Stress Effects on Bandgap in Si"). |
| EPS.XX | XX component of dielectric permittivity tensor used by vector Helmholtz solver. |
| EPS.YY | YY component of dielectric permittivity tensor used by vector Helmholtz solver. |
| EPS.ZZ | ZZ component of dielectric permittivity tensor, used by vector Helmholtz solver. |
| F.BANDCOMP | Specifies the name of a file containing a C-Interpreter function that defines temperature and composition dependent band parameter models. |
| F.CBDOSFN | Specifies the C-Interpreter file for the Conduction band effective density of states as a function of Lattice/Electron temperature. This function is called cbdosfn. |
| F.TCAP | Specifies the name of a file containing a C-Interpreter function that defines the lattice thermal capacity as a function of the lattice temperature, position, doping and fraction composition. |
| F.TCOND | Specifies the name of a file containing a C-Interpreter function that defines the lattice thermal conductivity as a function of the lattice temperature, position, doping and fraction composition. |
| F.EPSILON | Specifies the name of a file containing a C-Interpreter function that defines temperature and composition dependent static dielectric constant models. |
| F.FERRO | Specifies the name of a file containing a C-Interpreter function that defines dielectric permittivity as a function of electric field and position (x,y). You need a license to use this parameter. |
| F.VBDOSFN | Specifies the C-Interpreter file for the Valence band effective density of states as a function of Lattice/Hole temperature. This function is called vbdosfn. |
| M.DSN | specifies the electron density of states effective mass. When specified, it is in Equation 3-31 in Chapter 3: "Physics" to calculate electron density of states. |
| M.DSP | Specifies the hole density of states effective mass. When specified it is in Equation 3-32 in Chapter 3: "Physics" to calculate hole density of states. |

| | |
|---------------------------------------|--|
| M.VTHN | Specifies the electron effective mass for calculation of thermal velocity in the thermionic heterojunction model (see Chapter 5: “Blaze: Compound Material 2D Simulator”, Equation 5-51). |
| M.VTHP | Specifies the hole effective mass for calculation of thermal velocity in the thermionic heterojunction model (see Chapter 5: “Blaze: Compound Material 2D Simulator”, Equation 5-46). |
| ME.SBT and MH.SBT | These are aliases for ME.TUNNEL and MH.TUNNEL . |
| ME.TUNNEL and MH.TUNNEL | Specify the electron and hole effective masses for tunneling used in the universal Schottky tunneling model (see Chapter 3: “Physics”, Section 3.5.2: “Schottky Contacts”). The aliases for these parameters are ME.SBT and MH.SBT . |
| NC.F | Specifies the conduction band density of states temperature (see Chapter 3: “Physics”, Equation 3-31). |
| NV.F | Specifies the valence band density of states temperature (see Chapter 3: “Physics”, Equation 3-32). |
| NC300 | Specifies the conduction band density at 300K. (see Chapter 3: “Physics”, Equation 3-31). |
| NI.MIN | Specifies the minimum allowable value of the intrinsic carrier density. |
| NV300 | Specifies valence band density at 300K (see Chapter 3: “Physics”, Equation 3-32). |
| PERMITTIVITY | Specifies dielectric permittivity of the material. All materials in an ATLAS structure must have a defined permittivity. |

BQP Parameters

| | |
|---|---|
| BQP.NGAMMA and BQP.PGAMMA | These parameters allow you to set the γ parameter of the BQP model for electrons and holes respectively. |
| BQP.NALPHA and BQP.PALPHA | These parameters allow you to set the α parameter of the BQP model for electrons and holes respectively. |

Mobility Model Parameters

| | |
|--------------------|---|
| F.COMMUN | Specifies the name of a file containing a C-Interpreter function for the specification of temperature, composition and doping dependent electron mobility models. |
| F.COMMUP | Specifies the name of a file containing a C-Interpreter function for the specification of temperature, composition and doping dependent hole mobility models. |
| F.ENMUN | Specifies a C-Interpreter file for the electron mobility as a function of Electron Temperature and perpendicular field as well as other choice variables. The function itself is named <code>endepmun</code> and only applies to ATLAS2D. |
| F.ENMUP | Specifies a C-Interpreter file for the hole mobility as a function of Hole Temperature and perpendicular field as well as other choice variables. The function itself is named <code>endepmup</code> and only applies to ATLAS2D. |
| F.MUNSAT | Specifies the name of a file containing a C-Interpreter function for the specification of parallel field dependent electron mobility model for velocity saturation. |
| F.MUPSAT | Specifies the name of a file containing a C-Interpreter function for the specification of parallel field dependent hole mobility model for velocity saturation. |
| F.VSATN | Specifies the name of a file containing a C-Interpreter function for the specification of temperature and composition dependent electron saturation velocity models. |
| F.VSATP | Specifies the name of a file containing a C-Interpreter function for the specification of temperature and composition dependent hole saturation velocity models. |
| GSURF | Specifies a factor by which mobility is reduced at the semiconductor surface. This is a simple but not accurate alternative to the transverse field dependent or surface mobility models set on the <code>MODELS</code> statement. |
| MUN | Specifies low-field electron mobility. This parameter is only used if no concentration dependent mobility model is specified. |
| MUP | Specifies low-field hole mobility. This parameter is only used if no concentration dependent mobility model is specified. |
| VSATURATION | Specifies the saturation velocity for the electric field dependent mobility. |
| VSATN | Specifies the saturation velocity for electrons. |
| VSATP | Specifies the saturation velocity for holes. |

Recombination Model Parameters

| | |
|--|--|
| A.LANGEVIN | Specifies the prefactor for the bimolecular Langevin recombination model. See Chapter 15: “Organic Display and Organic Solar: Organic Simulators”, Equation 15-32. |
| A.TRAPCOULOMBIC and B.TRAP-COULOMBIC | Specify the Poole-Frenkel thermal emission enhancement factor parameters. See Chapter 3: “Physics”, Equations 3-90 and 3-91. |
| AN, AP, BN, BP, CN, EN, and EP | The parameter for the concentration dependent lifetime model (see Chapter 3: “Physics”, Equations 3-297 and 3-298). |
| AUG.CNL, AUG.CPL, and AUG.CHI | Specify the coefficients for the carrier and doping concentration dependent Auger rate coefficient models described in Equations 3-339 and 3-340. |
| AUGN | Specifies the Auger coefficient, cn (see Chapter 3: “Physics”, Equation 3-330). |
| AUGP | Specifies the Auger coefficient, cp (see Chapter 3: “Physics”, Equation 3-330). |
| AUGKN | The parameter of the narrow band-gap electron Auger recombination coefficient model. |
| AUGKP | The parameter of the narrow band-gap electron Auger recombination coefficient model. |
| BB.A, BB.B, and BB.GAMMA | Specify the band-to-band tunneling parameters (see Chapter 3: “Physics”, Equation 3-416). |
| C.DIRECT | This is an alias for COPT . |

See Equations 3-307 thru 3-310 to see how the following CDL parameters are used.

| | |
|---|---|
| CDL.ETR1 and CDL.ETR2 | There are the trap energy levels in the Coupled Defect Level model. They are relative to the intrinsic energy level and are in Electron Volts. |
| CDL.TN1, CDL.TN2, CDL.TP1, and CDL.TP2 | These are the recombination lifetimes for the two energy levels in the Coupled Defect Level model. |
| CDL.COUPLING | Specifies the coupling constant in units of $\text{cm}^{-3}\text{s}^{-1}$ for the Coupled Defect Level model. |
| COPT | Specifies the optical recombination rate for the material. This parameter has no meaning unless MODELS OPTR has been specified (see Chapter 3: “Physics”, Equation 3-326). The alias for this parameter is C.DIRECT . |
| ETRAP | Specifies the trap energy for SRH recombination |
| F.BBT | Specifies the name of a file containing a C-INTERPRETER function for the specification of the electric field and carrier concentration dependent band-to-band generation rate. |

| | |
|---|--|
| F.COPT | Specifies the name of a file containing a C-INTERPRETER function for the specification of composition and temperature dependence of the radiative recombination rate. |
| F.GAUN | Specifies the name of a file containing a C-INTERPRETER function for the specification of composition and temperature dependence of the electron Auger coefficient. |
| F.GAUP | Specifies the name of a file containing a C-INTERPRETER function for the specification of composition and temperature dependence of the hole Auger coefficient. |
| F.RECOMB | Specifies the name of a file containing a C-Interpreter function for the specification of temperature, composition, electron and hole concentration dependent recombination rate models. |
| F.TAUN | Specifies the name of a file containing a C-INTERPRETER function for the specification of position dependent electron lifetime models. |
| F.TAUP | Specifies the name of a file containing a C-INTERPRETER function for the specification of position dependent hole lifetime models. |
| F.TAURN | Specifies the name of a file containing a C-INTERPRETER function specifying the electron relaxation time as a function of electron energy. |
| F.TAURP | Specifies the name of a file containing a C-INTERPRETER function specifying the hole relaxation time as a function of hole energy. |
| HNS.AE, HNS.BE, HNS.CE, HNS.AH, HNS.BH, and HNS.CH | These are the temperature dependence parameters for HNSAUG model (see Equations 3-343 and 3-344). |
| HNS.HE and HNS.NOE | These are the Electron concentration dependence parameters for HNSAUG model (see Equations 3-343 and 3-344). |
| HNS.HH and HNS.NOH | These are the Hole concentration dependence parameters for HNSAUG model (see Equations 3-343 and 3-344). |
| N.SCH.MIN, P.SCH.MIN, N.SCH.MAX, P.SCH.MAX, N.SCH.GAMMA, P.SCH.GAMMA, and N.SCH.NREF, and P.SCH.NREF | These are used in the Scharfetter doping concentration dependent lifetime model. They are applied in Equations 3-301 and 3-302. |
| TCOEFF.N and TCOEFF.P | These are used in the alternative lifetime lattice temperature dependence model. |
| TAA.CN and TAA.CP | These are used in the carrier concentration dependent recombination lifetime model of Equations 3-311 and 3-312. |
| ZAMDMER.ZO | The nominal spatial separation of recombination centers in the ZAMDMER model of electron trap lifetime in LT-GaAs. |

Impact Ionization Parameters

| | |
|------------------------------|---|
| AN0.VALD | This is an alias for VAL.AN0. |
| AN1.VALD | This is an alias for VAL.AN1. |
| AN2.VALD | This is an alias for VAL.AN2. |
| AP0.VALD | This is an alias for VAL.AP0. |
| AP1.VALD | This is an alias for VAL.AP1. |
| AP2.VALD | This is an alias for VAL.AP2. |
| BETAN | This is for electrons and BETAP for holes correspond to coefficients for the power of ECRIT/E. The aliases for these parameters are EXN.II and EXP.II. |
| BN0.VALD | This is an alias for VAL.BN0. |
| BN1.VALD | This is an alias for VAL.BN1. |
| BP0.VALD | This is an alias for VAL.BP0. |
| BP1.VALD | This is an alias for VAL.BP1. |
| CN2, CP2, DN2 and DP2 | These are specifiable coefficients in the temperature dependent models described in Chapter 3: “Physics”, Equations 3-358 and 3-359. The aliases for these parameter are N.ION.1, P.ION.1, N.ION.2 and P.ION.2. |
| CN0.VALD | This is an alias for VAL.CN0. |
| CN1.VALD | This is an alias for VAL.CN1. |
| CN2.VALD | This is an alias for VAL.CN2. |
| CN3.VALD | This is an alias for VAL.CN3. |
| CP0.VALD | This is an alias for VAL.CP0. |
| CP1.VALD | This is an alias for VAL.CP1. |
| CP2.VALD | This is an alias for VAL.CP2. |
| CP3.VALD | This is an alias for VAL.CP3. |
| DN0.VALD | This is an alias for VAL.DN0. |
| DN1.VALD | This is an alias for VAL.DN1. |
| DN2.VALD | This is an alias for VAL.DN2. |
| DP0.VALD | This is an alias for VAL.DP0. |
| DP1.VALD | This is an alias for VAL.DP1. |
| DP2.VALD | This is an alias for VAL.DP2. |
| ECN.II | This is an alias for BN2. |
| ECP.II | This is an alias for BP2. |

| | |
|--|---|
| EXN.II | This is an alias for BETAN. |
| EXP.II | This is an alias for BETAP. |
| LAMBD AE | Specifies the mean free path for electrons. The alias for this parameter is LAN300. |
| LAMDAH | Specifies the mean free path for holes. The alias for this parameter is LAP300. |
| LAN300 | This is an alias for LAMBD AE. |
| LAP300 | This is an alias for LAMDAH. |
| N.ION.1, P.ION.1, N.ION.2 and P.ION.2 | These are the aliases for CN2, CP2, DN2 and DP2. |
| N.IONIZA | This is an alias for AN2. |
| OP.PH.EN | This is an alias for OPPHE. |
| OPPHE | Specifies the optical phonon energy. The alias for this parameter is OP.PH.EN. |
| P.IONIZA | This is an alias for AP2. |
| VAL.AN0 | Specifies the value of a temperature dependent impact ionization parameter in Chapter 3: "Physics", Equation 3-369. The alias for this parameter is AN0.VALD. |
| VAL.AN1 | Specifies the value of a temperature dependent impact ionization parameter in Chapter 3: "Physics", Equation 3-369. The alias for this parameter is AN1.VALD. |
| VAL.AN2 | Specifies the value of a temperature dependent impact ionization parameter in Chapter 3: "Physics", Equation 3-369. The alias for this parameter is AN2.VALD. |
| VAL.BN0 | Specifies the value of a temperature dependent impact ionization parameter in Chapter 3: "Physics", Equation 3-370. The alias for this parameter is BN0.VALD. |
| VAL.BN1 | Specifies the value of a temperature dependent impact ionization parameter in Chapter 3: "Physics", Equation 3-370. The alias for this parameter is BN1.VALD. |
| VAL.CN0 | Specifies the value of a temperature dependent impact ionization parameter in Chapter 3: "Physics", Equation 3-371. The alias for this parameter is CN0.VALD. |
| VAL.CN1 | Specifies the value of a temperature dependent impact ionization parameter in Chapter 3: "Physics", Equation 3-371. The alias for this parameter is CN1.VALD. |
| VAL.CN2 | Specifies the value of a temperature dependent impact ionization parameter in Chapter 3: "Physics", Equation 3-371. The alias for this parameter is CN2.VALD. |
| VAL.CN3 | Specifies the value of a temperature dependent impact ionization parameter in Chapter 3: "Physics", Equation 3-371. The alias for this parameter is CN3.VALD. |

| | |
|----------------|---|
| VAL.DN0 | Specifies the value of a temperature dependent impact ionization parameter in Chapter 3: “Physics”, Equation 3-372. The alias for this parameter is DN0.VALD. |
| VAL.DN1 | Specifies the value of a temperature dependent impact ionization parameter in Chapter 3: “Physics”, Equation 3-372. The alias for this parameter is DN1.VALD. |
| VAL.DN2 | Specifies the value of a temperature dependent impact ionization parameter in Chapter 3: “Physics”, Equation 3-372. The alias for this parameter is DN2.VALD. |
| VAL.AP0 | Specifies the value of a temperature dependent impact ionization parameter in Chapter 3: “Physics”, Equation 3-373. |
| VAL.AP1 | Specifies the value of a temperature dependent impact ionization parameter in Chapter 3: “Physics”, Equation 3-373. The alias for this parameter is AP1.VALD. |
| VAL.AP2 | Specifies the value of a temperature dependent impact ionization parameter in Chapter 3: “Physics”, Equation 3-373. The alias for this parameter is AP2.VALD. |
| VAL.BP0 | Specifies the value of a temperature dependent impact ionization parameter in Chapter 3: “Physics”, Equation 3-374. The alias for this parameter is BP0.VALD. |
| VAL.BP1 | Specifies the value of a temperature dependent impact ionization parameter in Chapter 3: “Physics”, Equation 3-374. The alias for this parameter is BP1.VALD. |
| VAL.CP0 | Specifies the value of a temperature dependent impact ionization parameter in Chapter 3: “Physics”, Equation 3-375. The alias for this parameter is CP0.VALD. |
| VAL.CP1 | Specifies the value of a temperature dependent impact ionization parameter in Chapter 3: “Physics”, Equation 3-375. The alias for this parameter is CP1.VALD. |
| VAL.CP2 | Specifies the value of a temperature dependent impact ionization parameter in Chapter 3: “Physics”, Equation 3-375. The alias for this parameter is CP2.VALD. |
| VAL.CP3 | Specifies the value of a temperature dependent impact ionization parameter in Chapter 3: “Physics”, Equation 3-375. The alias for this parameter is CP3.VALD. |
| VAL.DP0 | Specifies the value of a temperature dependent impact ionization parameter in Chapter 3: “Physics”, Equation 3-376. The alias for this parameter is DP0.VALD. |
| VAL.DP1 | specifies the value of a temperature dependent impact ionization parameter in Chapter 3: “Physics”, Equation 3-376. The alias for this parameter is DP1.VALD. |
| VAL.DP2 | Specifies the value of a temperature dependent impact ionization parameter in Chapter 3: “Physics”, Equation 3-376. The alias for this parameter is DP2.VALD. |

Klaassen Model parameters

| | |
|---------------|---|
| KSRHTN | Coefficient for Klaassen's concentration and temperature dependent SRH lifetime model. |
| KSRHTP | Coefficient for Klaassen's concentration and temperature dependent SRH lifetime model. |
| KSRHCN | Coefficient for Klaassen's concentration and temperature dependent SRH lifetime model. |
| KSRHCP | Coefficient for Klaassen's concentration and temperature dependent SRH lifetime model. |
| KSRHGN | Coefficient for Klaassen's concentration and temperature dependent SRH lifetime model. |
| KSRHGP | Coefficient for Klaassen's concentration and temperature dependent SRH lifetime model. |
| KAUCN | Coefficient for Klaassen's concentration dependent Auger model. |
| KAUGCP | Coefficient for Klaassen's concentration dependent Auger model. |
| KAUGDN | Coefficient for Klaassen's concentration dependent Auger model. |
| KAUGDP | Coefficient for Klaassen's concentration dependent Auger model. |
| NSRHN | Specifies the SRH concentration parameter for electrons (see Chapter 3: "Physics", Equation 3-297). |
| NSRHP | Specifies the SRH concentration parameter for holes (see Chapter 3: "Physics", Equation 3-298). |
| TAUN0 | Specifies SRH lifetime for electrons (see Chapter 3: "Physics", Equation 3-297). |
| TAUP0 | Specifies SRH lifetime for holes (see Chapter 3: "Physics", Equation 3-298). |

See also Chapter 3: "Physics", Equations 3-299 and 3-300 and Equations 3-331 and 3-333 for more information about Klaassen models.

Carrier Statistics Model Parameters

| | |
|-------------------------------|--|
| ASYMMETRY | Specifies the relative degree where band gap narrowing applies to the conduction band versus the valence band. The value of the ASYMMETRY parameter is multiplied by the total change in band gap due to band gap narrowing and that product is applied to the conduction band edge. For example, if the ASYMMETRY parameter has a value of 1.0, then the change in band gap due to band gap narrowing is applied only to the conduction band edge and the valence band edge remains unaffected. |
| BGN.E, BGN.N and BGN.C | Specify the parameters of the band gap narrowing model given in Chapter 3: “Physics”, Equation 3-46. The aliases for these parameters are V0.BGN, N0.BGN, and CON.BGN. BGN.E and BGN.N are also used in the Bennett-Wilson and del Alamo Bandgap narrowing models (see Equations 3-51 and 3-52). |
| CON.BGN | This is an alias for BGN.C. |
| EAB | Specifies acceptor energy level (see Chapter 3: “Physics”, Equation 3-55). |
| EDB | Specifies donor energy level (see Chapter 3: “Physics”, Equation 3-54). |
| F.BGN | Specifies the name of a file containing a C-INTERPRETER function for the specification of temperature, composition and doping dependent bandgap narrowing models. |
| GCB | Specifies the conduction-band degeneracy factor (see Chapter 3: “Physics”, Equation 3-54). |
| GVB | Specifies the valence-band degeneracy factor (see Chapter 3: “Physics”, Equation 3-55). |
| N0.BGN | This is an alias for BGN.N. |
| V0.BGN | This is an alias for BGN.E. |

Energy Balance Parameters

| | |
|------------------|---|
| TAUMOB.EL | Specifies the relaxation time for electrons in the temperature dependent mobility model (see Chapter 3: “Physics”, Equation 3-135). |
| TAUMOB.HO | Specifies the relaxation time for holes in the temperature dependent mobility model (Chapter 3: “Physics”, Equation 3-136). |

| | |
|---|---|
| TAUREL.EL | Specifies the relaxation time for electrons in the energy balance model (see Chapter 3: “Physics”, Equation 3-129). |
| TAUREL.HO | Specifies the relaxation time for holes in the energy balance model (see Chapter 3: “Physics”, Equation 3-130). |
| TRE.T1, TRE.T2, TRE.T3, TRE.W1, TRE.W2, TRE.W3, TRH.T1, TRH.T2, TRH.T3, TRH.W1, TRH.W2, and TRH.W3 | These are used in the temperature dependent energy relaxation time model based on table data from Laux-Fischetti Monte-Carlo simulation (see Chapter 3: “Physics”, Table 3-16). |

Hot Carrier Injection Parameters

| | |
|-----------------|--|
| IG.ELINR | Specifies the electron mean free path between redirecting collisions. The alias for this parameter is LAMRN. |
| IG.HLINR | Specifies the hole mean free path between redirecting collisions. The alias for this parameter is LAMRP. |
| IG.ELINF | Specifies the electron mean free path length for scattering by optical phonons. The alias for this parameter is LAMHN. |
| IG.HLINF | Specifies the hole mean free path length for scattering by optical phonons. The alias for this parameter is LAMHP. |
| LAMRN | This is an alias for IG.ELINR. |
| LAMRP | This is an alias for IG.HLINR. |
| LAMHN | This is an alias for IG.ELINF. |
| LAMHP | This is an alias for IG.HLINF. |

Lattice Temperature Dependence Parameters

| | |
|-----------------------------------|---|
| A.PASSLER | Specifies a parameter of the Passler temperature dependent bandgap model given in Chapter 3: “Physics”, Equation 3-39. |
| EGALPHA | Specifies the alpha coefficient for temperature dependence of bandgap (see Chapter 3: “Physics”, Equation 3-38). |
| EGBETA | Specifies the beta coefficient for temperature dependence of bandgap (see Chapter 3: “Physics”, Equation 3-38). |
| F.PDN | Uses C-Interpreter function for phonon drag contribution to the electron thermopower. |
| F.PDP | Uses C-Interpreter function for phonon drag contribution to the hole thermopower. |
| HC.A, HC.B, HC.C, and HC.D | Specify the values of the four coefficient of the heat capacity equation (see Chapter 7: “Giga: Self-Heating Simulator”, Equation 7-6). |

| | |
|--|---|
| HC.BETA, HC.C1, HC.C300, and HC.RHO | Specify user overrides for the parameters of Equation 7-7. |
| LT.TAUN | Specifies the temperature dependence for electron lifetimes (see Chapter 7: “Giga: Self-Heating Simulator”, Equation 7-31). |
| LT.TAUP | Specifies the temperature dependence for hole lifetimes (see Chapter 7: “Giga: Self-Heating Simulator”, Equation 7-32). |
| P.PASSLER | Specifies a parameter of the Passler temperature dependent bandgap model given in Chapter 3: “Physics”, Equation 3-39. |
| PCM.AEA | Specifies the activation energy for amorphization of a phase change material. |
| PCM.AP | Specifies the time exponent for amorphous change of a phase change material (see Section 7.2.9: “Phase Change Materials (PCMs)”). |
| PCM.ARHO | Specifies the amorphous resistivity of a phase change material (see Section 7.2.9: “Phase Change Materials (PCMs)”). |
| PCM.ATC | Specifies the critical temperature for amorphous change of a phase change material (see Section 7.2.9: “Phase Change Materials (PCMs)”). |
| PCM.CEA | Specifies the activation energy for crystallization of a phase change material. |
| PCM.CP | Specifies the time exponent for crystallization of a phase change material (see Section 7.2.9: “Phase Change Materials (PCMs)”). |
| PCM.CRHO | Specifies the crystalline resistivity of a phase change material (see Section 7.2.9: “Phase Change Materials (PCMs)”). |
| PCM.CTC | Specifies the critical temperature for crystallization of a phase change material (see Section 7.2.9: “Phase Change Materials (PCMs)”). |
| PCM.ATAU | Specifies the time constant for amorphous change of a phase change material (see Section 7.2.9: “Phase Change Materials (PCMs)”). |
| PCM.CTAU | Specifies the time constant for crystallization of a phase change material (see Section 7.2.9: “Phase Change Materials (PCMs)”). |
| PCM.LATHEAT | Specifies the latent of change from crystalline to amorphous state in a phase change material (see Section 7.2.9: “Phase Change Materials (PCMs)”). |
| PDA.N | Specifies the value of a parameter in the model of phonon drag contribution to the electron thermopower (see Chapter 7: “Giga: Self-Heating Simulator”, Equation 7-13). |
| PDA.P | Specifies the value of a parameter in the model of phonon drag contribution to the hole thermopower (see Chapter 7: “Giga: Self-Heating Simulator”, Equation 7-14). |

| | |
|-----------------------------|--|
| PDEXP.N | Specifies the value of a parameter in the model of phonon drag contribution to the electron thermopower (see Chapter 7: “Giga: Self-Heating Simulator”, Equation 7-13). |
| PDEXP.P | Specifies the value of a parameter in the model of phonon drag contribution to the hole thermopower (see Chapter 7: “Giga: Self-Heating Simulator”, Equation 7-14). |
| POWER | Specifies the value of thermal power generated in a power source associated with a region in THERMAL3D (see Chapter 17: “Thermal 3D: Thermal Packaging Simulator”). |
| T.PASSLER | Specifies a parameter of the Passler temperature dependent bandgap model given in Chapter 3: “Physics”, Equation 3-44. |
| TC.A, TC.B, and TC.C | Specify the three thermal conductivity coefficients (see Chapter 7: “Giga: Self-Heating Simulator”, Table 7-1). |
| TC.CONST | Specifies the equilibrium value of thermal conductivity, $k(T0)$, in Chapter 7: “Giga: Self-Heating Simulator”, Table 7-1. The synonym for this parameter is TC.CONST. TC.0 is an alias for TC.CONST. |
| TC.D | Specifies the value of the parameter D in Chapter 7: “Giga: Self-Heating Simulator”, Table 7-1. |
| TC.E | Specifies the value of the parameter E in Chapter 7: “Giga: Self-Heating Simulator”, Table 7-1. |
| TCON.CONST | Specifies that thermal conductivity should be modeled as constant with respect to temperature. The value of the thermal conductivity is given by the value of the TC.C0 parameter. |
| TCON.POWER | Specifies that the temperature dependence of thermal conductivity should be modeled using Table 7-1 in Chapter 7: “Giga: Self-Heating Simulator”. |
| TCON.POLY | Specifies that the temperature dependence of thermal conductivity should be modeled using Table 7-1 in Chapter 7: “Giga: Self-Heating Simulator”. |
| TCON.RECIP | Specifies that the temperature dependence of thermal conductivity should be modeled using Table 7-1 in Chapter 7: “Giga: Self-Heating Simulator”. |
| TC.NPOW | Specifies the value of the coefficient of temperature dependence of thermal conductivity, n , in Table 7-1 in Chapter 7: “Giga: Self-Heating Simulator”. |
| TMUN and TMUP | Specify the lattice temperature coefficients for the temperature dependence of electron lattice mobility, and of hole lattice mobility respectively. |
| UBGN.B and UBGN.C | Define the numerical values of the fitting parameters for Equation 3-50. |

Oxide Material Parameters

| | |
|--------------------|--|
| INSULATOR | Specifies that a semiconductor region is to be treated as an insulator. |
| OXCH.ONLY | Specifies that electron and hole concentrations are omitted from Poisson's Equation in oxides. |
| SEMICONDUCT | Specifies that an oxide region is to be treated as a semiconductor. |

Photogeneration Parameters

| | |
|--------------------------------------|---|
| A1.RAJ, A2.RAJ, and AD.RAJ | Specify parameters for Equation 3-529. |
| AADACHI, BADACHI, and DADACHI | These are the parameters for Adachi's refractive index model. See Chapter 3: "Physics", Equation 3-595. |
| BETA.RAJ and GAMMA.RAJ | Specify parameters in Equations 3-530 through 3-532. |
| C1.RAJ and C2.RAJ | Specify parameters of Equation 3-529. |
| E.CONDUC | Specifies the electric conductivity in all directions in mho/cm. |
| EG1.RAJ, EG2.RAJ, and EGD.RAJ | Specify parameters of Equations 3-530 through 3-532. |
| F.INDEX | Specifies the name of a file containing a C-INTERPRETER function for the specification of wavelength dependent complex index of refraction models. |
| J.ELECT | Specifies the electric current density in all directions in A/cm ² . |
| J.MAGNET | Specifies the equivalent magnetic current density in all directions in V/cm ² . |
| HNU1 and HNU2 | These are used to specify the range of energies over which to plot the complex index of refraction. You also should specify NHNU and OUT.INDEX. |
| IMAG.INDEX | Specifies the imaginary portion of the refractive index of the semiconductor (see Chapter 10: "Luminous: Optoelectronic Simulator", Equation 10-12). Wavelength dependent defaults exist for certain materials as documented in Appendix B: "Material Systems". |
| INDEX.FILE | Specifies the filename of an ASCII file from which complex refractive indices for a material are read. See Section 10.8.2: "Setting A Wavelength Dependent Refractive Index" for more information. |
| INDX.IMAG | Specifies the name of a file analogous to INDEX.FILE described above with only two columns wavelength and imaginary index. See Section 10.8.2: "Setting A Wavelength Dependent Refractive Index" for more information. |
| INDX.REAL | Specifies the name of a file analogous to INDEX.FILE described above with only two columns wavelength and real index. See Section 10.8.2: "Setting A Wavelength Dependent Refractive Index" for more information. |
| LAM1 and LAM2 | These are used to specify the range of wavelengths over which to plot the complex index of refraction. You also should specify NLAM and OUT.INDEX. |

| | |
|--|--|
| MAG.LOSS | Specifies the equivalent magnetic loss in all directions in Ω/cm . |
| NDX.ADACHI | Enables Adachi's refractive index model. See Chapter 3: "Physics", Equation 3-595. |
| NDX.SELLMEIER | Enables Sellmeier's refractive index model. See Chapter 3: "Physics", Equation 3-594. |
| NHNU | Specifies the number of energy samples between HNU1 and HNU2 to plotting the complex index of refraction. |
| NK.EV | Specifies that wavelengths included in index files specified by INDEX.FILE, INDX.IMAG, or INDX.REAL should be interpreted as energies in units of electron volts. |
| NK.NM | Specifies that wavelengths included in index files specified by INDEX.FILE, INDX.IMAG, or INDX.REAL should be interpreted as having units of nanometers. |
| NLAM | Specifies the number of wavelength samples between LAM1 and LAM2 to plotting the complex index of refraction. |
| OUT.INDEX | Specifies the root file name for output of wavelength dependent samples of complex index of refraction suitable for display in TONYPLOT (Section 10.8: "Defining Optical Properties of Materials"). |
| PERMEABILITY | Specifies the relative permeability. |
| S0SELL, S1SELL, S2SELL, L1SELL and L2SELL | These are parameters for Sellmeier's refractive index model. See Chapter 3: "Physics", Equation 3-594. |
| TLU.A, TLU.C, TLC.E0, TLU.EC, TLU.EG, and TLU.EPS | These are used to specify the parameters of the Tauc-Lorentz dielectric function model for complex index of refraction described in Section 3.10.3: "Tauc-Lorentz Dielectric Function with Optional Urbach Tail Model for Complex Index of Refraction" |

Note: The index file must be ordered by increasing wavelength.

| | |
|-------------------|---|
| REAL.INDEX | Specifies the real portion of the refractive index of the semiconductor. Wavelength dependent defaults exist for certain materials as documented in Appendix B: "Material Systems". |
|-------------------|---|

LASER Parameters

| | |
|-----------------------|---|
| ABSORPTION.SAT | Specifies the absorption saturation intensity used in the non-linear absorption loss model given in Chapter 8: "Laser: Edge Emitting Simulator", Equation 8-24. |
| ALPHAA | Specifies the bulk absorption coefficient in Chapter 8: "Laser: Edge Emitting Simulator", Equation 8-3. |
| ALPHAR | Specifies the line width broadening factor in Chapter 8: "Laser: Edge Emitting Simulator", Equation 8-3. |

| | |
|------------------------|--|
| EMISSION.FACTOR | Specifies a scale factor accounting the proportion of light directionally coupled into the lasing mode. |
| EPSINF | Specifies the high frequency relative dielectric permittivity (ϵ_{∞}) (see Chapter 8: “Laser: Edge Emitting Simulator”, Equation 8-3). If this parameter is not specified, it will be set equal to the static dielectric permittivity of the material. |
| F.ALPHAA | Specifies the name of a file containing a C-INTERPRETER function for the bulk absorption coefficient. |
| FCN | This is the free-carrier loss model parameter in Chapter 8: “Laser: Edge Emitting Simulator”, Equation 8-3. |
| FCP | This is the free-carrier loss model parameter in Chapter 8: “Laser: Edge Emitting Simulator”, Equation 8-3. |
| GAIN.SAT | Specifies the non-linear gain saturation factor used in Chapter 8: “Laser: Edge Emitting Simulator”, Equation 8-23. |
| GAIN0 | Specifies the parameter in Chapter 3: “Physics”, Sections 3.9.2: “The Default Radiative Recombination Model” and 3.9.3: “The Standard Gain Model”. |
| GAIN00 | Specifies the parameter in Chapter 3: “Physics”, Section 3.9.4: “The Empirical Gain Model”. |
| GAIN1N | Specifies the parameter in Chapter 3: “Physics”, Section 3.9.4: “The Empirical Gain Model”. |
| GAIN1P | Specifies the parameter in Chapter 3: “Physics”, Section 3.9.4: “The Empirical Gain Model”. |
| GAIN1MIN | Specifies the parameter in Chapter 3: “Physics”, Section 3.9.4: “The Empirical Gain Model”. |
| GAIN2NP | Specifies the parameter in Chapter 3: “Physics”, Section 3.9.4: “The Empirical Gain Model”. |
| GAMMA | Specifies the parameter in Chapter 3: “Physics”, Sections 3.9.2: “The Default Radiative Recombination Model” and 3.9.3: “The Standard Gain Model”. If this parameter is not specified, it will be calculated using Equation 3-539. |
| GN1 | Specifies the parameter in Chapter 3: “Physics”, Section 3.9.5: “Takayama's Gain Model”. |
| GN2 | Specifies the parameter in Chapter 3: “Physics”, Section 3.9.5: “Takayama's Gain Model”. |
| NTRANSPARENT | Specifies the parameter in Chapter 3: “Physics”, Section 3.9.5: “Takayama's Gain Model”. |

NOISE Parameters

| | |
|----------------------|---|
| F.MNSNDIFF | Specifies the name of a file containing a C-Interpreter function for the microscopic noise source for electron diffusion noise. |
| F.MNSPDIFF | Specifies the name of a file containing a C-Interpreter function for the microscopic noise source for hole diffusion noise. |
| F.MNSNFLICKER | Specifies the name of a file containing a C-Interpreter function for the microscopic noise source for electron flicker noise. |
| F.MNSPFlicker | Specifies the name of a file containing a C-Interpreter function for the microscopic noise source for hole flicker noise. |
| HOOGEN | Specifies the Hooge constant for electron flicker noise. |
| HOOGEp | Specifies the Hooge constant for hole flicker noise. |

Organic Transport Parameters

| | |
|-------------------|--|
| HOPN.BETA | Specifies the percolation constant for electrons. |
| HOPN.GAMMA | Specifies 1/carrier localization radius for electrons. |
| HOPN.V0 | Specifies the attempt-to-jump frequency for electrons. |
| HOPP.BETA | Specifies the percolation constant for holes. |
| HOPP.GAMMA | Specifies 1/carrier localization radius for holes. |
| HOPP.V0 | Specifies the attempt-to-jump frequency for holes. |

Exciton Material Parameters

| | |
|-----------------------|--|
| A.SINGLET | Specifies the singlet electron hole separation distance used in Equation 15-33. |
| DKCQ.EXCITON | Specifies the dopant concentration quenching rate. |
| DKNRS.EXCITON | Specifies the dopant non-radiative decay rate. |
| DKSS.EXCITON | Specifies the dopant bimolecular annihilation constant. |
| DOPE.SPECT | Specifies the file name of a second user defined spectrum file. See also USER.SPECT. |
| DPHEFF.EXCITON | Specifies the dopant photoluminescence quantum efficiency. |
| DRST.EXCITON | Specifies the fraction of dopant singlets formed. |
| DTAUS.EXCITON | Specifies the dopant singlet radiative decay lifetime. |
| KISC.EXCITON | Specifies the exciton intersystem crossing constant. |
| KNRS.EXCITON | Specifies the singlet non-radiative decay constant. |

| | |
|----------------------|---|
| KNRT.EXCITON | Specifies the triplet non-radiative decay constant. |
| KSP.EXCITON | Specifies the singlet-polaron constant. |
| KSS.EXCITON | Specifies the singlet-singlet constant. |
| KST.EXCITON | Specifies the singlet-triplet constant. |
| KTP.EXCITON | Specifies the triplet-polaron constant. |
| KTT.EXCITON | Specifies the triplet-triplet constant. |
| LDS.EXCITON | Specifies the singlet diffusion length. The synonym for this parameter is LD.EXCITON . |
| LDT.EXCITON | Specifies the triplet diffusion length. |
| OUT.DSPEC | Specifies the TONYPLOT compatible file name associated with the DOPE.SPECT parameter. |
| OUT.USPEC | Specifies the TONYPLOT compatible file name associated with the USER.SPECT parameter. |
| PHEFF.EXCITON | Specifies the photoluminescence quantum efficiency for the host material. |
| QE.EXCITON | Specifies the fraction of electron-hole photogeneration rate that goes to the generation of excitons. |
| QR.EXCITON | Specifies the quenching rate per unit metal density for electrode quenching. |
| RST.EXCITON | Specifies the fraction of singlets formed. |
| S.BINDING | Specifies the singlet binding energy used in Equation 15-33. |
| TAUS.EXCITON | Specifies the singlet radiative decay lifetime. The synonym for this parameter is TAU.EXCITON . |
| TAUT.EXCITON | Specifies the triplet radiative decay lifetime. |
| USER.SPECT | Specifies the file name of a user-defined spectrum file used during reverse raytrace. You can define a second user definable spectrum file using the DOPE.SPECT parameter. |

Miscellaneous Material Parameters

| | |
|---|--|
| A1, A2, A3, A4, A5 and A6 | Specify valence band effective mass parameters. |
| AC, AV and BBB | Specify cubic deformation potentials. |
| ALATTICE | Specifies the in plane lattice constant. |
| ASTR, BSTR, CSTR, DSTR, ESTR, and FSTR | These are user-definable parameters of the equations for heavy and light hole masses in Ishikawa's strain model (see Chapter 3: "Physics", Section 3.9.11: "Ishikawa's Strain Effects Model"). |
| C11, C12, C13, and C33 | Specify the elastic stiffness coefficients. |
| DEGENERACY | Specifies the spin degeneracy. |

| | |
|----------------------------------|---|
| DELTA1, DELTA2 and DELTA3 | Specify the valence band energy splits. |
| DGN.GAMMA and DGP.GAMMA | Specify the electron and hole tuning parameters for density gradient modeling. |
| DINDEXDT | Specifies the temperature coefficient of the index of refraction. |
| DRHODT | Specifies the temperature coefficient of conductor resistivity. |
| D1, D2, D3, and D4 | Specify shear deformation potentials. |
| E31, E33 and PSP | Specify piezo-electric constants. |
| EMISS.EFFI | Specifies the number of photons emitted per photon absorbed for frequency conversion materials (see Section 10.11: "Frequency Conversion Materials (2D Only)"). |
| EMISS.LAMB | Specifies the emission wavelength of the frequency conversion material described in (see Section 10.11: "Frequency Conversion Materials (2D Only)"). |
| EMISS.NANG | Specifies the number of angles evenly spaced around a circle of 360° in which emission centers emit light. |
| EMISS.NX | Specifies the number of emission centers in the x direction in a frequency conversion material. |
| EMISS.NY | Specifies the number of emission centers in the y direction in a frequency conversion material. |
| EMISS.WIDE | Specifies the width of each ray emitted in a frequency conversion material. |
| EP.MBULK | This is an energy parameter used to calculate the momentum matrix element (see Equation 3-542). |
| FB.MBULK | This is a correction factor used to calculate the momentum matrix element (see Equation 3-542). |
| HUANG.RHYS | This is a parameter of the Schenk trap assisted tunneling model. |
| LUTT1, LUTT2 and LUTT3 | Specify the luttinger parameters. |
| M.VTHN and M.VTHP | Specify the electron and hole effective masses used for calculation of thermal velocity. |
| MBULKSQ | This is the momentum matrix element. |
| MC | Specifies the conduction band effective mass. |
| MINIMA | Specifies the number of equavalent minima in the conduction band energy. |
| MHH | Specifies the heavy hole effective mass. |
| ML | Specifies the conduction band longitudinal effective mass. |
| MLH | Specifies the light hole effective mass. |
| MSO | Specifies the split off (crystal lattice) effective mass. |

| | |
|----------------------|---|
| MSTAR | Specifies the conduction band effective mass dispersion used in Equation 3-542. |
| MTT | Specifies the transverse effective mass (wurtzite). |
| MT1 and MT2 | Specify the transverse effective masses (zincblende). |
| MV | Specifies the valence band effective mass. |
| MZZ | Specifies the effective mass along the crystal axis (wurtzite). |
| PHONON.ENERGY | This is a parameter of the Schenk trap assisted tunneling model. |
| PIP.OMEGA | This is the phonon energy in eV for the Pipinys model. |
| PIP.ACC | This is the electron-phonon interaction constant for the Pipinys model. |
| PIP.ET | This is the trap depth in eV for the Pipinys model. |
| PIP.NT | This is the occupied interface state density for the Pipinys model. |
| PSP | Specifies the spontaneous polarization. |
| RESISTIVITY | Specifies the resistivity of conductor regions. |
| SO.DELTA | Specifies the spin orbital splitting energy in a quantum well. The alias for this parameter is WELL.DELTA. |
| SOPRA | Identifies the name of a file from the SOPRA database. See Section B.13.1: “SOPRA Database” |
| STABLE | Specifies the selected strain table for the Ishikawa strain effects model. See Chapter 3: “Physics”, Section 3.9.11: “Ishikawa's Strain Effects Model”. |
| TE.MODES | Specifies whether TE or TM modes will be used for calculation of asymmetry factors for the LI model. |
| USER.DEFAULT | Specifies which material the user-defined material should use for its default parameters. |
| USER.GROUP | Specifies the material group for the user-defined material. USER.GROUP can be either SEMICONDUCTOR, INSULATOR, or CONDUCTOR. |
| WELL.EPS | Specifies the high frequency permittivity used in calculating gain and radiative recombination in a quantum well. |
| WELL.GAMMA0 | Specifies the Lorentzian gain broadening factor from Chapter 3: “Physics”, Section 3.9.10: “Lorentzian Gain Broadening”. |
| WELL.TAUIIN | Specifies the Lorentzian gain broadening factor from Chapter 3: “Physics”, Section 3.9.10: “Lorentzian Gain Broadening”. |
| Z.SCHENK | This is a parameter of the Schenk trap assisted tunneling model. |

Conductor Parameters

| | |
|--------------------|--|
| DRHODT | Specifies the temperature coefficient of resistivity in $\mu\text{W}\cdot\text{cm}/\text{K}$. |
| RESISTIVITY | Specifies the material resistivity in μWcm . |

Defect Generation Material Parameters

| | |
|----------------|---|
| KD.LID | Specifies the light induced SiHD creation constant. See Chapter 14: "TFT: Thin-Film Transistor Simulator", Equation 14-52. |
| KH.LID | Specifies the disassociation constant of a hydrogen atom from a SiHD defect. See Chapter 14: "TFT: Thin-Film Transistor Simulator", Equation 14-52. |
| SIG.LID | Specifies the capture coefficient of free carriers by dangling bonds. See Chapter 14: "TFT: Thin-Film Transistor Simulator", Equation 14-52. |

Material Coefficient Definition Examples

Numbered region

This example specifies SRH lifetimes and concentration independent low-field mobilities for region number 2. All other parameters use default values and parameters in other regions are unaffected.

```
MATERIAL TAUN0=5.0E-6 TAUP0=5.0E-6 MUN=3000 MUP=500 REGION=2
```

All regions

This example defines carrier lifetimes and the refractive index for all semiconductor regions.

```
MATERIAL TAUP0=2.E-6 TAUN0=2.E-6 REAL.INDEX=3.7 \
IMAG.INDEX=1.0E-2
```

Named Material

This shows the definition of bandgap for all InGaAs regions in the structure:

```
MATERIAL MATERIAL=InGaAs EG300=2.8
```

All materials are divided into three classes: semiconductors, insulators and conductors. See Appendix B: "Material Systems" for more information about the parameters required for each material class.

Note: You can use the `MODEL PRINT` command to echo back default material parameters or `MATERIAL` parameter settings to the run-time output.

21.30: MEASURE

MEASURE extracts selected electrical data from the solution.

Note: This statement is almost obsolete. Its functions have been replaced by the `EXTRACT`, `OUTPUT`, or `PROBE` statement.

Syntax

```
MEASURE <dt> [<boundary>] [OUTFILE=<filename>]
```

| Parameter | Type | Default | Units |
|-------------|-----------|----------------|-------|
| CONTACT | Integer | | |
| E.CRIT | Real1E-8 | | |
| ELECTRON | Logical | False | |
| HOLE | Logical | False | |
| IONIZINT | Logical | False | |
| LRATIO | Real | 1.0 | |
| METAL.CH | Logical | False | |
| N.CURRENT | Logical | False | |
| N.LAYER | Real | 15 | |
| N.LINES | Integer | 50 | |
| N.RESIST | Logical | False | |
| NET.CARR | Logical | False | |
| NET.CHAR | Logical | False | |
| OUTFILE | Character | | |
| P.CURRENT | Logical | False | |
| P.RESIST | Logical | False | |
| REGIONS | Integer | All regions | |
| SUBSTR | Character | | |
| U.AUGER | Logical | False | |
| U.RADIATIVE | Logical | False | |
| U.SRH | Logical | False | |
| U.TOTAL | Logical | False | |
| X.MIN | Real | Left of device | μm |

| Parameter | Type | Default | Units |
|-----------|------|------------------|---------------|
| X.MAX | Real | Right of device | μm |
| Y.MIN | Real | Top of device | μm |
| Y.MAX | Real | Bottom of device | μm |

Description

| | |
|-----------------|---|
| dt | This is used to specify the type of information to be measured. |
| boundary | Specifies which nodes will be measured. |
| OUTFILE | Specifies a filename where simulation results and bias information will be written. |

Data Type Parameters

Net carrier concentration, charge concentration, electron concentration, or hole concentration can be integrated over a section of a device. The charge on part of an electrode can be calculated, just like the current through that part. This is useful for capacitance studies in conjunction with the difference mode of the `LOAD` statement. The resistance of a structure cross-section, such as a diffused line, can also be calculated.

| | |
|------------------|---|
| E.CRIT | Specifies the critical electric field used to calculate integration integrals. |
| ELECTRON | Extracts integrated electron concentration. |
| HOLE | Extracts integrated hole concentration. |
| IONIZINT | Enables the calculation of ionization integrals. Other integral ionization parameters will be ignored unless <code>IONIZINT</code> is specified. |
| LRATIO | Specifies the ratio between electric field lines used in ionization integral calculation. The value of this parameter should be set from 0.5 to 1.5. |
| METAL.CH | Extracts integrated charge on a contact. |
| N.CURRENT | Extracts n-current through an electrode. |
| N.LINES | Specifies the number of ionization integrals. |
| N.RESIST | Extracts n-resistance of a cross-section. |
| NET.CARR | Extracts integrated carrier concentration. |
| NET.CHAR | Extracts integrated net charge. |
| NLAYERS | Controls the distance from the contact where electric field lines start. |
| P.CURRENT | Extracts p-current through an electrode. |
| P.RESIST | Extracts p-resistance of a cross-section. |
| SUBSTR | Selects the substrate electrode for electric field lines. You don't need to specify this parameter if a substrate electrode has been defined in the <code>ELECTRODE</code> statement. |
| U.AUGER | Specifies that the integrated Auger recombination rate is to be extracted. |

| | |
|----------------------|--|
| U . RADIATIVE | Specifies that the integrated radiative recombination rate is to be extracted. |
| U . SRH | Specifies that the integrated SRH recombination rate is to be extracted. |
| U . TOTAL | Specifies that the integrated total recombination rate is to be extracted. |

Boundary Parameters

Boundary parameters: X.MIN, X.MAX, Y.MIN, and Y.MAX define a bounding box. Only nodes falling within this bounding box are included in the integration. The default bounds are the boundaries of the entire device.

| | |
|----------------|---|
| CONTACT | Specifies the contact number. For electrode quantities (current and metal charge), a contact must be selected. Only nodes falling within the bounds and belonging to the contact are included in the integration. When IONIZINT is specified, this is the electrode used to start electric field lines. |
| REGIONS | Specifies a particular set of regions. If REGIONS is specified, only nodes within the specified bounds that are part of a particular set of regions will be integrated. |
| X . MAX | Specifies the X coordinate of the right edge of the bounding box. |
| X . MIN | Specifies the X coordinate of the left edge of the bounding box. |
| Y . MAX | Specifies the Y coordinate of the top of the bounding box. |
| Y . MIN | Specifies the Y coordinate of the bottom of the bounding box. |

Resistance Example

This example extracts the resistance of a p-type line diffused into a lightly doped n-substrate. Since the p-conductivity of the substrate is negligible, the integration bounds can include the whole device.

```
MEASURE P.RESIST
```

Gate Charge Example

In this example, the charge on the lower surface of a gate electrode is integrated. There is 0.05 μm of gate oxide on the surface, which is located at $y=0$.

```
MEASURE METAL.CH CONT=1 X.MIN=-2.0 X.MAX=2.0 \
Y.MAX=-0.0499 Y.MIN=-0.0501
```

Ionization Integral Example

This example shows how to extract the maximum ionization integral in the device.

```
MEASURE IONIZINT CONTACT=3 SUSTR=4 N.LINES=200 \
NLAYERS=15 LRATIO=1.1
```

This syntax was the original implementation of ionization integrals in early ATLAS versions. It has been superseded. See Sections 21.53: “SOLVE” and 21.40: “OUTPUT” for the recommended approach to extract ionization integrals.

21.31: MESH

MESH generates a mesh or reads a previously generated mesh.

Syntax

MESH <prev>|<new> [<output>]

| Parameter | Type | Default | Units |
|--------------|-----------|----------|-------|
| ATHENA | Logical | False | |
| AUTO | Logical | False | |
| CONDUCTOR | Logical | False | |
| CYLINDRICAL | Logical | False | |
| DATAFILE.ISE | Character | | |
| DIAG.FLIP | Logical | True | |
| ELEC.BOT | Logical | False | |
| GRIDFILE.ISE | Character | | |
| FLIP.POS | Real | Midpoint | μm |
| FLIP.Y | Logical | False | |
| IN.FILE | Character | | |
| INFILE | Character | | |
| MASTER.IN | Logical | True | |
| MASTER.OUT | Logical | True | |
| MINOBTUSE | Logical | False | |
| NX | Integer | | |
| NY | Integer | | |
| NZ | Integer | | |
| OUT.FILE | Character | | |
| OUTFILE | Character | | |
| PERIODIC | Logical | False | |
| PISCES.IN | Logical | False | |
| RECTANGULAR | Logical | True | |
| SCALE | Integer | 1 | |
| SCALE.X | Integer | 1 | |
| SCALE.Y | Integer | 1 | |
| SCALE.Z | Integer | 1 | |

| Parameter | Type | Default | Units |
|------------|---------|---------|---------------|
| SMOOTH.KEY | Integer | | |
| SPACE.MULT | Real | 1.0 | |
| THREE.D | Logical | False | |
| TIF | Logical | False | |
| VERT.FLIP | Logical | False | |
| WIDTH | Real | 1.0 | μm |

Description

| | |
|---------------|--|
| prev | This is a set of parameters that allows you to read a previously generated mesh type. |
| new | This is a set of parameters that allow you to initiate the generation of a rectangular mesh. |
| output | This is a set of the parameters for saving the mesh. |

Mesh File Parameters

| | |
|---------------------|--|
| CONDUCTOR | Interprets metal regions loaded in with the <code>INFILE</code> parameter as conductors . |
| CYLINDRICAL | Specifies that the mesh being read in contains cylindrical symmetry. Since this information is not saved in the mesh file, the <code>CYLINDRICAL</code> parameter must be specified each time a structure with cylindrical symmetry is loaded. |
| DATAFILE.ISE | Specifies the name of the data file for ISE formatted structures. |
| FLIP.Y | Reverses the sign of the Y coordinate. |
| GRIDFILE.ISE | Specifies the name of the grid file for ISE formatted structures. |
| IN.FILE | This is a synonym for <code>INFILE</code> . |
| INFILE | Specifies the name of a previously generated mesh that has been saved to disk. The synonym for this parameter is <code>IN.FILE</code> . |
| MASTER.IN | Specifies a filename to read mesh and doping information in the Silvaco Standard Structure File (SSF) Format. This parameter is used to read ATHENA or DEVEDIT structure files. Typically, these files contain all <code>REGION</code> , <code>ELECTRODE</code> , and <code>DOPING</code> information. Although ATLAS allows you to modify the structure using these statements, this parameter is true by default and is the only file format supported by Silvaco. |
| PISCES.IN | Indicates that the mesh file is in the old PISCES-II format. This is not recommended or supported by Silvaco. |
| SCALE | Specifies a scale factor by which all X, Y, and Z coordinates are multiplied. |
| SCALE.X | Specifies a scale factor by which all X coordinates are multiplied. |

| | |
|---------------------|--|
| SCALE . Y | Specifies a scale factor by which all X and Y coordinates are multiplied. |
| SCALE . Z | Specifies a scale factor by which all Z coordinates are multiplied. |
| SPACE . MULT | This is a scale factor that is applied to all specified grid spacings. This parameter can be used to produce a coarse mesh and thereby reduce the simulation time. |
| ATHENA | Reads mesh and doping data generated by the ATHENA PISCES-II format file. This parameter and file format is obsolete. |

Mesh Parameters

| | |
|--------------------|--|
| AUTO | Specifies that mesh lines will be generated automatically from REGION statements. See Chapter 9: “VCSEL Simulator”, “Specifying the Mesh” Section on page 9-9 for more information on how to specify mesh lines. |
| CYLINDRICAL | Specifies that the mesh contains cylindrical symmetry. The exact meaning also depends on the state of the THREE . D parameter. If THREE . D is not set, the simulation will assume that a 2D mesh in X and Y coordinates is rotated by 360° about the Y axis. In this case, do not define mesh locations with negative X coordinates. Also, note that if such a structure is saved and re-loaded in subsequent simulations, the state of the CYLINDRICAL flag is lost and should be specified in each successive input deck. |
| DIAG . FLIP | Flips the diagonals in a square mesh about the center of the grid. If the parameter is negated, using DIAG . FLIP is specified, all diagonals will be in the same direction. |
| FLIP . POS | Works with DIAG . FLIP. If FLIP . POS is specified, the change of mesh diagonal direction occurs at the nearest mesh X coordinate to the value specified by FLIP . POS. If it is not specified, then the default value used is the average X coordinate of the device. |
| MINOBTUSE | Minimizes the generation of obtuse triangles during the 3D cylindrical meshing (see Section 2.6.9: “Specifying 3D Cylindrical Structures”). |
| NX | Specifies the number of nodes in the X direction. |
| NY | Specifies the number of nodes in the Y direction. |
| NZ | Specifies the number of nodes in the Z direction, used in DEVICE3D only. |
| PERIODIC | Specifies the left and right edges of the device will be modeled as periodic (i.e., the solution along the right edge wraps around to the left edge and vice-versa). |
| RECTANGULAR | Initiates the generation of a rectangular mesh. |
| THREE . D | Starts ATLAS3D. |
| TIF | Specifies that structure file is in TIF format. |
| VERT . FLIP | Flips the direction of mesh triangle diagonals. In other words, the diagonals of the mesh are mirrored in the vertical direction. This also works in the XY plane for 3D structures generated within ATLAS. |
| WIDTH | Specifies a scale factor to represent the un-simulated dimension for 2D simulations. This scale factor is applied to all run time and log file outputs. |

Output Parameters

| | |
|-------------------|---|
| OUT.FILE | This is a synonym for OUTFILE . |
| OUTFILE | Specifies the output filename to which the mesh is written. The synonym for this parameter is OUT.FILE . |
| MASTER.OUT | Specifies the format of the output file. This parameter is <code>true</code> by default so the output file will conform to the Silvaco Standard Structure File Format and can be plotted in TONYPLOT. |
| SMOOTH.KEY | <p>Specifies a smoothing index. The digits of the index are read in reverse order and interpreted as follows:</p> <ul style="list-style-type: none"> • Triangle smoothing. All region boundaries remain fixed. • Triangle smoothing. Only material boundaries are maintained. • Node averaging. • Improved triangle smoothing method. This method uses diagonal flipping to reduce the number of obtuse triangles. • Triangle smoothing by flipping diagonals according to electric field. <p>Usually option 1 is sufficient. Option 2 is useful only if a device has several regions of the same material and the border between different regions is unimportant. Option 3 is not recommended when the initial mesh is basically rectangular, such as mesh information usually obtained from SSUPREM4. Option 4 is similar to Option 1 but Option 4 usually creates less obtuse triangles.</p> |

Mesh Definition Example

This example initiates a rectangular mesh and stores the mesh in file, `MESH1.STR`.

```
MESH RECTANGULAR NX=40 NY=17 OUTF=MESH1.STR
```

ATHENA Interface Example

This syntax reads in a mesh from ATHENA or DEVEDIT:

```
MESH INFILE=NMOS.STR
```

When the **auto-** interface feature is used in DECKBUILD, the program will automatically insert the **MESH** statement to load the result of previous programs into ATLAS.

Note: See Chapter 2: "Getting Started with ATLAS", Sections 2.6.1: "Interface From ATHENA" and 2.6.2: "Interface From DevEdit", or the on-line examples for details of the interfaces from ATHENA or DEVEDIT to ATLAS.

21.32: METHOD

METHOD sets the numerical methods to be used to solve the equations and parameters associated with the these algorithms.

Syntax

METHOD <gp> <mdp>

| Parameter | Type | Default | Units |
|-------------|---------|--|------------------|
| 2NDORDER | Logical | True | |
| ACONTINU | Real | 0.5 | |
| ALT.SCHRO | Logical | False | |
| ATRAP | Real | 0.5 | |
| AUTONR | Logical | False | |
| BICGST | Logical | False | |
| BLOCK | Logical | False | |
| BLOCK.TRAN | Logical | False | |
| BQP.ALTEB | logical | false | |
| BQP.NMIX | Real | 1 | |
| BQP.NOFERMI | logical | false | |
| BQP.PMIX | Real | 1 | |
| BQPX.TOL | Real | 2.5×10^{-7} | |
| BQPR.TOL | Real | 1.0×10^{-26} (2D) 1.0×10^{-18} (3D) | |
| CARRIERS | Real | 2 | |
| C.ITLIMIT | Integer | 500 | |
| C.STABIL | Real | 1.0×10^{-10} | |
| C.RESID | Real | 1.0×10^{-8} | |
| CLIM.DD | Real | 4.5×10^{13} | cm^{-3} |
| CLIM.EB | Real | 0 | cm^{-3} |
| CLIM.LAT | Real | 10^5 | cm^{-3} |
| CLIMIT | Real | 10000 | |
| CONT.RHS | Logical | True | |
| CONTINV | Logical | True | |
| CR.TOLER | Real | 5.0×10^{-18} | |

| Parameter | Type | Default | Units |
|---------------|---------|-----------------------|-------|
| CUR.PROJ | Logical | False | |
| CX.TOLER | Real | 1.0×10^{-5} | |
| DIRECT | Logical | False | |
| DG.INIT | logical | false | |
| DG.N.INIT | logical | false | |
| DG.P.INIT | logical | false | |
| DT.MAX | Real | 2000 | s |
| DT.MIN | Real | 1.0×10^{-25} | s |
| DTUPDATE | Real | 10^{-9} | K |
| DVLIMIT | Real | 0.1 | |
| DVMAX | Real | 2.5 | V |
| EF.TOL | Real | 10^{-12} | |
| ELECTRONS | Logical | True | |
| ETR.TOLE | Real | 100 | |
| ETX.TOLE | Real | | |
| EXTRAPOLATE | Logical | False | |
| FAIL.QUIT | Logical | False | |
| FAIL.SAFE | Logical | True | |
| FGCNTRL | Logical | True | |
| FILL.LEVEL | Real | 0 | |
| FILL.RATIO | Real | 0.5 | |
| FIX.QF | Logical | False | |
| GCARR.ITLIMIT | Real | 1 | |
| GCON.ITLIMIT | Real | 0 | |
| GMRES | Logical | False | |
| GUM.INIT | Integer | 15 | |
| GUMITS | Integer | 100 | |
| GUMMEL | Logical | False | |
| GUMMEL.NEWTON | Logical | False | |
| HALFIMPLICIT | Logical | False | |
| HCIR.TOL | Real | 5.0×10^{-11} | |

| Parameter | Type | Default | Units |
|---------------|---------|-----------------------|-------|
| HCIX.TOL | Real | 5.0×10^{-4} | |
| HCTE.THERM | Logical | False | |
| HOLES | Logical | True | |
| ICCG | Logical | False | |
| IR.TOL | Real | 5.0×10^{-15} | |
| ITLIMIT | Integer | 25 | |
| IX.TOL | Real | 2.0×10^{-5} | |
| LAS.PROJ | Logical | False | |
| LTR.TOLE | Real | 100 | |
| LTX.TOLE | Real | | |
| LU1CRI | Real | 3.0×10^{-3} | |
| LU2CRI | Real | 3.0×10^{-2} | |
| L2NORM | Logical | True | |
| MAXTRAPS | Integer | 4 | |
| MAX.TEMP | Real | 2000 | K |
| MEINR | Logical | False | |
| MIN.TEMP | Real | 120 | K |
| NBLOCKIT | Integer | 15 | |
| NEG.CONC | Logical | False | |
| NEW.EI | Logical | False | |
| NEWTON | Logical | True | |
| NITGUMM | Integer | 5 | |
| NOGRADMSTAR | Logical | False | |
| NT0 | Integer | 4 | |
| NT1 | Integer | 10 | |
| NT2 | Integer | 25 | |
| NT3 | Integer | 100 | |
| NRCRITER | Real | 0.1 | |
| NO.POISSON | Logical | False | |
| PC.FILL_LEVEL | Real | 0 | |
| PC.SCALE | Real | 1 | |

| Parameter | Type | Default | Units |
|---------------|---------|-----------------------|-------|
| PCM | Logical | False | |
| PR.TOLER | Real | 1.0×10^{-26} | |
| PRECONDIT | Real | 0 | |
| PX.TOLER | Real | 1.0×10^{-5} | |
| RAT.FGCNTRL | Real | 1.0 | |
| RATIO.TIME | Real | 0.2 | |
| RHSNORM | Logical | False | |
| RXNORM | Logical | True | |
| QMAX.FGCNTRL | Real | 100.0 | Q |
| QUASI | Logical | True | |
| SEMIIMPLICIT | Logical | False | |
| SINGLEPOISSON | Logical | False | |
| STACK | Integer | 4 | |
| SP.NUMITER | Integer | 30 | |
| SP.NUMOSC | Integer | 30 | |
| SP.STAOSC | Integer | 3 | |
| SP.MINDIF | Real | 1.0×10^{-3} | |
| SPEEDS | Logical | False | |
| TAUTO | Logical | True | |
| TCR.TOL | Real | 100 | |
| TCX.TOL | Real | | |
| TLR.TOL | Real | 100 | |
| TLX.TOL | Real | | |
| TMIN.FACT | Real | 0.4 | |
| TOL.LTEMP | Real | 0.001 | |
| TOL.RELAX | Real | 1 | |
| TOL.TIME | Real | 5.0×10^{-3} | |
| TRAP | Logical | True | |
| TSTEP.INCR | Real | 2.0 | |
| TTNMA | Real | 60000.0 | K |
| TTPMA | Real | 60000.0 | K |

| Parameter | Type | Default | Units |
|-------------|---------|----------------------|-------|
| V.TOL | Real | 1.0×10^{-6} | |
| VSATMOD.INC | Real | 0.01 | |
| XNORM | Logical | False | |
| WEAK | Real | 200 | |
| ZIP.BICGST | Logical | False | |

Description

The **METHOD** statement is used to set the numerical methods for subsequent solutions. All structure and model definitions should precede the **METHOD** statement and all biasing conditions should follow it. Parameters in the **METHOD** statement are used to set the solution technique, specify options for each technique and tolerances for convergence.

Solution Method Parameters

| | |
|----------------------|--|
| ALT.SCHRO | Specifies that the alternative Schrodinger solver should be used. |
| BLOCK | Specifies that the block Newton solution method will be used as a possible solution method in subsequent solve statements until otherwise specified. The Block method only has meaning when either lattice heating or energy balance is included in the simulation. For isothermal drift diffusion simulations, BLOCK is equivalent to NEWTON . |
| BLOCK.TRAN | Specifies that the block Newton solution method will be used in subsequent transient solutions. |
| BICGST | Switches from the default ILUCGS iterative solver to the BICGST iterative solver for 3D simulations. |
| DIRECT | Specifies that a direct linear solver will be used to solve the linear problem during 3D simulation. By default, the ILUCGS iterative solver is used for 3D problems. |
| FILL.LEVEL | Specifies the fill level for the ILUK preconditioner (PRECONDIT =1) used by the ZIP.BIGST iterative solver. |
| FILL.RATIO | Specifies the fill ratio for the ILUP preconditioner (PRECONDIT =2) used by the ZIP.BIGST iterative solver. |
| GMRES | Switches from the default ILUCGS iterative solver to the GMRES iterative solver for 3D simulations. |
| GUMMEL | Specifies the Gummel method will be used as a solution method in subsequent SOLVE statements until otherwise specified. If other methods (BLOCK or NEWTON) are specified in the same METHOD statement, each solution method will be applied in succession until convergence is obtained. The order that the solution methods will be applied is GUMMEL then BLOCK then NEWTON . If no solution methods are specified NEWTON is applied by default. |
| GUMMEL.NEWTON | Specifies that a NEWTON solution will always be performed after a GUMMEL solution, even if GUMMEL has converged for all equations. |

| | |
|---------------------|---|
| HALFIMPLICIT | Specifies that a semi-implicit scheme will be used for transient solutions in 3D. In most cases this method is significantly less time consuming than the default TR-BDF method. |
| MEINR | Specifies the Meinerzhagens Method, whereby carrier temperature equations will be coupled with the associated carrier continuity equation and used during GUMMEL iterations. |
| NEWTON | Specifies that Newton's method will be used as the solution method in subsequent SOLVE statements unless specified otherwise. Certain models and boundary conditions settings require that the Newton's method is used. If no solution methods are specified, NEWTON is applied by default. |
| NEW.EI | Enables an alternative eigenvalue solver that obtains eigenvectors using the reverse iteration method. |
| PRECONDIT | Specifies the preconditioner used by the ZIP.BIGST iterative solver. PRECONDIT=0 specifies the ILU preconditioner (default). 1 specifies ILUK and 2 specifies ILUP. |
| SPEEDS | Specifies that the SPEEDS direct linear solve will be used. |
| ZIP.BICGST | Specifies that the ZIP library version of the BICGST iterative solver will be used for 3D solution. |

Note: Details on the different solution methods can be found in Chapter 20: "Numerical Techniques".

Equation Solver Parameters

| | |
|------------------|---|
| CARRIERS | Specifies the number of carrier continuity equations that will be solved. Valid values are 0, 1 and 2. CARRIERS=0 implies that only Poisson's Equation will be solved. CARRIERS=1 implies that only one carrier solution will be obtained. When this is specified, also specify either HOLES or ELECTRONS. CARRIERS=2 implies that solutions will be obtained for both electrons and holes. |
| ELECTRONS | Specifies that only electrons will be simulated for single carrier simulation. |
| HOLES | Specifies that only holes will be simulated for single carrier simulations. |

Solution Tolerance Parameters

The default convergence criteria used in ATLAS consists of a combination of relative and absolute values. The program will converge if either criterion is met. This is particularly useful when low-carrier concentrations would not converge using just relative criteria.

Current convergence criteria are also used. Terminal currents are monitored at each iteration and overall convergence is allowed if currents converge along with absolute potential error.

| | |
|-----------------|--|
| BQPX.TOL | This is the convergence criterion for the update vector in the BQP model. |
| BQPR.TOL | This is the convergence criterion for the Right hand side (residual) in the BQP model. |
| CR.TOLER | Specifies an absolute tolerance for the continuity equation. |

| | |
|-------------------------------|--|
| CX.TOL or C.TOL | This is the relative tolerance for the continuity equation. The XNORM parameter uses the CX.TOL and PX.TOL parameters to calculate convergence criteria. |
| EF.TOL | Specifies the Schrodinger solver tolerance when NEW.EI is specified. |
| ETR.TOLE | This is an alias for TCR.TOL . |
| ETX.TOLE | This is an alias for TCX.TOL . |
| HCIR.TOL | This is the absolute current convergence criteria for energy transport models. |
| HCIX.TOL | This is the relative current convergence criteria for energy transport models. |
| IR.TOL | Specifies absolute current convergence criteria. |
| IX.TOL | Specifies relative current convergence criteria. |
| LTR.TOLE | This is an alias for TLR.TOL . |
| LTX.TOLE | This is an alias for TLX.TOL . |
| PR.TOLER | Specifies an absolute tolerance for the Poisson Equation. |
| PX.TOL | This is the relative tolerance for the potential equation. The XNORM parameter uses the CX.TOL and PX.TOL parameters to calculate convergence criteria. |
| RHSNORM | Specifies that only absolute errors will be used to determine convergence. If RHSNORM is selected Poisson error are measured in C/ μm and the continuity error is measured in A/ μm . |
| RXNORM | Specifies that both relative and absolute convergence criteria will be used in the solution method. This is the equivalent of specifying both XNORM and RHSNORM . This is the default and it is not recommended to change this. |
| TCR.TOL | Specifies the absolute (RHSNORM) tolerance for convergence of the carrier temperature equations. The alias for this parameter is ETR.TOL . |
| TCX.TOL | Specifies the relative (XNORM) tolerance for convergence of the carrier temperature equations. The alias for this parameter is ETX.TOL . |
| TOL.TIME | Specifies maximum local truncation error for transient simulations. |
| TOL.LTEMP | Specifies the temperature convergence tolerance in block iterations using the lattice heat equation. |
| TOL.RELAX | Specifies a relaxation factor for all six Poisson, continuity, and current convergence parameters (PX.TOL , CX.TOL , PR.TOL , CR.TOL , IX.TOL , and IR.TOL). |
| TLR.TOL | Specifies the relative (XNORM) tolerance for convergence of the lattice temperature equation. The alias for this parameter is LTR.TOL . |
| TLX.TOL | Specifies the relative (XNORM) tolerance for convergence of the lattice temperature equation. The alias for this parameter is LTX.TOL . |
| WEAK | Specifies the multiplication factor for weaker convergence tolerances applied when current convergence is obtained. |
| XNORM | Specifies that only the relative errors will be used to determine convergence for the drift-diffusion equations. If XNORM is used Poisson updates are measured in kT/q. and carrier updates are measured relative to the local carrier concentration. |

Note: Generally, the solution tolerances should not be changed. Convergence problems should be tackled by improving the mesh or checking the model and method combinations. Chapter 2: “Getting Started with ATLAS” has useful hints.

General Parameters

| | |
|--|---|
| ACONTINU | This is an alias for ATRAP . |
| ATRAP | Specifies the multiplication factor which reduces the electrode bias steps when a solution starts to diverge. This parameter has no effect unless the TRAP parameter is specified. The alias for this parameter for ACONTINU . |
| BQP.NMIX and BQP.PMIX | Specify a mixing parameter with value between 0 and 1, which causes relaxation of fermi-dirac factor for electron and holes in the BQP model. |
| CLIM.DD | This is analogous to CLIMIT except it is expressed in a dimensional value representing the minimum carrier concentration that can be resolved. |
| CLIM.EB | This can be treated as a regularization parameter for the case of very small carrier concentrations for energy balance simulation. It specifies the minimum value of carrier concentration for which the relaxation term in the energy balance equation will still be properly resolved. Carrier temperatures for points where the concentration is much less than CLIM.EB , will tend to the lattice temperature. |
| CLIM.LAT | Specifies the minimum resolvable carrier concentration for Joule heating calculation. |
| CLIMIT | Specifies a concentration normalization factor. See Chapter 20: “Numerical Techniques”, the “Carrier Concentrations and CLIM.DD (CLIMIT)” Section on page 20-8 for a complete description. |
| CONT.RHS | This is an alias for TRAP . |
| CONTINU | This is an alias for TRAP . |
| CUR.PROJ | Enables the use of projection method for initial guesses with current boundary conditions. |
| DTUPDATE | Specifies the change in local temperature during lattice heating simulations, which local composition and temperature dependent physical models (such as mobility and bandgap) are recalculated. |
| FAIL.QUIT | Requires that premature due to excessive trapping during continuation will exit the simulator. |
| FAIL.SAFE | Requires that premature exit from a static ramp due to compliance or excessive trapping during continuation will exit with the device in the last converged state. |
| FIX.QF | Fixes the quasi-Fermi potential of each non-solved for carrier to a single value, instead of picking a value based on local bias. |
| FGCNTRL | Enables the FGCG model stabilisation algorithm for addition of charge to floating gate. |

| | |
|-------------------------------------|---|
| HCTE.THERM | Specifies that hot carrier simulation will use a thermodynamically correct Joule heating term. This term has the form $(\bar{J}_n \cdot \bar{J}_n)/(\mu_n N)$ rather than the default $(J_n \cdot E)$. |
| ITLIMIT or GITLIMIT | Specifies the maximum number of allowed outer loops (Newton loops or Gummel continuity iterations). |
| K.SHIFT | Specifies the energy shift applied to the input imaginary index spectrum in electron volts. |
| LAS.PROJ | Extrapolates that photon rates for the initial guess during bias ramp. |
| MAXTRAPS | Specifies the number of times the trap procedure will be repeated in case of divergence. The value of MAXTRAPS may range from 1 to 10. The alias for this parameter is STACK. |
| MIN.TEMP and MAX.TEMP | These are specified to control the absolute range of lattice temperatures allowed during Gummel loop iterations with lattice temperature. These parameters help insure that lattice temperatures converge during the outer loop iterations. |
| N.SHIFT | Specifies the energy shift applied to the input real index spectrum in electron volts. |
| NBLOCKIT | Specifies the maximum number of BLOCK iterations. If METHOD BLOCK NEWTON is specified, the solver will switch to Newton's method after NBLOCKIT Block-Newton iterations. |
| NEG.CONC | This flag allows negative carrier concentrations. |
| NK.SHIFT | Specifies the energy shift applied to the complex index of refraction in electron volts. |
| NO.POISSON | This flag allows you to omit the solution of the Poisson's Equation (see Chapter 3: "Physics", Equation 3-1). This feature doesn't work with Gummel's Method (see Chapter 20: "Numerical Techniques", Section 20.5.2: "Gummel Iteration"). |
| NOGRADMSTAR | Specifies that the gradient of the log of the effective mass will be omitted from drift-diffusion and hydrodynamic/energy balance calculations. This may help convergence properties. |
| PC.FILL_LEVEL | Specifies the fill level to be used in the ZIP.BICGST iterative solver. |
| PC.SCALE | Specifies the scaling method to be used in the ZIP.BICGST iterative solver. |
| PCM | Sets certain models and parameter values for optimal simulation of phase change materials (see Table 7-12). |
| QMAX.FGCNTRL | Threshold charge parameter for FGCNTRL stabilization algorithm. |
| RAT.FGCNTRL | Step size ratio parameter for FGCNTRL stabilization algorithm. |
| STACK | This is an alias for MAX.TRAPS. |
| TMIN.FACT | Specifies the minimum electron or hole temperature allowable during non-linear iteration updates. TMIN.FACT is normalized to 300K. |

| | |
|--------------------|---|
| TRAP | Specifies that if a solution process starts to diverge, the electrode bias steps taken from the initial approximation are reduced by the multiplication factor ATRAP. The aliases for this parameter is CONT.RHS and CONTINU. |
| TTNMA | Specifies the maximum allowable electron carrier temperature. |
| TTPMA | Specifies the maximum allowable hole carrier temperature. |
| VSATMOD.INC | Specifies that the derivatives of the negative differential mobility (MODEL FLDMOB EVSATMOD=1) will not be included into the Jacobian until the norm of Newton update for potential is less than the value specified by VSATMOD.INC. This is useful since the negative differential mobility model is highly nonlinear and causes numerical stability problems. |

Gummel Parameters

| | |
|--|---|
| DVLIMIT | Limits the maximum potential update for a single loop. |
| GCARR.ITLIMIT | Specifies the maximum number of iterations that the carrier continuity equations will solve when using GUMMEL. |
| GCON.ITLIMIT | Specifies the number of extra GUMMEL loop iterations that will be performed after all equations have converged. |
| GUM.INIT | Specifies the maximum number of Gummel iterations in order to obtain an initial approximation for successive Newton iterations. This parameter is used when METHOD GUMMEL NEWTON is specified |
| GUMITS | Specifies the maximum number of Gummel iterations. |
| LU1CRI, LU2CRI | Specifies amount of work per Poisson loop. The inner norm is required to either decrease by at least LU1CRI before returning, or reach a factor of LU2CRI below the projected Newton error, whichever is smaller. If the inner norm is exceeds the projected Newton error, the quadratic convergence is lost. |
| SINGLEPOISSON | Specifies that only a single Poisson iteration is to be performed per Gummel loop. In the default state, the continuity equation is only treated after the Poisson iteration has fully converged. This technique is useful where the carrier concentration and potential are strongly coupled but the initial guess is poor precluding the use of NEWTON. |
| NITGUMM, NT0, NT1, NT2, and NT3 | Specify Gummel iteration control parameters described in Chapter 20: “Numerical Techniques”, Section 20.5.10: “Detailed Convergence Criteria”. |

Newton Parameters

| | |
|---------------------|--|
| 2NDORDER | Specifies that second-order discretization will be used when transient simulations are performed. |
| AUTONR | Implements an automated Newton-Richardson procedure, which attempts to reduce the number of LU decompositions per bias point. We strongly recommend that you use this parameter to increase the speed of NEWTON solutions. Iterations using AUTONR will appear annotated with an A in the run-time output. Often an extra iteration is added when using this parameters since the final iteration of any converged solution cannot be done using AUTONR . |
| DT . MAX | Specifies the maximum time-step for transient simulation. |
| DT . MIN | Specifies the minimum time-step for transient simulations. |
| DVMAX | Sets the maximum allowed potential update per Newton iteration. Large voltage steps are often required when simulating high voltage devices. If any simulation requires voltage steps of 10V or more, set DVMAX to 100,000. Reducing DVMAX may serve to damp oscillations in solutions in some cases leading to more robust behavior. Excessive reduction, however, in DVMAX is not recommended since the maximum voltage step allowed will be limited by DVMAX*ITLIMIT . The alias for this parameter is N . DVLIM . |
| EXTRAPOLATE | Specifies the use of second-order extrapolation to compute initial estimates for successive time-steps for transient simulations. |
| L2NORM | Specifies the use of L2 error norms rather than infinity norms when calculating time steps for transient simulations. |
| NRCRITER | Specifies the ratio by which the norm from the previous Newton loop must decrease in order to be able to use the same Jacobian (LU decomposition) for the current Newton loop. |
| N . DVLIM | This is an alias for DVMAX . |
| RATIO . TIME | Specifies the minimum time step ratio allowed in transient simulations. If the calculated time step divided by the previous time step is less than RATIO . TIME , ATLAS will cut back the transient solution instead of continuing on to the next time point. |
| TAUTO | Selects automatic, adaptive timesteps for transient simulations from local truncation error estimates. Automatic time-stepping is the default for second-order discretization, but is not allowed for first-order. |
| TSTEP . INCR | Specifies the maximum allowable ratio between the time step sizes of successive (increasing) time steps during transient simulation. |
| QUASI | Specifies a quasistatic approximation for transient simulations. This is useful in simulating transient simulations with long timescales where the device is in equilibrium at each timestep. |

Quantum Parameters

| | |
|--------------------|--|
| BQP.NOFERMI | Forces the BQP model to only use its formulation derived using Maxwell Boltzmann statistics. If this is not set, then the BQP formulation used will be the same as the carrier statistics specified for the electrons or holes or both. |
| BQP.ALTEB | Enables an alternative iteration scheme that can be used when solving the BQP equation and the energy balance equation. This may produce a more robust convergence than for the default scheme. The scheme used with BQP.ALTEB set, however, will be slower. |
| DG.INIT | Enables an algorithm to initialize the Density Gradient method within the SOLVE INIT statement. This is not self-consistent with the solution of Poisson's equation, which makes it limited in usefulness. You can specify the carrier type to be initialized using either DG.N.INIT or DG.P.INIT. DG.INIT will enable both DG.N.INIT and DG.P.INIT. |
| SP.NUMITER | Sets the maximum number of Schrodinger-, NEGF- or DDMS-Poisson iterations, after which ATLAS proceeds to the next bias point. |
| SP.NUMOSC | The number of previous Schrodinger-Poisson iterations, whose residual is compared to the residual of the current iteration in order to check whether the residual is oscillating. |
| SP.STAOSC | The number of Schrodinger-Poisson iteration, after which ATLAS starts checking for oscillatory behavior of the residual. |
| SP.MINDIF | Minimum difference between logarithm of current and previous residuals of Schrodinger-Poisson below which the residual is regarded as oscillating and ATLAS proceeds to the next bias point. |

Numerical Method Definition Example

The default numerical method is the equivalent of:

```
METHOD NEWTON CARRIERS=2
```

For more complex problems including those involving floating regions the following is recommended

```
METHOD GUMMEL NEWTON GUM.INIT=5
```

When impact ionization is combined with floating regions as in SOI or guard ring breakdown simulation the above syntax can also be used. Quicker solutions, however, can be obtained using the following SINGLEPOISSON technique:

```
METHOD GUMMEL NEWTON GUM.INIT=5 SINGLE
```

TRAP Parameter Example

This example illustrates the trap feature (often used to capture knees of I-V curves for junction breakdown).

The first SOLVE statement solves for the initial, zero bias case. In the second SOLVE statement, we attempt to solve for V2=3 volts and V3=5 volts. If such a large bias change caused the solution algorithms to diverge for this bias point, the bias steps would be multiplied by ATRAP (0.5).

An intermediate point (V2=1.5 volts, V3=2.5 volts) would be attempted before trying to obtain V2=3 volts and V3=5 volts again. If the intermediate point can not be solved for either case, then the program will continue to reduce the bias step (the next would be V2=0.75 volts and V3=1.25 volts) up to MAXTRAPS times.

```
METHOD TRAP ATRAP=0.5
SOLVE INIT
SOLVE V2=3 V3=5 OUTFILE=OUTA
```

Transient Method Example

In this transient simulation example, second-order discretization is used (by default), but the required LTE (10^{-3}) is smaller than the default. Since the Jacobian is exact for the second part (BDF-2) of the composite timestep, there should be very few factorizations for the BDF-2 interval when AUTONR is specified.

```
METHOD NEWTON TOL.TIME=1E-3 AUTONR
```

Note: For recommendations on METHOD parameters for different simulations, see Chapter 2: “Getting Started with ATLAS” or the on-line examples.

21.33: MOBILITY

MOBILITY allows specification of mobility model parameters.

Syntax

```
MOBILITY [NUMBER=<n>] [REGION=<n>] [MATERIAL=<name>]
        [NAME=<region_name>] <parameters>
```

| Parameter | Type | Default | Units |
|--------------|---------|-----------------------|------------------------|
| A.BROOKS | Real | 1.56×10^{21} | $(\text{cm V s})^{-1}$ |
| ACCN.SF | Real | 0.87 | |
| ACCP.SF | Real | 0.87 | |
| ALBRCT.N | Logical | False | |
| ALBRCT.P | Logical | False | |
| AL1N.WATT | Real | -0.16 | |
| AL1P.WATT | Real | -0.296 | |
| AL2N.WATT | Real | -2.17 | |
| AL2P.WATT | Real | -1.62 | |
| AL3N.WATT | Real | 1.07 | |
| AL3P.WATT | Real | 1.02 | |
| ALPHAN | Real | 0.0 | |
| ALPHAN.ARORA | Real | -0.57 | |
| ALPHAN.CAUG | Real | 0.0 | |
| ALPHAP | Real | 0.0 | |
| ALPHAP.ARORA | Real | -0.57 | |
| ALPHAP.CAUG | Real | 0.0 | |
| ALPHAN.FLD | Real | 2.4×10^7 | cm/s |
| ALPHAP.FLD | Real | 2.4×10^7 | cm/s |
| ALPHA1N.KLA | Real | 0.68 | |
| ALPHA1P.KLA | Real | 0.719 | |
| ALPHAN.TAS | Real | 2 | |
| ALPHAP.TAS | Real | 3.4 | |
| ALPHN.CVT | Real | 0.680 | |
| ALPHP.CVT | Real | 0.71 | |

| Parameter | Type | Default | Units |
|-------------|---------|------------------------|------------------|
| ALN.CVT | Real | 6.85×10^{-21} | |
| ALP.CVT | Real | 7.82×10^{-21} | |
| ALPN.UM | Real | 0.68 | |
| ALPP.UM | Real | 0.719 | |
| AN.PLBRCT | Real | | |
| AN.CCS | Real | 4.61×10^{17} | cm^{-3} |
| AN.CVT | Real | 2.58 | |
| AN.IIS | Real | 4.61×10^{17} | cm^{-3} |
| AP.IIS | Real | 1.0×10^{17} | cm^{-3} |
| ANALYTIC.N | Logical | False | |
| ANALYTIC.P | Logical | False | |
| AP.CCS | Real | 1.0×10^{17} | cm^{-3} |
| AP.CVT | Real | 2.18 | |
| ARORA.N | Logical | False | |
| ARORA.P | Logical | False | |
| ASN.YAMA | Real | 1.54×10^{-5} | cm/V |
| ASP.YAMA | Real | 5.35×10^{-5} | cm/V |
| B.BROOKS | Real | 7.63×10^{19} | cm^{-3} |
| B1N.TAS | Real | 1.75 | |
| B1P.TAS | Real | 1.5 | |
| B2N.TAS | Real | -0.25 | |
| B2P.TAS | Real | -0.3 | |
| BETAN | Real | 2.0 | |
| BETAP | Real | 1.0 | |
| BETAN.ARORA | Real | -2.33 | |
| BETAP.ARORA | Real | -2.33 | |
| BETAN.CAUG | Real | -2.3 | |
| BETAP.CAUG | Real | -2.2 | |
| BETAN.CVT | Real | 2.00 | |
| BETAP.CVT | Real | 2.00 | |
| BETAN.TAS | Real | 2 | |

| Parameter | Type | Default | Units |
|-----------|---------|------------------------|---|
| BETAP.TAS | Real | 1 | |
| BN.CCS | Real | 1.52×10^{15} | cm^{-3} |
| BP.CCS | Real | 6.25×10^{14} | cm^{-3} |
| BN.CVT | Real | 4.75×10^7 | $\text{cm}/(\text{K} \cdot \text{s})$ |
| BN.IIS | Real | 1.52×10^{15} | cm^{-3} |
| BN.LSM | Real | 4.75×10^7 | $\text{cm}^2/(\text{V} \cdot \text{s})$ |
| BP.CVT | Real | 9.925×10^6 | $\text{cm}/(\text{K} \cdot \text{s})$ |
| BP.IIS | Real | 6.25×10^{14} | cm^{-3} |
| BP.LSM | Real | 9.925×10^6 | $\text{cm}^2/(\text{V} \cdot \text{s})$ |
| CA.KLA | Real | 0.50 | |
| CCSMOB.N | Logical | False | |
| CCSMOB.P | Logical | False | |
| CD.KLA | Real | 0.21 | |
| CONMOB.N | Logical | False | |
| CONMOB.P | Logical | False | |
| CVT.N | Logical | False | |
| CVT.P | Logical | False | |
| CN.ARORA | Real | 1.432×10^{17} | cm^{-3} |
| CN.CVT | Real | 1.74×10^5 | |
| CN.LSM | Real | 1.74×10^5 | |
| CN.UCHIDA | Real | 0.78125 | $\text{cm}^2/\text{Vsum}^6$ |
| CP.ARORA | Real | 2.67×10^{17} | cm^{-3} |
| CP.CVT | Real | 8.842×10^5 | |
| CP.LSM | Real | 8.842×10^5 | |
| CP.UCHIDA | Real | 0.78125 | $\text{cm}^2/\text{Vsum}^6$ |
| CRN.CVT | Real | 9.68×10^{16} | cm^{-3} |
| CRN.LSM | Real | 9.68×10^{16} | cm^{-3} |
| CRP.CVT | Real | 2.23×10^{17} | cm^{-3} |
| CRP.LSM | Real | 2.23×10^{17} | cm^{-3} |

| Parameter | Type | Default | Units |
|-------------|-----------|-------------------------|---|
| CSN.CVT | Real | 3.43×10^{20} | cm^{-3} |
| CSN.LSM | Real | 3.43×10^{20} | cm^{-3} |
| CSP.CVT | Real | 6.10×10^{20} | cm^{-3} |
| CSP.LSM | Real | 6.10×10^{20} | cm^{-3} |
| D.CONWELL | Real | 1.04×10^{21} | $(\text{cm} \times \text{Vs})^{-1}$ |
| DELN.CVT | Real | 5.82×10^{14} | V/s |
| DELP.CVT | Real | 2.0546×10^{14} | V/s |
| DELTAN.CAUG | Real | 0.73 | |
| DELTAP.CAUG | Real | 0.70 | |
| DEVICE | Character | | |
| DP.CVT | Real | 1/3 | |
| DN.CVT | Real | 1/3 | |
| DN.LSM | Real | 3.58×10^{18} | $\text{cm}^2 / (\text{V} \cdot \text{s})$ |
| DN.TAS | Real | 3.2×10^{-9} | |
| DP.LSM | Real | 4.1×10^{15} | $\text{cm}^2 / (\text{V} \cdot \text{s})$ |
| DP.TAS | Real | 2.35×10^{-9} | |
| EON | Real | 4.0×10^3 | V/cm |
| E1N.SHI | Real | 6.3×10^3 | V/cm |
| E2N.SHI | Real | 0.77×10^6 | V/cm |
| EOP | Real | 4.0×10^3 | V/cm |
| E1P.SHI | Real | 8.0×10^3 | V/cm |
| E2P.SHI | Real | 3.9×10^5 | V/cm |
| ECRITN | Real | 4.0×10^3 | V/cm |
| ECRITP | Real | 4.0×10^3 | V/cm |
| ECN.MV | Real | 6.48×10^4 | V/cm |
| ECP.MV | Real | 1.87×10^4 | V/cm |
| EGLEY.N | Logical | False | |
| EGLEY.P | Logical | False | |
| EGLEY.R | Real | 2.79 | |

| Parameter | Type | Default | Units |
|------------|---------|------------------------|------------------|
| EN.CVT | Real | 1.0 | |
| EP.CVT | Real | 1.0 | |
| ESRN.TAS | Real | 2.449×10^7 | |
| ESRP.TAS | Real | 1.0×10^9 | |
| ETAN.CVT | Real | 0.0767 | |
| ETAP.CVT | Real | 0.123 | |
| ETAN | Real | | |
| ETAN.WATT | Real | 0.50 | |
| ETAP.WATT | Real | 0.33 | |
| EVSATMOD | Real | 0 | |
| EX1N.SHI | Real | 0.3 | |
| EX1P.SHI | Real | 2.9 | |
| EXN1.ARO | Real | -0.57 | |
| EXN1.LSM | Real | 0.680 | |
| EXN2.ARO | Real | -2.33 | |
| EXN2.LSM | Real | 2.0 | |
| EXN3.ARO | Real | 2.546 | |
| EXN3.LSM | Real | 2.5 | |
| EXN4.LSM | Real | 0.125 | |
| EXN8.LSM | Real | | |
| EXP1.ARO | Real | -0.57 | |
| EXP1.LSM | Real | 0.71 | |
| EXP2.ARO | Real | -2.33 | |
| EXP2.LSM | Real | 2.0 | |
| EXP3.ARO | Real | 2.546 | |
| EXP3.LSM | Real | 2.2 | |
| EXP4.LSM | Real | 0.0317 | |
| EXP8.LSM | Real | | |
| EXP.WATT.N | Logical | False | |
| EXP.WATT.P | Logical | False | |
| F.CONWELL | Real | 7.452×10^{13} | cm^{-2} |

| Parameter | Type | Default | Units |
|--------------|-----------|----------------------|------------------------------------|
| F.CONMUN | Character | | |
| F.CONMUP | Character | | |
| F.ENMUN | Character | | |
| F.ENMUP | Character | | |
| F.LOCALMUN | Character | | |
| F.LOCALMUP | Character | | |
| F.TOFIMUN | Character | | |
| F.TOFIMUP | Character | | |
| F.MUNSAT | Character | | |
| F.MUPSAT | Character | | |
| F.VSATN | Character | | |
| F.VSATP | Character | | |
| FBH.KLA | Real | 3.828 | |
| FCW.KLA | Real | 2.459 | |
| FELN.CVT | Real | 1.0×10^{50} | $V^2 / (\text{cm} \cdot \text{s})$ |
| FELP.CVT | Real | 1.0×10^{50} | $V^2 / (\text{cm} \cdot \text{s})$ |
| FLDMOB.N | Logical | False | |
| FLDMOB.P | Logical | False | |
| FLDMOB | Integer | 0 | |
| GAMMAN | Real | 4.0 | |
| GAMMAP | Real | 1.0 | |
| GAMMAN.ARORA | Real | 2.546 | |
| GAMMAP.ARORA | Real | 2.546 | |
| GAMMAN.CAUG | Real | -3.8 | |
| GAMMAP.CAUG | Real | -3.7 | |
| GAMN.CVT | Real | 2.5 | |
| GAMP.CVT | Real | 2.2 | |
| GN.YAMA | Real | 8.8 | |
| GP.YAMA | Real | 1.6 | |
| GSURFN | Real | 1.0 | |
| GSURFP | Real | 1.0 | |
| HOPMOB.N | Logical | False | |

| Parameter | Type | Default | Units |
|-------------|-----------|---------|---|
| HOPMOB.P | Logical | False | |
| HVSATMOD | Real | 0 | |
| KAPPAN.CVT | Real | 1.7 | |
| KAPPAP.CVT | Real | 0.9 | |
| KLA.N | Logical | False | |
| KLA.P | Logical | False | |
| INVN.SF | Real | 0.75 | |
| INVP.SF | Real | 0.75 | |
| MATERIAL | Character | | |
| ME.KLA | Real | 1.0 | |
| MH.KLA | Real | 1.258 | |
| MIN.NHANCE | Real | 0.1 | |
| MIN.PHANCE | Real | 0.1 | |
| MMNN.UM | Real | 52.2 | $\text{cm}^2 / (\text{V} \cdot \text{s})$ |
| MMNP.UM | Real | 44.9 | $\text{cm}^2 / (\text{V} \cdot \text{s})$ |
| MMXN.UM | Real | 1417.0 | $\text{cm}^2 / (\text{V} \cdot \text{s})$ |
| MMXP.UM | Real | 470.5 | $\text{cm}^2 / (\text{V} \cdot \text{s})$ |
| MOBMOD.N | Real | 1 | |
| MOBMOD.P | Real | 1 | |
| MOD.WATT.N | Logical | False | |
| MOD.WATT.P | Logical | False | |
| MREF1N.WATT | Real | 481.0 | $\text{cm}^2 / (\text{V} \cdot \text{s})$ |
| MREF1P.WATT | Real | 92.8 | $\text{cm}^2 / (\text{V} \cdot \text{s})$ |
| MREF2N.WATT | Real | 591.0 | $\text{cm}^2 / (\text{V} \cdot \text{s})$ |
| MREF2P.WATT | Real | 124.0 | $\text{cm}^2 / (\text{V} \cdot \text{s})$ |
| MREF3N.WATT | Real | 1270.0 | $\text{cm}^2 / (\text{V} \cdot \text{s})$ |
| MREF3P.WATT | Real | 534.0 | $\text{cm}^2 / (\text{V} \cdot \text{s})$ |
| MSTI.PHOS | Logical | False | |
| MTN.ALPHA | Real | 0.68 | |
| MTN.BETA | Real | 2.0 | |

| Parameter | Type | Default | Units |
|------------|------|------------------------|---|
| MTN.CR | Real | 9.68×10^{-16} | cm^{-3} |
| MTN.CS | Real | 3.34×10^{20} | cm^{-3} |
| MTN.MAX | Real | 1417 | $\text{cm}^2 / (\text{Vs})$ |
| MTN.MIN1 | Real | 52.2 | $\text{cm}^2 / (\text{Vs})$ |
| MTN.MIN2 | Real | 52.2 | $\text{cm}^2 / (\text{Vs})$ |
| MTN.MU1 | Real | 43.4 | $\text{cm}^2 / (\text{Vs})$ |
| MTN.PC | Real | 0.0 | cm^{-3} |
| MTP.ALPHA | Real | 0.719 | |
| MTP.BETA | Real | 2.0 | |
| MTP.CR | Real | 2.23×10^{17} | cm^{-3} |
| MTP.CS | Real | 6.1×10^{20} | cm^{-3} |
| MTP.MAX | Real | 470.5 | $\text{cm}^2 / (\text{Vs})$ |
| MTP.MIN1 | Real | 44.9 | $\text{cm}^2 / (\text{Vs})$ |
| MTP.MIN2 | Real | 0.0 | $\text{cm}^2 / (\text{Vs})$ |
| MTP.MU1 | Real | 29.0 | $\text{cm}^2 / (\text{Vs})$ |
| MTP.PC | Real | 9.23×10^{-16} | cm^{-3} |
| MU0N.SHI | Real | 1430.0 | $\text{cm}^2 / (\text{V} \cdot \text{s})$ |
| MU0P.SHI | Real | 500.0 | $\text{cm}^2 / (\text{V} \cdot \text{s})$ |
| MU1N.ARORA | Real | 88.0 | $\text{cm}^2 / (\text{V} \cdot \text{s})$ |
| MU1P.ARORA | Real | 54.3 | $\text{cm}^2 / (\text{V} \cdot \text{s})$ |
| MU2N.ARORA | Real | 1252.0 | $\text{cm}^2 / (\text{V} \cdot \text{s})$ |
| MU2P.ARORA | Real | 407.0 | $\text{cm}^2 / (\text{V} \cdot \text{s})$ |
| MU1N.CAUG | Real | 55.24 | $\text{cm}^2 / (\text{V} \cdot \text{s})$ |
| MU1P.CAUG | Real | 49.7 | $\text{cm}^2 / (\text{V} \cdot \text{s})$ |
| MU2N.CAUG | Real | 1429.23 | $\text{cm}^2 / (\text{V} \cdot \text{s})$ |
| MU2P.CAUG | Real | 479.37 | $\text{cm}^2 / (\text{V} \cdot \text{s})$ |
| MU0N.CVT | Real | 52.2 | $\text{cm}^2 / (\text{V} \cdot \text{s})$ |
| MU0P.CVT | Real | 44.9 | $\text{cm}^2 / (\text{V} \cdot \text{s})$ |

| Parameter | Type | Default | Units |
|------------|------|---------|---|
| MU1N.CVT | Real | 43.4 | $\text{cm}^2 / (\text{V} \cdot \text{s})$ |
| MU1P.CVT | Real | 29.0 | $\text{cm}^2 / (\text{V} \cdot \text{s})$ |
| MUBN.TAS | Real | 1150 | |
| MUBP.TAS | Real | 270 | |
| MUDEG.N | Real | 1.0 | |
| MUDEG.P | Real | 1.0 | |
| MULN.YAMA | Real | 1400.0 | $\text{cm}^2 / (\text{V} \cdot \text{s})$ |
| MULP.YAMA | Real | 480.0 | $\text{cm}^2 / (\text{V} \cdot \text{s})$ |
| MUMAXN.CVT | Real | 1417.0 | $\text{cm}^2 / (\text{V} \cdot \text{s})$ |
| MUMAXP.CVT | Real | 470.5 | $\text{cm}^2 / (\text{V} \cdot \text{s})$ |
| MUMAXN.KLA | Real | 1417.0 | $\text{cm}^2 / (\text{V} \cdot \text{s})$ |
| MUMAXP.KLA | Real | 470.5.0 | $\text{cm}^2 / (\text{V} \cdot \text{s})$ |
| MUMINN.KLA | Real | 52.2 | $\text{cm}^2 / (\text{V} \cdot \text{s})$ |
| MUMINP.KLA | Real | 44.9 | $\text{cm}^2 / (\text{V} \cdot \text{s})$ |
| MUN | Real | 1000 | $\text{cm}^2 / (\text{V} \cdot \text{s})$ |
| MUN.MAX | Real | 1429.23 | $\text{cm}^2 / (\text{V} \cdot \text{s})$ |
| MUN.MIN | Real | 55.24 | $\text{cm}^2 / (\text{V} \cdot \text{s})$ |
| MUN0.LSM | Real | 52.2 | $\text{cm}^2 / (\text{V} \cdot \text{s})$ |
| MUN1.ARO | Real | 88.0 | $\text{cm}^2 / (\text{V} \cdot \text{s})$ |
| MUN2.ARO | Real | 1252.0 | $\text{cm}^2 / (\text{V} \cdot \text{s})$ |
| MUN1.LSM | Real | 43.4 | $\text{cm}^2 / (\text{V} \cdot \text{s})$ |
| MUN2.LSM | Real | 1417.0 | $\text{cm}^2 / (\text{V} \cdot \text{s})$ |
| MUP | Real | 500 | $\text{cm}^2 / (\text{V} \cdot \text{s})$ |
| MUP.MAX | Real | 479.37 | $\text{cm}^2 / (\text{V} \cdot \text{s})$ |
| MUP.MIN | Real | 49.7 | $\text{cm}^2 / (\text{V} \cdot \text{s})$ |
| MUP0.LSM | Real | 44.9 | $\text{cm}^2 / (\text{V} \cdot \text{s})$ |
| MUP1.ARO | Real | 54.3 | $\text{cm}^2 / (\text{V} \cdot \text{s})$ |
| MUP1.LSM | Real | 29.0 | $\text{cm}^2 / (\text{V} \cdot \text{s})$ |

| Parameter | Type | Default | Units |
|--------------|-----------|-------------------------------|---|
| MUP2.ARO | Real | 407.0 | $\text{cm}^2 / (\text{V} \cdot \text{s})$ |
| MUP2.LSM | Real | 470.5 | $\text{cm}^2 / (\text{V} \cdot \text{s})$ |
| N.ANGLE | Real | 0.0 | Degrees |
| N.BETA0 | Real | 1.109 (CANALI) 0.6 (MEINR) | |
| N.BETAEXP | Real | 0.66 (CANALI) 0.01 (MEINR) | |
| N.BROOKS | Logical | False | |
| N.CANALI | Logical | False | |
| N.CONWELL | Logical | False | |
| N.LCRIT | Real | 1.0 | cm |
| N.MASETTI | Logical | False | |
| N.MEINR | Logical | False | |
| N2N.TAS | Real | 1.1×10^{21} | |
| N2P.TAS | Real | 1.4×10^{18} | |
| N1N.TAS | Real | 2.0×10^{19} | |
| N1P.TAS | Real | 8.4×10^{16} | |
| NAME | Character | | |
| NCRITN.ARORA | Real | 1.432×10^{17} | cm^{-3} |
| NCRITP.ARORA | Real | 2.67×10^{17} | cm^{-3} |
| NCRITN.CAUG | Real | 1.072×10^{17} | cm^{-3} |
| NCRITP.CAUG | Real | 1.606×10^{17} | cm^{-3} |
| NEWCVT.N | Logical | False | |
| NEWCVT.P | Logical | False | |
| NHANCE | Logical | False | |
| NREF1N.KLA | Real | 9.68×16 | cm^{-3} |
| NREF1P.KLA | Real | 2.23×17 | cm^{-3} |
| NREFD.KLA | Real | 4.0×20 | cm^{-3} |
| NREFA.KLA | Real | 7.2×20 | cm^{-3} |
| NREFN | Real | 1.072×10^{17} | cm^{-3} |

| Parameter | Type | Default | Units |
|------------|---------|-------------------------------|------------------|
| NREFN.YAMA | Real | 3.0×10^{16} | cm^{-3} |
| NREFP | Real | 1.606×10^{17} | cm^{-3} |
| NREFP.YAMA | Real | 4.0×10^{16} | cm^{-3} |
| NRFN.UM | Real | 9.68×10^{16} | cm^{-3} |
| NRFP.UM | Real | 2.23×10^{17} | cm^{-3} |
| NUN | Real | -2.3 | |
| NUP | Real | -2.2 | |
| OLDSURF.N | Logical | False | |
| OLDSURF.P | Logical | False | |
| OXLEFTN | Real | | μm |
| OXLEFTP | Real | | μm |
| OXRIGHTN | Real | | μm |
| OXRIGHTP | Real | | μm |
| OXBOTTOMN | Real | | μm |
| OXBOTTOMP | Real | | μm |
| P.BETA0 | Real | 1.213 (CANALI) 0.6 (MEINR) | |
| P.BETAEXP | Real | 0.17 (CANALI) 0.01 (MEINR) | |
| P.BROOKS | Logical | False | |
| P.CANALI | Logical | False | |
| P.CONWELL | Logical | False | |
| P.LCRIT | Real | 1.0 | cm |
| P.MASETTI | Logical | False | |
| P.MEINR | Logical | False | |
| P1N.SHI | Real | 0.28 | |
| P1P.SHI | Real | 0.3 | |
| P2N.SHI | Real | 2.9 | |
| P2P.SHI | Real | 1.0 | |
| P1N.TAS | Real | 0.09 | |
| P1P.TAS | Real | 0.334 | |
| P2N.TAS | Real | 4.53×10^{-8} | |

| Parameter | Type | Default | Units |
|-----------|---------|-----------------------|------------------|
| P2P.TAS | Real | 3.14×10^{-7} | |
| P.ANGLE | Real | 0.0 | Degrees |
| PC.LSM | Real | 9.23×10^{16} | cm^{-3} |
| PCN.CVT | Real | 0.0 | cm^{-3} |
| PCP.CVT | Real | 0.23×10^{16} | cm^{-3} |
| PHANCE | Logical | False | |
| PFMOB.N | Logical | False | |
| PFMOB.P | Logical | False | |
| PRINT | Logical | False | |
| R1.KLA | Real | 0.7643 | |
| R2.KLA | Real | 2.2999 | |
| R3.KLA | Real | 6.5502 | |
| R4.KLA | Real | 2.3670 | |
| R5.KLA | Real | -0.8552 | |
| R6.KLA | Real | 0.6478 | |
| RN.TAS | Real | 2 | |
| RP.TAS | Real | 3 | |
| REGION | Integer | | |
| S1.KLA | Real | 0.89233 | |
| S2.KLA | Real | 0.41372 | |
| S3.KLA | Real | 0.19778 | |
| S4.KLA | Real | 0.28227 | |
| S5.KLA | Real | 0.005978 | |
| S6.KLA | Real | 1.80618 | |
| S7.KLA | Real | 0.72169 | |
| SCHWARZ.N | Logical | False | |
| SCHWARZ.P | Logical | False | |
| SHI.N | Logical | False | |
| SHI.P | Logical | False | |
| SN.YAMA | Real | 350 | |
| SP.YAMA | Real | 81.0 | |

| Parameter | Type | Default | Units |
|------------|-----------|---------------------|-------|
| STRUCTURE | Character | | |
| SURFMOB.N | Logical | False | |
| SURFMOB.P | Logical | False | |
| TASCH.N | Logical | False | |
| TASCH.P | Logical | False | |
| TAUN.CVT | Real | 0.125 | |
| TAUP.CVT | Real | 0.0317 | |
| TETN.UM | Real | -2.285 | |
| TETP.UM | Real | -2.247 | |
| THETAN.FLD | Real | 0.8 | |
| THETAP.FLD | Real | 0.8 | |
| THETAN.KLA | Real | 2.285 | |
| THETAN.SHI | Real | 2.285 | |
| THETAP.KLA | Real | 2.247 | |
| THETAP.SHI | Real | 2.247 | |
| TMUBN.TAS | Real | 2.5 | |
| TMUBP.TAS | Real | 1.4 | |
| TMUN | Real | 1.5 | |
| TMUP | Real | 1.5 | |
| TNOMN.FLD | Real | 600.0 | K |
| TNOMP.FLD | Real | 600.0 | K |
| TN.UCHIDA | Real | 4.0 | nm |
| TP.UCHIDA | Real | 4.0 | nm |
| ULN.YAMA | Real | 4.9×10^6 | cm/s |
| ULP.YAMA | Real | 2.928×10^6 | cm/s |
| VSATN | Real | | cm/s |
| VSATP | Real | | cm/s |
| VSN.YAMA | Real | 1.036×10^7 | cm/s |
| VSP.YAMA | Real | 1.200×10^7 | cm/s |
| VTHN.PFMOB | Real | | cm/s |
| VTHP.PFMOB | Real | | cm/s |

| Parameter | Type | Default | Units |
|-------------|---------|-----------------------|-------|
| UCHIDA.N | Logical | False | |
| UCHIDA.P | Logical | False | |
| XIN | Real | -3.8 | |
| XIP | Real | -3.7 | |
| XMINN.WATT | Real | -1.0×32 | μm |
| XMAXN.WATT | Real | 1.0×32 | μm |
| YMAXN.WATT | Real | -1.0×32 | μm |
| XMINP.WATT | Real | -1.0×32 | μm |
| XMAXP.WATT | Real | 1.0×32 | μm |
| YMAXP.WATT | Real | -1.0×32 | μm |
| YCHARN.WATT | Real | 1.0×32 | μm |
| YCHARP.WATT | Real | 1.0×32 | μm |
| Z11N.TAS | Real | 0.0388 | |
| Z11P.TAS | Real | 0.039 | |
| Z22N.TAS | Real | 1.73×10^{-5} | |
| Z22P.TAS | Real | 1.51×10^{-5} | |

Description

| | |
|-----------------|--|
| MATERIAL | Specifies which material from Table B-1 in Appendix B: “Material Systems” should be applied to the MOBILITY statement. If a material is specified, then all regions defined as being composed of that material will be affected. |
|-----------------|--|

Note: You can specify the following logical parameters to indicate the material instead of assigning the MATERIAL parameter: SILICON, GAAS, POLYSILI, GERMANIU, SIC, SEMICON, SIGE, ALGAAS, A-SILICO, DIAMOND, HGCDTE, INAS, INGAAS, INP, S.OXIDE, ZNSE, ZNTE, ALINAS, GAASP, INGAP and MINASP.

| | |
|---------------|--|
| DEVICE | Specifies the device in MIXEDMODE simulation (see Chapter 12: “MixedMode: Mixed Circuit and Device Simulator”) to be applied to the MOBILITY statement. The synonym for this parameter is STRUCTURE. |
| NAME | Specifies the name of the region to be applied to the MOBILITY statement. Note that the name must match the name specified in the NAME parameter of the REGION statement or the region number. |

| | |
|------------------|---|
| REGION | Specifies the number of the region to be applied to the MOBILITY statement. |
| PRINT | Acts the same as PRINT on the MODELS statement. |
| STRUCTURE | This is a synonym for DEVICE. |

Mobility Model Flags

| | |
|--|--|
| ALBRCT.N and ALBRCT.P | Enable the Albrecht mobility model (see Chapter 5: “Blaze: Compound Material 2D Simulator”, “The Albrecht Model” Section on page 5-38). |
| ANALYTIC.N | Specifies that the analytic concentration dependent model is to be used for electrons (see Chapter 3: “Physics”, Equation 3-174). |
| ANALYTIC.P | Specifies that the analytic concentration dependent model is to be used for holes (see Chapter 3: “Physics”, Equation 3-175). |
| ARORA.N | Specifies that the Arora analytic concentration dependent model is to be used for electrons (see Chapter 3: “Physics”, Equation 3-176). |
| ARORA.P | Specifies that the Arora analytic concentration dependent model is to be used for electrons (see Chapter 3: “Physics”, Equation 3-177). |
| CONMOB.N | Specifies that doping concentration dependent model to be used for electrons. |
| CONMOB.P | Specifies that a doping concentration dependent model is to be used for holes. |
| CCSMOB.N | Specifies that carrier-carrier scattering model is to be used for electrons (see Chapter 3: “Physics”, Equations 3-180-3-184). |
| CCSMOB.P | Specifies that carrier-carrier scattering model is to be used for holes (see Chapter 3: “Physics”, Equations 3-180-3-184). |
| EGLEY.N | Enables the low field strained silicon mobility model for electrons (see Section 3.6.13: “Low-Field Mobility in Strained Silicon”). |
| EGLEY.P | Enables the low field strained silicon mobility model for holes (see Section 3.6.13: “Low-Field Mobility in Strained Silicon”). |
| EVSATMOD | <p>Specifies which parallel field dependent mobility model (see Chapter 3: “Physics”, Equation 3-274 and Chapter 5: “Blaze: Compound Material 2D Simulator”, Equation 5-59) should be used for electrons. The value of EVSATMOD should be assigned as follows:</p> <ul style="list-style-type: none"> • 0 - Use the standard saturation model (Equation 3-274). You also can apply the option parameter, MOBTEM.SIMPL (see Chapter 3: “Physics”, the “Carrier Temperature Dependent Mobility” Section on page 3-79 for more information). • 1 - Use the negative differential velocity saturation model (Equation 5-59). • 2 - Use a simple velocity limiting model. <p>In most cases, the default value of 0 should be used.</p> |

| | |
|-------------------|--|
| HVSATMOD | <p>Specifies which parallel field dependent mobility model (see Chapter 3: “Physics”, Equation 3-275 and Chapter 5: “Blaze: Compound Material 2D Simulator”, Equation 5-60) should be used for holes. The value of HVSATMOD should be assigned as follows:</p> <ul style="list-style-type: none"> 0 - Use the standard saturation model (Equation 3-275). 1 - Use the negative differential velocity saturation model (Equation 5-60). 2 - Use a simple velocity limiting model. <p>In most cases, the default value of 0 should be used.</p> |
| EXP.WATT.N | Turns on exponential modification to Watt’s mobility model for electrons (see Chapter 3: “Physics”, Equation 3-270). |
| EXP.WATT.P | Turns on exponential modification to Watt’s mobility model for holes (see Chapter 3: “Physics”, Equation 3-271). |
| FLDMOB | <p>Specifies transverse field degradation for electrons as follows:</p> <ol style="list-style-type: none"> 1. No transverse degradation. 2. Use the Watt or Tasch transverse field models depending on the settings of FIELDMOB1 and FIELDMOB2. 3. Use the Yamaguchi transverse field dependent model. 4. Use the CVT transverse field dependent model. |
| FLDMOB.N | Specifies a lateral electric field dependent model for electrons (see Chapter 3: “Physics”, Equation 3-274). |
| FLDMOB.P | Specifies a lateral electric field dependent model for holes (see Chapter 3: “Physics”, Equation 3-275). |
| KLA.N | Turns on Klaassen’s mobility model for electrons (see Chapter 3: “Physics”, Equations 3-192 through 3-217). |
| KLA.P | Turns on Klaassen’s mobility model for holes (see Chapter 3: “Physics”, Equations 3-192 through 3-217). |
| MOBMOD.N | <p>Specifies transverse field degradation for electrons as follows:</p> <ol style="list-style-type: none"> 1. No transverse degradation. 2. Use the Watt or Tasch transverse field models depending on the settings of FIELDMOB1 and FIELDMOB2. 3. Use the Yamaguchi transverse field dependent model. 4. Use the CVT transverse field dependent model. |
| MOBMOD.P | <p>Specifies transverse field degradation for holes as follows:</p> <ol style="list-style-type: none"> 1. No transverse degradation. 2. Use the Watt or Tasch transverse field models depending on the settings of FIELDMOB1 and FIELDMOB2. 3. Use the Yamaguchi transverse field dependent model. 4. Use the CVT transverse field dependent model. |
| MOD.WATT.N | Turns on modified Watt mobility model for electrons (see Chapter 3: “Physics”, Equation 3-270). |
| MOD.WATT.P | Turns on modified Watt Mobility Model for holes (see Chapter 3: “Physics”, Equation 3-271). |

| | |
|--------------------|--|
| MSTI . PHOS | Selects the parameter set for Phosphorous doping in Masetti model. For more information about this parameter, see Chapter 3: “Physics”, Tables 3-28, 3-29 and 3-30. |
| N . ANGLE | Specifies angle for application of electron mobility parameters in simulation of anisotropic mobility. |
| N . CANALI | Specifies that the Canali velocity saturation model is to be used for electrons (see Chapter 3: “Physics”, Equations 3-278 through 3-281). |
| N . CONWELL | Specifies that the Conwell-Weisskopf carrier-carrier scattering model is to be used for electrons (see Chapter 3: “Physics”, Equation 3-186). |
| N . MASETTI | Enables Masetti mobility model for electrons. For more information about this parameter, see Chapter 3: “Physics”, Tables 3-28, 3-29 and 3-30. |
| N . MEINR | Specifies that the Meinerzhagen-Engl hydrodynamic scattering model is to be used for electrons (see Chapter 3: “Physics”, Equation 3-290). |
| NEWCVT . N | Specifies that a new surface mobility degradation calculation is used in the CVT mobility model for electrons in place of the original (see Chapter 3: “Physics”, the “Darwish CVT Model” Section on page 3-65). |
| NEWCVT . P | Specifies that a new surface mobility degradation calculation is used in the CVT mobility model for holes in place of the original (see Chapter 3: “Physics”, the “Darwish CVT Model” Section on page 3-65). |
| NHANCE | Specifies that low field mobility values will be modified by mobility enhancement values contained in the mesh structure file. |
| P . ANGLE | Specifies angle for application of hole mobility parameters in simulation of anisotropic mobility. |
| P . BROOKS | Specifies that the Brooks-Herring carrier-carrier scattering model is to be used for holes (see Chapter 3: “Physics”, Equation 3-189). |
| P . CANALI | Specifies that the Canali velocity saturation model is to be used for holes (see Chapter 3: “Physics”, Equations 3-278 through 3-281). |
| P . CONWELL | Specifies that the Conwell-Weisskopf carrier-carrier scattering model is to be used for holes (see Chapter 3: “Physics”, Equation 3-186). |
| P . MASETTI | Enables Masetti mobility model for holes. For more information about this parameter, see Chapter 3: “Physics”, Tables 3-28, 3-29 and 3-30. |
| P . MEINR | Specifies that the Meinerzhagen-Engl hydrodynamic scattering model is to be used for holes (see Chapter 3: “Physics”, Equation 3-291). |
| PHANCE | Specifies that low field hole mobilities will be modified by mobility enhancement factors contained in the mesh structure file. |
| SURFMOB . N | Invokes the effective field based surface mobility model for electrons (see Equation 3-266). |
| SURFMOB . P | Invokes the effective field based surface mobility model for holes (see Equation 3-267). |
| SCHWARZ . N | Specifies the use of transverse electric field-dependent mobility models for electrons. See TFLDMB1 or SCHWARZ in the MODELS statement. |

| | |
|--------------------|--|
| SCHWARZ . P | Specifies the use of transverse electric field-dependent mobility models for holes. See TFLDMB1 or SCHWARZ in the MODELS statement. |
| SHI . N | Turns on Shirahata's Mobility Model for electrons (see Chapter 3: "Physics", Equation 3-272). |
| SHI . P | Turns on Shirahata's Mobility Model for holes (see Chapter 3: "Physics", Equation 3-273). |
| TASCH . N | Specifies a transverse electric field dependent mobility model for electrons based on Tasch [212,213] (see Chapter 3: "Physics", Equations 3-247 through 3-265). |
| TASCH . P | Specifies a transverse electric field dependent mobility model for holes based on Tasch [212,213] (see Chapter 3: "Physics", Equations 3-247 through 3-265). |

Temperature Dependent Low Field Mobility Parameters

For information about these parameters, see Chapter 3: "Physics", Table 3-24.

Albrecht Model Parameters

For information about these parameters, see Chapter 5: "Blaze: Compound Material 2D Simulator", "The Albrecht Model" Section on page 5-38.

Caughey-Thomas Concentration Dependent Model Parameters

For more information about these parameters, see Chapter 3: "Physics", Table 3-26.

Arora Concentration Dependent Mobility Model Parameters

For more information about these parameters, see Chapter 3: "Physics", Table 3-27.

Brooks Model Parameters

For more information about these parameters, see Chapter 3: "Physics", Table 3-33.

Canali Model Parameters

For more information about these parameters, see Chapter 3: "Physics", Table 3-52.

Carrier-Carrier Scattering Model Parameters

For more information about these parameters, see Chapter 3: "Physics", Table 3-31.

Conwell Model Parameters

For more information about these parameters, see Chapter 3: "Physics", Table 3-32.

Masetti Model Parameters

For more information about these parameters, see Chapter 3: "Physics", Tables 3-28, 3-29, 3-30.

Meinerzhagen-Engl Model Parameters

For more information about these parameters, see Chapter 3: "Physics", Table 3-55.

Parallel Field Dependent Model Parameters

For more information about these parameters, see Chapter 3: “Physics”, Table 3-52 and Chapter 5: “Blaze: Compound Material 2D Simulator”, Tables 5-3 and 5-10.

Perpendicular Field Dependent Model Parameters

For more information about these parameters, see Table 3-42.

Yamaguchi Transverse Field Dependent Model Parameters

For more information about these parameters, see Chapter 3: “Physics”, Table 3-47.

CVT Transverse Field Dependent Model Parameters

For more information about these parameters, see Chapter 3: “Physics”, Table 3-43.

Darwish CVT Transverse Field Dependent Model Parameters

For more information about these parameters, see Chapter 3: “Physics”, Table 3-44.

Watt Effective Transverse Field Dependent Model Parameters

For more information about these parameters, see Chapter 3: “Physics”, Table 3-49.

Tasch Mobility Model Parameters

For more information about these parameters, see Chapter 3: “Physics”, Table 3-48.

Klaassen’s Mobility Model Parameters

For more information about these parameters, see Chapter 3: “Physics”, Tables 3-35 and 3-40.

The Modified Watt Mobility Model Parameters

For more information about these parameters, see Chapter 3: “Physics”, Table 3-50.

Shirahata’s Mobility Model Parameters

For more information about these parameters, see Chapter 3: “Physics”, Table 3-51.

Uchida’s Mobility Model Parameters

For more information about these parameters, see Chapter 3: “Physics”, Table 3-41.

Poole-Frenkel Mobility Model Parameters

For more information about these parameters, see Chapter 15: “Organic Display and Organic Solar: Organic Simulators”, Table 15-6.

SCHWARZ and TASCH Transverse Field Dependent Model Parameters

| | |
|------------------|--|
| ACCN.SF | Specifies the accumulation saturation factor which describes the ratio of the electron concentration in the accumulation layer before and after bending of conductivity and valence bands for electron mobility. |
| ACCN.SF | Specifies the accumulation saturation factor which describes the ratio of the hole concentration in the accumulation layer before and after bending of conductivity and valence bands for hole mobility. |
| INVN.SF | Specifies the inversion saturation factor which describes the ratio of the electron concentration in the inversion layer before and after the bending of conductivity and valence bands for electron mobility. |
| INVN.SF | Specifies the inversion saturation factor which describes the ratio of the hole concentration in the inversion layer before and after the bending of conductivity and valence bands for hole mobility. |
| OXBOTTOMN | Specifies the coordinate of the bottom edge of the gate oxide for a MOSFET transistor for electron mobility. |
| OXBOTTOMP | Specifies the coordinate of the bottom edge of the gate oxide for a MOSFET transistor for hole mobility. |
| OXLEFTN | Specifies the coordinate of the left edge of the gate oxide for a MOSFET transistor for electron mobility. |
| OXLEFTP | Specifies the coordinate of the left edge of the gate oxide for a MOSFET transistor for hole mobility. |
| OXRIGHTN | Specifies the coordinate of the right edge of the gate oxide for a MOSFET transistor for electron mobility. |
| OXRIGHTP | Specifies the coordinate of the right edge of the gate oxide for a MOSFET transistor for hole mobility. |

Miscellaneous Mobility Model Parameters

| | |
|-------------------|--|
| EGLEY.R | Specifies the ratio of unstrained light hole mobility model to the unstrained net mobility. |
| MIN.NHANCE | Specifies the minimum electron mobility after strain enhancement relative to the unstrained value (i.e., this is the minimum of the ratio of the strain enhanced mobility to the enhanced mobility). |
| MIN.PHANCE | Specifies the minimum hole mobility after strain enhancement relative to the unstrained value (i.e., this is the minimum of the ratio of the enhanced mobility to the enhanced mobility). |

Interpreter Functions

| | |
|-------------------|---|
| F.CONMUN | Specifies the name of a file containing a C-INTERPRETER function for the specification of temperature, composition and doping dependent electron mobility model. |
| F.CONMUP | Specifies the name of a file containing a C-INTERPRETER function for the specification of temperature, composition and doping dependent hole mobility model. |
| F.ENMUN | Specifies a C-Interpreter file for the electron mobility as a function of Electron Temperature and perpendicular field as well as other choice variables. The function itself is named <code>endepmun</code> and only applies to ATLAS2D. |
| F.ENMUP | Specifies a C-Interpreter file for the hole mobility as a function of Hole Temperature and perpendicular field as well as other choice variables. The function itself is named <code>endepmup</code> and only applies to ATLAS2D. |
| F.LOCALMUN | Specifies the name of a file containing a C-Interpreter function for the specification of electron mobility, which can depend explicitly on position. |
| F.LOCALMUP | Specifies the name of a file containing a C-Interpreter function for the specification of Hole mobility, which can depend explicitly on position. |
| F.TOFIMUN | Specifies the name of a file containing a C-Interpreter function for the specification of electron mobility, which can depend on both parallel and perpendicular electric field. |
| F.TOFIMUP | Specifies the name of a file containing a C-Interpreter function for the specification of hole mobility, which can depend on both parallel and perpendicular electric field. |
| F.MUNSAT | Specifies the name of a file containing a C-INTERPRETER function for the specification of parallel field dependent electron mobility model for velocity saturation. |
| F.MUPSAT | Specifies the name of a file containing a C-INTERPRETER function for the specification of parallel field dependent hole mobility model for velocity saturation. |
| F.VSATN | Specifies the name of a file containing a C-INTERPRETER function for the specification of temperature and composition dependent electron saturation velocity models. |
| F.VSATP | Specifies the name of a file containing a C-INTERPRETER function for the specification of temperature and composition dependent electron saturation velocity models. |

Mobility Model Aliases

Aliases are available for certain parameters on the MOBILITY statement. Table 21-2 lists these aliases.

Table 21-2. Mobility Model Aliases

| Parameter | Alias | Parameter | Alias |
|--------------|----------|-------------|----------|
| MU1N.CAUG | MUN.MIN | THETAN.KLA | TETN.UM* |
| MU1P.CAUG | MUP.MIN | THETAP.KLA | TETP.UM* |
| MU2N.CAUG | MUN.MAX | MUMAXN.KLA | MMXN.UM |
| MU2P.CAUG | MUP.MAX | MUMAXP.KLA | MMXP.UM |
| BETAN.CAUG | NUN | MUMINN.KLA | MMNN.UM |
| BETAP.CAUG | NUP | MUMINP.KLA | MMNP.UM |
| DELTAN.CAUG | ALPHAN | NREF1N.KLA | NRFN.UM |
| DELTAP.CAUG | ALPHAP | NREF1P.KLA | NRFP.UM |
| GAMMAN.CAUG | XIN | ALPHA1N.KLA | ALPN.UM |
| GAMMAP.CAUG | XIP | ALPHA1P.KLA | ALPP.UM |
| NCRITN.CAUG | NREFN | BN.CVT | BN.LSM |
| NCRITP.CAUG | NREFP | BP.CVT | BP.LSM |
| MU1N.ARORA | MUN1.ARO | CN.CVT | CN.LSM |
| MU1P.ARORA | MUP1.ARO | CP.CVT | CP.LSM |
| MU2N.ARORA | MUN2.ARO | TAUN.CVT | EXN4.LSM |
| MU2P.ARORA | MUP2.ARO | TAUP.CVT | EXP4.LSM |
| ALPHAN.ARORA | EXN1.ARO | MU0N.CVT | MUN0.LSM |
| ALPHAP.ARORA | EXP1.ARO | MU0P.CVT | MUP0.LSM |
| BETAN.ARORA | EXN2.ARO | MU1N.CVT | MUN1.LSM |
| BETAP.ARORA | EXP2.ARO | MU1P.CVT | MUP1.LSM |
| GAMMAN.ARORA | EXN3.ARO | CRN.CVT | CRN.LSM |
| GAMMAP.ARORA | EXP3.ARO | CRP.CVT | CRP.LSM |
| NCRITN.ARORA | CN.ARORA | CSN.CVT | CSN.LSM |
| NCRITP.ARORA | CP.ARORA | CSP.CVT | CSP.LSM |
| AN.CCS | AN.IIS | ALPHAN.CVT | EXN1.LSM |
| AP.CCS | AP.IIS | ALPHAP.CVT | EXP1.LSM |
| BN.CCS | BN.IIS | BETAN.CVT | EXN2.LSM |
| BP.CCS | BP.IIS | BETAP.CVT | EXP2.LSM |
| P1N.SHI | EX1N.SHI | MUMAXN.CVT | MUN2.LSM |
| P1P.SHI | EX1P.SHI | MUMAXP.CVT | MUP2.LSM |

Table 21-2. Mobility Model Aliases

| Parameter | Alias | Parameter | Alias |
|-----------|----------|-----------|----------|
| ECRITN | EON | GAMN.CVT | EXN3.LSM |
| ECRITP | EOP | GAMP.CVT | EXP3.LSM |
| KN.CVT | EXN8.LSM | DELN.CVT | DN.LSM |
| KP.CVT | EXP8.LSM | DELP.CVT | DP.LSM |
| PCP.CVT | PC.LSM | | |

Note: These aliases are negated with respect to the primary parameter.

Modified Watt Model Example

The following example sets the Modified Watt Surface mobility model for MOSFETs. The `MOBILITY` statement is used to set the models and to specify the value of the depth of action of the Modified Watt model.

```
MODELS CONMOB FLDMOB SRH MIN.SURF PRINT
MOBILITY WATT.N MOD.WATT.N YMAXN.WATT=0.01
```

21.34: MODELS

MODELS specifies model flags to indicate the inclusion of various physical mechanisms, models, and other parameters such as the global temperature for the simulation.

Syntax

MODELS <mf> <gp> <mdp>

| Parameter | Type | Default | Units |
|--------------|---------|------------------------|--|
| 2DXY.SCHRO | Logical | False | |
| A.BBT.SCHENK | Real | 8.977×10^{20} | $\text{cm}^2 \text{s}^{-1} \text{V}^{-2}$ |
| A.TEMP | Logical | False | |
| ACC.SF | Real | 0.87 | |
| ALBRCT | Logical | False | |
| ALL | Logical | True | |
| ALN1 | Real | -0.160 | |
| ALN2 | Real | -2.17 | |
| ALN3 | Real | 1.07 | |
| ALP1 | Real | -0.296 | |
| ALP2 | Real | -1.62 | |
| ALP3 | Real | 1.02 | |
| ALPHA.DOS | Logical | False | |
| ALT.SCHRO | Logical | False | |
| ANALYTIC | Logical | False | |
| AR.MU1N | Real | 88 | |
| AR.MU2N | Real | 1252 | |
| AR.MU1P | Real | 54.3 | |
| AR.MU2P | Real | 407 | |
| ARORA | Logical | False | |
| ASUB | Real | 1.0 | Å |
| AUGER | Logical | False | |
| AUGGEN | Logical | False | |
| AUTOBBT | Logical | False | |
| B.BBT.SCHENK | Real | 2.14667×10^7 | $\text{eV}^{(-3/2)} \text{V} \cdot \text{cm}^{-1}$ |
| B.DORT | Real | 1.0 | |

| Parameter | Type | Default | Units |
|--------------|---------|-----------------------|-----------------------------|
| B.ELECTRONS | Real | 2 | |
| B.HOLES | Real | 1 | |
| BARLN | Real | 2.59×10^{-4} | $(V \cdot cm)^{0.5}$ |
| BARLN | Real | 2.59×10^{-4} | $(V \cdot cm)^{0.5}$ |
| BB.A | Real | 4.0×10^{14} | $cm^{-1/2} V^{-5/2} s^{-1}$ |
| BB.B | Real | 1.97×10^7 | V/cm |
| BB.GAMMA | Real | 2.5 | |
| BBT.A_KANE | Real | 3.5×10^{21} | $eV^{1/2}/cm-s-V^2$ |
| BBT.B_KANE | Real | 2.25×10^7 | $V/cm-eV^{3/2}$ |
| BBT.FORWARD | Logical | False | |
| BBT.GAMMA | Real | 2.5 | |
| BBT.HURKX | Logical | False | |
| BBT.KANE | Logical | False | |
| BBT.KL | Logical | False | |
| BBT.NLDERIVS | Logical | False | |
| BBT.NONLOCAL | Logical | False | |
| BBT.STD | Logical | False | |
| BBT1 | Logical | False | |
| BBT2 | Logical | False | |
| BBT3 | Logical | False | |
| BC.QUANT | Logical | False | |
| BGN | Logical | False | |
| BEAM.LID | Logical | False | |
| BGN2 | Logical | False | |
| BGN.ALAMO | Logical | False | |
| BGN.BENNETT | Logical | False | |
| BGN.KLA | Logical | False | |
| BGN.KLAASSEN | Logical | False | |
| BGN.SLOTBOOM | Logical | False | |
| BH.FNONOS | Real | 3.07 | eV |
| BIPOLAR | Logical | False | |

| Parameter | Type | Default | Units |
|---------------|---------|-----------------------|---------------|
| BIPOLAR2 | Logical | False | |
| BOLTZMANN | Logical | True | |
| BOUND.TRAP | Logical | False | |
| BQP.N | Logical | False | |
| BQP.P | Logical | False | |
| BQP.NALPHA | Real | 0.5 | |
| BQP.NGAMMA | Real | 1.2 | |
| BQP.NEUMANN | Logical | True | |
| BQP.PALPHA | Real | 0.5 | |
| BQP.PGAMMA | Real | 1.0 | |
| BQP.QDIR | Integer | 2 | |
| BROOKS | Logical | False | |
| BTBT | Logical | False | |
| BX | Real | 0.0 | Tesla |
| BY | Real | 0.0 | Tesla |
| BZ | Real | 0.0 | Tesla |
| C0 | Real | 2.5×10^{-10} | |
| CALC.FERMI | Logical | False | |
| CALC.STRAIN | Logical | False | |
| CARRIERS | Real | | |
| CAVITY.LENGTH | Real | | μm |
| CCS.EA | Real | 4.61×10^{17} | |
| CCS.EB | Real | 1.52×10^{15} | |
| CCS.HA | Real | 1.0×10^{17} | |
| CCS.HB | Real | 6.25×10^{14} | |
| CCSMOB | Logical | False | |
| CCSNEW | Logical | False | |
| CCSSURF | Logical | False | |
| CDL | Logical | False | |
| CGATE.N | Real | $5.0 \text{e}4$ | |
| CGATE.P | Real | $3.0 \text{e}8$ | |

| Parameter | Type | Default | Units |
|------------|-----------|----------------------|---------------|
| CHI.HOLES | Real | 4.6×10^4 | |
| CHIA | Real | 3×10^5 | |
| CHIB | Real | 5.0×10^4 | |
| CHUANG | Logical | False | |
| CONCDL | Logical | False | |
| CONMOB | Logical | False | |
| CONSRH | Logical | False | |
| CONSRH.LAW | Logical | False | |
| CONWELL | Logical | False | |
| CUBIC35 | Logical | False | See Table 5-5 |
| CVT | Logical | False | |
| D.DORT | Real | 2.5×10^{-6} | |
| DEC.C1 | Real | 0.0 | eV |
| DEC.C2 | Real | 0.0 | eV |
| DEC.C3 | Real | 0.0 | eV |
| DEC.ISO | Real | 0.0 | eV |
| DEC.D2 | Real | 0.0 | eV |
| DEC.D4 | Real | 0.0 | eV |
| DEV.HH | Real | 0.0 | eV |
| DEV.LH | Real | 0.0 | eV |
| DEV.ISO | Real | 0.0 | eV |
| DEV.SO | Real | 0.0 | eV |
| DG.N | Logical | False | |
| DG.P | Logical | False | |
| DGN.GAMMA | Real | 3.6 | |
| DGP.GAMMA | Real | 3.6 | |
| DEVDEG.E | Logical | False | |
| DEVDEG.H | Logical | False | |
| DEVDEG.B | Logical | False | |
| DEVICE | Character | | |
| DGLOG | Logical | True | |

| Parameter | Type | Default | Units |
|--------------|---------|-----------------------|-------------------------------|
| DGROOT | Logical | False | |
| DRIFT.DIFF | Logical | True | |
| DT.CBET | Logical | False | |
| DT.CUR | Logical | False | |
| DT.METH | Real | 1 | |
| DT.VBET | Logical | False | |
| DT.VBHT | Logical | False | |
| DTPP | Logical | False | |
| E.BENDING | Logical | False | |
| E.TAUR.VAR | Logical | False | |
| E0.TCOEF | Real | | |
| E0.TCOEF | Real | | |
| ECRIT | Real | 4000.0 | V/cm |
| EF.TOL | Real | 10×10^{-10} | |
| E.FGCGTUN | Logical | False | |
| EIGENS | Integer | 15 | |
| ELECTRONS | Logical | True | |
| ENERGY.STEP | Real | 0.0025 | eV |
| ERASE | Logical | False | |
| E.SC.FGCGTUN | Logical | False | |
| ESIZE.NEGF | Real | 2001 | |
| ET.MODEL | Logical | False | |
| ETA.FNONOS | Real | 1.0 | |
| ETAN | Real | 0.50 | |
| ETAP | Real | 0.33 | |
| ETA.NEGF | Real | 0.0066 | eV |
| EQUIL.NEGF | Logical | False | |
| EXCITONS | Logical | False | |
| EVSATMOD | Integer | 0 | |
| F.AE | Real | 1.82×10^{-7} | $\text{CV}^{-2}\text{s}^{-1}$ |
| F.BE | Real | 1.90×10^8 | V/cm |

| Parameter | Type | Default | Units |
|------------------|-----------|-----------------------|-------------------------------|
| F.AH | Real | 1.82×10^{-7} | $\text{CV}^{-2}\text{s}^{-1}$ |
| F.BH | Real | 1.90×10^8 | V/cm |
| F.EFEMIS | Character | | |
| F.HFEMIS | Character | | |
| F.KSN | Character | | |
| F.KSP | Character | | |
| F.PCM | Character | | |
| F.PDN | Character | | |
| F.PDP | Character | | |
| F.TRAP.COULOMBIC | Character | | |
| F.TRAP.TUNNEL | Character | | |
| FAST.EIG | Logical | False | |
| FC.ACCURACY | Real | 10^{-6} | |
| FERMIDIRAC | Logical | False | |
| FERRO | Logical | False | |
| FG.RATIO | Real | | |
| FILE.LID | Character | | |
| FIXED.FERMI | Logical | False | |
| FLDMOB | Logical | False | |
| FN.CUR | Logical | False | |
| FNHOLES | Logical | False | |
| FNHPP | Logical | False | |
| FNONOS | Logical | False | |
| FNORD | Logical | False | |
| FNPP | Logical | False | |
| FREQ.CONV | Logical | False | |
| G.EMPIRICAL | Logical | False | |
| G.STANDARD | Logical | False | |
| GAINMOD | Logical | 0 | |
| GATE1 | Logical | False | |
| GATE2 | Logical | False | |

| Parameter | Type | Default | Units |
|---------------|---------|-----------------------|--|
| GENERATE.LID | Real | 0 | $\text{cm}^{-3}\text{s}^{-1}$ |
| GR.HEAT | Logical | False | |
| HANSCHQM | Logical | False | |
| H.BENDING | Logical | False | |
| H.FGCGTUN | Logical | False | |
| H.SC.FGCGTUN | Logical | False | |
| H.TAUR.VAR | Logical | False | |
| HCTE | Logical | False | |
| HCTE.EL | Logical | False | |
| HCTE.HO | Logical | False | |
| HEAT.FULL | Logical | False | |
| HEAT.PETHOM | Logical | False | |
| HEI | Logical | False | |
| HHI | Logical | False | |
| HNSAUG | Logical | False | |
| HOLE | Logical | False | |
| HOPMOB | Logical | False | |
| HVSATMOD | Integer | 0 | |
| HW.BBT.SCHENK | Real | 0.0186 | eV |
| IG.ELINR | Real | 6.16×10^{-6} | cm |
| IG.HLINR | Real | 6.16×10^{-6} | cm |
| IG.ELINF | Real | 9.2×10^{-7} | cm |
| IG.HLINF | Real | 9.2×10^{-7} | cm |
| IG.EBETA | Real | 2.59×10^{-4} | $(\text{V} \cdot \text{cm})^{0.5}$ |
| IG.HBETA | Real | 2.59×10^{-4} | $(\text{V} \cdot \text{cm})^{0.5}$ |
| IG.EETA | Real | 2.0×10^{-5} | $\text{V}^{1/3} \cdot \text{cm}^{2/3}$ |
| IG.HTETA | Real | 2.0×10^{-5} | $\text{V}^{1/3} \cdot \text{cm}^{2/3}$ |
| IG.EEOX | Real | 9.0×10^4 | V/cm |
| IG.HEOX | Real | 9.0×10^4 | V/cm |
| IG.EB0 | Real | 3.2 | V |

| Parameter | Type | Default | Units |
|------------|---------|----------------------|----------|
| IG.HB0 | Real | 4.0 | V |
| IG.LRELE | Real | 3.0×10^{-6} | [Q=1] cm |
| IG.LRELH | Real | 2.0×10^{-6} | [Q=1] cm |
| II.NODE | Logical | False | |
| II.VALDI | Logical | False | |
| IMPACT | Logical | False | |
| INC.ION | Logical | False | |
| INCOMPLETE | Logical | False | |
| INFINITY | Real | 0.001 | |
| IONIZ | Logical | False | |
| INV.SF | Real | 0.75 | |
| ISHIKAWA | Logical | False | |
| JOULE.HEAT | Logical | True | |
| K.P | Logical | False | |
| KAUGCN | Real | | |
| KAUGCP | Real | | |
| KAUGDN | Real | | |
| KAUGDP | Real | | |
| KSRHCN | Real | | |
| KSRHCP | Real | | |
| KSRHGN | Real | | |
| KSRHGP | Real | | |
| KSRHTN | Real | | |
| KSRHTP | Real | | |
| KSN | Integer | -1 | |
| KSP | Integer | -1 | |
| KLA | Logical | False | |
| KLAAUG | Logical | False | |
| KLASRH | Logical | False | |
| L.TEMP | Logical | False | |
| LAMHN | Real | 9.2×10^{-7} | cm |

| Parameter | Type | Default | Units |
|------------------|---------|-----------------------|------------------|
| LAMHP | Real | 9.2×10^{-7} | cm |
| LAMRN | Real | 6.16×10^{-6} | cm |
| LAMRP | Real | 6.16×10^{-6} | cm |
| LAS.ABSOR_SAT | Logical | False | |
| LAS.ABSORPTION | Logical | False | |
| LAS.EFINAL | Real | | eV |
| LAS.EINIT | Real | | eV |
| LAS.ESEP | Real | | eV |
| LAS.ETRANS | Logical | False | |
| LAS.FCARRIER | Logical | False | |
| LAS.GAIN_SAT | Logical | False | |
| LAS.ITMAX | Integer | 30 | |
| LAS.LOSSES | Real | 0 | cm^{-1} |
| LAS.MIRROR | Real | 90 | % |
| LAS.MULTISAVE | Logical | False | |
| LAS.NEFF | Real | 3.57 | |
| LAS.OMEGA | Real | 2.16×10^{15} | 1/sec |
| LAS.NMODE | Integer | 1 | |
| LAS.NX | Real | | |
| LAS.NY | Real | | |
| LAS.REFLECT | Logical | False | |
| LAS.RF | Real | | |
| LAS.RR | Real | | |
| LAS.SIN | Real | 1.0×10^4 | cm^{-1} |
| LAS.SPECSAVE | Integer | 1 | |
| LAS.SPONTANEOUS | Real | | |
| LAS.TAUSS | Real | 0.05 | |
| LAS.TIMERATE | Logical | True | |
| LAS.TOLER | Real | 0.01 | |
| LAS.TRANS_ENERGY | Real | | |
| LAS.XMAX | Real | | |

| Parameter | Type | Default | Units |
|--------------|-----------|---------|---------------------|
| LAS.XMIN | Real | | |
| LAS.YMAX | Real | | |
| LAS.YMIN | Real | | |
| LAS_MAXCH | Real | 2.5 | |
| LASER | Logical | False | |
| LAT.TEMP | Logical | False | |
| LED | Logical | False | |
| LI | Logical | False | |
| LMODE | Logical | False | |
| LORENTZ | Logical | False | |
| LSMMOB | Logical | False | |
| MASS.TUNNEL | Real | 0.25 | |
| MASETTI | Logical | False | |
| MATERIAL | Character | | |
| MIN.SURF | Logical | False | |
| MOB.INCOMPL | Logical | False | |
| MOBMOD | Integer | | |
| MOBTEM.SIMPL | Logical | False | |
| MOS | Logical | False | |
| MOS2 | Logical | False | |
| MREFN1 | Real | 481.0 | cm ² /Vs |
| MREFN2 | Real | 591.0 | cm ² /Vs |
| MREFN3 | Real | 1270.0 | cm ² /Vs |
| MREFP1 | Real | 92.8 | cm ² /Vs |
| MREFP2 | Real | 124. | cm ² /Vs |
| MREFP3 | Real | 534. | cm ² /Vs |
| MIMTUN | Logical | False | |
| N.CONCANNON | Logical | False | |
| N.DORT | Logical | False | |
| N.HOTSONOS | Logical | False | |
| N.KSI.VAR | Logical | False | |

| Parameter | Type | Default | Units |
|-------------|-----------|-----------|-------|
| N.KSI_VAR | Logical | False | |
| N.NEGF_PL | Logical | False | |
| N.NEGF_PL1D | Logical | False | |
| N.QUANTUM | Logical | False | |
| N.TEMP | Logical | False | |
| NAME | Character | | |
| NEARFLG | Logical | False | |
| NEGF_CMS | Logical | False | |
| NEGF_MS | Logical | False | |
| NEGF_UMS | Logical | False | |
| NEW.EIG | Logical | False | |
| NEW.SCHRO | Logical | False | |
| NEW.DORT | Logical | False | |
| NEWIMPACT | Logical | False | |
| NI.FERMI | Logical | False | |
| NPRED.NEGF | Real | 7 | |
| NT.FNONOS | Real | 0.0 | μm |
| NUM.BAND | Real | | |
| NUM.DIRECT | Real | | |
| NUMBER | Integer | 0 | |
| NUMCARR | Real | | |
| OLDIMPACT | Logical | False | |
| OPTR | Logical | False | |
| ORTH.SCHRO | Real | 10^{-3} | |
| OX.BOTTOM | Real | 0.0 | μm |
| OX.LEFT | Real | | μm |
| OX.MARGIN | Real | 0.0003 | μm |
| OX.POISSON | Logical | False | |
| OX.RIGHT | Real | | μm |
| OX.SCHRO | Logical | False | |
| PFREQ.CONV | Logical | False | |
| P.CONCANNON | Logical | False | |

| Parameter | Type | Default | Units |
|---------------|---------|-----------------------|------------------|
| P.DORT | Logical | False | |
| P.HOTSONOS | Logical | False | |
| P.KSI_VAR | Logical | False | |
| P.KSI_VAR | Logical | False | |
| P.NEGF_PL | Logical | False | |
| P.NEGF_PL1D | Logical | False | |
| P.SCHRODING | Logical | False | |
| P.TEMP | Logical | False | |
| PASSLER | Logical | False | |
| PATH.N | Real | 3.4×10^7 | microns |
| PATH.P | Real | 2.38×10^{-7} | microns |
| PATRIN | Logical | False | |
| PCM | Logical | False | |
| PCM.LOG | Logical | True | |
| PEFF.N | Real | 3.2 | eV |
| PEFF.P | Real | 4.8 | eV |
| PF.NITRIDE | Logical | False | |
| PFMOB | Logical | False | |
| PHONONDRAG | Logical | False | |
| PHOTON.ENERGY | Real | | eV |
| PHUMOB | Logical | False | |
| PIC.AUG | Logical | False | |
| PIEZOELECTRIC | Logical | False | |
| PIEZO.SCALE | Real | 1.0 | |
| POISSON | Logical | False | |
| POLAR.CHARGE | Real | 0.0 | cm^{-2} |
| POLAR.SCALE | Real | 1.0 | |
| POLARIZATION | Logical | False | |
| POST.SCHRO | Logical | False | |
| PRINT | Logical | False | |
| PRINT.REGION | Integer | | |

| Parameter | Type | Default | Units |
|----------------|-----------|-----------------------|------------------|
| PRINT.MATERIAL | Character | | |
| PRPMOB | Logical | False | |
| PROGRAM | Logical | False | |
| PRT.BAND | Logical | False | |
| PRT.COMP | Logical | False | |
| PRT.FLAGS | Logical | False | |
| PRT.IMPACT | Logical | False | |
| PRT.RECOM | Logical | False | |
| PRT.THERM | Logical | False | |
| PSP.SCALE | Real | 1.0 | |
| PT.HEAT | Logical | False | |
| QCRIT.NEGF | Real | 3×10^{-3} | |
| QMINCONC | Real | 1.0×10^{-10} | cm^{-3} |
| QTNL.DERIVS | Logical | False | |
| QTNLSC.BBT | Logical | False | |
| QTNLSC.EL | Logical | False | |
| QTNLSC.HO | Logical | False | |
| QTUNN | Logical | False | |
| QTUNN.BBT | Logical | False | |
| QTUNN.DIR | Real | 0 | |
| QTUNN.EL | Logical | False | |
| QTUNN.HO | Logical | False | |
| QTUNNSC | Logical | False | |
| QUANTUM | Logical | False | |
| QWELL | Logical | False | |
| QWNUM | Integer | -1 | |
| QX.MAX | Real | RHS of device | μm |
| QX.MIN | Real | LHS of device | μm |
| QY.MAX | Real | Bottom of device | μm |
| QY.MIN | Real | Bottom of device | μm |

| Parameter | Type | Default | Units |
|-------------|-----------|---------|-------|
| RAJKANAN | Logical | False | |
| REGION | Integer | 0 | |
| R.ELEC | Real | 1.1 | |
| R.HOLE | Real | 0.7 | |
| S.DISSOC | Logical | False | |
| SBT | Logical | False | |
| SCHENK.BBT | Logical | False | |
| SCHENK.EL | Logical | False | |
| SCHENK.HO | Logical | False | |
| SCHENK | Logical | False | |
| SCHKSC.EL | Logical | False | |
| SCHKSC.HO | Logical | False | |
| SCHKSC | Logical | False | |
| SCHSRH | Logical | False | |
| SCHRO | Logical | False | |
| SHAPEOX | Logical | False | |
| SHI | Logical | False | |
| SHIRAMOB | Logical | False | |
| SINGLET | Logical | False | |
| SIS.EL | Logical | False | |
| SIS.HO | Logical | False | |
| SIS.REVERSE | Logical | False | |
| SIS.TAT | Logical | False | |
| SISTAT.TN | Real | 1.0e-6 | s |
| SISTAT.TP | Real | 1.0e-6 | s |
| SP.BAND | Logical | True | |
| SP.CHECK | Logical | False | |
| SP.DIR | Integer | 0 | |
| SP.EXCORR | Logical | False | |
| SP.FAST | Logical | False | |
| SP.GEOM | Character | 1DX | |
| SP.SMOOTH | Logical | True | |

| Parameter | Type | Default | Units |
|----------------|-----------|----------------------|---------------------------------|
| SPEC.NAME | Character | | |
| SPONTANEOUS | Logical | False | |
| SRH | Logical | False | |
| SRH.EXPTTEMP | Logical | False | |
| STRESS | Logical | False | |
| STRUCTURE | Character | | |
| SUBSTRATE | Logical | False | |
| SURFMOB | Logical | False | |
| TAT.NLDEPTH | Real | 0 | eV |
| TAT.NONLOCAL | Logical | False | |
| TAT.RELEI | Logical | False | |
| TAUMOB | Logical | False | |
| TAUTEM | Logical | False | |
| TAYAMAYA | Logical | False | |
| TEMPERATURE | Real | 300 | K |
| TFLDMB1 | Logical | False | |
| TFLDMB2 | Logical | False | |
| THETA.N | Real | 60.0 | degrees |
| THETA.P | Real | 60.0 | degrees |
| TIME.EP | Real | 0 | s |
| TIME.LID | Real | 0 | s |
| TLU.INDEX | Logical | False | |
| TRAP.AUGER | Logical | False | |
| TRAP.COULOMBIC | Logical | False | |
| TRAP.LID | Logical | False | |
| TRAP.TUNNEL | Logical | False | |
| TRIPLET | Logical | False | |
| TSQ.ZAIDMAN | Real | 1.1 | |
| TUNLN | Real | 2.0×10^{-5} | $V^{1/3} \cdot \text{cm}^{2/3}$ |
| TUNLP | Real | 2.0×10^{-5} | $V^{1/3} \cdot \text{cm}^{2/3}$ |
| UBGN | Logical | False | |
| UST | Logical | False | |

| Parameter | Type | Default | Units |
|--------------|---------|---------|-------|
| UNSAT.FERRO | Logical | False | |
| VALDINOCI | Logical | False | |
| WELL.CNBS | Integer | 1 | |
| WELL.DEBUG | Logical | False | |
| WELL.DENERGY | Real | 0.01 | eV |
| WELL.FIELD | Logical | True | |
| WELL.GAIN | Real | 1.0 | |
| WELL.MARGIN | Real | 0.01 | μm |
| WELL.NX | Integer | 10 | |
| WELL.NY | Integer | 10 | |
| WELL.NZ | Integer | 10 | |
| WELL.OVERLAP | Real | | |
| WELL.VNBS | Integer | 1 | |
| YAMAGUCHI | Logical | False | |
| YAN | Logical | False | |
| ZAIDMAN | Logical | False | |
| ZAMDMER | Logical | False | |

Description

| | |
|------------|--|
| mf | This is one or more of the model flags described on the next page. |
| gp | This is one or more of the general parameters described in the “General Parameters” Section on page 21-257. These parameters are used to specify general information used during the simulation. |
| mdp | This is one or more of the model dependent parameters described in the “Model Dependent Parameters” Section on page 21-260. |

Mobility Model Flags

| | |
|-----------------|---|
| ALBRCT | Enables the Albrecht mobility model for electrons and holes (see Chapter 5: “Blaze: Compound Material 2D Simulator”, Equation 5-140). |
| ANALYTIC | Specifies an analytic concentration dependent mobility model for silicon which includes temperature dependence (see Chapter 3: “Physics”, Equations 3-174 and 3-175). |
| ARORA | Specifies an analytic concentration and temperature dependent model according to Arora (see Chapter 3: “Physics”, Equations 3-176 and 3-177). |

| | |
|-------------------------|---|
| BROOKS | Enables the Brooks-Herring mobility model for both electrons and holes (Chapter 3: “Physics”, Equation 3-189). |
| CCSMOB | Specifies carrier-carrier scattering model according to Dorkel and Leturq (see Chapter 3: “Physics”, Equations 3-180-3-184). |
| CONMOB | Specifies that a concentration dependent mobility model be used for silicon and gallium arsenide. This model is a doping versus mobility table valid for 300K only. |
| CVT | Specifies that the CVT transverse field dependent mobility model is used for the simulation. The alias for this parameter is <code>LSMMOB</code> . |
| FLDMOB | Specifies a lateral electric field-dependent model (see Chapter 3: “Physics”, Equation 3-274 and Chapter 5: “Blaze: Compound Material 2D Simulator”, Equation 5-57). The <code>EVSATMOD</code> parameter may be used to define which field dependent equation is used. |
| HOPMOB | Specifies that the hopping mobility model will be used for electrons and holes (see Chapter 15: “Organic Display and Organic Solar: Organic Simulators”). |
| KLA | Specifies that the Klaassen Mobility Model (see Chapter 3: “Physics”, Equations 3-192-3-217) will be used for electrons and holes. |
| LSMMOB | This is an alias for <code>CVT</code> . |
| MASETTI | Enables the Masetti mobility model for electrons and holes (see Chapter 3: “Physics”, Equations 3-178 and 3-179). |
| MIN.SURF | Specifies that the <code>WATT</code> , <code>TASCH</code> , or <code>SHI</code> mobility models should only apply to minority carriers. |
| MOBMOD | Specifies mobility degradation by longitudinal electric field only (<code>MOBMOD=1</code>), or by both longitudinal and transverse electric fields (<code>MOBMOD=2</code>). When <code>MOBMOD=2</code> , specify the <code>ACC.SF</code> , <code>INV.SF</code> , <code>OX.BOTTOM</code> , <code>OX.LEFT</code> , and <code>OX.RIGHT</code> parameters. This parameter is only used with <code>TFLDMB1</code> and <code>TFLDMB2</code> . |
| MOB.INCOMPL | Causes the low field mobility models having a dependence on doping level to depend on ionized dopant density rather than total dopant density. See “Incomplete Ionization and Doping Dependent Mobility” Section on page 3-55. |
| PF.NITRIDE | Enables a model for steady-state conduction in Silicon-Nitride that behaves like Poole-Frenkel emission at high fields. |
| PFGMOB | Specifies that the Poole-Frenkel mobility model will be used for electrons and holes (see Chapter 15: “Organic Display and Organic Solar: Organic Simulators”). |
| PHUMOB | This is an alias for <code>KLA</code> . |
| PRPMOB | Enables the perpendicular field dependent mobility model as described in Equations 3-220 and 3-221. |
| SHIRAMOB | Specifies that the Shirahata Mobility Model (see Chapter 3: “Physics”, Equation 3-273) will be used for electrons and holes. |
| SURFGMOB or WATT | Invokes the effective field based surface mobility model (see Chapter 3: “Physics”, Equations 3-266 and 3-267). <code>SURFGMOB</code> parameters are used in the calculation of surface mobility according to the Watt Model [247]. Do not specify this parameter unless <code>S-PISCES</code> is installed on your system. |

| | |
|----------------------------------|---|
| TFLDMB1 or SCHWARZ | Specifies the use of transverse electric field-dependent mobility models. The electron model is based on the Schwarz and Russe equations [204] and is implemented in [212]. The hole model, which is used only when MOBMOD =2, is based on the Watt and Plummer equations [248]. |
| TFLDMB2 or TASCH | Specifies a transverse electric field dependent mobility model for electrons and holes based on a semi-empirical equation [212, 213]. |
| YAMAGUCHI | Specifies that the Yamaguchi transverse field dependent mobility model is used in the simulation. |

Note: See Section 21.33: “MOBILITY” for alternative ways to set mobility models.

Recombination Model Flags

| | |
|---|--|
| AUGER | Specifies Auger recombination (see Chapter 3: “Physics”, Equation 3-330). |
| AUGGEN | Specifies that the Auger recombination model will be used as a generation and a recombination term. |
| CDL , CONCDL | Enables the Coupled defect level recombination model. CONCDL additionally enables concentration dependence of the recombination lifetimes used in this model. |
| CONSRH | Specifies Shockley-Read-Hall recombination using concentration dependent lifetimes (see Equations 3-296, 3-297, and 3-298). |
| CONSRH.LAW | Enables the concentration dependent Shockley-Read-Hall recombination model using the alternate parameter set given in Table 3-60. |
| HNSAUG | Enables Auger recombination model that has co-efficients depending on Lattice temperature and carrier concentration (see Equations 3-339 and 3-341). |
| KLAAUG | Enables Klaassen’s model for concentration dependent auger coefficients (see Chapter 3: “Physics”, Equations 3-328, 3-329, and 3-330). |
| KAUGCN , KAUGCP , KAUGDN and KAUGDP | Specify parameters of Klaassen's Auger recombination model (see Chapter 3: “Physics”, Equations 3-175 and 3-176). |
| KLASRH | Enables Klaassen’s model for concentration dependent lifetimes for Shockley Read Hall recombination (Chapter 3: “Physics”, Equations 3-299 and 3-300). |
| KSRHCN , KSRHCP , KSRHGN , KSRHGP , KSRHTN and KSRHTP | Specify parameters of Klaassen's SRH recombination model (see Chapter 3: “Physics”, Equations 3-299 and 3-300). |
| NI.FERMI | Includes the effects of Fermi statistice into the calculation of the intrinsic concentration in expressions for SRH recombination. |

| | |
|-----------------------|--|
| OPTR | Selects the optical recombination model (see Chapter 3: “Physics”, Equation 3-326). When this parameter is specified, the COPT parameter of the MATERIAL statement should be specified. |
| PIC.AUG | Enables the carrier and doping concentration dependent Auger rate coefficient model given by Equations 3-339 and 3-340. |
| S.DISSOC | Enables the singlet dissociation model described in Section 15.3.3: “Exciton Dissociation”. |
| SCHSRH | Enables Scharfetter concentration dependent lifetime model. |
| SRH | Specifies Shockley-Read-Hall recombination using fixed lifetimes (see Chapter 3: “Physics”, Equation 3-295). |
| SRH.EXPTEMP | Enables the alternative model for the Lattice Temperature dependence of the recombination lifetimes. |
| TRAP.AUGER | Enables the dependence of recombination lifetime on carrier density as given by Equations 3-311 and 3-312. |
| TRAP.COULOMBIC | Specifies that the Poole-Frenkel barrier lowering for columbic wells will be used for traps. |
| TRAP.TUNNEL | Specifies that the trap-assisted tunneling model will be used for traps. |
| TAT.NLDEPTH | Allows you to specify the trap energy used in the TAT.NONLOCAL model. Its units are in eV and how it is interpreted depends on whether the flag TAT.RELEI is specified. If TAT.NLDEPTH is not specified, the trap energy is the same as the Intrinsic Fermi energy. |
| TAT.NONLOCAL | Enables the non-local tunneling model in the calculation of the field effect enhancement factors. Setting this flag will also set the TRAP.TUNNEL flag. |
| TAT.RELEI | This flag affects how the TAT.NLDEPTH parameter is used to calculate the trap energy. See the “Trap-Assisted Tunneling” Section on page 3-18 for details. |
| ZAMDMER | Enables the electron lifetime model for TRAP states in LT-GaAs. |

Direct Tunneling Flags

An alternative set of direct quantum tunneling models for calculating gate current can be set using **DT.CUR** on the **MODELS** statement. If you set this parameter, then select the particular model using **DT.METH**. The allowed values of **DT.METH** are 1, 2 and 3. The default value of **DT.METH** is 1.

| | |
|------------------|--|
| DT.METH=1 | Selects a Fowler-Nordheim type model, with a correction for the trapezoidal, rather than the triangular shape of the potential barrier. |
| DT.METH=2 | Selects a WKB model with the assumption of a linearly varying potential. It involves a calculation of the classical turning points and integration between those limits. |
| DT.METH=3 | Selects an exact formula for a trapezoidal barrier that involves Airy function solutions. |

You may also need to specify the type of tunneling taking place by using at least one of the following flags.

| | |
|----------------|--|
| DT.CBET | Specifies electron tunneling from conduction band to conduction band. |
| DT.CUR | Enables the self-consistent version of Direct Tunneling. |
| DT.VBHT | Specifies holes tunneling from valence band to valence band. |
| DT.VBET | Specifies Band-to-Band tunneling. |
| DTTPP | Specify this along with DT.CUR to enable the Post-Processing version of Direct tunneling. |

Note: Specifying **DT.CUR** on the **MODELS** statement will invoke the self-consistent version of these models. You can also specify **DT.CUR** and associated parameters on the **SOLVE** statement, which will invoke the post processing version of this model for the particular **SOLVE** statement.

Note: The effective masses used in the tunneling calculations are the default or specified effective masses for the materials in question, unless you set the **ME.DT** and **MH.DT** parameters on the **MATERIAL** statement.

Generation Model Flags

| | |
|---------------------|---|
| A.BBT.SCHENK | This is the schenk band-to-band tunneling parameter (see Equation 3-406). |
| AUTOBBT | Causes band-to-band tunneling parameters to be calculated from first principals (see Chapter 3: “Physics”, Equations 3-418 and 3-419). |
| B.BBT.SCHENK | This is the Schenk band-to-band tunneling parameter (see Equation 3-421). |
| BBT.FORWARD | Avoids convergence problems (if using BBT.NONLOCAL in a forward biased junction). |
| BBT.HURKX | Enables the Hurkx model (see Chapter 3: “Physics”, Equation 3-412). |
| BBT.KANE | Specifies a Band-to-Band tunneling model according to Kane. |
| BBT.KL | Specifies a band-to-band tunneling model according to Klaassen. |
| BBT.NONLOCAL | Enables the non-local band-to-band tunneling model. No other band-to-band tunneling models should be enabled in the same region. |
| BBT.NLDERIVS | Enables the inclusion of non-local derivatives in the Jacobian matrix (if you set BBT.NONLOCAL). |
| BBT.STD | Specifies a standard band-to-band tunneling model (see Chapter 3: “Physics”, Equation 3-416). The alias for this parameter is BTBT . |
| BBT1 | This is an alias for BBT.KL . |
| BBT2 | This is an alias for BBT.STD . |
| BBT3 | This is an alias for BBT.HURKX . |

| | |
|------------------|--|
| BH.FNONOS | This is the barrier height parameter for the FNONOS model. |
| BTBT | This is an alias for BBT.KANE. |
| DEVDEG.E | Activates the device degradation caused by hot electron injection current. HEI should also be specified in this case. |
| DEVDEG.H | Activates the device degradation caused by hot hole injection current. HHI should also be specified in this case. |
| DEVDEG.B | Activates the device degradation caused by both the hot electron and hot hole injection currents. HEI and HHI should also be specified in this case. |

Note: The specification of either DEVDEG.E, DEVDEG.H, or DEVDEG.B will initialize the density of electron (hole) like traps on the interface and will clear out the trapped electron (hole) density on the interface if any.

| | |
|-------------------------|--|
| E.BENDING | Specifies that electron band bending will be taken into account for electron injection. |
| E.FGCGTUN | Enables the Floating Gate to Control Gate (FGCG) tunneling model for electrons. |
| E.SC.FGCGTUN | Enables the self-consistent version of the Floating Gate to Control Gate (FGCG) tunneling model for electrons. |
| ETA.FNONOS | This is the trap capture efficiency for the FNONOS model. |
| FERRO | Enables the ferroelectric permittivity model (see Section 3.6.8: “The Ferroelectric Permittivity Model”). |
| FG.RATIO | Specifies the ratio of the floating gate extent in the Z direction to the channel width in Z direction for 2D simulation. |
| FN.CUR | Enables both FNORD and FNHOLES. |
| FNHOLES | Enables self-consistent analysis of hole Fowler-Nordheim currents. |
| FNONOS | Enables model for gate tunneling in SONOS structures. |
| F.TRAP.TUNNEL | Specifies the name of a file containing a C-interpreter function to simulate trap assisted tunneling. The alias for this parameter is F.TRAP.DIRAC. |
| F.TRAP.COULOMBIC | Specifies the name of a file containing a C-interpreter function to simulate trap assisted tunneling with Coulombic wells. |
| FNORD | Selects a self-consistent Fowler-Nordheim tunneling model for electrons (see Chapter 3: “Physics”, Equation 3-433). This is the recommended approach for calculating Fowler-Nordheim current. |
| FNHPP | Selects a post-processing Fowler-Nordheim tunneling model for holes (see Chapter 3: “Physics”, Equation 3-434). Generally, the Fowler-Nordheim current does not cause convergence problems so this approach is not required. |
| FNPP | Selects a post-processing Fowler-Nordheim tunneling model for electrons (see Chapter 3: “Physics”, Equation 3-433). Generally, the Fowler-Nordheim current does not cause convergence problems so this approach is not required. |

| | |
|----------------------|---|
| GATE1 | Enables both HEI and HHI. |
| GATE2 | This is an alias for GATE1. |
| H.BENDING | Specifies that hole band bending will be taken into account for hole injection (see Chapter 3: “Physics”, Equation 3-441). |
| H.FGCGTUN | Enables the Floating Gate to Control Gate (FGCG) tunneling model for holes. |
| H.SC.FGCGTUN | Enables the self-consistent version of the Floating Gate to Control Gate (FGCG) tunneling model for holes. |
| HEI | Specifies the calculation of hot electron injection into oxides. This parameter can be used to simulate MOS gate current or EPROM programming. In transient mode, the oxide current is self-consistently added to the floating gate charge (see Chapter 3: “Physics”, Equation 3-436). |
| HHI | Specifies the calculation of hot hole current into an oxide in a similar manner to HEI (see Chapter 3: “Physics”, Equation 3-437). |
| HW.BBT.SCHENK | This is the schenk band-to-band tunneling parameter (see Equation 3-406). |
| II.NODE | This is an alias for OLDIMPACT. |
| II.VALDI | This is an alias for VALDINOCI. |
| IMPACT | Invokes the empirical impact ionization model with ionization coefficients taken from [82]. More rigorous impact ionization models may be specified with the IMPACT statement. |
| MASS.TUNNEL | Specifies the effective mass for band to band tunneling (see Chapter 3: “Physics”, Equations 3-84 and 3-85). |
| MIMTUN | Enables the Metal-Insulator-Metal direct tunneling model for Interelectrode tunneling. |
| N.CONCANNON | Enables the Concannon gate current model for electrons. |
| NEARFLG | Specifies the model used for oxide transport when HEI, HHI or FNSONOS are used. The default is <code>false</code> which sets a purely drift based model assigning gate current to the electrodes where the electric field lines through the oxide terminate. Setting NEARFLG replaces this model with one assuming the gate current is flowing to the electrode physically nearest the point of injection. This assumes a purely diffusion transport mechanism. Setting NEARFLG for devices with only one gate or a coarse mesh is advised. |
| NEWIMPACT | Specifies that impact ionization should use the form described in Chapter 3: “Physics”, Equation 3-350. |
| N.HOTSONOS | Alternative hot electron gate current model to be used with DYNASONOS model. |
| NT.FNONOS | This is the trap area density for saturation mode of the FNONOS model. |
| OLDIMPACT | Specifies that the impact ionization should use the form described in Chapter 3: “Physics”, Equation 3-349. The alias for parameter is II.NODE. |

| | |
|--------------------|--|
| P.CONCANNON | Enables the Concannon gate current model for holes. |
| P.HOTSONOS | Alternative hot electron gate current model to be used with DYNASONOS model. |
| QTNL.DERIVS | Enables non-local couplings in the Jacobian matrix in the self-consistent direct quantum tunneling models. |
| QTNLSC.BBT | Enables band-to-band mode of the self-consistent direct quantum tunneling model. |
| QTNLSC.EL | Enables the self-consistent direct quantum tunneling model for electrons. |
| QTNLSC.HO | Enables the self-consistent direct quantum tunneling model for holes. |
| QTUNN.BBT | Enables the band-to-band mode of the direct quantum tunneling model. This does not work with the quantum confined variant of quantum tunneling. |
| QTUNN.DIR | specifies the tunneling current direction if you specify a rectangular mesh using the QTX.MESH and QTY.MESH statements. A value of 0 means the Y direction (default) and a value of 1 means the X direction. |
| QTUNN.EL | Enables direct quantum tunneling model for electrons (see Chapter 3: “Physics”, Section 3.6.6: “Gate Current Models”). |
| QTUNN.HO | Enables direct quantum tunneling model for holes. |
| QTUNN | This is the same as specifying QTUNN.EL, QTUNN.HO, and QTUNN.BBT. These models calculate the quantum tunneling current through an oxide. |
| QTUNNSC | Enables the self-consistent versions of the direct quantum tunneling models for gate current. These include the tunneling current self-consistently in the carrier continuity equations. QTUNNSC is the same as specifying QTNLSC.EL, QTNLSC.HO, and QTNLSC.BBT. |
| SBT | This is an alias for UST. |
| SCHENK.BBT | This is the schenk band-to-band tunneling model. |
| SCHENK.EL | This is the schenk post-processing oxide tunneling current for electrons. |
| SCHENK.HO | This is the schenk post-processing oxide tunneling current for holes. |
| SCHENK | This is the schenk post-processing oxide tunneling current for bipolar. |
| SCHKSC.EL | This is the schenk self-consistent oxide tunneling current for electrons. |
| SCHKSC.HO | This is the schenk self-consistent oxide tunneling current for holes. |
| SCHKSC | This is the schenk self-consistent oxide tunneling current for bipolar. |
| SHAPEOX | Specifies which algorithm will be used for calculating quantum tunneling current on a non-rectangular mesh. If this parameter is not specified, then the current is calculated in a direction normal to each segment of the semiconductor/oxide interface. If SHAPEOX is specified, then the minimum distance is found between each segment and a contact or a polysilicon region. The quantum tunneling current is calculated along the direction that gives this minimum distance. |

| | |
|--------------------|---|
| SIS.EL | Enables direct electron quantum tunneling through an insulator between two semiconductor regions. This requires a QT mesh. |
| SIS.HO | Enables direct hole quantum tunnelling through an insulator between two semiconductor regions. This requires a QT mesh. |
| SIS.REVERSE | Causes the SIS.EL and SIS.HO models to use the quasi-Fermi levels at the start and end of the mesh slices. This may increase stability in some cases. |
| SIS.TAT | Enables Trap-Assisted-Tunnelling for structures that have an insulator layer between two semiconductors. |
| SISTAT.TN | Basic electron recombination time for SIS.TAT model. |
| SISTAT.TP | Basic hole recombination time for SIS.TAT model. |
| TSQ.ZAIDMAN | Parameter for the Zaidman model. |
| UST | Enables the universal Schottky tunneling model (see Chapter 3: “Physics”, Section 3.5.2: “Schottky Contacts”). The alias for this parameter is SBT. |
| VALDINOCI | Enables the Valdinoci impact ionization model. See Chapter 3: “Physics”, Equations 3-355, 3-368, and 3-376. The alias for this parameter is II.VALDI. |
| ZAIDMAN | Specifies the tunneling model for surface field emission. |

Carrier Statistics Model Flags

| | |
|---------------------|---|
| BGN | Specifies band-gap narrowing (see Chapter 3: “Physics”, Equation 3-46). |
| BGN2 | This is an alias for BGN. |
| BGN.ALAMO | Enables del Alamo Bandgap Narrowing model (see Section 3.2.11: “Bennett-Wilson and del Alamo Bandgap models”). |
| BGN.BENNETT | Enables Bennett-Wilson Bandgap Narrowing model (see Section 3.2.11: “Bennett-Wilson and del Alamo Bandgap models”). |
| BGN.KLA | Specifies that the bandgap narrowing model will use the Klaassen coefficients. The alias for this parameter is BGN2. |
| BGN.KLAASSEN | Enables the use of Klaassen's parameters for defaults for bandgap narrowing parameters (see Chapter 3: “Physics”, Table 3-3). |
| BGN.SLOTBOOM | Specifies band-gap narrowing using the original Slotboom coefficients (see Chapter 3: “Physics”, Equation 3-46). |
| BOLTZMANN | Specifies that Boltzmann carrier statistics be used (see Chapter 3: “Physics”, Equations 3-25 and 3-26). |
| BQP.N | Enables the BQP model for electrons. |
| BQP.P | Enables the BQP model for holes. |
| BQP.NGAMMA | Sets the value of BQP γ factor for electrons. |
| BQP.NALPHA | Sets the value of BQP α factor for electrons. |

| | |
|----------------------|---|
| BQP . NEUMANN | Uses explicitly enforced Neumann boundary conditions instead of the implicit implementation. |
| BQP . PALPHA | Sets the value of BQP α factor for holes. |
| BQP . PGAMMA | Sets the value of BQP γ factor for holes. |
| BQP . QDIR | Sets the direction of principal quantization. |
| FERMIDIRAC | Specifies that Fermi-Dirac carrier statistics be used (see Chapter 3: “Physics”, Equations 3-25 – 3-80). |
| INCOMPLETE | Accounts for incomplete ionization of impurities in Fermi-Dirac statistics (see Chapter 3: “Physics”, Equations 3-54 and 3-55). |
| INC . ION | Specifies that Equations 3-59 and 3-60 should be used for calculations of incomplete ionization. |
| IONIZ | Accounts for complete ionization of heavily doped silicon when using INCOMPLETE. |
| UBGN | Enables the universal bandgap narrowing model given in Equation 3-50. |

Quantum Model Parameters

| | |
|---------------------|--|
| 2DXY . SCHRO | This is the flag that tells ATLAS to solve a 2D Schrodinger equation in XY plane when you also specify the SCHRODINGER or P . SCHRODINGER flag. When it is off, 1D Schrodinger equations will be solved at each slice perpendicular to X axis. |
| ALT . SCHRO | Specifies usage of an alternate Schrodinger solver. |
| BC . QUANT | Specifies Dirichlet boundary conditions for all insulator interfaces for the quantum transport equation. |
| CALC . FERMI | Specifies that the Fermi level used in calculation of the quantum carrier concentration in the Schrodinger-Poisson model is calculated from the classic carrier concentrations. |
| DEC . C1 | This is a conduction band shift for 1st pair of electron valleys. |
| DEC . C2 | This is a conduction band shift for 2nd pair of electron valleys. |
| DEC . C3 | This is a conduction band shift for 3rd pair of electron valleys. |
| DEC . D2 | This is a conduction band shift for $\Delta 2$ electron valleys if DEC . C1 is not set. |
| DEC . D4 | This is a conduction band shift for $\Delta 4$ electron valleys if DEC . C2 is not set. |
| DEC . ISO | This is a conduction band shift for isotropic electron band, when NUM . DIRECT=1. |
| DEV . HH | This is a valence band shift for heavy holes. |
| DEV . LH | This is a valence band shift for light holes. |
| DEV . ISO | This is a valence band shift for isotropic hole band, when NUM . BAND=1. |
| DEV . SO | This is a valence band shift for split-off holes. |
| DG . N | This is an alias for QUANTUM (see Chapter 13: “Quantum: Quantum Effect Simulator”, Section 13.3: “Density Gradient (Quantum Moments Model)”). |

| | |
|--------------------|---|
| DG.P | This is an alias for P.QUANTUM (see Chapter 13: “Quantum: Quantum Effect Simulator”, Section 13.3: “Density Gradient (Quantum Moments Model)”). |
| DGN.GAMMA | Specifies the fit factor for electrons for the electron density gradient model (see Chapter 13: “Quantum: Quantum Effect Simulator”, Equation 13-9). |
| DGP.GAMMA | Specifies the fit factor for holes for the hole density gradient model (see Chapter 13: “Quantum: Quantum Effect Simulator”, Equation 13-10). |
| DGLOG | Specifies that the gradient of the log of concentration is to be used in the calculation of the quantum potential in the density gradient model (see Chapter 13: “Quantum: Quantum Effect Simulator”, Equation 13-9). |
| DGROOT | Specifies that the gradient of the root of the concentration is to be used in the calculation of the quantum potential in the density gradient model (see Chapter 13: “Quantum: Quantum Effect Simulator”, Equation 13-10). |
| EIGENS | Specifies the number of eigenstates solved for by the Poisson-Schrodinger solver (see Chapter 13: “Quantum: Quantum Effect Simulator”, Section 13.2: “Self-Consistent Coupled Schrodinger Poisson Model”). |
| EF.TOL | Controls the eigenvector tolerance on numerical accuracy for the alternate eigenvalue solver enabled by the NEW.EIG parameter. |
| EQUIL.NEGF | Specified that the region will be treated as quasi-equilibrium in planar NEGF model. |
| ESIZE.NEGF | Sets the number energy grid points in the NEGF solver. |
| ETA.NEGF | An imaginary optical potential, added to Hamiltonian of quasi-equilibrium regions in planar NEGF model. |
| EV.TOL | Controls eigenvalue tolerance on numerical accuracy for the alternate eigenvalue solver enabled by the NEW.EIG parameter. |
| FAST.EIG | Enables a computationally efficient version of the eigen-value solver. |
| FIXED.FERMI | Specifies that a constant Fermi level is used along each individual slice in the Y direction for carrier concentration calculation in the Schrodinger-Poisson Model. |
| HANSCHQM | Turns on the Hansch quantum effects approximation model for N channel MOS devices (see Chapter 13: “Quantum: Quantum Effect Simulator”, Section 13.5.1: “Hansch’s Model”). |
| LED | Specifies that the region is to be treated as a light emitting region and included in postprocessing for LED analysis. See Chapter 11: “LED: Light Emitting Diode Simulator”. |
| N.DORT | Turns on the Van Dort quantum effects approximation model for N channel MOS devices (see Chapter 13: “Quantum: Quantum Effect Simulator”, Section 13.5.2: “Van Dort’s Model”). |
| N.NEGF_PL | Activates planar NEGF solver for electrons. Solution is done in all 1D slices. |
| N.NEGF_PL1D | Activates planar NEGF solver for electrons. Solution is done for the first 1D slice and copied to all other slices. |
| N.QUANTUM | This is an alias for QUANTUM (see Chapter 13: “Quantum: Quantum Effect Simulator”, Section 13.3: “Density Gradient (Quantum Moments Model)”). |

| | |
|--------------------|--|
| NEGF_CMS | Enforces coupled mode space NEGF approach. |
| NEGF_MS | Activates a mode-space NEGF solver. See Chapter 13: “Quantum: Quantum Effect Simulator” for more information. |
| NEGF_UMS | Enforces uncoupled mode space NEGF approach. |
| NPRED.NEGF | Sets a number of predictor iterations in the predictor-corrector scheme of Schrodinger and NEGF solvers. |
| NEW.SCHRO | Specifies that the new non-rectilinear self-consistent Schrodinger-Poisson solver will be used for an ATLAS mesh (see Chapter 13: “Quantum: Quantum Effect Simulator”, Section 13.2: “Self-Consistent Coupled Schrodinger Poisson Model”). When this is specified, the Schrodinger solver mesh should also be specified using the <code>SX.MESH</code> and <code>SY.MESH</code> statements. |
| NEW.EIG | Enables an alternate eigenvalue solver that obtains eigenvectors using the <code>INVERSE ITERATION</code> method. |
| NUM.BAND | Specifies the number of valence bands to retain for Schrodinger Poisson solutions. |
| NUM.DIRECT | Specifies the number of conduction band directions in the k space to retain for Schrodinger Poisson solutions. |
| ORTH.SCHRO | Specifies the critical value used for determination of the orthogonality of eigenvectors (wavefunctions) resulting from Schrodinger equation solutions. The orthogonality measurement is done by taking the sum of the product of individual samples from two eigenvectors in question and dividing the sum by the number of samples. If that measure exceeds the value specified by <code>ORTH.SCHRO</code> , then an error message will be issued during any subsequent output of structure files. This message indicates that you should carefully check any wavefunction data contained in the structure file and make adjustments as necessary. |
| OX.MARGIN | This is the maximum electron penetration into oxide. You can use it with <code>OX.SCHRO</code> in non-planar semiconductor-oxide interface or nonrectangular channel crosssection (ATLAS3D) to reduce the number of nodes used in the solution of the Schrodinger equation. |
| OX.POISSON | Calculates the quasi-Fermi levels in insulators for Schrodinger Poisson solutions. |
| OX.SCHRO | Specifies that the band edges of insulators are included in the solution of Schrodinger's Equation in self-consistent solutions of the Schrodinger-Poisson Model (see Chapter 13: “Quantum: Quantum Effect Simulator”, Section 13.2: “Self-Consistent Coupled Schrodinger Poisson Model”). |
| P.DORT | Turns on the Van Dort quantum effects approximation model for P channel MOS devices (see Chapter 13: “Quantum: Quantum Effect Simulator”, Section 13.5.2: “Van Dort's Model”). |
| P.NEGF_PL | Activates planar NEGF solver for holes. Solution is done in all 1D slices. |
| P.NEGF_PL1D | Activates planar NEGF solver for holes. Solution is done for the first 1D slice and copied to all other slices. |
| P.SCHRODING | Computes the self consistent Schrodinger Poisson for holes. |
| PIEZO.SCALE | This is an alias for <code>POLAR.SCALE</code> . |

| | |
|-----------------------|---|
| PIEZOELECTRIC | This is an alias for POLARIZATION. |
| POLARIZATION | Enables the automatic calculation of added interface charge due to spontaneous and piezoelectric polarization. The alias for this parameter is PIEZOELECTRIC. See Chapter 3: “Physics”, Section 3.6.11: “Polarization in Wurtzite Materials [26]”. |
| POLAR.CHARG | Specifies polarization charge densities to replace the density calculated using Equations 3-331 and 3-332. |
| POLAR.SCALE | Specifies a constant scale factor multiplied by the calculated spontaneous and piezoelectric polarization charges when you enable polarization by setting the POLARIZATION parameter of the REGION statement. The alias for this parameter is PIEZO.SCALE. See Chapter 3: “Physics”, Section 3.6.11: “Polarization in Wurtzite Materials [26]”. |
| POST.SCHRO | Specifies to calculate the Schrodinger Equation (see Chapter 13: “Quantum: Quantum Effect Simulator”, Section 13.2: “Self-Consistent Coupled Schrodinger Poisson Model”) for quantum effects as a post processing step. |
| PSP.SCALE | Specifies a constant scale factor similar to POLAR.SCALE but applied only to spontaneous polarization. |
| QMINCONC | Specifies the minimum carrier concentration considered in the gradient calculations of the density gradient model or in Poisson's Equation in the self-consistent Schrodinger-Poisson Model (see Chapter 13: “Quantum: Quantum Effect Simulator”, Sections 13.2: “Self-Consistent Coupled Schrodinger Poisson Model” and 13.3: “Density Gradient (Quantum Moments Model)”). |
| QCRIT.NEGF | Sets a convergence criterium for potential in case of NEGF or Schrodinger solver. |
| QUANTUM | Enables the density gradient (see Chapter 13: “Quantum: Quantum Effect Simulator”, Section 13.3: “Density Gradient (Quantum Moments Model)”). |
| QWELL | Specifies that the region is treated as a quantum well for calculation of radiative recombination or gain or both for certain optoelectronic models. |
| QWNUM | Optionally sets the number of the quantum well region. |
| QX.MAX, QX.MIN | Specify the minimum and maximum extent of the Poisson-Schrodinger solver along the X axis direction (see Chapter 13: “Quantum: Quantum Effect Simulator”, Section 13.2: “Self-Consistent Coupled Schrodinger Poisson Model”). |
| QY.MAX, QY.MIN | Specify the minimum and maximum extent of the domain of the Schrodinger solver (see Chapter 13: “Quantum: Quantum Effect Simulator”, Section 13.2: “Self-Consistent Coupled Schrodinger Poisson Model”). |
| SCHRO | Enables the Poisson-Schrodinger solver (see Chapter 13: “Quantum: Quantum Effect Simulator”, Section 13.2: “Self-Consistent Coupled Schrodinger Poisson Model”). This can be used for zero carrier solutions only (specified by METHOD CARRIERS=0). This is typically combined with the EIGENS parameter to control the number of eigenstates calculated. This is a 1D solver that is solved within the mesh between limits set by QX.MIN and QX.MAX. |
| SP.BAND | This is a flag that turns on a banded matrix solver used to solve the 2D Schrodinger equation in ATLAS3D. Otherwise, a full matrix solver is used. |

| | |
|--|--|
| SP.CHECK | Enables checking of orthogonality of wavefunctions for Schrodinger - Poisson solutions. |
| SP.DIR | <p>Specifies direction of quantum confinement in Schrodinger equation and used in materials with single electron band but with anisotropic effective mass. It is active only when you set <code>SCHRODINGER</code> and <code>NUM.DIRECT=1</code> on the <code>MODELS</code> statement. The values of effective mass(es) in quantization direction(s) and DOS effective mass are give below.</p> <p>In ATLAS, quantization is in Y direction:</p> $\text{SP.DIR}=0 \quad m_y = M_C, \quad \text{dos_mass} = M_C$ $\text{SP.DIR}=1 \quad m_y = M_L, \quad \text{dos_mass} = \sqrt{M_{T1} \cdot M_{T2}}$ $\text{SP.DIR}=2 \quad m_y = M_{T1}, \quad \text{dos_mass} = \sqrt{M_L \cdot M_{T2}}$ $\text{SP.DIR}=3 \quad m_y = M_{T2}, \quad \text{dos_mass} = \sqrt{M_{T1} \cdot M_{T2}}$ <p>In ATLAS, quantization is in XY plane (with <code>SCHRO.2DXY</code> on <code>MODELS</code> statement):</p> $\text{SP.DIR}=0 \quad (m_x, m_y) = (M_C, M_C), \quad \text{dos_mass} = M_C$ $\text{SP.DIR}=1 \quad (m_x, m_y) = (M_{T1}, M_L), \quad \text{dos_mass} = M_{T2}$ $\text{SP.DIR}=2 \quad (m_x, m_y) = (M_{T2}, M_{T1}), \quad \text{dos_mass} = M_L$ $\text{SP.DIR}=3 \quad (m_x, m_y) = (M_L, M_{T2}), \quad \text{dos_mass} = M_{T1}$ <p>In ATLAS3D, quantization is in YZ plane:</p> $\text{SP.DIR}=0 \quad (m_y, m_z) = (M_C, M_C), \quad \text{dos_mass} = M_C$ $\text{SP.DIR}=1 \quad (m_y, m_z) = (M_L, M_{T2}), \quad \text{dos_mass} = M_{T1}$ $\text{SP.DIR}=2 \quad (m_y, m_z) = (M_{T1}, M_L), \quad \text{dos_mass} = M_{T2}$ $\text{SP.DIR}=3 \quad (m_y, m_z) = (M_{T2}, M_{T1}), \quad \text{dos_mass} = M_L$ |
| SP.EXCORR | Activates exchange-correlation correction in Schrodinger solvers. |
| SP.FAST | Activates a fast product-space approach in a 2D Schrodinger solver. |
| SP.GEOM | Sets a dimensionality and direction of a Schrodinger solver. See Chapter 13: "Quantum: Quantum Effect Simulator" for more information. |
| SP.SMOOTH | Enables smoothing of quantum carrier calculations. When you set the <code>SP.SMOOTH</code> parameter on the <code>MODELS</code> statement, the SP solver will use the degeneracy factor and effective mass evaluated at the location of the maximum value of the primary wave function for calculation of carrier concentration. This removes any discontinuities due to abrupt changes in mass or degeneracy. |
| WELL.DENERGY | Energy spacing for numerical integration of spontaneous emission spectrum to radiative recombination. |
| WELL.NX, WELL.NY, and WELL.NZ | Specifies the number of grid points in x, y, and z directions for Schrodinger equation in a quantum well region. |

Energy Balance Simulation Flags

| | |
|---------------------------------|---|
| A.TEMP | This is an alias for HCTE. |
| E.TAUR.VAR | Specifies that electron temperature dependent energy relaxation time is used. Use the TRE.T1, TRE.T2, TRE.T3, TRE.W1, TRE.W2, and TRE.W3 parameters on the material statement to specifies the energy relaxation time. |
| ET.MODEL | This is an alias for HCTE. |
| H.TAUR.VAR | Specifies that hole temperature dependent energy relaxation time is used. Use TRH.T1, TRH.T2, TRH.T3, TRH.W1, TRH.W2, and TRH.W3 parameters on the MATERIAL statement to specifies the energy relaxation time. |
| HCTE | Specifies that both electron and hole temperature will be solved. The aliases for this parameter are A.TEMP and ET.MODEL. |
| HCTE.EL | Specifies that electron temperature will be solved. |
| HCTE.HO | Specifies that hole temperature will be solved. |
| F.KSN | Specifies the name of a file containing a C-INTERPRETER function specifying the electron Scattering Law Exponent as a function of electron energy. This is the value of Scattering Law Exponent. Values other than 0 or -1 are permitted. |
| F.KSP | Specifies the name of a file containing a C-INTERPRETER function specifying the hole Scattering Law Exponent as a function of hole energy. This is the value of Scattering Law Exponent. Values other than 0 or -1 are permitted. |
| GR.HEAT | Includes generation/recombination heat source terms in the lattice heat flow equation. |
| JOULE.HEAT | Includes the Joule heat source terms in the lattice heat flow equation. |
| KSN | Specifies which hot carrier transport model will be used for electrons. KSN=0 selects the hydrodynamic model and KSN=-1 selects the energy balance model. |
| KSP | Specifies which hot carrier transport model will be used for holes. KSP=0 selects the hydrodynamic model and KSP=-1 selects the energy balance model. |
| TAUMOB | Specifies the dependence of relaxation times with carrier temperature in the mobility definition. If TAUMOB is specified, the values of MATERIAL statement parameters TAUMOB.EL and TAUMOB.HO are dependent on the carrier temperature. |
| TAUTEM | Specifies the dependence of relaxation times with carrier temperature. If TAUTEM is specified, the values of MATERIAL statement parameters TAUREL.EL and TAUREL.HO are dependent on carrier temperature. |
| N.TEMP or HCTE.EL | Specifies that the electron temperature equation will be solved. |

| | |
|-------------------------------------|--|
| P . TEMP or HCTE . HO | Specifies that the hole temperature equation will be solved. |
| PASSLER | Enables Passler's bandgap versus temperature model. |
| PT . HEAT | Includes Peltier-Thomson heat sources in the lattice heat flow equation. |

Lattice Heating Simulation Flags

| | |
|--------------------------------------|--|
| F . PDN | Uses C-Interpreter function for phonon drag contribution to electron thermopower. |
| F . PDP | Uses C-Interpreter function for phonon drag contribution to hole thermopower. |
| HEAT . FULL | Enables all thermal sources and sinks (Joule heat, generation-recombination heat, and Peltier Thomson heat). |
| HEAT . PETHOM | This can be used to turn off the Peltier-Thomson heat source in the HEAT . FULL option. |
| LAT . TEMP or L . TEMP | Specifies that the lattice temperature equation will be solved. For lattice heating simulation there must be at least one thermal contact defined using the THERMCONTACT statement. |
| PCM | Specifies that the phase change material temperature dependent resistivity is to be used. |
| PCM . LOG | Specifies that for phase change materials the interpolation for resistivity between the low temperature value (PCM . CTC and PCM . CRHO) and the high value (PCM . ATC and PCM . ARHO) is logarithmic. |
| PHONONDRAG | Enables the phonon drag contribution to thermopower. |

Note: These parameters should only be specified if **GIGA** or **GIGA3D** is enabled on your system.

Defect Generation Model

| | |
|-----------------------|--|
| BEAM . LID | Specifies that the generation rate for the light induced defect generation model is calculated only from active BEAM statements, which have the LID parameter specified. |
| FILE . LID | Specifies the file name where the dangling bond density of states distribution, as a function of energy, will be stored. |
| GENERATE . LID | Specifies the generation rate for the light induced defect generation model. |

| | |
|-----------------|--|
| TIME.EP | Specifies the bias stress time value used in the amphoteric defect generation model. |
| TIME.LID | Specifies the time value used in the light induced defect generation model. |
| TRAP.LID | Specifies the light induced defect generation model will be used. |

Magnetic Field Model

| | |
|---------------|---|
| BX | This is the X Component of Magnetic Field Vector (Tesla). |
| BY | This is the Y Component of Magnetic Field Vector (Tesla). |
| BZ | This is the Z Component of Magnetic Field Vector (Tesla). |
| R.ELEC | This is the Hall scattering factor for electrons . |
| R.HOLE | This is the Hall scattering factor for holes. |

Model Macros

| | |
|-----------------|--|
| BIPOLAR | Selects a default set of models which are used when simulating bipolar devices. The bipolar models are CONMOB, FLDMOB, BGN, CONSRH, and AUGER. |
| BIPOLAR2 | Selects an alternative default set of models which are used when simulating bipolar devices. The bipolar models are FERMI, KLA, KLASRH, KLAAUG, FLDMOB, and BGN. |
| ERASE | Specifies a default set of models which are used to simulate EEPROM erasure. When it's specified, the MOS, FNORD, IMPACT, and BBT.KL models will be used. |
| MOS | Specifies a default set of models for MOS devices. The MOS models are CVT, SRH and FERMI. |
| MOS2 | Specifies a default set of models for MOS devices. The MOS2 models are KLA, SHI, SRH, FERMI and BGN. |
| PROGRAM | Specifies a default set of models used when writing to EEPROMS. When PROGRAM is specified, the MOS, HEI, and IMPACT models will be used. |

General Parameters

| | |
|------------------|---|
| ALPHA.DOS | Specifies that density of states data should be extracted from the absorption spectra during output of complex index of refraction using OUT.INDEX on the MATERIAL statement. |
| ALL | Enables solution for both electrons and holes. |
| ASUB | Specifies the substrate lattice constant for strain calculations as described in Section 3.6.10: "Epitaxial Strain Tensor Calculation in Wurtzite". |
| BB.GAMMA | Specify the band-to-band tunneling parameters (see Chapter 3: "Physics", Equation 3-416). |

| | |
|--------------------|--|
| BBT.GAMMA | This is an alias for BB.GAMMA . |
| BOUND.TRAP | Enables modeling of traps coincident with ohmic boundaries. |
| CARRIERS | Specifies the number of carriers to simulate, which should be 0, 1 or 2. The alias is NUMCARR . |
| CHUANG | Enables the Chuang gain/radiative recombination model (GAINMOD=5). |
| CUBIC35 | Specifies to use the material dependent band parameter model discussed in Section 5.3.1: "Cubic III-V Semiconductors". |
| DEVICE | Specifies which device in MIXEDMODE simulation the MODELS statement should apply to. The synonym for this parameter is STRUCTURE . |
| DRIFT.DIFF | Specifies that the drift-diffusion transport model is to be used. This implies that the electron and hole carrier temperature equations will not be solved. |
| ELECTRONS | Specifies that the electron continuity equation is included in simulation. |
| FC.ACCURACY | This is the maximum ratio of the change in integrated photogeneration to the total that is acceptable during iterations for calculation of frequency conversion material emission (see Section 10.11: "Frequency Conversion Materials (2D Only)"). |
| FREQ.CONV | Enables the frequency conversion material model. |
| F.PCM | Specifies the file name of a C-Interpreter function that models the resistivity of a conductor as a function of time, temperature, and history. |
| G.EMPIRICAL | Enables the empirical gain model from Chapter 3: "Physics", Section 3.9.4: "The Empirical Gain Model" (GAINMOD=2). |
| G.STANDARD | Enables the gain model from Chapter 3: "Physics", Section 3.9.3: "The Standard Gain Model" (GAINMOD=1). |
| HOLE | Specifies that the hole continuity equation is included in simulation. |
| ISHIKAWA | Enables Ishikawa's strain model for InGaAs/InGaAsP/InGaP (see Chapter 3: "Physics", Section 3.9.11: "Ishikawa's Strain Effects Model"). |
| K.P | Enables using the $k \cdot p$ model effective masses and band edge energies for drift-diffusion simulation. |
| LI | Enables the Li gain/radiative recombination model (GAINMOD=5). |
| LORENTZ | Enables Lorentz gain broadening. |
| MATERIAL | Specifies which material from Table B-1 in Appendix B: "Material Systems", will apply to the MODELS statement. If a material is specified, then all regions defined as being composed of that material will be affected. |
| NAME | Specifies which region will be applied to the MODELS statement. Note that the name must match the name specified in the NAME parameter of the REGION statement or the region number. |
| PATRIN | Enables the strain dependence of bandgap in the Raykanan silicon absorption model in Equation 3-529. |

| | |
|-----------------------|---|
| PFREQ.CONV | Specifies that the ray trace for emissions from a frequency conversion material are periodic with respect to the boundaries at the minimum and maximum x coordinates. |
| PRT.BAND | Enables run-time output of regional band parameter model information. |
| PRT.COMP | Enables run-time output of regional composition information. |
| PRT.FLAGS | Enables run-time output of regional model flag information. |
| PRT.IMPACT | Enables run-time output of regional impact ionization model information. |
| PRT.RECOM | Enables run-time output of regional recombination model information. |
| PRT.THERM | Enables run-time output of regional thermal model information. |
| PRINT | Prints the status of all models, a variety of coefficients, and constants. We recommended that you include this parameter in all ATLAS runs. |
| PRINT.REGION | Prints the model status and coefficients for the specified region. |
| PRINT.MATERIAL | Prints the model status and coefficients for the specified material. |
| REGION | Specifies the region number for this MODELS statement. The alias is NUMBER. |
| RAJKANAN | Enables the analytic absorption model for silicon given by Equation 3-529. |
| SPEC.NAME | Specifies the name of a file to collect the emission spectrum from the LASER simulator. |
| SPONTANEOUS | Includes the radiative recombination rates derived from the LI, YAN or CHUANG model into the drift diffusion. |

Note: You need additional computational resources since the radiative rate must be numerically integrated for each grid point.

| | |
|--------------------|---|
| STRUCTURE | This is a synonym for DEVICE. |
| STRESS | Enables the silicon stress dependent bandgap model from Section 3.6.12: “Stress Effects on Bandgap in Si”. |
| SUBSTRATE | This is a logical parameter indicating that the specified region should be considered as the substrate for strain calculations described in Section 3.6.10: “Epitaxial Strain Tensor Calculation in Wurtzite”. |
| TAYAMAYA | Enables the model from Chapter 3: “Physics”, Section 3.9.5: “Takayama's Gain Model” (GAINMOD=3). |
| TEMPERATURE | Specifies the temperature in Kelvin. |
| TLU.INDEX | Specifies that the Tauc-Lorentz dielectric function (see Section 3.10.3: “Tauc-Lorentz Dielectric Function with Optional Urbach Tail Model for Complex Index of Refraction”) should be used for calculation of the complex index of refraction. |
| UNSAT.FERRO | Enables unsaturated loop modeling for ferroelectrics. |
| YAN | Enables the Li gain/radiative recombination model (GAINMOD=5). |

Model Dependent Parameters

ARORA Model Parameters

The parameters that can only be used with the ARORA model (see Chapter 3: “Physics”, Equations 3-176 and 3-177) are AR.MU1N, AR.MU2N, AR.MU1P, and AR.MU2P.

BBT.KL and BBT.STD Model Parameters

The parameters used with the BBT.KL model are BB.A1 and BB.B. The BB.A2 and BB.B parameters are used with the BBT.STD model. The BB.A1 and BB.A2 parameters are the pre-exponential coefficients in the band-to-band tunneling models. The BB.B parameter is the exponential coefficient used in both models. The default value of BB.B depends on which model is chosen (see Chapter 3: “Physics”, Equation 3-416).

CCSMOB Model Parameters

The CCS.EA, CCS.EB, CCS.HA, and CCS.HB parameters describe the dependence of mobility on doping, carrier concentration, and temperature (see Chapter 3: “Physics”, Equations 3-180 – 3-184).

FLDMOB Model Parameters

| | |
|--------------------|--|
| B.ELECTRONS | This is used in the field-dependent mobility (see Chapter 3: “Physics”, Equation 3-274). See also BETAN on the MOBILITY statement. |
| B.HOLES | This is used in the field-dependent mobility expression (see Chapter 3: “Physics”, Equation 3-275). See also BETAP on the MOBILITY statement. |
| E0 | This is used in the field dependent mobility model for EVSATMOD=1 (see Chapter 5: “Blaze: Compound Material 2D Simulator”, Equation 5-57). |
| EVSATMOD | <p>Specifies which parallel field dependent mobility model (see Chapter 3: “Physics”, Equation 3-274 and Chapter 5: “Blaze: Compound Material 2D Simulator”, Equation 5-59) should be used for electrons. The value of EVSATMOD should be assigned as follows:</p> <ul style="list-style-type: none"> 0 - Use the standard saturation model (Equation 3-274). You also can apply the option parameter, MOBTEM.SIMPL (see Chapter 3: “Physics”, the “Carrier Temperature Dependent Mobility” Section on page 3-79 for more information). 1 - Use the negative differential velocity saturation model (Equation 5-59). 2 - Use a simple velocity limiting model. <p>In most cases, the default value of 0 should be used.</p> |
| HVSATMOD | <p>Specifies which parallel field dependent mobility model (see Chapter 3: “Physics”, Equation 3-275 and Chapter 5: “Blaze: Compound Material 2D Simulator”, Equation 5-60) should be used for holes. The value of HVSATMOD should be assigned as follows:</p> <ul style="list-style-type: none"> 0 - Use the standard saturation model (Equation 3-275). 1 - Use the negative differential velocity saturation model (Equation 5-60). 2 - Use a simple velocity limiting model. <p>In most cases, the default value of 0 should be used.</p> |

Fowler-Nordheim Tunneling Model Parameters

The parameters used in this model are `F.AE` and `F.BE`. `F.AE` is the pre-exponential factor and `F.BE` is the exponential coefficient (see Chapter 3: “Physics”, Equation 3-433).

WATT or SURFMOB Model Parameters

The parameters that can be used with the `WATT` model, include: `ALN1`, `ALN2`, `ALN3`, `ALP1`, `ALP2`, `ALP3`, `ETAN`, `ETAP`, `MREFN1`, `MREFN2`, `MREFN3`, `MREFP1`, `MREFP2`, and `MREFP3` (see Chapter 3: “Physics”, Equations 3-266 and 3-267).

TFLDMB1 and TFLDMB2 Model Parameters

| | |
|------------------|--|
| ACC.SF | Specifies the accumulation saturation factor which describes the ratio of the majority carrier concentration in the accumulation layer before and after bending of conductivity and valance bands. |
| INV.SF | Specifies the inversion saturation factor which describes the ratio of the majority carrier concentration in the inversion layer before and after the bending of conductivity and valance bands. |
| OX.BOTTOM | Specifies the coordinate of the bottom edge of the gate oxide for a MOSFET transistor. |
| OX.LEFT | Specifies the coordinate of the left edge of the gate oxide for a MOSFET transistor. |
| OX.RIGHT | Specifies the coordinate of the right edge of the gate oxide for a MOSFET transistor. |

CONCANNON Model Parameters

| | |
|--------------------|---|
| CGATE.N | Specifies an empirical tuning factor for electrons in the Concannon gate current model. |
| CGATE.P | Specifies an empirical tuning factor for holes in the Concannon gate current model. |
| PEFF.N | Specifies an effective barrier height for electrons in the Concannon gate current model. An alias for <code>IG.EB0</code> . |
| PEFF.P | Specifies an effective barrier height for holes in the Concannon gate current model. An alias for <code>IG.HB0</code> . |
| THETA.N | Specifies the critical rejection angle for electrons in the Concannon gate current model. |
| THETA.P | Specifies the critical rejection angle for electrons in the Concannon gate current model. |
| C0 | Specifies the electron distribution weight factor in the Concannon gate current model. |
| CHIA | Specifies the electron distribution function constant in the Concannon gate current model. |
| CHIB | Specifies the electron distribution function constant in the Concannon gate current model. |
| CHI.HOLES | Specifies the hole distribution function constant in the Concannon gate current model. |
| ENERGY.STEP | Specifies the energy step for numeric integration in the Concannon gate current model. |

| | |
|-----------------|--|
| INFINITY | Specifies the highest energy in numeric integration in the Concannon gate current model. |
| PATH.N | Specifies the mean free path in the oxide for electrons in the Concannon gate current model. |
| PATH.P | Specifies the mean free path in the oxide for holes in the Concannon gate current model. |

HEI Model Parameters

The parameters that may be used with the HEI model include: IG.ELINR, IG.HLINR, IG.ELINF, IG.HLINF, IG.EBETA, IG.HBETA, IG.EETA, IG.ETA, IG.EEOX, IG.HEOX, IG.EB0, IG.HB0.

Table 21-3 lists aliases for parameters of the HEI model.

| Table 21-3. HEI model aliases | | | |
|-------------------------------|-------|-----------|-------|
| Parameter | Alias | Parameter | Alias |
| IG.ELINF | LAMHN | IG.EBETA | BARLN |
| IG.ELINR | LAMRN | IG.HBETA | BARLP |
| IG.HLINF | LAMHP | IG.EETA | TUNLN |
| IG.HLINR | LAMRP | IG.ETA | TUNLP |

N.DORT and P.DORT Model Parameters

| | |
|---------------|--|
| B.DORT | User-specifiable model parameter for the Van Dort quantum effects approximation model. |
| D.DORT | User-specifiable model parameter for the Van Dort quantum effects approximation model. |

BBT.KANE Model Parameters

The parameters used with the BBT.KANE model are BBT.A_KANE (aliases BB.A_KANE or A.BTBT), BBT.B_KANE (aliases BB.B_KANE or B.BTBT), and BBT.GAMMA (alias BB.GAMMA).

LASER Simulation Parameters

| | |
|------------------------------|---|
| CAVITY.LENGTH | Specifies the cavity length in the longitudinal direction (in mm). |
| GAINMOD | Specifies the local optical gain model to be used. GAINMOD=0 specifies that no optical gain model will be used. GAINMOD=1 specifies that the simple gain model will be used (see Chapter 3: “Physics”, Section 3.9.3: “The Standard Gain Model”). GAINMOD=2 specifies that the complex frequency-dependent gain model will be used (see Chapter 3: “Physics”, Section 3.9.4: “The Empirical Gain Model”). GAINMOD=3 specifies that Takayama’s gain model will be used (see Chapter 3: “Physics”, Section 3.9.5: “Takayama’s Gain Model”). GAINMOD=5 specifies that the Yam’s, Li’s, or Chuang’s gain model will be used (see Chapter 3: “Physics”, Sections 3.9.7: “Unstrained Zincblende Models for Gain and Radiative Recombination” and 3.9.9: “Strained Wurtzite Three-Band Model for Gain and Radiative Recombination”). |
| LAS.ABSOR_SAT | Enables the non-linear absorption loss saturation model. |
| LAS.ABSORPTION | Enables the absorption loss model in LASER. |
| LAS.EINIT, LAS.EFINAL | Specify the lower and upper photon energies. LASER will calculate multiple longitudinal photon rates within this range. Using wide ranges can slow down simulation. |
| LAS.ESEP | Specifies the photon energy separation. If this is not specified, LASER will automatically calculate the number of longitudinal modes based on the cavity length and the energy range. |
| LAS.ETRANS | Specifies that the Helmholtz solver should use the transverse mode with the eigen-energy closes to the energy specified by the LAS.TRANS_ENERGY parameter. |
| LAS.FCARRIER | Enables the free carrier loss model in LASER. |
| LAS.GAIN_SAT | Enables the non-linear gain saturation model. |
| LAS.ITMAX | Specifies the maximum number of iterations allowed for LASER simulation at each bias point. |
| LAS.LOSSES | Specifies the total losses in Equation 8-13. |
| LAS.MIRROR | Specifies the percentage facet reflectivity (both facets are assumed to have this value of reflectivity) for the mirror loss in Laser. 100% reflectivity is equivalent to no mirror loss. |
| LAS.NEFF | Specifies the effective refractive index in Equation 9-2. |
| LAS.NMODE | Specifies the number of transverse modes simulated. |
| LAS.NX | Specifies the number of discrete samples in the laser mesh in the X direction. |
| LAS.NY | Specifies the number of discrete samples in the laser mesh in the Y direction. |

| | |
|---|--|
| LAS.OMEGA | Specifies the lasing frequency to be used in Chapter 8: “Laser: Edge Emitting Simulator”, Equation 8-1. If model 2 is used for simulation, then this parameter specifies an estimate of the lasing frequency. Instead of using this parameter, PHOTON.ENERGY can be used to specify photon energy. |
| LAS.REFLECT | Specifies that the Helmholtz equation should be solved with the Y axis (X=0) as an axis of symmetry. |
| LAS.RF | Specifies the front mirror reflectivity in percent. |
| LAS.RR | Specifies the rear mirror reflectivity in percent. |
| LAS.SIN | Specifies an initial photon density in the fundamental lasing mode. This value provides an initial guess for subsequent iterations. This parameter is used only when the single frequency model has been selected. |
| LAS.SPECSAVE | The spectrum file will be saved after every LAS.SPECSAVE LASER solution steps. |
| LAS.SPONTANEOUS | Enables the physically based model for spontaneous emission to be used. |
| LAS.TAUSS | Specifies the iteration parameter to be used for the photon rate equation when solving Equation 9-8. |
| LAS.TIMERATE | Specifies that the time dependent photon rate equation will be used in a transient laser simulation. |
| LAS.TOLER | Specifies the desired accuracy in photon areas. |
| LAS.TRANS_ENERGY | Specifies the transverse mode energy for mode selection with LAS.ETRANS set. |
| LAS.XMAX, LAS.XMIN, LAS.YMAX, and LAS.YMIN | Specify the maximum and minimum limits on the laser Helmholtz solution mesh. |
| LAS_MAXCH | Specifies the maximum allowable relative change in photon densities between iterations. Rapid changes of the photon densities can cause convergence problems. |
| LASER | Enables the LASER simulation. |
| LMODE | Specifies that multiple longitudinal models are to be taken into account during the LASER simulation. |
| PHOTON.ENERGY | Specifies the energy of photons. If model 2 is used for simulation, this parameter specifies only an initial estimate of the photon energy. Instead of using this parameter, LAS.OMEGA can be used to specify the lasing frequency. |
| SPEC.NAME | Specifies the name of a spectrum file, which LASER will produce for each bias point if the LMODES parameter has been specified. |

Exciton Model Flags

| | |
|-----------------|---|
| EXCITONS | Specifies that singlet and triplet exciton continuity equations will be solved. |
| SINGLET | Specifies that the singlet exciton continuity equation will be solved. |
| TRIPLET | Specifies that the triplet exciton continuity equation will be solved. |

Model Selection Example

This example selects concentration and field dependent mobilities, SRH recombination, and Auger recombination. This is a typical model set for bipolar simulation. The simulation temperature is 290K.

```
MODELS CONMOB FLDMOB SRH AUGER TEMP=290
```

Confirming Model Selection

To echo back model selections, parameters and material constants use

```
MODELS PRINT
```

Note: For the best model selection for different applications, see the Standard Examples set (see also Chapter 2: “Getting Started with ATLAS”, Section 2.4: “Accessing The Examples” for more information about to how to access these examples).

21.35: MQW

MQW defines multiple quantum well structures in an existing device structure. This statement should follow all other structure definition statements (i.e., MESH, REGION, ELECTRODE, and DOPING).

Syntax

MQW <parameters>

| Parameter | Type | Default | Units |
|-----------|-----------|----------------------|------------------|
| ACCEPTORS | Real | 0.0 | cm ⁻³ |
| ALT.SCHRO | Logical | False | |
| ASTR | Real | 0.0 | |
| BSTR | Real | 0.0 | |
| CSTR | Real | 0.0 | |
| DELTA | Real | 0.341 | eV |
| DONORS | Real | 0.0 | cm ⁻³ |
| DSTR | Real | 0.0 | |
| EPSILON | Real | 0.0 | |
| ESTR | Real | 0.0 | |
| FSTR | Real | 0.0 | |
| GAIN0 | Real | 1.0 | |
| GAMMA0 | Real | 2.0×10 ⁻³ | eV |
| GSCALE | Real | 1.0 | |
| ISHIKAWA | Logical | False | |
| LI | Logical | False | |
| LORENTZ | Logical | False | |
| MATERIAL | Character | | |
| MC | Real | 0.067 | |
| MHH | Real | 0.62 | |
| MLH | Real | 0.087 | |
| MSTAR | Real | 0.053 | |
| NBS | Integer | 15 | |
| NWELL | Integer | 1 | |
| NX | Integer | 10 | |
| NY | Integer | 10 | |

| | | | |
|-------------|---------|-----------------------|---------|
| RESOLVE | Logical | True | |
| SPONTANEOUS | Logical | False | |
| STRAIN | Real | 0.0 | |
| STABLE | Integer | 0 | |
| SY | Real | | μm |
| TAU.IN | Real | 3.3×10^{-13} | seconds |
| TE.MODES | Logical | True | |
| WB | Real | | μm |
| WW | Real | | μm |
| XCOMP | Real | 0.0 | |
| XMAX | Real | | μm |
| XMIN | Real | | μm |
| YAN | Logical | False | |
| YCOMP | Real | 0.0 | |
| YMAX | Real | | μm |
| YMIN | Real | | μm |

Description

The MQW regions will be added to ATLAS when you specify the `MQW` statement. This statement is necessary to correctly model the recombination and gain effects of these MQW regions.

The multiple quantum well structure is restricted to place the quantum wells only parallel to the X axis (perpendicular to the Y axis). Also, if more than one well is specified, then each well will have the same width defined by the `WW` parameter. Each barrier between wells will then have the same width defined by the `WB` parameter.

The `MQW` structure is located within the rectangle defined by the `XMIN`, `XMAX`, `YMIN`, and `YMAX` parameters. In the Y direction, the wells are centered within the span of `YMIN` to `YMAX`. Make sure that the difference between `YMIN` and `YMAX` is larger than the sum of the well width (`WW`) and the barrier width (`WB`) multiplied by the number of wells (`NWELL`). In the X direction, the wells extend the entire length from `XMIN` to `XMAX`.

The quantum well material is specified by the `MATERIAL` parameter, modified by the composition fractions: `XCOMP` and `YCOMP`. The barrier material is given by the material specified in the region, where the wells are defined.

This implementation solves the Schrodinger's equation (see Chapter 13: “Quantum: Quantum Effect Simulator”, Equations 13-2 and 13-3) for each quantum well, in order to calculate the quantum well-bound state energies and carrier distributions in the wells. You can specify the number of bound states to use for this calculation with the `NBS` parameter. For laser gain calculations, only the lowest bound state energy in the conduction band and the highest bound state energy in the valence band are used. These bound state energies feed directly into the gain model and spontaneous emission models are shown in Chapter 3: “Physics”, Section 3.9: “Optoelectronic Models”

MQW Parameters

| | |
|---|--|
| ACCEPTORS | Specifies a uniform density of ionized acceptors in the quantum wells. |
| ALT.SCHRO | Specifies that the alternative Schrodinger solver should be used in the calculations. |
| ASTR, BSTR, CSTR, DSTR, ESTR, and FSTR | Specify coefficients to calculate the effective masses in the strained quantum well. |
| DELTA | Specifies the spin orbital splitting energy in the quantum well. |
| DONORS | Specifies the uniform density of ionized donors in the quantum wells. |
| EPSILON | Specifies the high frequency permittivity to used in calculating the gain and radiative recombinations. |
| GAIN0 | Scaling factor for the MQW gain models. |
| GAMMA0 | Specifies the width in eV (Note: $GAMMA0 = h / TAU.IN$). |
| GSCALE | Specifies a scale factor to be multiplied by the optical gain. |
| ISHIKAWA | Specifies that the Ishikawa model [104] is used to account for strain effects (see Chapter 3: “Physics”, Section 3.9.11: “Ishikawa's Strain Effects Model” for more information). |
| LI | Specifies that the Li model [38] be used for spontaneous emission in multiple quantum wells. The DELTA, MSTAR, MC and MHH parameters can be used with this model. |
| LORENTZ | This is the Lorentzian line broadening model for MQW gain. The half width of the Lorentzian shape function is controlled by the GAMMA0 parameter of the MQW statement. You can also set the TAU.IN parameter to specify the intraband relaxation time in seconds. For more information about the Lorentzian line broadening model, see Chapter 3: “Physics”, Section 3.9.10: “Lorentzian Gain Broadening”. |
| MATERIAL | Specifies the name of the material to be used in the wells. The barrier material is taken from whatever material is already in the structure at the MQW location. |
| MC | This is the conduction band effective mass. |
| MHH | This is the heavy hole effective mass. |
| MLH | This is the light hole effective mass. |
| MSTAR | Disperses energy in the conduction band. This doesn't necessarily equate to the conduction band effective mass, see [266]. |
| NBS | Defines the number of bound states used in solving the Schrodinger equation. |
| NWELL | Specifies the number of quantum wells. |
| NX, NY | Specify the number of mesh points in the X and Y direction for resolving the MQW structure. Make sure that these are specified large enough to resolve the individual quantum wells. NY is defined as: |

$$N_Y = \left\lceil \frac{Y_{MAX} - Y_{MIN}}{\langle YGridSpacing(\mu m) \rangle} \right\rceil + 1$$

21-5

| | |
|-------------------------------|---|
| RESOLVE | Specifies whether the band edge discontinuities at the well edges are resolved by the device equations. |
| SPONTANEOUS | Specifies whether the quantum well spontaneous recombination is included in the device continuity equations. |
| STABLE | Specifies the table row to be used for coefficients to calculate the effective masses in strained quantum wells. |
| STRAIN | Specifies the strain percentage in the quantum well. |
| SY | Specifies the maximum mesh spacing to be applied in the Y direction through the quantum wells. |
| TAU.IN | Specifies the intraband relaxation time in seconds (Note: $GAMMA0 = h / TAU.IN$). |
| TE.MODES | Specifies whether TE or TM modes will be used in calculating the asymmetrical factors in the LI model. |
| WB | Specifies the individual barrier width between wells in microns. |
| WW | Specifies the individual quantum well width in microns. |
| XCOMP | Defines the X composition fraction for the wells for ternary and quaternary materials. |
| XMIN, XMAX, YMIN, YMAX | Specify a rectangular box where the quantum wells are to be simulated. The units of these parameters are in microns. |
| YCOMP | Defines the Y composition fraction for the wells for quaternary materials. |
| YAN | Specifies that the Yan model [266] be used for spontaneous emission in multiple quantum wells. The DELTA, MSTAR, MC and MHH parameters can be used with this model (GAINMOD=5). |

21.36: NITRIDECHARGE

NITRIDECHARGE specifies the parameters describing the properties of traps in Silicon Nitride in the DYNASONOS model and the PF.NITRIDE model.

The parameters apply to all Silicon Nitride regions.

Syntax

NITRIDECHARGE [<params>]

| Parameter | Type | Default | Units |
|------------|------|-----------------------|-----------------|
| NT.N | Real | 0.0 | cm ³ |
| NT.P | Real | 0.0 | cm ³ |
| TAU.N | Real | 1.0×10 ³⁰⁰ | s |
| TAU.P | Real | 1.0×10 ³⁰⁰ | s |
| ELEC.DEPTH | Real | -999.0 | eV |
| HOLE.DEPTH | Real | -999.0 | eV |
| SIGMAN.P | Real | 1.0×10 ⁻¹⁵ | cm ² |
| SIGMAP.N | Real | 1.0×10 ⁻¹⁴ | cm ² |
| SIGMAT.N | Real | 1.0×10 ⁻¹⁶ | cm ² |
| SIGMAT.P | Real | 1.0×10 ⁻¹⁴ | cm ² |
| PF.BARRIER | Real | | eV |
| PF.A | Real | 1.0×10 ⁵ | s |
| PF.B | Real | 1.0e13 | Hertz |

Description

The NITRIDE charge allows you to set up the properties of electron and hole traps in Silicon Nitride. It is used in the DYNASONOS model and also the steady state version of the PF.NITRIDE model.

Trap Density

| | |
|-------------|---|
| NT.N | Sets the value of the uniform density of electron traps (acceptor states) in the Silicon Nitride. |
| NT.P | Sets the value of the uniform density of hole traps (donor states) in the Silicon Nitride. |

Cross-Section

| | |
|-----------------|---|
| SIGMAT.N | A factor in determining the rate at which the acceptor states capture electrons from the conduction band. |
| SIGMAT.P | A factor in determining the rate at which the donor states capture holes from the valence band. |
| SIGMAN.P | A factor in determining the rate at which the acceptor states capture holes from the valence band. |
| SIGMAP.N | A factor in determining the rate at which the donor states capture electrons from the conduction band. |

Trap Depth

| | |
|-------------------|--|
| ELEC.DEPTH | Energy below conduction band edge of acceptor traps. |
| HOLE.DEPTH | Energy above valence band of donor traps. |

Lifetimes

| | |
|-------------------|---|
| TAU.N | Lifetime for electron detrapping from acceptor states to conduction band. |
| TAU.P | Lifetime for hole detrapping from donor states to valence band. |
| PF.A | Constant of proportionality for the ohmic part of the electron generation rate in the PF.NITRIDE model. |
| PF.B | Constant of proportionality for electron detrapping rate when Poole-Frenkel model is enabled. |
| PF.BARRIER | If specified, it overrides ELEC.DEPTH in calculation of electron detrapping rate when Poole-Frenkel model is enabled. |

21.37: ODEFFECTS

ODEFFECTS activates the bandgap defect model for organic polymer materials and sets the parameter values. This model can be used when simulating organic polymer devices using the ORGANIC DISPLAY AND ORGANIC SOLAR modules (see Chapter 15: “Organic Display and Organic Solar: Organic Simulators”).

Syntax

ODEFFECTS [<parameters>]

| Parameter | Type | Default | Units |
|------------|-----------|-----------------------|------------------|
| AFILE | Character | | |
| CONTINUOUS | Logical | False | |
| DEVICE | Character | | |
| DFILE | Character | | |
| DOPANT | Logical | False | |
| EA | Real | 0 | eV |
| ED | Real | 0 | eV |
| F.OTFTACC | Character | | |
| F.OTFTDON | Character | | |
| HA | Real | 0 | cm ⁻³ |
| HD | Real | 0 | cm ⁻³ |
| HOPPING | Logical | False | |
| INT_LIM1 | Real | 0.0 | eV |
| INT_LIM2 | Real | 0.0 | eV |
| MATERIAL | Character | | |
| NA | Real | 0 | cm ⁻³ |
| ND | Real | 0 | cm ⁻³ |
| NIA | Real | 0 | cm ⁻³ |
| NID | Real | 0 | cm ⁻³ |
| NUMA | Real | 12 | |
| NUMD | Real | 12 | |
| REGION | Real | All | |
| SIGAE | Real | 1.0×10^{-16} | cm ² |
| SIGAH | Real | 1.0×10^{-14} | cm ² |

| Parameter | Type | Default | Units |
|-----------|-----------|-----------------------|-----------------|
| SIGDE | Real | 1.0×10^{-14} | cm ² |
| SIGDH | Real | 1.0×10^{-16} | cm ² |
| SIGMA | Real | 0 | eV |
| SIGMD | Real | 0 | eV |
| SIGMAIA | Real | 0 | eV |
| SIGMAID | Real | 0 | eV |
| STRUCTURE | Character | | |
| TCA | Real | 0.0 | K |
| TCD | Real | 0.0 | K |
| TFILE | Character | | |
| X.MIN | Real | | μm |
| X.MAX | Real | | μm |
| Y.MIN | Real | | μm |
| Y.MAX | Real | | μm |
| Z.MIN | Real | | μm |
| Z.MAX | Real | | μm |

Description

| | |
|-------------------|---|
| AFILE | Specifies the acceptor state density output file. |
| CONTINUOUS | Specifies that the continuous defect model will be used. |
| DEVICE | Specifies which device in MIXEDMODE simulation will apply to the ODEFECTS statement. The synonym for this parameter is STRUCTURE. |
| DFILE | Specifies the donor state density output file. |
| DOPANT | Specifies that the defects defined using NA and ND are to be used in the dopant singlet exciton calculation. Only one dopant is allowed per region. |
| EA | Specifies the energy shift between the intrinsic and dopant states for acceptor-like traps. |
| ED | Specifies the energy shift between the intrinsic and dopant states for donor-like traps. |
| F.OTFTACC | Specifies the C-Interpreter file for the acceptor states energy distribution function. |
| F.OTFTDON | Specifies the C-Interpreter file for the donor states energy distribution function. |
| HA | Specifies the total acceptor-like trap density. |

| | |
|---|---|
| HD | Specifies the total donor-like trap density. |
| HOPPING | Specifies the effective transport hopping energy model is to be used. |
| INT_LIM1 | Specifies the lower limit for the numerical integration of the CONTINUOUS model. |
| INT_LIM2 | Specifies the upper limit for the numerical integration of the CONTINUOUS model. |
| MATERIAL | Specifies which material will apply to the ODEFFECTS statement. If a material is specified, then all regions defined as being composed of that material will be affected. |
| NA | Specifies the total dopant density for acceptor-like traps. |
| ND | Specifies the total dopant density for donor-like traps. |
| NIA | Specifies the total intrinsic dopant density for acceptor-like traps. |
| NID | Specifies the total intrinsic dopant density for donor-like traps. |
| NUMA | Specifies the number of discrete levels that will be used to simulate the continuous distribution of acceptor states. |
| NUMD | Specifies the number of discrete levels that will be used to simulate the continuous distribution of donor states. |
| REGION | Specifies the region to which the ODEFFECTS statement applies. |
| SIGAE | Specifies the electron capture cross-section for acceptor traps. |
| SIGAH | Specifies the hole capture cross-section for acceptor traps. |
| SIGAE | Specifies the electron capture cross-section for donor traps. |
| SIGAH | Specifies the hole capture cross-section for donor traps. |
| SIGMAA | Specifies the Gaussian width for the acceptor-like traps dopant distribution. |
| SIGMAD | Specifies the Gaussian width for the donor-like traps dopant distribution. |
| SIGMAIA | Specifies the Gaussian width for the acceptor-like traps intrinsic distribution. |
| SIGMAID | Specifies the Gaussian width for the donor-like traps intrinsic distribution. |
| STRUCTURE | This is a synonym for DEVICE. |
| TCA | Specifies the characteristic temperature for the acceptor-like trap states. |
| TCD | Specifies the characteristic temperature for the acceptor-like trap states. |
| TFILE | Specifies the file name where the acceptor and donor state density distributions will be stored. |
| X.MIN, X.MAX, Y.MIN, Y.MAX, Z.MIN, and Z.MAX | Specify the bounding box for the ODEFFECTS statement. |

21.38: OINTDEFECTS

OINTDEFECTS activates the bandgap interface defect model for organic polymer materials and sets the parameter values. This model can be used when simulating organic polymer devices using the OTFT module (see Chapter 15: “Organic Display and Organic Solar: Organic Simulators”).

Syntax

OINTDEFECTS [<parameters>]

| Parameter | Type | Default | Units |
|-------------|-----------|---------|------------------|
| AFILE | Character | | |
| CONTINUOUS | Logical | False | |
| DEVICE | Character | | |
| DFILE | Character | | |
| EA | Real | 0 | eV |
| ED | Real | 0 | eV |
| F.OTFTACC | Character | | |
| F.OTFTDON | Character | | |
| HA | Real | 0 | cm ⁻² |
| HD | Real | 0 | cm ⁻² |
| HOPPING | Logical | False | |
| INT_LIM1 | Real | 0.0 | eV |
| INT_LIM2 | Real | 0.0 | eV |
| INTMATERIAL | Character | | |
| INTNAME | Character | | |
| INTNUMBER | Character | | |
| INTREGION | Character | | |
| MATERIAL | Character | | |
| NA | Real | 0 | cm ⁻³ |
| ND | Real | 0 | cm ⁻³ |
| NIA | Real | 0 | cm ⁻³ |
| NID | Real | 0 | cm ⁻³ |
| NUMA | Real | 12 | |
| NUMD | Real | 12 | |
| R1MATERIAL | Character | | |

| Parameter | Type | Default | Units |
|------------|-----------|-----------------------|-----------------|
| R1NAME | Character | | |
| R1NUMBER | Integer | | |
| R1REGION | Character | | |
| R2MATERIAL | Character | | |
| R2NAME | Character | | |
| R2NUMBER | Integer | | |
| R2REGION | Character | | |
| REGION | Real | All | |
| SIGAE | Real | 1.0×10^{-16} | cm ² |
| SIGAH | Real | 1.0×10^{-14} | cm ² |
| SIGDE | Real | 1.0×10^{-14} | cm ² |
| SIGDH | Real | 1.0×10^{-16} | cm ² |
| SIGMA | Real | 0 | eV |
| SIGMD | Real | 0 | eV |
| SIGMAIA | Real | 0 | eV |
| SIGMAID | Real | 0 | eV |
| STRUCTURE | Character | | |
| TCA | Real | 0.0 | K |
| TCD | Real | 0.0 | K |
| TFILE | Character | | |
| X.MIN | Real | | μm |
| X.MAX | Real | | μm |
| Y.MIN | Real | | μm |
| Y.MAX | Real | | μm |
| Z.MIN | Real | | μm |
| Z.MAX | Real | | μm |

Description

| | |
|--------------------|---|
| AFILE | Specifies the acceptor state density output file. |
| CONTINUOUS | Specifies that the continuous defect model will be used. |
| DEVICE | Specifies which device in MIXEDMODE simulation will apply to the OINTDEFECTS statement. The synonym for this parameter is STRUCTURE. |
| DFILE | Specifies the donor state density output file. |
| EA | Specifies the energy shift between the intrinsic and dopant states for acceptor-like traps. |
| ED | Specifies the energy shift between the intrinsic and dopant states for donor-like traps. |
| F.OTFTACC | Specifies the C-Interpreter file for the acceptor states energy distribution function. |
| F.OTFTDON | Specifies the C-Interpreter file for the donor states energy distribution function. |
| HA | Specifies the total acceptor-like trap density. |
| HD | Specifies the total donor-like trap density. |
| HOPPING | Specifies the effective transport hopping energy model is to be used. |
| INT_LIM1 | Specifies the lower limit for the numerical integration of the CONTINUOUS model. |
| INT_LIM2 | Specifies the upper limit for the numerical integration of the CONTINUOUS model. |
| INTMATERIAL | Specifies that the interface models defined on this command should be applied to every interface between the two given materials. For example, INTMATERIAL="oxide/silicon". |
| INTNAME | Specifies that the interface models defined on this command should be applied to every interface between the two given regions (where the regions are defined by their region name). For example, INTNAME="channel/substrate". |
| INTNUMBER | Specifies that the interface models defined on this command should be applied to every interface between the two given regions (where the regions are defined by their region number). For example, INTNUMBER="2/3". |
| INTREGION | Specifies that the interface models defined on this command should be applied to every interface between the two given regions (where the regions are defined by either their region name or their region number). For example, INTREGION="channel/substrate". |
| MATERIAL | Specifies which material will apply to the OINTDEFECTS statement. If a material is specified, then all regions defined as being composed of that material will be affected. |
| NA | Specifies the total dopant density for acceptor-like traps. |
| ND | Specifies the total dopant density for donor-like traps. |
| NIA | Specifies the total intrinsic dopant density for acceptor-like traps. |
| NID | Specifies the total intrinsic dopant density for donor-like traps. |

| | |
|---|---|
| NUMA | Specifies the number of discrete levels that will be used to simulate the continuous distribution of acceptor states. |
| NUMD | Specifies the number of discrete levels that will be used to simulate the continuous distribution of donor states. |
| R1MATERIAL and R2MATERIAL | Specifies that the interface models defined on this command should be applied to every interface between the two given materials. For example, R1MATERIAL=oxide R2MATERIAL=silicon. |
| R1NAME and R2NAME | Specifies that the interface models defined on this command should be applied to every interface between the two given regions (where the regions are defined by their region name). For example, R1NAME=channel R2NAME=substrate. |
| R1NUMBER and R2NUMBER | Specifies that the interface models defined on this command should be applied to every interface between the two given regions (where the regions are defined by their region number). For example, R1NUMBER=2 R2NUMBER=3. |
| R1REGION and R2REGION | Specifies that the interface models defined on this command should be applied to every interface between the two given regions (where the regions are defined by either their region name or their region number). For example, R1REGION=channel R2REGION=substrate. |
| REGION | Specifies the region to which the OINTDEFECTS statement applies. |
| SIGAE | Specifies the electron capture cross-section for acceptor traps. |
| SIGAH | Specifies the hole capture cross-section for acceptor traps. |
| SIGDE | Specifies the electron capture cross-section for donor traps. |
| SIGDH | Specifies the hole capture cross-section for donor traps. |
| SIGMAA | Specifies the Gaussian width for the acceptor-like traps dopant distribution. |
| SIGMAD | Specifies the Gaussian width for the donor-like traps dopant distribution. |
| SIGMAIA | Specifies the Gaussian width for the acceptor-like traps intrinsic distribution. |
| SIGMAID | Specifies the Gaussian width for the donor-like traps intrinsic distribution. |
| STRUCTURE | This is a synonym for DEVICE. |
| TCA | Specifies the characteristic temperature for the acceptor-like trap states. |
| TCD | Specifies the characteristic temperature for the acceptor-like trap states. |
| TFILE | Specifies the file name where the acceptor and donor state density distributions will be stored. |
| X.MIN, X.MAX, Y.MIN, Y.MAX, Z.MIN, and Z.MAX | Specify the bounding box for the OINTDEFECTS statement. |

21.39: OPTIONS

OPTIONS sets options for an entire run.

Syntax

OPTIONS [**<parameters>**]

| Parameter | Type | Default | Units |
|-------------|-----------|---------|-------|
| CINT.CHAR | Character | | |
| CINT.DLL | Logical | False | |
| CINT.DOUBLE | Real | 0 | |
| CINT.INT | Real | 0 | |
| CINT.MODE | Integer | | |
| CINT.PARAM | Character | | |
| FAIL.QUIT | Logical | False | |
| NORMAL | Logical | True | |
| OUTLOGS | Logical | False | |
| QUIET | Logical | False | |
| TRANSITION | Logical | False | |
| VERBOSE | Logical | False | |

Description

| | |
|--------------------|---|
| CINT.CHAR | Specifies the value of a C-Interpreter global character parameter. CINT.PARAM must be defined along with CINT.CHAR and only one C-Interpreter global parameter can be defined per OPTIONS statement. The value of CINT.CHAR can be accessed in a C-Interpreter function by using <code>get_global_char()</code> . The function prototype is <code>char* get_global_char(char *param_name);</code> |
| CINT.DLL | Specifies that ATLAS should treat subsequent C-Interpreter files with the extension ".so" (on UNIX based machines) or ".dll" (on Windows based machines) as shared object libraries instead of C code files. The shared object libraries will be dynamically loaded at run-time. |
| CINT.DOUBLE | Specifies the value of a C-Interpreter global double parameter. CINT.PARAM must be defined along with CINT.DOUBLE and only one C-Interpreter global parameter can be defined per OPTIONS statement. The value of CINT.DOUBLE can be accessed in a C-Interpreter function by using <code>get_global_double()</code> . The function prototype is <code>double get_global_double(char *param_name);</code> |

| | |
|-------------------|--|
| CINT.INT | Specifies the value of a C-Interpreter global integer parameter. <code>CINT.PARAM</code> must be defined along with <code>CINT.INT</code> and only one C-Interpreter global parameter can be defined per <code>OPTIONS</code> statement. The value of <code>CINT.INT</code> can be accessed in a C-Interpreter function by using <code>get_global_int()</code> . The function prototype is <code>int get_global_int(char *param_name);</code> |
| CINT.MODE | Specifies the C-Interpreter compilation mode. If <code>CINT.MODE</code> is set to 0, all subsequent C-Interpreter files will be compiled in optimize mode. If <code>CINT.MODE</code> is set to 1, all subsequent C-Interpreter files will be compiled in command-line debug mode. If <code>CINT.MODE</code> is set to 2, all subsequent C-Interpreter files will be compiled in GUI debug mode. The default compilation mode is optimize. |
| CINT.PARAM | Specifies the name of a C-Interpreter global parameter. Either <code>CINT.CHAR</code> , <code>CINT.INT</code> , or <code>CINT.DOUBLE</code> must be defined along with <code>CINT.PARAM</code> . Only one C-Interpreter global parameter can be defined per <code>OPTIONS</code> statement. |
| FAIL.QUIT | If enabled, it will cause the simulation to quit if the number of cutbacks exceeds the number specified by the <code>MAXTRAP</code> parameter of the <code>METHOD</code> statement and <code>TRAP</code> is enabled. |
| parameters | This is one or more of the run control parameters described below. These parameters, which are not normally used, specify debugging options. |
| NORMAL | This is the default specification for run-time output filtering. At this setting ATLAS prints out the most relevant information (e.g., mesh statistics, terminal voltages, currents, warnings, and error messages). |
| OUTLOGS | Specifies that complex index of refraction data is to be automatically output into logfiles similar to the use of <code>OUT.INDEX</code> on the <code>MATERIAL</code> statement. |
| QUIET | Specifies the maximum of filtering of run-time output. |
| TRANSITION | Specifies that during calculation of bound state energies for optical transitions. The allowable transitions are printed to the run-time output. |
| VERBOSE | Specifies the minimum filtering of run-time output. You should specify <code>VERBOSE</code> if you want output of residual norms. |

Example

```
options cint.param=filename cint.char="a.in"
options cint.param=debug_flag cint.int=1
options cint.param="time" cint.double=10.5

char *filename;
int debug_flag;
double time;
filename = get_global_char("filename");
debug_flag = get_global_int("debug_flag");
time = get_global_double("time");
```

The following syntax can be used to provide extra debugging output.

```
OPTION VERBOSE
```


21.40: OUTPUT

OUTPUT allows you to specify the data that will be stored in standard structure format files.

Syntax

OUTPUT <parameters>

| Parameter | Type | Default | Units |
|---------------|---------|---------|-------|
| ANGLE | Logical | False | |
| AREA | Logical | False | |
| BAND.PARAM | Logical | False | |
| BAND.TEMP | Logical | false | |
| CHARGE | Logical | False | |
| CON.BAND | Logical | False | |
| CONTACT | Integer | | |
| DELTAV | Real | 0.1 | |
| DEVDEG | Logical | False | |
| E.FIELD | Logical | True | |
| E.LINES | Logical | False | |
| E.MOBILITY | Logical | False | |
| E.TEMP | Logical | True | |
| E.VELOCITY | Logical | False | |
| EFIELD | Logical | True | |
| EIGENS | Integer | 5 | |
| ESIZEOUT.NEGF | Real | 500 | |
| EX.FIELD | Logical | True | |
| EX.VELOCITY | Logical | False | |
| EY.FIELD | Logical | True | |
| EY.VELOCITY | Logical | False | |
| EZ.FIELD | Logical | True | |
| EZ.VELOCITY | Logical | False | |
| FLOWLINES | Logical | False | |
| H.MOBILITY | Logical | False | |
| H.TEMP | Logical | True | |
| H.VELOCITY | Logical | False | |

| Parameter | Type | Default | Units |
|-------------|-----------|---------|-------|
| HCTE.JOULE | Logical | False | |
| HEI | Logical | False | |
| HHI | Logical | False | |
| HX.VELOCITY | Logical | False | |
| HY.VELOCITY | Logical | False | |
| HZ.VELOCITY | Logical | False | |
| IMPACT | Logical | True | |
| INV.AREA | Logical | False | |
| INV.ANGLE | Logical | False | |
| INAME | Character | | |
| J.CONDUC | Logical | True | |
| J.DISP | Logical | False | |
| J.DRIFT | Logical | False | |
| J.DIFFUSION | Logical | False | |
| J.ELECTRON | Logical | True | |
| J.HOLE | Logical | True | |
| J.TOTAL | Logical | True | |
| JX.CONDUC | Logical | False | |
| JX.ELECTRON | Logical | True | |
| JX.HOLE | Logical | True | |
| JX.TOTAL | Logical | True | |
| JY.CONDUC | Logical | False | |
| JY.ELECTRON | Logical | True | |
| JY.HOLE | Logical | True | |
| JY.TOTAL | Logical | True | |
| JZ.CONDUC | Logical | True | |
| JZ.ELECTRON | Logical | True | |
| JZ.HOLE | Logical | True | |
| JZ.TOTAL | Logical | True | |
| KSN | Logical | False | |
| KSP | Logical | False | |
| L.TEMPER | Logical | True | |

| Parameter | Type | Default | Units |
|--------------|---------|---------|-------|
| LRATIO | Real | 1.0 | |
| MINSET | Logical | False | |
| N.LINES | Integer | 20 | |
| NLTAT.GAMMA | Logical | False | |
| NOISE | Logical | False | |
| NOISE.IMP | Logical | False | |
| NOISE.ALL | Logical | False | |
| OPT.INTENS | Logical | False | |
| OX.CHARGE | Logical | False | |
| OLD.AVG | Logical | True | |
| P.QUANTUM | Logical | False | |
| PERMITTIVITY | Logical | False | |
| PHOTOGEN | Logical | True | |
| POLAR.CHARGE | Logical | False | |
| QFN | Logical | True | |
| QFP | Logical | True | |
| QSS | Logical | False | |
| QTUNN.BBT | Logical | False | |
| QTUNN.EL | Logical | False | |
| QTUNN.HO | Logical | False | |
| RECOMB | Logical | True | |
| SCHOTTKY | Logical | False | |
| SONOS.RATES | Logical | False | |
| T.QUANTUM | Logical | False | |
| TAURN | Logical | False | |
| TAURP | Logical | False | |
| TOT.DOPING | Logical | False | |
| TRAPS | Logical | True | |
| TRAPS.FT | Logical | False | |
| U.AUGER | Logical | False | |
| U.BBT | Logical | False | |
| U.LANGEVIN | Logical | False | |

| Parameter | Type | Default | Units |
|-------------|---------|---------|-------|
| U.RADIATIVE | Logical | False | |
| U.SRH | Logical | False | |
| U.TRANTRAP | Logical | False | |
| U.TRAP | Logical | False | |
| VAL.BAND | Logical | False | |
| VECTORS | Logical | False | |
| X.COMP | Logical | True | |
| Y.COMP | Logical | True | |

Description

| | |
|---------------------------------|---|
| BAND.PARAM | Specifies that the band parameters (E_g , n_i , N_c , N_v , and χ) are included in the standard structure file. |
| BAND.TEMP | Outputs the following temperature dependent band parameters. <ul style="list-style-type: none"> • $\text{Sqrt}(\text{electron concentration} * \text{hole concentration}) \text{ (cm}^{-3}\text{)}$ • Conduction band effective density of states (cm^{-3}) • Valence band effective density of states (cm^{-3}) • Energy band gap (eV) • Conduction Band Energy (eV) • Valence Band Energy (eV) |
| CHARGE | Specifies that the net charge will be included in the standard structure file. |
| CON.BAND | Specifies that the conduction band edge will be included in the standard structure file. |
| DEVDEG | Causes the distribution of acceptor/donor like traps on the interface, hot electron/hole current density on the interface, and trapped electron/holes to be written to the structure file. |
| E.FIELD or EFIELD | Specifies that total electric field will be included in the standard structure file. |
| E.LINES | Specifies the electric field lines will be included in the standard structure file. |
| E.MOBILITY | Specifies that electron mobility will be included in the standard structure file. |
| E.TEMP | Specifies that the electron temperature will be included in the standard structure file. |
| E.VELOCITY | Specifies that the total electron velocity will be included in the standard structure file. |
| EIGENS | Specifies the maximum number of eigen energies and eigen functions to be written to the structure file from a Poisson- Schrodinger solution. |

| | |
|----------------------|---|
| ESIZEOUT.NEGF | Sets the number of energy grid points in the output file where transmission, DOS, current and carrier densities versus energy are stored. |
| EX.FIELD | Specifies that the x-component of electric field will be included in the standard structure file. |
| EX.VELOCITY | Specifies that the x-component of electron velocity will be included in the standard structure file. |
| EY.FIELD | Specifies that the y-component of electric field will be included in the standard structure file. |
| EY.VELOCITY | Specifies that the y-component of electron velocity will be included in the standard structure file. |
| EZ.FIELD | Specifies that the z-component of the electric field will be included in the standard structure file. |
| EZ.VELOCITY | Specifies that the z-component of the electron velocity will be included in the standard structure file. |
| FLOWLINES | Specifies that the current flowlines will be included in the standard structure file. |
| H.MOBILITY | Specifies that hole mobility will be included in the standard structure file. |
| H.TEMP | Specifies that the hole temperature will be included in the standard structure file. |
| H.VELOCITY | Specifies that the total hole velocity will be included in the standard structure file. |
| HCTE.JOULE | Specifies that the volumetrically averaged Joule heating will be included in the standard structure file. |
| HEI | Specifies that the hot electron current density will be included in the standard structure file. |
| HHI | Specifies that the hot hole current density will be included in the standard structure file. |
| HX.VELOCITY | Specifies that the x-component of hole velocity will be included in the standard structure file. |
| HY.VELOCITY | Specifies that the y-component of hole velocity will be included in the standard structure file. |
| HZ.VELOCITY | Specifies that the z-component of the hole velocity will be included in the standard structure file. |
| IMPACT | Specifies that the impact ionization rate will be included in the standard structure file. |
| J.CONDUC | Specifies that the total conduction current density will be included in the standard structure file. |
| J.DISP | Specifies that the total displacement current density will be included in the standard structure file. |
| J.ELECTRON | Specifies that the total electron current density will be included in the standard structure file. |

| | |
|--------------------|--|
| J.HOLE | Specifies that the total hole current density will be included in the standard structure file. |
| J.TOTAL | Specifies that the total current density will be included in the standard structure file. |
| JX.CONDUC | Specifies that the x-component of the total conduction current density will be included in the standard structure file. |
| J.DRIFT | Specifies that the drift current density will be included in the standard structure file. |
| J.DIFFUSION | Specifies that diffusion current density will be included in the standard structure file. |
| JX.ELECTRON | Specifies that the x-component of electron current density will be included in the standard structure file. |
| JX.HOLE | Specifies that the x-component of hole current density will be included in the standard structure file. |
| JX.TOTAL | Specifies that the x-component of total current density will be included in the standard structure file. |
| JY.CONDUC | Specifies that the y-component of the total conduction current density will be included in the standard structure file. |
| JY.ELECTRON | Specifies that the y-component of electron current density will be included in the standard structure file. |
| JY.HOLE | Specifies that the y-component of hole current density will be included in the standard structure file. |
| JY.TOTAL | Specifies that the y-component of total current density will be included in the standard structure file. |
| JZ.CONDUC | Specifies that the z-component of the conduction current density will be included in the standard structure file. |
| JZ.ELECTRON | Specifies that the z-component of the electron current density will be included in the standard structure file. |
| JZ.HOLE | Specifies that the z-component of the hole current density will be included in the standard structure file. |
| JZ.TOTAL | Specifies that the z-component of the total current density will be included in the standard structure file. |
| KSN | Specifies that electron Scattering Law Exponent is to be written to any saved structure file. |
| KSP | Specifies that hole Scattering Law Exponent is to be written to any saved structure file. |
| L.TEMPER | Specifies that lattice temperature will be included in the standard structure file. |
| MINSET | This is the minimum set of data (potential, carrier concentration, and electric field) that will be included in the standard structure file. |

| | |
|---------------------|--|
| NLTAT.GAMMA | Specifies that the Nonlocal trap-assisted-tunneling Gamma factors are written to any saved structure file. The values written have been interpolated onto the device mesh. |
| OPT.INTENS | Specifies that optical intensity is included in the standard structure file. |
| OX.CHARGE | Specifies that fixed oxide charge is include in the standard structure file. |
| P.QUANTUM | Specifies that the Bohm quantum potential is included in the solution file. |
| PERMITTIVITY | Specifies the dielectric permittivity is saved. |
| PHOTOGEN | Specifies that the photogeneration rate will be included in the standard structure file. |
| POLAR.CHARGE | Specifies that polarization charge will be included in the structure file. |
| QFN | Specifies that the electron quasi-fermi level will be included in the standard structure file. |
| QFP | Specifies that the hole quasi-fermi level will be included in the standard structure file. |
| QSS | Specifies that the surface charge will be included in the standard structure file. |
| QTUNN.BBT | Specifies that the direct quantum tunneling band-to-band current density at each interface node is written to any saved structure file. |
| QTUNN.EL | Specifies that the direct quantum tunneling electron current density at each interface node is written to any saved structure file. |
| QTUNN.HO | Specifies that the direct quantum tunneling hole current density at each interface node is written to any saved structure file. |
| RECOMB | Specifies that the recombination rate will be included in the standard structure file. |
| SCHOTTKY | Specifies that recombination velocities and barrier lowering will be included in the standard structure file. |
| SONOS.RATES | This causes the output of four quantities to the structure file. These are the Generation and Recombination rates for the trapped electron states and the trapped hole states in the DYNSAONOS model. This requires the DYNASONOS or BESONOS models. |
| T.QUANTUM | Specifies that quantum temperatture from the density gradient model is included in the solution file. |
| TAURN | Specifies that electron relaxation times are to be written to any saved structure file. |
| TAURP | Specifies that hole relaxation times are to be written to any saved structure file. |
| TOT.DOPING | Specifies that total doping will be included in the standard structure file. |
| TRAPS | Specifies that trap density information will be included in the standard structure file. |

| | |
|--------------------|---|
| TRAPS.FT | Specifies that the trap probability of occupation will be included in the standard structure file. |
| U.AUGER | Specifies that the Auger component of recombination is to be written to solution files. |
| U.BBT | Specifies that the band to band tunneling rate will be included in the standard structure file. |
| U.LANGEVIN | Specifies that the Langevin recombination rate will be included in the standard structure file. |
| U.RADIATIVE | Specifies that the radiative component of recombination is to be written to solution files. |
| U.SRH | Specifies that the SRH component of recombination is to be written to solution files. |
| U.TRANTRAP | Specifies that both electron recombination rate and the hole recombination rate into transient traps will be included in the SILVACO standard structure file. |
| U.TRAP | Specifies that the trap recombination/generation rate will be included in the standard structure file. |
| VAL.BAND | Specifies that the valence band edge will be included in the standard structure file. |
| VECTORS | Specifies that only vector components will be included in the standard structure file. |
| X.COMP | Specifies that the composition fraction, x , is to be written to solution files. |
| Y.COMP | Specifies that the composition fraction, y, is to be written to solution files. |

Ionization Integral Parameters

| | |
|----------------|--|
| INAME | Specifies the name of a contact for which electric field lines are calculated. |
| CONTACT | Specifies a contact number for which electric field lines are calculated. |
| LRATIO | Specifies the spacing ratio between adjacent electric field lines. Defaults to 1.0 for uniform spacing. |
| N.LINES | Specifies the number of electric field lines. |
| DELTAV | Since the electric field is near zero at the contact, the electric field line calculations begin at a distance from the contact at which the contact voltage has changed by DELTAV. Defaults to 0.1 V. |

Note: See Section 21.53: "SOLVE" and the on-line examples for instructions on using ionization integrals.

NOISE Parameters

| | |
|------------------|---|
| NOISE | Selects the total local noise source for output. |
| NOISE.IMP | Selects the impedance fields for output. |
| NOISE.ALL | Selects everything for output. Currently, the local noise source, the impedance fields, the short-circuit current Green's function, the individual microscopic noise sources, and the individual local noise sources. |

Averaging Parameters for Vector Quantities

| | |
|------------------|---|
| OLD.AVG | Specifies that the current and field quantities will be averaged using an older algorithm (from version 3.0.0.R and back). By default the new method is used. |
| ANGLE | Specifies that averaging of current and fields will be weighted by the size of the angle of triangles intersecting at the node. |
| INV.ANGLE | Specifies that averaging of current and fields will be weighted by the inverse of the size of the angle of triangles intersecting at the node. |
| AREA | Specifies that averaging of current and fields will be weighted by the areas of triangles intersecting at the node. |
| INV.AREA | Specifies that averaging of current and fields will be weighted by the inverse of areas of triangles intersecting at the node. |

Note: Certain quantities that can be output into the structure file and subsequently displayed using TONYPLOT need special mention. These quantities are evaluated within ATLAS along the links between grid points. They are represented in the structure file at the grid points themselves. As such these quantities are subject to averaging. In particular, electric field and currents are averaged so as to take into account the vector nature of these values. Mobility is simply summed up over all the links surrounding the grid point and divided by the total number of links. Carrier velocities are derived by dividing the averaged current by the carrier density at the grid point and the fundamental electron charge, q .

An Example of Combining OUTPUT with SOLVE and SAVE

The OUTPUT statement is often used in conjunction with the SAVE statement. The following statement lines specify that current flowlines and electron velocity components are saved in all subsequent standard structure solution files.

```
OUTPUT FLOWLINES EX.VELO EY.VELO
SOLVE PREVIOUS V5=2 OUTF=data1.str MASTER
SAVE OUTF=data2.str
```

21.41: PHOTOGENERATE

PHOTOGENERATE statement specifies photogeneration of carriers inside the device. It ensures TMA compatibility with the PHOTOGEN statement.

Syntax

PHOTOGENERATE <parameters>

| Parameter | Type | Default | Units |
|-----------|------|-----------------|------------------------------|
| A1 | Real | 0.0 | cm^{-3} |
| A2 | Real | 0.0 | $\text{cm}^{-3}/\mu\text{m}$ |
| A3 | Real | 0.0 | cm^{-3} |
| A4 | Real | 0.0 | μm^{-1} |
| CONSTANT | Real | 0.0 | cm^{-3} |
| EXPONENT | Real | 0.0 | μm^{-1} |
| FACTOR | Real | 0.0 | cm^{-3} |
| LINEAR | Real | 0.0 | $\text{cm}^{-3}/\mu\text{m}$ |
| RADIAL | Real | ∞ | μm |
| R.CHAR | Real | ∞ | μm |
| X.END | Real | Min x of device | μm |
| X.MAX | Real | Max x of device | μm |
| X.MIN | Real | Min x of device | μm |
| X.ORIGIN | Real | Min x of device | μm |
| X.START | Real | Min x of device | μm |
| Y.END | Real | Max y of device | μm |
| Y.MAX | Real | Max y of device | μm |
| Y.MIN | Real | Min y of device | μm |
| Y.ORIGIN | Real | Min y of device | μm |
| Y.START | Real | Min y of device | μm |

Description

| | |
|-----------|--|
| A1 | This is the synonym for CONSTANT. Added for TMA compatibility. |
| A2 | This is the synonym for LINEAR. Added for TMA compatibility. |
| A3 | This is the synonym for FACTOR. Added for TMA compatibility. |

| | |
|-----------------|--|
| A4 | This is the synonym for EXPONENT . Added for TMA compatibility. |
| CONSTANT | Specifies the constant photogeneration rate. |
| EXPONENT | Specifies the exponential coefficient for depth dependent photogeneration. |
| FACTOR | Specifies the pre-exponential factor for depth dependent photogeneration. |
| LINEAR | Specifies the linear factor for depth dependent photogeneration. |
| RADIAL | Specifies the characteristic radial distance for Gaussian dependence of photogeneration rate in the direction perpendicular to the line along which the carriers are injected. |
| R.CHAR | This is the synonym for RADIAL . Added for TMA compatibility. |
| X.END | Specifies the X coordinate of the end of the line along which photogenerated carriers are injected. |
| X.MAX | This is the maximum X coordinate at which photogeneration occurs. Generation of carriers is zero for $x > X.MAX$. |
| X.MIN | This is the minimum X coordinate at which photogeneration occurs. Generation of carriers is zero for $x < X.MIN$. |
| X.ORIGIN | Specifies the X coordinate of the origin of the line along which photogenerated carriers are injected. |
| X.START | This is the synonym of X.ORIGIN . Added for TMA compatibility. |
| Y.END | Specifies the Y coordinate of the end of the line along which photogenerated carriers are injected. |
| Y.MAX | This is the maximum Y coordinate at which photogeneration occurs. Generation of carriers is zero for $y > Y.MAX$. |
| Y.MIN | This is the minimum Y coordinate at which photogeneration occurs. Generation of carriers is zero for $y < Y.MIN$. |
| Y.ORIGIN | Specifies the Y coordinate of the origin of the line along which photogenerated carriers are injected. |
| Y.START | This is the synonym of Y.ORIGIN . Added for TMA compatibility. |

21.42: PML

The PML statement allows definition of perfectly matched layers for finite-difference time-domain (FDTD) analysis.

Syntax

PML [parameters]

| Parameter | Type | Default | Units |
|--------------|-----------|---------|-------|
| ALL | Logical | False | |
| ALPHA | Real | 0.0 | 1/cm |
| BACK | Logical | False | |
| BEAM | Integer | All | |
| BOTTOM | Logical | True | |
| DEGREE | Integer | 2 | |
| FRONT | Logical | False | |
| LEFT | Logical | False | |
| MATERIAL | Character | | |
| NSAMP | Integer | 100 | |
| PERMEABILITY | Real | 1.0 | |
| PERMITTIVITY | Real | 1.0 | |
| R90 | Real | 0.0 | |
| REAL.INDEX | Real | 1.0 | |
| TOP | Logical | False | |
| RIGHT | Logical | False | |
| WIDTH | Real | 0.0 | μm |
| XDIR | Logical | False | |
| YDIR | Logical | False | |

Description

| | |
|--------------|--|
| ALL | Specifies that the PML is applied to all sides (TOP, BOTTOM, LEFT and RIGHT) of the FDTD domain. |
| ALPHA | Specifies the maximum absorption coefficient of the PML. |
| BACK | Specifies that the PML is added at the XY plane at the minimum value of z. |
| BEAM | Specifies the index for the beam that the PML will be applied. If BEAM is unspecified, then PML will be applied to all previously defined beams. |

| | |
|---------------------|---|
| BOTTOM | Specifies that the PML is added at the XZ plane at the maximum value of y. |
| DEGREE | Specifies the degree of Equation 10-68 |
| FRONT | Specifies that the PML is added at the XY plane at the maximum of z. |
| LEFT | Specifies that the PML is added at the YZ plane at the minimum X coordinate. |
| MATERIAL | Specifies the material name to use to determine the real part of the complex index of refraction versus wavelength for the PML. |
| NSAMP | Specifies the number of samples in the PML in the direction of the coordinate axis specified by X.DIR or Y.DIR. |
| PERMEABILITY | Specifies the relative permeability to use within the PML. |
| PERMITTIVITY | Specifies the relative permittivity to use within the PML. |
| R90 | Specifies the desired value of the normal reflection coefficient. This is $R(\Theta)$ at $\Theta=90^\circ$ in Equation 10-69. |
| REAL . INDEX | Specifies the real part of the complex index of refraction of the PML. |
| RIGHT | Specifies that the PML is added at the YZ plane at the maximum X coordinate. |
| TOP | Specifies that the PML is added at the XZ plane at the minimum value of y. |
| WIDTH | Specifies the thickness of the PML in microns. |
| XDIR | Specifies that the PML will be added at the maximum and minimum x coordinates. |
| YDIR | Specifies that the PML will be added at the maximum and minimum y coordinates. |

21.43: PROBE

PROBE allows you to output the value of several distributed quantities to the log file. The value at a specified location or the minimum, maximum, or integrated value within a specified area of the device will be saved to the log file at each bias or time point.

Note: PROBE is the most accurate way to determine the value of many parameters calculated by ATLAS. Parameters stored on node points in the structure files for TonyPlot are often interpolated and subject to noise.

Syntax

```
PROBE [MIN|MAX|INTEGRATED|x=<n> y=<n> z=<n> [DIR=<n>]] [POLAR=<n>]<parameters>
```

| Parameter | Type | Default | Units |
|---------------|-----------|-----------------|-------|
| ACC.CTRAP | Logical | False | |
| ACC.TRAP | Logical | False | |
| ALPHAN | Logical | False | |
| ALPHAP | Logical | False | |
| APCURRENT | Logical | False | |
| AUGER | Logical | False | |
| BACK | Real | maximum z coord | μm |
| BAND | Integer | 1 | |
| BAND.GAP | Logical | False | |
| BEAM | Integer | | |
| BND.ENER | Logical | False | |
| BOTTOM | Real | maximum y coord | μm |
| CHARGE | Logical | False | |
| COMPLIANCE | Real | | |
| CON.BAND | Logical | False | |
| CONCACC.CTRAP | Logical | False | |
| CONCACC.TRAP | Logical | False | |
| CONCDON.CTRAP | Logical | False | |
| CONCDON.TRAP | Logical | False | |
| CURDVSE | Logical | False | |
| DENSUSE | Logical | False | |
| DEVICE | Character | | |

| Parameter | Type | Default | Units |
|----------------|-----------|-----------------|---------|
| DIR | Real | 0.0 | degrees |
| DON.CTRAP | Logical | | |
| DON.TRAP | Logical | | |
| DOPANT.EXCITON | Logical | False | |
| DOPRAD.EXCITON | Logical | False | |
| DOSVSE | Logical | False | |
| E.TRANTRAP | Logical | False | |
| EMAX | Real | | eV |
| EMIN | Real | | eV |
| ENERGY | Real | | eV |
| EXCITON | Logical | False | |
| FILENAME | Character | "TransvsE" | |
| FIELD | Logical | False | |
| FRONT | Real | minimum z coord | μm |
| FTACC.CTRAP | Logical | False | |
| FTACC.TRAP | Logical | False | |
| FTDON.CTRAP | Logical | False | |
| FTDON.TRAP | Logical | False | |
| GENERATION | Logical | False | |
| GR.HEAT | Logical | False | |
| H.CONC | Logical | False | |
| H.TRANTRAP | Logical | False | |
| INTEGRATED | Logical | False | |
| INTENSITY | Logical | False | |
| J.CONDUCTION | Logical | False | |
| J.DISP | Logical | False | |
| J.ELECTRON | Logical | False | |
| J.HOLE | Logical | False | |
| J.PROTON | Logical | False | |
| J.TOTAL | Logical | False | |
| JOULE.HEAT | Logical | False | |
| KX | Logical | False | |

| Parameter | Type | Default | Units |
|--------------------|-----------|-----------------|-------|
| KY | Logical | False | |
| KZ | Logical | False | |
| LAYER.ABSO | Logical | False | |
| LAYER.REFL | Logical | False | |
| LAYER.TRAN | Logical | False | |
| LMAX | Real | | μm |
| LMIN | Real | | μm |
| LANGEVIN | Logical | False | |
| LASER.INTENSITY | Logical | False | |
| LASER.GAIN | Logical | False | |
| LASER.MODE | Real | | |
| LAT.TEMP | Logical | False | |
| LEFT | Real | minimum x coord | μm |
| LUMINOUS.INTENSITY | Logical | False | |
| MATERIAL | Character | | |
| MAX | Logical | False | |
| MIN | Logical | False | |
| MAX.XITION | Logical | False | |
| MIN.XITION | Logical | False | |
| N.CONC | Logical | False | |
| N.MOB | Logical | False | |
| N.TEMP | Logical | False | |
| NAME | Character | | |
| NWELL | Logical | False | |
| P.CONC | Logical | False | |
| P.MOB | Logical | False | |
| P.TEMP | Logical | False | |
| PERMITTIVITY | Logical | False | |
| PHOTOGEN | Logical | False | |
| POLARIZATION | Logical | False | |
| POTENTIAL | Logical | False | |
| PT.HEAT | Logical | False | |

| Parameter | Type | Default | Units |
|--------------|-----------|-----------------|-------|
| PWELL | Logical | False | |
| QFN | Logical | False | |
| QFP | Logical | False | |
| R.TRAP | Logical | False | |
| R.BBT | Logical | False | |
| RADIATIVE | Logical | False | |
| RAUGER | Logical | False | |
| RECOMBIN | Logical | False | |
| REGION | Integer | | |
| RESISTIVITY | Logical | False | |
| RIGHT | Real | maximum x coord | μm |
| RNAME | Character | | |
| SONOS.CHARGE | Logical | False | |
| SRH | Logical | False | |
| STATE | Integer | 1 | |
| STRUCTURE | Character | | |
| TOTAL.HEAT | Logical | False | |
| TOP | Real | minimum y coord | μm |
| TRANSMISSION | Logical | False | |
| VAL.BAND | Logical | False | |
| VEL.ELECTRON | Logical | False | |
| VEL.HOLE | Logical | False | |
| WAVE.FUN | Logical | False | |
| WAVELENGTH | Logical | False | |
| X | Real | | μm |
| X.MAX | Real | maximum x coord | μm |
| X.MIN | Real | minimum x coord | μm |
| Y | Real | maximum x coord | μm |
| Y.MAX | Real | maximum x coord | μm |
| Y.MIN | Real | minimum y coord | μm |
| Z.MAX | Real | maximum z coord | μm |
| Z.MIN | Real | minimum z coord | μm |

Description

| | |
|-----------------------|---|
| ACC.CTRAP | Specifies that the continuous acceptor trap density of states is to be probed. |
| ACC.TRAP | Specifies that the acceptor trap density of states is to be probed. If multiple trap levels are present the ENERGY parameter should be set to the desired energy level that is to be probed. |
| ALPHAN | Specifies that the electron impact ionization coefficient is to be probed. The DIR parameter should also be specified as this is a vector quantity. |
| ALPHAN, ALPHAP | Specify that the electron or hole impact ionization constant alpha is to be probed. |
| ALPHAP | Specifies that the hole impact ionization coefficient is to be probed. The DIR parameter should also be specified as this is a vector quantity. |
| APCURRENT | Specifies that the available photocurrent is probed. |
| AUGER | Specifies that Auger recombination rate is probed. |
| BAND | <p>This is the number of the electron or hole band characterized by effective mass. Generally, the electron valley or hole band is characterized by values of effective mass (mx,my,mz) along main axes, which are given below for different values of BAND on the PROBE statement and the SCHRODINGER, P.SCHRODINGER, NUM.DIRECT, NUM.BAND and SP.DIR parameters on the MODELS statement.</p> <pre>(mx, my, mz) . (MT1, ML, MT2) (BAND=1 AND SCHRODINGER AND NUM.DIRECT>1) (MT2, MT1, ML) (BAND=2 AND SCHRODINGER AND NUM.DIRECT>1) (ML, MT2, MT1) (BAND=3 AND SCHRODINGER AND NUM.DIRECT=3) (MC, MC, MC) (BAND=1 AND SCHRODINGER AND NUM.DIRECT=1) (MHH, MHH, MHH) (BAND=1 AND P.SCHRODINGER AND NUM.BAND>1) (MLH, MLH, MLH) (BAND=2 AND P.SCHRODINGER AND NUM.BAND>1) (MSO, MSO, MSO) (BAND=3 AND P.SCHRODINGER AND NUM.BAND=3) (MV, MV, MV) (BAND=1 AND P.SCHRODINGER AND NUM.BAND=1)</pre> <p>If BAND<0 , it defaults to BAND=1.</p> <p>If BAND>NUM.DIRECT and SCHRODINGER, it defaults to BAND=NUM.DIRECT.</p> <p>If BAND>NUM.BAND and P.SCHRODINGER, it defaults to BAND=NUM.BAND.</p> <p>For materials with one band but with anisotropic electron effective mass, you can change the effective mass in the case of BAND=1 and SCHRODINGER=1 and NUM.DIRECT=1 using the SP.DIR parameter on the MODELS statement.</p> |
| BAND.GAP | Specifies that the bandgap is to be probed. If the probe is located in a equation well, the probe returns the energy associated with the minimum allowable transition. |

| | |
|-----------------------|--|
| BEAM | Specifies a beam number to focus the application of the probe to that specific beam. |
| BND.ENER | Probes the bound state energy characterized by the BAND and STATE parameters. |
| CHARGE | Specifies that the net charge is to be probed. |
| COMPLIANCE | Specifies the probed quantity compliance value. When the probed quantity reaches the specifies value, the SOLVE statement (or .DC or .TRANS statement in MIXEDMODE) will terminate and will execute the next statement. |
| CON.BAND | Probes the conduction band. |
| CONCACC.CTRAP | Specifies that the continuous acceptor trap concentration is to be probed. |
| CONCACC.TRAP | Specifies that the acceptor trap concentration is to be probed. You can use the ENERGY parameter to specify the trap energy level to be probed. If ENERGY is not specified, then the total value of all acceptor energy levels will be probed. |
| CONCDON.CTRAP | Specifies that the continuous donor trap concentration is to be probed. |
| CONCDON.TRAP | Specifies that the donor trap concentration is to be probed. You can use the ENERGY parameter to specify the trap energy level to be probed. If ENERGY is not specified, then the total value of all donor energy levels will be probed. |
| CURDVSE | Stores current density versus energy for each solution of NEGF solver. |
| DENSVSE | Stores carrier density versus energy for each solution of NEGF solver. |
| DEVICE | Specifies which device in MIXEDMODE simulation the PROBE statement should apply to. The synonym for this parameter is STRUCTURE . |
| DIR | Specifies the direction relative to the X axis in degrees associated with certain directed quantities. These quantities include FIELD , N.MOB , P.MOB , and POLARIZATION . |
| DON.CTRAP | Specifies that the continuous donor trap density of states is to be probed. |
| DON.TRAP | Specifies that the ionized donor trap density is to be probed. If multiple trap levels are present the ENERGY parameter should be set to the desired energy level that is to be probed. |
| DOPANT.EXCITON | Specifies that the singlet dopant exciton density is to be probed. |
| DOPRAD.EXCITON | Specifies that the singlet dopant exciton radiative rate is to be probed. |
| DOSVSE | Stores density of states (DOS) versus energy for each solution of NEGF solver. |
| E.TRANTRAP | Specifies that the electron recombination rate into transient traps is to be probed. |

| | |
|---------------------|---|
| EMAX, EMIN | Specifies the range of energies to search for peak emission wavelength when the WAVELENGTH parameter is set on the PROBE statement. |
| FILENAME | Specifies the name of file where Transmission, DOS, carrier, and current density versus energy are stored. |
| TRANSMISSION | Stores Transmission versus energy for each solution of NEGF solver. See Chapter 13: “Quantum: Quantum Effect Simulator” for more information. |

Note: The algorithm used finds the triangle in the mesh containing the specified X and Y values. Then the value of the **DIR** parameter is used to find which edge of the triangle lies in the direction nearest that value.

| | |
|---------------------|--|
| EXCITON | Specifies that the exciton density is probed. |
| FIELD | Specifies that a value of electric field is probed. The DIR parameter should also be specified if FIELD is used. |
| FTACC.CTRAP | Specifies that the continuous trap probability of occupation is to be probed. |
| FTACC.TRAP | Specifies that the acceptor trap probability of occupation is to be probed. You can use the ENERGY parameter to specify the trap energy level to be probed. If ENERGY is not specified, then the total value of all acceptor energy levels will be probed. |
| FTDON.CTRAP | Specifies that the continuous donor trap probability of occupation is to be probed. |
| FTDON.TRAP | Specifies that the donor trap probability of occupation is to be probed. You can use the ENERGY parameter to specify the trap energy level to be probed. If ENERGY is not specified, then the total value of all donor energy levels will be probed. |
| GENERATION | Specifies that the generation rate due to impact ionization is probed. |
| GR.HEAT | Requests a PROBE of Generation-Recombination heat in GIGA. |
| H.CONC | Specifies that proton concentration is probed. |
| H.TRANTRAP | Specifies that the hole recombination rate into transient traps is to be probed. |
| INTEGRATED | Specifies that the probed value is to be integrated over all mesh points inside a box defined with the parameters X.MIN , X.MAX , Y.MIN , Y.MAX , Z.MIN and Z.MAX . |
| INTENSITY | Evaluates optical intensity of an optical beam in LUMINOUS . If this is a multispectral source, this value accounts for the subsampling, while the intensity already in the logfile will only reflect the integrated input spectrum. |
| J.CONDUCTION | Requests a PROBE of Conduction current (J.ELEC + J.HOLE). |
| J.DISP | Requests a PROBE of Displacement current. |
| J.ELECTRON | Requests a PROBE of Electron Current density. |
| J.HOLE | Requests a PROBE of Hole Current density. |

| | |
|---|---|
| J . PROTON | Specifies that the proton current density is probed. |
| J . TOTAL | Requests a PROBE of Total Current density (J . TOTAL+J . DISP). |
| JOULE . HEAT | Requests a PROBE of Joule-Heating in GIGA. |
| KX, KY, and KZ | Specify directions in k space associated with probing conduction and valence band bound state energies. See also NWELL and PWELL. |
| LANGVIN | Specifies that the Langevin recombination rate is probed. |
| LAYER . ABSO, LAYER . REFL, and LAYER . TRAN | Specify that the absorption, reflection, or transmission coefficient is probed for LUMINOUS ray trace or transfer matrix. When specifying one of these values, you also need to specify the BEAM and REGION parameters. |
| LASER . GAIN | Specifies that the probe will operate on the LASER optical gain. For more information about LASER, see Chapter 8: “Laser: Edge Emitting Simulator”. |
| LASER . INTENSITY | Specifies that the probe will operate on the LASER optical intensity. For more about information LASER, see Chapter 8: “Laser: Edge Emitting Simulator”. |
| LASER . MODE | Specifies the optical mode for LASER . INTENSITY and LASER . GAIN. |
| LAT . TEMP | Specifies that the probe will operate on lattice temperature. |
| LMAX, LMIN | Specifies the range of wavelengths to search for peak emission wavelength when the WAVELENGTH parameter is set on the PROBE statement. |
| LUMINOUS . INTENSITY | Specifies that the probe will operate on the LUMINOUS optical intensity. For more information about LUMINOUS, see Chapter 10: “Luminous: Optoelectronic Simulator”. |
| MATERIAL | This is assigned to a specific material name that will act to direct the probe to only address regions composed of the specified material. |
| MAX | Specifies that the probe will find the maximum value on the mesh. |
| MIN | Specifies that the probe will find the minimum value on the mesh. |
| MAX . XITION | Specifies that the maximum allowable transition between bound state energies is to be probed. If there are no allowable transitions between bound state energies, the band gap is probed. |
| MIN . XITION | Specifies that the minimum allowable transition between bound state energies is to be probed. If there are no allowable transitions between bound state energies, the band gap is probed. |
| NAME | Sets a character string that allows you to specify the description displayed by TONYPLOT. |
| N . CONC | Specifies that the probe will operate on electron concentration. |
| N . MOB | Specifies that the probe will operate on the electron mobility. The DIR parameter should also be specified if N . MOB is used. |
| N . TEMP | Specifies that the probe will operate on electron temperature. |

| | |
|---------------------|--|
| NWELL | Specifies that the a specified conduction bound state energy is to be probed. To specify the bound state, you must also specify which bound state is to be probed with the <code>STATE</code> parameter (where 0 specifies the lowest bound state) and the direction in k space using the <code>KX</code> , <code>KY</code> or <code>KZ</code> parameters. |
| P.CONC | Specifies that the probe will operate on hole concentration. |
| P.MOB | Specifies that the probe will operate on the hole mobility. The <code>DIR</code> parameters should also be specified if <code>P.MOB</code> is used. |
| P.TEMP | Specifies that the probe will operate on hole temperature. |
| PT.HEAT | Requests a <code>PROBE</code> of Peltier-Thomson Heat in GIGA. |
| PERMITTIVITY | Specifies that material permittivity is probed. |
| PHOTOGEN | Specifies that photogeneration or SEU generation rate is probed. |
| POLARIZATION | Specifies that the probe will operate on ferroelectric polarization. The <code>DIR</code> parameter should also be specified if <code>POLARIZATION</code> is used. |
| POTENTIAL | Specifies that the probe will operate on electrostatic potential. |
| PWELL | Specifies that the a specified valence bound state energy is to be probed. To specify the bound state, you must also specify which bound state is to be probed with the <code>STATE</code> parameter (where 0 specifies the highest bound state) and the direction in k space using the <code>KX</code> , <code>KY</code> or <code>KZ</code> parameters. |
| QFN | Specifies that the probe will operate on the electron quasi-Fermi level. |
| QFP | Specifies that the probe will operate on the hole quasi-Fermi level. |
| R.TRAP | Specifies that the trap recombination is to be probed. |
| R.BBT | Specifies tha the band-to-band tunneling rate is to be probed. |
| RADIATIVE | Specifies that the probe will operate on radiative recombination rate. |
| RECOMBIN | Specifies that the probe will operate on net recombination rate. |
| REGION | Limits the application of the probe to a specific region of a specified index. |
| RESISTIVITY | Specifies that the resistivity of metals and semiconductors is probed. The resistivity in insulators is returned as 0. |
| SONOS.CHARGE | Specifies that the net trapped carrier density in a Silicon-Nitride region is to be probed. The net density is defined as the electron density minus the hole density. |
| SRH | Specifies that the probe will operate on SRH recombination rate. |
| STATE | This is the number of the bound state. It can take values from 1 to the maximum number of bound states, which is specified by the <code>EIGENS</code> parameter on the <code>MODELS</code> statement. |
| STRUCTURE | This is a synonym for <code>DEVICE</code> . |
| TOTAL.HEAT | Requests a <code>PROBE</code> of Total heat in GIGA (<code>GR.HEAT+PT.HEAT+JOULE.HEAT</code>). |

| | |
|---------------------|---|
| VAL.BAND | Probes the valence band. |
| VEL.ELECTRON | Specifies that the probe will operate on electron velocity. |
| VEL.HOLE | Specifies that the probe will operate on hole velocity. |
| WAVE.FUN | Probes the wavefunction characterized by the BAND and STATE parameters. |
| WAVELENGTH | Specifies that the radiative emission wavelength is probed. |

Region Parameters

| | |
|---------------|---|
| BACK | This is a synonym for Z.MAX . |
| BOTTOM | This is a synonym for Y.MAX . |
| FRONT | This is a synonym for Z.MIN . |
| LEFT | This is a synonym for X.MIN . |
| RIGHT | This is a synonym for X.MAX . |
| TOP | This is a synonym for Y.MIN . |
| X, Y | Specifies the location of a point probe. |
| X.MAX | Specifies the maximum X coordinate for the minimum, maximum, or integrated probe. |
| X.MIN | Specifies the minimum X coordinate for the minimum, maximum, or integrated probe. |
| Y.MAX | Specifies the maximum Y coordinate for the minimum, maximum, or integrated probe. |
| Y.MIN | Specifies the minimum Y coordinate for the minimum, maximum, or integrated probe. |
| Z.MAX | Specifies the maximum Z coordinate for the minimum, maximum, or integrated probe. |
| Z.MIN | Specifies the minimum Z coordinate for the minimum, maximum, or integrated probe. |

Example of Probing the Maximum Value

The following line will cause the maximum electron concentration on the grid to be output to the log file:

```
PROBE NAME=peak_electrons MAX N.CONC
```

Probing at a location Example

This syntax will cause the potential at the location $x=0.5$ $y=0.1$ to be output to the log file.

```
PROBE NAME=mypotential X=0.5 Y=0.1 POTENTIAL
```

Vector Quantity Example

For vector quantities, the direction parameter, DIR, must be specified. These two lines allow a lateral mobility and vertical field in a MOSFET.

```
PROBE NAME=channel_mobility x=1 y=0.001 N.MOB DIR=0
```

```
PROBE NAME=channel_field x=1 y=0.001 FIELD DIR=90
```

In ATLAS3D, you can add a parameter POLAR to the PROBE statement. Its default value is 90°, which means the direction lies within the XY plane. POLAR gives the angle respect to the Z axis. A value of zero means that the probed direction is along the Z axis. A value of POLAR between 0 and 90° will PROBE along a direction vector with a z-component of $\cos(\text{POLAR})$.

```
PROBE NAME=electroncurrent dir=45 polar=60 j.electron x=0.5 y=0.5 z=0.0
```

This probes the electron current at the specified position along the direction (0.61237, 0.61237, 0.5).

21.44: QTREGION

This allows you to specify one or more polygonal regions as regions where non-local band-to-band tunneling will occur. Each QTREGION statement sets up a quadrilateral region. The polygon is built up from one or more quadrilaterals. ATLAS deletes the mesh inside the polygonal regions and replaces it with another, which is more suitable for the non-local band-to-band tunneling calculation. The modified mesh is also the mesh to be outputted by any SAVE statements.

Syntax

```
QTREGION NUMBER [X1 Y1] X2 Y2 X3 Y3 [X4 Y4]
PTS.TUNNEL | STNL.BEG STNL.END | F.RESOLUTION
PTS.NORMAL | SNRM.BEG SNRM.END
```

| Parameter | Type | Default | Units |
|--------------|------|---------|---------------|
| F.RESOLUTION | Char | | |
| NUMBER | Real | 1 | |
| PTS.NORMAL | Real | -1 | |
| PTS.TUNNEL | Real | -1 | |
| SNRM.BEG | Real | 0 | μm |
| SNRM.END | Real | 0 | μm |
| STNL.BEG | Real | 0 | μm |
| STNL.END | Real | 0 | μm |
| X1 | Real | 0 | μm |
| X2 | Real | 0 | μm |
| X3 | Real | 0 | μm |
| X4 | Real | 0 | μm |
| Y1 | Real | 0 | μm |
| Y2 | Real | 0 | μm |
| Y3 | Real | 0 | μm |
| Y4 | Real | 0 | μm |

Description

| | |
|---------------------|---|
| F.RESOLUTION | Specifies a text file that contains a column of numbers between 0 and 1. This determines the mesh spacing in the tunneling direction and is an alternative to <code>PTS.TUNNEL</code> . The numbers give the mesh points relative to the corners, 0.0 maps to the starting corner, and 1.0 maps to the ending corner. Intermediate mesh points are calculated according to a linear mapping from the supplied coordinates in [0,1]. |
| NUMBER | This is the index of the polygonal region that the <code>QTREGION</code> statement applies to. |
| PTS.NORMAL | This is the number of points in quadrilateral in direction perpendicular to tunneling direction. This dictates a regular mesh spacing along the sides from corner 1 to corner 2 and from corner 3 to corner 4. See Figure 3-7 in Section 3.6.5: “Band-to-Band Tunneling” for an example. |
| PTS.TUNNEL | This is the number of points in quadrilateral in direction parallel to tunneling direction. This dictates a regular mesh spacing along the sides from corner 1 to corner 4 and from corner 2 to corner 3. |
| SNRM.BEG | Along with <code>SNRM.END</code> , is one way of specifying the mesh spacing in the direction normal to tunneling. <code>SNRM.BEG</code> specifies the mesh spacing at the corner 1 (4). <code>SNRM.END</code> specifies it at the corner 2 (3). |
| SNRM.END | See <code>SNRM.BEG</code> . |
| STNL.BEG | Along with <code>STNL.END</code> , is one way of specifying the mesh spacing in the direction parallel to tunneling. <code>STNL.BEG</code> specifies the mesh spacing at the corner 1 (2). <code>STNL.END</code> specifies it at the corner 4 (3). |
| STNL.END | See <code>STNL.BEG</code> . |
| X1 | This is the X coordinate of the first corner of the quadrilateral. |
| X2 | This is the X coordinate of the second corner of the quadrilateral. |
| X3 | This is the X coordinate of the third corner of the quadrilateral. |
| X4 | This is the X coordinate of the fourth corner of the quadrilateral. |
| Y1 | This is the Y coordinate of the first corner of the quadrilateral. |
| Y2 | This is the Y coordinate of the second corner of the quadrilateral. |
| Y3 | This is the Y coordinate of the third corner of the quadrilateral. |
| Y4 | This is the Y coordinate of the fourth corner of the quadrilateral. |

Note: The corners must be specified in counter-clockwise order.

Examples

The following four QTREGION statements make up a polygonal region similar in shape to that in Figure 3-8 in Section 3.6.5: “Band-to-Band Tunneling”. You need to specify all four corners in the first statement.

Subsequent statements may omit (x1, y1) and (x4, y4). In the tunneling direction, only one specification of mesh spacing in the tunneling direction is allowed per polygonal region. In this case, a regular spacing with 51 points is requested.

```
QTREGION NUMBER=1 PTS.TUNNEL=51 X1=0.0 Y1=0.45 X2=0.9 Y2=0.45
X3=0.9 Y3=0.55 X4=0.0 Y4=0.55 SNRM.BEG=0.2 SNRM.END=0.02
```

```
QTREGION NUMBER=1 PTS.NORMAL=9 X1=0.9 Y1=0.45 X2=0.94 Y2=0.38 X3=1.03 Y3=0.45
X4=0.9 Y4=0.55
```

```
QTREGION NUMBER=1 PTS.NORMAL=9 X2=0.975 Y2=0.25
X3=1.075 Y3=0.25
```

```
QTREGION NUMBER=1 PTS.NORMAL=3 X2=0.975 Y2=0.0
X3=1.075 Y3=0.0 SNRM.BEG=0.05 SNRM.END=0.1
```

The following example uses a data file, mesh.dat, to specify the mesh spacing in the tunneling direction.

```
QTREGION NUMBER=2 X1=0.0 Y1=1.55 X2=0.8 Y2=1.55 \
X3=0.8 Y3=1.65 X4=0.0 Y4=1.65 SNRM.BEG=0.2 SNRM.END=0.02 F.RESOLUTION=MESH.DAT
```

The mesh.dat file should have a format such as

```
0.0
0.2
0.4
0.45
0.5
0.55
0.6
0.8
1.0
```

In the direction normal to tunneling, the spacing is 0.2 at one end and 0.02 at the other.

21.45: QTX.MESH, QTY.MESH

QTX.MESH and QTY.MESH allow you to specify a rectangular mesh in order to calculate quantum tunneling current in either the X direction or Y direction. It is required in some situations for the direct quantum tunneling model for gate insulators. It is also required for non-local band-to-band and trap assisted tunneling models.

Syntax

```
QTX.MESH NODE=<n> LOCATION=<n>
```

```
QTX.MESH SPACING=<n> LOCATION=<n>
```

```
QTY.MESH NODE=<n> LOCATION=<n>
```

```
QTY.MESH SPACING=<n> LOCATION=<n>
```

| Parameter | Type | Default | Units |
|-----------|---------|---------|-------|
| LOCATION | Real | | μm |
| NODE | Integer | | |
| SPACING | Real | | μm |

Description

| | |
|-----------------|---|
| NODE | Specifies the mesh line index. These mesh lines are assigned consecutively. |
| LOCATION | Specifies the location of the grid line. |
| SPACING | Specifies the mesh spacing at the mesh locations specified by the LOCATION parameter. If the SPACING parameter is specified, then the NODE parameter should not be specified. |

Example

```
qtx.mesh loc=0.0 spac=0.25
```

```
qtx.mesh loc=1.0 spac=0.25
```

```
qty.mesh loc=1.5 spac=0.05
```

```
qty.mesh loc=2.0 spac=0.01
```

```
qty.mesh loc=3.0 spac=0.01
```

```
qty.mesh loc=3.5 spac=0.05
```

will set up a mesh in the rectangle bounded by $x=0.0$, $x=1.0$, $y=1.5$ and $y=3.5$. The mesh is finer in the Y direction because it is intended to calculate the tunneling current in this direction.

21.46: QUIT

QUIT stops execution of ATLAS.

Syntax

QUIT

Synonyms

STOP

END

EXIT

Description

The QUIT statement may be placed anywhere in an input file. ATLAS will stop execution upon encountering the QUIT statement. All input lines after the occurrence of the QUIT statement will be ignored for that execution of ATLAS.

Note: To quit and immediately restart ATLAS inside of DECKBUILD, use the GO ATLAS statement. Full details on the GO syntax statement are found in the DECKBUILD USER'S MANUAL.

21.47: REGION

REGION specifies the location of materials in a previously defined mesh. Every triangle must be defined as a material.

Syntax

```
REGION NUMBER=<n> <material> [<position>]
```

| Parameter | Type | Default | Units |
|--------------|---------|---------|------------------|
| A.MAX | Real | | degrees |
| A.MIN | Real | | degress |
| A-SILICO | Logical | False | |
| ACCEPTORS | Real | 0.0 | cm ⁻³ |
| ALGAAS | Logical | False | |
| ALINAS | Logical | False | |
| ASUB | Real | 1.0 | Å |
| BOTTOM | Logical | False | |
| CALC.STRAIN | Logical | False | |
| COMPX.BOTTOM | Real | 0.0 | |
| COMPY.BOTTOM | Real | 0.0 | |
| COMPX.TOP | Real | 0.0 | |
| COMPY.TOP | Real | 0.0 | |
| CONDUCTOR | Logical | False | |
| CONVERT | Logical | False | |
| DEC.C1 | Real | 0.0 | eV |
| DEC.C2 | Real | 0.0 | eV |
| DEC.C3 | Real | 0.0 | eV |
| DEC.D2 | Real | 0.0 | eV |
| DEC.D4 | Real | 0.0 | eV |
| DEC.ISO | Real | 0.0 | eV |
| DEV.HH | Real | 0.0 | eV |
| DEV.LH | Real | 0.0 | eV |
| DEV.SO | Real | 0.0 | eV |
| DEV.ISO | Real | 0.0 | eV |
| DIAMOND | Logical | False | |

| Parameter | Type | Default | Units |
|-------------|---------|---------------------|------------------|
| DONORS | Real | 0.0 | cm ⁻³ |
| ETA.NEGF | Real | 0.0066 | eV |
| EQUIL.NEGF | Logical | False | |
| FIXED.FERMI | Logical | False | |
| FN.SIS | Logical | False | |
| HELMHOLTZ | Logical | True | |
| GAAS | Logical | False | |
| GAASP | Logical | False | |
| GERMANIU | Logical | False | |
| GRAD.12 | Real | | μm |
| GRAD.23 | Real | | mm |
| GRAD.34 | Real | | μm |
| GRAD.41 | Real | | μm |
| GRADED | Logical | False | |
| HGCDTE | Logical | False | |
| INGAAS | Logical | False | |
| INAS | Logical | False | |
| INASP | Logical | False | |
| INGAP | Logical | False | |
| INP | Logical | False | |
| INSULATO | Logical | False | |
| IX.LOW | Integer | left of structure | |
| IX.HIGH | Integer | right of structure | |
| IX.MAX | Integer | right of structure | |
| IX.MIN | Integer | left of structure | |
| IY.LOW | Integer | top of structure | |
| IY.HIGH | Integer | bottom of structure | |
| IY.MAX | Integer | top of structure | |
| IY.MIN | Integer | bottom of structure | |
| IZ.HIGH | Real | | |
| IZ.LOW | Real | | |
| IZ.MAX | Integer | | |

| Parameter | Type | Default | Units |
|---------------|-----------|---------|------------------|
| IZ.MIN | Integer | | |
| LED | Logical | False | |
| MATERIAL | Character | | |
| MODIFY | Logical | False | |
| NAME | Character | | |
| NA.TOP | Real | 0.0 | cm^{-3} |
| ND.TOP | Real | 0.0 | cm^{-3} |
| NA.BOTTOM | Real | 0.0 | cm^{-3} |
| ND.BOTTOM | Real | 0.0 | cm^{-3} |
| NITRIDE | Logical | False | |
| NUMBER | Integer | | |
| NX | Real | 2 | |
| NY | Real | 2 | |
| OXIDE | Logical | False | |
| OXYNITRI | Logical | False | |
| P1.X | Real | | μm |
| P1.Y | Real | | μm |
| P2.X | Real | | μm |
| P2.Y | Real | | μm |
| P3.X | Real | | μm |
| P3.Y | Real | | μm |
| P4.X | Real | | μm |
| P4.Y | Real | | μm |
| PIEZOELECTRIC | Logical | False | |
| PIEZO.SCALE | Real | 1.0 | |
| POLAR.CHARGE | Real | 0.0 | cm^{-2} |
| POLAR.SCALE | Real | 1.0 | |
| POLARIZATION | Logical | False | |
| POLYSILICON | Logical | False | |
| PSP.SCALE | Real | 1.0 | |
| QWELL | Logical | False | |

| Parameter | Type | Default | Units |
|---------------|-----------|---------|-------|
| QWNUM | Integer | -1 | |
| R.MAX | Real | | μm |
| R.MIN | Real | | μm |
| S.OXIDE | Logical | False | |
| SAPPHIRE | Logical | False | |
| SCHRO | Logical | True | |
| SEMICOND | Logical | False | |
| SELF | Logical | False | |
| SI3N4 | Logical | False | |
| SIC | Logical | False | |
| SIGE | Logical | False | |
| SILICON | Logical | False | |
| SIO2 | Logical | False | |
| STAY | Logical | False | |
| STRAIN | Real | 0.0 | |
| STR.BOT | Real | 0.0 | |
| STR.TOP | Real | 0.0 | |
| SUBSTRATE | Logical | False | |
| SX | Real | 0.0 | |
| SY | Real | 0.0 | |
| THICKNESS | Real | 0.0 | μm |
| TOP | Logical | False | |
| TRAPPY | Logical | False | |
| USER.GROUP | Character | | |
| USER.MATERIAL | Character | | |
| WELL.CNBS | Integer | 1 | |
| WELL.DEBUG | Logical | False | |
| WELL.FIELD | Logical | True | |
| WELL.GAIN | Real | 1.0 | |
| WELL.NX | Integer | 10 | |
| WELL.NY | Integer | 10 | |
| WELL.NZ | Integer | 10 | |

| Parameter | Type | Default | Units |
|--------------|---------|---------------------|---------------|
| WELL.OVERLAP | Real | | |
| WELL.VNBS | Integer | 1 | |
| X.COMP | Real | 0.0 | |
| X.MAX | Real | right of structure | μm |
| X.MIN | Real | left of structure | μm |
| X.MOLE | Real | 0.0 | |
| Y.MOLE | Real | 0.0 | |
| Y.COMP | Real | 0.0 | |
| Y.MIN | Real | top of structure | μm |
| Y.MAX | Real | bottom of structure | μm |
| Z.MAX | Real | | |
| Z.MIN | Real | | |
| ZEROBP | Logical | False | |
| ZNSE | Logical | False | |
| ZNTE | Logical | False | |

Description

| | |
|-----------------|---|
| n | Specifies a region number from 1 to 200. |
| material | This is one or more of the material names described below. |
| position | This is one or more of the position parameters described below. |

Material Parameters

| | |
|---|---|
| ACCEPTORS | Specifies a uniform density of ionized acceptors in the region. |
| ASUB | Specifies the substrate lattice constant for strain calculations as described in Section 3.6.10: “Epitaxial Strain Tensor Calculation in Wurtzite”. |
| CALC.STRAIN | Specifies that the strain in the region is calculated from the lattice mismatch with adjacent regions. |
| COMPX.BOTTOM, COMPY.BOTTOM, COMPX.TOP, and COMPY.TOP | Specify the composition fractions at the top and bottom of a region when linearly graded. Linear grading is specified by the GRADED parameter. See Chapter 2: “Getting Started with ATLAS”, Section 2.6.4: “Automatic Meshing (Auto-meshing) Using The Command Language”. |
| CONDUCTOR | Specifies that the region is to be simulated as a conductor. This means that the conduction equation is solved for the region. |

| | |
|-----------------------|--|
| CONVERT | This is an alias for MODIFY . |
| DEC.C1 | This is a conduction band shift for 1st pair of electron valleys. |
| DEC.C2 | This is a conduction band shift for 2nd pair of electron valleys. |
| DEC.C3 | This is a conduction band shift for 3rd pair of electron valleys. |
| DEC.D2 | This is a conduction band shift for $\Delta 2$ electron valleys if DEC.C1 is not set. |
| DEC.D4 | This is a conduction band shift for $\Delta 4$ electron valleys if DEC.C2 is not set. |
| DEC.ISO | This is a conduction band shift for isotropic electron band, when NUM.DIRECT =1. |
| DEV.HH | This is a valence band shift for heavy holes. |
| DEV.LH | This is a valence band shift for light holes. |
| DEV.ISO | This is a valence band shift for isotropic hole band, when NUM.BAND =1. |
| DEV.SO | This is a valence band shift for split-off holes. |
| DONORS | Specifies a uniform density of ionized donors in the region. |
| ETA.NEGF | An imaginary optical potential, added to Hamiltonian of quasi-equilibrium regions in planar NEGF model. |
| EQUIL.NEGF | Specified that the region will be treated as quasi-equilibrium in planar NEGF model. |
| GRAD.<n> | <p>Specifies the compositional gradings for heterojunctions along each side of the region rectangle or quadrilateral. The value of the GRAD parameters specifies the distance at which the composition fraction reduces to zero. A value of 0.0 specifies that the heterojunction is abrupt. The value of <n> can be the numbers: 12, 23, 34, and 41. The meanings of these numbers is down below.</p> <ul style="list-style-type: none"> • 12 = top surface • 23= right hand side • 34= bottom surface • 41 = left hand side <p>These correspond to the point indices around the rectangular region working clockwise from top left.</p> |
| GRADED | Specifies that the region has linear compositional or doping variation or both. See also COMPX.BOTTOM , COMPY.BOTTOM , COMPX.TOP , COMPY.TOP , ND.BOTTOM , ND.TOP , NA.BOTTOM and NA.TOP . |
| HELMHOLTZ | Allows (default) or prevents a solution of vector Helmholtz equation in the region. |
| LED | Specifies that the region is to be treated as a light emitting region and included in postprocessing for LED analysis. See Chapter 11: “LED: Light Emitting Diode Simulator”. |
| MATERIAL | Specifies the material used for the region. Valid material names are listed in Appendix B: “Material Systems”, Table B-1. All materials are divided into three classes: semiconductors, insulators and conductors. |

Note: You can specify the following logical parameters to indicate the region material instead of assigning the MATERIAL parameter: SILICON, GAAS, POLYSILI, GERMANIU, SIC, SEMICON, SIGE, ALGAAS, A-SILICO, DIAMOND, HGCDTE, INAS, INGAAS, INP, S.OXIDE, ZNSE, ZNTE, ALINAS, GAASP, INGAP, INASP, OXIDE, SIO2, NITRIDE, SI3N4, INSULATO, SAPPHIRE, and OXYNITRI.

| | |
|---|---|
| MODIFY | This is used to modify the characteristics of regions imported into the simulator. See Chapter 2: “Getting Started with ATLAS”, Section 2.6.5: “Modifying Imported Regions”. The alias for this parameter is CONVERT. |
| NAME | Specifies the name of the region. The name can be used in the MODELS, MATERIAL, and IMPACT statements to provide regionally dependent models. This name is just a label. It doesn’t imply any material parameter settings. |
| ND.BOTTOM, ND.TOP, NA.BOTTOM, and NA.TOP | Specify the doping concentrations at the top and bottom of a region when linearly graded. Linear grading is specified by the GRADED parameter. See Chapter 2: “Getting Started with ATLAS”, Section 2.6.4: “Automatic Meshing (Auto-meshing) Using The Command Language”. |
| NUMBER | Assigns a region number. Multiple REGION lines with the same number can be used to define region shapes made from several rectangles. |
| PIEZO.SCALE | This is an alias for POLAR.SCALE. |
| PIEZOELECTRIC | This is an alias for POLARIZATION. |
| POLARIZATION | Enables the automatic calculation of added interface charge due to spontaneous and piezoelectric polarization. The alias for this parameter is PIEZOELECTRIC. See Chapter 3: “Physics”, Section 3.6.11: “Polarization in Wurtzite Materials [26]”. |
| POLAR.CHARGE | Specifies polarization charge densities to replace the density calculated using Equations 3-506 and 3-507. |
| POLAR.SCALE | Specifies a constant scale factor multiplied by the calculated spontaneous and piezoelectric polarization charges when you enable polarization by setting the POLARIZATION parameter of the REGION statement. The alias for this parameter is PIEZO.SCALE. See Chapter 3: “Physics”, Section 3.6.11: “Polarization in Wurtzite Materials [26]”. |
| PSP.SCALE | Specifies a constant scale factor similar to POLAR.SCALE but applied only to spontaneous polarization. |
| QWELL | Specifies that the region is treated as a quantum well for calculation of radiative recombination or gain or both for certain optoelectronic models. |
| QWNUM | Optionally sets the number of the quantum well region. |
| SCHRO | Allows (default) or prevents a solution of Schrodinger in the region. Switch it off, if the region is to be treated classically. |
| STRAIN | Specifies the strain in the region. (Negative strain is compressive). |
| STR.BOT and STR.TOP | Specify the strain at the bottom and top of the region for calculations of the k.p model. The strain values between the top and bottom of the region are linearly interpolated. |

| | |
|--|---|
| SUBSTRATE | This is a logical parameter indicating that the specified region should be considered as the the substrate for strain calculations as described in Section 3.6.10: “Epitaxial Strain Tensor Calculation in Wurtzite”. |
| TRAPPY | Used only with the BESONOS model. This indicates that a Silicon-Nitride region will be able to trap electrons and holes. |
| USER.GROUP | Specifies the material group for the user-defined material. USER.GROUP can be either SEMICONDUCTOR , INSULATOR , or CONDUCTOR . |
| USER.MATERIAL | Specifies a user-defined material name. The specified material name can be any name except that of a default material, such as Silicon. You should define each material with an accompanying definition in the MATERIAL statement. You can define up to 50 user-defined materials. |
| WELL.CNBS and WELL.VNBS | Specify the number of bound states retained for calculation of radiative recombination or gain if the region is treated as a quantum well as specified by the QWELL parameter. |
| WELL.FIELD | Specifies that the calculations of bound state energies should include the effects of the local field. |
| WELL.GAIN | Specifies a constant scale factor multiplied by the calculated gain to give the net gain used for certain optoelectronic calculations. |
| WELL.NX , WELL.NY , and WELL.NZ | Specifies the number of grid points in x, y, and z directions for Schrodinger equation in a quantum well region. |
| WELL.OVERLAP | Specifies the wavefunction overlap integral. If WELL.OVERLAP is not specified, then the overlap integral is calculated from the wavefunctions. |

Note: The highest region number takes precedence if **REGION** definitions overlap.

| | |
|----------------|--|
| ZEROBQP | Specifies that in the given region the Bohm quantum potential is not solved and is assigned to zero. |
|----------------|--|

Position Parameters

You can use grid indices to define a region only when the mesh is rectangular. To define a region with a rectangular mesh, use the `X.MESH` and `Y.MESH` statements to specify grid indices.

You can also use the `IX.HIGH`, `IX.LOW`, `IY.HIGH`, and `IY.LOW` parameters to specify x and y mesh line number values.

Note: To add regions to irregular meshes, such as those from ATHENA, specify the boundaries with the `X.MAX`, `X.MIN`, `Y.MAX`, and `Y.MIN` parameters.

| | |
|---|---|
| A.MAX | Specifies the maximum angle of a 3D cylindrical region. |
| A.MIN | Specifies the minimum angle of a 3D cylindrical region. |
| BOTTOM | Specifies that the region is to be added at the bottom (starting at the maximum previously specified Y coordinate and extending in the positive Y direction) of the structure. |
| FN.SIS | Applies to the Fowler-Nordheim model for an interface to the insulator region having this attribute. Any Fowler-Nordheim current being evaluated is not assigned to a contact. Instead, it is assumed to pass from one semiconductor region to another through the tagged region. |
| IX.HIGH | Specifies the maximum x value of the grid index. The alias for this parameter is <code>IX.MAX</code> . |
| IX.LOW | Specifies the minimum x value of the grid index. The alias for this parameter is <code>IX.MIN</code> . |
| IY.HIGH | Specifies the maximum y value of the grid index. The alias for this parameter is <code>IY.MAX</code> . |
| IY.LOW | Specifies the minimum y value of the grid index. The alias for this parameter is <code>IY.MIN</code> . |
| IZ.HIGH | Specifies the maximum z value of the grid index. The alias for this parameter is <code>IZ.MAX</code> . |
| IZ.LOW | Specifies the minimum z value of the grid index. The alias for this parameter is <code>IZ.MIN</code> . |
| IX.MAX, IX.MIN, IY.MAX, IY.MIN, IZ.MAX, and IZ.MIN | These are aliases for <code>IX.HIGH</code> , <code>IX.LOW</code> , <code>IY.HIGH</code> , <code>IY.LOW</code> , <code>IZ.HIGH</code> , and <code>IZ.LOW</code> . |
| NX | Specifies the number of uniformly spaced mesh lines to be added to resolve the region in the X direction. |
| NY | Specifies the number of uniformly spaced mesh lines to be added to resolve the region in the Y direction. |
| STAY | This is used in automeshing to create material variations in the X direction. See Chapter 2: “Getting Started with ATLAS”, Section 2.6.4: “Automatic Meshing (Auto-meshing) Using The Command Language”. |
| SX | Specifies the spacing between mesh lines to be applied at the edges of the region in the X direction. |

| | |
|-----------------------|---|
| SY | Specifies the spacing between mesh lines to be applied at the edges of the region in the Y direction. |
| P1.X | X coordinate of 1st corner of REGION. |
| P1.Y | Y coordinate of 1st corner of REGION. |
| P2.X | X coordinate of 2nd corner of REGION. |
| P2.Y | Y coordinate of 2nd corner of REGION. |
| P3.X | X coordinate of 3rd corner of REGION. |
| P3.Y | Y coordinate of 3rd corner of REGION. |
| P4.X | X coordinate of the last corner of REGION. |
| P4.Y | Y coordinate of the last corner of REGION. |
| THICKNESS | Specifies the thickness of the region in the Y direction. This parameter must accompany the specification of the TOP or BOTTOM parameters. |
| TOP | Specifies that the region is to be added at the top (starting at the minimum previously specified Y coordinate and extending in the negative Y direction) of the structure. |
| R.MAX | Specifies the maximum radius of a 3D cylindrical region. |
| R.MIN | Specifies the minimum radius of a 3D cylindrical region. |
| X.MAX | Specifies the maximum x-boundary. |
| X.MIN | Specifies the minimum x-boundary. |
| X.COMP, X.MOLE | This is the composition fraction (X) for a region with a composition dependent cations (e.g., AlGaAs). |
| Y.COMP, Y.MOLE | This is the composition fraction (Y) for a region with a composition dependent anions(e.g., InGaAsP). |
| Y.MAX | Specifies the maximum y-boundary. |
| Y.MIN | Specifies the minimum x-boundary. |
| Z.MIN | Specifies the minimum z-boundary. |
| Z.MAX | Specifies the maximum z-boundary. |

Grid Indices Example

Define a silicon region extending from nodes 1 to 25 in the X direction and from nodes 1 to 20 in the Y direction.

```
REGION NUM=1 IX.LO=1 IX.HI=25 IY.LO= 1 IY.HI=20 MATERIAL=SILICON
```

Non-Rectangular Region Example

Define a region that's composed of two separate rectangular areas. Note that REGION statements are cumulative.

```
REGION NUM=1 IX.LO=4 IX.HI=5 IY.LO=1 IY.HI=20 MATERIAL=OXIDE
```

```
REGION NUM=1 IX.LO=1 IX.HI=30 IY.LO=1 IY.HI=37 MATERIAL=OXIDE
```

Typical MOS Example

Define regions for a typical MOS structure.

```
REGION NUM=1 Y.MAX=0 MATERIAL=OXIDE
REGION NUM=2 Y.MIN=0 MATERIAL=SILICON
```

3D Region Definition Example

Define a cube of oxide within a region silicon in 3D.

```
REGION NUM=1 MATERIAL=SILICON
REGION NUM=2 Y.MAX=0.5 X.MIN=0.5 \
X.MAX=1.0 Z.MIN=0.5 Z.MAX=1.0 MATERIAL = OXIDE
```

Graded Heterojunction Definition Example

Define a graded heterojunction of AlGaAs/GaAs.

```
REGION NUM=1 MATERIAL=GaAs Y.MIN=1
REGION NUM=2 MATERIAL=AlGaAs Y.MAX=0.9 X.COMP=0.2 GRAD.34=0.1
```

In this case, the area between $y=0.9$ and 1.0 is graded in composition from 0.2 to 0.0 . The $Y.MAX$ parameter refers to the bottom of the uniform composition region. The actual bottom of the AlGaAs region is $Y.MAX+GRAD.34$

Graded x.comp and y.comp Material Definition Example

Define a graded $x.comp$ and $y.comp$ region in ATLAS using the `comp.x.top`, `comp.x.bottom`, `comp.y.top`, and the `comp.y.bottom` keywords on the `REGION` statement. The following example shows the use of `comp.x.top`, `comp.x.bottom` functions. Similar use, however, can be made of the `comp.y.top` and `comp.y.bottom` keywords.

You can use the following code to create a graded $x.comp$ AlGaAs region where the $x.comp$ falls off linearly in value from 0.4 to 0.2 from the top of the region to the bottom of the region.

```
region num=1 material=algaas comp.x.top=0.4 comp.x.bottom=0.1
```


21.48: REGRID

REGRID allows you to refine a crude mesh. A triangle is refined when the chosen variable changes by more than one specified criteria.

Syntax

```
REGRID RATIO=<n> <var> [<lp>] [<cp>] [<io>]
```

| Parameter | Type | Default | Units |
|------------|-----------|--------------------------|------------------|
| ABSOLUTE | Logical | False | |
| ASCII | Logical | False | |
| CHANGE | Logical | True | |
| COS.ANG | Real | 2.0 | |
| DOPFILE | Character | | |
| DOPING | Logical | | cm ⁻³ |
| E.TEMP | Logical | False | |
| EL.FIELD | Logical | | V/cm |
| ELECTRON | Logical | | cm ⁻³ |
| H.TEMP | Logical | False | |
| HOLE | Logical | | cm ⁻³ |
| IGNORE | Integer | | |
| IN.GREEN | Character | | |
| LOCALDOP | Logical | False | |
| LOGARITHM | Logical | False | |
| MAX.LEVEL | Integer | 1+ maximum level of grid | |
| MIN.CARR | Logical | | cm ⁻³ |
| NET.CARR | Logical | | cm ⁻³ |
| NET.CHRG | Logical | | cm ⁻³ |
| PISCES.OUT | Logical | False | |
| OUT.GREEN | Character | value of OUTFILE + tt | |
| OUTFILE | Character | | |
| POTENTIAL | Logical | | V |
| QFN | Logical | | V |
| QFP | Logical | | V |
| REGION | Integer | | All |

| Parameter | Type | Default | Units |
|-----------|---------|---------|---------------|
| SMOOTH.K | Integer | | |
| STEP | Real | | |
| X.MAX | Real | Right | μm |
| X.MIN | Real | Left | μm |
| Y.MAX | Real | Bottom | μm |
| Y.MIN | Real | Top | μm |

Description

| | |
|-----------------------------|--|
| RATIO or STEP | Specifies the maximum allowed variance across one element. |
| var | This is one of the variable parameters described below. The selected parameter is used as the basis for regridding. |
| lp | This is one of more of the location parameters described below. These parameters are used to select the areas which are to be refined. |
| cp | This is one or more of the control parameters. These parameters are used to control the plotted output. |
| io | This is one or more of the File I/O parameters. |

Variable Parameters

| | |
|-------------------|---|
| DOPING | Selects net doping. |
| E . TEMP | Select electron temperature. |
| EL . FIELD | Selects electric field. |
| ELECTRON | Selects electron concentration. |
| H . TEMP | Selects hole temperature. |
| HOLE | Selects hole concentration. |
| MIN . CARR | Selects minority carrier concentration. |
| NET . CARR | Selects net carrier concentration. |
| NET . CHRG | Selects net charge. |
| POTENTIAL | Selects mid-gap potential. |
| QFN | Selects the electron quasi-Fermi level. |
| QFP | Selects the hole quasi-Fermi level. |

Location Parameters

If no location parameters are specified, refinement will include:

- All regions for potential and electric field regrid
- All semiconductor regions for regrid which depend on the other variables

| | |
|----------------|---|
| IGNORE | Specifies regions that are not to be refined. |
| REGION | Specifies regions which are refined according to the specified criterion. Other regions may be refined to maintain well-shaped triangles. |
| X . MAX | Uses device coordinates to specify the maximum x-value for refinement. |
| X . MIN | Uses device coordinates to specify the minimum x-value for refinement. |
| Y . MAX | Uses device coordinates to specify the maximum y-value for refinement. |
| Y . MIN | Uses device coordinates to specify the minimum y-value for refinement. |

Control Parameters

| | |
|--------------------|--|
| ABSOLUTE | Specifies that the absolute value of the variable be used. |
| CHANGE | Determines whether to use the magnitude or the difference of a triangle variable as the refinement criterion. This parameter defaults to "difference". |
| COS . ANGLE | Limits the creation of obtuse angles in the mesh by specifying obtuse criterion. If this parameter is used, nodes are added to the mesh so that the number of obtuse triangles is reduced. |

Note: Be careful when using the `COS . ANGLE` parameter. Recommended values are from 0.8 to 0.95. Smaller values may dramatically increase the number of nodes.

| | |
|-----------------|--|
| LOCALDOP | Specifies that if minority carrier concentration exceeds local doping, the grid will be refined. This parameter is used in conjunction with minority carrier regrid. |
|-----------------|--|

| | |
|---------------------|--|
| LOGARITHM | Specifies a logarithmic refinement scale. Since many of the quantities may become negative, numerical problems are avoided by using $\log(x)=\text{sign}(x)\cdot\log_{10}(1+ x)$. If you wish to obtain the true logarithm of a quantity, the ABSOLUTE parameter must be specified before the LOGARITHM parameter is specified. The absolute value of a quantity is computed first, thereby eliminating negative arguments. |
| MAX . LEVEL | Specifies the maximum level of any triangle relative to the original mesh. This parameter defaults to one more than the maximum level of the grid, but can be set to a smaller value to limit refinement. Values less than or equal to zero are interpreted relative to the current maximum grid level. |
| SMOOTH . KEY | <p>Specifies a smoothing index. The digits of the index are read in reverse order and interpreted as follows:</p> <ol style="list-style-type: none"> 1. Triangle smoothing: All region boundaries remain fixed. 2. Triangle smoothing: Only material boundaries are maintained. 3. Node averaging. 4. Improved triangle smoothing method: This method uses diagonal flipping to reduce the number of obtuse triangles. 5. Aligns triangles with electric field gradient. <p>Usually option 1 is sufficient. Option 2 is useful only if a device has several regions of the same material and the border between different regions is unimportant. Option 3 is not recommended when the initial mesh is basically rectangular, such as mesh information usually obtained from SSUPREM4. Option 4 is similar to option 1, but option 4 usually creates less obtuse triangles.</p> |

File I/O Parameters

| | |
|---------------------|---|
| ASCII | Specifies that mesh files and triangle trees will be written in an ASCII rather than a binary format. This parameter has no effect on the device doping file (see the DOPFILE parameter). |
| DOPFILE | Specifies the name of a file, which contains device doping information. This file is created on the DOPING statement. Specifying DOPFILE avoids linear interpolation of doping values at newly created grid points by using the initial doping specification to apply doping to the new grid points. |
| IN . GREEN | Specifies a triangle tree for the mesh which will be used in this regrid. If this parameter is not specified, the program will look for a file with the same name as the current mesh plus, <i>tt</i> , at the end. If no such file exists, the program will not use a triangle tree for the previous mesh. |
| MASTER . OUT | Saves mesh and doping information in a standard structure file format. |
| OUTFILE | Specifies the name of a standard structure output file where mesh information will be stored. This parameter must be specified if the mesh is to be used for subsequent runs. |
| OUT . GREEN | Specifies the name of the file that holds the history of the triangle tree. This history is used in further regrid steps. |
| PISCES . OUT | Saves mesh and doping information in a binary PISCES-II format. Files in this format cannot be displayed in TONYPLOT. |

Doping Regrid Examples

Starting with an initial grid, we refine twice so that all triangles with large doping steps are refined.

```
REGRID LOG DOPING RATIO=6 OUTF=grid1 DOPF=dopxx SMOOTH=4
REGRID LOG DOPING RATIO=6 OUTF=grid2 DOPF=dopxx SMOOTH=4
```

A similar effect could be obtained with just one regrid statement.

```
REGRID LOG DOPING RATIO=6 OUTF=grid2 DOPF=dopxx MAX.LEVEL=2
```

In both cases, two levels of refinement are performed. The first example is recommended because new doping information is introduced at each level of refinement. This produces better refinement criterion and fewer triangles.

Potential Regrid Example

Next, an initial solution is produced and triangles which exhibit large potential steps are refined.

```
SOLVE INIT
REGRID POTENTIAL RATIO=0.2 OUTF=grid3.str SMOOTH=4
```

Re-initializing after Regrid example

Often you need to re-solve the same bias point after a REGRID using the following style of syntax.

```
SOLVE VDRAIN=3.0
REGRID POTENTIAL RATIO=0.25 SMOOTH=4 OUTF=mygrid.str
SOLVE PREV
```

Occasionally, you need to quit and restart ATLAS with the new mesh. To do this, type syntax such as:

```
SOLVE VDRAIN=3.0
REGRID POTENTIAL RATIO=0.25 SMOOTH=4 OUTF=mygrid.str
go atlas
MESH INF=mygrid.str
```

After this MESH statement all models, material parameters and numerical methods have to be re-specified before any SOLVE statement.

21.49: SAVE

SAVE saves all node point information into an output file.

Note: In all cases the region boundaries, electrodes, mesh and doping are saved. If a SOLVE statement has preceded the SAVE statement all electrical data from the last solution is stored.

Syntax

SAVE OUTFILE=<filename> [MASTER]

| Parameter | Type | Default | Units |
|--------------|-----------|---------|---------|
| ABSORB | Logical | False | |
| AMBIEN.IMAG | Real | 0.0 | |
| AMBIEN.REAL | Real | 1.0 | |
| ANGLE.OUTPUT | Real | 30.0 | degrees |
| ANGPOWER | Character | | |
| COMPARE | Logical | False | |
| COUPLING3D | Logical | False | |
| CUTPLANE | Logical | False | |
| DIPOLE | Logical | False | |
| DDMS.LOG | Logical | False | |
| EDGE_ONLY | Logical | False | |
| EDGE_REFLECT | Logical | False | |
| EMAX | Real | | eV |
| EMIN | Real | | eV |
| FAST | Logical | False | |
| HORIZONTAL | Real | 2/3 | |
| INCOHERENT | Logical | False | |
| INCOH.TOP | Logical | False | |
| INTERFERE | Logical | False | |
| L.WAVE | Real | 0.8 | μm |
| LMAX | Real | | μm |
| LMIN | Real | | μm |
| MASTER | Character | True | |
| MIR.BOTTOM | Logical | False | |

| Parameter | Type | Default | Units |
|--------------|-----------|--------------------|---------------|
| MIN.POWER | Real | 1×10^{-4} | |
| MIR.TOP | Logical | False | |
| MQWELLS | Character | | |
| NEAR.FIELD | Character | | |
| NEGF.LOG | Logical | False | |
| NSAMP | Integer | 100 | |
| NUMRAYS | Integer | 180 | |
| OUT.FILE | Character | | |
| OUTFILE | Character | | |
| PATTERNS | Character | | |
| PISCES | Logical | False | |
| POLAR | Real | 45.0 | |
| RAYPLOT | Character | | |
| REFLECTS | Integer | 0 | |
| SIDE | Logical | False | |
| SMOOTHNESS | Real | 8.0 | |
| SOURCE.TERM | Logical | False | |
| SOURCE_TERM | Logical | False | |
| SPECT.ANGLE | Character | | |
| SPECTRUM | Character | | |
| STRUCTURE | Character | False | |
| SURFACE_ONLY | Logical | False | |
| TEMPER | Real | 300.0 | |
| TR.MATRIX | Logical | False | |
| TRAP.FILE | Character | | |
| USER.SPECT | Character | | |
| X | Real | 0.0 | μm |
| X.CUTPLANE | Real | 0.0 | μm |
| XMAX | Real | 0.0 | μm |
| XMIN | Real | 0.0 | μm |
| XNUM | Integer | 0 | |
| Y | Real | 0.0 | μm |

| Parameter | Type | Default | Units |
|------------|---------|---------|---------------|
| Y.CUTPLANE | Real | 0.0 | μm |
| YMAX | Real | 0.0 | μm |
| Y.MAX | Real | 0.0 | μm |
| YMIN | Real | 0.0 | μm |
| Y.MIN | Real | 0.0 | μm |
| YNUM | Integer | 0 | |
| Z | Real | 0.0 | μm |
| Z.CUTPLANE | Real | | μm |
| ZMAX | Real | 0.0 | μm |
| Z.MAX | Real | 0.0 | μm |
| ZMIN | Real | 0.0 | μm |
| Z.MIN | Real | 0.0 | μm |

Description

| | |
|---------------------|---|
| ABSORB | Takes absorption into account in reverse ray-tracing (see Chapter 11: “LED: Light Emitting Diode Simulator”, Section 11.5: “Reverse Ray-Tracing”). The absorption is assumed to be constant specified for each material by the imaginary part of the refractive index. |
| AMBIEN.IMAG | Specifies the imaginary index of refraction for the ambient outside the device domain for LED reverse ray tracing. |
| AMBIEN.REAL | Specifies the real index of refraction for the ambient outside the device domain for LED reverse ray tracing. |
| ANGLE.OUTPUT | Specifies the angular interval in degrees where spectrum versus angle are written to the file specified by the SPECT.ANGLE parameter. |
| ANGPOWER | Enables the reverse ray-tracing algorithm (see Chapter 11: “LED: Light Emitting Diode Simulator”, Section 11.5: “Reverse Ray-Tracing”) for analysis of output coupling of light from the structure of a Light Emitting Diode. ANGPOWER specifies the name of the output file for the angular power density vs. output angle dependence. |
| COUPLING3D | Calculates an output coupling coefficient, assuming a cylindrically symmetric light output with the light source located on the axis of symmetry (see Chapter 11: “LED: Light Emitting Diode Simulator”, Section 11.5: “Reverse Ray-Tracing”). Takes into account the 3D nature of the problem with output coupling calculation. |

| | |
|---------------------|---|
| CUTPLANE | Specifies that a 2D cutplane will be saved from a 3D structure to the file specified by the <code>OUTFILE</code> parameter. The direction of the cutplane depends on the value specified on either the <code>X.CUTPLANE</code> , <code>Y.CUTPLANE</code> or <code>Z.CUTPLANE</code> parameter. If you specify the <code>X.CUTPLANE</code> parameter, the output cutplane will be perpendicular to the X axis. If you specify the <code>Y.CUTPLANE</code> parameter, the output cutplane will be perpendicular to the Y axis. If you specify the <code>Z.CUTPLANE</code> parameter, the output cutplane will be perpendicular to the Z axis. |
| DIPOLE | Specifies a particular angular distribution of the internal radiating field that corresponds to a preferred in-plane orientation of dipoles often relevant to OLED devices (see Chapter 11: “LED: Light Emitting Diode Simulator”, Section 11.5: “Reverse Ray-Tracing”). |
| DDMS.LOG | Specifies that in case of DDMS model (see Section 13.8: “Drift-Diffusion Mode-Space Method (DD_MS)”), an additional log file with subband-resolved quantities will be stored along with structure file. |
| EDGE_ONLY | Specifies that for LED reverse ray tracing only the rays exiting from the edges are considered. Rays exiting at the top and bottom surfaces are not shown. |
| EDGE_REFLECT | Specifies the rays in reverse ray tracing reaching the edges of the device are totally reflected. |
| EMAX, EMIN | Specify the energy range for saving a spectrum file. |
| FAST | Specifies that a fast algorithm should be used for LED reverse ray tracing. In this case, the ray tracing is performed from region boundary to region boundary rather than the default element by element trace. |
| HORIZONTAL | Specifies the proportion of horizontally oriented dipoles for the dipole emission model. |
| INCOHERENT | Specifies that an incoherent material in LED/OLED structure is used for the purpose of combined transfer matrix method/reverse ray tracing (TTM+RRT) optical analysis. |
| INCOH.TOP | When specified with the <code>SOURCE.TERM</code> parameter, this allows a combination of transfer matrix method in thin coherent layers and ray tracing in thick incoherent layers for LED reverse ray tracing. |
| INTERFERE | Specifies that rays originating in the same point are fully coherent in reverse ray-tracing (see Chapter 11: “LED: Light Emitting Diode Simulator”, Section 11.5: “Reverse Ray-Tracing”). In this case, the phase information upon propagation is preserved. Phase change upon reflection is also considered. Thus, interference of rays exiting the device at the same angle are taken into account. |
| L.WAVE | Specifies the wavelength for reverse ray-tracing (see Chapter 11: “LED: Light Emitting Diode Simulator”, Section 11.5: “Reverse Ray-Tracing”). |
| LMAX, LMIN | Specify the range of wavelength for saving spectrum files. |
| MASTER | Specifies that the output file will be written in a standard structure format. Files in this format can be plotted in TONYPLOT. |

| | |
|-------------------|--|
| MIN.POWER | Specifies the minimum relative power of a ray (see Chapter 11: “LED: Light Emitting Diode Simulator”, Section 11.5: “Reverse Ray-Tracing”). The ray is not traced after its power falls below MIN.POWER value. This is useful to limit the number of rays traced. The default value is MIN.POWER=1e-4. |
| MIR.TOP | Specifies that the top surface of the device be treated as an ideal mirror in reverse ray-tracing (see Chapter 11: “LED: Light Emitting Diode Simulator”, Section 11.5: “Reverse Ray-Tracing”). |
| MIR.BOTTOM | Specifies that the bottom surface of the device be treated as an ideal mirror in reverse ray-tracing (see Chapter 11: “LED: Light Emitting Diode Simulator”, Section 11.5: “Reverse Ray-Tracing”). |
| NEAR.FIELD | Specifies the output file name where LED near field distribution is saved. A file for each surface where light exits is created. |
| NEGF.LOG | Specifies that spectra of transmission, DOS, density and and curent obtained from NEGF model need to be saved. |
| NSAMP | Specifies the number of samples to use for a spectrum plot. |
| NUMRAYS | Specifies the number of rays starting from the origin in reverse ray-tracing (see Chapter 11: “LED: Light Emitting Diode Simulator”, Section 11.5: “Reverse Ray-Tracing”). The default is 180. Acceptable range is 36-3600. |
| OUT.FILE | This is a synonym for OUTFILE. |
| OUTFILE | Specifies the name of an output file name. The synonym for this parameter is OUT.FILE. |
| PISCES | Specifies that the output file will be written in the original PISCES-II format. |
| PATTERNS | Specifies a character string representing the root of the file names where near and far field patterns are written for LASER or VCSEL. The near field pattern file is appended with the string <i>.nfp</i> and the far field pattern file is appended with the string <i>.ffp</i> . |
| POLAR | Specifies polarization of the emitted photons in degrees while linearly polarized light is assumed (see Chapter 11: “LED: Light Emitting Diode Simulator”, Section 11.5: “Reverse Ray-Tracing”). Parallel (TM-mode, POLAR=0.0) and perpendicular (TE-mode, POLAR=90.0) polarizations result in significantly different output coupling values. Use the default value (POLAR=45.0) if there is no preferred direction of polarization of emitted photons (unpolarized light emission). |
| RAYPLOT | Specifies the name of the output file containing the information on each ray exiting the device in single origin reverse ray-tracing (see Chapter 11: “LED: Light Emitting Diode Simulator”, Section 11.5: “Reverse Ray-Tracing”). This file is only created when the single origin for all rays is assumed. The information includes ray output angle, relative ray power (TE and TM-polarization and total), and initial internal angle at the origin (only if INTERFERE parameter is unspecified). 0° angle corresponds to the rays in the X axis direction. 90° angle corresponds to the rays in the Y axis direction. |
| REFLECTS | Specifies a number of reflections to be traced for each ray in reverse ray-tracing (see Chapter 11: “LED: Light Emitting Diode Simulator”, Section 11.5: “Reverse Ray-Tracing”). The default value is REFLECTS=0. The maximum allowed value is REFLECTS=10. Setting the number of reflections to 3 or 4 is often a good choice. |

| | |
|---------------------|---|
| SIDE | Specifies that the rays reaching the sides of the device are terminated there and do not contribute to the total light output (see Chapter 11: “LED: Light Emitting Diode Simulator”, Section 11.5: “Reverse Ray-Tracing”). |
| SOURCE_TERM | Indicates that dipole source terms are combined with transfer matrix calculation of light output for LEDs. The alias is SOURCE_TERM. |
| SPECT_ANGLE | Specifies the output file name where LED spectrum is written as a function of emission angle. |
| SPECTRUM | Specifies the name of a file for saving spectrum plots. |
| STRUCTURE | This is a synonym for SAVE. |
| SURFACE_ONLY | Specifies that for LED reverse ray tracing only the rays exiting from the top and bottom surfaces are considered. Rays exiting at the edges are not shown. |
| TEMPER | This is the temperature (needed for using appropriate refractive indexes of the materials in reverse ray-tracing). The default setting of 300 K will be used if TEMPER is unspecified. |
| TRAP_FILE | Specifies a file name to which all trap densities at the location specified by X,Y, and Z are to be saved. |
| TR_MATRIX | Specifies that the transfer matrix method should be used to handle thin film LEDs. |
| X | This is the X coordinate of light origin for a single point reverse ray-tracing (see Chapter 11: “LED: Light Emitting Diode Simulator”, Section 11.5: “Reverse Ray-Tracing”). |
| X.CUTPLANE | Specifies the X coordinate for a YZ cutplane. The region and nodal data from the nearest X plane to this X coordinate will be saved in the structure file. |
| XMAX | This is the maximum X coordinate of a rectangular area containing multiple origin points in reverse ray-tracing (see Chapter 11: “LED: Light Emitting Diode Simulator”, Section 11.5: “Reverse Ray-Tracing”). |
| XMIN | This is the minimum X coordinate of a rectangular area containing multiple origin points in reverse ray-tracing (see Chapter 11: “LED: Light Emitting Diode Simulator”, Section 11.5: “Reverse Ray-Tracing”). |
| XNUM | Specifies the number of points along X axis within a rectangular area in multiple origin reverse ray-tracing (see Chapter 11: “LED: Light Emitting Diode Simulator”, Section 11.5: “Reverse Ray-Tracing”). |
| Y | This is the Y coordinate of light origin for a single point reverse ray-tracing (see Chapter 11: “LED: Light Emitting Diode Simulator”, Section 11.5: “Reverse Ray-Tracing”). |
| Y.CUTPLANE | Specifies the Y coordinate for a XZ cutplane. The region and nodal data from the nearest Y plane to this Y coordinate will be saved in the structure file. |
| YMAX | This is the maximum Y coordinate of a rectangular area containing multiple origin points in reverse ray-tracing (see Chapter 11: “LED: Light Emitting Diode Simulator”, Section 11.5: “Reverse Ray-Tracing”). |
| YMIN | This is the minimum Y coordinate of a rectangular area containing multiple origin points in reverse ray-tracing (see Chapter 11: “LED: Light Emitting Diode Simulator”, Section 11.5: “Reverse Ray-Tracing”). |

| | |
|-------------------|--|
| YNUM | Specifies the number of points along Y axis within a rectangular area in multiple origin reverse ray-tracing (see Chapter 11: “LED: Light Emitting Diode Simulator”, Section 11.5: “Reverse Ray-Tracing”). |
| Z | Specifies the Z coordinate. |
| Z.CUTPLANE | Specifies the Z coordinate for a XY cutplane. The region and nodal data from the nearest Z plane to this Z coordinate will be saved in the structure file. |

Basic Save Example

```
SOLVE V1=5
SAVE OUTF=data1.str
```

is equivalent to

```
SOLVE V1=5 OUTF=data1.str MASTER
```

Save Example with User-Defined Output

In the second example, the SAVE and OUTPUT commands are used to produce two output files for the same bias. The OUTPUT statement selects which data will be stored in each file. The first file (data1.str) contains the default contents, total electric field, and components of electron velocity. The second file (data2.str) contains components of hole velocity and band edge potentials. Note that the EX.VELO and EY.VELO parameters are used to prevent electron velocity components from being stored in file data2.

```
OUTPUT E.FIELD EX.VELO EY.VELO
SAVE OUTF=data1.str
OUTPUT HX.VELO HY.VELO CON.BAND VAL.BAND ^EX.VELO ^EY.VELO
SAVE OUTF=data2.str
```

Note: You can customize the contents of the saved file by using the OUTPUT statement.

21.50: SET

The SET statement is used to define variables for substitution into ATLAS syntax. SET commands are executed by DECKBUILD.

Note: Full documentation of the SET statement is found in the DECKBUILD USER'S MANUAL.

Numeric Variable Example

Define a numerical variable. Use it in a calculation and substitute it into the ATLAS syntax for REGION definition

```
SET MYLENGTH=0.1
SET HALFLENGTH= $"MYLENGTH"*0.5
...
REGION NUM=1 MATERIAL=SILICON X.MIN=$"HALFLENGTH" X.MAX=$"MYLENGTH"
```

String Variable Example

Define a string variable to use as part of a filename

```
SET LABEL=testcase1
..
LOG OUTF=$"LABEL".log
..
SAVE OUTF=bias_$"LABEL"_25.str
```

This will produce files called testcase1.log and bias_testcase1_25.str

21.51: SINGLEEVENTUPSET

SINGLEEVENTUPSET specifies the values of parameters used in Single Event Upset modeling.

Syntax

SINGLEEVENTUPSET <parameters>

| Parameter | Type | Default | Units |
|-------------|-----------|---------|------------------|
| A1 | Real | | |
| A2 | Real | | |
| A3 | Real | | |
| A4 | Real | | |
| B1 | Real | | |
| B2 | Real | | |
| B3 | Real | | |
| B4 | Real | | |
| B.DENSITY | Real | 0 | cm ⁻³ |
| BEAM.RADIUS | Real | 0 | μm |
| DENSITY | Real | | cm ⁻³ |
| DEVICE | Character | | |
| STRUCTURE | Character | | |
| ENTRYPOINT | Real | vector | μm |
| EXITPOINT | Real | vector | μm |
| F.SEU | Character | | |
| PCUNITS | Logical | False | |
| RADIALGAUSS | Logical | False | |
| RADIUS | Real | | μm |
| RESCALE | Logical | False | |
| TFINAL.SEU | Real | | |
| T0 | Real | | s |
| TC | Real | | s |
| TF | Real | | s |
| UNIFORM | Logical | False | |

Description

| | |
|--------------------------|--|
| A1, A2, A3 and A4 | The first set of parameters for the length dependence of the charge generation pulse. |
| B1, B2, B3 and B4 | The second set of parameters for the length dependence of the charge generation pulse. |
| B.DENSITY | Specifies the number of electron-hole pairs per unit volume or generated charge in pico Coulombs per micron if the PCUNITS parameter is specified. |
| BEAM.RADIUS | This is the radius of the beam where the generation rate is maintained constant. Beyond this point the generation will decay by either an exponential or by a Gaussian function. |
| DENSITY | Specifies the number of electron-hole pairs per unit volume generated along the alpha particle track. |
| DEVICE | Specifies which device the SINGLEEVENTUPSET statement applies to in MixedMode. The synonym for this parameter is STRUCTURE. |
| ENTRYPOINT | Specifies the X, Y, and Z coordinates of the beginning of the alpha particle track. The specified point should belong to the semiconductor region. |
| EXITPOINT | Specifies the X, Y, and Z coordinates of the end of the alpha particle track. The specified point should belong to the semiconductor region. |
| F.SEU | Specifies the name of C-Interpreter function describing the SEU generation rate as a function of position and time. |
| PCUNITS | Sets the units of B.DENSITY to be pC per micron. |
| RADIALGAUSS | Specifies the Gaussian radial dependence of the charge generation pulse. By default, the exponential dependence is used. |
| RADIUS | Specifies the radius of the alpha particle track. |
| RESCALE | This causes nodal generation rates to be scaled by the ratio of the integral of the analytic generation rate divided by the numerically integrated value. |
| STRUCTURE | This is a synonym for DEVICE. |
| TFINAL.SEU | Specifies the finish time for the track, this defaults to the finish time of the transient simulation if TFINAL.SEU is not specified. |
| T0 | Specifies the peak in time of the charge generation pulse. |
| TC | Specifies the width of the charge generation pulse. |
| UNIFORM | Specifies that a uniform generation rate corresponding to that specified by the DENSITY parameter is applied. |

SEU Example

This statement specifies a track path, radius and density:

```
SINGLEEVENTUPSET ENTRYPOINT="1.5,2.0,0.0"\  
EXITPOINT="1.0,1.0,4.0" RADIUS=0.05" \  
DENSITY=1E18
```

Note: For user-defined Single Event Generation profiles, the C-INTERPRETER function `F.SEU` on the `SINGLEEVENTUPSET` statement can be used.

21.52: SOLAR

The SOLAR statement is used to simplify standard analysis of solar cells.

Syntax

SOLAR <parameters>

| Parameter | Type | Default | Units |
|------------|-----------|---------|---------|
| ANODE | Integer | | |
| AZIMUTH | Real | 0.0 | Degrees |
| BEAM | Integer | | |
| DV | Integer | 0.05 | Volts |
| ELEVATION | Real | 90.0 | Degrees |
| IA | Character | | |
| IV | Character | | |
| IW | Character | | |
| LATTITUDE | Real | 35.0 | Degrees |
| MAX.ANGLE | Real | 85.0 | Degrees |
| MAX.WAVE | Real | microns | |
| MIN.DV | Real | 0.002 | Volts |
| MIN.WAVE | Real | microns | |
| RTO | Character | | |
| STEP.ANGLE | Real | 5.0 | Degrees |
| STEP.WAVE | Real | microns | |
| VANODE | Real | 0.5 | Volts |

Description

| | |
|----------------|--|
| ANODE | Specifies the electrode index of the "anode". The "anode" is the electrical contact where positive voltages are applied to extract the standard current-voltage characteristic of a solar cell. If the ANODE parameter is left unspecified, the simulator will search for a contact named "anode". |
| AZIMUTH | Specifies the solar cell azimuth angle (angle with respect to due south) for orbital simulation of annual energy collection. |
| BEAM | Specifies the beam index of the beam used as a solar source. If the BEAM parameter is left unspecified, the simulator will automatically choose the first beam defined on a BEAM statement. |

| | |
|-------------------|---|
| DV | Specifies the initial voltage step increment for extraction of the standard IV characteristic. |
| ELEVATION | Specifies the solar cell elevation angles (angle from the horizon) for orbital simulation of annual energy collection. |
| IA | Specifies the name of a file for collection of efficiency versus angle data. You must specify the IA parameter to perform the efficiency versus angles extraction. |
| IV | Specifies the name of a file for collection of the standard current-voltage characteristics of the solar cell. You must specify the IV parameter to perform standard current voltage extraction including the extraction of Voc, Isc, Pmax, and FF. |
| IW | Specifies the name of a file for collection of solar cell efficiency versus wavelength. If you specify this parameter, you must also specify the MIN.WAVE , MAX.WAVE , and STEP.WAVE parameters. |
| LATTITUDE | Specifies the latitude of the solar cell for orbital simulation of the annual energy collection. |
| MAX.ANGLE | Specifies the maximum angle for angular efficiency collection (see IA). This value must be less than 90° and greater than 0°. |
| MAX.WAVE | Specifies the maximum wavelength for collection of spectral response of the solar cell (see IW). |
| MIN.DV | Specifies minimum voltage step at open circuit conditions for the extraction of standard solar cell current-voltage characteristics (see IV). |
| MIN.WAVE | Specifies the minimum wavelength for collection of spectral response of the solar cell (see IW). |
| RTO | Specifies the name of a file where the solar cell run-time output will separately be written. |
| STEP.ANGLE | Specifies the angle step in degrees for angular efficiency collection (see IA). |
| STEP.WAVE | Specifies the wavelength step for collection of spectral response of the solar cell (see IW). |
| VANODE | Specifies the anode operating voltage for extraction of angular response (see IA) or spectral response (see IW) or both. If the current-voltage characteristics are extracted (see IV) the voltage at maximum power, Pmax, will be used as the operating voltage. |

21.53: SOLVE

SOLVE instructs ATLAS to perform a solution for one or more specified bias points.

Syntax

SOLVE [<ion>] <dc> [<fp>][<ep>][<tp>][<ac>][<photo>] [<thermal>]

| Parameter | Type | Default | Units |
|--------------|-----------|----------------------|-------------------|
| AC.ANALYSIS | Logical | False | |
| AFINAL | Real | 85.0 | Degrees |
| ANAME | Character | | |
| ANGLE | Real | 0.0 | Degrees |
| ASCII | Logical | False | |
| ASTEP | Real | 5.0 | Degrees |
| AUTO | Logical | True | |
| B<n> | Real | 0.0 | W/cm ² |
| BEAM | Integer | | |
| BRANIN | Logical | True | |
| C.IMAX | Real | 10 ⁻⁴ | A |
| C.IMIN | Real | -10 ⁻⁴ | A |
| C.VSTEP | Real | 0.0 | V |
| C.VMAX | Real | 5.0 | V |
| C.VMIN | Real | -5.0 | V |
| CNAME | Character | | |
| COMPLIANCE | Real | | |
| CONTINUE | Logical | False | |
| CURVETRACE | Logical | False | |
| CYCLES | Integer | 1 | |
| CYCLIC.BIAS | Logical | False | |
| CYCLIC.RELAX | Real | 0.2 | |
| CYCLIC.TOL | Real | 1.0×10 ⁻⁵ | |
| DDMS.LOG | Logical | False | |
| DECAY | Real | | s |
| DELTAV | Real | 0.1 | V |

| Parameter | Type | Default | Units |
|---------------|-----------|----------------------|------------------|
| DIRECT | Logical | False | |
| DT | Real | 0 | s |
| DT.CBET | Logical | False | |
| DT.CUR | Logical | False | |
| DT.METH | Real | 1 | |
| DT.VBET | Logical | False | |
| DT.VBHT | Logical | False | |
| E.CHECK | Integer | | |
| E.COMPL | Real | | |
| E.CRIT | Real | 1.0×10^{-8} | |
| ELECTRODE | Integer | | |
| EMAX | Real | 0.0 | eV |
| EMIN | Real | 0.0 | eV |
| ENDRAMP | Real | | s |
| FREQUENCY | Real | | Hz |
| FSTEP | Real | 0 | Hz |
| GRAD | Logical | False | |
| I<n> | Real | | A/ μm |
| IFINAL | Real | | A/ μm |
| IMPACT.I | Logical | False | |
| IMULT | Logical | False | |
| INAME | Character | | |
| INDEX.CHECK | Logical | False | |
| INITIAL | Logical | False | |
| ION.CRIT | Real | 1.0 | |
| ION.ELEC | Integer | see Description | |
| IONIZINT | Logical | False | |
| IONLINES | Integer | 50 | none |
| IONSTOP | Logical | True | |
| ISTEP | Real | 0.0 | A/ μm |
| INT.INCREMENT | Logical | False | |
| IT.SAVE | Character | | |

| Parameter | Type | Default | Units |
|-----------|-----------|------------------|------------------------|
| LAMBDA1 | Real | | μm |
| LIT.STEP | Real | | W/cm^2 |
| LMAX | Real | 0.0 | μm |
| LMIN | Real | 0.0 | μm |
| LOCAL | Logical | False | |
| LRATIO | Real | 1.0 | |
| L.WAVE | Real | | μm |
| MASTER | Logical | False | |
| MAX.INNER | Integer | 25 | |
| MLOCAL | Logical | False | |
| MONOTONIC | Logical | False | |
| MULT.FREQ | Logical | False | |
| N.BIAS | Real | | V |
| NAME | Character | | |
| NB1 | Real | | V |
| NB2 | Real | | V |
| NB3 | Real | | V |
| NB4 | Real | | V |
| NB5 | Real | | V |
| NB6 | Real | | V |
| NB7 | Real | | V |
| NB8 | Real | | V |
| NEGATIVE | Logical | False | |
| NEGF.LOG | Logical | False | |
| NFSTEPS | Integer | 0 | |
| NIT.N | Real | 0.0 | cm^{-3} |
| NIT.P | Real | 0.0 | cm^{-3} |
| NET.XMAX | Real | right hand side | μm |
| NIT.XMIN | Real | left hand side | μm |
| NIT.YMAX | Real | top of region | μm |
| NIT.YMIN | Real | bottom of region | μm |

| Parameter | Type | Default | Units |
|--------------|-----------|-----------------------|------------------|
| NLAYERS | Real | 15 | |
| NOCONTACT | Logical | False | |
| NOCURRENT | Logical | False | |
| NOINTERFACE | Logical | False | |
| NOISE.SS | Logical | False | |
| NSAMP | Integer | 100 | |
| NSTEPS | Integer | 0 | |
| OFFSET.ANGLE | Real | 0.0 | Degrees |
| ONEFILEONLY | Logical | See Description | |
| OUT.FILE | Character | | |
| OUTFILE | Character | | |
| P.BIAS | Real | | |
| PB1 | Real | | V |
| PB2 | Real | | V |
| PB3 | Real | | V |
| PB4 | Real | | V |
| PB5 | Real | | V |
| PB6 | Real | | V |
| PB7 | Real | | V |
| PB8 | Real | | V |
| PIEZSCALE | Real | 1.0 | |
| POSITIVE | Logical | False | |
| POWER<n> | Real | | Ω |
| POWERFINAL | Real | | Ω |
| PREVIOUS | Logical | False | |
| PROJ.MOD | Logical | False | |
| PROJECT | Logical | False | |
| PULSE.WIDTH | Real | | s |
| Q<n> | Real | | C/ μm |
| QFACTOR | Real | 1.0 or previous value | |
| QFINAL | Real | | C/ μm |

| Parameter | Type | Default | Units |
|--------------|-----------|----------------------|-------------------|
| QSCV | Logical | False | |
| QSTEP | Real | | C/ μm |
| RAMPTIME | Real | | s |
| RAMP.LIT | Logical | False | |
| RELATIVE | Logical | False | |
| SCAN.SPOT | Real | | |
| S.OMEGA | Real | 1.0 | |
| SINUAMP.COMP | Real | 0.0 | |
| SINUVAR.COMP | Real | 0.0 | |
| SONOS | Logical | False | |
| SOR | Logical | False | |
| SPECTRUM | Character | | |
| SQPULSE | Logical | False | |
| SP.LAST | Logical | False | |
| SS.LIGHT | Real | 0.001 | W/cm ² |
| SS.PHOT | Logical | False | |
| T<n> | Real | | K |
| T.COMP | Real | 0 | K |
| T.SAVE | Real | 0.0 | s |
| TABLE | Character | | |
| TDELAY | Real | 0.0 | s |
| TFALL | Real | 0.0 | s |
| TRISE | Real | 0.0 | s |
| TSAVE.MULT | Real | 1.0 | |
| TERMFINAL | Real | | K |
| TERMINAL | Integer | all contacts | |
| TIMESPAN | Real | ∞ | seconds |
| TOLERANCE | Real | 1.0×10^{-5} | |
| TRANS.ANALY | Logical | False | |
| TSTOP | Real | | |
| TWOFILESONLY | Logical | False | |
| V<n> | Real | | V |

| Parameter | Type | Default | Units |
|-----------|-----------|---------|---------|
| VFINAL | Real | | V |
| VSTEP | Real | 0.0 | V |
| VSS | Real | 0.1 | KT/Q |
| WAVE<n> | Logical | False | |
| WFINAL | Real | | microns |
| WAVEFORMS | Character | | |
| WSTEP | Real | | microns |

Description

Each SOLVE statement must specify an initial bias condition. Once any DC condition has been solved, either a transient or AC analysis may be performed. You may also solve for carrier generation due to incident light under DC, or AC analysis transient conditions.

| | |
|-----------------|---|
| dc | This is one or more of the DC bias parameters |
| fp | This is one or more of the file parameters |
| ep | This is one or more of the initial guess or estimate parameters. Estimate parameters are used to specify how the initial approximation for the solution is to be obtained. |
| tp | This is one or more of the transient parameters. These parameters are used to specify data for transient analysis. |
| ac | This is one or more of the AC parameters. AC parameters are used to specify data for AC analysis. |
| ion | This is a set of the ionization integral parameters. |
| NEGF.LOG | Specifies that spectra of transmission, DOS, density and and curent obtained from NEGF model need to be saved. |
| photo | This is one or more of the photogeneration parameters. Photogeneration parameters are used to specify illumination data. |
| SP.LAST | Allows to solve Schrodinger equation in the last point of a bias sweep, as a post processing step after classical solution is obtained. When the parameter is off, a Schrodinger solution for each bias point is performed. |
| therm | This is one or more of the thermal parameters. Thermal parameters are used for obtaining solutions in THERMAL3D. |

DC Parameters

| | |
|----------------|---|
| C.IMAX | Specifies the maximum current for curve tracing. |
| C.IMIN | Specifies the minimum current for curve tracing. |
| C.VSTEP | Specifies the initial voltage step for curve tracing. |
| C.VMAX | Specifies the maximum voltage for curve tracing. |

| | |
|---|---|
| C.VMIN | Specifies the minimum voltage for curve tracing. |
| CONTINUE | This is an alias for CURVETRACE. |
| CURVETRACE | Initiates curve tracing. See also the CURVETRACE statement. The alias for this parameter is CONTINUE. |
| DDMS.LOG | Specifies that in case of DDMS model (see Section 13.8: “Drift-Diffusion Mode-Space Method (DD_MS)”), an additional log file with subband-resolved quantities will be stored along with structure file. MASTER and UTF also have to be set. |
| ELECTRODE | Specifies electrodes that you wish to add voltage and current increments (VSTEP and ISTEP) to. If n electrodes are to be stepped, ELECTRODE should be an n-digit integer, where each of the digits is a separate electrode number. See also the NAME parameter. |
| I<name> or I(<name>) | Specifies the applied current for a named electrode. One of several commonly used terminal names should be specified. These names are as follows: gate, gg, drain, dd, source, bulk, substrate, emitter, ee, collector, cc, base, bb, anode, cathode, fgate, cgate, ngate, pgate, well, nwell, pwell, channel, and ground. No other user-defined names are allowed. This parameter is used when current boundary conditions are selected (see Section 21.5: “CONTACT”) |
| I<n> | Specifies the terminal current for electrode, n. This parameter is used when current boundary conditions are selected (see Section 21.5: “CONTACT”). Normally, I defaults to the current from the previous bias point. It is more usual to use electrode names rather than numbers. This parameter is superseded by I<name>. |
| IFINAL | Specifies the final current value for a set of bias increments. If IFINAL is specified, either ISTEP or NSTEPS must be specified. |
| IMULT | Specifies that the current (for current boundary conditions) be multiplied by ISTEP rather than incremented. |
| ISTEP | Specifies a current increment to be added to one or more electrodes, as specified by the electrode name applied to the NAME parameter. If ISTEP is specified, either IFINAL or NSTEPS must also be specified. |
| N.BIAS | Specifies fixed electron quasi-Fermi potentials if electron continuity is not being solved. If N.BIAS is not specified, then local quasi-Fermi potentials based on bias and doping are used. But if FIX.QF is set in the METHOD statement, the quasi-Fermi levels will be set to the maximum bias. |
| NB<n> | Allows region by region specification of N.BIAS. The n index corresponds to the region index for which the specified value of electron quasi-fermi level applies. |
| NAME | Specifies that the named electrode is to be ramped. Custom electrode names are supported by name. See also the V<name> parameter. |
| NSTEPS | Specifies the number of DC bias increments. |

| | |
|---|--|
| P.BIAS | Specifies fixed hole quasi-Fermi potentials if hole continuity is not being solved. If P.BIAS is not specified, then local quasi-Fermi potentials based on bias and doping are used. But if FIX.QF is set in the METHOD statement, the quasi-Fermi levels will be set to the minimum bias. |
| PB<n> | Allows region by region specification of P.BIAS. The n index corresponds to the region index for which the specified value of hole quasi-fermi level applies. |
| Q<name> or Q(<name>) | Specifies the charge on a named electrode. These names are as follows: gate, gg, fgate, cgate, ngate, and pgate. No other user-defined names are allowed. This parameter is used when floating or charge boundary conditions are selected (see Section 21.5: "CONTACT"). |
| Q<n> | Specifies the charge on electrode number, n. It is more usual to use electrode names rather than numbers. This parameter is superseded by Q<name>. |
| QFINAL | Specifies the final charge for a set of bias increments. If QFINAL is specified, either QSTEP or NSTEPS must also be specified. |
| QSCV | Specifies the Quasi-static Capacitance calculation. This only has meaning when the SOLVE statement is ramping a bias. This requires a small voltage increment between solutions for best results. |
| QSTEP | specifies a charge increment to be added to one or more electrodes, as specified by the electrode name applied to the NAME parameter. If QSTEP is specified, either QFINAL or NSTEPS must also be specified. |
| TIMESPAN | Specifies the simulated time for a bias ramp in the HEIMAN model. The ramp is assumed to be linear in time, and so the time taken to change by VSTEP volts is TIMESPAN times VSTEP divided by Total Bias Change. |
| V<name> or V(<name>) | Specifies the bias voltage for a named electrode. One of several commonly used terminal names should be specified. These names are as follows: gate, gg, drain, dd, source, bulk, substrate, emitter, ee, collector, cc, base, bb, anode, cathode, fgate, cgate, ngate, pgate, well, nwell, pwell, channel, and ground. No other user-defined names are allowed. |
| V<n> | Specifies the bias voltage for electrode, n. Normally, Vn, defaults to the potential from the previous bias point. It is more usual to use electrode names rather than numbers. This parameter is superseded by V<name>. |
| VFINAL | Specifies the final voltage for a set of bias increments. If VFINAL is specified, either VSTEP or NSTEPS must also be specified. |
| VSTEP | Specifies a voltage increment to be added to one or more electrodes, as specified by the electrode name applied to the NAME parameter. If VSTEP is specified, you must either specify VFINAL or NSTEPS. |

File Output Parameters

| | |
|------------------------|---|
| EMAX, EMIN | Specify the energy range for output of spectral data in the file named by the SPECTRUM parameter. |
| IMPACT . I | Specifies that impact ionization rate should be saved to the structure file. If impact ionization is not enabled, these results will not be self-consistent. |
| INT . INCREMENT | Specifies that the last character of OUTFILE will not be incremented for each structure file. Instead an integer corresponding to the bias point number will be appended to the OUTFILE along with .str. |
| IT . SAVE | Specifies the name of an output file where the structure information will be stored after every GUMMEL or NEWTON iteration. The ASCII code of the last non-blank character of the supplied file name will be incremented by one for each iteration, resulting in a unique file per iteration. |
| LMAX, LMIN | Specify the wavelength range for spectral output in the file named by the SPECTRUM parameter. |
| MASTER | Specifies that the output file selected by the OUTFILE parameter will be written in a standard structure file rather than in the older PISCES-II binary format. |
| ONEFILEONLY | Specifies that only one filename will be used to save solutions during a bias ramp. If this parameter is specified, filename incrementing described under OUTFILE is not applied. This parameter is true by default unless the NAME or ELECTRODE parameters or transient simulations specified. When CURVETRACE is used, you need to explicitly set this parameter to false using ^ONEFILEONLY to save a different filename at each bias point. |
| OUT . FILE | This is an alias for OUTFILE. |
| OUTFILE | Specifies the name of the output file where bias point solution information will be stored. If an electrode is stepped so that more than one solution is generated by the SOLVE statement, the ASCII code of the last non-blank character of the supplied file name will be incremented by one for each bias point in succession, resulting in a unique file per bias point. The alias for this parameter is OUT . FILE. |
| SPECTRUM | Specifies the name of an output file where LED spectral data are stored after each step. |

Note: The output file specified by OUTFILE has a limit of 132 characters on a UNIX system and eight characters on a PC system.

Initial Guess Parameters

| | |
|------------------|---|
| INITIAL | Sets all voltages to zero. If this parameter is not specified for the first bias point in a given structure a SOLVE INIT statement is automatically inserted. The SOLVE INIT statement is always solved in zero carrier mode with no external elements attached. It is used to provide a good initial guess to subsequent solutions. |
| LOCAL | Specifies that the initial approximation should use local values of quasi-Fermi levels. See Chapter 20: “Numerical Techniques”, Section 20.6: “Initial Guess Strategies” for more detailed information. |
| MLOCAL | Specifies the modified local initial guess. This parameter is used when solved for carrier temperatures in the energy balance models. If any energy balance model is specified, MLOCAL defaults to true. |
| NOCURRENT | Specifies an initial guess strategy that solves the non-linear Poisson equation and uses this solution as the initial guess. This will typically give good results for situations where the quasi-fermi levels are almost flat and the current is consequently low. Under these conditions, you can solve almost any desired bias point directly. |
| PREVIOUS | Specifies that the previous solution as the initial approximation. |
| PROJ.MOD | Gives an alternative to the PROJ initial guess strategy in the case of one carrier type solution by making a different update for the unsolved carrier concentration. |
| PROJ | Specifies that an extrapolation from the last two solutions will be used as an initial approximation. This parameter may be used if there are two or more existing solutions and equivalent bias steps are taken on any electrodes that are changed. |

Note: If no initial guess parameters are specified, ATLAS will use PROJ wherever possible.

| | |
|----------------|--|
| QFACTOR | Specifies as scaling factor to improve initial guesses when the QUANTUM model is used. This parameter should be ramped slowly from zero to unity at the start of quantum effect simulations. |
|----------------|--|

Compliance Parameters

Compliance parameters define a current limit for a DC bias ramp or transient simulation. You can terminate the simulation by monitoring the current and checking against a user-defined limit.

| | |
|---------------------|---|
| COMPLIANCE | Sets a limit on the current from the electrode which has been specified by the CNAME or E.COMPLIANCE parameter. When the COMPLIANCE value is reached, any bias ramp is stopped and the program continues with the next line of the input file. The COMPLIANCE parameter is normally specified in A. If the GRAD parameter is specified, COMPLIANCE is specified in A/V. |
| E.COMPLIANCE | Specifies the electrode number to be used by the COMPLIANCE parameter. See also CNAME. |
| CNAME | Specifies the name of the electrode used by the COMPLIANCE. |
| GRAD | Specifies that the compliance value is a current/voltage gradient, and not a current value. |

| | |
|------------------|--|
| E.CHECK | Specifies the electrode number for compliance testing for monotonicity, positiveness or negativeness. |
| MONOTONIC | Specifies that current in the electrode associated with the index specified on the E.CHECK parameter must remain monotonic during a static ramp. If this condition is violated, the solution ramp is immediately exited. |
| POSITIVE | Specifies that current in the electrode associated with the index specified on the E.CHECK parameter must remain positive during a static ramp. If this condition is violated, the solution ramp is immediately exited. |
| NEGATIVE | Specifies that current in the electrode associated with the index specified on the E.CHECK parameter must remain negative during a static ramp. If this condition is violated, the solution ramp is immediately exited. |

Transient Parameters

| | |
|--------------------|---|
| CYCLES | Specifies the number of periods to be simulated (both FREQUENCY and TRANS.ANALY must be specified when this parameter is used). The synonym for this parameter is PERIODS. |
| CYCLIC.BIAS | Specifies that a cyclic bias [225] simulation is being performed. Cyclic biasing allows the effects of repeated trapezoidal/square transient pulses (see SQPULSE) on the output characteristics to be determined, without having to do the extremely large numbers of cycles. When CYCLIC.BIAS is specified, ATLAS will calculate a series of trapezoidal/square pulses using the SQPULSE parameters. At the end of the third cycle (and at all subsequent cycles) the values of the potential (V), electron concentration (n), hole concentration (p) and trap probability of occupation (f_T) will be modified according to the equation: |

$$x(k+1) = x(k) - \text{CYCLIC.RELAX} * ((x(k) - x(k-1)) * dx(k) / (dx(h) - dx(k-1))) \quad 21-6$$

where x is a parameter such as V , n , p or f_T at every node point, $x(k)$ is the updated value calculated from the equation, k is the cycle number (with $k+1$ being the new update for parameter x), CYCLIC.RELAX is the relaxation factor, $\delta x(k)$ is the difference between the simulated values of x at the start and beginning of the current cycle, while $\delta x(k-1)$ is the equivalent for the previous cycle.

Steady state cyclic convergence is determined by comparing the normalizing sum of the updated values of V , n , p , and f_T with a tolerance value (CYCLIC.TOL).

| | |
|---------------------|--|
| CYCLIC.RELAX | Specifies the CYCLIC.BIAS relaxation factor (the recommended range for this parameter to ensure stable convergence is between 0.2 and 1). |
| CYCLIC.TOL | Specifies the CYCLIC.BIAS tolerance factor. |
| DECAY | Specifies the time constant used for defining an exponential change in bias for transient simulation. |
| ENDRAMP | Applies any bias changes as linear ramps. ENDRAMP specifies the exact end of the ramp in running time (i.e., the ramp will start at $t=t_0$ and end at $t=\text{ENDRAMP}$). |

| | |
|---------------------|---|
| NSTEPS | This can be used to signal the end of the run (i.e., the final time would be $t = t + \text{NSTEPS} * \text{DT}$). You can use this parameter instead of the TSTOP parameter. |
| PULSE.WIDTH | Specifies the time constant used for sinusoidal non-linear time domain simulation. If SQPULSE is specified, PULSE.WIDTH is the width of the trapezoidal/square pulse not including the rise and fall times. |
| RAMPTIME | Applies any bias changes as linear ramps. RAMPTIME specifies a ramp interval in seconds (i.e., the ramp will begin at $t=t_0$ and ends at $t=t_0 + \text{RAMPTIME}$). |
| RELATIVE | Specifies that the TSTOP value is relative to the current time value. |
| SINUAMP.COMP | Specifies that sinusoidal amplitude compliance will be used. The transient simulation will stop if the amplitude of a sinusoidal waveform is less than the value of SINUAMP.COMP . |
| SINUVAR.COMP | Specifies that sinusoidal variance compliance will be used. The transient simulation will stop if the change in amplitude of a sinusoidal waveform is less than SINUVAR.COMP . |
| SQPULSE | Specifies that multiple trapezoidal/square transient pulses will be applied. The pulse is controlled by the TDELAY , TRISE , PULSE.WIDTH , TFALL , and FREQUENCY parameters. |
| T.COMP | Specifies a temperature for temperature compliance. Once the specified temperature is obtained at some location on the mesh the solution process is discontinued. |
| T.SAVE | Specifies a time increment at which the device structure files are saved. |

Note: Actual time steps may not correspond to the user-specified increment.

| | |
|--------------|--|
| TABLE | <p>Specifies the filename of a table of time and bias values for the specified electrode. The following format must be used for the TABLE file.</p> <pre> time1 bias1 time2 bias2 time3 bias3 end </pre> <p>The time value should be in seconds. The value of the bias should be in the same units as displayed in ATLAS (i.e., Volts for a voltage controlled electrode, A/um for a current controlled electrode, and A for a current controlled electrode in DEVICE3D or ATLAS with the WIDTH parameter specified on the MESH statement). There's no limit to the number of time/bias pairs that can be defined in the table file. The keyword, END, must be placed after the last time/bias pair. Linear interpolation will be used to determine the bias for time points that aren't specified in the table file.</p> |
|--------------|--|

Note: An electrode must also be specified when using the `TABLE` parameter. The electrode can be specified either by name (e.g., `NAME=anode`) or by number (e.g., `ELECTRODE=1`).

| | |
|---------------------------|--|
| TDELAY | Specifies the time delay before the first cycle of multiple trapezoidal/square transient pulses (<code>SQPULSE</code>) will be applied. |
| TFALL | Specifies the fall time for trapezoidal/square transient pulses (<code>SQPULSE</code>). |
| TRISE | Specifies the rise time for trapezoidal/square transient pulses (<code>SQPULSE</code>). |
| TRANS.ANALY | Specifies that transient analysis is being performed and that a sinusoid with a frequency, specified by the <code>FREQUENCY</code> parameter, should be applied. |
| TSAVE.MULT | Specifies a multiplier the save time increment, <code>T.SAVE</code> , is multiplied by after each time a structure is saved. |
| TSTEP or DT | Specifies the time-step to be used. For automatic time-step runs, <code>DT</code> is used to select only the first time step (see Section 21.32: “METHOD”). |
| TSTOP | Specifies the end of the time interval. If simulation begins at $t=t_0$ and <code>RELATIVE</code> is specified, it will end at $t=TSTOP+t_0$. |
| WAVE<n> | Specifies that the <code>WAVEFORM</code> , <code>n</code> (where <code>n</code> is between 1 and 10), will be enabled for the current <code>SOLVE</code> statement. This parameter should appear on every <code>SOLVE</code> statement where the specified <code>WAVEFORM</code> is to be applied. |

Note: You can solve more than one `WAVEFORM` at the same time.

| | |
|------------------|---|
| WAVEFORMS | Specifies multiple <code>WAVEFORMS</code> to be enabled for the current <code>SOLVE</code> statement. The <code>WAVEFORM</code> numbers should be specified as a comma separated list. For example, <code>SOLVE WAVEFORMS= "1, 2, 12" TFINAL=1e-6</code> . This will enable <code>WAVEFORM</code> numbers 1, 2, and 12. |
|------------------|---|

AC Parameters

| | |
|--------------------|--|
| AC.ANALYSIS | Specifies that AC sinusoidal small-signal analysis should be performed after solving for the DC condition. The full Newton method must be used for this analysis. This is typically specified with the statement: <code>METHOD NEWTON CARRIERS=2</code> |
| ANAME | Specifies the name of the electrode to which the AC bias will be applied. See also <code>TERMINAL</code> . If no <code>ANAME</code> is specified, all electrodes have AC bias applied in turn. |
| AUTO | Selects an automatic AC analysis method. This method initially uses <code>SOR</code> . The <code>DIRECT</code> method will be used if convergence problems occur. We strongly recommend the use of the <code>AUTO</code> parameter. |
| DIRECT | Selects the direct AC solution method. This method is robust at all frequencies, but slow. |

| | |
|------------------|---|
| FREQUENCY | Specifies the AC analysis frequency. Analysis may be repeated at a number of different frequencies (without solving for the DC condition again) by specifying <code>FSTEP</code> . <code>FREQUENCY</code> can also be used to specify a sinusoidal or square pulse frequency for transient simulations. |
| FSTEP | Specifies a frequency increment which is added to the previous frequency. If <code>MULT.FREQ</code> is specified, the frequency will be multiplied by <code>FSTEP</code> . |
| MAX.INNER | Specifies the maximum number of SOR iterations. |
| MULT.FREQ | Specifies that the frequency will be multiplied by <code>FSTEP</code> , instead of added to <code>FSTEP</code> . |
| NFSTEPS | Specifies the number of times that the frequency is to be incremented by <code>FSTEP</code> . |
| S.OMEGA | Specifies the SOR parameter. This parameter is not the AC frequency. |
| SOR | Selects the SOR AC solution method. Although SOR is fast, it should only be used when you are performing simulations at low frequencies. Low frequency can be defined here as at least an order of magnitude below the cutoff frequency. |
| TERMINAL | Specifies the electrode number to which the AC bias will be applied. Although more than one contact number may be specified (via concatenation), each will be solved separately. Each contact that is specified generates a column of the admittance matrix. If no <code>TERMINAL</code> is specified, all electrodes have AC bias applied in turn. See also <code>ANAME</code> . |
| TOLERANCE | Specifies SOR convergence criterion. |
| VSS | Specifies the magnitude of the applied small-signal bias. The approach used for small-signal analysis constructs a linear problem based on derivatives calculated during Newton iterations, so adjusting <code>VSS</code> will generally not affect the results. |

NOISE Parameters

| | |
|--------------------|--|
| BRANIN | Specifies that Branin's method should be used in the calculation of the impedance field. The direct method (which is the alternative to Branin's method) is very slow. Therefore, we recommend that <code>BRANIN</code> is never set to <code>False</code> . |
| NOINTERFACE | Specifies that any element which is adjacent to an interface should be ignored in the noise calculation. |
| NOCONTACT | Specifies that any element which is adjacent to a contact should be ignored in the noise calculation. |
| NOISE.SS | Specifies that a small-signal noise simulation should be performed. |

Direct Tunneling Parameters

An alternative set of direct quantum tunneling models for calculating gate current can be set using `DT.CUR` on the `SOLVE` statement. If you set this parameter, then select the particular model using `DT.METH`. The allowed values of `DT.METH` are 1, 2 and 3. The default value of `DT.METH` is 1.

| | |
|------------------|--|
| DT.METH=1 | Selects a Fowler-Nordheim type model, with a correction for the trapezoidal, rather than the triangular shape of the potential barrier. |
| DT.METH=2 | Selects a WKB model with the assumption of a linearly varying potential. It involves a calculation of the classical turning points and integration between those limits. |
| DT.METH=3 | Selects an exact formula for a trapezoidal barrier that involves Airy function solutions. |

You can also need to specify the type of tunneling taking place by using at least one of the following flags.

| | |
|----------------|---|
| DT.CBET | Specifies electron tunneling from conduction band to conduction band. |
| DT.VBHT | Specifies holes tunneling from valence band to valence band. |
| DT.VBET | Specifies Band-to-Band tunneling. |

Note: Specifying `DT.CUR` on the `SOLVE` statement invokes the post-processing version of Direct tunneling calculation of Gate current. Specifying the same parameters on the `MODELS` statement enables a self-consistent version.

Ionization Integral Parameters

Ionization parameters are used to calculate ionization integrals. No calculation will take place unless the `IONIZINT` parameter is specified.

| | |
|-----------------|--|
| DELTAV | Since the electric field can be near zero at electrodes, the electric field line calculations begin at a distance from the electrode. A potential contour is drawn around the electrode at a distance where the potential is <code>DELTAV</code> less than the applied bias on the contact. Defaults to 0.1 V, but will typically need to be increased especially for power devices and heavily doped contact regions. |
| E.CRIT | Specifies the minimum electric field used to calculate integration integrals. Field lines will terminate when the field drops below <code>E.CRIT</code> . |
| INAME | Specifies the electrode name from which the electric field lines are calculated. The default is to use the same as electrode as specified in <code>NAME</code> . |
| ION.CRIT | Specifies the critical value of the ionization integral used by <code>IONSTOP</code> to terminate the simulation. When the critical value is reached, any bias ramp will be terminated and the next line of the input file will be executed. |
| ION.ELEC | Specifies the electrode from which the electric field lines are calculated. This parameter defaults to the electrode which is being ramped (if any). |
| IONIZINT | Enables the calculation of ionization integrals along electric field lines. |

| | |
|-----------------|---|
| IONLINES | Specifies the number of electric field lines to be calculated. Ionization integrals are calculated along each line. |
| IONSTOP | Stops the bias ramp if integral is greater than 1.0 |
| LRATIO | Specifies the ratio between the starting points of the electric field lines. An LRATIO value of between 0.5 and 1.5 is recommended. LRATIO=1 means that the spacing between the starting points of the electric field lines is equal. LRATIO < 1 means more lines start towards the left hand side of the structure. LRATIO > 1 means more lines start towards the right hand side. |

Photogeneration Parameters

All these parameters require LUMINOUS to be licensed for correct operation.

| | |
|---------------------|---|
| AFINAL | Specifies the final angle for angular dependence analysis. |
| ANGLE | This is an alias for OFFSET.ANGLE. |
| ASTEP | Specifies the step size for angular analysis. |
| B<n> | Specifies the optical spot power associated with optical beam number, n. The beam number must be an integer from 1 to 10. |
| BEAM | Specifies the beam number of the optical beam when AC angular or spectral photogeneration analysis is performed. Unlike the ELECTRODE parameter, this parameter can only be used to specify a single beam. |
| INDEX.CHECK | Specifies that the real and imaginary refractive indices used in the ray tracing of each beam will be printed to the run-time output. This parameter can be used as confirmation of the input of user-defined refractive indices or to check the default parameters. The indices are only printed when you perform the ray trace at the first reference to a given beam on the SOLVE statement. |
| L.WAVE | Specifies the luminous wavelength to use to calculate the luminous power estimate for radiative recombination. If a positive value of L.WAVE is specified the luminous power will be saved in any log file specified for that solution. |
| LAMBDA1 | Specifies the wavelength of the optical source (beam) number 1 for this solution. This parameter can be used to perform analysis of spectral response as a function of wavelength. |
| LIT.STEP | Selects the light intensity increment of all optical beams which have been specified. This parameter is used when light intensity varies by stepping (similar to the VSTEP parameter). If LIT.STEP is specified, the NSTEP parameter should be used to select the number of steps. |
| OFFSET.ANGLE | Specifies the offset angle for LUMINOUS angular response modeling (see Section 10.12.14: "Obtaining Angular Response"). The angle of propagation is the sum of the angle specified on the BEAM statement and the value of this parameter. |
| RAMP.LIT | Specifies that the light intensity is to be ramped when transient simulations are performed. If RAMP.LIT is specified, transient mode parameters such as RAMPTIME, TSTEP, and TSTOP must also be specified. The RAMP.LIT parameter affects all specified optical beams (i.e., all beams are ramped). |

| | |
|------------------|---|
| SCAN.SPOT | Specifies a beam number for spot scanning. Spot scanning requires you to specify the RAYS parameter of the BEAM statement. With this specification, the incident light is split into the user-specified number of rays. During the spot scan, solutions are obtained with the beam energy applied to each of the rays in sequence. |
| SS.LIGHT | Specifies the intensity in the small signal part of the optical beam when small signal AC photogeneration analysis is performed. |
| SS.PHOT | Specifies that small signal AC analysis will be performed on the optical beam selected by the BEAM parameter. When SS.PHOT is specified, other AC parameters (e.g., FREQUENCY, FSTEP, MAX.INNER, MULT.FREQ, NFSTEPS, S.OMEGA, and TOLERANCE) should also be specified. You don't need to specify the AC.ANALYSIS parameter when performing small signal AC analysis on optical beams. |
| WFINAL | Specifies the final wavelength in a spectral analysis ramp. |
| WSTEP | Specifies the wavelength step size in a spectral analysis ramp. |

SONOS Parameters

| | |
|-----------------|--|
| NIT.N | Specifies the trapped electron concentration in a Silicon-Nitride region for the steady-state SOLVE. This can be used in conjunction with the SONOS models or independently from them. |
| NIT.P | Specifies the trapped hole concentration in a Silicon-Nitride region for the steady-state SOLVE. This can be used in conjunction with the SONOS models or independently from them. |
| NIT.XMAX | Maximum x-coordinate for applying density specified by NIT.N or NIT.P. |
| NIT.XMIN | Minimum x-coordinate for applying density specified by NIT.N or NIT.P. |
| NIT.YMAX | Maximum y-coordinate for applying density specified by NIT.N or NIT.P. |
| NIT.YMIN | Minimum y-coordinate for applying density specified by NIT.N or NIT.P. |
| SONOS | Only used in the case of SOLVE INIT with a SONOS structure. Helps prevent SOLVE INIT introducing large carrier concentrations in a charged Silicon Nitride region. |

Thermal3D Parameters

| | |
|-----------------------|--|
| POWER<n> | Specifies the power in watts on the n-th heat source. |
| POWERFINAL | Specifies the final power for a linearly ramped heat source. |
| T<n> | Specifies the temperature in K on the n-th heat sink. |
| TEMPFINAL | Specifies the final temperature for a linearly ramped heat sink. |

For more information about these parameters, see also Chapter 17: “Thermal 3D: Thermal Packaging Simulator”, Section 17.4: “Obtaining Solutions In THERMAL3D”.

DC Conditions Example

The following statement solves for a defined bias point and saves the solution to output file, *OutA*. The voltages on electrodes other than the gate will keep the value from the previous SOLVE statement.

```
SOLVE VGATE=0.1 OUTFILE=OutA
```

Bias Stepping Example

In the next example, the bias stepping is illustrated. The two SOLVE statements produce the following bias conditions.

| Bias Point | Vgate | Vdrain | Vsub |
|------------|-------|--------|------|
| 1 | 0.0 | 0.5 | -0.5 |
| 2 | 1.0 | 0.5 | -0.5 |
| 3 | 2.0 | 0.5 | -0.5 |
| 4 | 3.0 | 0.5 | -0.5 |
| 5 | 4.0 | 0.5 | -0.5 |
| 6 | 5.0 | 0.5 | -0.5 |

The solutions for these bias points will be saved to the files: OUT1, OUTA, OUTB, OUTC, OUTD, and OUTE. The initial approximation for each bias point is obtained directly from the preceding solution.

For bias points 4, 5, and 6, the program will use a PROJ to obtain an initial approximation. Since, starting with bias point 4, both of its preceding solutions (bias points 2 and 3) only had the same electrode bias (number 1) altered.

```
SOLVE Vdrain=.5 Vsub=-.5 OUTF=OUT1
```

```
SOLVE Vgate=1 VSTEP=1 VFINAL=5 NAME=gate OUTF=OUTA
```

Transient Simulation Example

The following sequence is an example of a time dependent solution. The METHOD statement specifies second-order discretization, automatic time-step selection, and an automated Newton-Richardson procedure.

The first SOLVE statement then computes the solution for a device with 1V on the base electrode and 2V on the collector in steady-state. The second SOLVE statement specifies that the base electrode is to be ramped to 2V over a period of 10 ns and is left on until 25 ns. Each solution is written to a file. The name of the file is incremented in a manner similar to that described for a DC simulation (UP1, UP2, and so on). Note that an initial time step had to be specified in this statement.

The third SOLVE statement ramps the base down from 2V to -0.5V in 20 ns (end of ramp is at 45 ns). The device is then solved at this bias for another 55 ns (out to 100 ns). Each solution is again saved in a separate file (DOWN1, DOWN2, and so on).

No initial timestep was required since one had been estimated from the last transient solution from the previous SOLVE statement.

Finally, the fourth SOLVE statement performs the steady-state solution at $V_{be} = -0.5V$ and $V_{ce} = 2V$.

```
METHOD 2ND TAUTO AUTONR
```

```
SOLVE Vbase=1 Vcollector=2
```

```
SOLVE Vbase=2 DT=1E-12 TSTOP=25E-9 RAMPTIME=10E-9 OUTF=UP1
SOLVE Vbase= -0.5 TSTOP=100E-9 RAMPTIME=20E-9 OUTF=DOWN1
SOLVE Vbase= -0.5 Vcollector=2
```

AC Analysis Example

The following example illustrates an application of the SOLVE statement for AC analysis. It is assumed that the device has three electrodes. This analysis is being performed after DC conditions are solved at $V_1 = 0V, 0.5V, 1.0V, 1.5V,$ and $2.0V$. A series of 10mV AC signals with frequencies of 1 MHz, 10 MHz, 100 MHz, 1 GHz, 10 GHz, and 100 GHz are applied to each electrode in the device.

Ninety AC solutions will be performed ($5 \times 6 \times 3 = 90$).

```
SOLVE V1=0 V2=0 V3=0 VSTEP=0.5 NSTEPS=4 ELECT=1 \
AC FREQ=1E6 FSTEP=10 MULT.F NFSTEP=5 VSS=0.01
```

Photogeneration Examples

The following statement simulates two DC optical beams incident on the device with optical spot powers of 15 and 25 W/cm².

```
SOLVE B1=15 B3=25
```

The next example shows how DC spot power of the two optical beams can be stepped simultaneously. Beam #1 will increase to 35 W/cm² and beam #3 will increase to 45 W/cm².

```
SOLVE LIT.STEP=5.0 NSTEP=4
```

In the next example, the beams are ramped in the time domain. Beam #1 is ramped down to 0 W/cm² and beam #3 is ramped up to 100 W/cm². The duration of the ramp is 1 ns. After the ramp, simulation will continue for 4 ns.

```
SOLVE B1=0 B3=100 RAMP.LIT TSTEP=2E-11 RAMPTIME=1E-9 TSTOP=5E-9
```

Next, the small signal response of a single beam is analyzed. First, ATLAS will solve the DC characteristics at the specified optical spot powers. Then, the AC response of beam #1 will be calculated at a frequency of 10 MHz.

```
SOLVE B1=10 B3=20 BEAM=1 FREQUENCY=1e7 SS.PHOT SS.LIGHT=0.01
```

Frequency stepping is used to look at the small signal AC frequency response of one of the beams. AC response is calculated at frequencies from 1kHz to 100MHz at each decade. The MULT.F parameter is used to geometrically increase the frequency.

```
SOLVE B1=10 B3=5 BEAM=1 SS.PHOT SS.LIGHT=0.01 \
MULT.F FREQUENCY=1E3 FSTEP=10 NFSTEP=6
```

The following illustrates the specification of analysis of angular response of beam number 2 at angles from 0 to 80° in 1° increments.

```
SOLVE BEAM=2 ANGLE=0 AFINAL=80 ASTEP=1
```

Similarly, the following illustrates the specification of analysis of spectral response over the wavelength range from 1 to 3 microns in steps of 0.05 microns.

```
SOLVE BEAM=1 LAMBDA=1 WFINAL=3 WSTEP=0.05
```

Ionization Integral Example

Ionization integrals are used to estimate the breakdown voltage from analysis of the electric field. They can be used in zero carrier mode providing much faster simulation than conventional breakdown analysis. The ionization syntax uses the parameter `IONIZ` to enable the ionization integral calculation. An equipotential contour is calculated at a potential `DELTAV` from the contact `NAME` (or `INAME`). Electric field lines are started at distances along this potential contour. `IONLINES` sets the number of lines and `LRATIO` is the ratio of the distance between the starting points of the lines. The following syntax is for a PMOS transistor. See the on-line examples for other cases using ionization integrals.

```
IMPACT SELB
METHOD CARR=0
SOLVE VDRAIN=-1 VSTEP=-1 VFINAL=-20.0 NAME=DRAIN \
IONIZ IONLINES=50 LRATIO=0.9 DELTAV=1.2
```

Note: There are over 300 on-line examples supplied with `ATLAS` to provide examples of sequences of `SOLVE` statements applied to practical problems for a variety of device technologies.

21.54: SPX.MESH, SPY.MESH, SPZ.MESH

S<n>.MESH specifies the location of grid lines along the <n>-axis in a rectangular mesh used in self-consistent Schrodinger-Poisson Model simulation (see Chapter 13: “Quantum: Quantum Effect Simulator”, Section 13.2: “Self-Consistent Coupled Schrodinger Poisson Model”). The syntax is equivalent for all directions. SPX.MESH and SPY.MESH should always be set or nor set together, while SPZ.MESH is always optional.

Syntax

```
SPX.MESH NODE=<n> LOCATION=<n>
```

```
SPX.MESH SPACING=<n> LOCATION=<n>
```

```
SPY.MESH NODE=<n> LOCATION=<n>
```

```
SPY.MESH SPACING=<n> LOCATION=<n>
```

| Parameter | Type | Default | Units |
|-----------|---------|---------|-------|
| LOCATION | Real | | μm |
| NODE | Integer | | |
| SPACING | Real | | μm |

Description

| | |
|-----------------|---|
| NODE | Specifies the mesh line index. These mesh lines are assigned consecutively. |
| LOCATION | Specifies the location of the grid line. |
| SPACING | Specifies the mesh spacing at the mesh locations specified by the LOCATION parameter. If the SPACING parameter is specified, then the NODE parameter should not be specified. |

Note: The mesh defined in these statements for the Self-Consistent Schrodinger-Poisson Model is entirely separate from the electrical device simulation mesh defined on the MESH statement.

Setting Locally Fine Grids Example

This example shows how to space grid lines closely around a topological feature such as a junction at y=0.85 microns.

```
SPY.MESH LOC=0.0 SPAC=0.2
```

```
SPY.MESH LOC=0.85 SPAC=0.01
```

```
SPY.MESH LOC=2 SPAC=0.35
```

21.55: SYMBOLIC

Note: In versions 3.0 and greater, the `SYMBOLIC` statement is no longer needed. All functions have been moved to the `METHOD` statement.

21.56: SPREAD

SPREAD distorts rectangular grids defined by ATLAS in the vertical direction to follow surface and junction contours.

Note: The use of this parameter is not recommended by SILVACO.

Syntax

```
SPREAD LEFT|RIGHT WIDTH=<r> UPPER=<i> LOWER=<i>
Y.LOWER|THICKNESS [<options>]
```

| Parameter | Type | Default | Units |
|-----------|---------|---------------------------------|-------|
| ENCROACH | Real | 1.0 | |
| GRADING | Real | 1.0 | |
| GR1 | Real | 1.0 | |
| GR2 | Real | 1.0 | |
| LEFT | Logical | False | |
| LOWER | Integer | | |
| MIDDLE | Integer | Halfway between UPPER and LOWER | |
| RIGHT | Logical | False | |
| THICKNESS | Real | | μm |
| UPPER | Integer | | |
| VOL.RATIO | Real | 0.44 | |
| WIDTH | Real | | μm |
| Y.LOWER | Real | | μm |
| Y.MIDDLE | Real | 0.50 | μm |

Description

SPREAD can reduce the grid complexity of specific simulations. Since the SPREAD statement is somewhat complicated, we suggest that you follow the supplied examples carefully until you're confident to understand the workings of this statement.

Mandatory Parameters

| | |
|------------------|--|
| LEFT | Distorts the left side of the grid. If LEFT is specified, RIGHT must not be specified. |
| LOWER | Specifies the lower y-grid line above which distortion will take place. |
| RIGHT | Distorts the right side of the grid. If RIGHT is specified, LEFT must not be specified. |
| THICKNESS | Specifies the thickness of the distorted region. Unless VOL.RATIO is set to 0 or 1, THICKNESS will usually move the positions of both the UPPER and LOWER grid lines. The Y.LOWER and THICKNESS parameters define the distorted grid region. Only one of these parameters should be specified. |
| UPPER | Specifies the upper y-grid line under which distortion will take place. |
| WIDTH | Specifies the width from the left or right edge (depending on whether LEFT or RIGHT is selected) of the distorted area. The actual X coordinate specified by WIDTH ($\min[x] + \text{WIDTH}$ for LEFT , $\max[x] + \text{WIDTH}$ for RIGHT) will lie in the middle of the transition region between distorted and undistorted grid regions. |
| Y.LOWER | Specifies the physical location in the distorted region to which the line specified by LOWER will be moved. The line specified by UPPER is not moved. The Y.LOWER and THICKNESS parameters define the distorted grid region. Only one of these parameters should be specified. |

Optional Parameters

| | |
|-----------------|---|
| ENCROACH | Defines the abruptness of the transition between a distorted and non-distorted grid. The transition region becomes more abrupt with smaller ENCROACH factors (the minimum is 0.1). |
|-----------------|---|

Note: Depending on the characteristics of the undistorted grid, long, thin, or obtuse triangles may result if too low an **ENCROACH** value is used.

| | |
|---------------------------|---|
| GRADING | Specifies a grid ratio which produces a non-uniform grid in the distorted region. This parameter is identical to the RATIO parameter in the X.MESH and Y.MESH statements. |
| GR1 and GR2 | These may be used instead of the GRADING parameter. GR1 and GR2 may be specified in conjunction with MIDDLE (y grid line) and Y.MIDDLE (location) so that GR1 specifies grading in the spread region from UPPER to MIDDLE , and GR2 specifies grading from MIDDLE to LOWER . |
| MIDDLE | Specifies the y-grid line that serves as a boundary between the grading specified by GR1 and the grading specified by GR2 . |
| VOL.RATIO | Specifies the ratio of the downward displacement of the lower grid line to the net increase in thickness. The default (0.44) should be used for oxide-silicon interfaces. VOL.RATIO is ignored if Y.LOWER is specified. |
| Y.MIDDLE | Specifies the physical location in the distorted grid to which the line specified by MIDDLE will be moved. |

Examples

This example spreads a uniform 400 Å of oxide to 1000 Å on the left side of the device. This increases oxide thickness by 600 Å. Because VOL.RATIO is not specified, the default (0.44) is used. Therefore, $0.44 \times 600 = 264$ Å of the net increase will lie below the original 400 Å and $0.56 \times 600 = 336$ Å of the net increase will lie above the original 400 Å. The width of the spread region is 0.5 μm, and the oxide taper is quite gradual because of the high encroachment factor. The grid is left uniform in the spread region.

```
# *** Mesh definition ***
MESH NX=30 NY=20 RECT
X.M N=1 L=0
X.M N=30 L=5
Y.M N=1 L=-.04
Y.M N=5 L=0
Y.M N=20 L=1 R=1.4
# *** Thin oxide ***
REGION IY.H=5 OXIDE NUM=1
# *** Silicon substrate ***
REGION IY.L=5 SILICON NUM=2
# *** Spread ***
SPREAD LEFT W=0.7 UP=1 LO=4 THICK=0.1 MID=2 Y.MID=0.05
```

In the second example, the right side of the grid is distorted in order to follow a junction contour. The initial grid is assumed to be above. Y.LOWER is used so that there is no increase in the size of the device, just grid redistribution. When Y.LOWER is set to the junction, choose the ENCROACH parameter so that the lower grid line (LOWER=10) follows the junction as closely as possible. The grid is graded so that grid lines are spaced closer together as they approach the junction. Because the point specified by WIDTH lies in the middle of the transition region, it should be chosen to be slightly larger than the width of the doping box.

```
# *** Doping ***
DOPING UNIFORM N.TYPE CONC=1E15
DOPING GAUSS P.TYPE X.LEFT=1.5 X.RIGHT=2 \
PEAK= CONC=1.e19 RATIO=.75 JUNC=0.3
# *** Spread ***
SPREAD RIGHT W=0.7 UP=1 LO=4 THICK=0.3 MID=2 Y.MID=0.10
```

21.57: SYSTEM

SYSTEM allows execution of any UNIX command within an input file

Note: The SYSTEM statement is executed by DECKBUILD and is fully documented in the DECKBUILD USER'S MANUAL. To enable SYSTEM command, select **Category: Options** in the DeckBuild Main Control menu.

Examples

The following command will remove all files test*.str before a SOLVE statement where the OUTF parameter is used.

```
system \rm -rf test*.str  
SOLVE .... OUTF=test0
```

The system command and the UNIX commands are case sensitive.

UNIX commands may be concatenated on a single line using the semicolon (;) operator. For example to run a third party program that reads and writes Silvaco format files with fixed names input.str and output.str.

```
SAVE OUTF=mysave.str  
system mv mysave.str input.str; source myprog.exe; mv output.str  
myrestart.str  
EXTRACT INIT INF=myrestart.str
```

The UNIX re-direct symbol > is not supported by the system command. The UNIX echo and sed syntax can be used instead to output values or variables to a given filename. For example to save the extracted value of variable \$myvariable to the file myfile.

```
system echo "$myvariable" | sed -n " w myfile"
```

21.58: THERMCONTACT

THERMCONTACT specifies the position and properties of thermal contacts. This statement must be used when lattice heating solutions are specified using GIGA or GIGA3D.

Syntax

```
THERMCONTACT NUMBER=<n> <position> [EXT.TEMPER=<n>] [ALPHA=<n>]
```

| Parameter | Type | Default | Units |
|-------------|-----------|-------------------------|---------------------------|
| ALPHA | Real | | W / (cm ² · K) |
| BOUNDARY | Logical | True | |
| DEVICE | Character | | |
| ELEC.NUMBER | Integer | | |
| EXT.TEMPER | Real | 300 | K |
| F.CONTEMP | Character | | |
| NAME | Character | | |
| NUMBER | Integer | 1 | |
| STRUCTURE | Character | | |
| X.MAX | Real | Right side of structure | μm |
| X.MIN | Real | Left side of structure | μm |
| Y.MAX | Real | Bottom of structure | μm |
| Y.MIN | Real | Top of structure | μm |
| Z.MAX | Real | Back | μm |
| Z.MIN | Real | Front | μm |

Description

At least one THERMCONTACT statement must be specified when simulating lattice heating effects (MODELS LAT.TEMP). The THERMCONTACT statement must appear in the input deck before any METHOD statement.

| | |
|-----------------|--|
| position | This is a set of the position parameters described below. Use either the X.MIN, X.MAX, Y.MIN, and Y.MAX parameters to specify the exact position of the contact or the ELEC.NUMBER parameter to specify an electrode number that coincides with the thermal contact. |
| NUMBER | Specifies a thermal contact number from 1 to 20. Contact numbers should be specified in increasing order. This parameters must be specified on all THERMCONTACT statements. |

| | |
|-------------------|--|
| ALPHA | Specifies the reverse value of thermal resistance ($a=1/R_{TH}$). |
| EXT.TEMPER | Specifies the external temperature. The synonym for this parameter is TEMPERATURE. |
| F.CONTEMP | Specifies the name of a file containing a C-Interpreter function describing the contact temperature as a function of time. |

Position Parameters

| | |
|--------------------|--|
| BOUNDARY | Specifies which parts of the thermal contact the thermal boundary conditions are applied at. See Chapter 7: “Giga: Self-Heating Simulator”, Section 7.2.7: “Thermal Boundary Conditions” for a full description. |
| NAME | Specifies an electrode name that the thermal contact is coincident with. See Section Section 21.12: “ELECTRODE” for more information. |
| DEVICE | Specifies which device in MIXEDMODE simulation the THERMCONTACT statement applies to. The synonym for this parameter is STRUCTURE. |
| ELEC.NUMBER | Specifies an electrode number that the thermal contact is coincident with. |
| STRUCTURE | This is a synonym for DEVICE. |
| X.MAX | Specifies the right edge of the contact. |
| X.MIN | Specifies the left edge of the contact. |
| Y.MAX | Specifies the bottom edge of the contact. |
| Y.MIN | Specifies the top edge of the contact. |
| Z.MAX | Specifies the location of the rear edge of the thermal contact. |
| Z.MIN | Specifies the location of the front edge of the thermal contact. |

Coordinate Definition Example

A thermal contact is located where Y coordinate values range from 10 μm to the bottom side of the structure and X coordinate values range from the left edge of the structure to the right edge of the structure (be default). The external temperature is set to 300K and a thermal resistance of 1 is added. Thus, the temperature at $y = 10 \mu\text{m}$ will be greater than 300K once lattice heating effects occur.

```
THERMCONTACT NUM=1 Y.MIN=10 EXT.TEMP=300 ALPHA=1
```

Setting Thermal and Electrical Contacts Coincident Example

The next statement line creates a thermal contact at the location of electrode #4. An external temperature of 400K is specified.

```
THERMCONTACT NUM=2 ELEC.NUM=4 EXT.TEMP=400
```

Note: Location and Parameters of thermal contacts are not stored in the ATLAS solution files. Therefore, THERMCONTACT statements must be defined in each ATLAS run involving lattice heating.

21.59: TITLE

`TITLE` specifies the title (up to 29 characters) that will appear in the standard output. If used, the `TITLE` command should be the first statement in the ATLAS input file.

Syntax

```
TITLE <string>
```

Example

This example causes the text, `*** CMOS p-channel device ***`, to be printed at the top of all ATLAS printouts and screen displays.

```
TITLE *** CMOS p-channel device ***
```

Note: `TITLE` cannot be used with the automatic ATHENA to ATLAS interface feature of `DECKBUILD`

21.60: TONYPLOT

TONYPLOT starts the graphical post-processor TONYPLOT

Note: The TONYPLOT statement is executed by DECKBUILD and is fully described in the DECKBUILD USER'S MANUAL.

Examples

All graphics in ATLAS is performed by saving a file and loading the file into TONYPLOT. The TONYPLOT command causes ATLAS to automatically save a structure file and plot it in TONYPLOT. The TonyPlot window will appear displaying the material boundaries. Use the **Plot:Display** menu to see more graphics options.

This command will display the file, *myfile.str*.

```
tonyplot -st myfile.str
```

This command will overlay the results of *myfile1.str* and *myfile2.str*.

```
tonyplot -overlay myfile1.str myfile2.str
```

Note: For documentation of the extensive features of TONYPLOT for graphical display and analysis, see TONYPLOT USER'S MANUAL.

21.61: TRAP

TRAP activates bulk traps at discrete energy levels within the bandgap of the semiconductor and sets their parameter values.

Syntax

```
TRAP DONOR|ACCEPTOR E.LEVEL=<r> DENSITY=<r> DEGEN=<v>
<capture parameters> REGION|NUMBER
```

| Parameter | Type | Default | Units |
|-----------|-----------|-----------------|------------------|
| ACCEPTOR | Logical | False | |
| DEGEN.FAC | Real | undefined | |
| DENSITY | Real | | cm ⁻³ |
| DEVICE | Character | | |
| DONOR | Logical | False | |
| E.LEVEL | Real | | eV |
| F.DENSITY | Character | | |
| FAST | Logical | False | |
| MIDGAP | Logical | False | |
| MATERIAL | Character | | |
| NUMBER | Integer | 0 | |
| REGION | Integer | 0 | |
| SIGN | Real | | cm ² |
| SIGP | Real | | cm ² |
| STRUCTURE | Character | | |
| TAUN | Real | | s |
| TAUP | Real | | s |
| X.MAX | Real | Maximum X coord | μm |
| X.MIN | Real | Minimum X coord | μm |
| Y.MAX | Real | Maximum Y coord | μm |
| Y.MIN | Real | Minimum Y coord | μm |
| Z.MAX | Real | Maximum X coord | μm |
| Z.MIN | Real | Minimum Z coord | μm |

Description

| | |
|------------------|--|
| ACCEPTOR | Specifies an acceptor-type trap level. |
| DEGEN.FAC | Specifies the degeneracy factor of the trap level used to calculate the density. |
| DENSITY | Sets the maximum density of states of the trap level. |
| DEVICE | Specifies which device the statement applies to in MIXEDMODE simulation. The synonym for this parameter is STRUCTURE . |
| DONOR | Specifies a donor-type trap level. |
| E.LEVEL | Sets the energy of the discrete trap level. For acceptors, E.LEVEL is relative to the conduction band edge. For donors, it depends on the valence band edge. |
| F.DENSITY | Specifies the name of a file containing a C-Interpreter function describing the density of donor/acceptor traps as a function of position. |
| FAST | Specifies that the trap densities are static even during transient simulation (i.e., they reach equilibrium instantaneously). |
| MATERIAL | Specifies which material from the table in Appendix B: "Material Systems" will apply to the TRAP statement. If a material is specified, then all regions defined as being composed of that material will be affected. |
| MIDGAP | Specifies that the energy of the discrete trap be set to the middle of the bandgap. |
| NUMBER | This is the synonym for REGION . |
| REGION | Specifies which region the traps apply to. If unspecified, the traps apply to all regions. |
| STRUCTURE | This is a synonym for DEVICE . |
| X.MAX | Specifies the maximum X coordinate of a box where traps are to be applied. |
| X.MIN | Specifies the minimum X coordinate of a box where traps are to be applied. |
| Y.MAX | Specifies the maximum Y coordinate of a box where traps are to be applied. |
| Y.MIN | Specifies the minimum Y coordinate of a box where traps are to be applied. |
| Z.MAX | Specifies the maximum Z coordinate of a box where traps are to be applied. |
| Z.MIN | Specifies the minimum Z coordinate of a box where traps are to be applied. |

Capture Parameters

Either the cross section or lifetime parameters should be used to define the capture parameters.

| | |
|-------------|--|
| SIGN | Specifies the capture cross section of the trap for electrons. |
| SIGP | Specifies the capture cross section of the trap for holes. |
| TAUN | Specifies the lifetime of electrons in the trap level. |
| TAUP | Specifies the lifetime of holes in the trap level. |

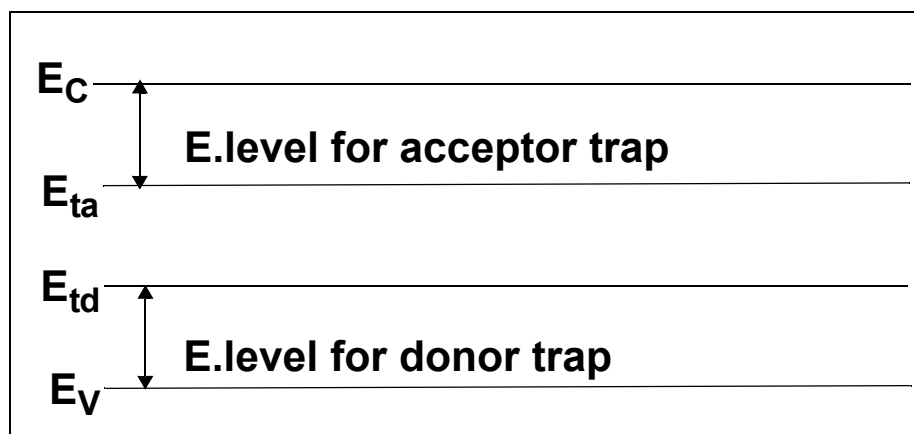


Figure 21-8: Acceptor and Donor Trap Energy Levels

Multiple Trap Level Definition Example

The following example sets three discrete trap levels within the silicon bandgap. These trap levels will capture carriers, slowing the switching speed of any device. In this example the capture cross sections are used to define the properties of each trap.

```
trap e.level=0.49 acceptor density=2.e15 degen=12 \
sign=2.84e-15 sigp=2.84e-14
trap e.level=0.41 acceptor density=1.e15 degen=12 \
sign=7.24e-16 sigp=7.24e-15
trap e.level=0.32 donor density=1.e15 degen=1 \
sign=1.00e-16 sigp=1.00e-17
```

Note: For distributed trap levels, see Section 21.8: "DEFECTS". For interface traps, see Section 21.22: "INTTRAP". Also, spatial TRAP distributions in X, Y, or Z directions must be defined in the DOPING statement.

21.62: UTMOST

UTMOST converts data from a ATLAS logfile format into an UTMOST logfile format.

Note: UTMOST 12.3.4 or later can read ATLAS format logfiles directly in batch mode. This statement is obsolete and its use is not recommended.

Syntax

```
UTMOST BIP|DIODE|MOS <input> OUTFILE=<fn> WIDTH=<n>
[<elec>] <cntrl>
[TRANSLATE INFILE1=<filename>][<analysis>] [<parasites>]
```

| Parameter | Type | Default | Units |
|-----------|-----------|------------|-------|
| AC | Logical | False | |
| ANODE | Integer | 1 | |
| APPEND | Logical | False | |
| BASE | Integer | | |
| BIP | Logical | False | |
| BULK | Integer | | |
| CATHODE | Integer | | |
| COLLECTOR | Integer | | |
| DEVICE | Integer | 1 | |
| DIODE | Logical | False | |
| DRAIN | Integer | | |
| EMITTER | Integer | | |
| GATE | Integer | | |
| INFILE | Character | | |
| INTERNAL | Logical | False | |
| LENGTH | Real | 1.0 | μm |
| MESFET | Logical | False | |
| MINSTEP | Real | 0.01 | V |
| MOS | Logical | False | |
| OUTFILE | Character | | |
| POLARITY | Integer | 1 (n-type) | |
| ROUTINE | Integer | 1 | |

| Parameter | Type | Default | Units |
|-------------|---------|---------|---------------|
| SOURCE | Integer | | |
| TEMPERATURE | Real | 300 | K |
| WELL | Integer | | |
| WIDTH | Real | 1.0 | μm |

Description

Specify a technology parameter (BIP, DIODE, or MOS), an input file (INFILE1=), and an output file (OUTFILE=). You can also specify one or more of the optional electrode parameters.

| | |
|----------------|--|
| INFILE | This is used to convert up to nine ATLAS logfiles into a single UTMOST logfile. The ATLAS logfiles must be specified in the form: INFILE1=<fn> INFILE2=<fn> INFILE3=<fn> . . . where fn is the name of the logfile that you wish to convert. |
| OUTFILE | Specifies the name of a file where I-V data will be stored in an UTMOST file format. |
| APPEND | Specifies that I-V data should be appended to the output file specified by OUTFILE2. |
| WIDTH | This is used to specify the width of the device. Electrode current is multiplied by the value of WIDTH before being saved in the logfile. |

Technology Parameters

| | |
|---------------|--|
| BIP | Creates an UTMOST bipolar transistor log file. |
| DIODE | Creates an UTMOST diode log file. |
| MOS | Creates an UTMOST MOSFET log file. |
| MESFET | Creates an UTMOST MESFET log file. |

Electrode Parameters

Different electrode parameters may be specified with different technologies.

| | |
|-----------------------|---|
| BIP | Technology |
| BASE | Specifies the base electrode number. |
| COLLECTOR | Specifies the collector electrode numb. |
| EMITTER | Specifies the emitter electrode numb. |
| POLARITY | Indicates the device type. POLARITY=1 specifies npn. POLARITY=-1 specifies pnp. |
| MOS and MESFET | Technologies |

Note: If you have used the `NAME` parameter of the `ELECTRODE` statement to assign standard electrode names (bulk, drain, gate, and source), you don't need to re-specify these names in the `UTMOST` statement.

| | |
|--------------------------|---|
| BULK or SUBSTRATE | Specifies the bulk electrode number. |
| DRAIN | Specifies the drain electrode number. |
| GATE | Specifies the gate electrode number. |
| POLARITY | Indicates the device type. <code>POLARITY=1</code> specifies nmos. <code>POLARITY=-1</code> specifies pmos. |
| SOURCE | Specifies the source electrode number. |

Control Parameters

The optional control parameters are used to specify what type of information will be converted to an UTMOST logfile.

| | |
|--------------------|---|
| AC | Specifies that input logfiles contain AC parameters and that the UTMOST routine numbers refer to the UTMOST capacitance routines. |
| DEVICE | Specifies the device (or row) number used to identify different devices in UTMOST. The synonym for this parameter is <code>ROW</code> . |
| INTERNAL | Specifies that internal contact voltage will be used instead of applied bias. |
| LENGTH | Specifies the length of the device. |
| MINSTEP | Specifies the minimum voltage step between data points. |
| TEMPERATURE | Specifies the simulation temperature. |
| ROUTINE | Specifies which UTMOST routine number data will be saved for. The following routines are supported. |

BIP Technology

| | |
|-------------------|---|
| ROUTINE=1 | Specifies I_C vs. V_{CE} curves. Each input file holds I-V data for a solution with a fixed base current and V_{CE} stepped. (UTMOST IC/VCE routine). |
| ROUTINE=9 | Specifies a B_F vs. V_{BE} plot. Each input file holds I-V data for a solution with constants V_{CE} and V_{BE} stepped. (UTMOST BF vs. IC routine) |
| ROUTINE=10 | Specifies a B_F vs. V_{BC} plot. Each input file holds I-V data for a solution with constants V_{CE} and V_{BC} stepped. (UTMOST BR routine) |

| | |
|-------------------|---|
| ROUTINE=14 | Specifies a I_C, I_B vs. V_{BE} (Gummel) plot. Each input file holds I-V data for a solution with constant V_{CE} and V_{BE} stepped. (UTMOST gummel routine) |
| ROUTINE=15 | Specifies a I_E, I_B vs. V_{BC} (Reverse Gummel) plot. Each input file holds I-V data for a solution with constants V_{EC} and V_{BC} stepped. (UTMOST rgummel routine) |
| ROUTINE=29 | Specifies I_E vs. V_{EC} plot. Each input file holds I-V data for a solution with a fixed base current and V_{EC} stepped. (UTMOST IE/VEC routine) |

MOS Technology

| | |
|-------------------|--|
| ROUTINE=1 | Specifies a I_D vs. V_{DS} plot. V_B is constant and V_G is stepped. (UTMOST ID/VD-VG routine) |
| ROUTINE=2 | Specifies a I_D vs. V_{GS} plot. V_D is constant and V_B is stepped. (UTMOST ID/VG-VB routine) |
| ROUTINE=3 | Specifies the L_{EFF} , R_{SD} routine. Two devices of different lengths are needed. The I_D/V_{GS} data should be used. |
| ROUTINE=5 | Specifies a I_D vs. V_{GS} plot. V_D is constant and $V_B=0$. (UTMOST VTH routine) |
| ROUTINE=9 | Specifies a I_D vs. V_{GS} plot. V_D is constant and V_B is stepped. (UTMOST NSUB routine). |
| ROUTINE=10 | Specifies the IS routine. The forward diode characteristics of the drain to bulk junction are required. |
| ROUTINE=11 | Specifies the LAMBDA routine. An I_D/V_D curve is required. |
| ROUTINE=12 | Specifies the ETA routine. A set of I_D/V_{GS} data for different V_{DS} is required. |
| ROUTINE=13 | Specifies the VMAX routine. A set of I_D/V_{GS} curves for small changes in V_{DS} are required. |
| ROUTINE=14 | Specifies the U0 routine. A set of I_D/V_{GS} data is required. |
| ROUTINE=26 | Specifies a I_D vs. V_{GS} plot. V_B is constant and V_D is stepped. (UTMOST ID/VG-VD routine). |

MOS Capacitances

The following routines may be specified if both MOS and AC parameters are selected.

| | |
|-------------------|---|
| ROUTINE=1 | Specifies the CGSO routine. C_{GS} vs. V_{GS} data is required. |
| ROUTINE=2 | Specifies the CGDO routine. C_{GD} vs. V_{GS} data is required. |
| ROUTINE=5 | Specifies the CJ routine. C_{BD} vs. V_{DS} data is required. |
| ROUTINE=6 | Specifies the CJSW routine. C_{BD} vs. V_{DS} data is required. |
| ROUTINE=12 | Specifies the CJ/CJSW routine. C_{GD} vs. V_{GS} data is required for two different size drain areas. |

Diode Technology

| | |
|------------------|--|
| ROUTINE=1 | Specifies an I vs. V plot. V is stepped. (UTMOST ID vs. VD routine). |
|------------------|--|

21.63: VCSEL

The VCSEL statement specifies certain VCSEL simulation parameters.

Syntax

VCSEL <parameters>

| Parameter | Type | Default | Units |
|------------------|---------|---------|-------|
| ABSORPTION | Logical | False | |
| CHECK | Logical | False | |
| EFINAL | Real | | eV |
| EINIT | Real | | eV |
| FCARRIER | Logical | | |
| INDEX.BOTTOM | Real | 1.0 | |
| INDEX.TOP | Real | 1.0 | |
| ITMAX | Integer | 30 | |
| MAXCH | Real | 2.5 | |
| LOSSES | Real | 0.0 | |
| NEFF | Real | 1.0 | |
| NMODE | Integer | 1 | |
| NSPEC | Integer | 100 | |
| OMEGA | Real | | |
| PERTURB | Logical | False | |
| PHOTON.ENERGY | Real | | eV |
| PROJ | Logical | False | |
| TAUSS | Real | 0.05 | s |
| TOLER | Real | 0.01 | |
| VCSEL.CHECK | Logical | False | |
| VCSEL.INCIDENTCE | Integer | 1 | |

Description

| | |
|----------------------|--|
| ABSORPTION | Enables the absorption loss model in VCSEL. |
| CHECK | Enables reflectivity test simulation of the VCSEL structure |
| EFINAL, EINIT | Specify the lower and upper photon energies in reflectivity test. The default values are EINIT=0.8 PHOTON.ENERGY and EFINAL=1.2 PHOTON.ENERGY. |

| | |
|-------------------------|---|
| INDEX.BOTTOM | Specifies the refractive index of the medium below the structure. The default value is 1.0. |
| INDEX.TOP | Specifies the refractive index of the medium above the structure. The default value is 1.0. |
| ITMAX | Sets maximum number of external VCSEL iterations during photon density calculation. The default value is 30. |
| MAXCH | Specifies the maximum allowed relative change in photon densities between iterations. Rapid changes of the photon densities can cause convergence problems. |
| LOSSES | Specifies additional losses in Chapter 9: “VCSEL Simulator”, Equation 9-16. |
| NEFF | Specifies the effective refractive index in Chapter 9: “VCSEL Simulator”, Equation 9-11. |
| NMODE | Specifies the number of transverse modes of interest. The default value is NMODE=1. |
| NSPEC | Specifies the number of sampling points between EINIT and EFINAL in reflectivity test. The default value is NSPEC=100. |
| OMEGA | Specifies the reference frequency (see Equation 9-2 in Chapter 9: “VCSEL Simulator”). The reference frequency can change after the reflectivity test to correspond to the resonant frequency of the structure. |
| PERTURB | Enables faster solution of the Helmholtz equation. When it is specified, the program solves the longitudinal wave equation only once. The perturbational approach is used to account for the refractive index changes. |
| PHOTON.ENERGY | Specifies the reference photon energy. The reference photon energy can change after reflectivity test to correspond to the resonant photon energy of the structure. This parameter is related to OMEGA parameter. |
| PROJ | Enables faster solution of the photon rate equations below threshold. You should disable this solution scheme when the bias reaches lasing threshold. To do this, specify ^PROJ in a VCSEL statement. |
| TAUSS | This is an iteration parameter used in the calculation of photon densities. Using a larger value of this parameter can speed up the calculation but may cause convergence problems. |
| TOLER | Sets the desired relative tolerance of the photon density calculation. The default value is 0.01. Setting this parameter to a lower value may slow down the calculation significantly. Using a larger value will result in a faster but less accurate calculations. |
| VCSEL.CHECK | This is the same as CHECK. |
| VCSEL.INCIDENTCE | Specifies the direction of light incident on the structure. VCSEL.INCIDENTCE=1 is the light incident from the top. VCSEL.INCIDENTCE=0 is the light incident from the bottom. VCSEL.INCIDENTCE=2 or >2 means both directions of light incidence are considered. By default, light is incident from the top of the structure. |

21.64: WAVEFORM

WAVEFORM defines transient waveforms, which can then be enabled by specifying WAVE1 . . WAVE10 on the SOLVE statement.

Syntax

WAVEFORM [<parameters>]

| Parameter | Type | Default | Units |
|-------------|-----------|---------|-------|
| AMPLITUDE | Real | 0 | |
| BEAM | Real | | |
| CONTINUE | Logical | True | |
| DECAY | Real | 0 | |
| ELEC.NAME | Character | | |
| ELEC.NUMBER | Real | 0 | |
| F.WAVE | Character | | |
| FREQUENCY | Real | 0 | Hz |
| NUMBER | Real | 0 | |
| OFFSET | Logical | False | |
| PERIODS | Real | | |
| PHASE | Real | 0 | Deg |
| PWL | Character | | |
| SINUSOID | Logical | False | |

Description

| | |
|--------------------|--|
| AMPLITUDE | Specifies the sinusoidal amplitude. |
| BEAM | Specifies the optical BEAM number to which the WAVEFORM parameters will apply. |
| CONTINUE | Specifies that the waveform will continue (i.e. retain the phase) across multiple SOLVE statements. This is the default. |
| DECAY | Specifies an optional decay value. |
| ELEC.NAME | Specifies the electrode name. |
| ELEC.NUMBER | Specifies the electrode number (either ELEC.NAME or ELEC.NUMBER must be specified). |

| | |
|------------------|---|
| F.WAVE | <p>Specifies the C-Interpreter file. The function prototype is:</p> <pre>int workf(double time, double dt, double *bias)</pre> <p>where time is the transient time, dt is the time step and bias is the bias calculated by the C-Interpreter function.</p> |
| FREQUENCY | Specifies the frequency. |
| NUMBER | Specifies the waveform number. This must be specified on each WAVEFORM statement. |
| OFFSET | <p>Specifies that a phase offset is to be used. If you use a non-zero phase in a sinusoidal definition, then SOLVE statement will go immediately to this bias. For example, if PHASE=90, AMPLITUDE=1 and the DC bias is 1V, the transient SOLVE statement will start at 2V and vary from 2V to 0V. If you specify OFFSET, then the bias will vary from 1V to -1V.</p> |
| PERIODS | Specifies the maximum number of sinusoidal periods (default is unlimited). |
| PHASE | Specifies the phase. |
| PWL | <p>Specifies a list of time and bias value points. The time values must be in ascending order (e.g., PWL="1e-9, 1 2e-9, 2 3e-9, 3"). This specifies that the bias will change to 1V at 1ns, 2V at 2ns, and 3V at 3ns.</p> |
| SINUSOID | <p>Specifies that a sinusoidal waveform will be generated according to:</p> <pre>AMPLITUDE*exp(-time*DECAY) *sin(2*PI*(FREQUENCY*time+PHASE/360.0))</pre> |

21.65: WAVEGUIDE

WAVEGUIDE defines geometry and physical models for a stand-alone optical mode simulation, which is done by solving the Helmholtz equation. For information about WAVEGUIDE, see Section 8.3: “WAVEGUIDE Statement”.

Syntax

WAVEGUIDE <parameters>

| Parameter | Type | Default | Units |
|---------------|-----------|----------------|-------|
| DISP.NAME | Character | dispersion.log | |
| DISPERSION | Logical | False | |
| E.INIT | Real | -999 | eV |
| E.FINAL | Real | -999 | eV |
| FAR.NX | Integer | 100 | |
| FAR.NY | Integer | 100 | |
| LX.MAX | Real | 999 | μm |
| LX.MIN | Real | -999 | μm |
| LY.MAX | Real | 999 | μm |
| LY.MIN | Real | -999 | μm |
| NDISP | Integer | 10 | |
| NMODE | Integer | 1 | |
| NB.ITEREIG | Integer | 4 | |
| NEAR.NX | Integer | 100 | |
| NEAR.NY | Integer | 100 | |
| OMEGA | Real | -999 | 1/s |
| OMEGA.FINAL | Real | -999 | 1/s |
| OMEGA.INIT | Real | -999 | 1/s |
| PHOTON.ENERGY | Real | -999 | eV |
| PRT.ITEREIG | Logical | False | |
| REFLECT | Logical | False | |
| V.HELM | Logical | False | |

Description

| | |
|----------------------|---|
| DISP.NAME | Specifies the log file name for waveguide dispersion. |
| E.INIT | Sets the lower photon energy boundary for dispersion calculation. |
| E.FINAL | Sets the upper photon energy boundary for dispersion calculation. |
| FAR.NX | Sets the number of X-samples for far-field pattern. |
| FAR.NY | Sets the number of Y-samples for far-field pattern. |
| LX.MAX | Sets the upper X boundary of solution domain for vector Helmholtz solver. |
| LX.MIN | Sets the lower X boundary of solution domain for vector Helmholtz solver. |
| LY.MAX | Sets the upper Y boundary of solution domain for vector Helmholtz solver. |
| LY.MIN | Sets the lower Y boundary of solution domain for vector Helmholtz solver. |
| NB.ITEREIG | Sets the ratio of basis size of iterative Helmholtz eigensolver to the number of requested transverse modes, given by parameter NMODES. |
| NDISP | Sets the number of photon energy samples for dispersion calculation. |
| NEAR.NX | Sets the number of X-samples for near-field pattern. |
| NEAR.NY | Sets the number of Y-samples for near-field pattern. |
| NMODE | Sets the number of requested optical modes in vector Helmholtz solver. |
| OMEGA | Sets the photon frequency in vector Helmholtz solver. |
| OMEGA.INIT | Sets the lower frequency boundary for dispersion calculation. |
| OMEGA.FINAL | Sets the upper frequency boundary for dispersion calculation. |
| PHOTON.ENERGY | Sets the photon energy in vector Helmholtz solver. |
| PRT.ITEREIG | Specifies that iterative Helmholtz eigensolver prints information about its internal parameters and convergence. |
| REFLECT | Specifies that the structure is mirror-symmetrical around x=0 axis. |
| V.HELM | Specifies that vector Helmholtz solver will be used for solution for transverse optical modes. |

A.1: Overview

ATLAS has a built-in C language interpreter that allows many of the models contained in ATLAS to be modified. To use the SILVACO C-INTERPRETER, (SCI), you must write C language functions containing analytic descriptions of the model. The C-INTERPRETER uses the ANSI standard definition of C. If you are not familiar with the C language, we suggest that you refer to any of the popular C language references such as the one written by Kernighan and Ritchie [115]. Additional information about the C-INTERPRETER can be found in the SILVACO C-INTERPRETER MANUAL.

The function arguments of the C-INTERPRETER functions and return values are fixed in ATLAS. Make sure that the arguments and the return values for the functions match those expected by ATLAS. To help you, this release of ATLAS includes a set of templates for the available functions. The C-INTERPRETER function template can be obtained by typing:

```
atlas -T filename
```

where `filename` is the name of a file where you want the template to be copied. You can also get the C-INTERPRETER function template by accessing the template file through DECKBUILD.

This template file should be copied and edited when implementing user-defined C-INTERPRETER functions. To use the C-INTERPRETER function, specify the file name containing this function in the appropriate ATLAS statement. The relevant statement names and parameters are listed in the template file. The template function prototypes are defined in the include file `template.in`.

The following example shows how the C-INTERPRETER function `munsat` can be used to describe velocity saturation for electrons.

First, examine the template file and find the template for `munsat`. The template should look something like this:

```
/*
 * Electron velocity saturation model.
 * Statement: MATERIAL
 * Parameter: F.MUNSAT
 * Arguments:
 * t1      lattice temperature (K)
 * na      acceptor concentration (per cc)
 * nd      donor concentration (per cc)
 * e       electric field (V/cm)
 * v       saturation velocity (cm/s)
 * mu0     low field mobility (cm^2/Vs)
 * *mu     return: field dependent mobility (cm^2/Vs)
 * *dmde   return: derivative of mu with e
 */
int munsat(double t1, double na, double nd, double e,
           double v, double mu0, double *mu, double *dmde)
{
    return(0);          /* 0 - ok */
}
```

Here, we see that the function is passed the lattice temperature, the acceptor and donor concentrations, the electric field, the saturation velocity, and the low field mobility. The function returns the field dependent mobility and the derivative of mobility with respect to electric field.

Note: It is important to properly calculate and return derivative values when specified, since the convergence algorithms in ATLAS require these derivatives.

The return value is an error flag. In this case, it is set to zero indicating that the function was successful (0=OK, 1=fail).

In this example, the C-INTERPRETER implements a standard model for velocity saturation. This particular model is already built into ATLAS. If you want to compare the user-defined version with the standard version, you can activate the built-in model by setting the B.ELECTRONS parameter to 1.

To implement the model, two lines additional lines of C code in the body of the function are specified as follows:

```
/*
 * Electron velocity saturation model.
 * Statement: MATERIAL
 * Parameter: F.MUNSAT
 * Arguments:
 * t1      lattice temperature (K)
 * na      acceptor concentration (per cc)
 * nd      donor concentration (per cc)
 * e       electric field (V/cm)
 * v       saturation velocity (cm/s)
 * mu0     low field mobility (cm^2/Vs)
 * *mu     return: field dependent mobility (cm^2/Vs)
 * *dmde   return: derivative of mu with e
 */

int munsat(double t1, double na, double nd, double e,
           double v, double mu0, double *mu, double *dmde)
{
    *mu = mu0/(1.0+mu0*e/v);
    *dmde = (*mu)*(*mu)/v;
    return(0);          /* 0 - ok */
}
```

The function will then need to be stored in a file. For example, the function can be stored in the file: test.lib. The function is then introduced into a specific example by specifying the file name on the F.MUNSAT parameter in the MATERIAL statement as follows:

```
MATERIAL F.MUNSAT="test.lib"
```


In this case, you will also need to activate the calculation of the field dependent mobility by adding the `FLDMOB` parameter to a `MODELS` statement. For example:

```
MODELS FLDMOB
```

When the input deck is executed, your C-INTERPRETER functions will be used in place of the built in function. When trying this example, place `PRINT` statements (using the `printf` C command) in the function to check that the function is working correctly.

Table A-1 shows a complete list of all the interpreter functions available in ATLAS.

| Table A-1. Complete list of available C-Interpreter functions in ATLAS | | | |
|--|------------|------------------|--|
| Statement | Parameter | Template | Description |
| BEAM | F.IMAGE | image () | Specifies 2D relative intensity versus offset at the source perpendicular to the direction of propagation for ray tracing in LUMINOUS3D. |
| BEAM | F.RADIATE | radiate () | Generation rate as a function of position. |
| BEAM | F3.RADIATE | radiate3 () | Generation rate as a function of position (3D). |
| BEAM | F.REFLECT | reflect () | Reflection coefficient. |
| DEFECT | F.TFTACC | tftacc () | TFT acceptor trap density as a function of energy. |
| CONTACT | F.ETUNNEL | fetunnel () | Schottky contact electron tunneling. |
| CONTACT | F.HTUNNEL | fhtunnel () | Schottky contact hole tunneling. |
| CONTACT | F.WORKF | workf () | Electrical Field dependent workfunction. |
| DEFECT | F.TFTDON | tftdon () | TFT donor trap density as a function of energy. |
| DEGRE DAT | F.NTA | devdeg_nta () | Interface acceptor trap density as a function of location. |
| DEGRE DAT | F.NTD | devdeg_ntd () | Interface donor trap density as a function of location. |
| DEGRE DAT | F.SIGMAE | devdeg_sigmae () | Interface electron capture cross-section. |
| DEGRE DAT | F.SIGMAH | devdeg_sigmah () | Interface hole capture cross-section. |
| DOPING | F.COMPOSIT | composition () | Position dependent composition fractions. |
| DOPING | F.DOPING | doping () | Position dependent net doping. |

Table A-1. Complete list of available C-Interpreter functions in ATLAS

| Statement | Parameter | Template | Description |
|-----------|--------------|---------------------|---|
| DOPING | F.DOPING | doping3 () | Position dependent net doping. |
| IMPACT | F.IIAN | iian() | Electron impact ionization coefficient as a function of composition, temperature, and electric field. |
| IMPACT | F.IIAP | iiap() | Hole impact ionization coefficient as a function of composition, temperature, and electric field. |
| INTERFACE | F.QF | int_fixed_charge () | Interface fixed charge as a function of position. |
| INTERFACE | F.HTE.N | hten() | Electron heterojunction thermionic emission current. |
| INTERFACE | F.HTE.P | htep() | Hole heterojunction thermionic emission current. |
| INTERFACE | F.HTFE.N | htfen() | Electron heterojunction thermionic field emission delta term. |
| INTERFACE | F.HTFE.P | htfep() | Hole heterojunction thermionic field emission delta term. |
| INTTRAP | F.DENSITY | inte_acc_trap () | Interface ACCEPTOR trap density as a function of position. |
| INTTRAP | F.DENSITY | inte_don_trap () | Interface DONOR trap density as a function of position. |
| IMPACT | F.EDIIN | ediin () | Electron temperature coefficients for impact ionization. |
| IMPACT | F.EDIIP | ediip () | Hole temperature coefficients for impact ionization. |
| INTTRAP | F.INTACCEPTO | intacceptor () | Initial interface acceptor trap density and so on as a function of position. |
| LASER | F.MIRROR | mirror | Mirror facet reflectivities on a function of wavelength. |
| LENS | F.LENS | lenslet () | Lenslet surface as a function of position. |
| MATERIAL | F.BANDCOMP | bandcomp () | Temperature and composition dependent band parameters. |
| MATERIAL | F.BBT | bbt () | Electric field and carrier concentration dependent band-to-band generation rate. |

Table A-1. Complete list of available C-Interpreter functions in ATLAS

| Statement | Parameter | Template | Description |
|-----------|---------------|----------------|---|
| MATERIAL | F.BGN | bgn () | Composition, temperature, and doping dependent band gap narrowing. |
| MATERIAL | F.CBDOSFN | cbdosfn | Electron temperature dependent effective conduction band density of states. |
| MATERIAL | F.COMMUN | commun () | Composition, temperature, position, and doping dependent electron mobility. |
| MATERIAL | F.COMMUP | commup () | Composition, temperature, position, and doping dependent hole mobility. |
| MATERIAL | F.COPT | copt () | Radiative recombination rate as a function of composition and temperature. |
| MATERIAL | F.EPSILON | epsilon () | Composition and temperature dependent permittivity. |
| MATERIAL | F.FERRO | ferro () | Position and field dependent permittivity. |
| MATERIAL | F.GAUN | gaun () | Electron Auger rate as a function of composition and temperature. |
| MATERIAL | F.GAUP | gaup () | Hole Auger rate as a function of composition and temperature. |
| MATERIAL | F.INDEX | index () | Wavelength dependent complex index of refraction. |
| MATERIAL | F.MNSNDIFF | mnsndiff () | Microscopic noise source for electron diffusion noise. |
| MATERIAL | F.MNSPDIF | mnspdiff () | Microscopic noise source for hole diffusion noise. |
| MATERIAL | F.MNSNFlicker | mnsnflicker () | Microscopic noise source for electron flicker noise. |
| MATERIAL | F.MNSPFlicker | mnspflicker () | Microscopic noise source for hole flicker noise. |
| MATERIAL | F.MUNSAT | munsat () | Electron velocity saturation model. |
| MATERIAL | F.MUPSAT | mupsat () | Hole velocity saturation model. |

Table A-1. Complete list of available C-Interpreter functions in ATLAS

| Statement | Parameter | Template | Description |
|-----------------------|-----------|--------------------------|--|
| MATERIAL | F.PDN | fphonondrag () | Adds a phonon drag term to the electron thermopower in GIGA. Function of lattice temperature and electron density. |
| MATERIAL | F.PDP | fphonondragp () | Adds a phonon drag term to the hole thermopower in GIGA. Function of lattice temperature and hole density. |
| MATERIAL | F.RECOMB | recomb () | Position, temperature, and concentration dependent recombination. |
| MATERIAL | F.TARUP | taurp () | Energy dependent hole relaxation time. |
| MATERIAL | F.TAUN | taun () | Position, temperture, and doping dependent electron SRH lifetime. |
| MATERIAL | F.TAUP | taup () | Position, temperture, and doping dependent hole SRH lifetime. |
| MATERIAL | F.TAURN | taurn () | Energy dependent electron relaxation time. |
| MATERIAL | F.TCAP | TCAP () | Lattice Thermal Capacity as a function of lattice temperature, position, doping, and fraction composition. |
| MATERIAL | F.TCOND | TCOND () | Lattice Thermal Conductivity as a function of lattice temperature, position, doping, and fraction composition. |
| MATERIAL | F.VSATN | vsatn () | Composition and temperature dependent electron saturation velocity. |
| MATERIAL | F.VSATP | vsatp () | Composition and temperature dependent hole saturation velocity. |
| MATERIAL | F.VBDOSFN | vbdosfn | Hole temperature dependent effective valence band density of states. |
| MATERIAL/ MOBILITY | F.ENMUN | endepmun | Electron mobility as a function of electron temperature and a few other choice variables. |
| MATERIAL/ MOBILITY | F.ENMUP | endepmup | Hole mobility as a function of hole temperature and a few other choice variables. |

Table A-1. Complete list of available C-Interpreter functions in ATLAS

| Statement | Parameter | Template | Description |
|-----------------------|------------------|----------------|--|
| MATERIAL/ MOBILITY | F.LOCALMUN | localmun | Electron mobility with an explicit position dependence. |
| MATERIAL/ MOBILITY | F.LOCALMUP | localmup | Hole mobility with an explicit position dependence. |
| MATERIAL/ MOBILITY | F.TOFIMUN | tofimun | Electron mobility with a dependence on both parallel and perpendicular electric field. |
| MATERIAL/ MOBILITY | F.TOFIMUP | tofimup | Hole mobility with a dependence on both parallel and perpendicular electric field. |
| MODELS | F.ALPHAA | bulk_absorb() | Bulk absorption coefficient versus carrier density and photon energy. |
| MODELS | F.KSN | fksn() | Energy dependent electron Scattering Law Exponent. |
| MODELS | F.KSP | fksp() | Energy dependent hole Scattering Law Exponent. |
| MODELS | F.PDN | fphonondrag() | Adds a phonon drag term to the electron thermopower in GIGA. Function of lattice temperature and electron density. |
| MODELS | F.PDP | fphonondragp() | Adds a phonon drag term to the hole thermopower in GIGA. Function of lattice temperature and hole density. |
| MODELS | F.TRAPTUNNEL | ftraptunnel | Energy and electric field dependent Dirac enhancement factor. |
| MODELS | F.TRAP.COULOMBIC | ftrapcoulombic | Energy and electric field dependent Coulombic enhancement factor. |
| SINGLEEVENT | F.SEU | seu() | Time and position dependent SEU generation. |
| TRAP | F.DENSITY | acc_trap() | ACCEPTOR trap density as a function of position. |
| TRAP | F.DENSITY | don_trap() | DONOR trap density as a function of position. |
| LASER | F.LGAIN | lgain() | Laser gain as a function of position, composition, carrier concentration, quasi-Fermi level and current. |

Table A-1. Complete list of available C-Interpreter functions in ATLAS

| Statement | Parameter | Template | Description |
|-----------|-----------|-----------|--|
| LASER | F.OMODE | omode () | Laser transverse optical mode distribution as a function of position. |
| MODELS | F.PCM | pcm () | Phase change material resistivity as a function of time step, temperature, previous temperature, and previous resistivity. |

B.1: Overview

ATLAS understands a library of materials for reference to material properties and models of various regions in the semiconductor device. These materials are chosen to represent those most commonly used by semiconductor physicists today. BLAZE or DEVICE3D users will have access to all of these materials. S-PISCES users will have only access to Silicon and Polysilicon.

S-PISCES is designed to maintain backward compatibility with the standalone program, SPISCES2 Version 5.2. In the SPISCES2 syntax, certain materials can be used in the `REGION` statement just by using their name as logical parameters. This syntax is still supported.

B.2: Semiconductors, Insulators, and Conductors

All materials in ATLAS are strictly defined into three classes: semiconductor materials, insulator materials, or conductors. Each class of materials has particular properties.

B.2.1: Semiconductors

All equations specified by your choice of models are solved in semiconductor regions. All semiconductor regions must have a band structure defined in terms of bandgap, density of states, affinity, and so on. The parameters used for any simulation can be echoed to the run-time output using `MODELS PRINT`. For complex cases with mole fraction dependent models, these quantities can be seen in TONYPLOT by specifying `OUTPUT BAND.PARAM` and saving a solution file.

Any semiconductor region that is defined as an electrode is then considered to be a conductor region. This is typical for polysilicon gate electrodes.

B.2.2: Insulators

In insulator materials, only the Poisson and lattice heat equations are solved. Therefore for isothermal simulations, the only parameter required for an insulator is dielectric permittivity defined using `MATERIAL PERM=<n>`.

Materials usually considered as insulators (e.g., SiO_2) can be treated as semiconductors using BLAZE, however all semiconductor parameters are then required.

B.2.3: Conductors

All conductor materials must be defined as electrodes, and all electrode regions are defined as conductor material regions. If a file containing regions of a material known to be a conductor are read in, these regions will automatically become un-named electrodes. As noted below, if the file contains unknown materials, these regions will become insulators.

During electrical simulation, only the electrode boundary nodes are used. Nodes that are entirely within an electrode region are not solved. Any quantities seen inside a conductor region in TONYPLOT are spurious. Only optical ray tracing and absorption for LUMINOUS and lattice heating are solved inside of conductor/electrode regions.

B.2.4: Unknown Materials

If a mesh file is read containing materials not in Table B-1, these will automatically become insulator regions with a relative permittivity of 3.9. All user-defined materials from ATHENA, regardless of the material name chosen, will also become such insulator materials.

B.2.5: Specifying Unknown or User-Defined Materials in ATLAS

As mentioned previously, all materials in ATLAS are classified as a semiconductor, an insulator, or a conductor. These classes are termed user groups. In order to correctly define a new material in ATLAS, you must specify the name of the material, the user group it belongs to, and the known ATLAS material it is to take as a default material. Once you set these three elements up in their appropriate places in the input deck, you can change the specific properties of them using `MATERIAL` statements as you would normally do.

A user groups takes one of the following definitions:

```
user.group=semiconductor
user.group=insulator
user.group=conductor
```


The name of the material is specified using:

```
user.material=material_name
```

The default material that the new material is to be based on is specified using:

```
user.default=known_atlas_material_name
```

As an example of the syntax required to define a new material, we will define a new material called `my_oxynitride`. For simplicity, we will omit all the other code for the complete ATLAS deck and only include code for deck structure purposes.

Defining a new insulator called `my_oxynitride`.

```
go atlas

mesh
.
.
.
region num=1 x.min=1 x.max=2 y.min=0 y.max=2 user.material=my_oxynitride

electrode ...

doping ...

material material=my_oxynitride user.group=insulator user.default=oxide
permittivity=9

.
.
.
```

After creating your new material in ATLAS, it is advised to include a print on your `MODELS` statement to echo the parameter values used for the material.

B.3: ATLAS Materials

This section lists the materials in ATLAS. The superscripted numbers (e.g., Silicon⁽¹⁾) on these tables refer to the notes on the next page.

| Table B-1. The ATLAS Materials | | | |
|------------------------------------|---------------------|-----------|----------|
| Single Element Semiconductors | | | |
| Silicon ⁽¹⁾ | Poly ⁽²⁾ | Germanium | Diamond |
| Binary Compound Semiconductors | | | |
| GaAs ⁽³⁾ | GaP | CdSe | SnTe |
| SiGe | InP | CdTe | ScN |
| SiC-6H | InSb | HgS | GaN |
| SiC-3C | InAs | HgSe | AlN |
| SiC-4H | | | |
| AlP | ZnS | HgTe | InN |
| AlAs | ZnSe | PbS | BeTe |
| AlSb | ZnTe | PbSe | ZnO |
| GaSb | CdS | PbTe | IGZO |
| Ternary Compound Semiconductors | | | |
| AlGaAs | GaSbP | InAlAs | GaAsP |
| InGaAs | GaSbAs | InAsP | HgCdTe |
| InGaP | InGaN | AlGaN | CdZnTe |
| InAlP | InGaSb | InAlSb | AlGaSb |
| InAsSb | GaAsSb | AlAsSb | InPSb |
| AlPSb | AlPAs | AlGaP | AlInN |
| Quaternary Compound Semiconductors | | | |
| InGaAsP | AlGaAsP | AlGaAsSb | InAlGaN |
| InGaNAs | InGaNp | AlGaNAs | AlGaNp |
| AlInNAs | AlInNP | InAlGaAs | InAlGaP |
| InAlAsP | | | |
| Insulators | | | |
| Vacuum | Oxide | Nitride | Si3N4 |
| Air | SiO2 | SiN | Sapphire |
| Ambient | InPAsSb | InGaAsSb | InAlAsSb |

| Table B-1. The ATLAS Materials | | | |
|--------------------------------|------------|--------|------------------|
| CuInGaSe2 | HfO2 | HfSiO4 | OxyNitride |
| Al2O3 | BSG | BPSG | TiO |
| | | | SnO ₂ |
| Conductors ⁽⁴⁾ | | | |
| Polysilicon ⁽²⁾ | Palladium | TiW | TaSi |
| Aluminum | Cobalt | Copper | PaSi |
| Gold | Molybdenum | Tin | PtSi |
| Silver | Lead | Nickel | MoSi |
| AlSi | Iron | WSi | ZrSi |
| Tungsten | Tantalum | TiSi | AlSi |
| Titanium | AlSiTi | NiSi | Conductor |
| Platinum | AlSiCu | CoSi | Contact |
| ITO | In2O3 | | |
| TiON | GST | GaSbTe | PCM |
| Organics | | | |
| Organic | Pentacene | | Alq3 |
| TPD | PPV | | Tetracene |
| NPB | IGZO | | |

Notes

1: The material models and parameters of Silicon are identical to those of S-Pisces2 Version 5.2. Be aware that although these band parameters may be physically inaccurate compared to bulk silicon measurements, most other material parameters and models are empirically tuned using these band parameters.

2: Polysilicon is treated differently depending on how it is used. In cases where it's defined as an electrode, it's treated as a conductor. It can also be used as a semiconductor such as in a polysilicon emitter bipolars.

3: The composition of SiGe is the only binary compound that can be varied to simulate the effects of band gap variations.

4: Conductor names are only associated with electrodes. They are used for the specification of thermal conductivities and complex index of refraction and for display in TonyPlot.

B.3.1: Specifying Compound Semiconductors Rules

The rules for specifying the order of elements for compound semiconductors are derived from the rules used by the International Union of Pure and Applied Chemistry [163]. These rules are:

1. Cations appear before anions.
2. When more than one cation is present the order progresses from the element with the largest atomic number to the element with the smallest atomic number.
3. The order of anions should be the in order of the following list: B, Si, C, Sb, As, P, N, H, Te, Se, S, At, I, Br, Cl, O, and F.
4. The composition fraction x is applied to the cation listed first.
5. The composition y is applied to the anion listed first.

To accommodate popular conventions, there are several exceptions to these rules (see Table B-2).

| Table B-2. Exceptions to the Specifying Compound Semiconductor Rules | |
|--|---|
| Material | Description |
| SiGe | The composition fraction x applies to the Ge component. SiGe is then specified as $\text{Si}_{(1-x)}\text{Ge}_{(x)}$, an exception to rule #4. |
| AlGaAs | This is specified as $\text{Al}_{(x)}\text{Ga}_{(1-x)}\text{As}$. This is an exception to rule #2. |
| InGaAsP (system) | The convention $\text{In}_{(1-x)}\text{Ga}_{(x)}\text{As}_{(y)}\text{P}_{(1-y)}$ as set forth by Adachi [1] is used. This is an exception to rule #4. |
| InAlAs | The convention $\text{In}_{(1-x)}\text{Al}_{(x)}\text{As}$ as set forth by Ishikawi [104] is used. This is an exception to rule #4. |
| InAlGaN | Here we use the convention $\text{In}_y\text{Al}_x\text{Ga}_{(1-x-y)}\text{N}$. This is an exception to rule #4. |
| HgCdTe | Here we use the convention $\text{Hg}_{(1-x)}\text{C}_{(x)}\text{dTe}$. This is an exception to rule #4. |
| InAlN | Here we use the convention $\text{In}_{(1-x)}\text{Al}_{(x)}\text{N}$. This is an exception to rule #4. |

B.4: Silicon and Polysilicon

The material parameters defaults for Polysilicon are identical to those for Silicon. The following paragraphs describe some of the material parameter defaults for Silicon and Polysilicon.

Note: A complete description is given of each model Chapter 3: “Physics”. The parameter defaults listed in that chapter are all Silicon material defaults.

| Table B-3. Band parameters for Silicon and Poly | | | | | | |
|---|-------------|-----------------------|-------|----------------------|-----------------------|--------------|
| Material | Eg300 eV | a | b | Nc300 per cc | Nv300 per cc | χ eV |
| Silicon | 1.08 | 4.73×10^{-4} | 636.0 | 2.8×10^{19} | 1.04×10^{19} | 4.17 |
| Poly | 1.08 | 4.73×10^{-4} | 636.0 | 2.8×10^{19} | 1.04×10^{19} | 4.17 |

| Table B-4. Static dielectric constants for Silicon and Poly | |
|---|---------------------|
| Material | Dielectric Constant |
| Silicon | 11.8 |
| Poly | 11.8 |

The default mobility parameters for Silicon and Poly are identical in all cases. The defaults used depend on the particular mobility models in question. A full description of each mobility model and their coefficients are given in Chapter 3: “Physics”, Section 3.6.1: “Mobility Modeling”.

Table B-5 contains the silicon and polysilicon default values for the low field constant mobility model.

| Table B-5. Lattice Mobility Model Defaults for Silicon and Poly | | | | |
|---|----------------------------|----------------------------|------|------|
| Material | MUN cm ² /Vs | MUP cm ² /Vs | TMUN | TMUP |
| Silicon | 1000.0 | 500.0 | 1.5 | 1.5 |
| Poly | 1000.0 | 500.0 | 1.5 | 1.5 |

Table B-6 shows the silicon and polysilicon default values for the field dependent mobility model.

| Table B-6. Parallel Field Dependent Mobility Model Parameters for Silicon and Poly | | |
|--|-------|-------|
| Material | BETAN | BETAP |
| Silicon | 2 | 1 |
| Poly | 2 | 1 |

Table B-7 shows the default values used in the bandgap narrowing model for Silicon and Polysilicon.

| Table B-7. Bandgap Narrowing Parameters for Silicon and Poly | | | |
|--|-----------|-----------------------|------------------|
| Statement | Parameter | Defaults | Units |
| MATERIAL | BGN.E | 6.92×10^{-3} | V |
| MATERIAL | BGN.N | 1.3×10^{17} | cm^{-3} |
| MATERIAL | BGN.C | 0.5 | — |

Table B-8 shows the default parameters for Shockley-Read-Hall (SRH) recombination.

| Table B-8. SRH Lifetime Parameter Defaults for Silicon and Poly | | | | |
|---|----------------------|----------------------|----------------------------|----------------------------|
| Material | TAUN0 (s) | TAUP0 (s) | NSRHN (cm^{-3}) | NSRHP (cm^{-3}) |
| Silicon | 1.0×10^{-7} | 1.0×10^{-7} | 5.0×10^{16} | 5.0×10^{16} |
| Poly | 1.0×10^{-7} | 1.0×10^{-7} | 5.0×10^{16} | 5.0×10^{16} |

The default parameters for Auger recombination are given in Table B-9.

| Table B-9. Auger Coefficient Defaults for Silicon and Poly | | |
|--|-----------------------|-----------------------|
| Material | AUGN | AUGP |
| Silicon | 2.8×10^{-31} | 9.9×10^{-32} |
| Poly | 2.8×10^{-31} | 9.9×10^{-32} |

Table B-10 shows the default values for the SELB impact ionization coefficients.

| Table B-10. Impact Ionization Coefficients for Silicon and Poly | |
|--|---------------------|
| Parameter | Value |
| EGRAN | 4.0×10^5 |
| BETAN | 1.0 |
| BETAP | 1.0 |
| AN1 | 7.03×10^5 |
| AN2 | 7.03×10^5 |
| BN1 | 1.231×10^6 |
| BN2 | 1.231×10^6 |
| AP1 | 6.71×10^5 |
| AP2 | 1.582×10^6 |
| BP1 | 1.693×10^6 |
| BP2 | 2.036×10^6 |

Table B-11 shows the default Richardson coefficients.

| Table B-11. Effective Richardson Coefficients for Silicon and Poly | | |
|---|---|---|
| Material | ARICHN ($A/cm^2/K^2$) | ARICHP ($A/cm^2/K^2$) |
| Silicon | 110.0 | 30.0 |
| Poly | 110.0 | 30.0 |

B.5: The $\text{Al}_{(x)}\text{Ga}_{(1-x)}\text{As}$ Material System

Table B-12 shows the default recombination parameters for AlGaAs.

| Table B-12. Default Recombination Parameters for AlGaAs | | |
|---|-----------------------|----------|
| Parameter | Value | Equation |
| TAUN0 | 1.0×10^{-9} | 3-213 |
| TAUP0 | 1.0×10^{-8} | 3-213 |
| COPT | 1.5×10^{-10} | 3-226 |
| AUGN | 5.0×10^{-30} | 3-227 |
| AUGP | 1.0×10^{-31} | 3-227 |

Table B-13 shows the default values for the SELB impact ionization coefficients used for GaAs. AlGaAs uses the same values as GaAs.

| Table B-13. Impact Ionization Coefficients for GaAs | |
|---|---------------------|
| Parameter | Value |
| EGRAN | 0.0 |
| BETAN | 1.82 |
| BETAP | 1.75 |
| EGRAN | 0.0 |
| AN1 | 1.889×10^5 |
| AN2 | 1.889×10^5 |
| BN1 | 5.75×10^5 |
| BN2 | 5.75×10^5 |
| AP1 | 2.215×10^5 |
| AP2 | 2.215×10^5 |
| BP1 | 6.57×10^5 |
| BP2 | 6.57×10^5 |

The default values for the effective Richardson coefficients for GaAs are $6.2875 \text{ A/cm}^2/\text{K}^2$ for electrons and $105.2 \text{ A/cm}^2/\text{K}^2$ for holes.

B.6: The $\text{In}_{(1-x)}\text{Ga}_{(x)}\text{As}_{(y)}\text{P}_{(1-y)}$ System

The default material thermal models for InGaAsP assumes lattice-matching to InP. The material density is then given by

$$\rho = 4.791 + 0.575y.\text{composition} + 0.138y.\text{composition}$$

The specific heat for InGaAsP is given by

$$C_p = 0.322 + 0.026y.\text{composition} - 0.008y.\text{composition}$$

The thermal resistivities of InGaAsP are linearly interpolated from Table B-14.

| Table B-14. Thermal Resistivities for InGaAsP Lattice-Matched to InP | |
|--|--------------------------------|
| Composition Fraction y | Thermal Resistivity (deg/cm/w) |
| 0.0 | 1.47 |
| 0.1 | 7.05 |
| 0.2 | 11.84 |
| 0.3 | 15.83 |
| 0.4 | 19.02 |
| 0.5 | 21.40 |
| 0.6 | 22.96 |
| 0.7 | 23.71 |
| 0.8 | 23.63 |
| 0.9 | 22.71 |
| 1.0 | 20.95 |

The default thermal properties for the ternary compounds in the InGaAsP system: $\text{In}_{(1-x)}\text{Ga}_{(x)}\text{As}$, $\text{In}_{(1-x)}\text{Ga}_{(x)}\text{P}$, $\text{InAs}_{(y)}\text{P}_{(1-y)}$, and $\text{GaAs}_{(y)}\text{P}_{(1-y)}$, are given as a function of composition fraction by linear interpolations from these binary compounds.

B.7: Silicon Carbide (SiC)

Table B-15 shows the default values for the SELB impact ionization coefficients used for SiC.

| Table B-15. Impact Ionization Coefficients for SiC | |
|--|---------------------|
| Parameter | Value |
| EGRAN | 0.0 |
| BETAN | 1.0 |
| BETAP | 1.0 |
| AN1 | 1.66×10^6 |
| AN2 | 1.66×10^6 |
| BN1 | 1.273×10^7 |
| BN2 | 1.273×10^7 |
| AP1 | 5.18×10^6 |
| AP2 | 5.18×10^6 |
| BP1 | 1.4×10^7 |
| BP2 | 1.4×10^7 |

Table B-16 shows the default thermal parameters used for both 6H-SiC and 3C-SiC.

| Table B-16. Default Thermal Parameters for SiC | | |
|--|--------|--------|
| Parameter | Value | |
| | 3C-SiC | 6H-SiC |
| TCA | 0.204 | 0.385 |

B.8: Material Defaults for GaN/InN/AlN System

Tables B-17 through B-20 show the default values for the band structure parameters for InN, GaN and AlN for each of the user-defined parameter sets. To choose the parameters sets, specify KP.SET1 (Table B-20), KP.SET2 (Table B-21), KP.SET3 (Table B-22), and KP.SET4 (Table B-24). By default, the parameters in Table B-17 are used.

| Table B-17. Electronic Band-Structure Parameters for InN, GaN and AlN Using KP.SET1 (All Parameters Values are from [179] unless otherwise noted.) | | | | | | |
|---|----------|----------|-------|--------|---------|---------|
| Parameter | Symbol | Syntax | Units | InN | GaN | AlN |
| Electron eff. mass (z) | m_{cz} | MZZ | m_0 | 0.11 | 0.20 | 0.33 |
| Electron eff. mass (t) | m_{ct} | MTT | m_0 | 0.11 | 0.18 | 0.25 |
| Hole eff. mass param. | A1 | A1 | | -9.24 | -7.24 | -3.95 |
| Hole eff. mass param. | A2 | A2 | | -0.60 | -0.51 | -0.27 |
| Hole eff. mass param. | A3 | A3 | | 8.68 | 6.73 | 3.68 |
| Hole eff. mass param. | A4 | A4 | | -4.34 | -3.36 | -1.84 |
| Hole eff. mass param. | A5 | A5 | | -4.32 | -3.35 | -1.92 |
| Hole eff. mass param. | A6 | A6 | | -6.08 | -4.72 | -2.91 |
| Valence band reference | Ev0 | | eV | -1.59 | -2.64 | -3.44 |
| Direct band gap (300K) | Eg(300) | | eV | 1.89 | 3.42 | 6.28 |
| Spin-orbit split energy | D1 | DELTA1 | eV | 0.041 | 0.019 | -0.164 |
| Crystal-field split energy | D2 | DELTA2 | eV | 0.0013 | 0.01413 | 0.01913 |
| Lattice constant | a_0 | ALATTICE | Å | 3.548 | 3.189 | 3.112 |
| Elastic constant | C33 | C33 | GPa | 200 | 392 | 382 |
| Elastic constant | C13 | C13 | GPa | 94 | 100 | 127 |

Table B-17. Electronic Band-Structure Parameters for InN, GaN and AlN Using KP.SET1
(All Parameters Values are from [179] unless otherwise noted.)

| | | | | | | |
|-----------------------------------|----|----|----|-------|-------|-------|
| Hydrostatic deformation potential | ac | AC | eV | -4.08 | -4.08 | -4.08 |
| Shear deform. potential | D1 | D1 | eV | -0.89 | -0.89 | -0.89 |
| Shear deform. potential | D2 | D2 | eV | 4.27 | 4.27 | 4.27 |
| Shear deform. potential | D3 | D3 | eV | 5.18 | 5.18 | 5.18 |
| Shear deform. potential | D4 | D4 | eV | -2.59 | -2.59 | -2.29 |

Table B-18. Electronic Band-Structure Parameters for InN, GaN and AlN Using KP.SET2
(All Parameters Values are from [241] unless otherwise noted.)

| Parameter | Symbol | Syntax | Units | InN | GaN | AlN |
|-------------------------|----------|--------|-------|-------|-------|--------|
| Electron eff. mass (z) | m_{cz} | MZZ | m_0 | 0.12 | 0.20 | 0.32 |
| Electron eff. mass (t) | m_{ct} | MTT | m_0 | 0.12 | 0.20 | 0.28 |
| Hole eff. mass param. | A1 | A1 | | -8.21 | -6.56 | -3.95 |
| Hole eff. mass param. | A2 | A2 | | -0.68 | -0.91 | -0.27 |
| Hole eff. mass param. | A3 | A3 | | 7.57 | 5.65 | 3.68 |
| Hole eff. mass param. | A4 | A4 | | -5.23 | -2.83 | -1.84 |
| Hole eff. mass param. | A5 | A5 | | -5.11 | -3.13 | -1.92 |
| Hole eff. mass param. | A6 | A6 | | -5.96 | -4.86 | -2.91 |
| Valence band reference | Ev0 | | eV | -1.59 | -2.64 | -3.44 |
| Direct band gap (300K) | Eg(300) | | eV | 1.994 | 3.507 | 6.23 |
| Spin-orbit split energy | D1 | DELTA1 | eV | 0.041 | 0.019 | -0.164 |

Table B-18. Electronic Band-Structure Parameters for InN, GaN and AlN Using KP.SET2
(All Parameters Values are from [241] unless otherwise noted.)

| | | | | | | |
|-----------------------------------|----------------|----------|-----|--------|---------|---------|
| Crystal-field split energy | D2 | DELTA2 | eV | 0.0013 | 0.01413 | 0.01913 |
| Lattice constant | a ₀ | ALATTICE | Å | 3.548 | 3.189 | 3.112 |
| Elastic constant | C33 | C33 | GPa | 224 | 398 | 373 |
| Elastic constant | C13 | C13 | GPa | 92 | 106 | 108 |
| Hydrostatic deformation potential | ac | AC | eV | -4.08 | -4.08 | -4.08 |
| Shear deform. potential | D1 | D1 | eV | -0.89 | -3.0 | -0.89 |
| Shear deform. potential | D2 | D2 | eV | 4.27 | 3.6 | 4.27 |
| Shear deform. potential | D3 | D3 | eV | 5.18 | 8.82 | 5.18 |
| Shear deform. potential | D4 | D4 | eV | -2.59 | -4.41 | -2.29 |

Table B-19. Electronic Band-Structure Parameters for InN, GaN and AlN Using KP.SET3
(All Parameters Values are from [41] unless otherwise noted.)

| Parameter | Symbol | Syntax | Units | InN [241] | GaN | AlN |
|------------------------|-----------------|--------|-------|-----------|-------|-------------|
| Electron eff. mass (z) | m _{Cz} | MZZ | m0 | 0.12 | 0.20 | 0.32 |
| Electron eff. mass (t) | m _{Ct} | MTT | m0 | 0.12 | 0.20 | 0.28 |
| Hole eff. mass param. | A1 | A1 | | -8.21 | -6.56 | -3.95 [241] |
| Hole eff. mass param. | A2 | A2 | | -0.68 | -0.91 | -0.27 [241] |
| Hole eff. mass param. | A3 | A3 | | 7.57 | 5.65 | 3.68 [241] |
| Hole eff. mass param. | A4 | A4 | | -5.23 | -2.83 | -1.84 [241] |
| Hole eff. mass param. | A5 | A5 | | -5.11 | -3.13 | -1.92 [241] |

Table B-19. Electronic Band-Structure Parameters for InN, GaN and AlN Using KP.SET3
(All Parameters Values are from [41] unless otherwise noted.)

| | | | | | | |
|-----------------------------------|----------------|----------|-----|--------|---------|-------------|
| Hole eff. mass param. | A6 | A6 | | -5.96 | -4.86 | -2.91 [241] |
| Valence band reference | Ev0 | | eV | -1.59 | -2.64 | -3.44 |
| Direct band gap (300K) | Eg(300) | | eV | 1.994 | 3.44 | 6.28 |
| Spin-orbit split energy | D1 | DELTA1 | eV | 0.041 | 0.016 | -0.0585 |
| Crystal-field split energy | D2 | DELTA2 | eV | 0.0013 | 0.01213 | 0.020413 |
| Lattice constant | a ₀ | ALATTICE | Å | 3.548 | 3.189 | 3.112 [241] |
| Elastic constant | C33 | C33 | GPa | 224 | 267 | 395 |
| Elastic constant | C13 | C13 | GPa | 92 | 158 | 120 |
| Hydrostatic deformation potential | ac | AC | eV | -3.5 | -4.08 | -4.08 |
| Shear deform. potential | D1 | D1 | eV | -3.0 | 0.7 | 0.7 |
| Shear deform. potential | D2 | D2 | eV | 3.6 | 2.1 | 2.1 |
| Shear deform. potential | D3 | D3 | eV | 8.82 | 1.4 | 1.4 |
| Shear deform. potential | D4 | D4 | eV | -4.41 | -0.7 | -0.7 |

Table B-20. Electronic Band-Structure Parameters for InN, GaN and AlN Using KP.SET4
(All Parameters Values are from [43] unless otherwise noted.)

| Parameter | Symbol | Syntax | Units | InN [241] | GaN | AlN |
|------------------------|-----------------|--------|-------|-----------|-------|-------------|
| Electron eff. mass (z) | m _{Cz} | MZZ | m0 | 0.12 | 0.20 | 0.33 |
| Electron eff. mass (t) | m _{Ct} | MTT | m0 | 0.12 | 0.18 | 0.25 |
| Hole eff. mass param. | A1 | A1 | | -8.21 | -6.56 | -3.95 [241] |

**Table B-20. Electronic Band-Structure Parameters for InN, GaN and AlN Using KP.SET4
(All Parameters Values are from [43] unless otherwise noted.)**

| | | | | | | |
|-----------------------------------|----------------|----------|-----|---------|---------|-------------|
| Hole eff. mass param. | A2 | A2 | | -0.68 | -0.91 | -0.27 [241] |
| Hole eff. mass param. | A3 | A3 | | 7.57 | 5.65 | 3.68 [241] |
| Hole eff. mass param. | A4 | A4 | | -5.23 | -2.83 | -1.84 [241] |
| Hole eff. mass param. | A5 | A5 | | -5.11 | -3.13 | -1.92 [241] |
| Hole eff. mass param. | A6 | A6 | | -5.96 | -4.86 | -2.91 [241] |
| Valence band reference | Ev0 | | eV | -1.59 | -2.64 | -3.44 |
| Direct band gap (300K) | Eg(300) | | eV | 1.994 | 3.44 | 6.28 |
| Spin-orbit split energy | D1 | DELTA1 | eV | 0.041 | 0.021 | -0.0585 |
| Crystal-field split energy | D2 | DELTA2 | eV | 0.00113 | 0.01618 | 0.020413 |
| Lattice constant | a ₀ | ALATTICE | Å | 3.548 | 3.189 | 3.112 [241] |
| Elastic constant | C33 | C33 | GPa | 224 | 392 | 395 |
| Elastic constant | C13 | C13 | GPa | 92 | 100 | 120 |
| Hydrostatic deformation potential | ac | AC | eV | -35 | -4.08 | -4.08 |
| Shear deform. potential | D1 | D1 | eV | -3.0 | -0.89 | -0.89 |
| Shear deform. potential | D2 | D2 | eV | 3.6 | 4.27 | 4.27 |
| Shear deform. potential | D3 | D3 | eV | 8.82 | 5.18 | 5.18 |
| Shear deform. potential | D4 | D4 | eV | -4.41 | -2.59 | -2.29 |

Tables B-21 through B-23 show the default polarization parameters for InN, GaN and AlN for each of the user-defined parameter sets. To choose the parameter sets, specify POL.SET1 (Table B-24), POL.SET2 (Table B-25), or POL.SET3 (Table B-26) on the MATERIAL statement. By default, the parameter values in Table B-24 are used.

| Table B-21. Polarization Parameters for InN, GaN and AlN Using POL.SET1 (All Parameters Values are from [179] unless otherwise noted.) | | | | | | |
|---|---------------|---------------|------------------|------------|------------|------------|
| Parameter | Symbol | Syntax | Units | InN | GaN | AlN |
| Lattice constant | a_0 | ALATTICE | Å | 3.548 | 3.189 | 3.112 |
| Spontaneous polarization | P_{sp} | PSP | C/m ² | -0.042 | -0.034 | -0.09 |
| Piezoelectric const. (z) | e_{33} | E33 | C/m ² | 0.81 | 0.67 | 1.5 |
| Piezoelectric const. (x,y) | e_{31} | E31 | C/m ² | -0.41 | -0.34 | -0.53 |

| Table B-22. Polarization Parameters for InN, GaN and AlN Using POL.SET2 (All Parameters Values are from [241] unless otherwise noted.) | | | | | | |
|---|---------------|---------------|------------------|------------|------------|------------|
| Parameter | Symbol | Syntax | Units | InN | GaN | AlN |
| Lattice constant | a_0 | ALATTICE | Å | 3.545 | 3.189 | 3.112 |
| Spontaneous polarization | P_{sp} | PSP | C/m ² | -0.032 | -0.029 | -0.081 |
| Piezoelectric const. (z) | e_{33} | E33 | C/m ² | 0.97 | 1.27 | 1.79 |
| Piezoelectric const. (x,y) | e_{31} | E31 | C/m ² | -0.57 | -0.35 | -0.5 |

Table B-23. Polarization Parameters for InN, GaN and AlN Using POL.SET3
(All Parameters Values are from [42] unless otherwise noted.)

| Parameter | Symbol | Syntax | Units | InN | GaN | AlN |
|----------------------------|----------|----------|------------------|--------|--------|--------|
| Lattice constant | a_0 | ALATTICE | Å | 3.54 | 3.189 | 3.112 |
| Spontaneous polarization | P_{sp} | PSP | C/m ² | -0.032 | -0.029 | -0.081 |
| Piezoelectric const. (z) | e_{33} | E33 | C/m ² | 0.97 | 0.73 | 1.46 |
| Piezoelectric const. (x,y) | e_{31} | E31 | C/m ² | -0.57 | -0.49 | -0.6 |

B.9: Material Defaults for Compound Semiconductors

Tables B-24a and B-24b, and B-24c show the material defaults for binary compound semiconductors. Table B-25 shows Material defaults for ternary compound semiconductors.

Note: χ .comp is set to 0.3. See Chapter 5: "Blaze: Compound Material 2D Simulator", Section 5.3: "Material Dependent Physical Models" for more information.

Table B-24a. Materials Defaults for binary compound semiconductors

| Material | GaAs | GaP | CdSe | SnTe | InP | CdTe | ScN |
|---------------------------|----------|----------|----------|----------|----------|----------|----------|
| Epsilon | 13.2 | 11.1 | 10.6 | 0 | 12.5 | 10.9 | 0 |
| Eg (eV) | 1.42 | 2.26 | 1.74 | 0.18 | 1.35 | 1.5 | 2.15 |
| Chi (eV) | 4.07 | 4.4 | 0 | 0 | 4.4 | 4.28 | 0 |
| Nc (per cc) | 4.35E+17 | 1.76E+18 | 1.18E+18 | 1 | 5.68E+17 | 1 | 1 |
| Nv (per cc) | 8.16E+18 | 8.87E+18 | 7.57E+18 | 1 | 8.87E+18 | 1 | 1 |
| ni (per cc) | 2.12E+06 | 0.409 | 7.22E+03 | 0.0308 | 1.03E+07 | 2.51E-13 | 8.70E-19 |
| Gc | 2 | 2 | 2 | 2 | 2 | 2 | 2 |
| Gv | 4 | 4 | 4 | 4 | 4 | 4 | 4 |
| Ed (eV) | 0.044 | 0.044 | 0.044 | 0.044 | 0.044 | 0.044 | 0.044 |
| Ea (eV) | 0.045 | 0.045 | 0.045 | 0.045 | 0.045 | 0.045 | 0.045 |
| Lifetime (el) | 1.00E-09 | 1 | 1 | 1 | 1 | 1 | 1 |
| Lifetime (ho) | 2.00E-08 | 1 | 1 | 1 | 1 | 1 | 1 |
| Auger cn | 5.00E-30 | 0 | 0 | 0 | 0 | 0 | 0 |
| Auger cp | 1.00E-31 | 0 | 0 | 0 | 0 | 0 | 0 |
| Auger kn | 0 | 0 | 0 | 0 | 0 | 0 | 0 |
| Auger kp | 0 | 0 | 0 | 0 | 0 | 0 | 0 |
| Copt | 1.50E-10 | 0 | 0 | 0 | 0 | 0 | 0 |
| An** | 6.29 | 20.4 | 15.6 | 1.40E-11 | 9.61 | 1.40E-11 | 1.40E-11 |
| Ap** | 105 | 60.1 | 54.1 | 1.40E-11 | 60.1 | 1.40E-11 | 1.40E-11 |
| betan | 1.82 | 1 | 1 | 1 | 1 | 1 | 1 |
| betap | 1.75 | 1 | 1 | 1 | 1 | 1 | 1 |
| egran | 0 | 0 | 0 | 0 | 0 | 0 | 0 |
| an1 | 1.90E+05 | 7.30E+04 | 7.30E+04 | 7.03E+05 | 7.30E+04 | 7.03E+05 | 7.03E+05 |
| bn1 | 5.75E+05 | 1.23E+06 | 1.23E+06 | 1.23E+06 | 1.23E+06 | 1.23E+06 | 1.23E+06 |
| an2 | 1.90E+05 | 7.30E+04 | 7.30E+04 | 7.03E+05 | 7.30E+04 | 7.03E+05 | 7.03E+05 |
| an2 | 5.75E+05 | 1.23E+06 | 1.23E+06 | 1.23E+06 | 1.23E+06 | 1.23E+06 | 1.23E+06 |
| ap1 | 2.22E+05 | 6.71E+05 | 6.71E+05 | 6.71E+05 | 6.71E+05 | 6.71E+05 | 6.71E+05 |
| bp1 | 6.57E+05 | 1.69E+06 | 1.69E+06 | 1.69E+06 | 1.69E+06 | 1.69E+06 | 1.69E+06 |
| ap2 | 2.22E+05 | 1.58E+06 | 1.58E+06 | 1.58E+06 | 1.58E+06 | 1.58E+06 | 1.58E+06 |
| bp2 | 6.57E+05 | 2.40E+05 | 2.40E+05 | 2.04E+06 | 2.40E+05 | 2.04E+06 | 2.04E+06 |
| Vsatn (cm/s) : | 7.70E+06 | 1.00E+06 | 1.00E+06 | 1.00E+06 | 1.00E+06 | 1.00E+06 | 1.00E+06 |
| Vsatp (cm/s) : | 7.70E+06 | 1.00E+06 | 1.00E+06 | 1.00E+06 | 1.00E+06 | 1.00E+06 | 1.00E+06 |
| mun (cm ² /Vs) | 8000 | 300 | 800 | | 4600 | 1050 | |
| tmun | 1 | 1.5 | 1.5 | | 1.5 | 1.5 | |
| mup (cm ² /Vs) | 400 | 100 | | | 150 | 100 | |
| tmup | 2.1 | 1.5 | | | 1.5 | 1.5 | |

Table B-24b. Materials Defaults for binary compound semiconductors

| Material | GaAs | GaP | CdSe | SnTe | InP | CdTe | ScN |
|---------------------------|----------|----------|----------|----------|----------|----------|----------|
| Epsilon | 13.2 | 11.1 | 10.6 | 0 | 12.5 | 10.9 | 0 |
| Eg (eV) | 1.42 | 2.26 | 1.74 | 0.18 | 1.35 | 1.5 | 2.15 |
| Chi (eV) | 4.07 | 4.4 | 0 | 0 | 4.4 | 4.28 | 0 |
| Nc (per cc) | 4.35E+17 | 1.76E+18 | 1.18E+18 | 1 | 5.68E+17 | 1 | 1 |
| Nv (per cc) | 8.16E+18 | 8.87E+18 | 7.57E+18 | 1 | 8.87E+18 | 1 | 1 |
| ni (per cc) | 2.12E+06 | 0.409 | 7.22E+03 | 0.0308 | 1.03E+07 | 2.51E-13 | 8.70E-19 |
| Gc | 2 | 2 | 2 | 2 | 2 | 2 | 2 |
| Gv | 4 | 4 | 4 | 4 | 4 | 4 | 4 |
| Ed (eV) | 0.044 | 0.044 | 0.044 | 0.044 | 0.044 | 0.044 | 0.044 |
| Ea (eV) | 0.045 | 0.045 | 0.045 | 0.045 | 0.045 | 0.045 | 0.045 |
| Lifetime (el) | 1.00E-09 | 1 | 1 | 1 | 1 | 1 | 1 |
| Lifetime (ho) | 2.00E-08 | 1 | 1 | 1 | 1 | 1 | 1 |
| Auger cn | 5.00E-30 | 0 | 0 | 0 | 0 | 0 | 0 |
| Auger cp | 1.00E-31 | 0 | 0 | 0 | 0 | 0 | 0 |
| Auger kn | 0 | 0 | 0 | 0 | 0 | 0 | 0 |
| Auger kp | 0 | 0 | 0 | 0 | 0 | 0 | 0 |
| Copt | 1.50E-10 | 0 | 0 | 0 | 0 | 0 | 0 |
| An** | 6.29 | 20.4 | 15.6 | 1.40E-11 | 9.61 | 1.40E-11 | 1.40E-11 |
| Ap** | 105 | 60.1 | 54.1 | 1.40E-11 | 60.1 | 1.40E-11 | 1.40E-11 |
| betan | 1.82 | 1 | 1 | 1 | 1 | 1 | 1 |
| betap | 1.75 | 1 | 1 | 1 | 1 | 1 | 1 |
| egran | 0 | 0 | 0 | 0 | 0 | 0 | 0 |
| an1 | 1.90E+05 | 7.30E+04 | 7.30E+04 | 7.03E+05 | 7.30E+04 | 7.03E+05 | 7.03E+05 |
| bn1 | 5.75E+05 | 1.23E+06 | 1.23E+06 | 1.23E+06 | 1.23E+06 | 1.23E+06 | 1.23E+06 |
| an2 | 1.90E+05 | 7.30E+04 | 7.30E+04 | 7.03E+05 | 7.30E+04 | 7.03E+05 | 7.03E+05 |
| an2 | 5.75E+05 | 1.23E+06 | 1.23E+06 | 1.23E+06 | 1.23E+06 | 1.23E+06 | 1.23E+06 |
| ap1 | 2.22E+05 | 6.71E+05 | 6.71E+05 | 6.71E+05 | 6.71E+05 | 6.71E+05 | 6.71E+05 |
| bp1 | 6.57E+05 | 1.69E+06 | 1.69E+06 | 1.69E+06 | 1.69E+06 | 1.69E+06 | 1.69E+06 |
| ap2 | 2.22E+05 | 1.58E+06 | 1.58E+06 | 1.58E+06 | 1.58E+06 | 1.58E+06 | 1.58E+06 |
| bp2 | 6.57E+05 | 2.40E+05 | 2.40E+05 | 2.04E+06 | 2.40E+05 | 2.04E+06 | 2.04E+06 |
| Vsatsn (cm/s) : | 7.70E+06 | 1.00E+06 | 1.00E+06 | 1.00E+06 | 1.00E+06 | 1.00E+06 | 1.00E+06 |
| Vsatp (cm/s) : | 7.70E+06 | 1.00E+06 | 1.00E+06 | 1.00E+06 | 1.00E+06 | 1.00E+06 | 1.00E+06 |
| mun (cm ² /Vs) | 8000 | 300 | 800 | | 4600 | 1050 | |
| tmun | 1 | 1.5 | 1.5 | | 1.5 | 1.5 | |
| mup (cm ² /Vs) | 400 | 100 | | | 150 | 100 | |
| tmup | 2.1 | 1.5 | | | 1.5 | 1.5 | |

Table B-24c. Material Defaults for binary compound semiconductors

| Material | ZnS | HgTe | AlAs | ZnSe | PbS | BeTe | AlSb | ZnTe | PbSe | GaSb | PbTe | SiGe |
|------------------------------|----------|----------|----------|----------|----------|----------|----------|----------|----------|----------|----------|----------|
| Epsilon | 8.3 | 20 | 12 | 8.1 | 170 | 0 | 11 | 9.7 | 250 | 15.7 | 412 | 11.8 |
| Eg (eV) | 3.8 | 0 | 2.16 | 2.58 | 0.37 | 2.57 | 1.52 | 2.28 | 0.26 | 0.72 | 0.29 | 0.78 |
| Chi (eV) | 0 | 0 | 3.5 | 4.09 | 0 | 0 | 3.65 | 3.5 | 0 | 4.06 | 4.6 | 4.17 |
| Nc (per cc) | 6.35E+18 | 1 | 4.35E+17 | 1 | 3.14E+18 | 1 | 6.79E+18 | 1 | 1 | 5.68E+18 | 1.76E+18 | 1.92E+19 |
| Nv (per cc) | 1 | 1 | 8.16E+18 | 1 | 3.14E+18 | 1 | 6.35E+18 | 1 | 1 | 2.95E+18 | 2.24E+18 | 8.20E+18 |
| ni (per cc) | 3.02E-23 | 1 | 1.35 | 2.13E-22 | 2.45E+15 | 2.58E-22 | 1.12E+06 | 7.04E-20 | 0.00655 | 3.66E+12 | 7.28E+15 | 3.52E+12 |
| Gc | 2 | 2 | 2 | 2 | 2 | 2 | 2 | 2 | 2 | 2 | 2 | 2 |
| Gv | 4 | 4 | 4 | 4 | 4 | 4 | 4 | 4 | 4 | 4 | 4 | 4 |
| Ed (eV) | 0.044 | 0.044 | 0.044 | 0.044 | 0.044 | 0.044 | 0.044 | 0.044 | 0.044 | 0.044 | 0.044 | 0.044 |
| Ea (eV) | 0.045 | 0.045 | 0.045 | 0.045 | 0.045 | 0.045 | 0.045 | 0.045 | 0.045 | 0.045 | 0.045 | 0.045 |
| Recombination Parameters | | | | | | | | | | | | |
| Lifetime (el) | 1 | 1 | 1.00E-09 | 1 | 1 | 1 | 1 | 1 | 1 | 1 | 1 | 3.00E-05 |
| Lifetime (ho) | 1 | 1 | 2.00E-08 | 1 | 1 | 1 | 1 | 1 | 1 | 1 | 1 | 1.00E-05 |
| Auger cn | 0 | 0 | 5.00E-30 | 0 | 0 | 0 | 0 | 0 | 0 | 0 | 0 | 8.30E-32 |
| Auger cp | 0 | 0 | 1.00E-31 | 0 | 0 | 0 | 0 | 0 | 0 | 0 | 0 | 1.80E-31 |
| Auger kn | 0 | 0 | 0 | 0 | 0 | 0 | 0 | 0 | 0 | 0 | 0 | 0 |
| Auger kp | 0 | 0 | 0 | 0 | 0 | 0 | 0 | 0 | 0 | 0 | 0 | 0 |
| Copt | 0 | 0 | 1.50E-10 | 0 | 0 | 0 | 0 | 0 | 0 | 0 | 0 | 0 |
| An** | 48.1 | 1.40E-11 | 8.05 | 1.40E-11 | 30 | 1.40E-11 | 50.3 | 1.40E-11 | 1.40E-11 | 44.6 | 20.4 | 110 |
| Ap** | 1.40E-11 | 1.40E-11 | 56.8 | 1.40E-11 | 30 | 1.40E-11 | 48.1 | 1.40E-11 | 1.40E-11 | 28.8 | 24 | 30 |
| Impact Ionization Parameters | | | | | | | | | | | | |
| betan | 1 | 1 | 1.82 | 1 | 1 | 1 | 1 | 1 | 1 | 1 | 1 | 1 |
| betap | 1 | 1 | 1.75 | 1 | 1 | 1 | 1 | 1 | 1 | 1 | 1 | 1 |
| egran | 0 | 0 | 0 | 0 | 0 | 0 | 0 | 0 | 0 | 0 | 0 | 4.00E+05 |
| an1 | 7.03E+05 | 7.03E+05 | 1.90E+05 | 7.03E+05 | 7.30E+04 | 7.03E+05 | 7.30E+04 | 7.03E+05 | 7.03E+05 | 7.30E+04 | 7.30E+04 | 7.03E+05 |
| bn1 | 1.23E+06 | 1.23E+06 | 5.75E+05 | 1.23E+06 | 1.23E+06 | 1.23E+06 | 1.23E+06 | 1.23E+06 | 1.23E+06 | 1.23E+06 | 1.23E+06 | 1.23E+06 |
| an2 | 7.03E+05 | 7.03E+05 | 1.90E+05 | 7.03E+05 | 7.30E+04 | 7.03E+05 | 7.30E+04 | 7.03E+05 | 7.03E+05 | 7.30E+04 | 7.30E+04 | 7.03E+05 |
| an2 | 1.23E+06 | 1.23E+06 | 5.75E+05 | 1.23E+06 | 1.23E+06 | 1.23E+06 | 1.23E+06 | 1.23E+06 | 1.23E+06 | 1.23E+06 | 1.23E+06 | 1.23E+06 |
| ap1 | 6.71E+05 | 6.71E+05 | 2.22E+05 | 6.71E+05 | 6.71E+05 | 6.71E+05 | 6.71E+05 | 6.71E+05 | 6.71E+05 | 6.71E+05 | 6.71E+05 | 6.71E+05 |
| bp1 | 1.69E+06 | 1.69E+06 | 6.57E+05 | 1.69E+06 | 1.69E+06 | 1.69E+06 | 1.69E+06 | 1.69E+06 | 1.69E+06 | 1.69E+06 | 1.69E+06 | 1.69E+06 |
| ap2 | 1.58E+06 | 1.58E+06 | 2.22E+05 | 1.58E+06 | 1.58E+06 | 1.58E+06 | 1.58E+06 | 1.58E+06 | 1.58E+06 | 1.58E+06 | 1.58E+06 | 1.58E+06 |
| bp2 | 2.04E+06 | 2.04E+06 | 6.57E+05 | 2.04E+06 | 2.40E+05 | 2.04E+06 | 2.40E+05 | 2.04E+06 | 2.04E+06 | 2.40E+05 | 2.40E+05 | 2.04E+06 |
| Saturation Velocities | | | | | | | | | | | | |
| Vsatn (cm/s) | 1.00E+06 | 1.00E+06 | 7.70E+06 | 1.00E+06 | 1.00E+06 | 1.00E+06 | 1.00E+06 | 1.00E+06 | 1.00E+06 | 1.00E+06 | 1.00E+06 | 1.00E+07 |
| Vsatp (cm/s) | 1.00E+06 | 1.00E+06 | 7.70E+06 | 1.00E+06 | 1.00E+06 | 1.00E+06 | 1.00E+06 | 1.00E+06 | 1.00E+06 | 1.00E+06 | 1.00E+06 | 7.98E+06 |
| Mobility Parameters | | | | | | | | | | | | |
| mun (cm ² /Vs) | 165 | 22000 | 1000 | 100 | 600 | | 200 | 7 | 1020 | 4000 | 6000 | 1430 |
| tmun | 1.5 | 1.5 | 1.5 | 1.5 | 1.5 | | 1.5 | 1.5 | 1.5 | 1.5 | 1.5 | 1.5 |
| mup (cm ² /Vs) | 5 | 100 | 100 | | 700 | | 550 | | 930 | 1400 | 4000 | 480 |
| tmup | 1.5 | 1.5 | 1.5 | | 1.5 | | 1.5 | | 1.5 | 1.5 | 1.5 | 1.5 |

Note: α_{comp} is set to 0.3. See Chapter 5: "Blaze: Compound Material 2D Simulator", Section 5.3: "Material Dependent Physical Models" for more information.

Table B-25. Material Default for ternary compound semiconductors

| Material | AlGaAs | GaSbP | InAlAs | GaAsP | InGaAs | GaSbAs | InAsP | HgCdTe | InGaP |
|---|----------|----------|----------|----------|----------|----------|----------|----------|----------|
| Epsilon | 12.3 | 0 | 0 | 11.7 | 14.2 | 0 | 13.1 | 16.4 | 12.1 |
| Band Parameters | | | | | | | | | |
| Eg (eV) | 1.8 | 2.01 | 2.1 | 2.31 | 0.571 | 0.665 | 1.03 | 0.291 | 1.61 |
| Chi (eV) | 3.75 | 0 | 0 | 4.32 | 4.13 | 4.06 | 4.32 | 2.54 | 4.4 |
| Nc (per cc) | 4.35E+17 | 1 | 1 | 1.04E+18 | 1.15E+17 | 1 | 2.86E+17 | 7.58E+16 | 7.18E+17 |
| Nv (per cc) | 8.16E+18 | 1 | 1 | 8.54E+18 | 8.12E+18 | 1 | 8.54E+18 | 1.02E+19 | 8.87E+18 |
| ni (per cc) | 1.37E+03 | 1.24E-17 | 2.29E-18 | 0.125 | 1.56E+13 | 2.61E-06 | 3.56E+09 | 3.18E+15 | 7.43E+04 |
| Gc | 2 | 2 | 2 | 2 | 2 | 2 | 2 | 2 | 2 |
| Gv | 4 | 4 | 4 | 4 | 4 | 4 | 4 | 4 | 4 |
| Ed (eV) | 0.044 | 0.044 | 0.044 | 0.044 | 0.044 | 0.044 | 0.044 | 0.044 | 0.044 |
| Ea (eV) | 0.045 | 0.045 | 0.045 | 0.045 | 0.045 | 0.045 | 0.045 | 0.045 | 0.045 |
| Recombination Parameters | | | | | | | | | |
| Lifetime (el) | 1.00E-09 | 1 | 1 | 1 | 1 | 1 | 1 | 1 | 1 |
| Lifetime (ho) | 2.00E-08 | 1 | 1 | 1 | 1 | 1 | 1 | 1 | 1 |
| Auger cn | 5.00E-30 | 0 | 0 | 0 | 0 | 0 | 0 | 0 | 0 |
| Auger cp | 1.00E-31 | 0 | 0 | 0 | 0 | 0 | 0 | 0 | 0 |
| Auger kn | 0 | 0 | 0 | 0 | 0 | 0 | 0 | 0 | 0 |
| Auger kp | 0 | 0 | 0 | 0 | 0 | 0 | 0 | 0 | 0 |
| Copt | 1.50E-10 | 0 | 0 | 0 | 0 | 0 | 0 | 0 | 0 |
| An** | 8.05 | 1.40E-11 | 1.40E-11 | 14.4 | 3.32 | 1.40E-11 | 6.08 | 2.51 | 11.2 |
| Ap** | 56.8 | 1.40E-11 | 1.40E-11 | 58.6 | 56.6 | 1.40E-11 | 58.6 | 66.1 | 60.1 |
| Impact Ionization Model Parameters (Selberherr Model) | | | | | | | | | |
| betan | 1.82 | 1 | 1 | 1 | 1 | 1 | 1 | 1 | 1 |
| betap | 1.75 | 1 | 1 | 1 | 1 | 1 | 1 | 1 | 1 |
| egran | 0 | 0 | 0 | 0 | 0 | 0 | 0 | 0 | 0 |
| an1 | 1.90E+05 | 7.03E+05 | 8.60E+06 | 7.03E+05 | 7.03E+05 | 7.03E+05 | 7.03E+05 | 7.03E+05 | 7.03E+05 |
| bn1 | 5.75E+05 | 1.23E+06 | 3.50E+06 | 1.23E+06 | 1.23E+06 | 1.23E+06 | 1.23E+06 | 1.23E+06 | 1.23E+06 |
| an2 | 1.90E+05 | 7.03E+05 | 8.60E+06 | 7.03E+05 | 7.03E+05 | 7.03E+05 | 7.03E+05 | 7.03E+05 | 7.03E+05 |
| an2 | 5.75E+05 | 1.23E+06 | 3.50E+06 | 1.23E+06 | 1.23E+06 | 1.23E+06 | 1.23E+06 | 1.23E+06 | 1.23E+06 |
| ap1 | 2.22E+05 | 6.71E+05 | 2.30E+07 | 6.71E+05 | 6.71E+05 | 6.71E+05 | 6.71E+05 | 6.71E+05 | 6.71E+05 |
| bp1 | 6.57E+05 | 1.69E+06 | 4.50E+06 | 1.69E+06 | 1.69E+06 | 1.69E+06 | 1.69E+06 | 1.69E+06 | 1.69E+06 |
| ap2 | 2.22E+05 | 1.58E+06 | 2.30E+07 | 1.58E+06 | 1.58E+06 | 1.58E+06 | 1.58E+06 | 1.58E+06 | 1.58E+06 |
| bp2 | 6.57E+05 | 2.04E+06 | 4.50E+06 | 2.04E+06 | 2.04E+06 | 2.04E+06 | 2.04E+06 | 2.04E+06 | 2.04E+06 |
| Saturation Velocities | | | | | | | | | |
| Vsatn (cm/s) | 7.70E+06 | 1.00E+06 | 1.00E+06 | 1.00E+06 | 7.70E+06 | 1.00E+06 | 1.00E+06 | 1.00E+06 | 1.00E+06 |
| Vsatp (cm/s) | 7.70E+06 | 1.00E+06 | 1.00E+06 | 1.00E+06 | 7.70E+06 | 1.00E+06 | 1.00E+06 | 1.00E+06 | 1.00E+06 |

Note: α_{comp} is set to 0.3. See Chapter 5: “Blaze: Compound Material 2D Simulator”, Section 5.3: “Material Dependent Physical Models” for more information.

Table B-26 shows material defaults for quaternary compound semiconductors.

Table B-26. Material Defaults for quaternary compound semiconductors

| | | | | | | | | | | | | |
|---|----------|----------|----------|----------|----------|----------|----------|----------|----------|----------|----------|----------|
| Material : | InGaAsP | AlGaAsP | AlGaAsSb | InGaAs | InGaNP | AlGaAs | AlGaNP | AlInAs | AlInNP | InAlGaAs | InAlGaP | InAlAsP |
| Epsilon : | 12.7 | 0 | 0 | 0 | 0 | 0 | 0 | 0 | 0 | 0 | 0 | 0 |
| Band Parameters | | | | | | | | | | | | |
| Eg (eV) : | 1.27 | 0 | 0 | 0 | 0 | 0 | 0 | 0 | 0 | 1.34 | 0 | 0 |
| Chi (eV) : | 4.32 | 0 | 0 | 0 | 0 | 0 | 0 | 0 | 0 | 1.46 | 0 | 0 |
| Nc (per cc) : | 3.61E+17 | 1 | 1 | 1 | 1 | 1 | 1 | 1 | 1 | 1 | 1 | 1 |
| Nv (per cc) : | 8.54E+18 | 1 | 1 | 1 | 1 | 1 | 1 | 1 | 1 | 1 | 1 | 1 |
| ni (per cc) : | 3.72E+07 | 1 | 1 | 1 | 1 | 1 | 1 | 1 | 1 | 5.04E-12 | 1 | 1 |
| Gc : | 2 | 2 | 2 | 2 | 2 | 2 | 2 | 2 | 2 | 2 | 2 | 2 |
| Gv : | 4 | 4 | 4 | 4 | 4 | 4 | 4 | 4 | 4 | 4 | 4 | 4 |
| Ed (eV) : | 0.044 | 0.044 | 0.044 | 0.044 | 0.044 | 0.044 | 0.044 | 0.044 | 0.044 | 0.044 | 0.044 | 0.044 |
| Ea (eV) : | 0.045 | 0.045 | 0.045 | 0.045 | 0.045 | 0.045 | 0.045 | 0.045 | 0.045 | 0.045 | 0.045 | 0.045 |
| Recombination Parameters | | | | | | | | | | | | |
| Lifetime (el): | 1 | 1 | 1 | 1 | 1 | 1 | 1 | 1 | 1 | 1 | 1 | 1 |
| Lifetime (ho): | 1 | 1 | 1 | 1 | 1 | 1 | 1 | 1 | 1 | 1 | 1 | 1 |
| Auger cn : | 0 | 0 | 0 | 0 | 0 | 0 | 0 | 0 | 0 | 0 | 0 | 0 |
| Auger cp : | 0 | 0 | 0 | 0 | 0 | 0 | 0 | 0 | 0 | 0 | 0 | 0 |
| Auger kn : | 0 | 0 | 0 | 0 | 0 | 0 | 0 | 0 | 0 | 0 | 0 | 0 |
| Auger kp : | 0 | 0 | 0 | 0 | 0 | 0 | 0 | 0 | 0 | 0 | 0 | 0 |
| Copt : | 0 | 0 | 0 | 0 | 0 | 0 | 0 | 0 | 0 | 0 | 0 | 0 |
| An** : | 7.11 | 1.40E-11 | 1.40E-11 | 1.40E-11 | 1.40E-11 | 1.40E-11 | 1.40E-11 | 1.40E-11 | 1.40E-11 | 1.40E-11 | 1.40E-11 | 1.40E-11 |
| Ap** : | 58.6 | 1.40E-11 | 1.40E-11 | 1.40E-11 | 1.40E-11 | 1.40E-11 | 1.40E-11 | 1.40E-11 | 1.40E-11 | 1.40E-11 | 1.40E-11 | 1.40E-11 |
| Impact Ionization Parameters (Selberherr model) | | | | | | | | | | | | |
| betan : | 1 | 1 | 1 | 1 | 1 | 1 | 1 | 1 | 1 | 1 | 1 | 1 |
| betap : | 1 | 1 | 1 | 1 | 1 | 1 | 1 | 1 | 1 | 1 | 1 | 1 |
| egran : | 0 | 0 | 0 | 0 | 0 | 0 | 0 | 0 | 0 | 0 | 0 | 0 |
| an1 : | 7.03E+05 | 7.03E+05 | 7.03E+05 | 7.03E+05 | 7.03E+05 | 7.03E+05 | 7.03E+05 | 7.03E+05 | 7.03E+05 | 7.03E+05 | 7.03E+05 | 7.03E+05 |
| bn1 : | 1.23E+06 | 1.23E+06 | 1.23E+06 | 1.23E+06 | 1.23E+06 | 1.23E+06 | 1.23E+06 | 1.23E+06 | 1.23E+06 | 1.23E+06 | 1.23E+06 | 1.23E+06 |
| an2 : | 7.03E+05 | 7.03E+05 | 7.03E+05 | 7.03E+05 | 7.03E+05 | 7.03E+05 | 7.03E+05 | 7.03E+05 | 7.03E+05 | 7.03E+05 | 7.03E+05 | 7.03E+05 |
| an2 : | 1.23E+06 | 1.23E+06 | 1.23E+06 | 1.23E+06 | 1.23E+06 | 1.23E+06 | 1.23E+06 | 1.23E+06 | 1.23E+06 | 1.23E+06 | 1.23E+06 | 1.23E+06 |
| ap1 : | 6.71E+05 | 6.71E+05 | 6.71E+05 | 6.71E+05 | 6.71E+05 | 6.71E+05 | 6.71E+05 | 6.71E+05 | 6.71E+05 | 6.71E+05 | 6.71E+05 | 6.71E+05 |
| bp1 : | 1.69E+06 | 1.69E+06 | 1.69E+06 | 1.69E+06 | 1.69E+06 | 1.69E+06 | 1.69E+06 | 1.69E+06 | 1.69E+06 | 1.69E+06 | 1.69E+06 | 1.69E+06 |
| ap2 : | 1.58E+06 | 1.58E+06 | 1.58E+06 | 1.58E+06 | 1.58E+06 | 1.58E+06 | 1.58E+06 | 1.58E+06 | 1.58E+06 | 1.58E+06 | 1.58E+06 | 1.58E+06 |
| bp2 : | 2.04E+06 | 2.04E+06 | 2.04E+06 | 2.04E+06 | 2.04E+06 | 2.04E+06 | 2.04E+06 | 2.04E+06 | 2.04E+06 | 2.04E+06 | 2.04E+06 | 2.04E+06 |
| Saturation Velocities | | | | | | | | | | | | |
| Vsatn (cm/s) : | 1.00E+06 | 1.00E+06 | 1.00E+06 | 1.00E+06 | 1.00E+06 | 1.00E+06 | 1.00E+06 | 1.00E+06 | 1.00E+06 | 1.00E+06 | 1.00E+06 | 1.00E+06 |
| Vsatp (cm/s) : | 1.00E+06 | 1.00E+06 | 1.00E+06 | 1.00E+06 | 1.00E+06 | 1.00E+06 | 1.00E+06 | 1.00E+06 | 1.00E+06 | 1.00E+06 | 1.00E+06 | 1.00E+06 |

Table B-27 shows material defaults for organic materials.

Table B-27. Material Defaults for organic materials

| Material | Organic | Pentacene | Alq3 | TPD | PPV | Tetracene |
|-----------------------------------|-----------|-----------|-----------|-----------|-----------|-----------|
| Epsilon | 11.8 | 11.8 | 3.4 | 11.8 | 11.8 | 11.8 |
| Band Parameters | | | | | | |
| Eg (eV) | 1.08 | 1.08 | 2.4 | 1.08 | 1.08 | 1.08 |
| Chi (eV) | 4.17 | 4.17 | 4.17 | 4.17 | 4.17 | 4.17 |
| Nc (per cc) | 2.80E+19 | 2.80E+19 | 1.44E+20 | 2.80E+19 | 2.80E+19 | 2.80E+19 |
| Nv (per cc) | 1.04E+19 | 1.04E+19 | 1.44E+20 | 1.04E+19 | 1.04E+19 | 1.04E+19 |
| ni (per cc) | 1.45E+10 | 1.45E+10 | 0.998 | 1.45E+10 | 1.45E+10 | 1.45E+10 |
| Gc | 2 | 2 | 2 | 2 | 2 | 2 |
| Gv | 4 | 4 | 4 | 4 | 4 | 4 |
| Ed (eV) | 0.044 | 0.044 | 0.044 | 0.044 | 0.044 | 0.044 |
| Ea (eV) | 0.045 | 0.045 | 0.045 | 0.045 | 0.045 | 0.045 |
| An** | 129 | 129 | 385 | 129 | 129 | 129 |
| Ap** | 66.8 | 66.8 | 385 | 66.8 | 66.8 | 66.8 |
| Recombination Parameters | | | | | | |
| taun0 | 1 | 1 | 1 | 1 | 1 | 1 |
| taup0 | 1 | 1 | 1 | 1 | 1 | 1 |
| etrap | 0 | 0 | 0 | 0 | 0 | 0 |
| nsrhn | -1.00E+03 | -1.00E+03 | -1.00E+03 | -1.00E+03 | -1.00E+03 | -1.00E+03 |
| nsrhp | -1.00E+03 | -1.00E+03 | -1.00E+03 | -1.00E+03 | -1.00E+03 | -1.00E+03 |
| ksrhtn | 0.0025 | 0.0025 | 0.0025 | 0.0025 | 0.0025 | 0.0025 |
| ksrhtp | 0.0025 | 0.0025 | 0.0025 | 0.0025 | 0.0025 | 0.0025 |
| ksrhcn | 3.00E-13 | 3.00E-13 | 3.00E-13 | 3.00E-13 | 3.00E-13 | 3.00E-13 |
| ksrhcp | 1.18E-12 | 1.18E-12 | 1.18E-12 | 1.18E-12 | 1.18E-12 | 1.18E-12 |
| ksrhgn | 1.77 | 1.77 | 1.77 | 1.77 | 1.77 | 1.77 |
| ksrhgp | 0.57 | 0.57 | 0.57 | 0.57 | 0.57 | 0.57 |
| nsrhn | -1.00E+03 | -1.00E+03 | -1.00E+03 | -1.00E+03 | -1.00E+03 | -1.00E+03 |
| nsrhp | -1.00E+03 | -1.00E+03 | -1.00E+03 | -1.00E+03 | -1.00E+03 | -1.00E+03 |
| augn | 0 | 0 | 0 | 0 | 0 | 0 |
| augp | 0 | 0 | 0 | 0 | 0 | 0 |
| augkn | 0 | 0 | 0 | 0 | 0 | 0 |
| augkp | 0 | 0 | 0 | 0 | 0 | 0 |
| kaugcn | 1.83E-31 | 1.83E-31 | 1.83E-31 | 1.83E-31 | 1.83E-31 | 1.83E-31 |
| kaugcp | 2.78E-31 | 2.78E-31 | 2.78E-31 | 2.78E-31 | 2.78E-31 | 2.78E-31 |
| kaugd | 1.18 | 1.18 | 1.18 | 1.18 | 1.18 | 1.18 |
| kaugd | 0.72 | 0.72 | 0.72 | 0.72 | 0.72 | 0.72 |
| copt | 0 | 0 | 0 | 0 | 0 | 0 |
| Band-to-Band Tunneling Parameters | | | | | | |
| bb.a | 4.00E+14 | 4.00E+14 | 4.00E+14 | 4.00E+14 | 4.00E+14 | 4.00E+14 |
| bb.b | 1.90E+07 | 1.90E+07 | 1.90E+07 | 1.90E+07 | 1.90E+07 | 1.90E+07 |
| bb.gamma | 2.5 | 2.5 | 2.5 | 2.5 | 2.5 | 2.5 |
| mass.tunnel | 0.25 | 0.25 | 0.25 | 0.25 | 0.25 | 0.25 |
| me.tunnel | 1.08 | 1.08 | 3.21 | 1.08 | 1.08 | 1.08 |
| mh.tunnel | 0.556 | 0.556 | 3.21 | 0.556 | 0.556 | 0.556 |
| Saturation Velocities | | | | | | |
| Vsatn (cm/s) : | 1.00E+06 | 1.00E+06 | 1.00E+06 | 1.00E+06 | 1.00E+06 | 1.00E+06 |
| Vsatp (cm/s) : | 1.00E+06 | 1.00E+06 | 1.00E+06 | 1.00E+06 | 1.00E+06 | 1.00E+06 |

Note: `x.comp` and `y.comp` are both set to 0.3. See Chapter 5: “Blaze: Compound Material 2D Simulator”, Section 5.3: “Material Dependent Physical Models” for more information.

Table B-28. Lattice Parameters for Binary Zincblende Semiconductors [179]

| Parameter | a0 | da0/dT | C11 | C12 | b | av | ac |
|-----------|---------|------------------------|-------|-------|-------|------|-------|
| Unit | (Å) | (10 ⁻⁵ Å/K) | (GPa) | (GPa) | (eV) | (eV) | (eV) |
| GaAs | 5.65325 | 3.88 | 1221 | 566 | -2.0 | 1.16 | -7.17 |
| InP | 5.8697 | 2.79 | 1011 | 561 | -2.0 | 0.6 | -6.0 |
| AlAs | 5.6611 | 2.90 | 1250 | 534 | -2.3 | 2.47 | -5.64 |
| GaSb | 6.0959 | 4.72 | 884.2 | 402.6 | -2.0 | 0.8 | -7.5 |
| AlSb | 6.1355 | 2.60 | 876.9 | 434.1 | -1.35 | 1.4 | -4.5 |
| InAs | 6.0583 | 2.74 | 832.9 | 452.6 | -1.8 | 1.0 | -5.08 |
| GaP | 5.4505 | 2.92 | 1405 | 620.3 | -1.6 | 1.7 | -8.2 |
| AlP | 5.4672 | 2.92 | 1330 | 630 | -1.5 | 3.0 | -5.7 |
| InSb | 6.4794 | 3.48 | 684.7 | 373.5 | -2.0 | 0.36 | -6.94 |

Table B-29. Luttinger Parameters for Zincblende Semiconductors

| Parameter | γ_1 | γ_2 | γ_3 |
|-----------|------------|------------|------------|
| GaAs | 6.98 | 2.06 | 2.93 |
| InP | 5.08 | 1.60 | 2.10 |
| AlAs | 3.76 | 0.82 | 1.42 |
| GaSb | 13.4 | 4.7 | 6.0 |
| AlSb | 5.18 | 1.19 | 1.97 |
| InAs | 20.0 | 8.5 | 9.2 |
| GaP | 4.05 | 0.49 | 2.93 |
| AlP | 3.35 | 0.71 | 1.23 |
| InSb | 34.8 | 15.5 | 16.5 |

B.10: Miscellaneous Semiconductors

The remainder of the semiconductors available have defined default parameter values to various degrees of completeness [1]. The following tables describe those parameter defaults as they exist. Since many of the material parameters are currently unavailable, we recommended that you should be careful when using these materials. Make sure the proper values are used

Note: You can use the `MODEL PRINT` statement to echo the parameters used to the run-time output.

| Table B-30. Band Parameters for Miscellaneous Semiconductors | | | | | | | |
|--|---------|-----------|------------------------|----------|----------------|----------------|------|
| Material | Eg(0)eV | Eg(300)eV | a | b | m _c | m _v | χeV |
| Silicon | | | | | | | |
| Polysilicon | | | | | | | |
| Ge | 0.7437 | | 4.77×10^{-4} | 235.0 | 0.2225 | 0.2915 | 4.0 |
| Diamond | | 5.45 | 4.77×10^{-4} | 0.0 | (a) | (b) | 7.2 |
| 6H-SiC | 2.9 | 2.9 | 0.0 | 0.0 | 0.454 | 0.33 | 3.5 |
| 4H-SiC | 3.26 | 3.26 | 0.0 | 0.0 | 0.76 | 1.20 | 4.0 |
| 3C-SiC | 2.2 | 2.2 | 0.0 | 0.0 | 0.41 | 0.165 | 3.2 |
| AlP | 2.43 | 2.43 | 0.0 | 0.0 | | | |
| AlAs | 2.16 | 2.16 | 0.0 | 0.0 | | | 3.5 |
| AlSb | 1.6 | | 2.69×10^{-4} | 2.788 | (c) | 0.4 | |
| GaSb | 0.81 | | 3.329×10^{-4} | -27.6622 | (c) | 0.24 | 3.65 |
| InSb | 0.235 | | 2.817×10^{-4} | 90.0003 | 0.014 | 0.4 | 4.06 |
| ZnS | 3.8 | 3.8 | 0.0 | 0.0 | 0.4 | | 4.59 |
| ZnSe | 2.58 | 2.58 | 0.0 | 0.0 | 0.1 | 0.6 | |
| ZnTe | 2.28 | | 0.0 | 0.0 | 0.1 | 0.6 | 4.09 |
| CdS | 2.48 | 2.48 | 0.0 | 0.0 | 0.21 | 0.8 | 4.18 |
| CdSe | 1.74 | 1.74 | 0.0 | 0.0 | 0.13 | 0.45 | 4.5 |
| CdTe | 1.5 | 1.5 | 0.0 | 0.0 | 0.14 | 0.37 | |
| HgS | 2.5 | 2.5 | 0.0 | 0.0 | | | 4.28 |
| HgSe | | | | | | | |
| HgTe | | | | | | | |
| PbS | 0.37 | 0.37 | 0.0 | 0.0 | 0.25 | 0.25 | |

Table B-30. Band Parameters for Miscellaneous Semiconductors

| Material | E _g (0)eV | E _g (300)eV | a | b | m _c | m _v | χeV |
|----------|----------------------|------------------------|-----|-----|----------------|----------------|-----|
| PbSe | 0.26 | 0.26 | 0.0 | 0.0 | 0.33 | 0.34 | |
| PbTe | 0.29 | 0.29 | 0.0 | 0.0 | 0.17 | 0.20 | 4.6 |
| SnTe | 0.18 | 0.18 | 0.0 | 0.0 | | | |
| ScN | 2.15 | 2.15 | 0.0 | 0.0 | | | |
| BeTe | 2.57 | 2.57 | 0.0 | 0.0 | | | |

Notes

- $N_{c300} = 5.0 \times 10^{18}$
- $N_{v300} = 1.8 \times 10^{19}$
- $m_c(X) = 0.39$
 $m_c(G) = 0.09$
 $N_c = N_c(X) + N_c(G)$
- $m_c(G) = 0.047$
 $m_c(L) = 0.36$
 $N_c = N_c(G) + N_c(L)$

Table B-31. Static Dielectric Constants for Miscellaneous Semiconductors

| Material | Dielectric Constant |
|----------|---------------------|
| Ge | 16.0 |
| Diamond | 5.5 |
| 6H-SiC | 9.66 |
| 4H-SiC | 9.7 |
| 3C-SiC | 9.72 |
| AlP | 9.8 |
| AlAs | 12.0 |
| AlSb | 11.0 |
| GaSb | 15.7 |
| InSb | 18.0 |
| ZnS | 8.3 |
| ZnSe | 8.1 |
| CdS | 10 |

| Table B-31. Static Dielectric Constants for Miscellaneous Semiconductors | |
|---|----------------------------|
| Material | Dielectric Constant |
| CdSe | 10.6 |
| CdTe | 9.4 |
| HgS | |
| HgSe | 25.0 |
| HgTe | 20. |
| PbS | 170.0 |
| PbSe | 250.0 |
| PbTe | 412.0 |
| SnTe | 1770.0 |
| ScN | |
| BeTe | |
| ZnO | 2.0 |

| Table B-32. Mobility Parameters for Miscellaneous Semiconductors | | | | |
|---|---------------------------------|---------------------------------|--------------------|-------------------|
| Material | MUNO (cm²/Vs) | MUPO (cm²/Vs) | VSATN(cm/s) | VSAT(cm/s) |
| Ge | 3900.0 (a) | 1900.0 (b) | | |
| Diamond | 500.0 | 300.0 | 2.0×10^7 | |
| 6H-SiC | 330.0 | 300.0 | 2.0×10^7 | 1×10^7 |
| 4H-SiC | 460 | 124 | 2.2×10^7 | 1×10^7 |
| 3C-SiC | 1000.0 | 50.0 | 2.0×10^7 | 1×10^7 |
| AlP | 80.0 | | | |
| AlAs | 1000.0 | 100.0 | | |
| AlSb | 200.0 | 550.0 | | |
| GaSb | 4000.0 | 1400.0 | | |
| InSb | 7800.0 | 750.0 | | |
| ZnS | 165.0 | 5.0 | | |
| ZnSe | 100.0 | 16 | | |
| CdS | 340.0 | 50.0 | | |
| CdSe | 800.0 | | | |

| Table B-32. Mobility Parameters for Miscellaneous Semiconductors | | | | |
|--|----------------------------|----------------------------|-------------|------------|
| Material | MUNO (cm ² /Vs) | MUPO (cm ² /Vs) | VSATN(cm/s) | VSAT(cm/s) |
| CdTe | 1050.0 | 100.0 | | |
| HgS | | | | |
| HgSe | 5500.0 | | | |
| HgTe | 22000.0 | 100.0 | | |
| PbS | 600.0 | 700.0 | | |
| PbSe | 1020.0 | 930.0 | | |
| PbTe | 6000.0 | 4000.0 | | |
| SnTe | | | | |
| ScN | | | | |
| BeTe | | | | |

Notes

- Uses Equation B-4 with $\tau_{MUN}=1.66$.
- Uses Equation B-4 with $\tau_{MUP}=2.33$.

B.11: Insulators

The following tables show the default material parameters for insulator materials. As noted in the Section B.2: “Semiconductors, Insulators, and Conductors”, the only parameter required for electrical simulation in insulator materials is the dielectric constant. Thermal and optical properties are required in GIGA and LUMINOUS respectively.

| Table B-33. Default Static Dielectric Constants of Insulators | |
|---|---------------------|
| Material | Dielectric Constant |
| Vacuum | 1.0 |
| Air | 1.0 |
| Ambient | 1.0 |
| Oxide | 3.9 |
| SiO ₂ | 3.9 |
| BSG | 3.9 |
| BPSG | 3.9 |
| Nitride | 7.5 |
| SiN | 7.5 |
| Si ₃ N ₄ | 7.5 |
| OxyNitride | 7.5 |
| Sapphire | 12.0 |
| Al ₂ O ₃ | 9.3 |
| HfO ₂ | 22.0 |
| HfSiO ₄ | 12.0 |
| SnO ₂ | 9.0 |
| CuPc | 4.0 |
| NPD | 4.0 |
| CBP | 4.0 |
| Irppy | 4.0 |
| BAIq | 4.0 |

Table B-34. Default Thermal Parameters for Insulators at 300K

| Material | Thermal Capacity (J/cm ³ /K) | Thermal Conductivity (W/cm/K) |
|--------------------------------|---|-------------------------------|
| Vacuum | 0.0 | 0.0 |
| Air | 1.0 | 0.026×10^{-2} |
| Ambient | 1.0 | 0.026×10^{-2} |
| Oxide | 3.066 | 0.014 |
| SiO ₂ | 3.066 | 0.014 |
| BSG | 3.066 | 0.014 |
| BPSG | 3.066 | 0.014 |
| Nitride | 0.585 | 5.4 |
| SiN | 0.585 | 5.4 |
| Si ₃ N ₄ | 0.585 | 5.4 |
| OxyNitride | 0.585 | 5.4 |
| Sapphire | 1.97 | 33 |
| Al ₂ O ₃ | 1.97 | 33 |
| HfO ₂ | | |
| HfSiO ₂ | | |

B.12: Metals/Conductors

Table B-35 shows the default values for resistivities of metals and the temperature coefficients of resistivity [see also 249].

| Table B-35. Resistivity and Temperature Coefficient of Metals | | |
|---|--|--|
| Material | Resistivity ($\mu\Omega\cdot\text{cm}$) | Temperature Coefficient ($\mu\Omega\cdot\text{cm/K}$) |
| Aluminum | 2.6540 | 0.00429 |
| Gold | 2.35 | 0.004 |
| Silver | 1.59 | 0.0041 |
| Tungsten | 5.65 | |
| Titanium | 42.0 | |
| Platinum | 10.6 | 0.003927 |
| Palladium | 10.8 | 0.00377 |
| Cobalt | 6.24 | 0.00604 |
| Molibdinum | 5.2 | |
| Lead | 20.648 | 0.00336 |
| Iron | 9.71 | 0.00651 |
| Tantalum | 12.45 | 0.00383 |
| Copper | 6.24 | 0.00604 |
| Tin | 11.0 | 0.0047 |
| Nickel | 6.84 | 0.0069 |

B.13: Optical Properties

The default values for complex index of refraction in LUMINOUS are interpolated from the tables in [47, 92, 139, 171, 175, 268]. Rather than print the tables here, the ranges of optical wavelengths for each material are listed in Table B-36.

| Table B-36. Wavelength Ranges for Default Complex Index of Refraction | | | |
|---|-----------------|----------------------|-----------------------|
| Material | Temperature (K) | Composition Fraction | Wavelengths (microns) |
| Silicon | 300 | NA | 0.0103 - 2.0 |
| AlAs | 300 | NA | 0.2213 - 50.0 |
| GaAs | 300 | NA | 0.0 - 0.9814 |
| InSb | 300 | NA | 0.2296 - 6.5 |
| InP | 300 | NA | 0.1689 - 0.975 |
| Poly | 300 | NA | 0.1181 - 18.33 |
| SiO ₂ | 300 | NA | 0.1145 - 1.7614 |
| Alq ₃ | 300 | NA | 0.3 - 0.8 |
| ITO | 300 | NA | 0.3 - 0.8 |
| NPB | 300 | NA | 0.3 - 0.8 |
| CIGS | 300 | YES | 0.27 - 1.65 |
| CdS | 300 | NA | 0.2 - 1.6 |
| SnTe | 300 | NA | 0.2 - 1.6 |
| ZnO | 300 | NA | .349 - .898 |
| PPV | 300 | NA | 0.3 - 0.8 |

Table B-37 show the default parameters for the Sellmeier refractive index model (see Chapter 3: “Physics”, Equation 3-594) for various materials.

| Table B-37. Default Parameter Values [179] for the Sellmeier Refractive Index Model | | | | | |
|---|--------|---------|---------|---------|----------|
| Parameter | S0SELL | S1SELL | L1SELL | S2SELL | L2SELL |
| Si | 3.129 | 8.54297 | 0.33671 | 0.00528 | 38.72983 |
| Ge | 9.282 | 6.7288 | 0.66412 | 0.21307 | 62.20932 |
| GaAs | 3.5 | 7.4969 | 0.4082 | 1.9347 | 37.17526 |
| InP | 7.255 | 2.316 | 0.6263 | 2.756 | 32.93934 |
| AlAs | 2.616 | 5.56711 | 0.2907 | 0.49252 | 10.0 |
| GaSb | 13.1 | 0.75464 | 1.2677 | 0.68245 | 10.0 |

Table B-37. Default Parameter Values [179] for the Sellmeier Refractive Index Model

| | | | | | |
|------|-------|---------|---------|---------|----------|
| InAs | 11.1 | 0.71 | 2.551 | 2.75 | 45.6618 |
| GaP | 3.096 | 5.99865 | 0.30725 | 0.83878 | 17.32051 |
| InSb | 15.4 | 0.10425 | 7.15437 | 3.47475 | 44.72136 |
| GaN | 3.6 | 1.75 | 0.256 | 4.1 | 17.86057 |
| AlN | 3.14 | 1.3786 | 0.1715 | 3.861 | 15.0333 |

Table B-38 shows the default parameters for the Adachi refractive index model [1] (see Chapter 3: “Physics”, Equation 3-595) for various materials.

Table B-38. Default Parameter Values [105] for the Adachi Refractive Index Model

| Parameter | AADACHI | BADACHI | DADACHI |
|-----------|---------|---------|---------|
| GaAs | 6.3 | 9.4 | 0.34 |
| InP | 8.4 | 6.6 | 0.11 |
| AlAs | 25.3 | -0.8 | 0.28 |
| GaSb | 4.05 | 12.66 | 0.82 |
| AlSB | 59.68 | -9.53 | 0.65 |
| InAs | 5.14 | 10.15 | 0.38 |
| GaP | 22.25 | 0.9 | 0.08 |
| AlP | 24.1 | -2.0 | 0.07 |
| InSb | 7.91 | 13.07 | 0.81 |

B.13.1: SOPRA Database

The SOPRA database is a collection of complex refractive index for various materials sometimes as a function of temperature and composition. To access this data, you should specify the file name from Table B-39 using the SOPRA parameter of the MATERIAL statement. The SOPRA database is courtesy of SOPRA, a thin film metrology company located world wide (www.sopra-sa.com).

Table B-39. Contents of SOPRA Database

| File | Description | Default |
|------------|---|---------|
| 7059.nk | Glass 7059 | x |
| Ag.nk | Silver | x |
| Againp.all | $(\text{Al}_x\text{Ga}_{1-x})_{0.5}\text{In}_{0.5}\text{P}$ vs composition fraction x | x |
| Againp0.nk | $\text{Ga}_{0.5}\text{In}_{0.5}\text{P}$ | x |
| Againp1.nk | $(\text{Al}_{0.1}\text{Ga}_{0.9})_{0.5}\text{In}_{0.5}\text{P}$ | x |

Table B-39. Contents of SOPRA Database

| | | |
|-------------|---|---|
| Againp3.nk | $(\text{Al}_{0.3}\text{Ga}_{0.7})_{0.5}\text{In}_{0.5}\text{P}$ | x |
| Againp6.nk | $(\text{Al}_{0.6}\text{Ga}_{0.4})_{0.5}\text{In}_{0.5}\text{P}$ | x |
| Againp7.nk | $(\text{Al}_{0.7}\text{Ga}_{0.3})_{0.5}\text{In}_{0.5}\text{P}$ | x |
| Againp10.nk | $\text{Al}_{0.5}\text{In}_{0.5}\text{P}$ | x |
| Al.nk | Aluminum | |
| Al2o3.nk | Al_2O_3 | |
| Al2o3p.nk | Al_2O_3 (Palik) | |
| Alas.nk | AlAs | |
| Alas.all | AlAs vs temperature from 28K to 626K | x |
| Alas028t.nk | AlAs 28K | x |
| Alas052t.nk | AlAs 52K | x |
| Alas072t.nk | AlAs 72K | x |
| Alas098t.nk | AlAs 98K | x |
| Alas125t.nk | AlAs 125K | x |
| Alas152t.nk | AlAs 152K | x |
| Alas178t.nk | AlAs 178K | x |
| Alas204t.nk | AlAs 204K | x |
| Alas228t.nk | AlAs 228K | x |
| Alas305t.nk | AlAs 305K | x |
| Alas331t.nk | AlAs 331K | x |
| Alas361t.nk | AlAs 361K | x |
| Alas390t.nk | AlAs 390K | x |
| Alas421t.nk | AlAs 421K | x |
| Alas445t.nk | AlAs 445K | x |
| Alas469t.nk | AlAs 469K | x |
| Alas499t.nk | AlAs 499K | x |
| Alas527t.nk | AlAs 527K | x |
| Alas552t.nk | AlAs 552K | x |
| Alas578t.nk | AlAs 578K | x |
| Alas602t.nk | AlAs 602K | x |
| Alas626t.nk | AlAs 626K | x |

Table B-39. Contents of SOPRA Database

| | | |
|-------------|---|---|
| Alcu.nk | Aluminum Copper | x |
| Algaas.all | $\text{Al}_x\text{Ga}_{1-x}\text{As}$ vs composition fraction x | x |
| Algaas0.nk | GaAs | x |
| Algaas1.nk | $\text{Al}_{.1}\text{Ga}_{.9}\text{As}$ | x |
| Algaas2.nk | $\text{Al}_{.2}\text{Ga}_{.8}\text{As}$ | x |
| Algaas3.nk | $\text{Al}_{.3}\text{Ga}_{.7}\text{As}$ | x |
| Algaas4.nk | $\text{Al}_{.4}\text{Ga}_{.6}\text{As}$ | x |
| Algaas5.nk | $\text{Al}_{.5}\text{Ga}_{.5}\text{As}$ | x |
| Algaas6.nk | $\text{Al}_{.6}\text{Ga}_{.4}\text{As}$ | x |
| Algaas7.nk | $\text{Al}_{.7}\text{Ga}_{.3}\text{As}$ | x |
| Algaas8.nk | $\text{Al}_{.8}\text{Ga}_{.2}\text{As}$ | x |
| Algaas9.nk | $\text{Al}_{.9}\text{Ga}_{.1}\text{As}$ | x |
| Algaas10.nk | AlAs | x |
| Alon.nk | Aluminum Oxynitride | |
| Alsb.nk | AlSb | x |
| Alsi.nk | AlSi | x |
| Alsiti.nk | Aluminum Silicon Titanium | |
| Asi.nk | Aluminum Silicon | |
| Au.nk | Gold | |
| Baf2.nk | BaF_2 | |
| Bk7.nk | Glass BK7 | |
| Bk7_abs.nk | | |
| Caf2.nk | CaF_2 | |
| Carbam.nk | Amorphous Carbon | |
| Ccl4.nk | HexaChloromethane | |
| Cdse.nk | CdSe | x |
| Cdte.nk | CdTe | x |
| Co.nk | Co | x |
| Co_2.nk | Cobalt Hexagonal (Thin Flim) | |
| Cor7059.nk | Glass Corning 7059 | |
| Cosi2-4.nk | CoSi_2 | |

Table B-39. Contents of SOPRA Database

| | | |
|--------------|--------------------------------------|---|
| Cr.nk | Cr | |
| Cr3si.nk | CrSi ₃ | |
| Cr5si3.nk | Cr ₅ Si ₃ | |
| Crsi2el2.nk | Chromimum Silicide | |
| Cu.nk | Cu | x |
| Cu2o.nk | Cu ₂ O | |
| Cuo.nk | CuO | |
| Diam.nk | Diamond | x |
| Fesi2el1.nk | Iron Silicide | |
| Fesi2el2.nk | Iron Silicide | |
| Fesi2epi.nk | Iron Silicide | |
| Gaas.nk | GaAs | |
| Gaas100.nk | GaAs 100K | |
| Gaas111.nk | GaAs 111K | |
| GaasTemp.ALL | GaAs vs temperature from 31K to 634K | x |
| Gaas031t.nk | GaAs 31K | x |
| Gaas041t.nk | GaAs 41K | x |
| Gaas060t.nk | GaAs 60K | x |
| Gaas081t.nk | GaAs 81K | x |
| Gaas103t.nk | GaAs 103K | x |
| Gaas126t.nk | GaAs 126K | x |
| Gaas150t.nk | GaAs 150K | x |
| Gaas175t.nk | GaAs 175K | x |
| Gaas199t.nk | GaAs 199K | x |
| Gaas224t.nk | GaAs 224K | x |
| Gaas249t.nk | GaAs 249K | x |
| Gaas273t.nk | GaAs 273K | x |
| Gaas297t.nk | GaAs 297K | x |
| Gaas320t.nk | GaAs 320K | x |
| Gaas344t.nk | GaAs 344K | x |
| Gaas367t.nk | GaAs 367K | x |

Table B-39. Contents of SOPRA Database

| | | |
|-------------|--|---|
| Gaas391t.nk | GaAs 391K | x |
| Gaas415t.nk | GaAs 415K | x |
| Gaas443t.nk | GaAs 443K | x |
| Gaas465t.nk | GaAs 465K | x |
| Gaas488t.nk | GaAs 488K | x |
| Gaas515t.nk | GaAs 515K | x |
| Gaas546t.nk | GaAs 546K | x |
| Gaas579t.nk | GaAs 579K | x |
| Gaas603t.nk | GaAs 603K | x |
| Gaas634t.nk | GaAs 634K | x |
| Gaaso.nk | Gallium Arsenide Oxide | |
| Gaasox.nk | Gallium Arsenide Oxide | |
| Gan-uv.nk | GaN | |
| Gan01.nk | | |
| Gan02.nk | | |
| Gan03.nk | | |
| Gan60.nk | | |
| Gan70.nk | | |
| Gap.nk | GaP | x |
| Gap100.nk | GaP (100) | |
| Gapox.nk | Gallium Phosphide Oxide | |
| Gasb.nk | GaSb | x |
| Gasbox.nk | Gallium Antimonide Oxide | |
| Ge.nk | Ge | |
| Ge100.nk | Ge (100) | |
| H2o.nk | H ₂ O | |
| Hfo2.nk | H _F O ₂ | |
| Hfsi2.nk | HFSi ₂ | |
| Hgcdte.all | Hg _{1-x} Cd _x Te as a function of composition fraction x | x |
| Hgcdte0.nk | HgTe | x |
| Hgcdte2.nk | Hg _{.8} Cd _{.2} Te | x |

Table B-39. Contents of SOPRA Database

| | | |
|-------------|---|---|
| Hgcdte3.nk | $\text{Hg}_{.71}\text{Cd}_{.29}\text{Te}$ | x |
| Inas.nk | InAs | x |
| Inasox.nk | Indium Arsenide Oxide | |
| Ingaas.nk | $\text{In}_{0.53}\text{Ga}_{0.41}\text{As}$ | |
| Ingasb.all | $\text{In}_{1-x}\text{Ga}_x\text{Sb}$ as a function of composition fraction x | x |
| Ingasb0.nk | InSb | x |
| Ingasb1.nk | $\text{In}_{.9}\text{Ga}_{.1}\text{Sb}$ | x |
| Ingasb3.nk | $\text{In}_{.7}\text{Ga}_{.3}\text{Sb}$ | x |
| Ingasb5.nk | $\text{In}_{.5}\text{Ga}_{.5}\text{Sb}$ | x |
| Ingasb7.nk | $\text{In}_{.3}\text{Ga}_{.7}\text{Sb}$ | x |
| Ingasb9.nk | $\text{In}_{.1}\text{Ga}_{.9}\text{Sb}$ | x |
| Ingasb10.nk | GaSb | x |
| Inp.nk | InP | x |
| Inpox.nk | Indium Phosphide Oxide | |
| Insb.nk | InSb | x |
| Insbox.nk | Indium Antimonide Oxide | |
| Ir.nk | Ir | |
| Ir3si5e.nk | Indium Silicide | |
| Ir3si5p.nk | Indium Silicide | |
| Ito2.nk | Indium Tin Oxide | x |
| Kcl.nk | KCl | |
| Lasf9.nk | Glass LASF9 | |
| Li.nk | Li | |
| Lif.nk | LiF | |
| Mgf2.nk | MgF_2 | |
| Mo.nk | Mo | x |
| Mosi2-a.nk | Molybdenuin Silicide (Parallel) | |
| Mosi2-b.nk | Molybdenuin Silicide (Perpendicular) | |
| Nbsi-a.nk | Niobuim Silicide (Parallel) | |
| Nbsi-b.nk | Niobuim Silicide (Perpendicular) | |
| Ni.nk | Ni | x |

Table B-39. Contents of SOPRA Database

| | | |
|-------------|--|---|
| Ni2si.nk | Nickel Silicide | |
| Ni3si.nk | Nickel Silicide | |
| Nisi.nk | Nickel Silicide | x |
| Os.nk | Os | |
| P_sias.nk | Silicon Arsenide | |
| P_siud.nk | Polysilicon (heavy As doping) | |
| Pbs.nk | PbS | x |
| Pbse.nk | PbSe | x |
| Pd.nk | Pd | x |
| Pd2si-a.nk | Palladium Silicide (Parallel) | |
| Pd2si-b.nk | Palladium Silicide (Perpendicular) | |
| Pt.nk | Pt | x |
| Resil-75.nk | Si _{.75} Ge _{.25} | x |
| Resige.all | Si _x Ge _{1-x} as a function of composition fraction x | x |
| Resige0.nk | Ge | x |
| Resige1.nk | Si | x |
| Resige22.nk | Si _{.22} Ge _{.78} | x |
| Resige39.nk | Si _{.39} Ge _{.61} | x |
| Resige51.nk | Si _{.51} Ge _{.49} | x |
| Resige64.nk | Si _{.64} Ge _{.36} | x |
| Resige75.nk | Si _{.75} Ge _{.25} | x |
| Resige83.nk | Si _{.83} Ge _{.27} | x |
| Resige91.nk | Si _{.91} Ge _{.09} | x |
| Rh.nk | Rh | |
| Ringas.all | In _x Ga _{1-x} As as a function of composition fraction x | x |
| Ringas0.nk | GaAs | x |
| Ringas10.nk | In _{.1} Ga _{.9} As | x |
| Ringas20.nk | In _{.2} Ga _{.8} As | x |
| Ringas24.nk | In _{.24} Ga _{.78} As | x |
| Sf11.nk | Glass SF11 | |
| Si100_2.nk | Si (100) | |

Table B-39. Contents of SOPRA Database

| | | |
|-------------|---|---|
| Si110.nk | Si (110) | |
| Si111.nk | Si (111) | |
| Si11ge89.nk | Si _{0.11} Ge _{0.89} | |
| Si20ge80.nk | Si _{0.2} Ge _{0.8} | |
| Si28ge72.nk | Si _{0.88} Ge _{0.72} | |
| Si3n4.nk | Si ₃ N ₄ | x |
| Si65ge35.nk | Si _{0.35} Ge _{0.35} | |
| Si85ge15.nk | Si _{0.85} Ge _{0.15} | |
| Si98ge02.nk | Si _{0.98} Ge _{0.02} | |
| Siam1.nk | Amorphous Si | |
| Siam2.nk | Amorphous Si | |
| Sic.nk | SiC | x |
| Sicr-t.all | Si (0-450C) | x |
| Sicr-t02.nk | Si (20C) | x |
| Sicr-t10.nk | Si (100C) | x |
| Sicr-t15.nk | Si (150C) | x |
| Sicr-t20.nk | Si (200C) | x |
| Sicr-t25.nk | Si (250C) | x |
| Sicr-t30.nk | Si (300C) | x |
| Sicr-t35.nk | Si (350C) | x |
| Sicr-t40.nk | Si (400C) | x |
| Sicr-t45.nk | Si (450C) | x |
| Sicrir.nk | | |
| Sige_ge.nk | SiGe on Ge | |
| Sige_si.nk | SiGe on Si | |
| Singas.all | InGaAs (Strained) | |
| Singas0.nk | GaAs (Strained) | |
| Singas10.nk | In _{0.1} Ga _{0.9} As (Strained) | |
| Singas20.nk | In _{0.2} Ga _{0.8} As (Strained) | |
| Singas24.nk | In _{0.24} Ga _{0.76} As (Strained) | |
| Sio.nk | SiO | |

Table B-39. Contents of SOPRA Database

| | | |
|-------------|--|---|
| Sio2.nk | SiO ₂ | x |
| Sio2ir.nk | | |
| Sion0.nk | SiliconOxynitride (10% N) | |
| Sion20.nk | SiliconOxynitride (20% N) | |
| Sion40.nk | SiliconOxynitride (40% N) | |
| Sion60.nk | SiliconOxynitride (60% N) | |
| Sion80.nk | SiliconOxynitride (80% N) | |
| Siop.nk | SiO | |
| Sipoly.nk | Polysilicon | x |
| Sipoly10.nk | | |
| Sipoly20.nk | | |
| Sipoly30.nk | | |
| Sipoly40.nk | | |
| Sipoly50.nk | | |
| Sipoly60.nk | | |
| Sipoly70.nk | | |
| Sipoly80.nk | | |
| Sipoly90.nk | | |
| Sipore.nk | Porous Silicon | |
| Stsg.all | strained Si _x Ge _{1-x} verses composition fraction x | |
| Stsg0.nk | Ge(strained) | |
| Stsg064.nk | Si _{.064} Ge _{.936} (strained) | |
| Stsg123.nk | Si _{.123} Ge _{.877} (strained) | |
| Stsg169.nk | Si _{.169} Ge _{.831} (strained) | |
| Stsg229.nk | Si _{.229} Ge _{.771} (strained) | |
| Ta.nk | Ta | |
| Taox1.nk | Tantalum Oxide | |
| Taox2.nk | Tantalum Oxide | |
| Tasi2-a.nk | Tantalum Silicide (Parallel) | |
| Tasi2-b.nk | Tantalum Silicide (Perpendicular) | |
| Thf4.nk | ThF ₄ | |

Table B-39. Contents of SOPRA Database

| | | |
|-------------|--|---|
| Ti.nk | Ti | x |
| Tini.nk | TiN | |
| Tio2.nk | TiO ₂ | |
| Tio2b.nk | TiO ₂ | |
| Tisi-a.nk | TiSi _i | |
| V.nk | V | |
| Vsi2-a.nk | VS _{i2} (Parallel) | |
| Vsi2-b.nk | VS _{i2} (Perpendicular) | |
| W.nk | W | |
| Wsi2-a.nk | WS _{i2} (Parallel) | |
| Wsi2-b.nk | WS _{i2} (Perpendicular) | |
| Y2o3.nk | Y ₂ O ₃ | |
| Zncdte.all | Zn _{1-x} Cd _x Te as a function of composition fraction x | |
| Zncdte0.nk | ZnTe | |
| Zncdte1.nk | Zn _{.9} Cd _{.1} Te | |
| Zncdte10.nk | CdTe | |
| Zncdte3.nk | Zn _{.7} Cd _{.3} Te | |
| Zncdte5.nk | Zn _{.5} Cd _{.5} Te | |
| Zncdte7.nk | Zn _{.3} Cd _{.7} Te | |
| Zncdte9.nk | Zn _{.1} Cd _{.9} Te | |
| Znscub.nk | ZnS (Cubic) | |
| Znse.nk | ZnSe | x |
| Znsete.all | ZnSe _x Te _{1-x} as a function of composition fraction x | |
| Znsete0.nk | ZnTe | x |
| Znsete1.nk | ZnSe _{.1} Te _{.9} | |
| Znsete10.nk | ZnSe | |
| Znsete3.nk | ZnSe _{.3} Te _{.7} | |
| Znsete5.nk | ZnSe _{.5} Te _{.5} | |
| Znsete7.nk | ZnSe _{.7} Te _{.3} | |
| Znsete9.nk | ZnSe _{.9} Te _{.1} | |

Table B-39. Contents of SOPRA Database

| | | |
|------------|-------------------|--|
| Zro2.nk | ZrO ₂ | |
| Zrsi2.nk | ZrSi ₂ | |
| gan-tit.NK | | |
| sin_bf5.NK | | |

Note: You can add the INDEX.CHECK parameter to the SOLVE statement to list the values of real and imaginary index being used in each solution. The indices are only printed when you perform the ray trace at the first reference to a given beam on the SOLVE statement.

B.14: User Defined Materials

The current version of ATLAS doesn't directly support user-defined materials. A simple workaround can be done using the already existing user specifications. This workaround is based on the use of an already existing material name and modifying the material parameters as appropriate.

In ATLAS, material names are defined to give you a reasonable set of default material parameters. You can override any of these defaults using the `MATERIAL`, `IMPACT`, `MODEL`, and `MOBILITY` statements.

The key to defining new materials is to choose a material name defined in ATLAS. Then, modify the material parameters of that material to match the user material. Here, you should choose a material that has default parameter values that might best match the user material, while making sure to choose a material that is not already in the user device. Then, associate this material name with the device regions where the new material is present. To do this, either specify the chosen material name on the appropriate `REGION` statements (when the device is defined in the ATLAS syntax) or choose the material name from the materials menu when defining the region in `DEVEDIT`. Next, modify the material statements using `MATERIAL`, `IMPACT`, `MOBILITY`, and `MODEL` statements. When doing this, the `MATERIAL` parameter of the given statement should be assigned to the chosen material name.

For materials with variations in composition fraction, choose a defined material with X and/or Y composition fractions (i.e., a ternary or quaternary material). You may also find it convenient to use C interpreter functions to define the material parameters as a function of composition.

The C interpreter functions that are useful for this approach are: `F.MUNSAT`, `F.MUPSAT`, `F.BANDCOMP`, `F.VSATN`, `F.VSATP`, `F.RECOMB`, `F.INDEX`, `F.BGN`, `F.CONMUN`, `F.CONMUP`, `F.COPT`, `F.TAUN`, `F.TAUP`, `F.GAUN`, and `F.GAUP`.

When defining new materials, there is a minimum set of parameters that should be defined. This set includes bandgap (`EG300`), electron and hole density of states (`NC300` and `NV300`), dielectric permittivity (`PERMITIVITY`), and electron and hole mobilities (`MUN` and `MUP`). For bipolar devices, certain recombination parameters should also be defined such as: lifetimes (`TAUN` and `TAUP`), radiative recombination rates (`COPT`), and Auger coefficients (`AUGN` and `AUGP`).

For devices with variations in material composition, certain band-edge alignment parameters should also be defined: either electron affinity (`AFFINITY`) or edge alignment (`ALIGN`). See Section 5.1.5: "Temperature Dependence of Electron Affinity" if you're using `F.BANDCOMP` to specify a lattice temperature dependent `AFFINITY`. If impact ionization is considered, the impact ionization coefficients should also be defined.

As an example, consider the case where a device is simulating with an `AlInGaP` region. In Table B-1, we see that this material system is not defined in ATLAS. We then choose a material that's defined in ATLAS, which has default material parameters that best approximate the material parameters of the new material. In this case, we choose `InGaAsP` since, at least for this example, we feel that this material is closest to the `AlInGaP`. Next, we must specify `InGaAsP` as the material of the region(s) that is/are composed of `AlInGaP`. This can be done either on the `REGION` statement if the structure is defined in ATLAS syntax or from the material menu when the region is defined in `DEVEDIT`.

Supposing that we're satisfied with the default values of the parameters from the minimum set discussed above and that we're principally concerned with the recombination and heat flow parameters defaults, the following section of the input deck illustrates how these parameter defaults can be modified:

```
# new material AlInGaP
MATERIAL MATERIAL=InGaAsP
# SRH
MATERIAL MATERIAL=InGaAsP TAUN0=1.1e-9 TAUP0=2.3e-8
# Auger
MATERIAL MATERIAL=InGaAsP AUGN=5.8e-30 AUGP=1.1e-31
# Optical
```

```
material material=InGaAsP COPT=1.7e-30
# Thermoconductivity
MATERIAL MATERIAL=InGaAsP TC.A=2.49
# Heat capacity
MATERIAL MATERIAL=InGaAsP HC.A=1.9
```

This page is intentionally left blank.

Appendix C:

RF and Small Signal AC Parameter Extraction[239]

When performing small signal analysis, you can choose to capture various RF analysis parameters to the log file along with the default capacitance and conductance values. These include Y , Z , S , $ABCD$ and H parameters and certain gain parameters including GU_{max} (unilateral power gain), GT_{max} (maximum unilateral transducer power gain), k (stability factor), and h_{21} (current gain in dB). In all cases, these are calculated as two port parameters.

To include any of these parameters, set the appropriate parameters of the LOG statement (see Section 21.27: “LOG”).

All of the RF analysis parameters are calculated from the small signal capacitance and conductance values provided during small signal analysis (see Sections 2.9.3: “Small-Signal AC Solutions”, 2.10.3: “Parameter Extraction In DeckBuild” and 20.9: “Small Signal and Large Signal Analysis”).

An intermediate step in calculation of most of the RF parameters is the calculation of the Y parameters. Equations C-1 through C-8 describe the relationship between small signal capacitances and conductances and the complex Y parameters.

$$Re(Y_{11}) = G_{11} \cdot \text{IMPEDANCE} \cdot \text{WIDTH} \quad \text{C-1}$$

$$Im(Y_{11}) = 2\pi f C_{11} \cdot \text{IMPEDANCE} \cdot \text{WIDTH} \quad \text{C-2}$$

$$Re(Y_{12}) = G_{12} \cdot \text{IMPEDANCE} \cdot \text{WIDTH} \quad \text{C-3}$$

$$Im(Y_{12}) = 2\pi f C_{12} \cdot \text{IMPEDANCE} \cdot \text{WIDTH} \quad \text{C-4}$$

$$Re(Y_{21}) = G_{21} \cdot \text{IMPEDANCE} \cdot \text{WIDTH} \quad \text{C-5}$$

$$Im(Y_{21}) = 2\pi f C_{21} \cdot \text{IMPEDANCE} \cdot \text{WIDTH} \quad \text{C-6}$$

$$Re(Y_{22}) = G_{22} \cdot \text{IMPEDANCE} \cdot \text{WIDTH} \quad \text{C-7}$$

$$Im(Y_{22}) = 2\pi f C_{22} \cdot \text{IMPEDANCE} \cdot \text{WIDTH} \quad \text{C-8}$$

Here, IMPEDANCE is the matching impedance in ohms specified on the LOG statement. WIDTH is the device width in microns defined on the MESH statement. f is the frequency in Hz. C_{nm} is the small signal capacitance between ports n and m . G_{nm} is the small signal conductance between ports n and m . Y_{nm} is the complex Y parameter between ports n and m . $Re()$ indicates the real part of the argument. $Im()$ indicates the imaginary part of the argument.

The complex S parameters are calculated from the complex Y parameters as given in Equations C-9 through C-13.

$$\Delta_1 = \frac{1}{(1 + Y_{11})(1 + Y_{22}) - Y_{12}Y_{21}} \quad \text{C-9}$$

$$S_{11} = [(1 - Y_{11})(1 + Y_{22}) + Y_{12}Y_{21}]\Delta_1 \quad \text{C-10}$$

$$S_{12} - 2Y_{12}A_1 \quad \text{C-11}$$

$$S_{21} - 2Y_{21}A_1 \quad \text{C-12}$$

$$S_{22} = [(1 + Y_{11})(1 - Y_{22}) + Y_{12}Y_{21}]A_1 \quad \text{C-13}$$

During post-processing, you can choose to apply lumped resistances and inductances to the calculation of the complex S parameters. In the first step, ATLAS is programmed to convert the S parameters into complex Z parameters.

Equations C-14 through C-18 describe the conversion from S parameters to Z parameters.

$$A_2 = \frac{1}{(1 - S_{11})(1 - S_{22}) - S_{12}S_{21}} \quad \text{C-14}$$

$$Z_{11} = [(1 + S_{11})(1 - S_{22}) + S_{12}S_{21}]A_2 \quad \text{C-15}$$

$$Z_{12} = 2S_{12}A_2 \quad \text{C-16}$$

$$Z_{21} = 2S_{21}A_2 \quad \text{C-17}$$

$$Z_{22} = [(1 - S_{11})(1 + S_{22}) + S_{12}S_{21}]A_2 \quad \text{C-18}$$

Once you have Z parameters, you can apply the lumped resistances and inductances as described in Equations C-19 through C-26.

$$Re(Z'_{11}) = Re(Z_{11}) + (RIN + RCOM) / IMPEDANCE \quad \text{C-19}$$

$$I_m(Z'_{11}) = I_m(Z_{11}) + 2\pi f(LIN + LCOM) / IMPEDANCE \quad \text{C-20}$$

$$Re(Z'_{12}) = Re(Z_{12}) + RCOM / IMPEDANCE \quad \text{C-21}$$

$$I_m(Z'_{12}) = I_m(Z_{12}) + 2\pi fLCOM / IMPEDANCE \quad \text{C-22}$$

$$Re(Z'_{21}) = Re(Z_{21}) + RCOM / IMPEDANCE \quad \text{C-23}$$

$$I_m(Z'_{21}) = I_m(Z_{21}) + 2\pi fLCOM / IMPEDANCE \quad \text{C-24}$$

$$Re(Z'_{22}) = Re(Z_{22}) + (ROUT + RCOM) / IMPEDANCE \quad \text{C-25}$$

$$I_m(Z'_{22}) = I_m(Z_{22}) + 2\pi f(LOUT + LCOM) / IMPEDANCE \quad \text{C-26}$$

Here, RCOM, LCOM, RIN, LIN, ROUT and LOUT are the common, input and output resistances and inductances defined on the LOG statement.

Once you get the updated Z parameters, you can convert them back into S parameters as described in Equations C-27 through C-31.

$$\Delta_3 = \frac{1}{(1 + Z_{11})(1 + Z_{22}) - Z_{12}Z_{21}} \quad \text{C-27}$$

$$S_{11} = [(Z_{11} - 1)(Z_{22} + 1) - Z_{12}Z_{21}]\Delta_3 \quad \text{C-28}$$

$$S_{12} = 2Z_{12}\Delta_3 \quad \text{C-29}$$

$$S_{21} = 2Z_{21}\Delta_3 \quad \text{C-30}$$

$$S_{22} = [(Z_{11} + 1)(Z_{22} - 1) - Z_{12}Z_{21}]\Delta_3 \quad \text{C-31}$$

When not involving the application of lumped resistance and inductance to the S parameters, the Z parameters are calculated directly from the Y parameters as described by Equations C-32 through C-36.

$$\Delta_4 = \frac{1}{(Y_{11}Y_{22} - Y_{12}Y_{21})} \quad \text{C-32}$$

$$Z_{11} = Y_{22}\Delta_4 \quad \text{C-33}$$

$$Z_{12} = -Y_{12}\Delta_4 \quad \text{C-34}$$

$$Z_{21} = -Y_{21}\Delta_4 \quad \text{C-35}$$

$$Z_{22} = Y_{11}\Delta_4 \quad \text{C-36}$$

The H parameters can also be calculated directly from the Y parameters as described in Equations C-37 through C-40.

$$H_{11} = 1/Y_{11} \quad \text{C-37}$$

$$H_{12} = -Y_{12}/Y_{11} \quad \text{C-38}$$

$$H_{21} = Y_{21}/Y_{11} \quad \text{C-39}$$

$$H_{22} = (Y_{11}Y_{22} - Y_{12}Y_{21})/Y_{11} \quad \text{C-40}$$

The ABCD parameters are also directly calculated from the Y parameters as described by Equations C-41 through C-44.

$$A = -Y_{22}/Y_{21} \quad \text{C-41}$$

$$B = -1/Y_{21} \quad \text{C-42}$$

$$C = -(Y_{11}Y_{22} - Y_{12}Y_{21})/Y_{21} \quad \text{C-43}$$

$$D = -Y_{11}/Y_{21} \quad \text{C-44}$$

The gain parameters k , GU_{max} , GT_{max} and h_{21} are calculated from the S parameters as given by Equations C-45 through C-50.

$$\Delta_5 = S_{11}S_{22} - S_{12}S_{21} \quad \text{C-45}$$

$$k = \frac{1 - |S_{11}|^2 - |S_{22}|^2 + \Delta_5^2}{2|S_{12}||S_{21}|} \quad \text{C-46}$$

$$GU_{max} = \frac{0.5|S_{21}/S_{12} - 1|^2}{k|S_{21}/S_{12}| - \text{Re}(S_{21}/S_{12})} \quad \text{C-47}$$

$$GT_{max} = \frac{|S_{21}|^2}{(1 - |S_{11}|^2)(1 - |S_{22}|^2)} \quad \text{C-48}$$

$$\Delta_6 = \frac{-2|S_{21}|^2}{(1 - S_{11})(1 + S_{22}) + S_{12}S_{21}} \quad \text{C-49}$$

$$h_{21} = 20 \log_{10} (|\Delta_6|) \quad \text{C-50}$$

D.1: The Default Configuration File: defaults.in

```
#@@@@@@@@@@@@@@@@@@@@@@@@@@@@@@@@@@@@@@@@@@@@@@@@@@@@@@@@@@@@@@@@@@@@@@@@@@@@
# This is the default config file for the current version of moca.
# All parameters that make sense are assigned reasonable default values
# (e.g., temp = 300K  cut=(1,0,0)  etc).
# All others are set to illegal values (such as -1 or 0).
#@@@@@@@@@@@@@@@@@@@@@@@@@@@@@@@@@@@@@@@@@@@@@@@@@@@@@@@@@@@@@@@@@@@@@@@@@@@@

#-----
# General simulation parameters
# If maxwell=yes and restart=yes, positions are read from the
# the restart file, but momentums are given a Maxwellian distribution.
#-----

algo mode=-1 carrier=e dt=2e-15 iter=0 trans=0 restart=no seed=4212345 \
  maxwell=no

reflect mindist=-1E0

debug npick=0

output scatoutfile="scat.out" summaryoutfile="summary.out" \
  difflogfile="diff.log" currentlogfile="current.log" \
  difframplogfile="diff_ramp.log" currentramplogfile="current_ramp.log" \
  solstrfile="sol.str" \
  tstep=-1 xstep=(1,1,1) estep=50 restart=-1 wpstep=pinf \
  init=no hydro=no hist=yes qeta=no outfiles=no

#-----
# dz [=] cm.  If dz > 0.0, device width is fixed to this value,
# otherwise, if conc is set device width is set based on conc
# otherwise, width is set to achieve N particles using initial guess
# for particle concentration
#-----
particle n=0 nnorm=0 conc=0.0 dz=-1.0

# The threshold energy for DoS-dominated phonon scattering is fixed at
# 1.5eV, i.e., sufficiently above the L valley to account properly for
# XL scattering but still more or less within the validity of the k.p
# nonparabolic approximation for the first valley.
#
# bf eth=1.70, where non-parabolic dos and full-band dos do not differ
# bf eth=0.63, where non-parabolic dos and full-band dos do not differ
# bf eth=0.57, to get agreement with average over measured ii-coeff. (Kane)
# bf eth=0.42, to get agreement with lowest measured ii-coeff. (Cartier)
phon eth=0.42 model=0 file="dos_c.in"

#-----
# Interpolation of energy from k, using bandstructure tables
```

```
#
# 0 = most accurate cubic interpolation
# For strain model (when using "mmat type=1"):
#   Include the quad correction for energy and velocity WITHOUT USING
#   interpolated fitting parameters for energy/velocity as
#   a function of mole fraction.
#
# 1 = less accurate linear interpolation
# For strain model (when using "mmat type=1"):
#   Include the quad correction for energy and velocity USING
#   interpolated fitting parameters for energy/velocity as
#   a function of mole fraction.
#
# 2 = more accurate linear interpolation
# For strain model (when using "mmat type=1"):
#   Include the quad correction for energy and velocity USING
#   interpolated fitting parameters for energy/velocity as
#   a function of mole fraction.
#
#-----

bands interp=0 n=2 nk=40 file="eder40_2.in"
# The settings for the n, nk, and file parameters were moved
# from the bands2d.elec.in file to here.
# n=(2,3)
# nk=(40,40)
# interp=(0,0)
# file=("eder40_2.in","eder40_3v.in")

qbands interp=0 n=1 nk=100 file="qbandtest"
# The settings for the n, nk, and file parameters were moved
# from the bands2d.elec.in file to here.
# The file parameter on the qbands statement is not presently used.

#-----
# Bulk, 1-D, and 2-D simulation parameters
#-----

mat cut=(1.0,0.0,0.0) temp=300.0

bulk field=(0.0,0.0) doping=0.0 conc=0.0 memory=no mmfrac=0.0

oned mode=1 size=(0.0,0.0,0.0) nx=(100,0,0) conc=(0.0,0.0) reflect1d=(no,no)
vbias=0.0

enhan mode=0 tstep=-1 estep=100 xstep=(0,0,0) \
  damp=0.0 lothre=1e-20 hithre=1e20 relthre=0.05 ratio=2.0 n=10 nfrac=0.95

#-----
#traj: If mode is not 0, then particles will be initialized to be uniformly
#      distributed in the BOUND box. If mode=2, detailed information
#      will be stored about particle trajectories. If mode=1, detailed
#      will not be stored. If ZEROSCAT is not 0, all scattering
```

```

#           in the simulation will be disabled.
#-----
traj mode=0 zeroscat=no bound=(0.0,0.0,0.0,0.0) boundp=(0.0,0.0,0.0,0.0)

tunnel mode=0

excit energy=0.0 shape=0 width=0.0 rate=0.0 alpha=(0.0,0.0,0.0)

#-----
#cutoff: maximum cutoff for doping if complete ionization is used.
#-----
poisson tstep=5 iter=100 tol=(2e-4,1e-6) ioniz=no start=1 freeze=pinf \
    linpoi=no cutoff=1e25 ipoly=no hideplasmons=no

#-----
#negfield: If yes, getfield, will produce negative of the field calculated
#           from the potential. Useful in a hole frozen field simulation,
#           where potential is read in from an electron simulation.
#-----
field maxfield=(-1.0,-1.0) ramp=(-1,-1) negfield=no usebarr=no

quantum restart=no option=(no,no) decay=(100e-15,2000e-15) \
    minconc=(1e10,1e10) maxqv=-1.0 maxqf=-1.0 strength=1.0 \
    qld=(-1,-1,-1) freeze=pinf sigma=8e-8 radius=3 ladders=(1,0,0) \
    energy=no ttemp=no

import type=8 volt=false nconc=false pconc=false dop=false \
    avgvolt=false avgnconc=false avgpconc=false \
    mesh=false regions=false \
    dipsh=no adddop=no bound=(0,0,0,0) \
    boundp=(0.0,0.0,0.0,0.0) \
    voltfile="volt.in" concfile="conc.in" dopfile="dop.in" \
    gridfile="grid_filename" solfile="sol_filename" \
    verfile="ver_filename" triframe="tri_filename" \
    sdfile="sd_filename" retrofile="retro_filename" \
    strfile="str_filename"

#-----
# Physical models
#
# Phonon-scattering parameters from Tang and Hess, JAP 54:5139
# bf threshold in bands.elec.in is set so that xl vanishes
# this fairly reproduces the drift velocity versus field charac-
# teristics at 300 and 77K.
#-----

xxf temp=(220.0,550.0,685.0) defo=(3e7,2e8,2e8)

xxg temp=(140.0,215.0,720.0) defo=(5e7,8e7,11e8)

xl temp=(672.0,634.0,480.0,197.0) defo=(2e8,2e8,2e8,2e8)

ac defo=9.0

#-----

```

```
# Parameters for all four impact-ionization models
# (default=Cartier, then Cartier et al, APL 62(25):3339).
# model=Cartier
# final=no:      Sets all 3 particles after ii event to zero energy.
# weight=yes:    Doubles the weight of the primary impacting particle.
# sec=yes:       Generates a secondary particle equal in weight to
#               primary.
# csec=yes:      Generates a complementary secondary particle for slave
#               process.
# randsec=yes:   Secondary particles are randomly placed in rpos region.
# rpos=(min max): If randsec=yes, specifies minimum and maximum radii (cm)
#               of a ring-shaped region in which secondaries are placed.
#               The ring is centered about the location of ii.
#-----

impact model=cartier param=(6.25e10,3e12,6.8e14) eth=(1.2,1.8,3.45) \
  final=yes weight=no sec=no csec=no start=1000 randsec=no \
  rpos=(0.0,0.0)

#-----
# default scale = 1
# bf scale = 1.9 to get agreement with the experimental doping dependent
# low-field mobility of majority carriers
#-----
ridley tstep=-1 scale=1.9

#-----
# Parameters for analytic surface scattering model
# For more info, see
# J. Appl. Phys., vol. 79, Jan 1996, p. 911
#
# In some calibration tests, reducing SEXPL to 11.0e-10 reduced rolloff
# in mobility at high fields and gave a better fit to the universal
# mobility curves from Tagaki: Trans. on ED, 41, december 1992, p. 2357
#-----

ssparam sexpl=22.0e-10 sexpd=1.78e-10 ssfield=-1.0 file="ssphonon.dat" \
  surfphon=(0.0,0.0)
# surfphon=(7e10,0.34)
# Values above were used in a bulk example.

#-----
# Extra crossing estimators (energy distributions as a function of space)
# are calculated for the crossest region (ignored for crossreg = 0)
#-----

crossest crossreg=0

#-----
# Pipe sets up interprocess communication which lets an electron and a hole
# simulation exchange secondary particles created by impact ionization.
# If mode = master, the simulation proceeds as usual except that secondaries
# are exchanged. If mode=slave, the particles move in fields which are
# received from the master. The communication occurs in the pipe files
# designated by msfile and smfile. These files must be specified exactly
```

```

# the same in both the master and slave command files.  If initnlin = yes,
# non-linear poisson is solved once at the beginning of the simulation to
# determine the initial concentration of slave particles.  If initnlin=no,
# the concentration is set by charge neutrality.  initnlin must also be
# specified the same in slave and master command files.
#-----

bipolar comm=none msfile="msfile" smfile="smfile" nslave=0 nfracii=0.5
initnlin=yes

#-----
#INJECT block controls injection from contact
#
# dn: fraction of mesh to inject in normal direction
# dp: fraction of mesh to inject in parallel direction
# hemimax: if no, inject carriers on a full maxwellian distribution
# overinj: Maintain overinj fraction more carriers at interface than
#           required by charge neutrality
#-----
inject dn=0.0 dp=1.0 hemimax=no overinj=1e4 tstep=-1

#-----
# The treatment of broadening is a bit incomplete and inconsistent.
# Also, bulk simulations do not appear to be sensitive to cutoff, so,
# play it safe and turn off broadening. (cutoff = 0.0)
#-----
final cutoff=0.0 n=178152 nk=100 format=0 file="eord100_2.in"
# The setting for n, nk, format, and file parameter were moved
# from # bands2d.elec.in to here.
# NK= (100,100)
# N=(178152,267228)
# FORMAT=(0,0)
# FILE=("eord100_2.in","eord100_3v.in")

#-----
# Fullband numerical scattering rates
#-----

escat type=analytic fbproc=7 fbband=4 anproc=24 anband=1 \
  file="scatfl_c.uni.in" \
  phncplfile="phcpl_c.in" \
  phnfacfile="phon_fac_c.uni_300k.in" \
  plotfile="scateng_c.in"

hscat type=analytic fbproc=7 fbband=3 anproc=24 anband=1 \
  file="scatfl_v.in" \
  phncplfile="phcpl_v.in" \
  phnfacfile="phon_fac_v.in" \
  plotfile="scateng_v.in"

#-----
# Multimaterial options
#-----

mmat type=no

```

```
#-----
# Multimaterial for electrons for strained silicon
#-----

ssielec band="eder40_c_ssi_interp.in" \
  rate="rates_ssi_c_45_uni.in" phncpl="coupl_ssi_c.in" \
  latt="latts_ssi_c.in"

units length=um

#-----
# Material definition for 2-D simulation
#-----

#Note: Hard-coded associations exist (in mat.*) for materials
#       with n=1, 2, 3, 4, 5, 11, and 12. These should not be changed
#       to relate to different materials than their names below.
matdef n=1 name="Air"   eps= 1.0 barrier=0.0  rough=0.0 \
  egap=1.1245 affinity=4.17
matdef n=2 name="Si"    eps=11.7 barrier=0.0  rough=0.0 \
  egap=1.1245 affinity=4.17
matdef n=3 name="Poly"  eps=11.7 barrier=0.0  rough=0.0 \
  egap=1.1245 affinity=4.17
# For SiO2, use barrier=4.0 eV instead of barrier=3.15 for hole simulation.
# (For example, when simulating a p-MOSFET with "ALGO CARRIER=H".)
#matdef n=4 name="SiO2" eps= 3.9 barrier=3.15 rough=0.10 \
#  egap=1.1245 affinity=4.17
matdef n=4 name="SiO2"  eps= 3.9 barrier=3.15 rough=0.25 \
  egap=8.9000 affinity=1.02
matdef n=5 name="Si3N4" eps= 7.5 barrier=3.15 rough=0.0 \
  egap=1.1245 affinity=1.02
matdef n=6 name="Al"    eps= 1.0 barrier=0.69 rough=0.0 \
  egap=1.1245 affinity=3.48
matdef n=7 name="Pt"    eps= 1.0 barrier=0.85 rough=0.0 \
  egap=1.1245 affinity=3.32
matdef n=8 name="W"     eps= 1.0 barrier=0.65 rough=0.0 \
  egap=1.1245 affinity=3.52

#use barrier=0.34? for hole simulation
matdef n=9 name="Au"    eps= 1.0 barrier=0.79 rough=0.0 \
  egap=1.1245 affinity=3.38

# I will leave the two definitions below commented for now.
# Note that these already exist in the hard codes mentioned above.
#matdef n=11 name="SSi"  eps=11.7 barrier=0.0  rough=0.0 \
#  egap=1.1245 affinity=4.17
#matdef n=12 name="SiGe" eps=11.7 barrier=0.0  rough=0.0 \
#  egap=1.1245 affinity=4.17
```

D.2: File Formats

This appendix provides a description of input and output file formats used by MC DEVICE. By default, MC DEVICE writes `diff.log` files for bulk simulations and `current.log` and `sol.str` files for 2D simulations. Section D.2.1: “Silvaco Output Files” describes these file formats.

Many output files are written using the UIUC MOCA file formats. These output files use the suffix `.out` are only written when the `OUTFILES` parameter on the `OUTPUT` statement is set to `1|TRUE|YES`. By default, the `OUTFILES` parameter in the `OUTPUT` section is set to `0` and these output files are suppressed. In addition to the `OUTFILES` parameter, some `*.out` files have additional boolean control parameters (see Section 19.3.4: “Commonly-Used Statements”). Sections D.2.2: “General Output Files” through Section D.2.6: “Miscellaneous Input And Output Files” describe the UIUC MOCA output files.

Some input files use UIUC MOCA file formats. These input files use the suffix `.in` and have the same format as the corresponding UIUC MOCA output (`.out`) file.

Many files written in the UIUC MOCA file format consist of three columns. The first two columns are the x and y positions (in cm) and the third column is data field associated with that file in cgs units. You can see from the x and y values that the rows (all values of y) are scanned for each column (each value of x with y fixed) and then for each row (each value of y). Note that data (x and y values and data field) may be written at the nodes of the mesh (for potential and MC carrier concentration) or at the element centers (for the doping). Quantities are averaged over iterations greater than or equal to `ISTART` (or `time>=0`). All output files are in ASCII format.

D.2.1: Silvaco Output Files

***diff*.log** files with this extended suffix contain several time-dependent time-averaged quantities for a bulk simulation. They are as follows:

- Time = [s].
- Average Position = [cm].
- Variance of Position = [cm²].
- Diffusion Coefficient = [cm²/s].
- Diffusion-Derived Mobility = [cm²/V/s].
- Drift-derived Mobility = [cm²/V/s].

Here is the format of the columns:

```
Time      <X(t)>      <X(t)>2-<X>2      Diff_Coeff(t)      Mobility_D(t)      Mobility_E(t)
```

You can change this filename with the `DIFFLOGFILE` parameter on the `OUTPUT` statement (see Section 19.3.4: “Commonly-Used Statements”). We recommend you use the extended file suffix `diff.log` (as shown in the examples) to keep this filename consistent with this documentation.

Note: The first asterisk in the file name above represents the base file name. For example, `mcdeviceex01_diff.log`.
The second asterisk in the file name above represents a possible ramp step. For example, `mcdeviceex01_diff_field=1000.log`.

***diff_ramp.log** files with this extended suffix contain several time-averaged quantities for a bulk simulation for different bias voltages, which typically represent the steady-state solution for each bias voltage. The quantities are the same as those for ***diff*.log** but exclude the Time. Instead, they include the Electric Field = [V/cm].

You can change this filename with the `DIFFRAMPLOGFILE` parameter on the `OUTPUT` statement (see Section 19.3.4: “Commonly-Used Statements”). We recommend you use the extended file suffix `diff.log` (as shown in the examples) to keep this filename consistent with this documentation.

***current*.log** files with this extended suffix contain time-dependent time-averaged and space-averaged currents over CREGIONS defined in the input file. They are as follows:

- Time = [s].
- Current = [A/cm]. The sign convention is given at the end of the current regions section. See “Current Regions” on page 19-23.
- Velocity = [cm/s].
- Concentration-weighted force = [V/cm].
- Mobility = [cm²/V/s].

Each current, velocity, force, and mobility has first an x-directed, then a y-directed column denoted by dim=1 and dim=2 respectively. Each current, velocity, force, and mobility is also written for each current region and denoted by creg=1 up to creg=n, where n is the number of current regions.

Here is the format of the columns:

Time Current(t) Velocity(t) Force(t) Mobility(t)

You can change this filename with the CURRENTLOGFILE parameter on the OUTPUT statement (see Section 19.3.4: “Commonly-Used Statements”). We recommend you use the extended file suffix current.log (as shown in the examples) to keep this filename consistent with this documentation.

Note: The first asterisk in the file name above represents the base file name. For example, mcdeviceex02_current.log. The second asterisk in the file name above represents a possible ramp step. For example, mcdeviceex02_current_vdrain=1.log.

*current_ramp.log files with this extended suffix contain several time-averaged and space-averaged currents over CREGIONS defined in the input file for different bias voltages, which typically represent the steady-state solution for each bias voltage. The quantities are the same as those for *current*.log but exclude the Time. Instead, they include the contact voltage as vcontact_name = [V], where contact_name represents the name of the contacted for which the voltage is ramped. For example, vdrain.

You can change this filename with the CURRENTRAMPLOGFILE parameter on the OUTPUT statement (see Section 19.3.4: “Commonly-Used Statements”). We recommend you use the extended file suffix current_ramp.log (as shown in the examples) to keep this filename consistent with this documentation.

***sol*.str** files contain quantities for a 2D simulation. They are as follows:

- Arsenic = [cm⁻³] (when DOP=0 on IMPORT or IONIZ=1 on POISSON)
- Band gap = [eV]
- Boron = [cm⁻³] (when DOP=0 on IMPORT or IONIZ=1 on POISSON)
- Conduction Band DOS = [cm⁻³]
- Conduction Band Energy = [eV]
- e- Energy = [eV] (when CARRIER=E on ALGO)
- e- Velocity X = [cm/s]
- e- Velocity Y = [cm/s]
- E Field X = [V/cm]
- E Field Y = [V/cm]
- (EHP) Generation Rate = [s⁻¹]
- Electron Conc = [cm⁻³]
- Electron QFL = [eV]

-
- h+ Energy = [eV] (when CARRIER=H on ALGO)
 - h+ Velocity X = [cm/s]
 - h+ Velocity Y = [cm/s]
 - Hole Conc = [cm⁻³]
 - Hole QFL = [eV]
 - Impact (Ionization) Gen(eration) Rate = [cm⁻³/s]
 - Indium = [cm⁻³] (when DOP=0 on IMPORT or IONIZ=1 on POISSON)
 - Instant Electron Conc = [cm⁻³]
 - Instant Hole Conc = [cm⁻³]
 - Instant Potential = [V]
 - Net Doping = -Boron + Phosphorus - Indium + Arsenic = [cm⁻³]
 - Phosphorus = [cm⁻³] (when DOP=0 on IMPORT or IONIZ=1 on POISSON)
 - Potential = [V]
 - Relative Permittivity = [-]
 - Total Doping = B + P + In + As = [cm⁻³] (when DOP=0 on IMPORT or IONIZ=1 on POISSON)
 - Valence Band DOS = [cm⁻³]
 - Valence Band Energy = [eV]

All quantities above beginning with “Average” are time averages from time=0. These quantities are also Monte Carlo carrier-ensemble averages from the MC carriers, which resided in the rectangular box centered about each mesh node.

You can change this filename with the SOLSTRFILE parameter on the OUTPUT statement (see Section 19.3.4: “Commonly-Used Statements”). We recommend you use the extended file suffix sol.str (as shown in the examples) to keep this filename consistent with this documentation.

Note: The first asterisk in the file name above represents the base file name. For example, mcdeviceex02_sol.str. The second asterisk in the file name above represents a possible ramp step. For example, mcdeviceex02_sol_vdrain=1.str.

D.2.2: General Output Files

diff.out contains several time-dependent time-averaged quantities for a bulk simulation. They are as follows:

- Time = [s].
- Average Position = [cm].
- Variance of Position = [cm²].
- Diffusion Coefficient = [cm²/s].
- Diffusion-Derived Mobility = [cm²/V/s].
- Drift-derived Mobility = [cm²/V/s].

Here is the format of the columns:

```
Time    <X(t)>    <X(t)2>-<X>2    Diff_Coeff(t)    Mobility_D(t)    Mobility_E(t)
```

sol.out contains several time-averaged quantities for a 2D simulation. They are as follows:

- X/Y = [cm].
- Potential = [V].

- Force = [V/cm].
- Particle concentration = [cm^{-3}].
- Velocity = [cm/s].
- Energy = [eV].
- Impact Ionization Rate = [cm^{-3}/s].
- Electron-Hole Pair (EHP) generation rate = [s^{-1}].

Force is the electric field for holes and its negative for electrons. Force and velocity each have two components: the first is x-directed, the second is y-directed.

Here is the format of the columns:

```
X   Y   Potential   Force   Concentration   Velocity   Energy   Generation
```

xhist.out, **yhist.out** contain the energy distribution along slices in the X/Y directions. They are as follows:

- Energy = [eV].
- X/Y slice = [cm].
- Distribution = [$\text{cm}^{-3}\text{eV}^{-1}$].

Here is the format of the columns:

```
Energy   Position   Distribution
```

volt.out contains the instantaneous electric potential in V. You can import the contents of this file by copying it to another file (i.e., **volt.in**) and using an **IMPORT** statement. Importing the contents of this file may be useful when restarting a simulation or when starting with a better initial guess. The electric potential is written at each node in the mesh. Here is the format of the columns:

```
X   Y   Potential
```

avgvolt.out contains the time-averaged (for `time>=0`) electric potential in V. You can import the contents of this file by copying it to another file (i.e., **volt.in**) and using an **IMPORT** statement. Importing the contents of this file may be useful when performing simulations with a fixed electric potential (fixed field). The format of this file is the same as **volt.out**.

init*volt.out contains the instantaneous electric potential in V. Here * varies from 1 to 5 at different points during initialization. These files can be helpful to understand problems associated with initialization. The format of this file is the same as **volt.out**.

conc.out contains the instantaneous MC carrier concentration in cm^{-3} . You can import the contents of this file by copying it to another file (i.e., **conc.in**) and using an **IMPORT** statement. Importing the contents of this file may be useful when restarting a simulation or when starting with a better initial guess. The MC carrier concentration is written at each node in the mesh. Here is the format of the columns:

```
X   Y   Concentration
```

avgconc.out contains the time-averaged (for `time>=0`) MC carrier concentration in cm^{-3} . You can import the contents of this file by copying it to another file (i.e., **conc.in**) and using an **IMPORT** statement. Importing the contents of this file may be useful when starting with a better initial guess. The format of this file is the same as **conc.out**.

init*conc.out contains the instantaneous MC carrier concentration in cm^{-3} . Here * varies from 1 to 5 at different points during initialization. These files can be helpful to understand problems associated with initialization. The format of this file is the same as **conc.out**.

dop.out contains the doping in the device. They are as follows:

- X/Y = [cm].

- Doping = $[\text{cm}^{-3}]$.
- Total = $-B + P - \text{In} + \text{As}$.

Here is the format of the columns:

```
X      Y      Total      B      P      In      As
```

status.out contains the running statistics of every particle in the ensemble. The first two columns are the X and Y coordinates in [cm]. The third column is the band index of the particle. The next three columns are the components of k . The seventh column is the Monte Carlo particle weight. The last two columns are the total energy and quantum corrected energy in [eV].

Here is the format of the columns:

```
X      Y      band_num      kx      ky      kz      weight      Etot      Eq
```

xaxis.out, **yaxis.out** contain the coordinates of the grid lines in the X and Y directions. The last column is the half-way point between grid point i and $i+1$. Coordinate = [cm].

Here is the format of the columns:

```
grid_point      X      X(1/2)
```

runstats.out contains the running statistics of particles in the simulation. Here are the following statistics for every 5000 iterations:

- number of particles injected
- number of scattering events which occurred
- number of reflections during that iteration

Here is the format of the columns.

```
iteration      particles      scatterings      reflections
```

***summary.out** files with this extended suffix contain all MC DEVICE input related to an MC solve. You can change this filename with the SUMMARYOUTFILE parameter on the OUTPUT statement. We recommend you use the extended file suffix summary.out (as shown in the examples) to keep this filename consistent with this documentation. The *summary.out file will contain a summary of the input used for the last solve statement in your input file.

D.2.3: Current Output Files

current.out contains the time-averaged and space-averaged over “cregion” boxes defined in the command file. They are as follows:

- Cregion = #.
- Samples = #.
- Time = [s].
- Current = [A/cm].
- Velocity = [cm/s].
- Concentration-weighted force = [V/cm].
- Mobility = $[\text{cm}^2/\text{V/s}]$.

Each current, velocity, force and mobility has first an x-directed then a y-directed column. Here is the format of the columns:

```
Cregion      Samples      Time      Current      Velocity      Force      Mobility
```

To extract this into a file, which covers only a single cregion, you can use a statement such as the following.

```
awk '{if ($1 == 1) print $3, $4, $5, $6, $7, $8}' current.out > cbox1.out
```

creg.out contains physical properties of each current estimator region. *n* is the cregion number. *z* is the normalized width of the device. *x* and *y* are the length and depth of the cregion. Here is the format of the columns:

```
cbox  n    z    x    y
```

isub.out shows the impact ionization currents after the transient period has elapsed. The first column is the iteration number, the next column is the impact ionization current, and the last column is generation current. Here is the format of the columns:

```
iteration  II_current  generation_current
```

isub2.out contains the averaged impact ionization currents. The first line is the device width used. The second line has the impact ionization current. The second quantity is generation current.

D.2.4: Scattering Output Files

impact.out contains the running impact ionization statistics. The first column is the iteration during which the event occurred. The second column is the weight of the particle before impact ionization. The next two columns are the *x* and *y* coordinates of the particle before scattering in [cm]. The last two columns are the energies of the particle before and after the event in [eV]. Here is the format of the columns:

```
iter  weight  X    Y    Eb    Ea
```

scatmesh.out contains several time averaged scattering quantities. First, *X/Y* [cm]. The remaining columns are scattering rates.

***scat.out** files with this extended suffix contain the scattering rate table. See “Using Scattering Parameters” on page 19-55 for more information. You can change this filename with the `SCATOUTFILE` parameter on the `OUTPUT` statement. We recommend you use the extended file suffix `scat.out` to keep this filename consistent with this documentation.

sec.out contains the information about impact ionization secondary particles. The file contains the iteration number, weight of the particle, *X/Y* in [cm], and the last column is energy of the secondary particle in [eV].

```
iteration  weight  X    Y    energy
```

serest.out contains the scattering estimator output. The first column is the number of the scattering process and the remaining columns are the scattering rates in each of the different defined `seregion`'s. The last two scattering processes are inelastic and elastic empirical scattering respectively. For a description on the remaining processes, see Section 19.7.5: “Phonon Scattering”.

```
process_num  rate1  rate2  ...  rateN
```

ssrate.out contains surface scattering estimator output. The first column is the number of the `ssregion` region. The second column is the surface scattering iteration number. The third column is a factor. The last column is the region-dependent scattering rate.

```
region_num  iteration  ???  rate
```

surfphn.out contains surface phonon prefactor.

trackscat.out contains tracking information on the scattering in a specified `tsregion`. The first line is the total scattering rate in the chosen region. The remaining lines are the scattering from each process.

D.2.5: Quantum Output Files

calcsp2moca.out contains the transformation between the MC DEVICE solution grid and the Schrödinger grid. This file is only output if the quantum correction is turned on. The first column is the MC DEVICE grid point. The second column is the quantum correction grid point that falls closest to the MC DEVICE grid point. The third column is the relative distance of the SP grid point between MC grid point i and $i+1$. The last two columns are the real-space values of the quantum correction grid and the MC DEVICE grid.

Here is the format of the columns:

```
MC_grid    SP_grid    R    SP_dist    MC_dist
```

etabarr.out, **etabarr1.out** show the Eta barrier for each mesh area. The Eta barrier for each mesh area is taken to be the average of the eta barriers of the materials on each of the 4 sides of the mesh. The file is written as

```
for y=ymin:ymax {
  for x=xmin:xmax {
    write etabarr
  }
}
```

spgrid.out contains the definition of Schrödinger-Poisson grid. It is the same as with **xaxis.out**. The first column is the grid point index. The second column is the real-space coordinate in [cm].

```
grid_point    X
```

qatten.out contains quantum correction attenuation factor through the whole device traversing it one y-grid line at a time.

qcap.out contains quantum solution for simulation of a MOS capacitor with the same bounds as in **qregion**. The first two columns are the X and Y coordinates respectively, in Å. The next two columns are carrier concentration and energy respectively. Here is the format of the columns:

```
X    Y    Concentration    Energy
```

qhist.out contains quantum correction histogram. The first column is the energy bin in [eV] and the second is the energy histogram of particles in the quantum region.

qrestart.out shows the transient quantum correction particle status. The quantum Eta for each grid point in the device structure and traversed y-grid line by line.

qsol.out contains quantum correction throughout the entire device in [eV]. The results are written for each increasing y-grid line.

qsol.trans.out has exactly the same format as **qsol.out** but is the transient solution.

qstatus.out contains the quantum correction particle status. The quantum Eta for each grid point in the device structure, traversed y-grid line by line.

qvolt.out contains quantum corrected quantum potential. This may be used as an input by copying it to **qvolt.in** and using the import statement.

ttemp.out contains transverse temperature in [K] for the transverse grid lines. First column is the grid line number. The third column is the actual transverse temperature. Columns 2 and 4 are fitting parameters for the Marquardt fit method. Here is the format of the columns:

```
Grid_Line    Param1    Transverse_Temp    Param2
```

D.2.6: Miscellaneous Input And Output Files

inj_2.in contains parameters where you tell MC DEVICE how you want to simulate a Schottky barrier device. **bar_poisson** must equal the value of the silicide barrier height set in your input command (*.in) file. **hqflreg** is typically set to the substrate contact region. It is best not to modify any of the parameters relating to the Airy functions.

balance.out contains the variance reduction balancing grid. The file contains the size of the balancing grid and the number of energy bins.

oxide0x.out contains the oxide injection currents for the various current estimator regions.

crosshist.out, **xcross.out**, **ycross.out** contains tracked energies of particles that change regions.

fieldeff.out contains the effective electric field in a surface scattering region. The field is written along the x grid points only. The field is given in [V/cm].

geom.out contains the boundaries [cm] of all regions in the order they were loaded or defined in the input file. Unlike the *summary.out file (see Section D.2.2: “General Output Files”), which only contains region definitions in the input file, **geom.out** contains all region definitions including those obtained by importing the structure.

mat.out contains the location of the cell centers [cm], the relative permittivity [-], the band gap [eV], the density of states in the conduction band [cm^{-3}], the density of states in the valence band [cm^{-3}], and the quasi-Fermi potential [V]. The quasi-Fermi potential is used to calculate the density of non-MC carriers. It is also used to calculate the ionized doping concentration when using incomplete ionization.

mesh.out contains the node location [cm], mesh areas [cm^2] for 2D) inside cells of type MC (with a negative average area where it would be 0), the Poisson boundary conditions [V], and the Poisson boundary conditions types where 0=Dirichlet, 1=Neumann, 2=Interior.

D.2.7: Band Structure Input Files

Three types of band structure files are used in building the data files used in the MC simulation: band structure (used for high-resolution energy calculations), gradients, and eigenstates. Figure D-1 shows the formats. The files are located in the \$MCDEVICEDIR directory and are named **eder40_*.in**.

a.

| k_x | k_y | k_z | E_0 | E_1 | ... | E_{N_b-1} |
|-------|-------|-------|-------|-------|-----|-------------|
| . | . | . | . | . | . | . |

b.

| k_x | k_y | k_z | $\frac{\partial E_0}{\partial x}$ | ... | $\frac{\partial E_{N_b-1}}{\partial x}$ | ... | $\frac{\partial E_0}{\partial z}$ | ... | $\frac{\partial E_{N_b-1}}{\partial z}$ |
|-------|-------|-------|-----------------------------------|-----|---|-----|-----------------------------------|-----|---|
| . | . | . | . | . | . | . | . | . | . |

c.

| k_x | k_y | k_z | E_0 | ... | E_{N_b-1} |
|---------|---------|-------|-------|-----|-------------|
| c_0^0 | c_0^1 | ... | | | $c_0^{N_c}$ |
| . | | | | | |
| . | | | | | |
| . | | | | | |

Figure D-1: Formats of the band structure files: a. energies, b. gradients, c. eigenstates.

The final state is chosen based on final energy. To make this task efficient, the bandstructure tables are reordered according to energy. Figure D-2 shows the format. The files are in the `$MCDEVICEDIR` directory and are named `reord100_*.in`.

| k_x | k_y | k_z | E | n |
|-------|-------|-------|-----|-----|
| . | | | | |
| . | | | | |
| . | | | | |

Figure D-2: Format of the final-state table.

There is also a density of states table for electrons and holes. These files are located in the same directory as the bandstructure files and are named `dos_c.in` for the conduction band and `dos_v.in` for the valence band. The format of these files is a single column of probabilities of occupation discretized over 100 pts.

D.3: Examples

This appendix contains several example input files for MC DEVICE. These include: Section D.3.1: “Bulk n-type Silicon: mcdeviceex01”, Section D.3.2: “A 25-nm n-MOSFET: mcdeviceex02”, Section D.3.3: “A 25-nm n-MOSFET with Quantum Correction: mcdeviceex03”, Section D.3.4: “A 25-nm p-MOSFET: mcdeviceex04”, and Section D.3.5: “An imported 25-nm n-MOSFET: mcdeviceex05”. The example input files below and the sample output and TONYPLOT set files (for each output file) may be accessed with DECKBUILD (see Section 19.3.6: “Accessing The Examples”).

D.3.1: Bulk n-type Silicon: mcdeviceex01

```
go atlas
mcdevice
# Bulk simulation for electron transport in silicon at STP
algo mode=0 carrier=e iter=10000 dt=1e-15
# bulk simulation
bulk field=(5e2,5e2)
#bulk field=(1e3,1e3)
# write output
output tstep=1000 \
    difflogfile      ="mcdeviceex01_diff.log" \
    difframplogfile="mcdeviceex01_diff_ramp.log" \
    summaryoutfile  ="mcdeviceex01_summary.out"
# Set the number of particles (i.e. electrons).
particle n=10000

# Do a single solve at field=(5e2,5e2) V/cm.
solve
tonyplot mcdeviceex01_diff.log -set mcdeviceex01_diff_log.set

# Do a 1-step field ramp from field=5e2 V/cm to field=1e3 V/cm.
# with uniform spacing on a linear scale.
#solve fstep=5e2 ffinal=1e3
#tonyplot mcdeviceex01_diff_ramp.log -set mcdeviceex01_diff_ramp_log.set

# Do a 3-step field ramp from field=1e3 V/cm to field=1e6 V/cm.
# with uniform spacing on a logarithmic scale.
#bulk field=(1e3,1e3)
#solve nsteps=3 ffinal=1e6 uselog=1
#tonyplot mcdeviceex01_diff_ramp.log -set mcdeviceex01_diff_ramp_log.set

# Do a second solve at field=(1e3,1e3) V/cm.
#output difflogfile="mcdeviceex01_diff2.log"
#bulk field=(1e3,1e3)
#solve
#tonyplot mcdeviceex01_diff2.log -set mcdeviceex01_diff_log.set

quit
```

D.3.2: A 25-nm n-MOSFET: mcdeviceex02

```
go atlas
mcdevice
# 25-nm MOSFET definition
# see http://www-mtl.mit.edu/researchgroups/Well/
# MIT's "well-tempered" MOSFET
# Reduce from iter=200000 to iter=2500 to make a short test.
# Note that this test will not have fully reached staty-state at iter=2500.
algo mode=2 carrier=e iter=2500 dt=0.1e-15
poisson tstep=5
#Turn off enhancement for now!
#enhan mode=2 tstep=20 estep=300 xstep=(1,1,0) hithre=10.0 nfrac=0.8
# save output at regular intervals
# (-1 will default to a reasonable value)
output tstep=500 init=1 \
    currentlogfile      ="mcdeviceex02_current.log" \
    currenttramplogfile="mcdeviceex02_current_ramp.log" \
    solstrfile          ="mcdeviceex02_sol.str" \
    summaryoutfile      ="mcdeviceex02_summary.out"
# Set the maximum number of particles (i.e. electrons).
particle n=40000
# X Mesh Lines
xmesh node=1   loc=0.0000
xmesh node=45  loc=0.0225 ratio=1.00
xmesh node=145 loc=0.0725 ratio=1.00
xmesh node=189 loc=0.0950 ratio=1.00
# Y Mesh Lines
ymesh node=1   loc=-0.0615
ymesh node=6   loc=-0.0015 ratio=0.400
ymesh node=11  loc= 0.0000 ratio=0.800
ymesh node=90  loc= 0.0800 ratio=1.035
# Simulation Box
region n=1 mat=SiO2 type=out      boundp=(0.0,0.095,-0.0615,0.08)
# Substrate
region n=2 mat=Si   type=mc       boundp=(0.0,0.095,0.0,0.08)
# Gate oxide
region n=3 mat=SiO2 type=block    boundp=(0.0,0.095,-0.0015,0.0)
# Source contact
region n=4 mat=Si   type=contact  boundp=(0.0,0.0026,0.0026,0.0073) \
    name="source"
# Drain contact
region n=5 mat=Si   type=contact  boundp=(0.0924,0.095,0.0026,0.0073) \
    name="drain" usefermi=1
# Poly gate
region n=6 mat=Poly type=contact  boundp=(0.0225,0.0725,-0.0615,-0.0015) \
    name="gate"
# Substrate contact
region n=7 mat=Si   type=contact  boundp=(0.0,0.095,0.0771,0.08) \
    name="substrate"
# calculate current in cregions
cregion boundp=(0.0275,0.0675,0.0,0.08)
cregion boundp=(0.0325,0.0475,0.0,0.080)
cregion boundp=(0.0475,0.0625,0.0,0.08)
## background
```

```
doping dopant=B conc=1e15 boundp=(0.0000,0.0950,0.0,0.0800)
## source
doping dopant=As conc=2e20 \
    boundp=(0.0000,0.0293,0.0,      0.0001) \
    char =(0.0040,0.0040,0.0001,0.0170)
## source halo
doping dopant=B conc=1e19 \
    boundp=(0.0000,0.0293,0.0179,0.0181) \
    char =(0.0182,0.0182,0.0160,0.0160)
## drain
doping dopant=As conc=2e20 \
    boundp=(0.0657,0.0950,0.0,      0.0001) \
    char =(0.0040,0.0040,0.0001,0.0170)
## drain halo
doping dopant=B conc=1e19 \
    boundp=(0.0657,0.0950,0.0179,0.0181) \
    char =(0.0182,0.0182,0.0160,0.0160)
## gate
doping dopant=As conc=5e20 \
    boundp=(0.0225,0.0725,-0.0615,-0.0015)
#Uncomment to use surface scattering in this region
#ssregion boundp=(0.0153,0.0355,0.0,0.0006)
#Make rough=0.0 for the Si-SiO2 interface when using ssREGION
#matdef n=4 name="SiO2" eps=3.9 barrier=3.15 rough=0.0

# Do a single solve at vgate=vdrain=1.0 V.
solve vgate=1.0 vdrain=1.0
tonyplot mcdeviceex02_current.log -set mcdeviceex02_current_log.set
tonyplot mcdeviceex02_sol.str -set mcdeviceex02_sol_str.set

# Do a 3-step voltage ramp from vdrain=3.0 V to vdrain=0.0 V.
#solve vgate=1.0 vdrain=3.0 name="drain" vfinal=0.0 vstep=-1

# Do a 3-step voltage ramp from vdrain=0 V to vdrain=3 V.
#solve vgate=1.0 vdrain=0.0 name="drain" vfinal=3.0 vstep=1.0

# Do a longer 5-step voltage ramp from vdrain=5.0 V to vdrain=0.0 V.
#algo iter=7500
#solve vgate=1.0 vdrain=5.0 name="drain" vfinal=0.0 vstep=-1

# Do a second solve at Vgate=vdrain=2.0 V.
#output currentlogfile="mcdeviceex02_current2.log" \
#    solstrfile      ="mcdeviceex02_sol2.str"
#solve vgate=2.0 vdrain=2.0
#tonyplot mcdeviceex02_current2.log -set mcdeviceex02_current_log.set
#tonyplot mcdeviceex02_sol2.str -set mcdeviceex02_sol_str.set

quit
```

D.3.3: A 25-nm *n*-MOSFET with Quantum Correction: mcdeviceex03

```
go atlas
mcdevice
# This n-MOSFET example with quantum correction
# was created by adding input associated with the quantum
# correction model to the n-MOSFET example (mcdeviceex02).
# Please see comments in mcdeviceex02.in for a description
# of the key parameter settings.
algo mode=2 carrier=e iter=2500 dt=0.1e-15
poisson tstep=2
output restart=-1 outfiles=no init=1 \
    currentlogfile      ="mcdeviceex03_current.log" \
    currenttramplogfile="mcdeviceex03_current_ramp.log" \
    solstrfile          ="mcdeviceex03_sol.str" \
    summaryoutfile      ="mcdeviceex03_summary.out" \
    tstep=1000
particle n=60000
# X Mesh Lines
xmesh node=1   loc=0.0000
xmesh node=76  loc=0.0225 ratio=1.00
xmesh node=243 loc=0.0725 ratio=1.00
xmesh node=318 loc=0.0950 ratio=1.00
# Y Mesh Lines
ymesh node=1   loc=-0.0615
ymesh node=6   loc=-0.0015 ratio=0.4000
ymesh node=9   loc=-0.0008 ratio=0.4000
ymesh node=10  loc= 0.0000 ratio=0.8000
ymesh node=15  loc= 0.0005 ratio=1.0000
ymesh node=89  loc= 0.0800 ratio=1.0508
# Simulation Box
region n=1 mat=SiO2 type=out      boundp=(0.0,0.095,-0.0615,0.08)
# Substrate
region n=2 mat=Si   type=mc       boundp=(0.0,0.095,0.0,0.08)
# Gate oxide
region n=3 mat=SiO2 type=block    boundp=(0.0,0.095,-0.0015,0.0)
# Source contact
region n=4 mat=Si   type=contact  boundp=(0.0,0.0072,0.0033,0.0135) \
    name="source"
# Drain contact
region n=5 mat=Si   type=contact  boundp=(0.0878,0.095,0.0033,0.0135) \
    name="drain" usefermi=1
# Poly gate
region n=6 mat=Poly type=contact  boundp=(0.0225,0.0725,-0.0615,-0.0015) \
    name="gate"
# Substrate contact
region n=7 mat=Si type=contact    boundp=(0.0,0.095,0.0761,0.08) \
    name="substrate"
# calculate current in cregions
cregion boundp=(0.0285,0.0665,0.0,0.08)
cregion boundp=(0.0357,0.0506,0.0,0.08)
cregion boundp=(0.0447,0.0596,0.0,0.08)
# use quantum correction
qregion mode=schroedinger dir=y tstep=4000 xstep=1 boundp=(0.0,0.095,-
0.0008,0.0026)
```

```
# Regions for quantum correction
schrregion n=1 mat=SiO2 boundp=(-0.0015,0.0000)
schrregion n=2 mat=Si boundp=( 0.0000,0.0300)
#schroedinger mesh
schrmesh node=1 loc=-0.0015
schrmesh node=11 loc= 0.0000 ratio=0.84
schrmesh node=41 loc= 0.0050 ratio=1.069
schrmesh node=71 loc= 0.0300 ratio=1.043
#does nothing, set boundaries equal to device boundaries
ebregion boundp=(0.0,0.095,-0.0615,0.0178)
#surface scattering region
#ssregion boundp=(0.0225,0.0725,-0.0008,0.0014)
#Make rough = 0.0 for interface when using ssregion
#matdef N=4 name="SiO2" eps=3.9 barrier=3.15 rough=0.0
## background
doping dopant=B conc=1e15 \
    boundp=(0.0000,0.0950,0.0,0.0800)
## source
doping dopant=As conc=2e20 \
    boundp=(0.0000,0.0293,0.0, 0.0001) \
    char =(0.0040,0.0040,0.0001,0.0170)
## source halo
doping dopant=B conc=2.5e19 \
    boundp=(0.0000,0.0293,0.0179,0.0181) \
    char =(0.0182,0.0182,0.0160,0.0160)
## drain
doping dopant=As conc=2e20 \
    boundp=(0.0657,0.0950,0.0, 0.0001) \
    char =(0.0040,0.0040,0.0001,0.0170)
## drain halo
doping dopant=B conc=2.5e19 \
    boundp=(0.0657,0.0950,0.0179,0.0181) \
    char =(0.0182,0.0182,0.0160,0.0160)
## gate
doping dopant=As conc=2e20 \
    boundp=(0.0225,0.0725,-0.0615,-0.0015)

# Do a single solve for vgate=vdrain=1.0 V.
solve vgate=1.0 vdrain=1.0
tonyplot mcdeviceex03_current.log -set mcdeviceex03_current_log.set
tonyplot mcdeviceex03_sol.str -set mcdeviceex03_sol_str.set

# Do a 1-step voltage ramp from vdrain=1.0 V to vdrain=2.0 V.
#solve vgate=1.0 vdrain=1.0 name="drain" vfinal=2.0 vstep=1.0

# Do a second solve at Vgate=Vdrain=2.0 V.
#output currentlogfile="mcdeviceex03_current2.log" \
#    solstrfile ="mcdeviceex03_sol2.str"
#solve vgate=2.0 vdrain=2.0
#tonyplot mcdeviceex03_current2.log -set mcdeviceex03_current_log.set
#tonyplot mcdeviceex03_sol2.str -set mcdeviceex03_sol_str.set

quit
```

D.3.4: A 25-nm *p*-MOSFET: mcdeviceex04

```
go atlas
mcdevice
# This p-MOSFET example was created by changing the type
# of all dopants and the polarity of all applied biases for the
# the n-MOSFET example (mcdeviceex02). Please see comments
# in mcdeviceex02.in for a description of key parameter settings.
algo mode=2 carrier=h iter=2500 dt=0.1e-15
poisson tstep=5 linpoi=no
output outfiles=no tstep=500 \
    currentlogfile      ="mcdeviceex04_current.log" \
    currenttramplogfile="mcdeviceex04_current_ramp.log" \
    solstrfile          ="mcdeviceex04_sol.str" \
    summaryoutfile      ="mcdeviceex04_summary.out"
particle n=40000
# X Mesh Lines
xmesh node=1   loc=0.0000
xmesh node=45  loc=0.0225 ratio=1.00
xmesh node=145 loc=0.0725 ratio=1.00
xmesh node=189 loc=0.0950 ratio=1.00
# Y Mesh Lines
ymesh node=1   loc=-0.0615
ymesh node=6   loc=-0.0015 ratio=0.400
ymesh node=11  loc =0.0000 ratio=0.800
ymesh node=90  loc =0.0800 ratio=1.035
# Simulation Box
region n=1 mat=SiO2 type=out      boundp=(0.0,0.095,-0.0615,0.08)
# Substrate
region n=2 mat=Si   type=mc       boundp=(0.0,0.095,0.0,0.08)
# Gate oxide
region n=3 mat=SiO2 type=block    boundp=(0.0,0.095,-0.0015,0.0)
# Source contact
region n=4 mat=Si   type=contact  boundp=(0.0,0.0026,0.0026,0.0073) \
    name="source"
# drain contact
region n=5 mat=Si   type=contact  boundp=(0.0924,0.095,0.0026,0.0073) \
    name="drain" usefermi=1
# Poly gate
region n=6 mat=Poly type=contact  boundp=(0.0225,0.0725,-0.0615,-0.0015) \
    name="gate"
# Substrate contact
region n=7 mat=Si   type=contact  boundp=(0.0,0.095,0.0771,0.08) \
    name="substrate"
# calculate current in cregions
cregion boundp=(0.0275,0.0675,0.0,0.08)
cregion boundp=(0.0325,0.0475,0.0,0.080)
cregion boundp=(0.0475,0.0625,0.0,0.08)
## background
doping dopant=As conc=1e15 \
    boundp=(0.0000,0.0950,0.0,0.0800)
## source
doping dopant=B conc=2e20 \
    boundp=(0.0000,0.0293,0.0,      0.0001) \
    char   =(0.0040,0.0040,0.0001,0.0170)
```

```
## source halo
doping dopant=As conc=1e19 \
  boundp=(0.0000,0.0293,0.0179,0.0181) \
  char =(0.0182,0.0182,0.0160,0.0160)
## drain
doping dopant=B conc=2e20 \
  boundp=(0.0657,0.0950,0.0, 0.0001) \
  char =(0.0040,0.0040,0.0001,0.0170)
## drain halo
doping dopant=As conc=1e19 \
  boundp=(0.0657,0.0950,0.0179,0.0181) \
  char =(0.0182,0.0182,0.0160,0.0160)
## gate
doping dopant=B conc=5e20 \
  boundp=(0.0225,0.0725,-0.0615,-0.0015)
#Uncomment to use surface scattering in this region
##ssregion bound=(31,71,11,14)
#ssregion boundp=(0.0153,0.0355,0.0e+0,0.0006)
#Make rough=0.0 for the Si-SiO2 interface when using ssregion
#matdef n=4 name="SiO2" eps=3.9 barrier=3.15 rough=0.0
# These settings are for MC holes in unstrained silicon.
phon eth=1.5 model=0 file="dos_v.in"
bands n=3 nk=40 file="eder40_3v_so.in"
final n=267228 nk=100 format=0 file="eord100_3v_so.in"

# Do a single solve at Vgate=vdrain=-1.0 V.
solve vgate=-1.0 vdrain=-1.0
tonyplot mcdeviceex04_current.log -set mcdeviceex04_current_log.set
tonyplot mcdeviceex04_sol.str -set mcdeviceex04_sol_str.set

# Do a 1-step voltage ramp from vdrain=-1 V to vdrain=-2 V.
#solve vgate=-1.0 vdrain=-1.0 name="drain" vfinal=-2.0 vstep=-1.0

# Do a second solve at Vgate=vdrain=-2.0 V.
#output currentlogfile="mcdeviceex04_current2.log" \
#      solstrfile      ="mcdeviceex04_sol2.str"
#solve vgate=-2.0 vdrain=-2.0
#tonyplot mcdeviceex04_current2.log -set mcdeviceex04_current_log.set
#tonyplot mcdeviceex04_sol2.str -set mcdeviceex04_sol_str.set

quit
```

D.3.5: An imported 25-nm *n*-MOSFET: mcdeviceex05

```
go atlas
mcdevice
algo      mode=2 iter=2500 dt=0.1e-15
import    mesh=true regions=true dop=true \
          strfile="mcdeviceex05_atlas.str"
particle  n=40000
region    name="source"      type=contact
region    name="drain"       type=contact usefermi=1
region    name="gate"        type=contact
region    name="substrate"   type=contact
cregion    boundp=(0.0275,0.0675,0.0,0.08)
cregion    boundp=(0.0325,0.0475,0.0,0.08)
cregion    boundp=(0.0475,0.0625,0.0,0.08)
output    tstep=500 \
          currentlogfile      ="mcdeviceex05_current.log" \
          currentramplogfile="mcdeviceex05_current_ramp.log" \
          solstrfile          ="mcdeviceex05_sol.str" \
          summaryoutfile      ="mcdeviceex05_summary.out"

# Do a single solve at Vgate=vdrain=1.0 V.
solve     vgate=1.0 vdrain=1.0
tonyplot  mcdeviceex05_current.log -set mcdeviceex05_current_log.set
tonyplot  mcdeviceex05_sol.str -set mcdeviceex05_sol_str.set

# Do a 1-step voltage ramp from vdrain=1.0 V to vdrain=2.0 V.
#solve    vgate=1.0 vdrain=1.0 name="drain" vfinal=2.0 vstep=1.0

# Do a second solve at Vgate=Vdrain=2.0 V.
#output    currentlogfile="mcdeviceex05_current2.log" \
#          solstrfile      ="mcdeviceex05_sol2.str"
#solve     vgate=2.0 vdrain=2.0
#tonyplot  mcdeviceex05_current2.log -set mcdeviceex05_current_log.set
#tonyplot  mcdeviceex05_sol2.str -set mcdeviceex05_sol_str.set

quit
```

This page is intentionally left blank

This appendix is a collection of answers to commonly asked questions about the operation of ATLAS. This information has been previously published in articles in The Simulation StandardTM, Silvaco's trade publication. The original articles can be viewed at Silvaco's home page at <http://www.silvaco.com>.

Question:

Can ATLAS handle photogeneration from non-normally incident light? What syntax is used to determine the correct photogeneration rate?

Answer:

The models with LUMINOUS allow simulation of photogeneration within ATLAS. Arbitrary light sources are available within Luminous using the BEAM statement. The program uses geometric ray tracing to determine the path of a light beam including refraction and reflection of non-normally incident light. It then applies models for the absorption of the light to determine the photogeneration rate.

To use luminous the user should first define a light source using the BEAM statement and then choose the light intensity using a SOLVE statement. The BEAM statement can be explained by a simple example. The following syntax generates the ray trace in Figure C-1.

```
BEAM NUM=1 X.ORIGIN=3.0 Y.ORIGIN=-5.0 ANGLE=60.0 \  
MIN.W=-1 MAX.W=1 WAVEL=0.6 REFLECT=2
```

The parameter NUM sets the beam number. LUMINOUS can applications up to 10 independent beams. X.ORIGIN and Y.ORIGIN define the initial starting point for the light beam. This must be outside the device coordinates and for non-normal beams it is important to keep this point well away from the device. The ANGLE parameter determines the direction of the light beam relative to the X axis. ANGLE=90 gives normal incidence from the top of the device. The light is defined as coming from a line perpendicular to the direction set by ANGLE and passing through (X.ORIGIN, Y.ORIGIN). MAX.W and MIN.W set a window along this line through which the light passes. The default for these parameters is +/- infinity.

The wavelength of the light beam is defined in microns using the WAVEL parameter. It is also possible to specify spectral sources of light by replacing WAVEL with POWER.FILE={filename}, where the {file} is a UNIX text file defining the spectrum in terms of an XY list of wavelength vs intensity.

LUMINOUS automatically chooses the number of rays needed to resolve the geometry. In the case of Figure C-1, only one initial ray is needed. The number of rays used by LUMINOUS is purely a function of the geometry and is not related to optical intensity, photogeneration rate, or MIN.W and MAX.W. The REFLECT parameter is used to limit the number of reflections the light beam is allowed. In ATLAS Version 3.0.0.R an alternative parameter MIN.POWER is used to set a relative intensity below which no more rays are traced.

The user has a choice in LUMINOUS as to whether the rays should reflect from the sidewalls and bottom of the device structure. If the simulation is of a partial wafer (such as is typical for CCD simulation) the light should not reflect. This is the default shown in Figure C-1. If the simulation is of a complete device, such as is typical for solar cells, the light should reflect. The parameter BACK.REFL is used to enable back and side reflection. The result of adding this to the previous syntax is shown in Figure C-2. In this figure the limit set by REFLECT=2 is also clear as each ray reflects only two times.

The ray trace is only done once a SOLVE statement is used to turn on the light beam. For example, the syntax `SOLVE B1=0.5` sets the power of beam #1 to $0.5\text{W}/\text{cm}^2$. DC and transient ramps of light intensity can also be performed.

The refraction and reflection are determined by the real portion of the refractive index for each material. The imaginary portion on the refractive index controls the absorption of the light. Wavelength dependent defaults exist in ATLAS for common materials, but can be defined by the user as follows:

```
MATERIAL MATERIAL=Silicon REAL.INDEX={value} IMAG.INDEX={value}
```

From the ray trace information and the imaginary refractive indices, the photogeneration rate is calculated at each node in the structure. An integration method is used to ensure the charge generated is independent of the mesh density. The photogeneration rate from the ray trace in Figure C-2 is shown in Figure C-3. The electrons and holes generated are included in electrical simulations in ATLAS to determine collection efficiency, spectral response and other device parameters.

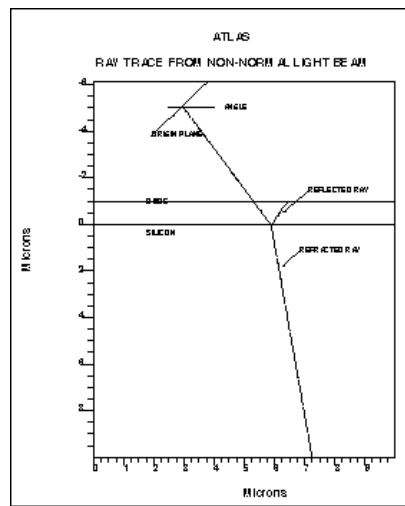


Figure C-1: Simple ray trace in LUMINOUS

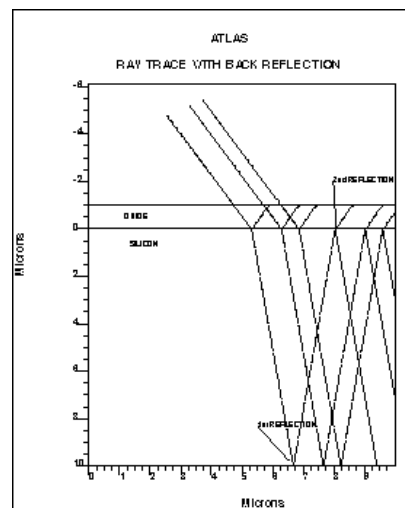


Figure C-2: Addition of back and sidewall reflection to Figure C-1

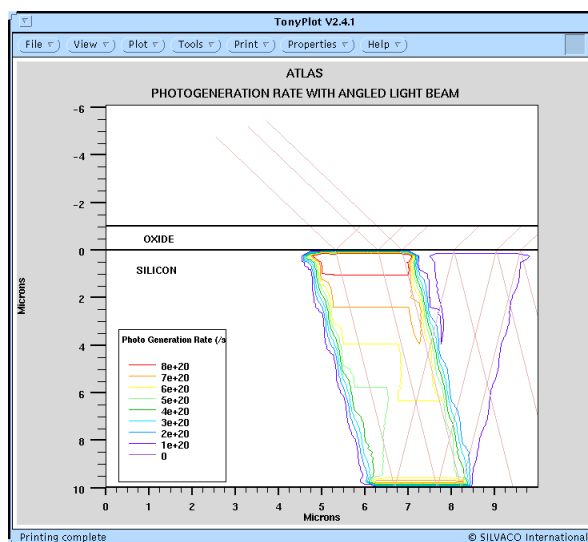


Figure C-3: Photogeneration contours based on ray trace in Figure C-2

Question:

What choices of numerical methods are available in ATLAS? When should each type of method be used?

Answer:

The latest release of ATLAS features more choices of numerical methods for users. It also has a new more logical syntax that clears up some of the previously confusing issues with the choice of numerical method for ATLAS solutions.

ATLAS has the ability to solve up to six equations on the simulation mesh. These are the Poisson equation, two carrier continuity equations, two carrier energy balance equations, and the lattice heat flow equation. The choice of numerical technique in solving these equations can strongly affect both the convergence and CPU time required to complete a simulation run.

In general equations can either be solved in a coupled manner with all equations solved at once or a decoupled manner with a subset of the equation solved whilst others are held constant. The coupled solutions are best when the interactions between the equations is strong (i.e., high current producing significant local heating). However they require a good initial guess to the solution variables for reliable convergence. Unless special techniques, such as projection, are used for calculating initial guesses this would mean that the voltage step size during a bias ramp might have to be rather small.

Decoupled methods can have advantages when the interaction between the equations is small (typically low current and voltage levels). They do not require such good initial guesses for convergence. They tend to either not converge or take excessive CPU time once the interactions become stronger.

ATLAS uses the `METHOD` statement to define numerical methods. The older `SYMBOLIC` statement is no longer required, although existing input files will run as before. To select the decoupled method for two carriers use:

```
method gummel carriers=2
```

To select the coupled method for two carriers use:

```
method newton carriers=2
```

This is the default. In fact users do not need to specify a `METHOD` statement at all for this case. For the majority of isothermal drift-diffusion simulations this choice of numerics is the recommended one.

ATLAS has the ability to switch automatically between different numerical methods. The syntax

```
method gummel newton
```

would start each bias point using a decoupled method and then switch to a coupled solution. This technique is extremely useful when the initial guess is not good. Typically this happens for devices with floating body effects (i.e., SOI).

For more complex simulation with energy balance or lattice heating other techniques are also available in ATLAS. A mixed technique where the poisson and continuity equations are solved coupled, and then the other equations are decoupled can be applied.

The syntax for this is:

```
method block
```

Typically this mixed technique is quicker and more robust at low lattice and carrier temperatures, whereas the fully coupled technique is better for high lattice and carrier temperatures. The mixed method can be combined very effectively with the fully coupled technique to provide improved speed and convergence for all ranges using:

```
method block newton
```

As an example of this Figure C-4 shows the CPU time taken for individual biasing points for a non-isothermal energy balance simulation of second breakdown of a sub-micron MOSFET. The device was constructed using ATHENA and the mesh contains a low number of obtuse triangles (not zero). The graph clearly shows that at initially the coupled method takes much longer to converge. This is because the initial guess is not good until two bias points are solved so that projection can be used. As the voltage is increased the block method has increasing convergence difficulty whereas the time taken for the newton method is flat. The time for the mixed method has the advantages of block at lower currents, but without the severe increases of block.

The ideal solution for most problems is the use of the mixed "block newton" method initially switching to the fully coupled "newton" method as the simulation proceeds. Of course the cross-over point, which is at $x=2.5$ in Figure C-4, varies from case to case. To avoid excessive user-interaction the "block newton" could be used throughout the simulation without a very excessive hit in terms of CPU time.

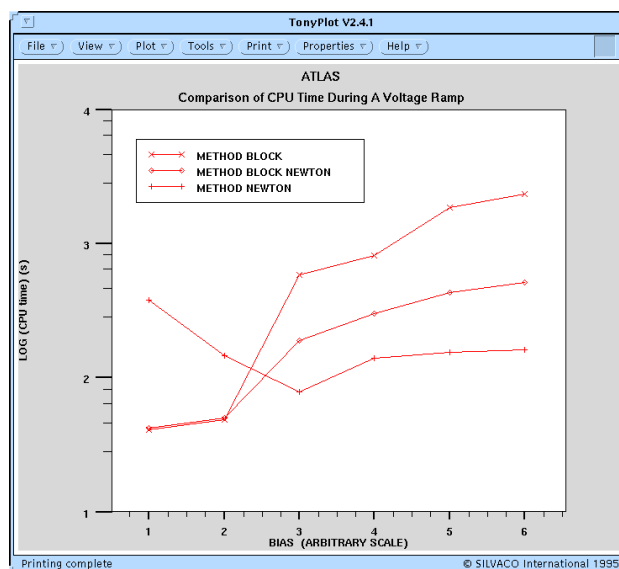


Figure C-4: Comparison of CPU time showing advantages of decoupled methods at low current and coupled method at high currents

Question:

Can the workfunction of the MOS polysilicon gate contact be calculated by ATLAS based on the doping? Can poly depletion effects be simulated in ATLAS?

Answer:

The polysilicon gate contact in MOS devices can be simulated in two distinct ways using ATLAS. These correspond to treating the polysilicon region as:

- A metal-like equipotential region with a specified workfunction.
- A semiconductor region with a potential defined by the doping level.

Most commonly the former approach is adopted. The polysilicon region acting as the gate is defined as an electrode in ATHENA.

The `electrode` statement is used with the `X` and `Y` parameters acting as crosshairs to target a particular region of the structure. The whole region, irrespective of shape, is then defined as an electrode.

```
ELECTRODE NAME=gate X={x value} Y={y value}
```

A region defined this way is now treated as equipotential in ATLAS. The potential of this region will be defined by the `VGATE` parameter of the `SOLVE` statement. Hence poly depletion cannot be modeled in gate contacts defined this way. The workfunction of this region must be set by the user. For example, a heavily n doped polysilicon contact can be defined by either of the two following statements:

```
CONTACT NAME=gate N.POLY
CONTACT NAME=gate WORK=4.17
```

The second approach of treating the polysilicon gate region as a semiconductor is achieved by placing a contact on the top of the gate. In ATHENA this is done by depositing a metal (or silicide) layer on top of the polysilicon. The `ELECTRODE` statement is then used to define this metal region as the gate electrode. In ATLAS a workfunction for the gate should not be specified on the `CONTACT` statement as this would give an undesirable workfunction difference between the metal and polysilicon. the

potential on the metal region is defined by the `VGATE` parameter of the `SOLVE` statement. The potential within the polysilicon gate region will depend on the doping level of the polysilicon. In non-degenerately doped polysilicon a voltage drop is seen across this region from top to bottom. The workfunction difference between the gate and the substrate can be derived from a potential profile through the channel region.

It is also possible for the polysilicon to be depleted starting at the gate oxide interface. Figure C-5 shows a comparison of high frequency CV curves between a MOS device with a uniform degenerately doped poly gate typical when tube doping is used and a lighter, non-uniformly doped gate typical when source/drain implants are used to dope the polysilicon. In the accumulation region the poly begins to deplete leading to an effectively thicker gate dielectric. This effect is illustrated in Figure C-6. The amount of poly depletion observed is dependent on the doping level. Accurate polysilicon diffusion models are available in ATHENA to simulate the doping. In addition the `SILICIDE` module allows simulation of the dopant redistribution during gate silicidation. Silicides can typically reduce the effective gate doping making poly depletion more likely.

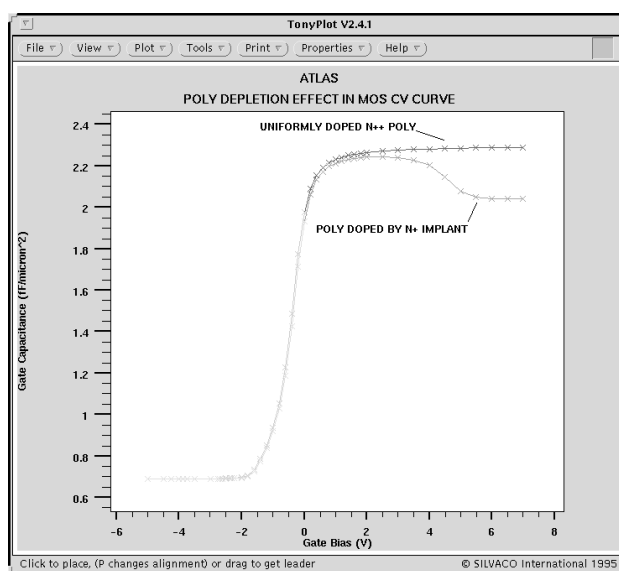


Figure C-5: High frequency CV curve showing poly depletion effects at positive V_{gs} .

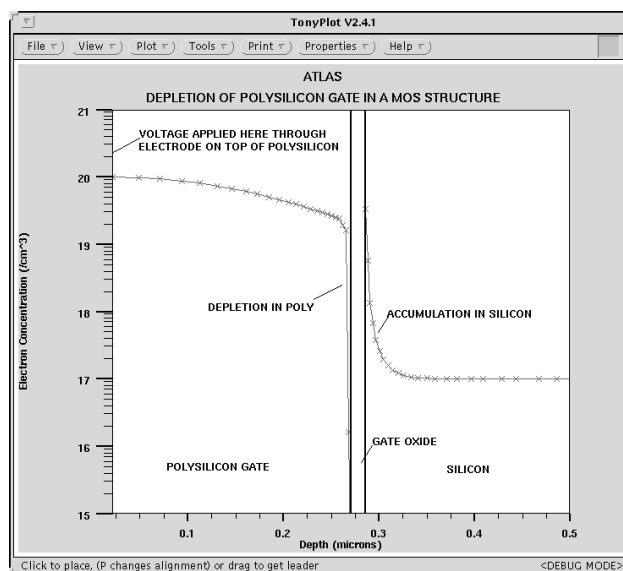


Figure C-6: Figure 2 Electron concentration profile of an NMOS transistor poly depletion occurs at the poly/gate oxide interface.

Question:

How can I remesh my process simulation result for device simulation?

Answer:

The structure editing and gridding tool DEVEDIT provides an effective way to remesh structures between process and device simulation.

DEVEDIT is able to read and write files to both ATHENA and ATLAS. In addition to the graphical user interface, DEVEDIT can operate in batch mode under DECKBUILD. The batch mode DEVEDIT features a powerful syntax that can be applied to remesh structures read directly from ATHENA. DEVEDIT employs a hierarchical method for remeshing existing structures. Users specify mesh parameters at each stage. Initially a base mesh is applied with the command:

```
BASE.MESH HEIGHT=<h1> WIDTH=<w1>
```

This mesh of h1 by w1 microns provides the coarsest mesh in the structure. On top of this base level mesh DEVEDIT determines which points must be added to ensure the geometry of all regions is preserved. Optional boundary conditioning to smooth region boundaries can be applied using the BOUND.COND statement.

Mesh constraints can be applied to arbitrary boxes with the device using the syntax:

```
constr.mesh x1=<n> x2=<n> y1=<n> y2=<n>\
max.height=<h2> max.width=<w2>
```

This sets the maximum mesh size to h2 by w2 microns the box with diagonal from (x1,y1) to (x2,y2). Using the constraint boxes in critical areas of the device is the most effective way to use DEVEDIT. In MOSFETS the constraint boxes can be applied to the silicon region under the gate. Typically vertical grid spacings of 5 are required for accurate simulation of channel conduction in sub-micron MOSFETs.

Use of multiple constraint boxes can be applied. For MOSFET breakdown constraint boxes can be applied to the drain/gate overlap area.

In addition to constraint boxes, DEVEDIT can refine on quantities such as individual doping species, net doping, potential. The `IMP.REFINE` statement allows users to select the critical value of a quantity for refinement and an associated minimum grid spacing.

This type of refinement is useful when key effects are located very close to junctions. For example the emitter-base junction in bipolar transistors.

The final level of grid refinement are "manual refine boxes" defined using:

```
Refine Mode={Both|x|y} P1=x1,y1 P2=x2,y2
```

These are boxes with a diagonal from (x1,y1) to (x2,y2), inside which the grid spacing is halved in the given direction. These can be used as a final customization to the mesh. In general, however, the constraint boxes described above are easier to use.

As a demonstration of the effectiveness of regriding using DEVEDIT. Figures C-7 and C-8 show meshes created from the same process simulation structure. Figures C-9 and C-10 show the I_d/V_d s and breakdown characteristics respectively of the device for each mesh. The mesh at the silicon surface is identical in both cases to a depth of 100Å. However the mesh below this is much coarser in Figure C-8.

However the device results show no significant change despite the reduction in the node count by a factor of two.

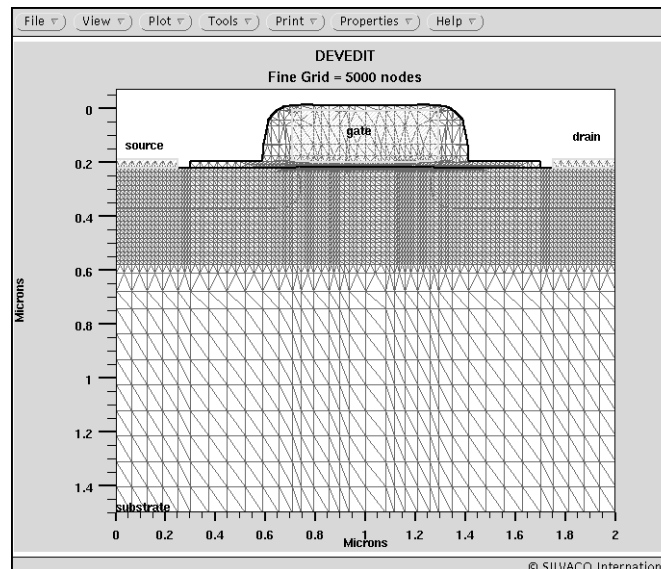


Figure C-7: Fine Grid - 5000 nodes

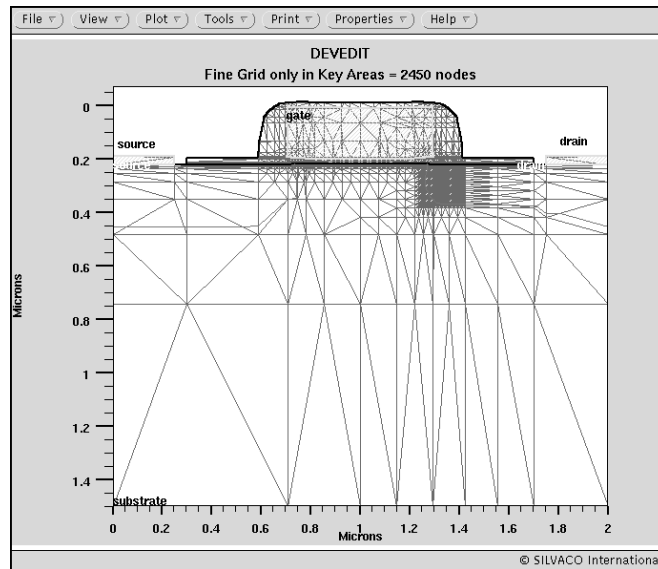


Figure C-8: Fine Grid only in Key Areas - 2450 nodes

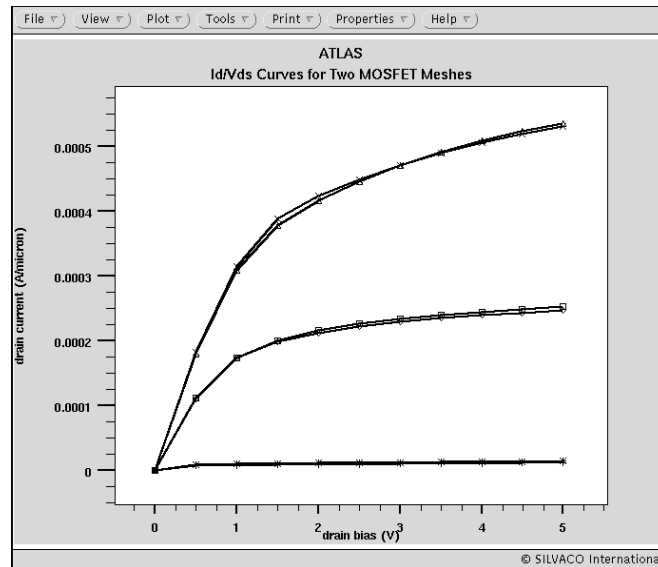


Figure C-9: Id-Vds Curves for two MOSFET Meshes

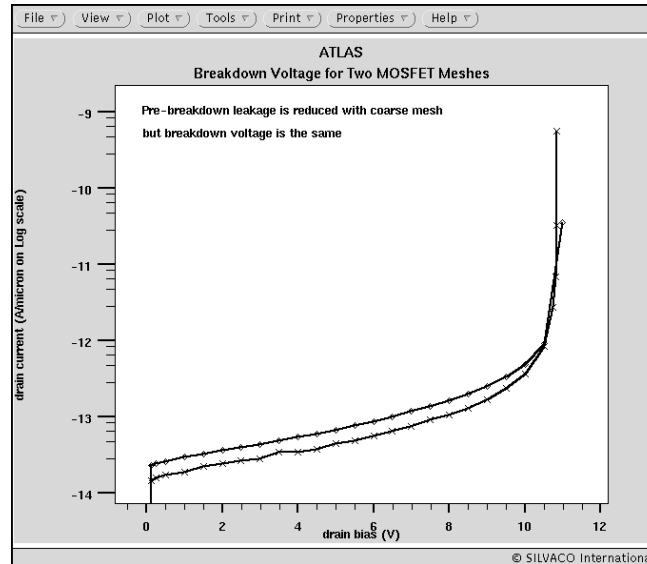


Figure C-10: Breakdown Voltage for Two MOSFET Meshes

Demonstration of optimized gridding using constraint boxes in DEVEDIT. Both very fine and optimized mesh produces equivalent results.

Question:

How can solution quantities such as Electric Field be saved for plotting against applied bias?

Answer:

There are two types of output files saved by ATLAS:

- Solution files contain physical quantities mapped to the simulation grid. One solution file is saved per bias point.
- Log files which traditionally have saved the terminal characteristics for all bias points.

A new feature of ATLAS 4.0 is the addition of a capability to save physical quantities at user-specified locations within the device grid to the log files. A new statement `PROBE` is used to specify the quantity to be saved and the location. For example, to save the electron concentration rate at a location [1,0.1] the syntax is:

```
PROBE NAME=my_e_conc N.CONC X=1.0 Y=0.5
```

The label specified by the `NAME` parameter is used to label the saved quantity in TONYPLOT and subsequent `EXTRACT` statements.

For vector quantities the `PROBE` statement also requires a direction to be given using the `DIR` parameter. This is specified as an angle in degrees with the X axis as `DIR=0`. To find the electric field across an oxide layer the syntax is:

```
PROBE X=1.2 Y=0.2 FIELD DIR=90 \ NAME=oxide_field
```

Figure C-11 shows the resultant plot of electric field in a MOSFET gate oxide during a transient ESD pulse. This result shows the probability of oxide breakdown during the ESD stress, without the need to examine many separate solution files.

Another advantage of the probe for vector quantities is that it reads the values directly from the simulator at the closest location to the specified XY coordinates. This avoids many issues of interpolation and averaging of vector quantities onto the simulation grid.

If two physical quantities are probed at the same location it is possible to plot them against each other to examine model settings. For example, impact ionization rate or mobility versus electric field. Figure C-12 shows a plot of channel electron mobility in a submicron NMOS transistor versus the transverse electric field from the gate.

All of the primary solution quantities can be probed. A full list is given in the manual under the PROBE statement. In addition to values at point locations the PROBE statement also supports MIN and MAX parameters to find the minimum and maximum of a given quantity.

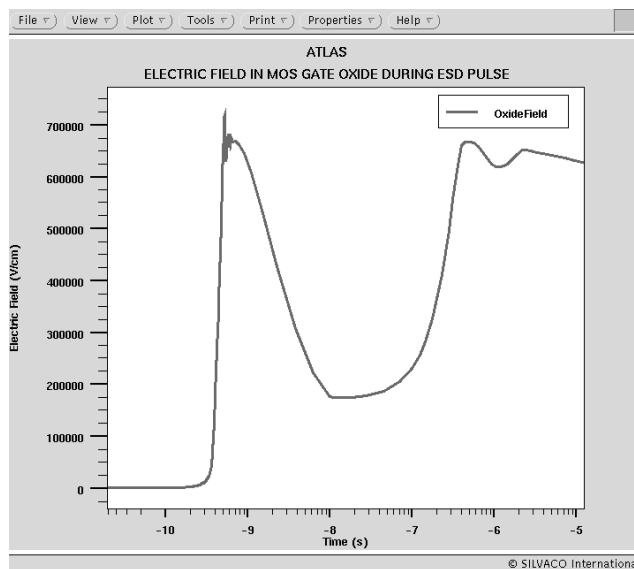


Figure C-11: Electric field in MOS gate oxide during a high current pulse on the drain.

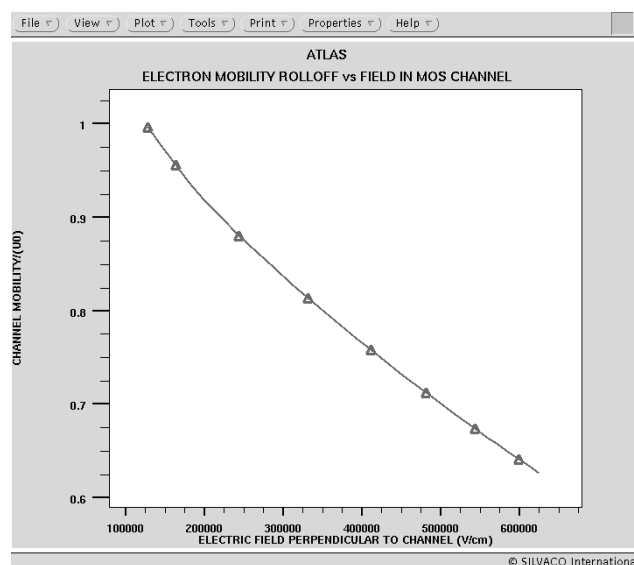


Figure C-12: Mobility (normalized) rolls off as a high gate electric field is applied

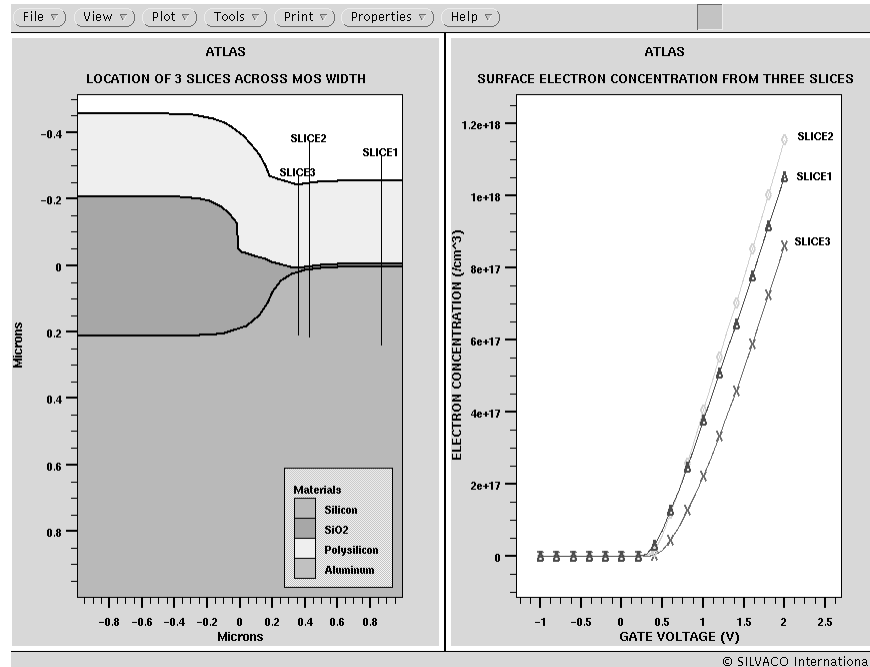


Figure C-13: Using a PROBE of electron concentration allows a study of MOS width effect using 2D simulation. An enhanced electron concentration is seen along slice 2.

Question:

What are the options for generating 3D structures for ATLAS device simulation?

Answer:

Currently there are three options for generating 3D device structures. In all cases the prismatic meshing of ATLAS/DEVICE3D permits arbitrary shaped device regions in 2 dimensions (typically X and Y) and rectangular regions in the other dimension (typically Z).

- Definition through the ATLAS syntax.

This limits the user to defining box shaped regions. Region definition is through statements such as:

```
region num=1 silicon x.min=0 \
x.max=1 y.min=0 y.max=1 z.min=0
\ z.max=1
```

Mesh generation is handled through the Z.MESH statement which is analogous to the X.MESH and Y.MESH statement used in 2D ATLAS simulations. Electrodes and doping can be defined using the same syntax as 2D ATLAS but with Z.MIN and Z.MAX parameters to control the Z extent. Doping profiles can be read from the formats supported in 2D ATLAS: ssuprem3, Athena, ascii.

- Use DEVEDIT to create a 3D mesh structure.

DEVEDIT3D is a 3D structure generation and meshing tool used to generate the mesh, regions, electrodes and doping used in ATLAS/DEVEDIT. It allows users to draw regions by hand in 2D and project them into the third direction.

DEVEDIT3D contains all the sophisticated meshing options available to 2D DEVEDIT. These include: mesh constraints by region, mesh constraints by a user defined box, refinement on doping and other

quantities, mouse controlled refine and unrefine boxes. DEVEDIT3D has both interactive and batch mode operation. This is the recommended approach for 3D power device simulation.

- Use ATHENA and DEVEDIT3D to extend a 2D process simulation to 3D.

A 2D process simulation from ATHENA can be extruded to form a 3D structure using DEVEDIT3D. In this mode DEVEDIT3D can be used to add extra regions and doping if required. This mode is commonly used for modeling MOS width effects in 3D (see Figure C-14). An ATHENA simulation of the isolation bird's beak and field stop implant is performed.

The 2D structure is loaded into DEVEDIT3D and extended in Z direction. The polysilicon gate is truncated in Z and aluminum source/drain contacts are added. The source/drain doping profiles can be read from analytical functions or other process simulation results. A worked example, named mos2ex04.in, is supplied with the Fall 96 release CDROM.

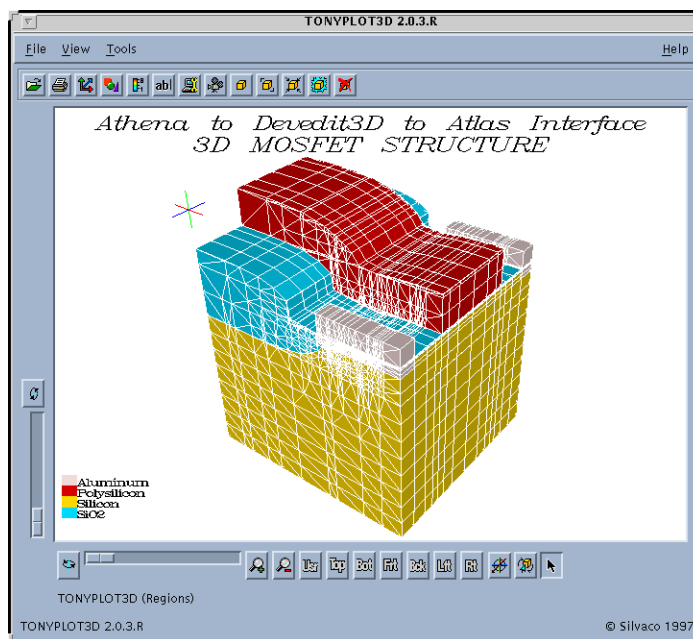


Figure C-14: 3D device simulation of MOS width effect can be performed on structures created Athena.

For devices with non-rectangular regions in the XZ plane such as pillar MOSFETs or cylindrically designed power structures DEVEDIT3D can also be used by drawing in the XZ plane and projecting into the Y direction.

The future release of Silvaco's 3D process/device simulator ODIN will provide a fourth option for 3D simulation problems. ODIN is based on tetrahedral mesh elements and will overcome the mesh restrictions described above.

Note: ODIN is now called Clever.

This page is intentionally left blank.

1. Adachi, S. *Physical Properties of III-V Semiconductor Compounds InP, InAs, GaAs, GaP, InGaAs, and InGaAsP*. New York: John Wiley and Sons, 1992.
2. Adachi, S., "Band gaps and refractive indices of AlGaAsSb, GaInAsSb, and InPAsSb: Key properties for a variety of the 2-4 μ m optoelectronic device applications", *J. Appl. Phys.*, Vol. 61, No. 10, 15 (May 1987): 4896-4876.
3. Adamsone A.I., and B.S. Polsky, "3D Numerical Simulation of Transient Processes in Semiconductor Devices", *COMPEL—The International Journal for Computation and Mathematics in Electrical and Electronic Engineering* Vol. 10, No. 3 (1991): 129-139.
4. Akira Hiroki, S. Odinaka et. al., "A Mobility Model for Submicrometer MOSFET Simulations, including Hot-Carrier Induced Device Degradation", *IEEE Trans. Electron Devices* Vol. 35 (1988): 1487-1493.
5. Alamo, J. del, S. Swirhun and R.M. Swanson, "Simultaneous measuring of hole lifetime, hole mobility and bandgap narrowing in heavily doped n-type silicon", *IEDM Technical Digest*, (December 1985): 290-293.
6. Albrecht, J.D. et al, "Electron transport characteristics of GaN for high temperature device modeling", *J. Appl. Phys.* Vol. 83 (1998): 4777-4781.
7. Allegretto, W., A.Nathan and Henry Baltes, "Numerical Analysis of Magnetic Field Sensitive Bipolar Devices", *IEEE Trans. on Computer-Aided Design*, Vol. 10, No. 4 (1991): 501-511.
8. Ambacher, O. et. al., "Two Dimensional Electron Gases Induced by Spontaneous and Piezoelectric Polarization in Undoped and Doped AlGaIn/GaN Heterosturctures", *J. Appl. Phys.* Vol. 87, No. 1, (1 Jan. 2000): 334-344.
9. Anderson, D.G., "Iterative Procedure for Nonlinear Integral Equations", *ACM Journal* Vol. 12, No. 4 (n.d.): 547-560.
10. Andrews, J.M., and M.P. Lepselter, "Reverse Current-Voltage Characteristics of Metal-Silicide Schottky Diodes", *Solid-State Electronics* 13 (1970): 1011-1023.
11. Antogneti, P., and G. Massobrio. *Semiconductor Device Modeling With SPICE*. McGraw-Hill Book Company, 1987.
12. Apanovich Y. et. al, "Numerical Simulation of Submicrometer Devices, Including Coupled Non-local Transport and Non-isothermal Effects," *IEEE Trans. Electron Devices* Vol. 42, No. 5 (1995): 890-898.
13. Apanovich Y. et. al, "Steady-State and Transient Analysis of Submircon Devices Using Energy Balance and Simplified Hydrodyamic Models," *IEEE Trans. Comp. Aided Design of Integrated Circuits and Systems* Vol. 13, No. 6 (June 1994): 702-710.
14. Arkhipov, V.I., P. Heremans, E.V. Emelianova, G.J. Adriaenssens, H. Bassler, "Charge carrier mobility in doping disordered organic semiconductors", *Journal of Non-Crystalline Solids*, Vol. 338-340 (2004): 603-606.
15. Arkhipov, V.I., P. Heremans, E.V. Emelianova, G.J. Adriaenssens, H. Bassler, "Charge carrier mobility in doped semiconducting polymers", *Applied Physics Letters*, Vol. 82, No. 19 (May 2003): 3245-3247.
16. Arora, N.D., J.R. Hauser, and D.J. Roulston, "Electron and Hole Mobilities in Silicon as a function of Concentration and Temperature", *IEEE Trans. Electron Devices* Vol. 29 (1982): 292-295.
17. Baccarani, G., M. Rudan, R. Guerrieri, and P. Ciampolini, "Physical Models for Numerical Device Simulation", *European School of Device Modeling*, University of Bologna, 1991.

18. Bank, R.E., and A.H. Sherman, "A Refinement Algorithm and Dynamic Data Structure for Finite Element Meshes", University of Texas at Austin Technical Report CS TR-159/CNA Tr-166, October 1980.
19. Bank, R., W.M. Coughran, W. Fichtner, E.H. Grosse, D.J. Rose, and R.K. Smith, "Transient Simulation of Silicon Devices and Circuits", *IEEE Trans. Electron Devices* Vol. 32 (October 1985): 1992-2007.
20. Baraff G.A., "Distribution Functions and Ionisation Rates for Hot Electrons in Semiconductors", *Appl. Phys. Rev.* 128 (1962): 2507-2517.
21. Barnes, J.J., R.J. Lomax, and G.I. Haddad, "Finite-element Simulation of GaAs MESFET's with Lateral Doping Profiles and Sub-micron Gates", *IEEE Trans. Electron Devices* Vol. 23 (September 1976): 1042-1048.
22. Beattie, A.R., and A.M. White, "An Analytical Approximation with a Wide Range of Applicability for Electron Initiated Auger Transitions in Narrow-gap Semiconductors." *J. Appl. Phys.* Vol. 79, No. 12 (1996): 802-813.
23. Behnen, E., "Quantitative examination of the thermoelectric power of n-type Si in the phonon drag regime", *J. Appl. Phys.*, Vol 87, (Jan 1990): 287-292.
24. Beinstman P. et al. "Comparision of Optical VCSEL Models on the Simulation at Oxide-Confined Devices." *IEEE J. of Quantum Electron* 37 (2001): 1618-1631.
25. Bennett, H.S., and C.L. Wilson, "Statistical comparisons of data on band-gap narrowing in heavily doped Silicon: Electrical and Optical measurements", *J. Appl. Phys.* Vol 55, No. 10, (1984): 3582-3587.
26. Bernardini, F., and V. Fiorentini, "Spontaneous Polarization and Piezoelectric Constants of III-V Nitrides", *Phys. Rev. B* Vol. 56, No. 16, 15 (Oct. 1997): R10024-R10027.
27. Berenger, J.P., "A Perfectly Matched Layer for the Absorption of Electromatic Waves", *Journal of Computational Physics*, Vol. 114 (1994): 185-200.
28. Blom, P.W.M., M.J.M. de Jong, and S. Breedijk, "Temperature Dependent Electron-Hole Recombination in Polymer Light-Emitting Diodes", *Applied Physics Letters* Vol. 71, No. 7 (August 1997): 930-932.
29. Blotekjaer, K., *IEEE Trans. Electron Devices* Vol. 17 (1970): 38.
30. Bonani, F., and G. Ghione. *Noise in Semiconductor Devices - Modeling and Simulation*. Berlin Heidelberg: Springer- Verlag (2001): 24-26.
31. Born, M., and E. Wolf. *Principles of Optics*. 6th ed., Cambridge Press, 1980.
32. Boyd, R.W. *Nonlinear Optics*. New York: Academic Press, 1992.
33. Buturla, E.M., and P.E. Cotrell, "Simulation of Semiconductor Transport Using Coupled and Decoupled Solution Techniques", *Solid State Electronics* 23, No. 4 (1980): 331-334.
34. Canali, C., C. Jacoboni, F. Nava, G. Ottaviani and A. Algerigi-Quaranta, "Electron Drift Velocity in Silicon", *Phys. Rev. B*, Vol. 12 (1975): 2265-2284.
35. Canali, C., G. Magni, R. Minder and G. Ottaviani, "Electron and Hole drift velocity measurements in Silicon and their empirical relation to electric field and temperature", *IEEE Trans. Electron Devices* ED-22 (1975): 1045-1047.
36. Carre, B.A., "The Determination of the Optimum Acceleration for Successive Over-Relaxation", *Computer Journal* Vol. 4, Issue 1 (1961): 73-79.
37. Caughey, D.M., and R.E. Thomas. "Carrier Mobilities in Silicon Empirically Related to Doping and Field." *Proc. IEEE* 55, (1967): 2192-2193.
38. Cassi C., and B. Ricco, "An Analytical Model of the Energy Distribution of Hot Electrons", *IEEE Trans. Electron Devices* Vol. 37 (1990): 1514-1521.
39. Chinn, S., P. Zory, and A. Reisinger, "A Model for GRIN-SCH-SQW Diode Lasers", *IEEE J. Quantum Electron.* Vol. 24, No. 11, November 1988.
40. Choo, S.C., "Theory of a Forward-Biased Diffused Junction P-L-N Rectifier -- Part 1: Exact Numerical Solutions", *IEEE Transactions on Electron Devices*, ED-19, 8 (1972): 954-966.

-
41. Chuang S.L., "Optical Gain of Strained Wurtzite GaN Quantum-Well Lasers", *IEEE J. Quantum Electron.* Vol. 32, No. 10 (Oct. 1996): 1791-1800.
 42. Chuang, S.L., and C.S. Chang, "k*p Method for Strained Wurtzite Semiconductors", *Phys. Rev. B* Vol. 54, No. 4, 15 (July 1996): 2491-2504.
 43. Chuang, S.L., and C.S. Chang, "A Band-Structure Model of Strained Quantum-Well Wurtzite Semiconductors", *Semicond. Sci. Technol.*, No. 12 (Nov. 1996): 252-262.
 44. Chung, Steve S., et. al., "A novel leakage current separation technique in a direct tunnelling regime Gate Oxide SONOS memory cell", *IEDM 2003 Technical Digest*, (2003): 26.6.1-26.6.4.
 45. Choi, Sangmoo et al, "Improved metal-oxide-nitride-oxide-silicon-type flash device with high-k dielectrics for blocking layer", *J. Appl. Phys.*, Vol 94, No. 8, (2003): 5408-5410.
 46. Chynoweth A.G., "Ionisation Rates for Electrons and Holes in Silicon", *Phys. Rev.* 109 (1958): 1537-1540.
 47. Cimrova, V, and D. Nehr, "Microcavity effects in single-layer light-emitting device based on poly (p-phenylene vinylene)", *J. Appl. Phys.* Vol. 79, No. 6 (March 15, 1996): 3299-3306.
 48. Clugston, D.A. and P.A. Basore, *Proceedings of the 26th IEEE Photovoltaic Specialists Conference*, Anaheim, CA, 1997.
 49. Cohen, M.L., and T. K. Bergstresser, *Phys. Rev.* Vol. 141 (1966): 789-796.
 50. Concannon, A., F. Piccinini, A. Mathewson, and C. Lombardi. "The Numerical Simulation of Substrate and Gate Currents in MOS and EPROMs." *IEEE Proc. IEDM* (1995): 289-292.
 51. Crofton, J., and S. Sriram, "Reverse Leakage Current Calculations for SiC Schottky Contacts", *IEEE Trans. Electron Devices* Vol. 43, No. 12: 2305-2307.
 52. Crowell, C.R., and S.M. Sze, "Current Transport in Metal-Semiconductor Barriers", *Solid State Electronics* 9 (1966): 1035-1048.
 53. Crowell, C.R., and S.M. Sze, "Temperature Dependence of Avalanche Multiplication in Semiconductors", *Applied Physics Letters* 9 (1966): 242-244.
 54. Darwish, M. et al, "An Improved Electron and Hole Mobility Model for General Purpose Device Simulation", *IEEE Trans. Electron Devices* Vol. 44, No. 9 (Sept. 1997): 1529-1537.
 55. Davydov, Y., et. al., "Band Gap of Hexagonal InN and InGaN Alloys", *Phys. Stat. Sol. (B)*, Vol. 234, No. 3 (2002): 787-795.
 56. De Mari, A., "An Accurate Numerical One-dimensional Solution of the P-N Junction Under Arbitrary Transient Conditions", *Solid-State Electronics* 11 (1968): 1021-1053.
 57. De Salvo, Barbara, et al., "Experimental and Theoretical Investigation of nano-Crystal and Nitride-Trap Memory Devices", *IEEE Transactions on Electron Devices*, Vol 48, No. 8, (2001): 1789-1799.
 58. Ding, Meng, et al, "Silicon Field Emission Arrays With Atomically Sharp Tips", *IEEE Transactions on Electron Devices*, Vol 49 (2002): 2333-2341.
 59. Dorkel, J., and Ph. Leturcq, "Carrier Mobilities in Silicon Semi-Empirically Related to Temperature Doping and Injection Level", *Solid-State Electronics* 24 (1981): 821-825.
 60. Dzierwior J. and W. Schmid, "Auger Coefficient for Highly Doped and Highly Excited Silicon", *Appl. Phys. Lett.* Vol. 31 (1977): 346-348.
 61. Erdelyi, M., et.al. "Generation of diffraction-free beams for applications in optical microlithography", *J. Vac. Sci. Technol. B*, Vol. 15, No. 2 (Mar/Apr 1997): 287-292.
 62. Gloeckler, M.A., "Device Physics of Cu(In, Ga)Se₂ Thin-Film Solar Cells" (Ph.D diss., Colorado State University, Summer 2005).
 63. Grant, W.N., "Electron and Hole Ionization Rates in Epitaxial Silicon at High Electric Fields", *Solid-State Electronics* 16 (1973): 1189-1203.
 64. J.L., Egley, and D., Chidambarrao, "Strain Effects on Device Characteristics: Implementation in Drift-Diffusion Simulators", *Solid-State Electronics*, Vol. 36, No. 12, (1993): 1653-1664.

65. Eisenstat, S.C., M.C. Gursky, M.H. Schultz, A.H. Sherman, Computer Science Department, Yale Univ. Tech. Rep. 112, 1977.
66. Engl, W.L., and H.K. Dirks, *Models of Physical Parameters in an Introduction to the Numerical Analysis of Semiconductor Devices and Integrated Circuits*, ed. J.J.H. Miller (Dublin: Boole Press, 1981).
67. Eriksson, J., N. Rorsman, and H. Zirath, "4H-Silicon Carbide Schottky Barrier Diodes for Microwave Applications", *IEEE Trans. on Microwave Theory and Techniques* Vol. 51, No. 3 (2003): 796-804.
68. Farahmand, M. et. al., "Monte Carlo Simulation of Electron Transport in the III-Nitride Wurtzite Phase Materials System: Binaries and Ternaries", *IEEE Trans. Electron Devices* Vol. 48, No. 3 (Mar. 2001): 535-542.
69. Feigna C., and Venturi F., "Simple and Efficient Modelling of EPROM Writing", *IEEE Trans. Electron Devices* Vol. 38 (1991): 603-610.
70. Fischetti, V., S.E. Laux, and E. Crabb, "Understanding hot-electron transport in silicon devices: Is there a shortcut?", *J. Appl. Phys.*, Vol. 78 (1995): 1050.
71. Foldyna, M., K. Postave, J. Bouchala, and J. Pistora, "Model dielectric functional of amorphous materials including Urbach tail", *Proc. SPIE*, Vol. 5445 (June 16, 2004): 301.
72. Fossum, J.G. and D.S. Lee, "A Physical Model for the Dependence of Carrier Lifetime on Doping Density in Nondegenerate Silicon", *Solid State Electronics* Vol. 25 (1982): 741-747.
73. Fossum, J.G., R.P. Mertens, D.S. Lee and J.F. Nijs, "Carrier recombination and lifetime in highly doped Silicon", *Solid State Electronics* Vol. 26, No 8 (1983): 569 -576.
74. Fujii, K., Y. Tanaka, K. Honda, H. Tsutsu, H. Koseki, and S. Hotta. "Process Techniques of 15 inch Full Color and High Resolution a-Si TFT LCD." 5th Int. MicroProcess Conf., Kawasaki, Japan, 1992.
75. Furnemont, A. et. al., "Model for electron redistribution in Silicon Nitride", *ESSDERC 2006* (2006):447-450.
76. Furnemont, A. et. al., "A consistent model for the SANOS programming operation", 22nd IEEE Non-volatile Semiconductor Memory Workshop, (2007): 96-97.
77. Gear, C.W. *Numerical Initial Value Problems in Ordinary Differential Equations*. Prentice-Hall, 1971.
78. Geballe T.H., and T.W. Hull, "Seebeck Effect in silicon", *Phys. Rev.* 98 (1955): 940-947.
79. Gill, W.D., "Drift Mobilities in Amorphous Charge-Transfer Complexes of Trinitrofluorenone and Poly-n-vinylcarbazole", *J. Appl. Phys.* Vol. 55, No. 12 (1972): 5033.
80. G.L., Bir, and G.E. Pikus, *Symmetry and Strain-Induced Effects in Semiconductors*, New York, Wiley, 1974.
81. Gossens, R.J. G., S. Beebe, Z. Yu and R.W. Dutton, "An Automatic Biasing Scheme for Tracing Arbitrarily Shaped I-V curves", *IEEE Trans. Computer-Aided Design* Vol. 13, No. 3 (1994): 310-317.
82. Grove, A.S. *Physics and Technology of Semiconductor Devices*. Wiley, 1967.
83. Gundlach, K. H., *Solid-State Electronics* Vol. 9 (1966): 949.
84. Hack, B.M. and J.G. Shaw. "Numerical Simulations of Amorphous and Polycrystalline Silicon Thin-Film Transistors." Extended Abstracts 22nd International Conference on Solid-State Devices and Materials, Sendai, Japan (1990): 999-1002.
85. Hacker R., and A. Hangleiter, "Intrinsic upper limits of the carrier lifetime in Silicon", *J. Appl. Physics*, Vol. 75 (1994): 7570-7572.
86. Hall, R.N., "Electron Hole Recombination in Germanium", *Phys. Rev.* 87 (1952): 387.
87. Hansch, W., Th. Vogelsang, R. Kirchner, and M. Orlowski, "Carrier Transport Near the Si/SiO₂ Interface of a MOSFET", *Solid-State Elec.* Vol. 32, No. 10 (1989): 839-849.

88. Hansch, W. et al., "A New Self-Consistent Modeling Approach to Investigating MOSFET Degradation", *IEEE Trans. Electron Devices* Vol. 11 (1990): 362.
89. Harper, J.G., H.E. Matthews, and R. H. Bube, "Photothermoelectric Effects in Semiconductors: n- and p-type Silicon", *J. Appl. Phys.*, Vol 41 (Feb 1970): 765 -770.
90. Harvey, J.E., "Fourier treatment of near-field scalar diffraction theory". *Am. J. Phys.* Vol. 47, No. 11 (1979): 974.
91. Hatakeyama, T., J. Nishio, C. Ota, and T. Shinohe, "Physical Modeling and Scaling Properties of 4H-SiC Power Devices", *Proc. SISPAD*, Tokyo (2005): 171-174.
92. Heavens, O.S. *Optical Properties of Thin Solid Films*. Dover Publishing, 1991.
93. Heiman, F.P. and G. Warfield, "The effects of Oxide Traps on the MOS Capacitance", *IEEE Trans. Electron Devices*, Vol. 12, No. 4, (April 1965): 167-178.
94. Herring, C., "Theory of the Thermoelectric Power of Semiconductors" *Phys. Rev.*, Vol 96, (Dec. 1954): 1163-1187.
95. Hockney, R.W., and J.W. Eastwood, *Computer Simulation Using Particles*, New York: McGraw Hill, 1981.
96. Horowitz, G., "Organic Field-Effect Transistors", *Advanced Materials* Vol. 10, No.5 (1998): 365-377.
97. Huldt, L., N. G. Nilsson and K.G.Svantesson, "The temperature dependence of band-to-band Auger recombination in Silicon", *Applied Physics Letters*, Vol. 35 (1979): 776-777.
98. Hurkx, G.A.M., D.B.M. Klaassen, and M.P.G. Knuvers, "A New Recombination Model for Device Simulation Including Tunneling," *IEEE Trans. Electron Devices* Vol. 39 (Feb. 1992): 331-338.
99. Hurkx, G.A.M., D.B.M. Klaassen, M.P.G. Knuvers, and F.G. O'Hara, "A New Recombination Model Describing Heavy-Doping Effects and Low Temperature Behaviour", *IEDM Technical Digest* (1989): 307-310.
100. Hurkx, G.A.M., H.C. de Graaf, W.J. Klosterman et. al. "A Novel Compact Model Description of Reverse Biased Diode Characteristics including Tunneling." *ESSDERC Proc.* (1990): 49-52.
101. Iannaccone, G., G. Curatola, and G. Fiori. "Effective Bohm Quantum Potential for device simulation based on drift-diffusion and energy transport." *SISPAD 2004*.
102. Jeong, M., Solomon, P., Laux, S., Wong, H., and Chidambarro, D., "Comparison of Raised and Schottky Source/Drain MOSFETs Using a Novel Tunneling Contact Model", *Proceedings of IEDM* (1998): 733-736.
103. Ioffe Physico-Technical Institute. "New Semiconductor Materials Characteristics and Properties". <http://www.ioffe.ru/SVA/NSM/introduction.html> (accessed January 7, 2009).
104. Ishikawa, T. and J. Bowers, "Band Lineup and In-Plane Effective Mass of InGaAsP or InGaAlAs on InP Strained-Layer Quantum Well", *IEEE J. Quantum Electron.* Vol. 30, No. 2 (Feb. 1994): 562-570.
105. Ismail, K., "Effect of dislocation in strained Si/SiGe on electron mobility," *J. Vac. Sci. Technol. B*, Vol. 14, No.4, 1996: 2776-2779.
106. Iwai, H., M.R. Pinto, C.S. Rafferty, J.E. Oristian, and R.W. Dutton, "Velocity Saturation Effect on Short Channel MOS Transistor Capacitance", *IEEE Electron Device Letters* EDL-6 (March 1985): 120-122.
107. Jacoboni, C., and L. Reggiani, "The Monte Carlo Method for the Solution of Charge Transport in Semiconductors with Applications to Covalent Materials", *Reviews of Modern Physics*, Vol. 55 (1983): 645-705.
108. Jaeger, R.C and F. H. Gaensslen, "Simulation of Impurity Freezeout through Numerical Solution of Poisson's Equations and Application to MOS Device Behavior", *IEEE Trans. Electron Devices* Vol. 27 (May 1980): 914-920.
109. Joyce, W.B., and R.W. Dixon, "Analytic Approximation for the Fermi Energy of an ideal Fermi Gas", *Appl. Phys Lett.* 31 (1977): 354-356.

110. Kahen, K.B., "Two-Dimensional Simulation of Laser Diodes in Steady State", *IEEE J. Quantum Electron.* Vol. 24, No. 4, April 1988.
111. Kane, E.O., "Zener tunneling in Semiconductors", *J. Phys. Chem. Solids*, Vol. 12, (1959): 181-188.
112. Katayama, K. and T. Toyabe, "A New Hot Carrier Simulation Method Based on Full 3D Hydrodynamic Equations", *IEDM Technical Digest* (1989): 135.
113. Keeney, S., F. Piccini, M. Morelli, A. Mathewson et. al., "Complete Transient Simulation of Flash EEPROM Devices", *IEDM Technical Digest* (1990): 201-204.
114. Kemp, A.M., M. Meunier, and C.G. Tannous, "Simulations of the Amorphous Silicon Static Induction Transistor", *Solid-State Elect.* Vol. 32, No. 2 (1989): 149-157.
115. Kernighan, Brian, W. and Dennis M. Ritchie, "The C Programming Language", Prentice-Hall, 1978.
116. Kerr, M.J., and A. Cuevas, "General Parameterization of Auger Recombination in Crystalline Silicon", *Jour. of Appl. Phys.*, Vol. 91, No. 4 (2002): 2473-2480.
117. Kimura M. et. al., "Development of Poly-Si TFT Models for Device Simulation: In-Plane Trap Model and Thermionic Emission Model", (Proceedings of Asia Display/IDW '01, 2001), 423.
118. Kimura M., R. Nozawa, S. Inoue, T. Shimoda, B.O-K. Lui, S.W-B. Tam, P. Migliorato, "Extraction of Trap States at the Oxide-Silicon Interface and Grain Boundary for Polycrystalline Silicon Thin-Film Transistors", *Jpn J. Appl. Phys.*, Vol. 40 (2001): 5227-5236.
119. Klaassen, D.B.M., *Physical Modeling Bipolar Device Simulation*, In: *Simulation of Semiconductor Devices and Processes* Vol. 4, ed. W. Fichtner and D. Aemmer (Harting-Gorre, 1991), 23-43.
120. Klaassen, D.B.M., "A Unified Mobility Model for Device Simulation- I. Model Equations and Concentration Dependence", *Solid-State Elect.* Vol. 35, No. 7 (1992): 953-959.
121. Klaassen, D.B.M., "A Unified Mobility Model for Device Simulation - II. Temperature Dependence of Carrier Mobility and Lifetime", *Solid-State Elect.* Vol. 35, No. 7 (1992): 961-967.
122. Klaassen, D.B.M., J.W. Slotboom, and H.C. De Graaff, "Unified Apparent Bandgap Narrowing in n- and p- type Silicon", *Solid-State Elect.* Vol. 35, No. 2 (1992):125-129.
123. Klausmeier-Brown, M., M. Lundstrom, M. Melloch, "The Effects of Heavy Impurity Doping on AlGaAs/GaAs Bipolar Transistors", *IEEE Trans. Electron Devices* Vol. 36, No. 10 (1989): 2146-2155.
124. Krc, J. et.al. "Optical Modeling and Simulation of Thin-Film Cu(In,Ga)Se₂ Solar Cells", NUSOD (2006): 33-34.
125. Krc, J. Zeman, M. Smole, F. and Topic, M. "Optical Modeling of a-Si:H Solar Cells Deposited on Textured Glass/SnO₂ Substrates", *J. Appl. Phys.*, Vol. 92. No. 2 (Feb. 2002): 749-755.
126. Krieger, G., and R.M. Swanson, "Fowler-Nordheim electron tunneling in thin Si-SiO₂-Al structures," *J. Appl. Phys.*, Vol. 52 (1981): 5710.
127. Kumagai, M., S.L. Chuang, and H. Ando, "Analytical Solutions of the Block-diagonalized Hamiltonian for Strained Wurtzite Semiconductors", *Phys. Rev. B* Vol. 57, No. 24, 15 (June 1998): 15303-15314.
128. Kuzmicz, W., "Ionization of Impurities In Silicon", *Solid-State Electronics*, Vol. 29, No. 12 (1986): 1223-1227.
129. Lackner, T., "Avalanche multiplication in semiconductors: A modification of Chynoweth's law", *Solid-State Electronics* Vol. 34 (1991): 33-42.
130. Lades M. and G. Wachutka. "Extended Anisotropic Mobility Model Applied to 4H/6H-SiC Devices." *Proc. IEEE SISPAD* (1997): 169-171.
131. Lambert, J. *Computational Methods in Ordinary Differential Equations*. Wiley, 1973.
132. Lang, D.V., "Measurement of the band gap of Ge_xSi_{1-x}/Si strained-layer heterostructures," *Appl. Phys. Lett.*, Vol. 47, No. 12, (1985): 1333-1335.

133. Larez, C, Bellabarba, C. and Rincon, C., "Allow composition and temperature dependence of the fundamental absorption edge in CuGa_xIn_{1-x}Se₂", *Appl. Pys. Lett.* Vol 65, No. 26 (Sept 1994): 1650-1652.
134. Laux, S.E., "Techniques for Small-Signal Analysis of Semiconductor Devices", *IEEE Trans. Electron Devices* Vol. 32 (October 1985): 2028-2037.
135. Laux, S.E., and M.V. Fischetti, "Monte Carlo Simulation of Submicron Si *n*-MOSFETs at 77 and 300", *IEEE Electron Device Letters*, Vol. 9, No. 9 (September 1988): 467-469.
136. Laux, S.E., and M.V. Fischetti, "Numerical aspects and implementation of the DAMOCLES Monte Carlo device simulation program" from *Monte Carlo Device Simulation: Full Band and Beyond*, Dordrecht: K.Hess, Ed. Kluwer Academic Publishers, 1991.
137. Law, M.E. et. al., Self-Consistent Model of Minority-Carrier Lifetime, Diffusion Length, and Mobility, *IEEE Electron Device Letters* Vol. 12, No. 8, 1991.
138. Lee, C.C., M.Y. Chang, P.T. Huang and S.W. Liu, "Electrical and optical simulation of organic light-emitting devices with fluorescent dopant in the emitting layer", *J. Appl Physics*, Vol. 101 (2007): 114501.
139. Lee, C., Chang, M., Jong, Y., Huang, T., Chu, C. and Chang, Y., "Numerical Simulation of Electrical and Optical Characteristics of Multilayer Organic Light-Emitting Devices", *Japanese Journal of Appl. Phys.*, Vol. 43, No. 11A (2004): 7560-7565.
140. Li, Z., K. Dzurko, A. Delage, and S. McAlister, "A Self-Consistent Two-Dimensional Model of Quantum-Well Semiconductor Lasers: Optimization of a GRIN-SCH SQW Laser Structure", *IEEE J. Quantum Electron.* Vol. 28, No. 4 (April 1992): 792-802.
141. Lindefelt U., "Equations for Electrical and Electrothermal Simulation of Anisotropic Semiconductors", *J. Appl. Phys.* 76 (1994): 4164-4167.
142. Littlejohn, M.J., J.R. Hauser, and T.H. Glisson, "Velocity-field Characteristics of GaAs with $\Gamma_6^c - L_6^c - X_6^c$ Conduction Band Ordering", *J. Appl. Phys.* 48, No. 11 (November 1977): 4587-4590.
143. Lombardi et al, "A Physically Based Mobility Model for Numerical Simulation of Non-Planar Devices", *IEEE Trans. on CAD* (Nov. 1988): 1164.
144. Lui O.K.B., and P. Migliorato, "A New Generation-Recombination Model For Device Simulation Including The Poole-Frenkel Effect And Phonon-Assisted Tunneling", *Solid-State Electronics* Vol. 41, No. 4 (1997): 575-583.
145. Lundstrom, Ingemar and Christer Svensson, "Tunneling to traps in insulators", *J. Appl. Phys.*, Vol.43. No. 12 (1972): 5045-5047.
146. Lundstrom M., and R. Shuelke, "Numerical Analysis of Heterostructure Semiconductor Devices", *IEEE Trans. Electron Devices* Vol. 30 (1983): 1151-1159.
147. Luo, J.K., H.Thomas, D.V.Morgan and D.Westwood, "Transport properties of GaAs layers grown by molecular beam epitaxy at low temperature and the effects of annealing", *J. Appl. Phys.*, Vol. 79, No. 7, (Apr 1996), pp. 3622-3629.
148. Manku, T., and A. Nathan, "Electron Drift Mobility Model for Devices Based on Unstrained and Coherently Strained Si_{1-x}Ge_x Grown on <001> Silicon Substrate", *IEEE Transaction on Electron Devices* Vol. 39, No. 9 (September 1992): 2082-2089.
149. Marques, M., Teles, L., Scolfaro, L., and Leite, J., "Lattice parameter and energy band gap of cubic Al_xGa_yIn_{1-x-y}N quaternary alloys", *Appl. Phys. Lett.*, Vol. 83, No. 5, 4 (Aug. 2003): 890-892.
150. Mars, P. "Temperature Dependence of Avalanche Breakdown Voltage in p-n Junctions", *International Journal of Electronics* Vol. 32, No. 1 (1963): 23-27.
151. Masetti G., M.Severi, and S.Solmi, "Modeling of Carrier Mobility Against Carrier Concentration in Arsenic , Phosphorous and Boron doped Silicon", *IEEE Trans. Elec. Dev. ED-* 30, (1983): 764-769.

152. Matsuzawa, K., Uchida, K., and Nishiyama, A., "A Unified Simulation of Schottky and Ohmic Contacts", *IEEE Trans. Electron Devices*, Vol. 47, No. 1 (Jan. 2000): 103-108.
153. Mayaram, K., "CODECS: A Mixed-Level Circuit and Device Simulator", Memo No. UCB/ERL M88/71, University of California, Berkeley, CA, November 1988.
154. Mayaram, K., and D.O. Pederson, "Coupling Algorithms for Mixed-Level Circuit and Device Simulation", *IEEE Transactions on Computer-Aided Design* Vol. 11, No. 8 (August 1992): 1003-1012.
155. Meinerzhagen, B., K. Bach, I. Bozk, and W.L. Engl. "A New Highly Efficient Nonlinear Relaxation Scheme for Hydrodynamic MOS Simulations." Proc. NUPAD IV (1992): 91.
156. Meinerzhagen, B., and W.L. Engl, "The Influence of Thermal Equilibrium Approximation on the Accuracy of Classical Two-Dimensional Numerical Modeling of Silicon Submicrometer MOS Transistors", *IEEE Trans. Electron Devices* Vol. 35, No. 5 (1988): 689-697.
157. Meftah, A.F., A.M. Meftah and A. Merazga, "A theoretical study of light induced defect creation, annealing and photoconductivity degradation in a-Si:H", *J. Phys.: Condens. Matter*, Vol.16 (2004): 3107-3116.
158. Miller et. al., "Device modeling of ferroelectric capacitors", *J. Appl. Phys.* 68, 12, 15 Dec. 1990.
159. Muth, J., et. al., "Absorption Coefficient, Energy Gap, Exciton Binding Energy, and Recombination Lifetime of GaN Obtained from Transmission Measurements", *Appl. Phys. Lett.* Vol. 71 (1997): 2572-2574.
160. Nakagawa, A., and H. Ohashi, "A Study on GTO Turn-off Failure Mechanism — A Time-and Temperature-Dependent 1D Model Analysis", *IEEE Trans. Electron Devices* Vol. 31, No. 3 (1984): 273-279.
161. Nemanich, R.J., et al, "Electron emission properties of crystalline diamond and III-Nitride surfaces", *Applied Surface Science*, (1998): 694-703.
162. Ning, T. H. , "High-field capture of electrons by Coulomb-attractive centres in Silicon dioxide", *J. Appl. Phys.*, Vol. 47, No. 7 (July 1976): 3203-3208.
163. Nomenclature of Inorganic Chemistry," *Journal of the American Chemical Society* No. 82 (1960): 5525.
164. Oguzman, I., et. al., "Theory of Hole Initiated Impact Ionization in Bulk Zincblende and Wurtzite GaN", *J. Appl. Phys.* V. 81, No. 12 (1997): 7827-7834.
165. Ohtoshi, T., K. Yamaguchi, C. Nagaoka, T. Uda, Y. Murayama, and N. Chionone, "A Two-Dimensional Device Simulator of Semiconductor Lasers", *Solid-State Electronics* Vol. 30, No.6 (1987): 627-638.
166. Okuto, Y., and R. Crowell, "Threshold energy effects on avalanche breakdown Voltage in semiconductor junctions", *Solid-State Electronics* Vol. 18 (1975): 161-168.
167. Pacelli, A., "On the Modeling of Quantization and Hot Carrier Effects in Scaled MOSFETs and Other Modern Devices." Dissertation, Polytechnic Institute of Milan, 1997.
168. Pacelli, A., W. Duncan, and U. Ravaioli. "A multiplication scheme with variable weights for Ensemble Monte Carlo simulation of hot-electron tails", Proc. IX Conference on Hot Carriers in Semiconductors, J.P. Leburton, K. Hess, and U. Ravaioli, Eds., Plenum Press (July 31-August 4, 1995):407-410.
169. Pacelli, A., and U. Ravaioli, "Analysis of variance-reduction schemes for Ensemble Monte Carlo simulation of semiconductor devices," *Solid-State Electronics*, Vol. 4, Issue 4 (April 1997): 599-605.
170. Palankovski, V., Schultheis, R. and Selberherr, S., "Simulation of Power Heterojunction Bipolar Transistors on Gallium Arsenide", *IEEE Trans. on Elec. Dev.*, Vol. 48, No. 6, 6 (June 2001): 1264-1269.
171. Palik, E.D., Ed. *Handbook of Optical Constants of Solids*. New York: Academic Press Inc., 1985.
172. Passler, R., *Phys.Stat.Solidi* (b) 216 (1999): 975.

173. Patil, M. B., "New Discretization Scheme for Two-Dimensional Semiconductor Device Simulation on Triangular Grid", *IEEE Trans. on CAD of Int. Cir. and Sys.* Vol. 17., No. 11 (Nov. 1998): 1160-1165.
174. Patrin, A. and M. Tarsik, "Optical-Absorption Spectrum of Silicon Containing Internal Elastic Stresses", *Journal of Applied Spectroscopy* Vol. 65, No. 4 (July 1998): 598- 603.
175. Paulson, P., R. Birkmire, and W. Shafarman, "Optical Characterization of CuIn_{1-x}Ga_xSe₂ Alloy Thin Films by Spectroscopic Ellipsometry", *Journal of Appl. Phys.*, V. 94, No. 2 (2003): 879-888.
176. Pearson, G.L., and J. Bardeen, "Electrical Properties of Pure Silicon and Silicon Alloys Containing Boron and Phosphorus", *Phys. Rev.*, Vol. 75, No. 5 (Mar. 1949): 865-883.
177. Pinto M.R., Conor S. Rafferty, and Robert W. Dutton, "PISCES2 - Poisson and Continuity Equation Solver", Stanford Electronics Laboratory Technical Report, Stanford University, September 1984.
178. Pipinys P., and V. Lapeika, "Temperature dependence of reverse-bias leakage current in GaN Schottky diodes as a consequence of phonon-assisted tunneling," *J.Appl. Phys.* 99 (2006): 093709.
179. Piprek, J., *Semiconductor Optoelectronic Devices: Introduction to Physics and Simulation*. UCSB: Academic Press (2003): 22.
180. Piprek, J., Peng, T., Qui, G., and Olowolafe, J., "Energy Gap Bowing and Refractive Index Spectrum of AlInN and AlGaInN". 1997 IEEE International Symposium on Compound Semiconductors (September 8-11, 1997): 227-229.
181. Polsky, B., and J. Rimshans, "Half-Implicit Scheme for Numerical Simulation of Transient Processes in Semiconductor Devices", *Solid-State Electronics* Vol. 29 (1986): 321-328.
182. Powell, M.J., and S.C. Deane, "Improved defect-pool model for charged defects in amorphous silicon", *Phy. Rev. B*, Vol. 48, No. 15 (1993): 10815-10827.
183. Powell, M.J., and S.C. Deane, "Defect-pool model and the hydrogen density of states in hydrogenated amorphous silicon", *Phy. Rev. B*, Vol. 53, No. 15 (1996): 10121-10132.
184. Price, C.H., "Two Dimensional Numerical Simulation of Semiconductor Devices", Ph.D. Dissertation, Stanford University, May 1982.
185. Price, P.J., and J. M. Radcliffe, "IBM Journal of Research and Development" 364, October 1959.
186. Prinz E.J., et. al, "An embedded 90 nm SONOS Flash EEPROM Utilizing Hot Electron Injection Programming and 2-sided Hot Hole Injection Erase", *IEDM Digest*, (2002): 927-930.
187. Rafferty, C.S., M.R. Pinto, and R.W. Dutton, "Iterative Methods in Semiconductor Device Simulation", *IEEE Trans. Electron Devices* Vol. 32 (October 1985): 2018-2027.
188. Rajkanan, K. R., Singh, and J. Shewchun, "Absorption Coefficient of Silicon for Solar Cell Calculations", *Sol. St. Elec.*, Vol. 22, (September 1979): 793-795.
189. Rakic, A.D., and M.L. Majewski. *Cavity and Mirror Design for Vertical-Cavity Surface-Emitting Lasers*, *Vertical-Cavity Surface-Emitting Laser Devices*. Springer Series in Photonics, 2003
190. Reggiani, S., M. Valdinoci, L. Colalongo, and G. Baccarani, " A unified analytical model for bulk and surface mobility in S n- and p-channel MOSFETs", ESSDERC, 1999.
191. Renewable Resource Data Center (RReDC). "Solar Spectra: Air Mass Zero". <http://rredc.nrel.gov/solar/spectra/am0/> (accessed January 16, 2009).
192. Renewable Resource Data Center (RReDC). "Reference Solar Spectral Irradiance: Air Mass 1.5". <http://rredc.nrel.gov/solar/spectra/am1.5/> (accessed January 16, 2009).
193. Rhoderick, E.H. and R.H. Williams. *Metal-Semiconductor Contacts*, 2nd ed. Oxford Science Publications, 1988.

194. Riccobene, C., G.Wachutka, J.Burgler, H.Baltes, "Operating principle of Dual Collector Magnetotransistors studied by Two-Dimensional Simulation", *IEEE Trans. Electron Devices*, Vol. 41, No. 7 (1994): 1136-1148.
195. Roblin, P., A. Samman, and S. Bibyk, "Simulation of Hot-Electron Trapping and Aging of n-MOSFETs", *IEEE Trans. Electron Devices* Vol. 35 (1988): 2229.
196. Rose, D.H., and R.E. Bank, "Global Approximate Newton Methods", *Numerische Mathematik* 37 (1981): 279-295.
197. Roulston, D.J., N.D. Arora, and S.G. Chamberlain, "Modeling and Measurement of Minority-Carrier Lifetime versus Doping in Diffused Layers of n \pm p Silicon Diodes", *IEEE Trans. Electron Devices* Vol. 29 (Feb. 1982): 284-291.
198. Ruhstaller, B., S.A. Carter, S. Barth, H. Riel, W. Riess, J.C. Scott, "Transient and Steady-State Behavior of Space Charges in Multilayer Organic Light-Emitting Diodes", *J. Appl. Phys.* Vol. 89, No. 8 (2001): 4575-4586.
199. Sangiorgi, E., C.S. Rafferty, M.R. Pinto, and R.W. Dutton, "Non-planar Schottky Device Analysis and Applications", (Proc. International Conference on Simulation of Semiconductor Devices and Processes, Swansea, U.K.), July 1984.
200. Scharfetter, D.L., and H.K. Gummel, "Large-Signal Analysis of a Silicon Read Diode Oscillator", *IEEE Trans. Electron Devices* Vol. 16 (January 1969): 64-77.
201. Schenk, A., and G. Heiser, "Modeling and simulation of tunneling through ultra-thin gate dielectrics", *J. Appl. Phys.* Vol. 81 (1997): 7900-7908.
202. Schenk, A., "A model for the field and temperature dependence of SRH lifetimes in Silicon", *Solid-State Electronics*, Vol. 35 (1992): 1585-1596.
203. Schenk, A., "Rigorous Theory and Simplified Model of the Band-to-Band Tunneling in Silicon", *Solid State Electronics* Vol. 36 (1993): 19-34.
204. Schwarz, S.A., and S.E. Russe, "Semi-Empirical Equations for Electron Velocity in Silicon: Part II — MOS Inversion Layer", *IEEE Trans. Electron Devices* Vol. 30, No. 12 (1983): 1634-1639.
205. Scott, J.C., S. Karg, and S.A. Carter, "Bipolar Charge and Current Distributions in Organic Light-Emitting Diodes", *J. Appl. Phys.* Vol. 82, No. 3 (August 1997): 1454-1460.
206. Seki, S., T. Yamanaka, and K. Yokoyama, "Two-Dimensional Analysis of Current Blocking Mechanism in InP Buried Heterostructure Lasers", *J. Appl. Phys.* Vol. 71, No. 7 (April 1992): 3572-3578.
207. Selberherr, S. *Analysis and Simulation of Semiconductor Devices*. Wien, New York: Springer-Verlag, 1984.
208. Selberherr, S., "Process and Device Modeling for VLSI", *Microelectron. Reliab.* 24 No. 2 (1984): 225-257.
209. Shaw, John G., and Michael Hack, "An Analytical Model For Calculating Trapped Charge in Amorphous Silicon", *J. Appl. Phys.* Vol. 64, No. 9 (1988): 4562-4566.
210. Shen J., and J. Yang, "Physical Mechanisms in Double-Carrier Trap-Charge Limited Transport Processes in Organic Electroluminescent Devices: A Numerical Study", *J. Appl. Phys.* Vol. 83, No. 12 (June 1998): 7706-7714.
211. Shih. I.B., and Z. Mi, "CIS, CIG, and Related Materials for Photovoltaic Applications" (Photovoltaic Workshop, McMaster University, Feb. 19, 2009).
212. Shin, H., A.F. Tasch, C.M. Maziar, and S.K. Banerjee, "A New Approach to Verify and Derive a Transverse-field-dependent Mobility Model for Electrons in MOS Inversion Layers", *IEEE Trans. Electron Devices* Vol. 36, No. 6 (1989): 1117-1123.
213. Shin, H., G.M. Yeric, A.F. Tasch, and C.M. Maziar. *Physically-based Models for Effective Mobility and Local-field Mobility of Electrons in MOS Inversion Layers* (to be published).

-
214. Shirahata M., H. Kusano, N. Kotani, S. Kusanoki, and Y. Akasaka, "A Mobility Model Including the Screening Effect in MOS Inversion Layer", *IEEE Trans. Computer-Aided Design* Vol. 11, No. 9 (Sept. 1992): 1114-1119.
215. Shockley W., and W.T. Read, "Statistics of the Recombination of Holes and Electrons", *Phys. Rev.* 87 (1952): 835-842.
216. Simmons, J.G., and G.W. Taylor, *Phys. Rev. B*, 4 (1971): 502.
217. Slotboom, J.W., "The PN Product in Silicon", *Solid State Electronics* 20 (1977): 279-283.
218. Slotboom, J.W. and H.C. De Graaf, "Measurements of Bandgap Narrowing in Silicon Bipolar Transistors", *Solid State Electronics* Vol. 19 (1976): 857-862.
219. Stratton, R., *Phys. Rev.*, 126, 6 (1962): 2002.
220. Stratton, R., "Semiconductor Current-Flow Equations (Diffusion and Degeneracy)", *IEEE Trans. Electron Devices* Vol. 19, No. 12 (1972): 1288-1292.
221. Sutherland, J., and F. Hauser, "A Computer Analysis of Heterojunction and Graded Composition Solar Cells", *IEEE Trans. Electron Devices* Vol. 24 (1977): 363-373.
222. Swirhun, S., Y.H. Kawark and R.M. Swanson, "Simultaneous measuring of hole lifetime, hole mobility and bandgap narrowing in heavily doped p-type silicon", *IEDM Technical Digest*, (December 1986): 24-27.
223. Sze, S.M. "Physics of Semiconductor Devices". Wiley, 1981.
224. Taflove, A. and S.C. Hagness, *Computational Electrodynamics The Finite-Difference Time-Domain Method*, Third Edition, Artech House, Boston and London, 2005.
225. Takahashi Y., K. Kunihiro, and Y. Ohno, "Two-Dimensional Cyclic Bias Device Simulator and Its Applications to GaAs HJFET Pulse Pattern Effect Analysis," *IEICE Journal C*, June 1999.
226. Takayama, T., "Low-Noise and High-Power GaAlAs Laser Diode with a New Real Refractive Index Guided Structure," *Japan J. Appl. Phys.* Vol. 34, No. 7A(1999): 3533-3542.
227. Tam, S., P-K Ko, and C. Hu, "Lucky-electron Model of Channel Hot-electron Injection in MOSFETs", *IEEE Trans. Electron Devices* Vol. 31, No. 9, September 1984.
228. Tan, G., N. Bewtra, K. Lee, Xu, and J.M., "A Two-Dimensional Nonisothermal Finite Element Simulation of Laser Diodes", *IEEE J. of Q.E.* Vol. 29, No.3 (March 1993): 822-835.
229. Uchida, K., and S. Takagi, "Carrier scattering induced by thickness fluctuation of silicon-on-insulator film in ultrathin-body metal-oxide-semiconductor field-effect transistors", *Applied Phys. Lett.*, Vol. 82, No. 17, 22 (April 2003): 2916-2918.
230. Uehara, K. and H. Kikuchi, "Generation of Nearly Diffraction-Free Laser Beams", *Appl. Phys. B*, Vol 48 (1989): 125-129.
231. *UTMOST III User's Manual* and *UTMOST III Extraction Manual*. Simucad Design Automation, Inc., 2008.
232. Vaillant, F., and D. Jousse, "Recombination at dangling bonds and steady-state photoconductivity in a-Si:H", *Phys. Rev. B*, Vol. 34, No. 6 (1986): 4088-4098.
233. Valdinoci, M., D. Ventura, M.C. Vecchi, M. Rudan, G. Baccarani, F. Illien, A. Stricker, and L. Zullino, "The Impact-ionization in Silicon at Large Operating Temperature". SISPAD '99, Kyoto, Japan, Sept. 6-8, 1999.
234. Van Dort, M.J., P.H. Woerlee, and A.J. Walker, "A Simple Model for Quantisation Effects in Heavily-Doped Silicon MOSFETs at Inversion Conditions", *Solid-State Elec.* Vol. 37, No. 3 (1994): 411-414.
235. Van Herwaarden A.W., and P.M.Sarro, "Thermal Sensors based on the Seebeck effect", *Sensors and Actuators* Vol.10, (1986): 321-346.
236. Van Overstraeten, R., and H. Deman, "Measurement of the Ionization Rates in Diffused Silicon p-n Junctions", *Solid-State Electronics* 13 (1970): 583-608.
237. Van Roey, J., J. Van Der Donk, P.E. Lagasse., "Beam-propagation method: analysis and assessment", *J. Opt. Soc. Am.* Vol. 71, No 7 (1981): 803.

- 238. Varga, R.S. *Matrix Iterative Analysis*. Prentice-Hall: Englewood Cliffs, NJ, 1962.
- 239. Vendelin, G. *Design of Amplifiers and Oscillators by the S-Parameter Method*. John Wiley & Sons, New York, 1982.
- 240. Verlaak, S., Cheyns D., Debucquoy M., Arkhipov, V. and Heremans P., "Numerical Simulation of Tetracene Light-Emitting Transistors: A Detailed Balance of Exciton Processes", *Applied Physics Letters* Vol. 85, No. 12 (Sep 2004): 2405-2407.
- 241. Vurgaftman, I. and J.R. Meyer, "Band Parameters for III-V Compound Semiconductors and their Alloys", *Applied Physics Review* Vol. 89, No. 11 (June 2001): 5815-5875.
- 242. Wachutka, G.K., "Rigorous Thermodynamic Treatment of Heat Generation in Semiconductor Device Modeling", *IEEE Trans., Computer-Aided Design* Vol. 9, No. 11 (1990): 1141-1149.
- 243. Wada, M. et al. "A Two-Dimensional Computer Simulation of Hot Carrier Effects in MOSFETs." *Proc. IEDM Tech. Dig.* (1981): 223-225.
- 244. Wegener et al., "Metal-insulator-semiconductor transistor as a nonvolatile storage ", *IEEE IEDM Abstract*, (1967): 58.
- 245. Walker, D., Zhang, X., Saxler, Z., Kung, P., Xj, J., Razeghi, M., "Al_xGa(1-x)N(0<=x,=1)Ultraviolet Photodetectors Grown on Sapphire by Metal-Organic Chemical-Vapor Deposition", *Appl. Phys. Lett.* Vol. 70, No. 8 (1997): 949-951.
- 246. Wu, J., et. al., "Unusual properties of the fundamental band gap of InN", *Applied Physics Letters*, Vol. 80, No. 21, 27 (May 2002): 3967-3969.
- 247. Watt, J.T., Ph.D., Thesis, Stanford University, 1989.
- 248. Watt, J.T., and J.D. Plummer. "Universal Mobility-Field Curves for Electrons and Holes in MOS Inversion Layers." 1987 Symposium on VLSI Technology, Karuizawa, Japan.
- 249. Weast, R. Ed. *CRC Handbook of Chemistry and Physics*. CRC Press, 1976.
- 250. Welser, J., J. L. Hoyt, S. Takagi, J.F. Gibbons, "Strain dependence of the performance enhancement in strained-Si *n*-MOSFETs", *IEDM Tech. Dig.*, 1994: 337-376.
- 251. Wenus, J., J. Rutkowski, and A. Rogalski, "Two-Dimensional Analysis of Double-Layer Heterojunction HgCdTe Photodiodes", *IEEE Trans. Electron Devices* Vol. 48, No.7 (July 2001): 1326-1332.
- 252. Wenzel, H., and H.J. Wünsche, "The effective frequency method in the analysis of vertical-cavity surface-emitting lasers," *IEEE J. Quantum Electron* 33 (1997): 1156-1162.
- 253. Wettstein, A., A. Schenk, and W. Fichtner, "Quantum Device-Simulation with the Density Gradient Model on Unstructured Grids", *IEEE Trans. Electron Devices* Vol. 48, No. 2 (Feb. 2001): 279-283.
- 254. White, Marvin H., Dennis A. Adams, and Jiankang Bu, "On the go with SONOS ", *IEEE Circuits and Devices Magazine*, Vol, 16, No. 4,(2000): 22-31.
- 255. White, W.T. et.al., *IEEE Trans. Electron Devices*. Vol. 37 (1990): 2532.
- 256. Wilt, D.P. and A. Yariv, "Self-Consistent Static Model of the Double-Heterostructure Laser," *IEEE J. Quantum Electron.* Vol. QE-17, No. 9 (1981): 1941-1949.
- 257. Wimp, T. *Sequence Transformation and their Application*. Academic Press, 1981.
- 258. Winstead, B., "Impact of source-side heterojunctions on MOSFET performance," M.S. thesis, University of Illinois at Urbana-Champaign, 1998.
- 259. Winstead, B., "Monte Carlo simulation of silicon devices including quantum correction and strain", Ph.D. Dissertation, University of Illinois at Urbana-Champaign, 2001.
- 260. Wünsche, H.J., H. Wenzel, U. Bandelow, J. Piprek, H. Gajewski, and J. Rehberg, "2D Modelling of Distributed Feedback Semiconductor Lasers," *Simulation of Semiconductor Devices and Processes* Vol. 4 (Sept. 1991): 65-70.
- 261. Wu, C.M., and E.S. Yang, "Carrier Transport Across Heterojunction Interfaces", *Solid-State Electronics* 22 (1979): 241-248.

-
262. Xiao, H. et. al., "Growth and characterization of InN on sapphire substrate by FR-MBE", *Journal of Crystal Growth*, Vol. 276 (2005): 401-406.
 263. Yamada, M., S. Ogita, M. Yamagishi, and K. Tabata, "Anisotropy and broadening of optical gain in a GaAs/AlGaAs multi-quantum-well laser," *IEEE J. Quantum Electron.* QE-21 (1985): 640-645.
 264. Yamada, T., J.R. Zhou, H. Miyata, and D.K. Ferry, "In-Plane Transport Properties of Si/Si(1-x)Ge(x) Structure and its FET Performance by Computer Simulation", *IEEE Trans. Electron Devices* Vol. 41 (Sept. 1994): 1513-1522.
 265. Yamaguchi, K. "A Mobility Model for Carriers in the MOS Inversion Layer", *IEEE Trans. Electron Devices* Vol. 30 (1983): 658-663.
 266. Yan, R., S. Corzine, L. Coldren, and I. Suemune, "Corrections to the Expression for Gain in GaAs", *IEEE J. Quantum Electron.* Vol. 26, No. 2 (Feb. 1990): 213-216.
 267. Yang K., J. East, and G. Haddad, "Numerical Modeling of Abrupt Heterojunctions Using a Thermionic-Field Emission Boundary Condition", *Solid-State Electronics* Vol. 36, No. 3 (1993): 321-330.
 268. Yariv, A. *Optical Electronics*. CBS College Publishing, 1985.
 269. Yee, K. S., "Numerical Solution of Initial Boundary Value Problems Involving Maxwell's Equations in Isotropic Media", *IEEE Trans. on Antennas and Propagation*, V. AP-14, No. 3 (May, 1966): 302-307.
 270. Yu, Z., D. Chen, L. So, and R.W. Dutton, "Pisces-2ET, Two Dimensional Device Simulation for Silicon and Heterostructures", Integrated Circuits Laboratory, Stanford University (1994): 27.
 271. Yu, Z., and R.W. Dutton, "SEDAN III-A Generalized Electronic Material Device Analysis Program", Stanford Electronics Laboratory Technical Report, Stanford University, July 1985.
 272. Zabelin, V., Zakheim, D., and Gurevich, S., "Efficiency Improvement of AlGaInN LEDs Advanced by Ray-Tracing Analysis", *IEEE Journal of Quantum Electronics*, Vol. 40, No. 12, (Dec. 2004): 1675-1686.
 273. Zaidman, Ernest G., "Simulation of Field Emission Microtriodes", *IEEE Transactions on Electron Devices*, Vol 40 (1993):1009-1015.
 274. Zamdmer, N., Qing Hu, K. A. McIntosh and S. Verghese, "Increase in response time of LT-GaAs photoconductive switches at high voltage bias", *Appl. Phys. Lett.*, Vol. 75, No. 15, (October 1999): 2313-2315.
 275. Zappa, F., Lovati, P., and Lacaita, A., "Temperature Dependence of Electron and Hole Ionization Coefficients in InP." (Eighth International Conference Indium Phosphide and Related Materials, IPRM '96, Schwabisch Gmund, Germany April 21-25, 1996), 628-631.
 276. Zeman, M., R. van Swaaij, and J. Metselaar, "Optical Modeling of a-Si:H Solar Cells with Rough Interfaces: Effect of Back Contact and Interface Roughness", *J. Appl. Phys.*, Vol. 88, No. 11 (Dec. 2000): 6436-6443.
 277. Zhou, B., Butcher, K., Li, X., Tansley, T., "Abstracts of Topical Workshop on III-V Nitrides". TWN '95, Nagoya, Japan, 1995.
 278. Zhou, J.R. and D.K. Ferry, "Simulation of Ultra-small GaAs MESFET Using Quantum Moment Equations," *IEEE Trans. Electron Devices* Vol. 39 (Mar. 1992): 473-478.
 279. Zhou, J.R. and D.K. Ferry, "Simulation of Ultra-small GaAs MESFET Using Quantum Moment Equations - II:Volocity Overshoot", *IEEE Trans. Electron Devices* Vol. 39 (Aug. 1992): 1793-1796.

This page is intentionally left blank.

A

| | |
|---|-----------------|
| Advanced Solution Techniques | 2-55 |
| Breakdown Voltage | 2-55 |
| Compliance Parameter | 2-56 |
| Current Boundary Conditions | 2-55–2-56 |
| Curvetrace | 2-56 |
| Affinity rule for the heterojunction | 5-10–5-11 |
| Alignment | 5-2 |
| Affinity Rule | 5-2 |
| EXAMPLE 1 | 5-3 |
| EXAMPLE 2 | 5-5 |
| EXAMPLE 3 | 5-7 |
| EXAMPLE 4 | 5-10 |
| Manually Adjusting Material Affinity | 5-3 |
| Angular Response | 10-58 |
| Anisotropic Impact Ionization | 5-36, 21-96 |
| Anisotropic. <i>See</i> Dielectric Permittivity and Lattice Heat Equation | |
| Anti-Reflective (AR) Coatings for Luminous3D | 10-40 |
| Anti-Reflective (AR) Coatings for Ray Tracing and Matrix Method | 10-38–10-40 |
| ATHENA | |
| Importing Conductors | 3-165 |
| ATHENA Examples | |
| 3D Doping | 21-59 |
| ATLAS Examples | 2-5–2-6 |
| ATLAS Modes | |
| Batch Mode with Deckbuild | 2-3 |
| Batch Mode Without DeckBuild | 2-4 |
| Interactive Mode with Deckbuild | 2-3 |
| ISE Compatibility | 2-4 |
| No Windows Batch Mode with Deckbuild | 2-3 |
| Running ATLAS inside Deckbuild | 2-4 |
| TMA Compatibility | 2-4 |
| ATLAS Syntax | 2-7, 12-3, 21-1 |
| Comments | 21-2 |
| Continuation Lines | 21-2 |
| Expressions | 21-3 |
| Mnemonics | 21-2 |
| Order of Commands | 2-7–2-8 |
| Parameters | 2-7 |
| Pseudonyms | 21-2 |
| Statements | 2-7 |
| Symbols | 21-3 |
| Synonyms | 21-2 |
| Syntax Replacements | 2-49 |
| ATLAS Tutorial | 2-1–2-64 |
| Auger Recombination | |
| Standard Auger Model | 3-94–3-95 |
| Auto-Meshing | |
| Composition and Doping Grading | 2-21 |
| Mesh And Regions | 2-16 |
| New Concepts | 2-16–2-18 |

| | |
|---|-----------|
| Non-uniformity In The X Direction | 2-18–2-20 |
| Quadrilateral REGION Definition | 2-35 |
| Superlattices and Distributed Bragg Reflectors DBRs | 2-22 |
| Auto-meshing | 2-16 |

B

| | |
|--|---------------------------------|
| Band Degeneracies | 19-41–19-42 |
| <i>See also</i> Band Structure | |
| Band Structure | 19-62, 19-74–19-75 |
| Band Degeneracies | 19-41–19-42 |
| Electron Dispersion | 19-42–19-43 |
| Interpolation Scheme Comparisons | 19-44–19-47 |
| Motion Equations | 19-42–19-43 |
| Silicon | 19-39–19-41 |
| <i>See also</i> Strain | |
| Band-to-Band Tunneling Models | |
| Kane | 3-118–3-119 |
| Non-Local | 3-119–3-126 |
| Schenk | 3-118 |
| Standard | 3-116–3-117 |
| Basic Heterojunction Definitions | 5-1 |
| Beam Examples | |
| Gaussian Intensity Profile | 21-20 |
| LUMINOUS3D Lens | 21-20 |
| Monochromatic Beam | 21-20 |
| Multi-spectral Beam | 21-20 |
| Beam Propagation Method (BPM) | 10-18–10-20 |
| Fast Fourier Transform (FFT) | 10-19–10-20 |
| Light Propagation | 10-19 |
| Biasing | 19-21 |
| <i>See also</i> Device Geometry | |
| Block Newton Method | 21-194, E-4 |
| Bohm Quantum Potential (BQP) | 13-9 |
| Post Calibration | 13-11–13-13 |
| Schrodinger-Poisson Model | 13-10–13-11 |
| Bowing | 3-9 |
| Bulk Simulations | 19-4, 19-15, 19-29, 19-76–19-77 |
| <i>See also</i> Strain | |

C

| | |
|--|-----------|
| Capture Parameters | 21-116 |
| Carrier Continuity Equations | 3-1 |
| Carrier Generation-Recombination Models | 3-84 |
| Auger Recombination | 3-94–3-95 |
| Auger Recombination Model for High and Low Injection Conditions | 3-96 |
| Auger Recombination Model With Temperature and Concentration Dependent Coefficients | 3-97 |
| Coupled Defect Level Recombination Model | 3-88–3-90 |
| Klaassen's Concentration Dependent Lifetime Model | 3-87 |
| Klaassen's Temperature-Dependent Auger Model | 3-95 |
| Klaassen's Temperature-dependent SRH Lifetime Model | 3-87 |

| | | | |
|--|-------------|--|-------------|
| Narrow Bandgap Auger Model | 3-96 | R | 12-25 |
| Optical Generation | 3-94 | T | 12-26 |
| Radiative Recombination | 3-94 | V | 12-26 |
| Scharfetter Concentration Dependent Lifetime Model | 3-87 | X | 12-27 |
| Shockley-Read-Hall (SRH) Recombination | 3-85 | Z | 12-28 |
| SRH Concentration-Dependent Lifetime Model | 3-85–3-86 | Circular Masks | 6-3 |
| Surface Recombination | 3-98 | Clever | E-13 |
| Trap Assisted Auger Recombination | 3-90 | Collisionality | 19-49–19-50 |
| Trap-Assisted Tunneling | 3-91 | Criterion | 19-50 |
| Zamdmr Model for LT-GaAs | 3-99–3-100 | Silicon Devices | 19-49 |
| Carrier Statistics | 3-5 | <i>See also</i> Coulomb Interaction | |
| Bandgap Narrowing | 3-9–3-10 | Common Physical Models | 5-16 |
| Boltzmann | 3-5 | Energy Balance Transport Model | 5-19 |
| Effective Density of States | 3-5–3-6 | Low Field Mobility Models | 5-16 |
| Energy Bandgap Rules | 3-7 | Parallel Electric Field-Dependent Mobility | 5-17–5-18 |
| Fermi-Dirac | 3-5 | Compound Semiconductors Rules | B-5 |
| Fermi-Dirac Integrals | 3-7 | Conduction | |
| General Ternary Bandgap Model with Bowing | 3-9 | Silicon Nitride | 3-192 |
| Intrinsic Carrier Concentration | 3-6–3-7 | Conductive Materials | 3-165 |
| Passler's Model | 3-8 | Interface Resistance | 3-165 |
| Universal Bandgap Narrowing Model | 3-11 | Conductors | B-33 |
| Universal Energy Bandgap | 3-8 | Confirming Model Selection | 21-265 |
| Carrier-Carrier Scattering Models | | CONTACT Examples | |
| Brooks-Herring | 3-54 | Floating Gate | 21-29 |
| Conwell-Weisskopf | 3-53–3-54 | Parasitic Resistance | 21-28 |
| Dorkel and Leturcq | 3-52–3-53 | Schottky Barrier | 21-28 |
| <i>See also</i> Low Field Mobility Models | | Surface Recombination | 21-28 |
| Channel Simulation | 18-9–18-12 | Contact Parasitics | 21-27 |
| Channel Current | 18-12 | Contacts | |
| Continuity Equation | 18-11–18-12 | Current Boundary | 2-37 |
| Poisson's Equation | 18-10–18-11 | External Resistors, Capacitors, or Inductors | 2-37 |
| <i>See also</i> Mercury and Quasi 2D-Simulator | | Floating | 2-37–2-38 |
| C-Interpreter | | Gates | 2-36 |
| Miscellaneous Mobility Model Parameters | 21-222 | Open Circuit Contact | 2-39 |
| Mobility Functions | 21-223 | Schottky | 2-36 |
| Model Specification | 2-45 | Shorting Two Contacts | 2-38 |
| Parser Functions | 5-48 | continuous density of states | 14-2 |
| Scattering Law Exponents | 7-20 | Control and Analysis Statements | 12-29 |
| C-Interpreter functions in ATLAS | A-3–A-7 | .AC | 12-29 |
| Circuit and Analysis | 12-4 | .BEGIN | 12-29 |
| Control Statements | 12-6 | .DC | 12-30 |
| Netlist Statements | 12-4–12-6 | .END | 12-30 |
| Special statements | 12-7 | .ENDL | 12-31 |
| Circuit Element Statements | | .GLOBAL | 12-31 |
| A | 12-14 | .IC | 12-31 |
| B | 12-15–12-16 | .INCLUDE | 12-32 |
| C | 12-17 | .LIB | 12-32 |
| D | 12-18 | .LOAD | 12-33 |
| E | 12-19 | .LOG | 12-33–12-34 |
| F | 12-19 | .MODEL | 12-34 |
| G | 12-20 | .NET | 12-35–12-36 |
| H | 12-20 | .NODESET | 12-36 |
| I | 12-21 | .NUMERIC | 12-37 |
| J | 12-21–12-22 | .OPTIONS | 12-38–12-41 |
| K | 12-22 | .PARAM | 12-42 |
| L | 12-22 | .PRINT | 12-41 |
| M | 12-23–12-24 | .SAVE | 12-42–12-43 |
| O | 12-24 | .SUBCKT | 12-43 |
| Q | 12-24–12-25 | | |

- .TRAN 12-44
- Convergence Criteria20-10, 20-12
 - Block Iteration 20-16
 - Gummel's Algorithms 20-12
 - Newton's Algorithm 20-14
- Coulomb Interaction
 - Collisionality 19-49–19-50
 - Discretization 19-49
 - General Scattering Statements 19-51
 - Types 19-48
- Coupled Mode Space (CMS) 13-18
- Crowell Model 21-94
- Cubic III-V Semiconductors 5-20–5-25
 - Density of States 5-24–5-25
 - Electron Affinity 5-23–5-24
 - Energy Bandgap 5-21–5-23
 - Static Permittivity 5-25
- Current Regions (C-Regions). *See* Regions
- Current-Density 19-36
 - See also* Self-Consistent Simulation
- curve tracing 21-30, 21-345
- Cylindrical Symmetry 9-9
- D**
- Dark Characteristics 10-54
 - Extrapolation from High Temperatures 10-54–10-55
 - Integrated Recombination 10-54
 - Numerical Solution Parameters 10-55
- DC
 - Contact Resistances 18-23
 - Input Matching Network 18-24
 - Output Matching Network 18-24
- DC and Small-Signal AC
 - Small-Signal AC 18-13
 - See also* Mercury
- DC Curve-Tracer Algorithm 20-20
- DC Solutions
 - Bias 2-50
 - Generating Families of Curves 2-51
- DeckBuild 2-3, 2-8, 2-57
- Deckbuild Examples Window 19-13
- Defect Generation
 - Amphoteric 14-15
 - Light Induced 14-15–14-16
- Defects 3-14–3-25
 - Amphoteric 14-11
- DEFECTS Example
 - TFT 21-43
- DEGRADATION Examples
 - MOS 21-44
- Density Gradient (Quantum Moments Model) 13-7–13-8
- Density Gradient Method (Quantum Moments Model) 13-9–13-13
- Density of States. *See* Phonon Scattering
- Dessis. *See* ISE Compatibility
- Detection Efficiency 10-55
- Internal and External Quantum Efficiency 10-55
- Device Geometry
 - Biasing 19-21
 - Doping 19-20
 - Grid 19-16
 - Materials 19-20
 - Regions 19-17–19-19
- Device Level Reliability Modeling
 - Hansch MOS Reliability Model 3-153
- Device 18-4–18-5
 - See also* Mercury
- Dielectric Permittivity
 - Anisotropic Relative 3-186–3-187
- Diffusion Noise
 - C-Interpreter 16-8–16-9
 - Einstein Diffusion Equation *See also* Noise 16-8
- Diode 21-376
- Diode Breakdown 21-32
- Discretization 19-49, 20-5
 - See also* Coulomb Interaction
- Disordered Materials 14-2
- Displacement Current Equation 3-4
- DOPING Examples
 - 1D ATHENA Interface 21-59
 - 3D Doping From ASCII 1D File 21-60–21-61
 - 3D Electrode Definition 21-72
 - Analytical Doping Definition 21-59
 - Athena Doping Interface 21-59
 - ATHENA2D Master Files from 3D Doping 21-61–21-65
 - MOS Electrode Definition 21-72
 - SSUPREM3 Interface 21-59
- Doping 19-20
 - See also* Device Geometry
- DOS 14-2
- Drift Diffusion
 - kp Modeling 11-5
- Drift Diffusion Transport Model
 - Position Dependent Band Structure 5-12–5-13
- Drift-Diffusion Transport Model 3-2, 3-2–3-3, 5-12
- E**
- EEPROMs 4-7
 - See also* Non-Volatile Memory Technologies
- EE-Regions. *See* Regions
- Electrode Linking 21-28
- ELECTRODE Statement 4-6
- Electron Affinity
 - Temperature Dependence 5-15
- Electron Dispersion 19-42–19-43
 - See also* Band Structure
- ELIMINATE Examples
 - Substrate Mesh Reduction 21-74
- Emission Spectra 11-15
 - See also* LED
- Energy Balance 21-95

| | |
|---|-----------------|
| Energy Balance Equations | |
| Energy Balance Equations | 3-26–3-28 |
| Energy Balance Transport Model | 3-26–3-31, 3-44 |
| Relaxation Times | 3-30–3-31 |
| Energy Regions (E-Regions). <i>See</i> Regions | |
| Error Estimation | |
| Energy Dissipation | 10-29 |
| Interference | 10-29 |
| Photogeneration | 10-28 |
| Run-Time Output | 10-27 |
| Time Domain Output | 10-28 |
| <i>See also</i> FDTD | |
| Error Measures | |
| Carrier Concentrations | 20-8 |
| CLIM.DD (CLIMIT) | 20-8 |
| CLIM.EB | 20-9 |
| Estimators | |
| Regions | 19-23–19-25 |
| Exciton Model Flags | 21-265 |
| Excitons | |
| Dissociation | 15-18–15-19 |
| Dopants | 15-17–15-18 |
| Light Generation | 15-18 |
| Metal Quenching | 15-19 |
| Singlet | 15-14–15-16 |
| Triplet | 15-14–15-16 |
| Expressions | |
| Functions | 12-49–12-50 |
| Operators | 12-51 |
| External Circuit | 18-2–18-3 |
| <i>See also</i> Mercury | |
| EXTRACT Examples | |
| Extractions from Previously Generated Results | 21-75 |
| Solution Quantities | 21-75 |
| Terminal Current | 21-75 |
| Eye Diagram | 21-76–21-77 |

F

| | |
|--|---------------------|
| Fast FET Simulator. <i>See</i> Mercury | |
| Fast Fourier Transform (FFT) | 20-23, 21-79 |
| Beam Propagation | 10-19–10-20 |
| FDTD | 21-18–21-20, 21-292 |
| Beam | 10-23 |
| Boundary Conditions | 10-23–10-27 |
| <i>See also</i> FDTD Boundary Conditions | |
| Error Estimation | 10-27–10-28 |
| Mesh | 10-23 |
| Physical Model | 10-21–10-22 |
| Static Solutions | 10-27–10-28 |
| FDTD Boundary Conditions | |
| Perfect Electrical Conductor (PEC) | 10-23 |
| Perfectly Matched Layer (PML) | 10-24–10-26 |
| Plane Source | 10-26–10-27 |
| Point Source | 10-27 |
| FDTD Mesh | 21-78 |
| FDTD Solution | 21-78 |

| | |
|--|-------------|
| FDX.MESH, FDY.MESH Examples | |
| FDTD Mesh | 21-78 |
| Setting Locally Fine Grids | 21-78 |
| FF | 10-62 |
| <i>See also</i> Solar Cells | |
| Field Emission | 3-191 |
| Field Emission Transport Model | 5-13–5-15 |
| Final State Selection. <i>See</i> Phonon Scattering | |
| Finite Difference Time Domain Analysis. <i>See</i> FDTD | |
| FLASH Memories | 4-7 |
| <i>See also</i> Non-Volatile Memory Technologies | |
| Flicker Noise | |
| C-Interpreter | 16-11–16-12 |
| Hooge | 16-11 |
| Floating Gate | 21-28 |
| Floating Gate to Control Gate (FCCG) Current. <i>See</i> Gate Current Models | |
| Fluctuations | |
| Current-Density | 19-36 |
| Potential | 19-37–19-39 |
| <i>See also</i> Self-Consistent Simulation | |
| Fourier Examples | 21-80 |
| Frequency Conversion Materials | |
| 2D | 10-46–10-48 |
| fundamental frequency | 18-15 |

G

| | |
|--|-------------|
| GaAs Physical Models | |
| Bandgap Narrowing | 5-26 |
| Low Field Mobility | 5-27–5-28 |
| Gain Models | |
| Empirical | 3-168 |
| Lorentzian Broadening | 3-177 |
| Standard | 3-167–3-168 |
| <i>See also</i> Optoelectronic Models | |
| Strained Wurtzite | 3-175–3-177 |
| Takayama's | 3-169 |
| Unstrained Zincblende | 3-171–3-173 |
| Gain Saturation | 8-7 |
| Gate Current Assignment | 4-8 |
| Gate Current Models | 3-126 |
| Concannon's Injection Model | 3-131–3-134 |
| Direct Quantum Tunneling | 3-134–3-140 |
| Floating Gate to Control Gate (FCCG) | 3-150–3-152 |
| Fowler-Nordheim Tunneling | 3-126–3-128 |
| Lucky Electron Hot Carrier Injection Model | 3-128–3-131 |
| Schenk | 3-140–3-142 |
| SONOS | 3-142 |
| Gather Algorithm | 19-69 |
| Gaussian Elimination | 20-8 |
| <i>See also</i> LU Decomposition | |
| General Quantum Well Model | 13-16 |
| Generation Models | 5-19 |
| Generation Rate Formula | 10-9 |
| Generation-Recombination Noise | |
| Direct GR | 16-10 |

| | |
|---------------------------------|------------------------------------|
| Impact Ionization | 16-11 |
| Trap Assisted GR | 16-10 |
| GO | 21-81, 21-309 |
| GO ATLAS | 21-309 |
| GO Examples | |
| Parallel ATLAS | 21-81 |
| Starting an ATLAS Version | 21-81 |
| Grid | 19-16, 21-5, 21-78, 21-141, 21-359 |
| <i>See also</i> Device Geometry | |
| Gummel | 21-194 |

H

| | |
|---|-----------|
| Harmonic Balance | |
| FastHarmonicBalance | 18-14 |
| Frequency Domain | 18-16 |
| Large-Signal Simulation's Problem | 18-17 |
| LOG | 18-14 |
| Method | 18-17 |
| Non-Linearity | 18-15 |
| <i>See also</i> Non-Linearity | |
| SOLVE | 18-14 |
| Time Domain | 18-16 |
| Heat Capacity | |
| Compositionally Dependent | 7-7–7-8 |
| Standard Model | 7-7 |
| Heat Generation | 7-12–7-13 |
| Heat Sink Layers | 7-8 |
| Helmholtz Equation | 8-2, 9-4 |
| Heterojunction Devices | 5-47 |
| Graded Junctions | 5-47 |
| Step Junctions | 5-47 |

I

| | |
|--|---------------|
| III-V Devices | 21-112 |
| Im. <i>See also</i> Solar Cells | 10-62 |
| IMPACT Example | |
| Selberherr Model | 21-97 |
| Impact Ionization | 21-167–21-169 |
| Parameters | 21-167 |
| Impact Ionization Models | 3-101 |
| Band-to-Band Tunneling | 3-116–3-126 |
| Geometrical Considerations | 3-101–3-102 |
| Local Electric Field Models | 3-102–3-110 |
| Non-Local Carrier Energy Models | 3-112–3-115 |
| Importing Conductors | 3-165 |
| Impurity Scattering | |
| Implementing | 19-59 |
| Incomplete Ionization of Impurities | 3-12–3-13 |
| Initial Guess | |
| First and Second Non-Zero Bias Solutions | 2-52 |
| Initial Solution | 2-52 |
| Parameters | 21-348 |
| Trap Parameter | 2-52–2-53 |
| Insulators | B-31–B-32 |

| | |
|--|-----------------|
| INTERFACE Examples | |
| Interface Charge for III-V Devices | 21-112 |
| MOS | 21-111 |
| SOI | 21-111 |
| Interpolation | 19-44–19-47 |
| Tricubic | 19-72 |
| Trilinear | 19-70–19-71 |
| <i>See also</i> Band Structure | |
| INTTRAP Examples | |
| Multiple Interface Trap States | 21-116 |
| Inversion Layer Mobility Models | |
| Darwish CVT Model | 3-65–3-67 |
| Lombardi CVT Model | 3-62–3-65 |
| Tasch Model | 3-69–3-72 |
| Yamaguchi Model | 3-67, 3-67–3-69 |
| Isc | 10-62 |
| <i>See also</i> Solar Cells | |
| ISE Compatibility | 2-4 |
| Ishikawa's Strain Effects Model | |
| InGaAlAs | 3-178–3-180 |
| InGaAs | 3-178 |
| InGaAsP | 3-178 |
| <i>See also</i> Optoelectronic Models | |

K

| | |
|---|--------|
| Klaassen Model Parameters | 21-170 |
| <i>See also</i> Carrier Generation-Recombination Models | |

L

| | |
|-----------------------------------|----------------------|
| Large Signal Analysis | 20-22–20-24 |
| Large-Signal | 18-14 |
| <i>See also</i> Harmonic Balance | |
| Laser Helmholtz Solver | 21-141 |
| LASER Mesh | 21-141 |
| Laser Simulation Problems | 8-10 |
| Laser Simulation Techniques | 8-12 |
| Lattice Heat Flow Equation | 7-2 |
| LED | 11-15, 21-125–21-129 |
| LED Data Extraction | |
| Emission Spectra | 11-7 |
| Emission Wavelength | 11-8 |
| Luminous Intensity | 11-6 |
| Lenslets | 10-44 |
| Anti-reflective Coatings | 10-45 |
| Aspheric | 10-42–10-43 |
| Composite | 10-42 |
| Ellipsoidal | 10-41 |
| Pyramid | 10-43 |
| Random Textured | 10-44 |
| Spherical | 10-41 |
| User-Definable | 10-45 |
| Li model. | 21-268 |
| <i>See also</i> Gain Models | |
| Light Absorption | 10-9 |

| | |
|---|-------------|
| Light Emitted Diode (LED) Simulation | |
| Reverse Ray-Tracing | 11-9 |
| <i>See also</i> LED Data Extraction and Reverse Ray-Tracing | |
| Light Emitted Diodes (LED) | |
| Data Extraction | 11-6–11-8 |
| <i>See also</i> LED Data Extraction and Reverse Ray-Tracing | |
| Models | 11-4 |
| <i>See also</i> Light Emitting Diode (LED) Models | |
| Statement | 11-15 |
| <i>See also</i> LED | |
| Light Emitting Diode (LED) Models | |
| kp Band Parameter Models | 11-5 |
| Polarization and Piezoelectric Effects | 11-4 |
| Radiative | 11-4–11-5 |
| <i>See also</i> LED Data Extraction and Reverse Ray-Tracing | |
| Light Emitting Diode (LED) Simulator | 11-1–11-14 |
| Light Propagation | |
| Fresnel formulae | 10-19 |
| Multiple Region Device | 10-19 |
| LOAD Examples | |
| Binary Format | 21-135 |
| Load | 21-135 |
| Simple Save | 21-135 |
| SOL.STR | 21-135 |
| Local Electric Field Models | |
| Crowell-Size Impact Ionization Model | 3-109–3-110 |
| Grant's Impact Ionization Model | 3-108–3-109 |
| Lackner Impact Ionization Model | 3-111–3-112 |
| Okuto-Crowell Impact Ionization Model | 3-110–3-111 |
| Selberherr's Impact Ionization Model | 3-102–3-104 |
| Valdinoci Impact Ionization Model | 3-105–3-107 |
| Van Overstraeten - de Man Impact Ionization Model | 3-105 |
| Zappa's Model for Ionization Rates in InP | 3-107–3-108 |
| Local Optical Gain | 8-5, 9-6 |
| Stimulated Emission | 9-6 |
| LOG Examples | |
| AC Logfile | 21-140 |
| Logfile Definition | 21-140 |
| RF Analysis | 21-140 |
| Transient | 21-140 |
| Log Files | |
| AC Parameter Extraction | 2-61 |
| Functions in TonyPlot | 2-61 |
| Parameter Extraction In Deckbuild | 2-60 |
| Units of Currents | 2-59 |
| UTMOST Interface | 2-60 |
| Lorentzian line broadening model | 21-268 |
| Lorentzian shape function | 21-268 |
| Low Field Mobility Models | |
| Albrecht Model | 5-38–5-39 |
| Analytic | 3-48–3-49 |
| Arora Model | 3-49–3-50 |
| Carrier-Carrier Scattering | 3-52–3-53 |
| Constant | 3-46 |
| Doping Dependent | 3-55 |
| Incomplete Ionization | 3-55 |
| Klaassen's | 3-55–3-60 |
| Masetti | 3-50–3-52 |
| Uchida's for Ultrathin SOI | 3-60 |
| Low Mobility Models | |
| Concentration-Dependent Tables | 3-46–3-47 |
| Faramand Modified Caughey Thomas | 5-39–5-41 |
| LU Decomposition | 20-8 |
| Luminous | 10-1, 11-6 |
| LUMINOUS3D | |
| Anti-Reflective (AR) Coatings | 10-40 |
| Diffusive Reflection | 10-8 |
| Luminous3D | 10-1 |
| Lumped Element | 3-41–3-42 |
| LX. MESH and LY.MESH Examples | |
| Setting Locally Fine Grids | 21-141 |
| LX.MESH, LY.MESH Examples | |
| LASER Mesh | 21-141 |
| M | |
| Magnetic Fields | |
| Carrier Transport | 3-184–3-185 |
| Material Coefficient Definition | 21-182 |
| All regions | 21-182 |
| Named Material | 21-182 |
| Numbered region | 21-182 |
| Material Defaults | B-20–B-25 |
| Material Dependent Physical Models | |
| Cubic III-V Semiconductors | 5-20–5-25 |
| <i>See also</i> Cubic III-V Semiconductors | |
| GaAs | 5-26–5-28 |
| <i>See also</i> GaAs Physical Models | |
| Material Parameters and Models Definition | 2-36 |
| Contact | 2-36 |
| Interface Properties | 2-40 |
| Material Properties | 2-39 |
| Physical Models | 2-40–2-41 |
| Material Properties | |
| Conductor | 2-39 |
| Heterojunction Materials | 2-40 |
| Insulator | 2-39 |
| Parameters | 2-39 |
| Semiconductor | 2-39 |
| Material Systems | |
| Al(x)Ga(1-x)As | 5-28–5-30 |
| Al/In/GaN | 5-37–5-45 |
| AlGaAs | B-10 |
| CIGS (CuIn(1-x)Ga(x)Se ₂), CdS, and ZnO | 5-46 |
| GaN/InN/AlN | B-13–B-19 |
| Hg(1-x)Cd(x)Te | 5-45 |
| In(1-x)Ga(x)As(y)P(1-y) | 5-30–5-32 |
| InGaAsP | B-11 |
| Polysilicon | B-7–B-9 |
| Si(1-x)Ge(x) | 5-32–5-34 |
| SiC | B-12 |
| Silicon | B-7–B-9 |
| Silicon Carbide (SiC) | 5-34–5-37 |
| Materials | 19-20 |
| <i>See also</i> Device Geometry | |
| Mathiessen's rule | 3-62 |

| | | | |
|---|-----------------------|--|--|
| Smoothing | 20-4 | TFLDMB2 Model | 21-261 |
| Mesh Cylindrical | 9-9 | WATT Model | 21-261 |
| MESH Examples | | Model Flags | |
| ATHENA Interface | 21-189 | Carrier Statistics | 21-249–21-250 |
| Mesh Definition | 21-189 | Defect Generation | 21-256–21-257 |
| Metals | B-33 | Direct Tunnelling | 21-244–21-245 |
| METHOD Examples | | Energy Balance Simulations | 21-255–21-256 |
| Numerical Method Definition | 21-201 | Generation | 21-245–21-249 |
| Transient Method | 21-202 | Lattice Heating Simulation | 21-256 |
| TRAP Parameter | 21-202 | Magnetic field model | 21-257 |
| Microscopic Noise Source Models | | Mobility | 21-217–21-220 |
| Diffusion Noise. <i>See</i> Diffusion Noise | | Recombination | 21-243–21-244 |
| Flicker Noise. <i>See</i> Flicker Noise | | Model Macros | 21-257 |
| Generation-Recombination Noise | 16-9–16-11 | Model Selection | 21-265 |
| Mixed Mode Recommendations | | Modifying Imported Regions | 2-23 |
| Extraction of Results | 12-10 | Monte Carlo. <i>See</i> MC Device | |
| Initial Settings | 12-11 | MOS | 21-44, 21-72, 21-111, 21-320, 21-375, 21-376 |
| Input Parsing | 12-7 | MOS Technologies | 4-2 |
| Multi-Device Structure Representation | 12-8–12-9 | Electrode | 4-4 |
| Numerics | 12-8 | Energy Balance Solutions | 4-5 |
| Scale and Suffixes | 12-8 | ESD Simulation | 4-5 |
| Using MixedMode inside the VWF Automation Tools | 12-10–12-11 | Gate Workfunction | 4-4 |
| MixedMode Command File | 12-12–12-13 | Interface Charge | 4-4 |
| Mobility | | Meshing | 4-2 |
| Canali Modification | 3-78–3-79 | Physical Models | 4-2 |
| Carrier Temperature Dependent Mobility | 3-79–3-81 | Single Carrier Solutions | 4-4 |
| C-interpretor Functions | 3-82 | Motion | 19-42–19-43 |
| Inversion Layer Mobility Models | 3-62–3-72 | <i>See also</i> Band Structure | |
| Low Field Mobility Models | 3-45–3-61 | Multiple Longitudinal Mode Model | 8-10 |
| Meinerzhagen-Engl | 3-81–3-82 | | |
| Model Flags | 21-241–21-243 | N | |
| Model Summary | 3-83 | Near-Field Pattern | 8-12 |
| Parallel Electric Field-Dependent Mobility | 3-77 | NEARFLG | 4-8 |
| Parallel Electric Field-Dependent Models | 5-17–5-18 | <i>See also</i> Gate Current Assignment | |
| Perpendicular Electric Field-Dependent Mobility | 3-73–3-76 | Negative Differential Mobility Model. | |
| Perpendicular Field Mobility Model | 3-61 | <i>See</i> Parallel Electric Field-Dependent Mobility Models | |
| MOBILITY Examples | | Newton-Richardson | 21-200 |
| Modified Watt Model | 21-225 | Nitride Charge | 21-270–21-271 |
| Mobility Models in TFT | 14-17 | Noise | |
| MOCA. <i>See</i> MC Device Input Files | | Calculating | 16-6 |
| MOCASIM Examples Window | 19-14 | <i>See also</i> Noise Calculation | |
| Mode Space (MS) | 13-18 | Circuit Level Description of | 16-3–16-5 |
| Model And Material Parameter Selection in 3D | 6-4–6-5 | Microscopic Analysis | 19-35 |
| Model Dependent Parameters | 21-260 | <i>See also</i> Self-Consistent Simulation | |
| ARORA Model | 21-260 | Outputting | 16-13–16-14 |
| BBT.KANE | 21-262 | <i>See also</i> Noise Output | |
| BBT.KL Model | 21-260 | Simulating | 16-2 |
| BBT.STD Model | 21-260 | Noise Calculation | |
| CCSMOB Model | 21-260 | Impedance Field | 16-6 |
| CONCANNON Model | 21-261–21-262 | Local Noise Source | 16-7 |
| FLDMOB Model | 21-217–21-218, 21-260 | Microscopic Noise Source | 16-7 |
| Fowler-Nordheim Tunneling Model | 21-261 | <i>See also</i> Microscopic Noise Source Models | |
| HEI Model | 21-262 | Noise Output | |
| LASER Simulation | 21-263–21-264 | Log Files | 16-13 |
| N.DORT Model | 21-262 | Structure Files | 16-14 |
| P.DORT Model | 21-262 | | |
| SURFMOB Model | 21-261 | | |
| TFLDMB1 Model | 21-261 | | |

-
- Non-Equilibrium Green's Function Approach (NEGF)
 Mode Space Approach 13-18–13-21
See also Quantum Transport
- Non-Isothermal Models
 Current Densities 7-9–7-10
 Effective Density Of States 7-9
 Seeback Effect 7-11
- Non-Linear Iteration 20-6
 Block 20-7
 Combining Iteration Methods 20-7
 Convergence Criteria 20-8
 Error Measures 20-8
 Gummel 20-6–20-7
 Linear Subproblems 20-7–20-8
 Newton 20-6
- Non-Linearity
 Linear Circuit 18-15
 Non-linear Circuit 18-16
 Real Devices 18-16
- Non-Local Carrier Energy Models
 Concannon's Impact Ionization Model 3-114–3-115, 21-96
 Hydrodynamic Models 3-115–3-116
 Non-Linear Hydrodynamic Model 21-90
 Toyabe Impact Ionization Model 3-112–3-113
- Non-Volatile Memory Technologies 4-7
 Floating Gates 4-7
 Gate Current Models 4-7–4-8
- Numerical Methods 21-190, E-3
- Numerical Solution Techniques
 (Numerical Techniques) 2-46–2-49, 20-1–20-25
 Basic Drift Diffusion Calculations 2-46
 Drift Diffusion Calculations with Lattice Heating 2-46
 Energy Balance Calculations 2-47
 Energy Balance Calculations with Lattice Heating 2-47
 Importatn Parameters of the METHOD Statement 2-48
 METHOD restrictions 2-48
 Pisces-II Compatibility 2-49
 Setting the Number of Carriers 2-47
- O**
- ODIN. *See* Clever
- Ohmic Contacts 19-22
- OLED 15-1
- Optical Generation/Radiative Recombination
 Photon Transition 3-94
- Optical Index Models
 Adachi's Dispersion 3-181
 Sellmeier Dispersion 3-181
 Tauc-Lorentz Dielectric Function with
 Optional Urbach Tail 3-182–3-183
- Optical Index Models 3-181
See also Laser, Luminous, Luminous3D, and VCSEL
- Optical Power 8-7, 9-7
- Optical Properties B-34
- Optical Properties of Materials 10-36
 Refractive Index 10-36
 Wavelength Dependent Refractive Index 10-36–10-37
- Optical Sources
 2D Sources 10-49
 3D Sources 10-49
 Aspheric Lenslets 10-42–10-43
 Composite Lenslets 10-42
 Ellipsoidal Lenslets 10-41
 Frequency Response 10-56
 Lenslet Anti-reflective Coatings 10-45
 Lenslets 10-41–10-43
 Luminous beam intensity in 2D 10-50–10-51
 Luminous3D Beam Intensity 10-51
 Monochromatic 10-51–10-53
 Multispectral 10-51–10-53
 Optical Beam 10-49
 Periodicity in the Ray Trace 10-50
 Pyramid 10-43
 Random Textured Lenslets 10-44
 Reflections 10-50
 Solar Sources 10-53
 Spherical Lenslets 10-41
 Transient Response 10-56
 User-Definable Lenslets 10-45
- Optoelectronic Models 3-166
 Band Stucture 3-170
 Default Radiative Recombination 3-167
 Empirical Gain 3-168
 General Radiative Recombination 3-166
 Ishikawa's 3-178–3-180
 Lorentzian Gain Broadening 3-177
 Standard Gain 3-167–3-168
 Strained Wurtzite Three-Band Model for Gain
 and Radiative Recombination 3-175–3-177
 Takayama's Gain 3-169
 Unstrained Zincblende Models for Gain
 and Radiative Recombination 3-171–3-173
- Organic Device Simulation. *See* Organic Display and Organic Solar
- Organic Display 15-1–15-2
- Organic Display and Organic Solar 15-1–15-18
 Organic Polymer Physical Models 15-5–15-13
- Organic Polymer Physical Models
 Bimolecular Langevin Recombination 15-13
 Exciton Dissociation 15-18–15-19
See also Excitons
 Excitons 15-14
See also Excitons
 Hopping Mobility 15-9–15-10
 Organic Defects 15-5–15-9
 Poole-Frenkel Mobility 15-10–15-13
- Organic Simulators. *See* Organic Display and Organic Solar
- Organic Solar 15-3–15-4
- OTFT 15-1
 ODEFECTS 21-272–21-274, 21-275
- OUTPUT Examples
 Combining OUTPUT with SOLVE and SAVE 21-289
-

P

Parallel ATLAS. *See* GO Statement

Parallel Momentum

Conservation 19-60–19-62
See also Tunneling

Parameter Type

1D Profile Modifications 21-53
 AC 21-351–21-352
 Albrecht Model Parameters 21-220
 Analytical Profile 21-51
 Angled Distribution 21-58
 Anisotropic Impact Ionization 21-96
 Arora Concentration Dependent Mobility Model 21-220
 Averaging Parameters 21-289
 Band Structure 21-161–21-163
 BIP Technology 21-374
 Boundary 21-73, 21-185
 Boundary Conditions 21-25–21-27, 21-106–21-110
 BQP 21-163
 Brooks Model Parameters 21-220
 Canali Model Parameters 21-220
 Cap Poisson Solution 18-28
 Capture 21-370
 Carrier Statistics Model 21-171
 Carrier-Carrier Scattering Model 21-220
 Caughey-Thomas Concentration Dependent Model 21-220
 Compliance 21-348
 Concannon Model 21-96
 Conductors 21-182
 Control 21-323, 21-374
 Conwell Model Parameters 21-220
 Cross-Section 21-271
 Crowell Model 21-94
 CVT Transverse Field Dependent Model 21-221
 Darwish CVT Transverse Field Dependent Model 21-221
 Data Type 21-184–21-185
 DC 21-344–21-346
 DC Contact Resistances 18-23
 DC Input Matching Network 18-24
 DC Output Matching Network 18-24
 Defect Generation Materials 21-182
 Diode Technology 21-376
 Direct Tunnelling 21-353
 Dopant Type Specification 21-54–21-55
 Electric Field Model Selection 21-90
 Electrode 21-373–21-374
 Energy Balance 21-95, 21-171–21-172
 Equation Solver 21-195
 Exciton Materials 21-178–21-179
 File 21-134–21-135
 File I/O 21-324
 File Import Profile 21-52–21-53
 File Output 21-137–21-138, 21-347
 Gate Poisson Solution 18-28
 General 21-197–21-199, 21-257–21-259
 Grid Indices 21-71–21-72
 Gummel 21-199
 Hot Carrier Injection 21-172
 Impact Ionization 21-167–21-169

Initial Guess 21-348
 Interface Doping Profile Location 21-50
 Ionization Integral 21-288, 21-353
 Klaassen Model 21-170
 Klaassen's Mobility Model 21-221
 Lackner Model Parameters 21-89
 LASER 21-176–21-177
 Laser Model 21-121–21-124
 Lateral Distribution 21-57–21-58
 Lateral Extent 21-56
 Lattice Temperature Dependence 21-172–21-174
 Lifetimes 21-271
 Localization 21-120
 Location 21-56, 21-303, 21-323
 Mandatory SPREAD Parameters 21-362
 Masetti Model Parameters 21-220
 Material 21-160, 21-314–21-317
 Meinerzhagen-Engl Model Parameters 21-220
 Mesh 21-188
 Mesh File 21-187
 Miscellaneous Material Parameters 21-179–21-181
 Mobility Model 21-164
 Mobility Model Aliases 21-223–21-225
 Model Dependent 21-260–21-264
 Model Localization 21-91
 Model Selection 21-88
 Modified Watt Mobility Model 21-221
 MOS Capacitances 21-376
 MOS Technology 21-375
 MQW Parameters 21-268–21-269
 Newton 21-200
 NOISE 21-139, 21-178, 21-289, 21-352
 Non-linear Hydrodynamic Model 21-90
 Okuto-Crowell 21-89
 Optional SPREAD Parameters 21-362
 Organic Transport 21-178
 Output 21-189
 Oxide Material 21-175
 Parallel Field Dependent Model 21-221
 Parasitic Element 21-139
 Perpendicular Field Dependent Model Parameters 21-221
 Photogeneration 21-175–21-176, 21-354–21-355
 Poisson Look-Up Table Calculation 18-29–18-30
 Poole-Frenkel Mobility Model 21-221
 Position .. 21-70, 21-110–21-111, 21-318–21-319, 21-366
 Quantum 21-201
 Quantum Model 21-250–21-254
 Recombination Model 21-165–21-166
 Region 21-71
 RF Analysis 21-138
 RF Contact Impedances 18-24
 RF Input Matching Network 18-25
 RF Output Matching Network 18-25
 SCHWARZ and TASCHE Transverse Field Dependent Model 21-222
 Selberrherr Model 21-94
 Shirahata's Mobility Model 21-221
 Solution Method 21-194–21-195
 Solution Tolerance 21-195–21-197
 Statement Applicability 21-50

- Tasch Mobility Model 21-221
 Technology 21-373
 Temperature Dependence 21-95
 Temperature Dependent Low Field Mobility 21-220
 Thermal3D 21-355
 Transient 12-44–12-45, 21-349–21-351
 Trap 21-58
 Trap Density 21-270
 Trap Depth 21-271
 Uchida's Mobility Model 21-221
 Valdinoci Models 21-91–21-93
 van Overstraeten de Man Model Parameters 21-89
 Variable 21-322
 Vertical Distribution 21-55–21-56
 Watt Effective Transverse Field Dependent Model 21-221
 Workfunction 21-24–21-25
 Yamaguchi Transverse Field Dependent Model 21-221
 Zappa Model 21-93–21-94
 PEC. *See* FDTD Boundary Conditions
 Perpendicular Electric Field-Dependent Mobility
 Shirahata's Model 3-75–3-76
 Watt Model 3-73–3-74
 Phase Change Materials (PCMs) 7-16–7-19
 phase-space balancing 19-29
 Phonon Scattering
 Density of States 19-54
 Final State Selection 19-55
 Modes 19-51–19-54
 See also Phonon Scattering Modes
 Parameters 19-55–19-57
 Strain 19-75
 See also Phonon Scattering Modes and Strain
 Phonon Scattering Modes
 Acoustic Phonons 19-52
 Hole Interband 19-54
 Hole Intraband 19-54
 Intervalley 19-53
 Optical 19-53
 Phonon-assisted Tunneling Model for
 GaN Schottky Diodes 3-38–3-39
 Photocurrent 10-35
 Defining Available Photocurrent 10-35
 Source 10-35
 Photodetectors 10-49–10-57
 Photogeneration 10-9, 10-28, E-1
 Contacts 10-9
 Exponential 10-33
 Non-uniform Mesh 10-9
 Tabular 10-34
 User-Defined 10-30–10-32
 Photon Rate Equations 8-5–8-7, 9-6–9-7
 Spontaneous Recombination Model 9-7
 Physical Models 3-45
 Carrier Generation-Recombination Models 3-84–3-98
 Device Level Reliability Modeling 3-153
 Energy Balance 2-41
 Epitaxial Strain Tensor Calculation in Wurtzite 3-156
 Ferroelectric Permittivity Model 3-154
 Gate Current 3-126–3-152
 Light Absorption in Strained Silicon 3-162–3-163
 Low Field Mobility in Strained Silicon 3-161
 Mobility 3-45–3-81
 Polarization in Wurtzite Materials 3-157–3-158
 Stress Effects on Bandgap in Si 3-158–3-160
 Summary 2-42–2-45
 Physically-Based Simulation 1-4
 PISCES-II 2-8–2-9
 Pm 10-62
 See also Solar Cells
 PML 21-292–21-293
 See also FDTD
 PML. *See* FDTD Boundary Conditions
 Poisson
 Cap Solution 18-28
 Gate Solution 18-28
 Look-Up Table Calculation 18-29–18-30
 Poisson's Equation 3-1
 Positionally-Dependent Band Structure 5-47
 Power Device Simulation Techniques 7-21
 External Inductors 7-21
 Floating Field Plates 7-21
 Floating Guard Rings 7-21
 PROBE Examples
 Maximum Value 21-303
 Probing at a Location 21-303
 Vector Quantity 21-304
Q
 Quantum Correction D-13, D-19
 Quantum Correction Models 13-14
 Hansch's 13-14
 Van Dort's 13-14–13-15
 Quantum Efficiency 10-35, 10-55
 Quantum Mechanical Models
 Self Consistent Coupled Schrodinger Poisson Model ... 13-2–13-6
 Quantum Transmitting Boundary Method (QTBM) 13-21
 Quantum Transport
 Drift-Diffusion Mode-Space Method (DD_MS) 13-22–13-23
 Non-Equilibrium Green's Function (NEGF) Approach ... 13-18–13-21
 Quasi-2D Simulation
 Channel Simulation 18-9–18-12
 Poisson Equation 18-6–18-8
 Quasi-2D Simulation 18-6–18-12
 See also Mercury
 Quasistatic Capacitance
 Voltage Profiles 3-164

R

| | |
|--|---------------------|
| Radiative Recombination Models | |
| Strained Wurtzite | 3-175–3-177 |
| Unstrained Zincblende | 3-171–3-173 |
| Radiative Recombination Models | 3-166–3-167 |
| <i>See also</i> Optoelectronic Models | |
| Rational Chebyshev approximation | 3-7 |
| Ray Tracing | 10-2–10-5 |
| 3D | 10-4–10-5 |
| Incident Beam | 10-2 |
| Outputting | 10-9 |
| Ray Splitting At Interfaces | 10-3 |
| <i>See also</i> Reverse Ray-Tracing | |
| Recombination Models | 5-19, 21-165–21-166 |
| Reflections | 10-7 |
| Back | 10-7 |
| Discontinuous Regions | 10-8 |
| Front | 10-7 |
| Sidewall | 10-7 |
| User Specified | 10-7 |
| refractive index | 21-107 |
| Region | |
| Modifying Imported Regions | 2-23 |
| REGION Examples | |
| 3D Region Definition | 21-320 |
| Graded Heterojunction Definition | 21-320 |
| Graded x.comp and y.comp Material Definition | 21-320 |
| Grid Indices | 21-319 |
| MOS | 21-320 |
| Non-Rectangular Region | 21-319 |
| Regions | |
| Current | 19-23–19-24 |
| Energy | 19-25 |
| <i>See also</i> Estimators | |
| Regions | 19-17–19-19 |
| <i>See also</i> Device Geometry | |
| Regrid Examples | 21-325 |
| Doping | 21-325 |
| Potential | 21-325 |
| Re-initializing | 21-325 |
| Regridding. <i>See</i> Remeshing the Structure | |
| Remeshing the Structure | 2-23–2-25, E-7 |
| Regrid on Doping | 2-24 |
| Regrid Using Solution Variables | 2-25 |
| Results | 2-58 |
| Log Files | 2-59 |
| Run-Time Output | 2-58 |
| Solution Files | 2-62 |
| Reverse Ray-Tracing | 11-9–11-14 |
| <i>See also</i> Ray-Tracing | |
| RF | |
| Contact Impedances | 18-24 |
| Input Matching Network | 18-25 |
| Output Matching Network | 18-25 |
| Running ATLAS | 2-4 |
| Parallel ATLAS | 2-4 |
| version number | 2-4 |

S

| | |
|--|---------------------------------|
| SAVE | 21-326–21-332 |
| SAVE Examples | |
| Basic Save | 21-332 |
| User-defined Output | 21-332 |
| Scalar Helmholtz Equation | 8-2 |
| Scatter Algorithm | 19-69 |
| Scattering | 19-51–19-60, D-12 |
| <i>See also</i> Impurity and Phonon Scattering | |
| Schottky Barrier Injection | 19-68–19-69 |
| Airy Function | 19-68 |
| Schottky Contacts | 19-69 |
| Schottky Contacts | 3-32 |
| Parabolic Field Emission Model | 3-36 |
| Phonon-assisted Tunneling Model for | |
| GaN Schottky Diodes | 3-38–3-39 |
| Universal Schottky Tunneling (UST) Model | 3-37–3-38 |
| Schrödinger Equation | 13-2, 19-64 |
| <i>See also</i> Size Quantization Correction | |
| Selberrher Model | 21-94 |
| Self-Consistent Schrodinger-Poisson | 21-359 |
| Self-Consistent Simulation | 19-32–19-39 |
| Current-Density | 19-36 |
| Noise | 19-35 |
| Potential | 19-37–19-39 |
| Velocity Autocorrelation | 19-35 |
| Semiconductor Equations | 3-1 |
| Semiconductor Laser Simulation Techniques | 9-15 |
| SET Examples | |
| Numeric Variable | 21-333 |
| String Variable | 21-333 |
| Silicon Bipolar Devices | 4-5 |
| Dual Base BJTs | 4-6 |
| Electrode Naming | 4-6 |
| Meshing | 4-5 |
| Open Circuit Electrode | 4-6 |
| Physical Models | 4-5 |
| Solution Techniques | 4-7 |
| Silicon Nitride | |
| Conduction | 3-192 |
| Silvaco C-Interpreter (SCI) | A-1 |
| <i>See also</i> C-Interpreter | |
| Simulations | 19-78 |
| Bulk. <i>See also</i> Strain | 19-76–19-77 |
| Device. <i>See also</i> Strain | 19-78 |
| Single Event Upset (SEU) | 3-188–3-190, 6-5, 21-334–21-336 |
| User-defined | 3-190 |
| SINGLEEVENTUPSET Examples | |
| SEU | 21-336 |
| six equation solver | 7-1 |
| Size Quantization Correction | 19-64–19-67 |
| Monte Carlo Schrodinger Formulation | 19-65–19-66 |
| Quantum | 19-66–19-67 |
| Schrödinger Equation | 19-64–19-65 |
| Small Signal Analysis | 20-22–20-24 |

-
- Small-Signal AC Solutions
 - Ramped Frequency At A Single Bias2-53
 - Single Frequency AC Solution During A DC Ramp2-53
 - smoothing21-189, 21-324
 - SOI Technologies4-8, 21-111
 - Meshing4-8
 - Numerical Methods4-10
 - Physical Models4-9
 - Physical Phenomena4-11
 - Solar Cells10-59
 - Extraction10-62–10-63
 - Optical Propagation Models10-59–10-61
 - Spectra10-59
 - Solution Files
 - Customizing Solution Files2-62
 - Interpreting Contour Plots2-62
 - Re-initializing ATLAS at a Given Bias Point2-63
 - Saving Quantities from the Structure at each Bias Point2-63
 - Solutions
 - DC2-50
 - Initial Guess2-51–2-53
 - Small-Signal AC2-53
 - Transient2-54
 - SOLVE Examples
 - AC Analysis21-357
 - Bias Stepping21-356
 - DC Conditions21-356
 - Ionization Integral21-358
 - Photogeneration21-357
 - Transient Simulation21-356–21-357
 - SONOS Type Structures
 - DYNASONOS Model3-144–3-149, 21-270
 - FNONOS Model3-142–3-143
 - SONOS Model3-143–3-144
 - See also Gate Current Models
 - SOPRA Database10-37, B-35–B-45
 - See also Optical Properties of Materials
 - Spatial Response10-57
 - Spectral Response10-57
 - Spontaneous Recombination Model8-7
 - SPREAD Examples21-363
 - Standard Mobility Model.
 - See Parallel Electric Field-Dependent Mobility Models
 - Statement allocation and usage19-4
 - Static Solutions
 - Energy Dissipation10-29
 - Interference10-29
 - Photogeneration10-28
 - Run-Time Output10-27
 - Time Domain Output10-28
 - See also FDTD
 - Statistical Enhancement19-29–19-31
 - Particle Compression19-31
 - Statements19-31
 - See also MC Device
 - Stimulated Emission8-5
 - Strain
 - Band Structure.19-74–19-75
 - Bulk Simulations19-76–19-77
 - Device Simulations19-78
 - Phonon Scattering19-75
 - Strain Effects. See Ishikawa's Strain Effects Model
 - Structure Definition
 - 2D Circular Structures2-25–2-28
 - 3D Cylindrical Structures2-29–2-33
 - 3D Structures2-29
 - ATHENA2-10
 - ATLAS Syntax2-11
 - DevEdit2-11
 - Extracting 2D Circular Structures
 - From 3D Cylindrical Structures2-33
 - Grids2-34
 - Maximum Numbers Of Nodes, Regions, and Electrodes2-34
 - Structure Definition Using ATLAS Syntax
 - 1D SSUPREM3 Doping Profiles2-15
 - 3D Structure Generation6-3
 - Analytical Doping Profiles2-14–2-15
 - Cylindrical Coordinates2-13
 - Doping2-13
 - Electrodes2-13
 - Initial Mesh2-11–2-12
 - Materials2-12
 - Regions2-12
 - Sub-sampling10-53
 - SUPERLATTICE9-10
 - SX.MESH and SY.MESH Examples
 - Setting Locally Fine Grids21-359
- ## T
- Temperature Dependent Material Parameters7-15–7-16
 - Terminal Current Criteria20-9
 - TFT14-1–14-17, 21-38–21-43
 - Amorphous Semiconductor Models14-1
 - Polycrystalline Semiconductor Models14-1
 - Simulation14-2–14-17
 - Thermal 3D
 - 3D Structure Generation17-1
 - Results17-5
 - Solutions17-4
 - Thermal Conductivity17-2
 - Thermal Simulation Model17-2
 - Thermal Boundary Conditions7-13–7-15
 - Thermal Capacity
 - C-Interpreter Defined7-8
 - Thermal Conductivity
 - Anisotropic7-5–7-6
 - C-Interpreter Defined7-5
 - Compositionally Dependent7-3–7-4
 - Standard Model7-2–7-3
 - THERMCONTACT Examples
 - Coordinate Definition21-366
 - Setting Thermal and Electrical Contacts Coincident21-366
 - Thermionic Emission Model5-13–5-15
-

| | |
|---|-----------------|
| Time Step Regions | 19-26 |
| TMA Compatibility | 2-4 |
| TonyPlot | 2-61, 21-368 |
| Track Boundary Crossings | 19-26 |
| Transient Parameters | |
| EXP | 12-44 |
| GAUSS | 12-45 |
| PULSE | 12-45–12-46 |
| PWL | 12-46 |
| PWLFILE | 12-46 |
| SFFM | 12-47 |
| SIN | 12-47 |
| TABLE | 12-48 |
| Transient Simulation | 20-21 |
| Transient Traps | 14-6–14-10 |
| Trap-Assisted Tunneling | 14-8–14-10 |
| Transport Equations | |
| Drift Diffusion Transport Model | 3-2–3-3 |
| Energy Balance Transport Model | 3-4 |
| TRAP Examples | |
| Multiple Trap Level Definition | 21-371 |
| Trap-Assisted Tunneling | |
| Poole Frenkel Barrier Lowering | 14-9 |
| Poole-Frenkel Barrier Lowering for Coulombic Wells | 3-21–3-22, 3-93 |
| Schenk | 3-91–3-93 |
| Traps | 3-14–3-25 |
| Traps and Defects | |
| Hysteresis of Interface Traps | 3-24–3-25 |
| Non-local Trap Assisted Tunneling | 3-19–3-22 |
| Recombination Models | 3-17–3-18 |
| Transient Traps | 3-23 |
| Trap-Assisted Tunneling | 3-18–3-19 |
| Trapped Charge in Poisson's Equation | 3-15–3-16 |
| TR-BDF | 6-6 |
| Tsu-esaki Model | 3-35 |
| Tunneling | |
| Band-Structure. <i>See also</i> Band Structure | 19-62 |
| Comparing Results | 19-63 |
| Parallel Momentum | 19-60–19-62 |
| Using the Statement | 19-64 |
| Two-Port Circuit | 18-15 |

U

| | |
|--|---------------|
| Uncoupled Mode Space (UMS) | 13-18 |
| Universal Schottky Tunneling (UST) Model | 3-37–3-38 |
| User Defined Materials | B-46–B-47 |
| User-Defined Two-Terminal Elements | |
| Input Parameters | 12-16 |
| Output Parameters | 12-16 |
| User-Defined Model | 12-15 |
| <i>See also</i> Circuit Element Statement B | |
| Using MC Device | 19-2 |
| UTMOST | 21-372–21-376 |

V

| | |
|--|---------------|
| VCSEL | 21-377–21-378 |
| Alternative Simulator | 9-13 |
| Far Field Patterns | 9-14 |
| Material Parameters | 9-11 |
| Numerical Parameters | 9-13 |
| Solution | 9-12 |
| VCSEL Physical Models | 9-2, 9-11 |
| Effective Frequency Model (EFM) | 9-2 |
| VCSEL Solution | |
| VCSEL Parameters | 9-12 |
| VCSEL Solution Mesh | 9-12 |
| Vector Helmholtz Equation | 8-4 |
| Vector Quantities | 21-289 |
| Velocity Autocorrelation | 19-35 |
| <i>See also</i> Self-Consistent Simulation | |
| Velocity Saturation | 5-19 |
| V _m | 10-62 |
| <i>See also</i> Solar Cells | |
| V _{oc} | 10-62 |
| <i>See also</i> Solar Cells | |

W

| | |
|-------------------------|---------------|
| Watt's Model | |
| Modifications | 3-74–3-75 |
| WAVEFORM | 21-379–21-380 |
| WKB approximation | 3-124, 3-150 |
| WKB Formula | 19-73 |
| WKB Method | 3-19 |

X

| | |
|---------------------------------------|------|
| X.MESH, Y.MESH, and Z.MESH Examples | |
| Setting Fine Grid at a Junction | 21-5 |

Y

| | |
|-----------------------------|--------|
| Yan model | 21-269 |
| <i>See also</i> Gain Models | |